

**Ongoing Face Recognition  
Vendor Test (FRVT)**  
**Part 1: Verification**

Patrick Grother  
Mei Ngan  
Kayee Hanaoka  
*Information Access Division  
Information Technology Laboratory*

This publication is available free of charge from:  
<https://www.nist.gov/programs-projects/face-recognition-vendor-test-frvt-ongoing>

2019/06/20

## ACKNOWLEDGMENTS

The authors are grateful to Wayne Salamon and Greg Fiumara at NIST for robust software infrastructure, particularly that which leverages [Berkeley DB Btrees](#) for storage of images and templates, and [Open MPI](#) for parallel execution of algorithms across our computers. Thanks also to Brian Cochran at NIST for providing highly available computers and network-attached storage.

## DISCLAIMER

Specific hardware and software products identified in this report were used in order to perform the evaluations described in this document. In no case does identification of any commercial product, trade name, or vendor, imply recommendation or endorsement by the National Institute of Standards and Technology, nor does it imply that the products and equipment identified are necessarily the best available for the purpose.

## FRVT STATUS

**This report** is a draft NIST Interagency Report, and is open for comment. It is the sixteenth edition of the report since the first was published in June 2017. Prior editions of this report are maintained on the FRVT website, and may contain useful information about older algorithms and datasets no longer used in FRVT.

**FRVT remains open:** All [four tracks](#) of the FRVT remain open to new algorithm submissions indefinitely. This report will be updated as new algorithms are evaluated, as new datasets are added, and as new analyses are included. Comments and suggestions should be directed to [frvt@nist.gov](mailto:frvt@nist.gov).

### Changes since April 2019:

- ▷ This report adds results for nine algorithms from nine developers submitted in early June 2019. These are from Tencent Deepsea, Hengrui, Kedacom, Moontime, Guangzhou Pixel, Rank One Computing, Synesis, Sensetime and Vocord.
- ▷ Another 23 algorithms have been submitted and are being evaluated. Results will be released in the next report, scheduled for July 3.
- ▷ Older algorithms for Rank One, Synesis, and Vocord have been retired, per the policy to list only two algorithms per developer.

### Changes since February 2019:

- ▷ This report adds results for 49 algorithms from 42 developers submitted in early March 2019.
- ▷ This report omits results for algorithms that we retired. We retired for three reasons: 1. The developer submitted a new algorithm, and we only list two. 2. The algorithm needs a GPU, and we no longer allow GPU-based algorithms. 3. Inoperable algorithms.
- ▷ Previous results for retired algorithms are available in older editions of this report linked [here](#).
- ▷ The mugshot database used from February 2017 to January 2019 has been replaced with an extract of the mugshot database documented in NIST Interagency Report 8238, November 2018. The new mugshot set is described in section [2.3](#) and is adopted because:
  - ▷▷ It has much better identity label integrity, so that false non-match rates are substantially lower than those reported in FRVT 1:1 reports to date - see [Figure 22](#).
  - ▷▷ It includes images collected over a 17 year period such that ageing can be much better characterized - - see [Figure 92](#).
- ▷ Using the new mugshot database, [Figure 92](#) shows accuracy for four demographic groups identified in the biographic metadata that accompanies the data: black females, black males, white females and white males.
- ▷ The report adds [Figure 4](#) with results for the twenty human-difficult pairs used in the May 2018 paper [Face recognition accuracy of forensic examiners, superrecognizers, and face recognition algorithms](#) by Phillips et al. [[1](#)].
- ▷ The report uses an update to the wild image database that corrects some ground truth labels.
- ▷ Some results for the child exploitation database are not complete. They are typically updated less frequently than for other image sets.

## Contents

<b>ACKNOWLEDGMENTS</b>	<b>1</b>
<b>DISCLAIMER</b>	<b>1</b>
<b>1 METRICS</b>	<b>19</b>
1.1 CORE ACCURACY . . . . .	19
<b>2 DATASETS</b>	<b>20</b>
2.1 CHILD EXPLOITATION IMAGES . . . . .	20
2.2 VISA IMAGES . . . . .	20
2.3 MUGSHOT IMAGES . . . . .	20
2.4 WILD IMAGES . . . . .	21
<b>3 RESULTS</b>	<b>21</b>
3.1 TEST GOALS . . . . .	21
3.2 TEST DESIGN . . . . .	22
3.3 FAILURE TO ENROLL . . . . .	24
3.4 RECOGNITION ACCURACY . . . . .	27
3.5 GENUINE DISTRIBUTION STABILITY . . . . .	99
3.5.1 EFFECT OF BIRTH PLACE ON THE GENUINE DISTRIBUTION . . . . .	99
3.5.2 EFFECT OF AGEING . . . . .	110
3.5.3 EFFECT OF AGE ON GENUINE SUBJECTS . . . . .	119
3.6 IMPOSTOR DISTRIBUTION STABILITY . . . . .	131
3.6.1 EFFECT OF BIRTH PLACE ON THE IMPOSTOR DISTRIBUTION . . . . .	131
3.6.2 EFFECT OF AGE ON IMPOSTORS . . . . .	344

## List of Tables

1 ALGORITHM SUMMARY . . . . .	12
2 ALGORITHM SUMMARY . . . . .	13
3 ALGORITHM SUMMARY . . . . .	14
4 FALSE NON-MATCH RATE . . . . .	15
5 FALSE NON-MATCH RATE . . . . .	16
6 FAILURE TO ENROL RATES . . . . .	25
7 FAILURE TO ENROL RATES . . . . .	26

## List of Figures

1 PERFORMANCE SUMMARY: FNMR VS. TEMPLATE SIZE TRADEOFF . . . . .	17
2 PERFORMANCE SUMMARY: FNMR VS. TEMPLATE TIME TRADEOFF . . . . .	18
3 EXAMPLE IMAGES . . . . .	21
(A) VISA . . . . .	21
(B) MUGSHOT . . . . .	21
(C) WILD . . . . .	21
4 PERFORMANCE ON 20 HUMAN-DIFFICULT PAIRS . . . . .	28
5 ERROR TRADEOFF CHARACTERISTIC: VISA IMAGES . . . . .	29
6 ERROR TRADEOFF CHARACTERISTIC: VISA IMAGES . . . . .	30
7 ERROR TRADEOFF CHARACTERISTIC: VISA IMAGES . . . . .	31
8 ERROR TRADEOFF CHARACTERISTIC: VISA IMAGES . . . . .	32
9 ERROR TRADEOFF CHARACTERISTIC: VISA IMAGES . . . . .	33

10	ERROR TRADEOFF CHARACTERISTIC: VISA IMAGES	34
11	ERROR TRADEOFF CHARACTERISTIC: VISA IMAGES	35
12	ERROR TRADEOFF CHARACTERISTIC: VISA IMAGES	36
13	ERROR TRADEOFF CHARACTERISTIC: VISA IMAGES	37
14	ERROR TRADEOFF CHARACTERISTIC: VISA IMAGES	38
15	ERROR TRADEOFF CHARACTERISTIC: VISA IMAGES	39
16	ERROR TRADEOFF CHARACTERISTIC: VISA IMAGES	40
17	ERROR TRADEOFF CHARACTERISTIC: MUGSHOT IMAGES	41
18	ERROR TRADEOFF CHARACTERISTIC: MUGSHOT IMAGES	42
19	ERROR TRADEOFF CHARACTERISTIC: MUGSHOT IMAGES	43
20	ERROR TRADEOFF CHARACTERISTIC: MUGSHOT IMAGES	44
21	ERROR TRADEOFF CHARACTERISTIC: MUGSHOT IMAGES	45
22	ERROR TRADEOFF CHARACTERISTIC: MUGSHOT IMAGES	46
23	ERROR TRADEOFF CHARACTERISTIC: WILD IMAGES	47
24	ERROR TRADEOFF CHARACTERISTIC: WILD IMAGES	48
25	ERROR TRADEOFF CHARACTERISTIC: WILD IMAGES	49
26	ERROR TRADEOFF CHARACTERISTIC: WILD IMAGES	50
27	ERROR TRADEOFF CHARACTERISTIC: WILD IMAGES	51
28	ERROR TRADEOFF CHARACTERISTICS: CHILD EXPLOITATION IMAGES	52
29	ERROR TRADEOFF CHARACTERISTICS: CHILD EXPLOITATION IMAGES	53
30	ERROR TRADEOFF CHARACTERISTICS: CHILD EXPLOITATION IMAGES	54
31	CMC CHARACTERISTICS: CHILD EXPLOITATION IMAGES	55
32	CMC CHARACTERISTICS: CHILD EXPLOITATION IMAGES	56
33	CMC CHARACTERISTICS: CHILD EXPLOITATION IMAGES	57
34	FALSE MATCH RATES WITHIN AND ACROSS DEMOGRAPHIC GROUPS	58
35	FALSE MATCH RATES WITHIN AND ACROSS DEMOGRAPHIC GROUPS	59
36	FALSE MATCH RATES WITHIN AND ACROSS DEMOGRAPHIC GROUPS	60
37	FALSE MATCH RATES WITHIN AND ACROSS DEMOGRAPHIC GROUPS	61
38	FALSE MATCH RATES WITHIN AND ACROSS DEMOGRAPHIC GROUPS	62
39	FALSE MATCH RATES WITHIN AND ACROSS DEMOGRAPHIC GROUPS	63
40	SEX AND RACE EFFECTS: MUGSHOT IMAGES	64
41	SEX AND RACE EFFECTS: MUGSHOT IMAGES	65
42	SEX AND RACE EFFECTS: MUGSHOT IMAGES	66
43	SEX AND RACE EFFECTS: MUGSHOT IMAGES	67
44	SEX AND RACE EFFECTS: MUGSHOT IMAGES	68
45	SEX AND RACE EFFECTS: MUGSHOT IMAGES	69
46	SEX EFFECTS: VISA IMAGES	70
47	SEX EFFECTS: VISA IMAGES	71
48	SEX EFFECTS: VISA IMAGES	72
49	SEX EFFECTS: VISA IMAGES	73
50	SEX EFFECTS: VISA IMAGES	74
51	SEX EFFECTS: VISA IMAGES	75
52	SEX EFFECTS: VISA IMAGES	76
53	SEX EFFECTS: VISA IMAGES	77
54	SEX EFFECTS: VISA IMAGES	78
55	SEX EFFECTS: VISA IMAGES	79
56	FALSE MATCH RATE CALIBRATION: MUGSHOT IMAGES	80
57	FALSE MATCH RATE CALIBRATION: MUGSHOT IMAGES	81
58	FALSE MATCH RATE CALIBRATION: MUGSHOT IMAGES	82
59	FALSE MATCH RATE CALIBRATION: MUGSHOT IMAGES	83
60	FALSE MATCH RATE CALIBRATION: MUGSHOT IMAGES	84
61	FALSE MATCH RATE CALIBRATION: MUGSHOT IMAGES	85
62	FALSE MATCH RATE CALIBRATION: VISA IMAGES	86
63	FALSE MATCH RATE CALIBRATION: VISA IMAGES	87
64	FALSE MATCH RATE CALIBRATION: VISA IMAGES	88
65	FALSE MATCH RATE CALIBRATION: VISA IMAGES	89
66	FALSE MATCH RATE CALIBRATION: VISA IMAGES	90

67	FALSE MATCH RATE CALIBRATION: VISA IMAGES	91
68	FALSE MATCH RATE CALIBRATION: VISA IMAGES	92
69	FALSE MATCH RATE CALIBRATION: VISA IMAGES	93
70	FALSE MATCH RATE CALIBRATION: VISA IMAGES	94
71	FALSE MATCH RATE CALIBRATION: VISA IMAGES	95
72	FALSE MATCH RATE CALIBRATION: VISA IMAGES	96
73	FALSE MATCH RATE CALIBRATION: VISA IMAGES	97
74	FALSE MATCH RATE CONCENTRATION: VISA IMAGES	98
75	EFFECT OF COUNTRY OF BIRTH ON FNMR	100
76	EFFECT OF COUNTRY OF BIRTH ON FNMR	101
77	EFFECT OF COUNTRY OF BIRTH ON FNMR	102
78	EFFECT OF COUNTRY OF BIRTH ON FNMR	103
79	EFFECT OF COUNTRY OF BIRTH ON FNMR	104
80	EFFECT OF COUNTRY OF BIRTH ON FNMR	105
81	EFFECT OF COUNTRY OF BIRTH ON FNMR	106
82	EFFECT OF COUNTRY OF BIRTH ON FNMR	107
83	EFFECT OF COUNTRY OF BIRTH ON FNMR	108
84	EFFECT OF COUNTRY OF BIRTH ON FNMR	109
85	ERROR TRADEOFF CHARACTERISTIC: MUGSHOT IMAGES	111
86	ERROR TRADEOFF CHARACTERISTIC: MUGSHOT IMAGES	112
87	ERROR TRADEOFF CHARACTERISTIC: MUGSHOT IMAGES	113
88	ERROR TRADEOFF CHARACTERISTIC: MUGSHOT IMAGES	114
89	ERROR TRADEOFF CHARACTERISTIC: MUGSHOT IMAGES	115
90	ERROR TRADEOFF CHARACTERISTIC: MUGSHOT IMAGES	116
91	ERROR TRADEOFF CHARACTERISTIC: MUGSHOT IMAGES	117
92	ERROR TRADEOFF CHARACTERISTIC: MUGSHOT IMAGES	118
93	EFFECT OF SUBJECT AGE ON FNMR	120
94	EFFECT OF SUBJECT AGE ON FNMR	121
95	EFFECT OF SUBJECT AGE ON FNMR	122
96	EFFECT OF SUBJECT AGE ON FNMR	123
97	EFFECT OF SUBJECT AGE ON FNMR	124
98	EFFECT OF SUBJECT AGE ON FNMR	125
99	EFFECT OF SUBJECT AGE ON FNMR	126
100	EFFECT OF SUBJECT AGE ON FNMR	127
101	EFFECT OF SUBJECT AGE ON FNMR	128
102	EFFECT OF SUBJECT AGE ON FNMR	129
103	WORST CASE REGIONAL EFFECT FNMR	132
104	IMPOSTOR DISTRIBUTION SHIFTS FOR SELECT COUNTRY PAIRS	134
105	ALGORITHM 3DIVI-003 CROSS REGION FMR	135
106	ALGORITHM ALCHERA-000 CROSS REGION FMR	136
107	ALGORITHM ALCHERA-001 CROSS REGION FMR	137
108	ALGORITHM ALLGOVISION-000 CROSS REGION FMR	138
109	ALGORITHM AMPLIFIEDGROUP-001 CROSS REGION FMR	139
110	ALGORITHM ANKE-002 CROSS REGION FMR	140
111	ALGORITHM ANKE-003 CROSS REGION FMR	141
112	ALGORITHM ANYVISION-002 CROSS REGION FMR	142
113	ALGORITHM ANYVISION-004 CROSS REGION FMR	143
114	ALGORITHM AWARE-003 CROSS REGION FMR	144
115	ALGORITHM AWARE-004 CROSS REGION FMR	145
116	ALGORITHM AYONIX-000 CROSS REGION FMR	146
117	ALGORITHM BM-001 CROSS REGION FMR	147
118	ALGORITHM CAMVI-002 CROSS REGION FMR	148
119	ALGORITHM CAMVI-003 CROSS REGION FMR	149
120	ALGORITHM CEIEC-001 CROSS REGION FMR	150
121	ALGORITHM COGENT-002 CROSS REGION FMR	151

122 ALGORITHM COGENT-003 CROSS REGION FMR . . . . .	152
123 ALGORITHM COGNITEC-000 CROSS REGION FMR . . . . .	153
124 ALGORITHM COGNITEC-001 CROSS REGION FMR . . . . .	154
125 ALGORITHM CYBEREXTRUDER-001 CROSS REGION FMR . . . . .	155
126 ALGORITHM CYBEREXTRUDER-002 CROSS REGION FMR . . . . .	156
127 ALGORITHM CYBERLINK-000 CROSS REGION FMR . . . . .	157
128 ALGORITHM CYBERLINK-001 CROSS REGION FMR . . . . .	158
129 ALGORITHM DAHUA-001 CROSS REGION FMR . . . . .	159
130 ALGORITHM DAHUA-002 CROSS REGION FMR . . . . .	160
131 ALGORITHM DERMALOG-005 CROSS REGION FMR . . . . .	161
132 ALGORITHM DERMALOG-006 CROSS REGION FMR . . . . .	162
133 ALGORITHM DIGITALBARIERS-002 CROSS REGION FMR . . . . .	163
134 ALGORITHM EVERAI-001 CROSS REGION FMR . . . . .	164
135 ALGORITHM EVERAI-002 CROSS REGION FMR . . . . .	165
136 ALGORITHM GLORY-000 CROSS REGION FMR . . . . .	166
137 ALGORITHM GLORY-001 CROSS REGION FMR . . . . .	167
138 ALGORITHM GORILLA-001 CROSS REGION FMR . . . . .	168
139 ALGORITHM GORILLA-002 CROSS REGION FMR . . . . .	169
140 ALGORITHM HIK-001 CROSS REGION FMR . . . . .	170
141 ALGORITHM HR-000 CROSS REGION FMR . . . . .	171
142 ALGORITHM ID3-003 CROSS REGION FMR . . . . .	172
143 ALGORITHM ID3-004 CROSS REGION FMR . . . . .	173
144 ALGORITHM IDEMIA-003 CROSS REGION FMR . . . . .	174
145 ALGORITHM IDEMIA-004 CROSS REGION FMR . . . . .	175
146 ALGORITHM IIT-000 CROSS REGION FMR . . . . .	176
147 ALGORITHM IMPERIAL-000 CROSS REGION FMR . . . . .	177
148 ALGORITHM IMPERIAL-001 CROSS REGION FMR . . . . .	178
149 ALGORITHM INCODE-002 CROSS REGION FMR . . . . .	179
150 ALGORITHM INCODE-003 CROSS REGION FMR . . . . .	180
151 ALGORITHM INNOVATRICS-004 CROSS REGION FMR . . . . .	181
152 ALGORITHM INNOVATRICS-005 CROSS REGION FMR . . . . .	182
153 ALGORITHM INTELLIVISION-001 CROSS REGION FMR . . . . .	183
154 ALGORITHM ISITYOU-000 CROSS REGION FMR . . . . .	184
155 ALGORITHM ISYSTEMS-001 CROSS REGION FMR . . . . .	185
156 ALGORITHM ISYSTEMS-002 CROSS REGION FMR . . . . .	186
157 ALGORITHM ITMO-005 CROSS REGION FMR . . . . .	187
158 ALGORITHM ITMO-006 CROSS REGION FMR . . . . .	188
159 ALGORITHM KAKAO-001 CROSS REGION FMR . . . . .	189
160 ALGORITHM LOOKMAN-002 CROSS REGION FMR . . . . .	190
161 ALGORITHM MEGVII-001 CROSS REGION FMR . . . . .	191
162 ALGORITHM MEGVII-002 CROSS REGION FMR . . . . .	192
163 ALGORITHM MEIYA-001 CROSS REGION FMR . . . . .	193
164 ALGORITHM MICROFOCUS-001 CROSS REGION FMR . . . . .	194
165 ALGORITHM MICROFOCUS-002 CROSS REGION FMR . . . . .	195
166 ALGORITHM NEUROTECHNOLOGY-004 CROSS REGION FMR . . . . .	196
167 ALGORITHM NEUROTECHNOLOGY-005 CROSS REGION FMR . . . . .	197
168 ALGORITHM NODEFLUX-000 CROSS REGION FMR . . . . .	198
169 ALGORITHM NODEFLUX-001 CROSS REGION FMR . . . . .	199
170 ALGORITHM NTECHLAB-005 CROSS REGION FMR . . . . .	200
171 ALGORITHM NTECHLAB-006 CROSS REGION FMR . . . . .	201
172 ALGORITHM PSL-001 CROSS REGION FMR . . . . .	202
173 ALGORITHM PSL-002 CROSS REGION FMR . . . . .	203
174 ALGORITHM RANKONE-006 CROSS REGION FMR . . . . .	204
175 ALGORITHM REALNETWORKS-001 CROSS REGION FMR . . . . .	205
176 ALGORITHM REALNETWORKS-002 CROSS REGION FMR . . . . .	206
177 ALGORITHM REMARKAI-000 CROSS REGION FMR . . . . .	207
178 ALGORITHM REMARKAI-001 CROSS REGION FMR . . . . .	208

179 ALGORITHM SAFFE-001 CROSS REGION FMR . . . . .	209
180 ALGORITHM SAFFE-002 CROSS REGION FMR . . . . .	210
181 ALGORITHM SENSETIME-001 CROSS REGION FMR . . . . .	211
182 ALGORITHM SENSETIME-002 CROSS REGION FMR . . . . .	212
183 ALGORITHM SHAMAN-000 CROSS REGION FMR . . . . .	213
184 ALGORITHM SHAMAN-001 CROSS REGION FMR . . . . .	214
185 ALGORITHM SIAT-002 CROSS REGION FMR . . . . .	215
186 ALGORITHM SIAT-004 CROSS REGION FMR . . . . .	216
187 ALGORITHM SMILART-002 CROSS REGION FMR . . . . .	217
188 ALGORITHM SMILART-003 CROSS REGION FMR . . . . .	218
189 ALGORITHM SYNESIS-004 CROSS REGION FMR . . . . .	219
190 ALGORITHM TECH5-001 CROSS REGION FMR . . . . .	220
191 ALGORITHM TECH5-002 CROSS REGION FMR . . . . .	221
192 ALGORITHM TEVIAN-003 CROSS REGION FMR . . . . .	222
193 ALGORITHM TEVIAN-004 CROSS REGION FMR . . . . .	223
194 ALGORITHM TIGER-002 CROSS REGION FMR . . . . .	224
195 ALGORITHM TIGER-003 CROSS REGION FMR . . . . .	225
196 ALGORITHM TOSHIBA-002 CROSS REGION FMR . . . . .	226
197 ALGORITHM TOSHIBA-003 CROSS REGION FMR . . . . .	227
198 ALGORITHM VCOG-002 CROSS REGION FMR . . . . .	228
199 ALGORITHM VD-001 CROSS REGION FMR . . . . .	229
200 ALGORITHM VERIDAS-001 CROSS REGION FMR . . . . .	230
201 ALGORITHM VERIDAS-002 CROSS REGION FMR . . . . .	231
202 ALGORITHM VIGILANTSOLUTIONS-005 CROSS REGION FMR . . . . .	232
203 ALGORITHM VIGILANTSOLUTIONS-006 CROSS REGION FMR . . . . .	233
204 ALGORITHM VION-000 CROSS REGION FMR . . . . .	234
205 ALGORITHM VISIONBOX-000 CROSS REGION FMR . . . . .	235
206 ALGORITHM VISIONBOX-001 CROSS REGION FMR . . . . .	236
207 ALGORITHM VISIONLABS-005 CROSS REGION FMR . . . . .	237
208 ALGORITHM VISIONLABS-006 CROSS REGION FMR . . . . .	238
209 ALGORITHM VOCORD-006 CROSS REGION FMR . . . . .	239
210 ALGORITHM YISHENG-004 CROSS REGION FMR . . . . .	240
211 ALGORITHM YITU-003 CROSS REGION FMR . . . . .	241
212 ALGORITHM 3DIVI-003 CROSS COUNTRY FMR . . . . .	242
213 ALGORITHM ALCHERA-000 CROSS COUNTRY FMR . . . . .	243
214 ALGORITHM ALCHERA-001 CROSS COUNTRY FMR . . . . .	244
215 ALGORITHM ALLGOVISION-000 CROSS COUNTRY FMR . . . . .	245
216 ALGORITHM ANKE-002 CROSS COUNTRY FMR . . . . .	246
217 ALGORITHM ANKE-003 CROSS COUNTRY FMR . . . . .	247
218 ALGORITHM ANYVISION-002 CROSS COUNTRY FMR . . . . .	248
219 ALGORITHM ANYVISION-004 CROSS COUNTRY FMR . . . . .	249
220 ALGORITHM AWARE-003 CROSS COUNTRY FMR . . . . .	250
221 ALGORITHM AWARE-004 CROSS COUNTRY FMR . . . . .	251
222 ALGORITHM AYONIX-000 CROSS COUNTRY FMR . . . . .	252
223 ALGORITHM BM-001 CROSS COUNTRY FMR . . . . .	253
224 ALGORITHM CAMVI-002 CROSS COUNTRY FMR . . . . .	254
225 ALGORITHM CAMVI-003 CROSS COUNTRY FMR . . . . .	255
226 ALGORITHM CEIEC-001 CROSS COUNTRY FMR . . . . .	256
227 ALGORITHM COGENT-002 CROSS COUNTRY FMR . . . . .	257
228 ALGORITHM COGENT-003 CROSS COUNTRY FMR . . . . .	258
229 ALGORITHM COGNITEC-000 CROSS COUNTRY FMR . . . . .	259
230 ALGORITHM COGNITEC-001 CROSS COUNTRY FMR . . . . .	260
231 ALGORITHM CYBEREXTRUDER-001 CROSS COUNTRY FMR . . . . .	261
232 ALGORITHM CYBEREXTRUDER-002 CROSS COUNTRY FMR . . . . .	262
233 ALGORITHM CYBERLINK-000 CROSS COUNTRY FMR . . . . .	263
234 ALGORITHM CYBERLINK-001 CROSS COUNTRY FMR . . . . .	264
235 ALGORITHM DAHUA-001 CROSS COUNTRY FMR . . . . .	265

236 ALGORITHM DAHUA-002 CROSS COUNTRY FMR . . . . .	266
237 ALGORITHM DERMALOG-005 CROSS COUNTRY FMR . . . . .	267
238 ALGORITHM DERMALOG-006 CROSS COUNTRY FMR . . . . .	268
239 ALGORITHM DIGITALBARRIERS-002 CROSS COUNTRY FMR . . . . .	269
240 ALGORITHM EVERAI-001 CROSS COUNTRY FMR . . . . .	270
241 ALGORITHM EVERAI-002 CROSS COUNTRY FMR . . . . .	271
242 ALGORITHM GLORY-000 CROSS COUNTRY FMR . . . . .	272
243 ALGORITHM GLORY-001 CROSS COUNTRY FMR . . . . .	273
244 ALGORITHM GORILLA-001 CROSS COUNTRY FMR . . . . .	274
245 ALGORITHM GORILLA-002 CROSS COUNTRY FMR . . . . .	275
246 ALGORITHM HIK-001 CROSS COUNTRY FMR . . . . .	276
247 ALGORITHM HR-000 CROSS COUNTRY FMR . . . . .	277
248 ALGORITHM ID3-003 CROSS COUNTRY FMR . . . . .	278
249 ALGORITHM ID3-004 CROSS COUNTRY FMR . . . . .	279
250 ALGORITHM IDEMIA-003 CROSS COUNTRY FMR . . . . .	280
251 ALGORITHM IDEMIA-004 CROSS COUNTRY FMR . . . . .	281
252 ALGORITHM IIT-000 CROSS COUNTRY FMR . . . . .	282
253 ALGORITHM IMPERIAL-000 CROSS COUNTRY FMR . . . . .	283
254 ALGORITHM IMPERIAL-001 CROSS COUNTRY FMR . . . . .	284
255 ALGORITHM INCODE-002 CROSS COUNTRY FMR . . . . .	285
256 ALGORITHM INCODE-003 CROSS COUNTRY FMR . . . . .	286
257 ALGORITHM INNOVATRICS-004 CROSS COUNTRY FMR . . . . .	287
258 ALGORITHM INNOVATRICS-005 CROSS COUNTRY FMR . . . . .	288
259 ALGORITHM INTELLIVISION-001 CROSS COUNTRY FMR . . . . .	289
260 ALGORITHM ISITYOU-000 CROSS COUNTRY FMR . . . . .	290
261 ALGORITHM ISYSTEMS-001 CROSS COUNTRY FMR . . . . .	291
262 ALGORITHM ISYSTEMS-002 CROSS COUNTRY FMR . . . . .	292
263 ALGORITHM ITMO-005 CROSS COUNTRY FMR . . . . .	293
264 ALGORITHM ITMO-006 CROSS COUNTRY FMR . . . . .	294
265 ALGORITHM KAKAO-001 CROSS COUNTRY FMR . . . . .	295
266 ALGORITHM LOOKMAN-002 CROSS COUNTRY FMR . . . . .	296
267 ALGORITHM MEGVII-001 CROSS COUNTRY FMR . . . . .	297
268 ALGORITHM MEGVII-002 CROSS COUNTRY FMR . . . . .	298
269 ALGORITHM MEIYA-001 CROSS COUNTRY FMR . . . . .	299
270 ALGORITHM MICROFOCUS-001 CROSS COUNTRY FMR . . . . .	300
271 ALGORITHM MICROFOCUS-002 CROSS COUNTRY FMR . . . . .	301
272 ALGORITHM NODEFLUX-001 CROSS COUNTRY FMR . . . . .	302
273 ALGORITHM NTECHLAB-005 CROSS COUNTRY FMR . . . . .	303
274 ALGORITHM NTECHLAB-006 CROSS COUNTRY FMR . . . . .	304
275 ALGORITHM PSL-001 CROSS COUNTRY FMR . . . . .	305
276 ALGORITHM PSL-002 CROSS COUNTRY FMR . . . . .	306
277 ALGORITHM RANKONE-006 CROSS COUNTRY FMR . . . . .	307
278 ALGORITHM REALNETWORKS-001 CROSS COUNTRY FMR . . . . .	308
279 ALGORITHM REALNETWORKS-002 CROSS COUNTRY FMR . . . . .	309
280 ALGORITHM REMARKAI-000 CROSS COUNTRY FMR . . . . .	310
281 ALGORITHM REMARKAI-001 CROSS COUNTRY FMR . . . . .	311
282 ALGORITHM SAFFE-001 CROSS COUNTRY FMR . . . . .	312
283 ALGORITHM SAFFE-002 CROSS COUNTRY FMR . . . . .	313
284 ALGORITHM SENSETIME-001 CROSS COUNTRY FMR . . . . .	314
285 ALGORITHM SENSETIME-002 CROSS COUNTRY FMR . . . . .	315
286 ALGORITHM SHAMAN-000 CROSS COUNTRY FMR . . . . .	316
287 ALGORITHM SHAMAN-001 CROSS COUNTRY FMR . . . . .	317
288 ALGORITHM SIAT-002 CROSS COUNTRY FMR . . . . .	318
289 ALGORITHM SIAT-004 CROSS COUNTRY FMR . . . . .	319
290 ALGORITHM SMILART-002 CROSS COUNTRY FMR . . . . .	320
291 ALGORITHM SMILART-003 CROSS COUNTRY FMR . . . . .	321
292 ALGORITHM TECH5-001 CROSS COUNTRY FMR . . . . .	322

293 ALGORITHM TECH5-002 CROSS COUNTRY FMR . . . . .	323
294 ALGORITHM TEVIAN-003 CROSS COUNTRY FMR . . . . .	324
295 ALGORITHM TEVIAN-004 CROSS COUNTRY FMR . . . . .	325
296 ALGORITHM TIGER-002 CROSS COUNTRY FMR . . . . .	326
297 ALGORITHM TIGER-003 CROSS COUNTRY FMR . . . . .	327
298 ALGORITHM TOSHIBA-002 CROSS COUNTRY FMR . . . . .	328
299 ALGORITHM TOSHIBA-003 CROSS COUNTRY FMR . . . . .	329
300 ALGORITHM VCOG-002 CROSS COUNTRY FMR . . . . .	330
301 ALGORITHM VD-001 CROSS COUNTRY FMR . . . . .	331
302 ALGORITHM VERIDAS-001 CROSS COUNTRY FMR . . . . .	332
303 ALGORITHM VERIDAS-002 CROSS COUNTRY FMR . . . . .	333
304 ALGORITHM VIGILANTSOLUTIONS-005 CROSS COUNTRY FMR . . . . .	334
305 ALGORITHM VIGILANTSOLUTIONS-006 CROSS COUNTRY FMR . . . . .	335
306 ALGORITHM VION-000 CROSS COUNTRY FMR . . . . .	336
307 ALGORITHM VISIONBOX-000 CROSS COUNTRY FMR . . . . .	337
308 ALGORITHM VISIONBOX-001 CROSS COUNTRY FMR . . . . .	338
309 ALGORITHM VISIONLABS-005 CROSS COUNTRY FMR . . . . .	339
310 ALGORITHM VISIONLABS-006 CROSS COUNTRY FMR . . . . .	340
311 ALGORITHM YISHENG-004 CROSS COUNTRY FMR . . . . .	341
312 ALGORITHM YITU-003 CROSS COUNTRY FMR . . . . .	342
313 IMPOSTOR COUNTS FOR CROSS COUNTRY FMR CALCULATIONS . . . . .	343
314 ALGORITHM 3DIVI-003 CROSS AGE FMR . . . . .	345
315 ALGORITHM ALCHERA-000 CROSS AGE FMR . . . . .	346
316 ALGORITHM ALCHERA-001 CROSS AGE FMR . . . . .	347
317 ALGORITHM ALLGOVISION-000 CROSS AGE FMR . . . . .	348
318 ALGORITHM AMPLIFIEDGROUP-001 CROSS AGE FMR . . . . .	349
319 ALGORITHM ANKE-002 CROSS AGE FMR . . . . .	350
320 ALGORITHM ANKE-003 CROSS AGE FMR . . . . .	351
321 ALGORITHM ANYVISION-002 CROSS AGE FMR . . . . .	352
322 ALGORITHM ANYVISION-004 CROSS AGE FMR . . . . .	353
323 ALGORITHM AWARE-003 CROSS AGE FMR . . . . .	354
324 ALGORITHM AWARE-004 CROSS AGE FMR . . . . .	355
325 ALGORITHM AYONIX-000 CROSS AGE FMR . . . . .	356
326 ALGORITHM BM-001 CROSS AGE FMR . . . . .	357
327 ALGORITHM CAMVI-002 CROSS AGE FMR . . . . .	358
328 ALGORITHM CAMVI-003 CROSS AGE FMR . . . . .	359
329 ALGORITHM CEIEC-001 CROSS AGE FMR . . . . .	360
330 ALGORITHM COGENT-002 CROSS AGE FMR . . . . .	361
331 ALGORITHM COGENT-003 CROSS AGE FMR . . . . .	362
332 ALGORITHM COGNITEC-000 CROSS AGE FMR . . . . .	363
333 ALGORITHM COGNITEC-001 CROSS AGE FMR . . . . .	364
334 ALGORITHM CYBEREXTRUDER-001 CROSS AGE FMR . . . . .	365
335 ALGORITHM CYBEREXTRUDER-002 CROSS AGE FMR . . . . .	366
336 ALGORITHM CYBERLINK-000 CROSS AGE FMR . . . . .	367
337 ALGORITHM CYBERLINK-001 CROSS AGE FMR . . . . .	368
338 ALGORITHM DAHUA-001 CROSS AGE FMR . . . . .	369
339 ALGORITHM DAHUA-002 CROSS AGE FMR . . . . .	370
340 ALGORITHM DERMALOG-005 CROSS AGE FMR . . . . .	371
341 ALGORITHM DERMALOG-006 CROSS AGE FMR . . . . .	372
342 ALGORITHM DIGITALBARRIERS-002 CROSS AGE FMR . . . . .	373
343 ALGORITHM EVERAI-001 CROSS AGE FMR . . . . .	374
344 ALGORITHM EVERAI-002 CROSS AGE FMR . . . . .	375
345 ALGORITHM GLORY-001 CROSS AGE FMR . . . . .	376
346 ALGORITHM GORILLA-001 CROSS AGE FMR . . . . .	377
347 ALGORITHM GORILLA-002 CROSS AGE FMR . . . . .	378
348 ALGORITHM HIK-001 CROSS AGE FMR . . . . .	379
349 ALGORITHM HR-000 CROSS AGE FMR . . . . .	380

350 ALGORITHM ID3-003 CROSS AGE FMR . . . . .	381
351 ALGORITHM ID3-004 CROSS AGE FMR . . . . .	382
352 ALGORITHM IDEMIA-003 CROSS AGE FMR . . . . .	383
353 ALGORITHM IDEMIA-004 CROSS AGE FMR . . . . .	384
354 ALGORITHM IIT-000 CROSS AGE FMR . . . . .	385
355 ALGORITHM IMPERIAL-000 CROSS AGE FMR . . . . .	386
356 ALGORITHM IMPERIAL-001 CROSS AGE FMR . . . . .	387
357 ALGORITHM INCODE-002 CROSS AGE FMR . . . . .	388
358 ALGORITHM INCODE-003 CROSS AGE FMR . . . . .	389
359 ALGORITHM INNOVATRICS-004 CROSS AGE FMR . . . . .	390
360 ALGORITHM INNOVATRICS-005 CROSS AGE FMR . . . . .	391
361 ALGORITHM INTELLIVISION-001 CROSS AGE FMR . . . . .	392
362 ALGORITHM ISITYOU-000 CROSS AGE FMR . . . . .	393
363 ALGORITHM ISYSTEMS-001 CROSS AGE FMR . . . . .	394
364 ALGORITHM ISYSTEMS-002 CROSS AGE FMR . . . . .	395
365 ALGORITHM ITMO-005 CROSS AGE FMR . . . . .	396
366 ALGORITHM ITMO-006 CROSS AGE FMR . . . . .	397
367 ALGORITHM KAKAO-001 CROSS AGE FMR . . . . .	398
368 ALGORITHM LOOKMAN-002 CROSS AGE FMR . . . . .	399
369 ALGORITHM MEGVII-001 CROSS AGE FMR . . . . .	400
370 ALGORITHM MEGVII-002 CROSS AGE FMR . . . . .	401
371 ALGORITHM MEIYA-001 CROSS AGE FMR . . . . .	402
372 ALGORITHM MICROFOCUS-001 CROSS AGE FMR . . . . .	403
373 ALGORITHM MICROFOCUS-002 CROSS AGE FMR . . . . .	404
374 ALGORITHM NEUROTECHNOLOGY-004 CROSS AGE FMR . . . . .	405
375 ALGORITHM NODEFLUX-001 CROSS AGE FMR . . . . .	406
376 ALGORITHM NTECHLAB-005 CROSS AGE FMR . . . . .	407
377 ALGORITHM NTECHLAB-006 CROSS AGE FMR . . . . .	408
378 ALGORITHM PSL-001 CROSS AGE FMR . . . . .	409
379 ALGORITHM PSL-002 CROSS AGE FMR . . . . .	410
380 ALGORITHM RANKONE-006 CROSS AGE FMR . . . . .	411
381 ALGORITHM REALNETWORKS-001 CROSS AGE FMR . . . . .	412
382 ALGORITHM REALNETWORKS-002 CROSS AGE FMR . . . . .	413
383 ALGORITHM REMARKAI-000 CROSS AGE FMR . . . . .	414
384 ALGORITHM REMARKAI-001 CROSS AGE FMR . . . . .	415
385 ALGORITHM SAFFE-001 CROSS AGE FMR . . . . .	416
386 ALGORITHM SAFFE-002 CROSS AGE FMR . . . . .	417
387 ALGORITHM SENSETIME-001 CROSS AGE FMR . . . . .	418
388 ALGORITHM SENSETIME-002 CROSS AGE FMR . . . . .	419
389 ALGORITHM SHAMAN-000 CROSS AGE FMR . . . . .	420
390 ALGORITHM SHAMAN-001 CROSS AGE FMR . . . . .	421
391 ALGORITHM SIAT-002 CROSS AGE FMR . . . . .	422
392 ALGORITHM SIAT-004 CROSS AGE FMR . . . . .	423
393 ALGORITHM SMILART-002 CROSS AGE FMR . . . . .	424
394 ALGORITHM SMILART-003 CROSS AGE FMR . . . . .	425
395 ALGORITHM SYNESIS-004 CROSS AGE FMR . . . . .	426
396 ALGORITHM TECH5-001 CROSS AGE FMR . . . . .	427
397 ALGORITHM TECH5-002 CROSS AGE FMR . . . . .	428
398 ALGORITHM TEVIAN-003 CROSS AGE FMR . . . . .	429
399 ALGORITHM TEVIAN-004 CROSS AGE FMR . . . . .	430
400 ALGORITHM TIGER-002 CROSS AGE FMR . . . . .	431
401 ALGORITHM TIGER-003 CROSS AGE FMR . . . . .	432
402 ALGORITHM TOSHIBA-002 CROSS AGE FMR . . . . .	433
403 ALGORITHM TOSHIBA-003 CROSS AGE FMR . . . . .	434
404 ALGORITHM VCOG-002 CROSS AGE FMR . . . . .	435
405 ALGORITHM VD-001 CROSS AGE FMR . . . . .	436
406 ALGORITHM VERIDAS-001 CROSS AGE FMR . . . . .	437

407 ALGORITHM VERIDAS-002 CROSS AGE FMR . . . . .	438
408 ALGORITHM VIGILANTSOLUTIONS-005 CROSS AGE FMR . . . . .	439
409 ALGORITHM VIGILANTSOLUTIONS-006 CROSS AGE FMR . . . . .	440
410 ALGORITHM VION-000 CROSS AGE FMR . . . . .	441
411 ALGORITHM VISIONBOX-000 CROSS AGE FMR . . . . .	442
412 ALGORITHM VISIONBOX-001 CROSS AGE FMR . . . . .	443
413 ALGORITHM VISIONLABS-005 CROSS AGE FMR . . . . .	444
414 ALGORITHM VISIONLABS-006 CROSS AGE FMR . . . . .	445
415 ALGORITHM VOCORD-006 CROSS AGE FMR . . . . .	446
416 ALGORITHM YISHENG-004 CROSS AGE FMR . . . . .	447
417 ALGORITHM YITU-003 CROSS AGE FMR . . . . .	448

Developer		Short	Seq.	Validation	Config <sup>1</sup>	Template		GPU	Comparison Time (ns) <sup>3</sup>	
Name		Name	Num.	Date	Data (KB)	Size (B)	Time (ms) <sup>2</sup>		Genuine	Impostor
1	3DiVi	3divi	003	2018-10-09	191636	<sup>109</sup> 4096 ± 0	<sup>80</sup> 650 ± 90	No	<sup>25</sup> 627 ± 11	<sup>28</sup> 623 ± 32
2	Alchera	alchera	000	2019-03-01	258450	<sup>66</sup> 2048 ± 0	<sup>72</sup> 587 ± 13	No	<sup>83</sup> 3189 ± 32	<sup>84</sup> 3031 ± 142
3	Alchera	alchera	000	2019-03-01	174013	<sup>63</sup> 2048 ± 0	<sup>75</sup> 627 ± 11	No	<sup>86</sup> 3342 ± 81	<sup>85</sup> 3243 ± 47
4	AllGoVision	allgovision	000	2019-03-01	172509	<sup>62</sup> 2048 ± 0	<sup>46</sup> 384 ± 8	No	<sup>112</sup> 29903 ± 406	<sup>113</sup> 29735 ± 194
5	Amplified Group	amplifiedgroup	001	2019-03-01	0	<sup>24</sup> 866 ± 2	<sup>39</sup> 93 ± 0	No	<sup>115</sup> 57803 ± 4210	<sup>115</sup> 56365 ± 1196
6	Anke Investments	anke	002	2018-10-19	798686	<sup>98</sup> 2072 ± 0	<sup>53</sup> 419 ± 30	No	<sup>17</sup> 501 ± 17	<sup>18</sup> 492 ± 17
7	Anke Investments	anke	003	2019-02-27	340160	<sup>95</sup> 2056 ± 0	<sup>104</sup> 811 ± 23	No	<sup>11</sup> 425 ± 28	<sup>13</sup> 437 ± 32
8	AnyVision	anyvision	002	2018-01-31	662659	<sup>29</sup> 1024 ± 0	<sup>20</sup> 248 ± 0	No	<sup>116</sup> 74069 ± 188	<sup>116</sup> 74019 ± 198
9	AnyVision	anyvision	004	2018-06-15	401001	<sup>33</sup> 1024 ± 0	<sup>30</sup> 355 ± 1	No	<sup>66</sup> 1891 ± 51	<sup>64</sup> 1829 ± 85
10	Aware	aware	003	2018-10-19	377729	<sup>105</sup> 3108 ± 0	<sup>101</sup> 783 ± 10	No	<sup>54</sup> 1392 ± 42	<sup>58</sup> 1334 ± 80
11	Aware	aware	004	2019-03-01	427829	<sup>100</sup> 2084 ± 0	<sup>116</sup> 900 ± 10	No	<sup>51</sup> 1279 ± 50	<sup>57</sup> 1287 ± 100
12	Ayonix	ayonix	000	2017-06-22	58505	<sup>35</sup> 1036 ± 0	<sup>18</sup> ± 2	No	<sup>24</sup> 621 ± 23	<sup>27</sup> 620 ± 26
13	Bitmain	bitmain	001	2018-10-17	287734	<sup>1</sup> 64 ± 0	<sup>55</sup> 444 ± 88	No	<sup>65</sup> 1887 ± 31	<sup>66</sup> 1877 ± 26
14	Camvi Technologies	camvitech	002	2018-10-19	236278	<sup>27</sup> 1024 ± 0	<sup>89</sup> 677 ± 7	No	<sup>23</sup> 612 ± 26	<sup>25</sup> 603 ± 20
15	Camvi Technologies	camvitech	003	2019-03-01	285657	<sup>26</sup> 1024 ± 0	<sup>96</sup> 750 ± 3	No	<sup>20</sup> 571 ± 23	<sup>22</sup> 565 ± 26
16	China Electronics Import-Export Corp	ceiec	001	2019-03-01	159618	<sup>28</sup> 1024 ± 0	<sup>33</sup> 314 ± 3	No	<sup>110</sup> 22831 ± 108	<sup>110</sup> 22813 ± 120
17	Gemalto Cogent	cogent	002	2018-10-19	696959	<sup>51</sup> 1979 ± 0	<sup>17</sup> 941 ± 0	No	<sup>104</sup> 14394 ± 134	<sup>104</sup> 14385 ± 176
18	Gemalto Cogent	cogent	003	2019-03-01	698290	<sup>25</sup> 973 ± 0	<sup>18</sup> 952 ± 0	No	<sup>101</sup> 12496 ± 75	<sup>101</sup> 11822 ± 163
19	Cognitec Systems GmbH	cognitec	000	2018-10-19	474759	<sup>83</sup> 2052 ± 0	<sup>17</sup> 224 ± 1	No	<sup>89</sup> 3835 ± 108	<sup>89</sup> 3782 ± 83
20	Cognitec Systems GmbH	cognitec	001	2019-03-01	476809	<sup>78</sup> 2052 ± 0	<sup>20</sup> 297 ± 17	No	<sup>91</sup> 4253 ± 59	<sup>91</sup> 4102 ± 167
21	Cyberextruder	cyberex	001	2017-08-02	121211	<sup>7</sup> 256 ± 0	<sup>115</sup> 893 ± 25	No	<sup>43</sup> 1083 ± 16	<sup>47</sup> 1079 ± 19
22	Cyberextruder	cyberex	002	2018-01-30	168909	<sup>57</sup> 2048 ± 0	<sup>62</sup> 532 ± 6	No	<sup>64</sup> 1803 ± 14	<sup>63</sup> 1779 ± 22
23	Cyberlink Corp	cyberlink	000	2019-03-01	221801	<sup>79</sup> 2052 ± 0	<sup>35</sup> 338 ± 6	No	<sup>72</sup> 2102 ± 40	<sup>73</sup> 2093 ± 32
24	Cyberline Corp	cyberlink	001	2019-03-01	222009	<sup>88</sup> 2052 ± 0	<sup>54</sup> 425 ± 29	No	<sup>70</sup> 2051 ± 32	<sup>71</sup> 2060 ± 31
25	Dahua Technology Co. Ltd	dahua	001	2018-10-19	283642	<sup>74</sup> 2048 ± 0	<sup>41</sup> 363 ± 6	No	<sup>76</sup> 367 ± 10	<sup>85</sup> 354 ± 16
26	Dahua Technology Co. Ltd	dahua	002	2019-03-01	526452	<sup>64</sup> 2048 ± 0	<sup>76</sup> 628 ± 7	No	<sup>13</sup> 461 ± 23	<sup>15</sup> 454 ± 20
27	Tencent Deepsea Lab	deepsea	001	2019-06-03	147497	<sup>30</sup> 1024 ± 0	<sup>77</sup> 630 ± 7	No	<sup>56</sup> 1401 ± 37	<sup>60</sup> 1467 ± 50
28	Dermalog	dermalog	005	2018-02-02	0	<sup>3</sup> 128 ± 0	<sup>5</sup> 130 ± 11	No	<sup>16</sup> 499 ± 22	<sup>19</sup> 500 ± 22
29	Dermalog	dermalog	006	2018-10-18	0	<sup>2</sup> 128 ± 0	<sup>6</sup> 1532 ± 12	No	<sup>18</sup> 506 ± 23	<sup>16</sup> 459 ± 23
30	Digital Barriers	barriers	002	2019-03-01	83002	<sup>90</sup> 2056 ± 0	<sup>14</sup> 209 ± 11	No	<sup>103</sup> 13409 ± 228	<sup>103</sup> 13267 ± 206
31	Ever AI	everai	001	2018-10-19	449149	<sup>58</sup> 2048 ± 0	<sup>90</sup> 701 ± 1	No	<sup>9</sup> 395 ± 11	<sup>11</sup> 404 ± 23
32	Ever AI	everai	002	2019-03-01	561727	<sup>111</sup> 4096 ± 0	<sup>97</sup> 758 ± 0	No	<sup>27</sup> 644 ± 14	<sup>29</sup> 624 ± 35
33	Glory Ltd	glory	000	2018-06-06	0	<sup>16</sup> 418 ± 0	<sup>8</sup> 165 ± 2	No	<sup>97</sup> 7003 ± 84	<sup>96</sup> 6978 ± 71
34	Glory Ltd	glory	001	2018-06-08	0	<sup>48</sup> 1726 ± 0	<sup>48</sup> 393 ± 2	No	<sup>100</sup> 9607 ± 128	<sup>100</sup> 9539 ± 182
35	Gorilla Technology	gorilla	001	2018-05-25	93768	<sup>102</sup> 2156 ± 0	<sup>7</sup> 160 ± 14	No	<sup>87</sup> 3429 ± 145	<sup>88</sup> 3288 ± 51
36	Gorilla Technology	gorilla	002	2018-10-17	93869	<sup>39</sup> 1132 ± 0	<sup>36</sup> 322 ± 14	No	<sup>81</sup> 2715 ± 68	<sup>82</sup> 2585 ± 84
37	Hikvision	hik	001	2019-03-01	667866	<sup>42</sup> 1408 ± 0	<sup>81</sup> 651 ± 0	No	<sup>15</sup> 488 ± 19	<sup>17</sup> 477 ± 22
38	Hengrui AI Technology Ltd	hr	000	2019-03-01	284600	<sup>97</sup> 2057 ± 0	<sup>73</sup> 600 ± 2	No	<sup>105</sup> 16747 ± 238	<sup>105</sup> 16627 ± 220
39	Hengrui AI Technology Ltd	hr	001	2019-06-04	346156	<sup>96</sup> 2057 ± 0	<sup>83</sup> 665 ± 3	No	<sup>107</sup> 17816 ± 260	<sup>107</sup> 17878 ± 464
40	ID3 Technology	id3	003	2018-10-05	265951	<sup>11</sup> 264 ± 0	<sup>34</sup> 316 ± 19	No	<sup>53</sup> 1330 ± 25	<sup>59</sup> 1354 ± 28
41	ID3 Technology	id3	004	2019-03-01	171526	<sup>12</sup> 264 ± 0	<sup>66</sup> 541 ± 11	No	<sup>45</sup> 1135 ± 23	<sup>51</sup> 1156 ± 32
42	Idemia	Idemia	003	2018-10-19	427244	<sup>15</sup> 352 ± 0	<sup>42</sup> 368 ± 6	No	<sup>96</sup> 6654 ± 75	<sup>92</sup> 4835 ± 90
43	Idemia	Idemia	004	2019-03-01	406924	<sup>14</sup> 352 ± 0	<sup>3</sup> 306 ± 5	No	<sup>94</sup> 5592 ± 518	<sup>95</sup> 5533 ± 426
44	Institute of Information Technologies	ittvision	000	2019-03-01	237317	<sup>34</sup> 1024 ± 0	<sup>13</sup> 197 ± 8	No	<sup>58</sup> 1537 ± 81	<sup>56</sup> 1282 ± 20

## Notes

- 1 The configuration size does not capture static data included in libraries. We do not count these because some algorithms include common ancillary libraries for image processing (e.g. openCV) or numerical computation (e.g. blas).
- 2 The median template creation times are measured on Intel® Xeon® CPU E5-2630 v4 @ 2.20GHz processors or, for GPU-enabled implementations, NVidia Tesla K40.
- 3 The comparison durations, in nanoseconds, are estimated using std::chrono::high\_resolution\_clock which on the machine in (2) counts 1ns clock ticks. Precision is somewhat worse than that however. The ± value is the median absolute deviation times 1.48 for Normal consistency.

Table 1: Summary of algorithms and properties included in this report. The red superscripts give ranking for the quantity in that column.

	Developer	Short	Seq.	Validation	Config <sup>1</sup>	Template		GPU	Comparison Time (ns) <sup>3</sup>	
	Name	Name	Num.	Date	Data (KB)	Size (B)	Time (ms) <sup>2</sup>		Genuine	Impostor
45	Imperial College London	imperial	000	2019-03-01	370120	<sup>73</sup> 2048 ± 0	<sup>85</sup> 669 ± 1	No	<sup>73</sup> 2130 ± 32	<sup>70</sup> 2052 ± 100
46	Imperial College London	imperial	001	2019-03-01	370260	<sup>70</sup> 2048 ± 0	<sup>87</sup> 671 ± 0	No	<sup>71</sup> 2090 ± 28	<sup>72</sup> 2062 ± 74
47	Incode Technologies Inc	incode	002	2018-10-18	73239	<sup>60</sup> 2048 ± 0	<sup>26</sup> 281 ± 15	No	<sup>59</sup> 1544 ± 38	<sup>61</sup> 1488 ± 69
48	Incode Technologies Inc	incode	003	2019-03-01	170632	<sup>110</sup> 4096 ± 0	<sup>48</sup> 384 ± 11	No	<sup>67</sup> 1928 ± 44	<sup>65</sup> 1876 ± 81
49	Innovatrics	innova	004	2018-10-19	0	<sup>37</sup> 1076 ± 0	<sup>47</sup> 391 ± 0	No	<sup>99</sup> 8573 ± 274	<sup>98</sup> 7929 ± 244
50	Innovatrics	innova	005	2019-03-01	0	<sup>38</sup> 1076 ± 0	<sup>70</sup> 577 ± 1	No	<sup>106</sup> 16880 ± 194	<sup>106</sup> 17232 ± 385
51	Intellivision	intellivision	001	2017-10-10	43692	<sup>93</sup> 2056 ± 0	<sup>2</sup> 62 ± 2	No	<sup>78</sup> 2573 ± 91	<sup>81</sup> 2544 ± 38
52	iQIYI Inc	iqface	000	2019-03-01	268819	<sup>117</sup> 4750 ± 32	<sup>63</sup> 538 ± 26	No	<sup>119</sup> 636433 ± 38446	<sup>119</sup> 632654 ± 85615
53	Is It You	isityou	000	2017-06-26	48010	<sup>118</sup> 19200 ± 0	<sup>4</sup> 113 ± 5	No	<sup>117</sup> 237517 ± 1318	<sup>117</sup> 237374 ± 1279
54	Innovation Systems	isystems	001	2018-06-12	274621	<sup>52</sup> 2048 ± 0	<sup>27</sup> 291 ± 9	No	<sup>19</sup> 557 ± 16	<sup>21</sup> 564 ± 22
55	Innovation Systems	isystems	002	2018-10-18	358984	<sup>59</sup> 2048 ± 0	<sup>107</sup> 822 ± 8	No	<sup>33</sup> 749 ± 31	<sup>30</sup> 632 ± 28
56	ITMO University	itmo	005	2018-10-19	482155	<sup>116</sup> 4173 ± 0	<sup>98</sup> 759 ± 1	No	<sup>102</sup> 13214 ± 164	<sup>102</sup> 12576 ± 257
57	ITMO University	itmo	006	2019-03-01	599187	<sup>101</sup> 2121 ± 0	<sup>105</sup> 814 ± 1	No	<sup>111</sup> 26154 ± 148	<sup>111</sup> 26217 ± 260
58	Kakao Corp	kakao	001	2019-03-01	107616	<sup>32</sup> 1024 ± 0	<sup>44</sup> 379 ± 1	No	<sup>40</sup> 930 ± 22	<sup>44</sup> 948 ± 38
59	Kedacom International Pte	kedacom	000	2019-06-03	245292	<sup>13</sup> 292 ± 0	<sup>58</sup> 506 ± 3	No	<sup>28</sup> 684 ± 14	<sup>32</sup> 682 ± 16
60	Lookman Electroplast Industries	lookman	002	2018-06-13	138200	<sup>22</sup> 548 ± 0	<sup>9</sup> 173 ± 1	No	<sup>22</sup> 610 ± 19	<sup>26</sup> 612 ± 22
61	Lookman Electroplast Industries	lookman	004	2019-06-03	244775	<sup>21</sup> 548 ± 0	<sup>59</sup> 507 ± 5	No	<sup>36</sup> 871 ± 29	<sup>41</sup> 878 ± 29
62	Megvii/Face++	megvii	001	2018-06-15	1361523	<sup>72</sup> 2048 ± 0	<sup>68</sup> 543 ± 0	No	<sup>93</sup> 5228 ± 32	<sup>94</sup> 5252 ± 60
63	Megvii/Face++	megvii	002	2018-10-19	1809564	<sup>114</sup> 4100 ± 0	<sup>79</sup> 644 ± 0	No	<sup>114</sup> 50630 ± 183	<sup>114</sup> 47591 ± 716
64	Xiamen Meiya Pico Information Co. Ltd	meiya	001	2019-03-01	280055	<sup>76</sup> 2049 ± 0	<sup>74</sup> 622 ± 12	No	<sup>98</sup> 8356 ± 615	<sup>99</sup> 8134 ± 97
65	MicroFocus	microfocus	001	2018-06-13	104524	<sup>10</sup> 256 ± 0	<sup>23</sup> 264 ± 18	No	<sup>1</sup> 215 ± 8	<sup>1</sup> 217 ± 10
66	MicroFocus	microfocus	002	2018-10-17	96288	<sup>6</sup> 256 ± 0	<sup>22</sup> 259 ± 18	No	<sup>53</sup> 37 ± 34	<sup>230</sup> 25 ± 25
67	Moontime Smart Technology	mt	000	2019-06-03	372169	<sup>77</sup> 2049 ± 0	<sup>92</sup> 724 ± 12	No	<sup>62</sup> 1678 ± 47	<sup>62</sup> 1614 ± 85
68	Neurotechnology	neurotech	004	2018-10-19	293384	<sup>9</sup> 256 ± 0	<sup>51</sup> 401 ± 0	No	<sup>219</sup> 8 ± 8	<sup>3</sup> 231 ± 13
69	Neurotechnology	neurotech	005	2019-03-01	270450	<sup>8</sup> 256 ± 0	<sup>50</sup> 399 ± 0	No	<sup>3</sup> 238 ± 10	<sup>4</sup> 237 ± 7
70	Nodeflux	nodeflux	000	2019-03-01	347079	<sup>56</sup> 2048 ± 0	<sup>67</sup> 542 ± 1	No	<sup>85</sup> 3283 ± 51	<sup>87</sup> 3285 ± 56
71	Nodeflux	nodeflux	001	2019-03-01	262553	<sup>55</sup> 2048 ± 0	<sup>19</sup> 247 ± 1	No	<sup>84</sup> 3242 ± 81	<sup>86</sup> 3255 ± 93
72	N-Tech Lab	ntech	005	2018-10-19	1726214	<sup>50</sup> 1940 ± 0	<sup>91</sup> 712 ± 1	No	<sup>39</sup> 882 ± 42	<sup>42</sup> 880 ± 29
73	N-Tech Lab	ntech	006	2019-03-01	7901590	<sup>104</sup> 2600 ± 0	<sup>95</sup> 749 ± 1	No	<sup>42</sup> 1055 ± 93	<sup>40</sup> 844 ± 48
74	Guangzhou Pixel Solutions Co. Ltd	pixelall	002	2019-06-06	0	<sup>103</sup> 2560 ± 0	<sup>12</sup> 191 ± 1	No	<sup>47</sup> 1223 ± 56	<sup>52</sup> 1230 ± 47
75	Panasonic R+D Center Singapore	psl	001	2018-10-12	382035	<sup>94</sup> 2056 ± 0	<sup>102</sup> 785 ± 16	No	<sup>4</sup> 298 ± 13	<sup>5</sup> 292 ± 14
76	Panasonic R+D Center Singapore	psl	002	2019-02-28	804934	<sup>85</sup> 2052 ± 0	<sup>114</sup> 888 ± 9	No	<sup>60</sup> 1590 ± 48	<sup>48</sup> 1133 ± 78
77	Rank One Computing	rankone	006	2019-02-27	0	<sup>5</sup> 165 ± 0	<sup>12</sup> 210 ± 1	No	<sup>12</sup> 443 ± 26	<sup>10</sup> 395 ± 22
78	Rank One Computing	rankone	007	2019-06-03	0	<sup>4</sup> 165 ± 0	<sup>18</sup> 245 ± 5	No	<sup>29</sup> 688 ± 20	<sup>24</sup> 601 ± 16
79	Realnetworks Inc	realnetworks	001	2018-10-19	99044	<sup>113</sup> 4100 ± 0	<sup>6</sup> 144 ± 2	No	<sup>76</sup> 2500 ± 47	<sup>78</sup> 2420 ± 34
80	Realnetworks Inc	realnetworks	002	2019-02-28	95328	<sup>49</sup> 1848 ± 0	<sup>21</sup> 250 ± 2	No	<sup>52</sup> 1285 ± 17	<sup>54</sup> 1247 ± 42
81	KanKan Ai	remarkai	000	2019-03-01	240152	<sup>53</sup> 2048 ± 0	<sup>108</sup> 829 ± 7	No	<sup>37</sup> 873 ± 4	<sup>39</sup> 835 ± 35
82	KanKan Ai	remarkai	001	2019-03-01	241857	<sup>89</sup> 2052 ± 0	<sup>109</sup> 831 ± 6	No	<sup>48</sup> 1229 ± 20	<sup>38</sup> 805 ± 56
83	Saffe Ltd	saffe	001	2018-10-19	85973	<sup>41</sup> 1280 ± 0	<sup>28</sup> 281 ± 1	No	<sup>50</sup> 1274 ± 19	<sup>53</sup> 1277 ± 26
84	Saffe Ltd	saffe	002	2019-03-01	260622	<sup>65</sup> 2048 ± 0	<sup>106</sup> 817 ± 11	No	<sup>32</sup> 717 ± 7	<sup>34</sup> 714 ± 29
85	Sensetime Group Ltd	sensetime	002	2018-10-19	531783	<sup>81</sup> 2052 ± 0	<sup>93</sup> 725 ± 3	No	<sup>77</sup> 2546 ± 102	<sup>76</sup> 2371 ± 45
86	Sensetime Group Ltd	sensetime	002	2018-10-19	531783	<sup>82</sup> 2052 ± 0	<sup>103</sup> 797 ± 3	No	<sup>80</sup> 2713 ± 90	<sup>75</sup> 2301 ± 25
87	Sensetime Group Ltd	sensetime	003	2019-06-04	534132	<sup>80</sup> 2052 ± 0	<sup>78</sup> 635 ± 33	No	<sup>82</sup> 2721 ± 47	<sup>83</sup> 2747 ± 26
88	Shaman Software	shaman	000	2017-12-05	0	<sup>108</sup> 4096 ± 0	<sup>82</sup> 653 ± 16	No	<sup>8</sup> 380 ± 25	<sup>9</sup> 379 ± 31

Notes

1 The configuration size does not capture static data included in libraries. We do not count these because some algorithms include common ancillary libraries for image processing (e.g. openCV) or numerical computation (e.g. blas).

2 The median template creation times are measured on Intel® Xeon® CPU E5-2630 v4 @ 2.20GHz processors or, for GPU-enabled implementations, NVidia Tesla K40.

3 The comparison durations, in nanoseconds, are estimated using std::chrono::high\_resolution\_clock which on the machine in (2) counts 1ns clock ticks. Precision is somewhat worse than that however. The ± value is the median absolute deviation times 1.48 for Normal consistency.

Table 2: Summary of algorithms and properties included in this report. The red superscripts give ranking for the quantity in that column.

	Developer	Short	Seq.	Validation	Config <sup>1</sup>	Template	GPU	Comparison Time (ns) <sup>3</sup>		
	Name	Name	Num.	Date	Data (KB)	Size (B)	Time (ms) <sup>2</sup>	Genuine	Impostor	
89	Shaman Software	shaman	001	2018-01-13	0	<sup>107</sup> 4096 ± 0	<sup>28</sup> 294 ± 2	No	<sup>26</sup> 635 ± 19	<sup>14</sup> 441 ± 25
90	Shenzhen Inst. Adv. Integrated Tech. CAS	SIAT	002	2018-06-13	486842	<sup>86</sup> 2052 ± 0	<sup>71</sup> 579 ± 0	No	<sup>34</sup> 769 ± 13	<sup>30</sup> 750 ± 13
91	Shenzhen Inst. Adv. Integrated Tech. CAS	SIAT	004	2019-03-01	940063	<sup>115</sup> 4100 ± 0	<sup>86</sup> 670 ± 0	No	<sup>90</sup> 4013 ± 45	<sup>90</sup> 3782 ± 173
92	Smilart	smilart	002	2018-02-06	111826	<sup>31</sup> 1024 ± 0	<sup>10</sup> 176 ± 16	No	<sup>109</sup> 18784 ± 136	<sup>109</sup> 18795 ± 151
93	Smilart	smilart	003	2018-06-18	67339	<sup>17</sup> 512 ± 0	<sup>11</sup> 180 ± 12	No	<sup>55</sup> 1395 ± 74	<sup>45</sup> 1027 ± 66
94	Synesis	synesis	004	2019-03-01	270628	<sup>71</sup> 2048 ± 0	<sup>94</sup> 735 ± 15	No	<sup>10</sup> 424 ± 14	<sup>12</sup> 430 ± 22
95	Synesis	synesis	005	2019-06-06	146509	<sup>54</sup> 2048 ± 0	<sup>16</sup> 211 ± 9	No	<sup>21</sup> 599 ± 23	<sup>23</sup> 581 ± 32
96	Tech5 SA	tech5	001	2018-10-19	636346	<sup>112</sup> 4096 ± 0	<sup>60</sup> 522 ± 5	No	<sup>44</sup> 1087 ± 34	<sup>37</sup> 799 ± 44
97	Tech5 SA	tech5	002	2019-03-01	1150887	<sup>40</sup> 1280 ± 0	<sup>99</sup> 780 ± 10	No	<sup>57</sup> 1406 ± 120	<sup>46</sup> 1048 ± 57
98	Tevian	tevian	003	2018-10-19	791725	<sup>75</sup> 2049 ± 0	<sup>52</sup> 404 ± 15	No	<sup>6</sup> 350 ± 11	<sup>7</sup> 338 ± 25
99	Tevian	tevian	004	2019-03-01	863474	<sup>67</sup> 2048 ± 0	<sup>57</sup> 506 ± 30	No	<sup>14</sup> 474 ± 31	<sup>6</sup> 326 ± 20
100	TigerIT Americas LLC	tiger	002	2018-06-13	341638	<sup>91</sup> 2056 ± 0	<sup>49</sup> 393 ± 20	No	<sup>74</sup> 2135 ± 29	<sup>74</sup> 2137 ± 38
101	TigerIT Americas LLC	tiger	003	2018-10-16	426164	<sup>92</sup> 2056 ± 0	<sup>56</sup> 458 ± 21	No	<sup>69</sup> 2031 ± 35	<sup>69</sup> 2029 ± 38
102	Toshiba	toshiba	002	2018-10-19	813606	<sup>45</sup> 1560 ± 0	<sup>65</sup> 541 ± 0	No	<sup>88</sup> 3521 ± 369	<sup>79</sup> 2449 ± 124
103	Toshiba	toshiba	003	2019-03-01	984125	<sup>46</sup> 1560 ± 0	<sup>64</sup> 540 ± 0	No	<sup>73</sup> 2390 ± 41	<sup>77</sup> 2407 ± 81
104	China University of Petroleum	upc	001	2019-06-05	0	<sup>36</sup> 1052 ± 0	<sup>69</sup> 552 ± 17	No	<sup>92</sup> 4900 ± 305	<sup>93</sup> 4990 ± 226
105	VCognition	vcog	002	2017-06-12	3229434	<sup>119</sup> 61504 ± 5	<sup>40</sup> 357 ± 25	No	<sup>118</sup> 296154 ± 3077	<sup>118</sup> 296436 ± 4183
106	Visidon	visidon	001	2019-02-26	170262	<sup>84</sup> 2052 ± 0	<sup>35</sup> 316 ± 6	No	<sup>49</sup> 1258 ± 38	<sup>49</sup> 1148 ± 109
107	Veridas Digital Authentication Solutions S.L.	veridas	001	2019-03-01	196540	<sup>69</sup> 2048 ± 0	<sup>88</sup> 671 ± 21	No	<sup>93</sup> 5748 ± 20	<sup>97</sup> 7111 ± 148
108	Veridas Digital Authentication Solutions S.L.	veridas	000	2019-03-01	193466	<sup>20</sup> 512 ± 0	<sup>84</sup> 669 ± 20	No	<sup>62</sup> 1733 ± 81	<sup>67</sup> 1934 ± 44
109	Vigilant Solutions	vigilant	005	2018-10-11	343048	<sup>43</sup> 1548 ± 0	<sup>110</sup> 837 ± 13	No	<sup>38</sup> 874 ± 22	<sup>31</sup> 637 ± 16
110	Vigilant Solutions	vigilant	006	2019-03-01	343048	<sup>44</sup> 1548 ± 0	<sup>111</sup> 841 ± 8	No	<sup>41</sup> 939 ± 32	<sup>33</sup> 711 ± 37
111	Beijing Vion Technology Inc	vion	000	2018-10-19	228219	<sup>87</sup> 2052 ± 0	<sup>37</sup> 333 ± 1	No	<sup>113</sup> 39839 ± 3561	<sup>112</sup> 26830 ± 2241
112	Vision-Box	visionbox	000	2019-02-26	176501	<sup>68</sup> 2048 ± 0	<sup>30</sup> 304 ± 7	No	<sup>61</sup> 1648 ± 57	<sup>52</sup> 1192 ± 42
113	Vision-Box	visionbox	001	2019-03-01	256869	<sup>61</sup> 2048 ± 0	<sup>13</sup> 983 ± 7	No	<sup>46</sup> 1161 ± 22	<sup>50</sup> 1154 ± 20
114	VisionLabs	visionlabs	005	2018-10-19	369602	<sup>18</sup> 512 ± 0	<sup>32</sup> 313 ± 0	No	<sup>35</sup> 848 ± 26	<sup>43</sup> 889 ± 37
115	VisionLabs	visionlabs	006	2019-03-01	353044	<sup>19</sup> 512 ± 0	<sup>24</sup> 270 ± 0	No	<sup>31</sup> 698 ± 19	<sup>35</sup> 734 ± 28
116	Vocord	vocord	006	2019-03-01	559457	<sup>23</sup> 768 ± 0	<sup>113</sup> 886 ± 1	No	<sup>68</sup> 2020 ± 72	<sup>68</sup> 1969 ± 62
117	Vocord	vocord	007	2019-06-06	587489	<sup>47</sup> 1664 ± 0	<sup>100</sup> 780 ± 2	No	<sup>79</sup> 2593 ± 83	<sup>80</sup> 2526 ± 59
118	Zhuhai Yisheng Electronics Technology	yisheng	004	2018-06-12	486351	<sup>106</sup> 3704 ± 0	<sup>43</sup> 378 ± 12	No	<sup>36</sup> 693 ± 137	<sup>20</sup> 526 ± 34
119	Shanghai Yitu Technology	yitu	003	2019-03-01	1525719	<sup>99</sup> 2082 ± 0	<sup>112</sup> 860 ± 0	No	<sup>108</sup> 18305 ± 71	<sup>108</sup> 18286 ± 62

## Notes

- 1 The configuration size does not capture static data included in libraries. We do not count these because some algorithms include common ancillary libraries for image processing (e.g. openCV) or numerical computation (e.g. blas).
- 2 The median template creation times are measured on Intel®Xeon®CPU E5-2630 v4 @ 2.20GHz processors or, for GPU-enabled implementations, NVidia Tesla K40.
- 3 The comparison durations, in nanoseconds, are estimated using std::chrono::high\_resolution\_clock which on the machine in (2) counts 1ns clock ticks. Precision is somewhat worse than that however. The ± value is the median absolute deviation times 1.48 for Normal consistency.

Table 3: Summary of algorithms and properties included in this report. The red superscripts give ranking for the quantity in that column.

	Algorithm	FALSE NON-MATCH RATE (FNMR)									
		CONSTRAINED, COOPERATIVE					LESS CONSTRAINED, NON-COOP.				
		Name	VISAMC	VISA	VISA	MUGSHOT	WILD	CHILD EXP			
	FMR	0.0001	1E-06	0.0001	1E-05	0.0001	0.0001	0.01			
1	3divi-003	0.0318	78	0.0588	79	0.0097	69	0.0389	77	0.0867	79
2	alchera-000	0.0165	50	0.0243	40	0.0086	64	0.0125	39	0.0370	36
3	alchera-001	0.0183	54	0.0299	53	0.0078	59	0.0142	46	0.0372	37
4	algovision-000	0.0346	80	0.0527	75	0.0210	86	0.0232	66	0.0607	72
5	amplifiedgroup-001	0.5034	111	0.5848	110	0.2999	112	0.6973	109	0.4250	104
6	anke-002	0.0402	82	0.0759	84	0.0136	78	0.0271	69	0.0664	74
7	anke-003	0.0131	36	0.0213	33	0.0056	40	0.0094	17	0.0302	15
8	anyvision-002	0.0660	87	0.0898	86	0.0387	92	0.0928	92	0.2227	94
9	anyvision-004	0.0267	71	0.0385	66	0.0081	60	0.0258	68	0.0470	54
10	aware-003	0.0793	89	0.1161	90	0.0288	90	0.1028	93	0.3180	101
11	aware-004	0.0690	88	0.0949	88	0.0257	88	0.0837	89	0.0516	63
12	ayonix-000	0.4351	108	0.4872	105	0.2299	109	0.6150	107	0.3635	102
13	bm-001	0.7431	114	0.9494	115	0.6188	115	0.9586	113	0.9935	108
14	camvi-002	0.0125	31	0.0221	37	0.0049	34	0.0089	15	0.0288	10
15	camvi-003	0.0184	55	0.0320	57	0.0062	44	0.0134	44	0.0300	13
16	ceiec-001	0.0328	79	0.0475	73	0.0163	81	0.0295	73	0.0847	76
17	cogent-002	0.0148	45	0.0321	58	0.0044	26	0.0095	18	0.0562	68
18	cogent-003	0.0091	16	0.0188	30	0.0032	14	0.0098	21	0.0406	41
19	cognitec-000	0.0116	26	0.0177	26	0.0036	17	0.0118	35	0.0953	83
20	cognitec-001	0.0126	32	0.0185	29	0.0047	31	0.0120	37	0.0598	71
21	cyberextruder-001	0.1972	100	0.2547	97	0.0755	101	0.4686	105	0.1747	91
22	cyberextruder-002	0.0811	90	0.1336	92	0.0265	89	0.1465	98	0.1000	85
23	cyberlink-000	0.0181	52	0.0274	48	0.0106	73	0.0125	40	0.1864	92
24	cyberlink-001	0.0131	35	0.0210	32	0.0050	35	0.0439	82	0.0318	24
25	dahua-001	0.0250	67	0.0466	72	0.0108	74	0.0228	64	0.0457	51
26	dahua-002	0.0129	33	0.0157	22	0.0090	66	0.0116	34	0.0323	26
27	deepsea-001	0.0136	38	0.0215	35	0.0071	55	0.0142	47	0.0347	34
28	dermalog-005	0.1526	97	0.1823	93	0.0658	99	0.2580	102	0.0855	78
29	dermalog-006	0.0253	68	0.0369	65	0.0172	84	0.0171	55	0.0623	73
30	digitalbarriers-002	0.3360	105	0.3690	102	0.0968	103	0.0877	90	0.0436	46
31	everai-001	0.0085	14	0.0156	20	0.0038	22	0.0072	7	0.0287	9
32	everai-002	0.0104	23	0.0159	23	0.0041	24	0.0063	4	0.0294	11
33	glory-000	0.1094	92	0.1286	91	0.0514	96	0.2179	100	0.4762	106
34	glory-001	0.0902	91	0.1082	89	0.0410	93	0.1642	99	0.4261	105
35	gorilla-001	0.0488	84	0.0756	82	0.0155	80	0.1218	97	0.0564	69
36	gorilla-002	0.0256	69	0.0413	67	0.0076	58	0.0478	85	0.0507	61
37	hik-001	0.0096	21	0.0125	14	0.0036	19	0.0093	16	0.0271	1
38	hr-000	0.0265	70	0.0434	68	0.0112	76	0.0340	75	0.1902	93
39	hr-001	0.0044	4	0.0072	5	0.0019	6	0.0073	8	0.0303	16
40	id3-003	0.0361	81	0.0757	83	0.0104	72	0.0292	72	0.0848	77
41	id3-004	0.0198	59	0.0344	60	0.0084	62	0.0238	67	-	-
42	idemia-003	0.0222	61	0.0316	56	0.0082	61	0.0188	57	0.0578	70
43	idemia-004	0.0160	49	0.0244	42	0.0065	45	0.0199	60	0.0309	20
44	iit-000	0.1516	96	0.1981	94	0.0620	98	0.0828	88	-	-
45	imperial-000	0.0067	9	0.0108	12	0.0022	8	0.0080	11	0.0281	5
46	imperial-001	0.0094	20	0.0154	19	0.0033	15	0.0072	6	0.0276	3
47	incode-002	0.0293	73	0.0548	78	0.0096	68	0.0436	81	0.0498	58
48	incode-003	0.0142	40	0.0249	44	0.0054	38	0.0448	83	0.0318	23
49	innovatrics-004	0.0194	57	0.0292	50	0.0068	52	0.0344	76	0.0454	49
50	innovatrics-005	0.0230	63	0.0353	62	0.0085	63	0.0398	79	0.0301	14
51	intellivision-001	0.1335	95	0.2205	95	0.0417	94	0.1090	95	0.2445	95
52	iqface-000	0.0091	17	0.0143	16	0.0043	25	0.0075	10	0.0381	38
53	isityou-000	0.5682	112	0.7033	111	0.4145	113	1.0000	115	1.0000	112
54	isystems-001	0.0149	46	0.0245	43	0.0067	51	0.0138	45	0.0524	66
55	isystems-002	0.0118	27	0.0182	28	0.0066	46	0.0111	28	0.0516	64
56	itmo-005	0.0182	53	0.0345	61	0.0067	50	0.0181	56	0.0433	44
57	itmo-006	0.0125	29	0.0220	36	0.0046	28	0.0149	49	0.0329	29
58	kakao-001	0.4553	110	0.5532	109	0.2034	108	0.6580	108	1.0000	118
59	kedacom-000	0.0055	6	0.0081	6	0.0027	10	0.0111	30	0.2511	97
60	lookman-002	0.0297	74	0.0547	77	0.0102	71	0.0339	74	0.2640	100

Table 4: FNMR is the proportion of mated comparisons below a threshold set to achieve the FMR given in the header on the fourth row. FMR is the proportion of impostor comparisons at or above that threshold. The light grey values give rank over all algorithms in that column. The green column applies to “matched-covariates” i.e. impostors of the same sex, age group, and country of birth. The pink column uses only same-sex impostors; All others are zero effort. The pink column includes effects of extended ageing, and is the most important. Missing entries for visa, mugshot and wild images generally mean the algorithm did not run to completion. For child exploitation, missing entries arise because NIST executes those runs only infrequently.

Algorithm Name	FMR	FALSE NON-MATCH RATE (FNMR)									
		CONSTRAINED, COOPERATIVE					LESS CONSTRAINED, NON-COOP.				
		VISAMC	VISA	VISA	MUGSHOT	WILD	CHILD EXP				
61	lookman-004	0.0074	12	0.0099	9	0.0037	20	0.0124	38	0.2516	98
62	megvii-001	0.0157	47	0.0244	41	0.0045	27	0.0392	78	0.0916	81
63	megvii-002	0.0104	24	0.0145	18	0.0036	18	0.0225	62	0.0692	75
64	meiya-001	0.0171	51	0.0275	49	0.0066	48	0.0159	53	0.0363	35
65	microfocus-001	0.4482	109	0.5524	108	0.2309	110	0.7256	111	0.2567	99
66	microfocus-002	0.3605	106	0.5057	106	0.1566	107	0.5783	106	0.1582	90
67	mt-000	0.0100	22	0.0170	24	0.0047	30	0.0074	9	0.0326	28
68	neurotechnology-004	0.0146	42	0.0297	51	0.0051	37	0.0107	24	0.0467	53
69	neurotechnology-005	0.0141	39	0.0300	54	0.0051	36	0.0108	26	0.0332	30
70	nodeflux-000	1.0000	117	1.0000	117	1.0000	117	1.0000	116	1.0000	114
71	nodeflux-001	1.0000	118	1.0000	118	1.0000	118	1.0000	117	1.0000	115
72	ntechlab-005	0.0093	19	0.0145	17	0.0024	9	0.0131	43	0.0466	52
73	ntechlab-006	0.0078	13	0.0111	13	0.0021	7	0.0112	31	0.0275	2
74	pixelall-002	0.0193	56	0.0340	59	0.0066	47	0.0127	41	0.0342	33
75	psl-001	0.0549	85	0.0927	87	0.0198	85	0.0096	19	0.0431	43
76	psl-002	0.0107	25	0.0180	27	0.0048	33	0.0089	14	0.0295	12
77	rankone-006	0.0242	64	0.0460	71	0.0070	54	0.0119	36	0.0538	67
78	rankone-007	0.0197	58	0.0366	64	0.0057	41	0.0113	32	0.0450	47
79	realnetworks-001	0.0315	77	0.0455	70	0.0116	77	0.0920	91	0.0500	59
80	realnetworks-002	0.0248	66	0.0358	63	0.0099	70	0.0513	86	0.0334	31
81	remarkai-000	0.0147	44	0.0257	46	0.0062	43	0.0102	22	0.0304	17
82	remarkai-001	0.0144	41	0.0256	45	0.0061	42	0.0102	23	0.0308	19
83	saffe-001	0.4339	107	0.5261	107	0.2340	111	0.7539	112	0.3887	103
84	saffe-002	0.0119	28	0.0206	31	0.0054	39	0.0107	25	0.0308	18
85	senstime-001	0.0063	8	0.0092	7	0.0030	13	0.0130	42	1.0000	111
86	senstime-002	0.0068	11	0.0098	8	0.0035	16	0.0143	48	0.9999	109
87	senstime-003	0.1187	93	0.8177	112	0.1015	104	0.7171	110	0.0976	84
88	shaman-000	0.9297	116	0.9774	116	0.9128	116	0.9990	114	0.9575	107
89	shaman-001	0.3346	104	0.4616	103	0.1360	106	0.2368	101	0.1498	89
90	siat-002	0.0091	18	0.0126	15	0.0039	23	0.0109	27	0.0520	65
91	siat-004	0.0067	10	0.0099	10	0.0028	11	0.0152	51	1.0000	110
92	smilart-002	0.2440	103	0.3532	101	0.0821	102	-	-	-	0.700
93	smilart-003	0.6944	113	0.8836	113	0.1088	105	0.0695	87	0.1190	86
94	synesis-004	0.0310	75	0.0480	74	0.0166	83	0.0476	84	0.1319	87
95	synesis-005	0.0147	43	0.0226	39	0.0073	57	0.0153	52	0.0334	32
96	tech5-001	0.0130	34	0.0176	25	0.0037	21	0.0218	61	0.0938	82
97	tech5-002	0.0046	5	0.0063	3	0.0009	2	0.0113	33	0.0310	21
98	tevian-003	0.0217	60	0.0298	52	0.0067	49	0.0230	65	0.0456	50
99	tevian-004	0.0228	62	0.0304	55	0.0069	53	0.0226	63	0.0394	40
100	tiger-002	0.0658	86	0.0889	85	0.0227	87	0.1083	94	0.0512	62
101	tiger-003	0.0313	76	0.0602	81	0.0087	65	0.0188	58	0.0482	56
102	toshiba-002	0.0134	37	0.0222	38	0.0048	32	0.0097	20	0.0434	45
103	toshiba-003	0.0125	30	0.0214	34	0.0047	29	0.0085	13	0.0282	6
104	upc-001	-	-	-	-	-	-	0.0291	71	0.0314	22
105	vcog-002	0.7522	115	0.9033	114	0.5040	114	-	-	0.752	36
106	vd-001	0.0243	65	0.0452	69	0.0093	67	0.0271	70	0.1389	88
107	veridas-001	0.1998	102	0.2724	98	0.0742	100	0.2987	104	0.0501	60
108	veridas-002	0.1733	99	0.2257	96	0.0528	97	0.2617	103	0.0450	48
109	vigilantsolutions-005	0.1613	98	0.4702	104	0.0166	82	0.0163	54	0.0497	57
110	vigilantsolutions-006	0.1264	94	0.3221	99	0.0136	79	0.0150	50	0.0321	25
111	vion-000	0.0419	83	0.0590	80	0.0288	91	0.0422	80	0.2479	96
112	visionbox-000	0.0293	72	0.0541	76	0.0110	75	0.0197	59	0.0476	55
113	visionbox-001	0.0159	48	0.0270	47	0.0072	56	0.0111	29	0.0389	39
114	visionlabs-005	0.0088	15	0.0156	21	0.0029	12	0.0048	2	0.0422	42
115	visionlabs-006	0.0037	2	0.0066	4	0.0012	3	0.0041	1	0.0285	8
116	vocord-006	0.0062	7	0.0102	11	0.0016	5	0.0082	12	0.0282	7
117	vocord-007	0.0039	3	0.0053	2	0.0012	4	0.0061	3	0.0280	4
118	yisheng-004	0.1988	101	0.3329	100	0.0475	95	0.1147	96	0.0908	80
119	yitu-003	0.0015	1	0.0026	1	0.0003	1	0.0066	5	0.0325	27

Table 5: FNMR is the proportion of mated comparisons below a threshold set to achieve the FMR given in the header on the fourth row. FMR is the proportion of impostor comparisons at or above that threshold. The light grey values give rank over all algorithms in that column. The green column applies to “matched-covariates” i.e. impostors of the same sex, age group, and country of birth. The pink column uses only same-sex impostors; All others are zero effort. The pink column includes effects of extended ageing, and is the most important. Missing entries for visa, mugshot and wild images generally mean the algorithm did not run to completion. For child exploitation, missing entries arise because NIST executes those runs only infrequently.

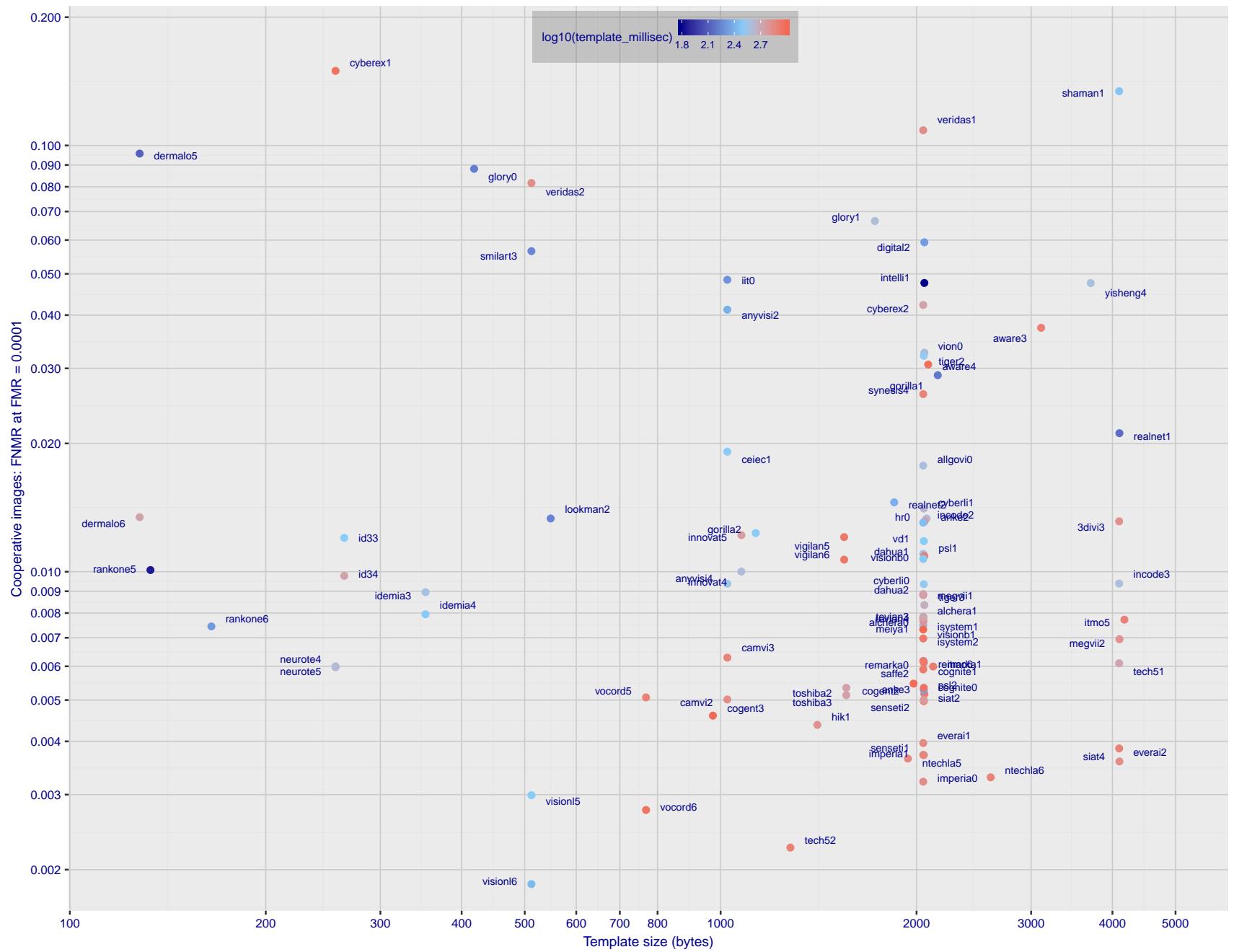
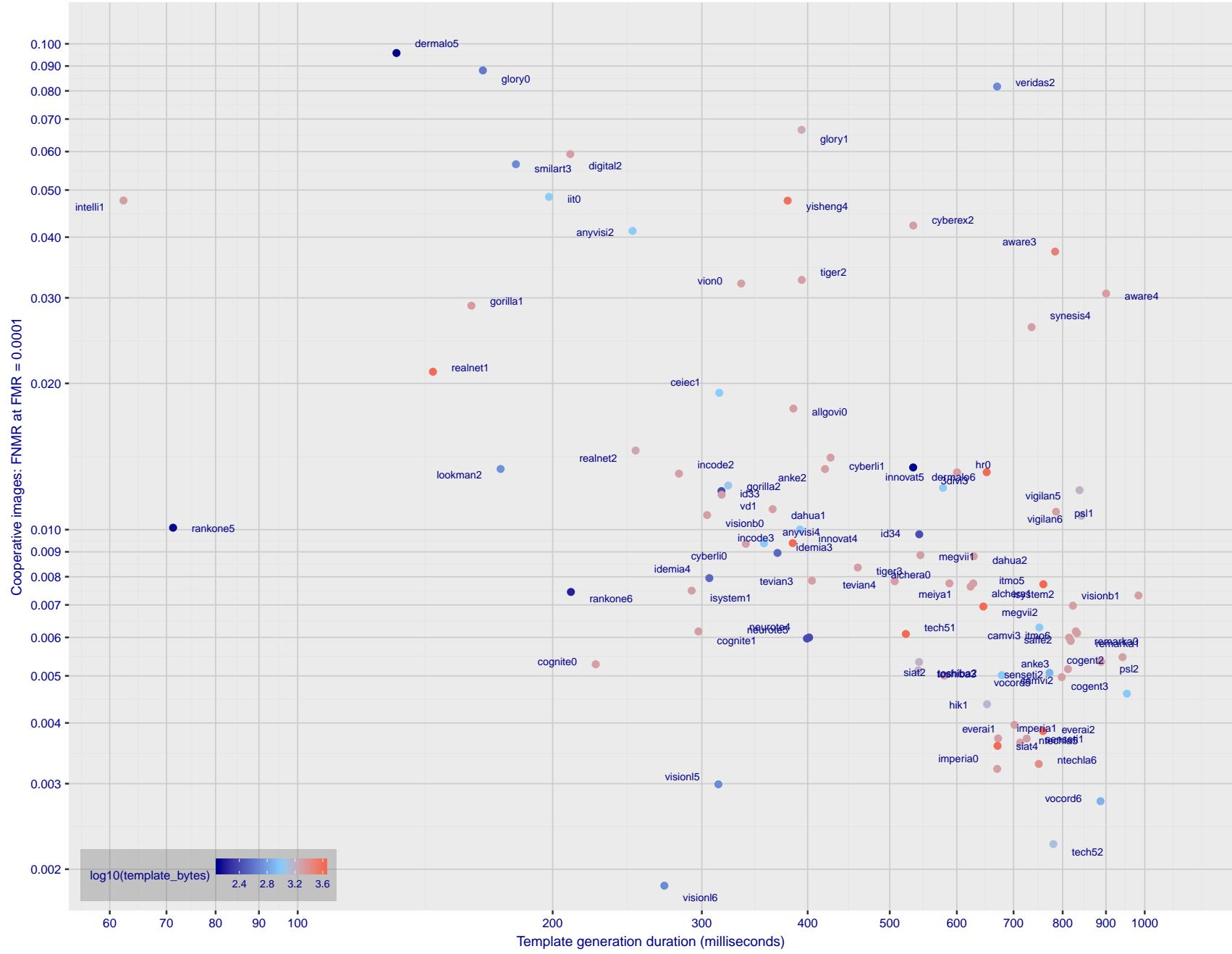


Figure 1: The points show false non-match rates (FNMR) versus the size of the encoded template. FNMR is the geometric mean of FNMR values for visa and mugshot images (from Figs. 16 and 22) at a false match rate (FMR) of 0.0001. The color of the points encodes template generation time - which spans at least one order of magnitude. Durations are measured on a single core of a c. 2016 Intel Xeon CPU E5-2630 v4 running at 2.20GHz. Algorithms with poor FNMR are omitted.



# 1 Metrics

## 1.1 Core accuracy

Given a vector of N genuine scores,  $u$ , the false non-match rate (FNMR) is computed as the proportion below some threshold, T:

$$\text{FNMR}(T) = 1 - \frac{1}{N} \sum_{i=1}^N H(u_i - T) \quad (1)$$

where  $H(x)$  is the unit step function, and  $H(0)$  taken to be 1.

Similarly, given a vector of N impostor scores,  $v$ , the false match rate (FMR) is computed as the proportion above T:

$$\text{FMR}(T) = \frac{1}{N} \sum_{i=1}^N H(v_i - T) \quad (2)$$

The threshold, T, can take on any value. We typically generate a set of thresholds from quantiles of the observed impostor scores,  $v$ , as follows. Given some interesting false match rate range,  $[\text{FMR}_L, \text{FMR}_U]$ , we form a vector of K thresholds corresponding to FMR measurements evenly spaced on a logarithmic scale

$$T_k = Q_v(1 - \text{FMR}_k) \quad (3)$$

where  $Q$  is the quantile function, and  $\text{FMR}_k$  comes from

$$\log_{10} \text{FMR}_k = \log_{10} \text{FMR}_L + \frac{k}{K} [\log_{10} \text{FMR}_U - \log_{10} \text{FMR}_L] \quad (4)$$

Error tradeoff characteristics are plots of FNMR(T) vs. FMR(T). These are plotted with  $\text{FMR}_U \rightarrow 1$  and  $\text{FMR}_L$  as low as is sustained by the number of impostor comparisons, N. This is somewhat higher than the “rule of three” limit  $3/N$  because samples are not independent, due to re-use of images.

## 2 Datasets

### 2.1 Child exploitation images

- ▷ The number of images is on the order of  $10^4$ .
- ▷ The number of subjects is on the order of  $10^3$ .
- ▷ The number of subjects with two images on the order of  $10^3$ .
- ▷ The images are operational. They are taken from ongoing investigations of child exploitation crimes. The images are arbitrarily unconstrained. Pose varies considerably around all three axes, including subject lying down. Resolution varies very widely. Faces can be occluded by other objects, including hair and hands. Lighting varies, although the images are intended for human viewing. Mis-focus is rare. Images are given to the algorithm without any cropping; faces may occupy widely varying areas.
- ▷ The images are usually large from contemporary cameras. The mean interocular distance (IOD) is 70 pixels.
- ▷ The images are of subjects from several countries, due to the global production of this imagery.
- ▷ The images are of children, from infancy to late adolescence.
- ▷ All of the images are live capture, none are scanned. Many have been cropped.
- ▷ When these images are input to the algorithm, they are labelled as being of type "EXPLOITATION" - see Table 4 of the FRVT API.

### 2.2 Visa images

- ▷ The number of images is on the order of  $10^5$ .
- ▷ The number of subjects is on the order of  $10^5$ .
- ▷ The number of subjects with two images on the order of  $10^4$ .
- ▷ The images have geometry in reasonable conformance with the ISO/IEC 19794-5 Full Frontal image type. Pose is generally excellent.
- ▷ The images are of size 252x300 pixels. The mean interocular distance (IOD) is 69 pixels.
- ▷ The images are of subjects from greater than 100 countries, with significant imbalance due to visa issuance patterns.
- ▷ The images are of subjects of all ages, including children, again with imbalance due to visa issuance demand.
- ▷ Many of the images are live capture. A substantial number of the images are photographs of paper photographs.
- ▷ When these images are input to the algorithm, they are labelled as being of type "ISO" - see Table 4 of the FRVT API.

### 2.3 Mugshot images

- ▷ The number of images is on the order of  $10^6$ .
- ▷ The number of subjects is on the order of  $10^6$ .
- ▷ The number of subjects with two images on the order of  $10^6$ .



Figure 3: The figure gives simulated samples of image types used in this report.

- ▷ The images have geometry in reasonable conformance with the ISO/IEC 19794-5 Full Frontal image type.
  - ▷ The images are of variable sizes. The median IOD is 105 pixels. The mean IOD is 113 pixels. The 1-st, 5-th, 10-th, 25-th, 75-th, 90-th and 99-th percentiles are 34, 58, 70, 87, 121, 161 and 297 pixels.
  - ▷ The images are of subjects from the United States.
  - ▷ The images are of adults.
  - ▷ The images are all live capture.
  - ▷ When these images are input to the algorithm, they are labelled as being of type "mugshot" - see Table 4 of the FRVT API.

## 2.4 Wild images

- ▷ The number of images is on the order of  $10^5$ .
  - ▷ The number of subjects is on the order of  $10^3$ .
  - ▷ The number of subjects with two images on the order of  $10^3$ .
  - ▷ The images include many photojournalism-style images. Images are given to the algorithm using a variable but generally tight crop of the head. Resolution varies very widely. The images are very unconstrained, with wide yaw and pitch pose variation. Faces can be occluded, including hair and hands.
  - ▷ The images are of adults.
  - ▷ All of the images are live capture, none are scanned.
  - ▷ When these images are input to the algorithm, they are labelled as being of type "WILD" - see Table 4 of the FRVT API.

3 Results

### 3.1 Test goals

- ▷ To state overall accuracy.
  - ▷ To compare algorithms.

### 3.2 Test design

**Method:** For visa images:

- ▷ The comparisons are of visa photos against visa photos.
- ▷ The number of genuine comparisons is on the order of  $10^4$ .
- ▷ The number of impostor comparisons is on the order of  $10^{10}$ .
- ▷ The comparisons are fully zero-effort, meaning impostors are paired without attention to sex, age or other covariates. However, later analysis is conducted on subsets.
- ▷ The number of persons is on the order of  $10^5$ .
- ▷ The number of images used to make 1 template is 1.
- ▷ The number of templates used to make each comparison score is two corresponding to simple one-to-one verification.

For mugshot images:

- ▷ The comparisons are of mugshot photos against mugshot photos.
- ▷ The number of genuine comparisons is on the order of  $10^6$ .
- ▷ The number of impostor comparisons is on the order of  $10^8$ .
- ▷ The impostors are paired by sex, but not by age or other covariates.
- ▷ The number of persons is on the order of  $10^6$ .
- ▷ The number of images used to make 1 template is 1.
- ▷ The number of templates used to make each comparison score is two corresponding to simple one-to-one verification.

**Method:** For wild images:

- ▷ The comparisons are of wild photos against wild photos.
- ▷ The number of genuine comparisons is on the order of  $10^6$ .
- ▷ The number of impostor comparisons is on the order of  $10^7$ .
- ▷ The comparisons are fully zero-effort, meaning impostors are paired without attention to sex, age or other covariates.
- ▷ The number of persons is on the order of  $10^4$ .
- ▷ The number of images used to make 1 template is 1.
- ▷ The number of templates used to make each comparison score is two corresponding to simple one-to-one verification.

For child exploitation images:

- ▷ The comparisons are of unconstrained child exploitation photos against others of the same type.

- ▷ The number of genuine comparisons is on the order of  $10^4$ .
- ▷ The number of impostor comparisons is on the order of  $10^7$ .
- ▷ The comparisons are fully zero-effort, meaning impostors are paired without attention to sex, age or other covariates.
- ▷ The number of persons is on the order of  $10^3$ .
- ▷ The number of images used to make 1 template is 1.
- ▷ The number of templates used to make each comparison score is two corresponding to simple one-to-one verification.
- ▷ We produce two performance statements. First, is a DET as used for visa and mugshot images. The second is a cumulative match characteristic (CMC) summarizing a simulated one-to-many search process. This is done as follows.
  - We regard  $M$  enrollment templates as items in a gallery.
  - These  $M$  templates come from  $M > N$  individuals, because multiple images of a subject are present in the gallery under separate identifiers.
  - We regard the verification templates as search templates.
  - For each search we compute the rank of the highest scoring mate.
  - This process should properly be conducted with a 1:N algorithm, such as those tested in NIST IR 8009. We use the 1:1 algorithms in a simulated 1:N mode here to a) better reflect what a child exploitation analyst does, and b) to show algorithm efficacy is better than that revealed in the verification DETs.

### 3.3 Failure to enroll

Algorithm Name	Failure to Enrol Rate <sup>1</sup>							
	CHILD-EXPLOIT	MUGSHOT	VISA	WILD				
3divi-003	0.1806	41	0.0007	75	0.0006	67	0.0294	85
alchera-000	-	119	0.0004	63	0.0014	93	0.0038	53
alchera-001	-	119	0.0004	62	0.0014	92	0.0038	52
allgovision-000	-	119	0.0026	96	0.0052	107	0.0131	77
amplifiedgroup-001	-	119	0.0189	110	0.0279	113	0.1390	104
anke-002	0.1371	35	0.0004	60	0.0009	77	0.0094	70
anke-003	-	119	0.0001	35	0.0004	46	0.0006	32
anyvision-002	0.4866	57	0.0070	104	0.0090	109	0.1146	98
anyvision-004	0.1660	38	0.0001	43	0.0004	51	0.0080	65
aware-003	0.3314	52	0.0016	91	0.0013	89	0.0745	97
aware-004	-	119	0.0002	45	0.0005	58	0.0014	43
ayonix-000	0.0000	4	0.0113	107	0.0137	111	0.1194	99
bm-001	0.0000	8	0.0000	19	0.0000	14	0.0000	11
camvi-002	0.0000	5	0.0000	3	0.0000	3	0.0000	2
camvi-003	-	119	0.0000	2	0.0000	2	0.0000	1
ceiec-001	-	119	0.0029	99	0.0023	99	0.0068	61
cogent-002	0.2096	43	0.0002	44	0.0004	55	0.0063	59
cogent-003	-	119	0.0001	34	0.0004	49	0.0009	41
cognitec-000	0.6342	60	0.0007	76	0.0007	73	0.0388	90
cognitec-001	-	119	0.0008	80	0.0010	78	0.0185	81
cyberextruder-001	0.5338	58	0.0024	94	0.0029	102	0.0597	95
cyberextruder-002	0.2672	50	0.0027	97	0.0028	101	0.0335	89
cyberlink-000	-	119	0.0006	73	0.0008	74	0.1374	102
cyberlink-001	-	119	0.0073	105	0.0005	59	0.0008	37
dahua-001	0.0000	14	0.0000	17	0.0000	19	0.0000	16
dahua-002	-	119	0.0024	95	0.0022	97	0.0009	39
dermalog-005	0.1796	39	0.0013	88	0.0041	104	0.0163	79
dermalog-006	0.1797	40	0.0013	87	0.0041	105	0.0163	80
digitalbarriers-002	-	119	0.0028	98	0.0027	100	0.0071	62
everai-001	-	119	0.0004	65	0.0004	54	0.0006	36
everai-002	-	119	0.0002	47	0.0004	34	0.0004	29
glory-000	0.0000	7	0.0053	102	0.0013	90	0.1565	105
glory-001	0.0000	10	0.0051	101	0.0010	79	0.1651	106
gorilla-001	0.1347	32	0.0003	56	0.0004	57	0.0117	73
gorilla-002	0.1347	33	0.0003	55	0.0004	56	0.0117	72
hik-001	-	119	0.0000	7	0.0000	8	0.0000	6
hr-000	-	119	0.0003	52	0.0008	75	0.0034	51
id3-003	0.3032	51	0.0016	92	0.0011	87	0.0317	87
id3-004	-	119	0.0015	90	0.0011	88	-	119
idemcia-003	0.0481	20	0.0000	23	0.0004	36	0.0042	56
idemcia-004	-	119	0.0000	26	0.0004	39	0.0003	27
iit-000	-	119	0.0007	74	0.0011	83	-	119
imperial-000	-	119	0.0000	16	0.0000	18	0.0000	15
imperial-001	-	119	0.0000	13	0.0000	15	0.0000	12
incode-002	0.2202	44	0.0004	67	0.0007	70	0.0081	66
incode-003	-	119	0.0004	66	0.0007	69	0.0014	42
innovatrics-004	0.1170	31	0.0000	29	0.0004	53	0.0041	55
innovatrics-005	-	119	0.0000	30	0.0004	52	0.0006	31
intellivision-001	0.5495	59	0.0048	100	0.0042	106	0.1358	101
isityou-000	0.4714	56	0.0023	93	0.0010	80	0.0663	96
isystems-001	0.1421	36	0.0010	82	0.0007	71	0.0128	75
isystems-002	0.1421	37	0.0010	83	0.0007	72	0.0128	76
itmo-005	0.1353	34	0.0005	70	0.0002	23	0.0075	63
itmo-006	-	119	0.0004	68	0.0004	50	0.0006	35
kakao-001	-	119	0.0002	48	0.0005	60	0.0310	86
lookman-002	-	119	0.0000	6	0.0000	7	0.0000	5
megvii-001	0.0274	18	0.0007	77	0.0004	41	0.0152	78
megvii-002	0.0274	17	0.0054	103	0.0004	40	0.0126	74
meiya-001	-	119	0.0004	69	0.0010	81	0.0025	46
microfocus-001	0.0791	30	0.0008	79	0.0016	95	0.0220	84

Table 6: FTE is the proportion of failed template generation attempts. Failures can occur because the software throws an exception, or because the software electively refuses to process the input image. This would typically occur if a face is not detected. FTE is measured as the number of function calls that give EITHER a non-zero error code OR that give a “small” template. This is defined as one whose size is less than 0.3 times the median template size for that algorithm. This second rule is needed because some algorithms incorrectly fail to return a non-zero error code when template generation fails.

<sup>1</sup>The effects of FTE are included in the accuracy results of this report by regarding any template comparison involving a failed template to produce a low similarity score. Thus higher FTE results in higher FNMR and lower FMR.

Algorithm Name	Failure to Enrol Rate <sup>1</sup>							
	CHILD-EXPLOIT	MUGSHOT	VISA	WILD				
microfocus-002	0.0791	29	0.0008	78	0.0016	94	0.0220	83
neurotechnology-004	0.0055	15	0.0000	22	0.0001	22	0.0026	47
neurotechnology-005	-	119	0.0004	59	0.0004	44	0.0018	44
nodeflux-000	-	119	0.0001	37	0.0002	25	0.0003	24
nodeflux-001	-	119	0.0001	36	0.0002	24	0.0003	23
ntechlab-005	0.0315	19	0.0000	21	0.0004	38	0.0032	50
ntechlab-006	-	119	0.0000	20	0.0004	33	0.0003	22
psl-001	0.0000	11	0.0000	14	0.0000	16	0.0000	13
psl-002	-	119	0.0000	12	0.0000	13	0.0000	10
rankone-006	-	119	0.0000	11	0.0000	12	0.0000	9
realnetworks-001	0.0076	16	0.0004	58	0.0003	28	0.0064	60
realnetworks-002	-	119	0.0004	57	0.0003	27	0.0004	28
remarkai-000	-	119	0.0000	5	0.0000	5	0.0000	19
remarkai-001	-	119	0.0000	18	0.0000	20	0.0000	20
saffe-001	0.0000	12	0.0000	15	0.0000	17	0.0000	14
saffe-002	-	119	0.0000	9	0.0000	10	0.0000	7
sensetime-001	0.0631	28	0.0000	25	0.0004	45	0.0003	25
sensetime-002	0.3345	53	0.0011	84	0.0005	65	0.0218	82
shaman-000	0.0000	6	0.0000	4	0.0000	4	0.0000	3
shaman-001	0.0000	1	0.0000	1	0.0000	1	0.0000	17
siat-002	0.0616	25	0.0000	28	0.0004	48	0.0048	57
siat-004	-	119	0.0000	27	0.0004	47	0.0003	26
smilart-002	0.2422	46	0.0003	54	0.0011	84	0.0575	94
smilart-003	-	119	0.0014	89	0.0013	91	0.0555	93
synesis-004	-	119	0.0164	109	0.0035	103	0.0485	92
tech5-001	0.0000	2	0.0004	61	0.0003	30	0.0409	91
tech5-002	-	119	0.0001	33	0.0003	26	0.0000	18
tevian-003	0.2430	48	0.0003	50	0.0005	66	0.0076	64
tevian-004	-	119	0.0002	46	0.0005	64	0.0057	58
tiger-002	0.0619	26	0.0001	38	0.0004	42	0.0082	67
tiger-003	0.0619	27	0.0001	39	0.0004	43	0.0082	68
toshiba-002	0.0000	13	0.0000	8	0.0000	9	-	119
toshiba-003	-	119	0.0001	40	0.0001	21	0.0002	21
vd-001	-	119	0.0004	64	0.0009	76	0.0024	45
veridas-001	-	119	0.0001	41	0.0005	62	0.0006	33
veridas-002	-	119	0.0001	42	0.0005	63	0.0006	34
vigilantsolutions-005	0.2538	49	0.0001	31	0.0004	35	0.0041	54
vigilantsolutions-006	-	119	0.0001	32	0.0004	37	0.0005	30
vion-000	0.6388	61	0.0130	108	0.0078	108	0.1389	103
visionbox-000	-	119	0.0005	72	0.0011	86	0.0028	49
visionbox-001	-	119	0.0005	71	0.0011	85	0.0028	48
visionlabs-005	0.1875	42	0.0002	49	0.0023	98	0.0085	69
visionlabs-006	-	119	0.0003	53	0.0005	61	0.0009	40
vocord-006	-	119	0.0003	51	0.0003	31	0.0008	38
yisheng-004	0.4279	54	0.0013	85	0.0006	68	0.0321	88
yitu-003	-	119	0.0009	81	0.0000	6	0.0000	4

Table 7: FTE is the proportion of failed template generation attempts. Failures can occur because the software throws an exception, or because the software electively refuses to process the input image. This would typically occur if a face is not detected. FTE is measured as the number of function calls that give EITHER a non-zero error code OR that give a “small” template. This is defined as one whose size is less than 0.3 times the median template size for that algorithm. This second rule is needed because some algorithms incorrectly fail to return a non-zero error code when template generation fails.

<sup>1</sup>The effects of FTE are included in the accuracy results of this report by regarding any template comparison involving a failed template to produce a low similarity score. Thus higher FTE results in higher FNMR and lower FMR.

### 3.4 Recognition accuracy

Core algorithm accuracy is stated via:

▷ **Cooperative subjects**

- The summary table of Figure 5;
- The visa image DETs of Figure 16;
- The mugshot DETs of Figure 22;
- The mugshot ageing profiles of Figure 92;
- The human-difficult pairs of Figure 4

▷ **Non-cooperative subjects**

- The photojournalism DET of Figure 27
- The child-exploitation DET of Figure 30;
- The child-exploitation CMC of Figure 32.

Figure 73 shows dependence of false match rate on algorithm score threshold. This allows a deployer to set a threshold to target a particular false match rate appropriate to the security objectives of the application.

Figure 61 likewise shows FMR(T) but for mugshots, and specially four subsets of the population.

Note that in both the mugshot and visa sets false match rates vary with the ethnicity, age, and sex, of the enrollee and impostor - see section 3.6. For example figure 39 summarizes FMR for impostors paired from four groups black females, black males, white females, white males.



Figure 4: The Figure shows, in blue, algorithms that correctly separate the 12 genuine and 8 impostor pairs used in the May 2018 paper Face recognition accuracy of forensic examiners, superrecognizers, and face recognition algorithms (Phillips et al. [1]). In red are algorithms that are imperfect. Some algorithms fail only because they failed to make a template e.g. due to face detection failure (shown as a triangle). Others fail because the pairs were selected for that study because they had been difficult for three leading algorithms used in FRVT 2006. Caution: Given the small sample size ( $n=20$ ) the figure may change substantially if larger or different sets were used.

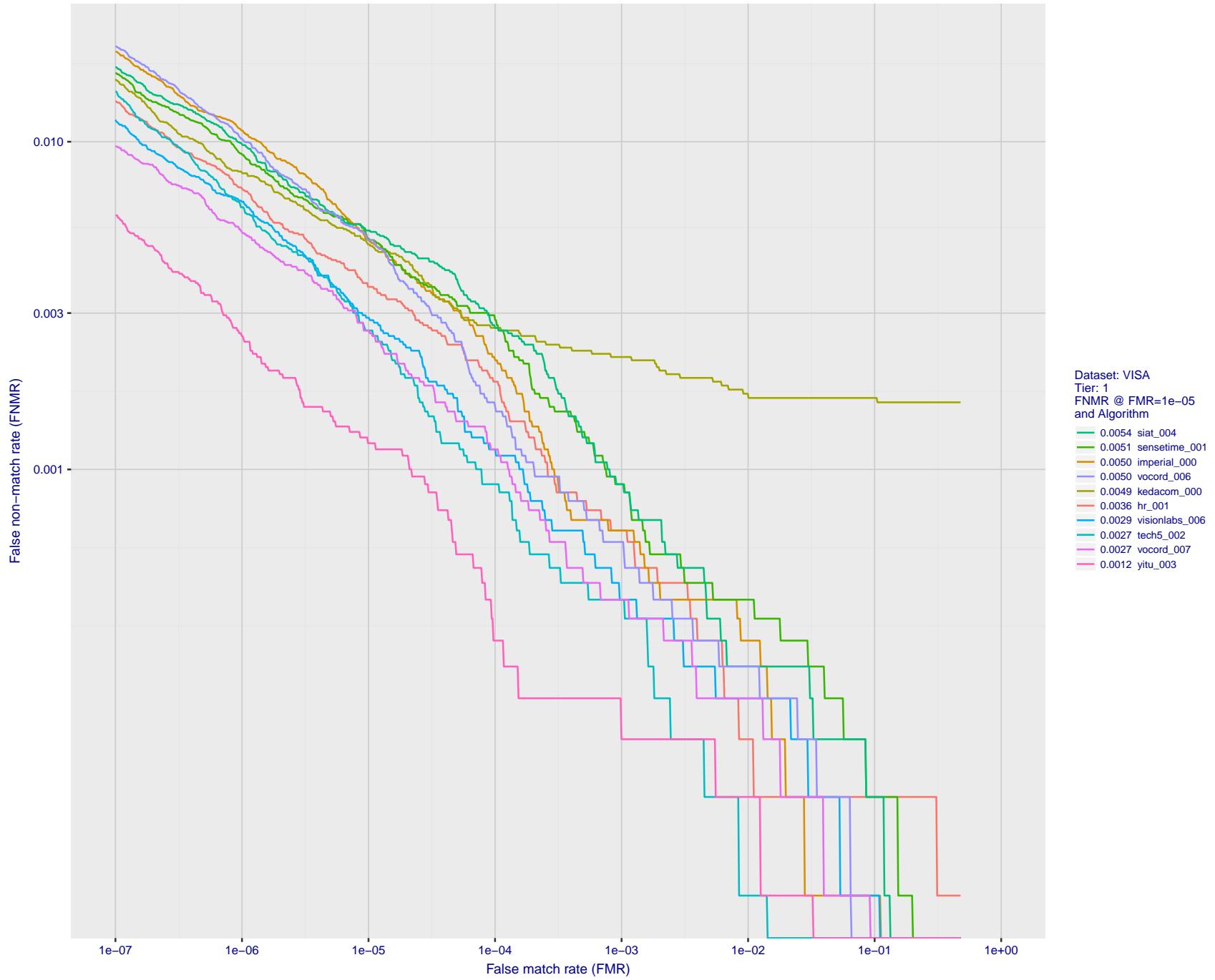


Figure 5: For the visa images, detection error tradeoff (DET) characteristics showing false non-match rate vs. false match rate plotted parametrically on threshold,  $T$ . The scales are logarithmic in order to show many decades of FMR.

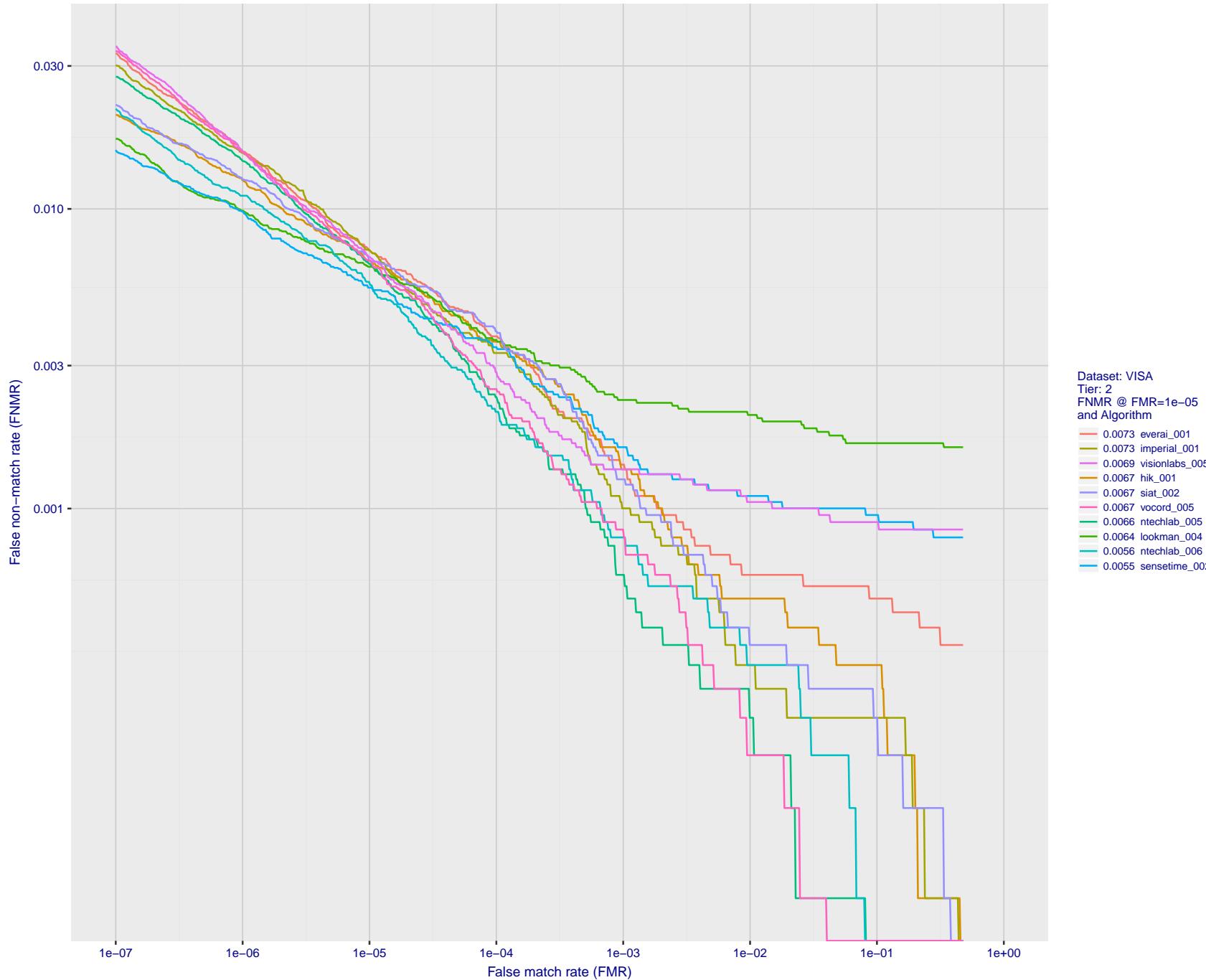


Figure 6: For the visa images, detection error tradeoff (DET) characteristics showing false non-match rate vs. false match rate plotted parametrically on threshold,  $T$ . The scales are logarithmic in order to show many decades of FMR.

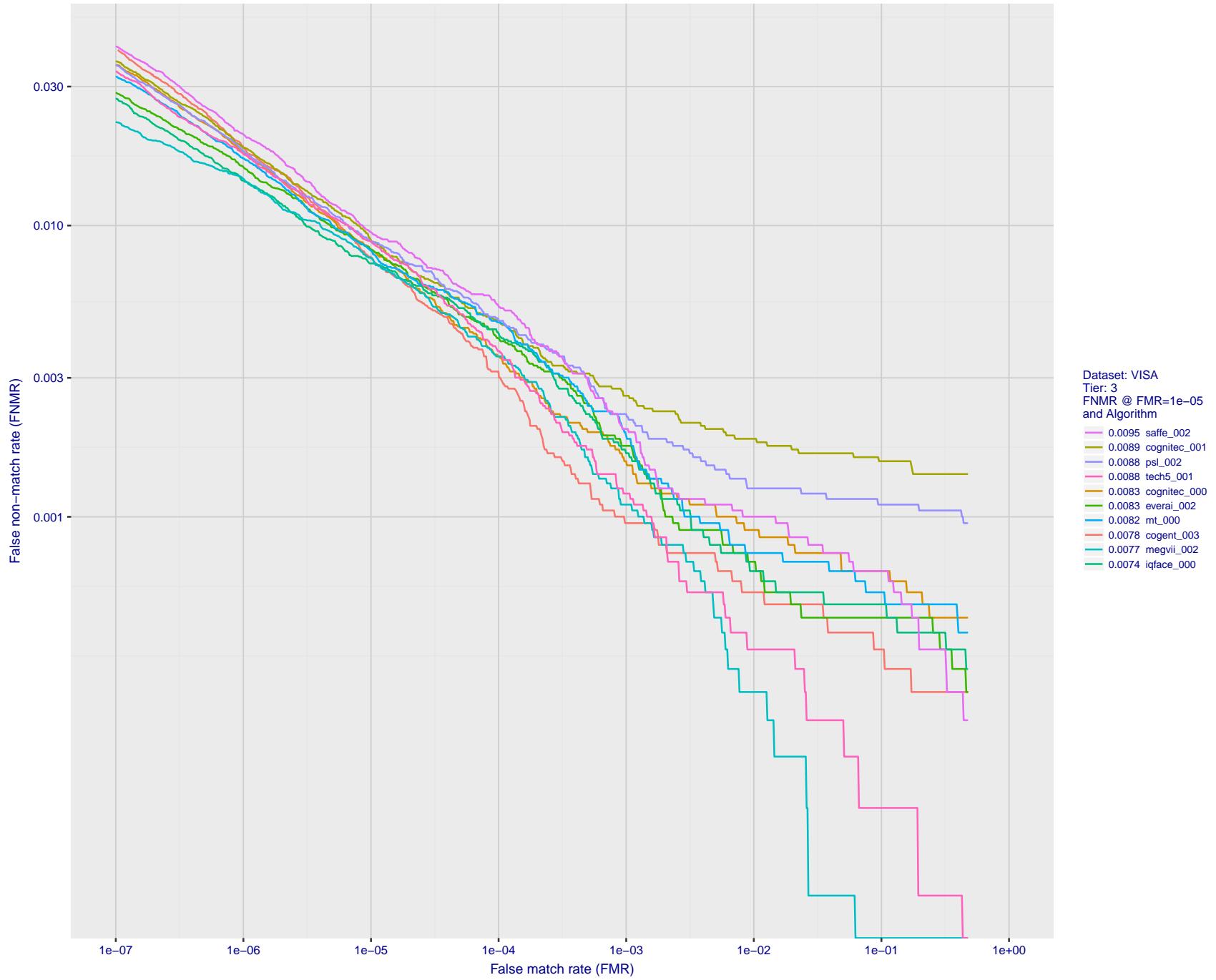


Figure 7: For the visa images, detection error tradeoff (DET) characteristics showing false non-match rate vs. false match rate plotted parametrically on threshold,  $T$ . The scales are logarithmic in order to show many decades of FMR.

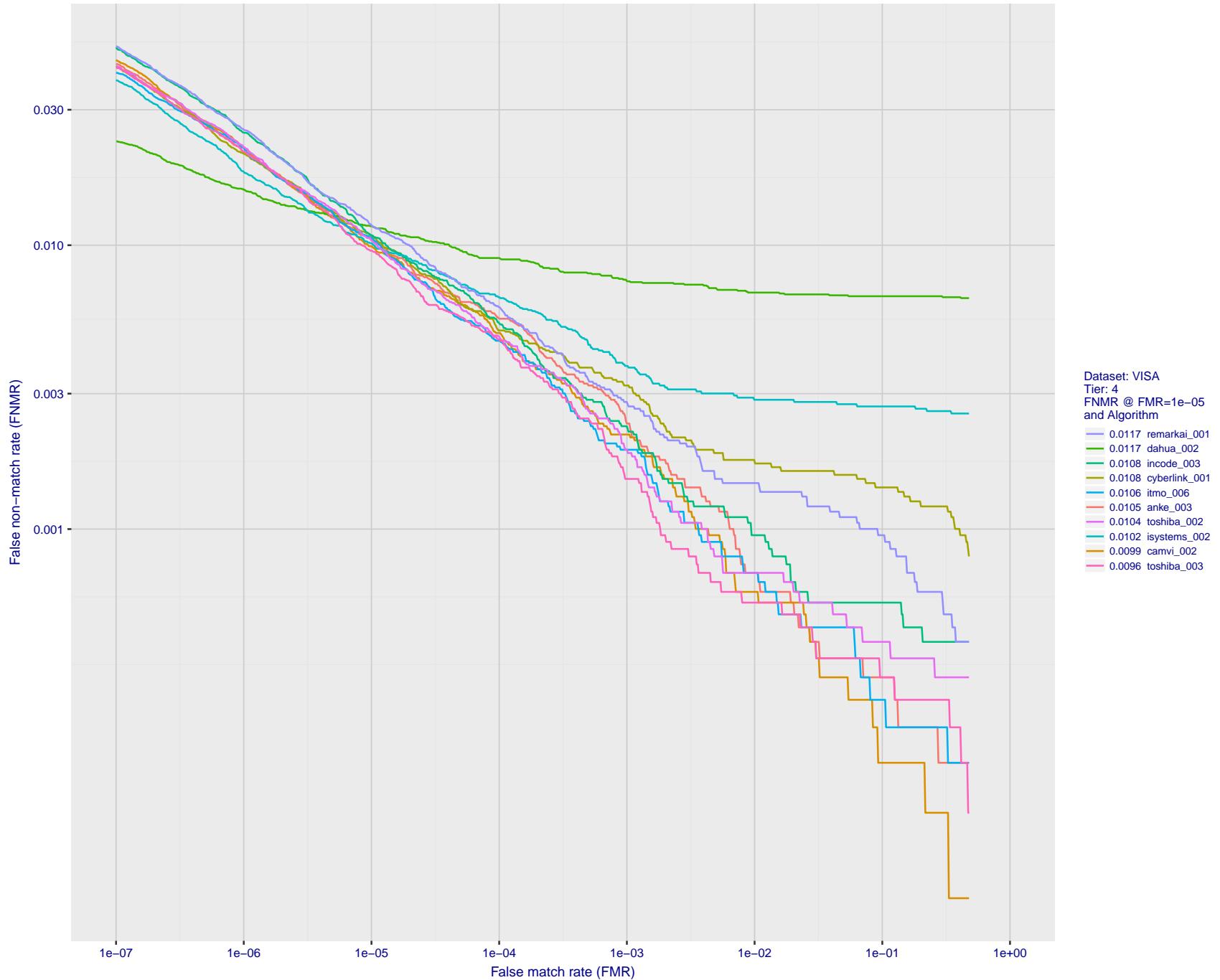


Figure 8: For the visa images, detection error tradeoff (DET) characteristics showing false non-match rate vs. false match rate plotted parametrically on threshold,  $T$ . The scales are logarithmic in order to show many decades of FMR.

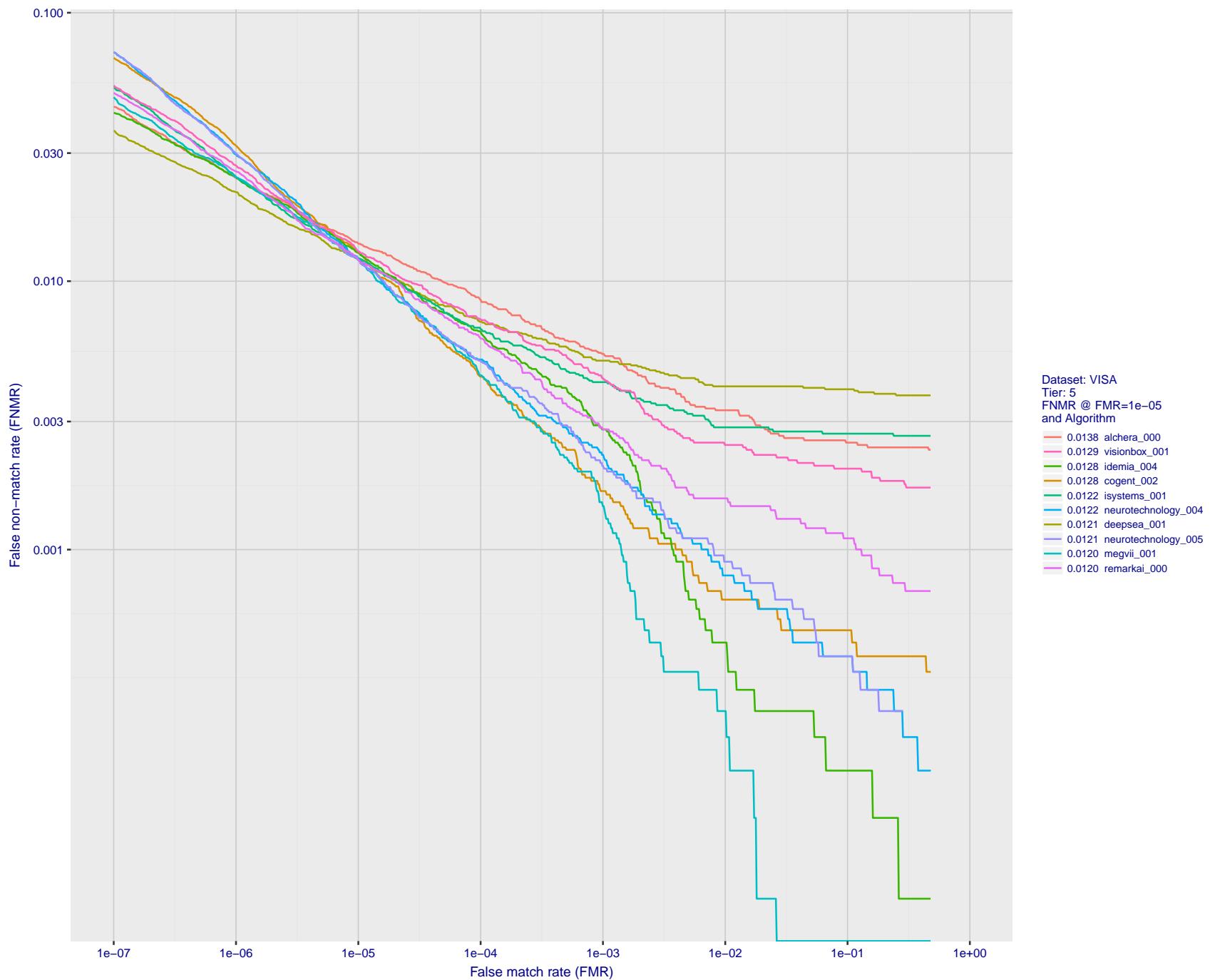


Figure 9: For the visa images, detection error tradeoff (DET) characteristics showing false non-match rate vs. false match rate plotted parametrically on threshold,  $T$ . The scales are logarithmic in order to show many decades of FMR.

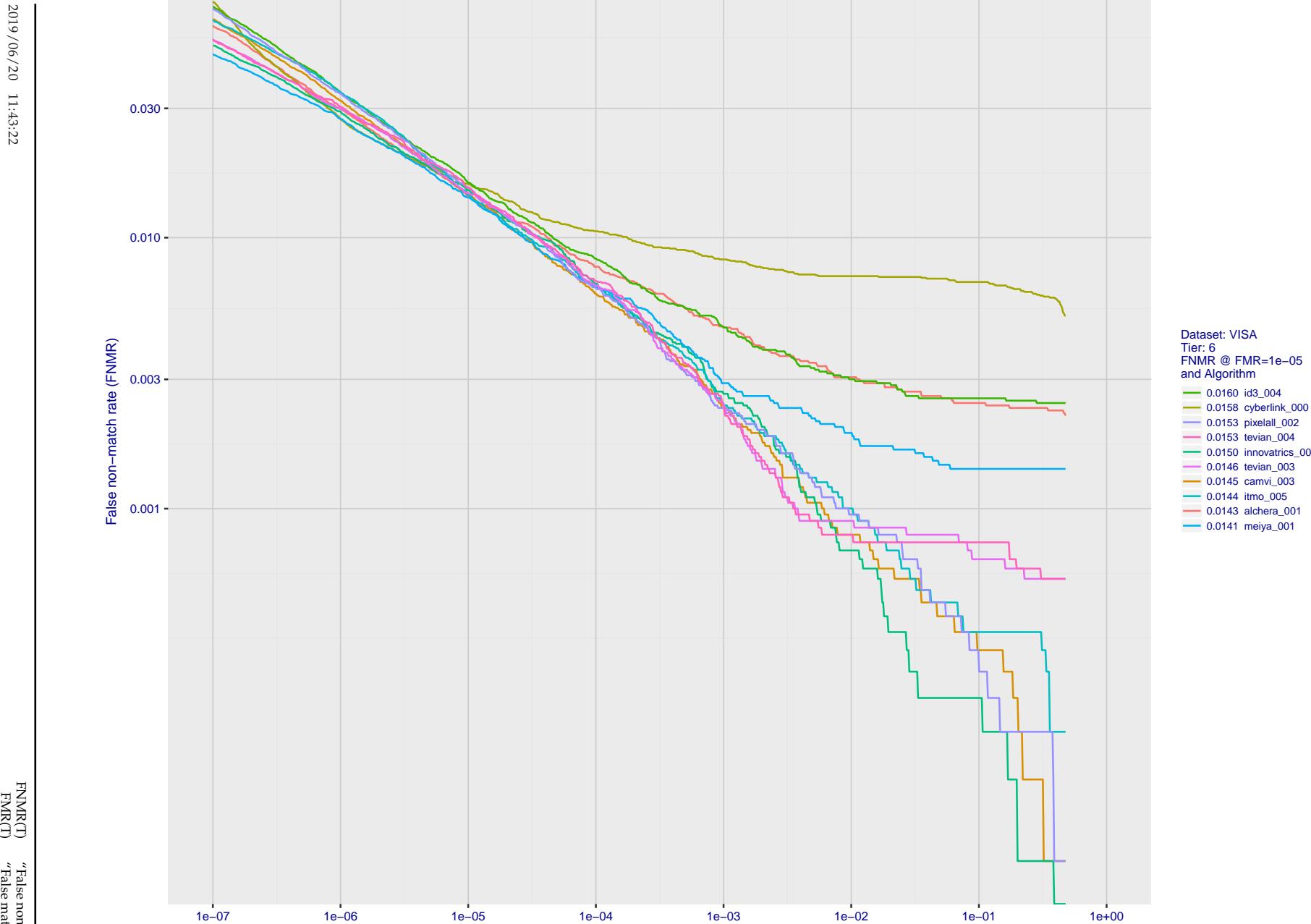


Figure 10: For the visa images, detection error tradeoff (DET) characteristics showing false non-match rate vs. false match rate plotted parametrically on threshold,  $T$ . The scales are logarithmic in order to show many decades of FMR.

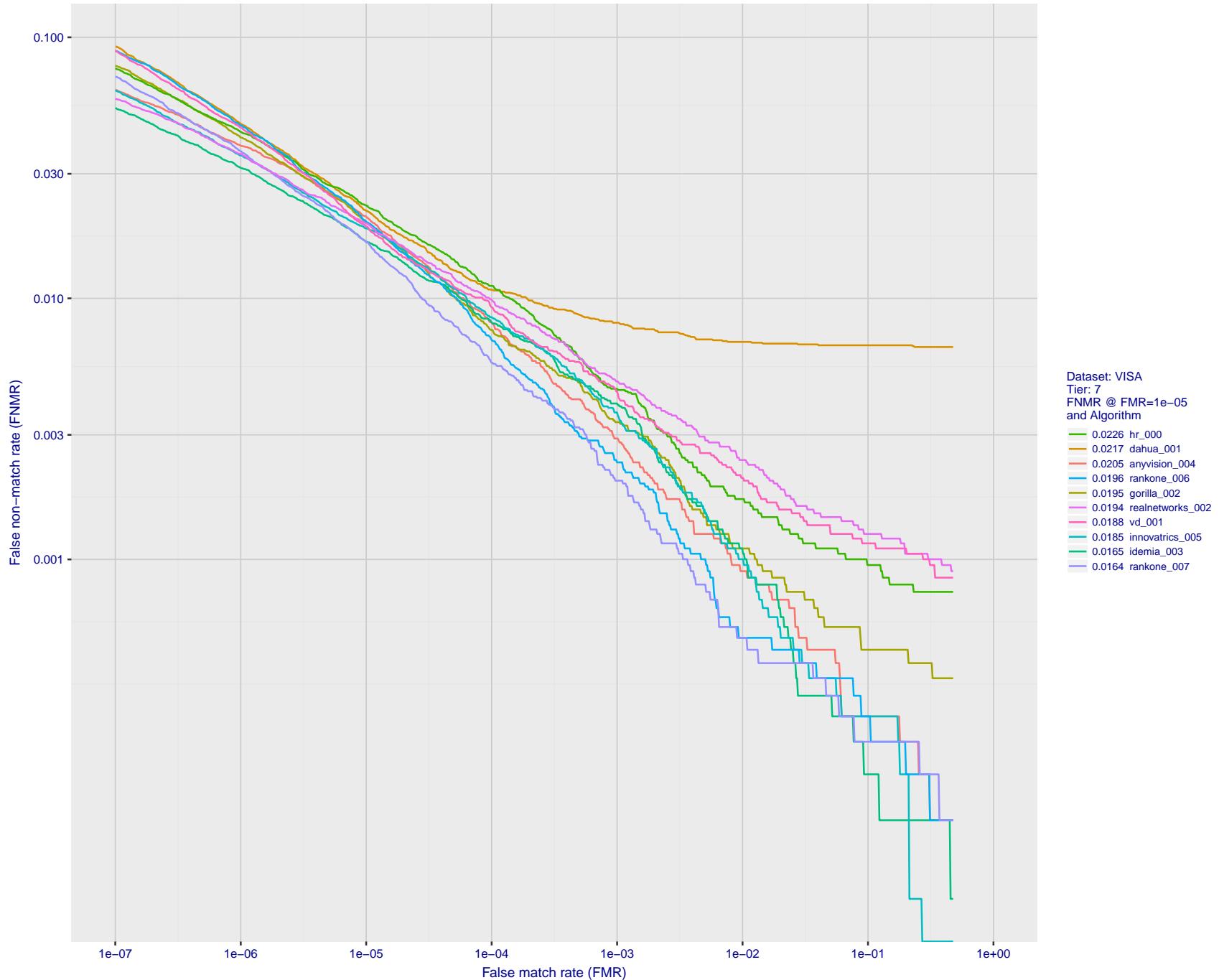


Figure 11: For the visa images, detection error tradeoff (DET) characteristics showing false non-match rate vs. false match rate plotted parametrically on threshold,  $T$ . The scales are logarithmic in order to show many decades of FMR.

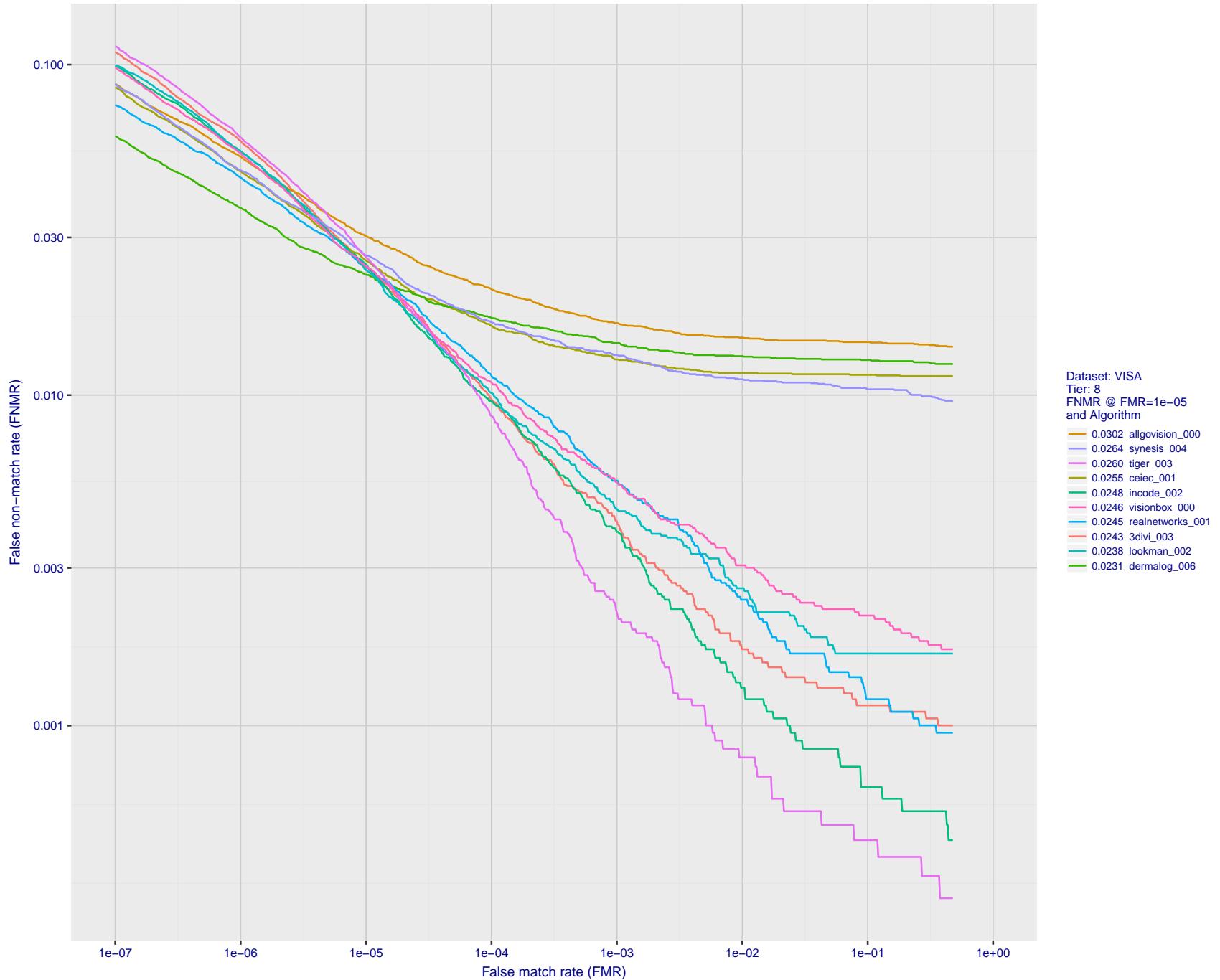


Figure 12: For the visa images, detection error tradeoff (DET) characteristics showing false non-match rate vs. false match rate plotted parametrically on threshold,  $T$ . The scales are logarithmic in order to show many decades of FMR.

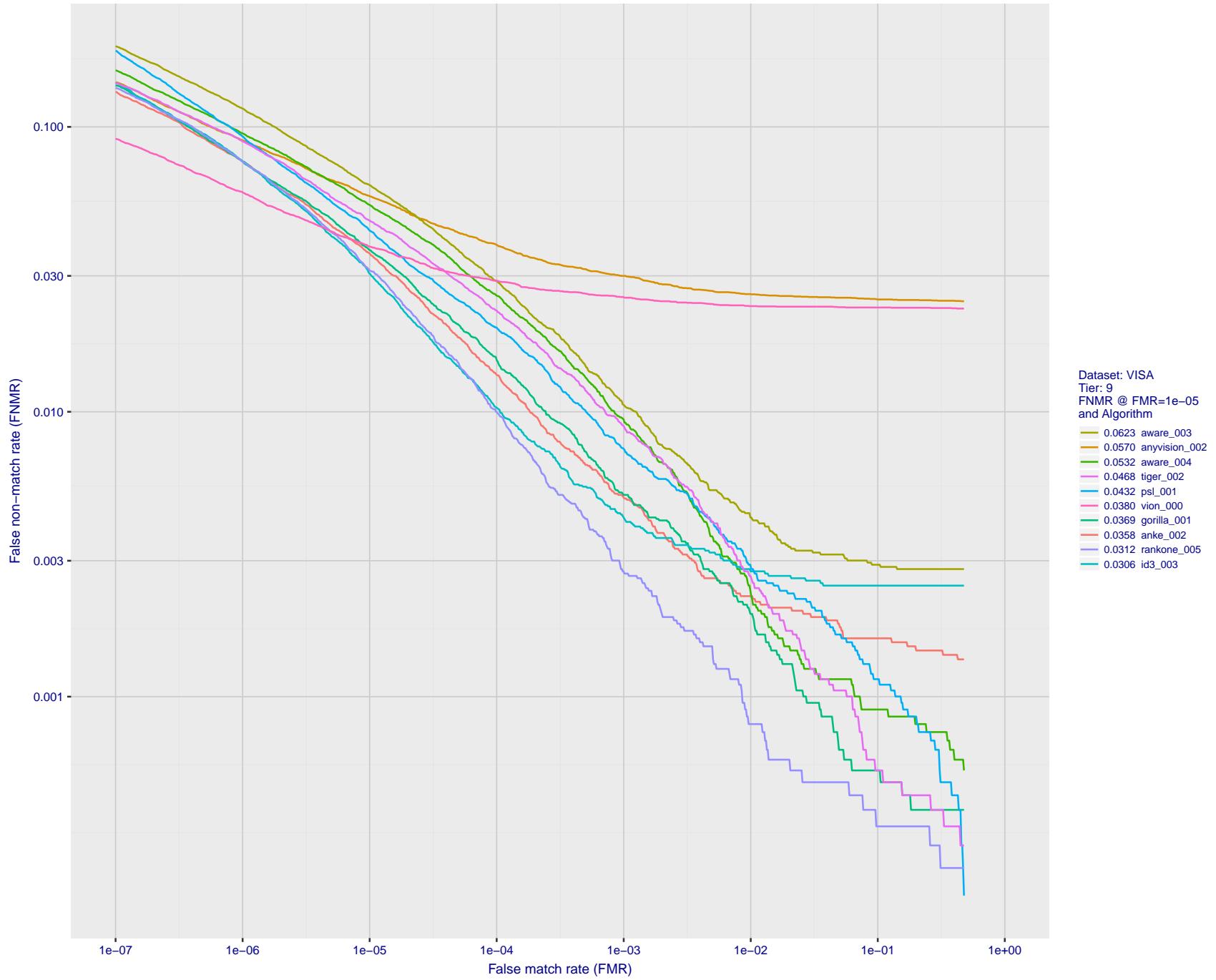


Figure 13: For the visa images, detection error tradeoff (DET) characteristics showing false non-match rate vs. false match rate plotted parametrically on threshold,  $T$ . The scales are logarithmic in order to show many decades of FMR.

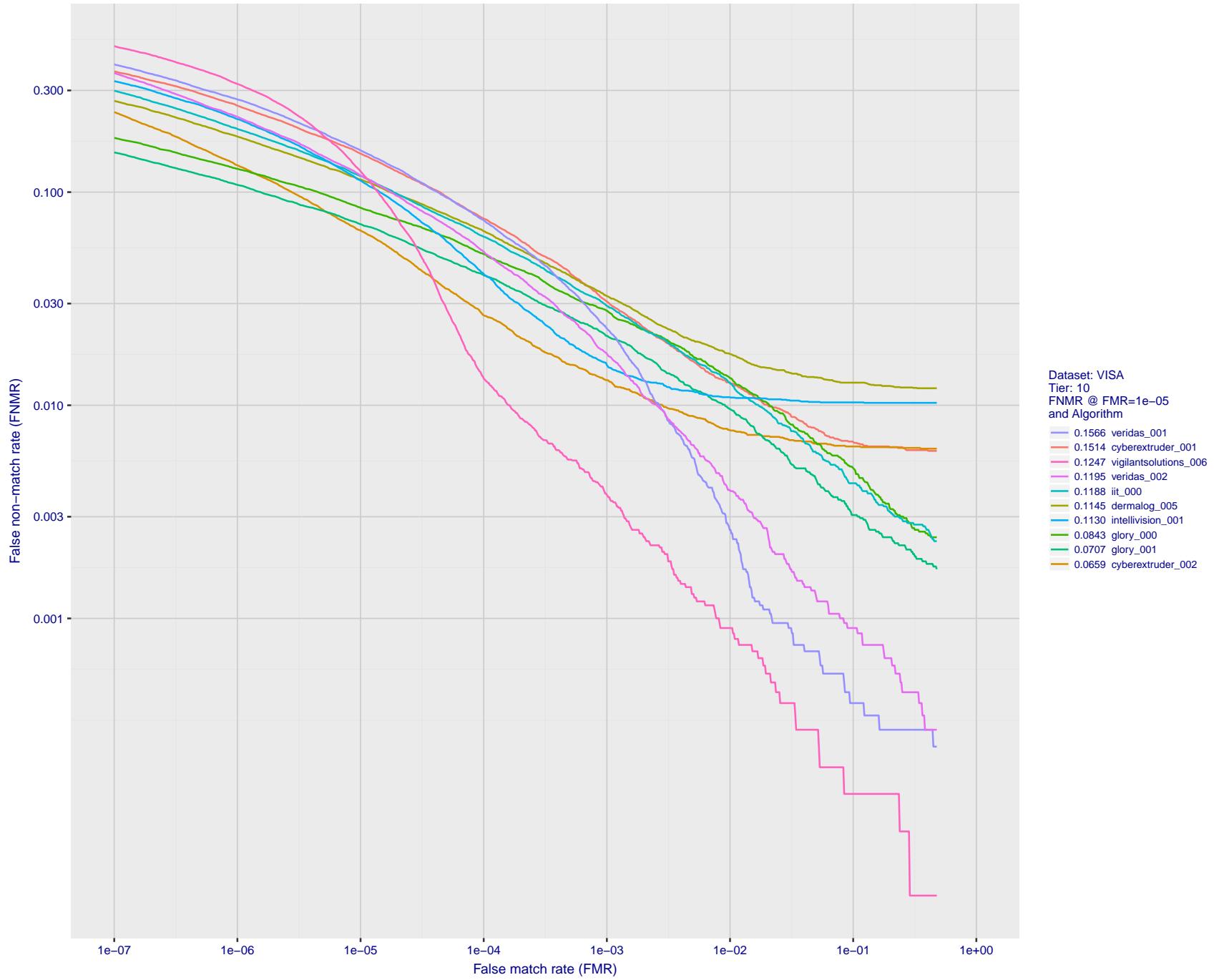


Figure 14: For the visa images, detection error tradeoff (DET) characteristics showing false non-match rate vs. false match rate plotted parametrically on threshold,  $T$ . The scales are logarithmic in order to show many decades of FMR.

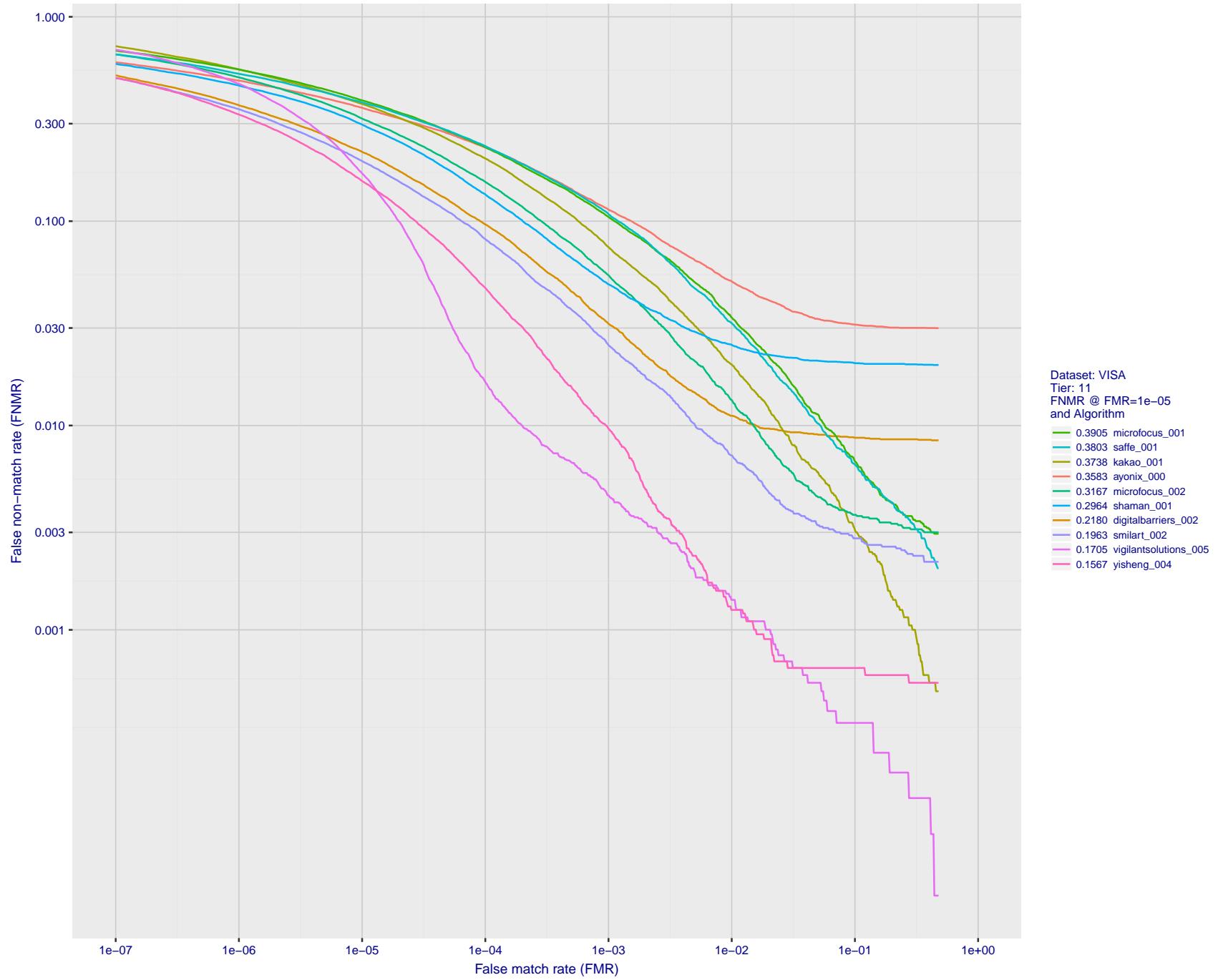


Figure 15: For the visa images, detection error tradeoff (DET) characteristics showing false non-match rate vs. false match rate plotted parametrically on threshold,  $T$ . The scales are logarithmic in order to show many decades of FMR.

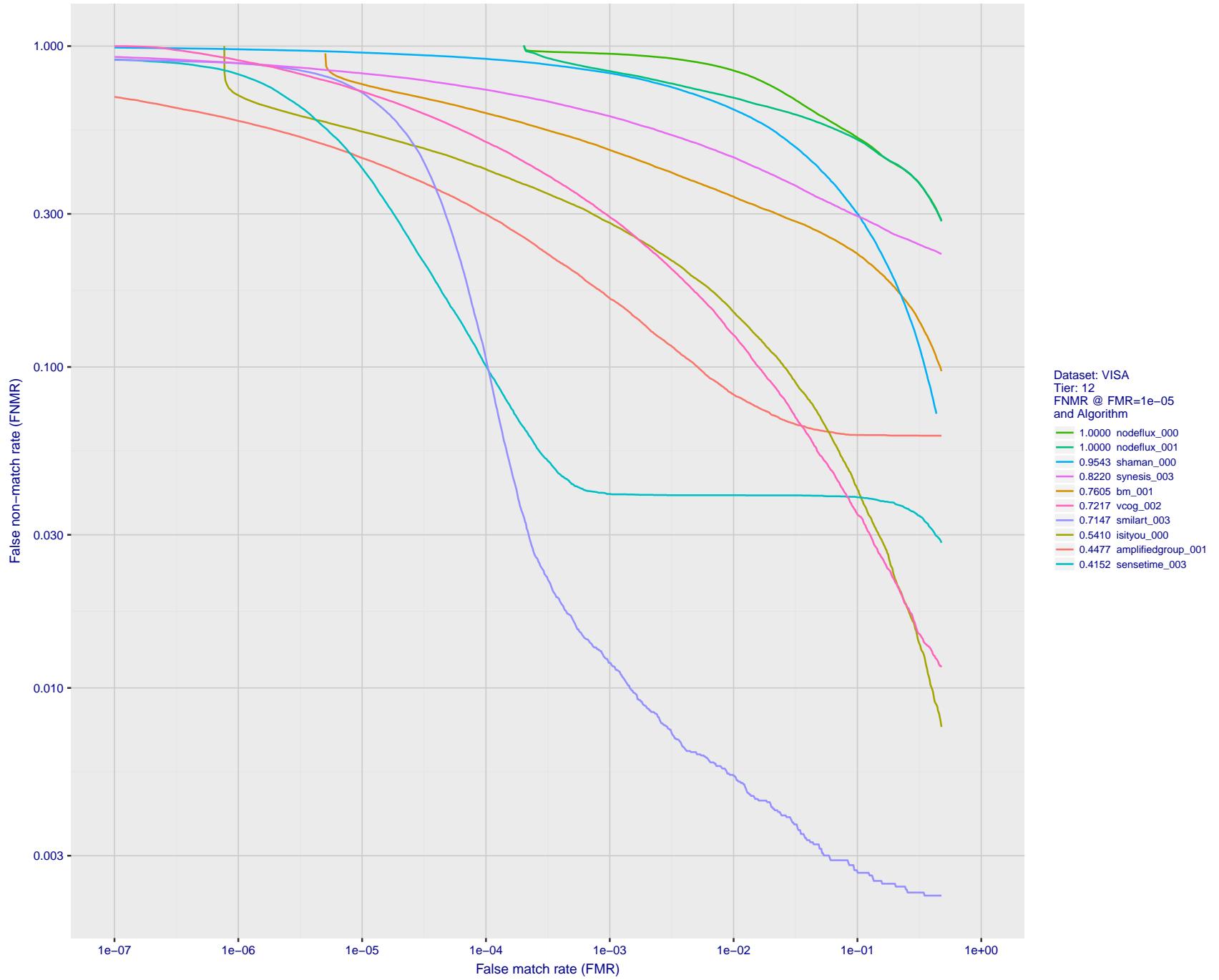


Figure 16: For the visa images, detection error tradeoff (DET) characteristics showing false non-match rate vs. false match rate plotted parametrically on threshold,  $T$ . The scales are logarithmic in order to show many decades of FMR.

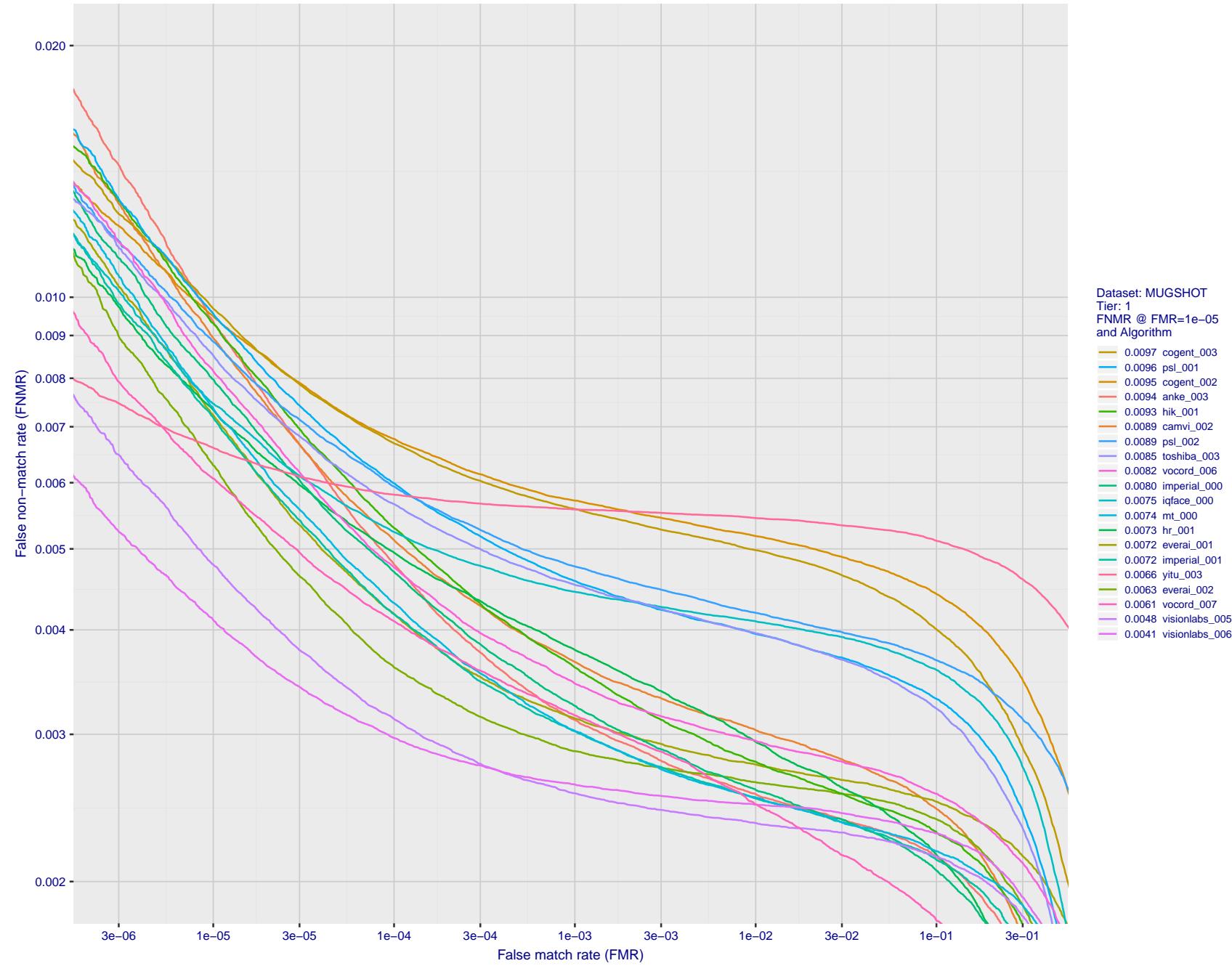


Figure 17: For the mugshot images, detection error tradeoff (DET) characteristics showing false non-match rate vs. false match rate plotted parametrically on threshold,  $T$ . The scales are logarithmic in order to show decades of FMR.

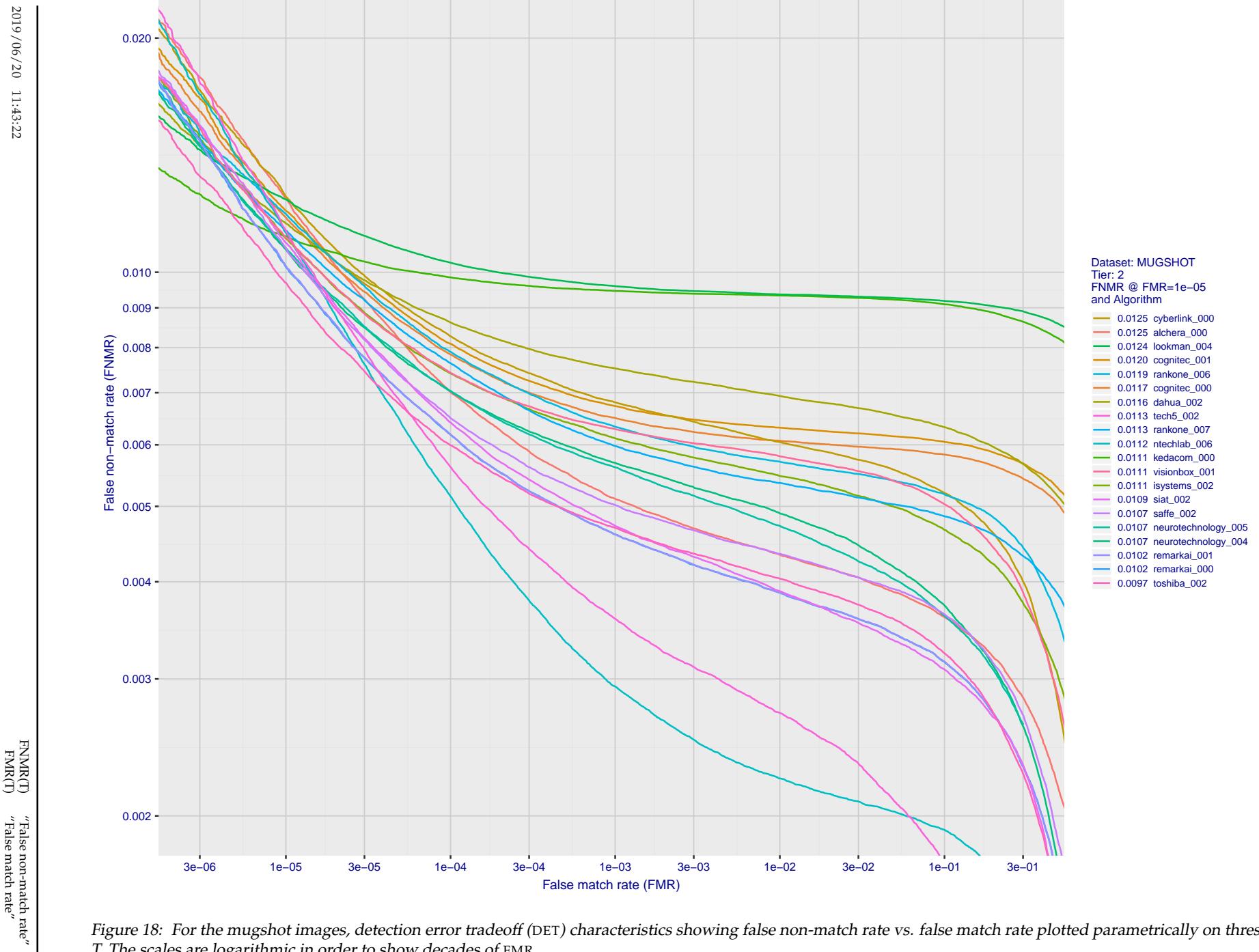


Figure 18: For the mugshot images, detection error tradeoff (DET) characteristics showing false non-match rate vs. false match rate plotted parametrically on threshold, T. The scales are logarithmic in order to show decades of FMR.

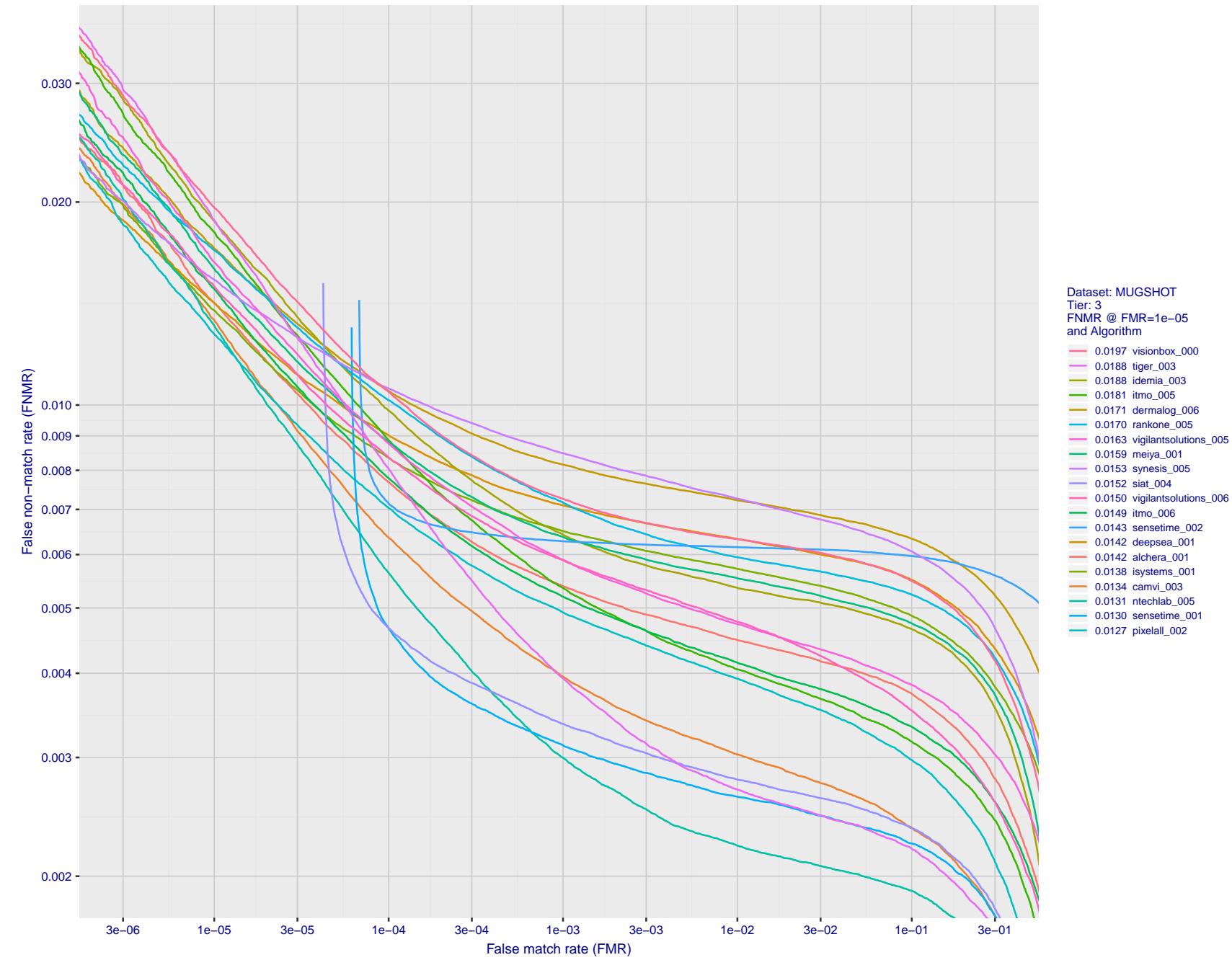


Figure 19: For the mugshot images, detection error tradeoff (DET) characteristics showing false non-match rate vs. false match rate plotted parametrically on threshold,  $T$ . The scales are logarithmic in order to show decades of FMR.

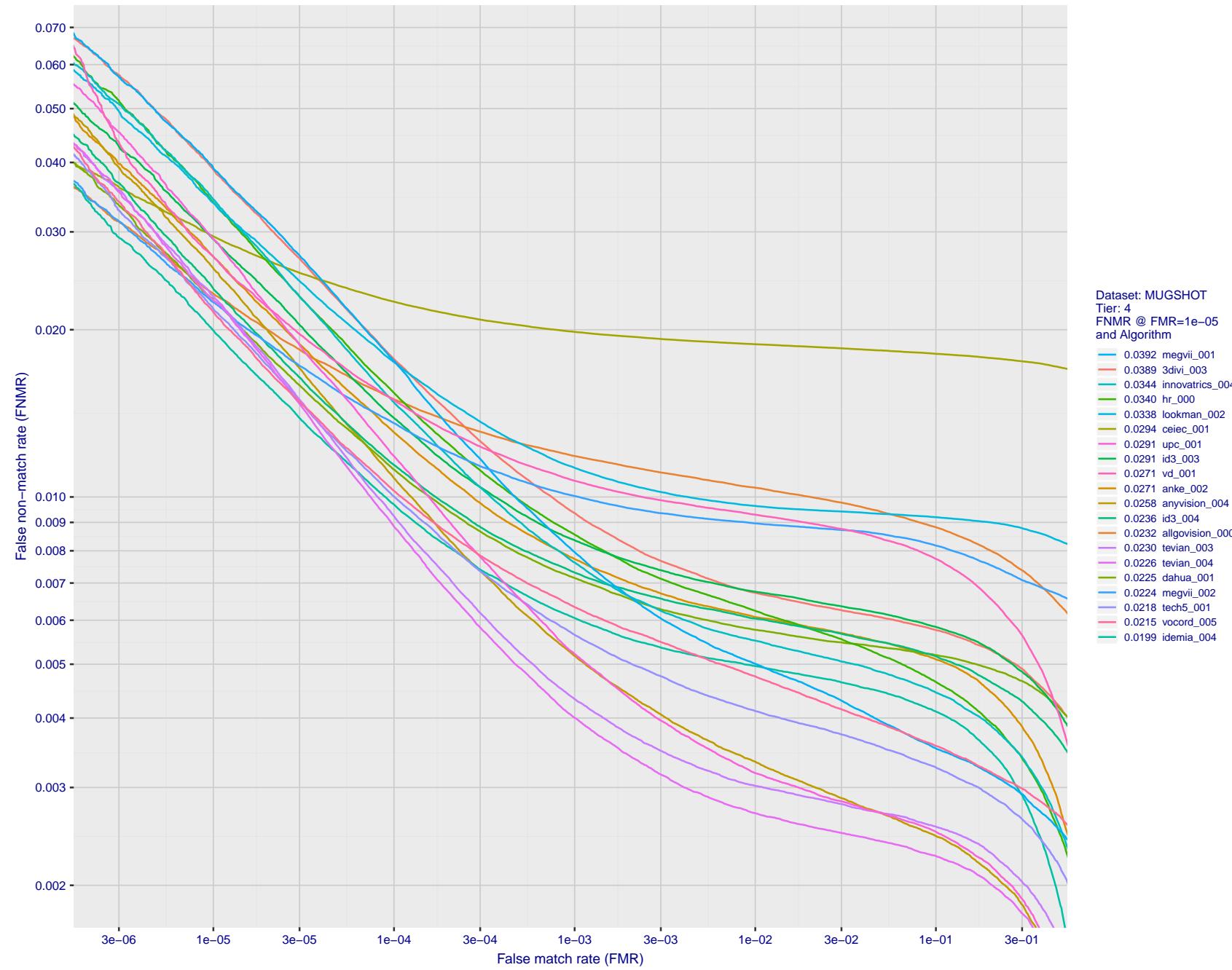


Figure 20: For the mugshot images, detection error tradeoff (DET) characteristics showing false non-match rate vs. false match rate plotted parametrically on threshold, T. The scales are logarithmic in order to show decades of FMR.

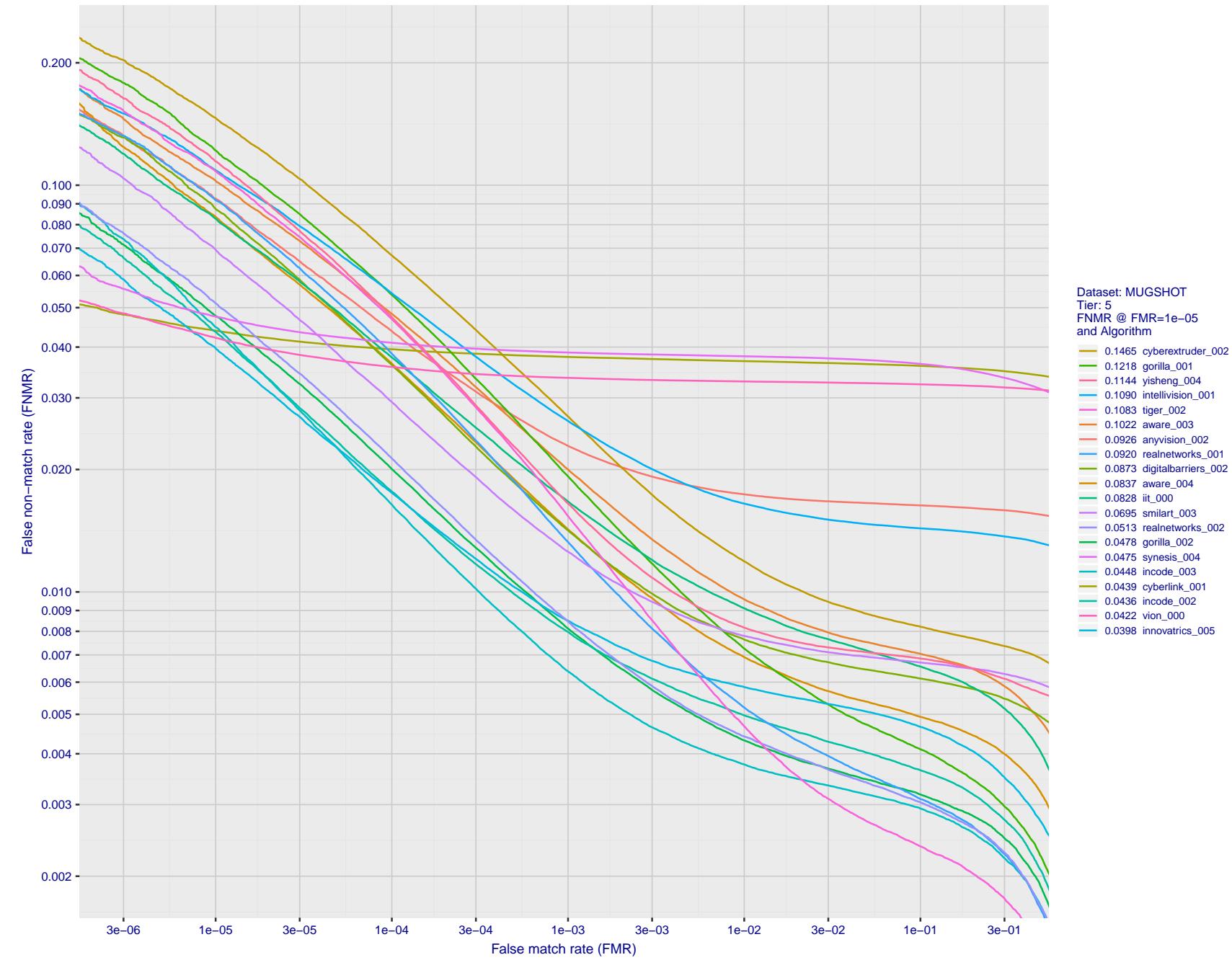


Figure 21: For the mugshot images, detection error tradeoff (DET) characteristics showing false non-match rate vs. false match rate plotted parametrically on threshold,  $T$ . The scales are logarithmic in order to show decades of FMR.

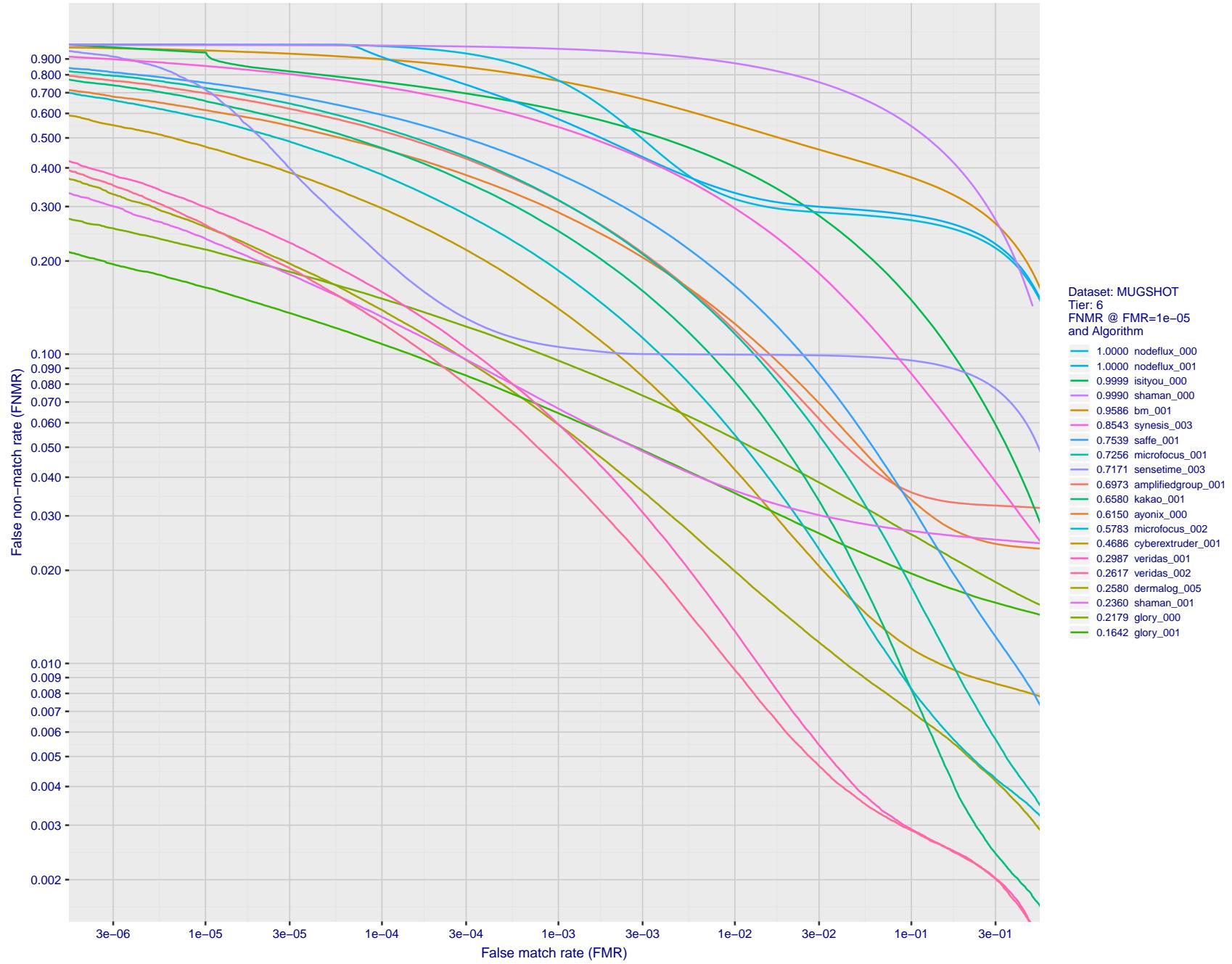


Figure 22: For the mugshot images, detection error tradeoff (DET) characteristics showing false non-match rate vs. false match rate plotted parametrically on threshold,  $T$ . The scales are logarithmic in order to show decades of FMR.

2019/06/20 11:43:22

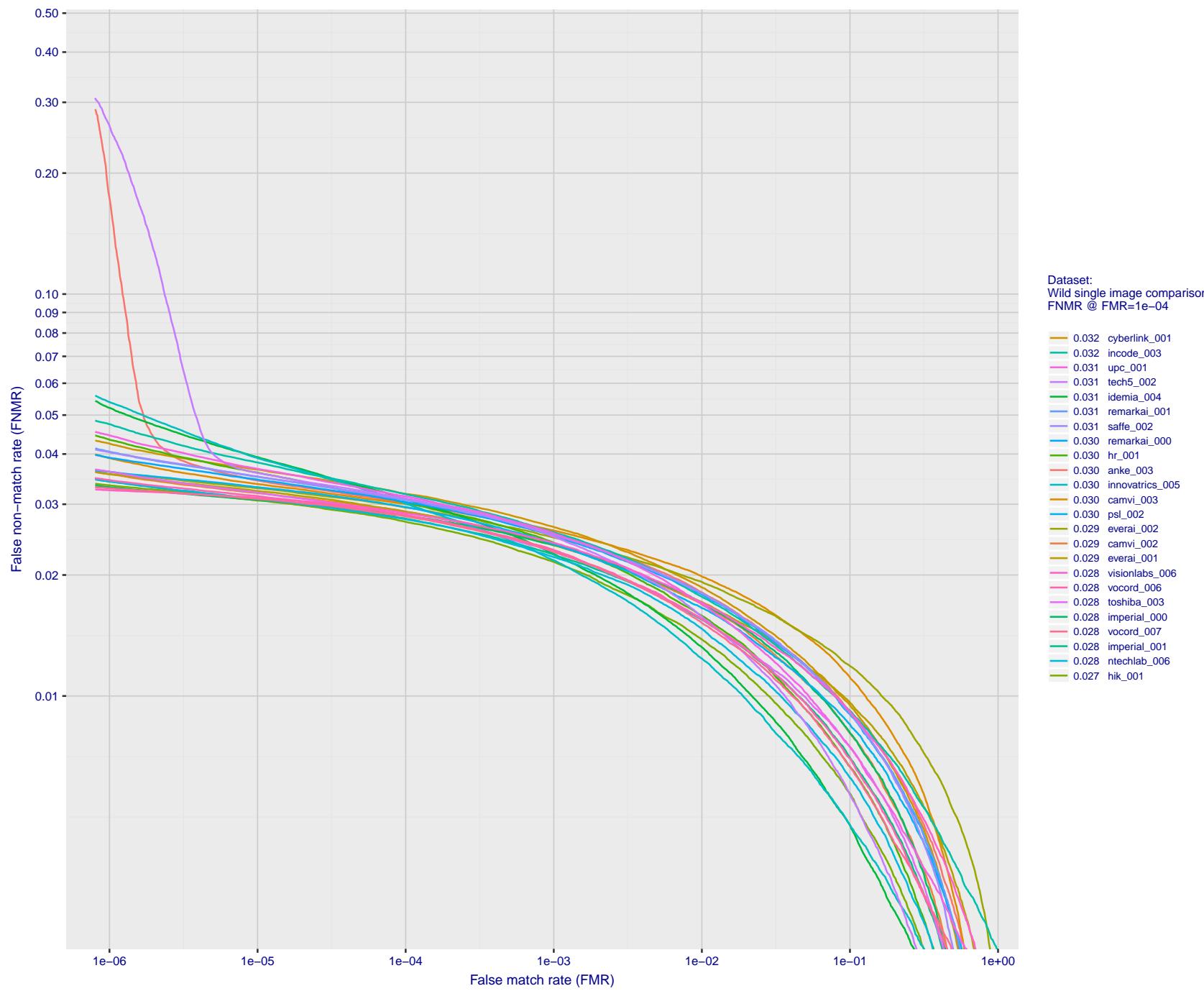


Figure 23: For the 2018 wild image comparisons, detection error tradeoff (DET) characteristics showing false non-match rate vs. false match rate plotted parametrically on threshold, T. The scales are logarithmic in order to show several decades of FMR.

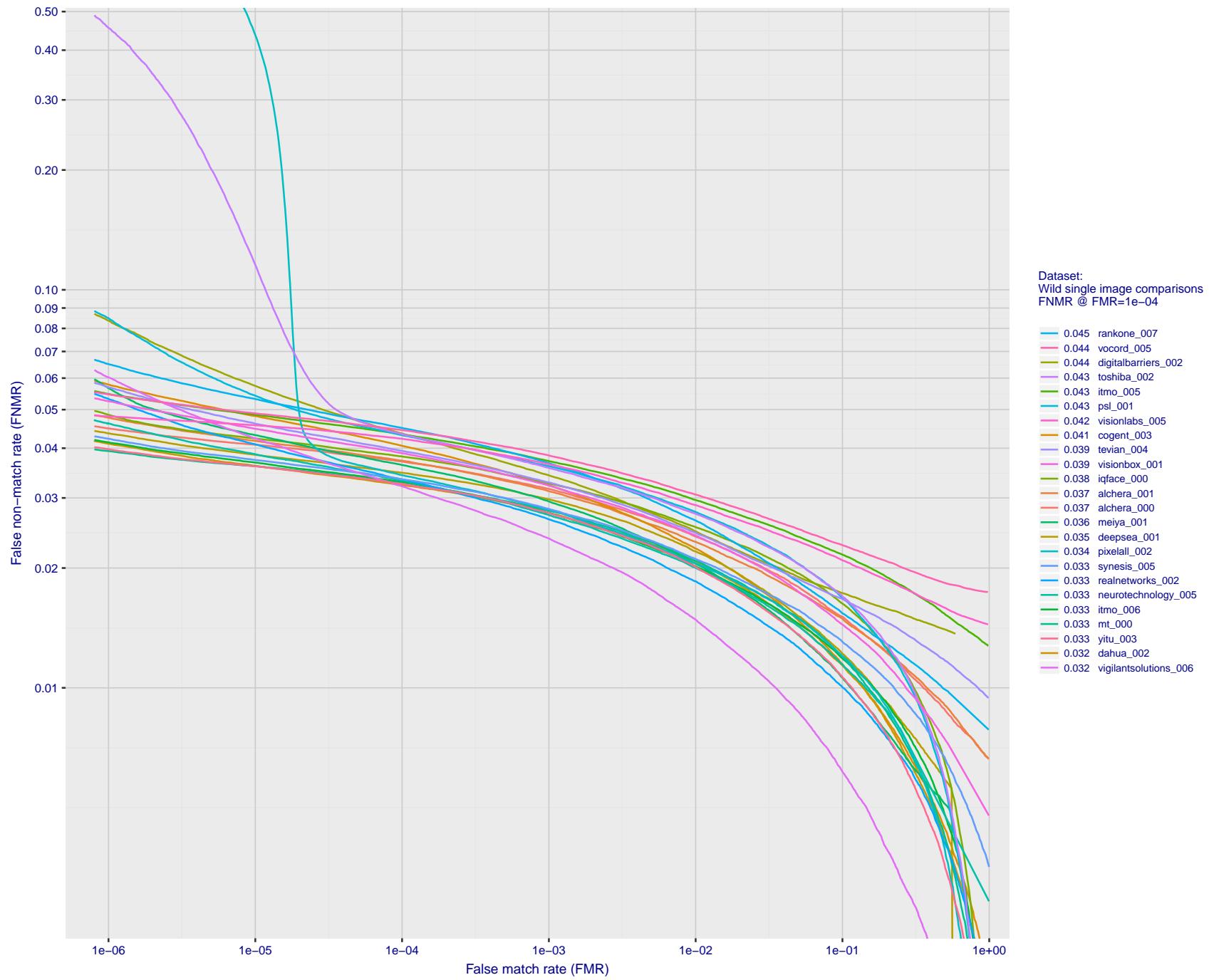


Figure 24: For the 2018 wild image comparisons, detection error tradeoff (DET) characteristics showing false non-match rate vs. false match rate plotted parametrically on threshold,  $T$ . The scales are logarithmic in order to show several decades of FMR.

2019/06/20 11:43:22

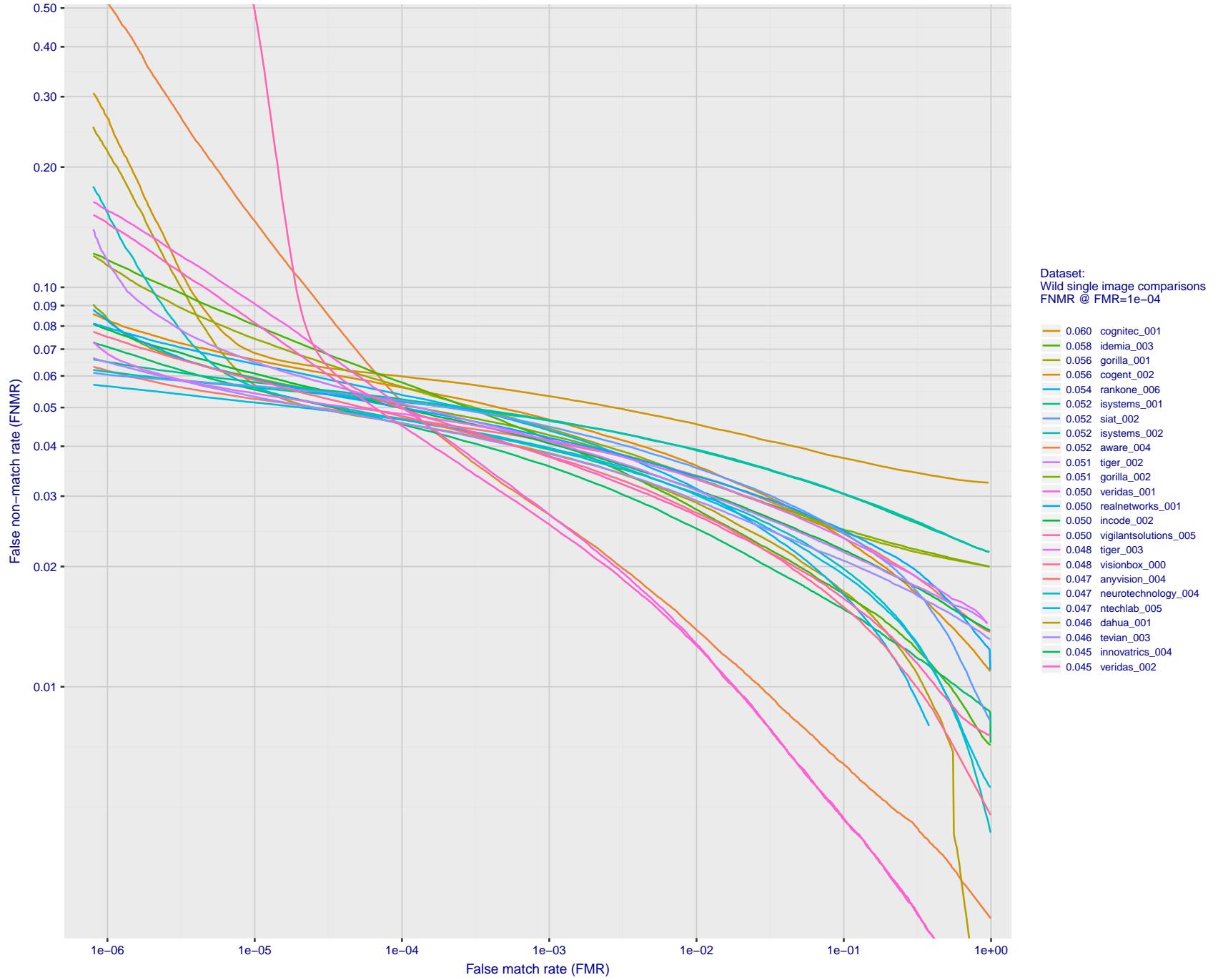


Figure 25: For the 2018 wild image comparisons, detection error tradeoff (DET) characteristics showing false non-match rate vs. false match rate plotted parametrically on threshold,  $T$ . The scales are logarithmic in order to show several decades of FMR.

2019/06/20 11:43:22

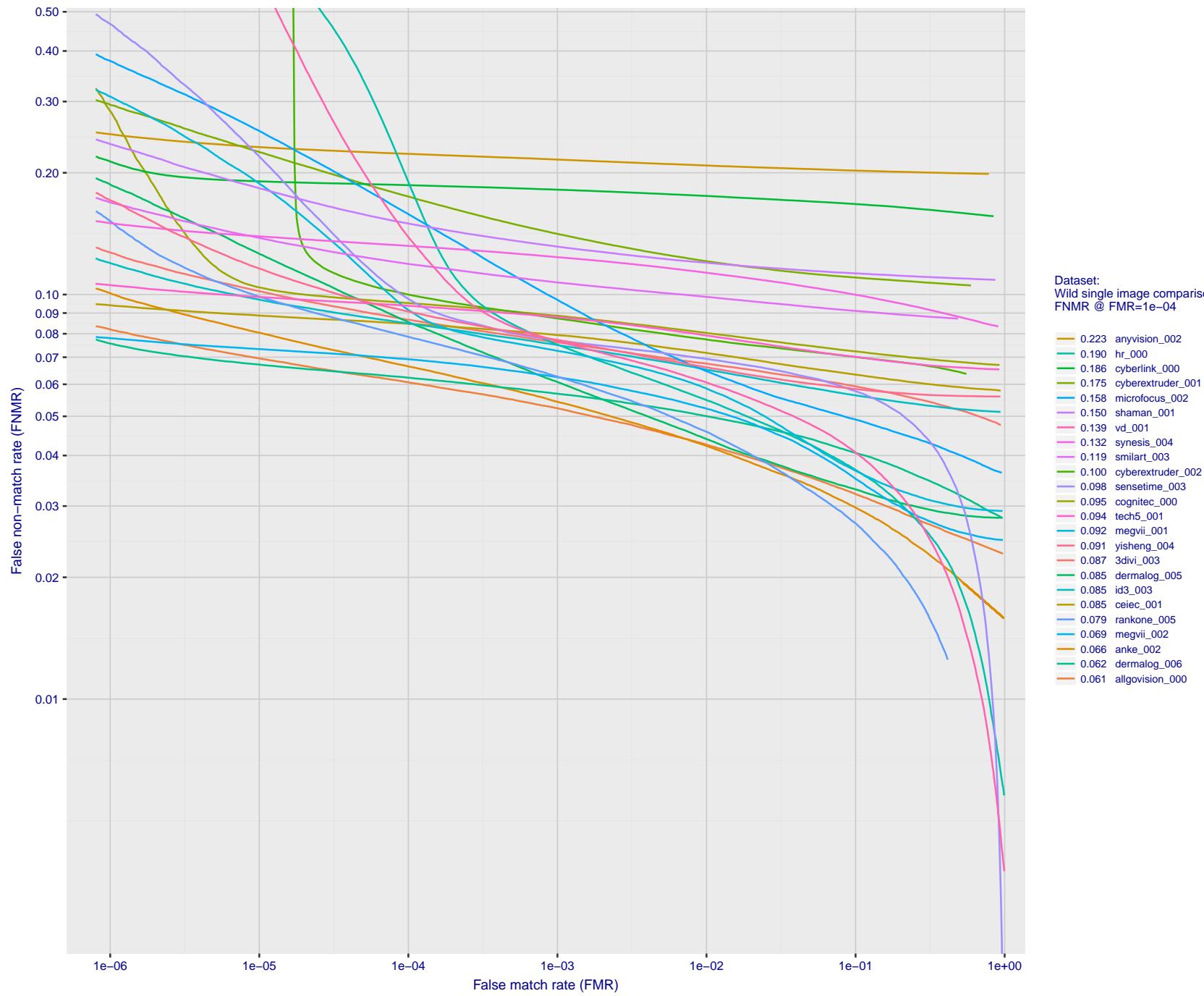


Figure 26: For the 2018 wild image comparisons, detection error tradeoff (DET) characteristics showing false non-match rate vs. false match rate plotted parametrically on threshold,  $T$ . The scales are logarithmic in order to show several decades of FMR.

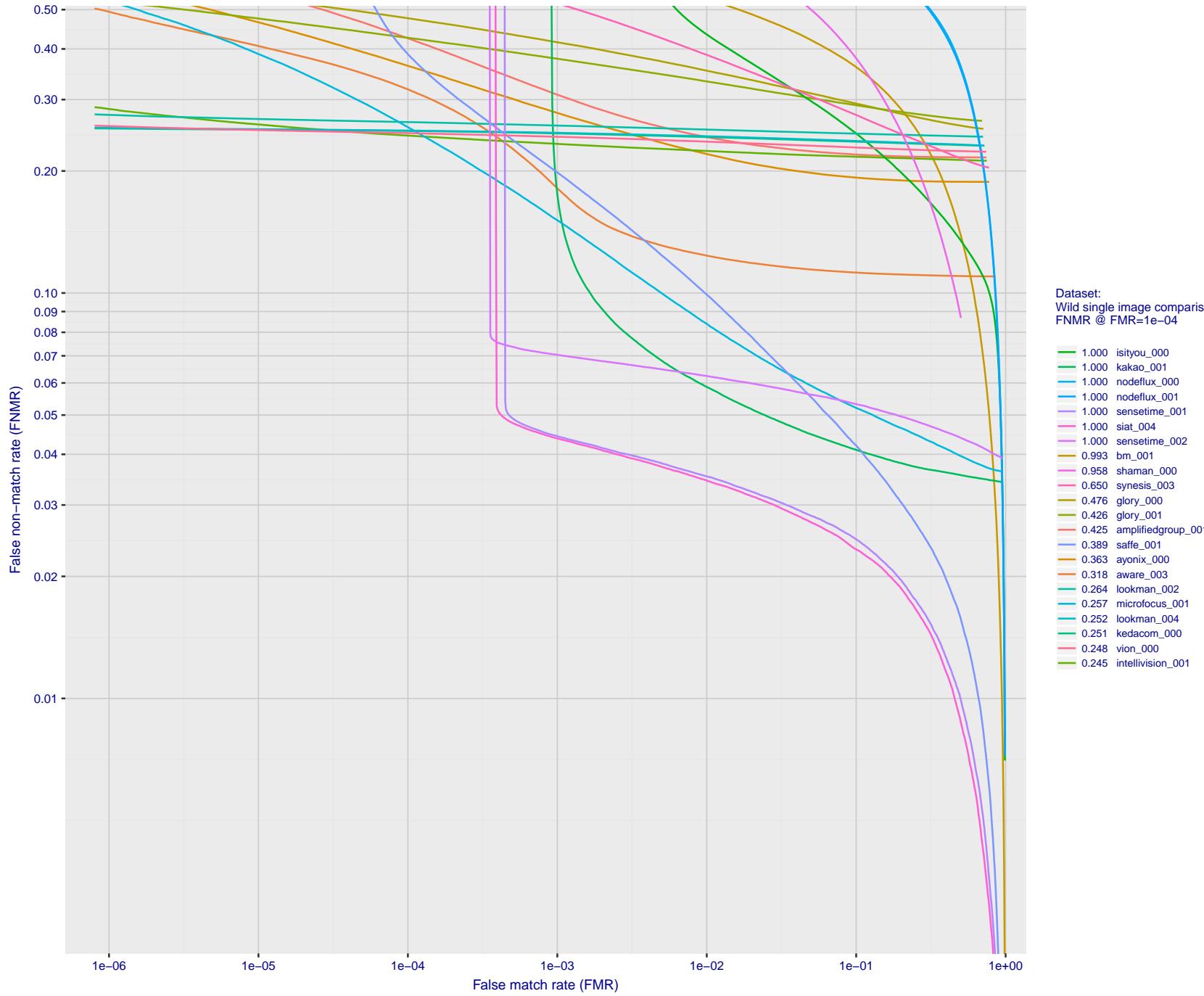


Figure 27: For the 2018 wild image comparisons, detection error tradeoff (DET) characteristics showing false non-match rate vs. false match rate plotted parametrically on threshold,  $T$ . The scales are logarithmic in order to show several decades of FMR.

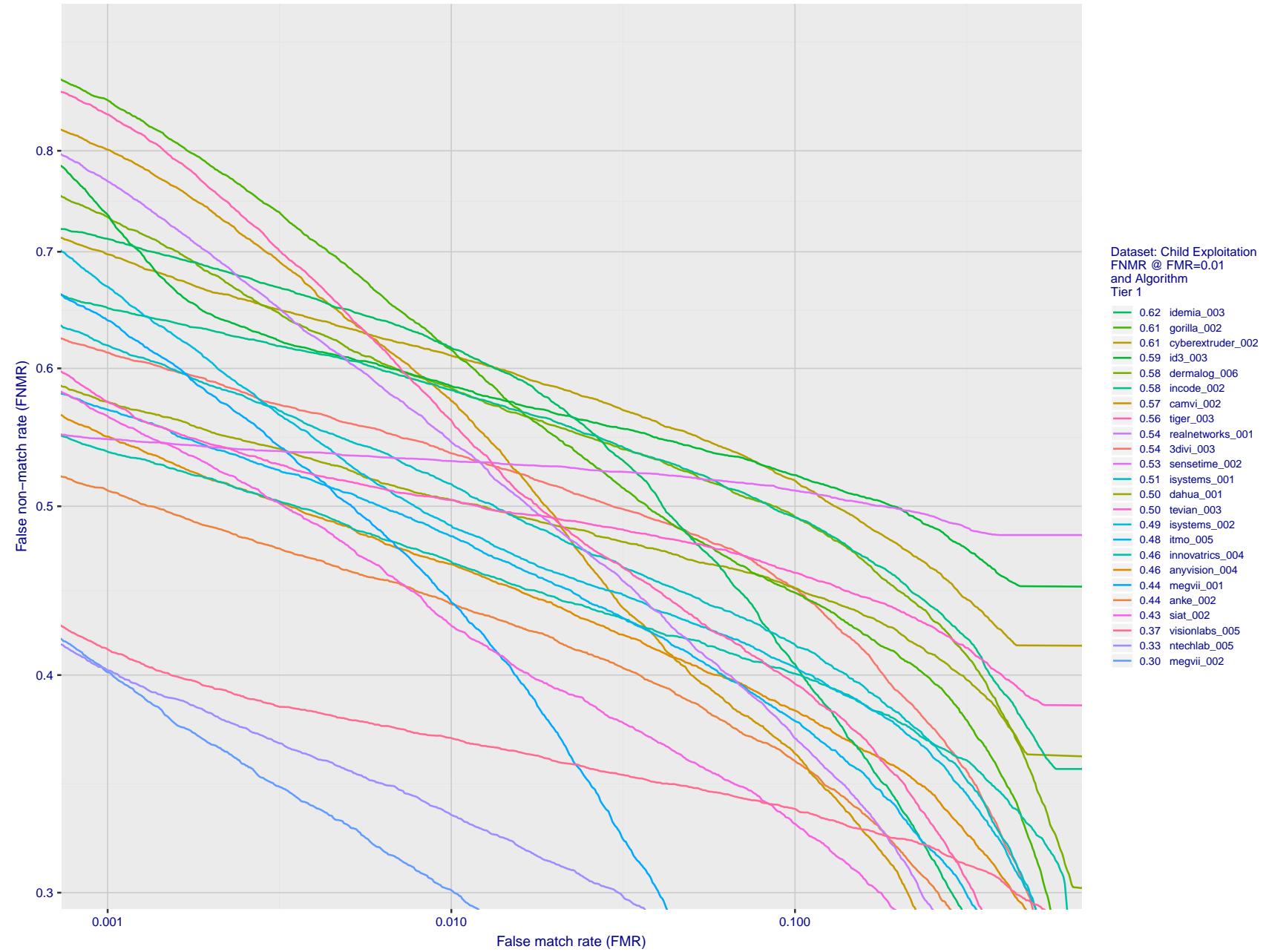


Figure 28: For child exploitation images, detection error tradeoff (DET) characteristics showing false non-match rate vs. false match rate plotted parametrically on threshold, T. The scales are logarithmic in order to show many decades of FMR. Accuracy is poor because many images have adverse quality characteristics, and because detection and enrollment fails.

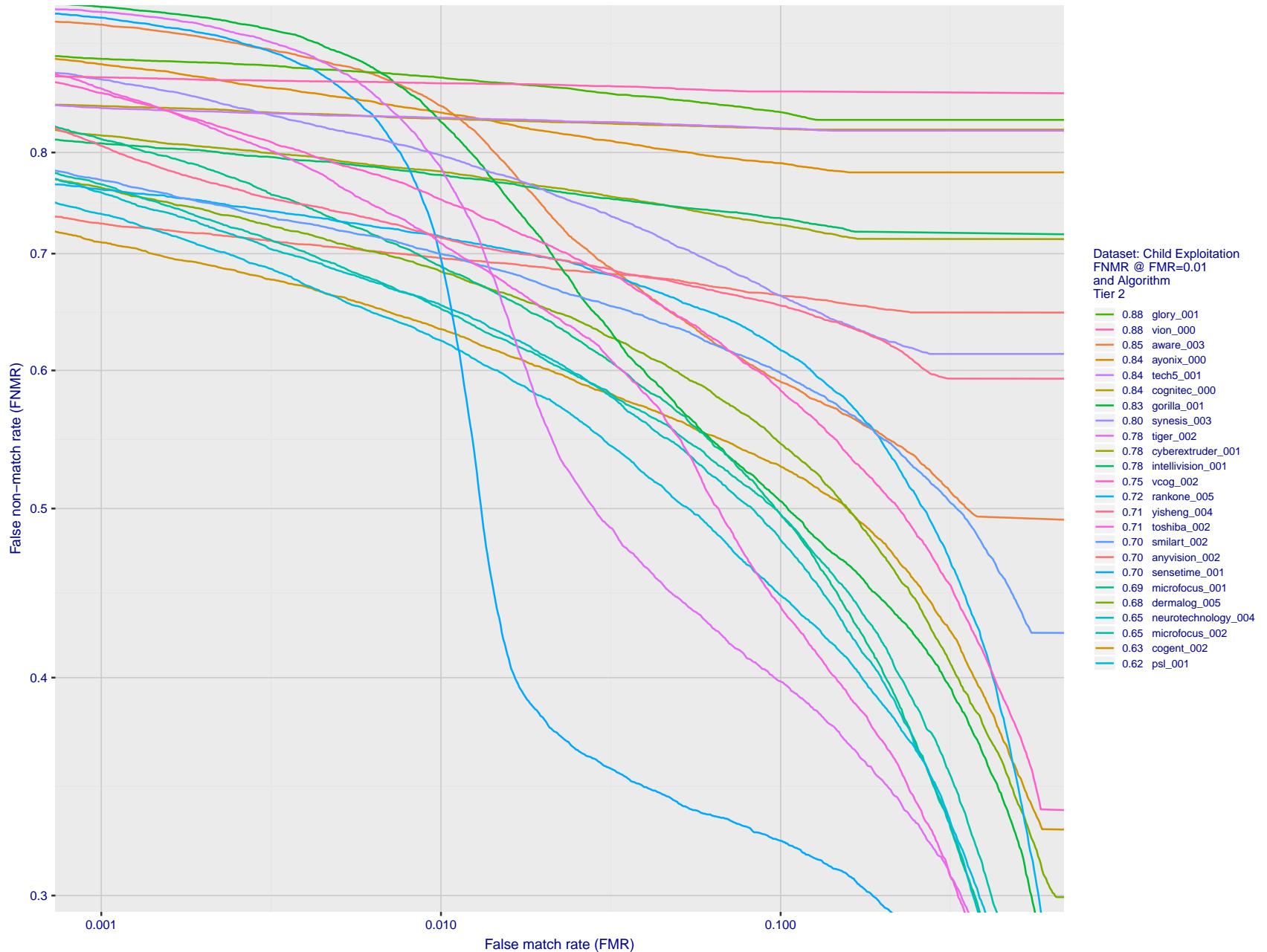


Figure 29: For child exploitation images, detection error tradeoff (DET) characteristics showing false non-match rate vs. false match rate plotted parametrically on threshold,  $T$ . The scales are logarithmic in order to show many decades of FMR. Accuracy is poor because many images have adverse quality characteristics, and because detection and enrollment fails.

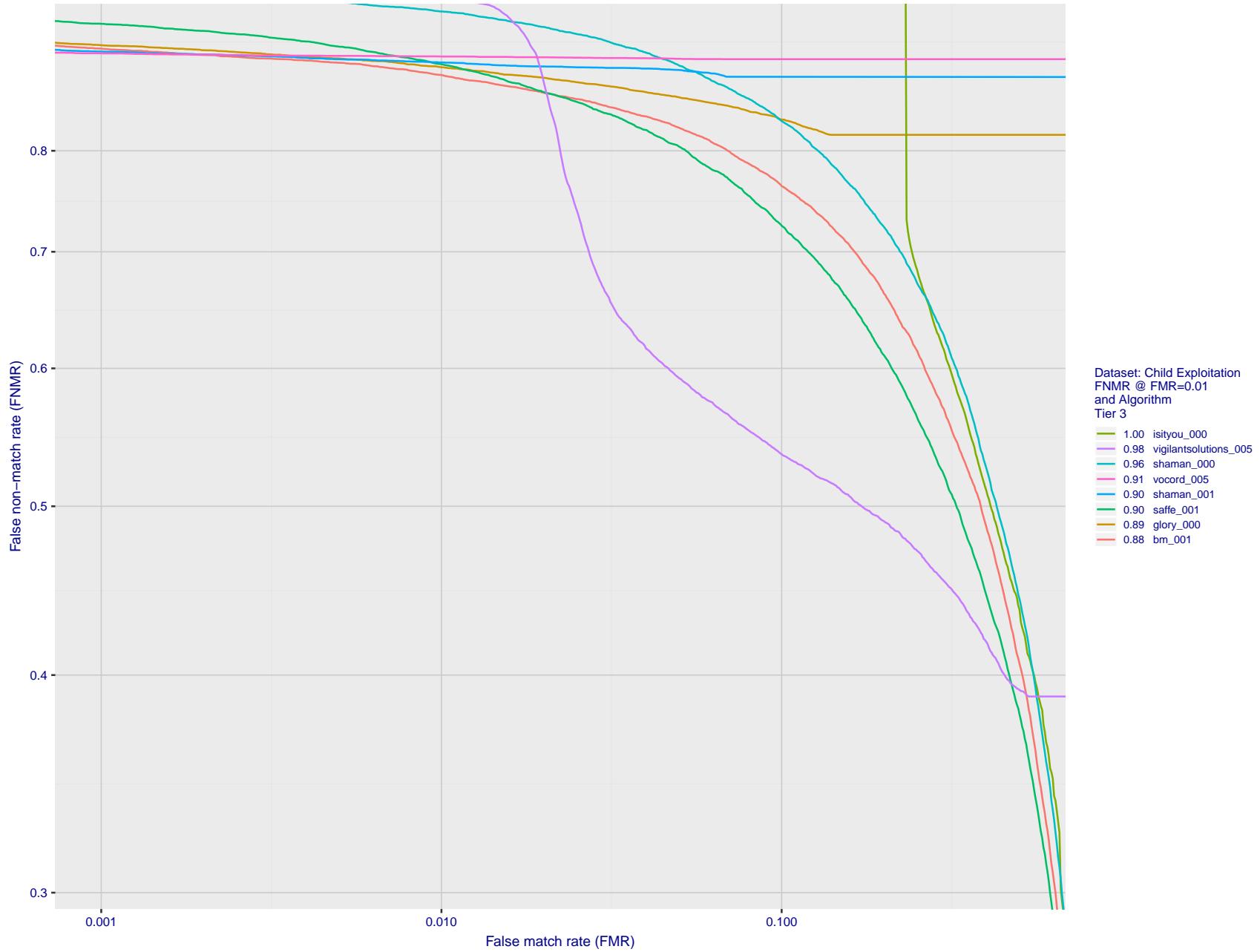


Figure 30: For child exploitation images, detection error tradeoff (DET) characteristics showing false non-match rate vs. false match rate plotted parametrically on threshold,  $T$ . The scales are logarithmic in order to show many decades of FMR. Accuracy is poor because many images have adverse quality characteristics, and because detection and enrollment fails.

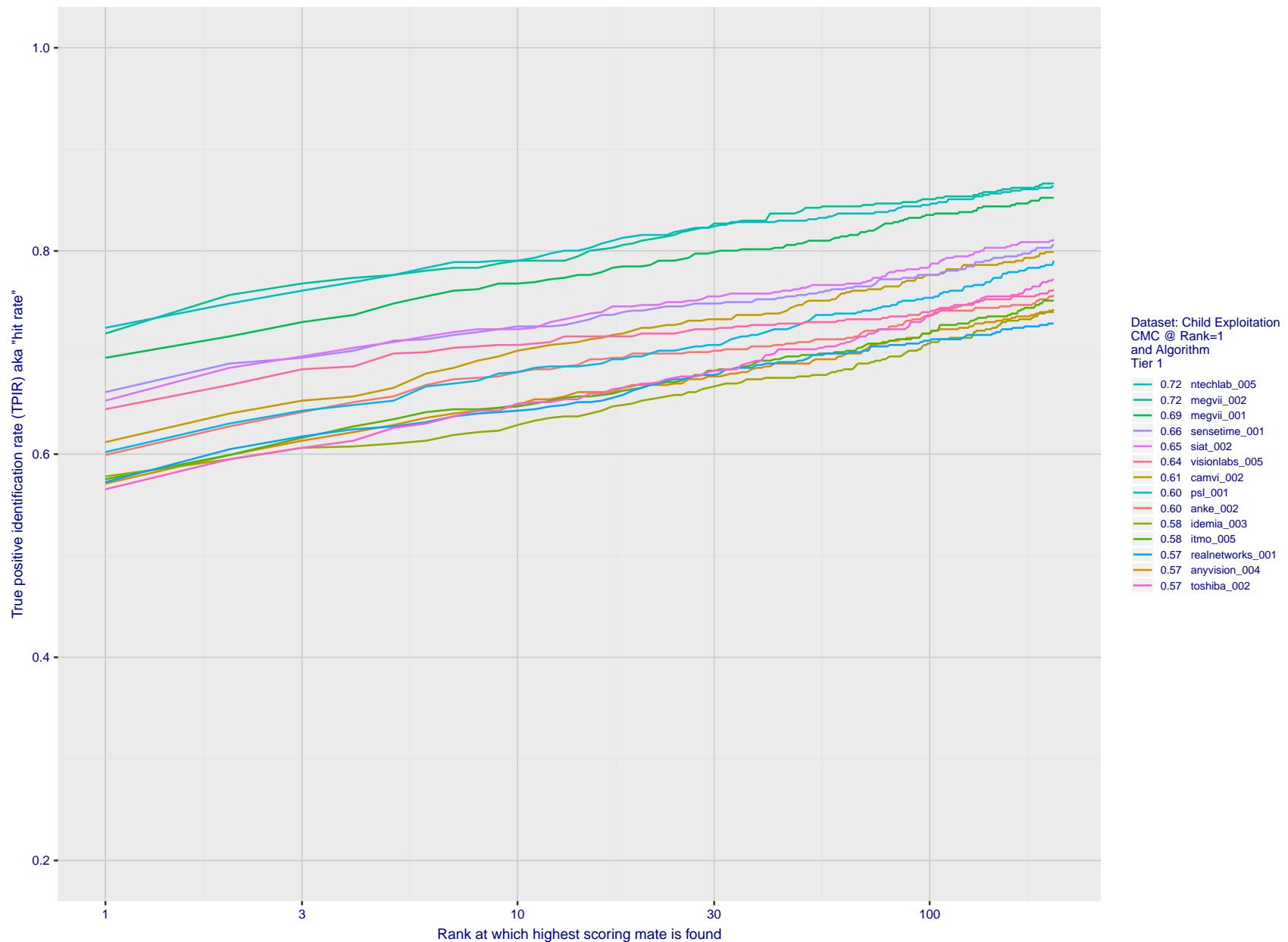


Figure 31: For child exploitation images, cumulative match characteristics (CMC) showing true positive identification rate vs. rank. This is simulation of a one-to-many search experiment - see discussion in section 3.2. The scales are logarithmic in order to show the effect of long candidate lists. Accuracy is poor but much improved relative to the 1:1 DETs of Fig. 30 because a search can succeed if any of a subject's several enrolled images matches the search image with a high score.

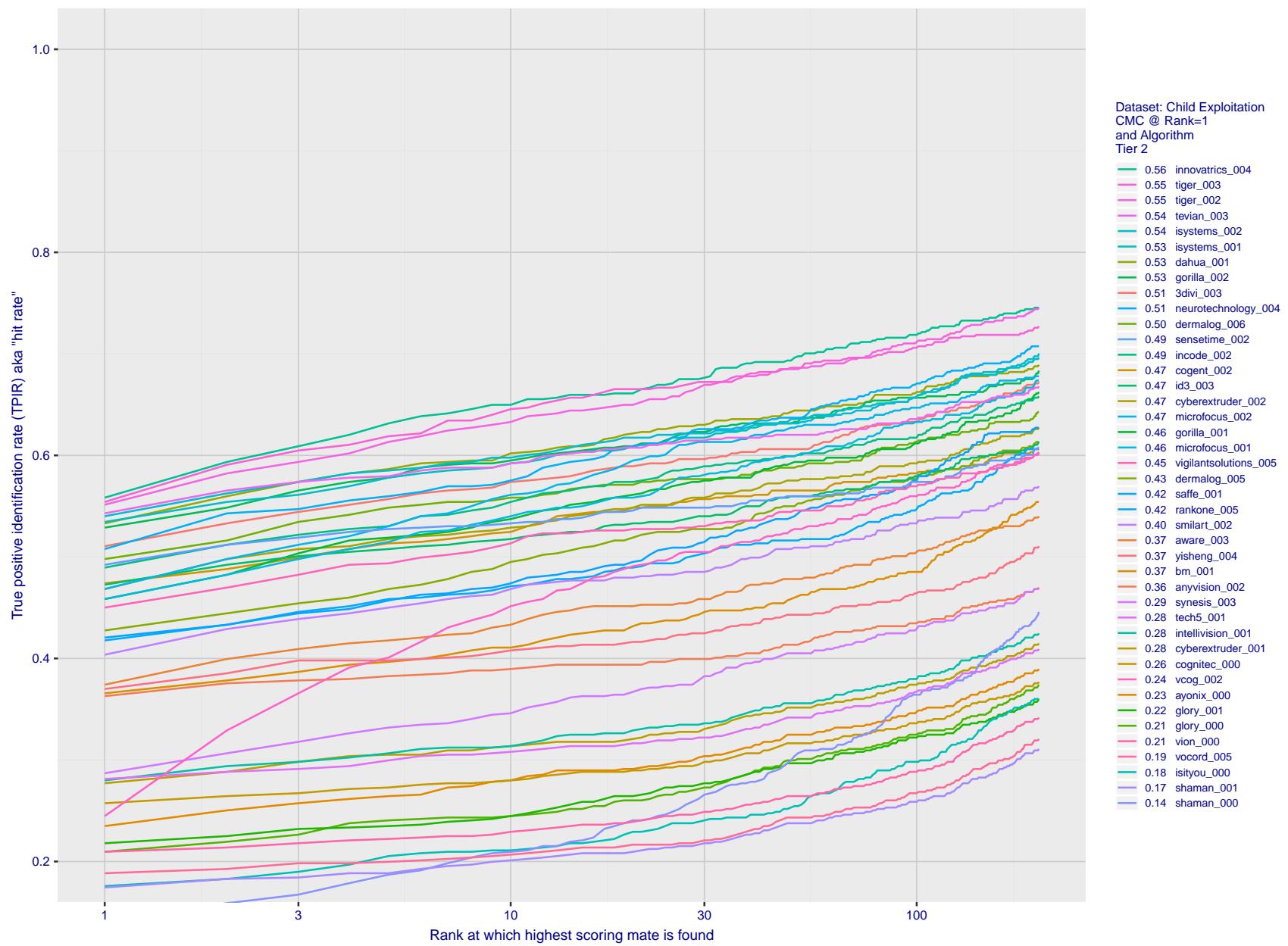


Figure 32: For child exploitation images, cumulative match characteristics (CMC) showing true positive identification rate vs. rank. This is simulation of a one-to-many search experiment - see discussion in section 3.2. The scales are logarithmic in order to show the effect of long candidate lists. Accuracy is poor but much improved relative to the 1:1 DETs of Fig. 30 because a search can succeed if any of a subject's several enrolled images matches the search image with a high score.

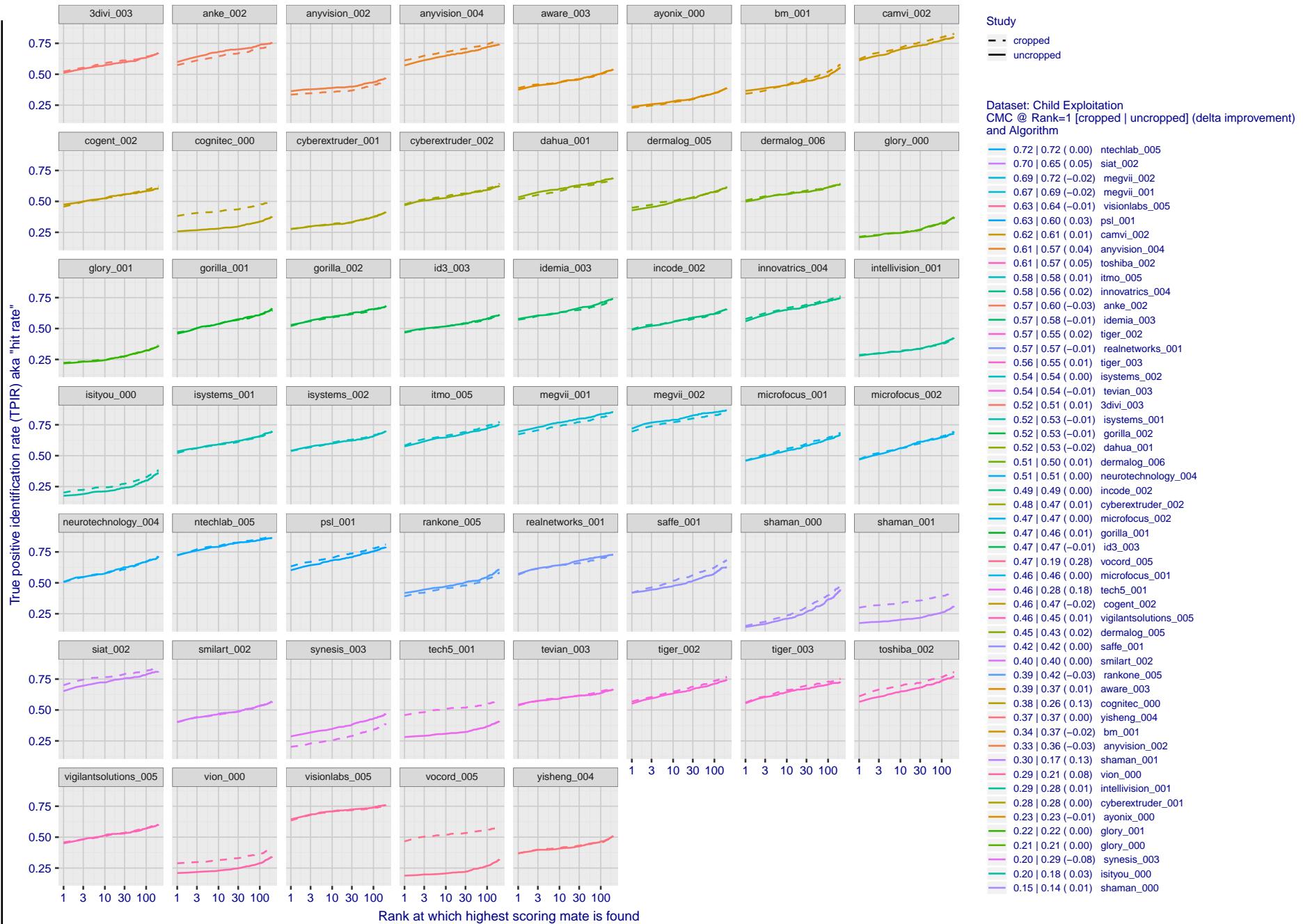


Figure 33: For child exploitation images, cumulative match characteristics (CMC) showing true positive identification rate vs. rank for two cases: 1. Whole image provided to the algorithm; 2. Human annotated rectangular region, cropped and provided to the algorithm. The difference between the traces is associated with detection of difficult faces, and fine localization.

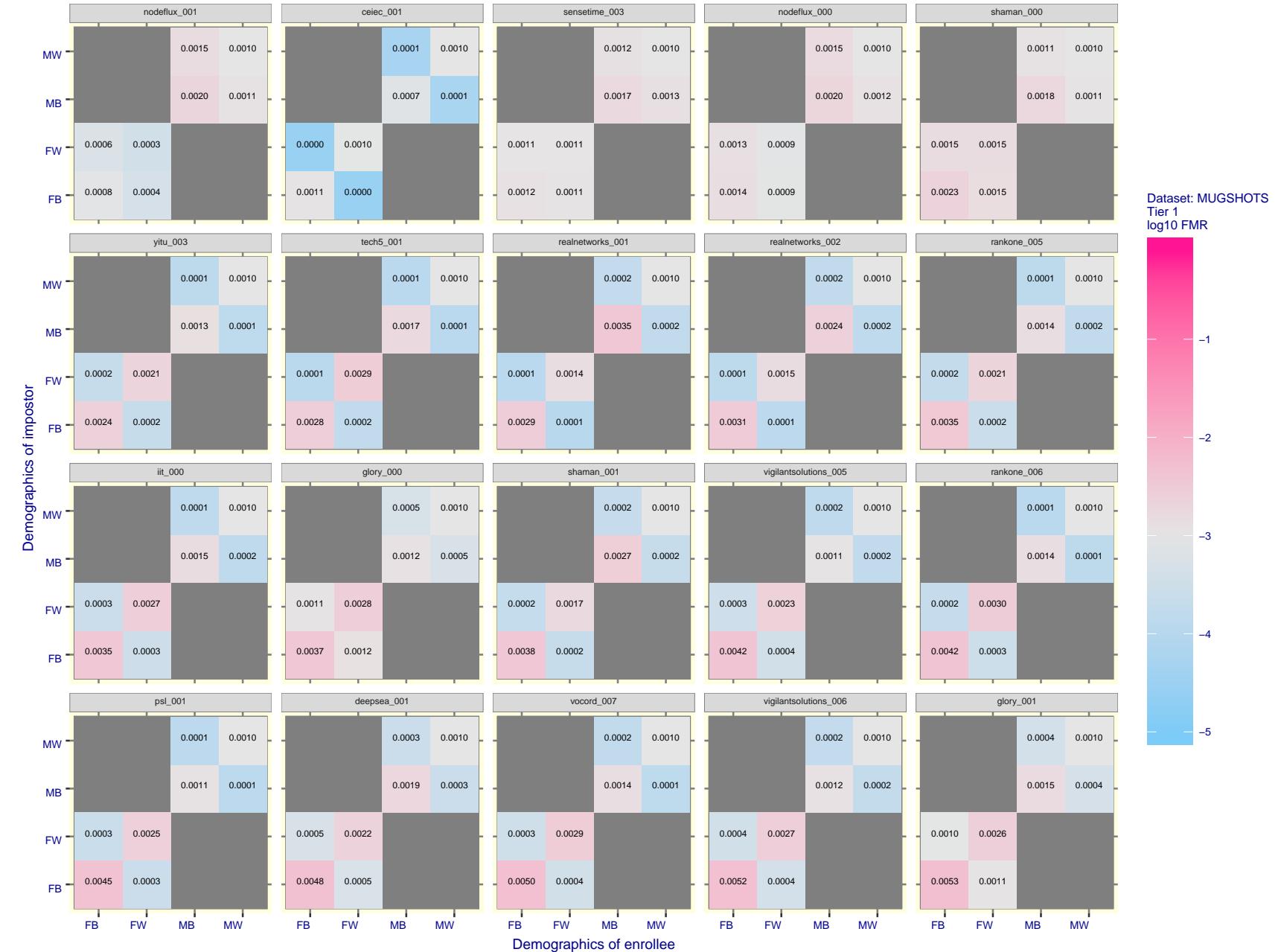


Figure 34: For the mugshot images, FMR for same-sex impostor pairs of images annotated with codes for black female, black male, white female, white male. The threshold is set for each algorithm to give  $FMR = 0.001$  for white males which is the demographic that usually gives the lowest FMR. This means the top right box is the same color in all panels. The panels are sorted over multiple pages in order of FMR on black females, which is the demographic that usually gives the highest FMR.

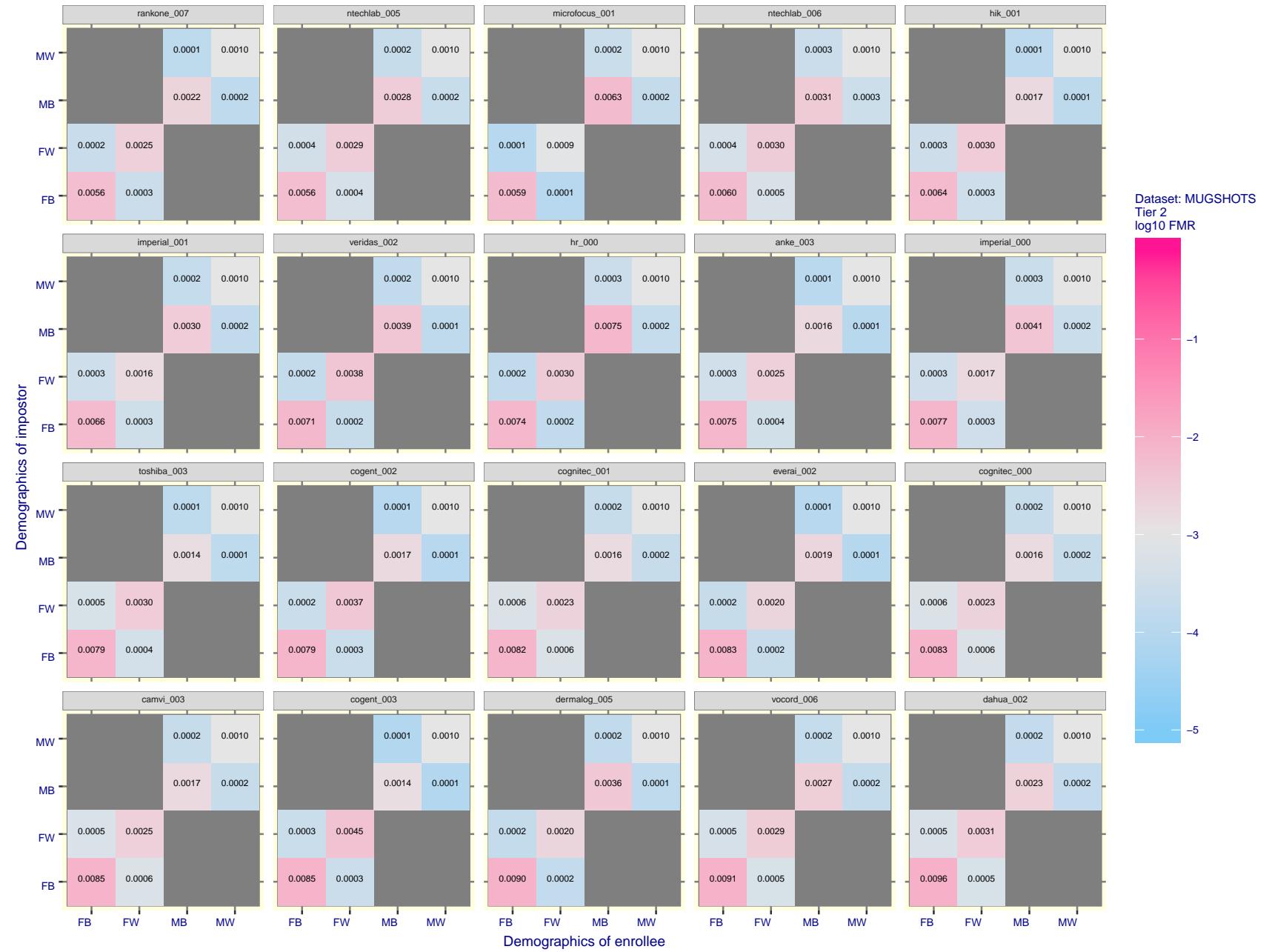


Figure 35: For the mugshot images, FMR for same-sex impostor pairs of images annotated with codes for black female, black male, white female, white male. The threshold is set for each algorithm to give  $FMR = 0.001$  for white males which is the demographic that usually gives the lowest FMR. This means the top right box is the same color in all panels. The panels are sorted over multiple pages in order of FMR on black females, which is the demographic that usually gives the highest FMR.

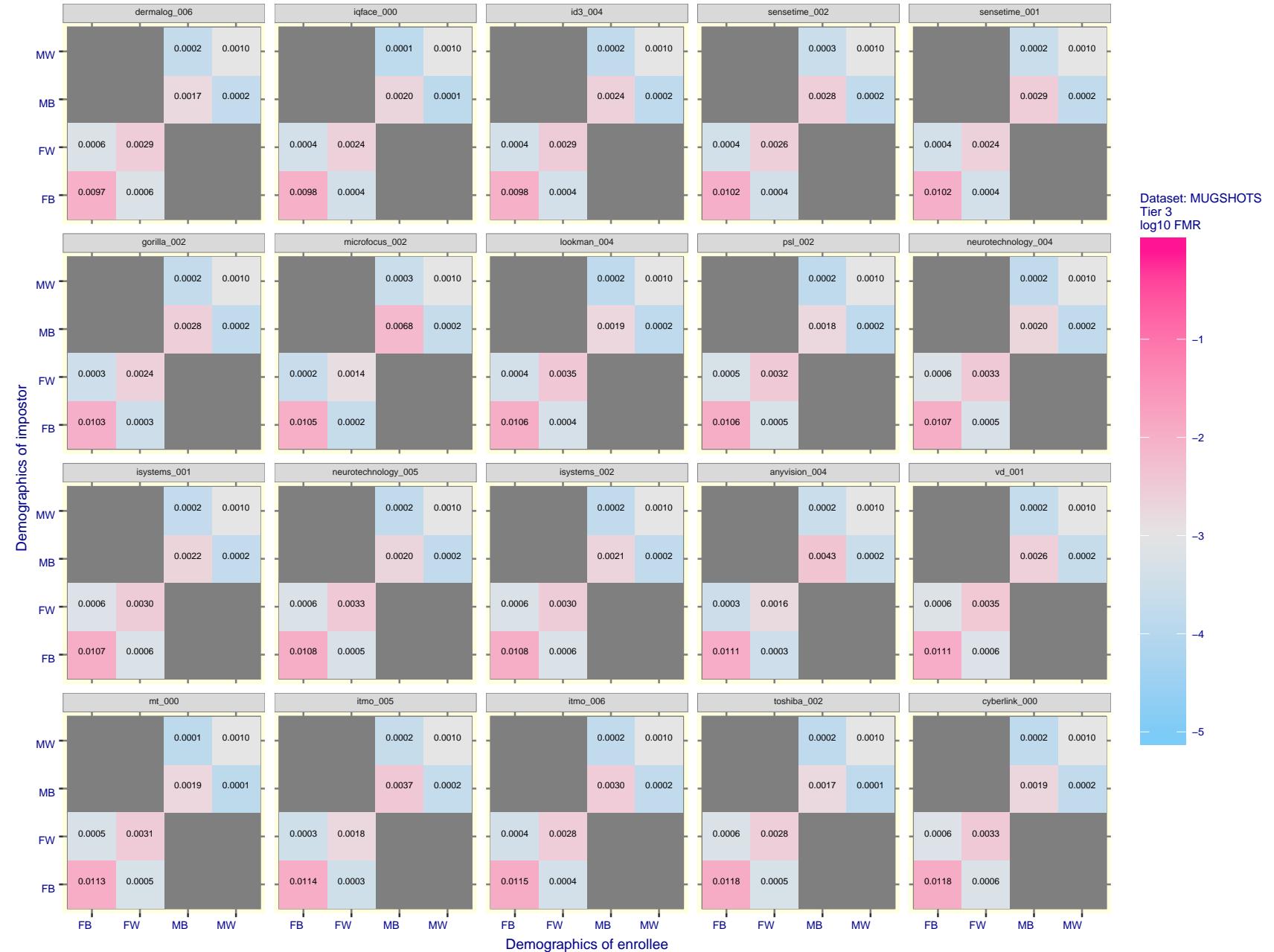


Figure 36: For the mugshot images, FMR for same-sex impostor pairs of images annotated with codes for black female, black male, white female, white male. The threshold is set for each algorithm to give  $FMR = 0.001$  for white males which is the demographic that usually gives the lowest FMR. This means the top right box is the same color in all panels. The panels are sorted over multiple pages in order of FMR on black females, which is the demographic that usually gives the highest FMR.

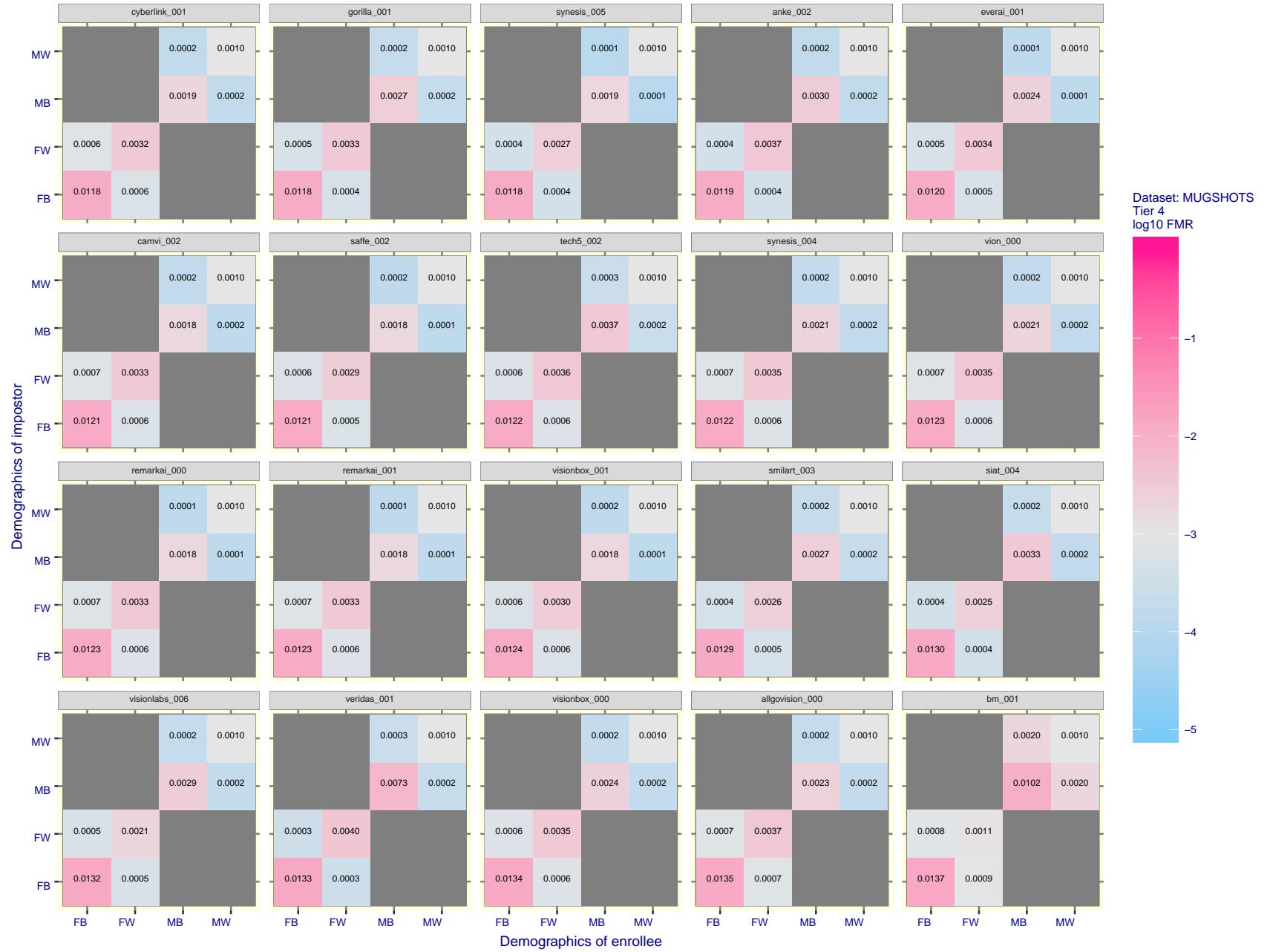


Figure 37: For the mugshot images, FMR for same-sex impostor pairs of images annotated with codes for black female, black male, white female, white male. The threshold is set for each algorithm to give  $FMR = 0.001$  for white males which is the demographic that usually gives the lowest FMR. This means the top right box is the same color in all panels. The panels are sorted over multiple pages in order of FMR on black females, which is the demographic that usually gives the highest FMR.

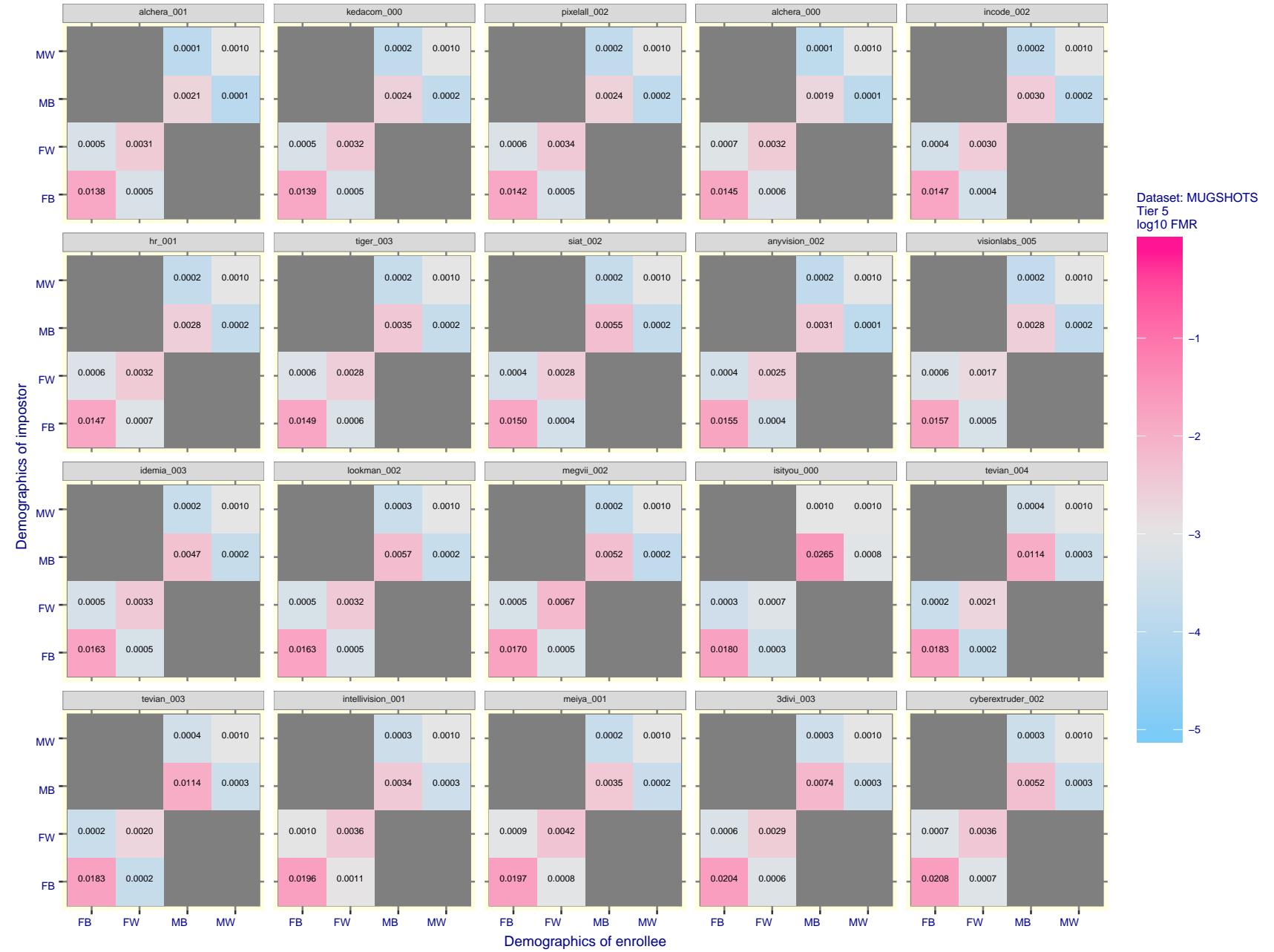


Figure 38: For the mugshot images, FMR for same-sex impostor pairs of images annotated with codes for black female, black male, white female, white male. The threshold is set for each algorithm to give  $FMR = 0.001$  for white males which is the demographic that usually gives the lowest FMR. This means the top right box is the same color in all panels. The panels are sorted over multiple pages in order of FMR on black females, which is the demographic that usually gives the highest FMR.

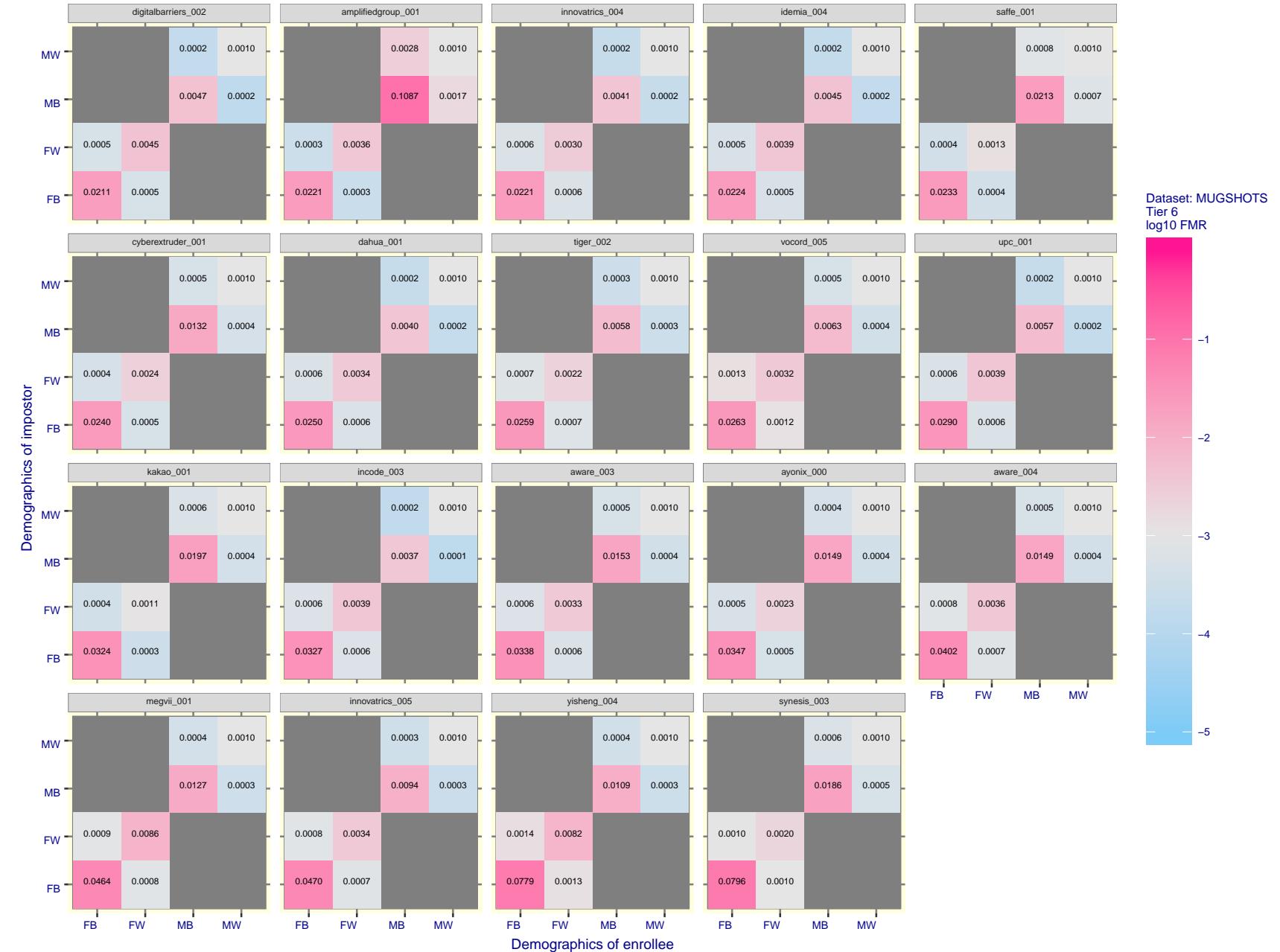


Figure 39: For the mugshot images, FMR for same-sex impostor pairs of images annotated with codes for black female, black male, white female, white male. The threshold is set for each algorithm to give  $FMR = 0.001$  for white males which is the demographic that usually gives the lowest FMR. This means the top right box is the same color in all panels. The panels are sorted over multiple pages in order of FMR on black females, which is the demographic that usually gives the highest FMR.

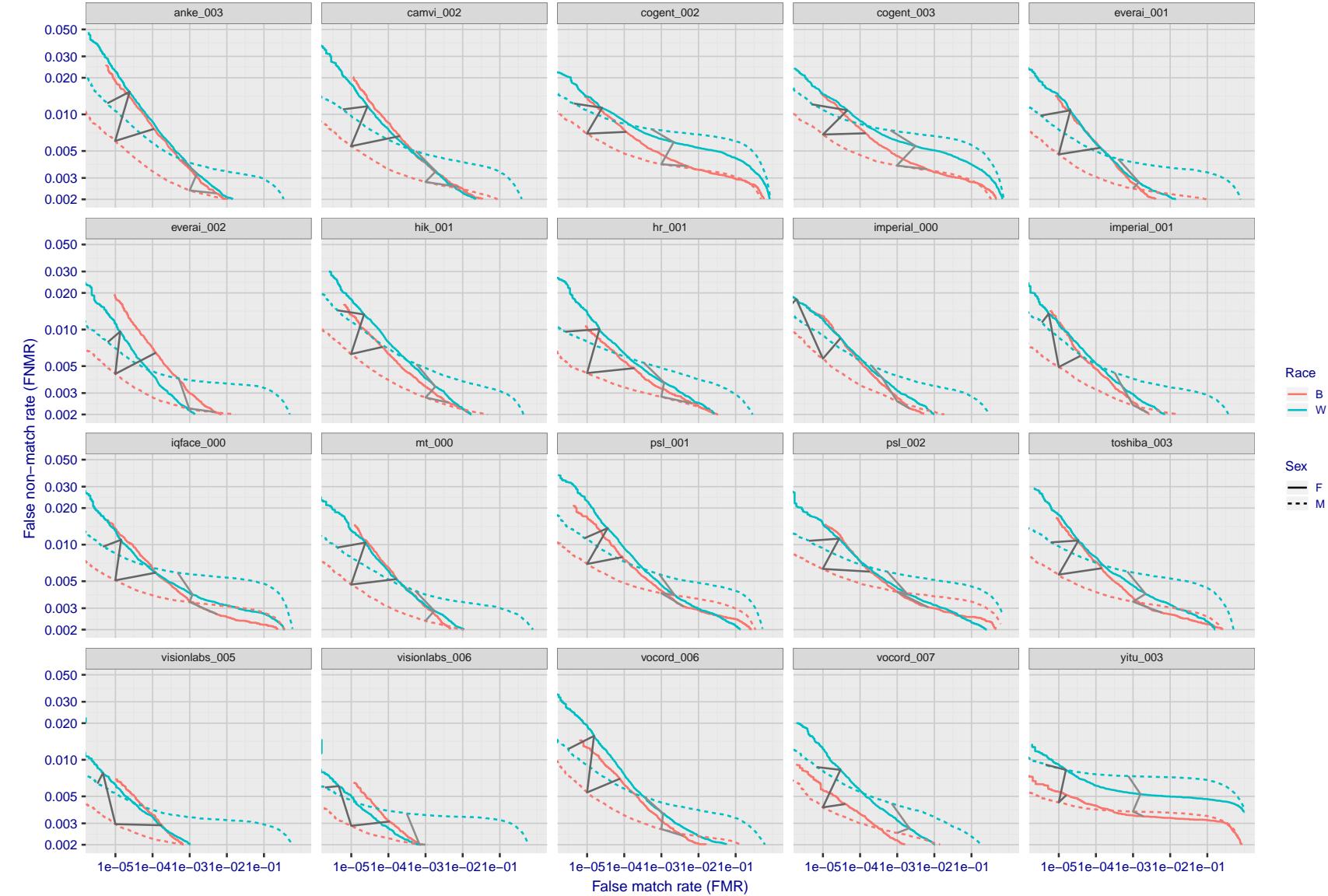


Figure 40: For the mugshot images, error tradeoff characteristics for white females, black females, black males and white males. The Z-shaped grey lines correspond to fixed thresholds, showing both FNMR and FMR vary at one T value. Note: Many of the plots will naively be read as saying women gives worse error rates than men because the solid traces lie above the dotted ones. However, this is misleading and incomplete: The grey lines show the traces reveal horizontal shifts. Thus for the cogent-003 algorithm FNMR for men is higher than for women at a fixed threshold but, at the same time, FMR is higher for women - see Figure 61. As access control systems almost always operate at a fixed threshold, the naive interpretation is incorrect.

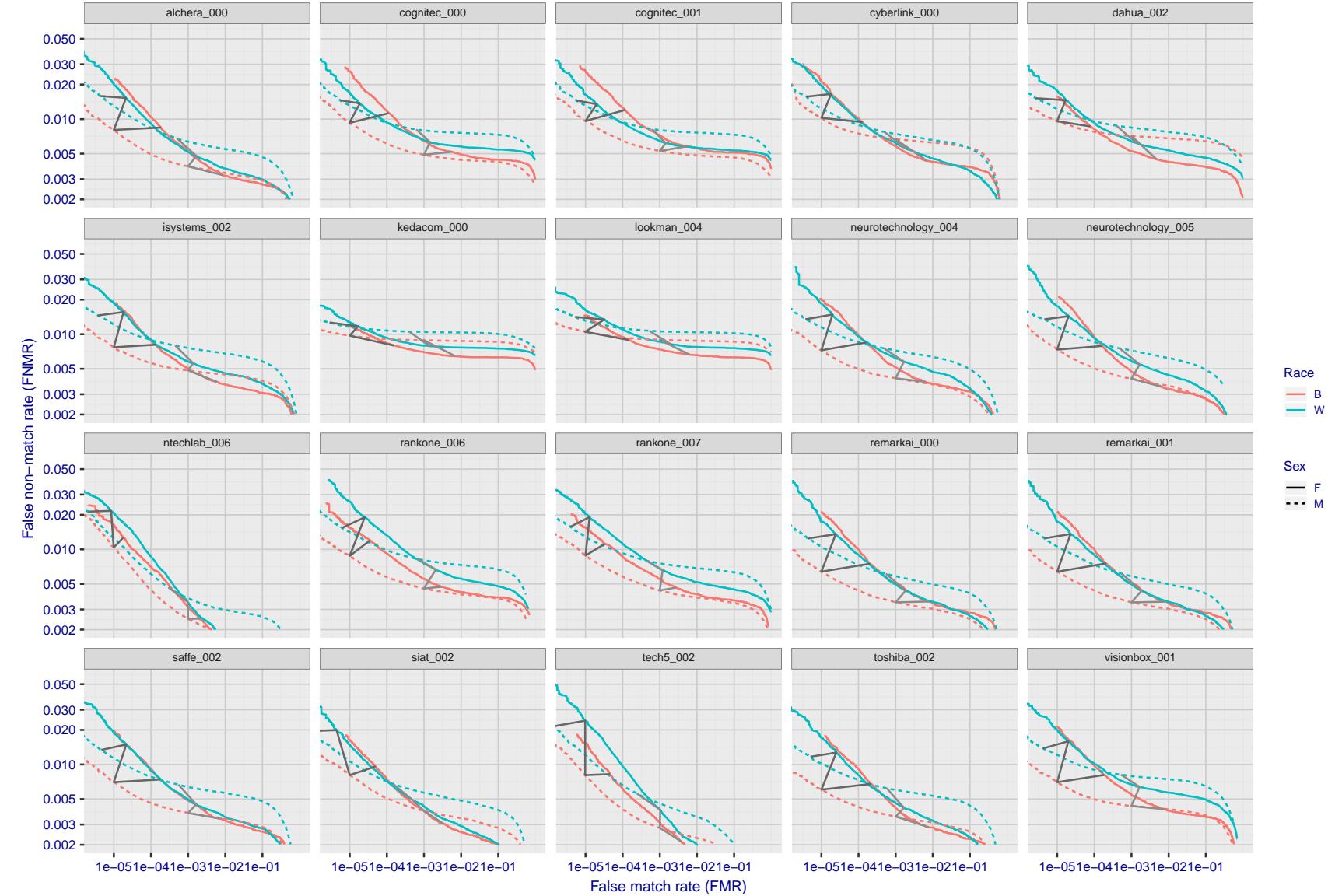


Figure 41: For the mugshot images, error tradeoff characteristics for white females, black females, black males and white males. The Z-shaped grey lines correspond to fixed thresholds, showing both FNMR and FMR vary at one T value. Note: Many of the plots will naively be read as saying women gives worse error rates than men because the solid traces lie above the dotted ones. However, this is misleading and incomplete: The grey lines show the traces reveal horizontal shifts. Thus for the cogent-003 algorithm FNMR for men is higher than for women at a fixed threshold but, at the same time, FMR is higher for women - see Figure 61. As access control systems almost always operate at a fixed threshold, the naive interpretation is incorrect.

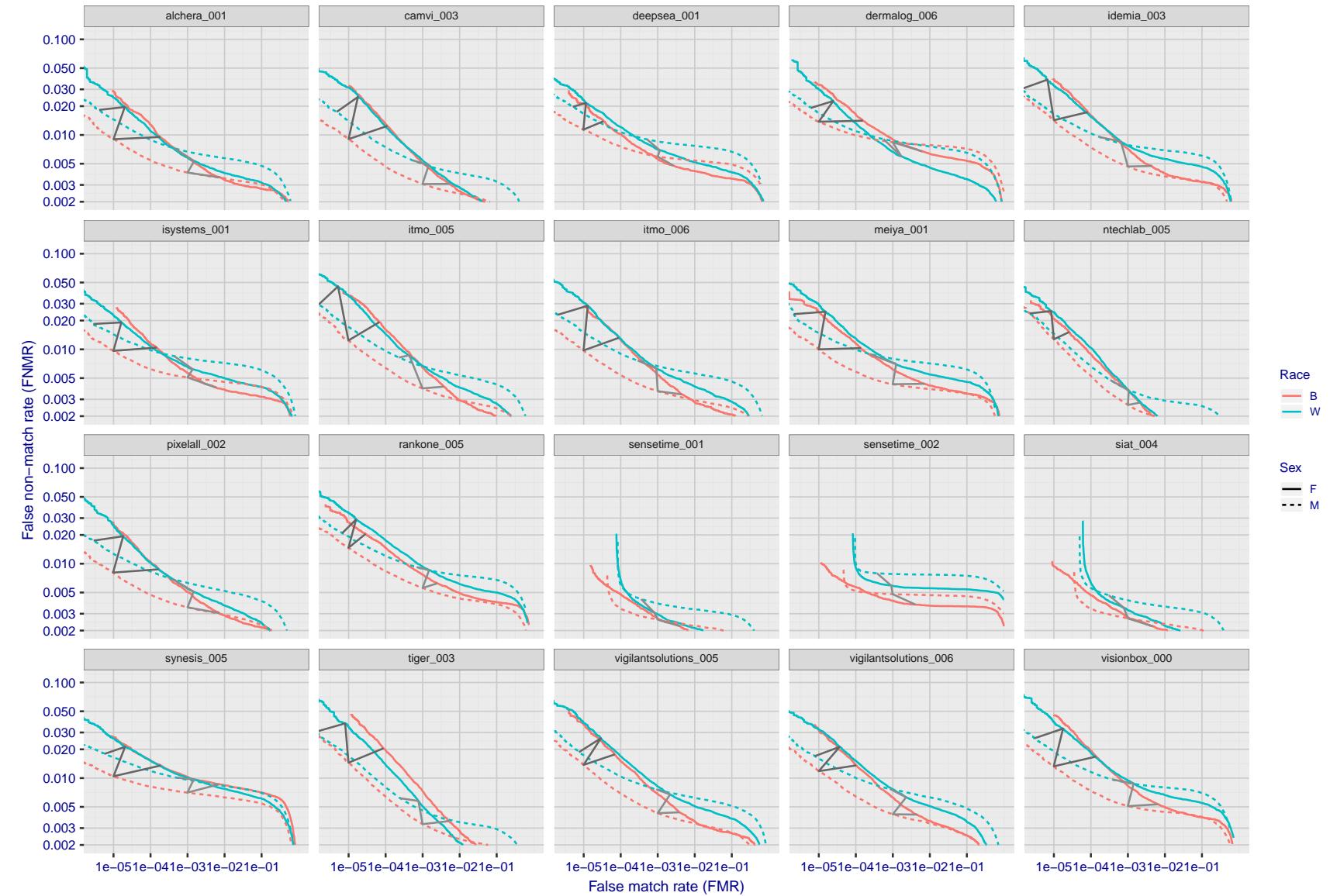


Figure 42: For the mugshot images, error tradeoff characteristics for white females, black females, black males and white males. The Z-shaped grey lines correspond to fixed thresholds, showing both FNMR and FMR vary at one T value. Note: Many of the plots will naively be read as saying women gives worse error rates than men because the solid traces lie above the dotted ones. However, this is misleading and incomplete: The grey lines show the traces reveal horizontal shifts. Thus for the cogent-003 algorithm FNMR for men is higher than for women at a fixed threshold but, at the same time, FMR is higher for women - see Figure 61. As access control systems almost always operate at a fixed threshold, the naive interpretation is incorrect.

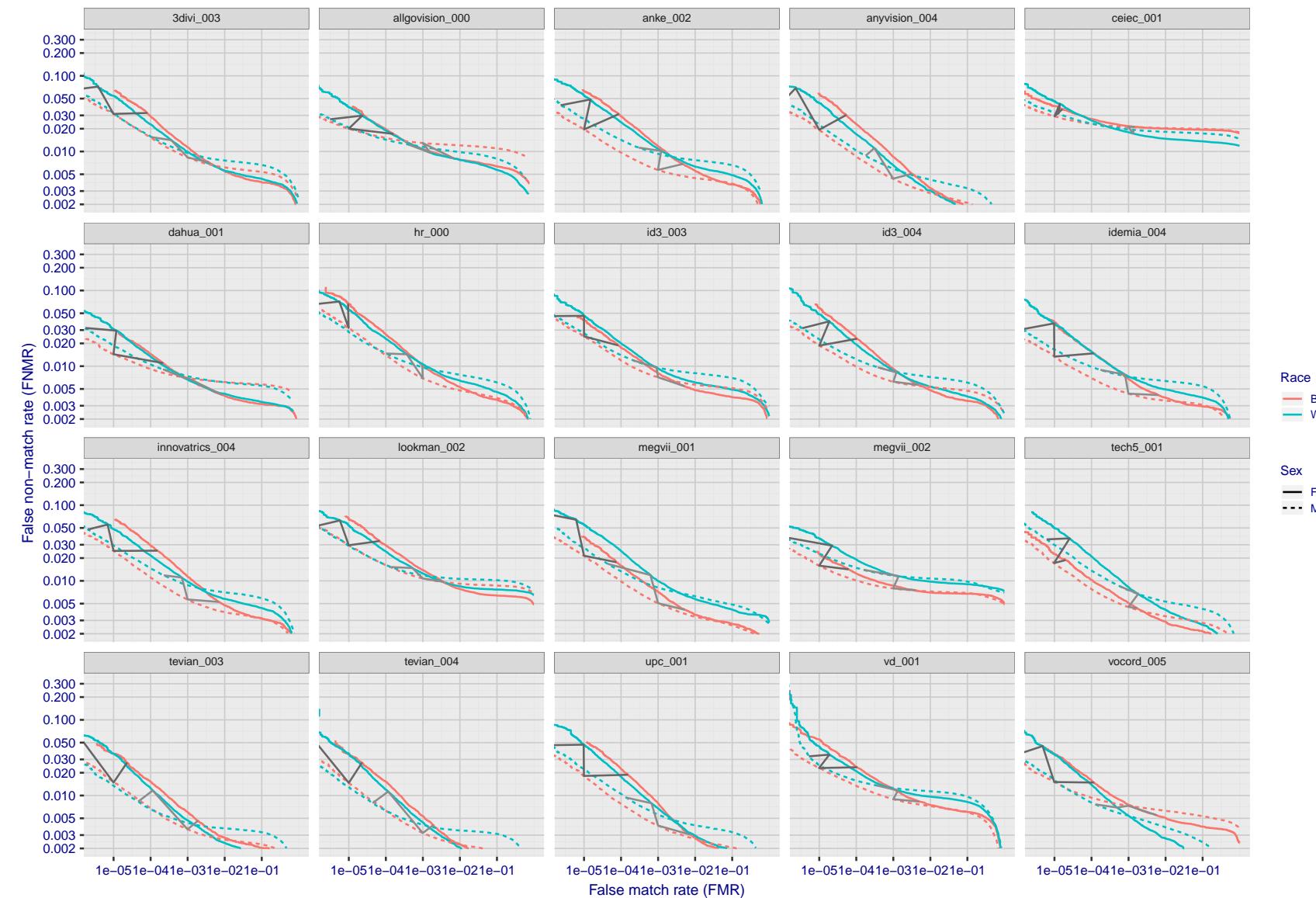


Figure 43: For the mugshot images, error tradeoff characteristics for white females, black females, black males and white males. The Z-shaped grey lines correspond to fixed thresholds, showing both FNMR and FMR vary at one T value. Note: Many of the plots will naively be read as saying women gives worse error rates than men because the solid traces lie above the dotted ones. However, this is misleading and incomplete: The grey lines show the traces reveal horizontal shifts. Thus for the cogent-003 algorithm FNMR for men is higher than for women at a fixed threshold but, at the same time, FMR is higher for women - see Figure 61. As access control systems almost always operate at a fixed threshold, the naive interpretation is incorrect.

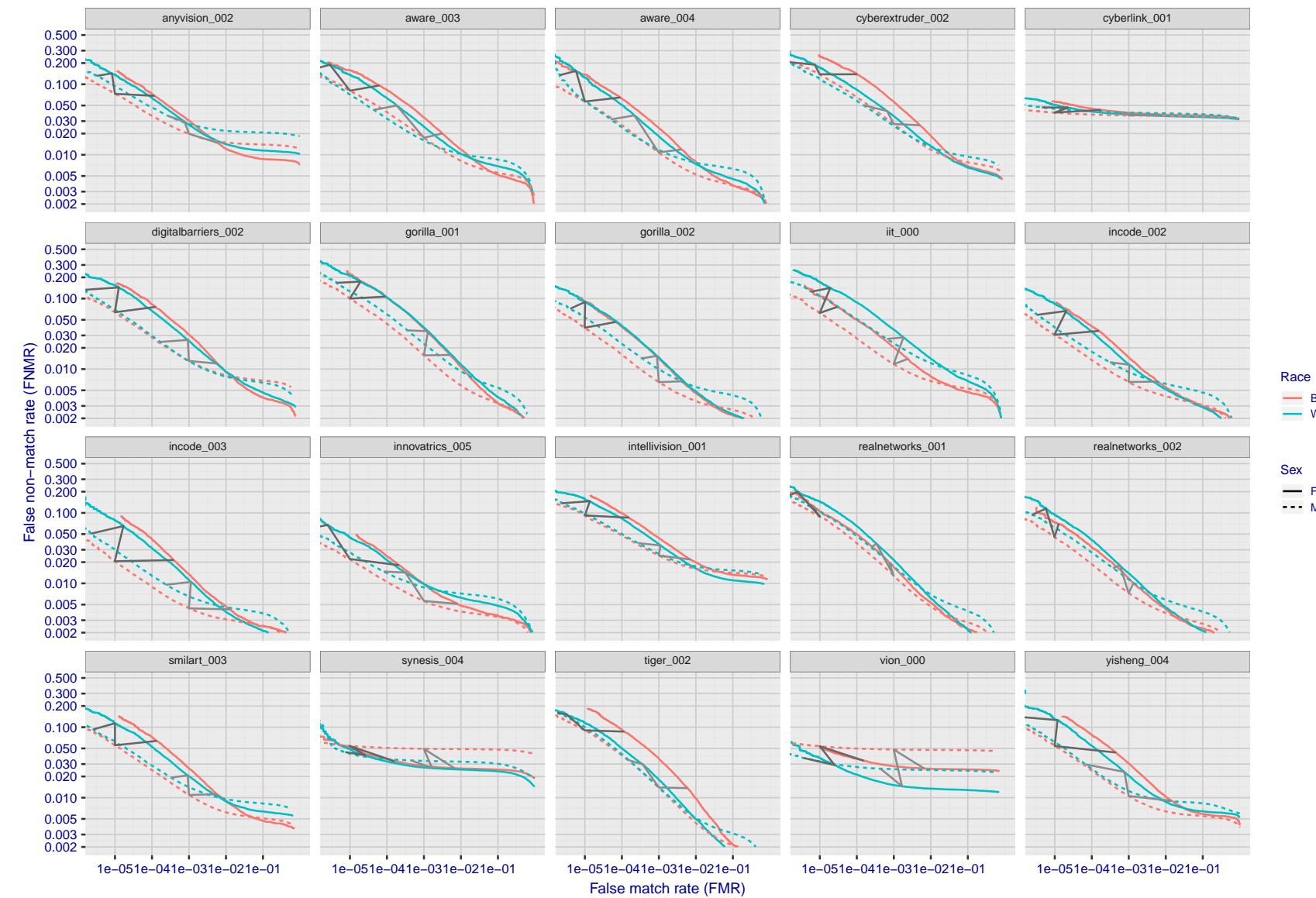


Figure 44: For the mugshot images, error tradeoff characteristics for white females, black females, black males and white males. The Z-shaped grey lines correspond to fixed thresholds, showing both FNMR and FMR vary at one T value. Note: Many of the plots will naively be read as saying women gives worse error rates than men because the solid traces lie above the dotted ones. However, this is misleading and incomplete: The grey lines show the traces reveal horizontal shifts. Thus for the cogent-003 algorithm FNMR for men is higher than for women at a fixed threshold but, at the same time, FMR is higher for women - see Figure 61. As access control systems almost always operate at a fixed threshold, the naive interpretation is incorrect.

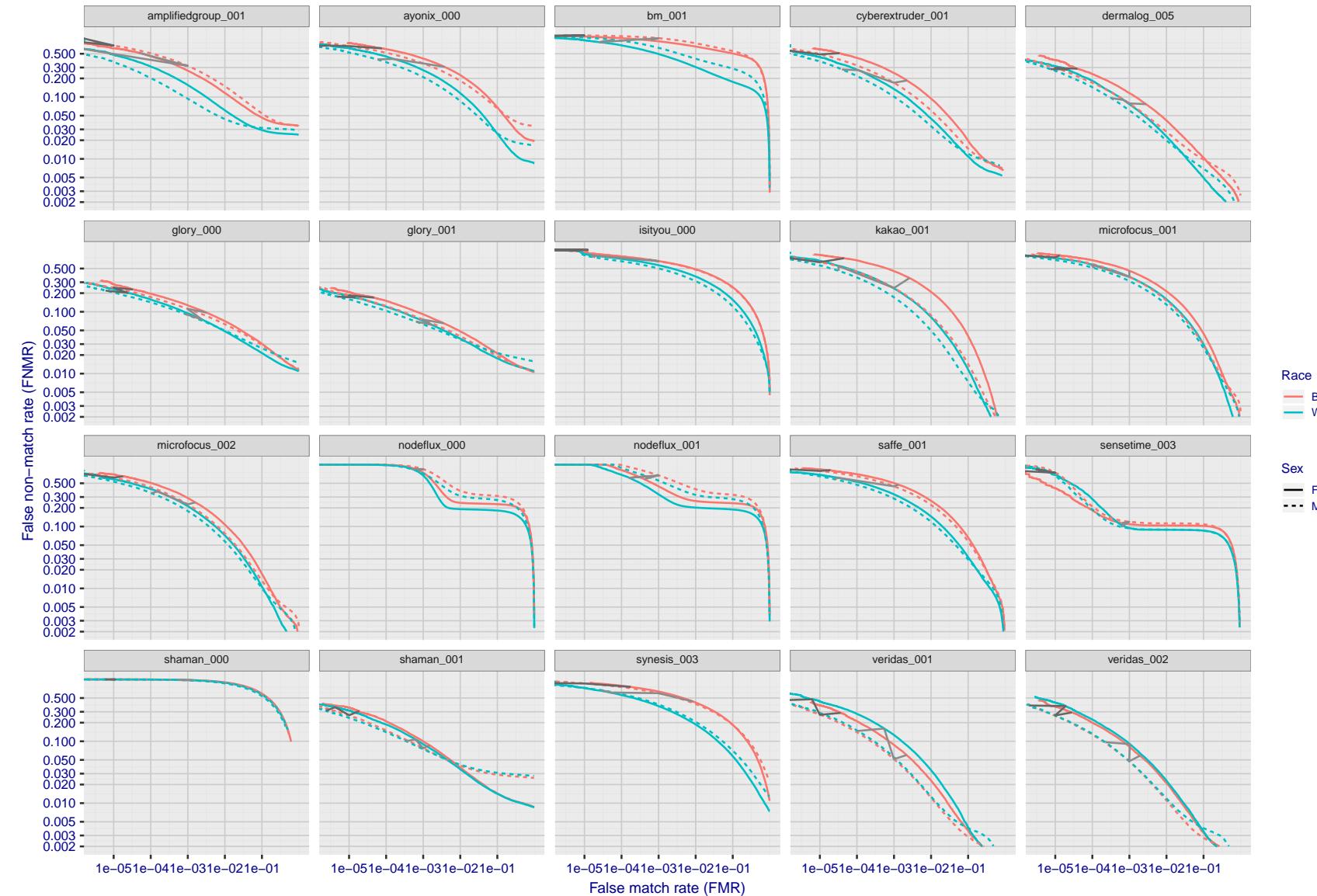


Figure 45: For the mugshot images, error tradeoff characteristics for white females, black females, black males and white males. The Z-shaped grey lines correspond to fixed thresholds, showing both FNMR and FMR vary at one T value. Note: Many of the plots will naively be read as saying women gives worse error rates than men because the solid traces lie above the dotted ones. However, this is misleading and incomplete: The grey lines show the traces reveal horizontal shifts. Thus for the cogent-003 algorithm FNMR for men is higher than for women at a fixed threshold but, at the same time, FMR is higher for women - see Figure 61. As access control systems almost always operate at a fixed threshold, the naive interpretation is incorrect.

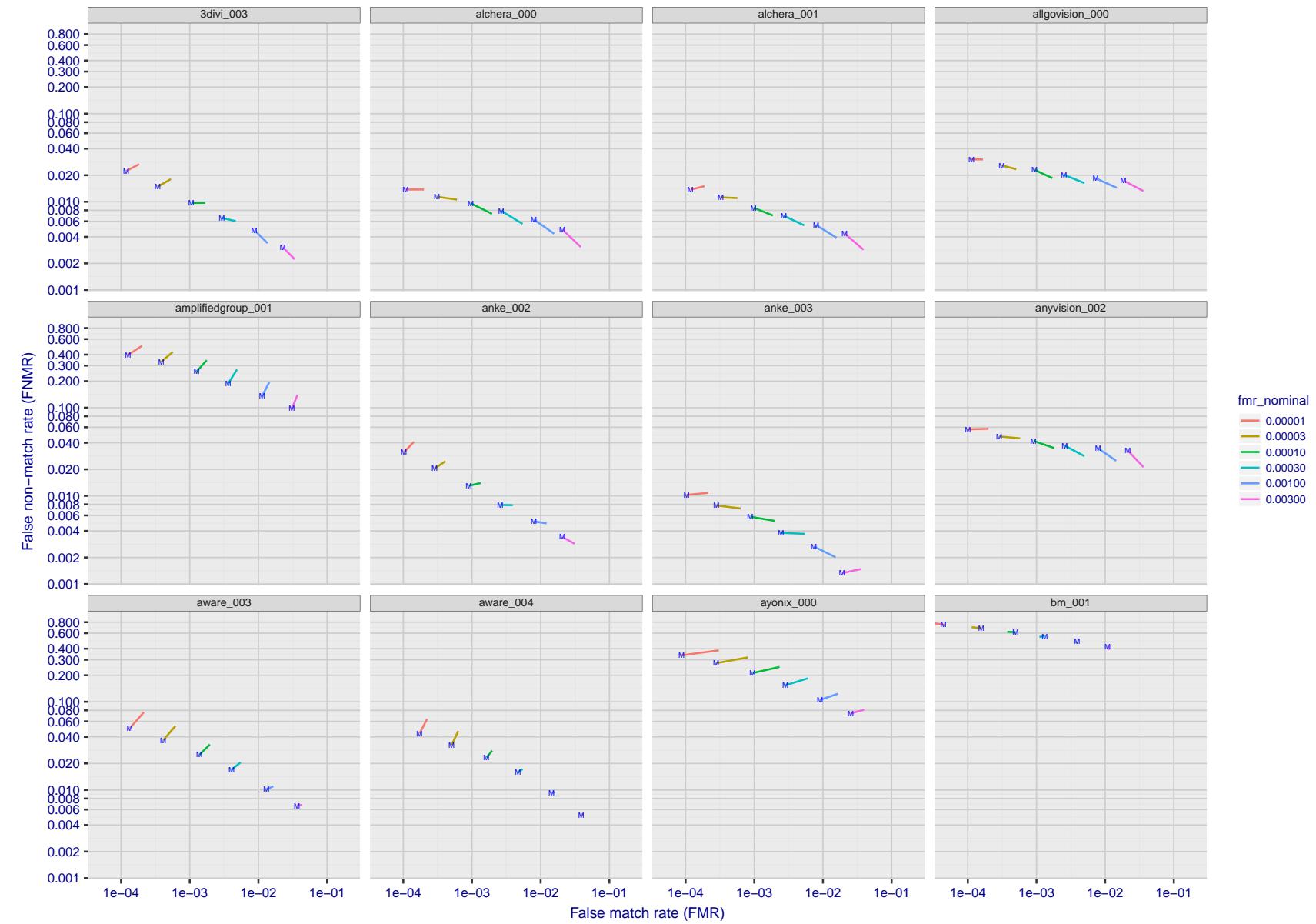


Figure 46: For the visa images, FNMR and FMR at six operating points along the DET characteristic. At each point a line is drawn between  $(FMR, FNMR)_{MALE}$  and  $(FMR, FNMR)_{FEMALE}$  showing how which sex has lower FMR and/or FNMR. The "M" label denotes male, the other end of the line corresponds to female. The six operating thresholds are selected to give the nominal false match rates given in the legend, and are computed over all impostor pairs regardless of age, sex, and place of birth. The plotted FMR values are broadly an order of magnitude larger than the nominal rates because FMR is computed over demographically-matched impostor pairs i.e individuals of the same sex, from the same geographic region (see section 3.6.1), and the same age group (see section 3.6.2).

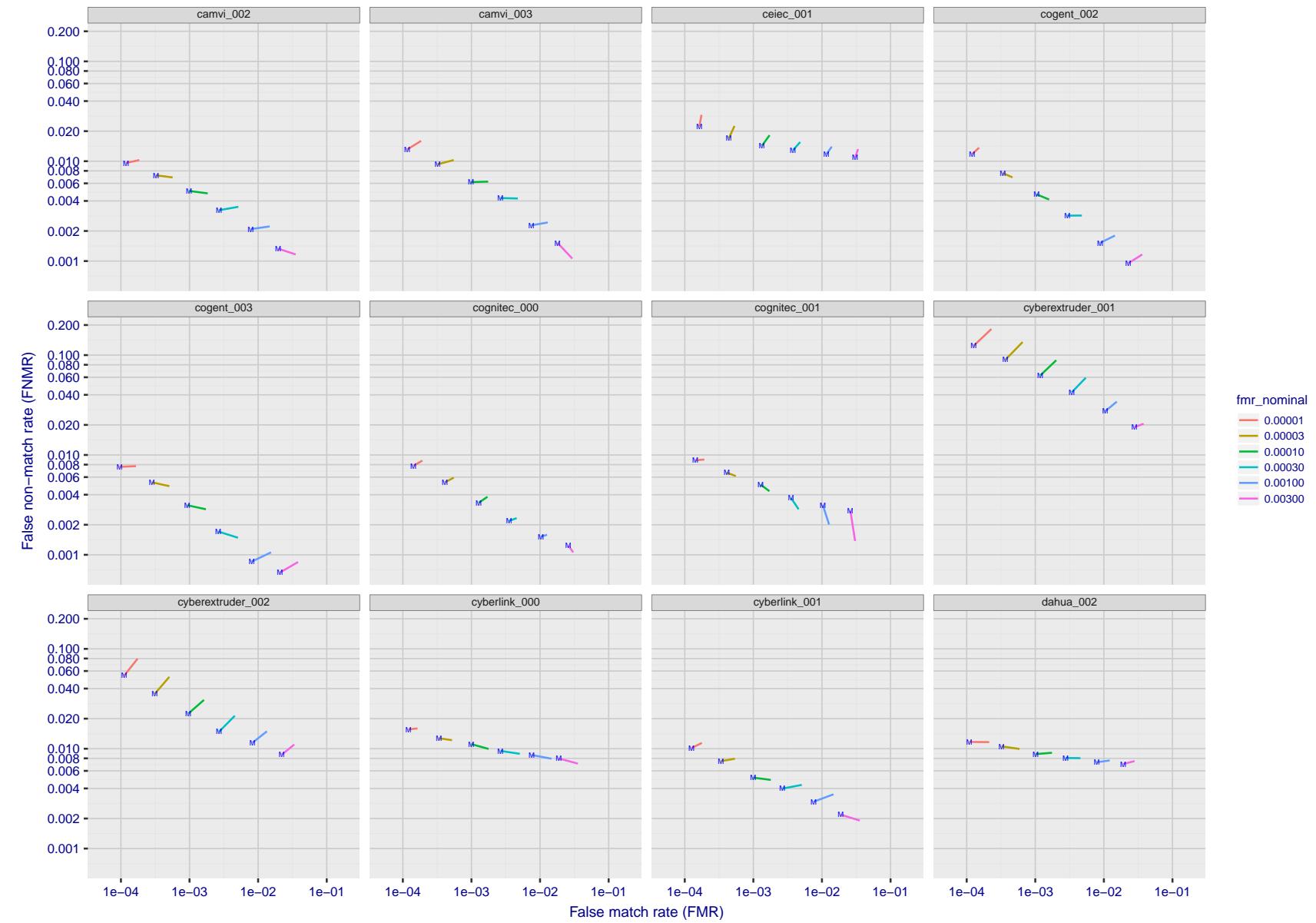


Figure 47: For the visa images, FNMR and FMR at six operating points along the DET characteristic. At each point a line is drawn between  $(FMR, FNMR)_{MALE}$  and  $(FMR, FNMR)_{FEMALE}$  showing how which sex has lower FMR and/or FNMR. The "M" label denotes male, the other end of the line corresponds to female. The six operating thresholds are selected to give the nominal false match rates given in the legend, and are computed over all impostor pairs regardless of age, sex, and place of birth. The plotted FMR values are broadly an order of magnitude larger than the nominal rates because FMR is computed over demographically-matched impostor pairs i.e individuals of the same sex, from the same geographic region (see section 3.6.1), and the same age group (see section 3.6.2).

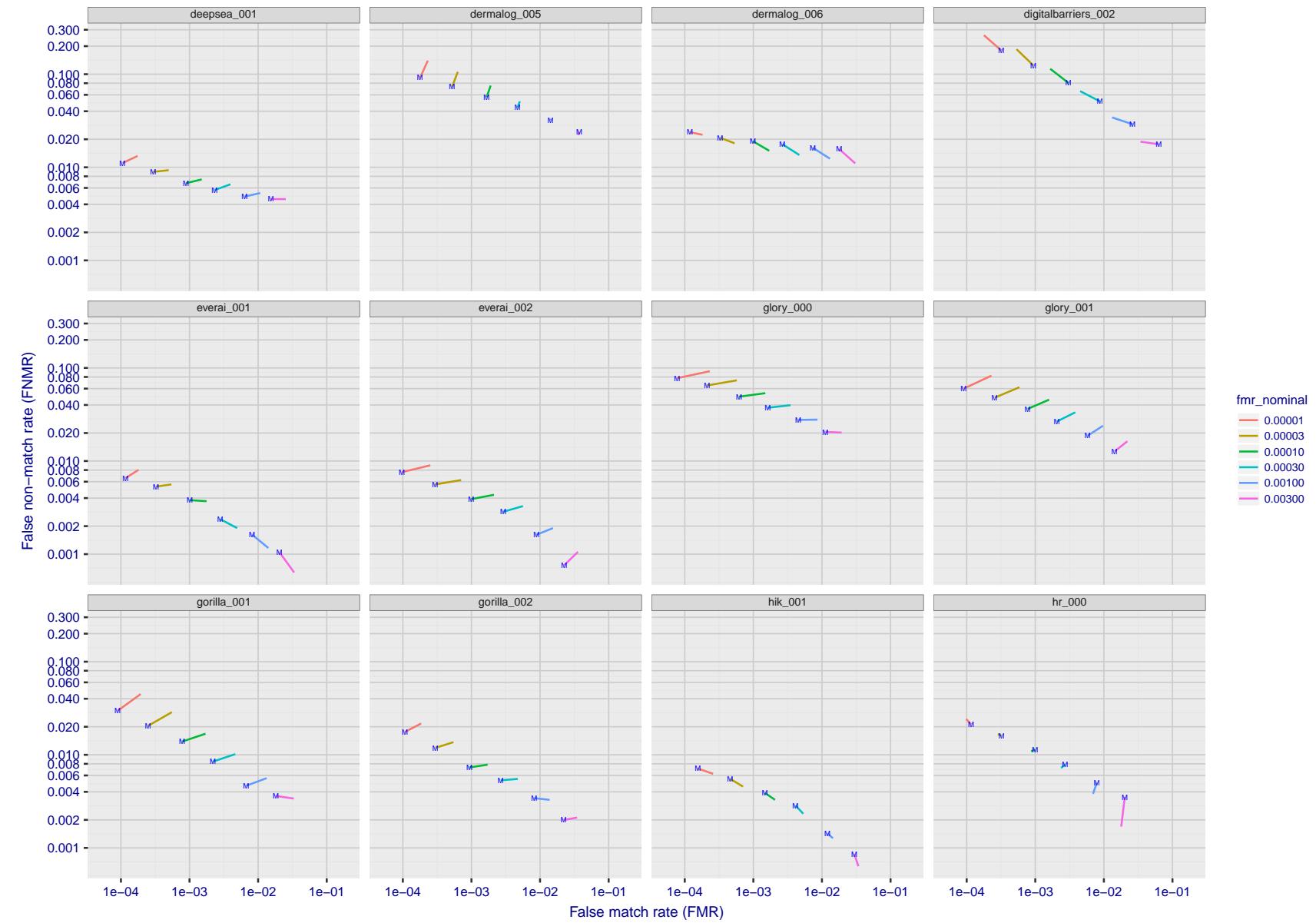


Figure 48: For the visa images, FNMR and FMR at six operating points along the DET characteristic. At each point a line is drawn between  $(FMR, FNMR)_{MALE}$  and  $(FMR, FNMR)_{FEMALE}$  showing how which sex has lower FMR and/or FNMR. The "M" label denotes male, the other end of the line corresponds to female. The six operating thresholds are selected to give the nominal false match rates given in the legend, and are computed over all impostor pairs regardless of age, sex, and place of birth. The plotted FMR values are broadly an order of magnitude larger than the nominal rates because FMR is computed over demographically-matched impostor pairs i.e individuals of the same sex, from the same geographic region (see section 3.6.1), and the same age group (see section 3.6.2).

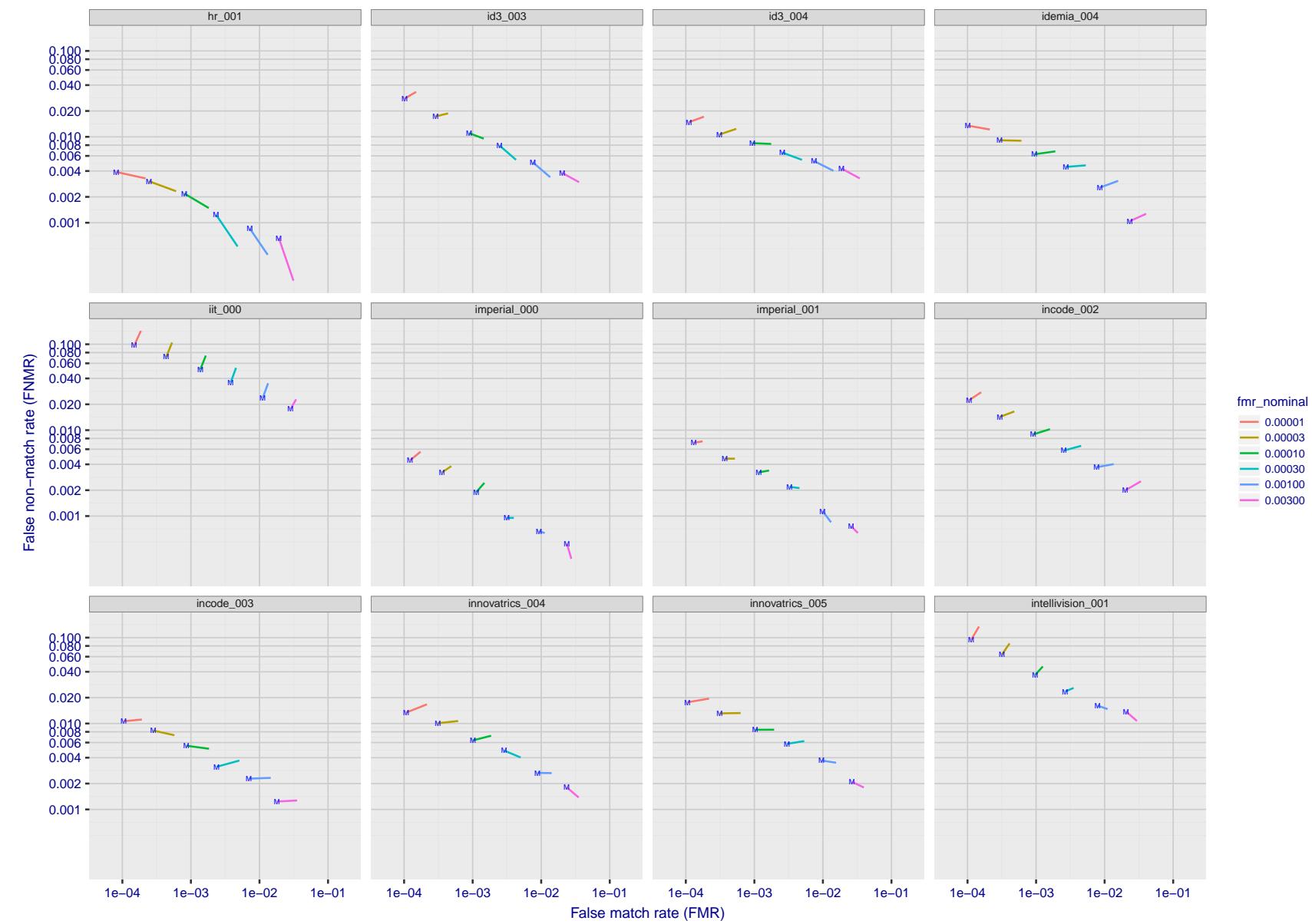


Figure 49: For the visa images, FNMR and FMR at six operating points along the DET characteristic. At each point a line is drawn between  $(FMR, FNMR)_{MALE}$  and  $(FMR, FNMR)_{FEMALE}$  showing how which sex has lower FMR and/or FNMR. The "M" label denotes male, the other end of the line corresponds to female. The six operating thresholds are selected to give the nominal false match rates given in the legend, and are computed over all impostor pairs regardless of age, sex, and place of birth. The plotted FMR values are broadly an order of magnitude larger than the nominal rates because FMR is computed over demographically-matched impostor pairs i.e individuals of the same sex, from the same geographic region (see section 3.6.1), and the same age group (see section 3.6.2).

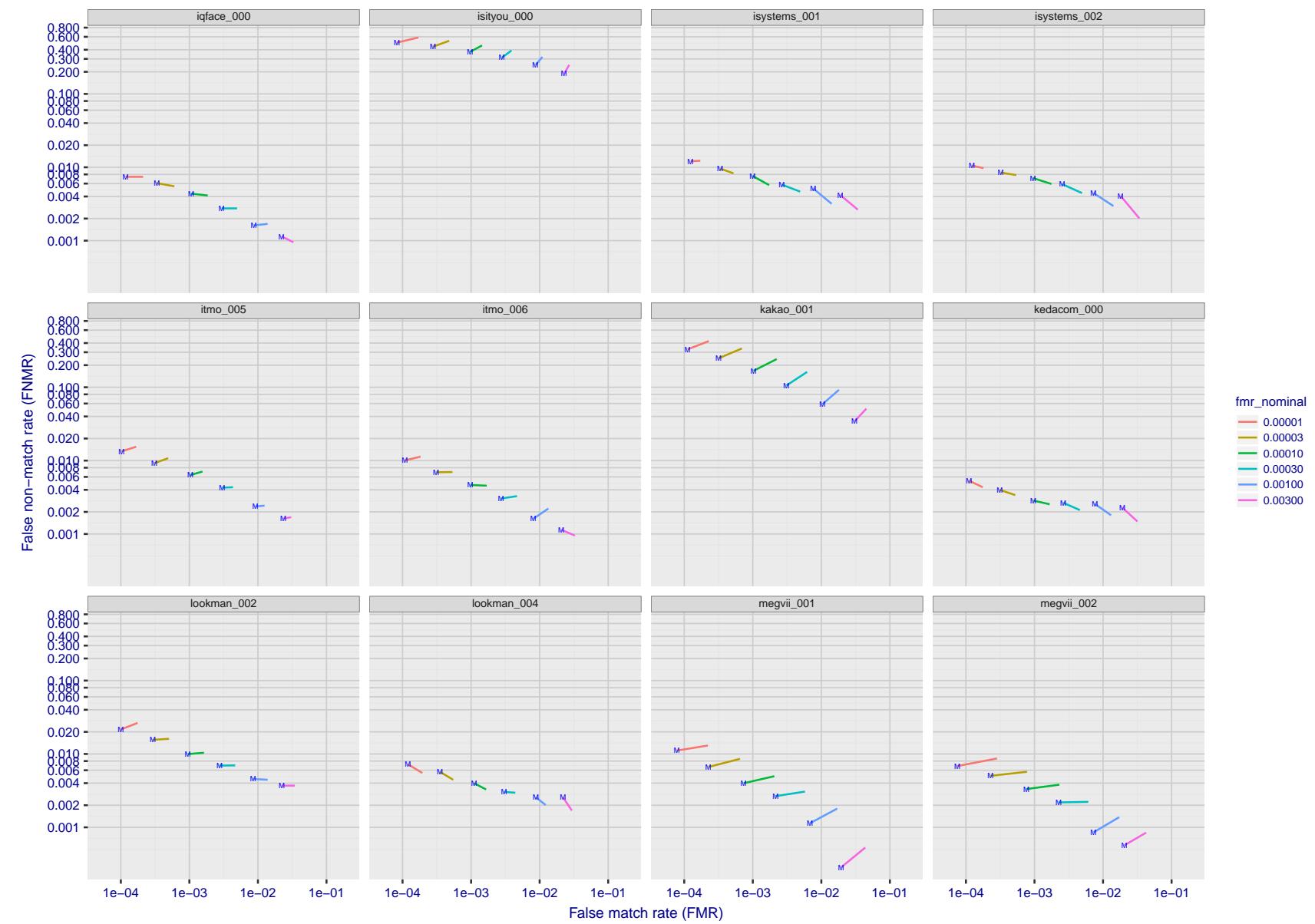


Figure 50: For the visa images, FNMR and FMR at six operating points along the DET characteristic. At each point a line is drawn between  $(FMR, FNMR)_{MALE}$  and  $(FMR, FNMR)_{FEMALE}$  showing how which sex has lower FMR and/or FNMR. The "M" label denotes male, the other end of the line corresponds to female. The six operating thresholds are selected to give the nominal false match rates given in the legend, and are computed over all impostor pairs regardless of age, sex, and place of birth. The plotted FMR values are broadly an order of magnitude larger than the nominal rates because FMR is computed over demographically-matched impostor pairs i.e individuals of the same sex, from the same geographic region (see section 3.6.1), and the same age group (see section 3.6.2).

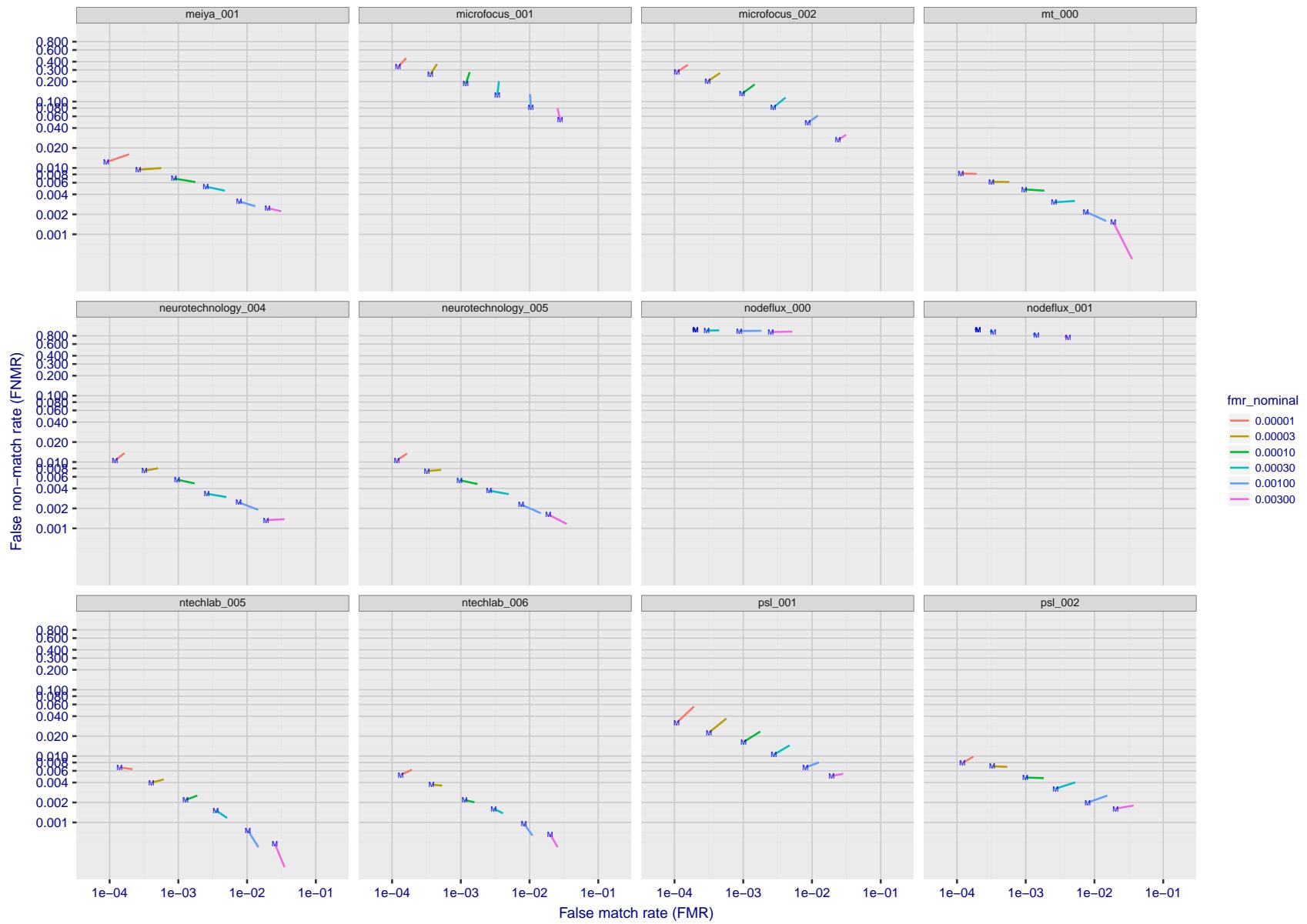


Figure 51: For the visa images, FNMR and FMR at six operating points along the DET characteristic. At each point a line is drawn between  $(FMR, FNMR)_{MALE}$  and  $(FMR, FNMR)_{FEMALE}$  showing how which sex has lower FMR and/or FNMR. The "M" label denotes male, the other end of the line corresponds to female. The six operating thresholds are selected to give the nominal false match rates given in the legend, and are computed over all impostor pairs regardless of age, sex, and place of birth. The plotted FMR values are broadly an order of magnitude larger than the nominal rates because FMR is computed over demographically-matched impostor pairs i.e individuals of the same sex, from the same geographic region (see section 3.6.1), and the same age group (see section 3.6.2).

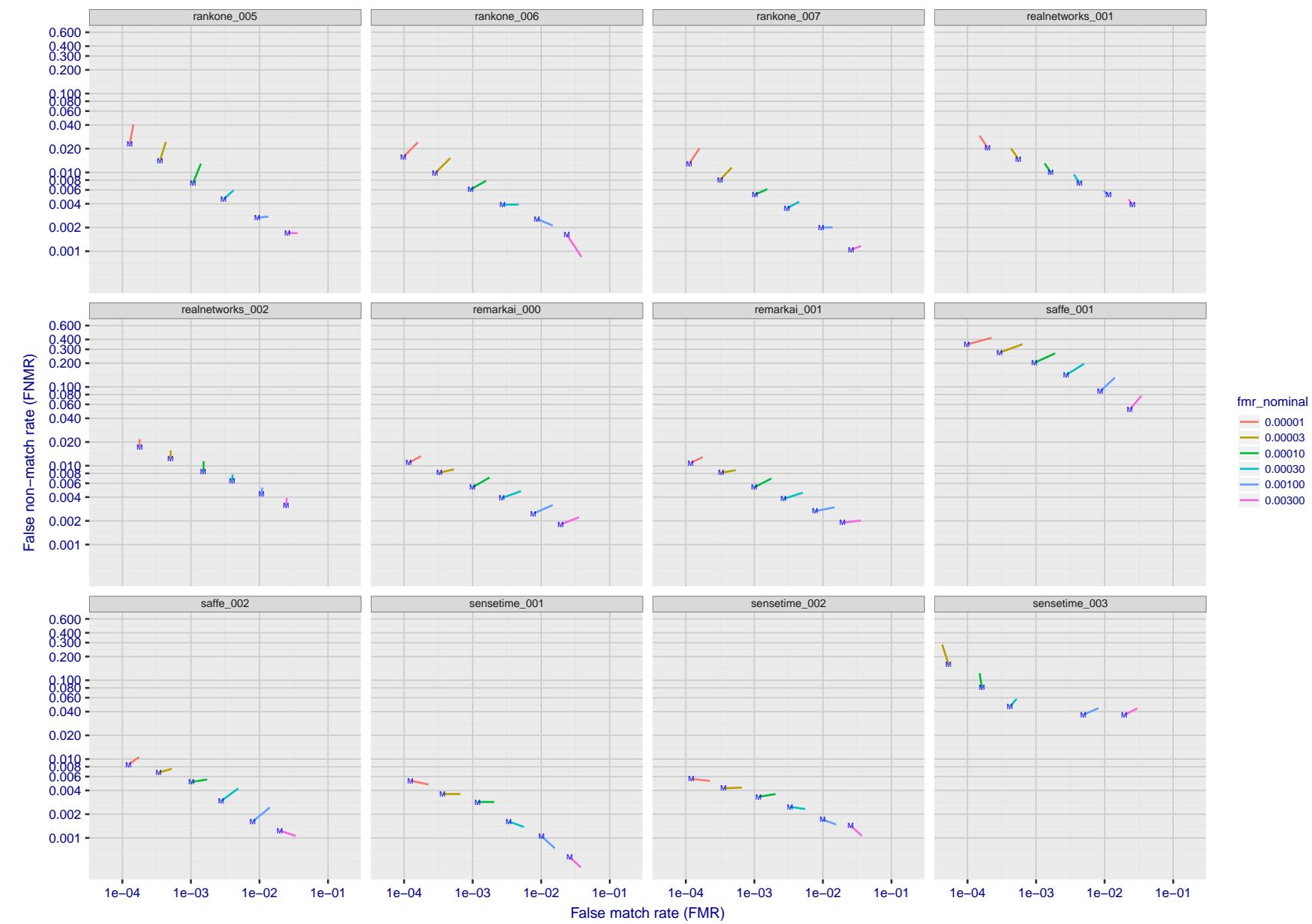


Figure 52: For the visa images, FNMR and FMR at six operating points along the DET characteristic. At each point a line is drawn between  $(FMR, FNMR)_{MALE}$  and  $(FMR, FNMR)_{FEMALE}$  showing how which sex has lower FMR and/or FNMR. The "M" label denotes male, the other end of the line corresponds to female. The six operating thresholds are selected to give the nominal false match rates given in the legend, and are computed over all impostor pairs regardless of age, sex, and place of birth. The plotted FMR values are broadly an order of magnitude larger than the nominal rates because FMR is computed over demographically-matched impostor pairs i.e individuals of the same sex, from the same geographic region (see section 3.6.1), and the same age group (see section 3.6.2).

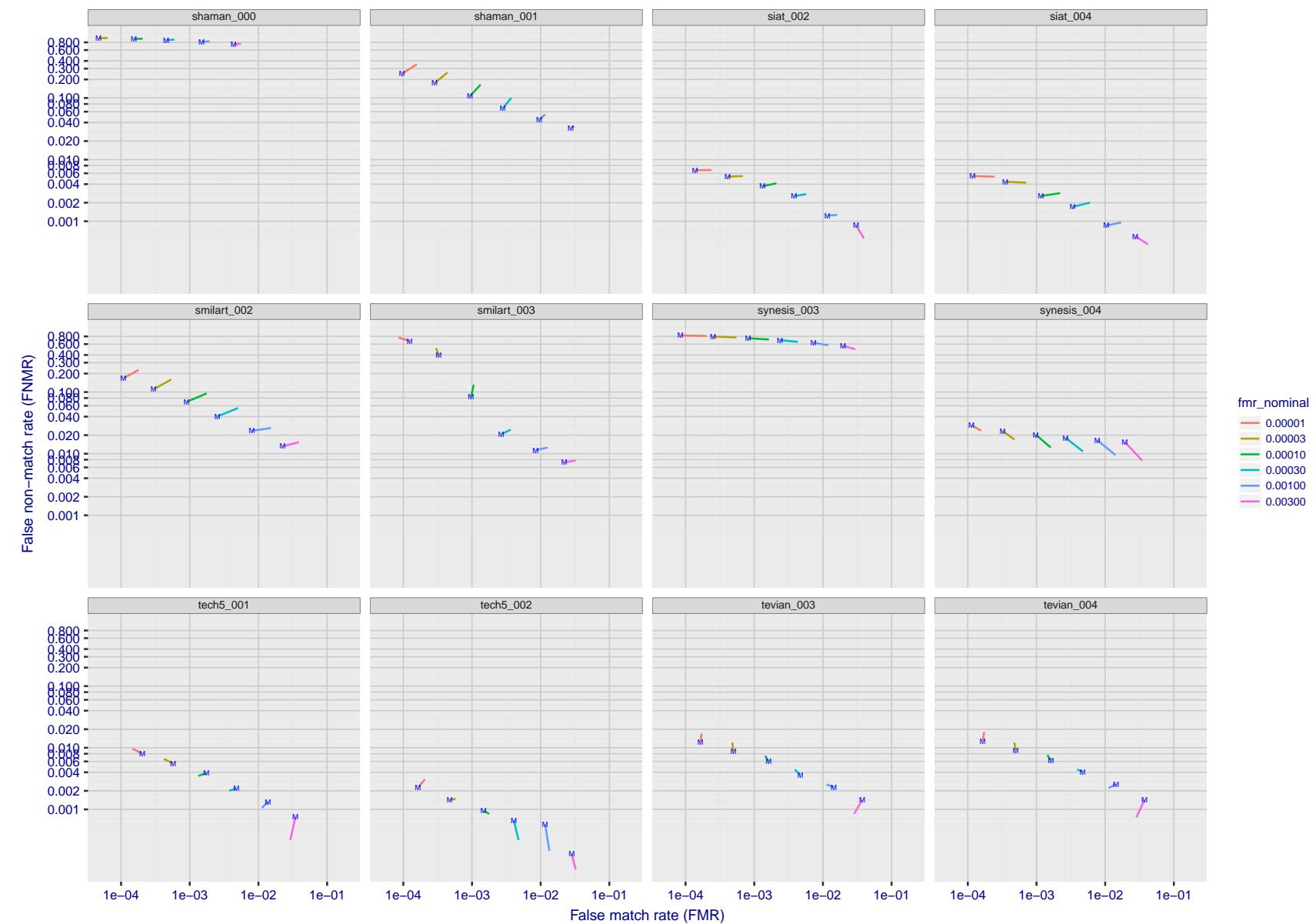


Figure 53: For the visa images, FNMR and FMR at six operating points along the DET characteristic. At each point a line is drawn between  $(FMR, FNMR)_{MALE}$  and  $(FMR, FNMR)_{FEMALE}$  showing how which sex has lower FMR and/or FNMR. The "M" label denotes male, the other end of the line corresponds to female. The six operating thresholds are selected to give the nominal false match rates given in the legend, and are computed over all impostor pairs regardless of age, sex, and place of birth. The plotted FMR values are broadly an order of magnitude larger than the nominal rates because FMR is computed over demographically-matched impostor pairs i.e individuals of the same sex, from the same geographic region (see section 3.6.1), and the same age group (see section 3.6.2).

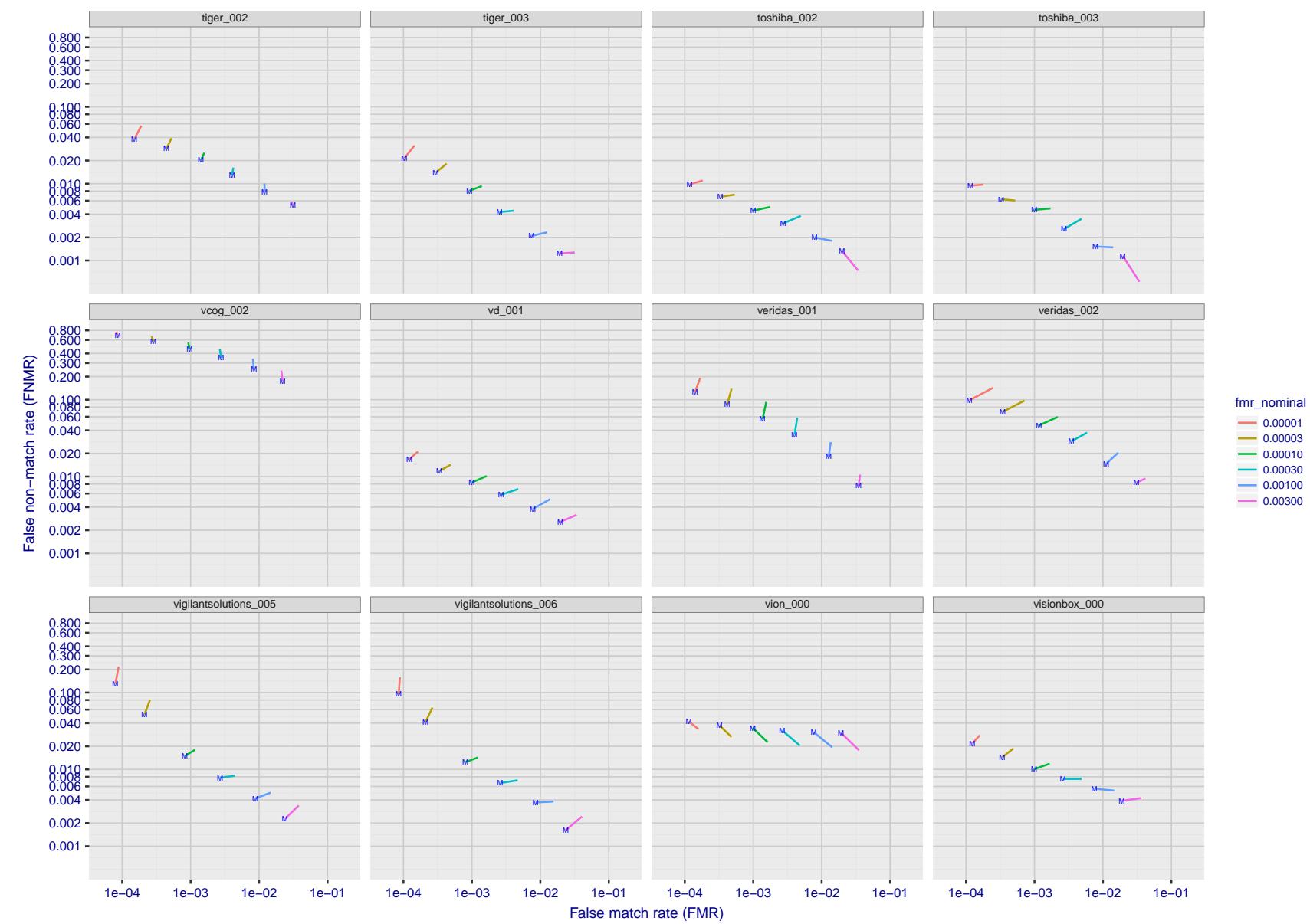


Figure 54: For the visa images, FNMR and FMR at six operating points along the DET characteristic. At each point a line is drawn between  $(FMR, FNMR)_{MALE}$  and  $(FMR, FNMR)_{FEMALE}$  showing how which sex has lower FMR and/or FNMR. The "M" label denotes male, the other end of the line corresponds to female. The six operating thresholds are selected to give the nominal false match rates given in the legend, and are computed over all impostor pairs regardless of age, sex, and place of birth. The plotted FMR values are broadly an order of magnitude larger than the nominal rates because FMR is computed over demographically-matched impostor pairs i.e individuals of the same sex, from the same geographic region (see section 3.6.1), and the same age group (see section 3.6.2).

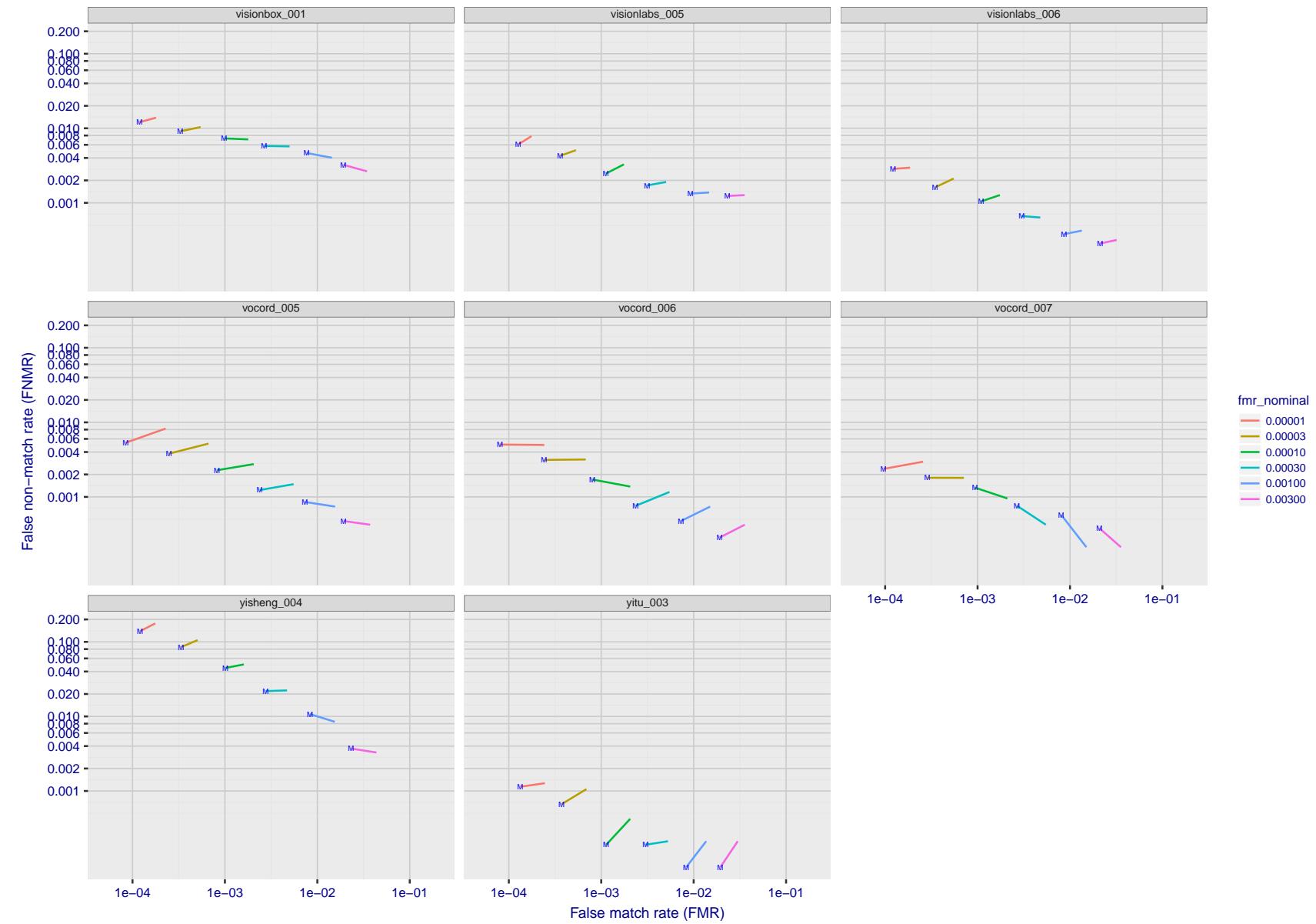


Figure 55: For the visa images, FNMR and FMR at six operating points along the DET characteristic. At each point a line is drawn between  $(FMR, FNMR)_{MALE}$  and  $(FMR, FNMR)_{FEMALE}$  showing how which sex has lower FMR and/or FNMR. The "M" label denotes male, the other end of the line corresponds to female. The six operating thresholds are selected to give the nominal false match rates given in the legend, and are computed over all impostor pairs regardless of age, sex, and place of birth. The plotted FMR values are broadly an order of magnitude larger than the nominal rates because FMR is computed over demographically-matched impostor pairs i.e individuals of the same sex, from the same geographic region (see section 3.6.1), and the same age group (see section 3.6.2).

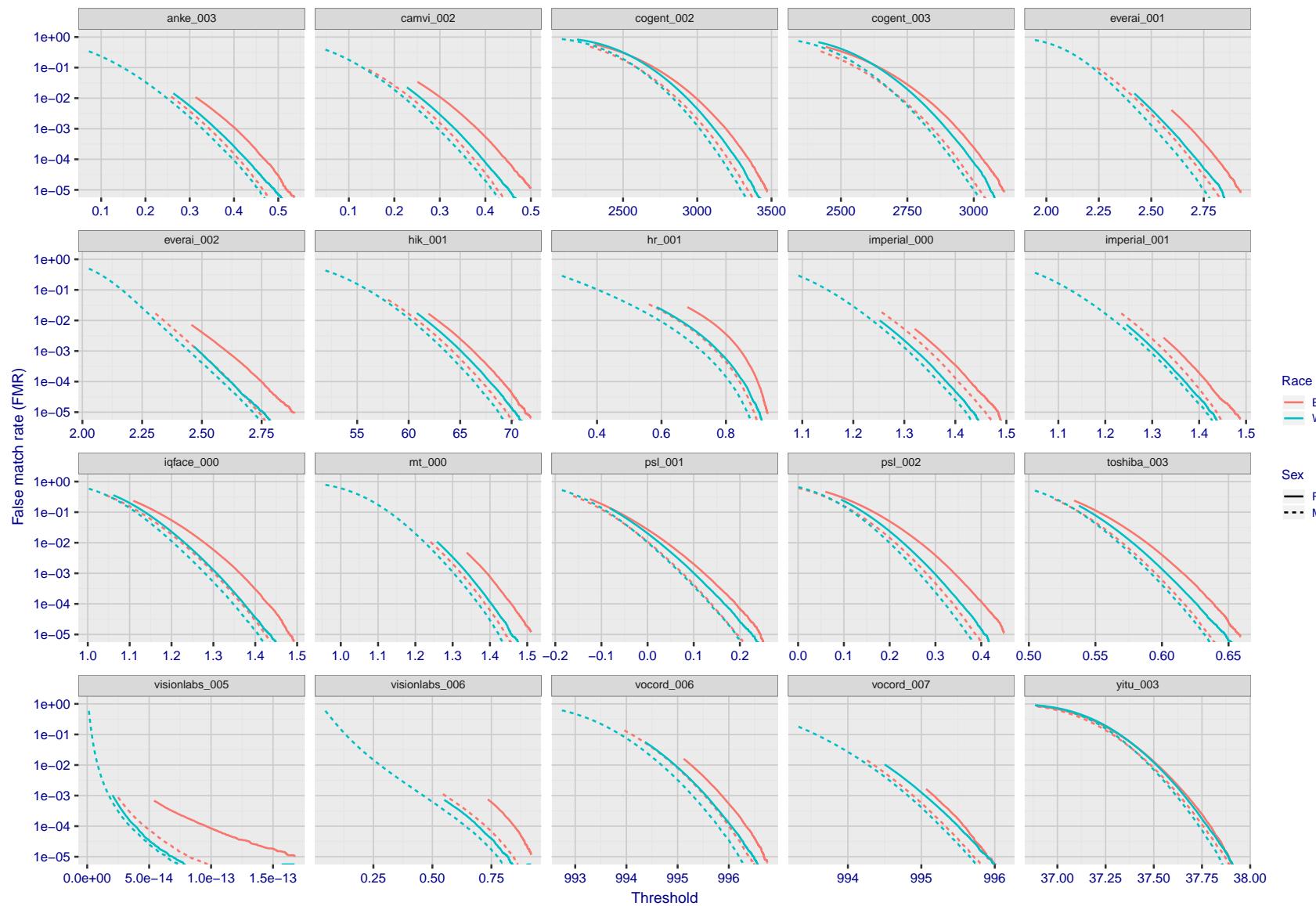


Figure 56: For the mugshot images, the false match calibration curves show false match rate vs. threshold. Separate curves appear for white females, black females, black males and white males.

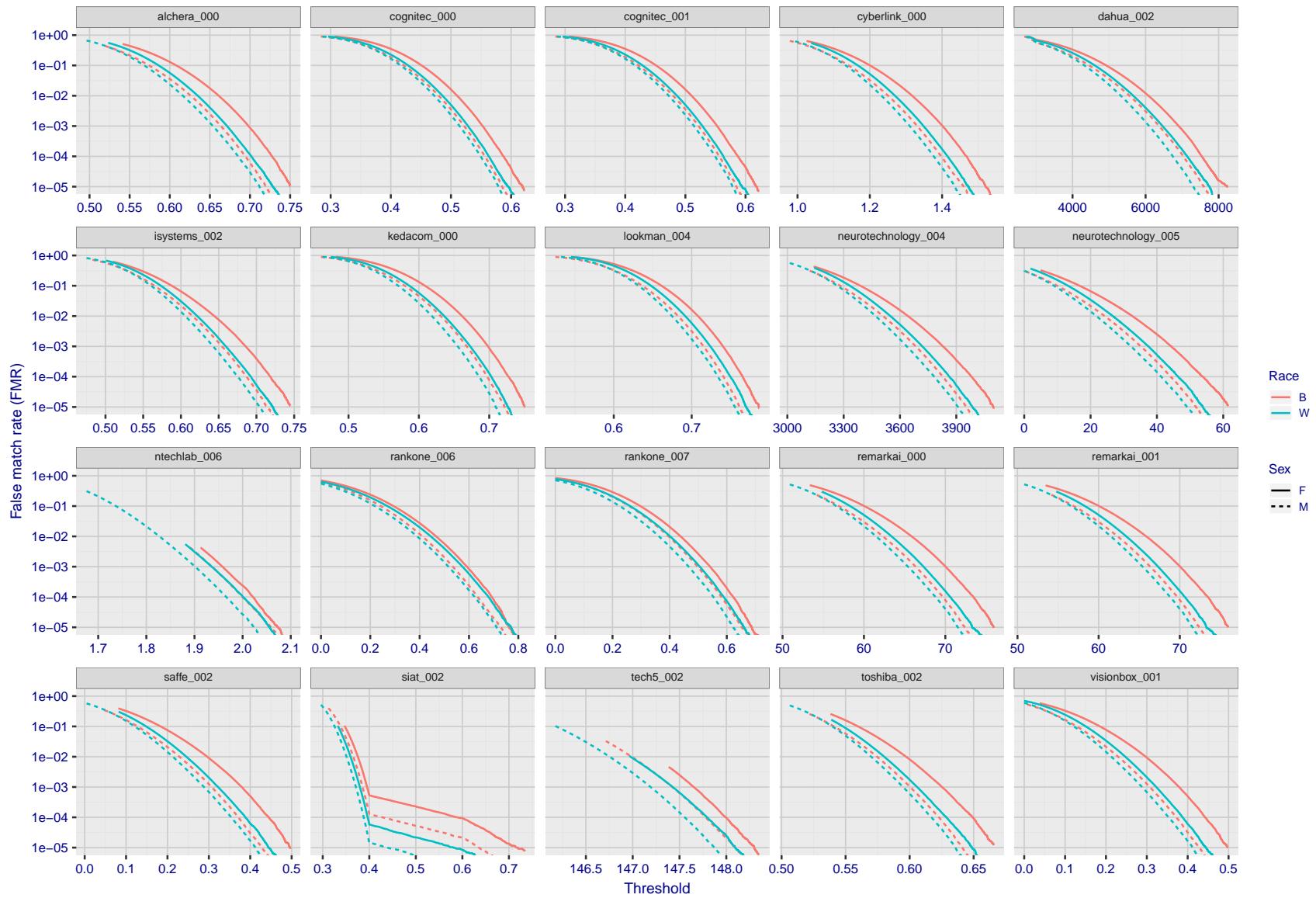


Figure 57: For the mugshot images, the false match calibration curves show false match rate vs. threshold. Separate curves appear for white females, black females, black males and white males.

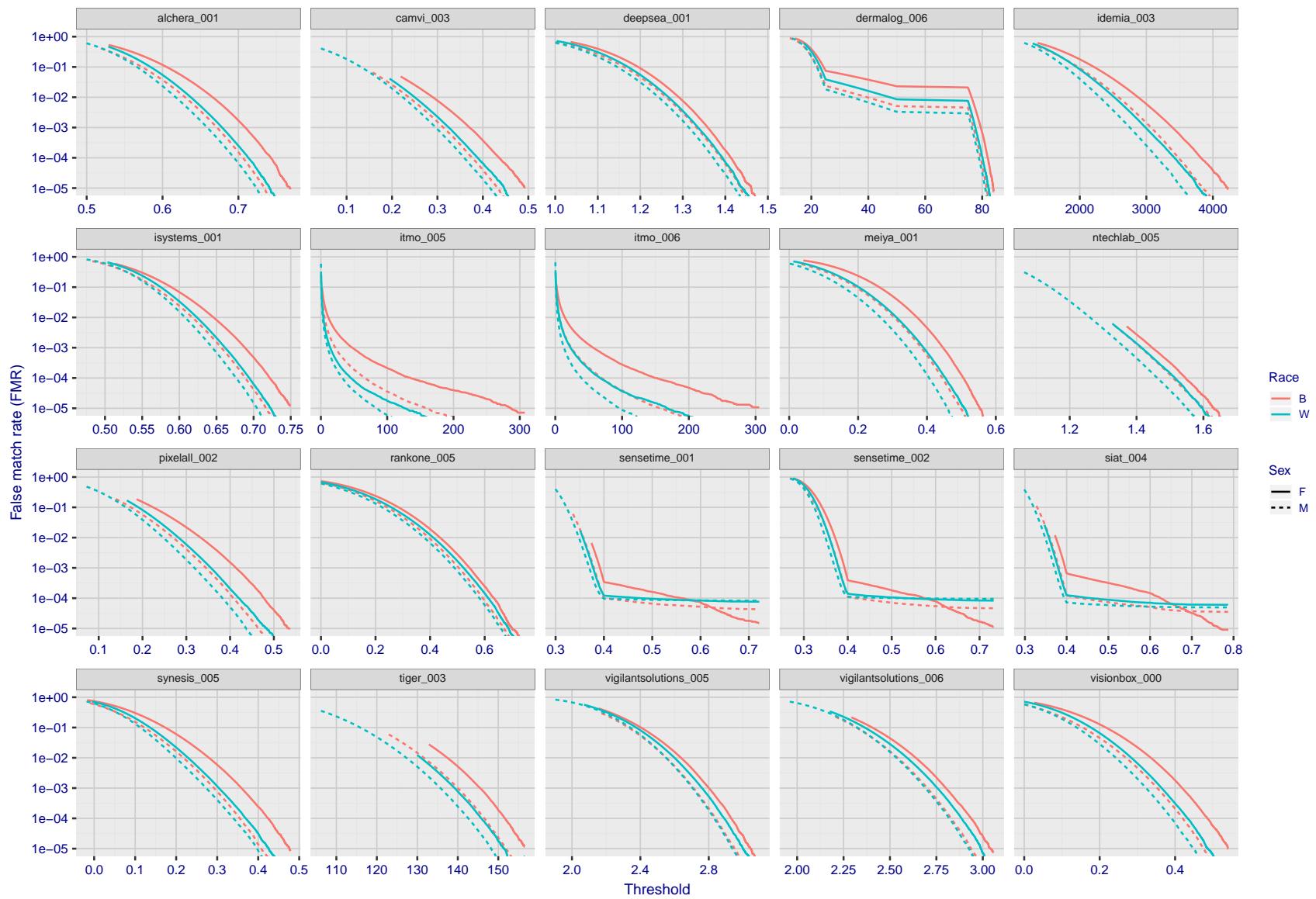


Figure 58: For the mugshot images, the false match calibration curves show false match rate vs. threshold. Separate curves appear for white females, black females, black males and white males.

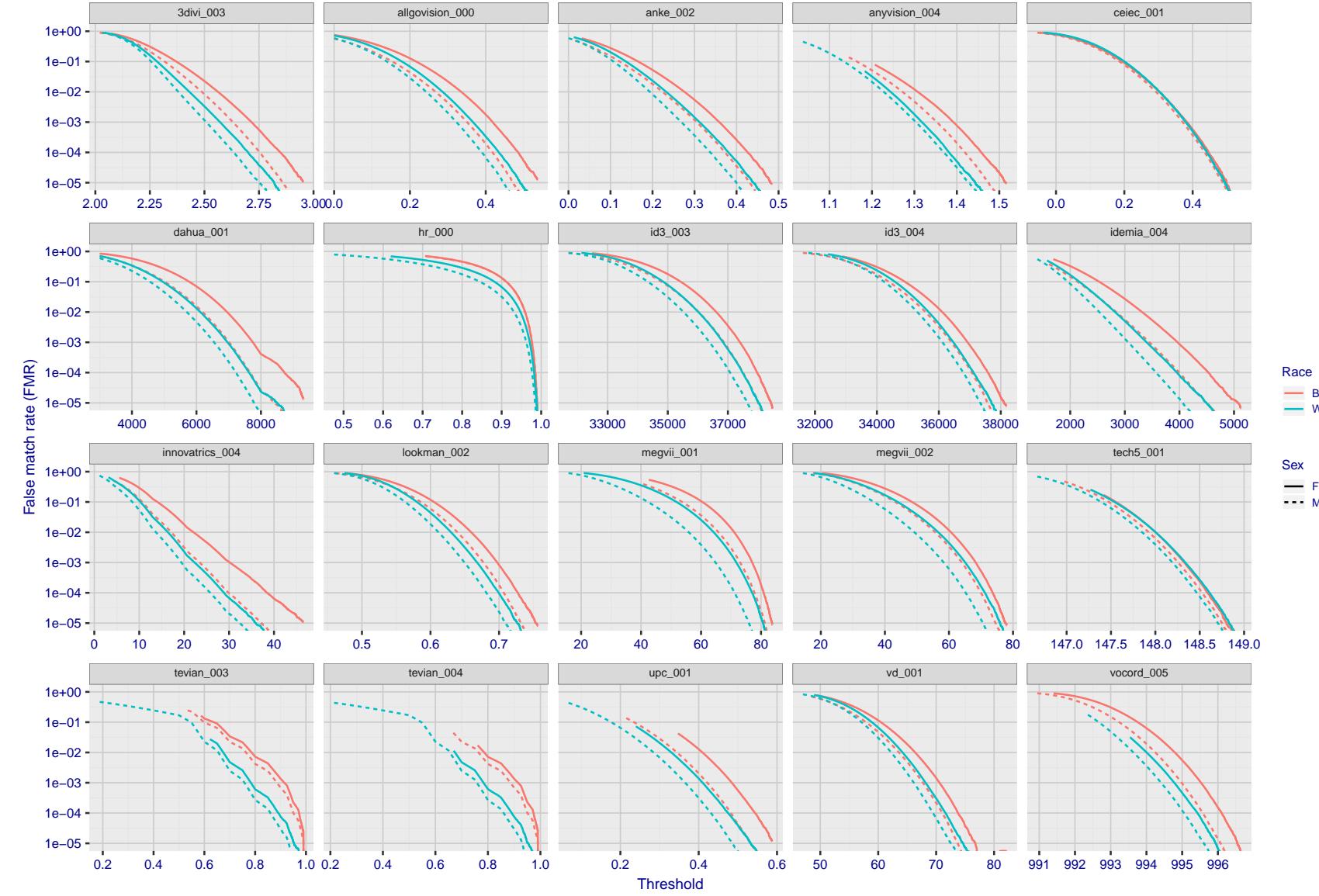


Figure 59: For the mugshot images, the false match calibration curves show false match rate vs. threshold. Separate curves appear for white females, black females, black males and white males.

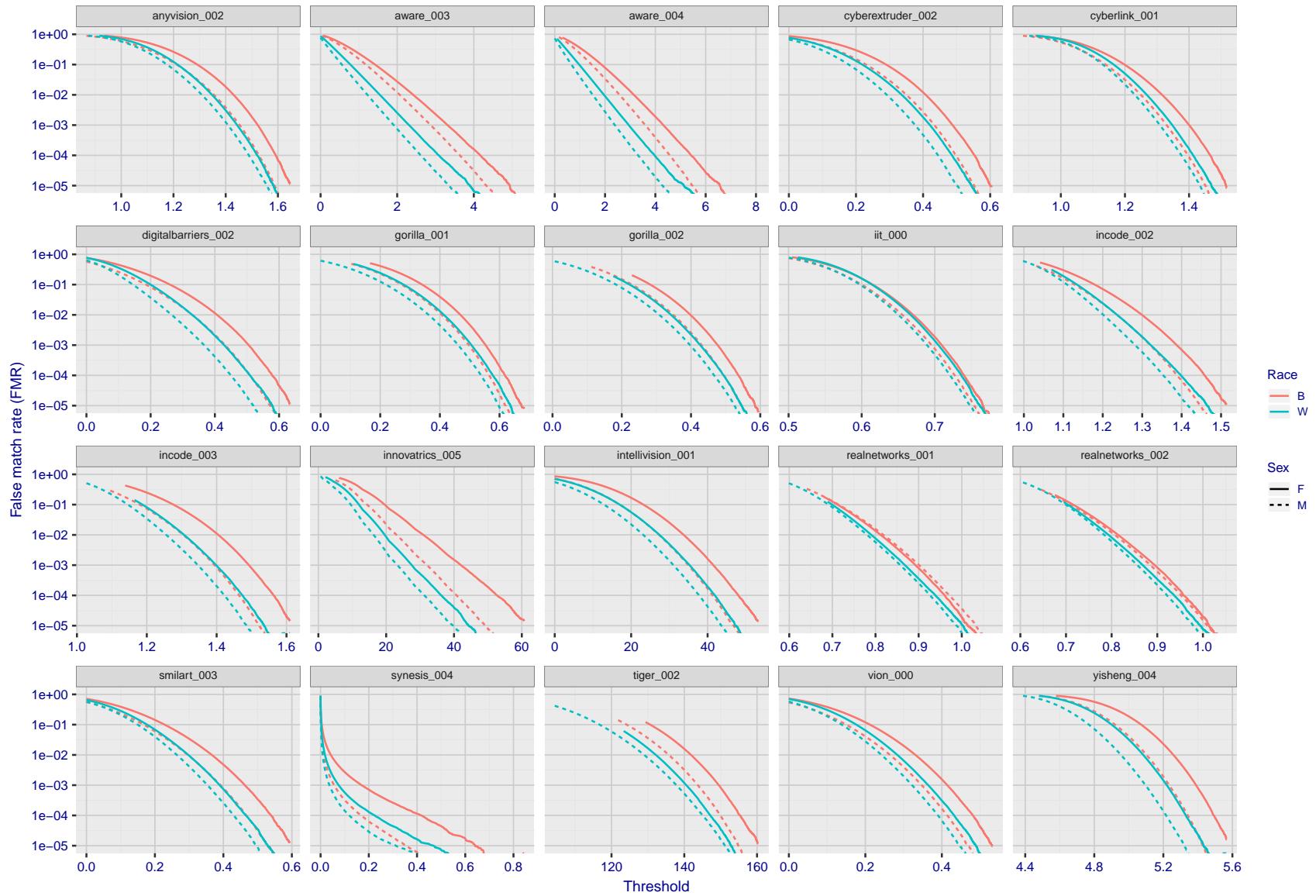


Figure 60: For the mugshot images, the false match calibration curves show false match rate vs. threshold. Separate curves appear for white females, black females, black males and white males.

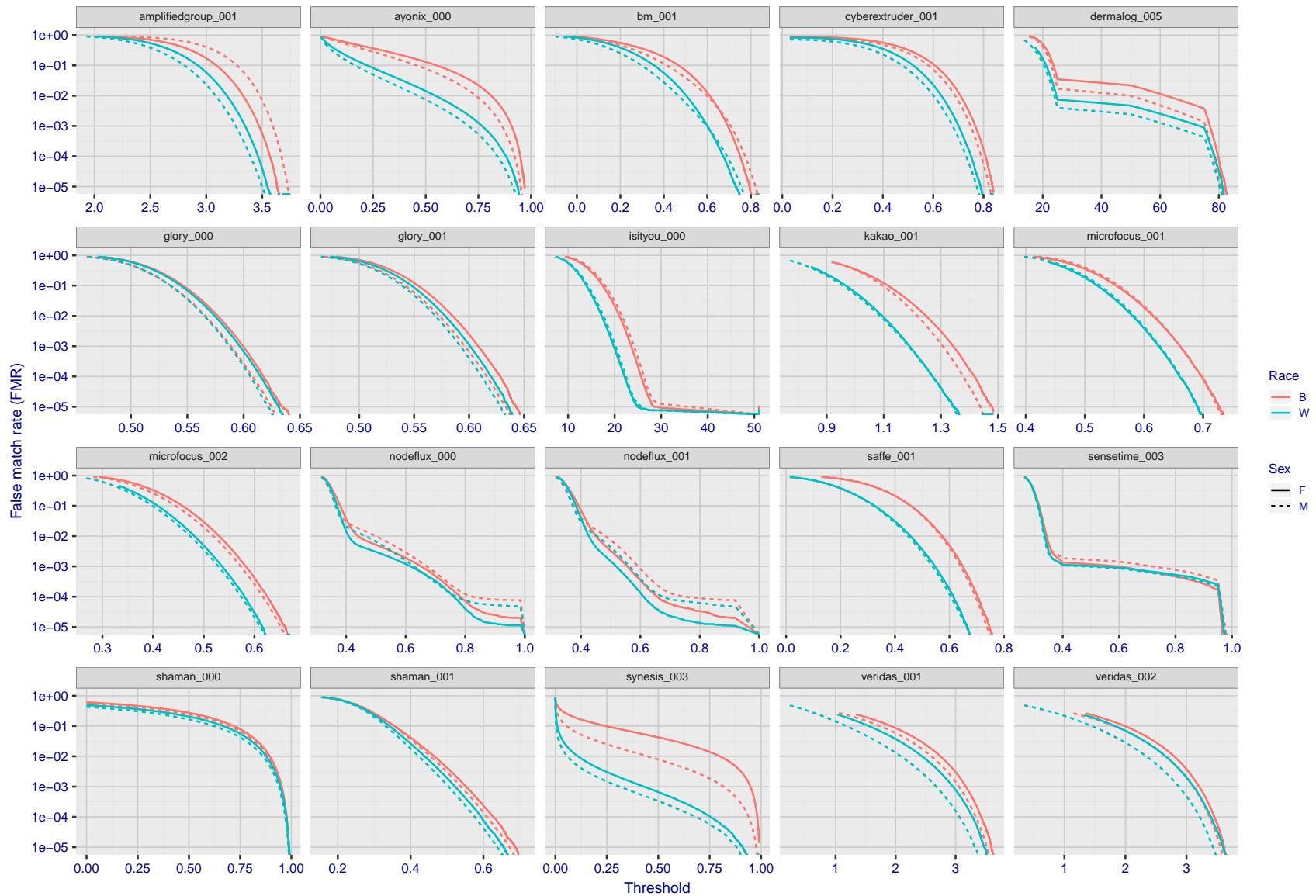


Figure 61: For the mugshot images, the false match calibration curves show false match rate vs. threshold. Separate curves appear for white females, black females, black males and white males.

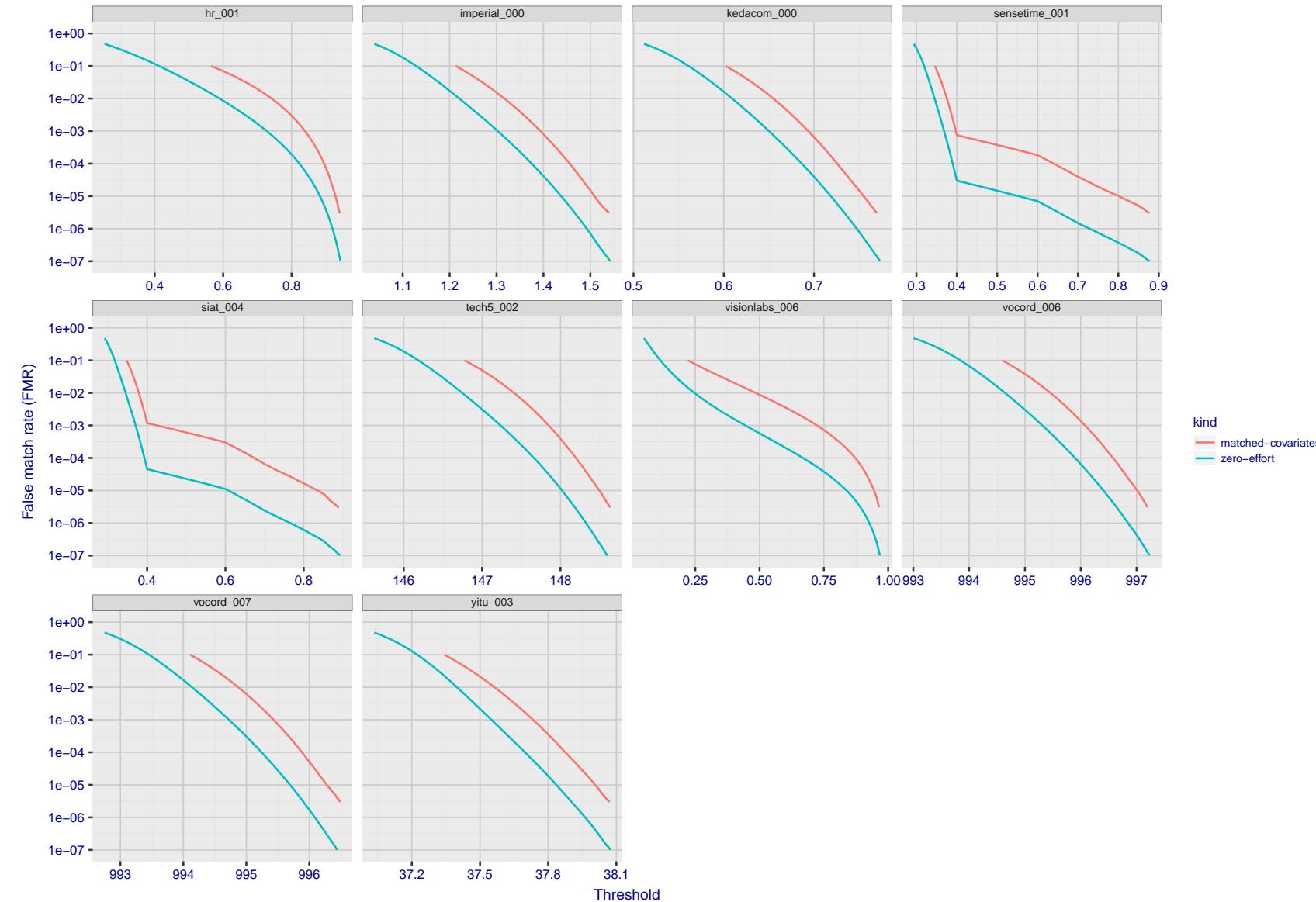


Figure 62: For the visa images, the false match calibration curves show FMR vs. threshold,  $T$ . The blue (lower) curves are for zero-effort impostors (i.e. comparing all images against all). The red (upper) curves are for persons of the same-sex, same-age, and same national-origin. This shows that FMR is underestimated (by a factor of 10 or more) by using a zero-effort impostor calculation to calibrate  $T$ . As shown later (sec. 3.6), FMR is higher for demographic-matched impostors.

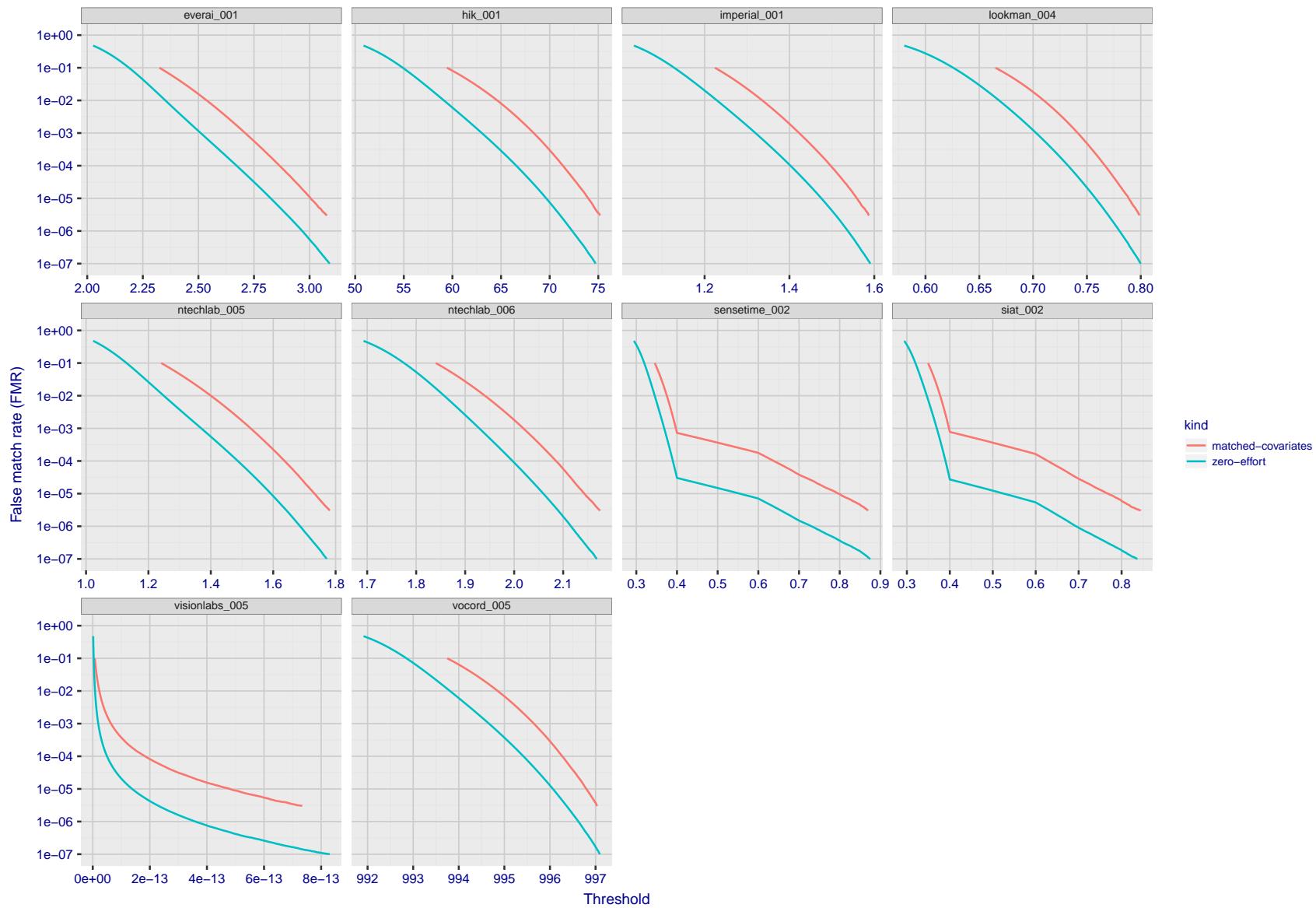


Figure 63: For the visa images, the false match calibration curves show FMR vs. threshold,  $T$ . The blue (lower) curves are for zero-effort impostors (i.e. comparing all images against all). The red (upper) curves are for persons of the same-sex, same-age, and same national-origin. This shows that FMR is underestimated (by a factor of 10 or more) by using a zero-effort impostor calculation to calibrate  $T$ . As shown later (sec. 3.6), FMR is higher for demographic-matched impostors.

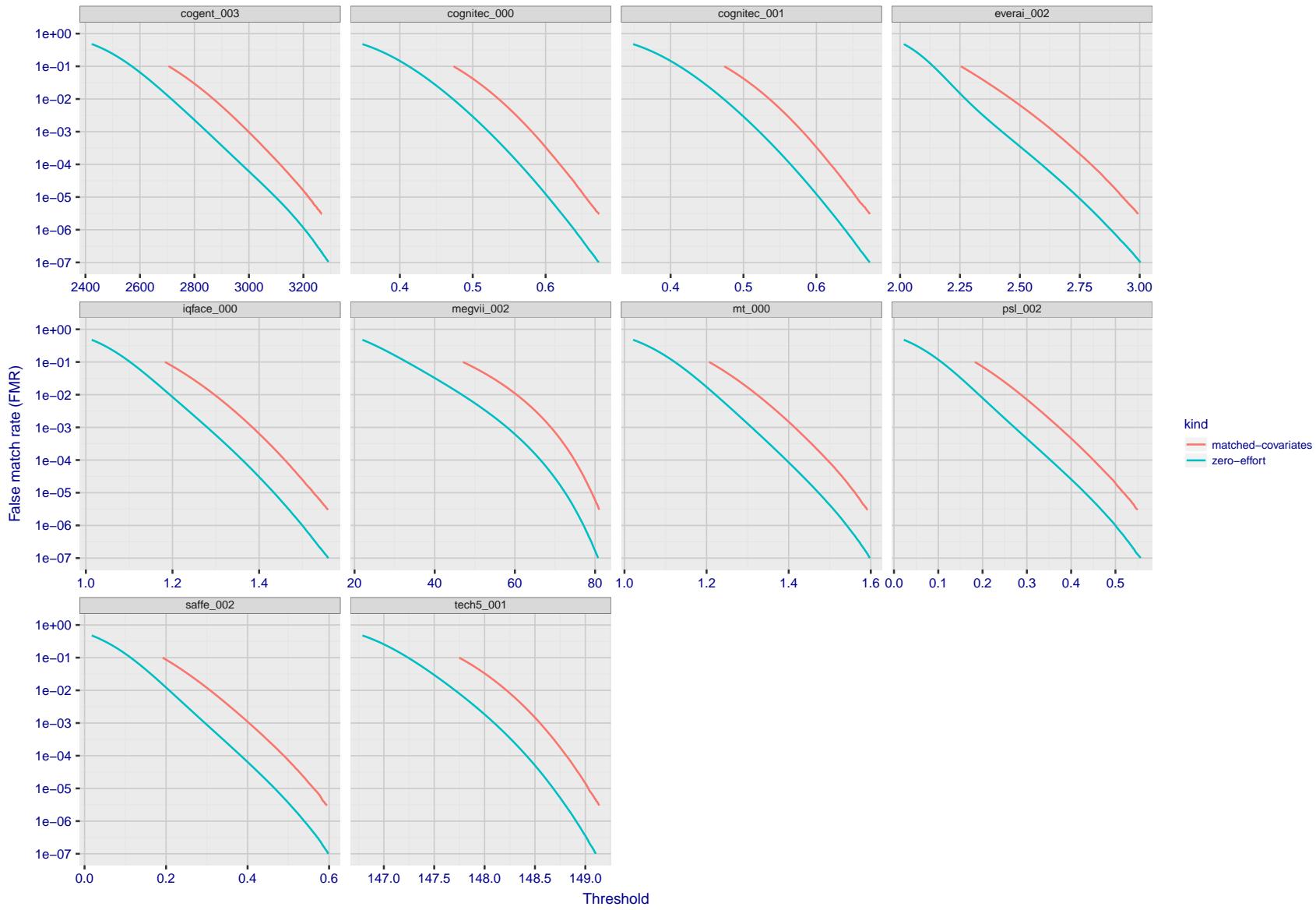


Figure 64: For the visa images, the false match calibration curves show FMR vs. threshold,  $T$ . The blue (lower) curves are for zero-effort impostors (i.e. comparing all images against all). The red (upper) curves are for persons of the same-sex, same-age, and same national-origin. This shows that FMR is underestimated (by a factor of 10 or more) by using a zero-effort impostor calculation to calibrate  $T$ . As shown later (sec. 3.6), FMR is higher for demographic-matched impostors.

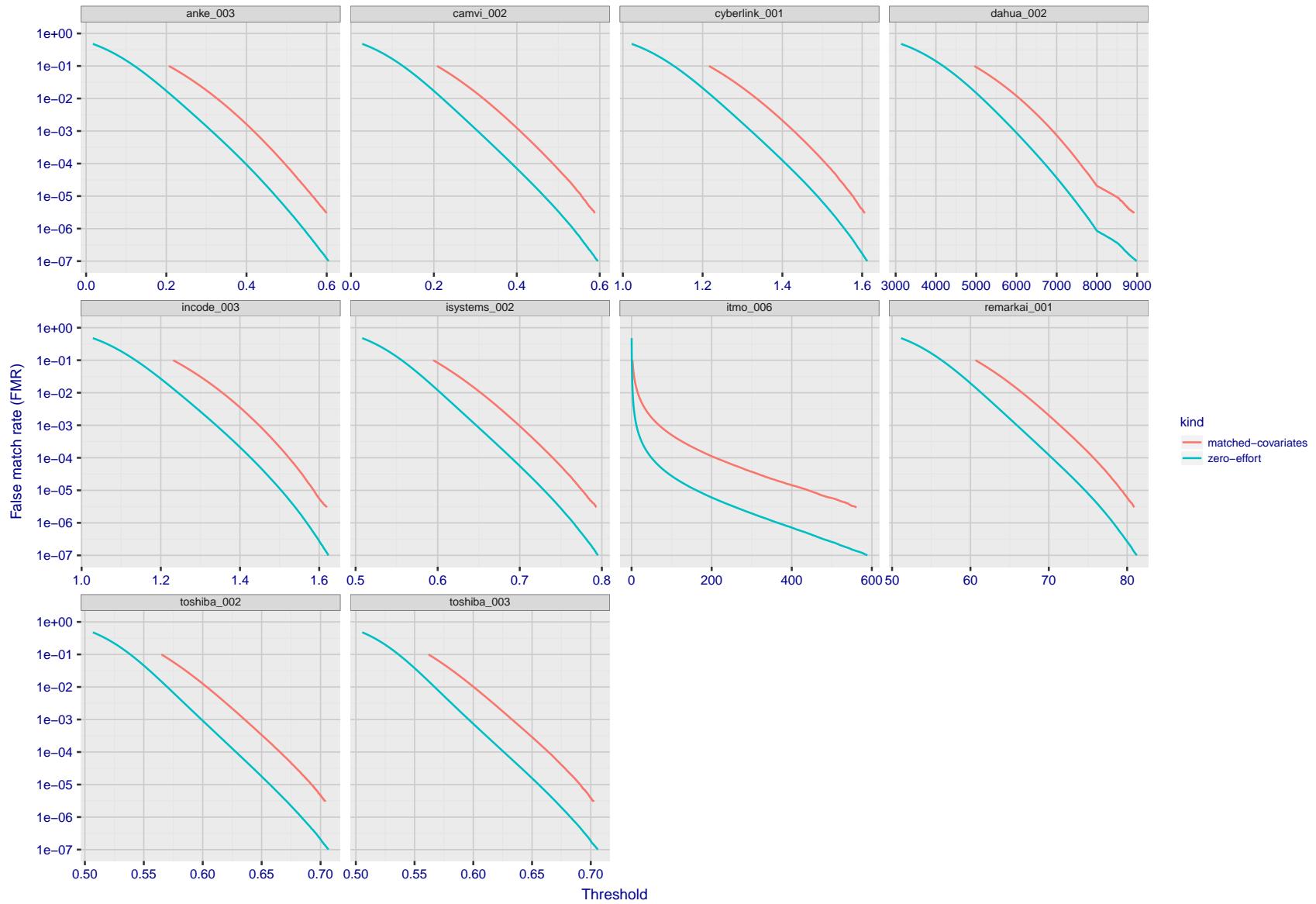


Figure 65: For the visa images, the false match calibration curves show FMR vs. threshold,  $T$ . The blue (lower) curves are for zero-effort impostors (i.e. comparing all images against all). The red (upper) curves are for persons of the same-sex, same-age, and same national-origin. This shows that FMR is underestimated (by a factor of 10 or more) by using a zero-effort impostor calculation to calibrate  $T$ . As shown later (sec. 3.6), FMR is higher for demographic-matched impostors.

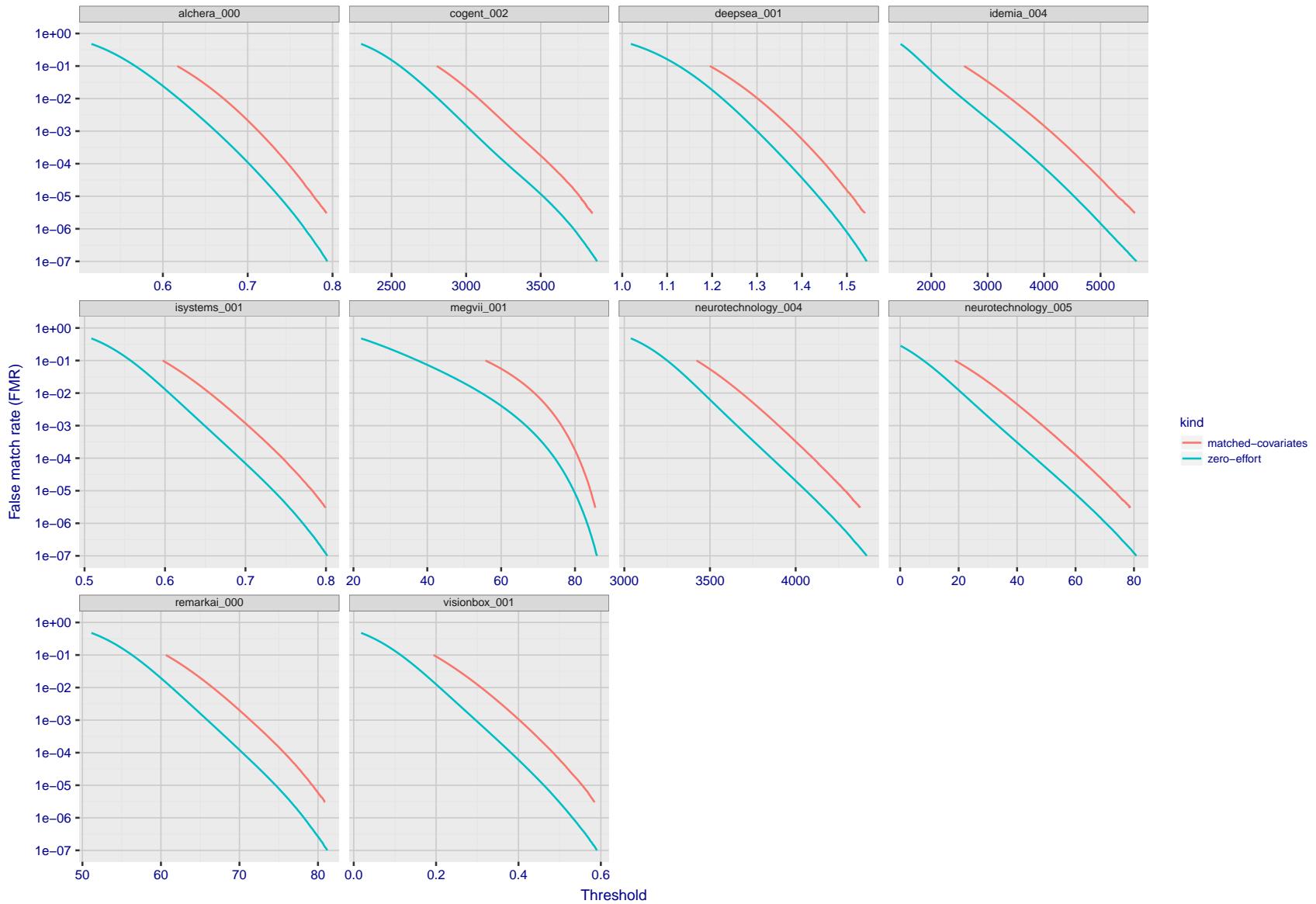


Figure 66: For the visa images, the false match calibration curves show FMR vs. threshold,  $T$ . The blue (lower) curves are for zero-effort impostors (i.e. comparing all images against all). The red (upper) curves are for persons of the same-sex, same-age, and same national-origin. This shows that FMR is underestimated (by a factor of 10 or more) by using a zero-effort impostor calculation to calibrate  $T$ . As shown later (sec. 3.6), FMR is higher for demographic-matched impostors.

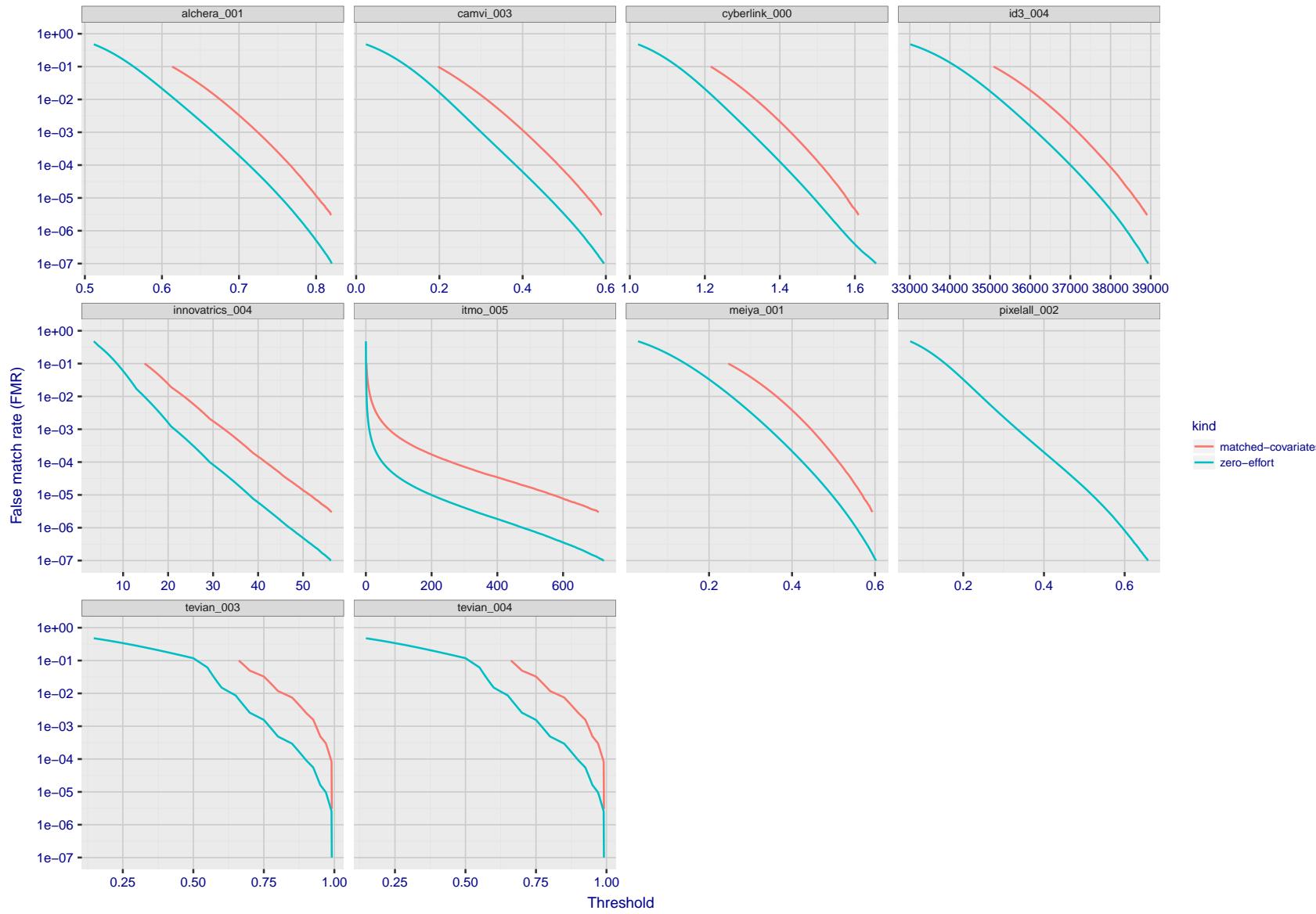


Figure 67: For the visa images, the false match calibration curves show FMR vs. threshold,  $T$ . The blue (lower) curves are for zero-effort impostors (i.e. comparing all images against all). The red (upper) curves are for persons of the same-sex, same-age, and same national-origin. This shows that FMR is underestimated (by a factor of 10 or more) by using a zero-effort impostor calculation to calibrate  $T$ . As shown later (sec. 3.6), FMR is higher for demographic-matched impostors.

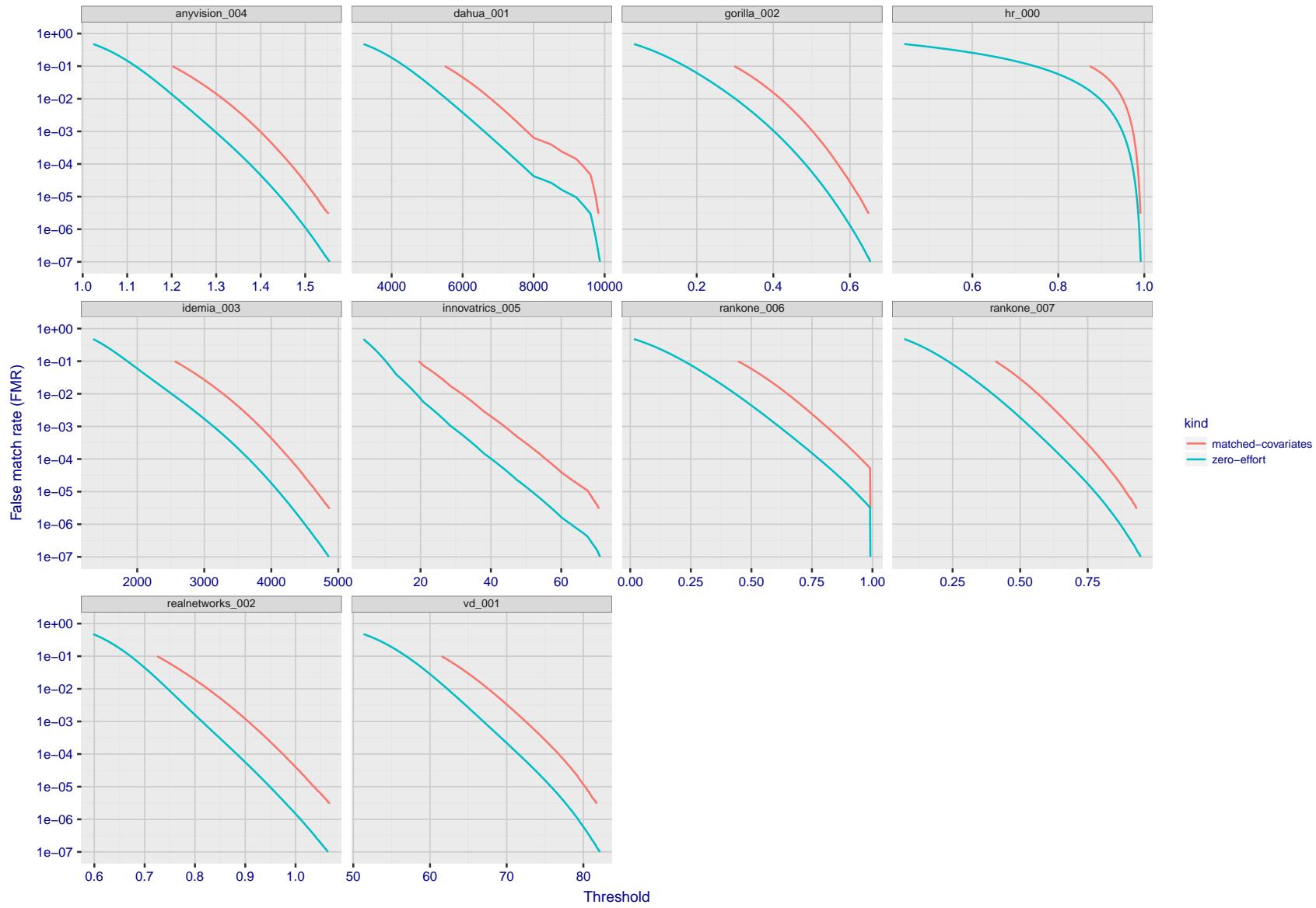


Figure 68: For the visa images, the false match calibration curves show FMR vs. threshold,  $T$ . The blue (lower) curves are for zero-effort impostors (i.e. comparing all images against all). The red (upper) curves are for persons of the same-sex, same-age, and same national-origin. This shows that FMR is underestimated (by a factor of 10 or more) by using a zero-effort impostor calculation to calibrate  $T$ . As shown later (sec. 3.6), FMR is higher for demographic-matched impostors.

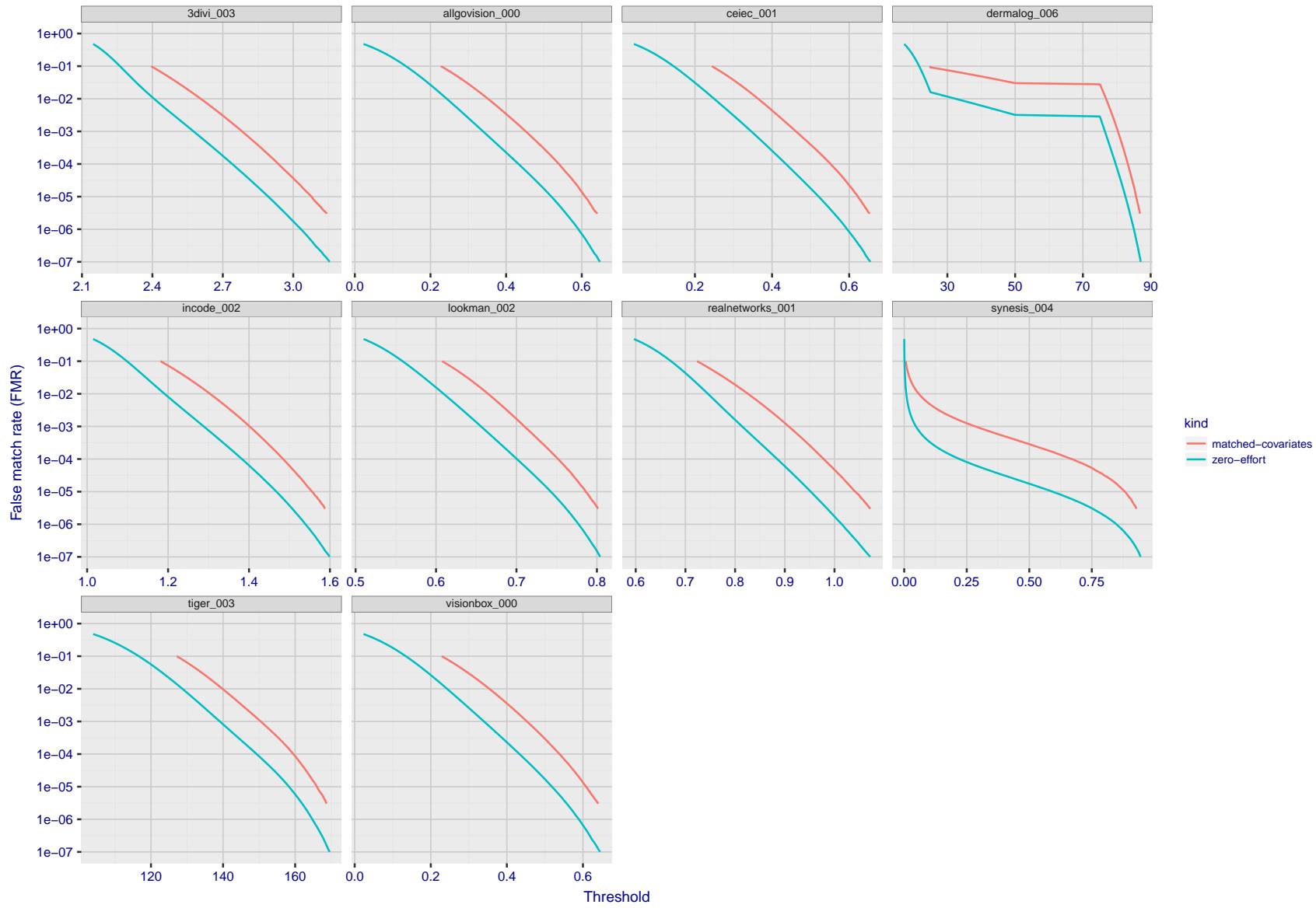


Figure 69: For the visa images, the false match calibration curves show FMR vs. threshold,  $T$ . The blue (lower) curves are for zero-effort impostors (i.e. comparing all images against all). The red (upper) curves are for persons of the same-sex, same-age, and same national-origin. This shows that FMR is underestimated (by a factor of 10 or more) by using a zero-effort impostor calculation to calibrate  $T$ . As shown later (sec. 3.6), FMR is higher for demographic-matched impostors.

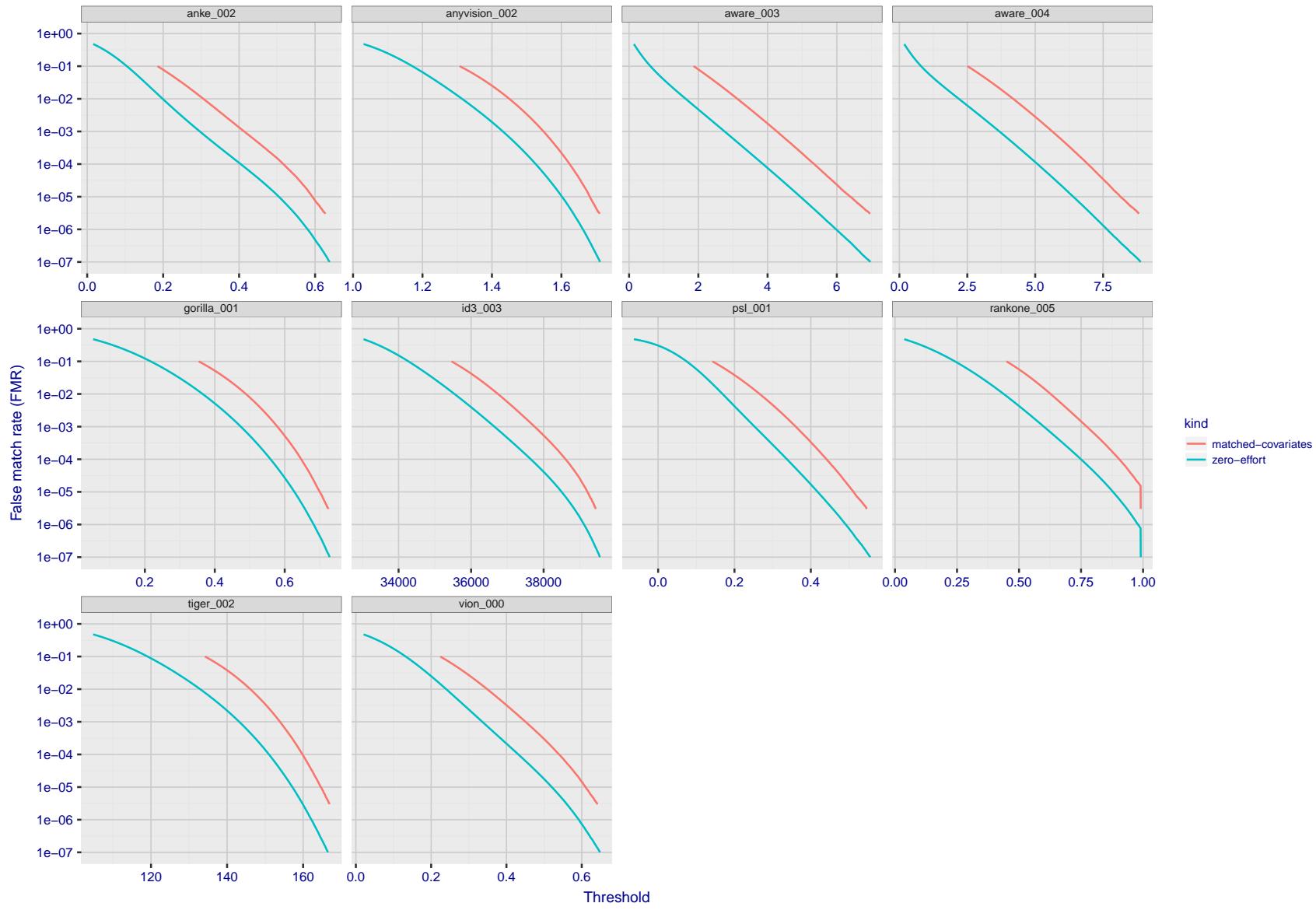


Figure 70: For the visa images, the false match calibration curves show FMR vs. threshold,  $T$ . The blue (lower) curves are for zero-effort impostors (i.e. comparing all images against all). The red (upper) curves are for persons of the same-sex, same-age, and same national-origin. This shows that FMR is underestimated (by a factor of 10 or more) by using a zero-effort impostor calculation to calibrate  $T$ . As shown later (sec. 3.6), FMR is higher for demographic-matched impostors.

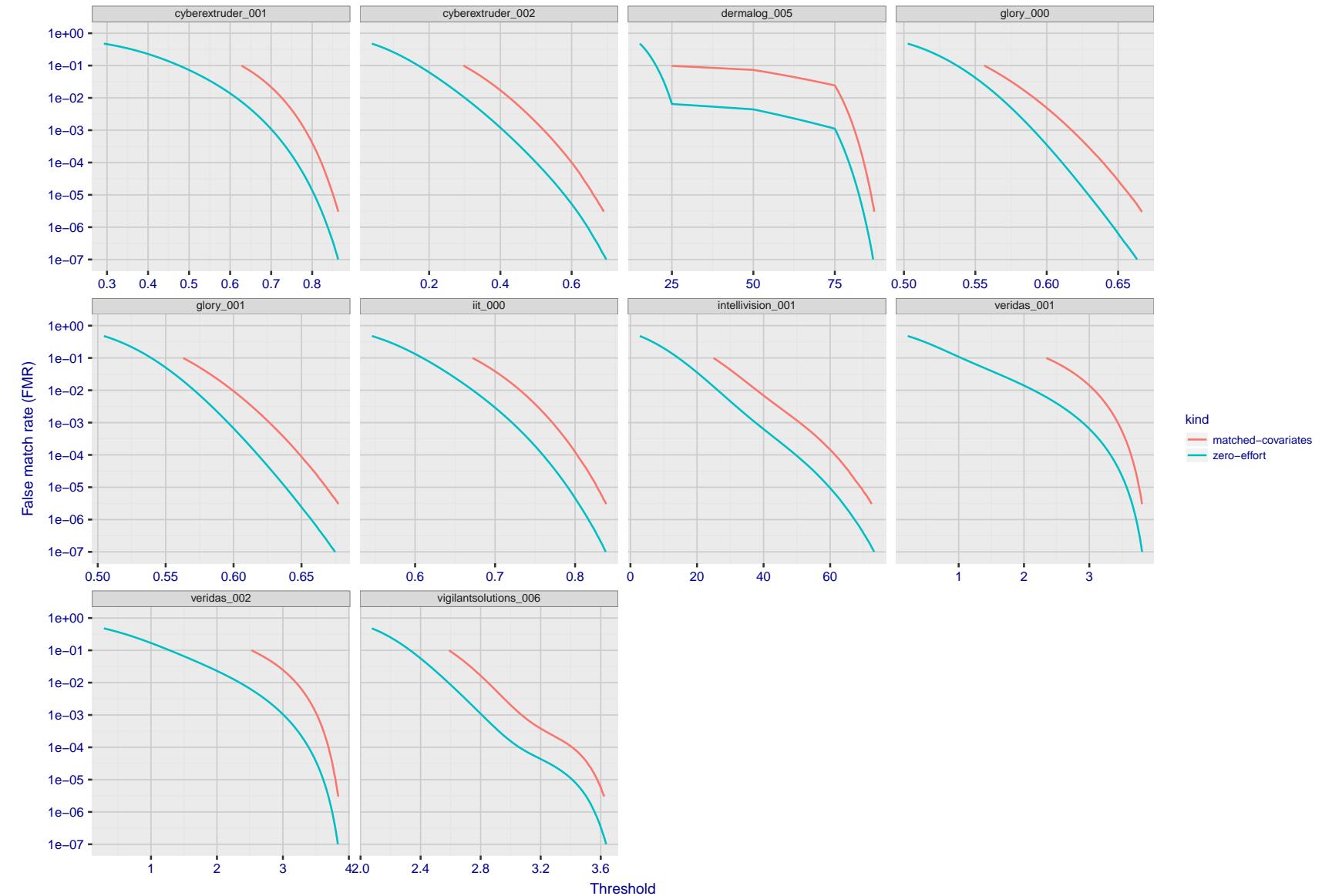


Figure 71: For the visa images, the false match calibration curves show FMR vs. threshold,  $T$ . The blue (lower) curves are for zero-effort impostors (i.e. comparing all images against all). The red (upper) curves are for persons of the same-sex, same-age, and same national-origin. This shows that FMR is underestimated (by a factor of 10 or more) by using a zero-effort impostor calculation to calibrate  $T$ . As shown later (sec. 3.6), FMR is higher for demographic-matched impostors.

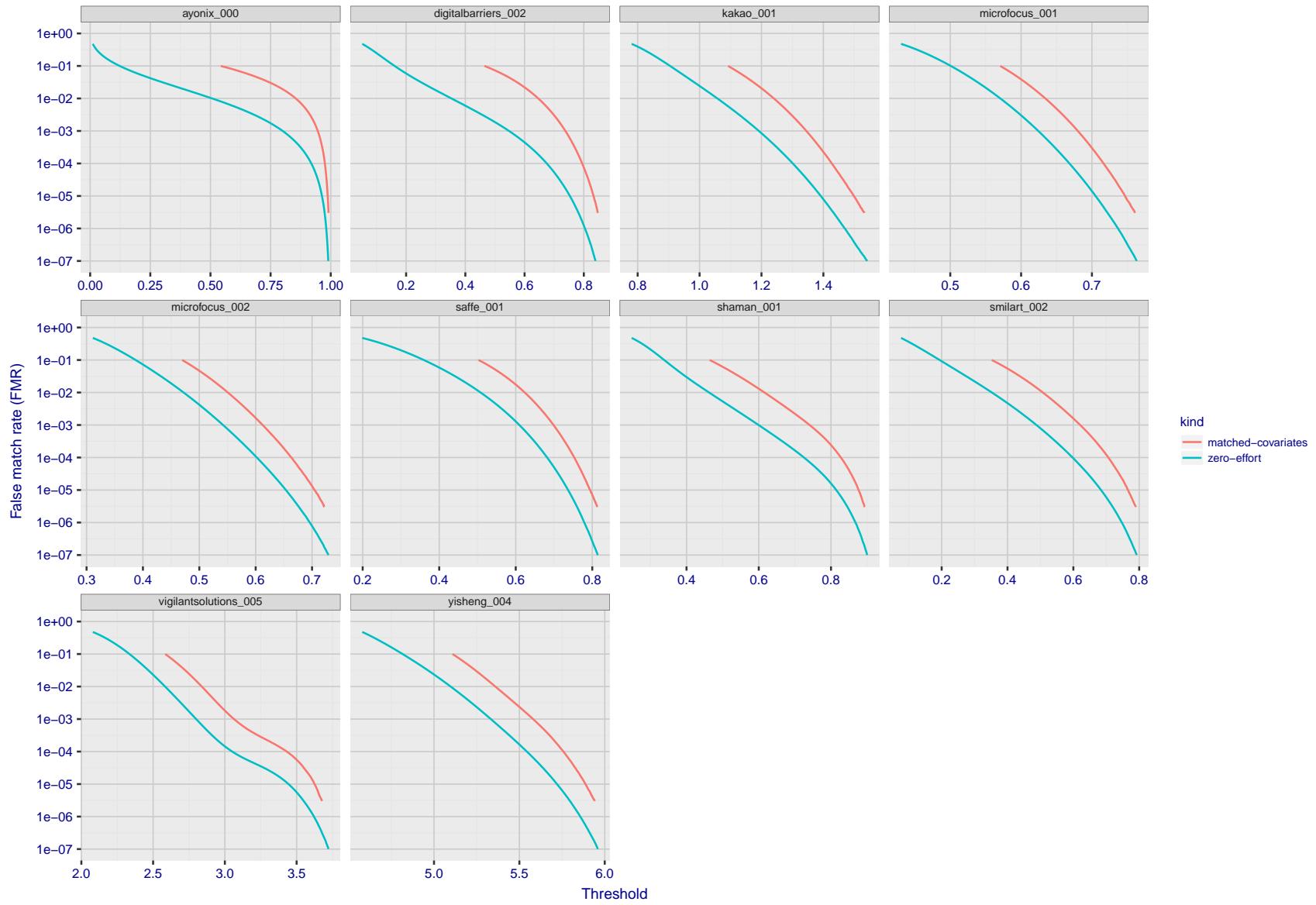


Figure 72: For the visa images, the false match calibration curves show FMR vs. threshold,  $T$ . The blue (lower) curves are for zero-effort impostors (i.e. comparing all images against all). The red (upper) curves are for persons of the same-sex, same-age, and same national-origin. This shows that FMR is underestimated (by a factor of 10 or more) by using a zero-effort impostor calculation to calibrate  $T$ . As shown later (sec. 3.6), FMR is higher for demographic-matched impostors.

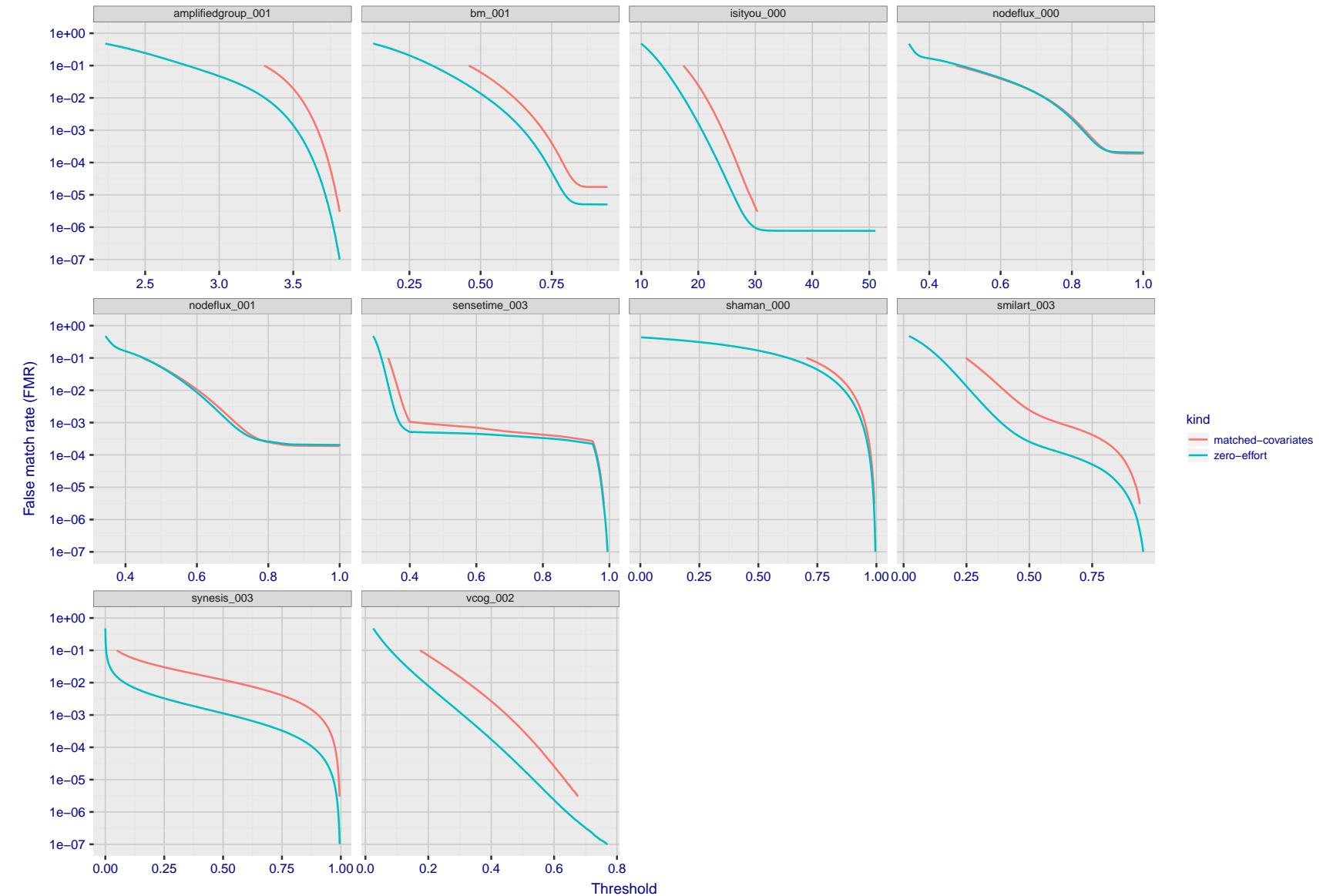


Figure 73: For the visa images, the false match calibration curves show FMR vs. threshold,  $T$ . The blue (lower) curves are for zero-effort impostors (i.e. comparing all images against all). The red (upper) curves are for persons of the same-sex, same-age, and same national-origin. This shows that FMR is underestimated (by a factor of 10 or more) by using a zero-effort impostor calculation to calibrate  $T$ . As shown later (sec. 3.6), FMR is higher for demographic-matched impostors.

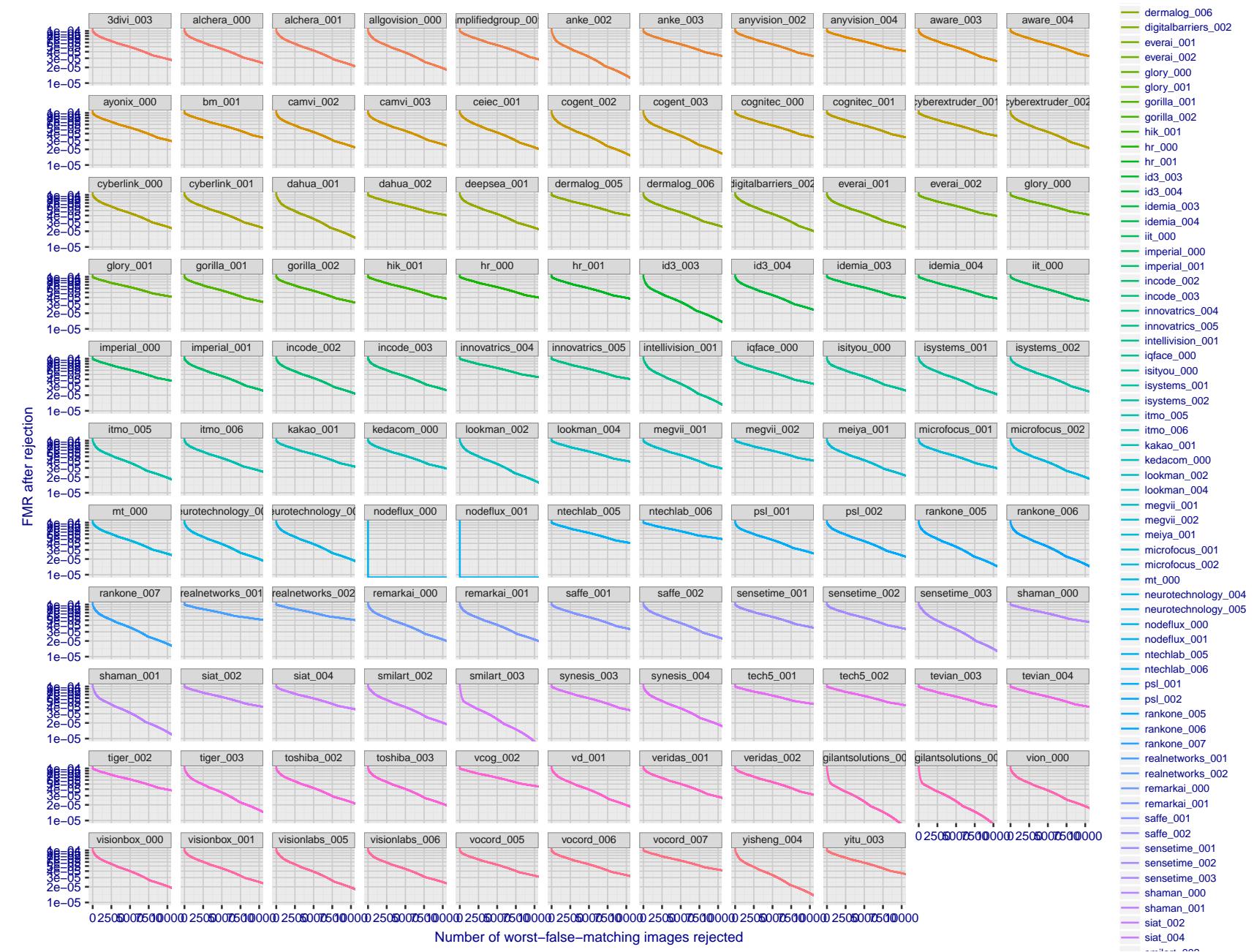


Figure 74: For the visa images, the curves show how false matches are concentrated in certain images. Specifically each line plots  $FMR(k)$  with  $k$  the number of images rejected in decreasing order of how many false matches that image was involved in.  $FMR(0) = 10^{-4}$ . In terms of the biometric zoo, the most “wolf-ish” images are rejected first i.e. those enrollment or verification images most often involved in false matches. A flatter response is considered superior. A steeply descending response indicates that certain kinds of images false match against others, e.g. if hypothetically images of men with particular mustaches would falsely match others.

## 3.5 Genuine distribution stability

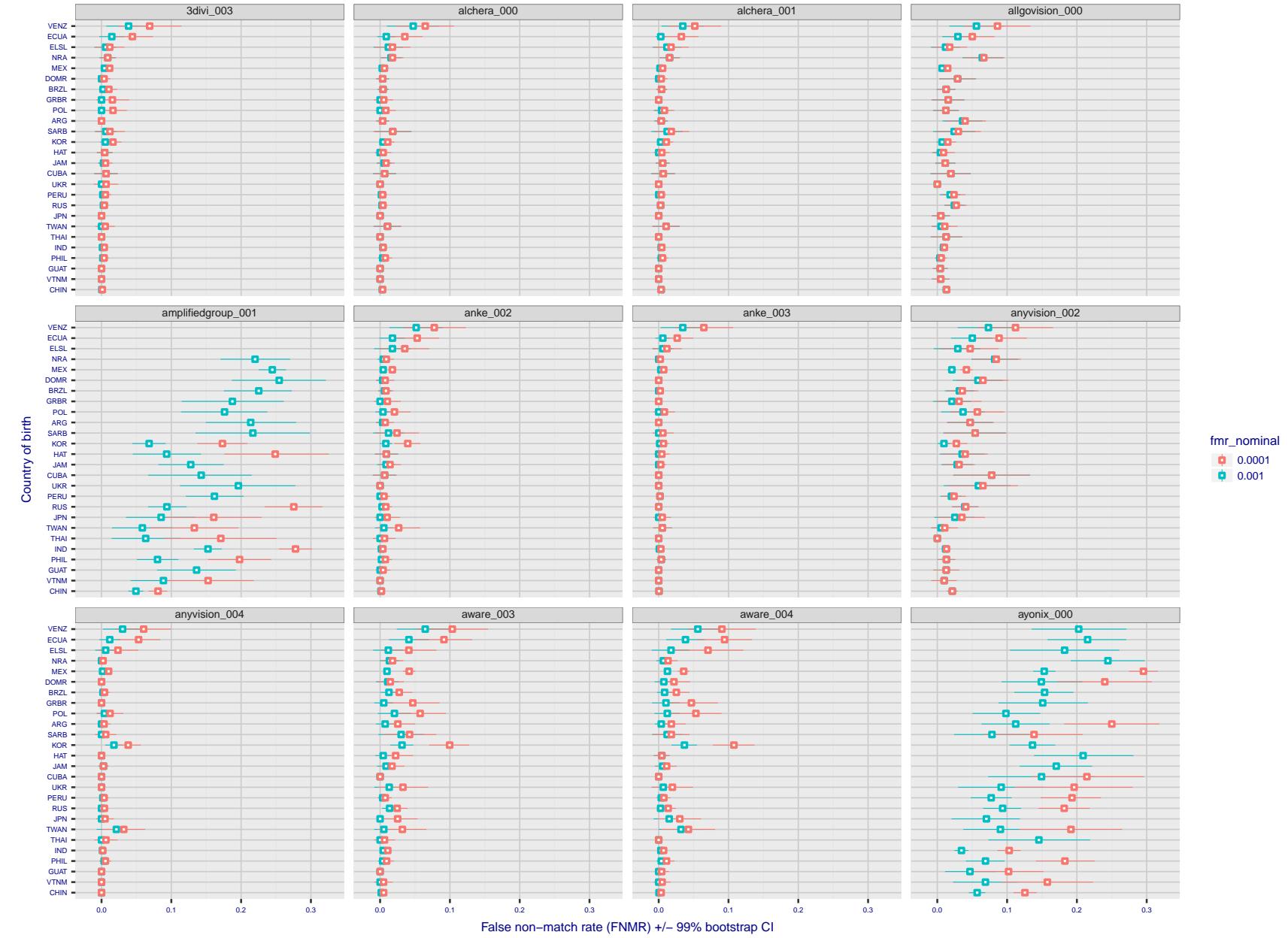
### 3.5.1 Effect of birth place on the genuine distribution

**Background:** Both skin tone and bone structure vary geographically. Prior studies have reported variations in FNMR and FMR.

**Goal:** To measure false non-match rate (FNMR) variation with country of birth.

**Methods:** Thresholds are determined that give  $FMR = \{0.001, 0.0001\}$  over the entire impostor set. Then FNMR is measured over 1000 bootstrap replications of the genuine scores. Only those countries with at least 140 individuals are included in the analysis.

**Results:** Figure 84 shows FNMR by country of birth for the two thresholds.



FNMR(T)  
FMR(T)  
"False non-match rate"  
"False match rate"

Figure 75: For the visa images, the dots show FNMR by country of birth for two globally set operating thresholds corresponding to  $FMR = \{0.001, 0.0001\}$  computed over all on the order of  $10^{10}$  impostor scores. The FMR in each bin will vary also - see subsequent impostor heatmaps in sec. 3.6.1. The figures shows an order of magnitude variation in FNMR across country of birth; these effects are likely due quality variations, then demographics like age and race. The error rates in some cases are zero, and in others the DET is flat so the error rates at the two thresholds are identical. The lines span 1% and 99% of bootstrap replicated FNMR estimates.

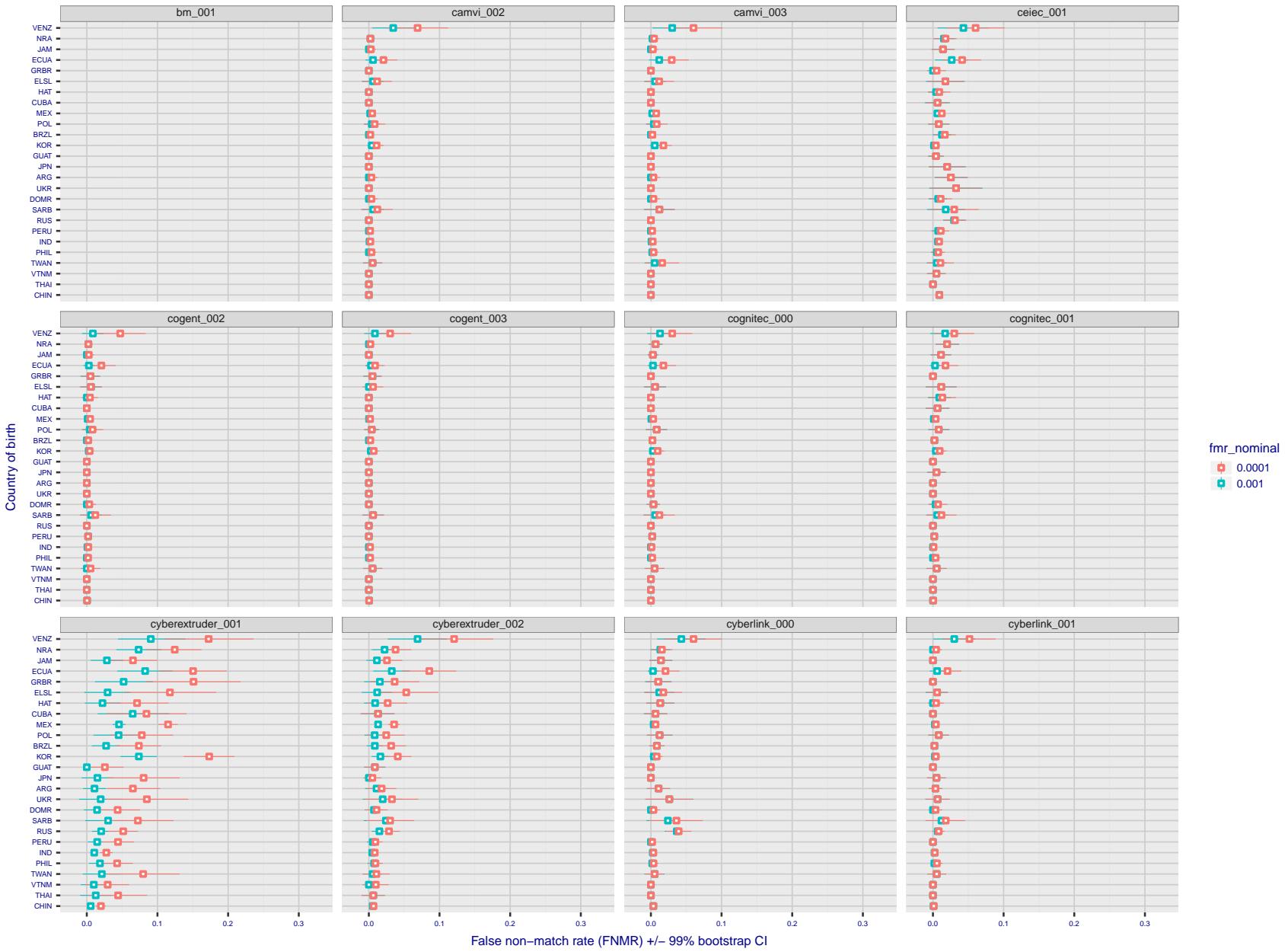


Figure 76: For the visa images, the dots show FNMR by country of birth for two globally set operating thresholds corresponding to  $FMR = \{0.001, 0.0001\}$  computed over all on the order of  $10^{10}$  impostor scores. The FMR in each bin will vary also - see subsequent impostor heatmaps in sec. 3.6.1. The figures shows an order of magnitude variation in FNMR across country of birth; these effects are likely due quality variations, then demographics like age and race. The error rates in some cases are zero, and in others the DET is flat so the error rates at the two thresholds are identical. The lines span 1% and 99% of bootstrap replicated FNMR estimates.

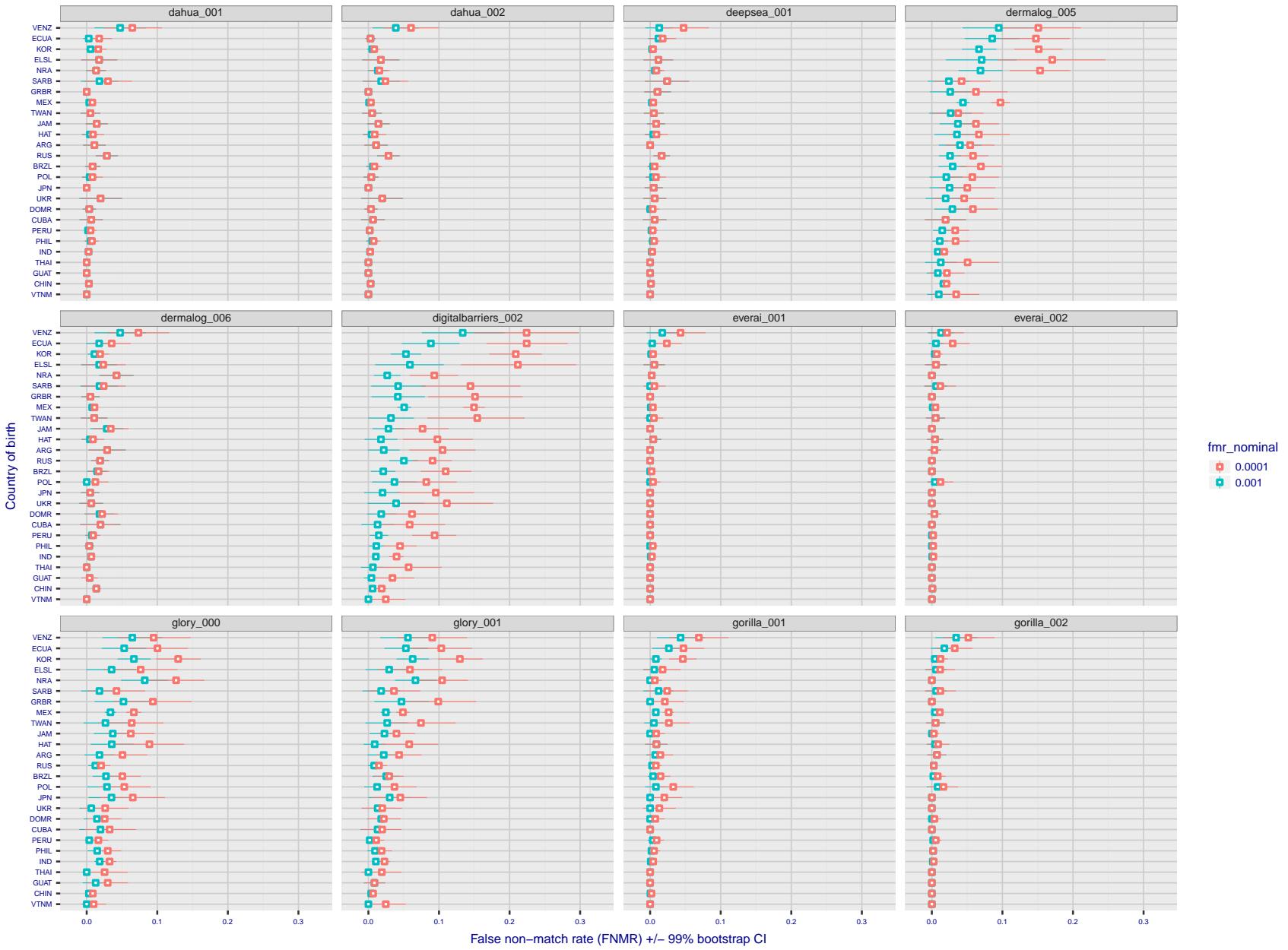


Figure 77: For the visa images, the dots show FNMR by country of birth for two globally set operating thresholds corresponding to  $FMR = \{0.001, 0.0001\}$  computed over all on the order of  $10^{10}$  impostor scores. The FMR in each bin will vary also - see subsequent impostor heatmaps in sec. 3.6.1. The figures shows an order of magnitude variation in FNMR across country of birth; these effects are likely due quality variations, then demographics like age and race. The error rates in some cases are zero, and in others the DET is flat so the error rates at the two thresholds are identical. The lines span 1% and 99% of bootstrap replicated FNMR estimates.

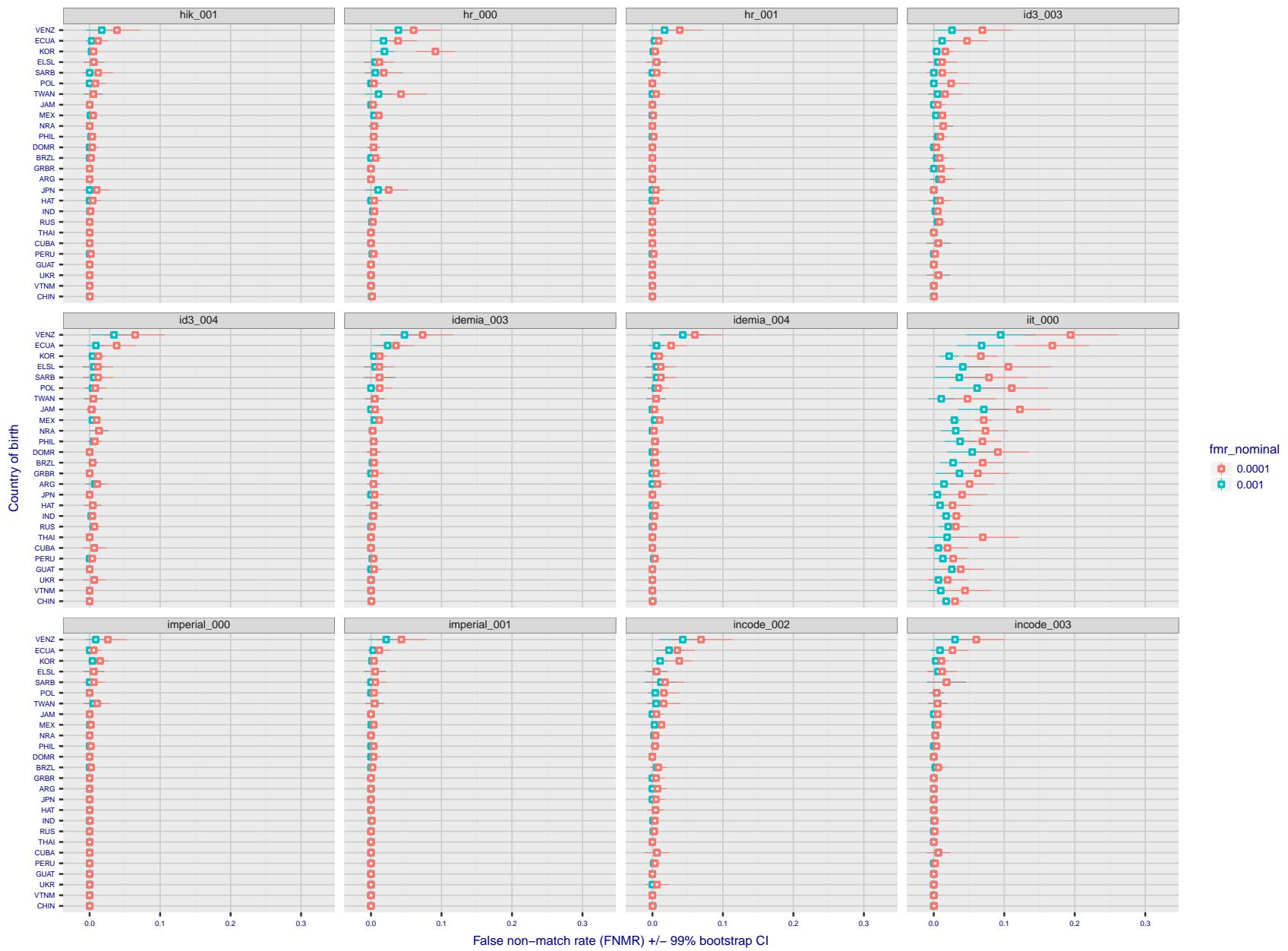


Figure 78: For the visa images, the dots show FNMR by country of birth for two globally set operating thresholds corresponding to  $FMR = \{0.001, 0.0001\}$  computed over all on the order of  $10^{10}$  impostor scores. The FMR in each bin will vary also - see subsequent impostor heatmaps in sec. 3.6.1. The figures shows an order of magnitude variation in FNMR across country of birth; these effects are likely due quality variations, then demographics like age and race. The error rates in some cases are zero, and in others the DET is flat so the error rates at the two thresholds are identical. The lines span 1% and 99% of bootstrap replicated FNMR estimates.

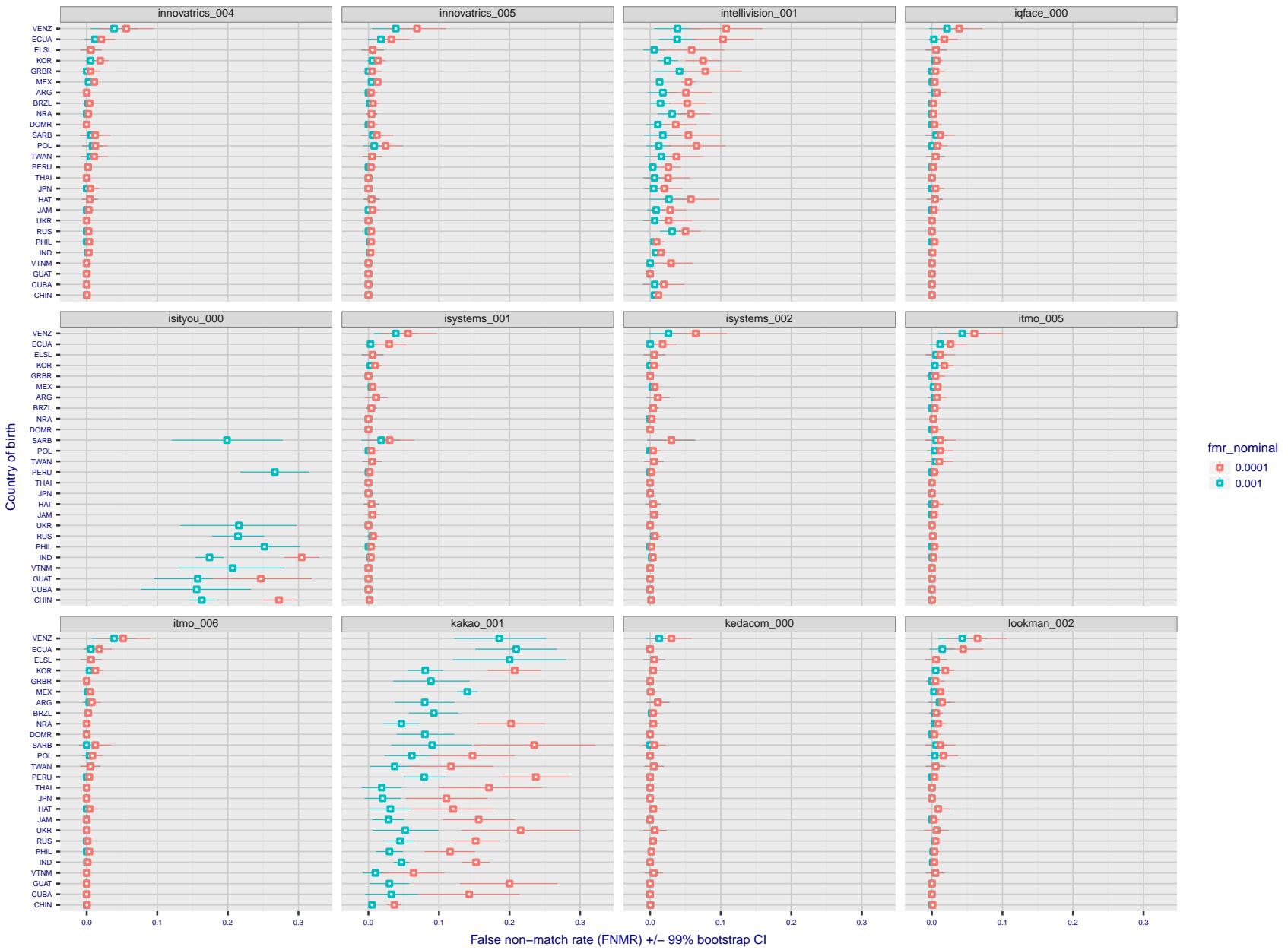


Figure 79: For the visa images, the dots show FNMR by country of birth for two globally set operating thresholds corresponding to  $FMR = \{0.001, 0.0001\}$  computed over all on the order of  $10^{10}$  impostor scores. The FMR in each bin will vary also - see subsequent impostor heatmaps in sec. 3.6.1. The figures shows an order of magnitude variation in FNMR across country of birth; these effects are likely due quality variations, then demographics like age and race. The error rates in some cases are zero, and in others the DET is flat so the error rates at the two thresholds are identical. The lines span 1% and 99% of bootstrap replicated FNMR estimates.

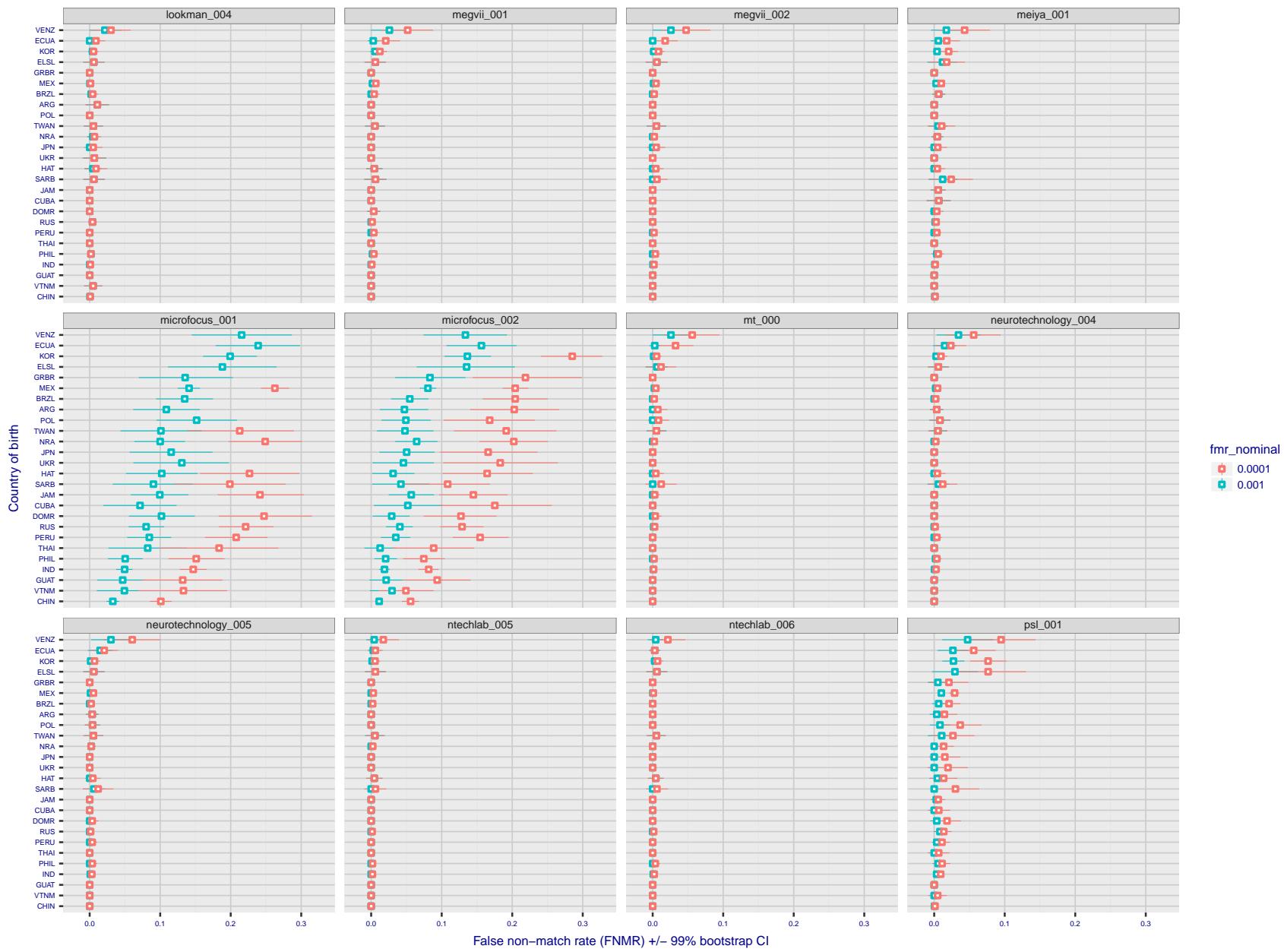


Figure 80: For the visa images, the dots show FNMR by country of birth for two globally set operating thresholds corresponding to  $FMR = \{0.001, 0.0001\}$  computed over all on the order of  $10^{10}$  impostor scores. The FMR in each bin will vary also - see subsequent impostor heatmaps in sec. 3.6.1. The figures shows an order of magnitude variation in FNMR across country of birth; these effects are likely due quality variations, then demographics like age and race. The error rates in some cases are zero, and in others the DET is flat so the error rates at the two thresholds are identical. The lines span 1% and 99% of bootstrap replicated FNMR estimates.

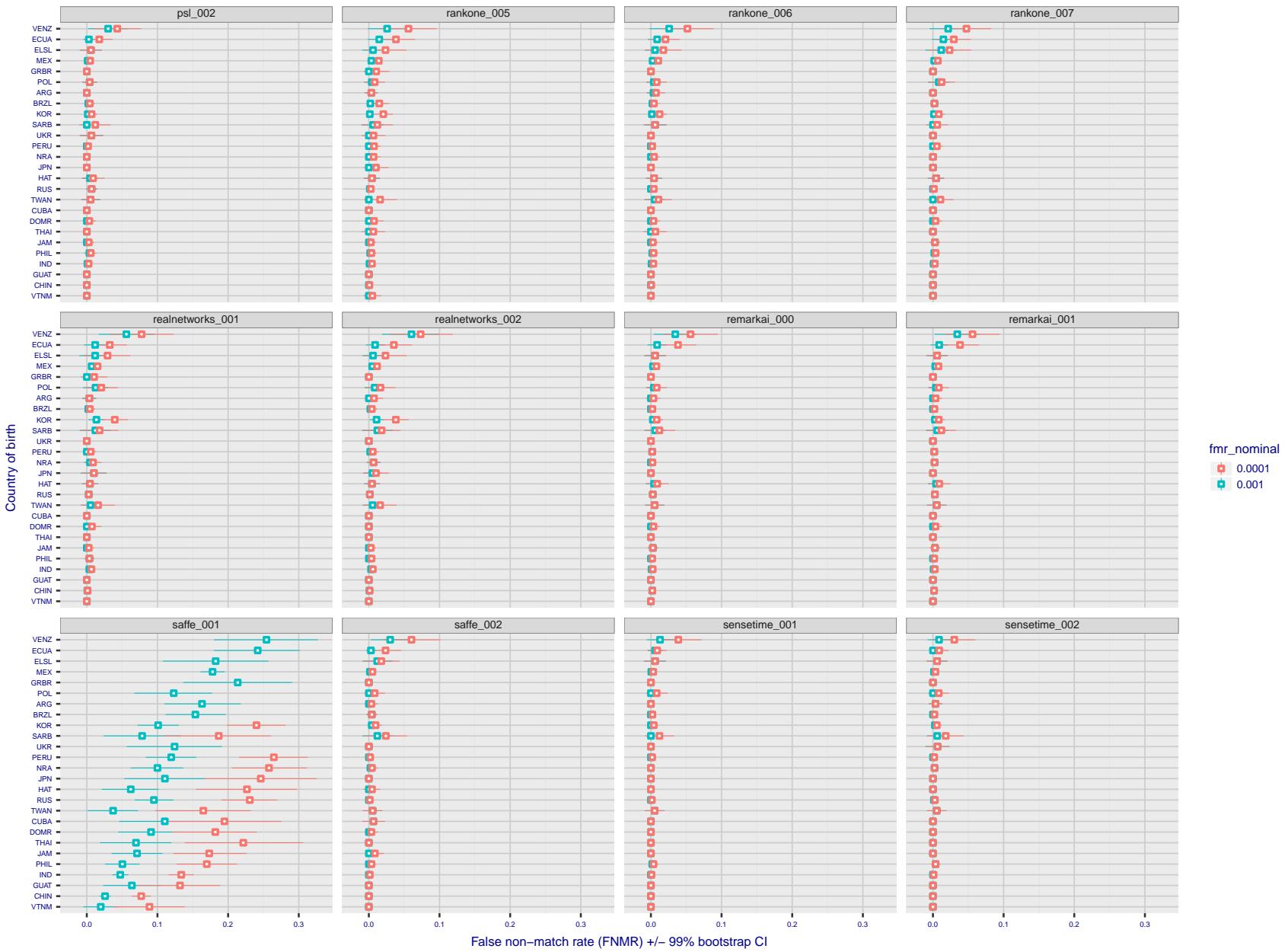


Figure 81: For the visa images, the dots show FNMR by country of birth for two globally set operating thresholds corresponding to  $FMR = \{0.001, 0.0001\}$  computed over all on the order of  $10^{10}$  impostor scores. The FMR in each bin will vary also - see subsequent impostor heatmaps in sec. 3.6.1. The figures shows an order of magnitude variation in FNMR across country of birth; these effects are likely due quality variations, then demographics like age and race. The error rates in some cases are zero, and in others the DET is flat so the error rates at the two thresholds are identical. The lines span 1% and 99% of bootstrap replicated FNMR estimates.

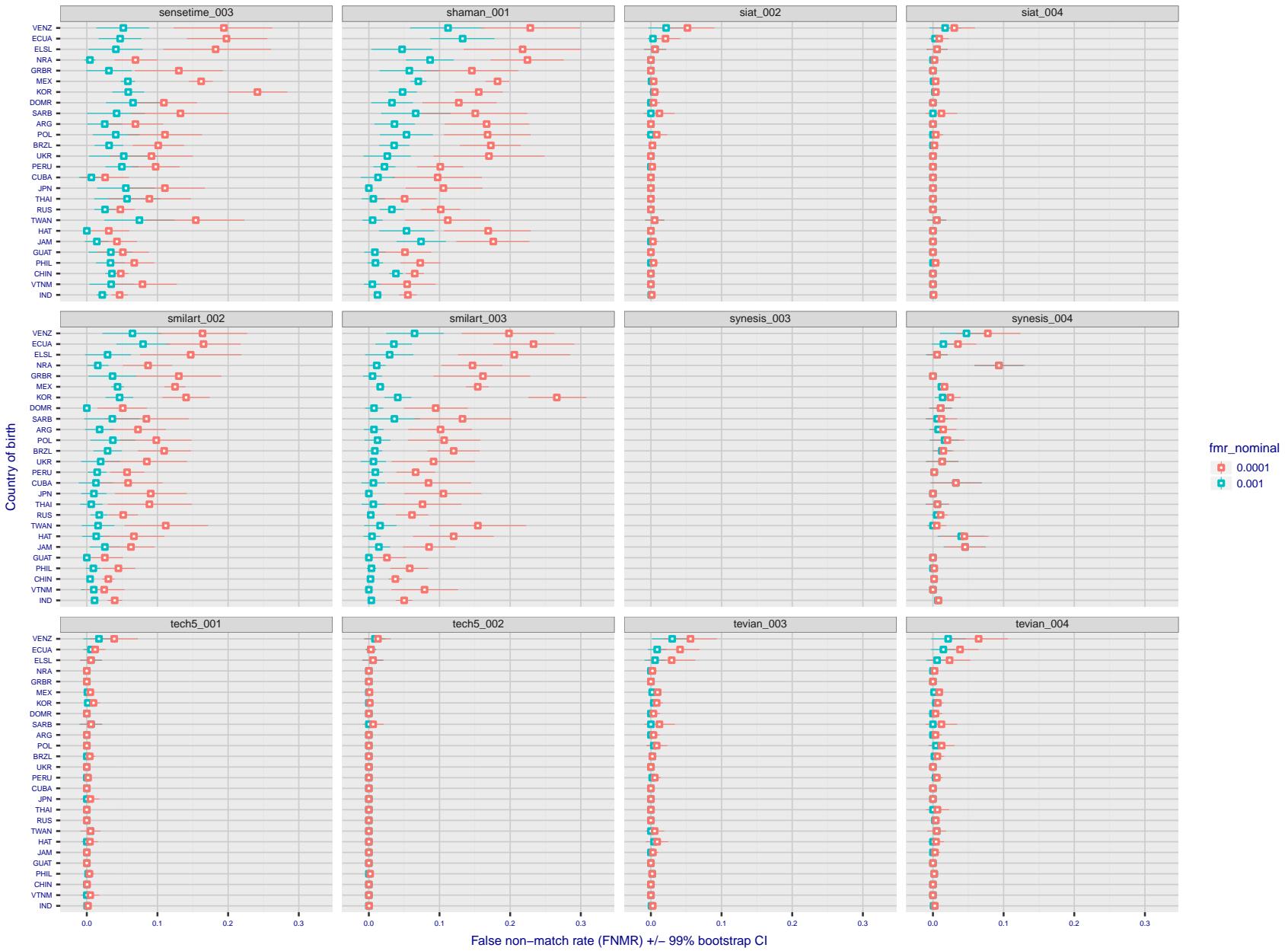


Figure 82: For the visa images, the dots show FNMR by country of birth for two globally set operating thresholds corresponding to  $FMR = \{0.001, 0.0001\}$  computed over all on the order of  $10^{10}$  impostor scores. The FMR in each bin will vary also - see subsequent impostor heatmaps in sec. 3.6.1. The figures shows an order of magnitude variation in FNMR across country of birth; these effects are likely due quality variations, then demographics like age and race. The error rates in some cases are zero, and in others the DET is flat so the error rates at the two thresholds are identical. The lines span 1% and 99% of bootstrap replicated FNMR estimates.

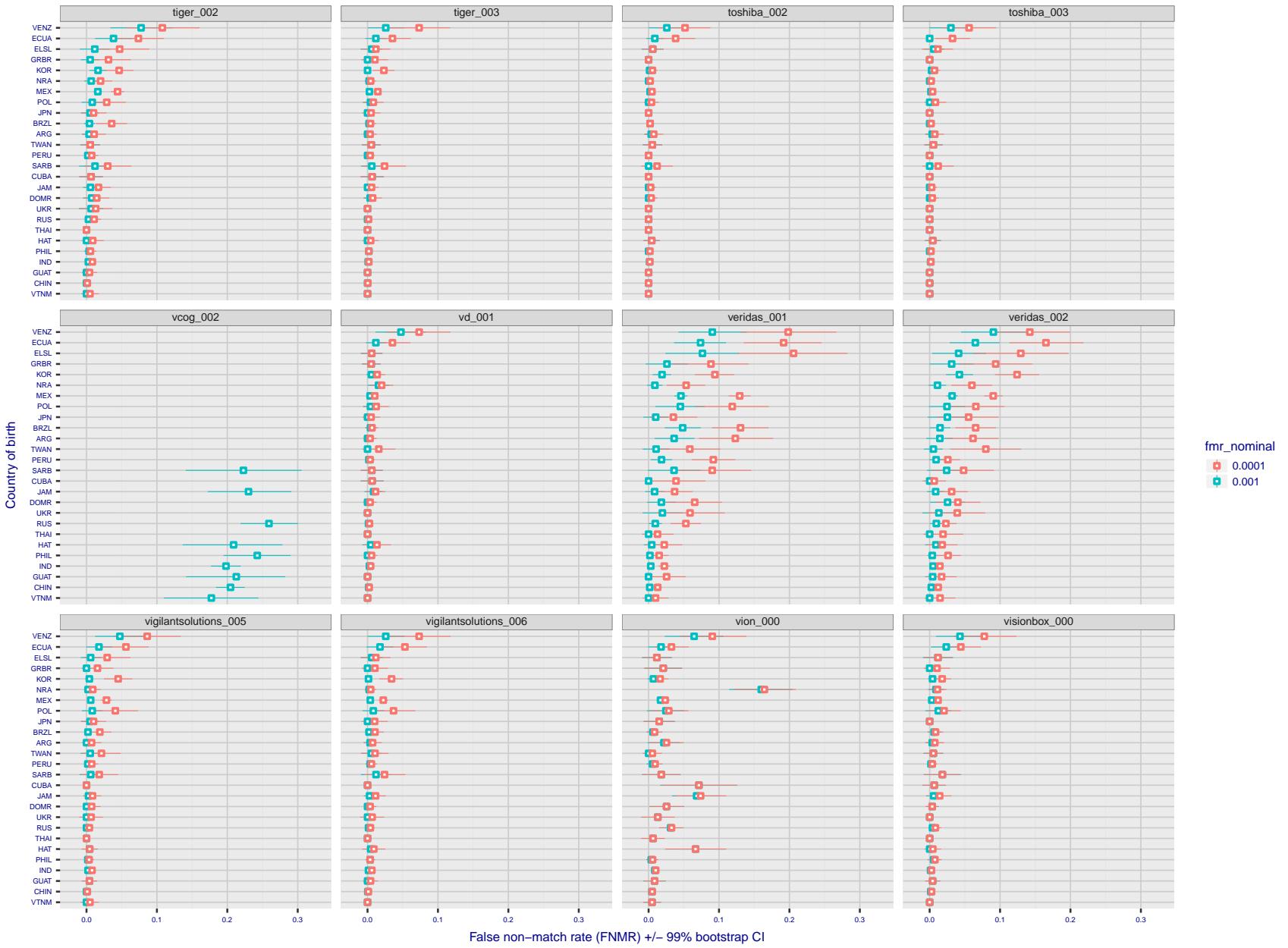


Figure 83: For the visa images, the dots show FNMR by country of birth for two globally set operating thresholds corresponding to  $FMR = \{0.001, 0.0001\}$  computed over all on the order of  $10^{10}$  impostor scores. The FMR in each bin will vary also - see subsequent impostor heatmaps in sec. 3.6.1. The figures shows an order of magnitude variation in FNMR across country of birth; these effects are likely due quality variations, then demographics like age and race. The error rates in some cases are zero, and in others the DET is flat so the error rates at the two thresholds are identical. The lines span 1% and 99% of bootstrap replicated FNMR estimates.

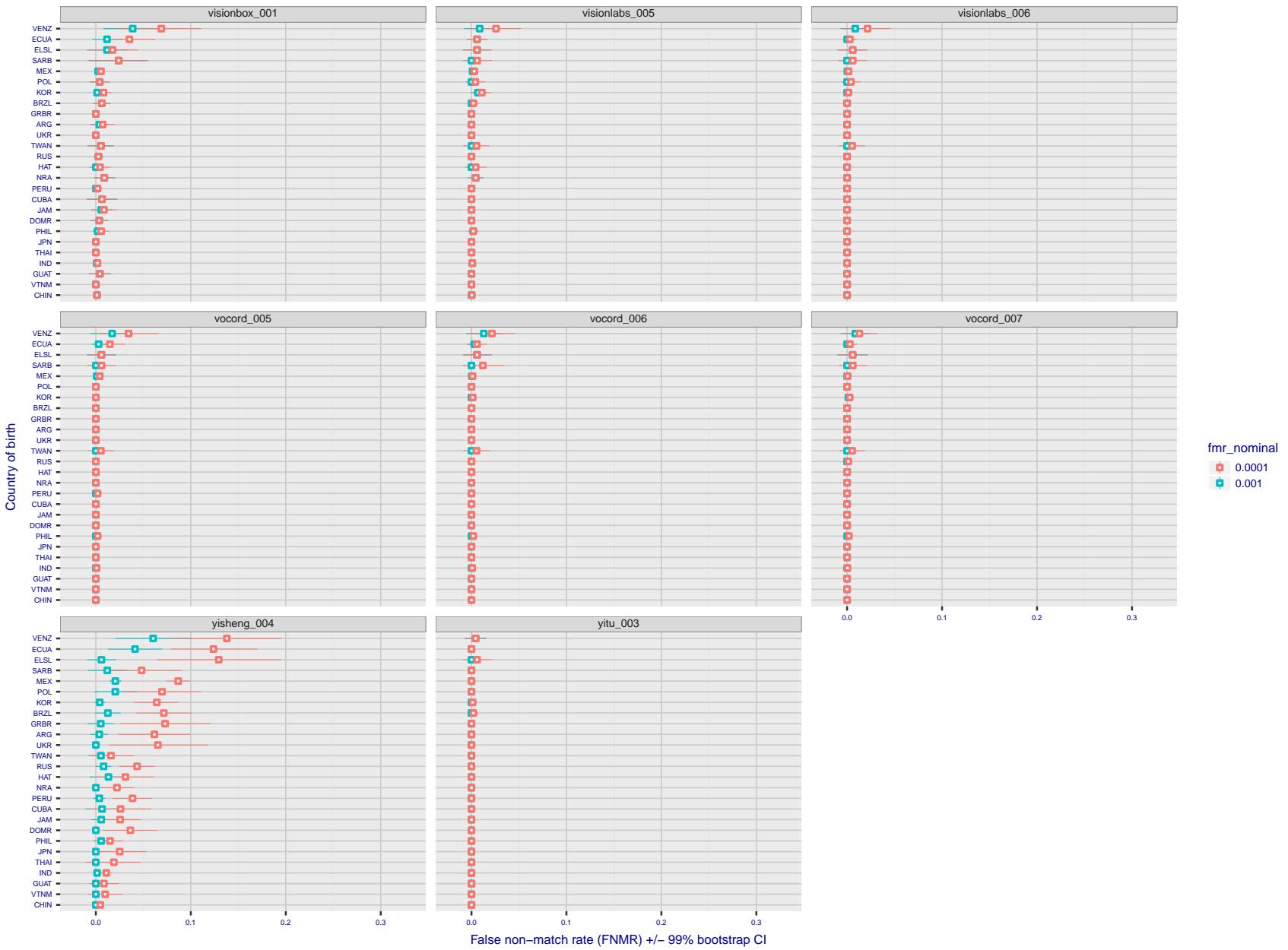


Figure 84: For the visa images, the dots show FNMR by country of birth for two globally set operating thresholds corresponding to  $FMR = \{0.001, 0.0001\}$  computed over all on the order of  $10^{10}$  impostor scores. The FMR in each bin will vary also - see subsequent impostor heatmaps in sec. 3.6.1. The figures shows an order of magnitude variation in FNMR across country of birth; these effects are likely due quality variations, then demographics like age and race. The error rates in some cases are zero, and in others the DET is flat so the error rates at the two thresholds are identical. The lines span 1% and 99% of bootstrap replicated FNMR estimates.

**Caveats:** The results may not relate to subject-specific properties. Instead they could reflect image-specific quality differences, which could occur due to collection protocol or software processing variations.

### 3.5.2 Effect of ageing

**Background:** Faces change appearance throughout life. This change gradually reduces similarity of a new image to an earlier image. Face recognition algorithms give reduced similarity scores and more frequent false rejections.

**Goal:** To quantify false non-match rates (FNMR) as a function of elapsed time in an adult population.

**Methods:** Using the mugshot images, a threshold is set to give FMR = 0.00001 over the entire impostor set. Then FNMR is measured over 1000 bootstrap replications of the genuine scores.

**Results:** For the visa images, Figure 92 shows how false non-match rates for genuine users, as a function of age group.

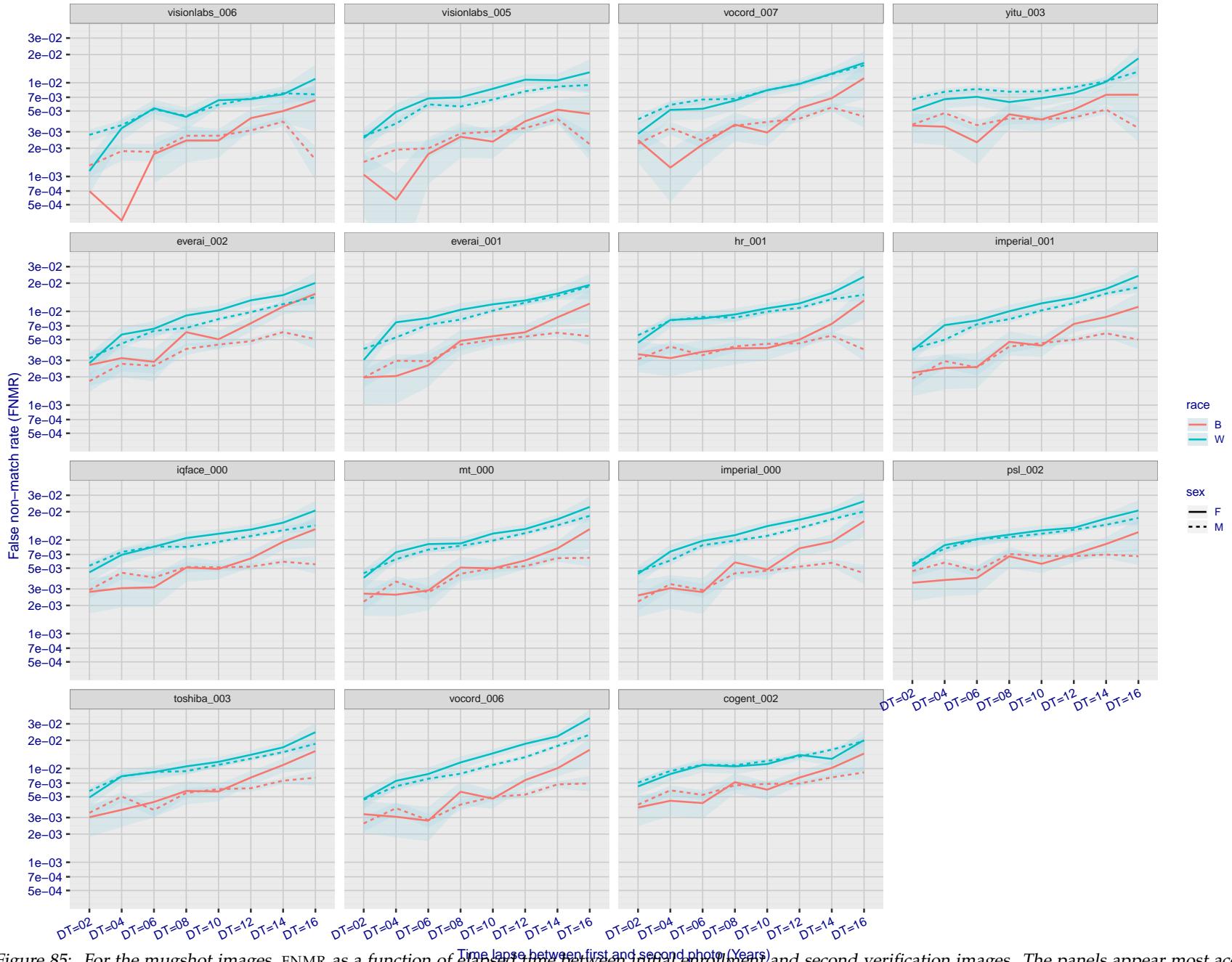


Figure 85: For the mugshot images, FNMR as a function of elapsed time between initial enrollment and second verification images. The panels appear most accurate first, and vertical scale changes on each page. The four traces correspond to images annotated with codes for black female, black male, white female, white male. The threshold is fixed for each algorithm to give  $FMR = 0.00001$  over all ( $10^8$ ) impostor comparisons. For short time-lapses, the most accurate algorithms give very few errors ( $FNMR < 0.001$ ) so that the uncertainty estimates are high.

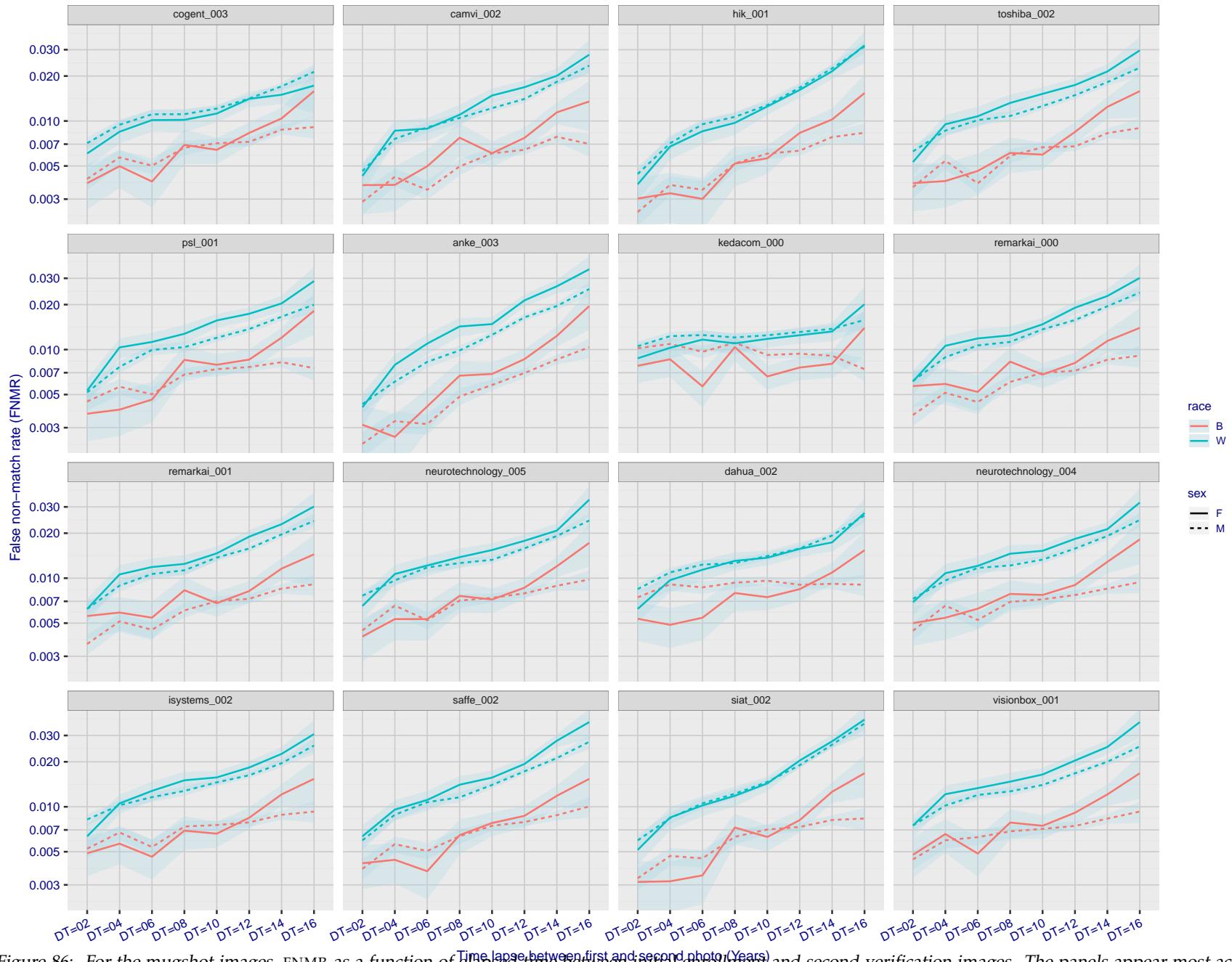


Figure 86: For the mugshot images, FNMR as a function of elapsed time between initial enrollment and second verification images. The panels appear most accurate first, and vertical scale changes on each page. The four traces correspond to images annotated with codes for black female, black male, white female, white male. The threshold is fixed for each algorithm to give FMR = 0.00001 over all ( $10^8$ ) impostor comparisons. For short time-lapses, the most accurate algorithms give very few errors (FNMR < 0.001) so that the uncertainty estimates are high.

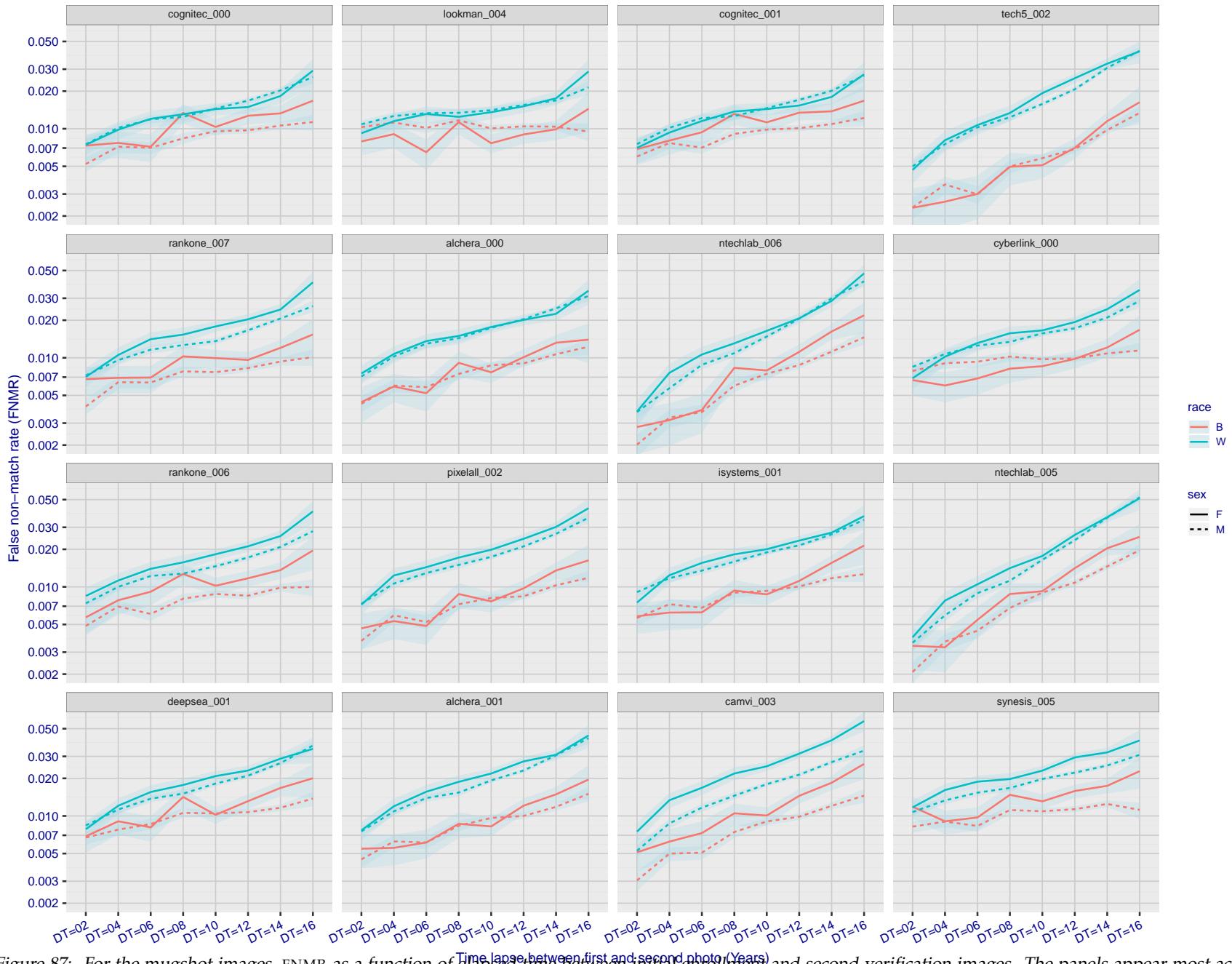
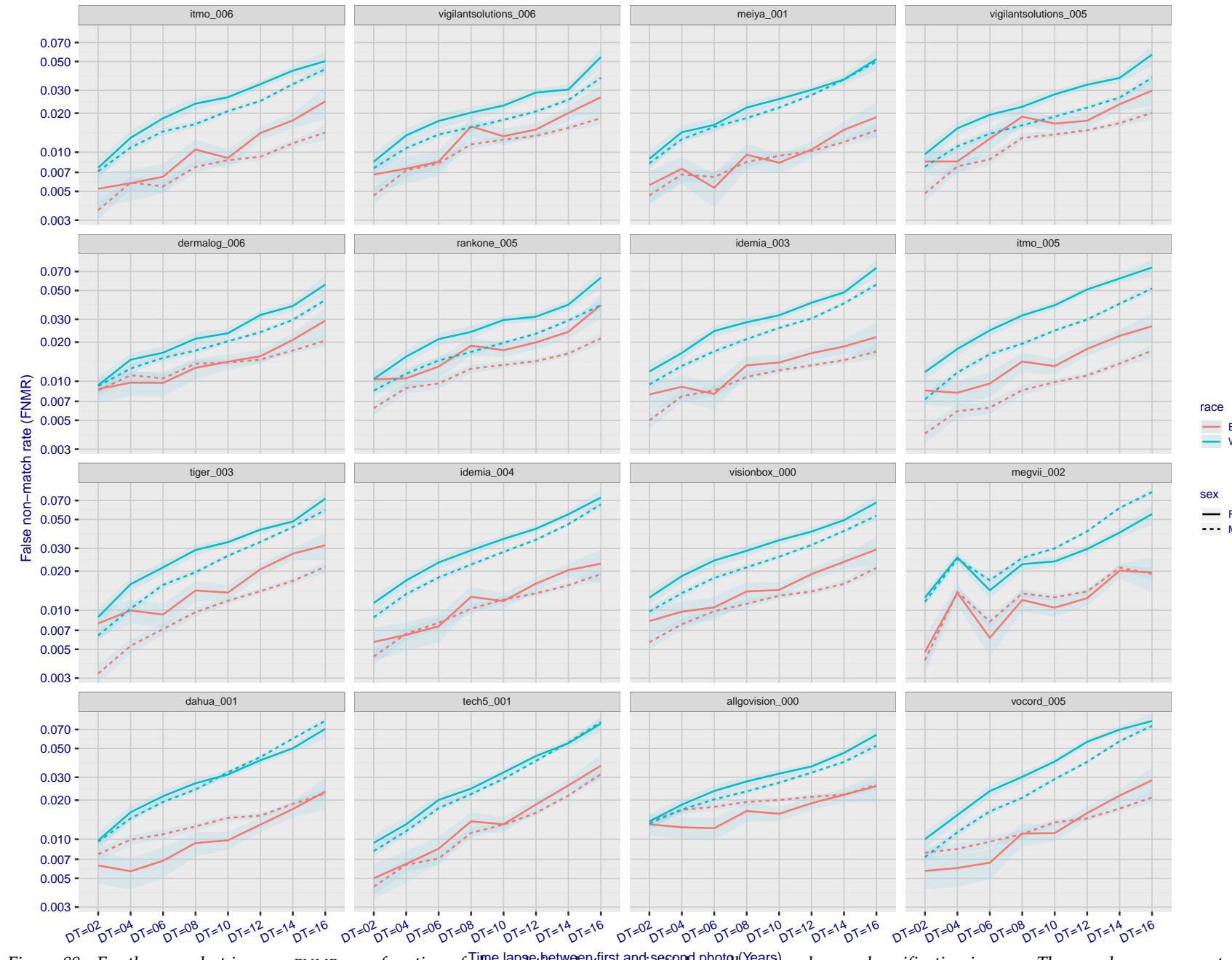


Figure 87: For the mugshot images, FNMR as a function of elapsed time between initial enrollment and second verification images. The panels appear most accurate first, and vertical scale changes on each page. The four traces correspond to images annotated with codes for black female, black male, white female, white male. The threshold is fixed for each algorithm to give FMR = 0.00001 over all ( $10^8$ ) impostor comparisons. For short time-lapses, the most accurate algorithms give very few errors (FNMR < 0.001) so that the uncertainty estimates are high.



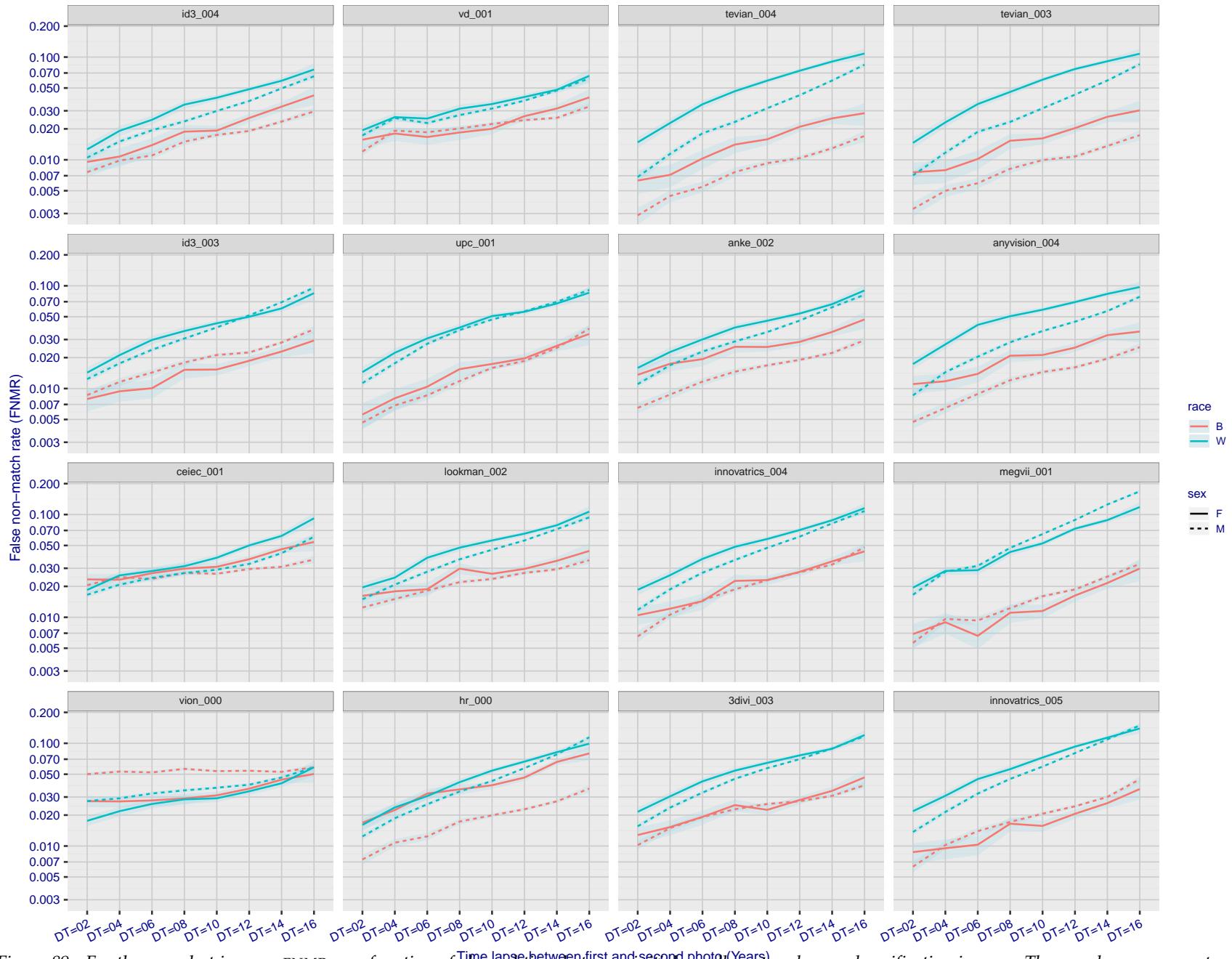


Figure 89: For the mugshot images, FNMR as a function of elapsed time between initial enrollment and second verification images. The panels appear most accurate first, and vertical scale changes on each page. The four traces correspond to images annotated with codes for black female, black male, white female, white male. The threshold is fixed for each algorithm to give  $FMR = 0.00001$  over all ( $10^8$ ) impostor comparisons. For short time-lapses, the most accurate algorithms give very few errors ( $FNMR < 0.001$ ) so that the uncertainty estimates are high.

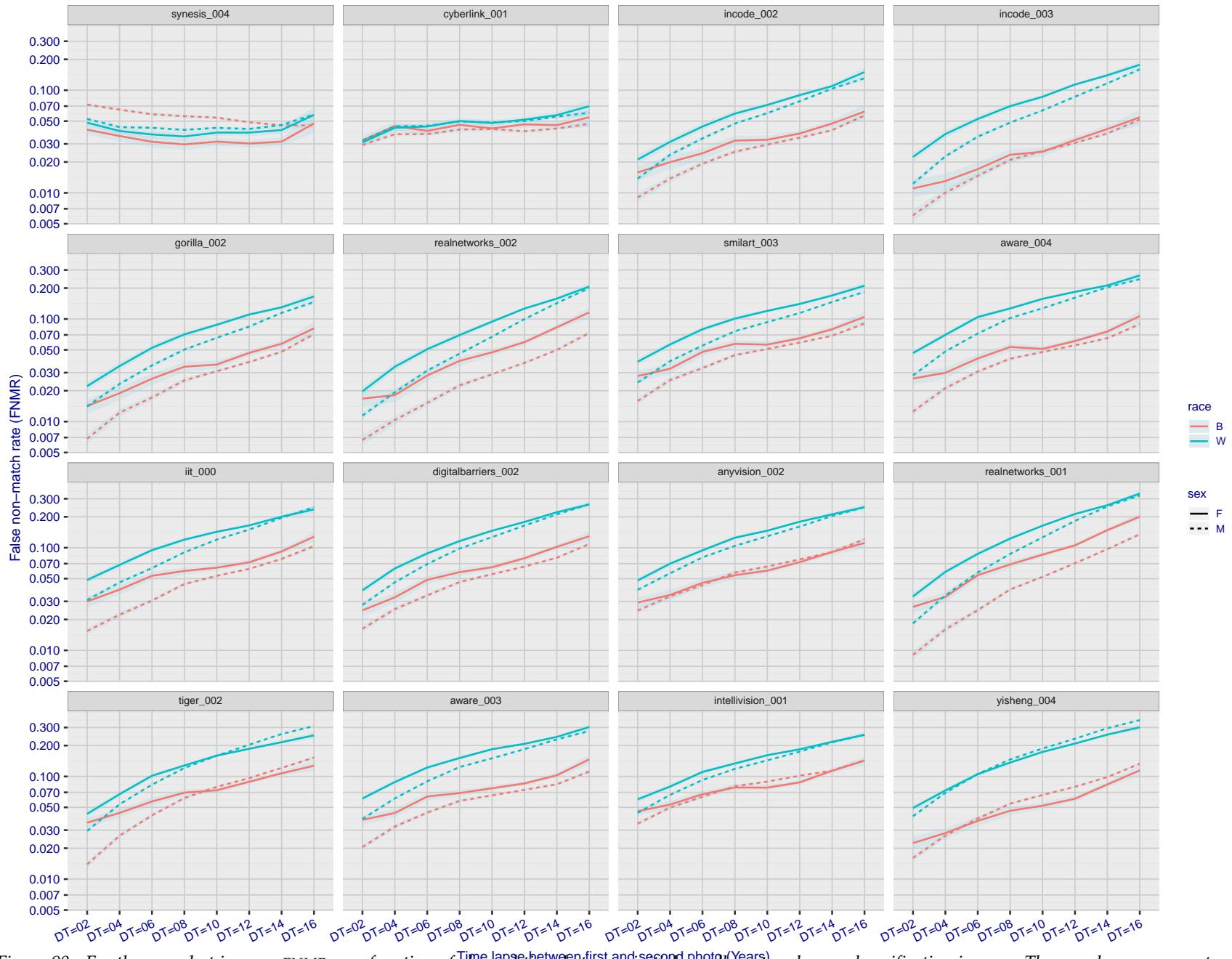


Figure 90: For the mugshot images, FNMR as a function of elapsed time between initial enrollment and second verification images. The panels appear most accurate first, and vertical scale changes on each page. The four traces correspond to images annotated with codes for black female, black male, white female, white male. The threshold is fixed for each algorithm to give FMR = 0.00001 over all ( $10^8$ ) impostor comparisons. For short time-lapses, the most accurate algorithms give very few errors (FNMR < 0.001) so that the uncertainty estimates are high.

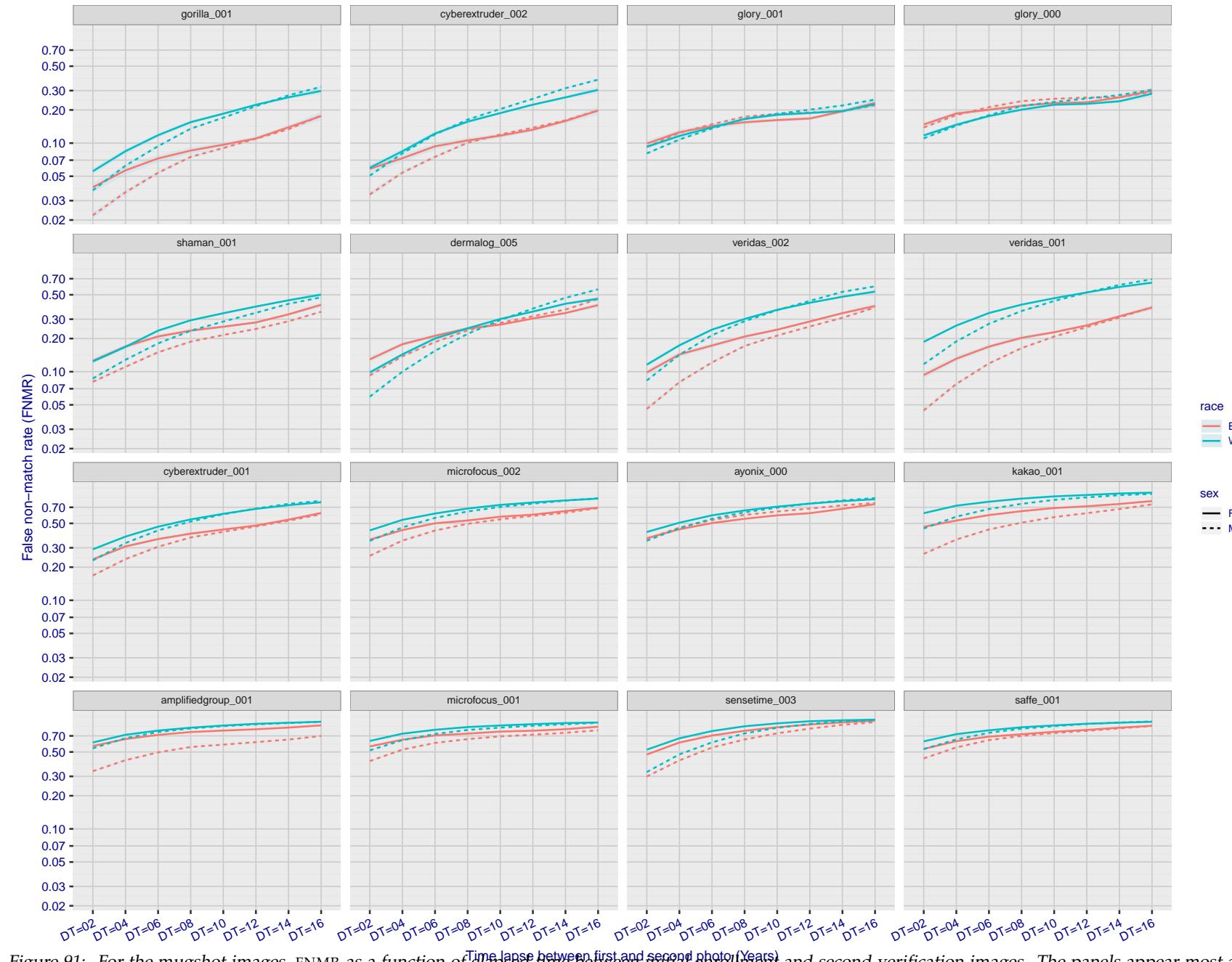


Figure 91: For the mugshot images, FNMR as a function of elapsed time between initial enrollment and second verification images. The panels appear most accurate first, and vertical scale changes on each page. The four traces correspond to images annotated with codes for black female, black male, white female, white male. The threshold is fixed for each algorithm to give FMR = 0.00001 over all ( $10^8$ ) impostor comparisons. For short time-lapses, the most accurate algorithms give very few errors (FNMR < 0.001) so that the uncertainty estimates are high.

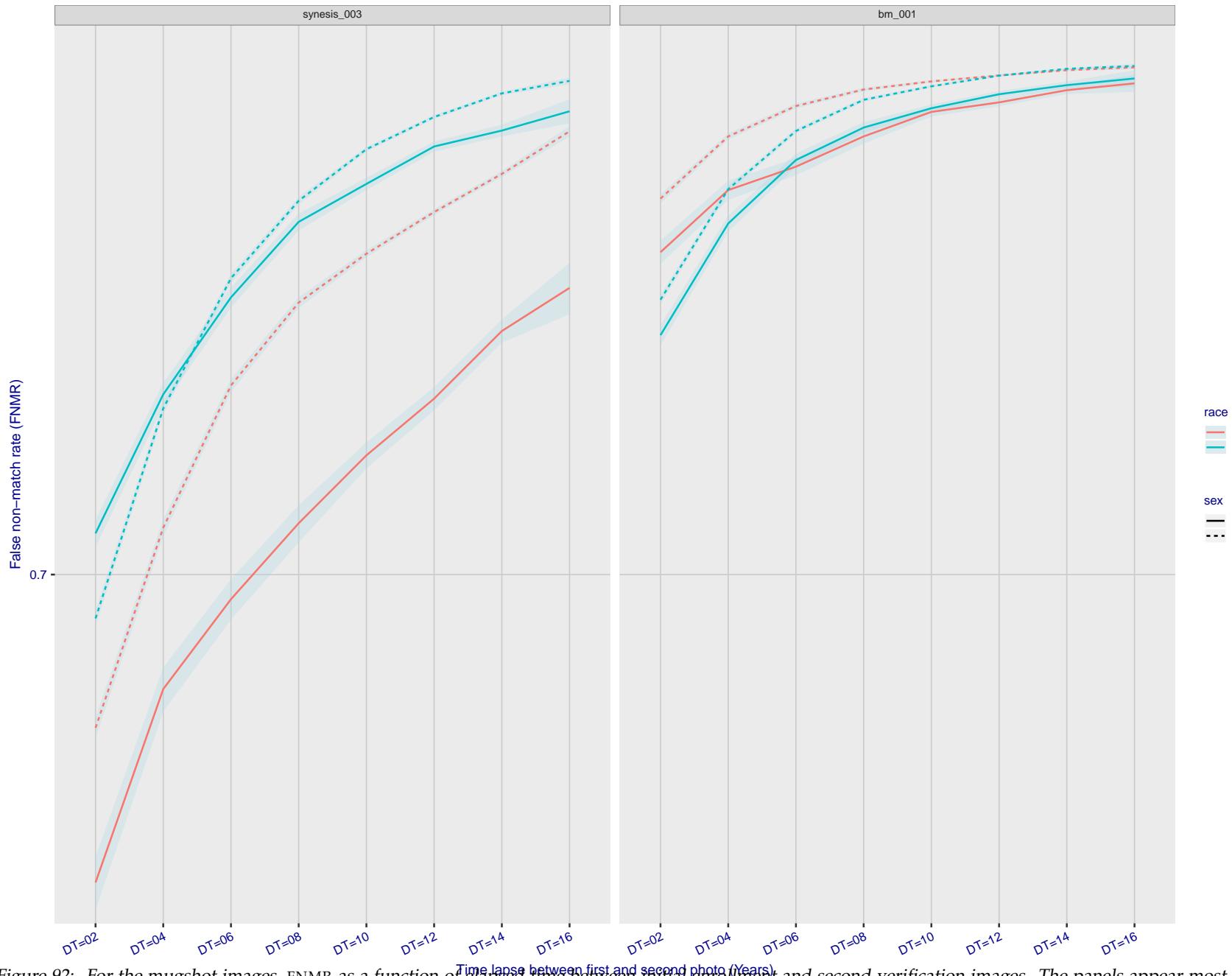


Figure 92: For the mugshot images, FNMR as a function of elapsed time between initial enrolment and second verification images. The panels appear most accurate first, and vertical scale changes on each page. The four traces correspond to images annotated with codes for black female, black male, white female, white male. The threshold is fixed for each algorithm to give  $FMR = 0.00001$  over all ( $10^8$ ) impostor comparisons. For short time-lapses, the most accurate algorithms give very few errors ( $FNMR < 0.001$ ) so that the uncertainty estimates are high.

### 3.5.3 Effect of age on genuine subjects

**Background:** Faces change appearance throughout life. Face recognition algorithms have previously been reported to give better accuracy on older individuals (See NIST IR 8009).

**Goal:** To quantify false non-match rates (FNMR) as a function of age, without an ageing component.

**Methods:** Using the visa images, which span fewer than five years, thresholds are determined that give FMR = 0.001 and 0.0001 over the entire impostor set. Then FNMR is measured over 1000 bootstrap replications of the genuine scores.

**Results:** For the visa images, Figure 102 shows how false non-match rates for genuine users, as a function of age group.

The notable aspects are:

- ▷ Younger subjects give considerably higher FNMR. This is likely due to rapid growth and change in facial appearance.
- ▷ FNMR trends down throughout life. The last bin, AGE > 72, contains fewer than 140 mated pairs, and may be affected by small sample size.

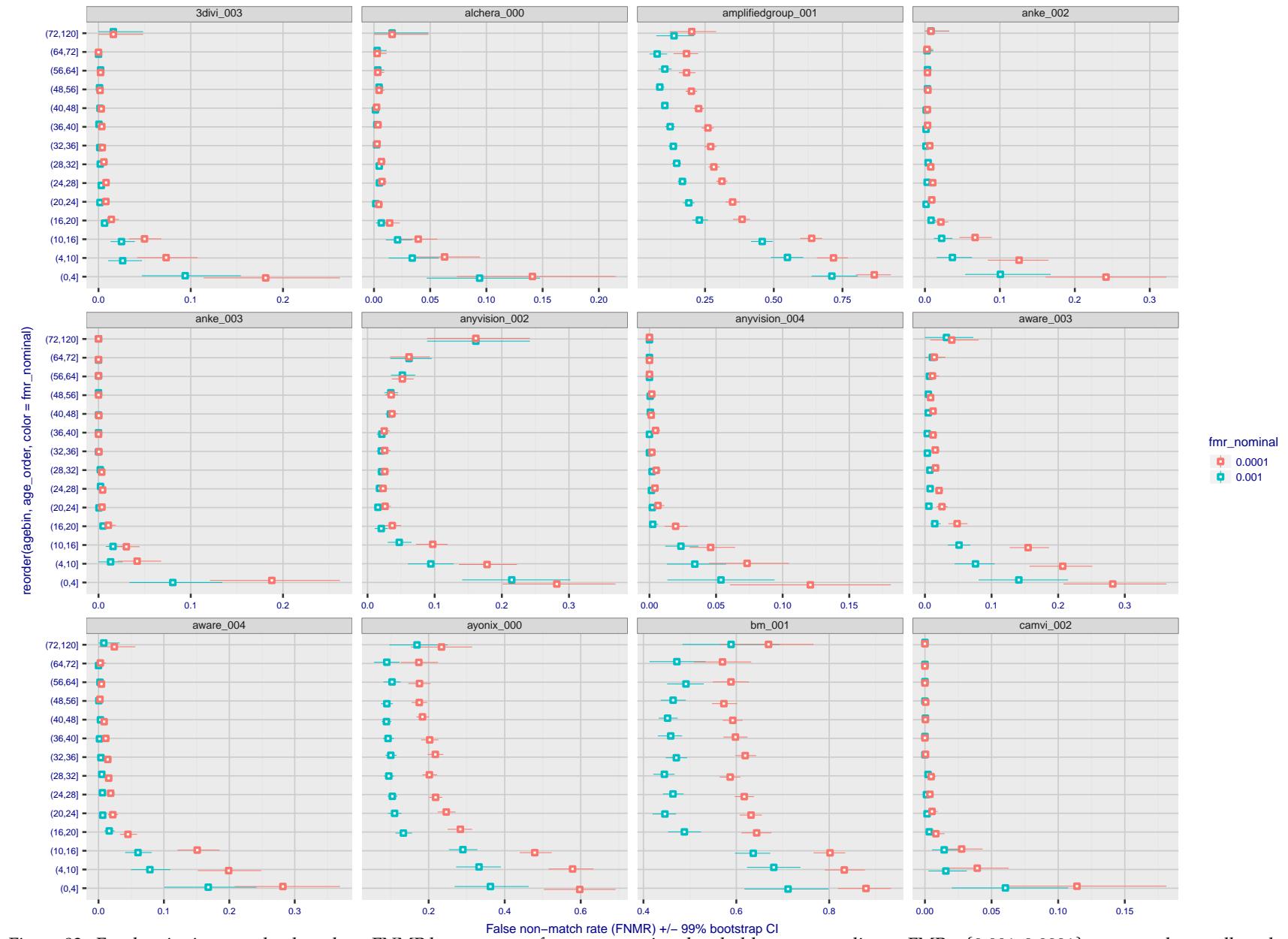


Figure 93: For the visa images, the dots show FNMR by age group for two operating thresholds corresponding to  $FMR = \{0.001, 0.0001\}$  computed over all on the order of  $10^{10}$  impostor scores. The FMR in each bin will vary also - see subsequent impostor heatmaps in sec. 3.6.2. Given a pair of face images taken at different times, we assign the comparison to the bin that is the arithmetic average of the subject's ages. This plot shows only the effect of age, not ageing. The number of comparisons in each bin is generally in the thousands, however the first and last bins are computed over 149 and 124 respectively. The error rates in some (adult) cases are zero, and in others the DET is flat so the error rates at the two thresholds are identical. The lines span 1% and 99% of bootstrap replicated FNMR estimates.

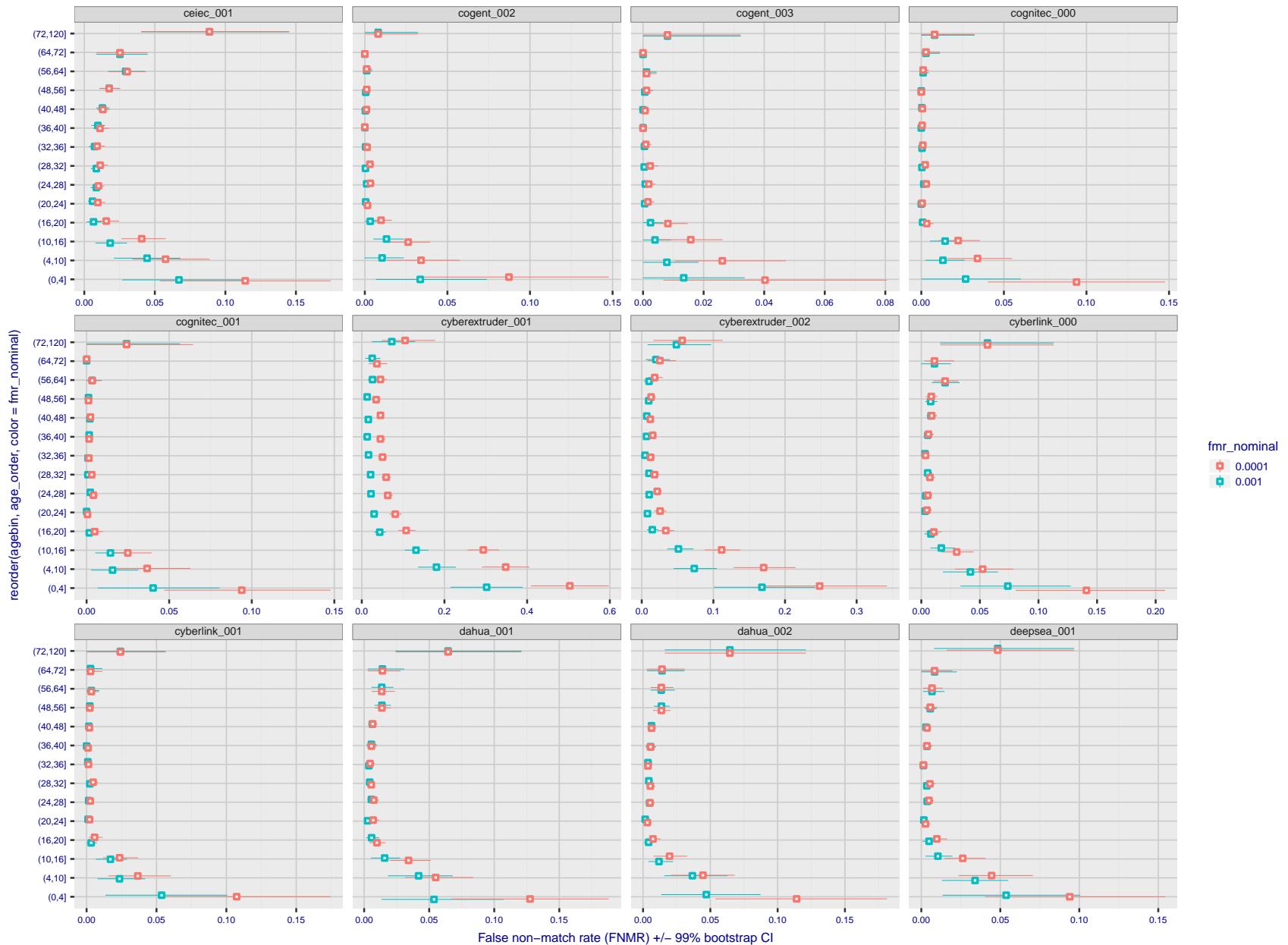


Figure 94: For the visa images, the dots show FNMR by age group for two operating thresholds corresponding to  $FMR = \{0.001, 0.0001\}$  computed over all on the order of  $10^{10}$  impostor scores. The FMR in each bin will vary also - see subsequent impostor heatmaps in sec. 3.6.2. Given a pair of face images taken at different times, we assign the comparison to the bin that is the arithmetic average of the subject's ages. This plot shows only the effect of age, not ageing. The number of comparisons in each bin is generally in the thousands, however the first and last bins are computed over 149 and 124 respectively. The error rates in some (adult) cases are zero, and in others the DET is flat so the error rates at the two thresholds are identical. The lines span 1% and 99% of bootstrap replicated FNMR estimates.

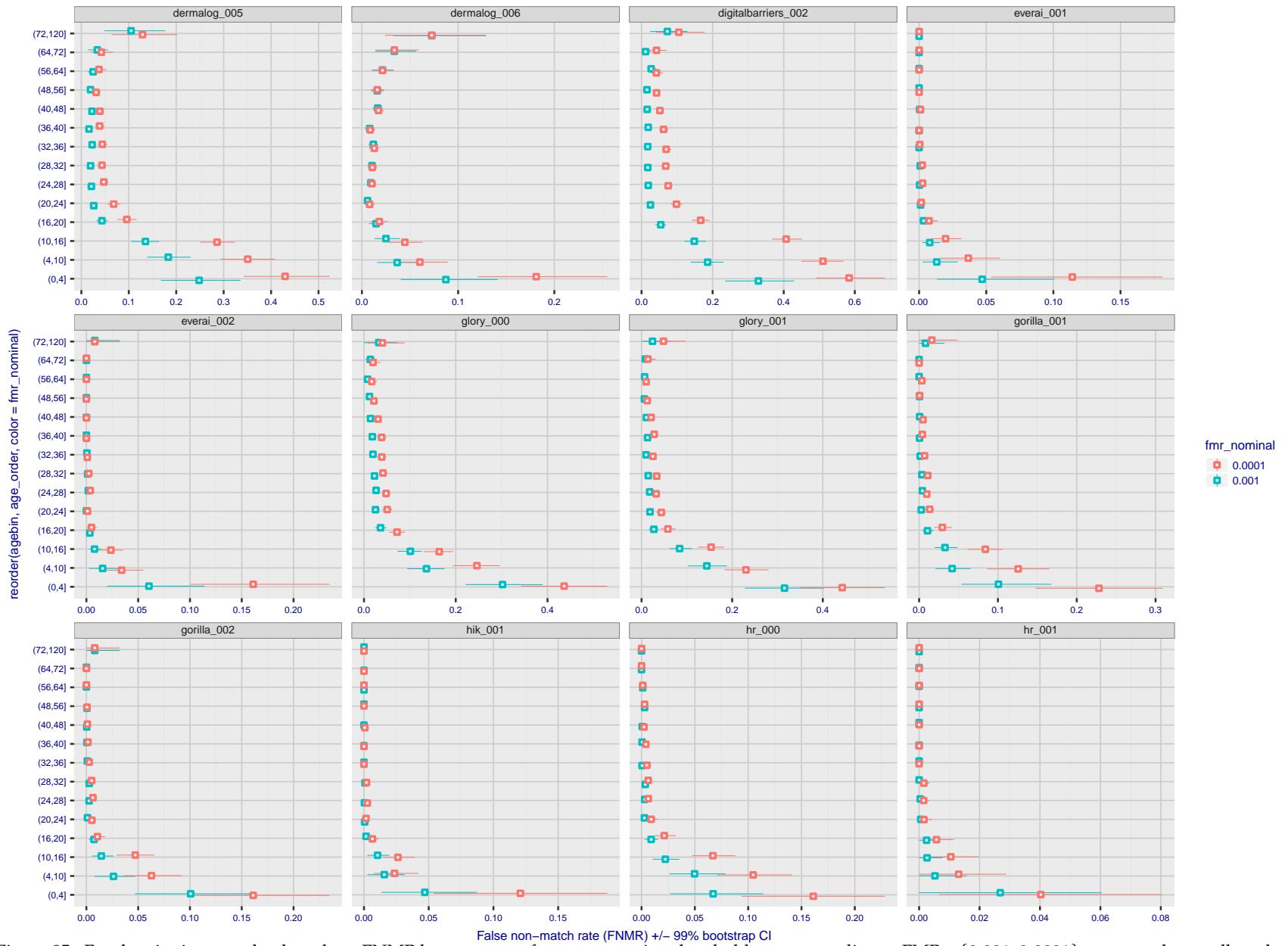


Figure 95: For the visa images, the dots show FNMR by age group for two operating thresholds corresponding to  $FMR = \{0.001, 0.0001\}$  computed over all on the order of  $10^{10}$  impostor scores. The FMR in each bin will vary also - see subsequent impostor heatmaps in sec. 3.6.2. Given a pair of face images taken at different times, we assign the comparison to the bin that is the arithmetic average of the subject's ages. This plot shows only the effect of age, not ageing. The number of comparisons in each bin is generally in the thousands, however the first and last bins are computed over 149 and 124 respectively. The error rates in some (adult) cases are zero, and in others the DET is flat so the error rates at the two thresholds are identical. The lines span 1% and 99% of bootstrap replicated FNMR estimates.

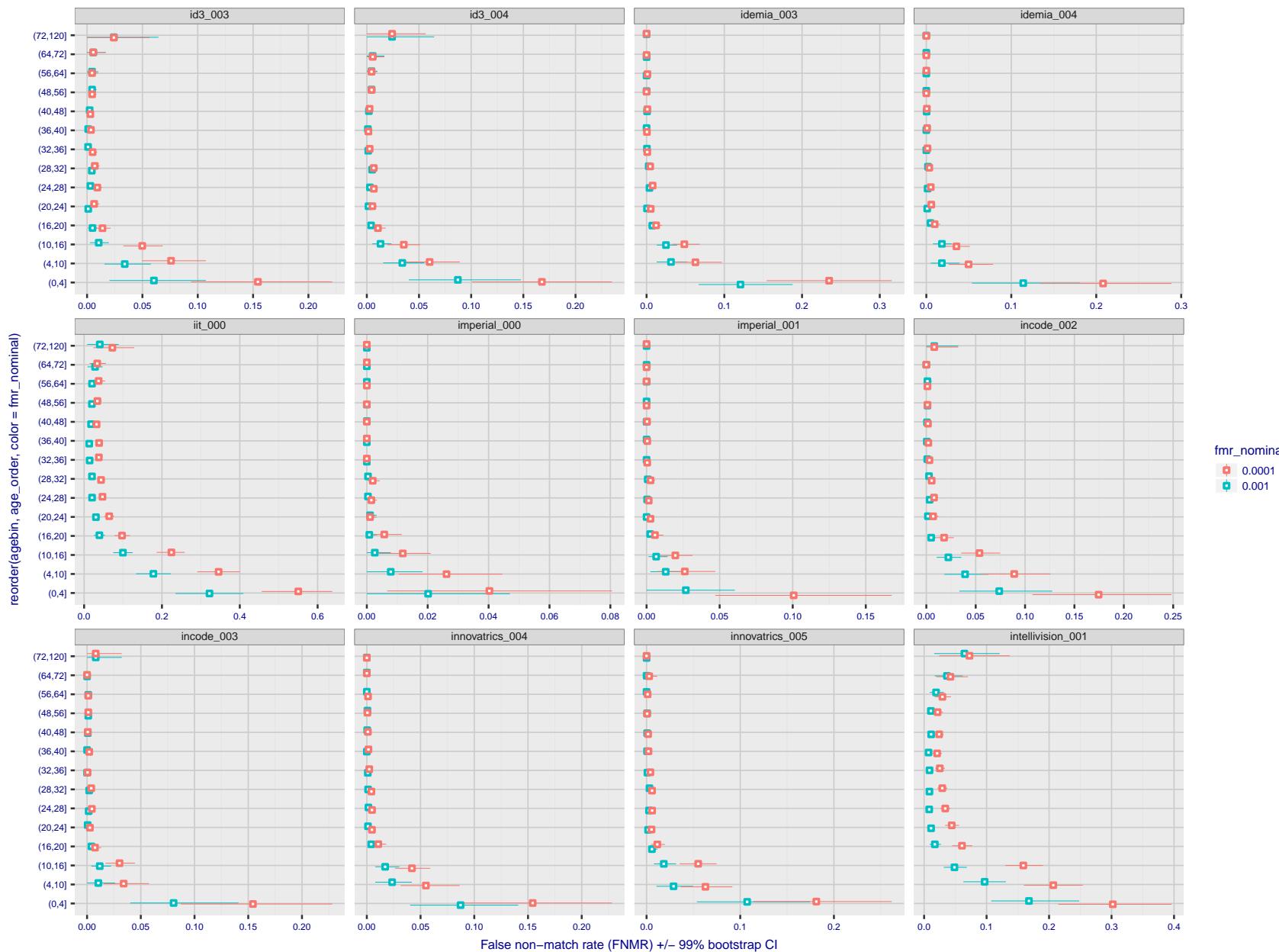


Figure 96: For the visa images, the dots show FNMR by age group for two operating thresholds corresponding to  $FMR = \{0.001, 0.0001\}$  computed over all on the order of  $10^{10}$  impostor scores. The FMR in each bin will vary also - see subsequent impostor heatmaps in sec. 3.6.2. Given a pair of face images taken at different times, we assign the comparison to the bin that is the arithmetic average of the subject's ages. This plot shows only the effect of age, not ageing. The number of comparisons in each bin is generally in the thousands, however the first and last bins are computed over 149 and 124 respectively. The error rates in some (adult) cases are zero, and in others the DET is flat so the error rates at the two thresholds are identical. The lines span 1% and 99% of bootstrap replicated FNMR estimates.

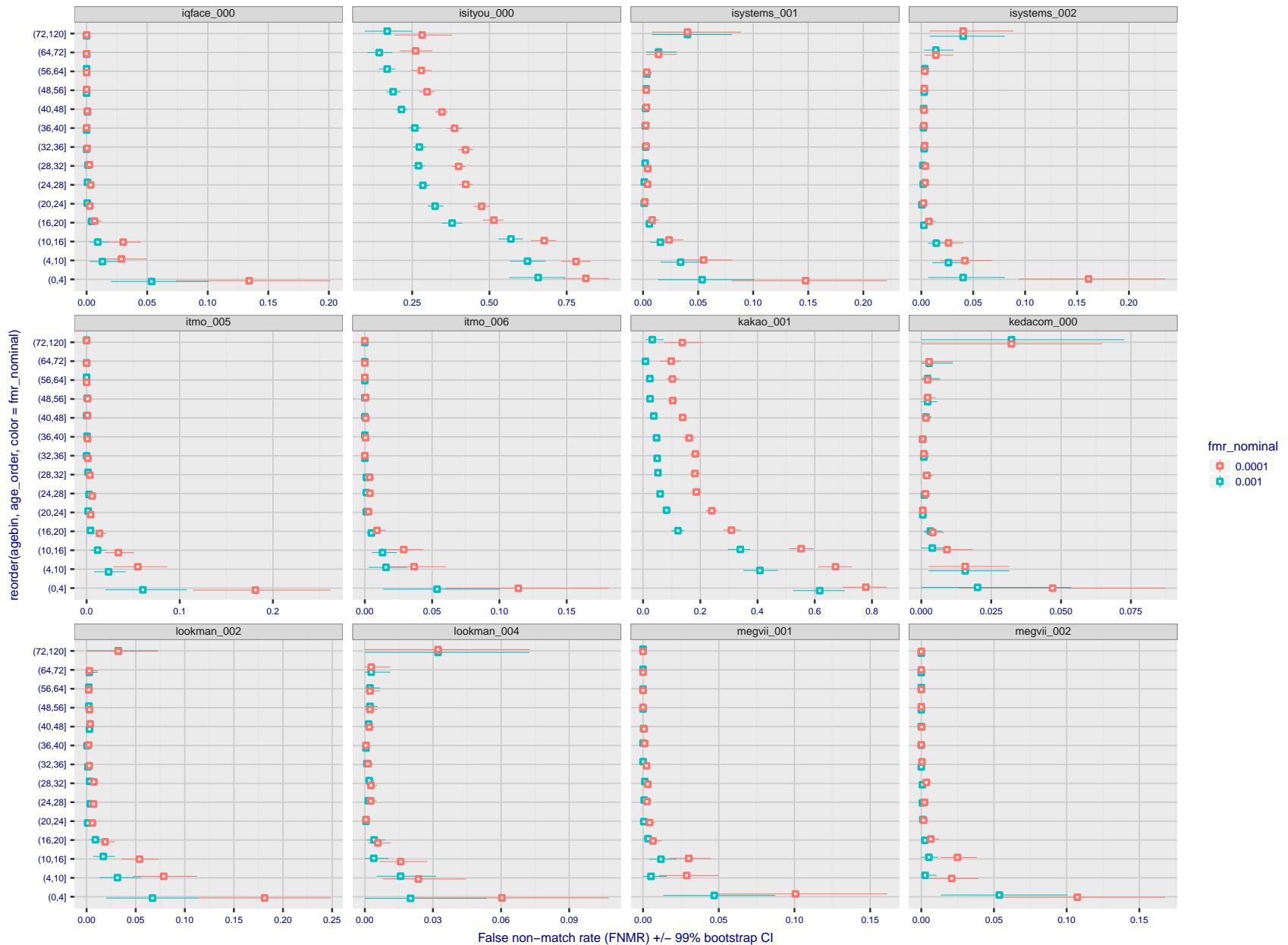


Figure 97: For the visa images, the dots show FNMR by age group for two operating thresholds corresponding to  $FMR = \{0.001, 0.0001\}$  computed over all on the order of  $10^{10}$  impostor scores. The FMR in each bin will vary also - see subsequent impostor heatmaps in sec. 3.6.2. Given a pair of face images taken at different times, we assign the comparison to the bin that is the arithmetic average of the subject's ages. This plot shows only the effect of age, not ageing. The number of comparisons in each bin is generally in the thousands, however the first and last bins are computed over 149 and 124 respectively. The error rates in some (adult) cases are zero, and in others the DET is flat so the error rates at the two thresholds are identical. The lines span 1% and 99% of bootstrap replicated FNMR estimates.

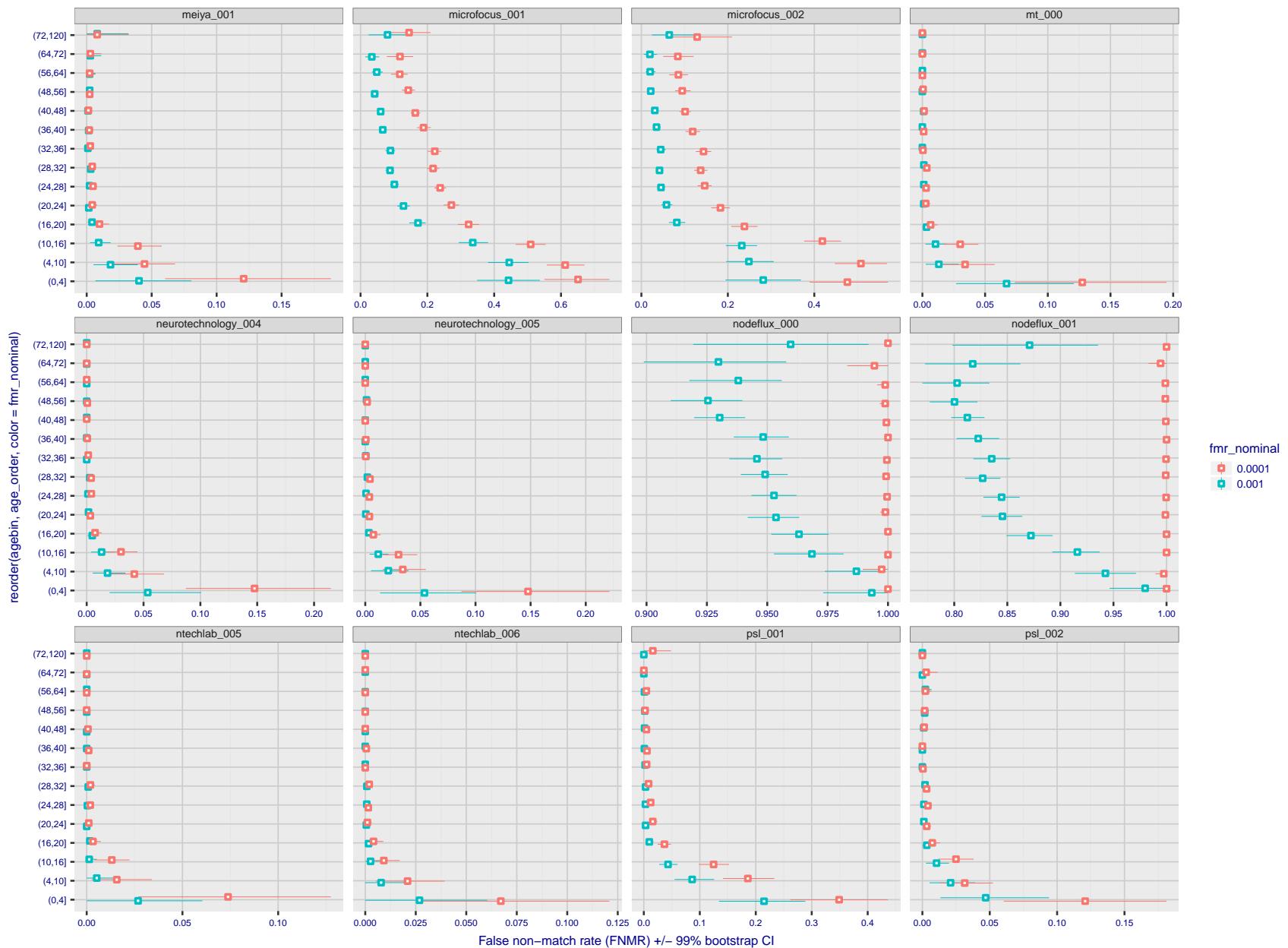


Figure 98: For the visa images, the dots show FNMR by age group for two operating thresholds corresponding to  $FMR = \{0.001, 0.0001\}$  computed over all on the order of  $10^{10}$  impostor scores. The FMR in each bin will vary also - see subsequent impostor heatmaps in sec. 3.6.2. Given a pair of face images taken at different times, we assign the comparison to the bin that is the arithmetic average of the subject's ages. This plot shows only the effect of age, not ageing. The number of comparisons in each bin is generally in the thousands, however the first and last bins are computed over 149 and 124 respectively. The error rates in some (adult) cases are zero, and in others the DET is flat so the error rates at the two thresholds are identical. The lines span 1% and 99% of bootstrap replicated FNMR estimates.

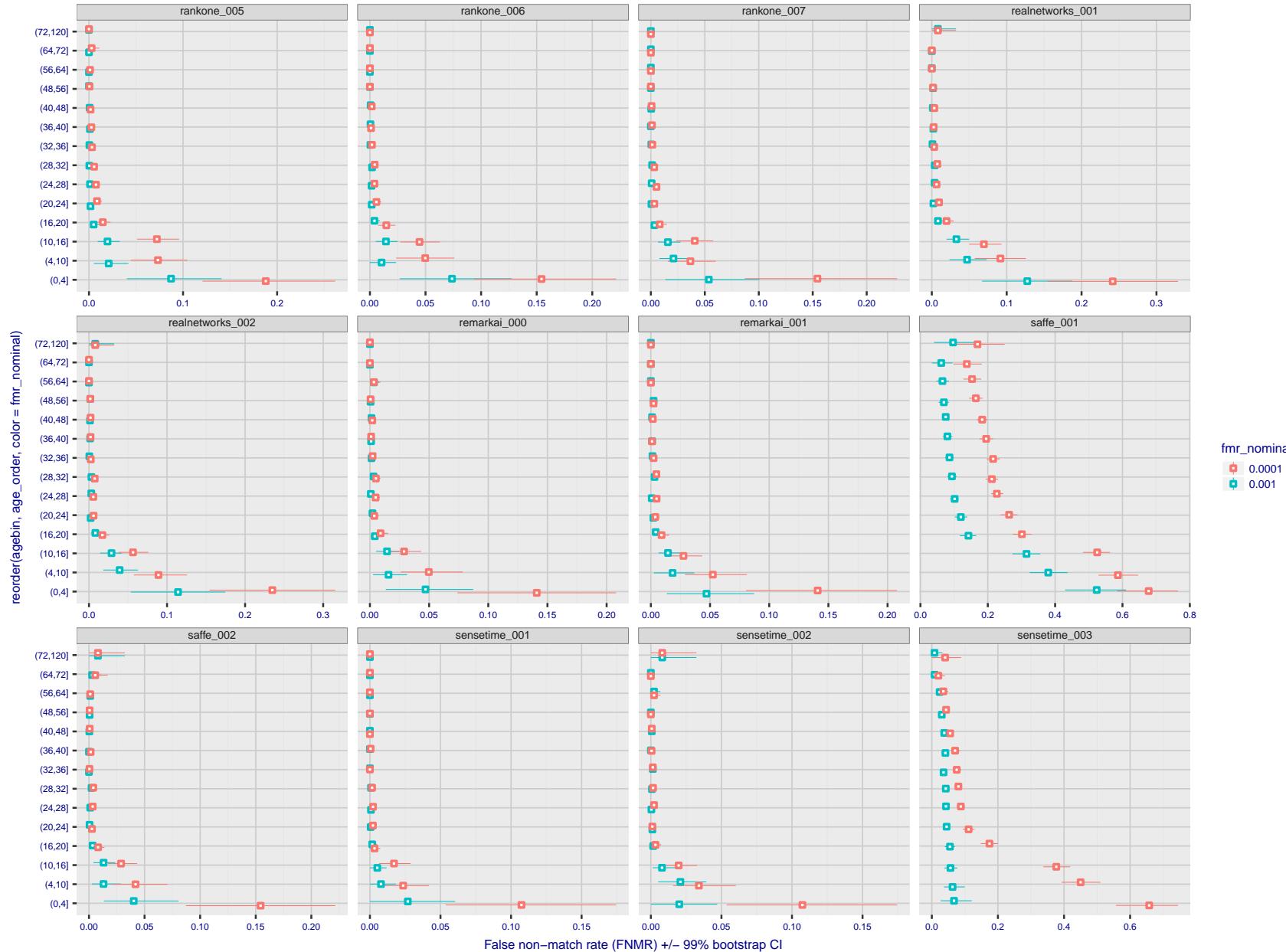


Figure 99: For the visa images, the dots show FNMR by age group for two operating thresholds corresponding to  $FMR = \{0.001, 0.0001\}$  computed over all on the order of  $10^{10}$  impostor scores. The FMR in each bin will vary also - see subsequent impostor heatmaps in sec. 3.6.2. Given a pair of face images taken at different times, we assign the comparison to the bin that is the arithmetic average of the subject's ages. This plot shows only the effect of age, not ageing. The number of comparisons in each bin is generally in the thousands, however the first and last bins are computed over 149 and 124 respectively. The error rates in some (adult) cases are zero, and in others the DET is flat so the error rates at the two thresholds are identical. The lines span 1% and 99% of bootstrap replicated FNMR estimates.

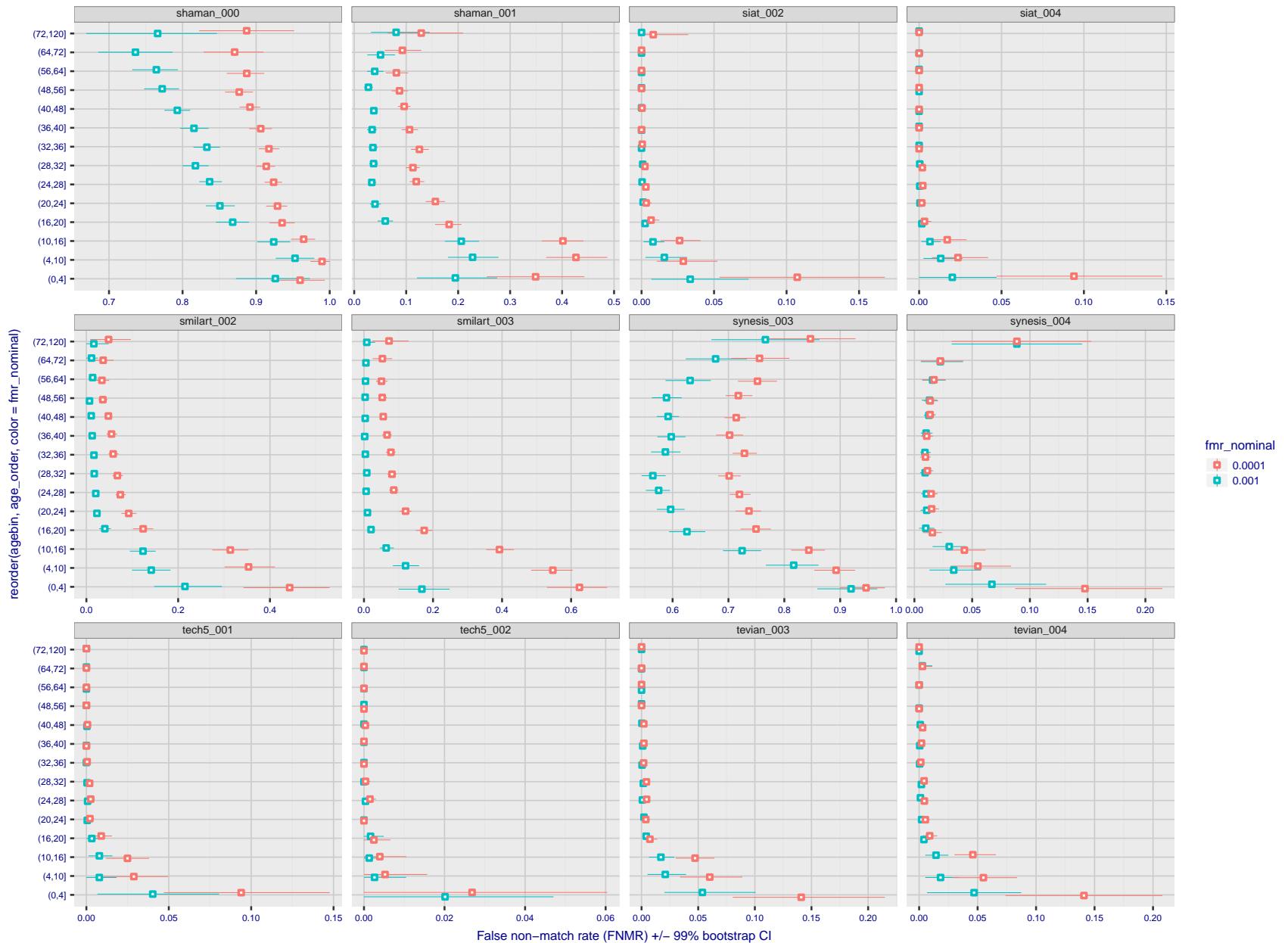


Figure 100: For the visa images, the dots show FNMR by age group for two operating thresholds corresponding to  $FMR = \{0.001, 0.0001\}$  computed over all on the order of  $10^{10}$  impostor scores. The FMR in each bin will vary also - see subsequent impostor heatmaps in sec. 3.6.2. Given a pair of face images taken at different times, we assign the comparison to the bin that is the arithmetic average of the subject's ages. This plot shows only the effect of age, not ageing. The number of comparisons in each bin is generally in the thousands, however the first and last bins are computed over 149 and 124 respectively. The error rates in some (adult) cases are zero, and in others the DET is flat so the error rates at the two thresholds are identical. The lines span 1% and 99% of bootstrap replicated FNMR estimates.

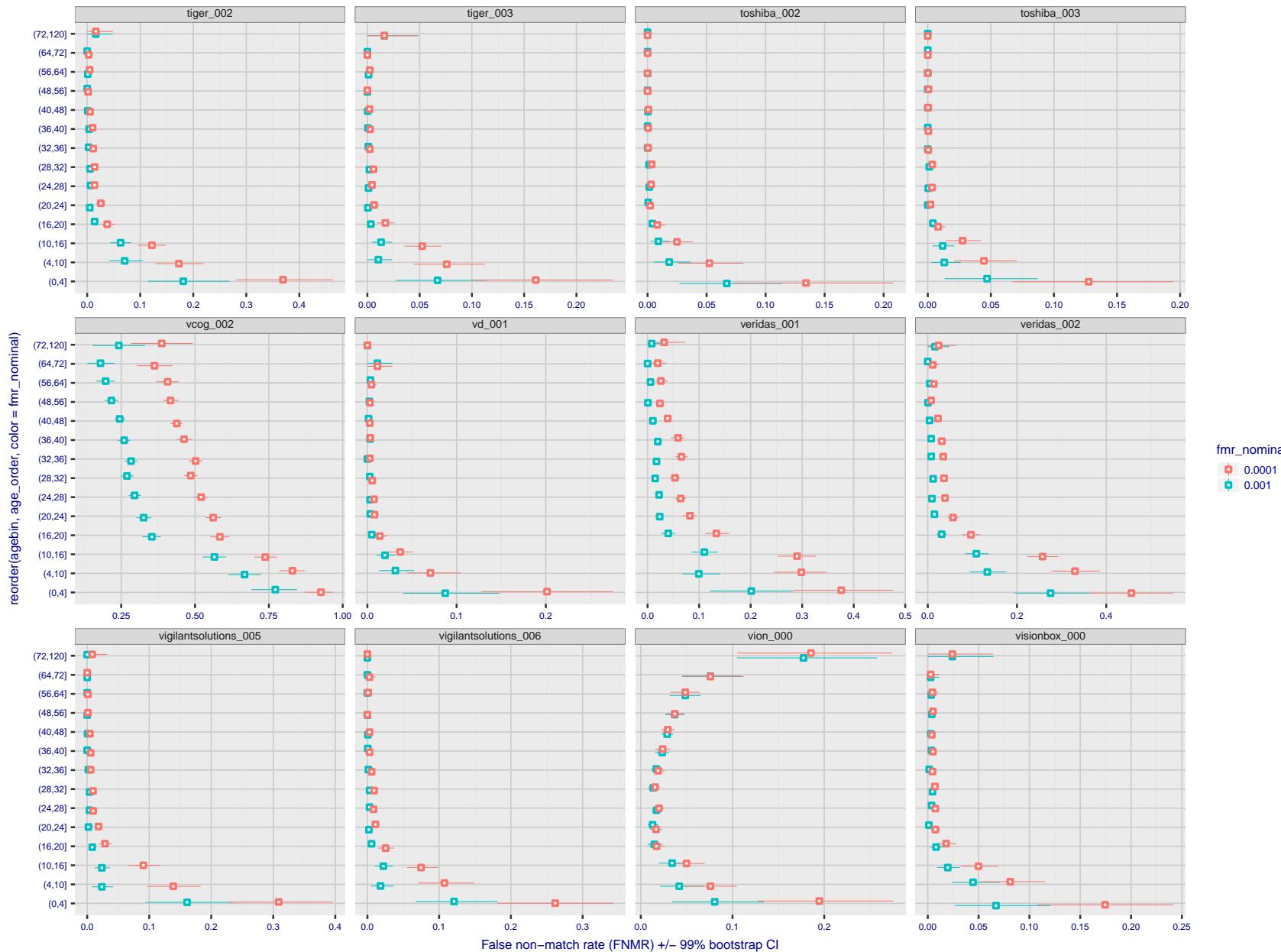


Figure 101: For the visa images, the dots show FNMR by age group for two operating thresholds corresponding to  $FMR = \{0.001, 0.0001\}$  computed over all on the order of  $10^{10}$  impostor scores. The FMR in each bin will vary also - see subsequent impostor heatmaps in sec. 3.6.2. Given a pair of face images taken at different times, we assign the comparison to the bin that is the arithmetic average of the subject's ages. This plot shows only the effect of age, not ageing. The number of comparisons in each bin is generally in the thousands, however the first and last bins are computed over 149 and 124 respectively. The error rates in some (adult) cases are zero, and in others the DET is flat so the error rates at the two thresholds are identical. The lines span 1% and 99% of bootstrap replicated FNMR estimates.

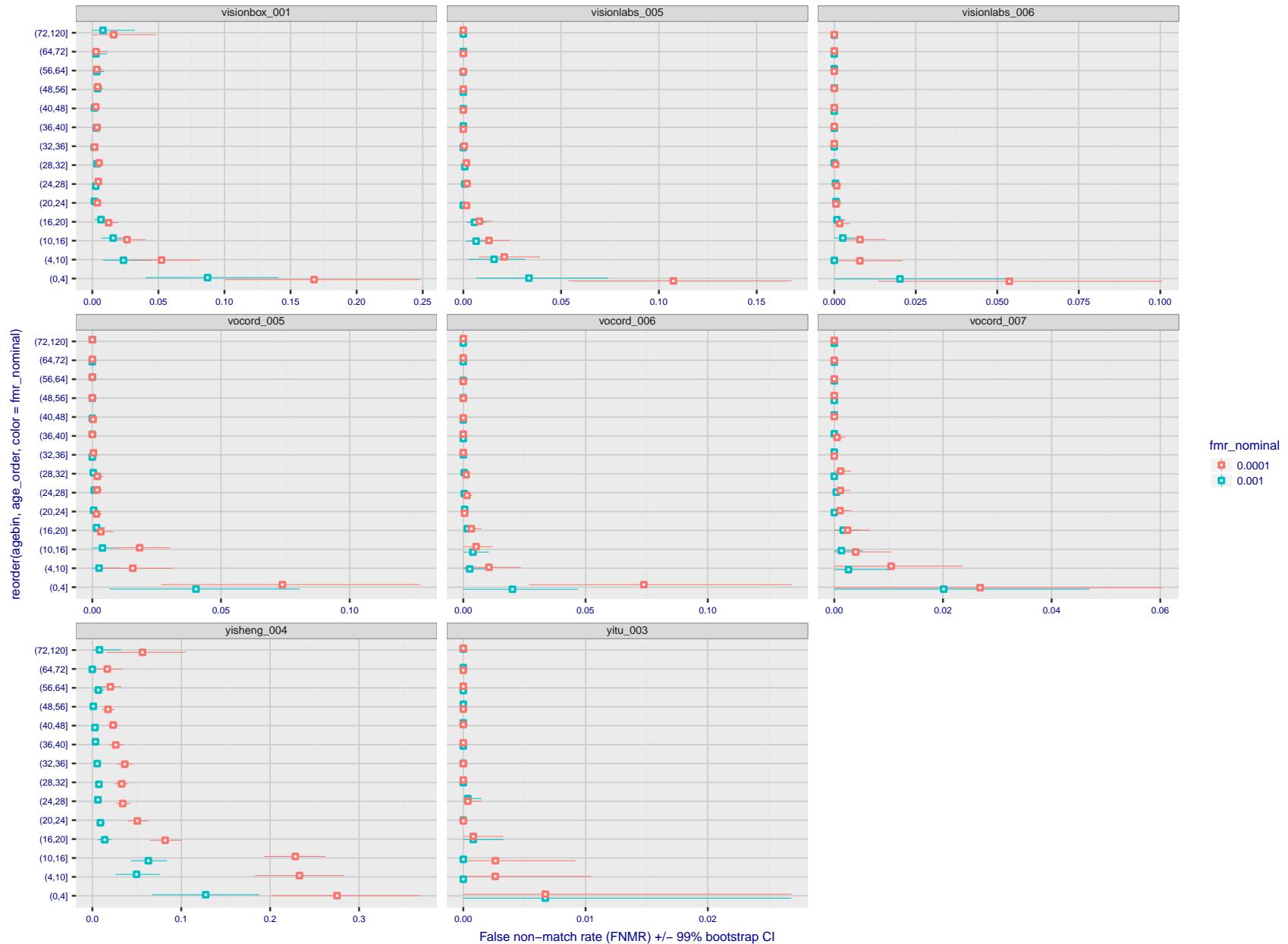


Figure 102: For the visa images, the dots show FNMR by age group for two operating thresholds corresponding to  $FMR = \{0.001, 0.0001\}$  computed over all on the order of  $10^{10}$  impostor scores. The FMR in each bin will vary also - see subsequent impostor heatmaps in sec. 3.6.2. Given a pair of face images taken at different times, we assign the comparison to the bin that is the arithmetic average of the subject's ages. This plot shows only the effect of age, not ageing. The number of comparisons in each bin is generally in the thousands, however the first and last bins are computed over 149 and 124 respectively. The error rates in some (adult) cases are zero, and in others the DET is flat so the error rates at the two thresholds are identical. The lines span 1% and 99% of bootstrap replicated FNMR estimates.

**Caveats:** None.

## 3.6 Impostor distribution stability

### 3.6.1 Effect of birth place on the impostor distribution

**Background:** Facial appearance varies geographically, both in terms of skin tone, cranio-facial structure and size. This section addresses whether false match rates vary intra- and inter-regionally.

**Goals:**

- ▷ To show the effect of birth region of the impostor and enrollee on false match rates.
- ▷ To determine whether some algorithms give better impostor distribution stability.

**Methods:**

- ▷ For the visa images, NIST defined 10 regions: Sub-Saharan Africa, South Asia, Polynesia, North Africa, Middle East, Europe, East Asia, Central and South America, Central Asia, and the Caribbean.
- ▷ For the visa images, NIST mapped each country of birth to a region. There is some arbitrariness to this. For example, Egypt could reasonably be assigned to the Middle East instead of North Africa. An alternative methodology could, for example, assign the Philippines to *both* Polynesia and East Asia.
- ▷ FMR is computed for cases where all face images of impostors born in region  $r_2$  are compared with enrolled face images of persons born in region  $r_1$ .

$$\text{FMR}(r_1, r_2, T) = \frac{\sum_{i=1}^{N_{r_1, r_2}} H(s_i - T)}{N_{r_1, r_2}} \quad (5)$$

where the same threshold,  $T$ , is used in all cells, and  $H$  is the unit step function. The threshold is set to give  $\text{FMR}(T) = 0.001$  over the entire set of visa image impostor comparisons.

- ▷ This analysis is then repeated by country-pair, but only for those country pairs where both have at least 1000 images available. The countries<sup>1</sup> appear in the axes of graphs that follow.
- ▷ The mean number of impostor scores in any cross-region bin is 33 million. The smallest number of impostor scores in any bin is 135000, for Central Asia - North Africa. While these counts are large enough to support reasonable significance, the number of individual faces is much smaller, on the order of  $N^{0.5}$ .
- ▷ The numbers of impostor scores in any cross-country bin is shown in Figure 313.

**Results:** Subsequent figures show heatmaps that use color to represent the base-10 logarithm of the false match rate. Red colors indicate high (bad) false match rates. Dark colors indicate benign false match rates. There are two series of graphs corresponding to aggregated geographical regions, and to countries. The notable observations are:

- ▷ The on-diagonal elements correspond to within-region impostors. FMR is generally above the nominal value of  $\text{FMR} = 0.001$ . Particularly there is usually higher FMR in, Sub-Saharan Africa, South Asia, and the Caribbean. Europe and Central Asia, on the other hand, usually give FMR closer to the nominal value.
- ▷ The off-diagonal elements correspond to across-region impostors. The highest FMR is produced between the Caribbean and Sub-Saharan Africa.
- ▷ Algorithms vary.

<sup>1</sup>These are Argentina, Australia, Brazil, Chile, China, Costa Rica, Cuba, Czech Republic, Dominican Republic, Ecuador, Egypt, El Salvador, Germany, Ghana, Great Britain, Greece, Guatemala, Haiti, Hong Kong, Honduras, Indonesia, India, Israel, Jamaica, Japan, Kenya, Korea, Lebanon, Mexico, Malaysia, Nepal, Nigeria, Peru, Philippines, Pakistan, Poland, Romania, Russia, South Africa, Saudi Arabia, Thailand, Trinidad, Turkey, Taiwan, Ukraine, Venezuela, and Vietnam.

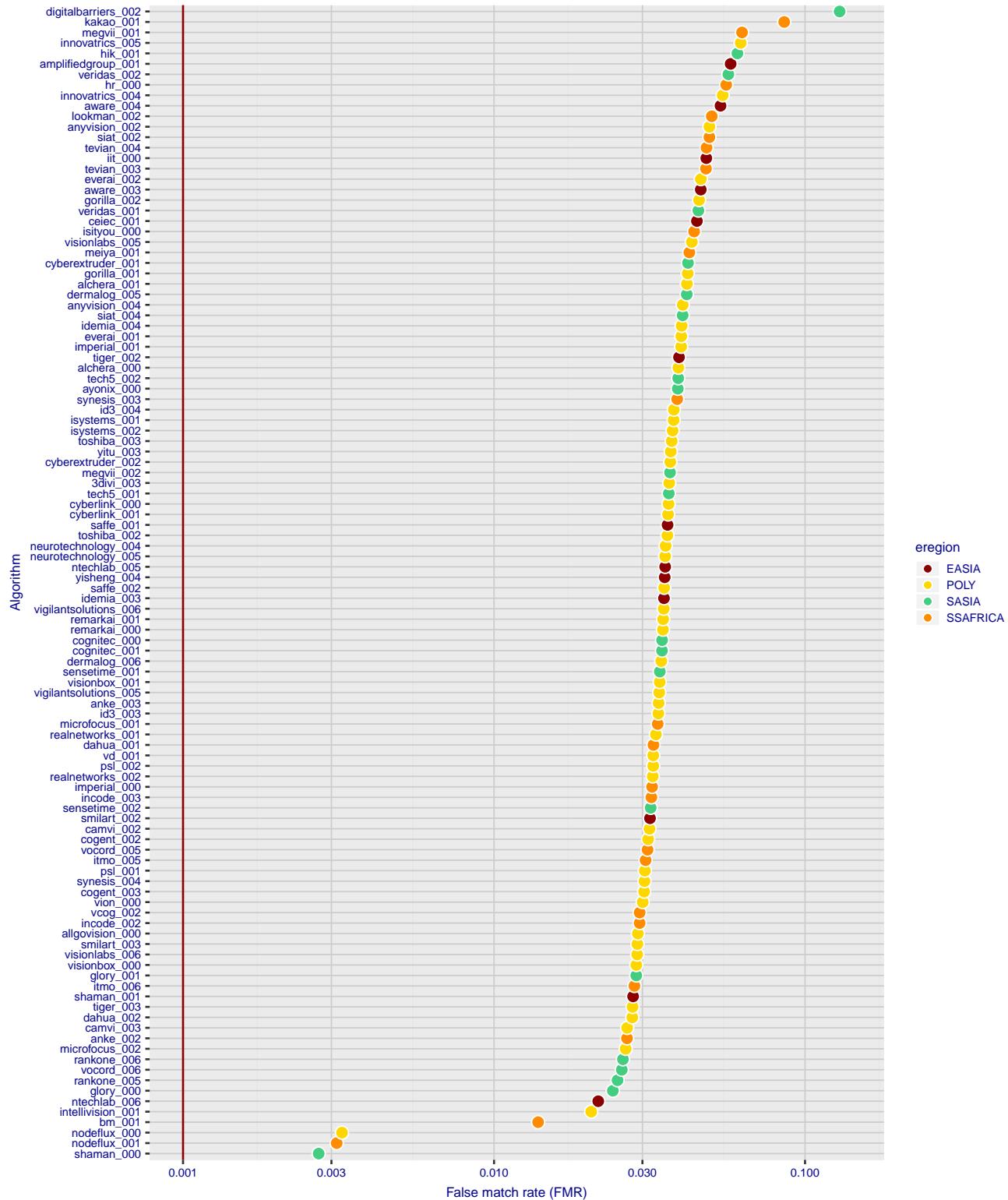


Figure 103: For the visa images, the dots show FMR for impostor comparisons of individuals of the same sex and same age group for the region of the world that gives the worst (highest) FMR when the threshold is set to give  $FMR = 0.001$  (red vertical line) over all on the order of  $10^{10}$  impostor scores i.e. zero-effort. The shift of the dots to right shows massive increases in FMR when impostors have the same sex, age, and region of birth. The color code indicates which region gives the worst case FMR. If the observed variation is due to the prevalence of one kind of images in the training imagery, then algorithms developed on one kind of data might be expected to give higher FMR on other kinds.

- ▷ We computed the same quantities for a global FMR = 0.0001. The effects are similar.

**Caveats:**

- ▷ The effects of variable impostor rates on one-to-many identification systems may well differ from what's implied by these one-to-one verification results. Two reasons for this are a) the enrollment galleries are usually imbalanced across countries of birth, age and sex; b) one-to-many identification algorithms often implement techniques aimed at stabilizing the impostor distribution. Further research is necessary.
- ▷ In principle, the effects seen in this subsection could be due to differences in the image capture process. We consider this unlikely since the effects are maintained across geography - e.g. Caribbean vs. Africa, or Japan vs. China.

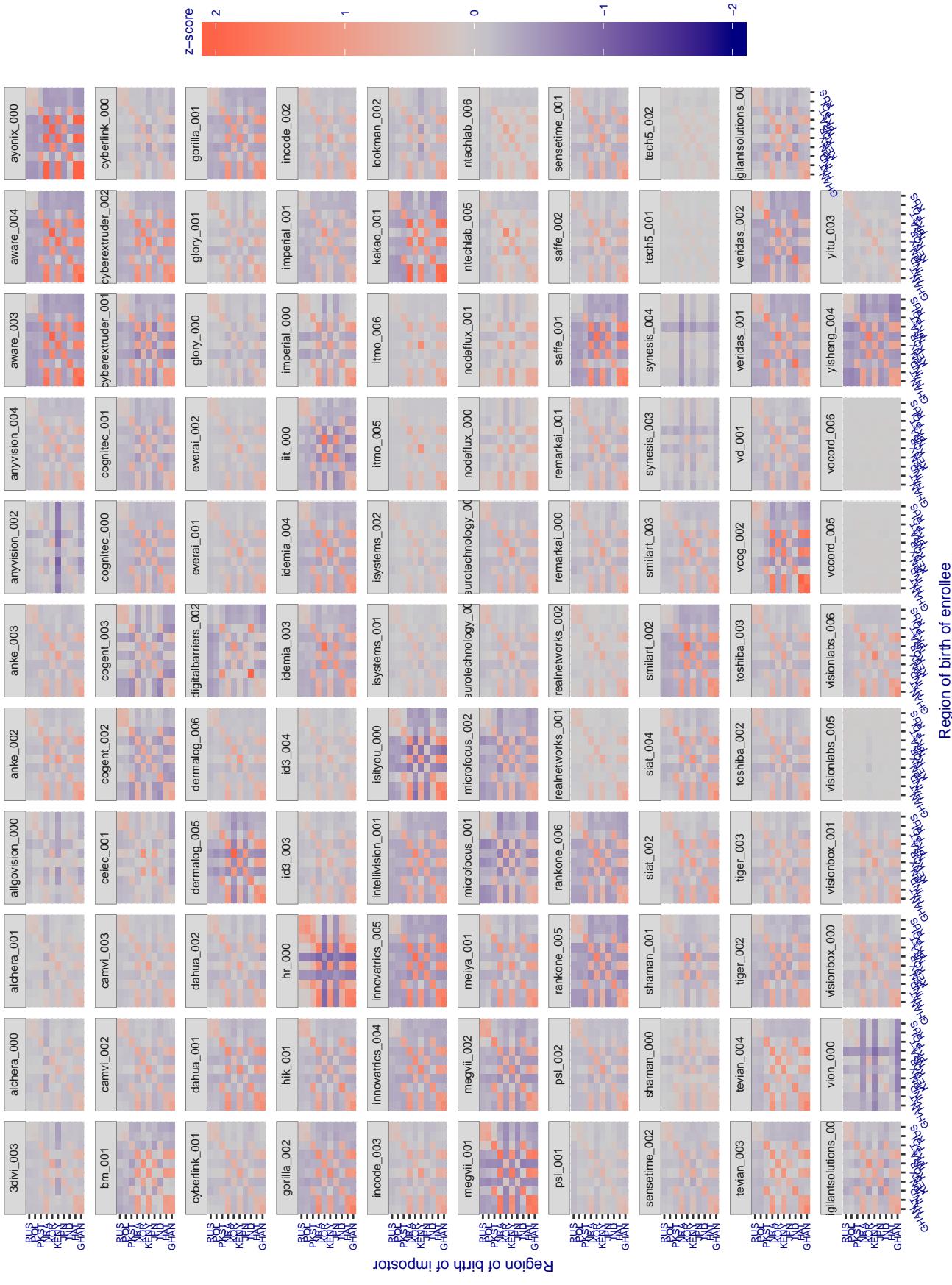


Figure 104. For visa images, the heatmap shows how the mean of the impostor distribution for the country pair  $(a,b)$  is shifted relative to the mean of the global impostor distribution, expressed as a number of standard deviations of the global impostor distribution. This statistic is designed to show shifts in the entire impostor distribution, not just tail effects that manifest as the anomalously high (or low) false match rates that appear in the subsequent figures. The countries are chosen to show that skin tone alone does not explain impostor distribution shifts. The reduced shift in Asian populations with the Yitu and TongYiTans algorithms, is accompanied by positive shifts in the European populations. This reversal relative to most other algorithms, may derive from use of nationally weighted training sets. The Visionlabs algorithm appears most insensitive to country effects. The figure is computed from same-sex and same-age impostor pairs.

### Cross region FMR at threshold T = 2.740 for algorithm 3divi\_003, giving FMR(T) = 0.0001 globally.

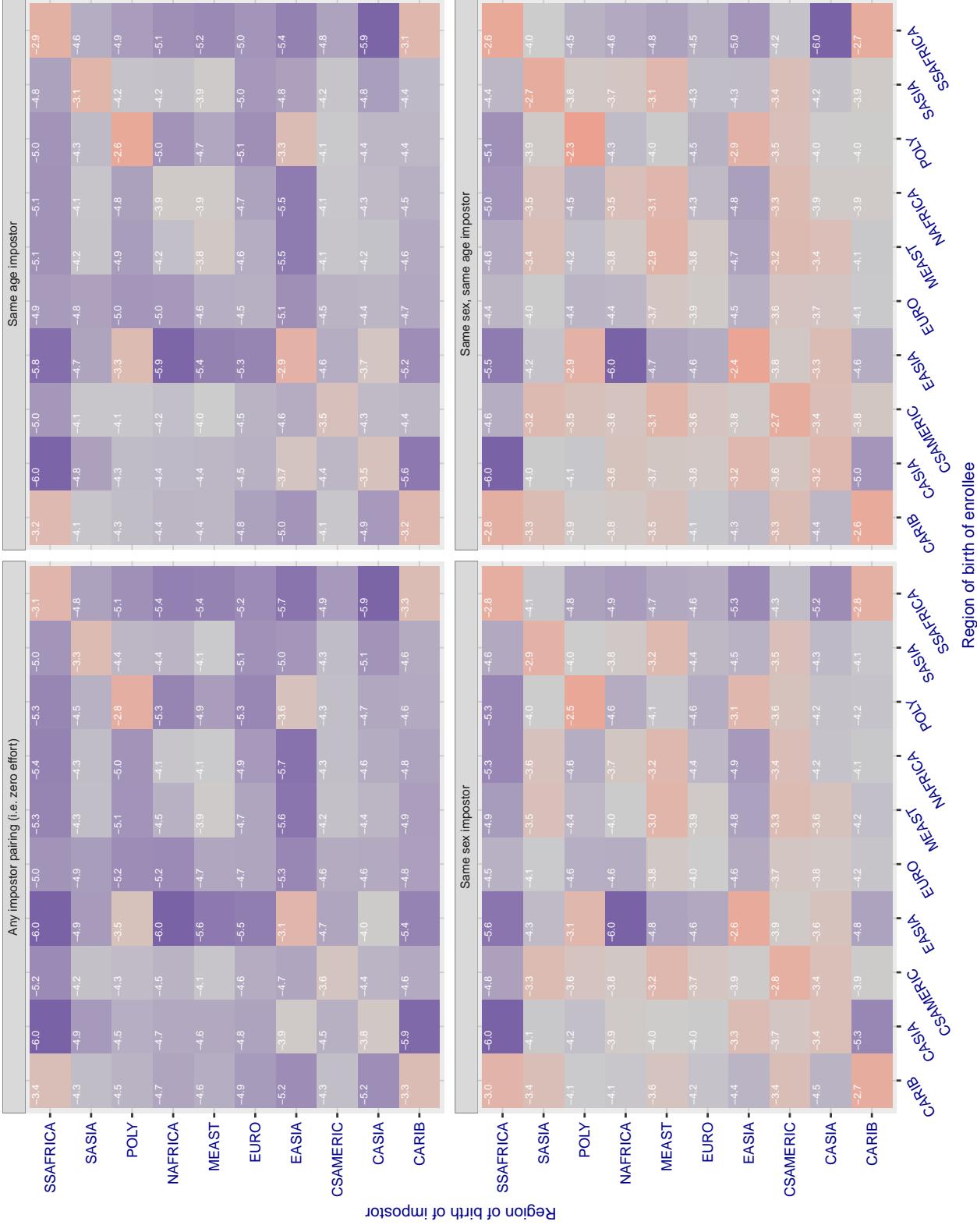


Figure 105: For algorithm 3divi-003 operating on visa images, the heatmap shows false match rates observed over impostor comparisons of faces from different individuals who were born in the given region pair. False matches are counted against a recognition threshold fixed globally to give the target FMR in the plot title, computed over all on the order of  $10^{10}$  impostor comparisons. If text appears in each box it give the same quantity as that coded by the color. Grey indicates FMR is at the intended FMR target level. Light red colors present a security vulnerability to, for example, a passport gate. Each +1 increase in  $\log_{10}$  FMR corresponds to a factor of 10 increase in FMR. The matrix is not quite symmetric because images in the enrollment and verification sets are different.

### Cross region FMR at threshold T = 0.702 for algorithm alchera\_000, giving FMR(T) = 0.0001 globally.

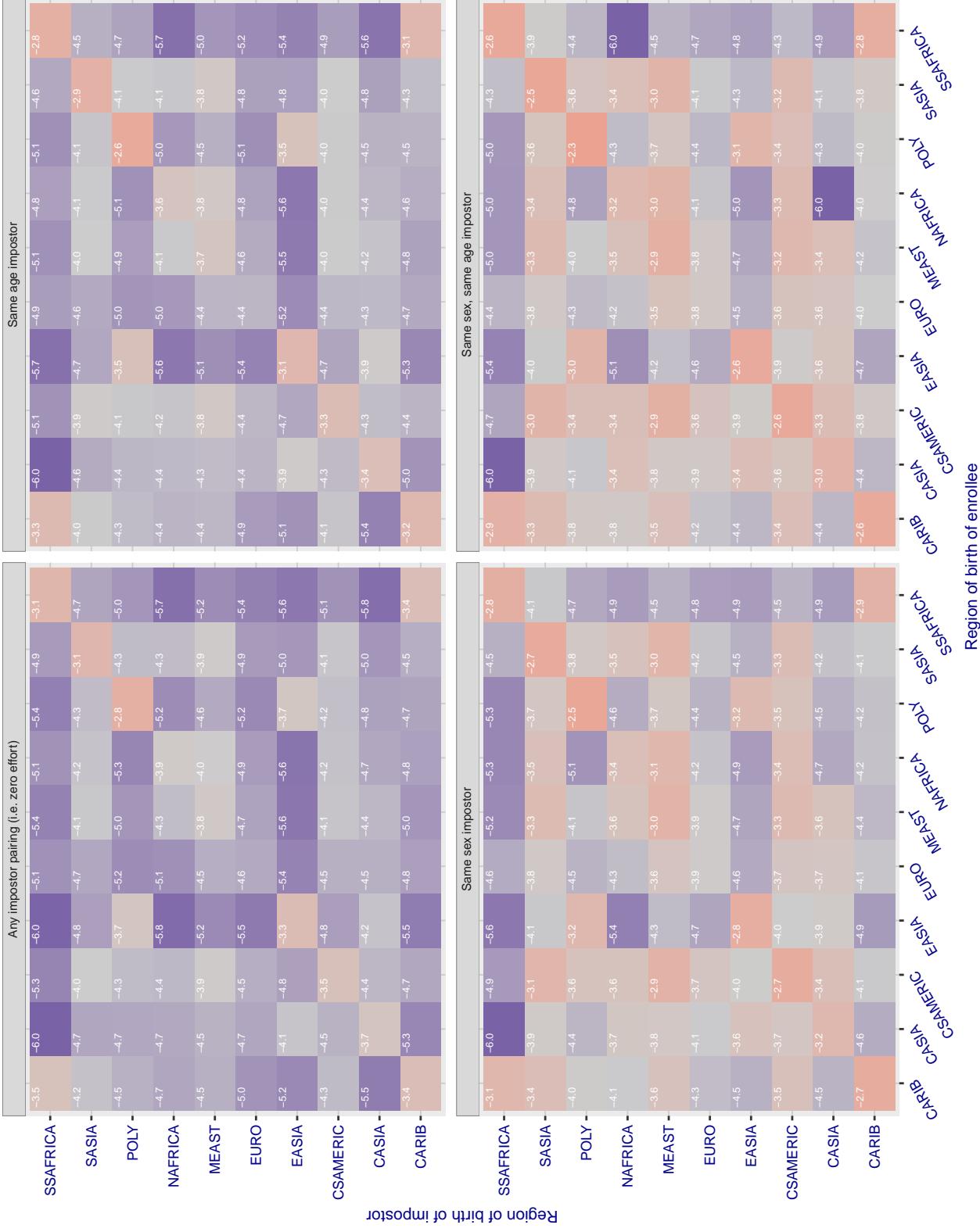


Figure 106: For algorithm alchera-000 operating on visa images, the heatmap shows false match rates observed over impostor comparisons of faces from different individuals who were born in the given region pair. False matches are counted against a recognition threshold fixed globally to give the target FMR in the plot title, computed over all on the order of  $10^{10}$  impostor comparisons. If text appears in each box it give the same quantity as that coded by the color. Grey indicates FMR is at the intended FMR target level. Light red colors present a security vulnerability to, for example, a passport gate. Each +1 increase in  $\log_{10} \text{FMR}$  corresponds to a factor of 10 increase in FMR. The matrix is not quite symmetric because images in the enrollment and verification sets are different.

### Cross region FMR at threshold T = 0.713 for algorithm alchera\_001, giving FMR(T) = 0.0001 globally.

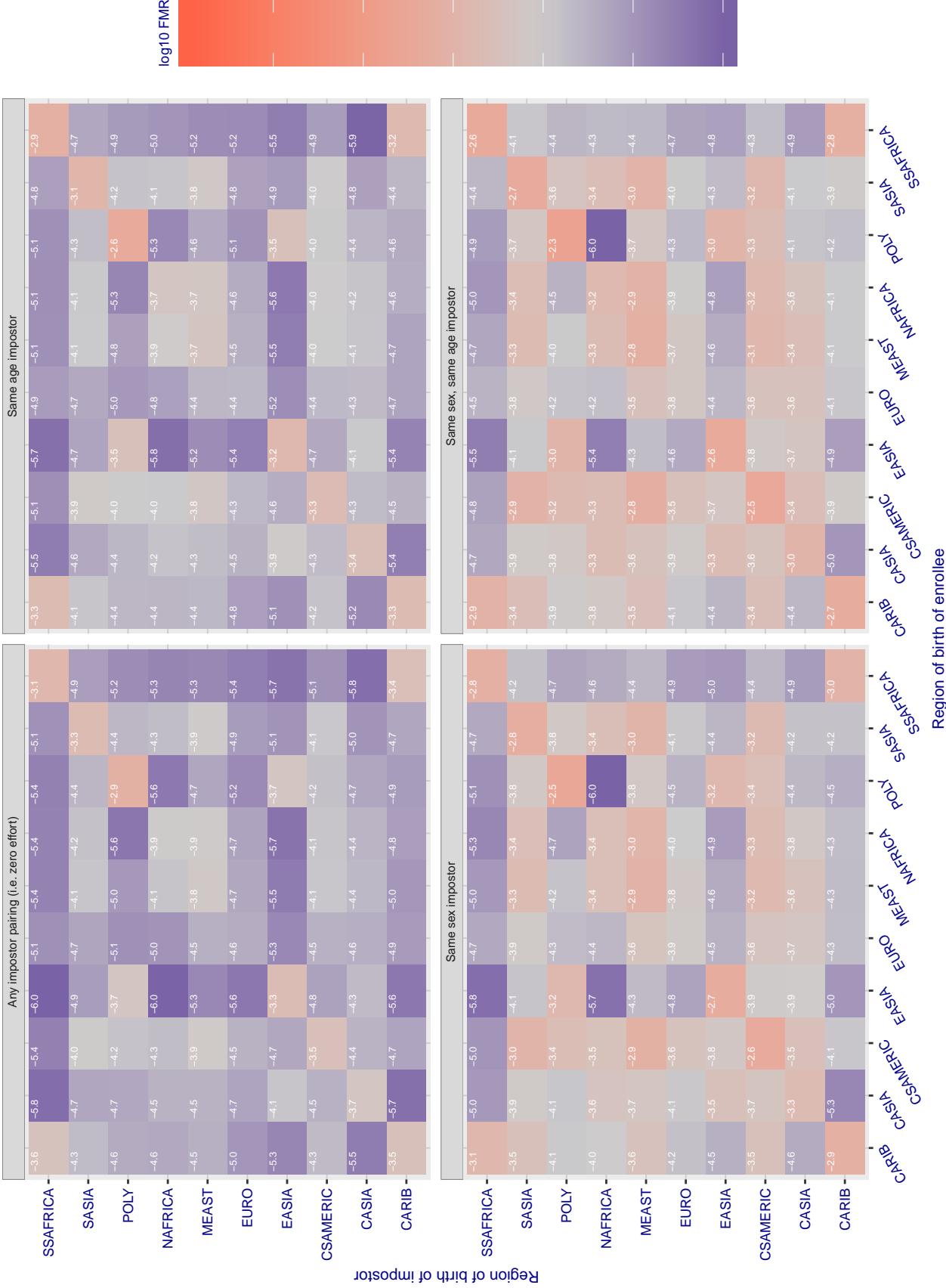


Figure 107: For algorithm alchera-001 operating on visa images, the heatmap shows false match rates observed over impostor comparisons of faces from different individuals who were born in the given region pair. False matches are counted against a recognition threshold fixed globally to give the target FMR in the plot title, computed over all on the order of  $10^{10}$  impostor comparisons. If text appears in each box it give the same quantity as that coded by the color. Grey indicates FMR is at the intended FMR target level. Light red colors present a security vulnerability to, for example, a passport gate. Each +1 increase in  $\log_{10} FMR$  corresponds to a factor of 10 increase in FMR. The matrix is not quite symmetric because images in the enrollment and verification sets are different.

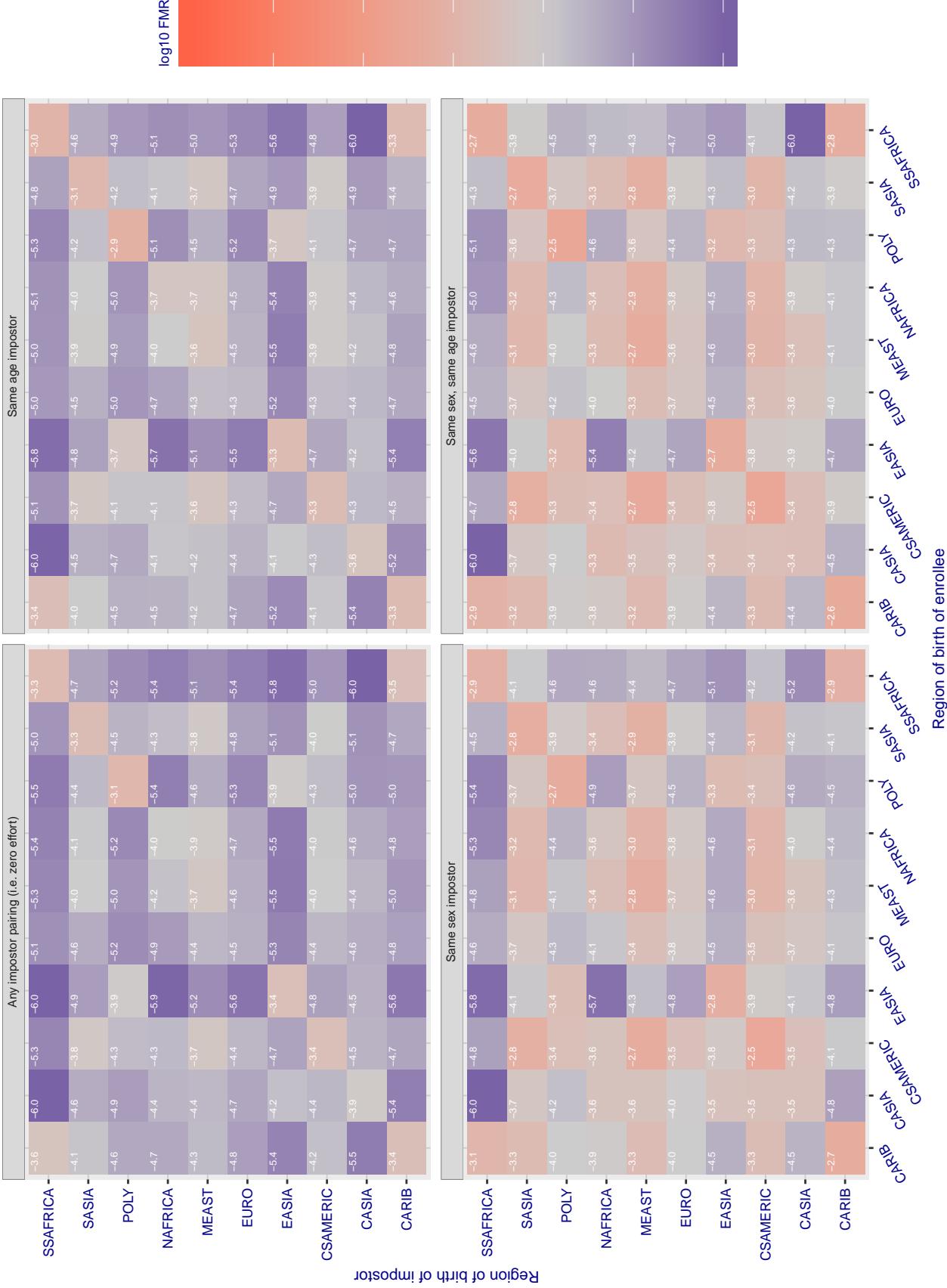
**Cross region FMR at threshold T = 0.433 for algorithm allgovision\_000, giving FMR(T) = 0.0001 globally.**

Figure 108: For algorithm allgovision-000 operating on visa images, the heatmap shows false match rates observed over impostor comparisons of faces from different individuals who were born in the given region pair. False matches are counted against a recognition threshold fixed globally to give the target FMR in the plot title, computed over all on the order of  $10^{10}$  impostor comparisons. If text appears in each box it give the same quantity as that coded by the color. Grey indicates FMR is at the intended FMR target level. Light red colors present a security vulnerability to, for example, a passport gate. Each +1 increase in  $\log_{10} FMR$  corresponds to a factor of 10 increase in FMR. The matrix is not quite symmetric because images in the enrollment and verification sets are different.

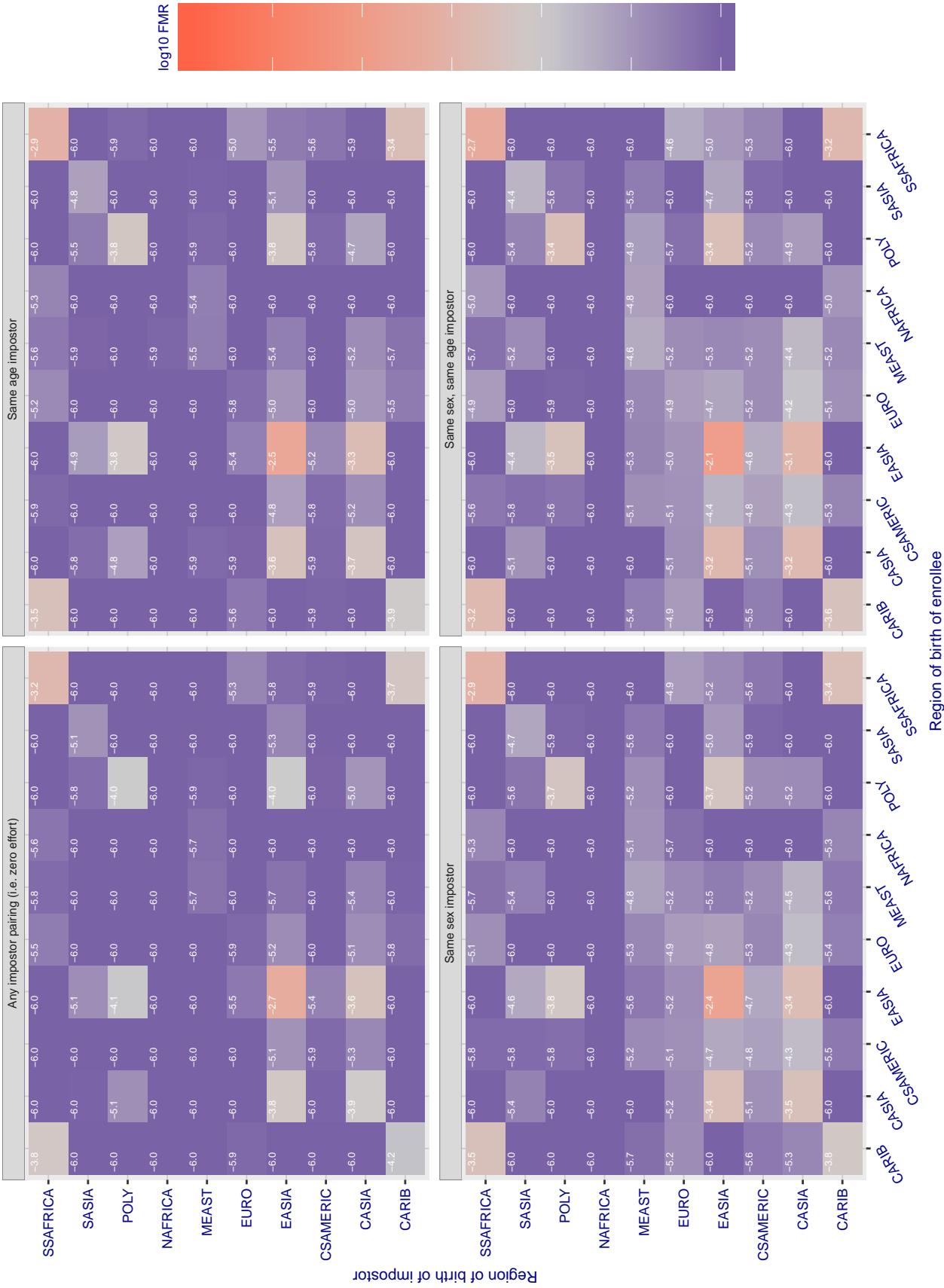
**Cross region FMR at threshold T = 3.640 for algorithm amplifiedgroup\_001, giving FMR(T) = 0.0001 globally.**

Figure 109: For algorithm amplifiedgroup-001 operating on visa images, the heatmap shows false match rates observed over impostor comparisons of faces from different individuals who were born in the given region pair. False matches are counted against a recognition threshold fixed globally to give the target FMR in the plot title, computed over all on the order of  $10^{10}$  impostor comparisons. If text appears in each box it give the same quantity as that coded by the color. Grey indicates FMR is at the intended FMR target level. Light red colors present a security vulnerability to, for example, a passport gate. Each +1 increase in  $\log_{10} \text{FMR}$  corresponds to a factor of 10 increase in FMR. The matrix is not quite symmetric because images in the enrollment and verification sets are different.

### Cross region FMR at threshold T = 0.404 for algorithm anke\_002, giving FMR(T) = 0.0001 globally.

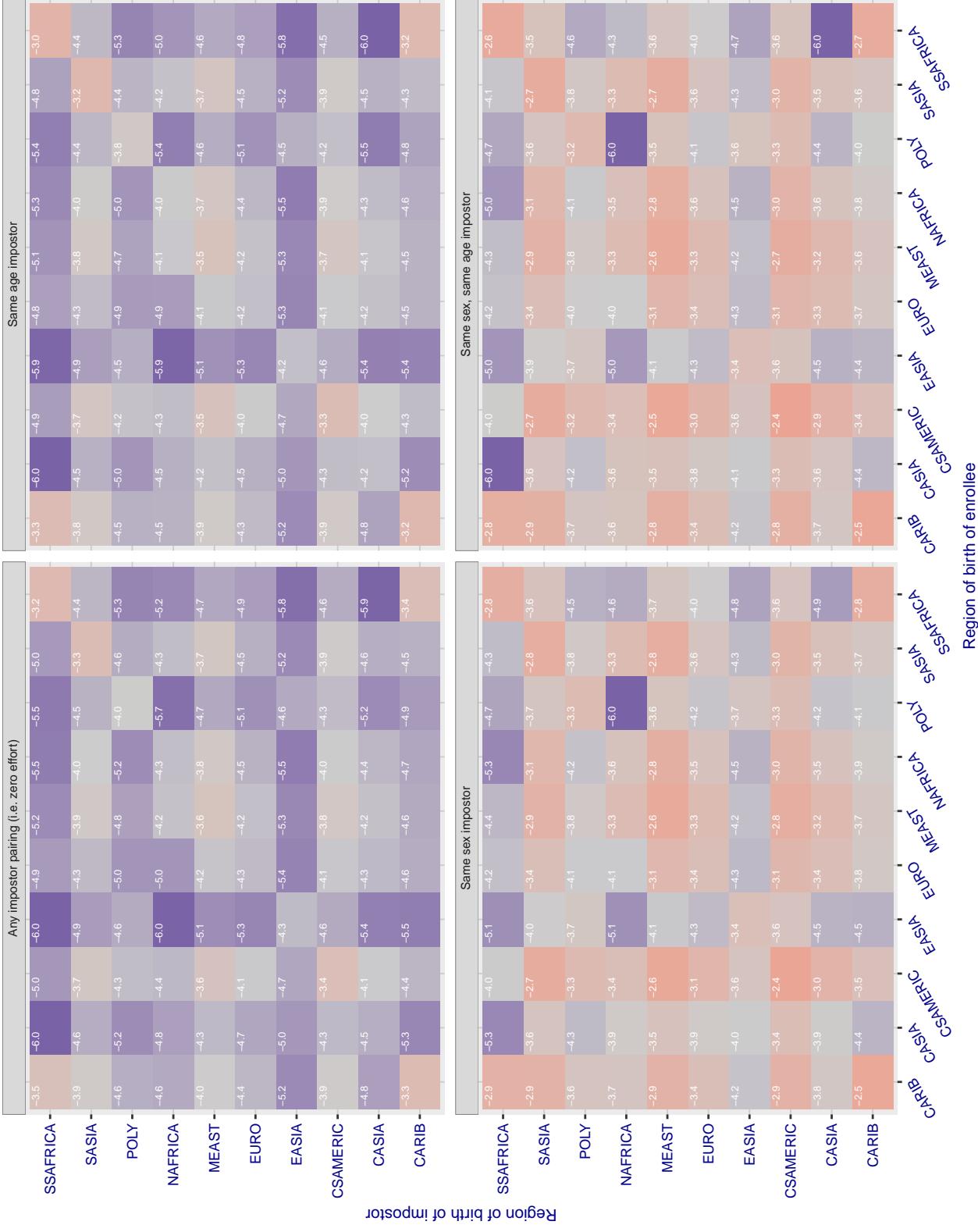


Figure 110: For algorithm anke-002 operating on visa images, the heatmap shows false match rates observed over impostor comparisons of faces from different individuals who were born in the given region pair. False matches are counted against a recognition threshold fixed globally to give the target FMR in the plot title, computed over all on the order of  $10^{10}$  impostor comparisons. If text appears in each box it give the same quantity as that coded by the color. Grey indicates FMR is at the intended FMR target level. Light red colors present a security vulnerability to, for example, a passport gate. Each +1 increase in  $\log 10$  FMR corresponds to a factor of 10 increase in FMR. The matrix is not quite symmetric because images in the enrollment and verification sets are different.

### Cross region FMR at threshold T = 0.397 for algorithm anke\_003, giving FMR(T) = 0.0001 globally.

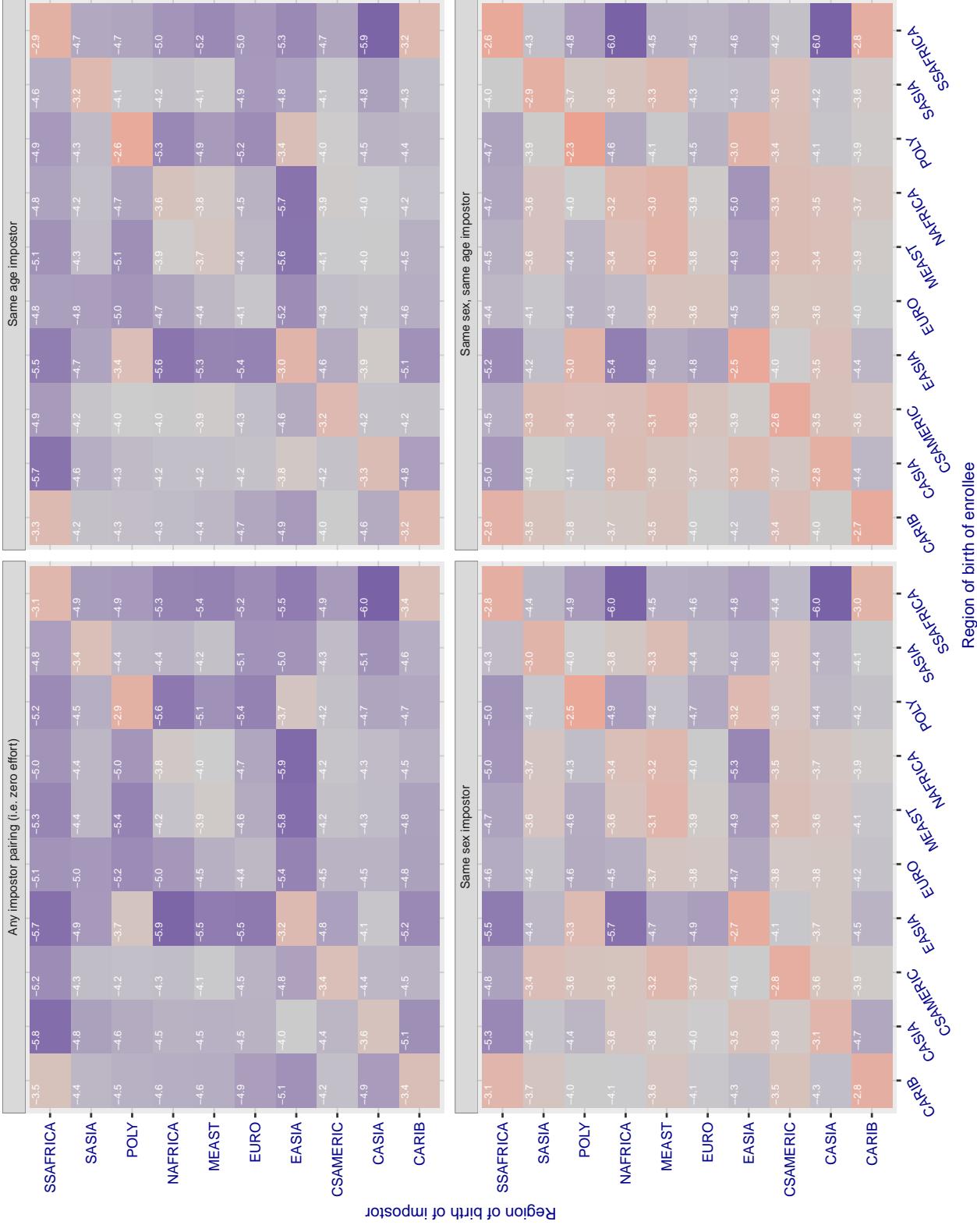


Figure 111: For algorithm anke-003 operating on visa images, the heatmap shows false match rates observed over impostor comparisons of faces from different individuals who were born in the given region pair. False matches are counted against a recognition threshold fixed globally to give the target FMR in the plot title, computed over all on the order of  $10^{10}$  impostor comparisons. If text appears in each box it give the same quantity as that coded by the color. Grey indicates FMR is at the intended FMR target level. Light red colors present a security vulnerability to, for example, a passport gate. Each +1 increase in  $\log_{10} \text{FMR}$  corresponds to a factor of 10 increase in FMR. The matrix is not quite symmetric because images in the enrollment and verification sets are different.

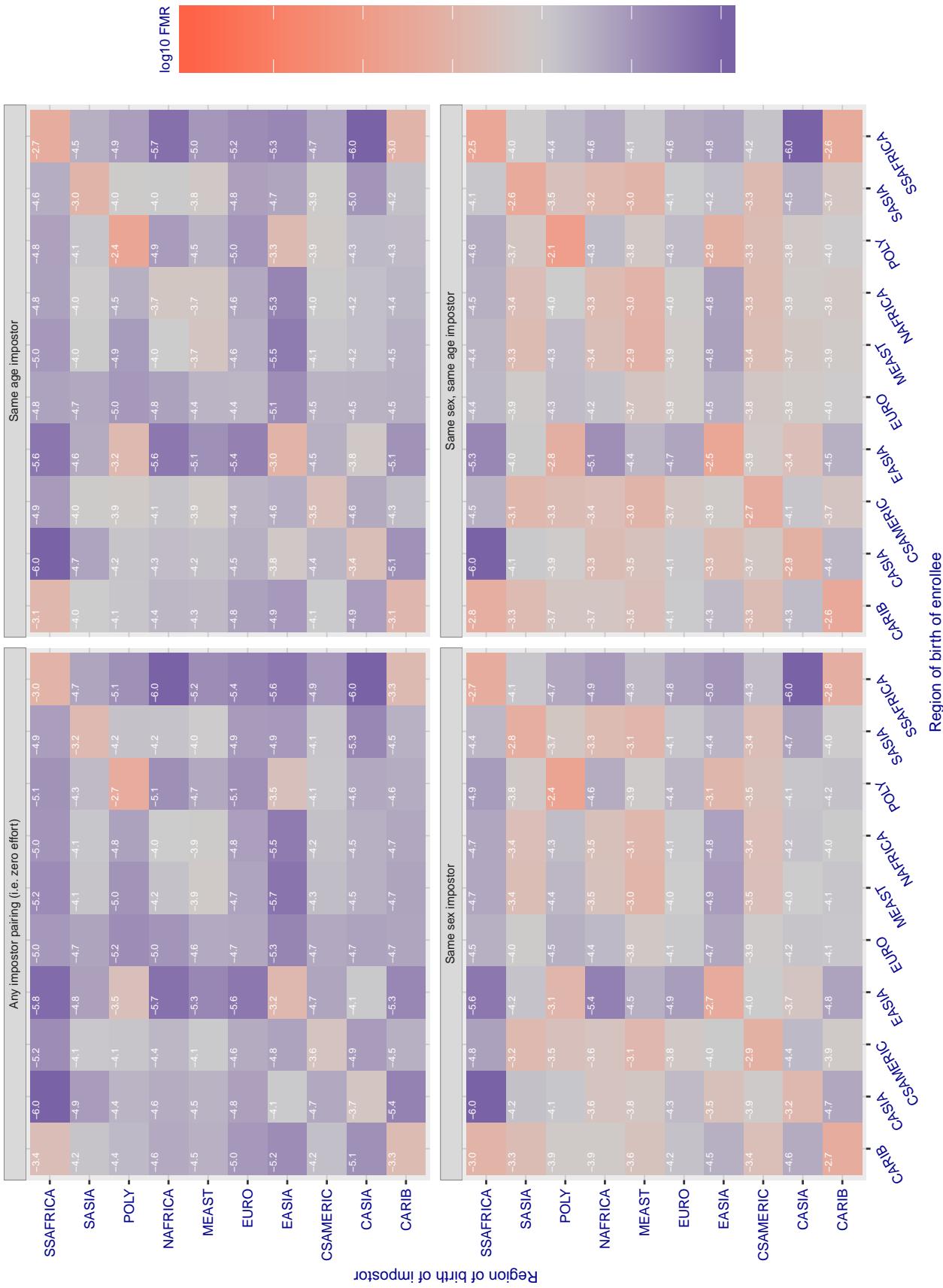
**Cross region FMR at threshold T = 1.526 for algorithm anyvision\_002, giving FMR(T) = 0.00001 globally.**

Figure 112: For algorithm anyvision-002 operating on visa images, the heatmap shows false match rates observed over impostor comparisons of faces from different individuals who were born in the given region pair. False matches are counted against a recognition threshold fixed globally to give the target FMR in the plot title, computed over all on the order of  $10^{10}$  impostor comparisons. If text appears in each box it give the same quantity as that coded by the color. Grey indicates FMR is at the intended FMR target level. Light red colors present a security vulnerability to, for example, a passport gate. Each +1 increase in  $\log_{10} FMR$  corresponds to a factor of 10 increase in FMR. The matrix is not quite symmetric because images in the enrollment and verification sets are different.

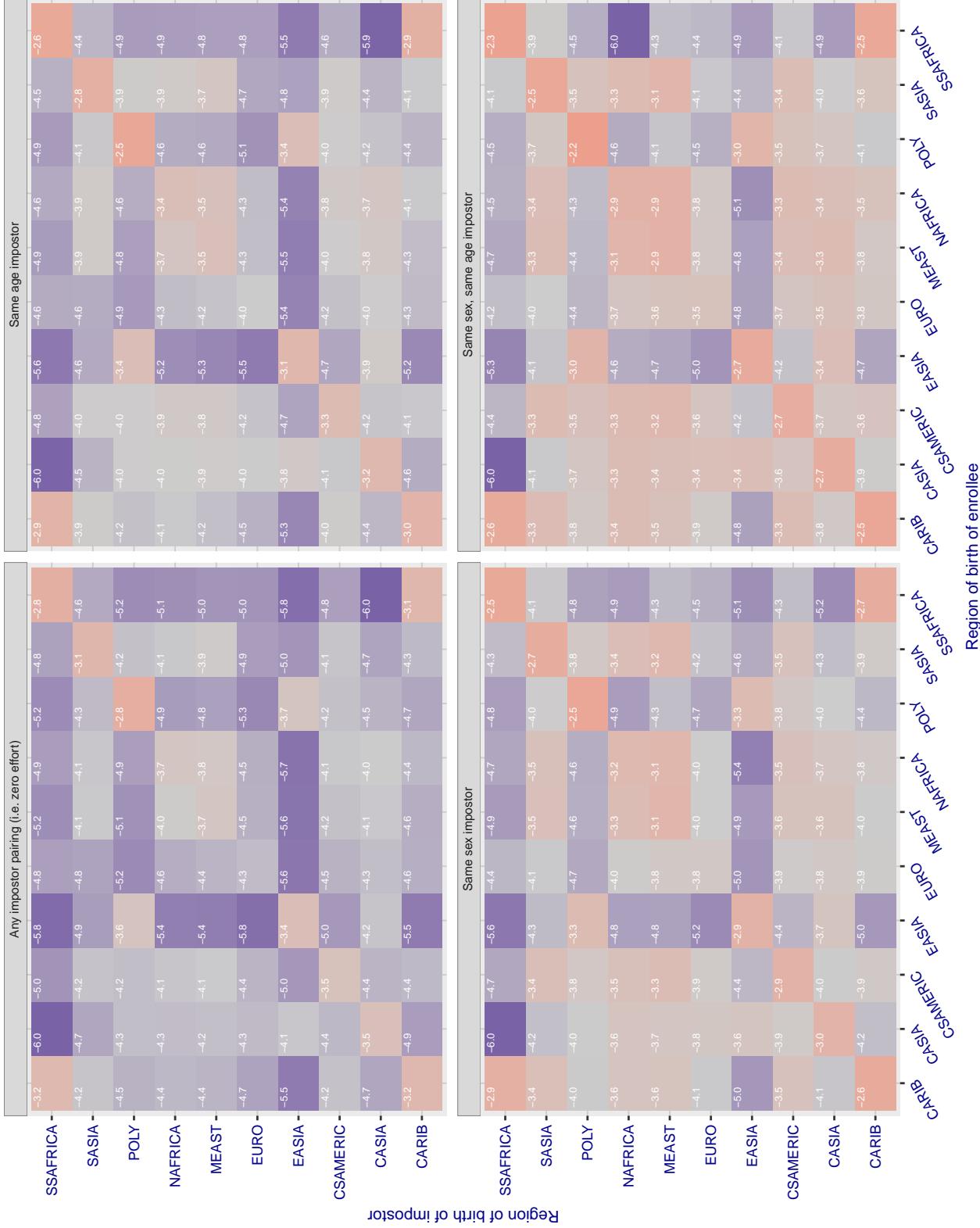
**Cross region FMR at threshold T = 1.375 for algorithm anyvision\_004, giving FMR(T) = 0.00001 globally.**

Figure 113: For algorithm anyvision-004 operating on visa images, the heatmap shows false match rates observed over impostor comparisons of faces from different individuals who were born in the given region pair. False matches are counted against a recognition threshold fixed globally to give the target FMR in the plot title, computed over all on the order of  $10^{10}$  impostor comparisons. If text appears in each box it give the same quantity as that coded by the color. Grey indicates FMR is at the intended FMR target level. Light red colors present a security vulnerability to, for example, a passport gate. Each +1 increase in  $\log_{10} FMR$  corresponds to a factor of 10 increase in FMR. The matrix is not quite symmetric because images in the enrollment and verification sets are different.

### Cross region FMR at threshold T = 3.868 for algorithm aware\_003, giving FMR(T) = 0.0001 globally.

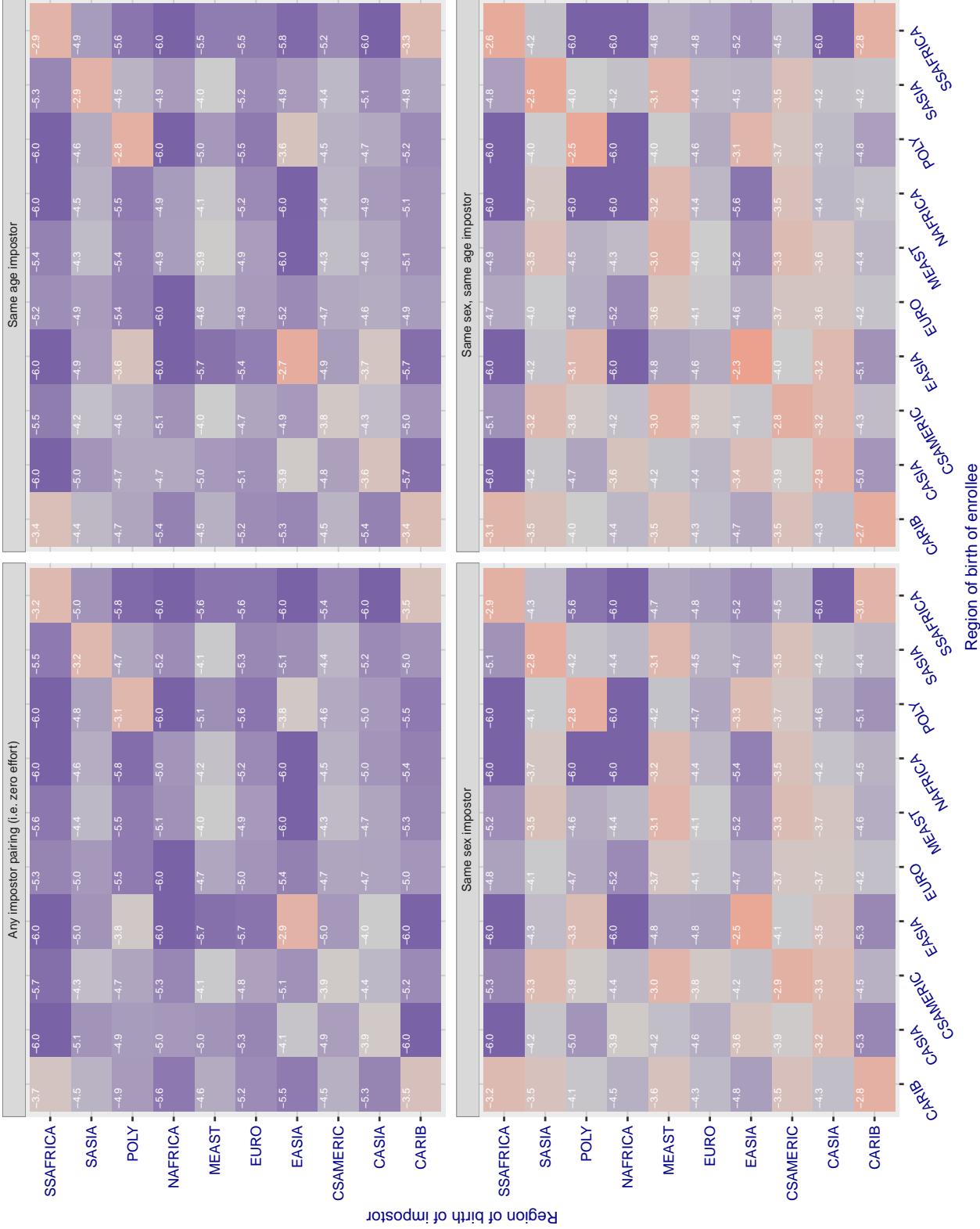


Figure 114: For algorithm aware-003 operating on visa images, the heatmap shows false match rates observed over impostor comparisons of faces from different individuals who were born in the given region pair. False matches are counted against a recognition threshold fixed globally to give the target FMR in the plot title, computed over all on the order of  $10^{10}$  impostor comparisons. If text appears in each box it give the same quantity as that coded by the color. Grey indicates FMR is at the intended FMR target level. Light red colors present a security vulnerability to, for example, a passport gate. Each +1 increase in  $\log_{10} \text{FMR}$  corresponds to a factor of 10 increase in FMR. The matrix is not quite symmetric because images in the enrollment and verification sets are different.

### Cross region FMR at threshold T = 5.084 for algorithm aware\_004, giving FMR(T) = 0.0001 globally.

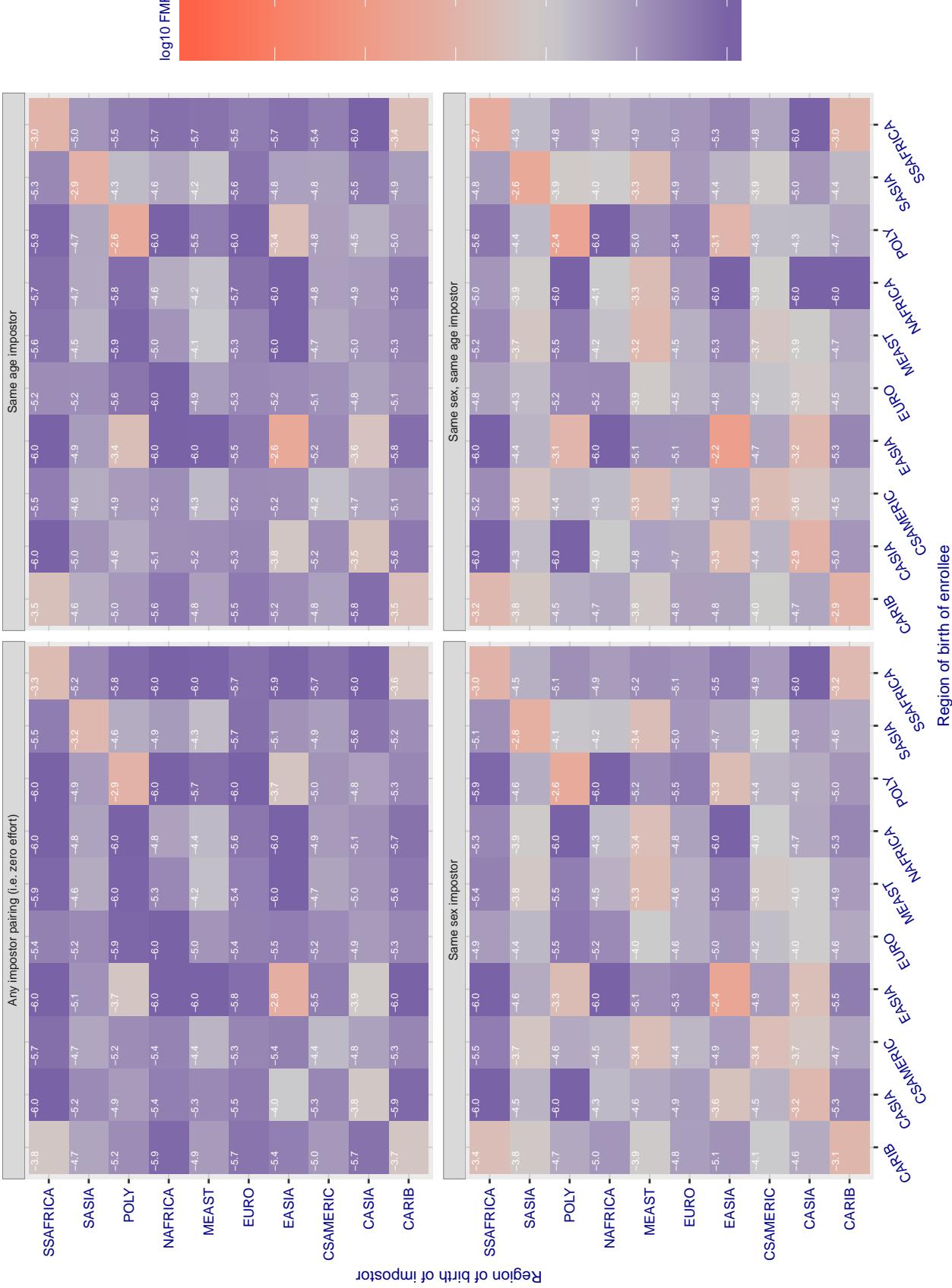


Figure 115: For algorithm aware-004 operating on visa images, the heatmap shows false match rates observed over impostor comparisons of faces from different individuals who were born in the given region pair. False matches are counted against a recognition threshold fixed globally to give the target FMR in the plot title, computed over all on the order of  $10^{10}$  impostor comparisons. If text appears in each box it give the same quantity as that coded by the color. Grey indicates FMR is at the intended FMR target level. Light red colors present a security vulnerability to, for example, a passport gate. Each +1 increase in  $\log_{10} FMR$  corresponds to a factor of 10 increase in FMR. The matrix is not quite symmetric because images in the enrollment and verification sets are different.

### Cross region FMR at threshold T = 0.919 for algorithm ayonix\_000, giving FMR(T) = 0.0001 globally.

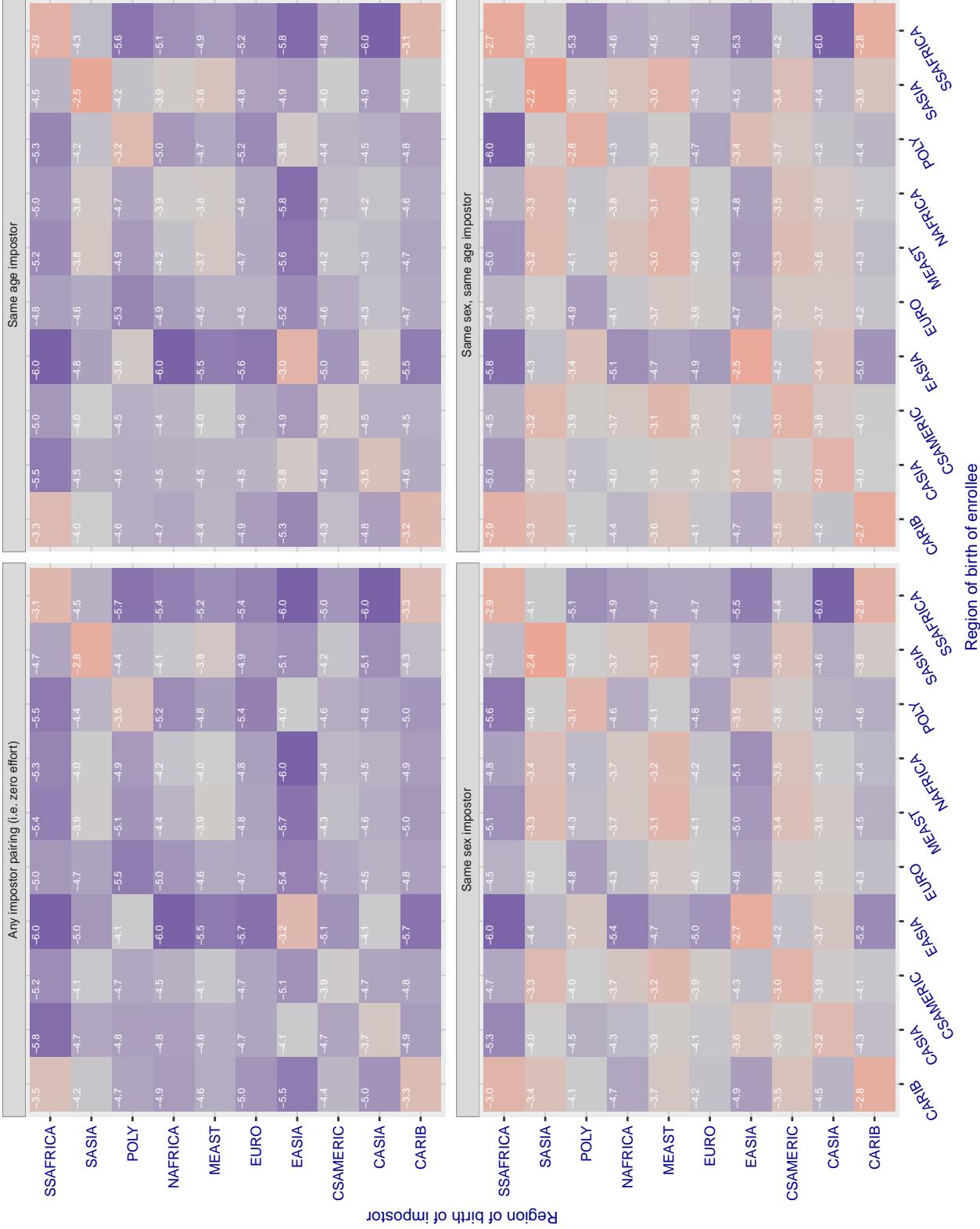


Figure 116: For algorithm ayonix-000 operating on visa images, the heatmap shows false match rates observed over impostor comparisons of faces from different individuals who were born in the given region pair. False matches are counted against a recognition threshold fixed globally to give the target FMR in the plot title, computed over all on the order of  $10^{10}$  impostor comparisons. If text appears in each box it give the same quantity as that coded by the color. Grey indicates FMR is at the intended FMR target level. Light red colors present a security vulnerability to, for example, a passport gate. Each +1 increase in  $\log_{10} FMR$  corresponds to a factor of 10 increase in FMR. The matrix is not quite symmetric because images in the enrollment and verification sets are different.

### Cross region FMR at threshold T = 0.731 for algorithm bm\_001, giving FMR(T) = 0.0001 globally.

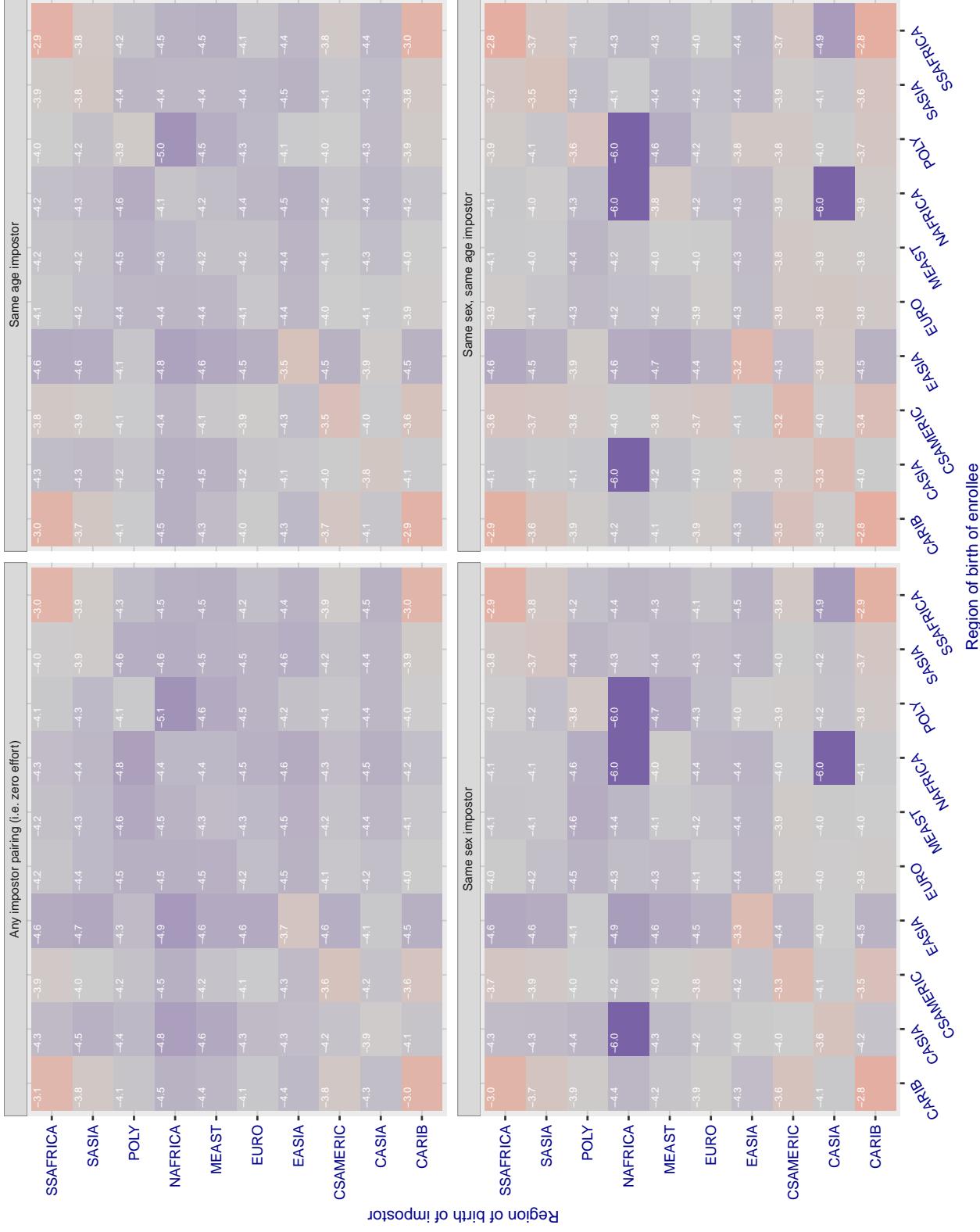


Figure 117: For algorithm bm-001 operating on visa images, the heatmap shows false match rates observed over impostor comparisons of faces from different individuals who were born in the given region pair. False matches are counted against a recognition threshold fixed globally to give the target FMR in the plot title, computed over all on the order of  $10^{10}$  impostor comparisons. If text appears in each box it give the same quantity as that coded by the color. Grey indicates FMR is at the intended FMR target level. Light red colors present a security vulnerability to, for example, a passport gate. Each +1 increase in  $\log_{10}$  FMR corresponds to a factor of 10 increase in FMR. The matrix is not quite symmetric because images in the enrollment and verification sets are different.

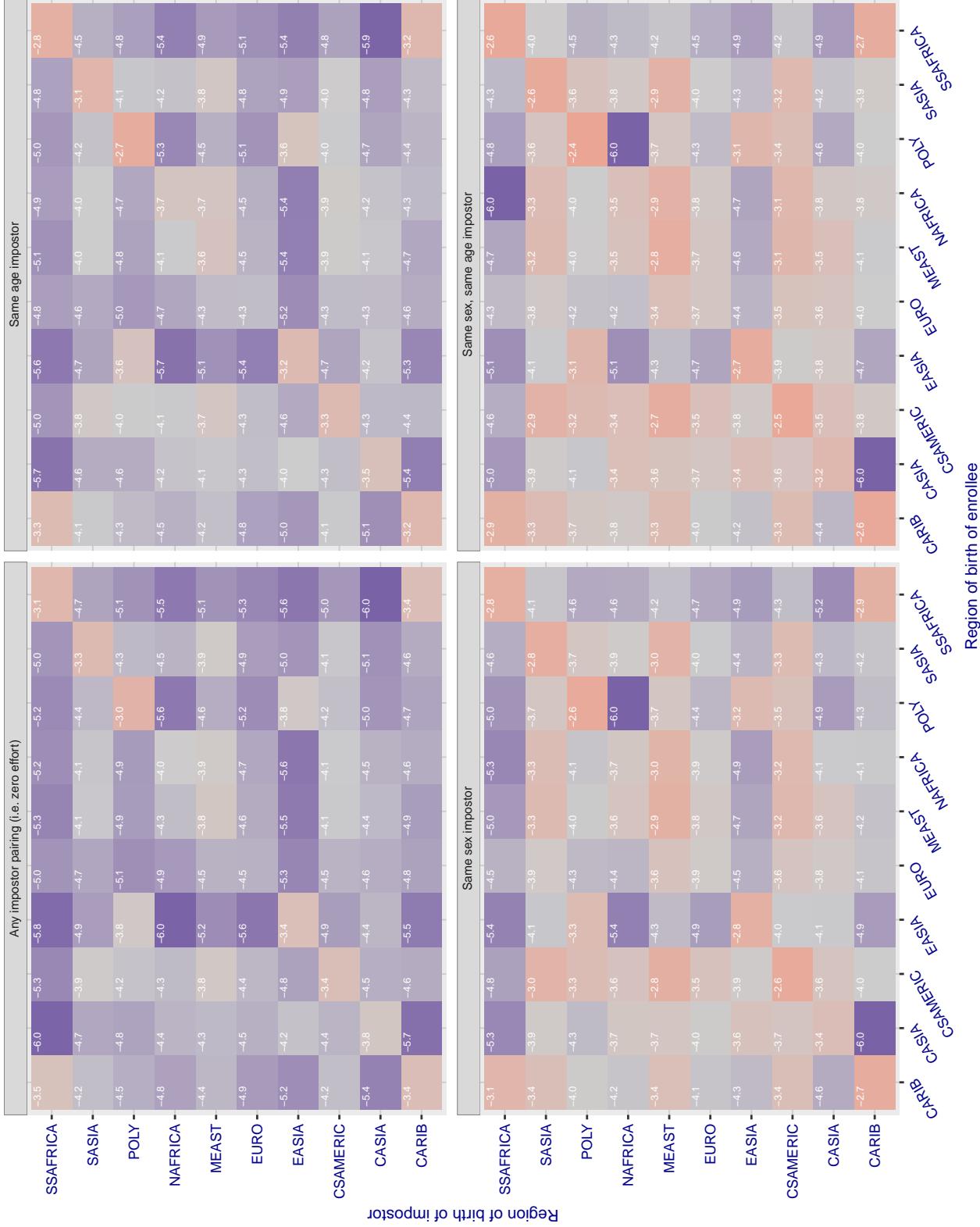
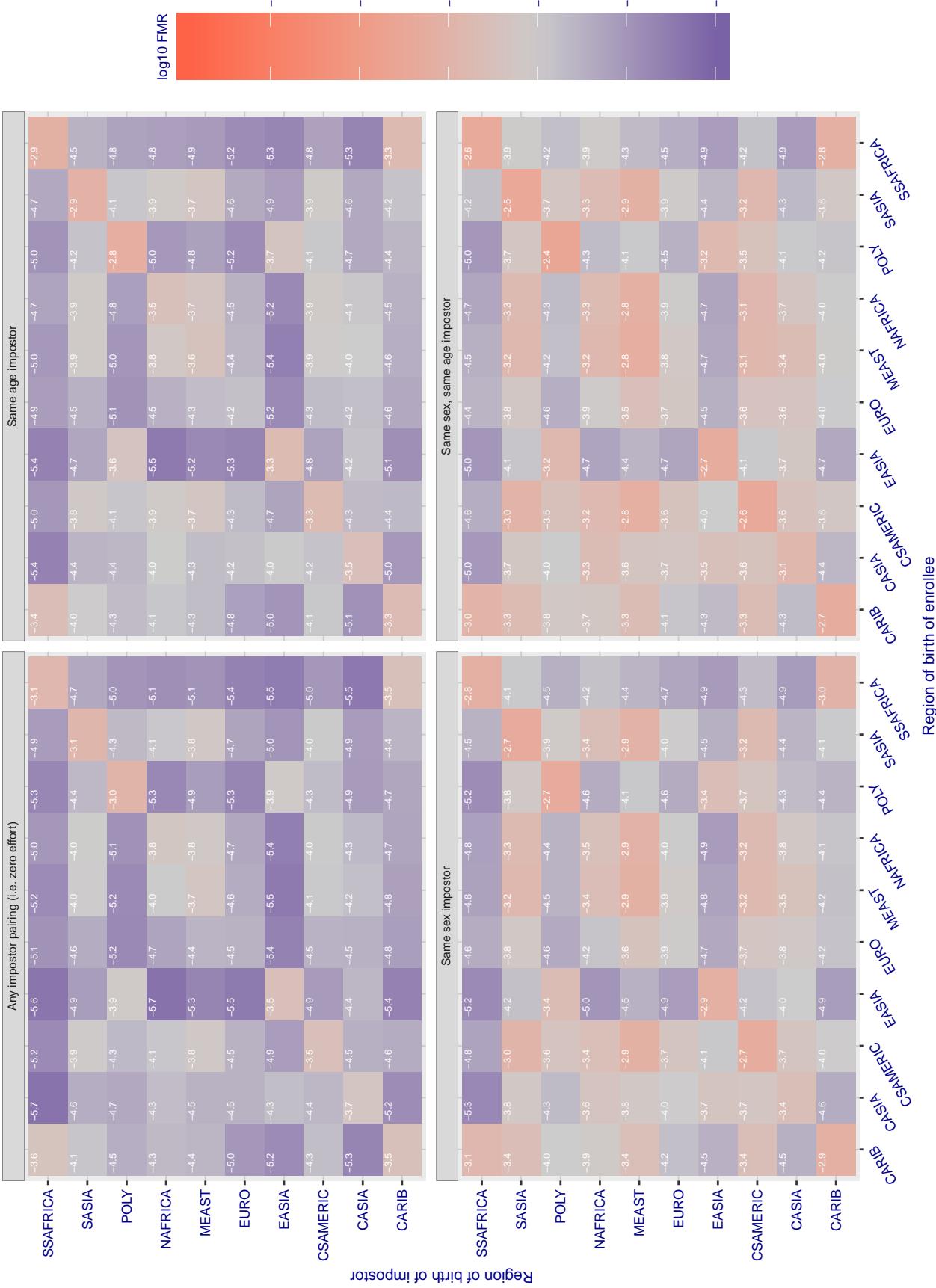
**Cross region FMR at threshold T = 0.388 for algorithm camvi\_002, giving FMR(T) = 0.0001 globally.**

Figure 118: For algorithm camvi-002 operating on visa images, the heatmap shows false match rates observed over impostor comparisons of faces from different individuals who were born in the given region pair. False matches are counted against a recognition threshold fixed globally to give the target FMR in the plot title, computed over all on the order of  $10^{10}$  impostor comparisons. If text appears in each box it give the same quantity as that coded by the color. Grey indicates FMR is at the intended FMR target level. Light red colors present a security vulnerability to, for example, a passport gate. Each +1 increase in  $\log_{10} FMR$  corresponds to a factor of 10 increase in FMR. The matrix is not quite symmetric because images in the enrollment and verification sets are different.

Cross region FMR at threshold  $T = 0.383$  for algorithm camvi\_003, giving  $FMR(T) = 0.0001$  globally.



**Figure 119:** For algorithm camvi-003 operating on visa images, the heatmap shows false match rates observed over impostor comparisons of faces from different individuals who were born in the given region pair. False matches are counted against a recognition threshold fixed globally to give the target  $FMR$  in the plot title, computed over all on the order of  $10^{10}$  impostor comparisons. If text appears in each box it give the same quantity as that coded by the color. Grey indicates  $FMR$  is at the intended  $FMR$  target level. Light red colors present a security vulnerability to, for example, a passport gate. Each +1 increase in  $\log_{10} FMR$  corresponds to a factor of 10 increase in  $FMR$ . The matrix is not quite symmetric because images in the enrollment and verification sets are different.

### Cross region FMR at threshold T = 0.436 for algorithm ceiec\_001, giving FMR( $\Gamma$ ) = 0.0001 globally.

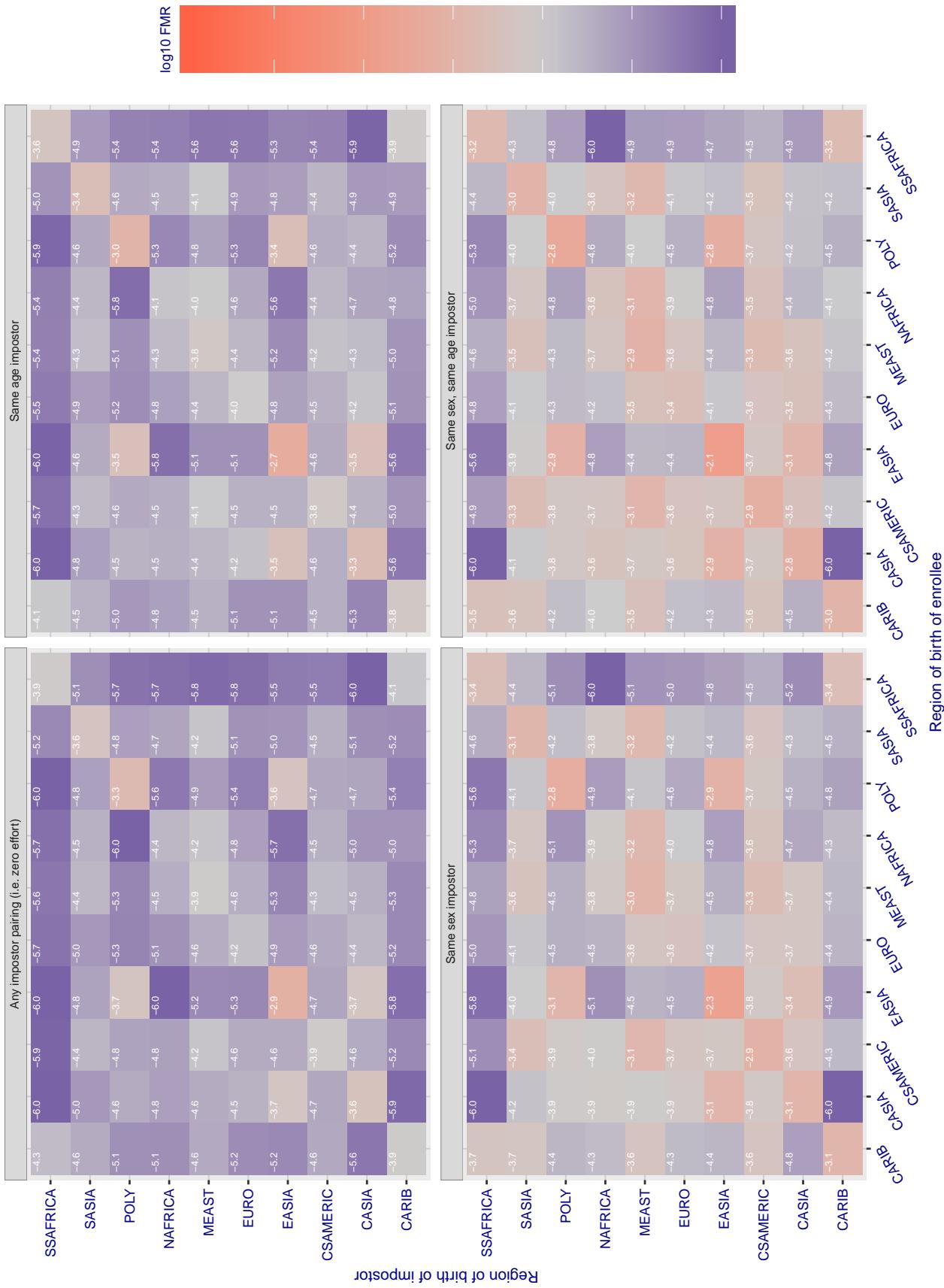


Figure 120: For algorithm ceiec-001 operating on visa images, the heatmap shows false match rates observed over impostor comparisons of faces from different individuals who were born in the given region pair. False matches are counted against a recognition threshold fixed globally to give the target FMR in the plot title, computed over all on the order of  $10^{10}$  impostor comparisons. If text appears in each box it give the same quantity as that coded by the color. Grey indicates FMR is at the intended FMR target level. Light red colors present a security vulnerability to, for example, a passport gate. Each +1 increase in  $\log 10$  FMR corresponds to a factor of 10 increase in FMR. The matrix is not quite symmetric because images in the enrollment and verification sets are different.

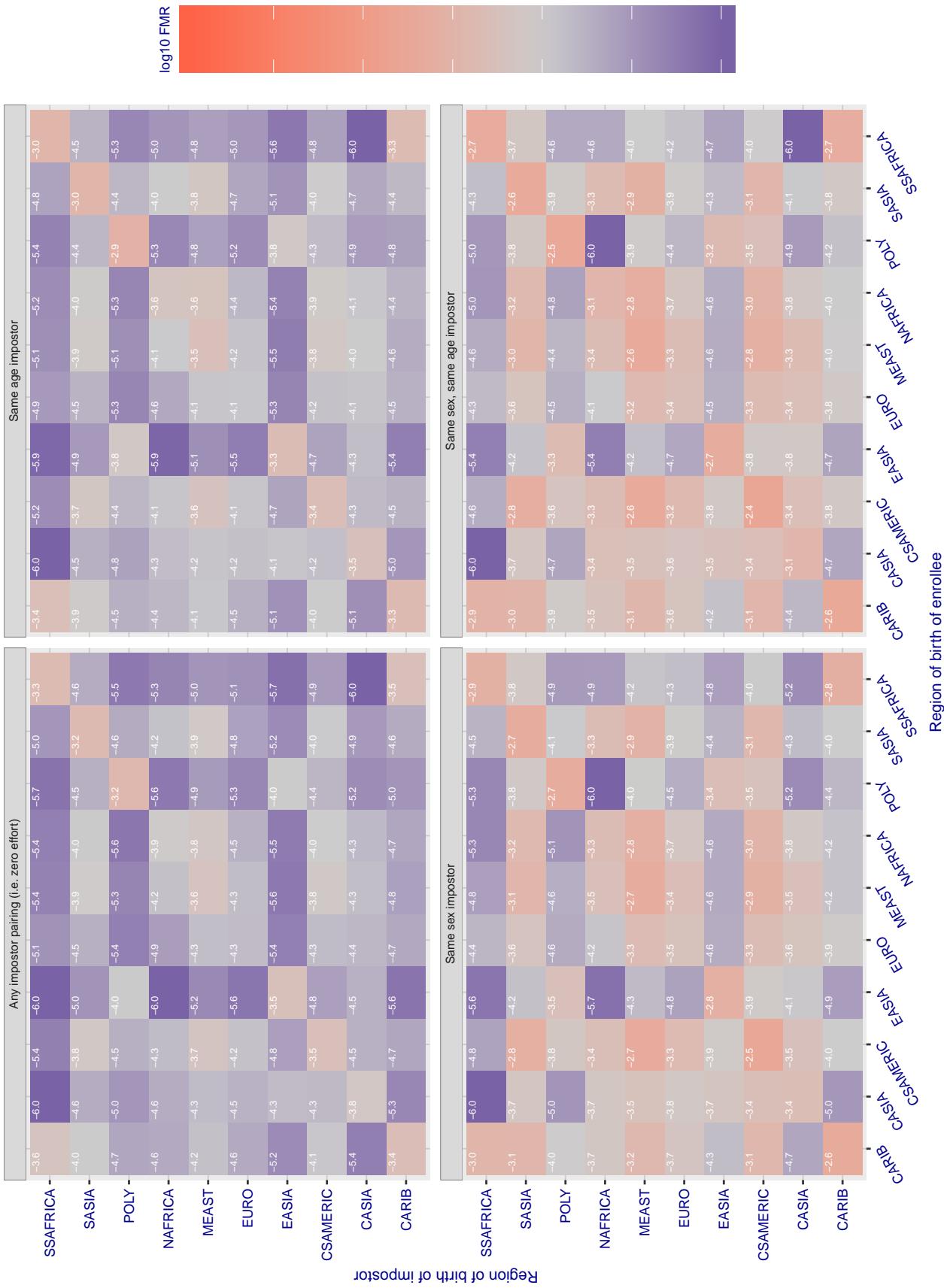
**Cross region FMR at threshold T = 3271.000 for algorithm cogent\_002, giving FMR(T) = 0.0001 globally.**

Figure 121: For algorithm cogent-002 operating on visa images, the heatmap shows false match rates observed over impostor comparisons of faces from different individuals who were born in the given region pair. False matches are counted against a recognition threshold fixed globally to give the target FMR in the plot title, computed over all on the order of  $10^{10}$  impostor comparisons. If text appears in each box it give the same quantity as that coded by the color. Grey indicates FMR is at the intended FMR target level. Light red colors present a security vulnerability to, for example, a passport gate. Each +1 increase in  $\log_{10} FMR$  corresponds to a factor of 10 increase in FMR. The matrix is not quite symmetric because images in the enrollment and verification sets are different.

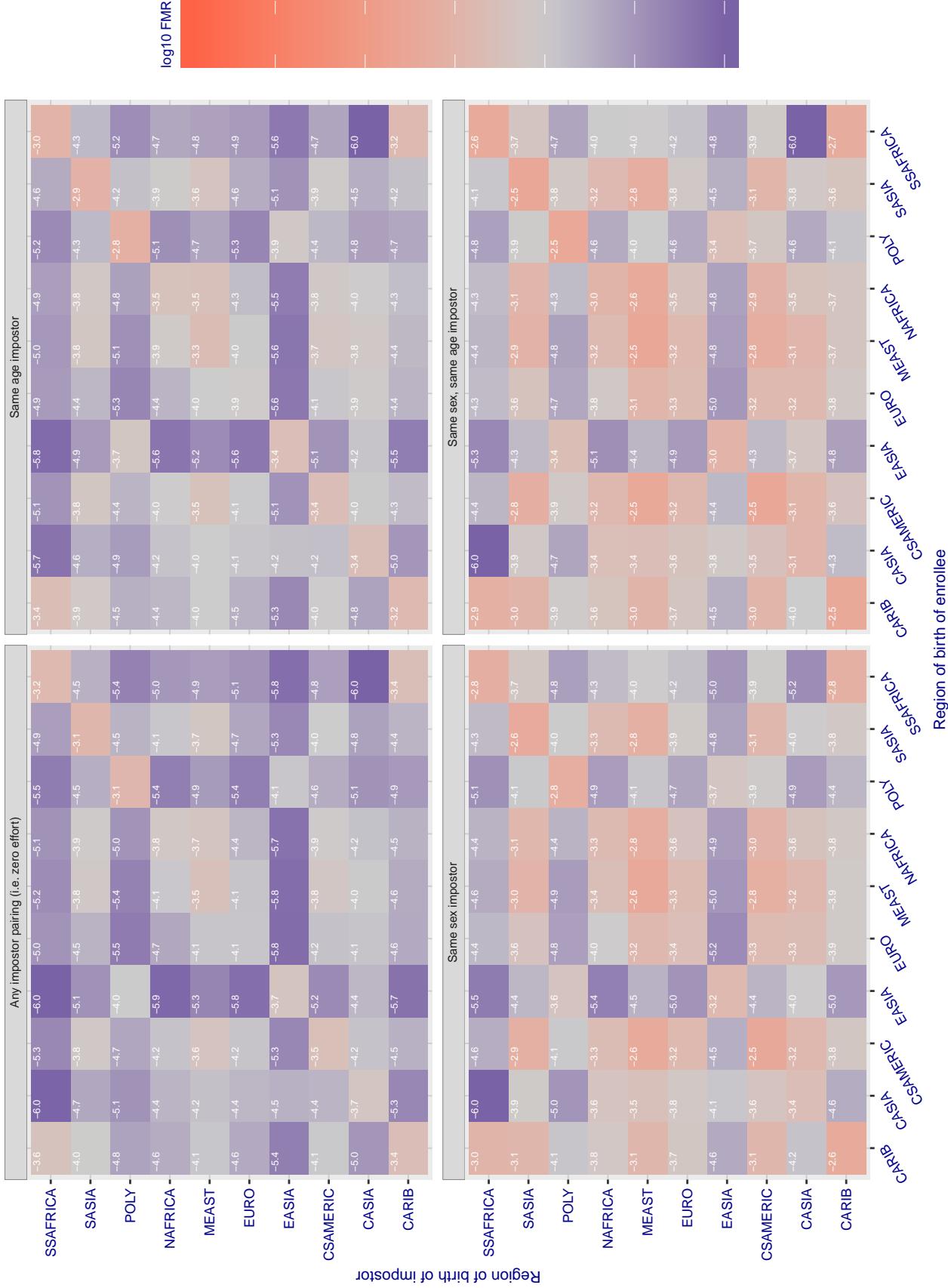
**Cross region FMR at threshold T = 2972.000 for algorithm cogent\_003, giving FMR(T) = 0.0001 globally.**

Figure 122: For algorithm cogent-003 operating on visa images, the heatmap shows false match rates observed over impostor comparisons of faces from different individuals who were born in the given region pair. False matches are counted against a recognition threshold fixed globally to give the target FMR in the plot title, computed over all on the order of  $10^{10}$  impostor comparisons. If text appears in each box it give the same quantity as that coded by the color. Grey indicates FMR is at the intended FMR target level. Light red colors present a security vulnerability to, for example, a passport gate. Each +1 increase in  $\log_{10} FMR$  corresponds to a factor of 10 increase in FMR. The matrix is not quite symmetric because images in the enrollment and verification sets are different.

### Cross region FMR at threshold T = 0.565 for algorithm cognitec\_000, giving FMR(T) = 0.0001 globally.

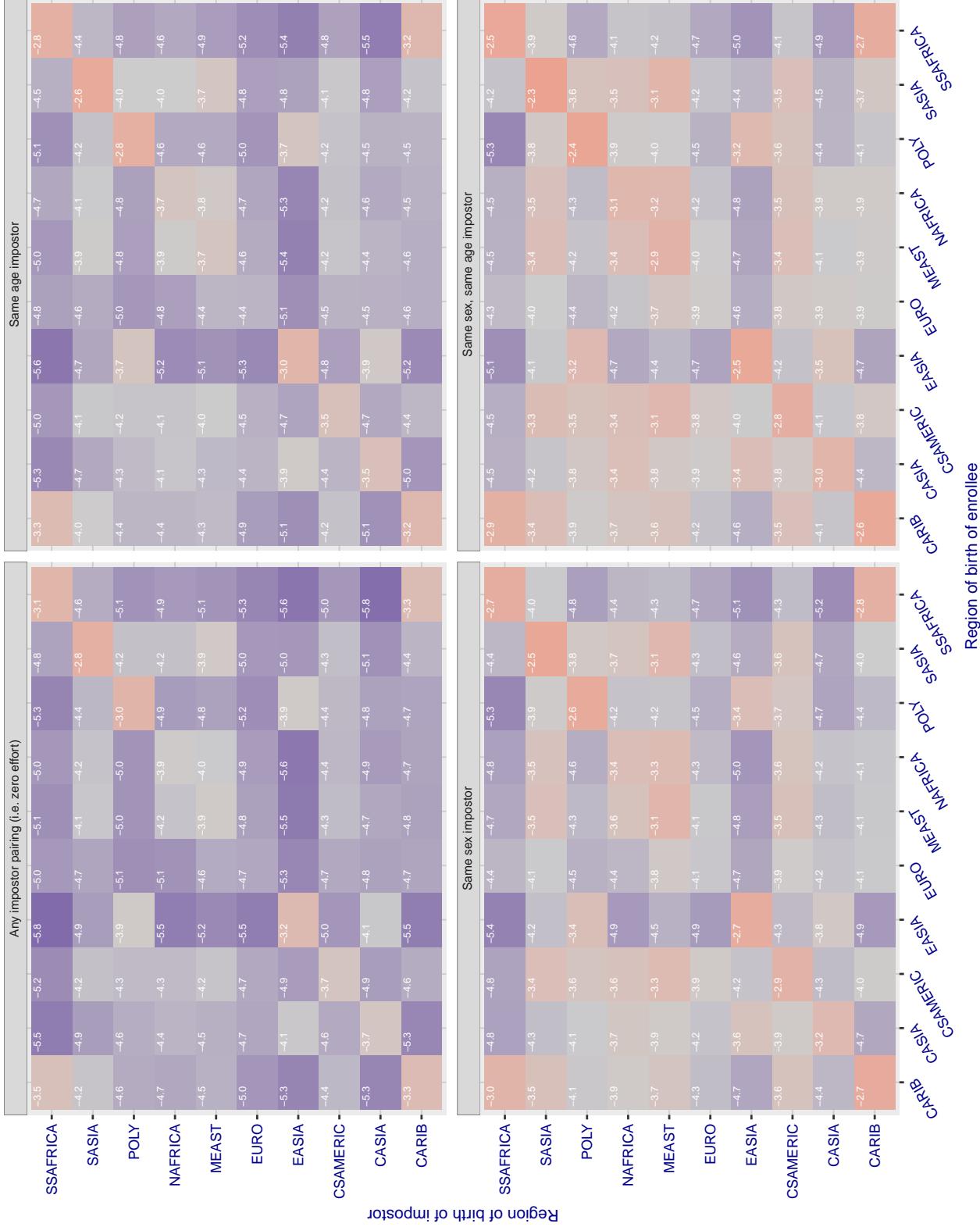


Figure 123: For algorithm cognitec-000 operating on visa images, the heatmap shows false match rates observed over impostor comparisons of faces from different individuals who were born in the given region pair. False matches are counted against a recognition threshold fixed globally to give the target FMR in the plot title, computed over all on the order of  $10^{10}$  impostor comparisons. If text appears in each box it give the same quantity as that coded by the color. Grey indicates FMR is at the intended FMR target level. Light red colors present a security vulnerability to, for example, a passport gate. Each +1 increase in  $\log_{10} FMR$  corresponds to a factor of 10 increase in FMR. The matrix is not quite symmetric because images in the enrollment and verification sets are different.

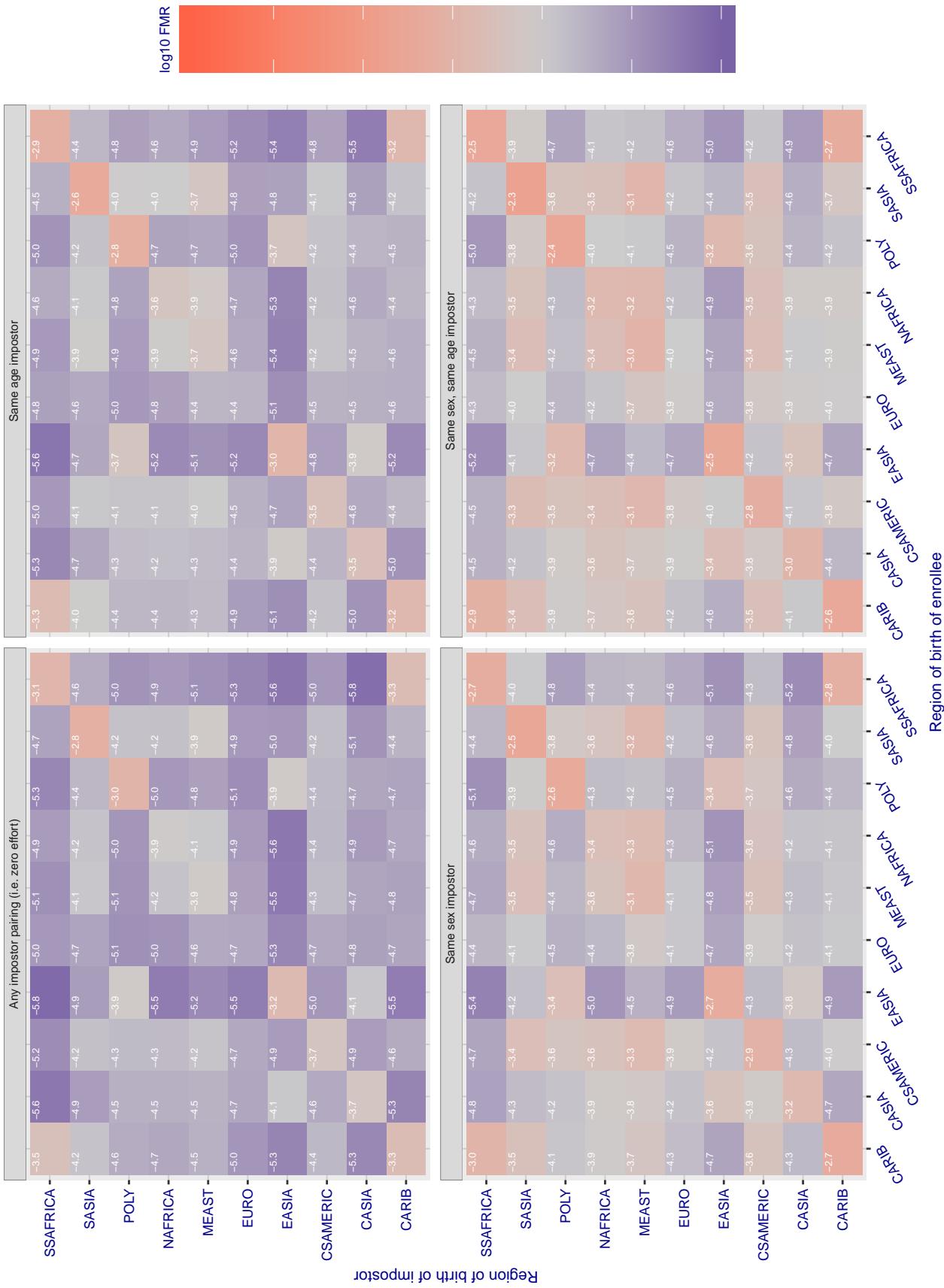
**Cross region FMR at threshold T = 0.565 for algorithm cognitec\_001, giving FMR(T) = 0.0001 globally.**

Figure 124: For algorithm cognitec-001 operating on visa images, the heatmap shows false match rates observed over impostor comparisons of faces from different individuals who were born in the given region pair. False matches are counted against a recognition threshold fixed globally to give the target FMR in the plot title, computed over all on the order of  $10^{10}$  impostor comparisons. If text appears in each box it give the same quantity as that coded by the color. Grey indicates FMR is at the intended FMR target level. Light red colors present a security vulnerability to, for example, a passport gate. Each +1 increase in  $\log_{10} FMR$  corresponds to a factor of 10 increase in FMR. The matrix is not quite symmetric because images in the enrollment and verification sets are different.

### Cross region FMR at threshold T = 0.762 for algorithm cyberextruder\_001, giving FMR(T) = 0.00001 globally.

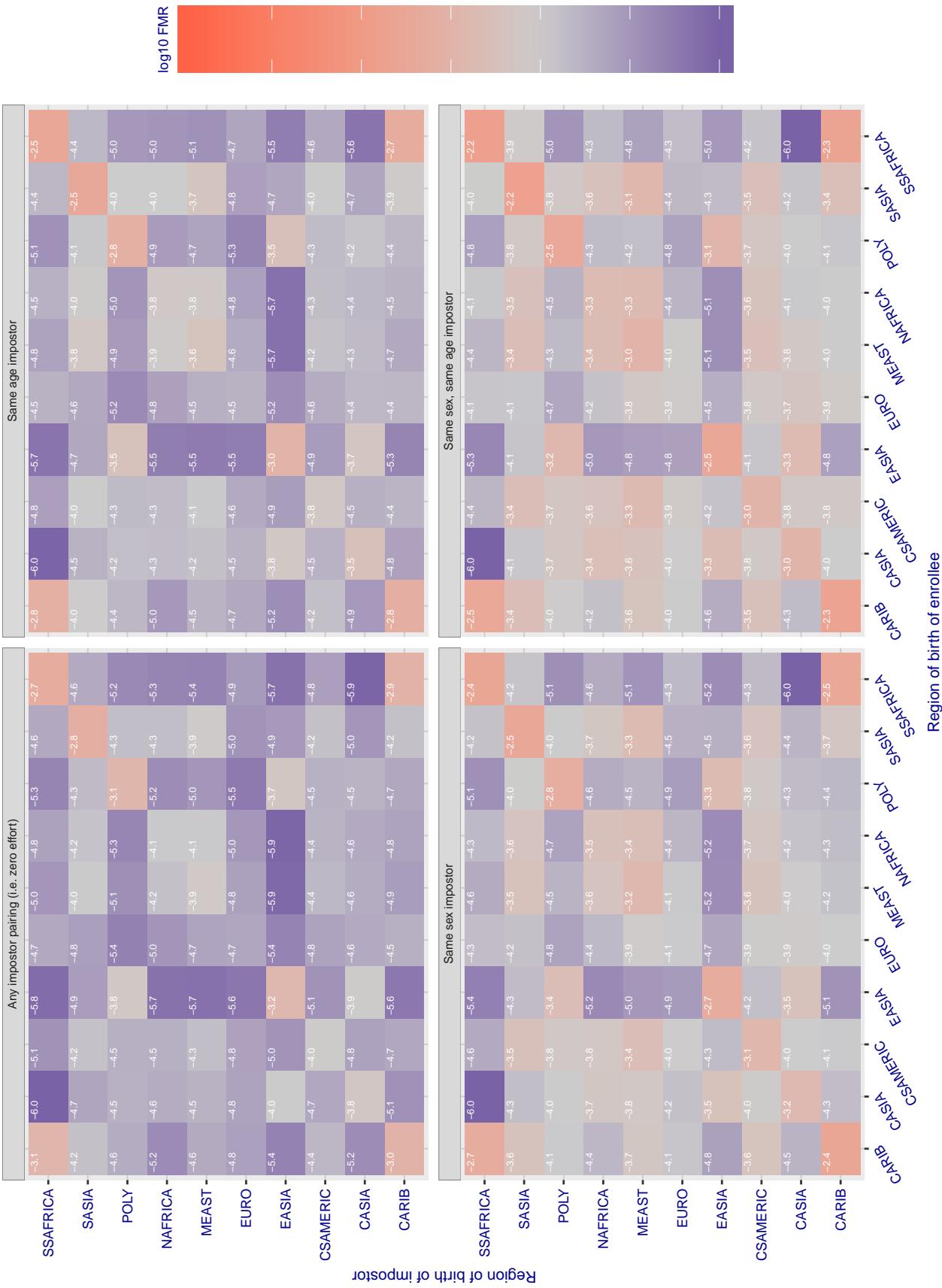


Figure 125: For algorithm cyberextruder-001 operating on visa images, the heatmap shows false match rates observed over impostor comparisons of faces from different individuals who were born in the given region pair. False matches are counted against a recognition threshold fixed globally to give the target FMR in the plot title, computed over all on the order of  $10^{10}$  impostor comparisons. If text appears in each box it give the same quantity as that coded by the color. Grey indicates FMR is at the intended FMR target level. Light red colors present a security vulnerability to, for example, a passport gate. Each +1 increase in  $\log_{10} FMR$  corresponds to a factor of 10 increase in FMR. The matrix is not quite symmetric because images in the enrollment and verification sets are different.

### Cross region FMR at threshold T = 0.500 for algorithm cyberextruder\_002, giving FMR(T) = 0.0001 globally.

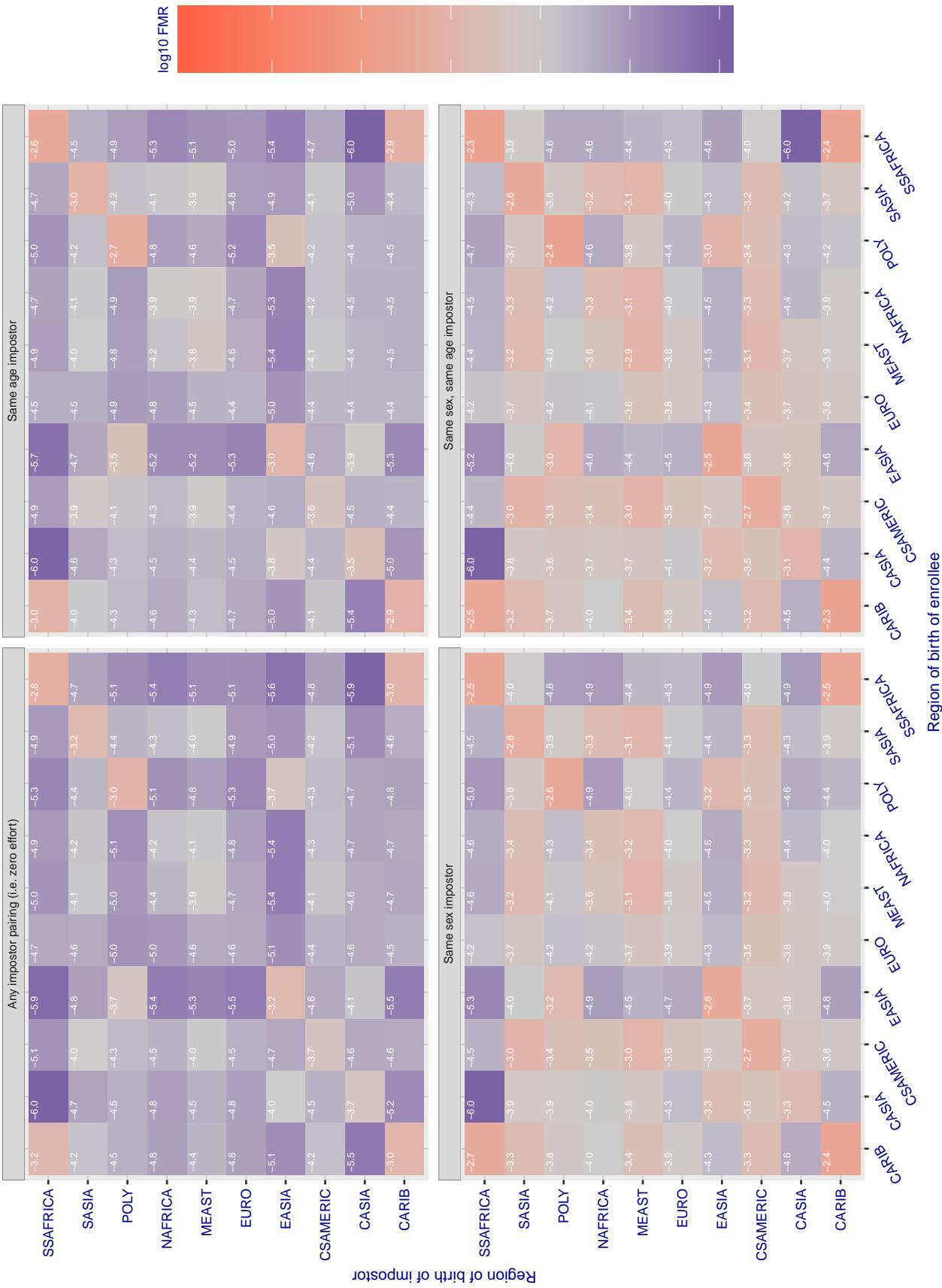


Figure 126: For algorithm cyberextruder-002 operating on visa images, the heatmap shows false match rates observed over impostor comparisons of faces from different individuals who were born in the given region pair. False matches are counted against a recognition threshold fixed globally to give the target FMR in the plot title, computed over all on the order of  $10^{10}$  impostor comparisons. If text appears in each box it give the same quantity as that coded by the color. Grey indicates FMR is at the intended FMR target level. Light red colors present a security vulnerability to, for example, a passport gate. Each +1 increase in  $\log_{10} FMR$  corresponds to a factor of 10 increase in FMR. The matrix is not quite symmetric because images in the enrollment and verification sets are different.

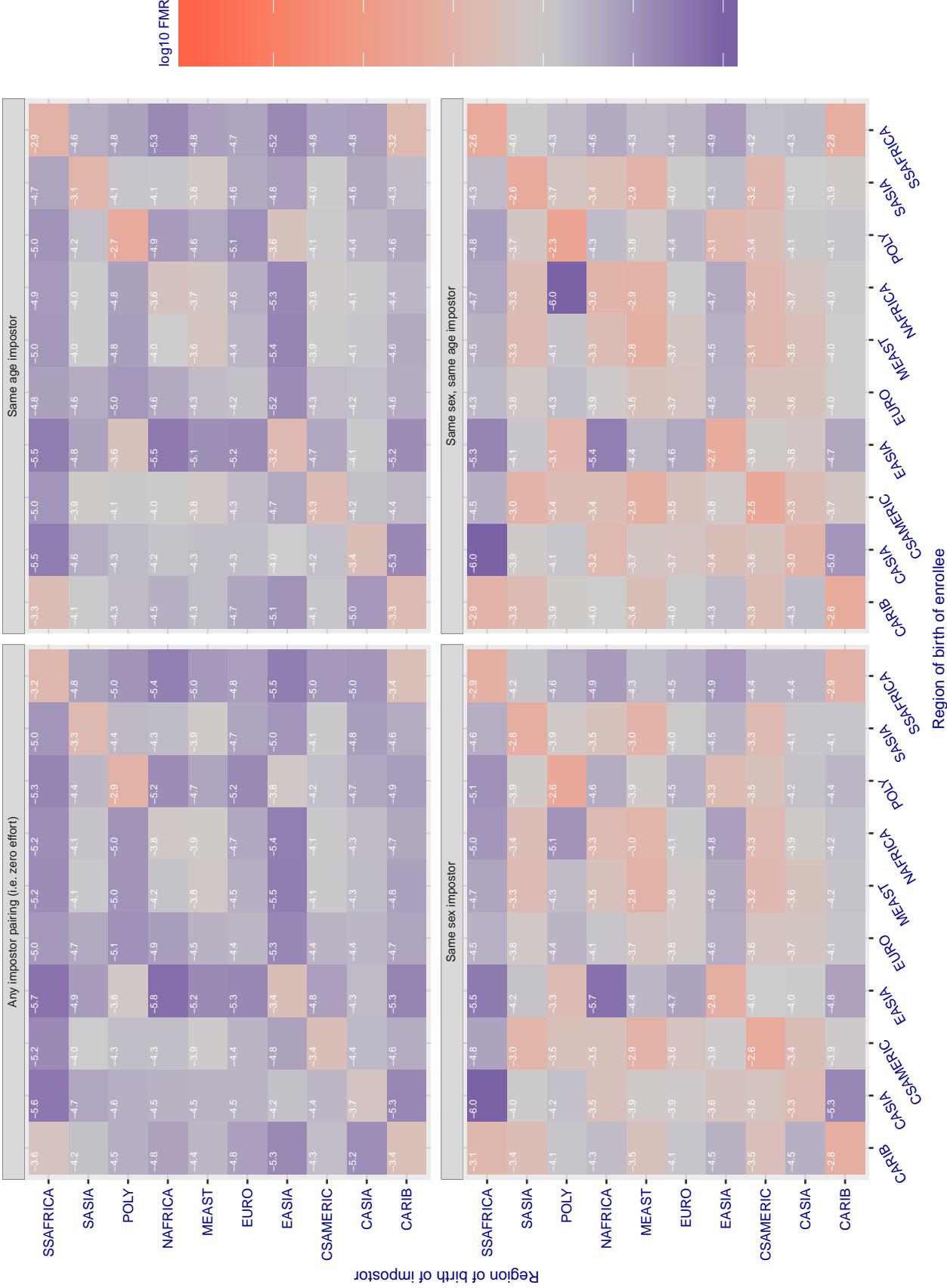
**Cross region FMR at threshold T = 1.409 for algorithm cyberlink\_000, giving FMR(T) = 0.0001 globally.**

Figure 127: For algorithm cyberlink-000 operating on visa images, the heatmap shows false match rates observed over impostor comparisons of faces from different individuals who were born in the given region pair. False matches are counted against a recognition threshold fixed globally to give the target FMR in the plot title, computed over all on the order of  $10^{10}$  impostor comparisons. If text appears in each box it give the same quantity as that coded by the color. Grey indicates FMR is at the intended FMR target level. Light red colors present a security vulnerability to, for example, a passport gate. Each +1 increase in  $\log_{10} FMR$  corresponds to a factor of 10 increase in FMR. The matrix is not quite symmetric because images in the enrollment and verification sets are different.

### Cross region FMR at threshold T = 1.408 for algorithm cyberlink\_001, giving $\text{FMR}(\text{T}) = 0.0001$ globally.

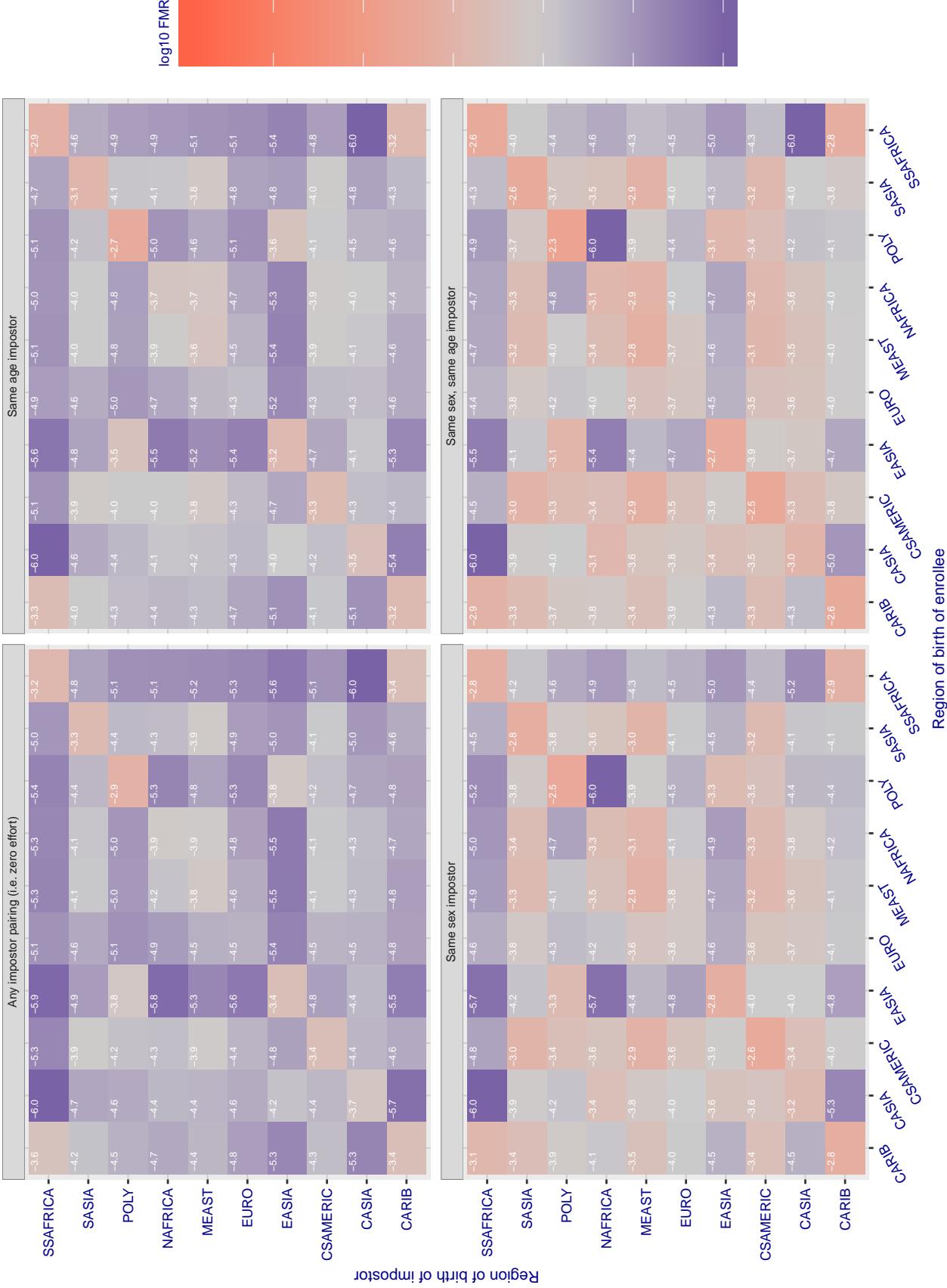
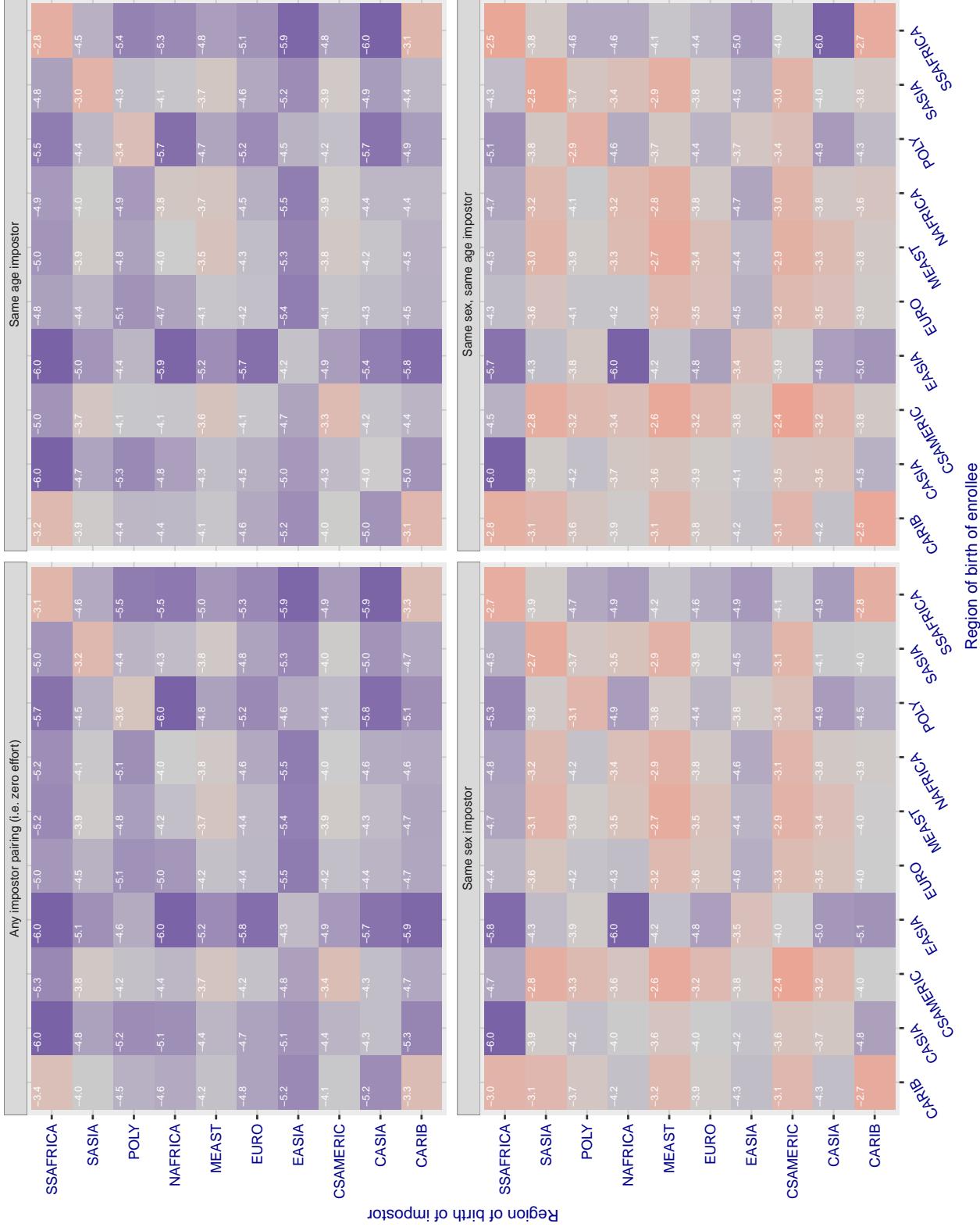


Figure 128: For algorithm cyberlink-001 operating on visa images, the heatmap shows false match rates observed over impostor comparisons of faces from different individuals who were born in the given region pair. False matches are counted against a recognition threshold fixed globally to give the target FMR in the plot title, computed over all on the order of  $10^{10}$  impostor comparisons. If text appears in each box it give the same quantity as that coded by the color. Grey indicates FMR is at the intended FMR target level. Light red colors present a security vulnerability to, for example, a passport gate. Each +1 increase in  $\log_{10} \text{FMR}$  corresponds to a factor of 10 increase in FMR. The matrix is not quite symmetric because images in the enrollment and verification sets are different.

**Cross region FMR at threshold T = 7630.000 for algorithm dahua\_001, giving FMR(T) = 0.00001 globally.**

FNMR(T)  
FMR(T) "False non-match rate"  
"False match rate"

Figure 129: For algorithm dahua\_001 operating on visa images, the heatmap shows false match rates observed over impostor comparisons of faces from different individuals who were born in the given region pair. False matches are counted against a recognition threshold fixed globally to give the target FMR in the plot title, computed over all on the order of  $10^{10}$  impostor comparisons. If text appears in each box it give the same quantity as that coded by the color. Grey indicates FMR is at the intended FMR target level. Light red colors present a security vulnerability to, for example, a passport gate. Each +1 increase in  $\log_{10} FMR$  corresponds to a factor of 10 increase in FMR. The matrix is not quite symmetric because images in the enrollment and verification sets are different.

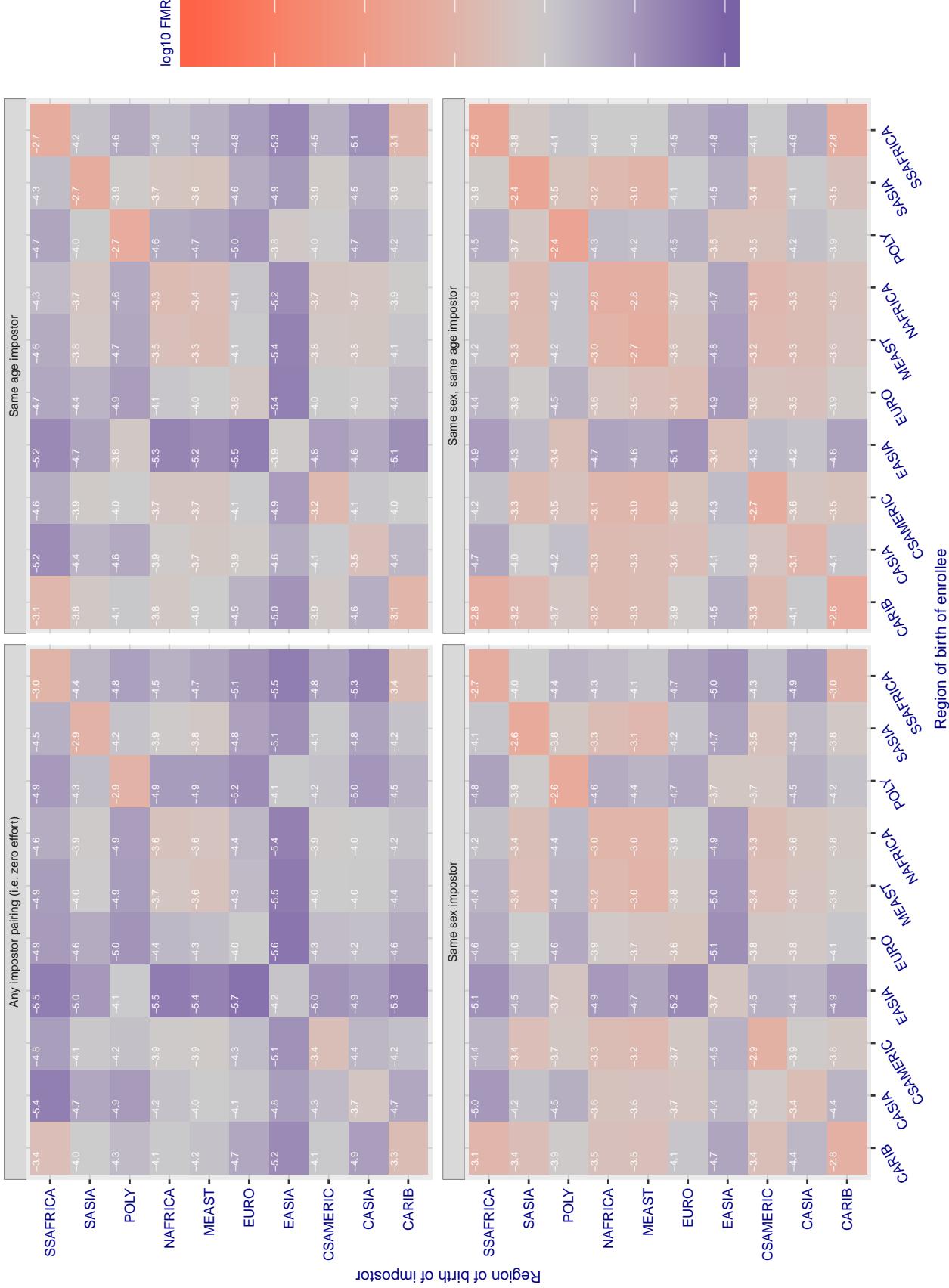
**Cross region FMR at threshold T = 6696.000 for algorithm dahua\_002, giving FMR(T) = 0.00001 globally.**

Figure 130: For algorithm dahua-002 operating on visa images, the heatmap shows false match rates observed over impostor comparisons of faces from different individuals who were born in the given region pair. False matches are counted against a recognition threshold fixed globally to give the target FMR in the plot title, computed over all on the order of  $10^{10}$  impostor comparisons. If text appears in each box it give the same quantity as that coded by the color. Grey indicates FMR is at the intended FMR target level. Light red colors present a security vulnerability to, for example, a passport gate. Each +1 increase in  $\log_{10} FMR$  corresponds to a factor of 10 increase in FMR. The matrix is not quite symmetric because images in the enrollment and verification sets are different.

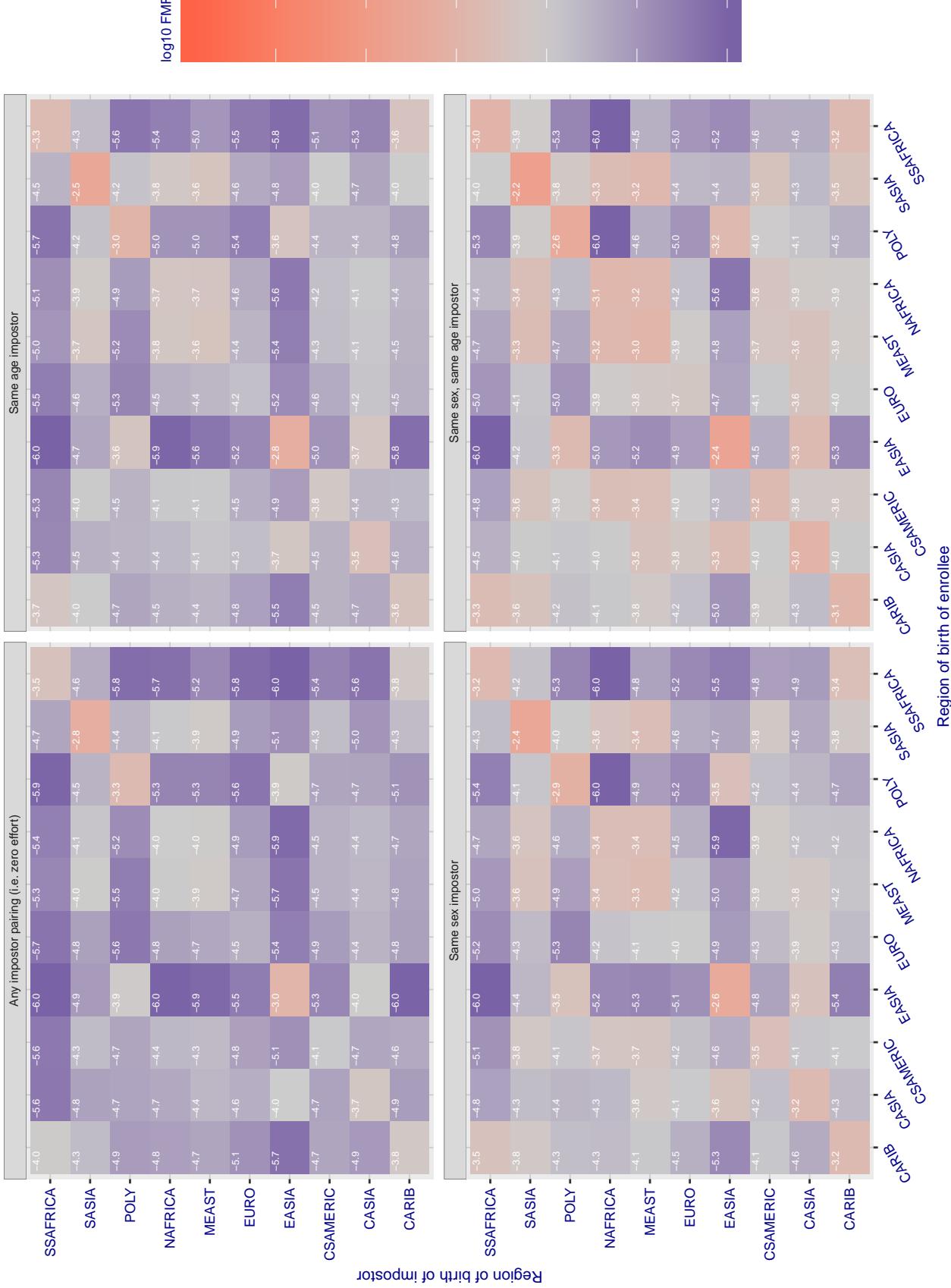
**Cross region FMR at threshold T = 79.344 for algorithm dermalog\_005, giving FMR(T) = 0.0001 globally.**

Figure 131: For algorithm dermalog-005 operating on visa images, the heatmap shows false match rates observed over impostor comparisons of faces from different individuals who were born in the given region pair. False matches are counted against a recognition threshold fixed globally to give the target FMR in the plot title, computed over all on the order of  $10^{10}$  impostor comparisons. If text appears in each box it give the same quantity as that coded by the color. Grey indicates FMR is at the intended FMR target level. Light red colors present a security vulnerability to, for example, a passport gate. Each +1 increase in  $\log_{10} FMR$  corresponds to a factor of 10 increase in FMR. The matrix is not quite symmetric because images in the enrollment and verification sets are different.

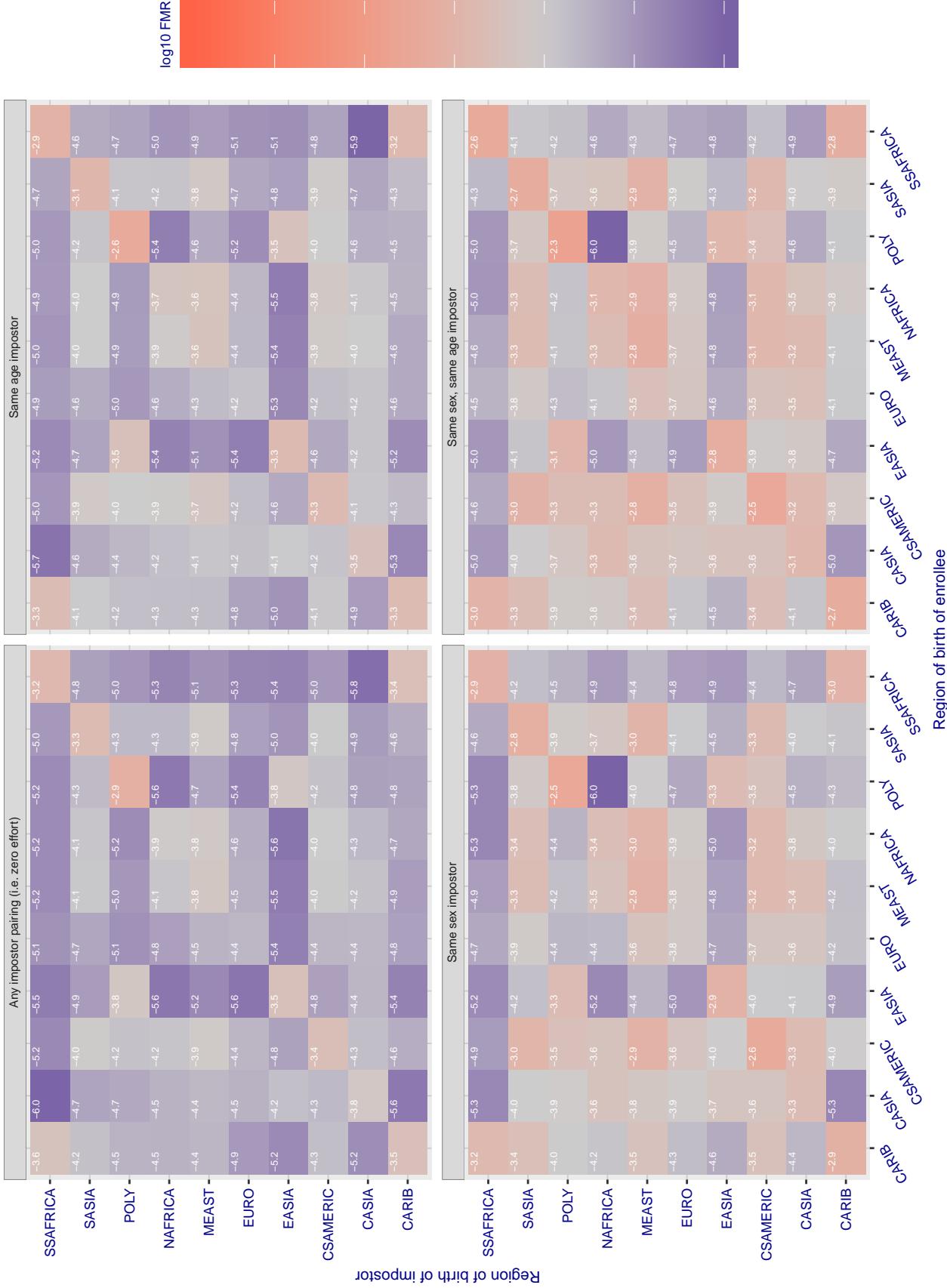
**Cross region FMR at threshold T = 79.670 for algorithm dermalog\_006, giving FMR(T) = 0.0001 globally.**

Figure 132: For algorithm dermalog-006 operating on visa images, the heatmap shows false match rates observed over impostor comparisons of faces from different individuals who were born in the given region pair. False matches are counted against a recognition threshold fixed globally to give the target FMR in the plot title, computed over all on the order of  $10^{10}$  impostor comparisons. If text appears in each box it give the same quantity as that coded by the color. Grey indicates FMR is at the intended FMR target level. Light red colors present a security vulnerability to, for example, a passport gate. Each +1 increase in  $\log_{10} FMR$  corresponds to a factor of 10 increase in FMR. The matrix is not quite symmetric because images in the enrollment and verification sets are different.

### Cross region FMR at threshold T = 0.675 for algorithm digitalbarriers\_002, giving FMR(T) = 0.00001 globally.

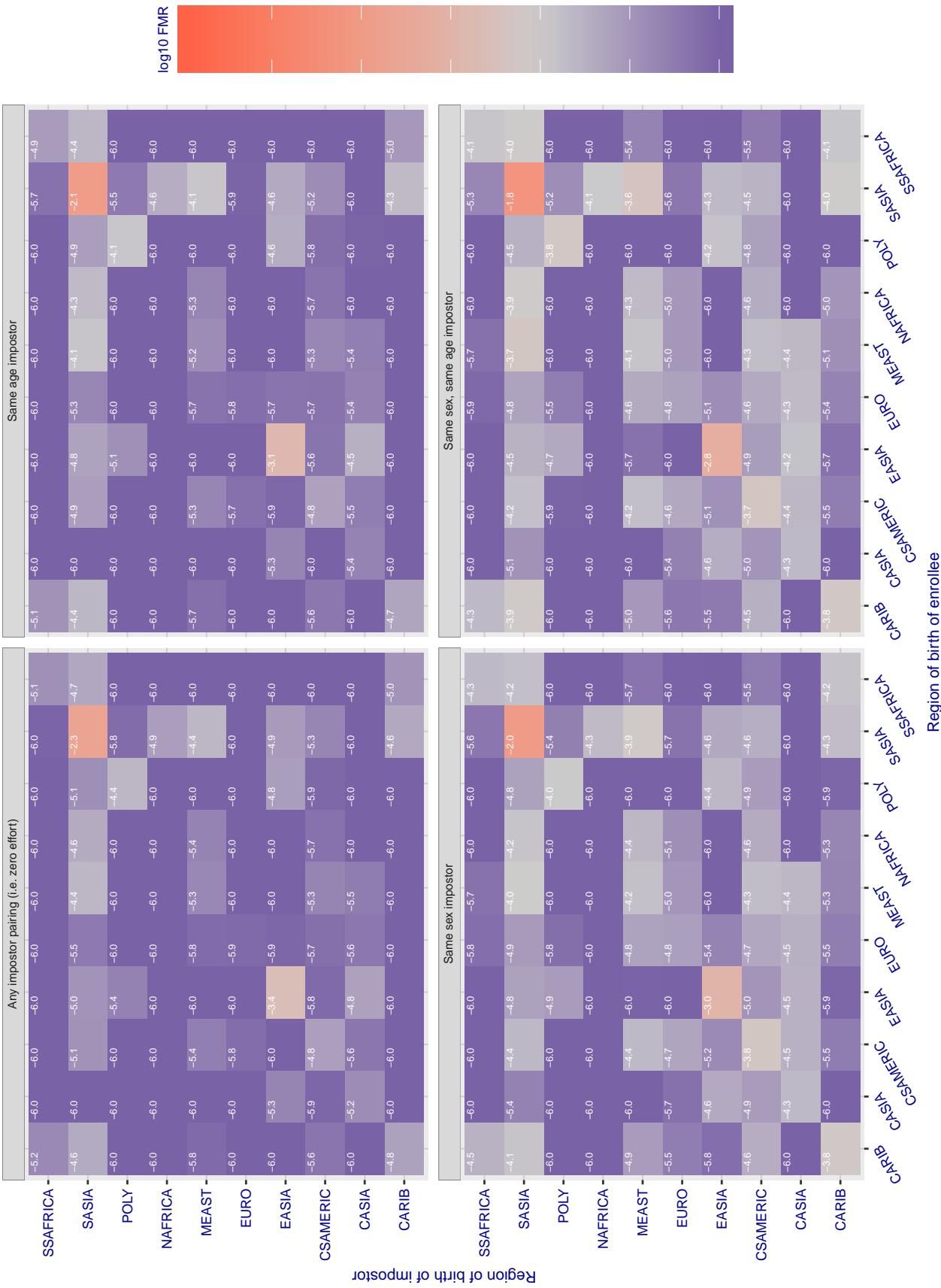


Figure 133: For algorithm digitalbarriers-002 operating on visa images, the heatmap shows false match rates observed over impostor comparisons of faces from different individuals who were born in the given region pair. False matches are counted against a recognition threshold fixed globally to give the target FMR in the plot title, computed over all on the order of  $10^{10}$  impostor comparisons. If text appears in each box it give the same quantity as that coded by the color. Grey indicates FMR is at the intended FMR target level. Light red colors present a security vulnerability to, for example, a passport gate. Each +1 increase in  $\log_{10} \text{FMR}$  corresponds to a factor of 10 increase in FMR. The matrix is not quite symmetric because images in the enrollment and verification sets are different.

### Cross region FMR at threshold T = 2.672 for algorithm everai\_001, giving FMR(T) = 0.0001 globally.

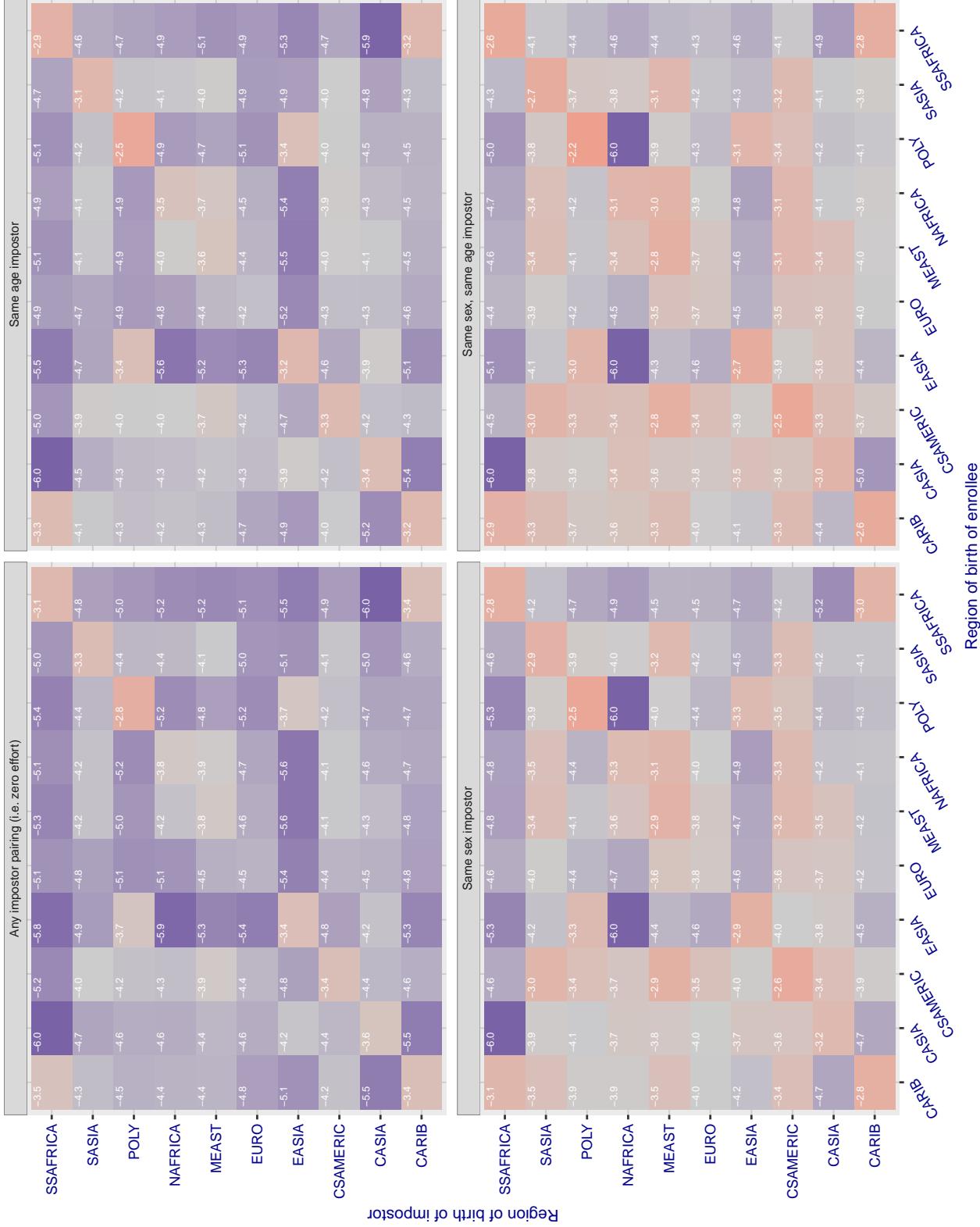


Figure 134: For algorithm everai-001 operating on visa images, the heatmap shows false match rates observed over impostor comparisons of faces from different individuals who were born in the given region pair. False matches are counted against a recognition threshold fixed globally to give the target FMR in the plot title, computed over all on the order of  $10^{10}$  impostor comparisons. If text appears in each box it give the same quantity as that coded by the color. Grey indicates FMR is at the intended FMR target level. Light red colors present a security vulnerability to, for example, a passport gate. Each +1 increase in  $\log_{10} \text{FMR}$  corresponds to a factor of 10 increase in FMR. The matrix is not quite symmetric because images in the enrollment and verification sets are different.

### Cross region FMR at threshold T = 2.589 for algorithm everai\_002, giving FMR(T) = 0.0001 globally.

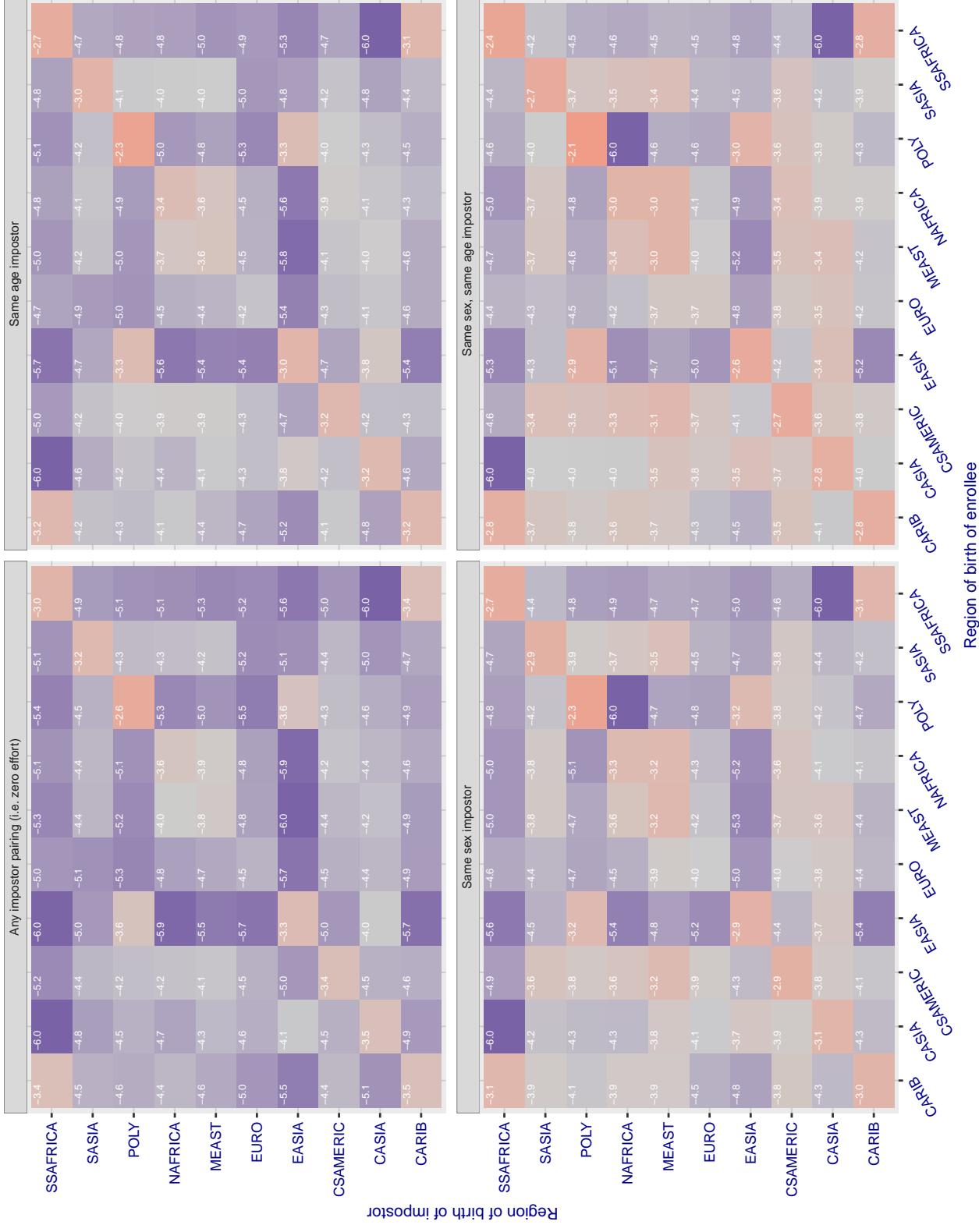


Figure 135: For algorithm everai-002 operating on visa images, the heatmap shows false match rates observed over impostor comparisons of faces from different individuals who were born in the given region pair. False matches are counted against a recognition threshold fixed globally to give the target FMR in the plot title, computed over all on the order of  $10^{10}$  impostor comparisons. If text appears in each box it give the same quantity as that coded by the color. Grey indicates FMR is at the intended FMR target level. Light red colors present a security vulnerability to, for example, a passport gate. Each +1 increase in  $\log_{10} FMR$  corresponds to a factor of 10 increase in FMR. The matrix is not quite symmetric because images in the enrollment and verification sets are different.

### Cross region FMR at threshold T = 0.611 for algorithm glory\_000, giving FMR(T) = 0.0001 globally.

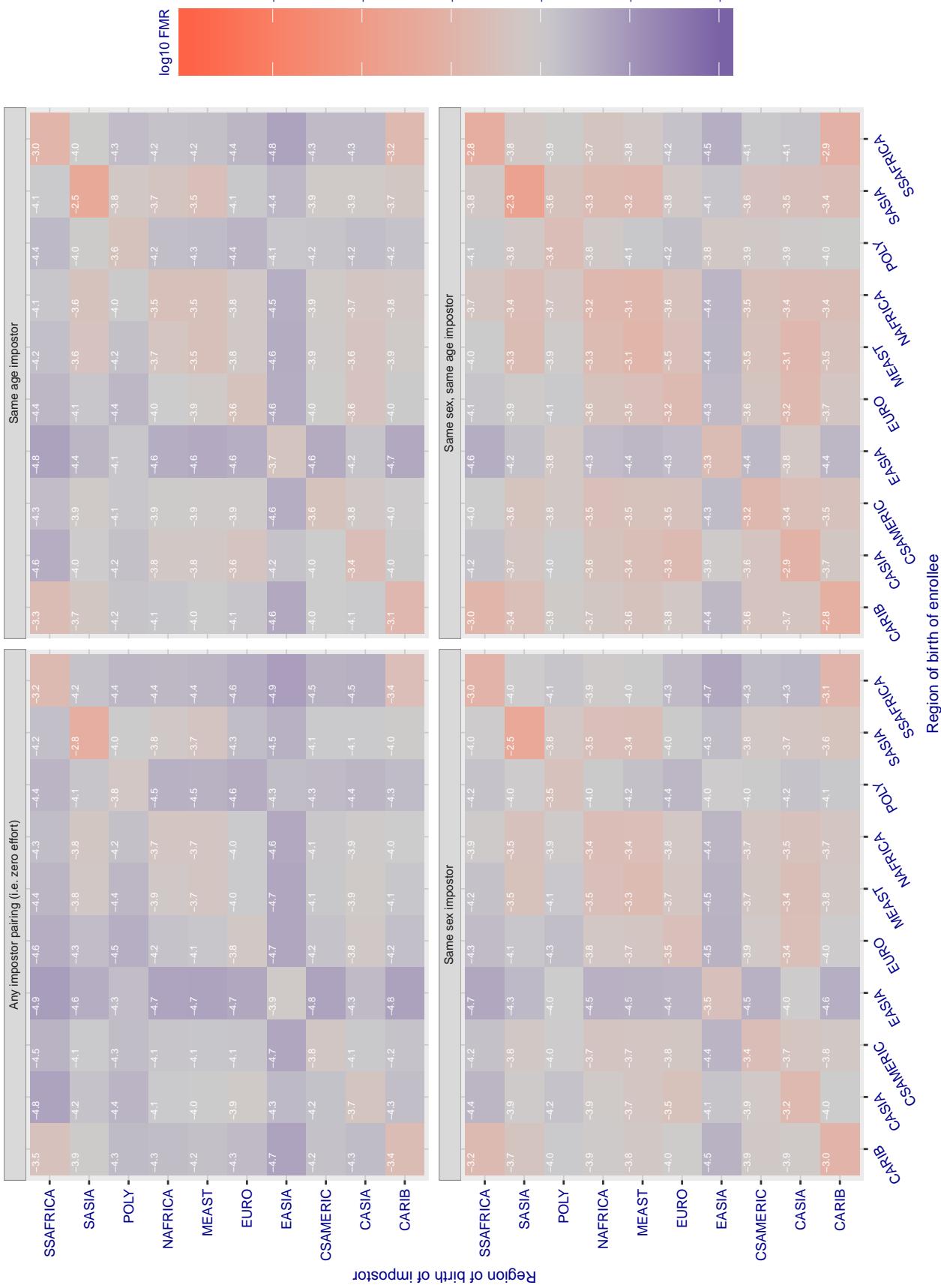


Figure 136: For algorithm glory-000 operating on visa images, the heatmap shows false match rates observed over impostor comparisons of faces from different individuals who were born in the given region pair. False matches are counted against a recognition threshold fixed globally to give the target FMR in the plot title, computed over all on the order of  $10^{10}$  impostor comparisons. If text appears in each box it give the same quantity as that coded by the color. Grey indicates FMR is at the intended FMR target level. Light red colors present a security vulnerability to, for example, a passport gate. Each +1 increase in  $\log_{10} FMR$  corresponds to a factor of 10 increase in FMR. The matrix is not quite symmetric because images in the enrollment and verification sets are different.

### Cross region FMR at threshold T = 0.618 for algorithm glory\_001, giving FMR(T) = 0.0001 globally.

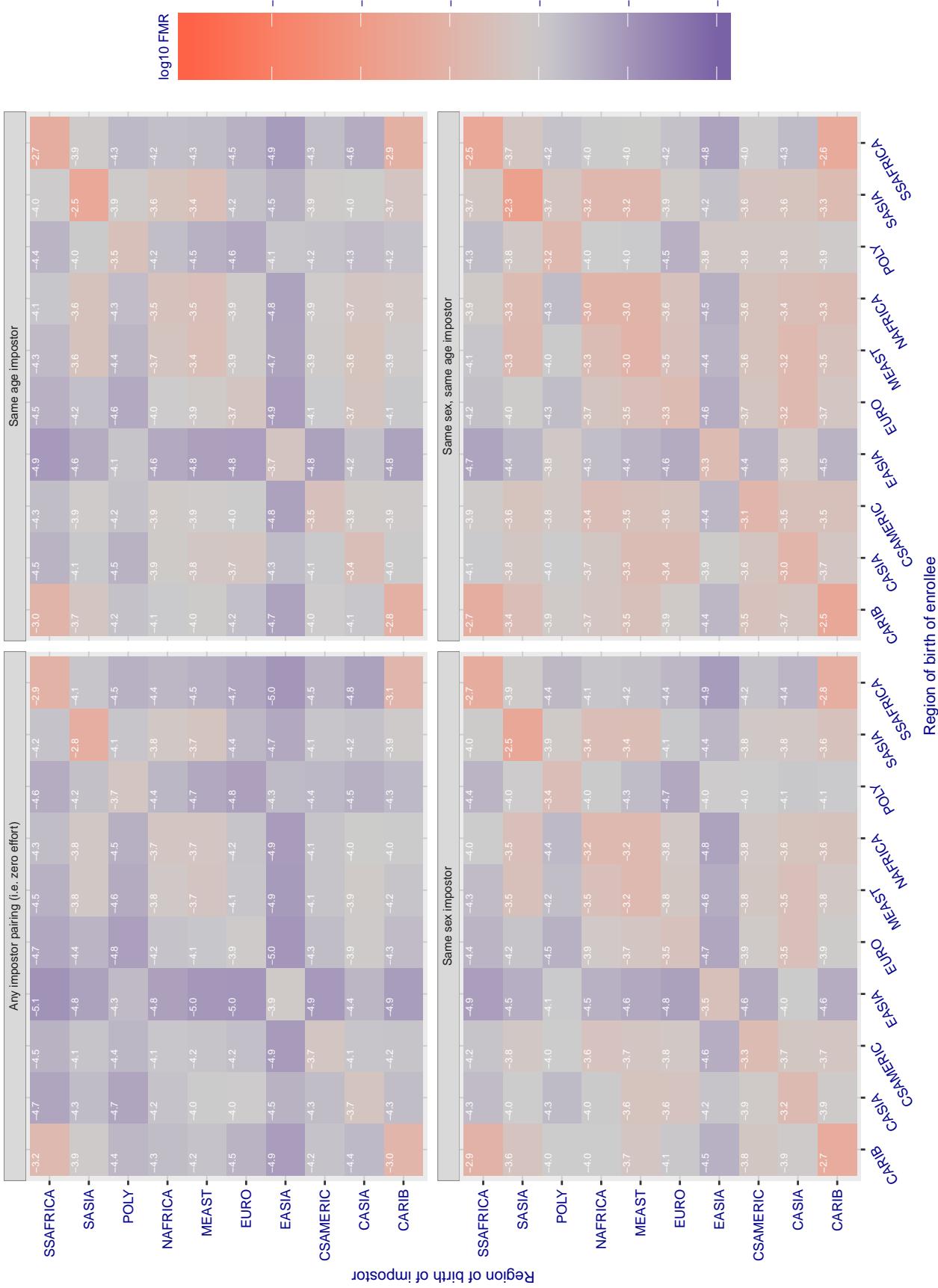


Figure 137: For algorithm glory-001 operating on visa images, the heatmap shows false match rates observed over impostor comparisons of faces from different individuals who were born in the given region pair. False matches are counted against a recognition threshold fixed globally to give the target FMR in the plot title, computed over all on the order of  $10^{10}$  impostor comparisons. If text appears in each box it give the same quantity as that coded by the color. Grey indicates FMR is at the intended FMR target level. Light red colors present a security vulnerability to, for example, a passport gate. Each +1 increase in  $\log_{10} \text{FMR}$  corresponds to a factor of 10 increase in FMR. The matrix is not quite symmetric because images in the enrollment and verification sets are different.

### Cross region FMR at threshold T = 0.559 for algorithm gorilla\_001, giving FMR(T) = 0.0001 globally.

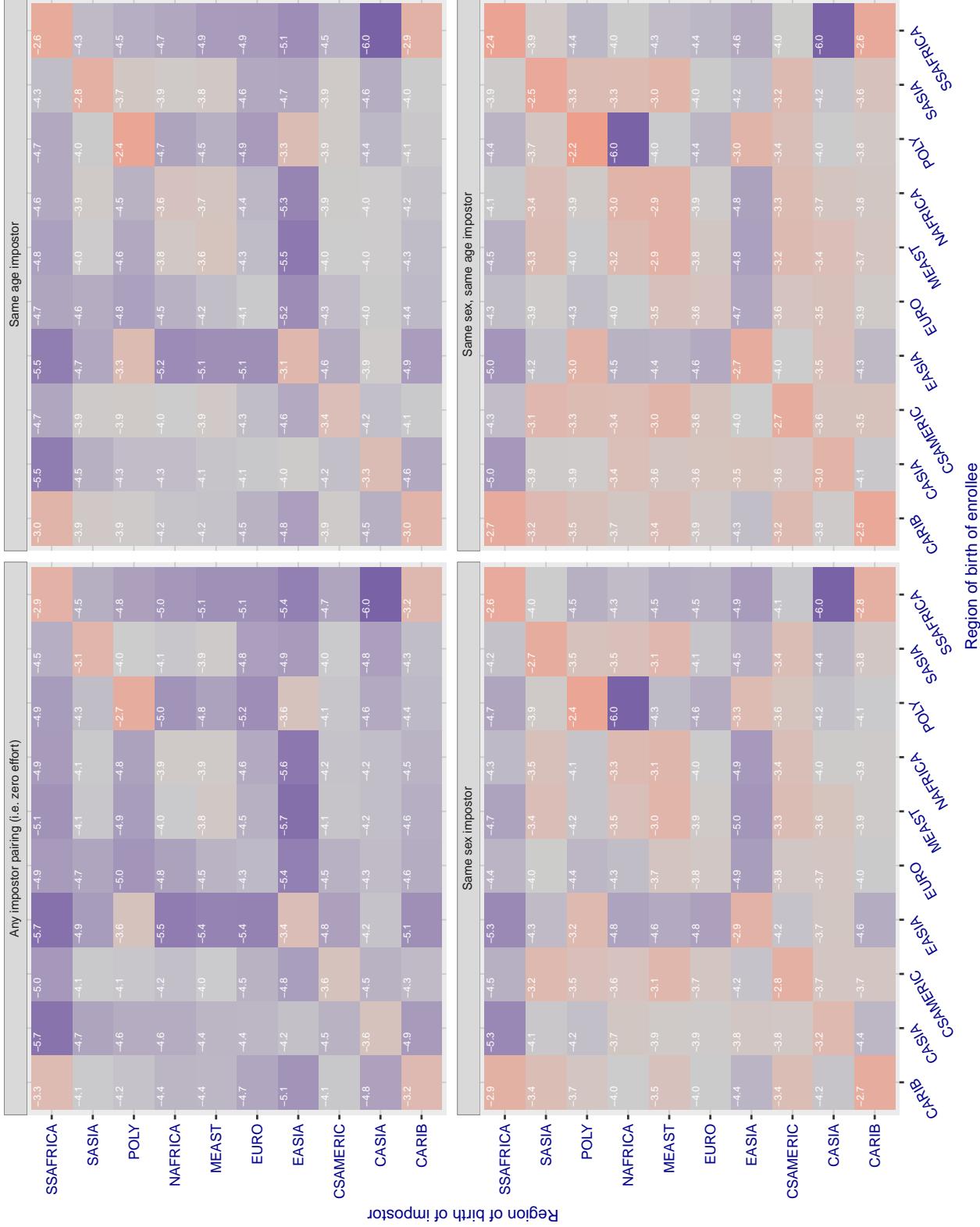


Figure 138: For algorithm gorilla-001 operating on visa images, the heatmap shows false match rates observed over impostor comparisons of faces from different individuals who were born in the given region pair. False matches are counted against a recognition threshold fixed globally to give the target FMR in the plot title, computed over all on the order of  $10^{10}$  impostor comparisons. If text appears in each box it give the same quantity as that coded by the color. Grey indicates FMR is at the intended FMR target level. Light red colors present a security vulnerability to, for example, a passport gate. Each +1 increase in  $\log_{10} FMR$  corresponds to a factor of 10 increase in FMR. The matrix is not quite symmetric because images in the enrollment and verification sets are different.

### Cross region FMR at threshold T = 0.483 for algorithm gorilla\_002, giving FMR(T) = 0.0001 globally.

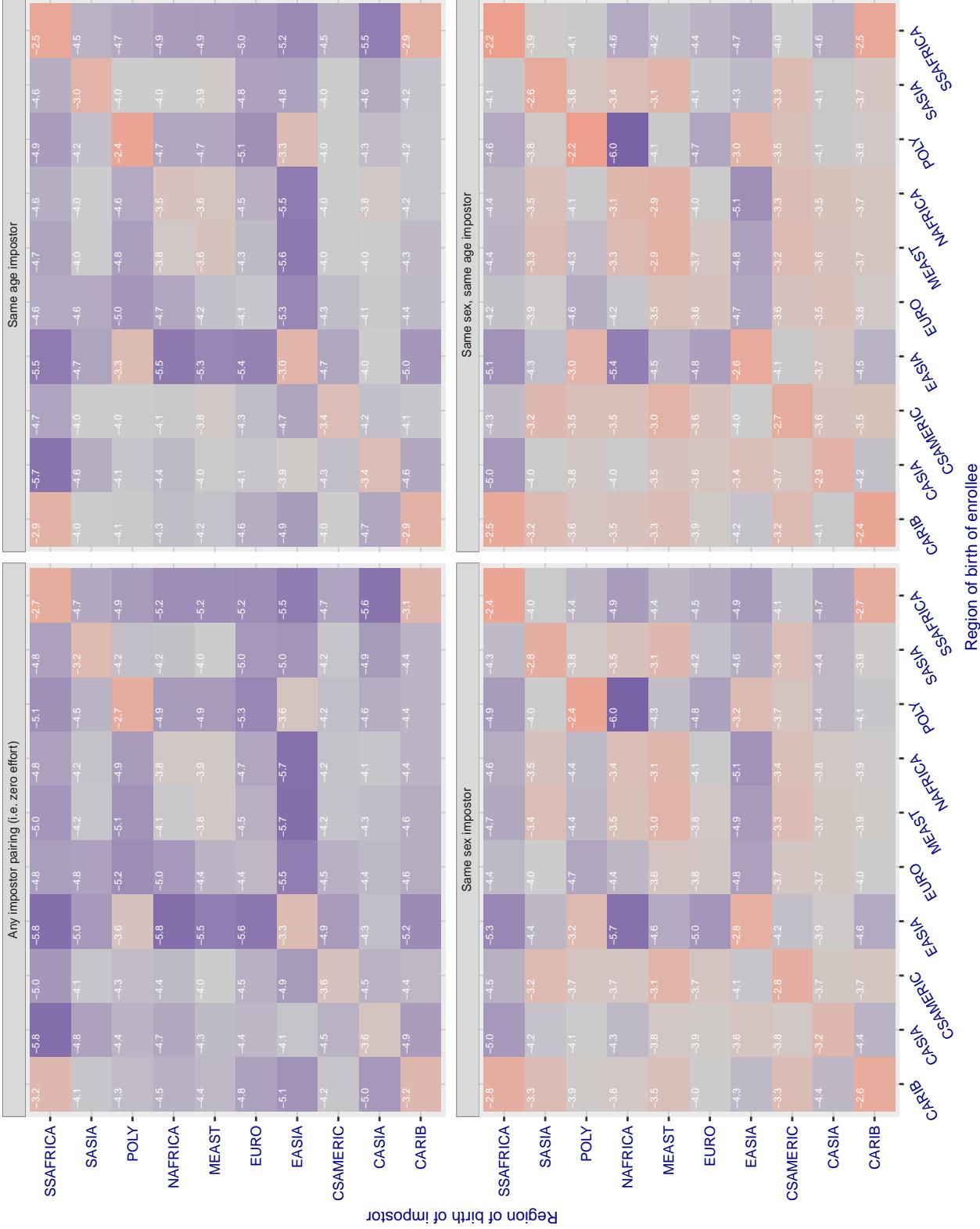


Figure 139: For algorithm gorilla-002 operating on visa images, the heatmap shows false match rates observed over impostor comparisons of faces from different individuals who were born in the given region pair. False matches are counted against a recognition threshold fixed globally to give the target FMR in the plot title, computed over all on the order of  $10^{10}$  impostor comparisons. If text appears in each box it give the same quantity as that coded by the color. Grey indicates FMR is at the intended FMR target level. Light red colors present a security vulnerability to, for example, a passport gate. Each +1 increase in  $\log_{10} FMR$  corresponds to a factor of 10 increase in FMR. The matrix is not quite symmetric because images in the enrollment and verification sets are different.

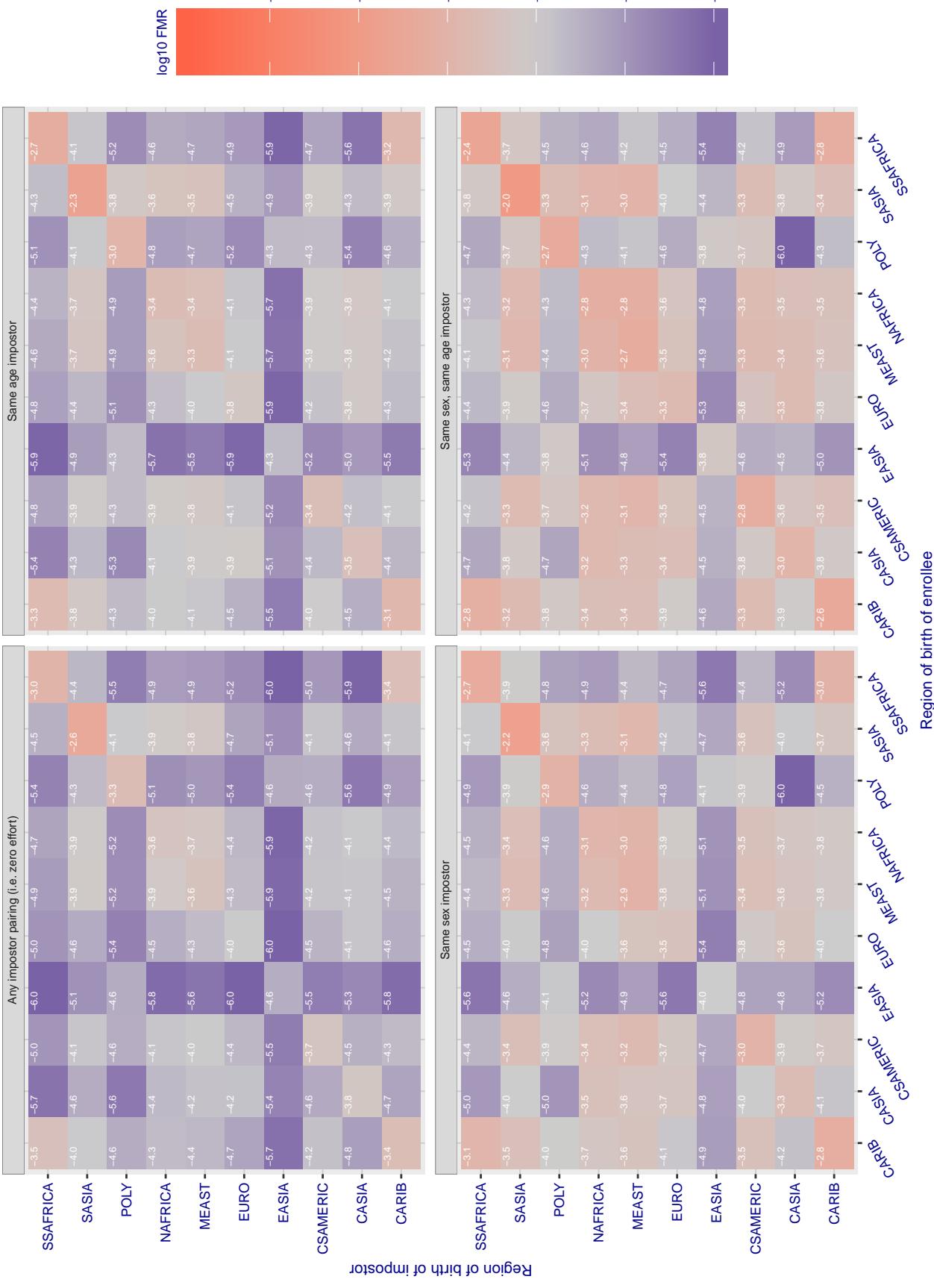
**Cross region FMR at threshold T = 66.565 for algorithm hik\_001, giving FMR(T) = 0.0001 globally.**

Figure 140: For algorithm hik-001 operating on visa images, the heatmap shows false match rates observed over impostor comparisons of faces from different individuals who were born in the given region pair. False matches are counted against a recognition threshold fixed globally to give the target FMR in the plot title, computed over all on the order of  $10^{10}$  impostor comparisons. If text appears in each box it give the same quantity as that coded by the color. Grey indicates FMR is at the intended FMR target level. Light red colors present a security vulnerability to, for example, a passport gate. Each +1 increase in  $\log 10 \text{ FMR}$  corresponds to a factor of 10 increase in FMR. The matrix is not quite symmetric because images in the enrollment and verification sets are different.

**Cross region FMR at threshold T = 0.971 for algorithm hr\_000, giving FMR(T) = 0.0001 globally.**

Figure 141: For algorithm hr-000 operating on visa images, the heatmap shows false match rates observed over impostor comparisons of faces from different individuals who were born in the given region pair. False matches are counted against a recognition threshold fixed globally to give the target FMR in the plot title, computed over all on the order of  $10^{10}$  impostor comparisons. If text appears in each box it give the same quantity as that coded by the color. Grey indicates FMR is at the intended FMR target level. Light red colors present a security vulnerability to, for example, a passport gate. Each +1 increase in  $\log 10$  FMR corresponds to a factor of 10 increase in FMR. The matrix is not quite symmetric because images in the enrollment and verification sets are different.

### Cross region FMR at threshold T = 37645.000 for algorithm id3\_003, giving FMR(T) = 0.0001 globally.

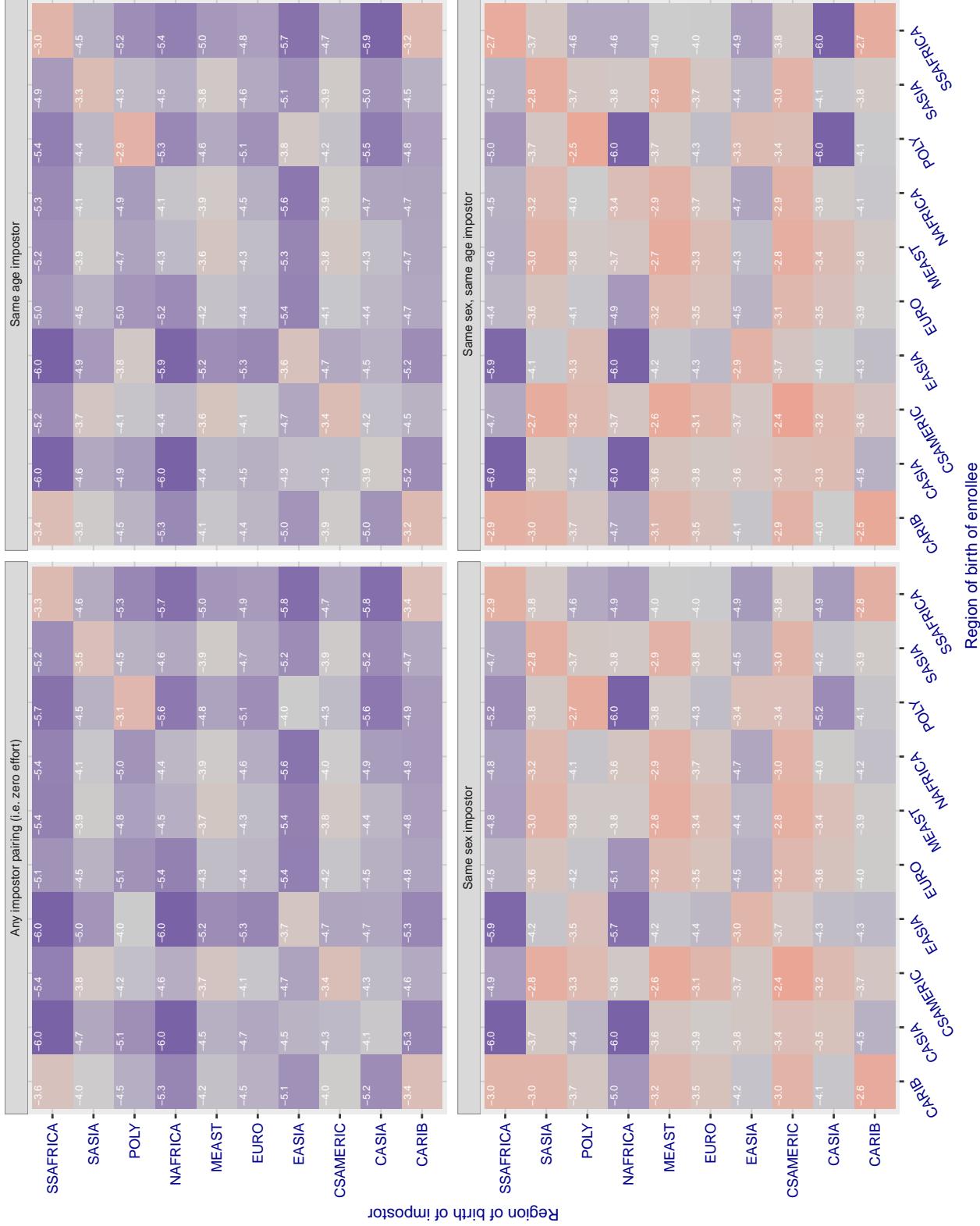


Figure 142: For algorithm id3\_003 operating on visa images, the heatmap shows false match rates observed over impostor comparisons of faces from different individuals who were born in the given region pair. False matches are counted against a recognition threshold fixed globally to give the target FMR in the plot title, computed over all on the order of  $10^{10}$  impostor comparisons. If text appears in each box it give the same quantity as that coded by the color. Grey indicates FMR is at the intended FMR target level. Light red colors present a security vulnerability to, for example, a passport gate. Each +1 increase in  $\log 10 \text{ FMR}$  corresponds to a factor of 10 increase in FMR. The matrix is not quite symmetric because images in the enrollment and verification sets are different.

### Cross region FMR at threshold T = 37001.000 for algorithm id3\_004, giving FMR(T) = 0.0001 globally.

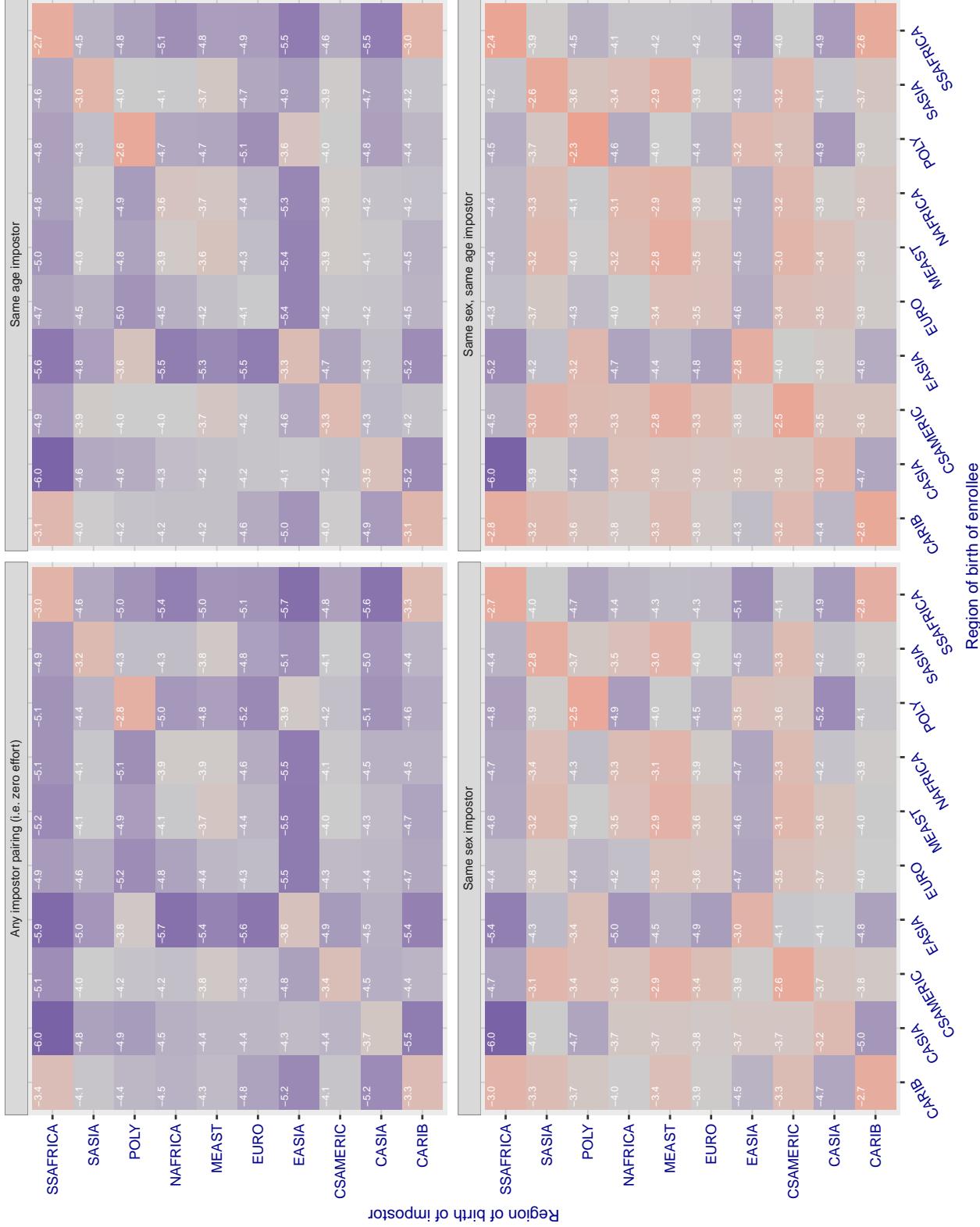


Figure 143: For algorithm id3\_004 operating on visa images, the heatmap shows false match rates observed over impostor comparisons of faces from different individuals who were born in the given region pair. False matches are counted against a recognition threshold fixed globally to give the target FMR in the plot title, computed over all on the order of  $10^{10}$  impostor comparisons. If text appears in each box it give the same quantity as that coded by the color. Grey indicates FMR is at the intended FMR target level. Light red colors present a security vulnerability to, for example, a passport gate. Each +1 increase in  $\log 10 \text{ FMR}$  corresponds to a factor of 10 increase in FMR. The matrix is not quite symmetric because images in the enrollment and verification sets are different.

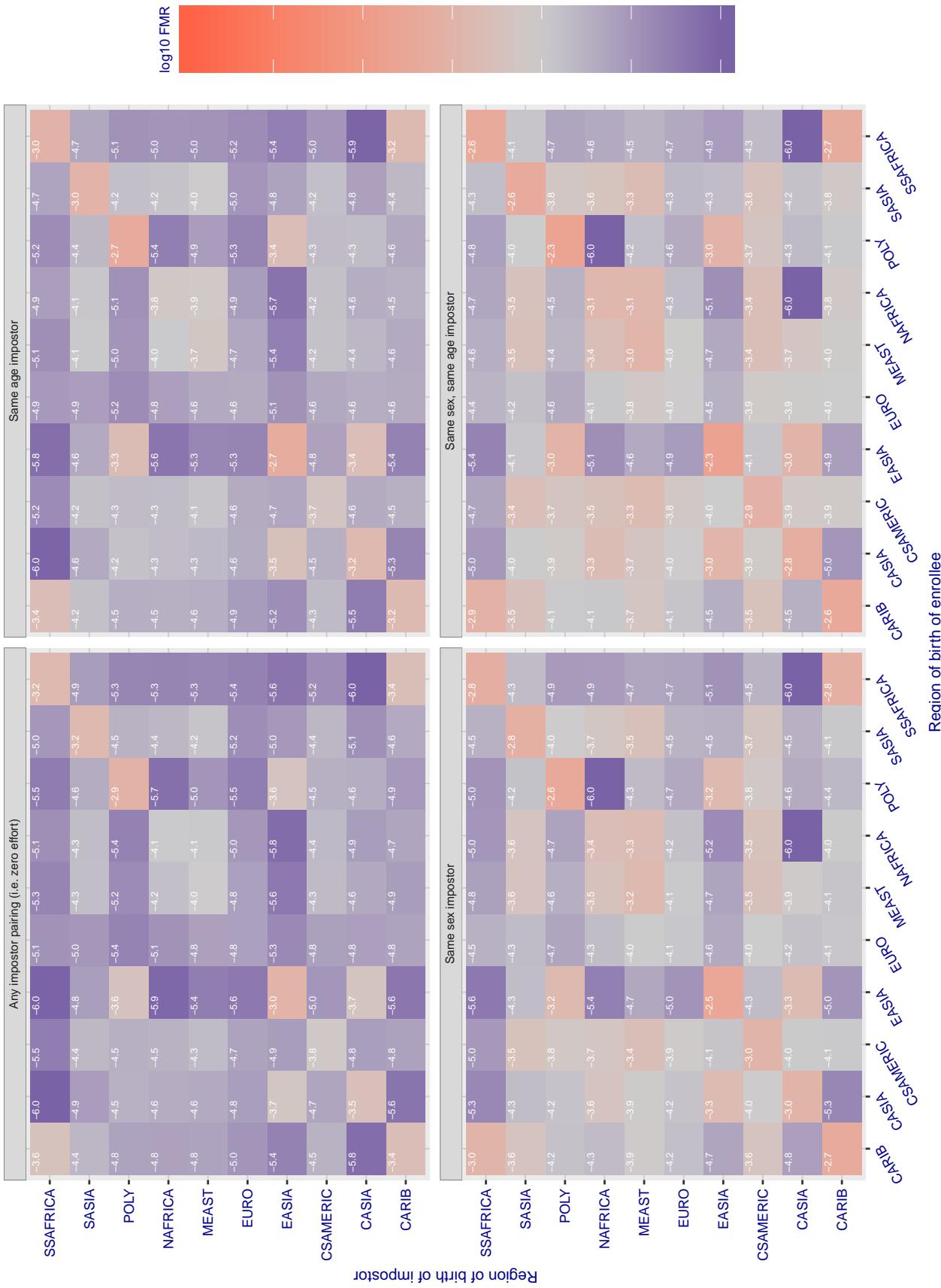
**Cross region FMR at threshold T = 3664.380 for algorithm idemia\_003, giving FMR(T) = 0.0001 globally.**

Figure 144: For algorithm idemia-003 operating on visa images, the heatmap shows false match rates observed over impostor comparisons of faces from different individuals who were born in the given region pair. False matches are counted against a recognition threshold fixed globally to give the target FMR in the plot title, computed over all on the order of  $10^{10}$  impostor comparisons. If text appears in each box it give the same quantity as that coded by the color. Grey indicates FMR is at the intended FMR target level. Light red colors present a security vulnerability to, for example, a passport gate. Each +1 increase in  $\log_{10} \text{FMR}$  corresponds to a factor of 10 increase in FMR. The matrix is not quite symmetric because images in the enrollment and verification sets are different.

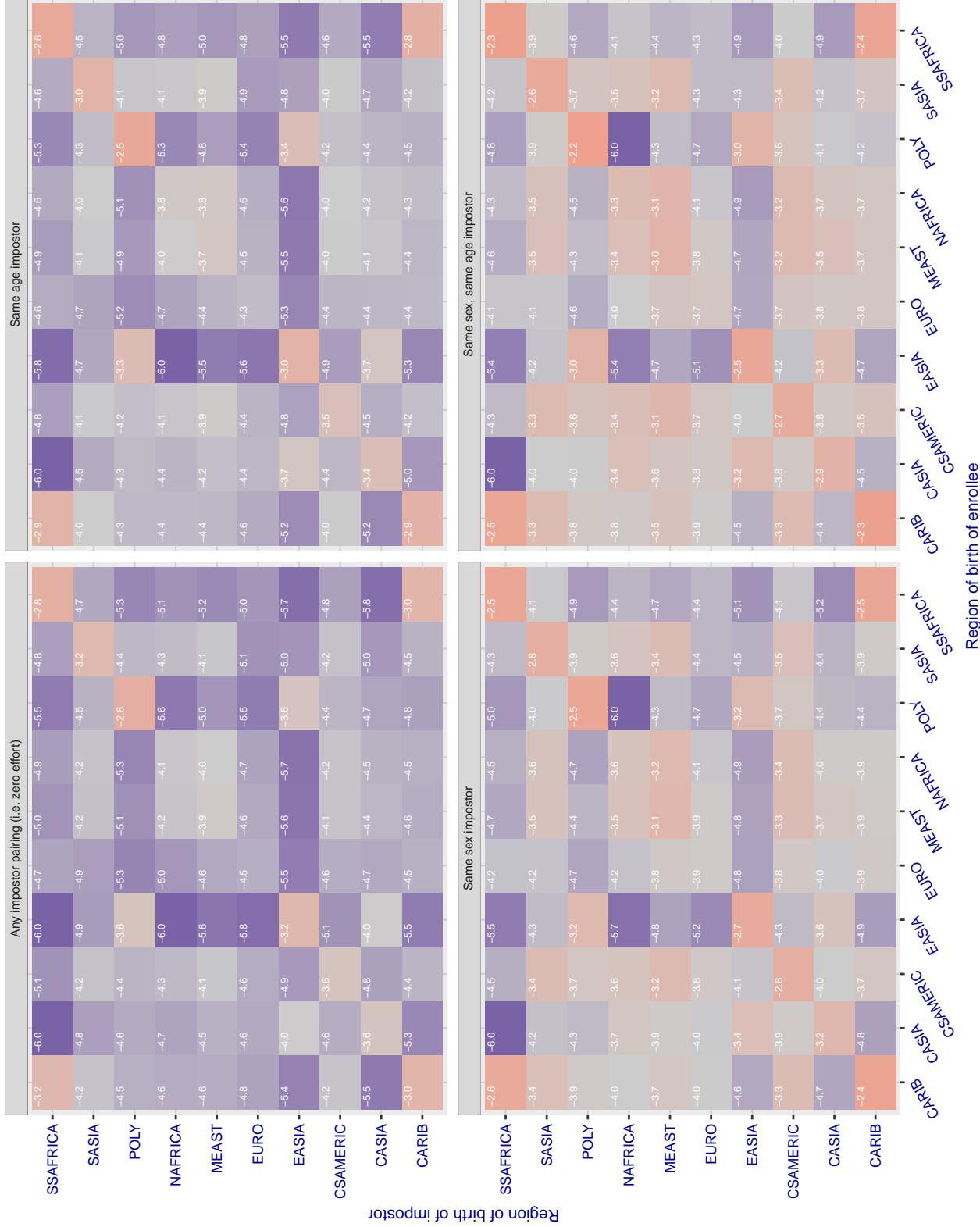
**Cross region FMR at threshold T = 3925.463 for algorithm idemia\_004, giving FMR(T) = 0.0001 globally.**

Figure 145: For algorithm idemia-004 operating on visa images, the heatmap shows false match rates observed over impostor comparisons of faces from different individuals who were born in the given region pair. False matches are counted against a recognition threshold fixed globally to give the target FMR in the plot title, computed over all on the order of  $10^{10}$  impostor comparisons. If text appears in each box it give the same quantity as that coded by the color. Grey indicates FMR is at the intended FMR target level. Light red colors present a security vulnerability to, for example, a passport gate. Each +1 increase in  $\log_{10} FMR$  corresponds to a factor of 10 increase in FMR. The matrix is not quite symmetric because images in the enrollment and verification sets are different.

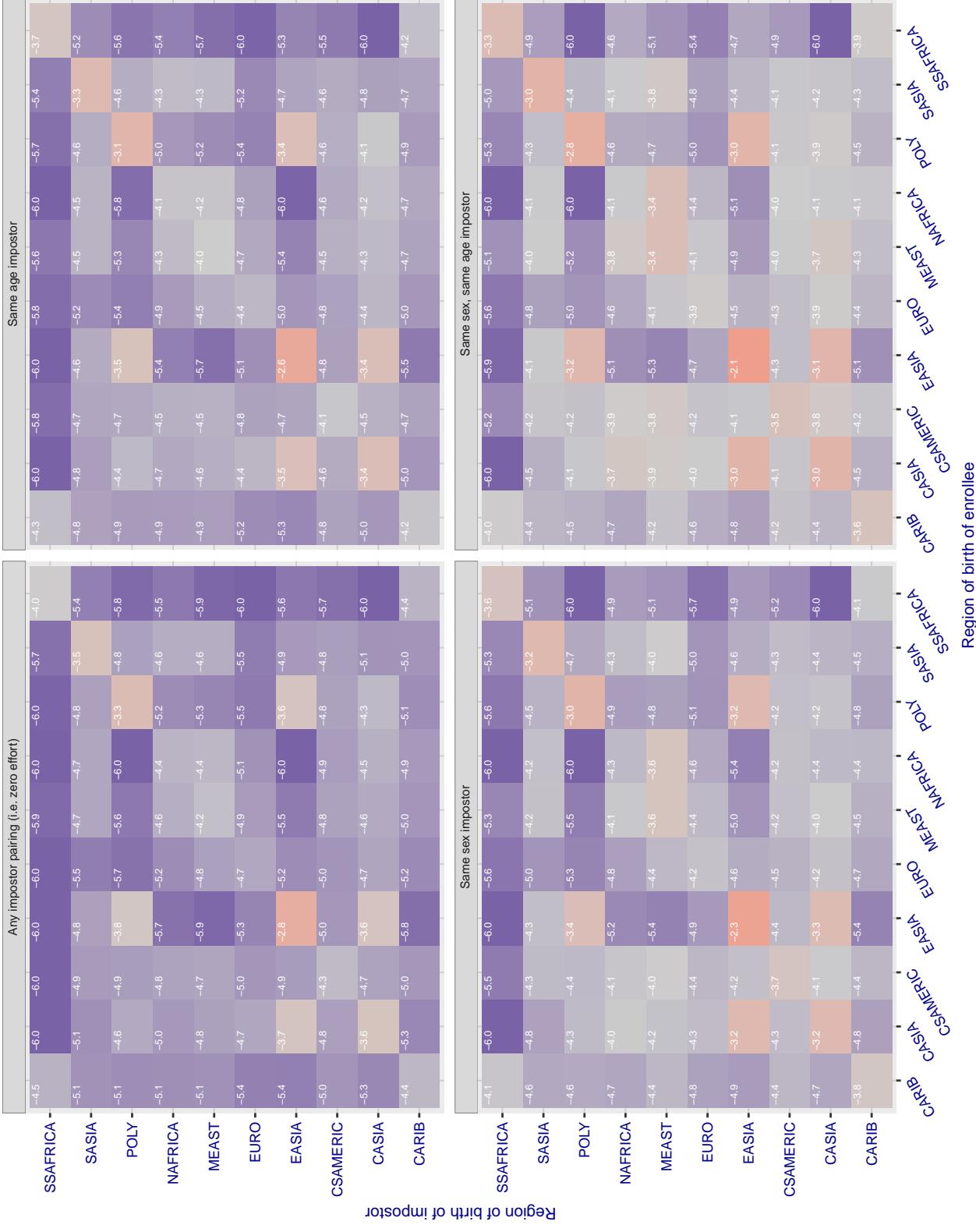
**Cross region FMR at threshold T = 0.760 for algorithm iit\_000, giving FMR(T) = 0.0001 globally.**

Figure 146: For algorithm iit-000 operating on visa images, the heatmap shows false match rates observed over impostor comparisons of faces from different individuals who were born in the given region pair. False matches are counted against a recognition threshold fixed globally to give the target FMR in the plot title, computed over all on the order of  $10^{10}$  impostor comparisons. If text appears in each box it give the same quantity as that coded by the color. Grey indicates FMR is at the intended FMR target level. Light red colors present a security vulnerability to, for example, a passport gate. Each +1 increase in  $\log_{10} \text{FMR}$  corresponds to a factor of 10 increase in FMR. The matrix is not quite symmetric because images in the enrollment and verification sets are different.

### Cross region FMR at threshold T = 1.375 for algorithm imperial\_000, giving FMR(T) = 0.0001 globally.

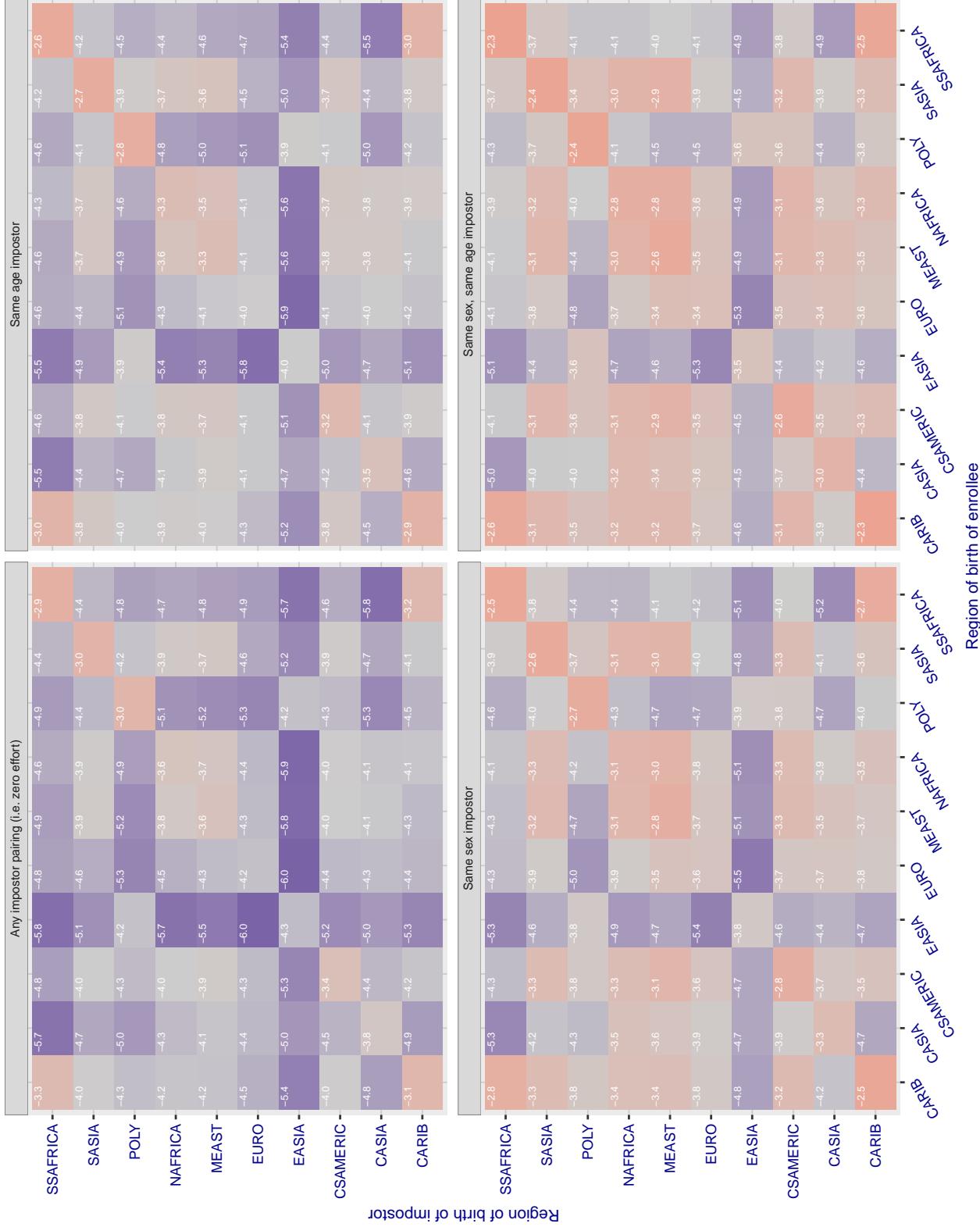


Figure 147: For algorithm imperial-000 operating on visa images, the heatmap shows false match rates observed over impostor comparisons of faces from different individuals who were born in the given region pair. False matches are counted against a recognition threshold fixed globally to give the target FMR in the plot title, computed over all on the order of  $10^{10}$  impostor comparisons. If text appears in each box it give the same quantity as that coded by the color. Grey indicates FMR is at the intended FMR target level. Light red colors present a security vulnerability to, for example, a passport gate. Each +1 increase in  $\log_{10} \text{FMR}$  corresponds to a factor of 10 increase in FMR. The matrix is not quite symmetric because images in the enrollment and verification sets are different.

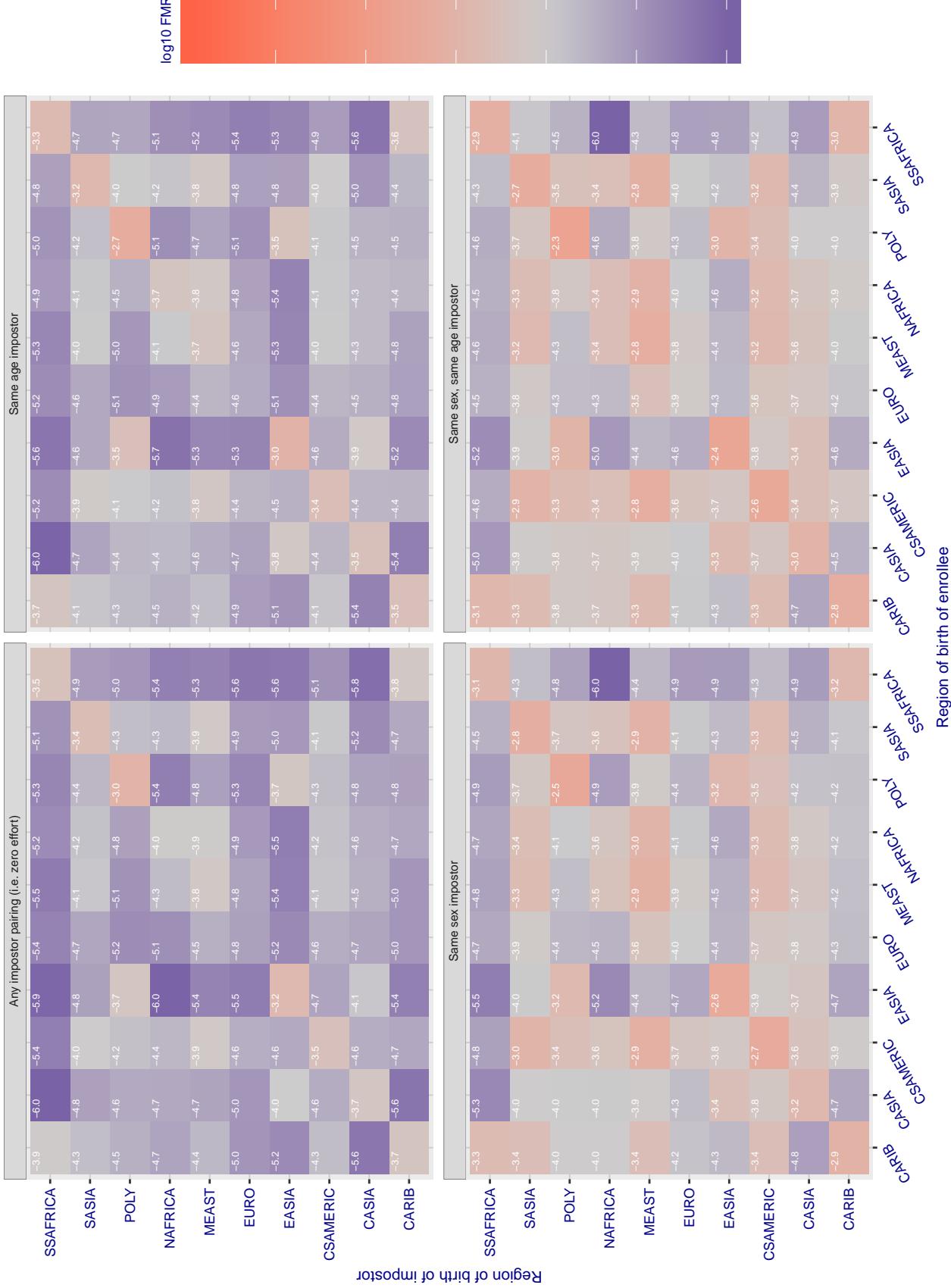
**Cross region FMR at threshold T = 1.402 for algorithm imperial\_001, giving FMR(T) = 0.0001 globally.**

Figure 148: For algorithm imperial-001 operating on visa images, the heatmap shows false match rates observed over impostor comparisons of faces from different individuals who were born in the given region pair. False matches are counted against a recognition threshold fixed globally to give the target FMR in the plot title, computed over all on the order of  $10^{10}$  impostor comparisons. If text appears in each box it give the same quantity as that coded by the color. Grey indicates FMR is at the intended FMR target level. Light red colors present a security vulnerability to, for example, a passport gate. Each +1 increase in  $\log_{10} FMR$  corresponds to a factor of 10 increase in FMR. The matrix is not quite symmetric because images in the enrollment and verification sets are different.

### Cross region FMR at threshold T = 1.382 for algorithm incode\_002, giving FMR(T) = 0.0001 globally.

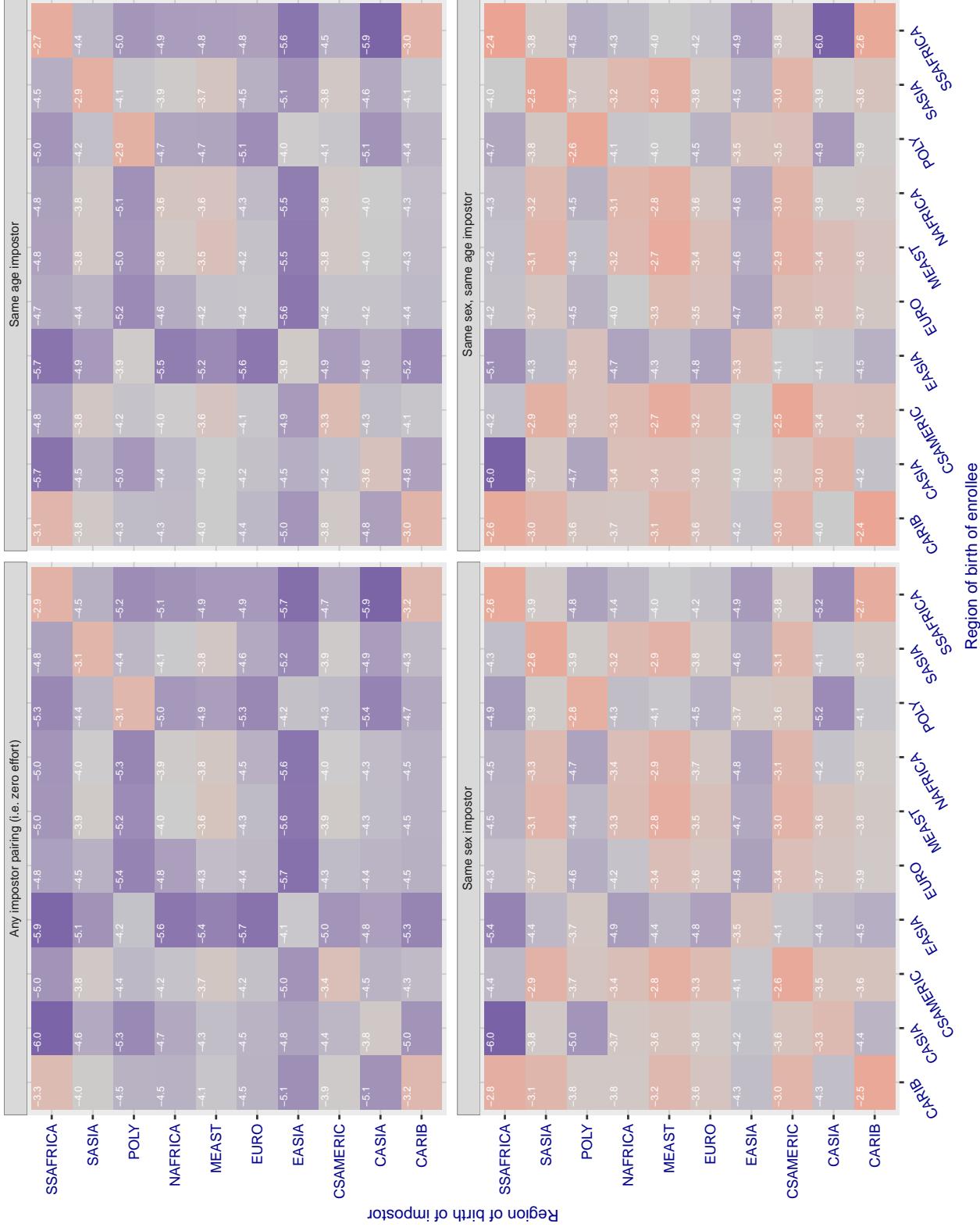


Figure 149: For algorithm incode-002 operating on visa images, the heatmap shows false match rates observed over impostor comparisons of faces from different individuals who were born in the given region pair. False matches are counted against a recognition threshold fixed globally to give the target FMR in the plot title, computed over all on the order of  $10^{10}$  impostor comparisons. If text appears in each box it give the same quantity as that coded by the color. Grey indicates FMR is at the intended FMR target level. Light red colors present a security vulnerability to, for example, a passport gate. Each +1 increase in  $\log_{10} \text{FMR}$  corresponds to a factor of 10 increase in FMR. The matrix is not quite symmetric because images in the enrollment and verification sets are different.

### Cross region FMR at threshold T = 1.427 for algorithm incode\_003, giving FMR(T) = 0.0001 globally.

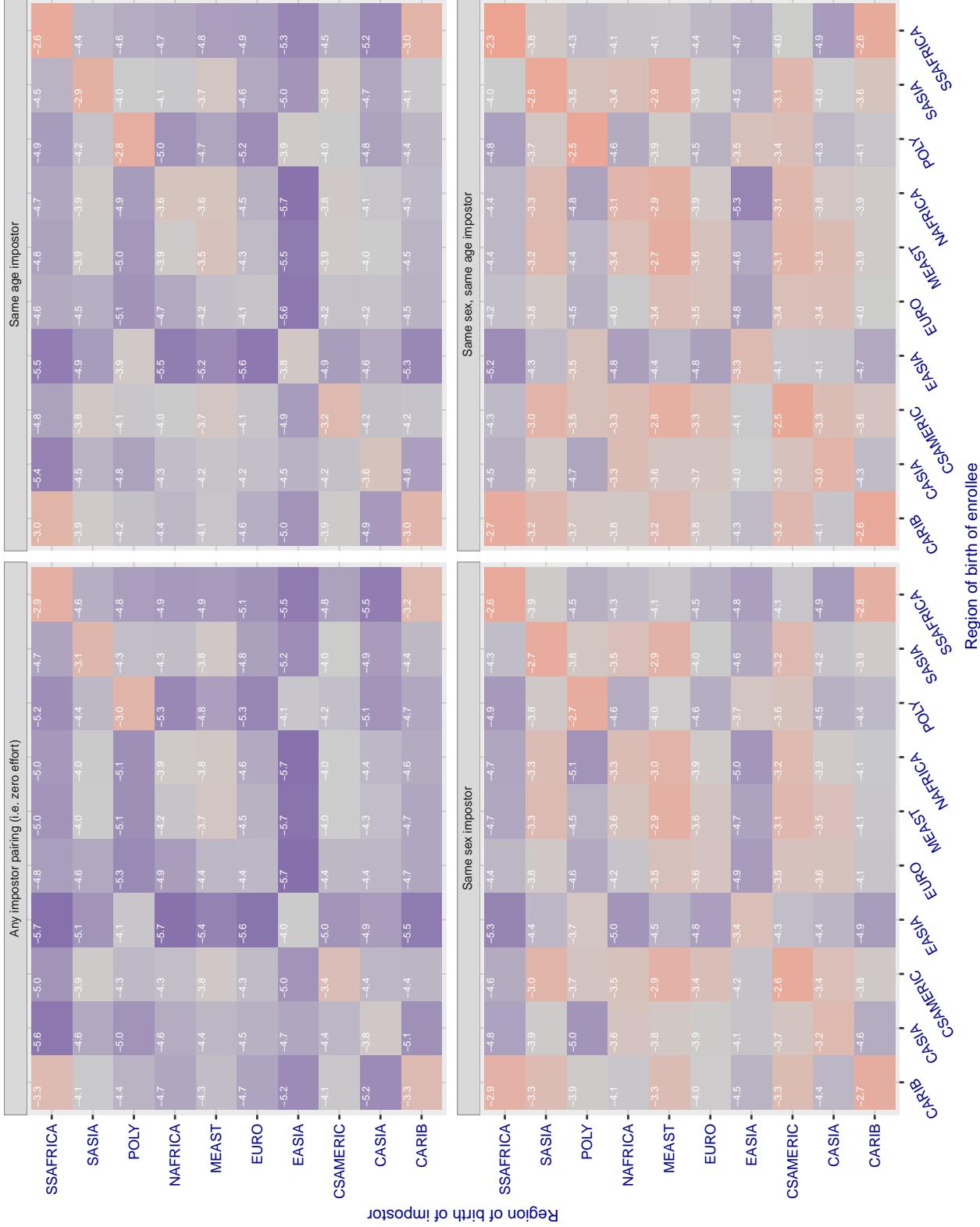


Figure 150: For algorithm incode-003 operating on visa images, the heatmap shows false match rates observed over impostor comparisons of faces from different individuals who were born in the given region pair. False matches are counted against a recognition threshold fixed globally to give the target FMR in the plot title, computed over all on the order of  $10^{10}$  impostor comparisons. If text appears in each box it give the same quantity as that coded by the color. Grey indicates FMR is at the intended FMR target level. Light red colors present a security vulnerability to, for example, a passport gate. Each +1 increase in  $\log_{10} \text{FMR}$  corresponds to a factor of 10 increase in FMR. The matrix is not quite symmetric because images in the enrollment and verification sets are different.

### Cross region FMR at threshold T = 29.232 for algorithm innovatrics\_004, giving FMR(T) = 0.0001 globally.

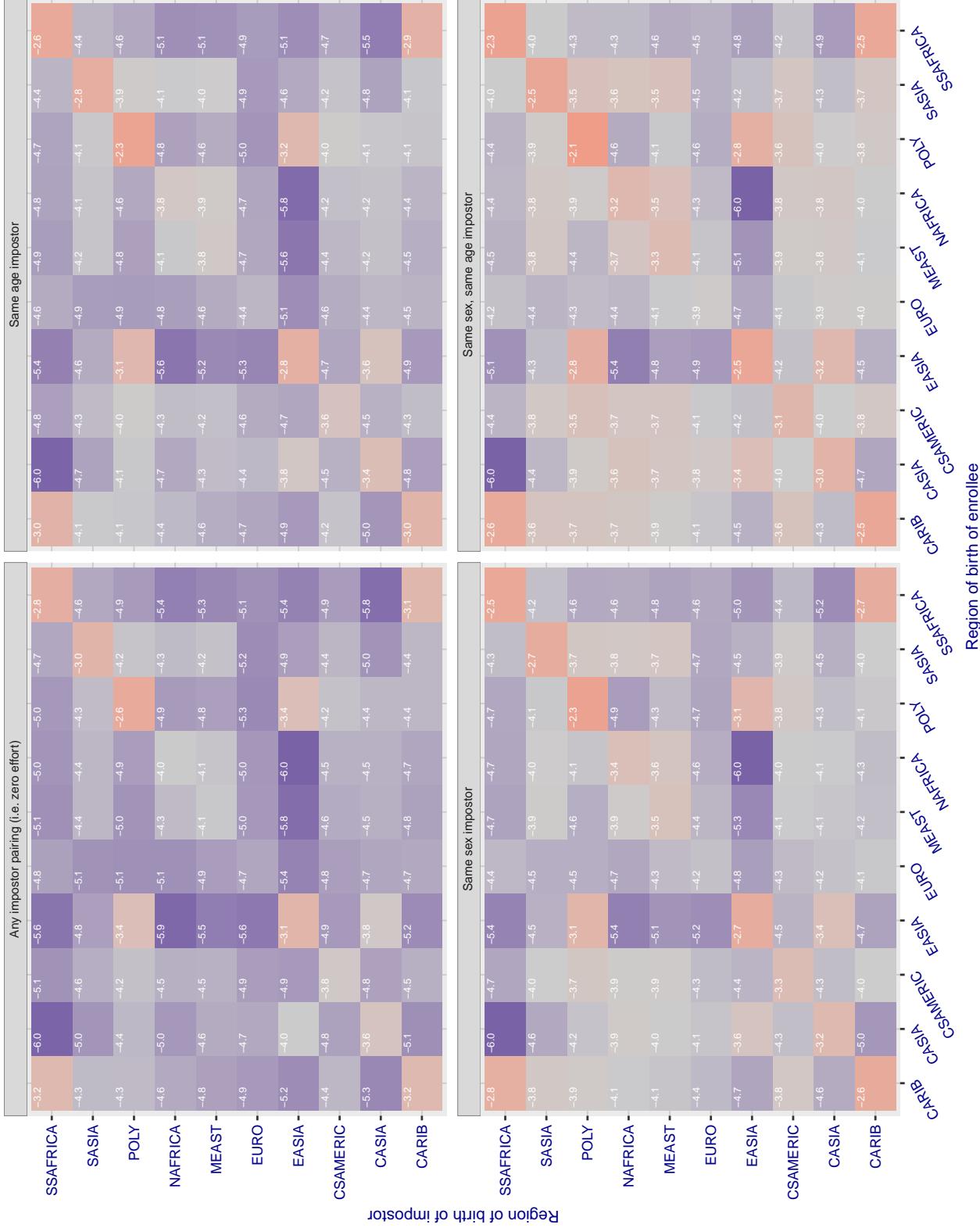


Figure 151: For algorithm innovatrics-004 operating on visa images, the heatmap shows false match rates observed over impostor comparisons of faces from different individuals who were born in the given region pair. False matches are counted against a recognition threshold fixed globally to give the target FMR in the plot title, computed over all on the order of  $10^{10}$  impostor comparisons. If text appears in each box it give the same quantity as that coded by the color. Grey indicates FMR is at the intended FMR target level. Light red colors present a security vulnerability to, for example, a passport gate. Each +1 increase in  $\log_{10} FMR$  corresponds to a factor of 10 increase in FMR. The matrix is not quite symmetric because images in the enrollment and verification sets are different.

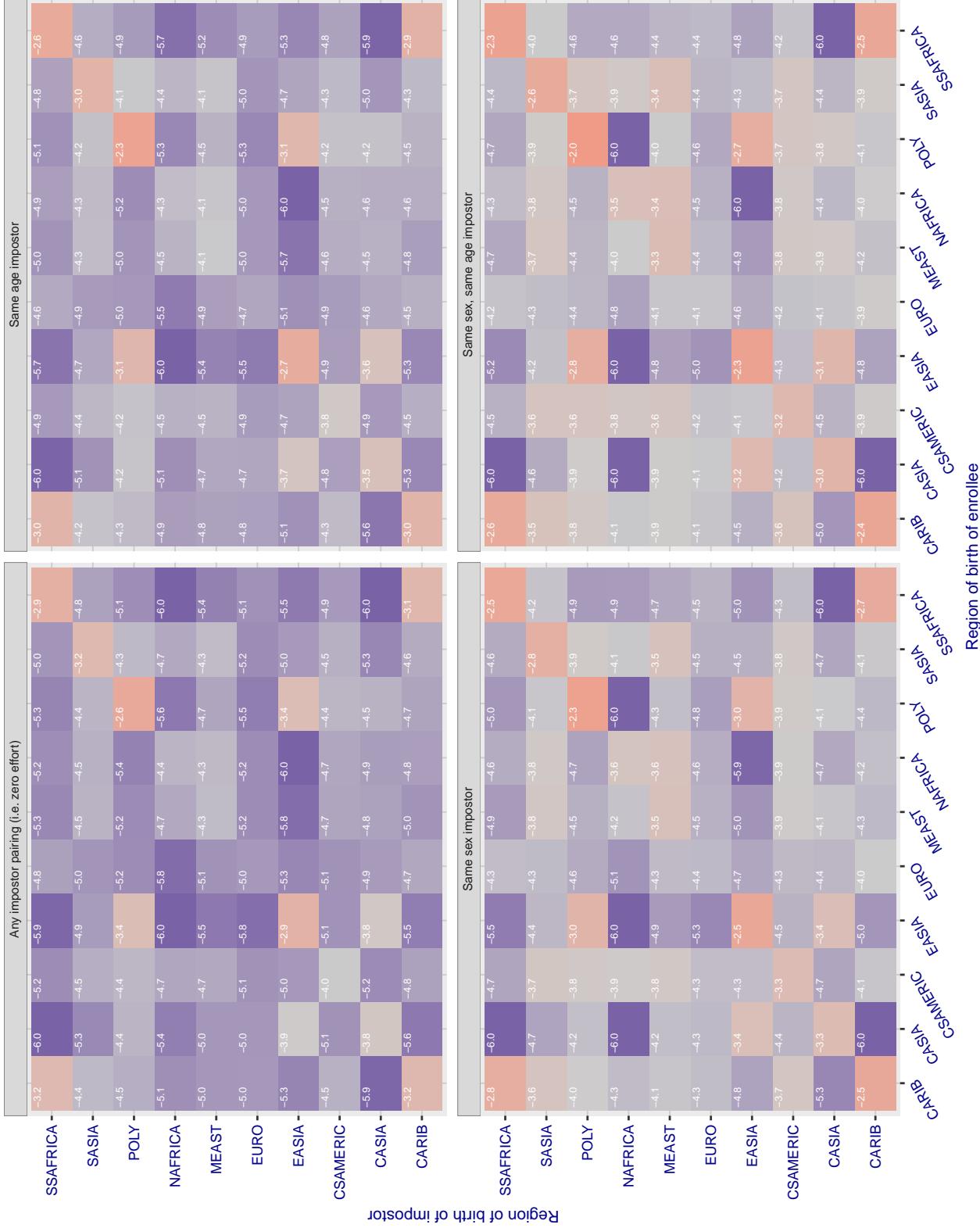
**Cross region FMR at threshold T = 40.157 for algorithm innovatrics\_005, giving FMR(T) = 0.0001 globally.**

Figure 152: For algorithm innovatrics\_005 operating on visa images, the heatmap shows false match rates observed over impostor comparisons of faces from different individuals who were born in the given region pair. False matches are counted against a recognition threshold fixed globally to give the target FMR in the plot title, computed over all on the order of  $10^{10}$  impostor comparisons. If text appears in each box it give the same quantity as that coded by the color. Grey indicates FMR is at the intended FMR target level. Light red colors present a security vulnerability to, for example, a passport gate. Each +1 increase in  $\log_{10} FMR$  corresponds to a factor of 10 increase in FMR. The matrix is not quite symmetric because images in the enrollment and verification sets are different.

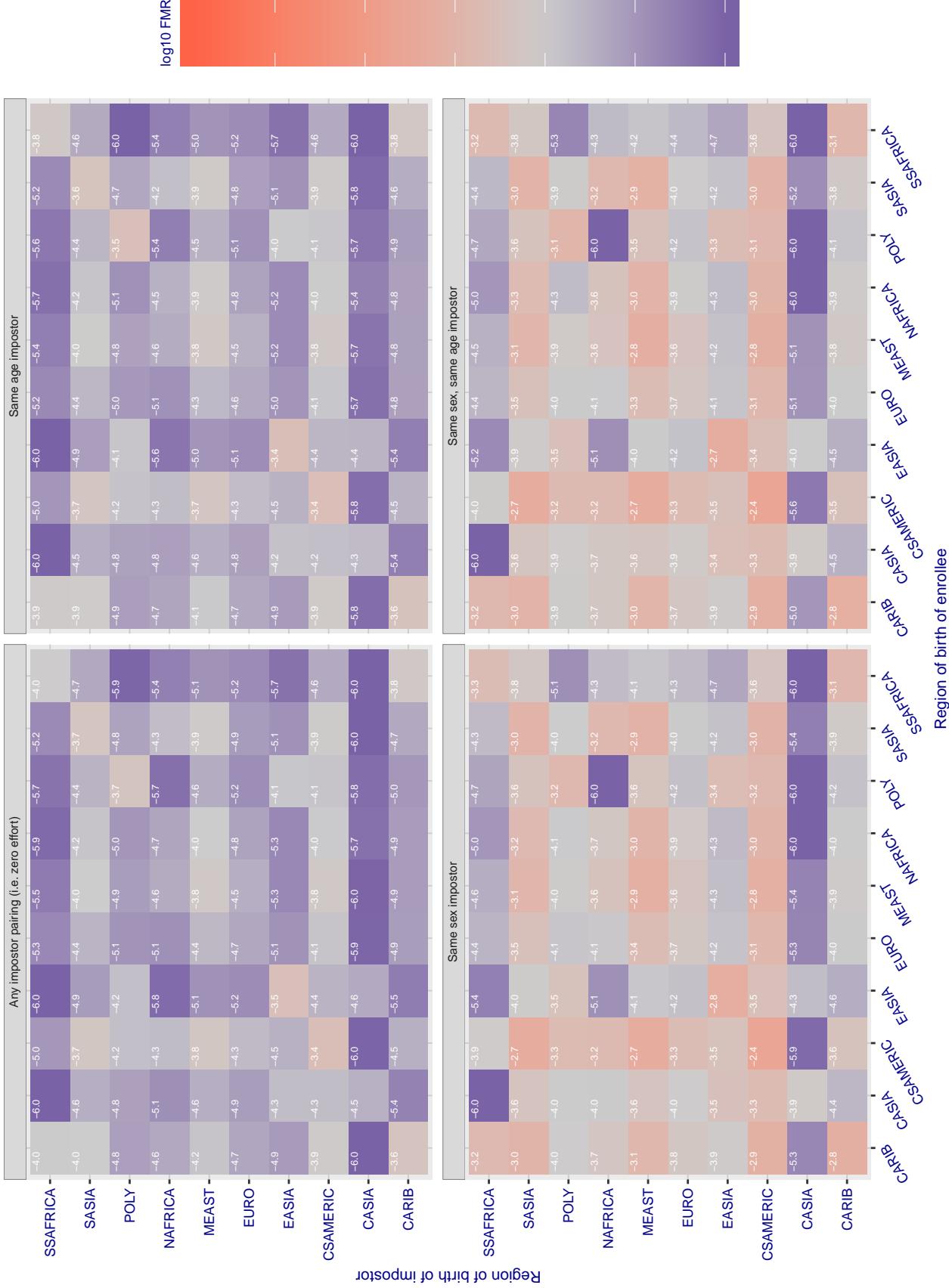
**Cross region FMR at threshold T = 49.664 for algorithm intellivision\_001, giving FMR(T) = 0.0001 globally.**

Figure 153: For algorithm intellivision-001 operating on visa images, the heatmap shows false match rates observed over impostor comparisons of faces from different individuals who were born in the given region pair. False matches are counted against a recognition threshold fixed globally to give the target FMR in the plot title, computed over all on the order of  $10^{10}$  impostor comparisons. If text appears in each box it give the same quantity as that coded by the color. Grey indicates FMR is at the intended FMR target level. Light red colors present a security vulnerability to, for example, a passport gate. Each +1 increase in  $\log_{10} FMR$  corresponds to a factor of 10 increase in FMR. The matrix is not quite symmetric because images in the enrollment and verification sets are different.

### Cross region FMR at threshold T = 23.498 for algorithm isityou\_000, giving FMR(T) = 0.0001 globally.

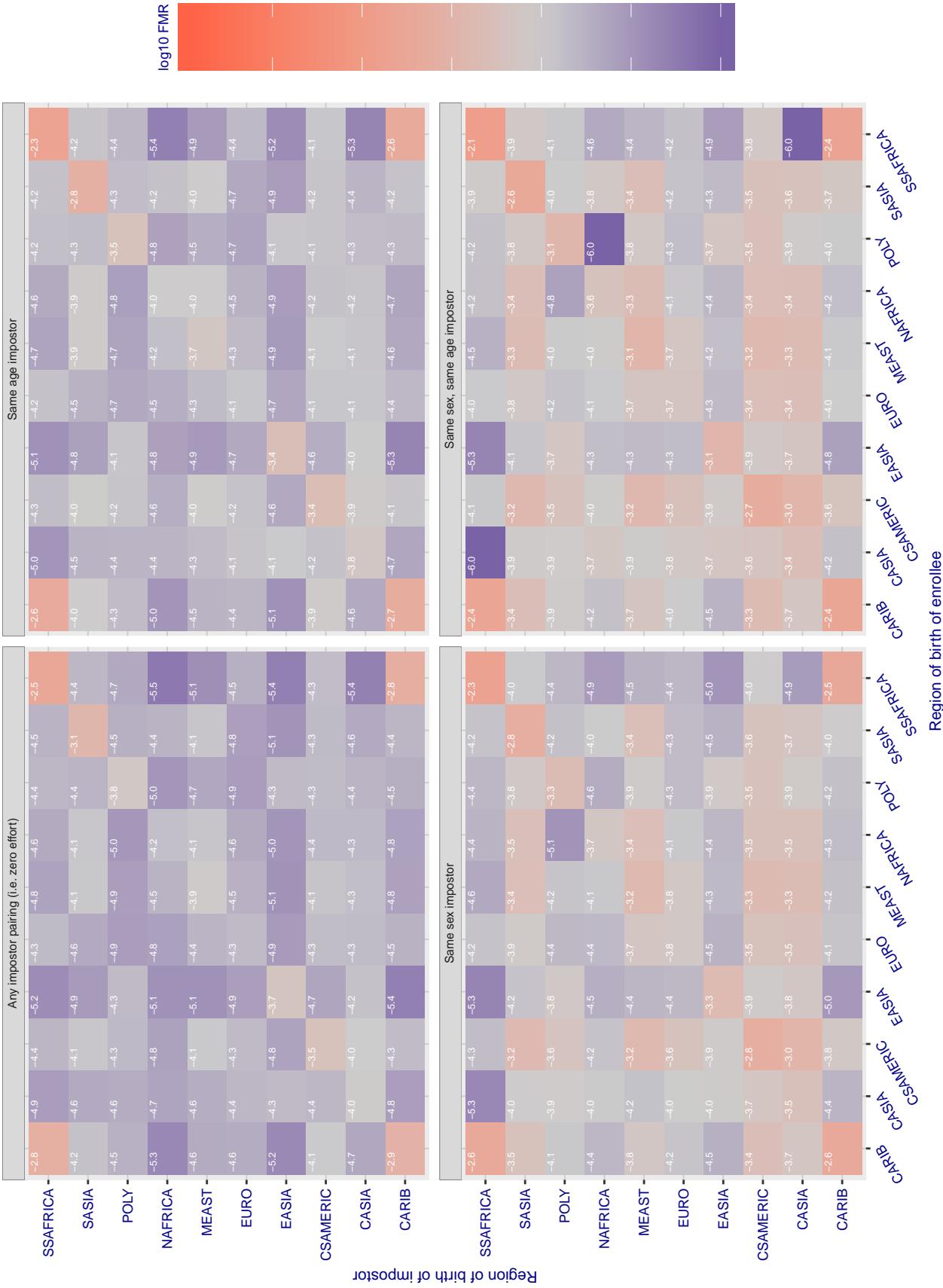


Figure 154: For algorithm isityou-000 operating on visa images, the heatmap shows false match rates observed over impostor comparisons of faces from different individuals who were born in the given region pair. False matches are counted against a recognition threshold fixed globally to give the target FMR in the plot title, computed over all on the order of  $10^{10}$  impostor comparisons. If text appears in each box it give the same quantity as that coded by the color. Grey indicates FMR is at the intended FMR target level. Light red colors present a security vulnerability to, for example, a passport gate. Each +1 increase in  $\log_{10} FMR$  corresponds to a factor of 10 increase in FMR. The matrix is not quite symmetric because images in the enrollment and verification sets are different.

### Cross region FMR at threshold T = 0.693 for algorithm isystems\_001, giving FMR(T) = 0.0001 globally.

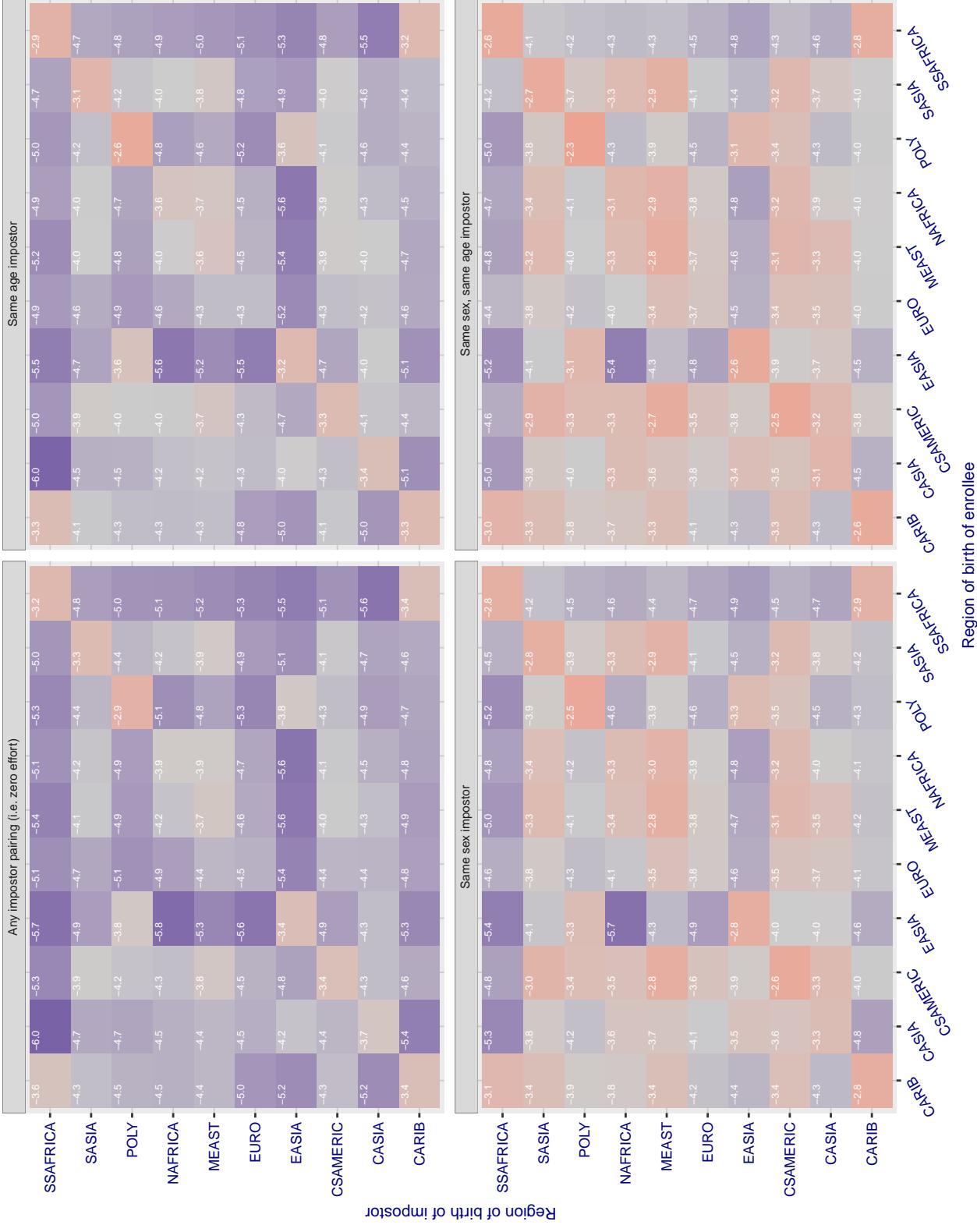


Figure 155: For algorithm isystems-001 operating on visa images, the heatmap shows false match rates observed over impostor comparisons of faces from different individuals who were born in the given region pair. False matches are counted against a recognition threshold fixed globally to give the target FMR in the plot title, computed over all on the order of  $10^{10}$  impostor comparisons. If text appears in each box it give the same quantity as that coded by the color. Grey indicates FMR is at the intended FMR target level. Light red colors present a security vulnerability to, for example, a passport gate. Each +1 increase in  $\log_{10} \text{FMR}$  corresponds to a factor of 10 increase in FMR. The matrix is not quite symmetric because images in the enrollment and verification sets are different.

### Cross region FMR at threshold T = 0.690 for algorithm isystems\_002, giving FMR(T) = 0.0001 globally.

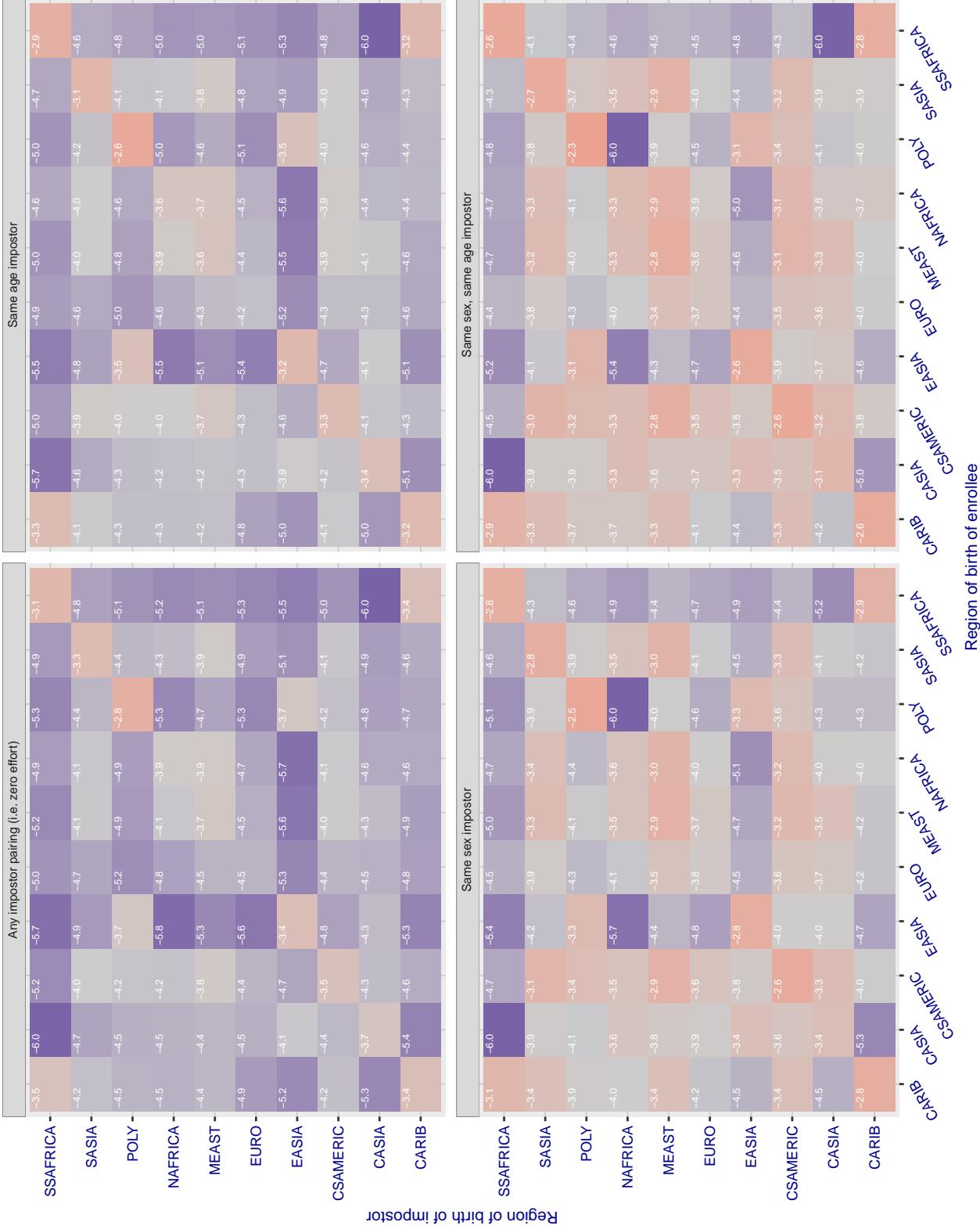


Figure 156: For algorithm isystems-002 operating on visa images, the heatmap shows false match rates observed over impostor comparisons of faces from different individuals who were born in the given region pair. False matches are counted against a recognition threshold fixed globally to give the target FMR in the plot title, computed over all on the order of  $10^{10}$  impostor comparisons. If text appears in each box it give the same quantity as that coded by the color. Grey indicates FMR is at the intended FMR target level. Light red colors present a security vulnerability to, for example, a passport gate. Each +1 increase in  $\log_{10} \text{FMR}$  corresponds to a factor of 10 increase in FMR. The matrix is not quite symmetric because images in the enrollment and verification sets are different.

### Cross region FMR at threshold T = 49.879 for algorithm itmo\_005, giving FMR(T) = 0.0001 globally.

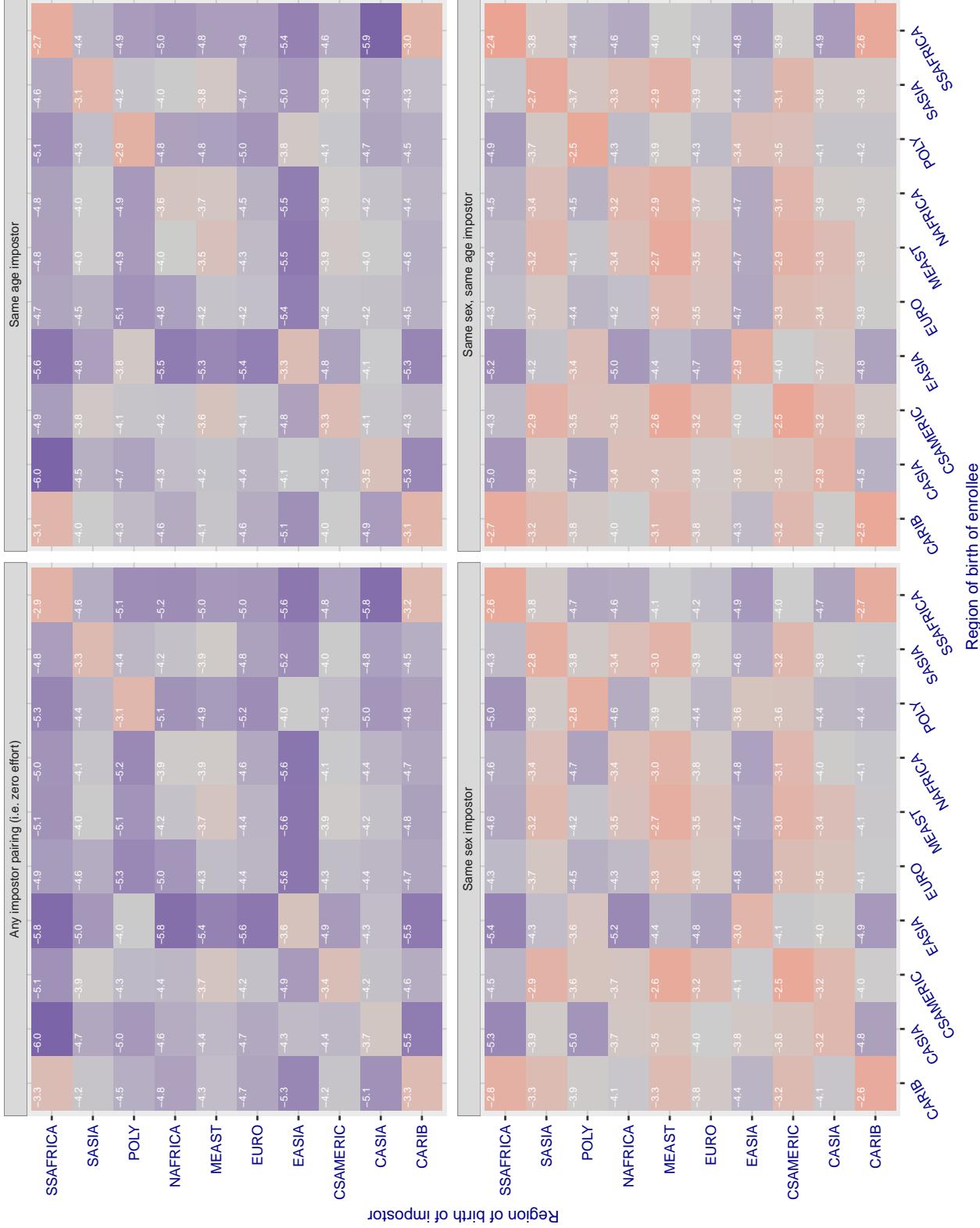


Figure 157: For algorithm itmo-005 operating on visa images, the heatmap shows false match rates observed over impostor comparisons of faces from different individuals who were born in the given region pair. False matches are counted against a recognition threshold fixed globally to give the target FMR in the plot title, computed over all on the order of  $10^{10}$  impostor comparisons. If text appears in each box it give the same quantity as that coded by the color. Grey indicates FMR is at the intended FMR target level. Light red colors present a security vulnerability to, for example, a passport gate. Each +1 increase in  $\log_{10}$  FMR corresponds to a factor of 10 increase in FMR. The matrix is not quite symmetric because images in the enrollment and verification sets are different.

### Cross region FMR at threshold T = 49.789 for algorithm itmo\_006, giving FMR(T) = 0.0001 globally.

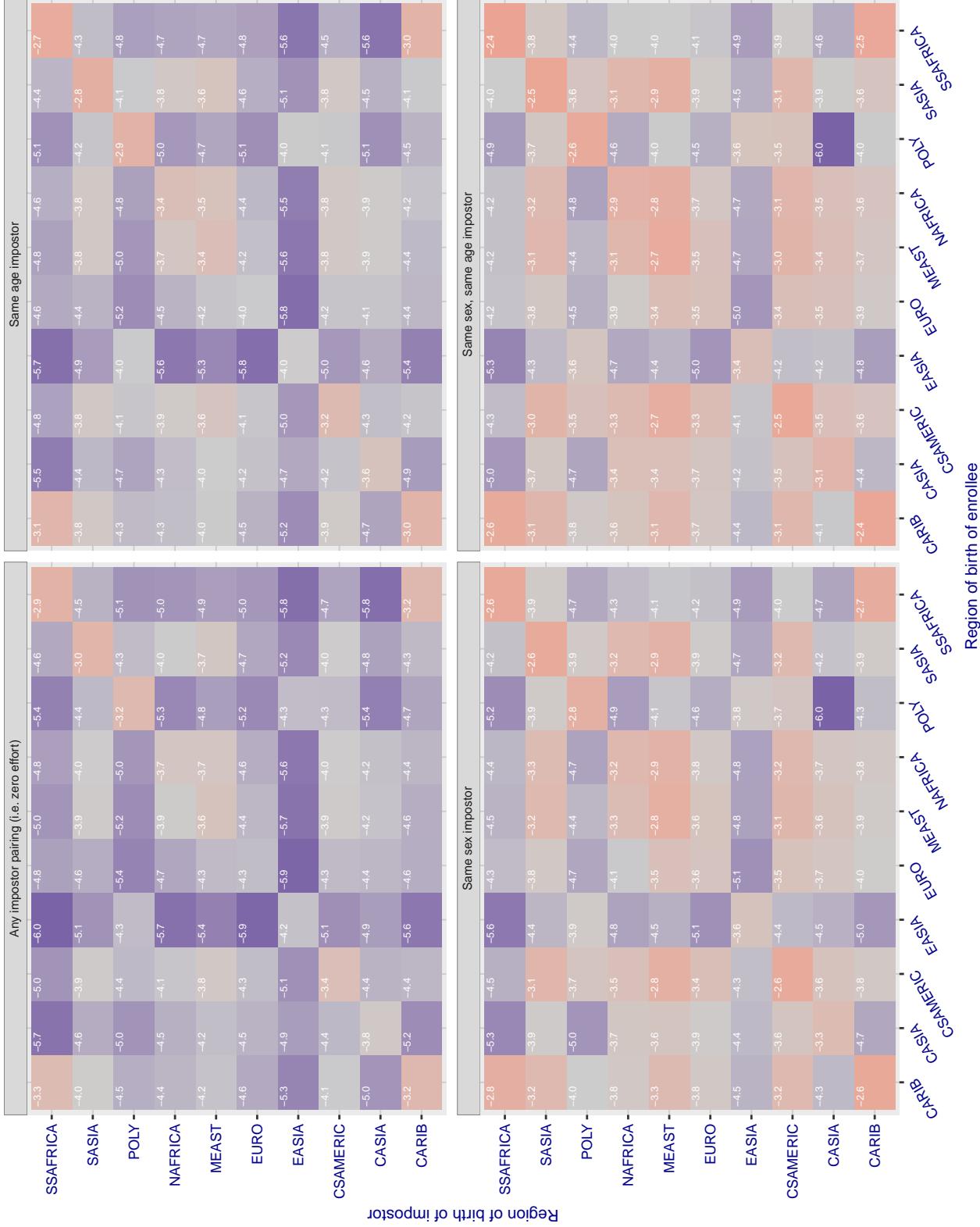


Figure 158: For algorithm itmo-006 operating on visa images, the heatmap shows false match rates observed over impostor comparisons of faces from different individuals who were born in the given region pair. False matches are counted against a recognition threshold fixed globally to give the target FMR in the plot title, computed over all on the order of  $10^{10}$  impostor comparisons. If text appears in each box it give the same quantity as that coded by the color. Grey indicates FMR is at the intended FMR target level. Light red colors present a security vulnerability to, for example, a passport gate. Each +1 increase in  $\log 10 \text{ FMR}$  corresponds to a factor of 10 increase in FMR. The matrix is not quite symmetric because images in the enrollment and verification sets are different.

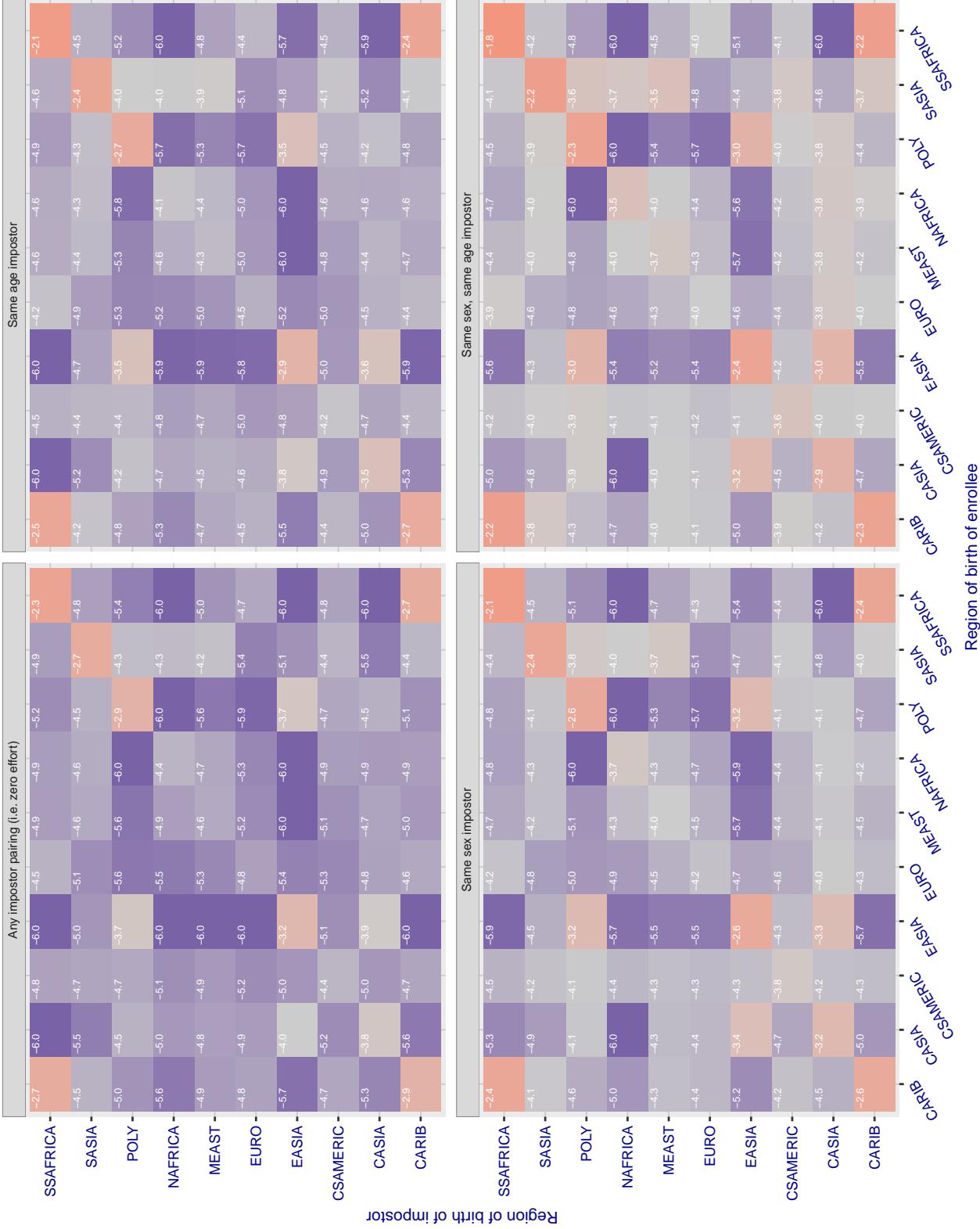
**Cross region FMR at threshold T = 1.301 for algorithm kakao\_001, giving FMR(T) = 0.0001 globally.**

Figure 159: For algorithm kakao-001 operating on visa images, the heatmap shows false match rates observed over impostor comparisons of faces from different individuals who were born in the given region pair. False matches are counted against a recognition threshold fixed globally to give the target FMR in the plot title, computed over all on the order of  $10^{10}$  impostor comparisons. If text appears in each box it give the same quantity as that coded by the color. Grey indicates FMR is at the intended FMR target level. Light red colors present a security vulnerability to, for example, a passport gate. Each +1 increase in  $\log_{10} FMR$  corresponds to a factor of 10 increase in FMR. The matrix is not quite symmetric because images in the enrollment and verification sets are different.

### Cross region FMR at threshold T = 0.701 for algorithm lookman\_002, giving FMR(T) = 0.0001 globally.

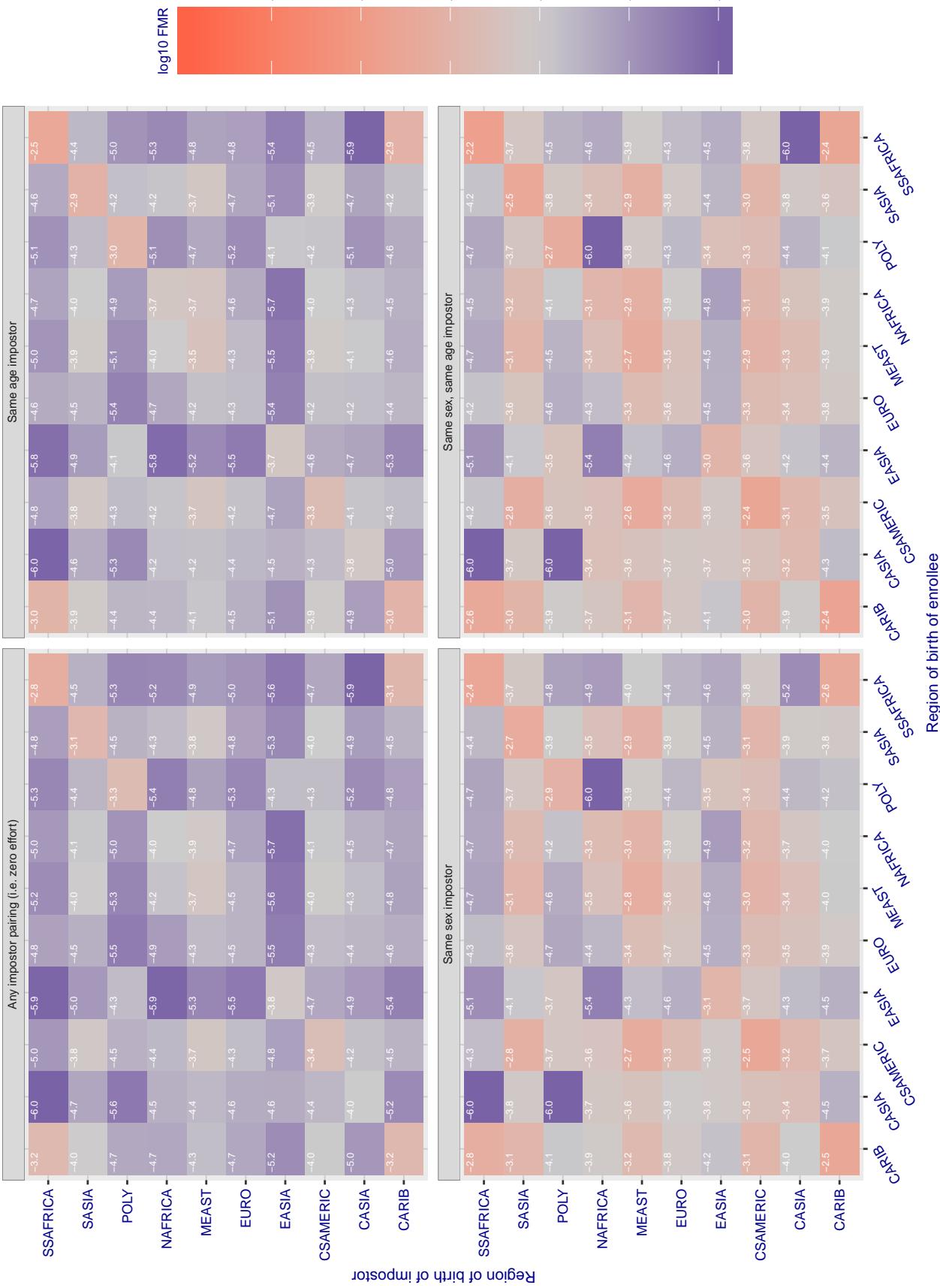


Figure 160: For algorithm lookman-002 operating on visa images, the heatmap shows false match rates observed over impostor comparisons of faces from different individuals who were born in the given region pair. False matches are counted against a recognition threshold fixed globally to give the target FMR in the plot title, computed over all on the order of  $10^{10}$  impostor comparisons. If text appears in each box it give the same quantity as that coded by the color. Grey indicates FMR is at the intended FMR target level. Light red colors present a security vulnerability to, for example, a passport gate. Each +1 increase in  $\log_{10} \text{FMR}$  corresponds to a factor of 10 increase in FMR. The matrix is not quite symmetric because images in the enrollment and verification sets are different.

### Cross region FMR at threshold T = 74.511 for algorithm megvii\_001, giving FMR(T) = 0.0001 globally.

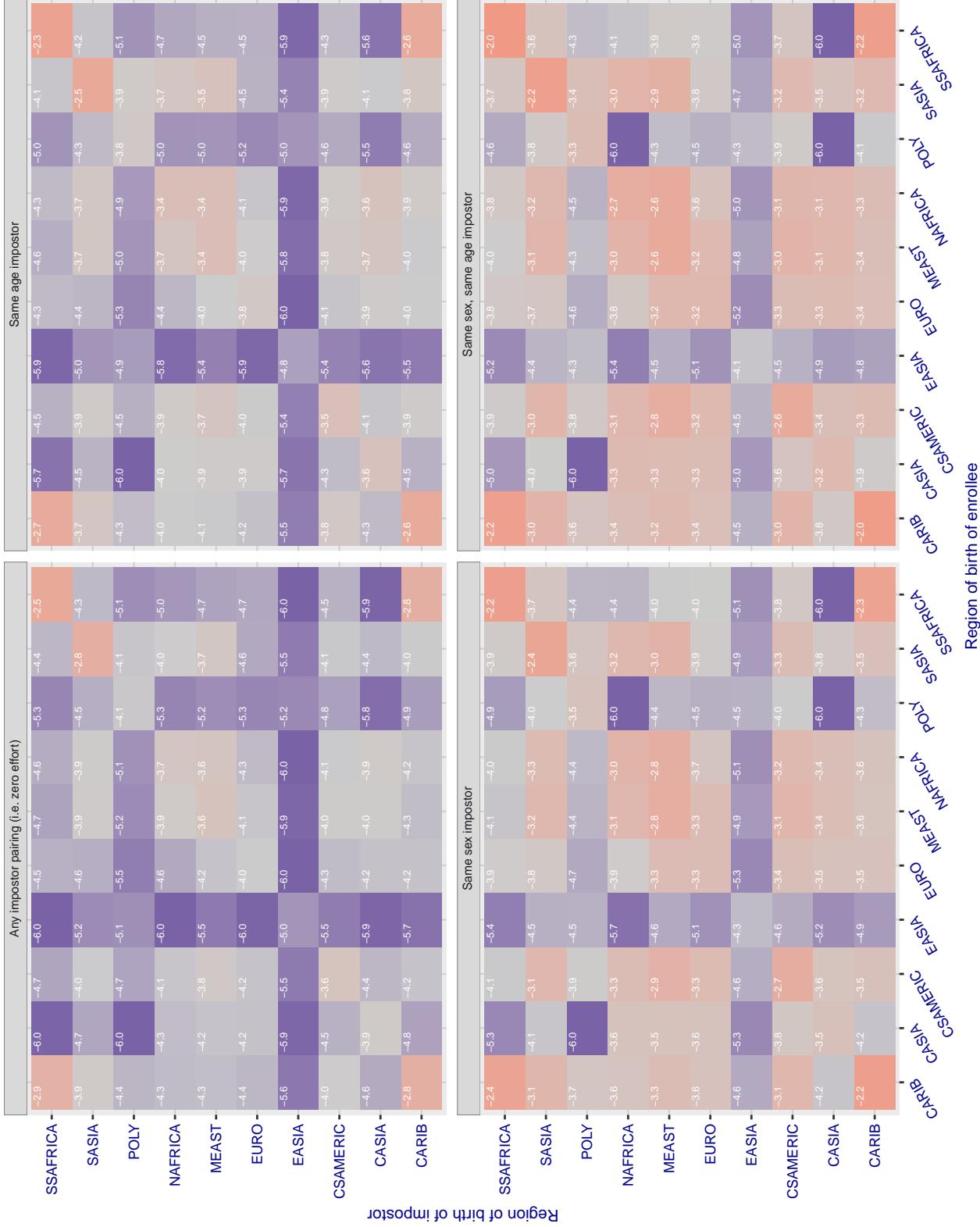


Figure 161: For algorithm megvii-001 operating on visa images, the heatmap shows false match rates observed over impostor comparisons of faces from different individuals who were born in the given region pair. False matches are counted against a recognition threshold fixed globally to give the target FMR in the plot title, computed over all on the order of  $10^{10}$  impostor comparisons. If text appears in each box it give the same quantity as that coded by the color. Grey indicates FMR is at the intended FMR target level. Light red colors present a security vulnerability to, for example, a passport gate. Each +1 increase in  $\log_{10} \text{FMR}$  corresponds to a factor of 10 increase in FMR. The matrix is not quite symmetric because images in the enrollment and verification sets are different.

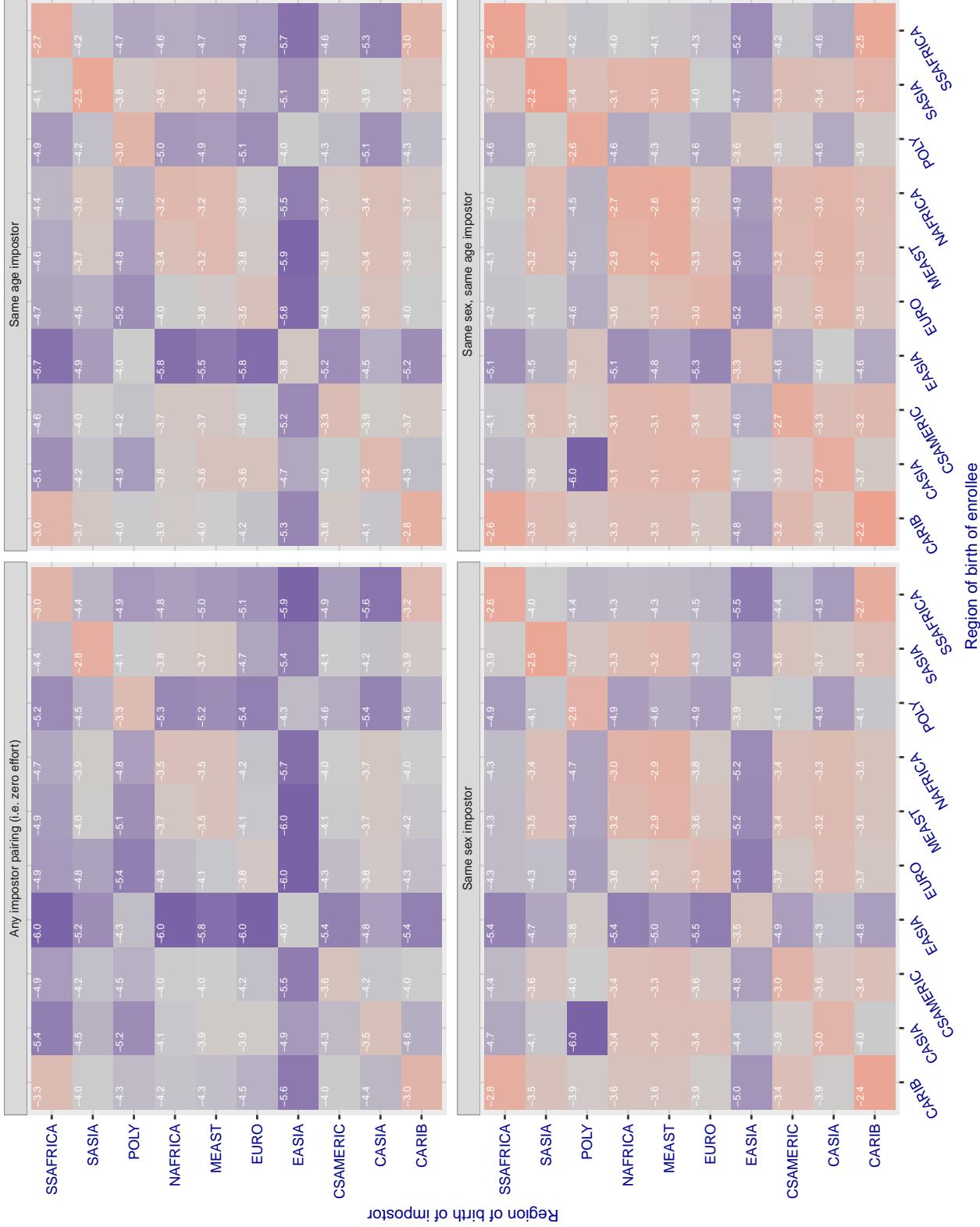
**Cross region FMR at threshold T = 66.384 for algorithm megvii\_002, giving FMR(T) = 0.0001 globally.**

Figure 162: For algorithm megvii-002 operating on visa images, the heatmap shows false match rates observed over impostor comparisons of faces from different individuals who were born in the given region pair. False matches are counted against a recognition threshold fixed globally to give the target FMR in the plot title, computed over all on the order of  $10^{10}$  impostor comparisons. If text appears in each box it give the same quantity as that coded by the color. Grey indicates FMR is at the intended FMR target level. Light red colors present a security vulnerability to, for example, a passport gate. Each +1 increase in  $\log_{10} FMR$  corresponds to a factor of 10 increase in FMR. The matrix is not quite symmetric because images in the enrollment and verification sets are different.

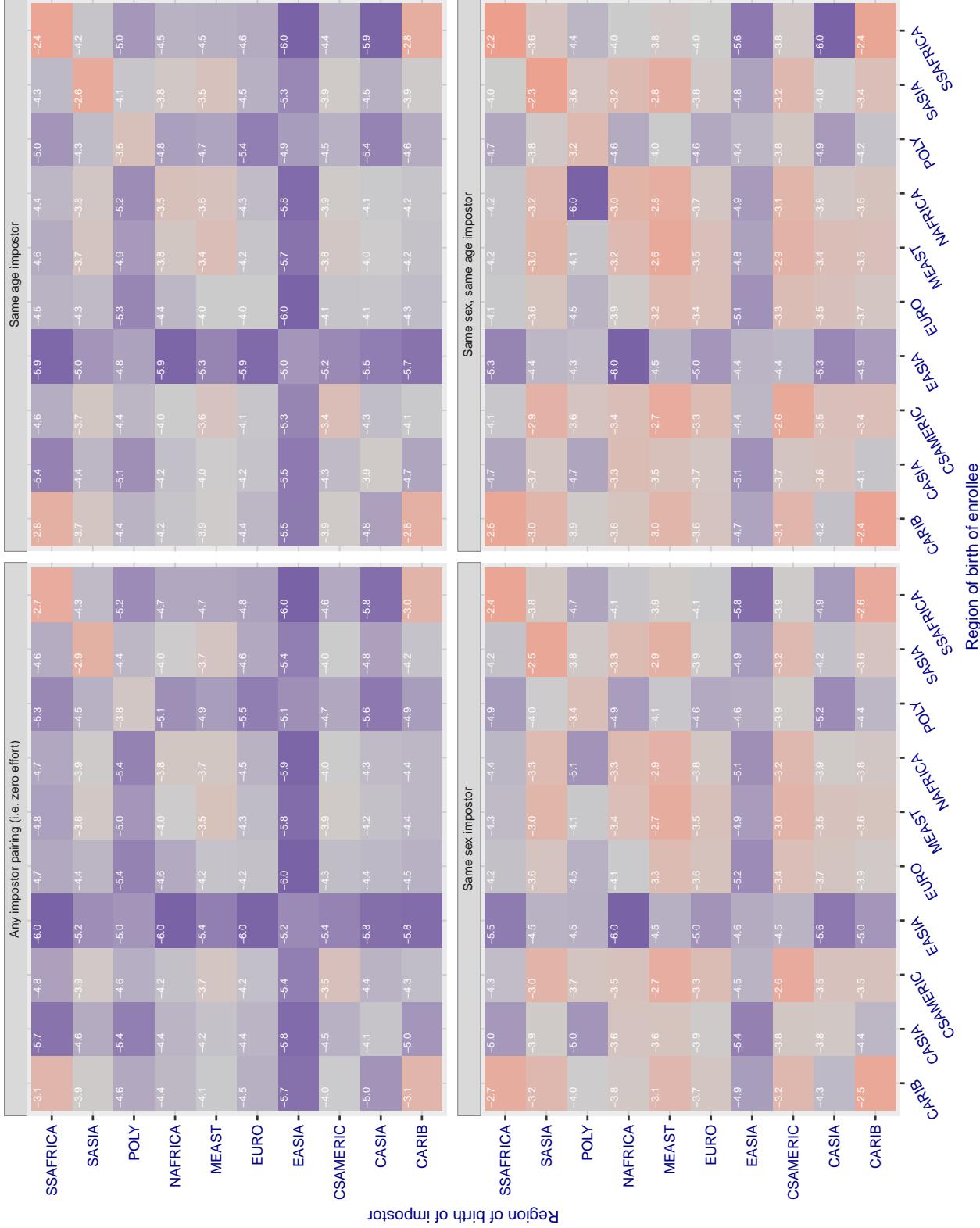
**Cross region FMR at threshold T = 0.425 for algorithm meiya\_001, giving FMR(T) = 0.0001 globally.**

Figure 163: For algorithm meiya-001 operating on visa images, the heatmap shows false match rates observed over impostor comparisons of faces from different individuals who were born in the given region pair. False matches are counted against a recognition threshold fixed globally to give the target FMR in the plot title, computed over all on the order of  $10^{10}$  impostor comparisons. If text appears in each box it give the same quantity as that coded by the color. Grey indicates FMR is at the intended FMR target level. Light red colors present a security vulnerability to, for example, a passport gate. Each +1 increase in  $\log_{10} FMR$  corresponds to a factor of 10 increase in FMR. The matrix is not quite symmetric because images in the enrollment and verification sets are different.

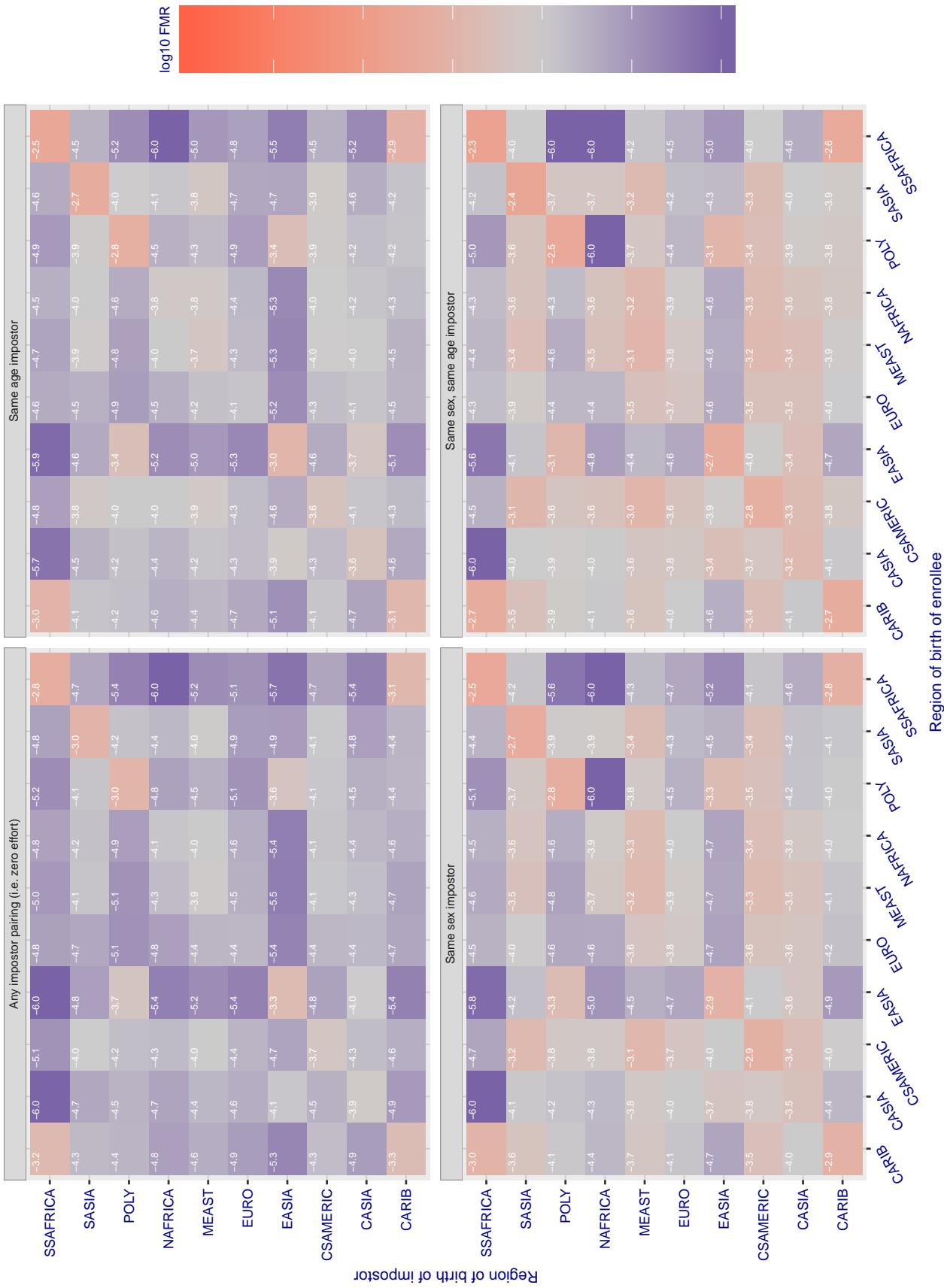
**Cross region FMR at threshold T = 0.668 for algorithm microfocus\_001, giving FMR(T) = 0.0001 globally.**

Figure 164: For algorithm microfocus-001 operating on visa images, the heatmap shows false match rates observed over impostor comparisons of faces from different individuals who were born in the given region pair. False matches are counted against a recognition threshold fixed globally to give the target FMR in the plot title, computed over all on the order of  $10^{10}$  impostor comparisons. If text appears in each box it give the same quantity as that coded by the color. Grey indicates FMR is at the intended FMR target level. Light red colors present a security vulnerability to, for example, a passport gate. Each +1 increase in  $\log_{10} FMR$  corresponds to a factor of 10 increase in FMR. The matrix is not quite symmetric because images in the enrollment and verification sets are different.

### Cross region FMR at threshold T = 0.602 for algorithm microfocus\_002, giving FMR(T) = 0.0001 globally.

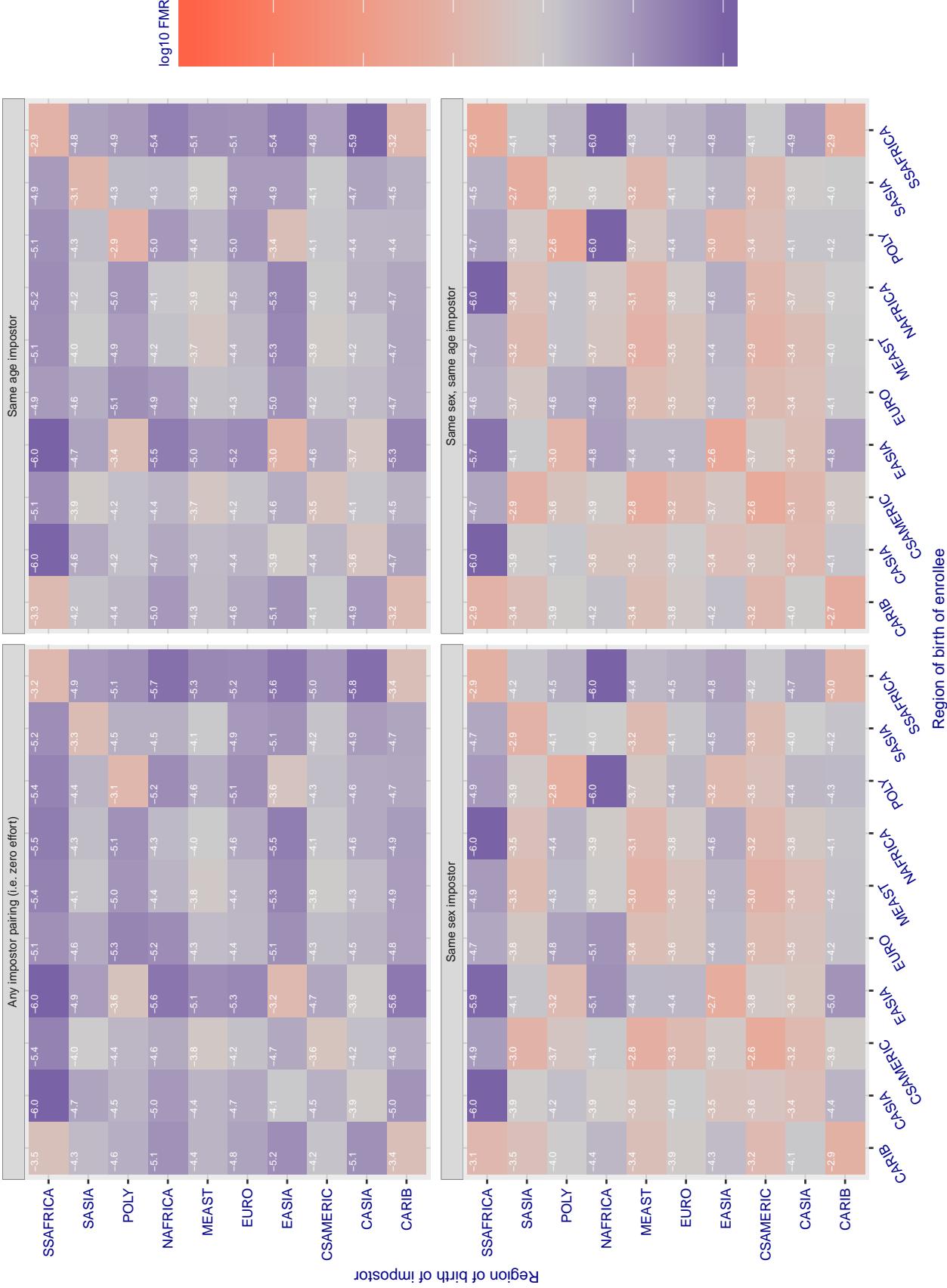


Figure 165: For algorithm microfocus-002 operating on visa images, the heatmap shows false match rates observed over impostor comparisons of faces from different individuals who were born in the given region pair. False matches are counted against a recognition threshold fixed globally to give the target FMR in the plot title, computed over all on the order of  $10^{10}$  impostor comparisons. If text appears in each box it give the same quantity as that coded by the color. Grey indicates FMR is at the intended FMR target level. Light red colors present a security vulnerability to, for example, a passport gate. Each +1 increase in  $\log_{10} \text{FMR}$  corresponds to a factor of 10 increase in FMR. The matrix is not quite symmetric because images in the enrollment and verification sets are different.

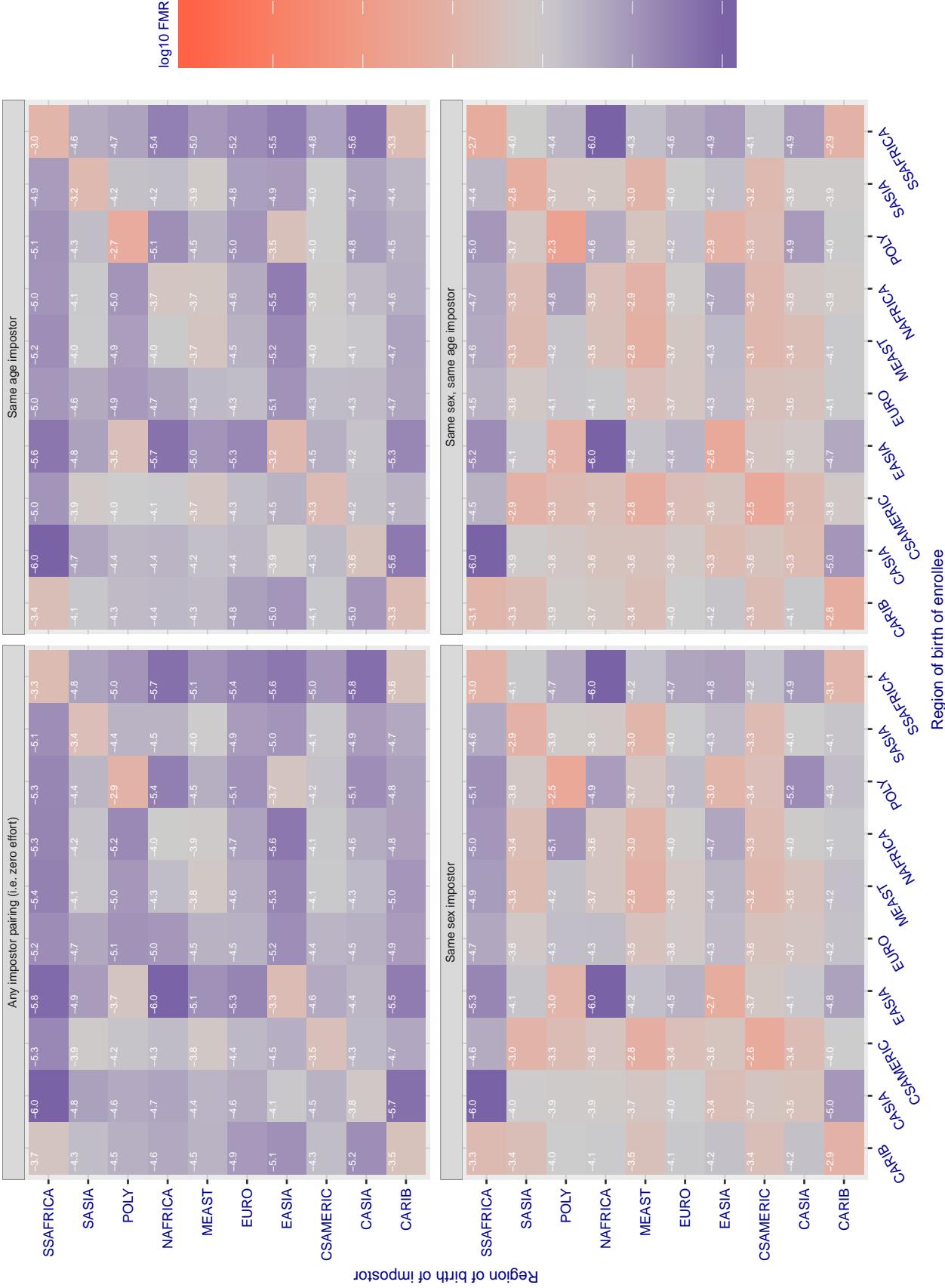
**Cross region FMR at threshold T = 3859.000 for algorithm neurotechnology\_004, giving FMR(T) = 0.0001 globally.**

Figure 166: For algorithm neurotechnology-004 operating on visa images, the heatmap shows false match rates observed over impostor comparisons of faces from different individuals who were born in the given region pair. False matches are counted against a recognition threshold fixed globally to give the target FMR in the plot title, computed over all on the order of  $10^{10}$  impostor comparisons. If text appears in each box it give the same quantity as that coded by the color. Grey indicates FMR is at the intended FMR target level. Light red colors present a security vulnerability to, for example, a passport gate. Each +1 increase in  $\log_{10} \text{FMR}$  corresponds to a factor of 10 increase in FMR. The matrix is not quite symmetric because images in the enrollment and verification sets are different.

### Cross region FMR at threshold T = 46.101 for algorithm neurotechnology\_005, giving FMR(T) = 0.0001 globally.

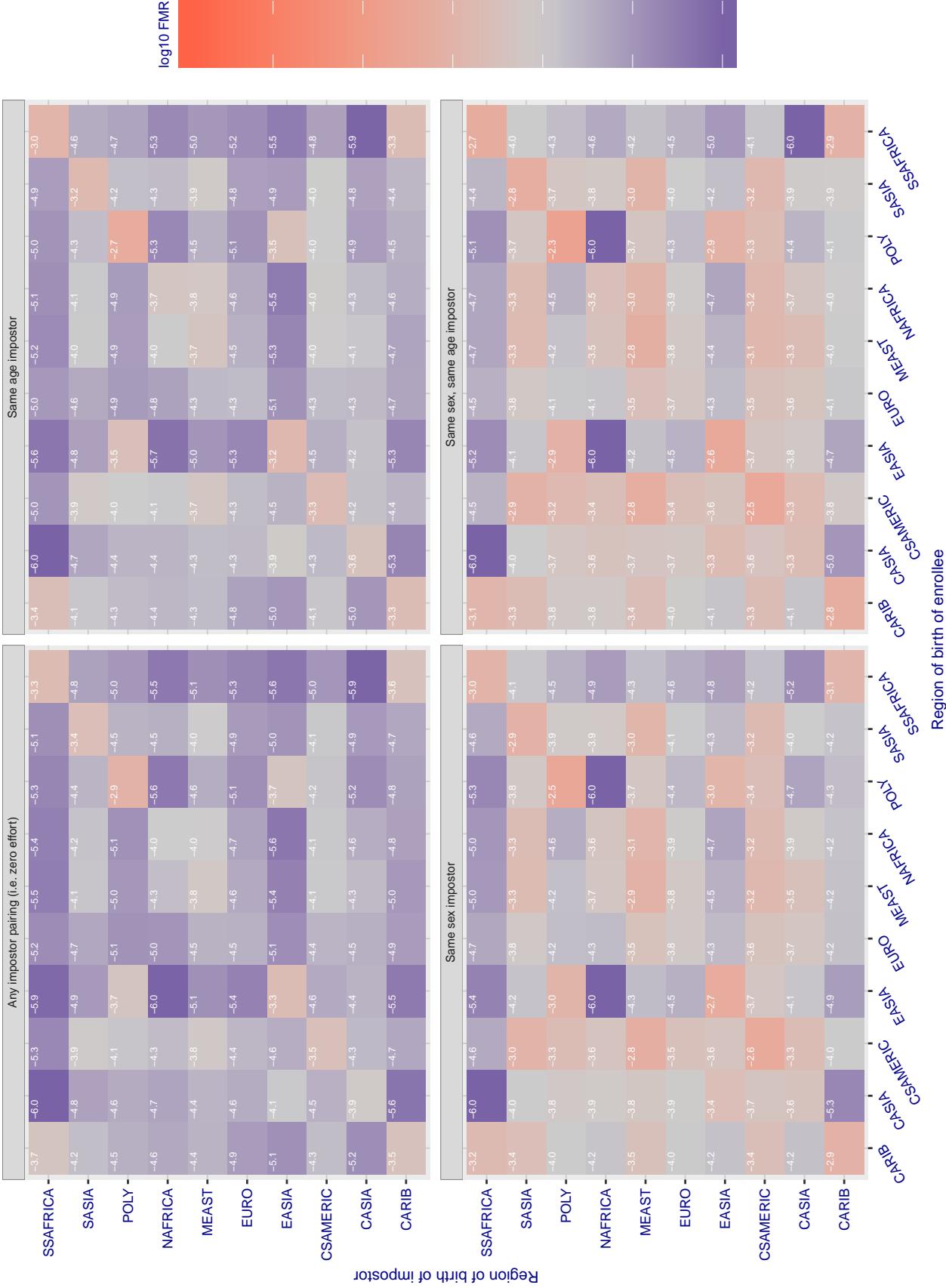


Figure 167: For algorithm neurotechnology-005 operating on visa images, the heatmap shows false match rates observed over impostor comparisons of faces from different individuals who were born in the given region pair. False matches are counted against a recognition threshold fixed globally to give the target FMR in the plot title, computed over all on the order of  $10^{10}$  impostor comparisons. If text appears in each box it give the same quantity as that coded by the color. Grey indicates FMR is at the intended FMR target level. Light red colors present a security vulnerability to, for example, a passport gate. Each +1 increase in  $\log_{10} FMR$  corresponds to a factor of 10 increase in FMR. The matrix is not quite symmetric because images in the enrollment and verification sets are different.

### Cross region FMR at threshold T = 1.000 for algorithm nodeflux\_000, giving FMR(T) = 0.0001 globally.

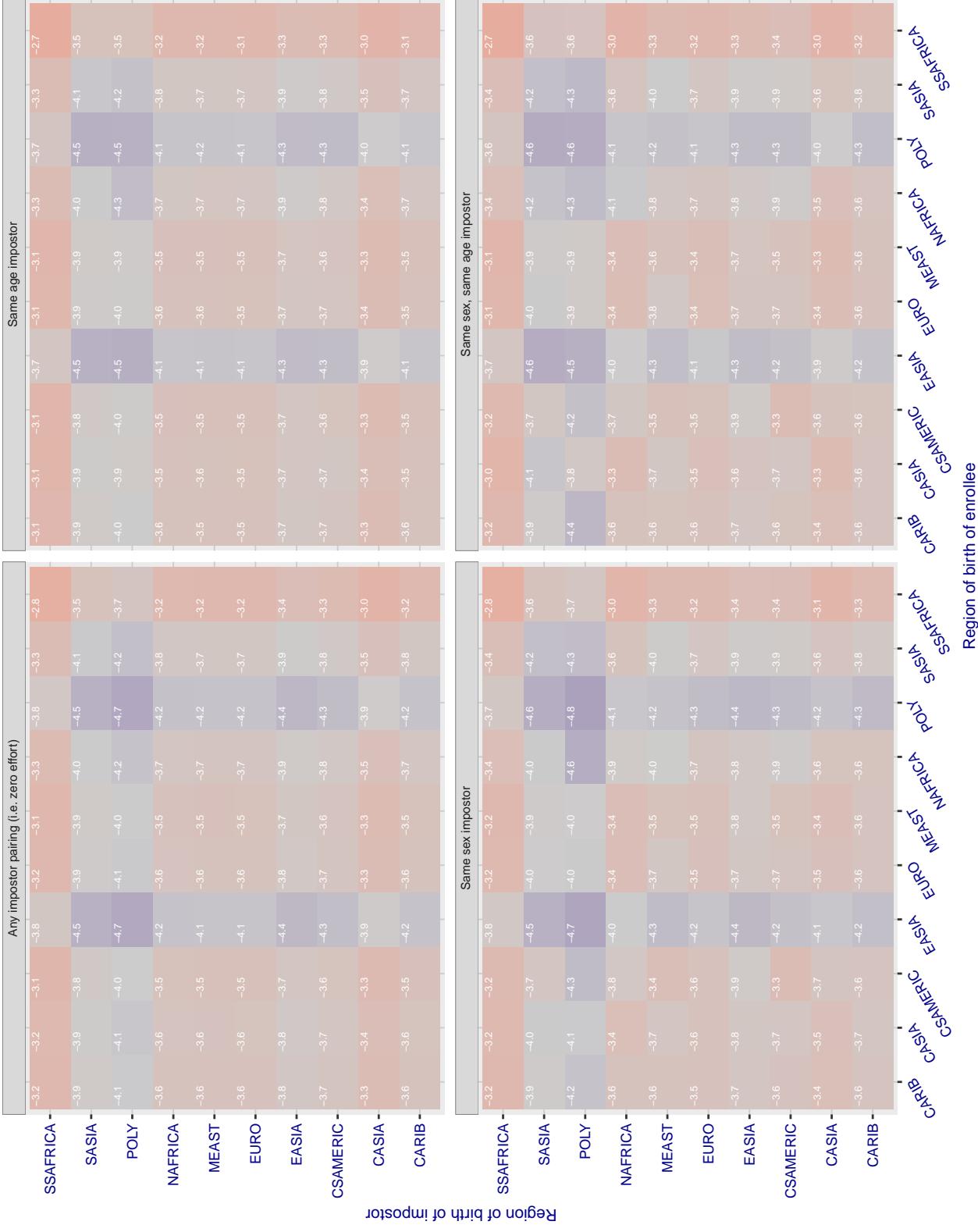


Figure 168: For algorithm nodeflux-000 operating on visa images, the heatmap shows false match rates observed over impostor comparisons of faces from different individuals who were born in the given region pair. False matches are counted against a recognition threshold fixed globally to give the target FMR in the plot title, computed over all on the order of  $10^{10}$  impostor comparisons. If text appears in each box it give the same quantity as that coded by the color. Grey indicates FMR is at the intended FMR target level. Light red colors present a security vulnerability to, for example, a passport gate. Each +1 increase in  $\log_{10} FMR$  corresponds to a factor of 10 increase in FMR. The matrix is not quite symmetric because images in the enrollment and verification sets are different.

### Cross region FMR at threshold T = 1.000 for algorithm nodeflux\_001, giving FMR(T) = 0.0001 globally.

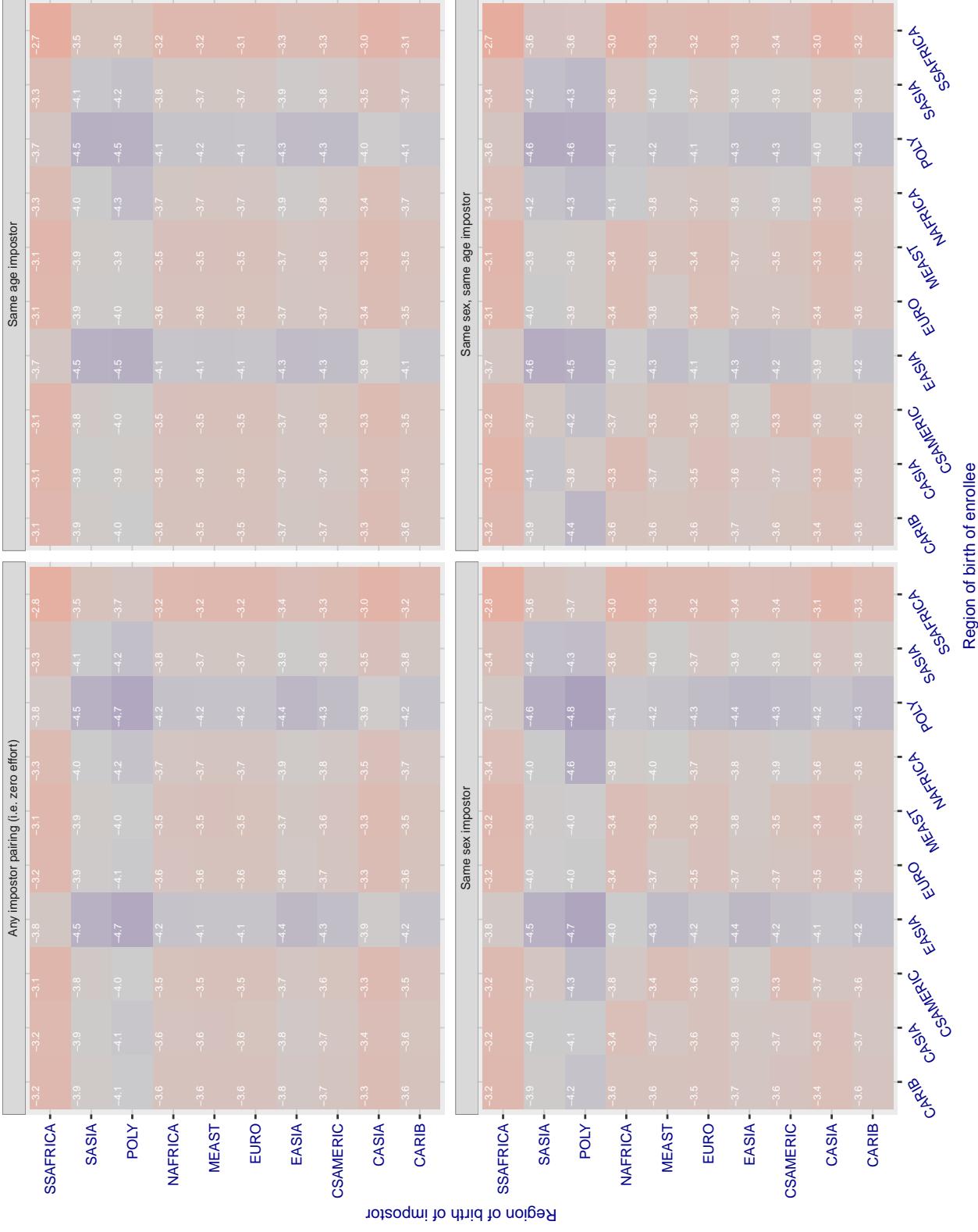


Figure 169: For algorithm nodeflux-001 operating on visa images, the heatmap shows false match rates observed over impostor comparisons of faces from different individuals who were born in the given region pair. False matches are counted against a recognition threshold fixed globally to give the target FMR in the plot title, computed over all on the order of  $10^{10}$  impostor comparisons. If text appears in each box it give the same quantity as that coded by the color. Grey indicates FMR is at the intended FMR target level. Light red colors present a security vulnerability to, for example, a passport gate. Each +1 increase in  $\log_{10} FMR$  corresponds to a factor of 10 increase in FMR. The matrix is not quite symmetric because images in the enrollment and verification sets are different.

### Cross region FMR at threshold T = 1.487 for algorithm ntechlab\_005, giving FMR(T) = 0.0001 globally.

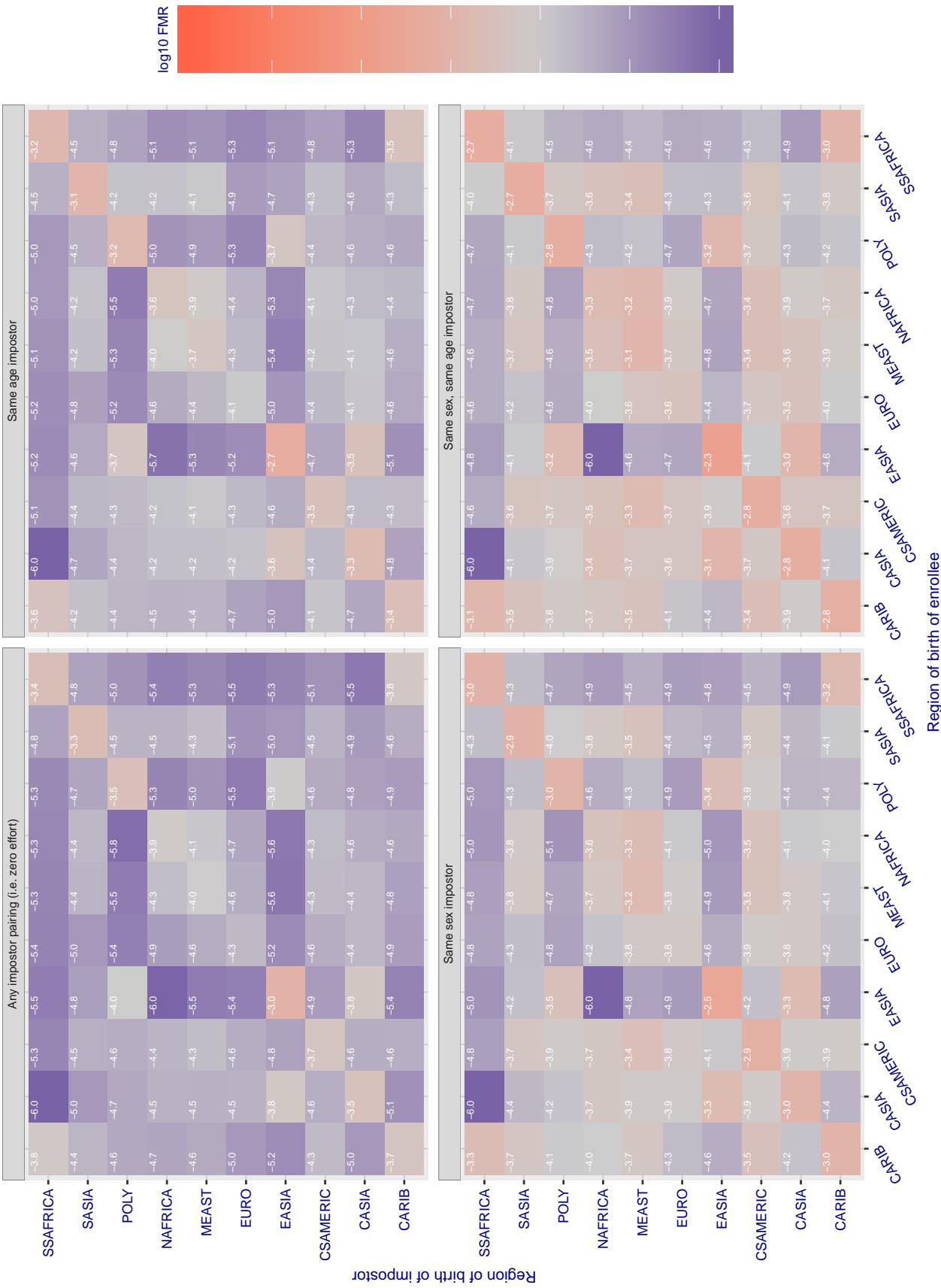


Figure 170: For algorithm ntechlab-005 operating on visa images, the heatmap shows false match rates observed over impostor comparisons of faces from different individuals who were born in the given region pair. False matches are counted against a recognition threshold fixed globally to give the target FMR in the plot title, computed over all on the order of  $10^{10}$  impostor comparisons. If text appears in each box it give the same quantity as that coded by the color. Grey indicates FMR is at the intended FMR target level. Light red colors present a security vulnerability to, for example, a passport gate. Each +1 increase in  $\log_{10} FMR$  corresponds to a factor of 10 increase in FMR. The matrix is not quite symmetric because images in the enrollment and verification sets are different.

### Cross region FMR at threshold T = 1.997 for algorithm ntechlab\_006, giving FMR(T) = 0.0001 globally.

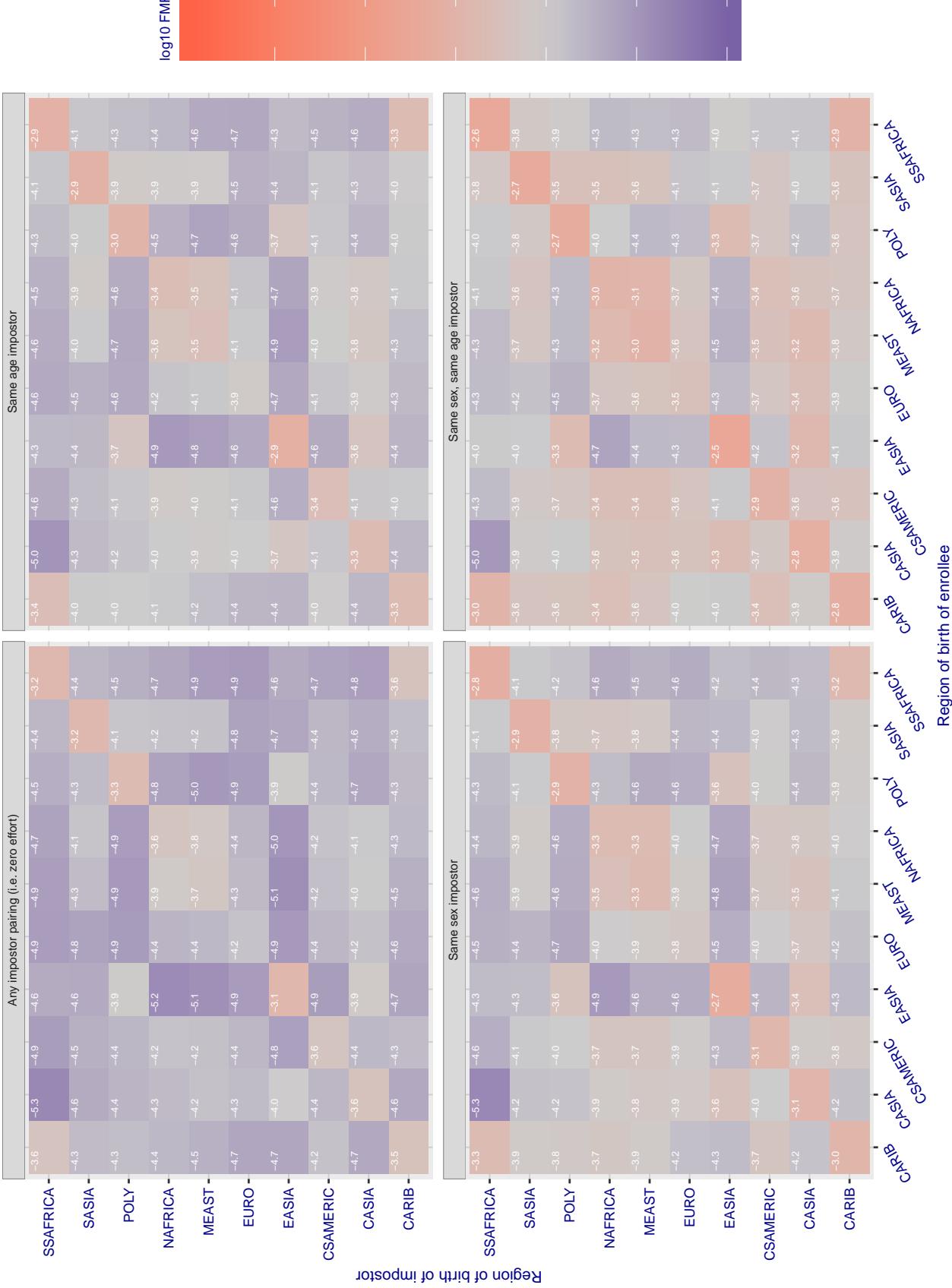


Figure 171: For algorithm ntechlab-006 operating on visa images, the heatmap shows false match rates observed over impostor comparisons of faces from different individuals who were born in the given region pair. False matches are counted against a recognition threshold fixed globally to give the target FMR in the plot title, computed over all on the order of  $10^{10}$  impostor comparisons. If text appears in each box it give the same quantity as that coded by the color. Grey indicates FMR is at the intended FMR target level. Light red colors present a security vulnerability to, for example, a passport gate. Each +1 increase in  $\log_{10} FMR$  corresponds to a factor of 10 increase in FMR. The matrix is not quite symmetric because images in the enrollment and verification sets are different.

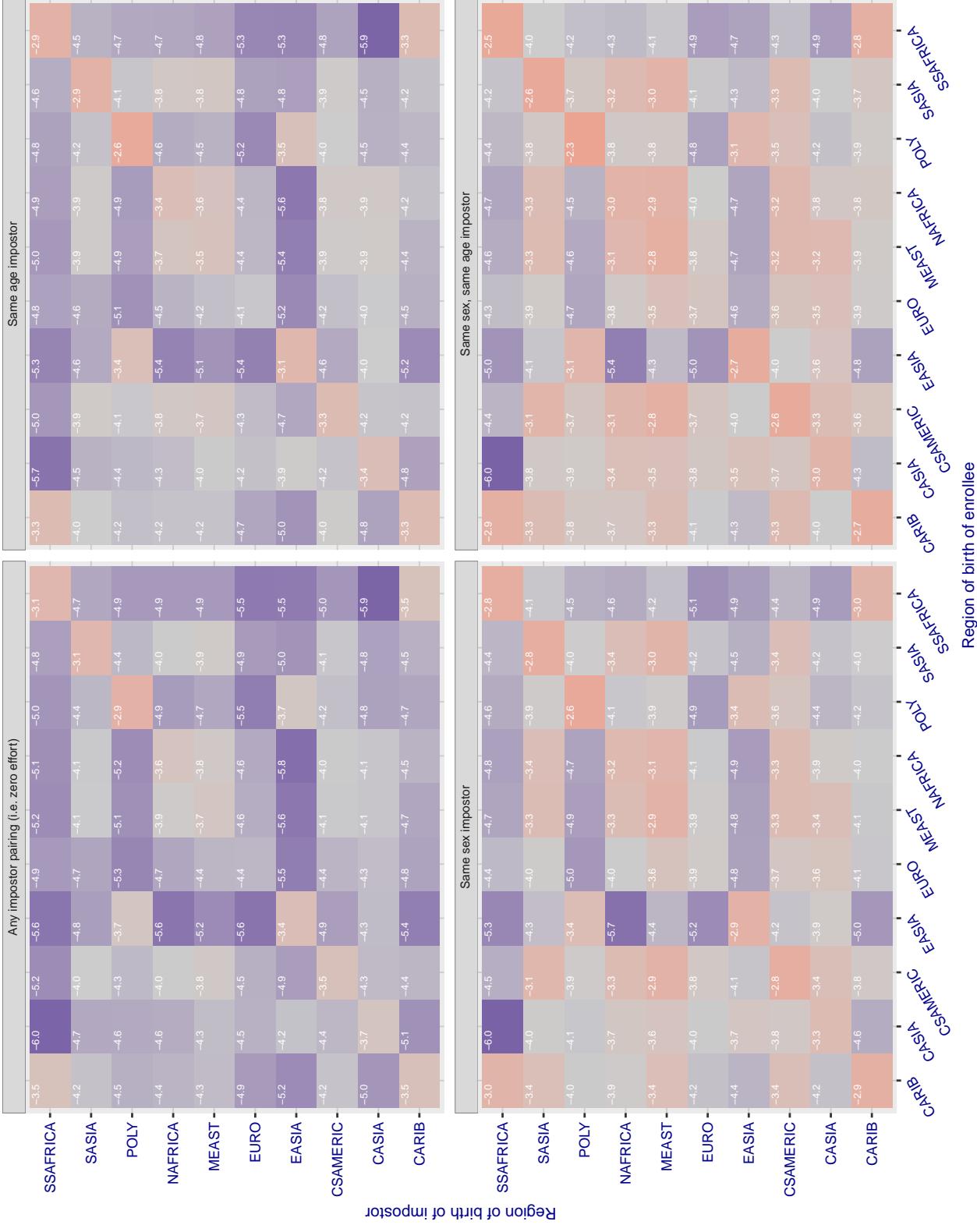
**Cross region FMR at threshold T = 0.337 for algorithm psl\_001, giving FMR(T) = 0.0001 globally.**

Figure 172: For algorithm psl-001 operating on visa images, the heatmap shows false match rates observed over impostor comparisons of faces from different individuals who were born in the given region pair. False matches are counted against a recognition threshold fixed globally to give the target FMR in the plot title, computed over all on the order of  $10^{10}$  impostor comparisons. If text appears in each box it give the same quantity as that coded by the color. Grey indicates FMR is at the intended FMR target level. Light red colors present a security vulnerability to, for example, a passport gate. Each +1 increase in  $\log_{10} \text{FMR}$  corresponds to a factor of 10 increase in FMR. The matrix is not quite symmetric because images in the enrollment and verification sets are different.

### Cross region FMR at threshold T = 0.353 for algorithm psl\_002, giving FMR(T) = 0.0001 globally.

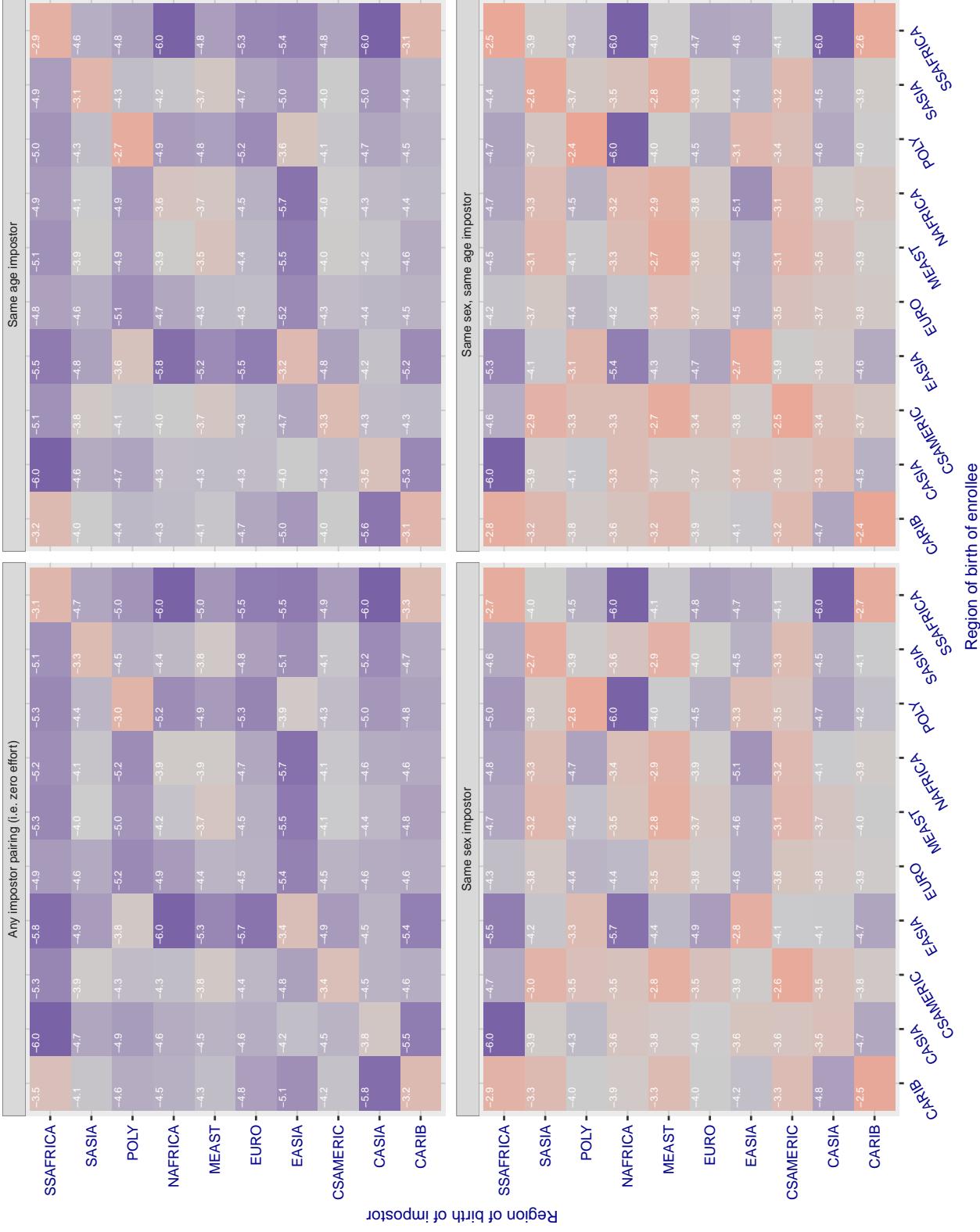


Figure 173: For algorithm psl-002 operating on visa images, the heatmap shows false match rates observed over impostor comparisons of faces from different individuals who were born in the given region pair. False matches are counted against a recognition threshold fixed globally to give the target FMR in the plot title, computed over all on the order of  $10^{10}$  impostor comparisons. If text appears in each box it give the same quantity as that coded by the color. Grey indicates FMR is at the intended FMR target level. Light red colors present a security vulnerability to, for example, a passport gate. Each +1 increase in  $\log 10$  FMR corresponds to a factor of 10 increase in FMR. The matrix is not quite symmetric because images in the enrollment and verification sets are different.

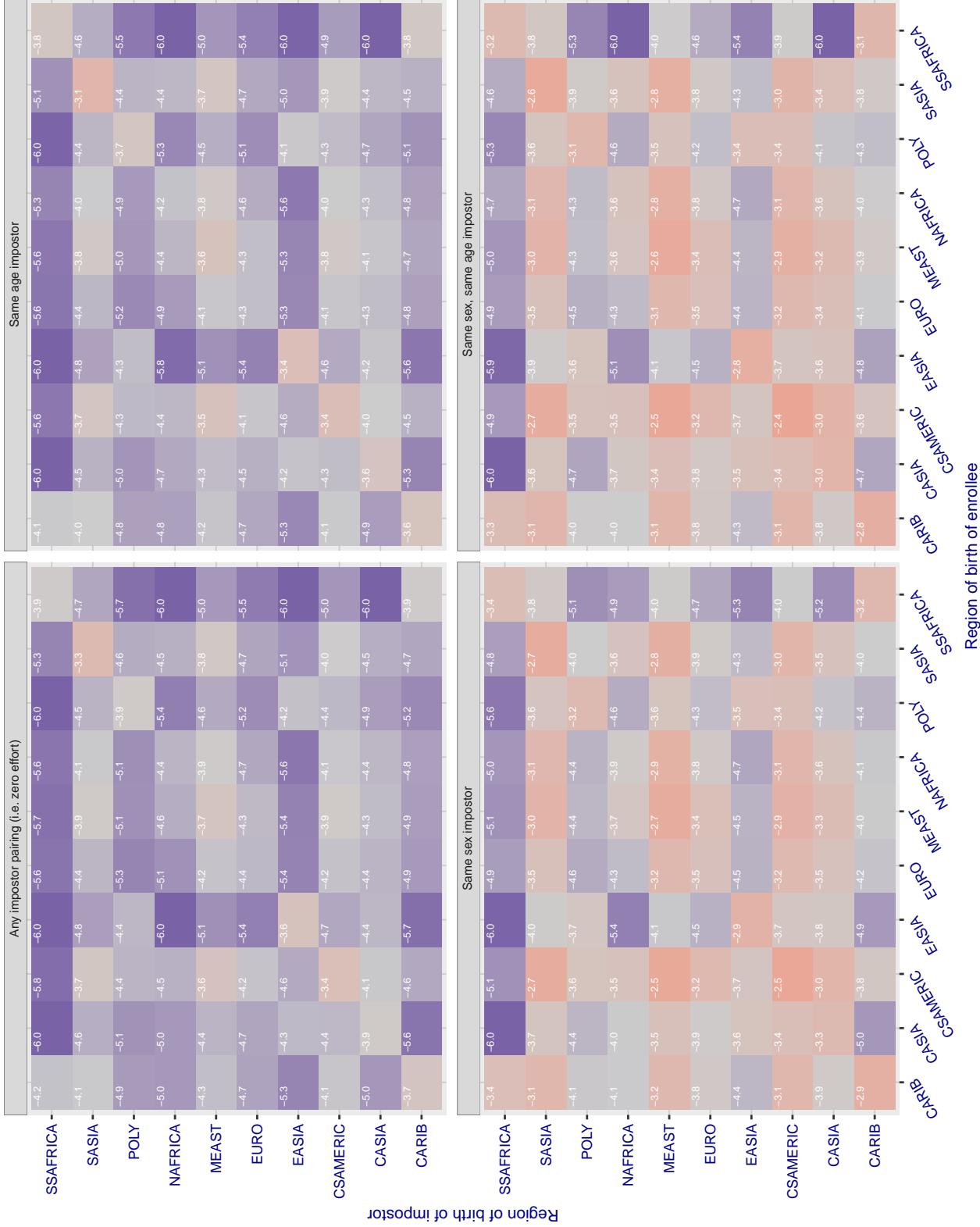
**Cross region FMR at threshold T = 0.779 for algorithm rankone\_006, giving FMR(T) = 0.0001 globally.**

Figure 174: For algorithm rankone-006 operating on visa images, the heatmap shows false match rates observed over impostor comparisons of faces from different individuals who were born in the given region pair. False matches are counted against a recognition threshold fixed globally to give the target FMR in the plot title, computed over all on the order of  $10^{10}$  impostor comparisons. If text appears in each box it give the same quantity as that coded by the color. Grey indicates FMR is at the intended FMR target level. Light red colors present a security vulnerability to, for example, a passport gate. Each +1 increase in  $\log_{10} \text{FMR}$  corresponds to a factor of 10 increase in FMR. The matrix is not quite symmetric because images in the enrollment and verification sets are different.

### Cross region FMR at threshold T = 0.885 for algorithm realnetworks\_001, giving FMR(T) = 0.00001 globally.

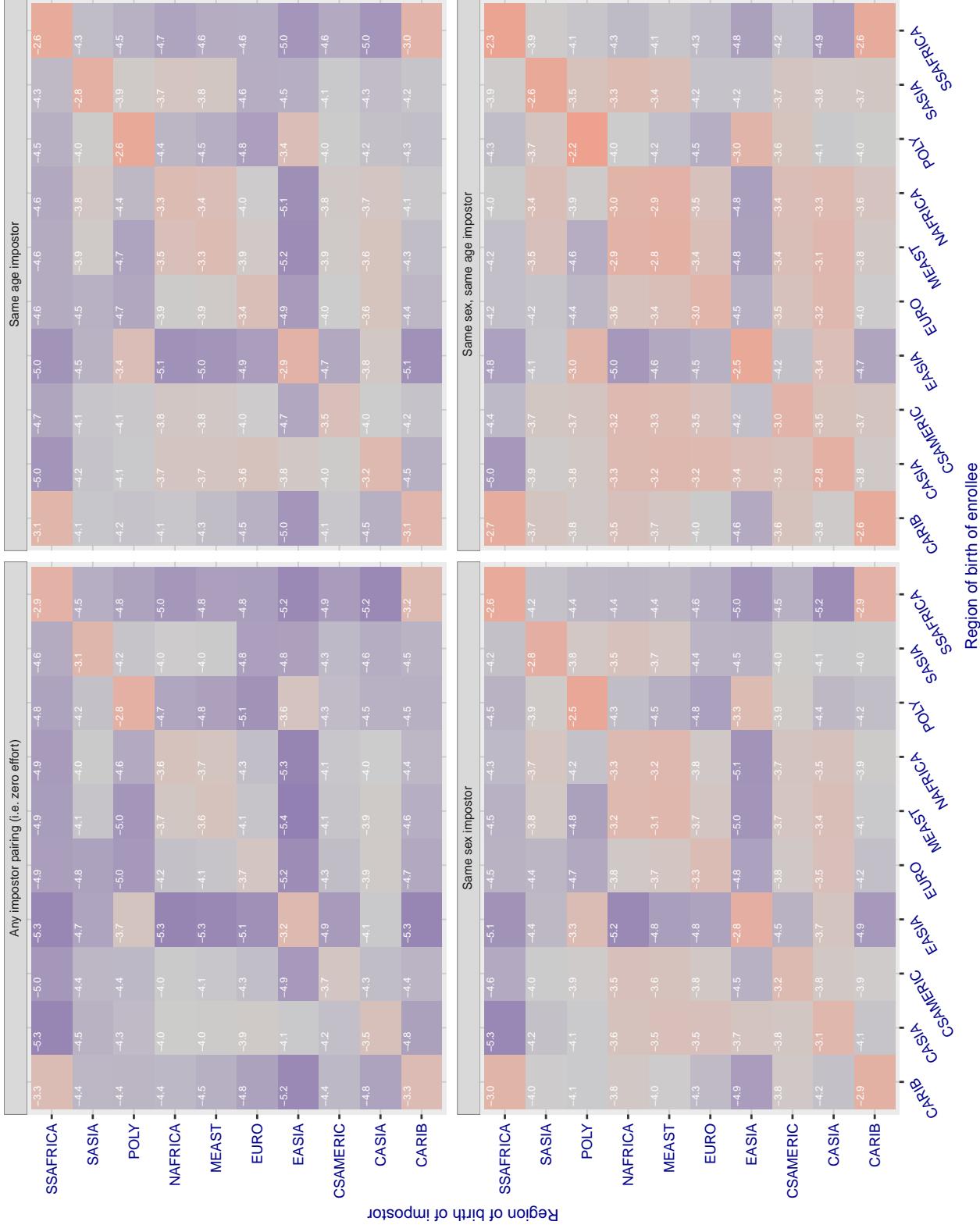


Figure 175: For algorithm realnetworks-001 operating on visa images, the heatmap shows false match rates observed over impostor comparisons of faces from different individuals who were born in the given region pair. False matches are counted against a recognition threshold fixed globally to give the target FMR in the plot title, computed over all on the order of  $10^{10}$  impostor comparisons. If text appears in each box it give the same quantity as that coded by the color. Grey indicates FMR is at the intended FMR target level. Light red colors present a security vulnerability to, for example, a passport gate. Each +1 increase in  $\log_{10} FMR$  corresponds to a factor of 10 increase in FMR. The matrix is not quite symmetric because images in the enrollment and verification sets are different.

### Cross region FMR at threshold T = 0.8883 for algorithm realnetworks\_002, giving FMR(T) = 0.00001 globally.

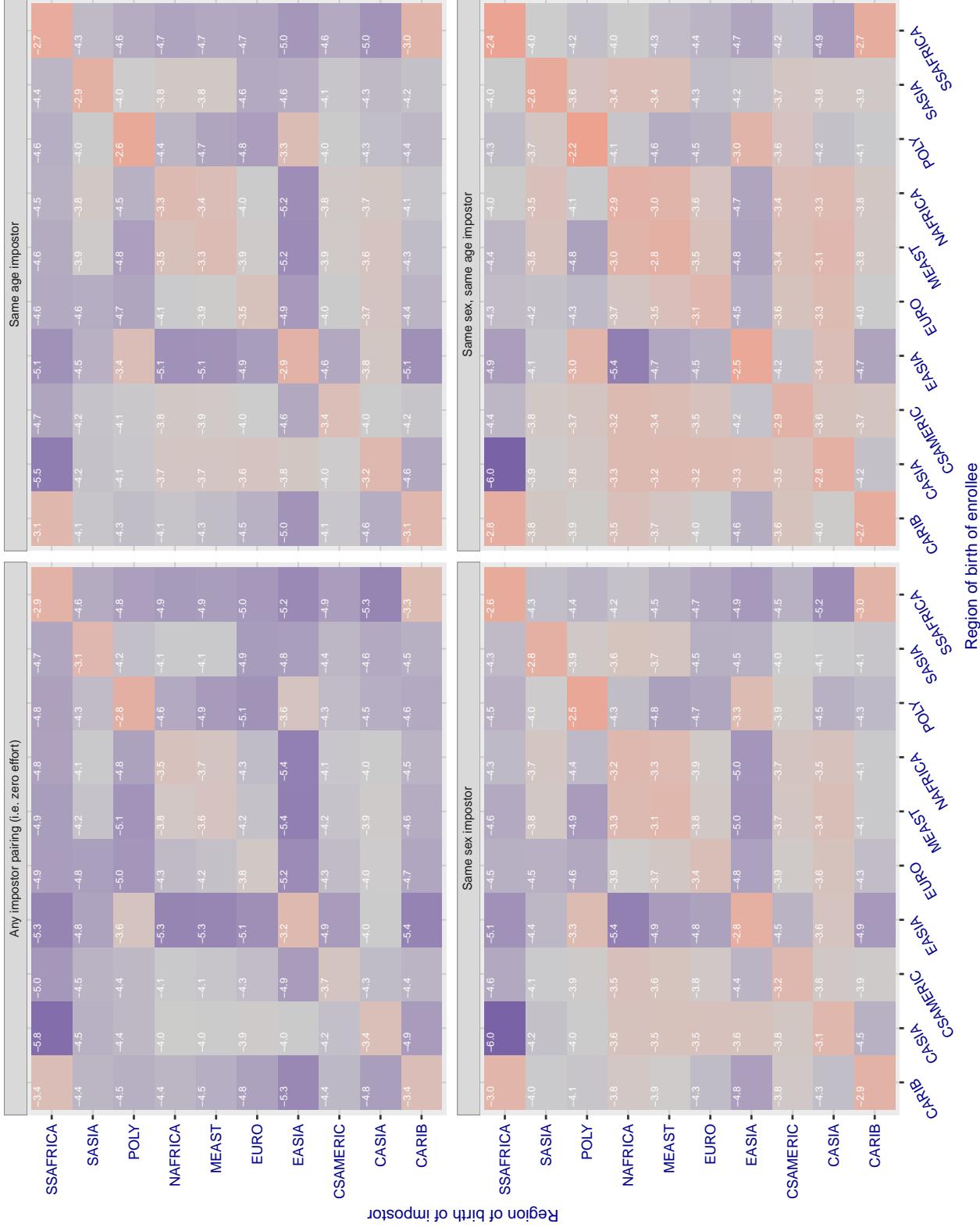


Figure 176: For algorithm realnetworks-002 operating on visa images, the heatmap shows false match rates observed over impostor comparisons of faces from different individuals who were born in the given region pair. False matches are counted against a recognition threshold fixed globally to give the target FMR in the plot title, computed over all on the order of  $10^{10}$  impostor comparisons. If text appears in each box it give the same quantity as that coded by the color. Grey indicates FMR is at the intended FMR target level. Light red colors present a security vulnerability to, for example, a passport gate. Each +1 increase in  $\log_{10} \text{FMR}$  corresponds to a factor of 10 increase in FMR. The matrix is not quite symmetric because images in the enrollment and verification sets are different.

### Cross region FMR at threshold T = 70.373 for algorithm remarkai\_000, giving FMR(T) = 0.0001 globally.

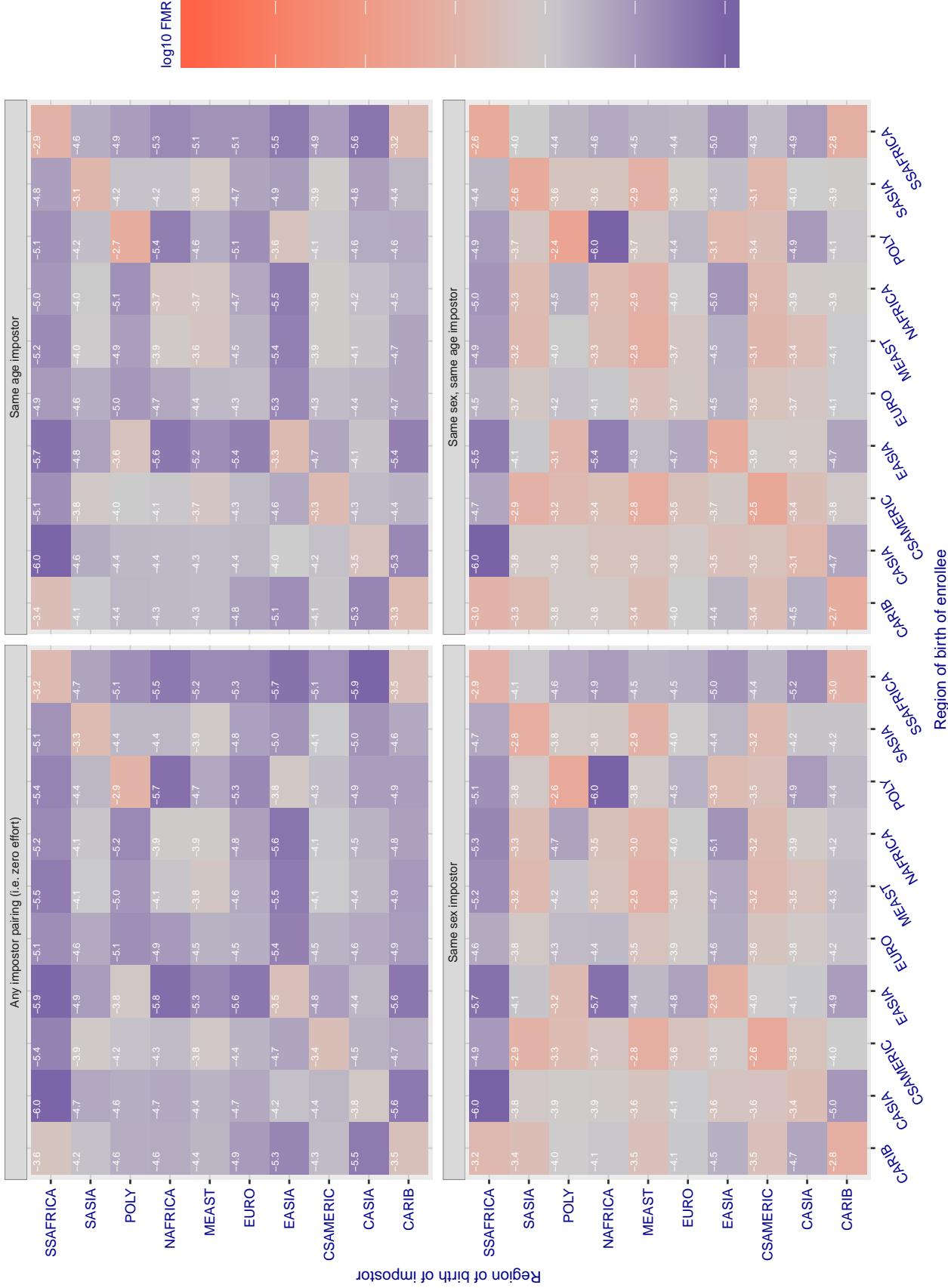


Figure 177: For algorithm remarkai-000 operating on visa images, the heatmap shows false match rates observed over impostor comparisons of faces from different individuals who were born in the given region pair. False matches are counted against a recognition threshold fixed globally to give the target FMR in the plot title, computed over all on the order of  $10^{10}$  impostor comparisons. If text appears in each box it give the same quantity as that coded by the color. Grey indicates FMR is at the intended FMR target level. Light red colors present a security vulnerability to, for example, a passport gate. Each +1 increase in  $\log_{10} \text{FMR}$  corresponds to a factor of 10 increase in FMR. The matrix is not quite symmetric because images in the enrollment and verification sets are different.

### Cross region FMR at threshold T = 70.384 for algorithm remarkai\_001, giving $FMR(T) = 0.0001$ globally.

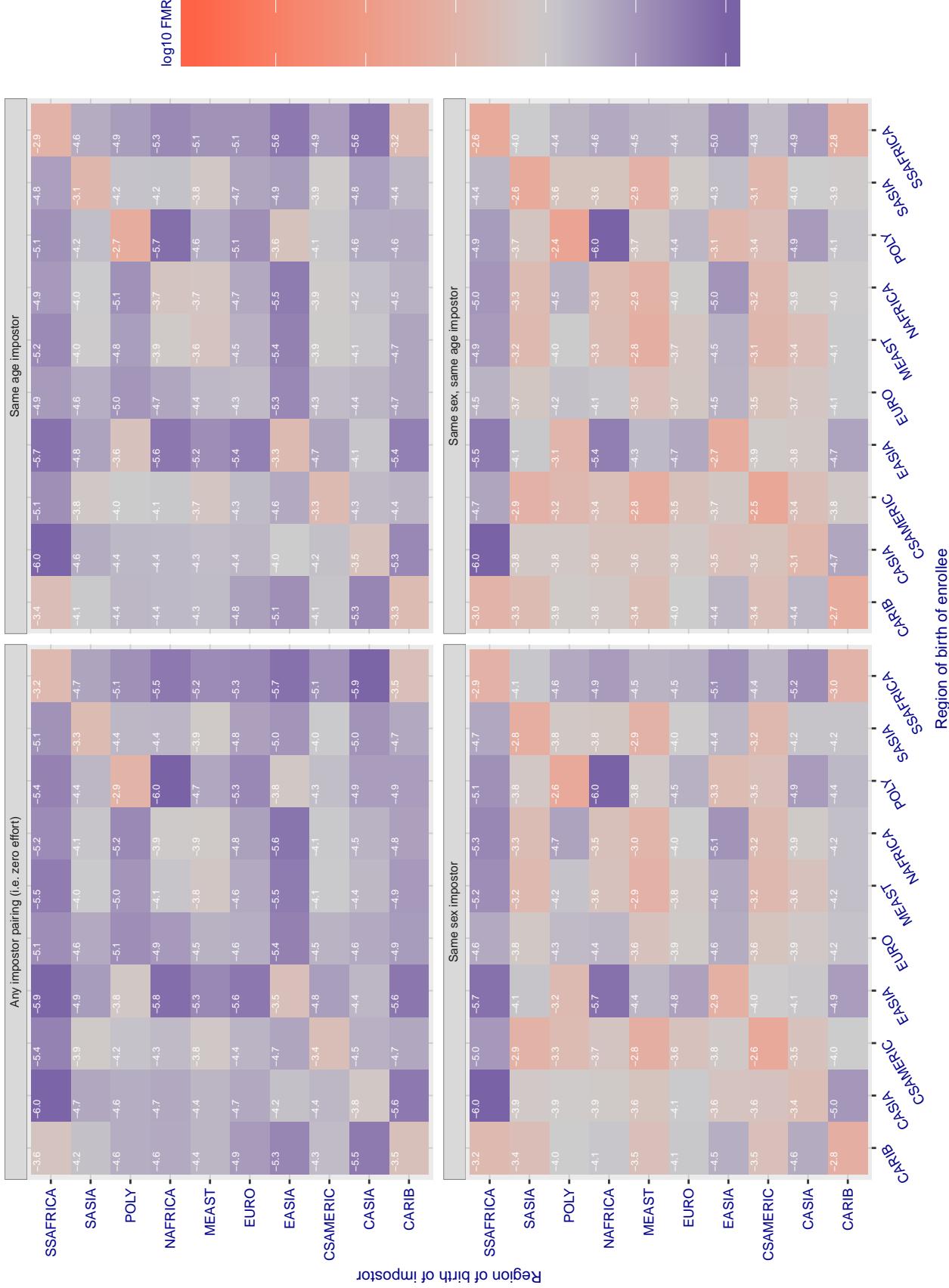


Figure 178: For algorithm remarkai-001 operating on visa images, the heatmap shows false match rates observed over impostor comparisons of faces from different individuals who were born in the given region pair. False matches are counted against a recognition threshold fixed globally to give the target FMR in the plot title, computed over all on the order of  $10^{10}$  impostor comparisons. If text appears in each box it give the same quantity as that coded by the color. Grey indicates FMR is at the intended FMR target level. Light red colors present a security vulnerability to, for example, a passport gate. Each +1 increase in  $\log_{10} FMR$  corresponds to a factor of 10 increase in FMR. The matrix is not quite symmetric because images in the enrollment and verification sets are different.

### Cross region FMR at threshold T = 0.682 for algorithm saffe\_001, giving FMR(T) = 0.0001 globally.

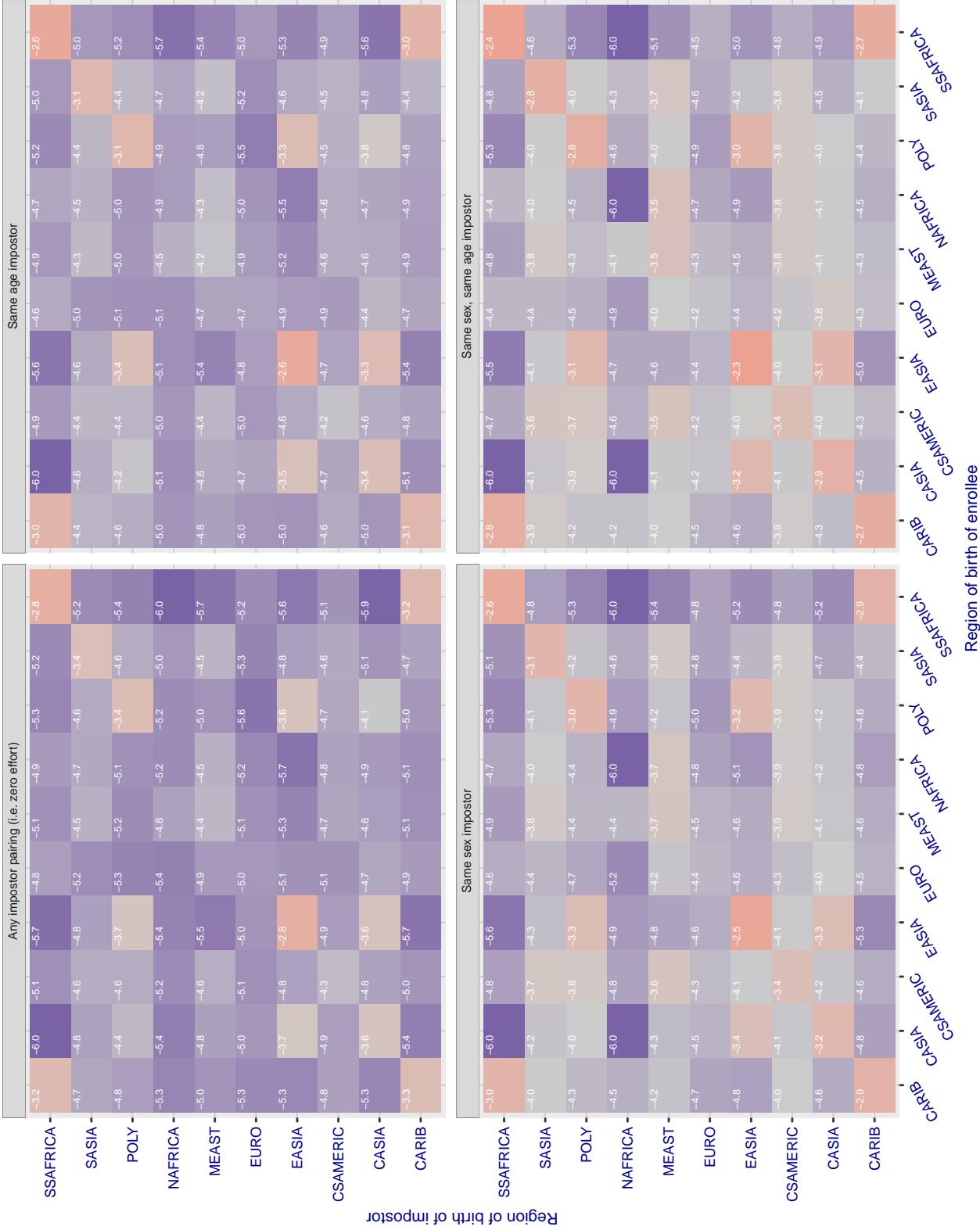


Figure 179: For algorithm saffe-001 operating on visa images, the heatmap shows false match rates observed over impostor comparisons of faces from different individuals who were born in the given region pair. False matches are counted against a recognition threshold fixed globally to give the target FMR in the plot title, computed over all on the order of  $10^{10}$  impostor comparisons. If text appears in each box it give the same quantity as that coded by the color. Grey indicates FMR is at the intended FMR target level. Light red colors present a security vulnerability to, for example, a passport gate. Each +1 increase in  $\log_{10}$  FMR corresponds to a factor of 10 increase in FMR. The matrix is not quite symmetric because images in the enrollment and verification sets are different.

**Cross region FMR** at threshold  $T = 0.383$  for algorithm *saffe\_002*, giving  $FMR(T) = 0.0001$  globally.

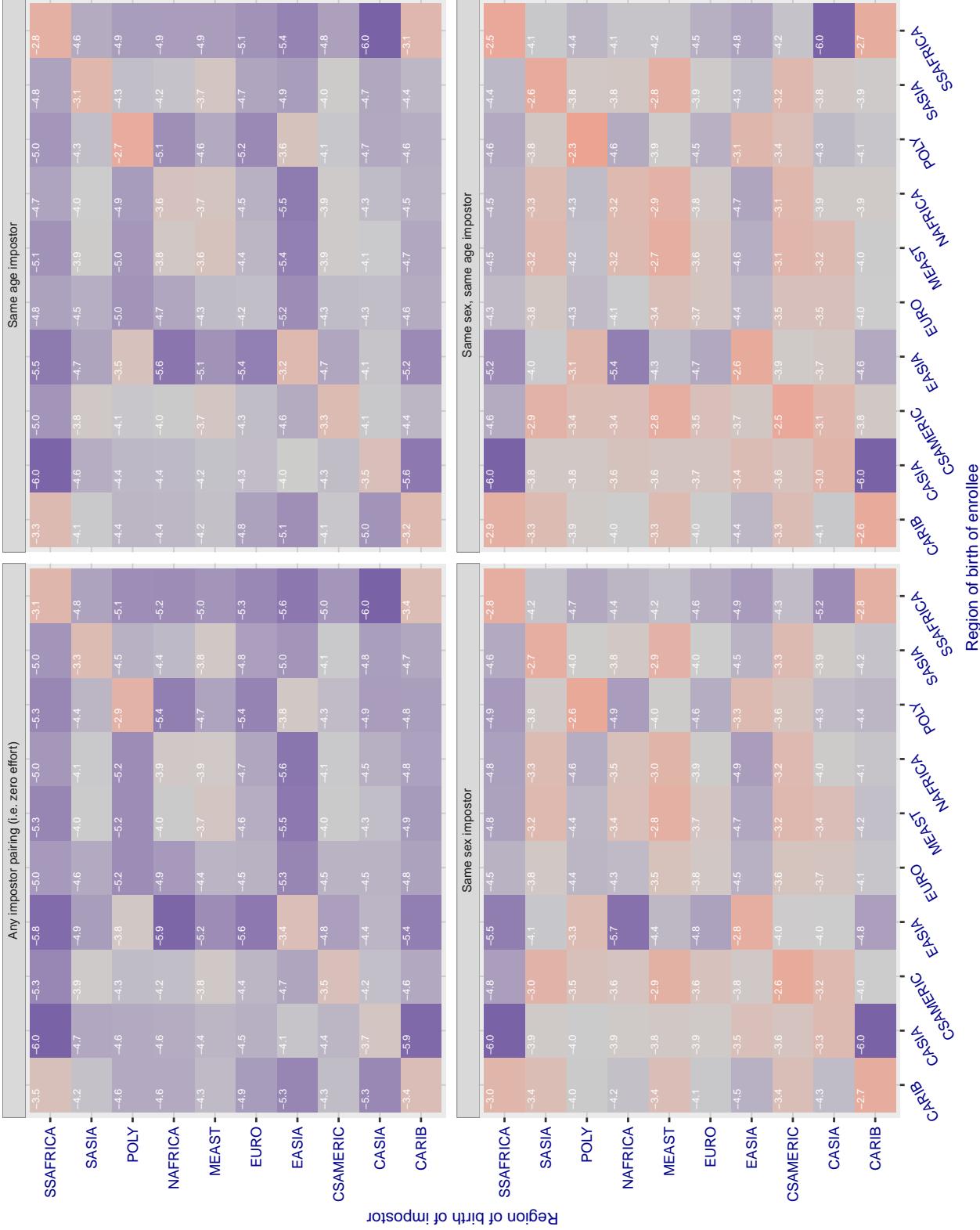


Figure 180: For algorithm saffe-002 operating on visa images, the heatmap shows false match rates observed over impostor comparisons of faces from different individuals who were born in the given region pair. False matches are counted against a recognition threshold fixed globally to give the target FMR in the plot title, computed over all on the order of  $10^{10}$  impostor comparisons. If text appears in each box it give the same quantity as that coded by the color. Grey indicates FMR is at the intended FMR target level. Light red colors present a security vulnerability to, for example, a passport gate. Each +1 increase in  $\log_{10} FMR$  corresponds to a factor of 10 increase in FMR. The matrix is not quite symmetric because images in the enrollment and verification sets are different.

### Cross region FMR at threshold T = 0.390 for algorithm sensetime\_001, giving FMR(T) = 0.0001 globally.

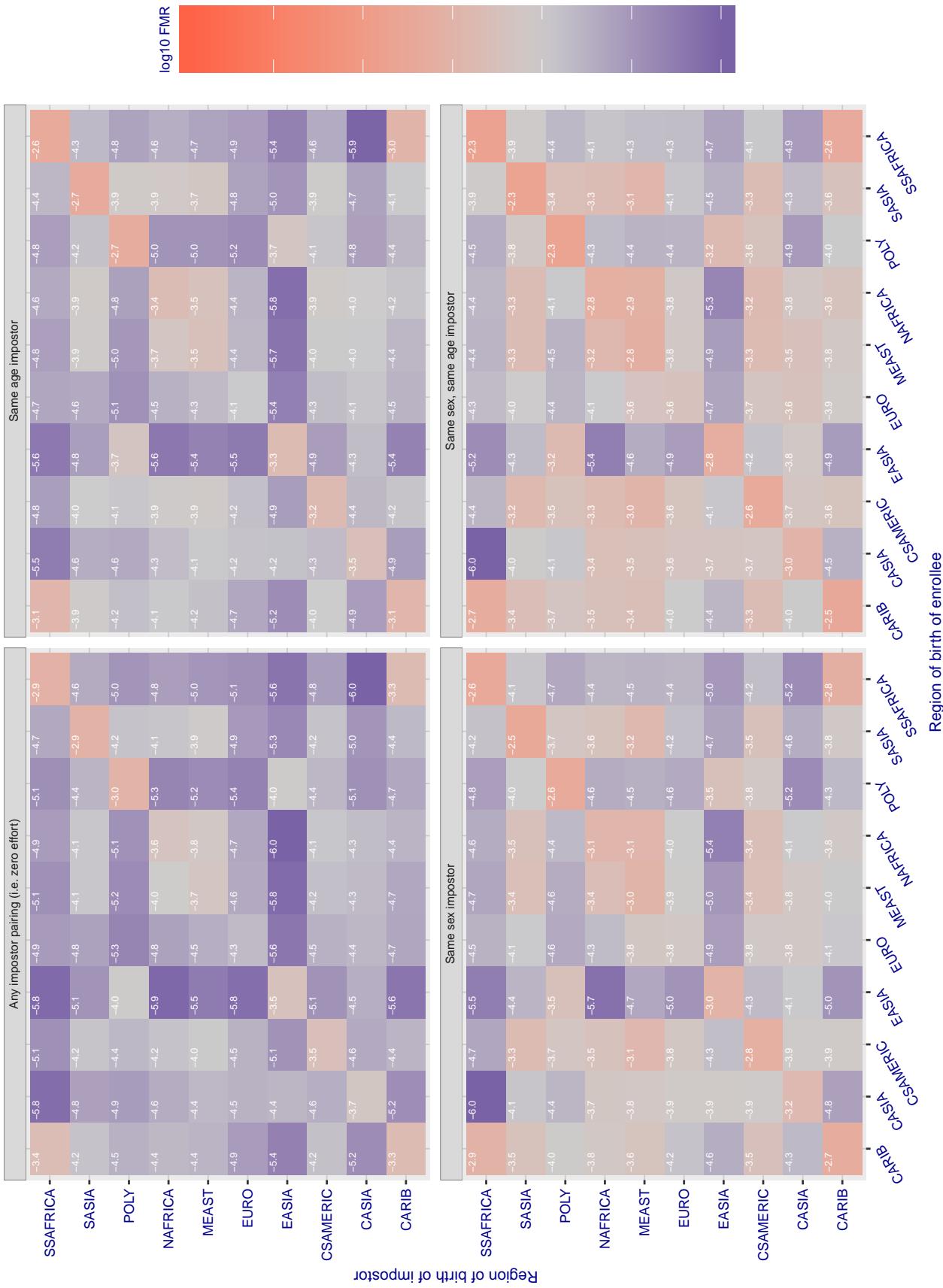


Figure 181: For algorithm sensetime-001 operating on visa images, the heatmap shows false match rates observed over impostor comparisons of faces from different individuals who were born in the given region pair. False matches are counted against a recognition threshold fixed globally to give the target FMR in the plot title, computed over all on the order of  $10^{10}$  impostor comparisons. If text appears in each box it give the same quantity as that coded by the color. Grey indicates FMR is at the intended FMR target level. Light red colors present a security vulnerability to, for example, a passport gate. Each +1 increase in  $\log_{10} \text{FMR}$  corresponds to a factor of 10 increase in FMR. The matrix is not quite symmetric because images in the enrollment and verification sets are different.

### Cross region FMR at threshold T = 0.390 for algorithm sensetime\_002, giving FMR(T) = 0.0001 globally.

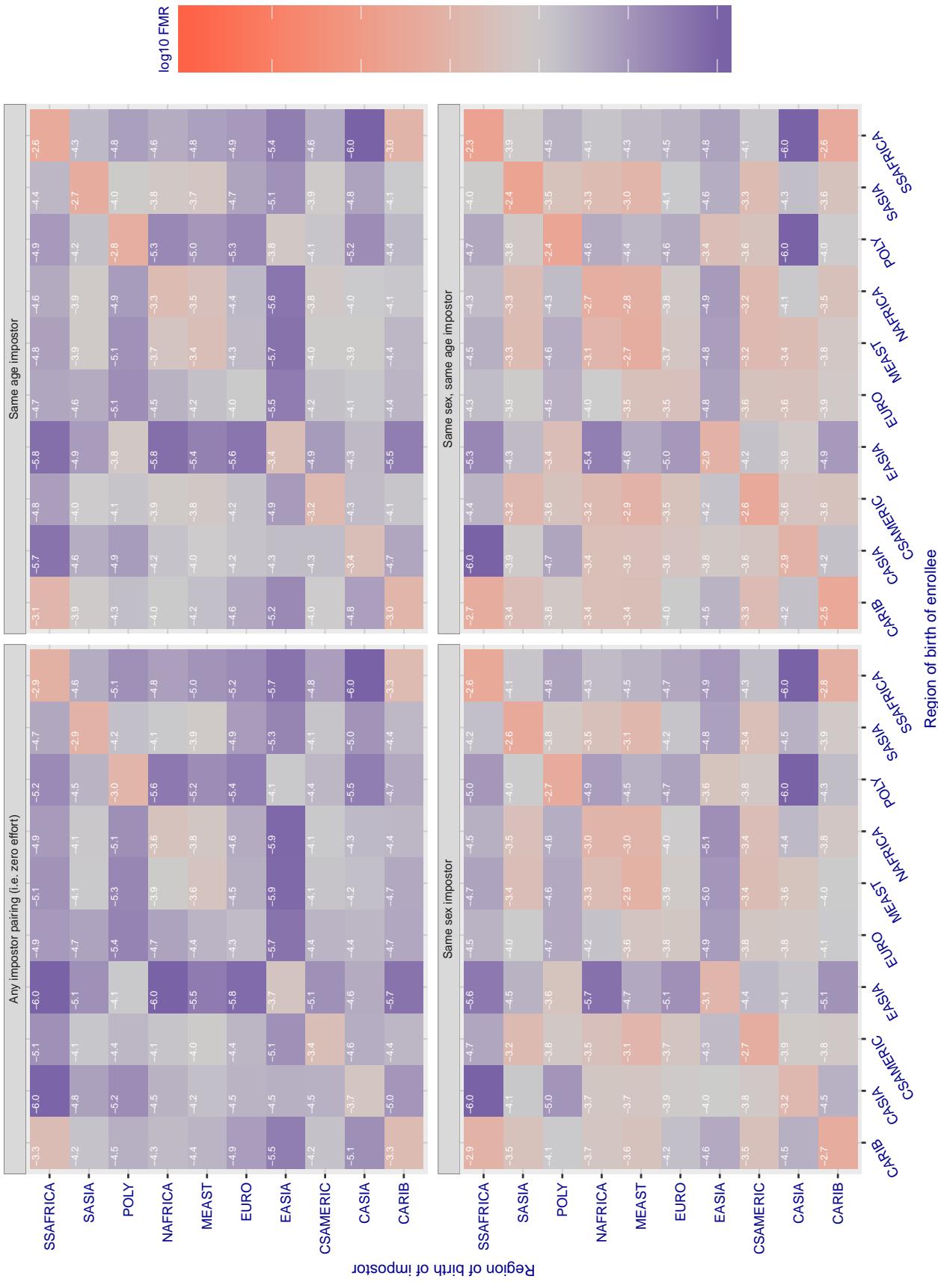


Figure 182: For algorithm sensetime-002 operating on visa images, the heatmap shows false match rates observed over impostor comparisons of faces from different individuals who were born in the given region pair. False matches are counted against a recognition threshold fixed globally to give the target FMR in the plot title, computed over all on the order of  $10^{10}$  impostor comparisons. If text appears in each box it give the same quantity as that coded by the color. Grey indicates FMR is at the intended FMR target level. Light red colors present a security vulnerability to, for example, a passport gate. Each +1 increase in  $\log_{10} \text{FMR}$  corresponds to a factor of 10 increase in FMR. The matrix is not quite symmetric because images in the enrollment and verification sets are different.

### Cross region FMR at threshold T = 0.970 for algorithm shaman\_000, giving FMR(T) = 0.0001 globally.

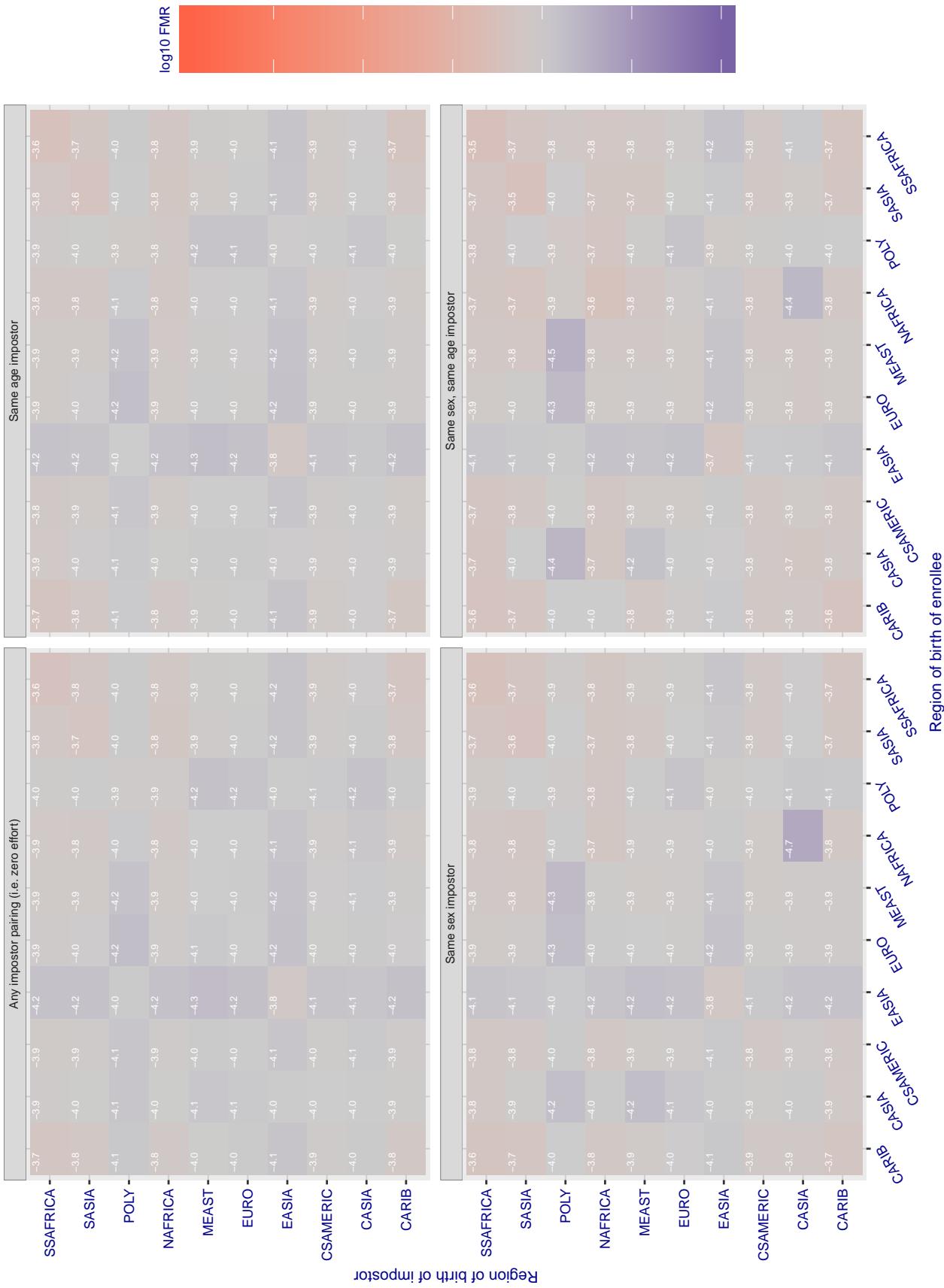


Figure 183: For algorithm shaman-000 operating on visa images, the heatmap shows false match rates observed over impostor comparisons of faces from different individuals who were born in the given region pair. False matches are counted against a recognition threshold fixed globally to give the target FMR in the plot title, computed over all on the order of  $10^{10}$  impostor comparisons. If text appears in each box it give the same quantity as that coded by the color. Grey indicates FMR is at the intended FMR target level. Light red colors present a security vulnerability to, for example, a passport gate. Each +1 increase in  $\log_{10} \text{FMR}$  corresponds to a factor of 10 increase in FMR. The matrix is not quite symmetric because images in the enrollment and verification sets are different.

### Cross region FMR at threshold T = 0.725 for algorithm shaman\_001, giving FMR(T) = 0.0001 globally.

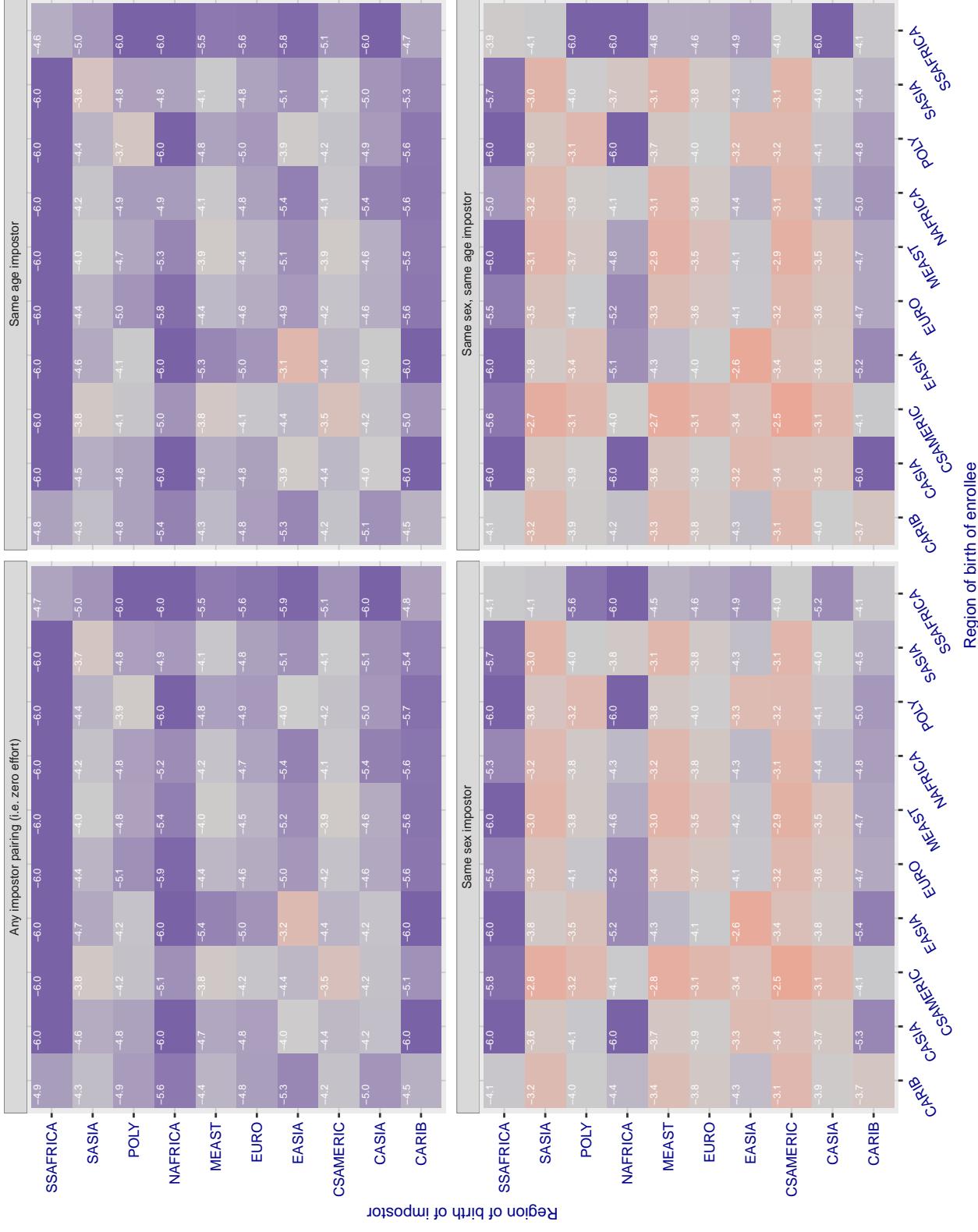


Figure 184: For algorithm shaman-001 operating on visa images, the heatmap shows false match rates observed over impostor comparisons of faces from different individuals who were born in the given region pair. False matches are counted against a recognition threshold fixed globally to give the target FMR in the plot title, computed over all on the order of  $10^{10}$  impostor comparisons. If text appears in each box it give the same quantity as that coded by the color. Grey indicates FMR is at the intended FMR target level. Light red colors present a security vulnerability to, for example, a passport gate. Each +1 increase in  $\log_{10} FMR$  corresponds to a factor of 10 increase in FMR. The matrix is not quite symmetric because images in the enrollment and verification sets are different.

### Cross region FMR at threshold T = 0.390 for algorithm siat\_002, giving FMR(T) = 0.0001 globally.

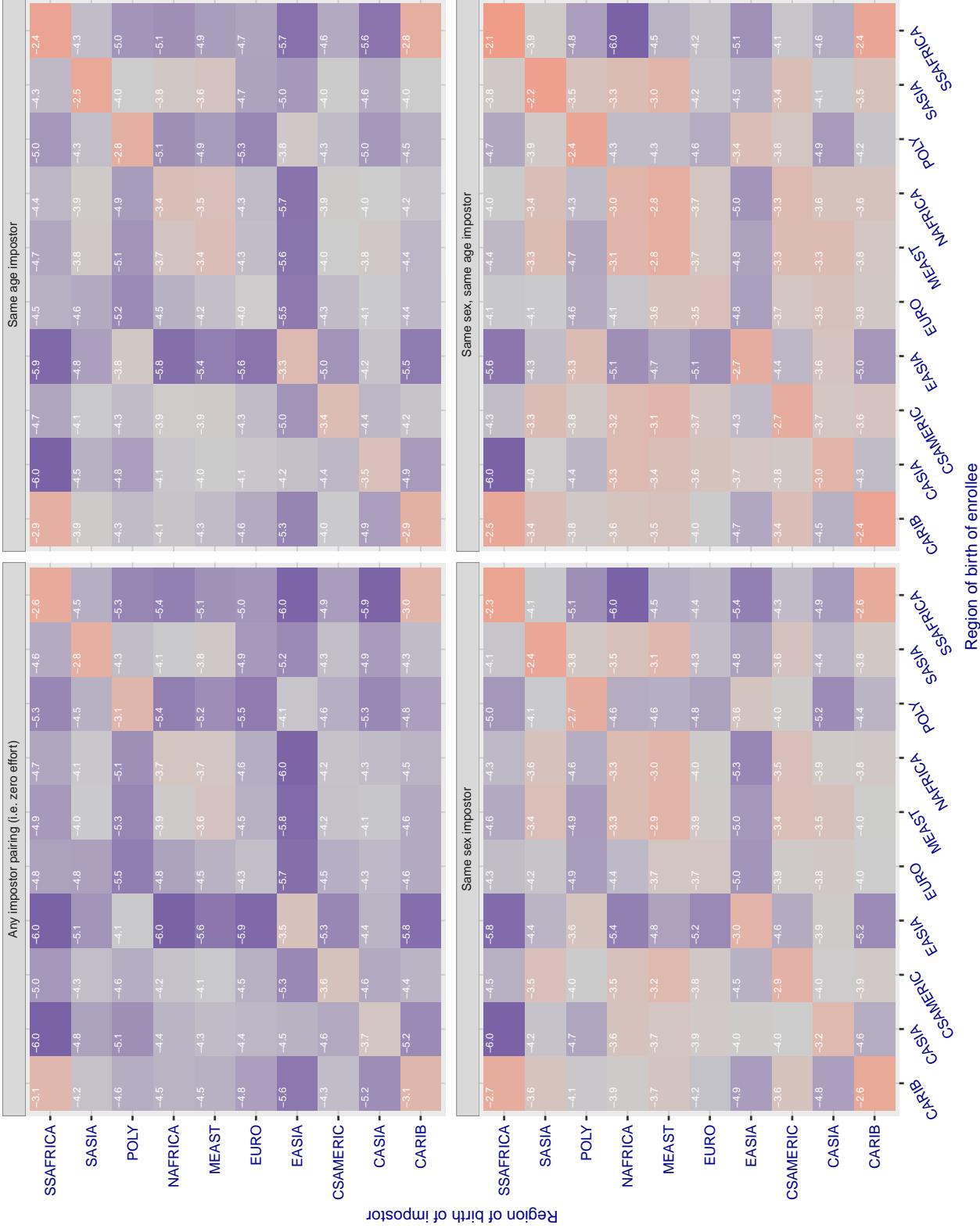


Figure 185: For algorithm siat-002 operating on visa images, the heatmap shows false match rates observed over impostor comparisons of faces from different individuals who were born in the given region pair. False matches are counted against a recognition threshold fixed globally to give the target FMR in the plot title, computed over all on the order of  $10^{10}$  impostor comparisons. If text appears in each box it give the same quantity as that coded by the color. Grey indicates FMR is at the intended FMR target level. Light red colors present a security vulnerability to, for example, a passport gate. Each +1 increase in  $\log_{10}$  FMR corresponds to a factor of 10 increase in FMR. The matrix is not quite symmetric because images in the enrollment and verification sets are different.

### Cross region FMR at threshold T = 0.393 for algorithm siat\_004, giving FMR(T) = 0.0001 globally.

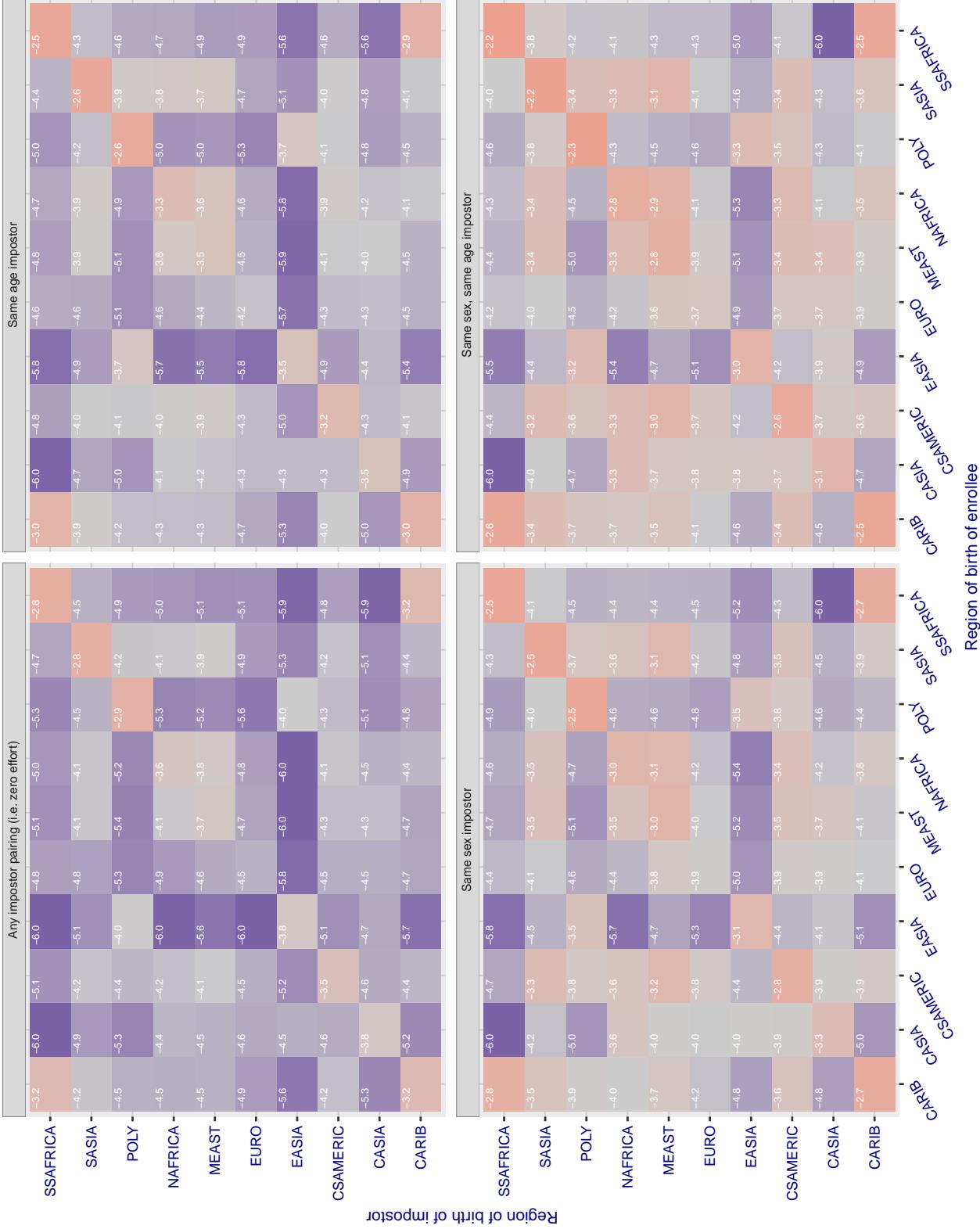


Figure 186: For algorithm siat-004 operating on visa images, the heatmap shows false match rates observed over impostor comparisons of faces from different individuals who were born in the given region pair. False matches are counted against a recognition threshold fixed globally to give the target FMR in the plot title, computed over all on the order of  $10^{10}$  impostor comparisons. If text appears in each box it give the same quantity as that coded by the color. Grey indicates FMR is at the intended FMR target level. Light red colors present a security vulnerability to, for example, a passport gate. Each +1 increase in  $\log 10$  FMR corresponds to a factor of 10 increase in FMR. The matrix is not quite symmetric because images in the enrollment and verification sets are different.

### Cross region FMR at threshold T = 0.598 for algorithm smilart\_002, giving $\text{FMR}(\text{T}) = 0.0001$ globally.

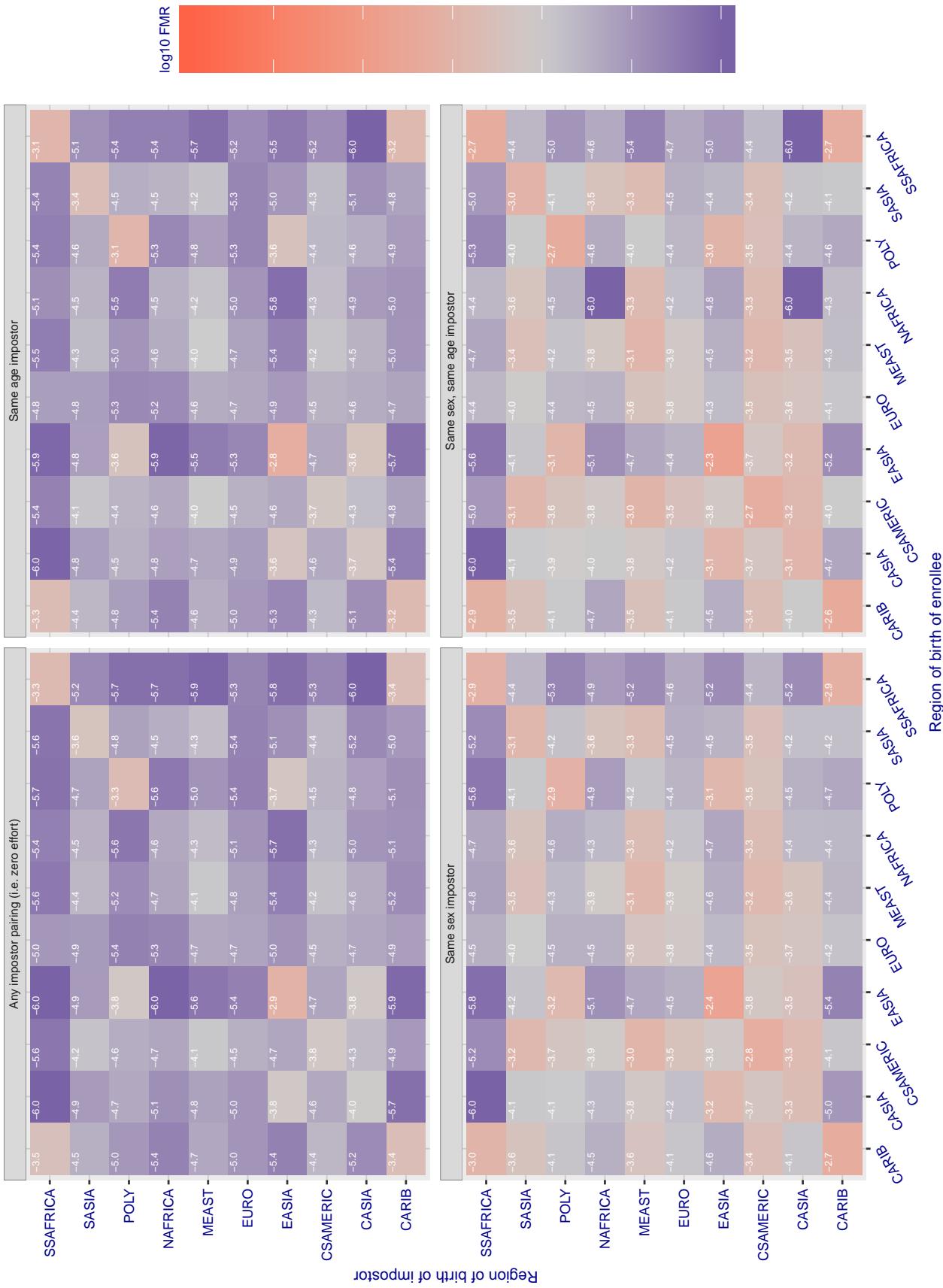


Figure 187: For algorithm smilart-002 operating on visa images, the heatmap shows false match rates observed over impostor comparisons of faces from different individuals who were born in the given region pair. False matches are counted against a recognition threshold fixed globally to give the target FMR in the plot title, computed over all on the order of  $10^{10}$  impostor comparisons. If text appears in each box it give the same quantity as that coded by the color. Grey indicates FMR is at the intended FMR target level. Light red colors present a security vulnerability to, for example, a passport gate. Each +1 increase in  $\log_{10} \text{FMR}$  corresponds to a factor of 10 increase in FMR. The matrix is not quite symmetric because images in the enrollment and verification sets are different.

### Cross region FMR at threshold T = 0.654 for algorithm smilart\_003, giving FMR(T) = 0.0001 globally.

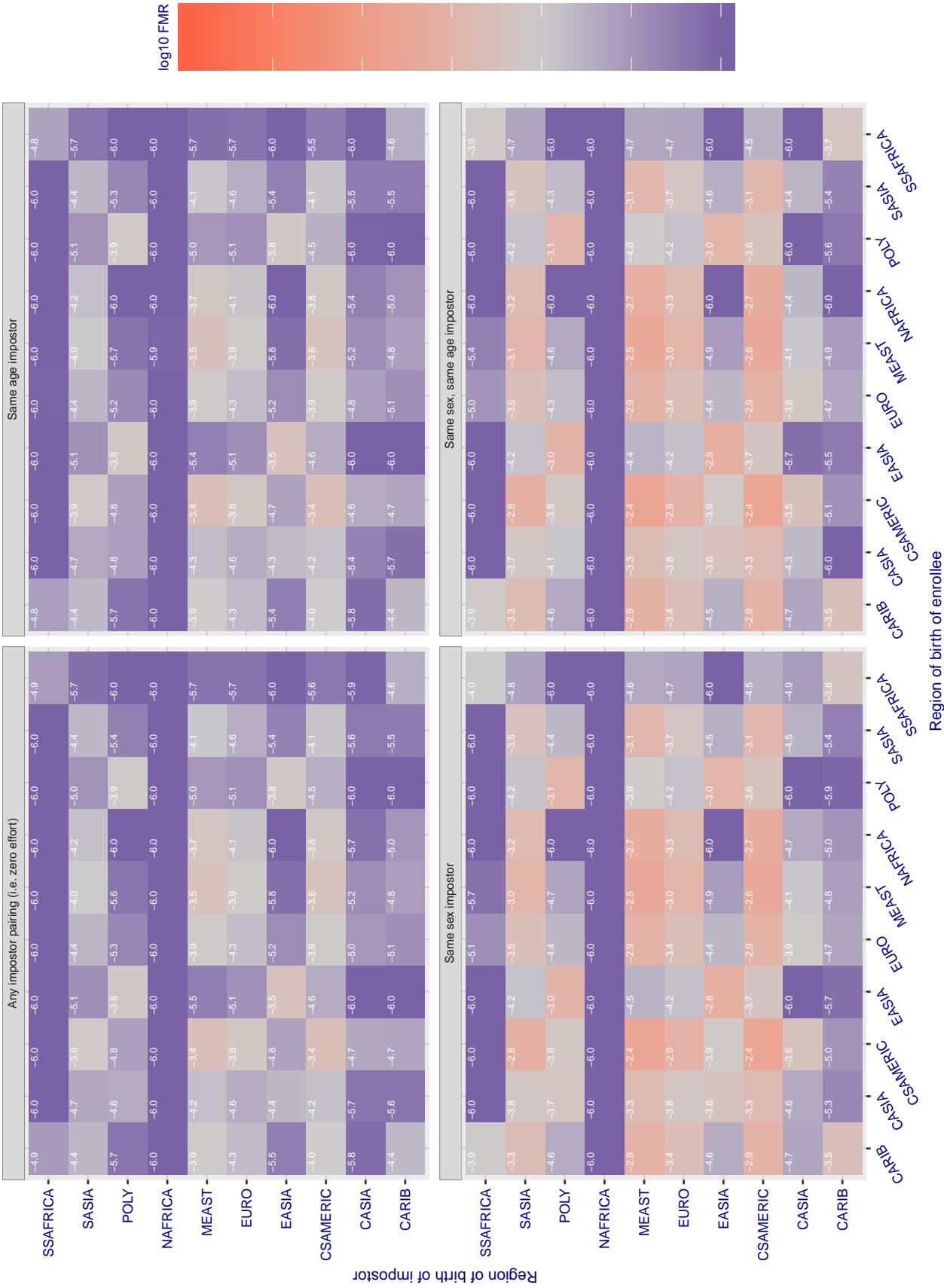


Figure 188: For algorithm smilart-003 operating on visa images, the heatmap shows false match rates observed over impostor comparisons of faces from different individuals who were born in the given region pair. False matches are counted against a recognition threshold fixed globally to give the target FMR in the plot title, computed over all on the order of  $10^{10}$  impostor comparisons. If text appears in each box it give the same quantity as that coded by the color. Grey indicates FMR is at the intended FMR target level. Light red colors present a security vulnerability to, for example, a passport gate. Each +1 increase in  $\log_{10} FMR$  corresponds to a factor of 10 increase in FMR. The matrix is not quite symmetric because images in the enrollment and verification sets are different.

### Cross region FMR at threshold T = 0.221 for algorithm **synesis\_004**, giving FMR(T) = 0.0001 globally.

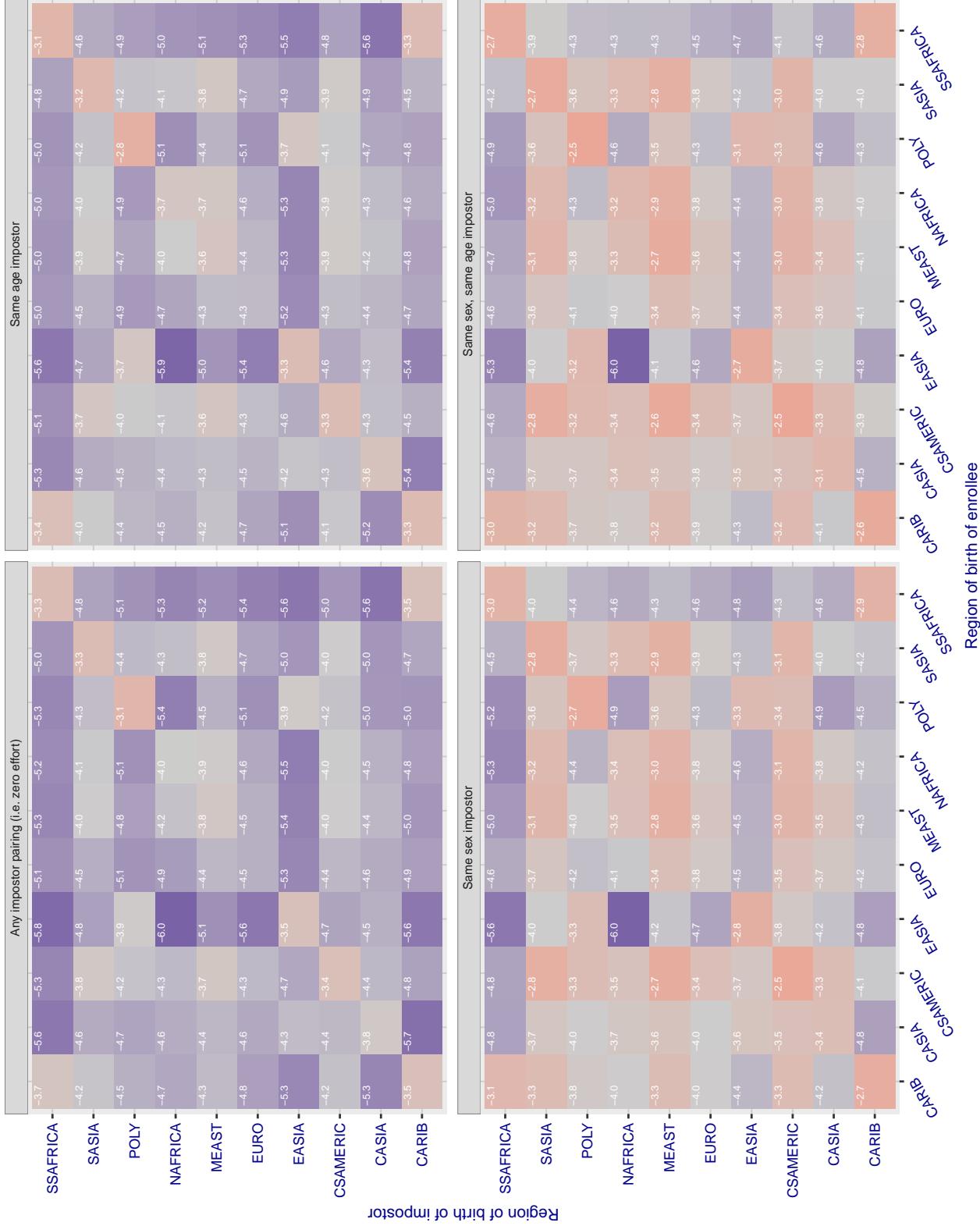


Figure 189: For algorithm **synesis-004** operating on visa images, the heatmap shows false match rates observed over impostor comparisons of faces from different individuals who were born in the given region pair. False matches are counted against a recognition threshold fixed globally to give the target FMR in the plot title, computed over all on the order of  $10^{10}$  impostor comparisons. If text appears in each box it give the same quantity as that coded by the color. Grey indicates FMR is at the intended FMR target level. Light red colors present a security vulnerability to, for example, a passport gate. Each +1 increase in  $\log_{10} FMR$  corresponds to a factor of 10 increase in FMR. The matrix is not quite symmetric because images in the enrollment and verification sets are different.

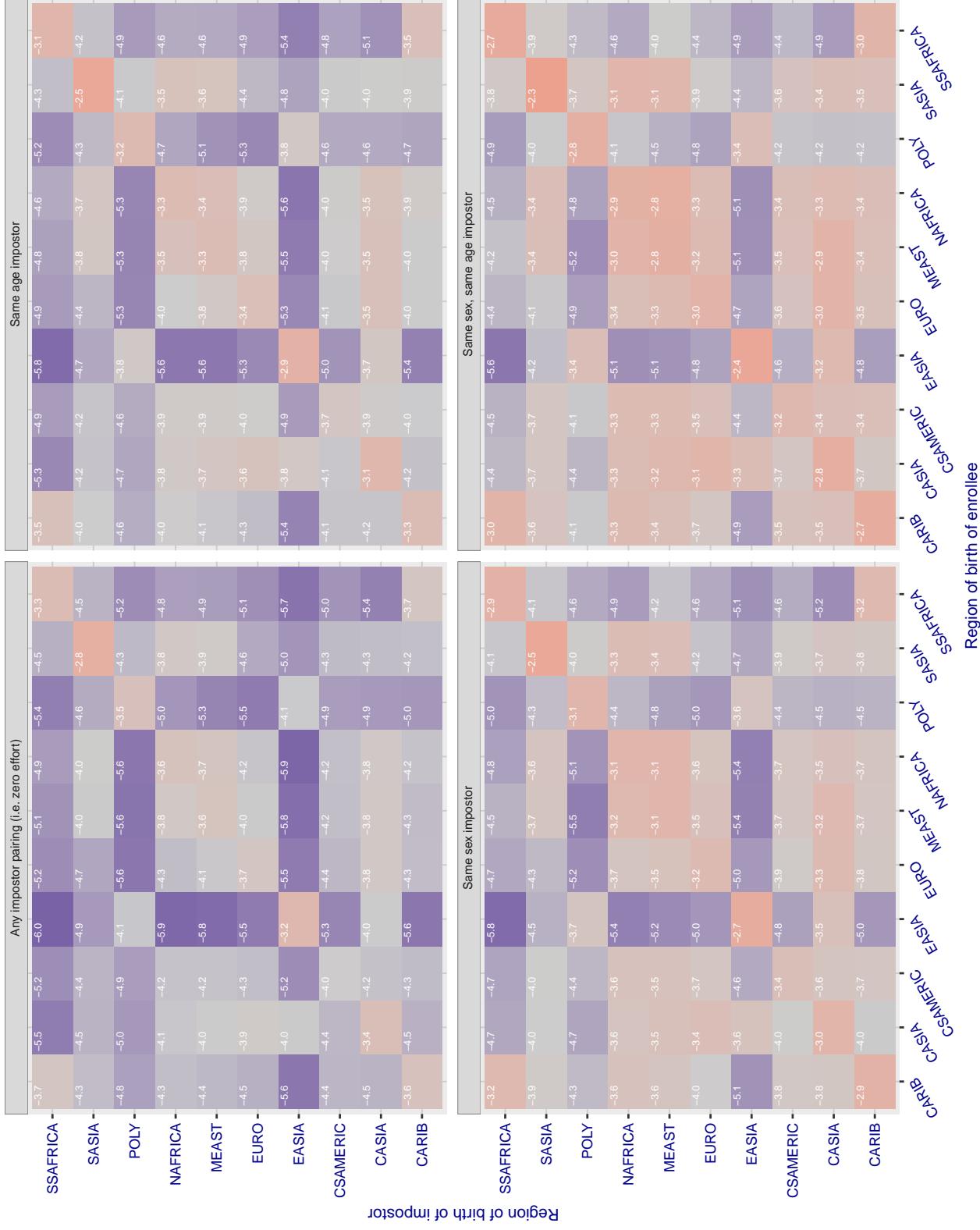
**Cross region FMR at threshold T = 148.416 for algorithm tech5\_001, giving FMR(T) = 0.0001 globally.**

Figure 190: For algorithm tech5-001 operating on visa images, the heatmap shows false match rates observed over impostor comparisons of faces from different individuals who were born in the given region pair. False matches are counted against a recognition threshold fixed globally to give the target FMR in the plot title, computed over all on the order of  $10^{10}$  impostor comparisons. If text appears in each box it give the same quantity as that coded by the color. Grey indicates FMR is at the intended FMR target level. Light red colors present a security vulnerability to, for example, a passport gate. Each +1 increase in  $\log_{10} FMR$  corresponds to a factor of 10 increase in FMR. The matrix is not quite symmetric because images in the enrollment and verification sets are different.

### Cross region FMR at threshold T = 147.661 for algorithm tech5\_002, giving FMR(T) = 0.0001 globally.

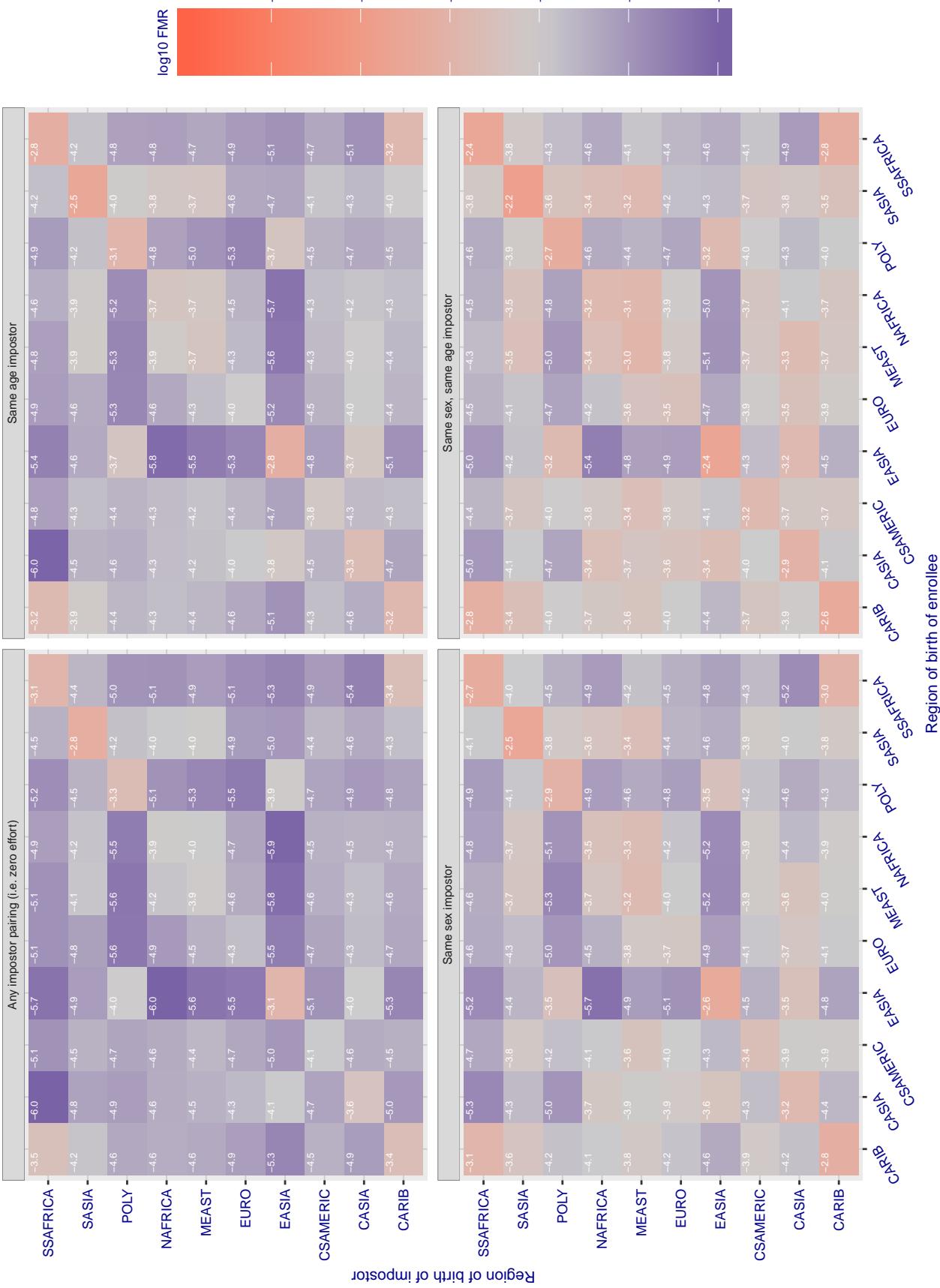


Figure 191: For algorithm tech5-002 operating on visa images, the heatmap shows false match rates observed over impostor comparisons of faces from different individuals who were born in the given region pair. False matches are counted against a recognition threshold fixed globally to give the target FMR in the plot title, computed over all on the order of  $10^{10}$  impostor comparisons. If text appears in each box it give the same quantity as that coded by the color. Grey indicates FMR is at the intended FMR target level. Light red colors present a security vulnerability to, for example, a passport gate. Each +1 increase in  $\log_{10} FMR$  corresponds to a factor of 10 increase in FMR. The matrix is not quite symmetric because images in the enrollment and verification sets are different.

### Cross region FMR at threshold T = 0.896 for algorithm tevian\_003, giving FMR(T) = 0.0001 globally.

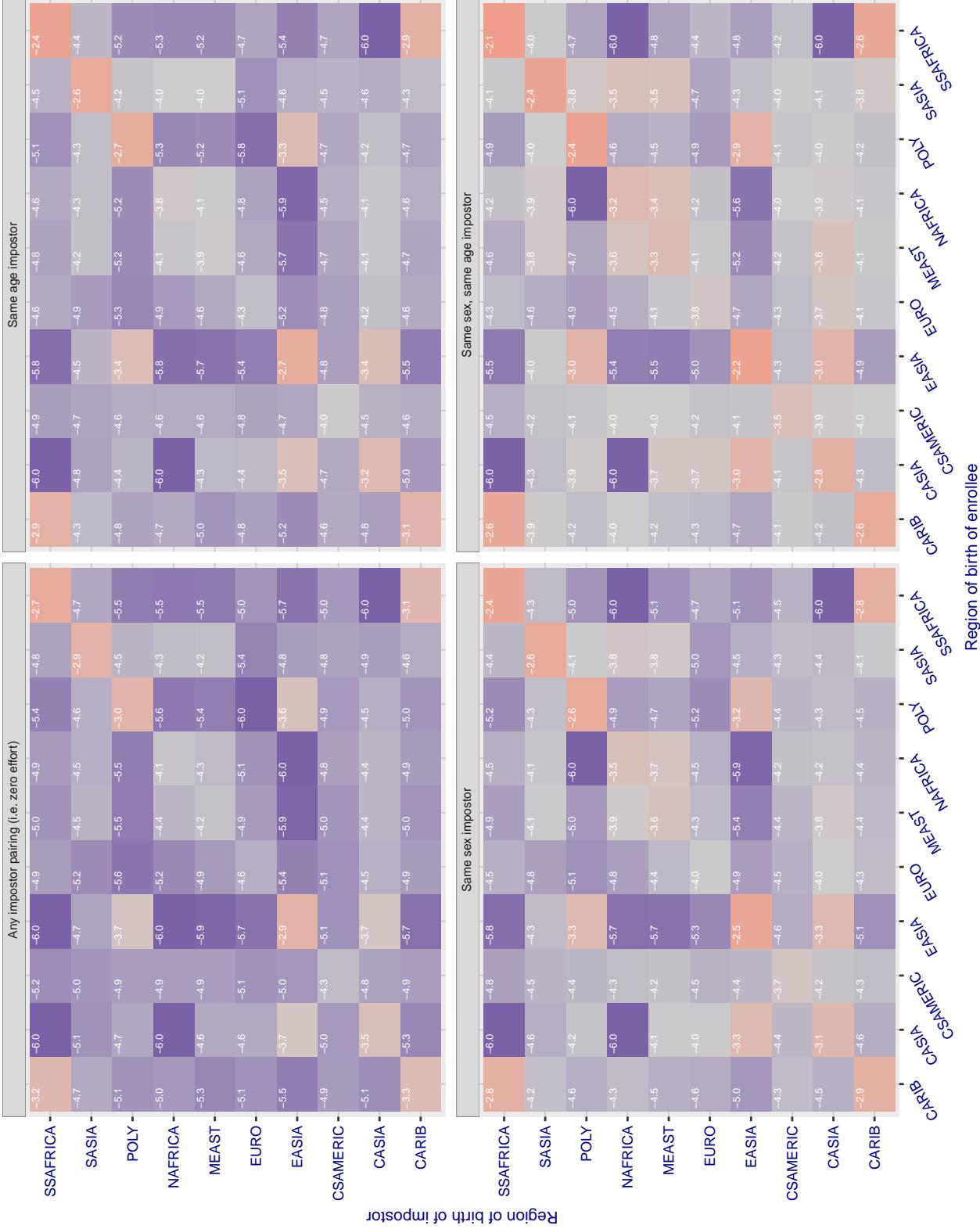


Figure 192: For algorithm tevian-003 operating on visa images, the heatmap shows false match rates observed over impostor comparisons of faces from different individuals who were born in the given region pair. False matches are counted against a recognition threshold fixed globally to give the target FMR in the plot title, computed over all on the order of  $10^{10}$  impostor comparisons. If text appears in each box it give the same quantity as that coded by the color. Grey indicates FMR is at the intended FMR target level. Light red colors present a security vulnerability to, for example, a passport gate. Each +1 increase in  $\log_{10} \text{FMR}$  corresponds to a factor of 10 increase in FMR. The matrix is not quite symmetric because images in the enrollment and verification sets are different.

### Cross region FMR at threshold T = 0.896 for algorithm tevian\_004, giving FMR(T) = 0.0001 globally.

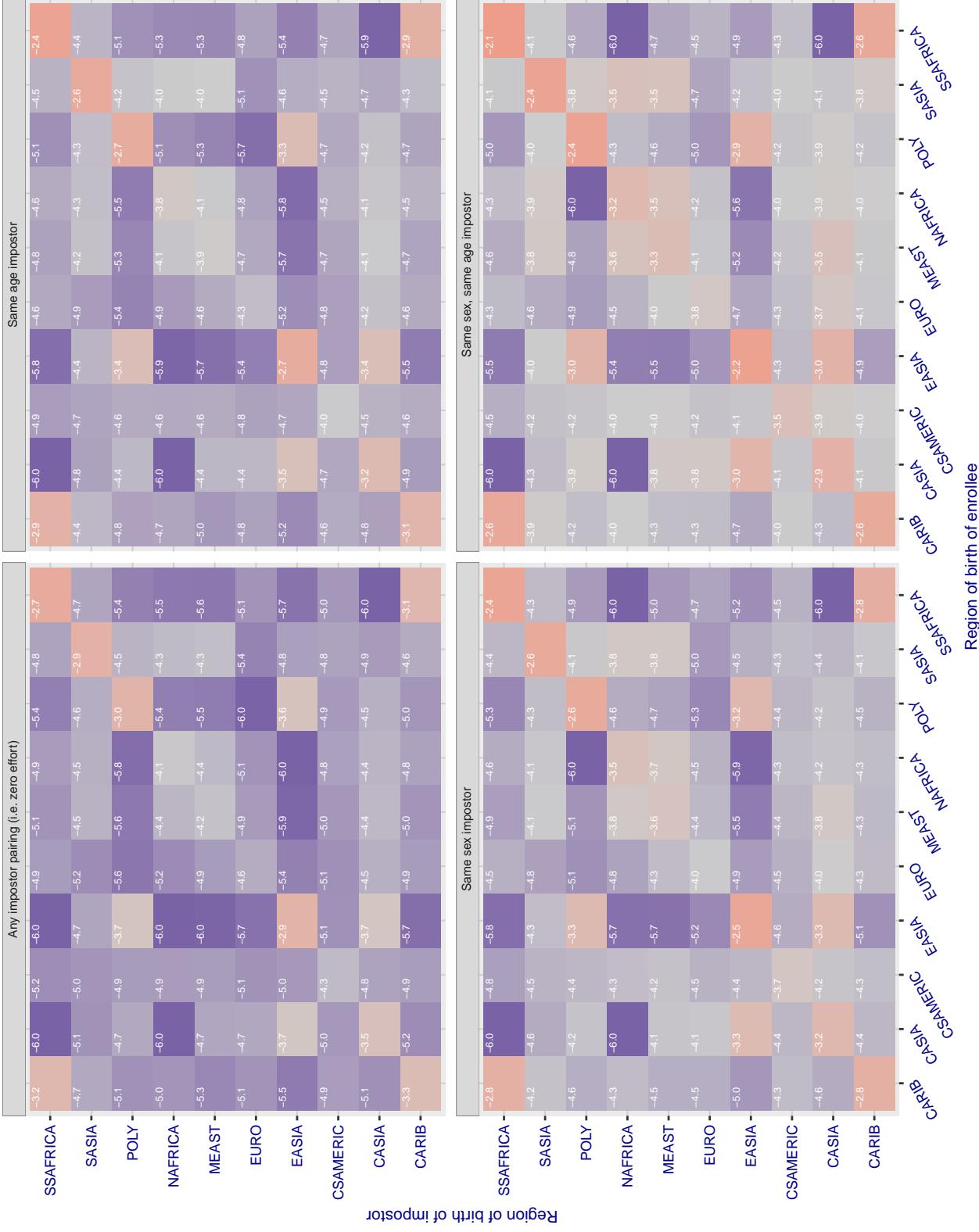


Figure 193: For algorithm tevian-004 operating on visa images, the heatmap shows false match rates observed over impostor comparisons of faces from different individuals who were born in the given region pair. False matches are counted against a recognition threshold fixed globally to give the target FMR in the plot title, computed over all on the order of  $10^{10}$  impostor comparisons. If text appears in each box it give the same quantity as that coded by the color. Grey indicates FMR is at the intended FMR target level. Light red colors present a security vulnerability to, for example, a passport gate. Each +1 increase in  $\log_{10} FMR$  corresponds to a factor of 10 increase in FMR. The matrix is not quite symmetric because images in the enrollment and verification sets are different.

### Cross region FMR at threshold T = 151.011 for algorithm tiger\_002, giving $\text{FMR}(\text{T}) = 0.0001$ globally.

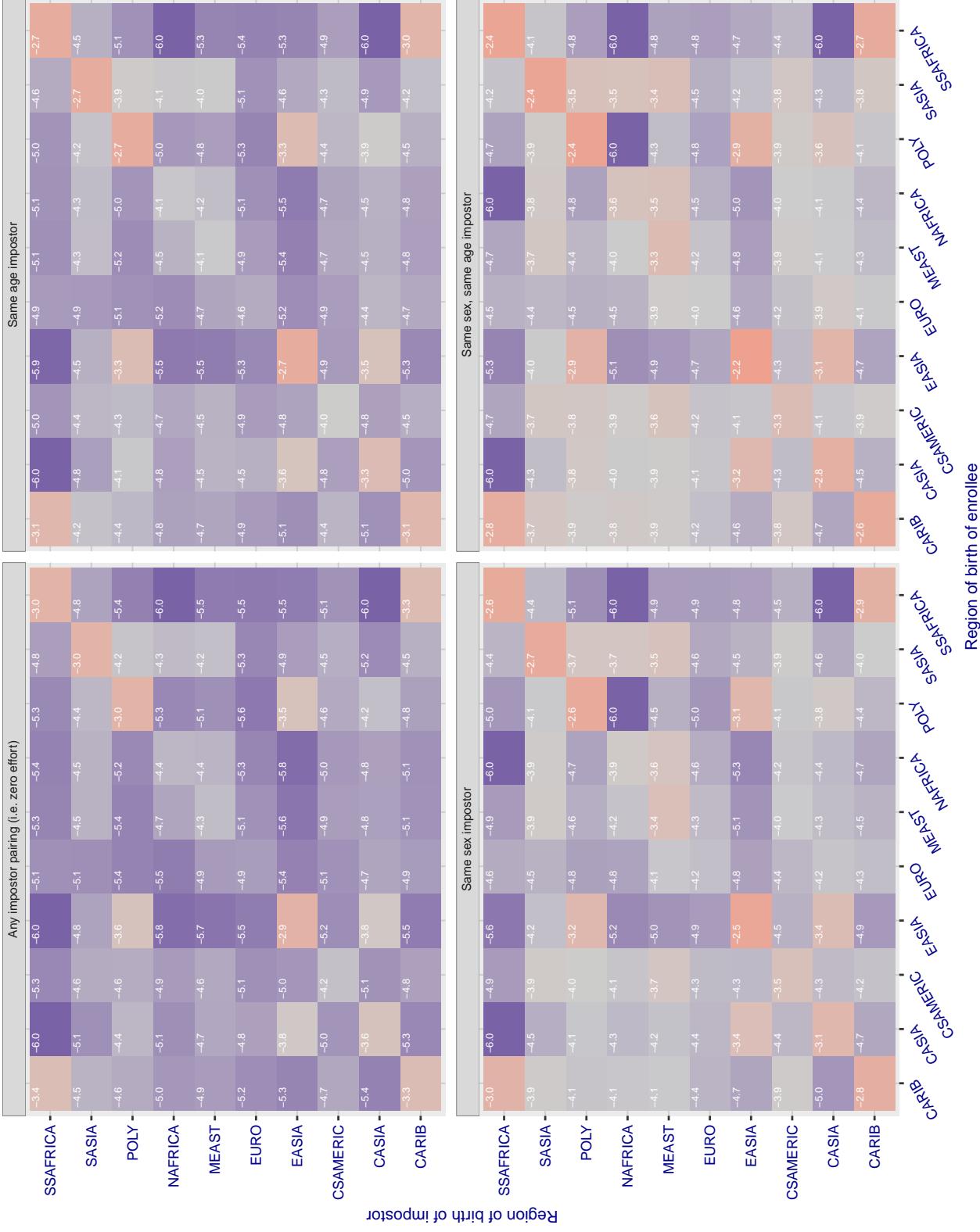


Figure 194: For algorithm tiger-002 operating on visa images, the heatmap shows false match rates observed over impostor comparisons of faces from different individuals who were born in the given region pair. False matches are counted against a recognition threshold fixed globally to give the target FMR in the plot title, computed over all on the order of  $10^{10}$  impostor comparisons. If text appears in each box it give the same quantity as that coded by the color. Grey indicates FMR is at the intended FMR target level. Light red colors present a security vulnerability to, for example, a passport gate. Each +1 increase in  $\log 10 \text{ FMR}$  corresponds to a factor of 10 increase in FMR. The matrix is not quite symmetric because images in the enrollment and verification sets are different.

### Cross region FMR at threshold T = 149.313 for algorithm tiger\_003, giving $\text{FMR}(\text{T}) = 0.0001$ globally.

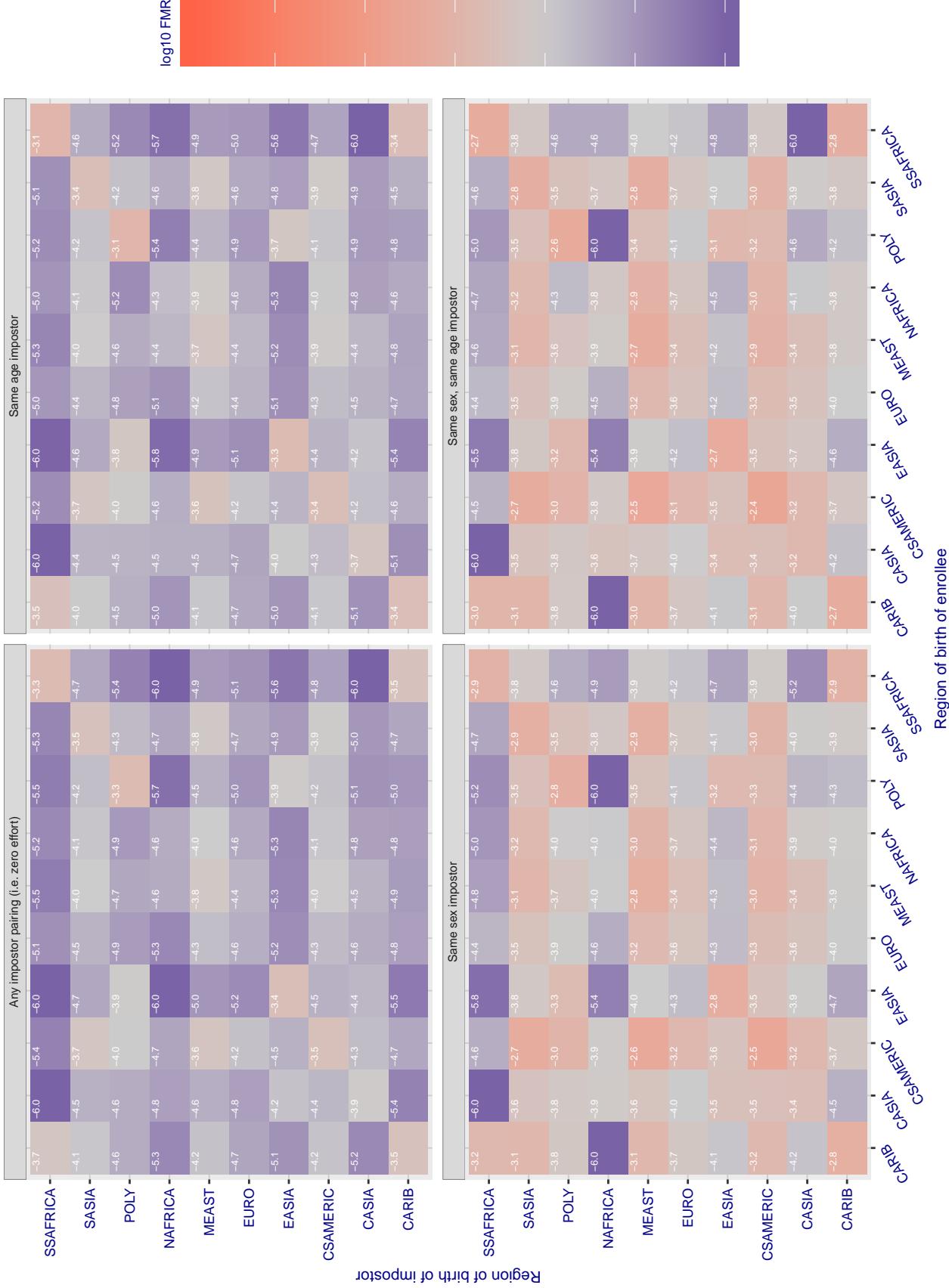


Figure 195: For algorithm tiger-003 operating on visa images, the heatmap shows false match rates observed over impostor comparisons of faces from different individuals who were born in the given region pair. False matches are counted against a recognition threshold fixed globally to give the target FMR in the plot title, computed over all on the order of  $10^{10}$  impostor comparisons. If text appears in each box it give the same quantity as that coded by the color. Grey indicates FMR is at the intended FMR target level. Light red colors present a security vulnerability to, for example, a passport gate. Each +1 increase in  $\log 10 \text{ FMR}$  corresponds to a factor of 10 increase in FMR. The matrix is not quite symmetric because images in the enrollment and verification sets are different.

### Cross region FMR at threshold T = 0.628 for algorithm toshiba\_002, giving FMR(T) = 0.0001 globally.

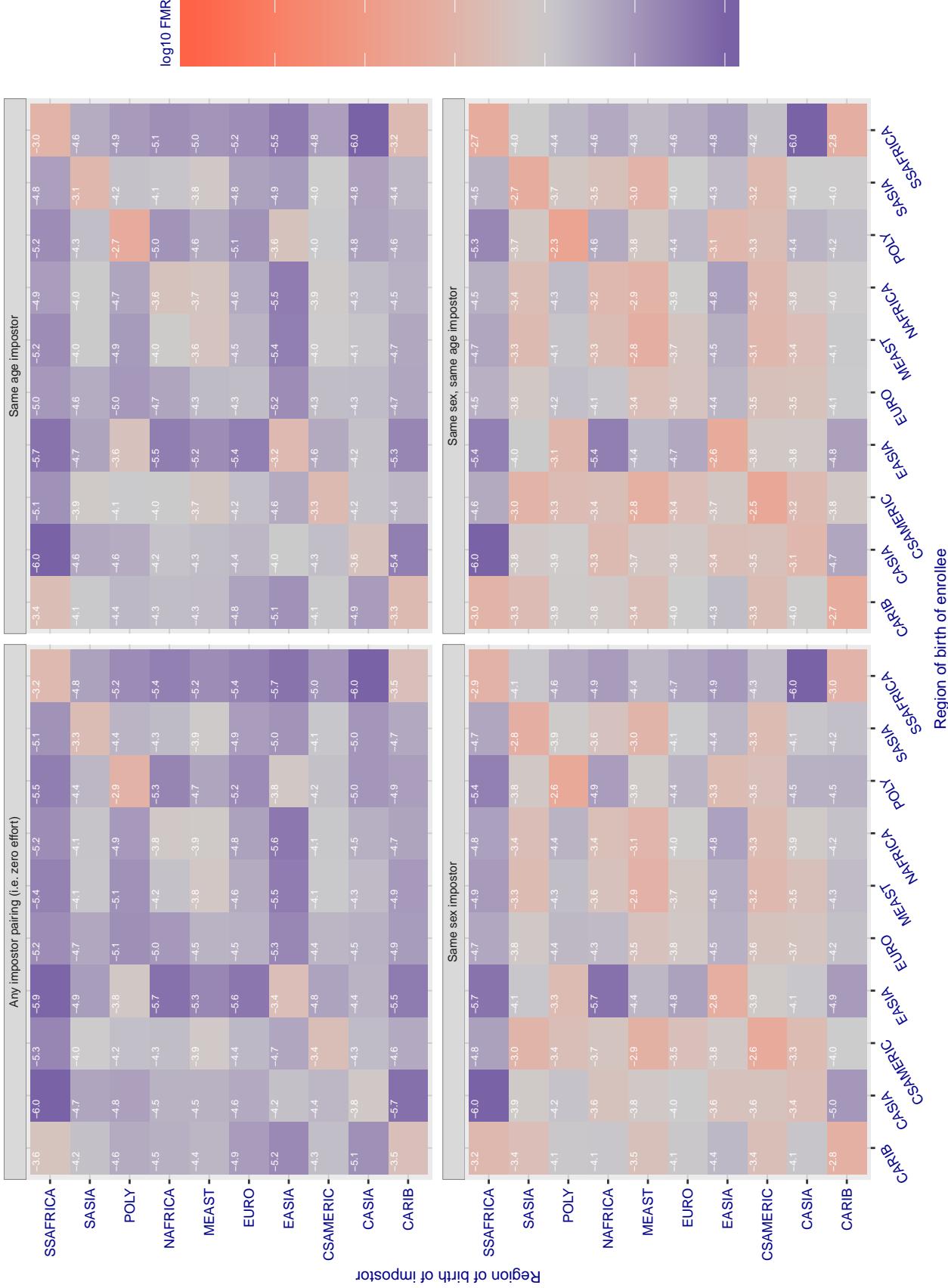


Figure 196: For algorithm toshiba-002 operating on visa images, the heatmap shows false match rates observed over impostor comparisons of faces from different individuals who were born in the given region pair. False matches are counted against a recognition threshold fixed globally to give the target FMR in the plot title, computed over all on the order of  $10^{10}$  impostor comparisons. If text appears in each box it give the same quantity as that coded by the color. Grey indicates FMR is at the intended FMR target level. Light red colors present a security vulnerability to, for example, a passport gate. Each +1 increase in  $\log_{10} FMR$  corresponds to a factor of 10 increase in FMR. The matrix is not quite symmetric because images in the enrollment and verification sets are different.

### Cross region FMR at threshold T = 0.626 for algorithm toshiba\_003, giving FMR(T) = 0.0001 globally.

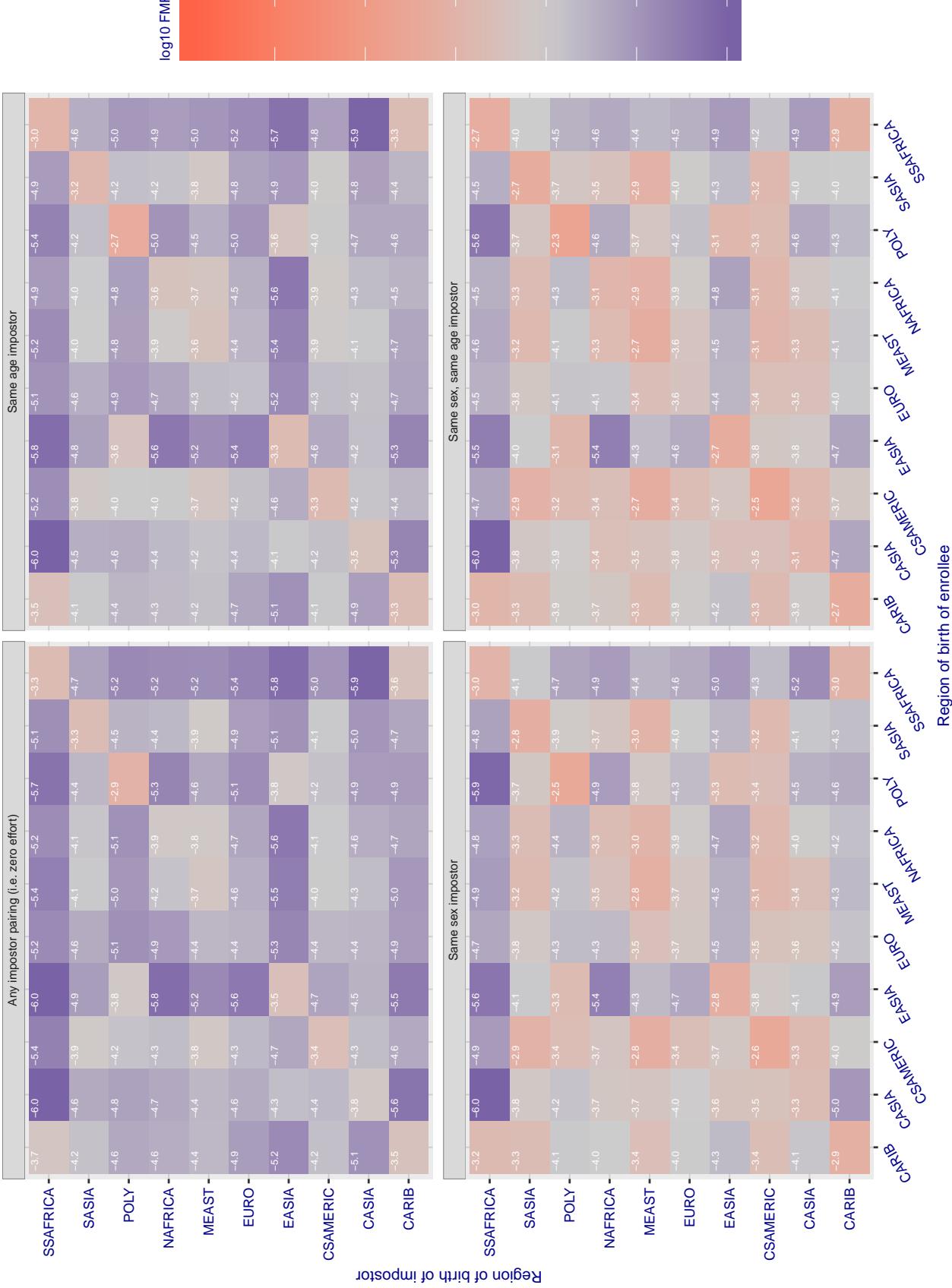


Figure 197: For algorithm toshiba-003 operating on visa images, the heatmap shows false match rates observed over impostor comparisons of faces from different individuals who were born in the given region pair. False matches are counted against a recognition threshold fixed globally to give the target FMR in the plot title, computed over all on the order of  $10^{10}$  impostor comparisons. If text appears in each box it give the same quantity as that coded by the color. Grey indicates FMR is at the intended FMR target level. Light red colors present a security vulnerability to, for example, a passport gate. Each +1 increase in  $\log_{10} \text{FMR}$  corresponds to a factor of 10 increase in FMR. The matrix is not quite symmetric because images in the enrollment and verification sets are different.

### Cross region FMR at threshold T = 0.428 for algorithm vcog\_002, giving FMR(T) = 0.0001 globally.

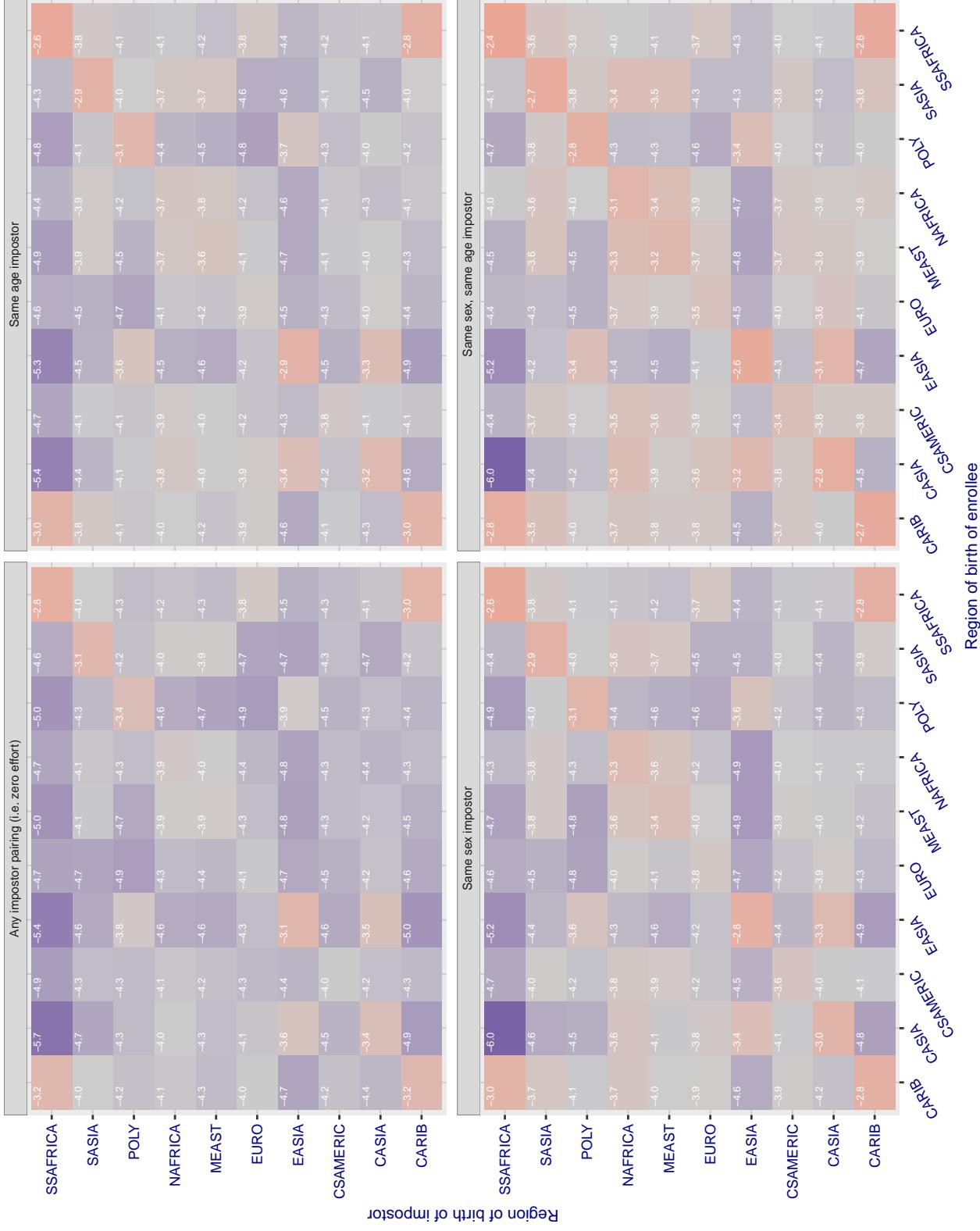


Figure 198: For algorithm vcog-002 operating on visa images, the heatmap shows false match rates observed over impostor comparisons of faces from different individuals who were born in the given region pair. False matches are counted against a recognition threshold fixed globally to give the target FMR in the plot title, computed over all on the order of  $10^{10}$  impostor comparisons. If text appears in each box it give the same quantity as that coded by the color. Grey indicates FMR is at the intended FMR target level. Light red colors present a security vulnerability to, for example, a passport gate. Each +1 increase in  $\log_{10} \text{FMR}$  corresponds to a factor of 10 increase in FMR. The matrix is not quite symmetric because images in the enrollment and verification sets are different.

### Cross region FMR at threshold T = 71.529 for algorithm vd\_001, giving FMR(T) = 0.0001 globally.

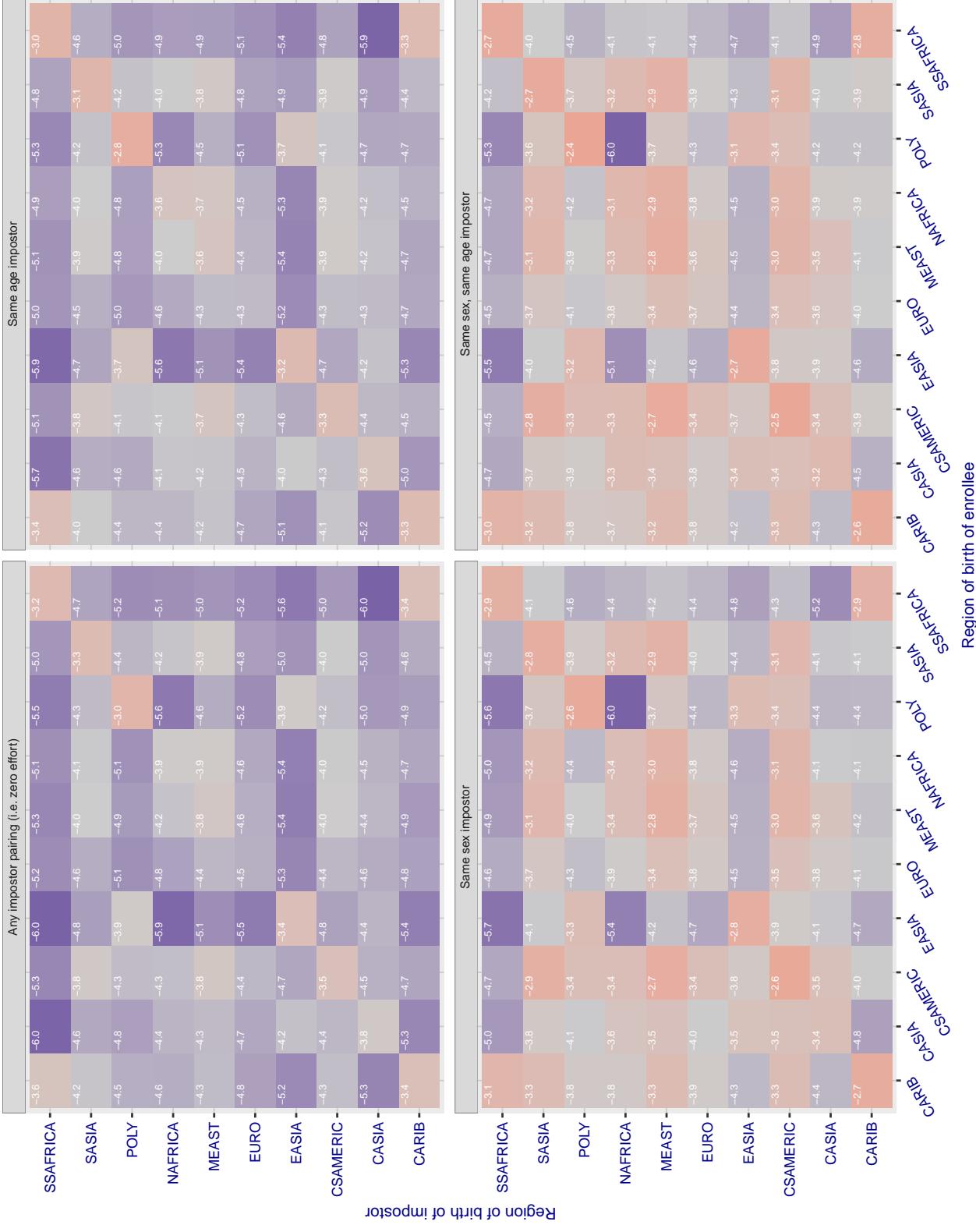


Figure 199: For algorithm vd\_001 operating on visa images, the heatmap shows false match rates observed over impostor comparisons of faces from different individuals who were born in the given region pair. False matches are counted against a recognition threshold fixed globally to give the target FMR in the plot title, computed over all on the order of  $10^{10}$  impostor comparisons. If text appears in each box it give the same quantity as that coded by the color. Grey indicates FMR is at the intended FMR target level. Light red colors present a security vulnerability to, for example, a passport gate. Each +1 increase in  $\log_{10}$  FMR corresponds to a factor of 10 increase in FMR. The matrix is not quite symmetric because images in the enrollment and verification sets are different.

### Cross region FMR at threshold T = 3.325 for algorithm veridas\_001, giving FMR(T) = 0.00001 globally.

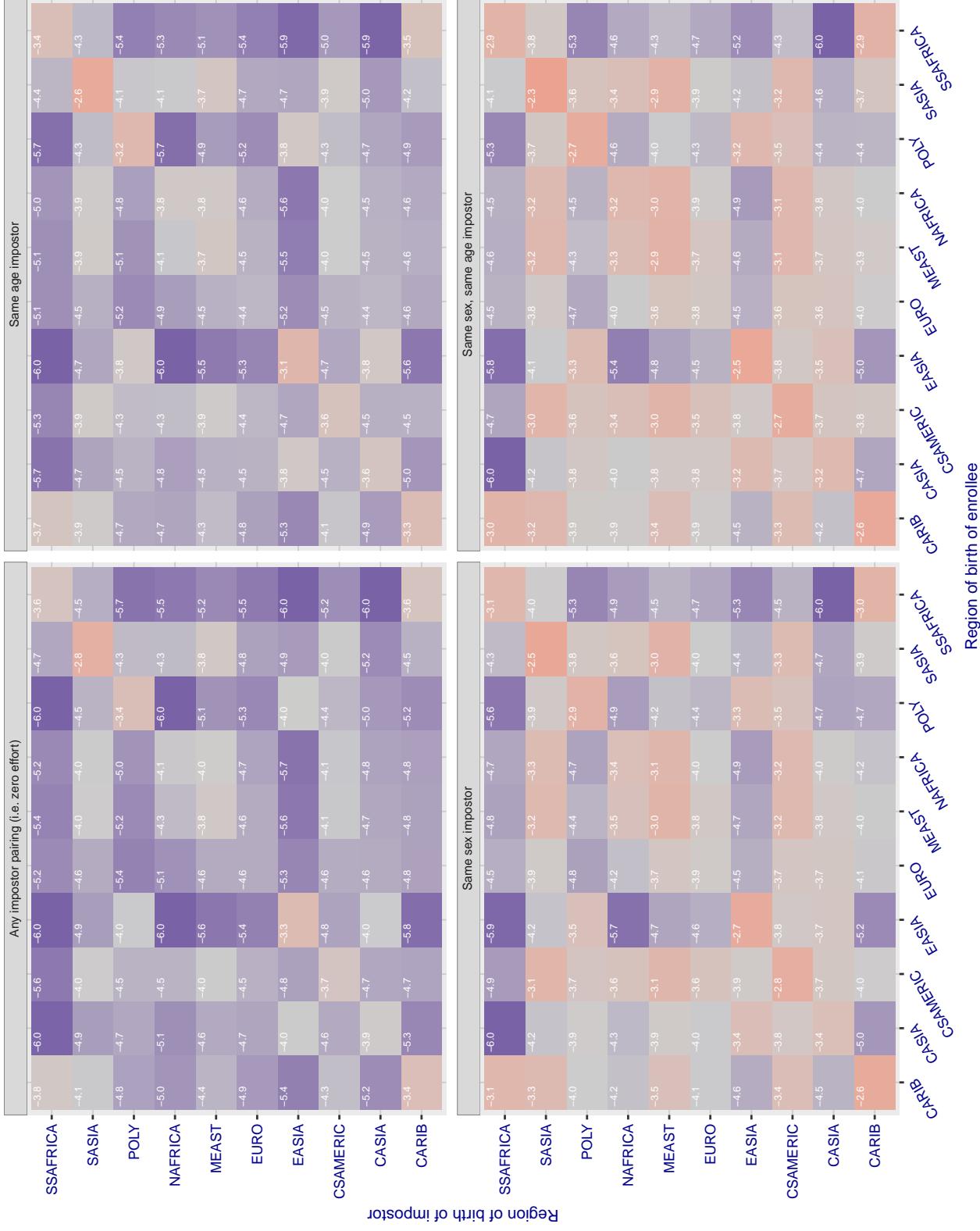


Figure 200: For algorithm veridas-001 operating on visa images, the heatmap shows false match rates observed over impostor comparisons of faces from different individuals who were born in the given region pair. False matches are counted against a recognition threshold fixed globally to give the target FMR in the plot title, computed over all on the order of  $10^{10}$  impostor comparisons. If text appears in each box it give the same quantity as that coded by the color. Grey indicates FMR is at the intended FMR target level. Light red colors present a security vulnerability to, for example, a passport gate. Each +1 increase in  $\log_{10} \text{FMR}$  corresponds to a factor of 10 increase in FMR. The matrix is not quite symmetric because images in the enrollment and verification sets are different.

### Cross region FMR at threshold T = 3.389 for algorithm veridas\_002, giving FMR(T) = 0.0001 globally.

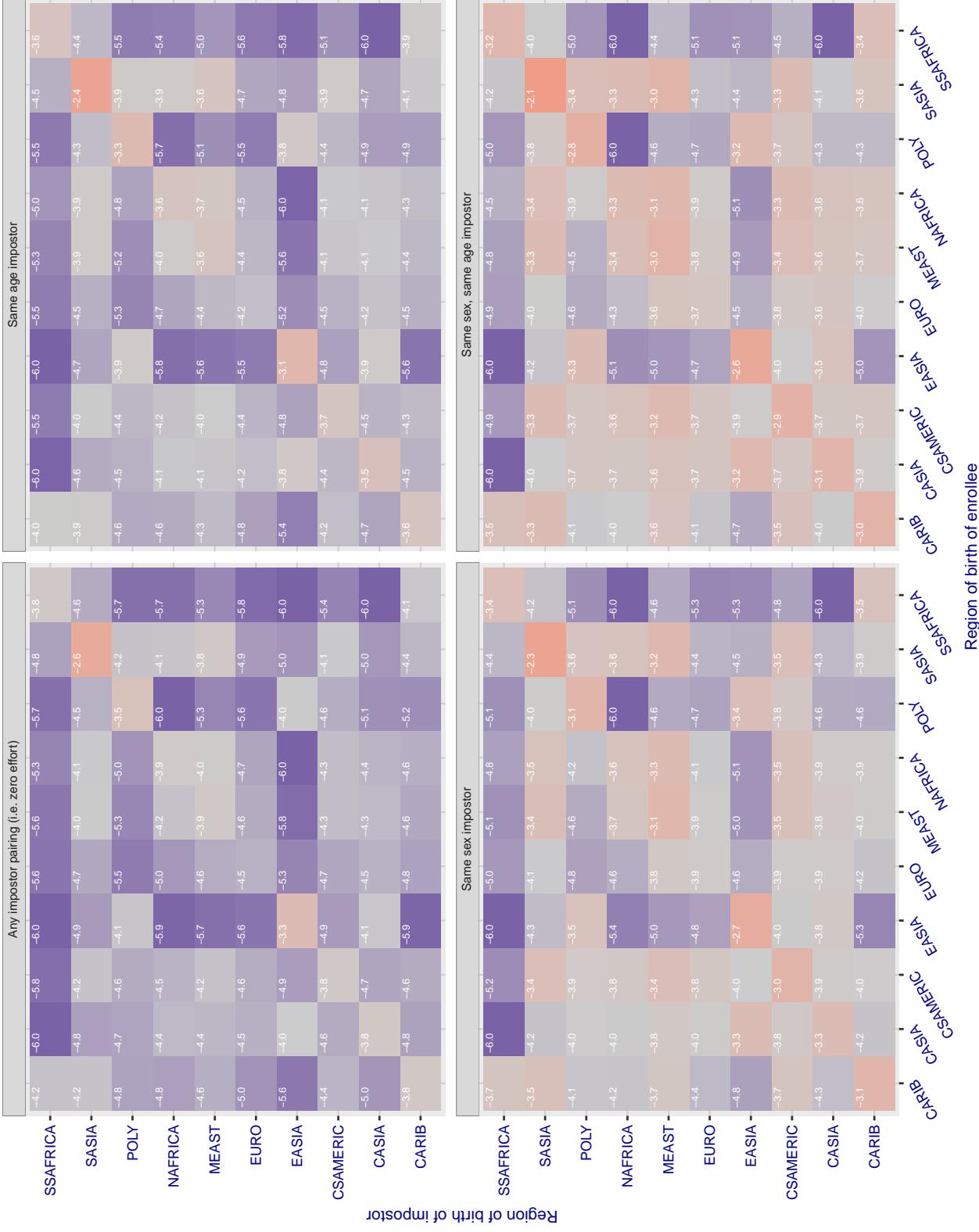


Figure 201: For algorithm veridas-002 operating on visa images, the heatmap shows false match rates observed over impostor comparisons of faces from different individuals who were born in the given region pair. False matches are counted against a recognition threshold fixed globally to give the target FMR in the plot title, computed over all on the order of  $10^{10}$  impostor comparisons. If text appears in each box it give the same quantity as that coded by the color. Grey indicates FMR is at the intended FMR target level. Light red colors present a security vulnerability to, for example, a passport gate. Each +1 increase in  $\log_{10} FMR$  corresponds to a factor of 10 increase in FMR. The matrix is not quite symmetric because images in the enrollment and verification sets are different.

### Cross region FMR at threshold T = 3.051 for algorithm vigilantsolutions\_005, giving FMR(T) = 0.0001 globally.

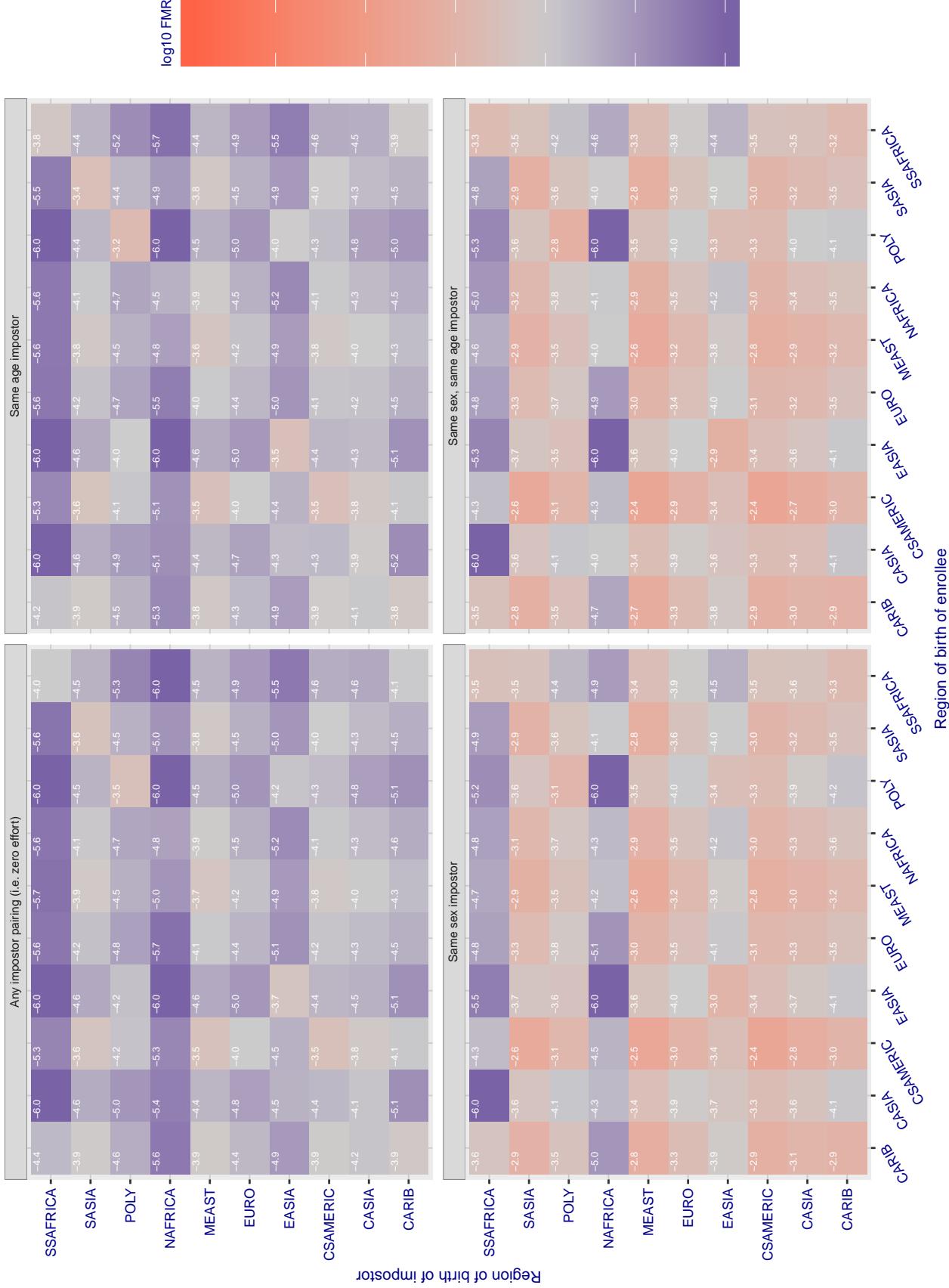


Figure 202: For algorithm vigilantsolutions-005 operating on visa images, the heatmap shows false match rates observed over impostor comparisons of faces from different individuals who were born in the given region pair. False matches are counted against a recognition threshold fixed globally to give the target FMR in the plot title, computed over all on the order of  $10^{10}$  impostor comparisons. If text appears in each box it give the same quantity as that coded by the color. Grey indicates FMR is at the intended FMR target level. Light red colors present a security vulnerability to, for example, a passport gate. Each +1 increase in  $\log_{10} FMR$  corresponds to a factor of 10 increase in FMR. The matrix is not quite symmetric because images in the enrollment and verification sets are different.

### Cross region FMR at threshold T = 3.057 for algorithm vigilantsolutions\_006, giving FMR(T) = 0.0001 globally.

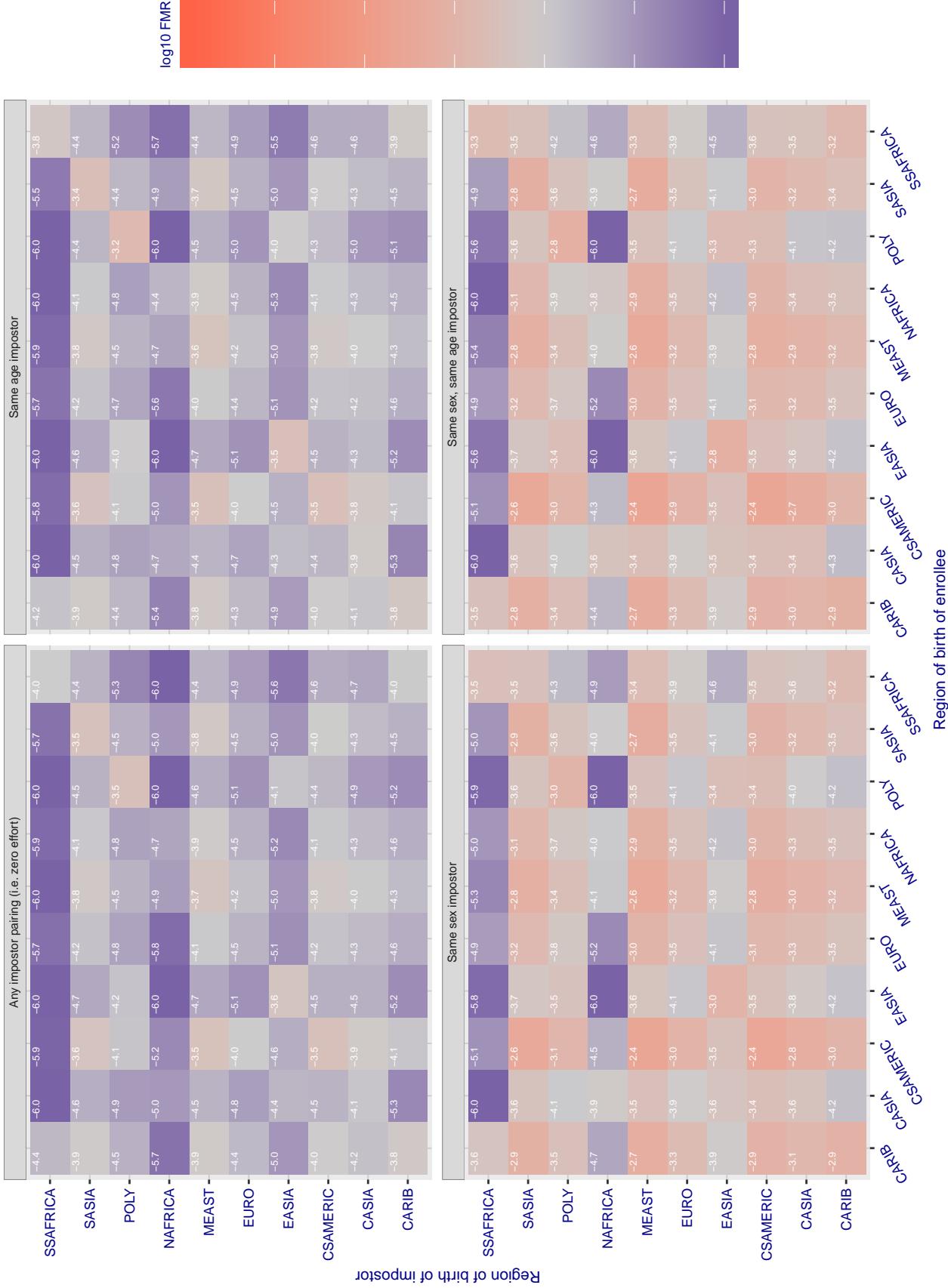


Figure 203: For algorithm vigilantsolutions-006 operating on visa images, the heatmap shows false match rates observed over impostor comparisons of faces from different individuals who were born in the given region pair. False matches are counted against a recognition threshold fixed globally to give the target FMR in the plot title, computed over all on the order of  $10^{10}$  impostor comparisons. If text appears in each box it give the same quantity as that coded by the color. Grey indicates FMR is at the intended FMR target level. Light red colors present a security vulnerability to, for example, a passport gate. Each +1 increase in  $\log_{10} \text{FMR}$  corresponds to a factor of 10 increase in FMR. The matrix is not quite symmetric because images in the enrollment and verification sets are different.

### Cross region FMR at threshold T = 0.432 for algorithm vion\_000, giving FMR(T) = 0.0001 globally.

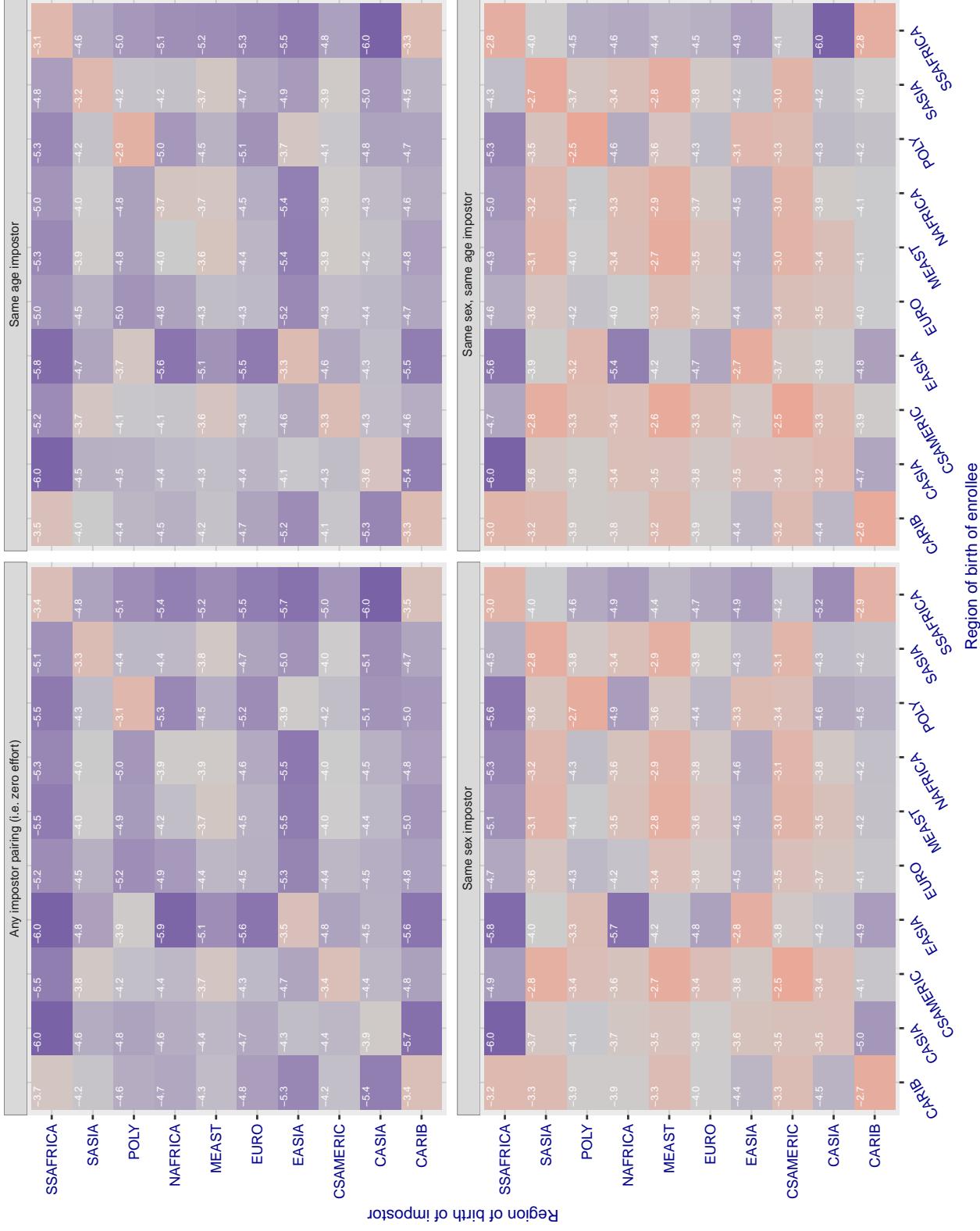


Figure 204: For algorithm vion\_000 operating on visa images, the heatmap shows false match rates observed over impostor comparisons of faces from different individuals who were born in the given region pair. False matches are counted against a recognition threshold fixed globally to give the target FMR in the plot title, computed over all on the order of  $10^{10}$  impostor comparisons. If text appears in each box it give the same quantity as that coded by the color. Grey indicates FMR is at the intended FMR target level. Light red colors present a security vulnerability to, for example, a passport gate. Each +1 increase in  $\log_{10}$  FMR corresponds to a factor of 10 increase in FMR. The matrix is not quite symmetric because images in the enrollment and verification sets are different.

### Cross region FMR at threshold T = 0.433 for algorithm visionbox\_000, giving FMR(T) = 0.0001 globally.

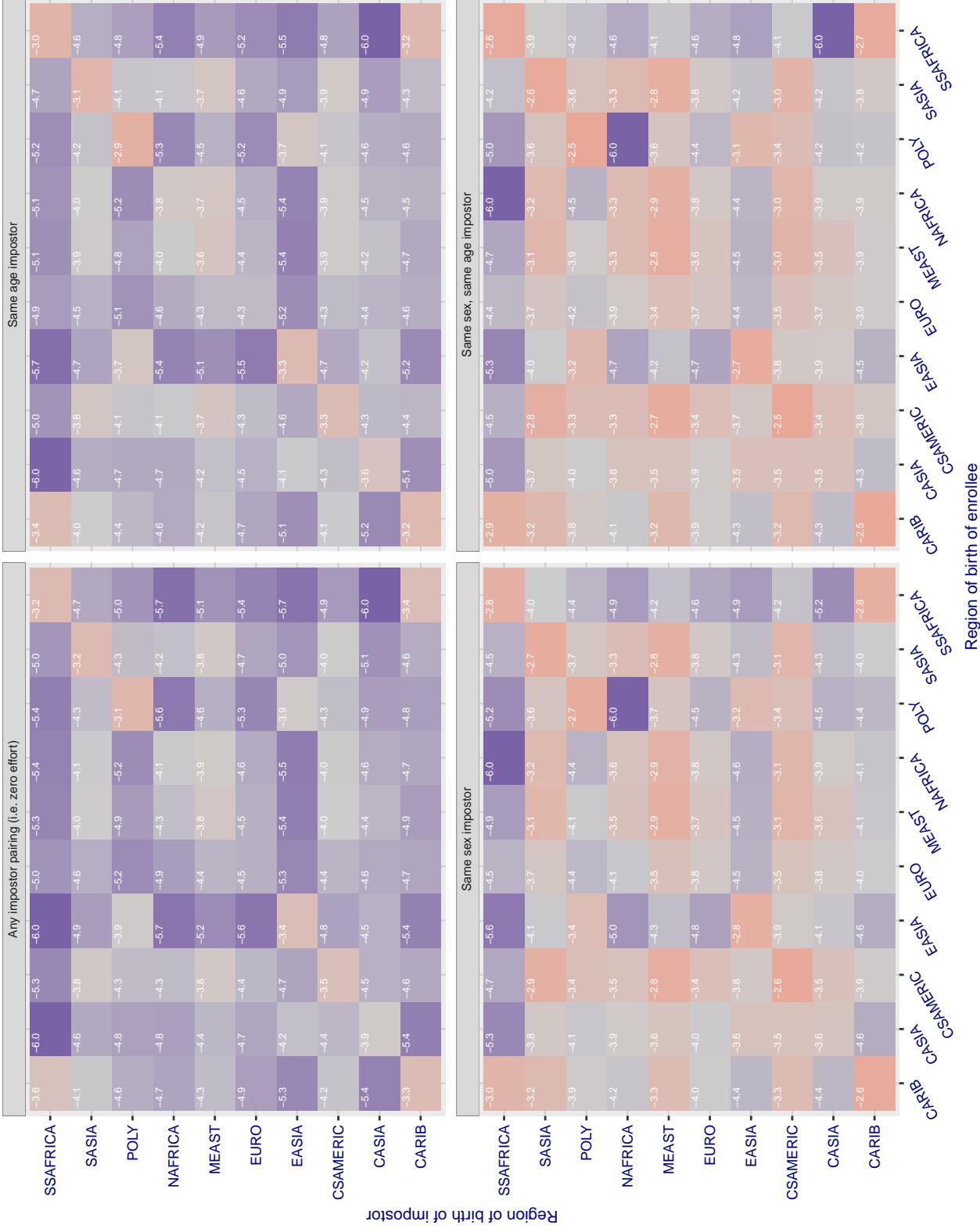


Figure 205: For algorithm visionbox-000 operating on visa images, the heatmap shows false match rates observed over impostor comparisons of faces from different individuals who were born in the given region pair. False matches are counted against a recognition threshold fixed globally to give the target FMR in the plot title, computed over all on the order of  $10^{10}$  impostor comparisons. If text appears in each box it give the same quantity as that coded by the color. Grey indicates FMR is at the intended FMR target level. Light red colors present a security vulnerability to, for example, a passport gate. Each +1 increase in  $\log_{10} FMR$  corresponds to a factor of 10 increase in FMR. The matrix is not quite symmetric because images in the enrollment and verification sets are different.

### Cross region FMR at threshold T = 0.382 for algorithm visionbox\_001, giving FMR(T) = 0.00001 globally.

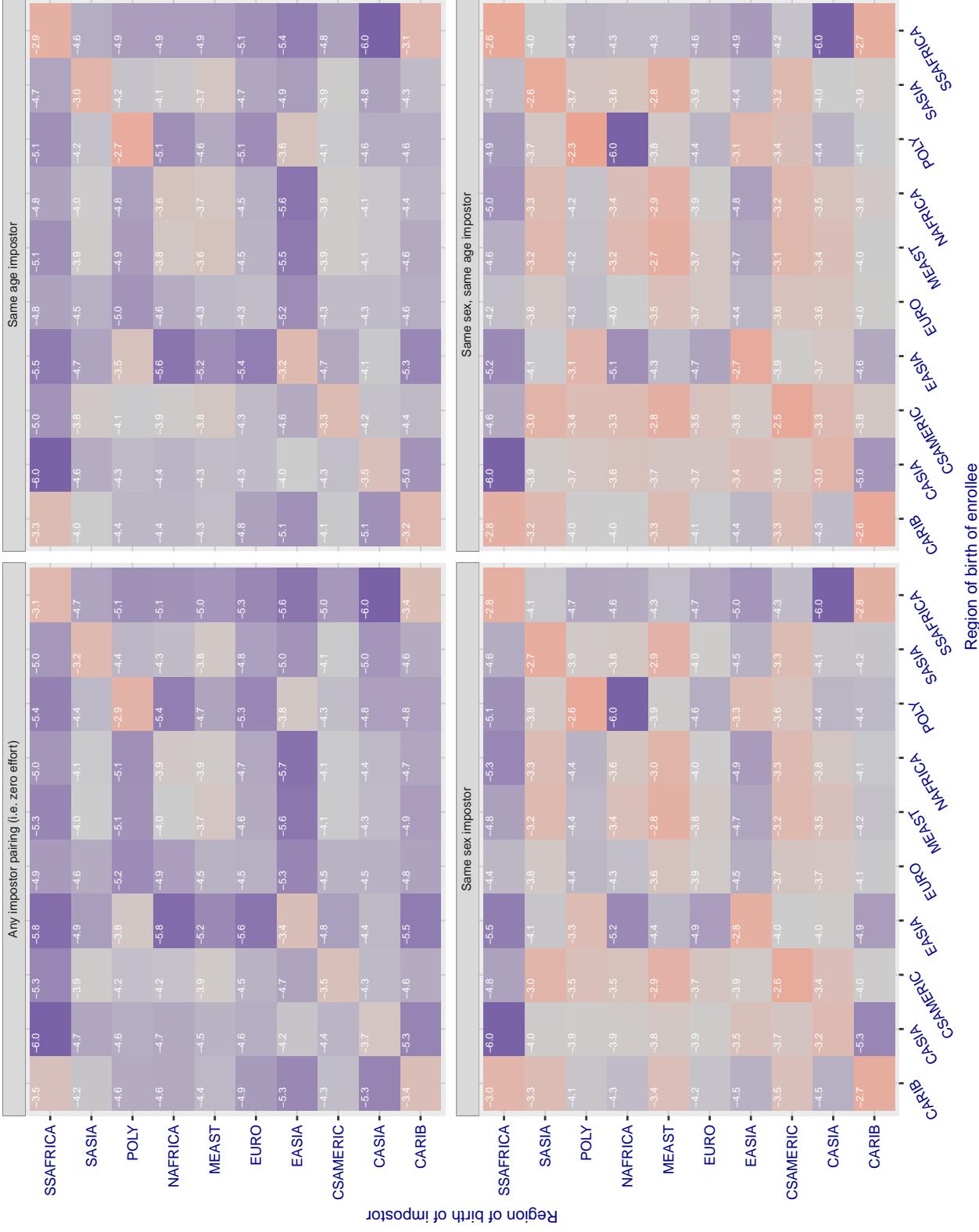


Figure 206: For algorithm visionbox\_001 operating on visa images, the heatmap shows false match rates observed over impostor comparisons of faces from different individuals who were born in the given region pair. False matches are counted against a recognition threshold fixed globally to give the target FMR in the plot title, computed over all on the order of  $10^{10}$  impostor comparisons. If text appears in each box it give the same quantity as that coded by the color. Grey indicates FMR is at the intended FMR target level. Light red colors present a security vulnerability to, for example, a passport gate. Each +1 increase in  $\log_{10} FMR$  corresponds to a factor of 10 increase in FMR. The matrix is not quite symmetric because images in the enrollment and verification sets are different.

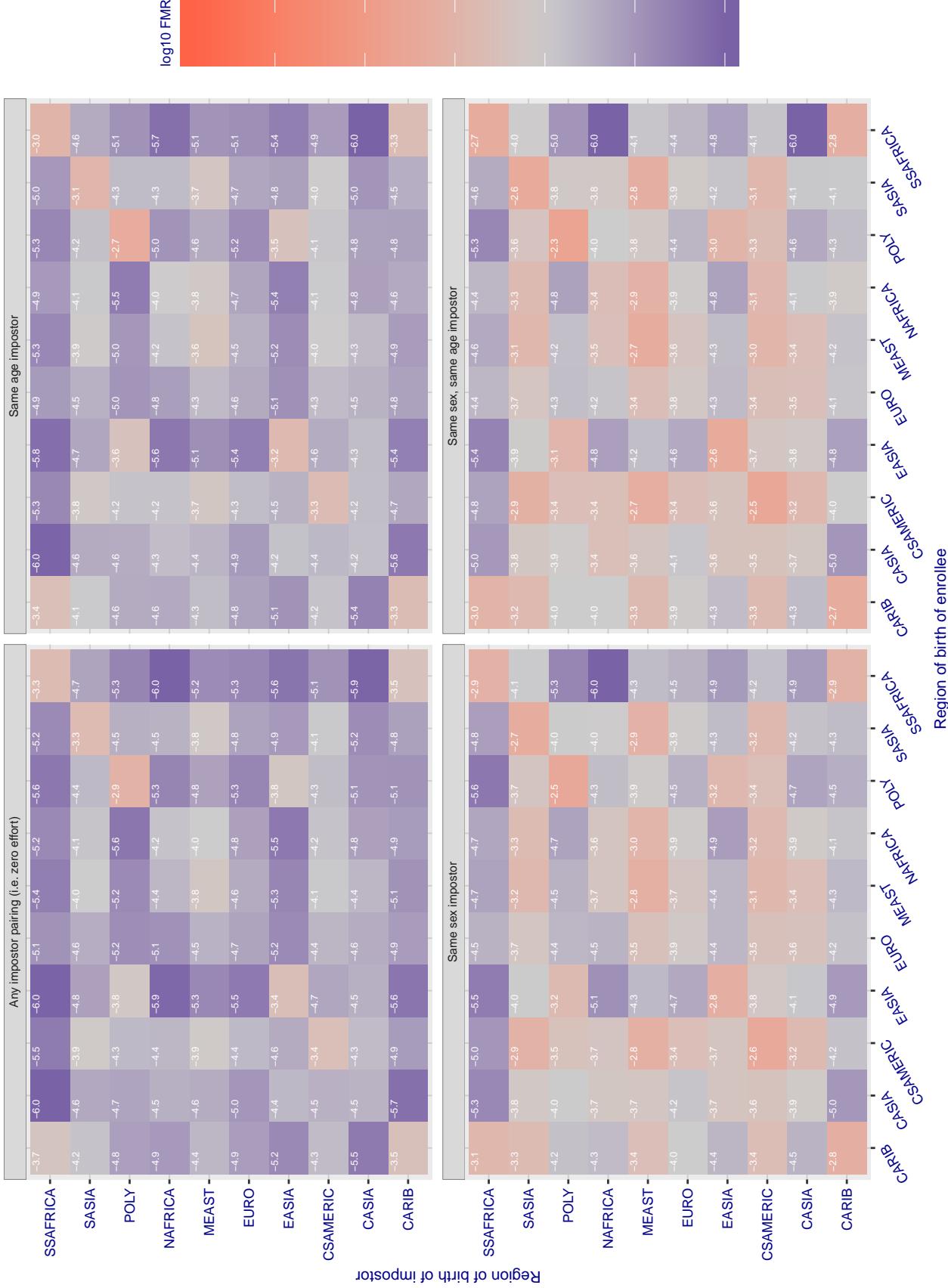
**Cross region FMR at threshold T = 0.000 for algorithm visionlabs\_005, giving FMR(T) = 0.0001 globally.**

Figure 207: For algorithm visionlabs-005 operating on visa images, the heatmap shows false match rates observed over impostor comparisons of faces from different individuals who were born in the given region pair. False matches are counted against a recognition threshold fixed globally to give the target FMR in the plot title, computed over all on the order of  $10^{10}$  impostor comparisons. If text appears in each box it give the same quantity as that coded by the color. Grey indicates FMR is at the intended FMR target level. Light red colors present a security vulnerability to, for example, a passport gate. Each +1 increase in  $\log_{10} FMR$  corresponds to a factor of 10 increase in FMR. The matrix is not quite symmetric because images in the enrollment and verification sets are different.

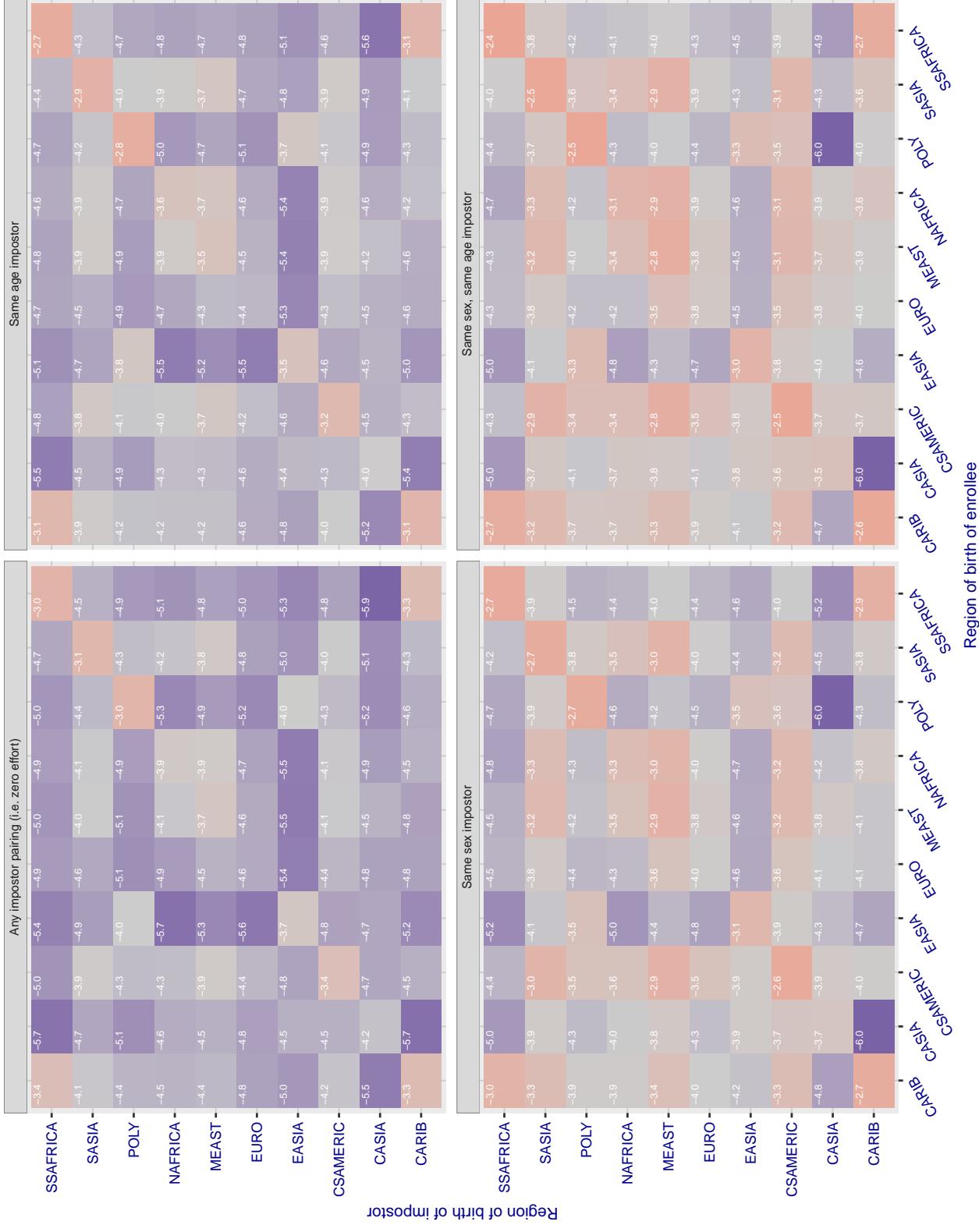
**Cross region FMR at threshold T = 0.669 for algorithm visionlabs\_006, giving FMR(T) = 0.0001 globally.**

Figure 208: For algorithm visionlabs-006 operating on visa images, the heatmap shows false match rates observed over impostor comparisons of faces from different individuals who were born in the given region pair. False matches are counted against a recognition threshold fixed globally to give the target FMR in the plot title, computed over all on the order of  $10^{10}$  impostor comparisons. If text appears in each box it give the same quantity as that coded by the color. Grey indicates FMR is at the intended FMR target level. Light red colors present a security vulnerability to, for example, a passport gate. Each +1 increase in  $\log_{10} FMR$  corresponds to a factor of 10 increase in FMR. The matrix is not quite symmetric because images in the enrollment and verification sets are different.

### Cross region FMR at threshold T = 995.898 for algorithm vocord\_006, giving FMR(T) = 0.0001 globally.

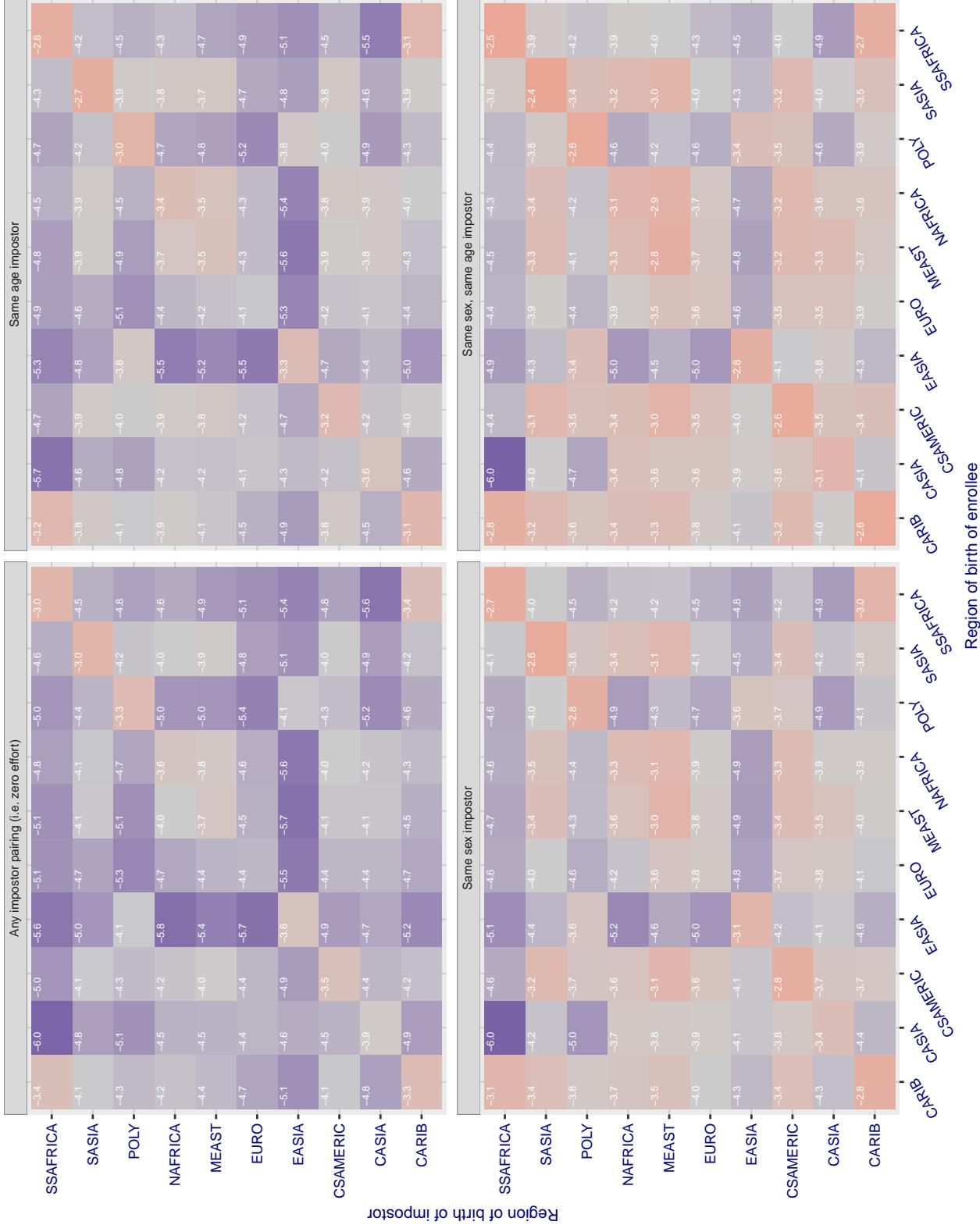


Figure 209: For algorithm vocord-006 operating on visa images, the heatmap shows false match rates observed over impostor comparisons of faces from different individuals who were born in the given region pair. False matches are counted against a recognition threshold fixed globally to give the target FMR in the plot title, computed over all on the order of  $10^{10}$  impostor comparisons. If text appears in each box it give the same quantity as that coded by the color. Grey indicates FMR is at the intended FMR target level. Light red colors present a security vulnerability to, for example, a passport gate. Each +1 increase in  $\log_{10} \text{FMR}$  corresponds to a factor of 10 increase in FMR. The matrix is not quite symmetric because images in the enrollment and verification sets are different.

Cross region FMR at threshold  $T = 5.544$  for algorithm *yisheng\_004*, giving  $FMR(T) = 0.0001$  globally.

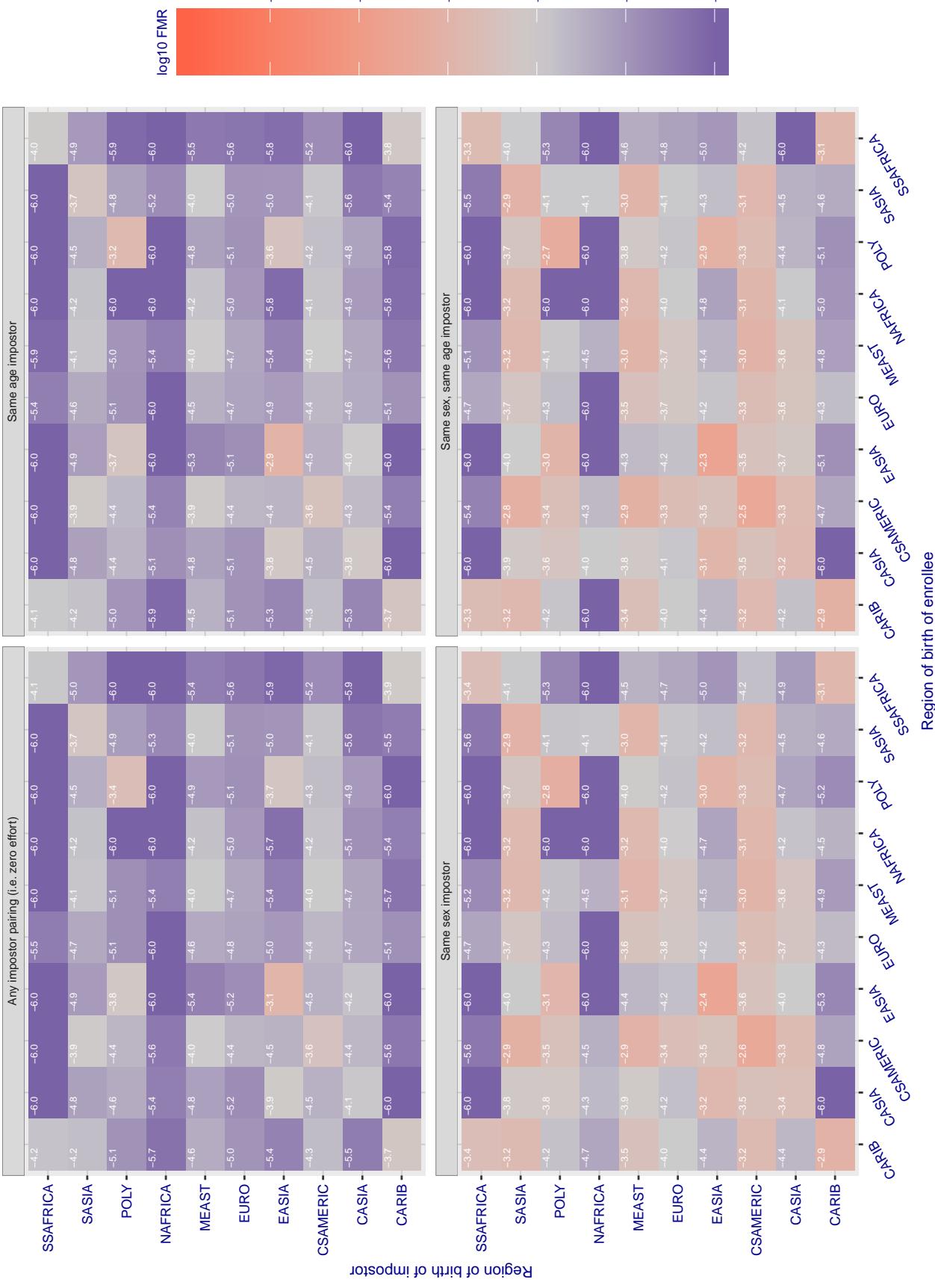


Figure 210: For algorithm *yisheng-004* operating on visa images, the heatmap shows false match rates observed over impostor comparisons of faces from different individuals who were born in the given region pair. False matches are counted against a recognition threshold fixed globally to give the target FMR in the plot title, computed over all on the order of  $10^{10}$  impostor comparisons. If text appears in each box it give the same quantity as that coded by the color. Grey indicates FMR is at the intended FMR target level. Light red colors present a security vulnerability to, for example, a passport gate. Each +1 increase in  $\log_{10}$  FMR corresponds to a factor of 10 increase in FMR. The matrix is not quite symmetric because images in the enrollment and verification sets are different.

### Cross region FMR at threshold T = 37.698 for algorithm yitu\_003, giving FMR(T) = 0.0001 globally.

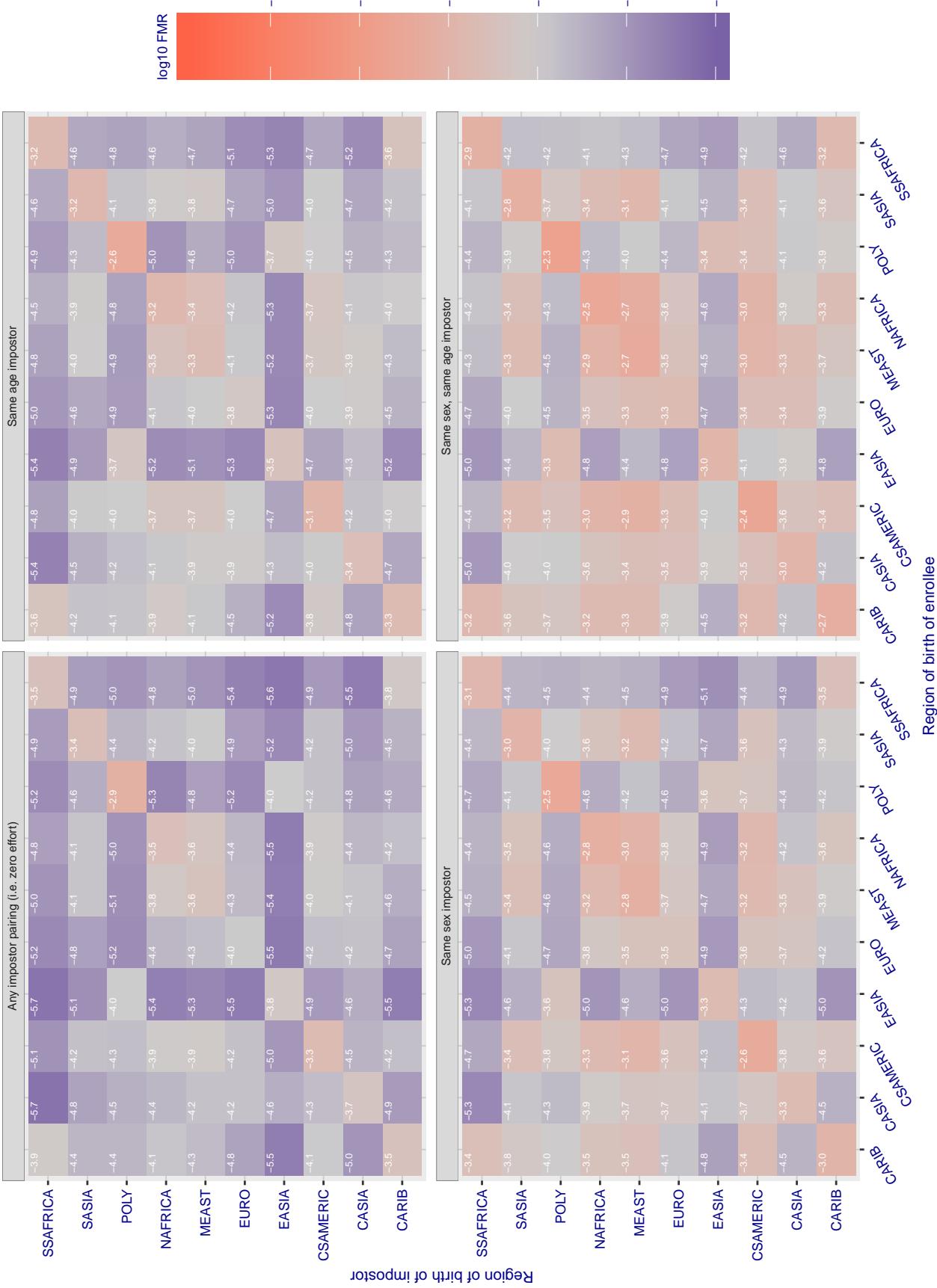


Figure 211: For algorithm yitu-003 operating on visa images, the heatmap shows false match rates observed over impostor comparisons of faces from different individuals who were born in the given region pair. False matches are counted against a recognition threshold fixed globally to give the target FMR in the plot title, computed over all on the order of  $10^{10}$  impostor comparisons. If text appears in each box it give the same quantity as that coded by the color. Grey indicates FMR is at the intended FMR target level. Light red colors present a security vulnerability to, for example, a passport gate. Each +1 increase in  $\log_{10} \text{FMR}$  corresponds to a factor of 10 increase in FMR. The matrix is not quite symmetric because images in the enrollment and verification sets are different.

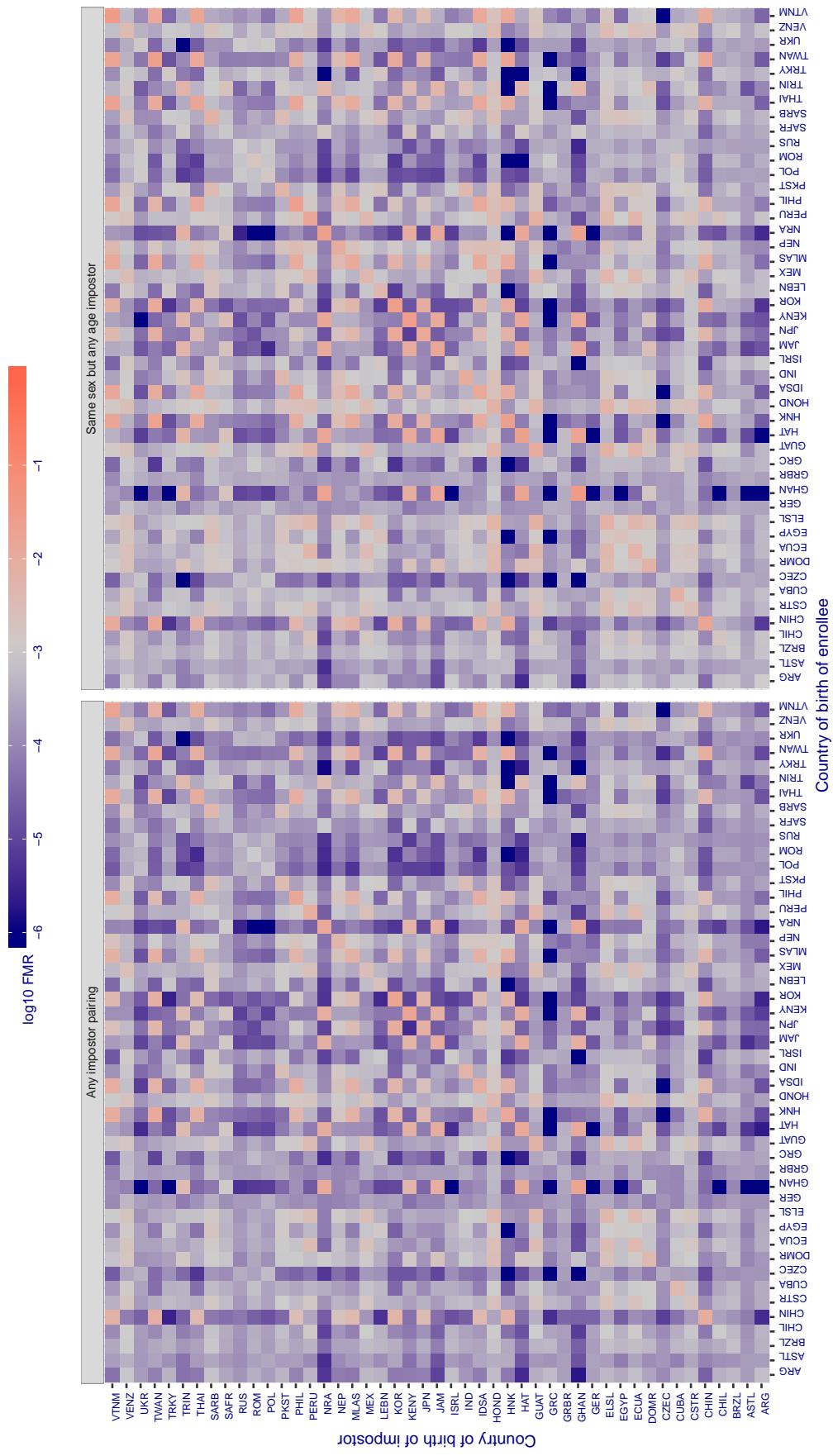
**Cross country FMR at threshold T = 2.575 for algorithm 3divi\_003, giving  $\text{FMR}(T) = 0.001$  globally.**

Figure 212: For algorithm 3divi-003 operating on visa images, the heatmap shows false match rates observed over impostor comparisons of faces from different individuals who were born in the given country pair. False matches are counted against a recognition threshold fixed globally to give the target FMR in the plot title, computed over all on the order of  $10^{10}$  impostor comparisons. If text appears in each box it give the same quantity as that coded by the color. Grey indicates FMR is at the intended FMR target level. Light red colors present a security vulnerability to, for example, a passport gate. Each +1 increase in  $\log_{10} \text{FMR}$  corresponds to a factor of 10 increase in FMR. The matrix is not quite symmetric because images in the enrollment and verification sets are different.

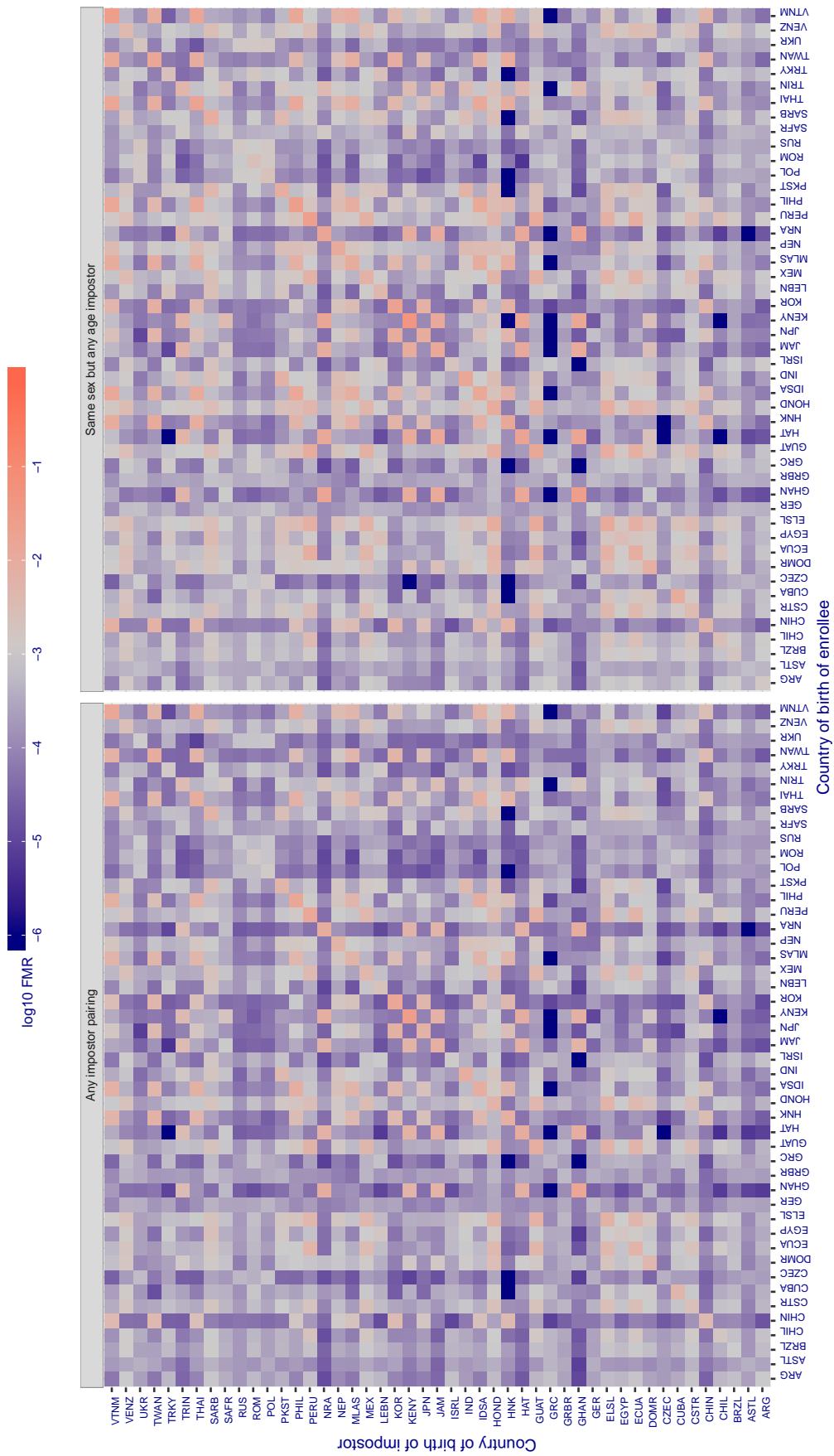
**Cross country FMR at threshold T = 0.662 for algorithm alchera\_000, giving FMR(T) = 0.001 globally.**

Figure 213: For algorithm alchera-000 operating on visa images, the heatmap shows false match rates observed over impostor comparisons of faces from different individuals who were born in the given country pair. False matches are counted against a recognition threshold fixed globally to give the target FMR in the plot title, computed over all on the order of  $10^{10}$  impostor comparisons. If text appears in each box it give the same quantity as that coded by the color. Grey indicates FMR is at the intended FMR target level. Light red colors present a security vulnerability to, for example, a passport gate. Each +1 increase in  $\log_{10} \text{FMR}$  corresponds to a factor of 10 increase in FMR. The matrix is not quite symmetric because images in the enrollment and verification sets are different.

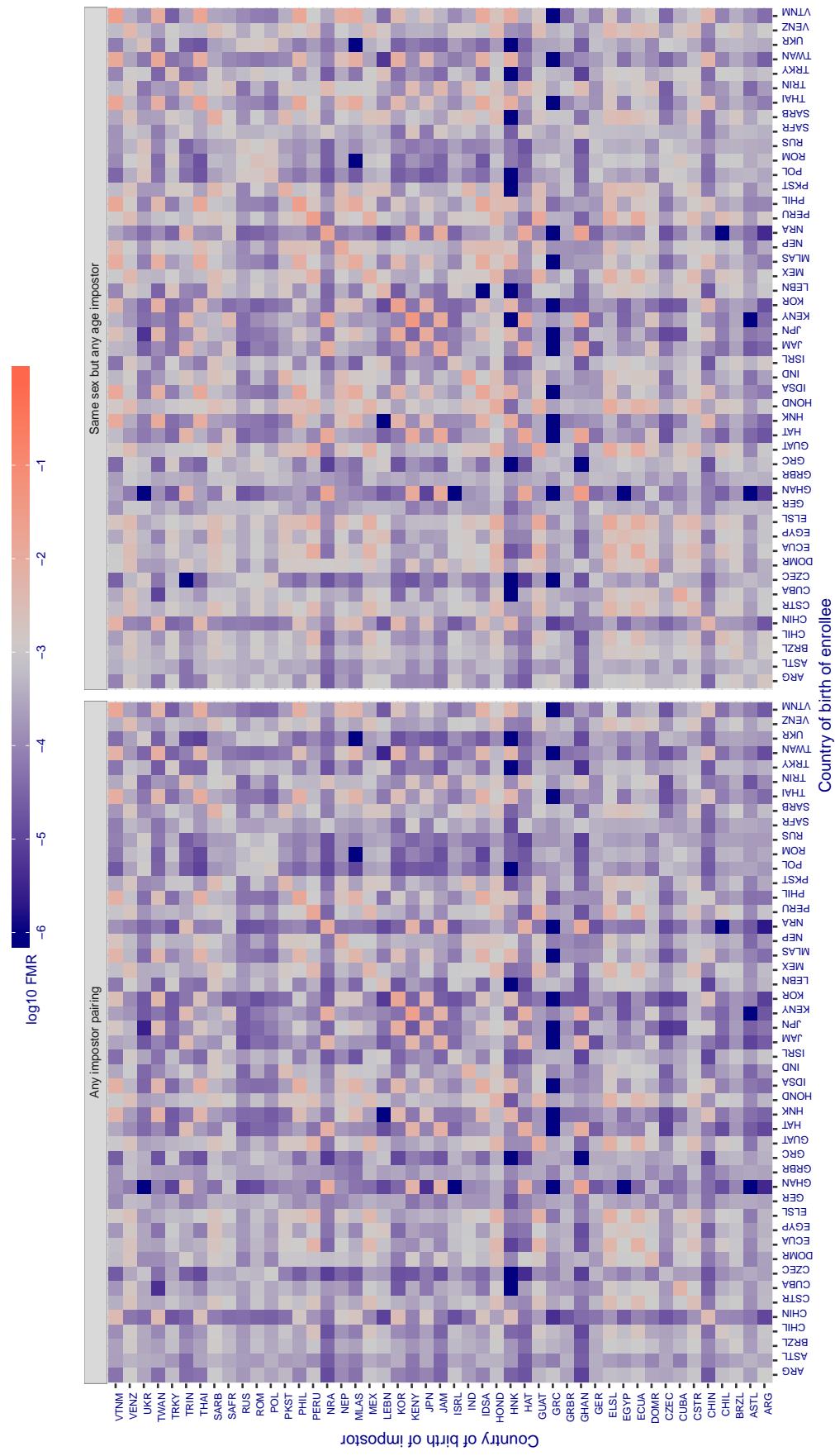
**Cross country FMR at threshold  $T = 0.667$  for algorithm alchera\_001, giving  $FMR(T) = 0.001$  globally.**

Figure 214: For algorithm alchera-001 operating on visa images, the heatmap shows false match rates observed over impostor comparisons of faces from different individuals who were born in the given country pair. False matches are counted against a recognition threshold fixed globally to give the target  $FMR$  in the plot title, computed over all on the order of  $10^{10}$  impostor comparisons. If text appears in each box it give the same quantity as that coded by the color. Grey indicates  $FMR$  is at the intended  $FMR$  target level. Light red colors present a security vulnerability to, for example, a passport gate. Each +1 increase in  $\log_{10} FMR$  corresponds to a factor of 10 increase in  $FMR$ . The matrix is not quite symmetric because images in the enrollment and verification sets are different.

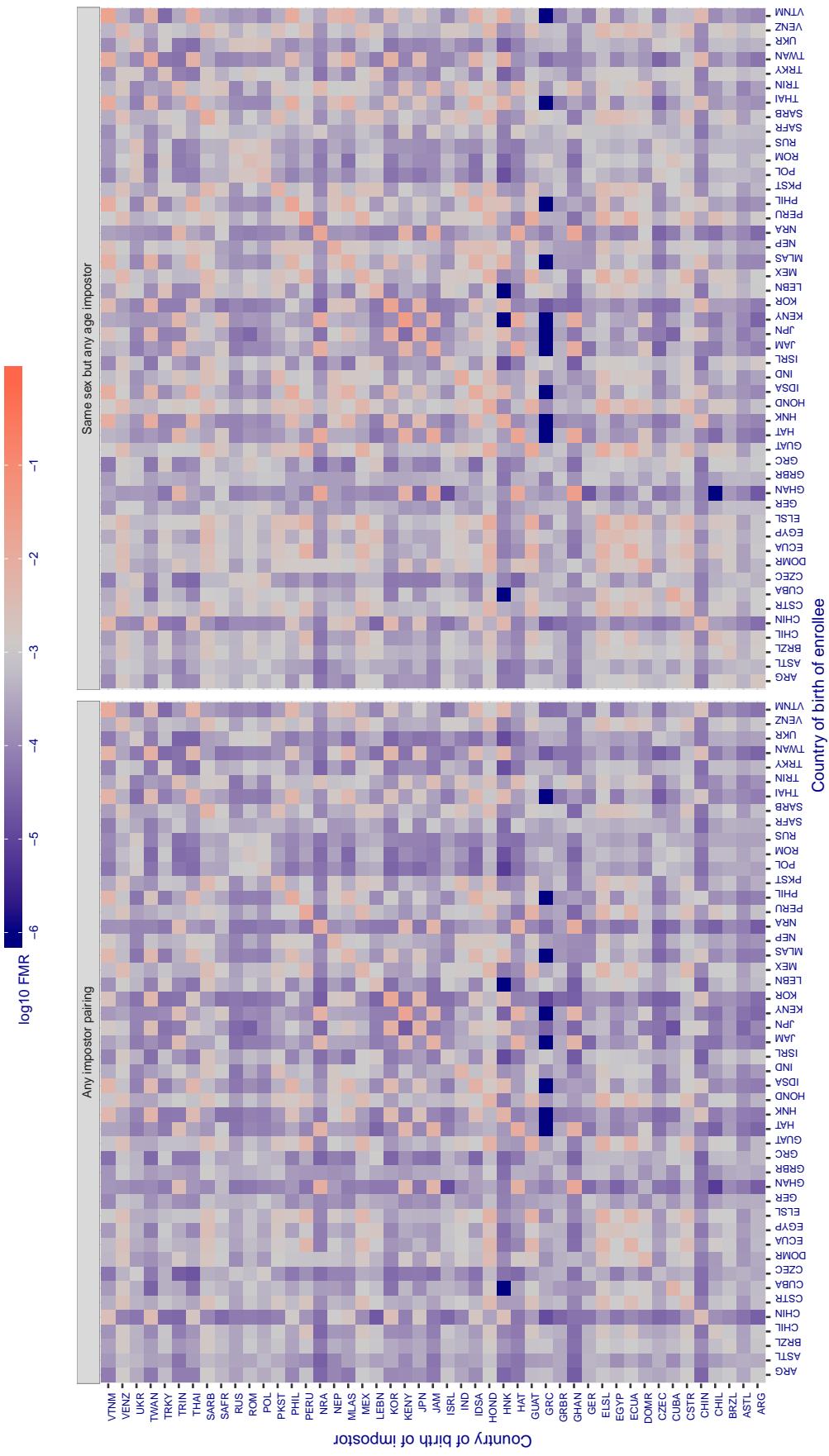
**Cross country FMR at threshold T = 0.339 for algorithm allgovision\_000, giving FMR(T) = 0.001 globally.**

Figure 215: For algorithm allgovision-000 operating on visa images, the heatmap shows false match rates observed over impostor comparisons of faces from different individuals who were born in the given country pair. False matches are counted against a recognition threshold fixed globally to give the target FMR in the plot title, computed over all on the order of  $10^{10}$  impostor comparisons. If text appears in each box it give the same quantity as that coded by the color. Grey indicates FMR is at the intended FMR target level. Light red colors present a security vulnerability to, for example, a passport gate. Each +1 increase in  $\log_{10}$  FMR corresponds to a factor of 10 increase in FMR. The matrix is not quite symmetric because images in the enrollment and verification sets are different.

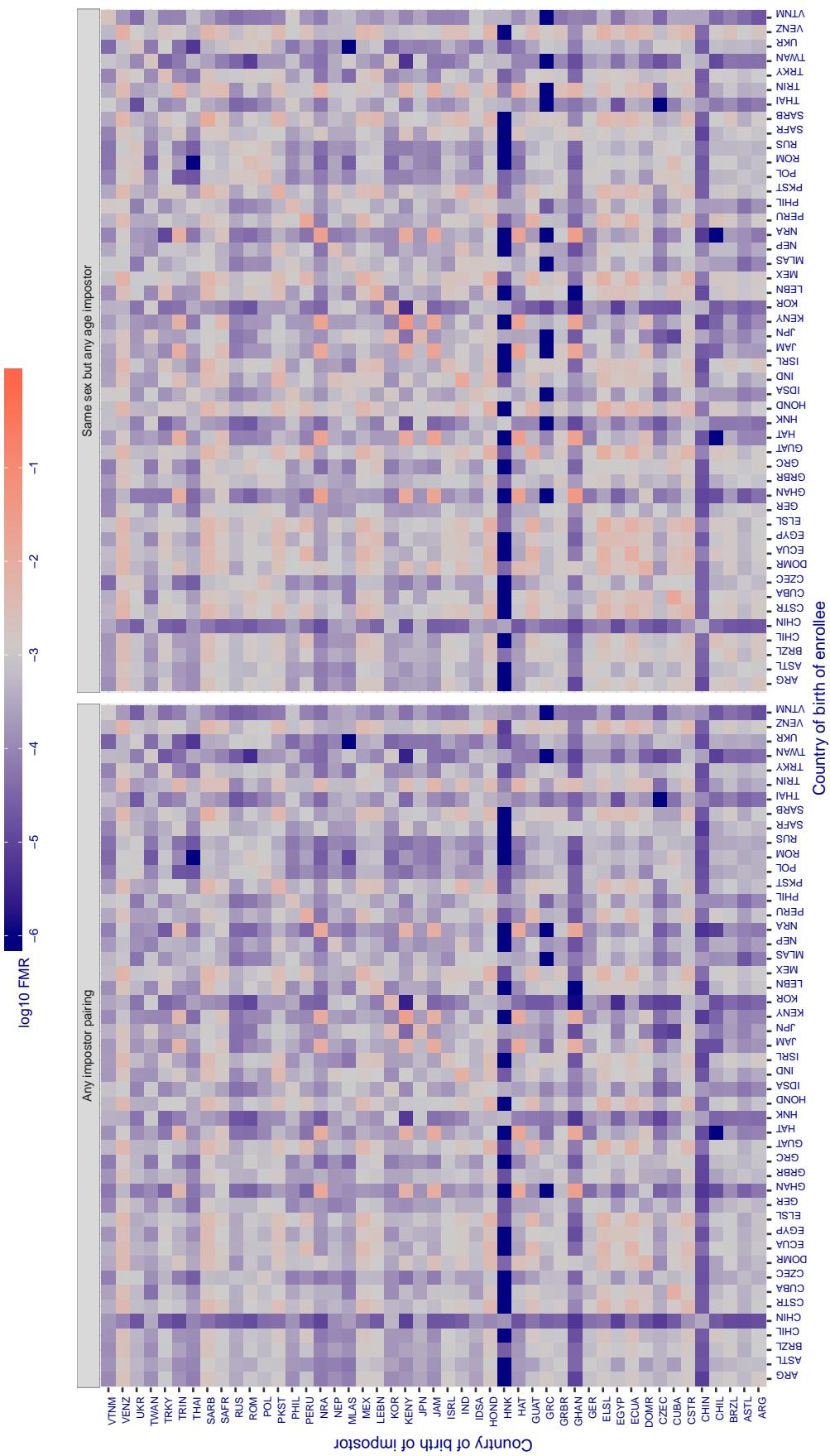
**Cross country FMR at threshold T = 0.297 for algorithm anke\_002, giving  $\text{FMR}(T) = 0.001$  globally.**

Figure 216: For algorithm anke-002 operating on visa images, the heatmap shows false match rates observed over impostor comparisons of faces from different individuals who were born in the given country pair. False matches are counted against a recognition threshold fixed globally to give the target FMR in the plot title, computed over all on the order of  $10^{10}$  impostor comparisons. If text appears in each box it give the same quantity as that coded by the color. Grey indicates FMR is at the intended FMR target level. Light red colors present a security vulnerability to, for example, a passport gate. Each +1 increase in  $\log_{10} \text{FMR}$  corresponds to a factor of 10 increase in FMR. The matrix is not quite symmetric because images in the enrollment and verification sets are different.

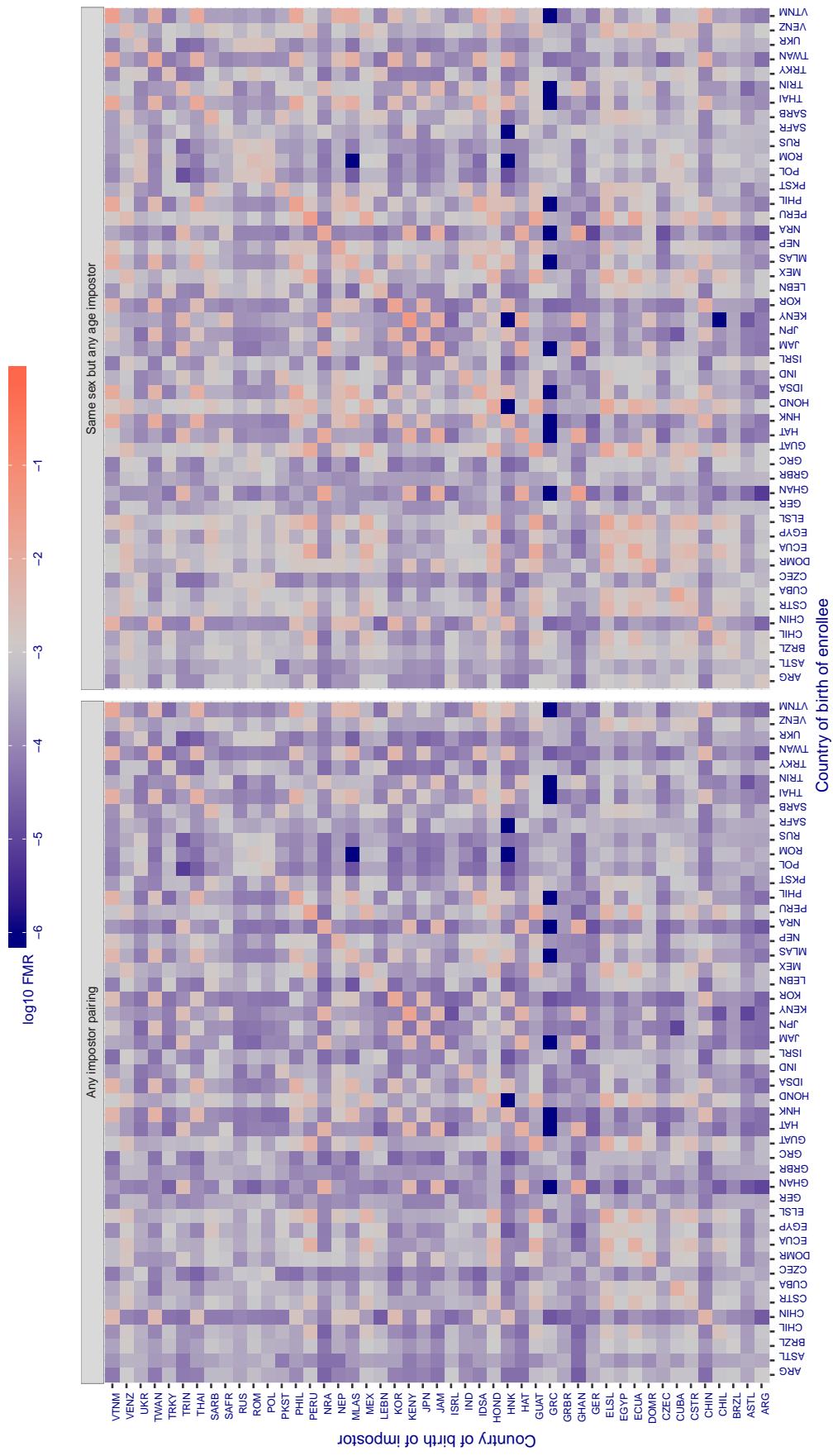
**Cross country FMR at threshold T = 0.313 for algorithm anke\_003, giving  $\text{FMR}(T) = 0.001$  globally.**

Figure 217: For algorithm anke-003 operating on visa images, the heatmap shows false match rates observed over impostor comparisons of faces from different individuals who were born in the given country pair. False matches are counted against a recognition threshold fixed globally to give the target FMR in the plot title, computed over all on the order of  $10^{10}$  impostor comparisons. If text appears in each box it give the same quantity as that coded by the color. Grey indicates FMR is at the intended FMR target level. Light red colors present a security vulnerability to, for example, a passport gate. Each +1 increase in  $\log_{10} \text{FMR}$  corresponds to a factor of 10 increase in FMR. The matrix is not quite symmetric because images in the enrollment and verification sets are different.

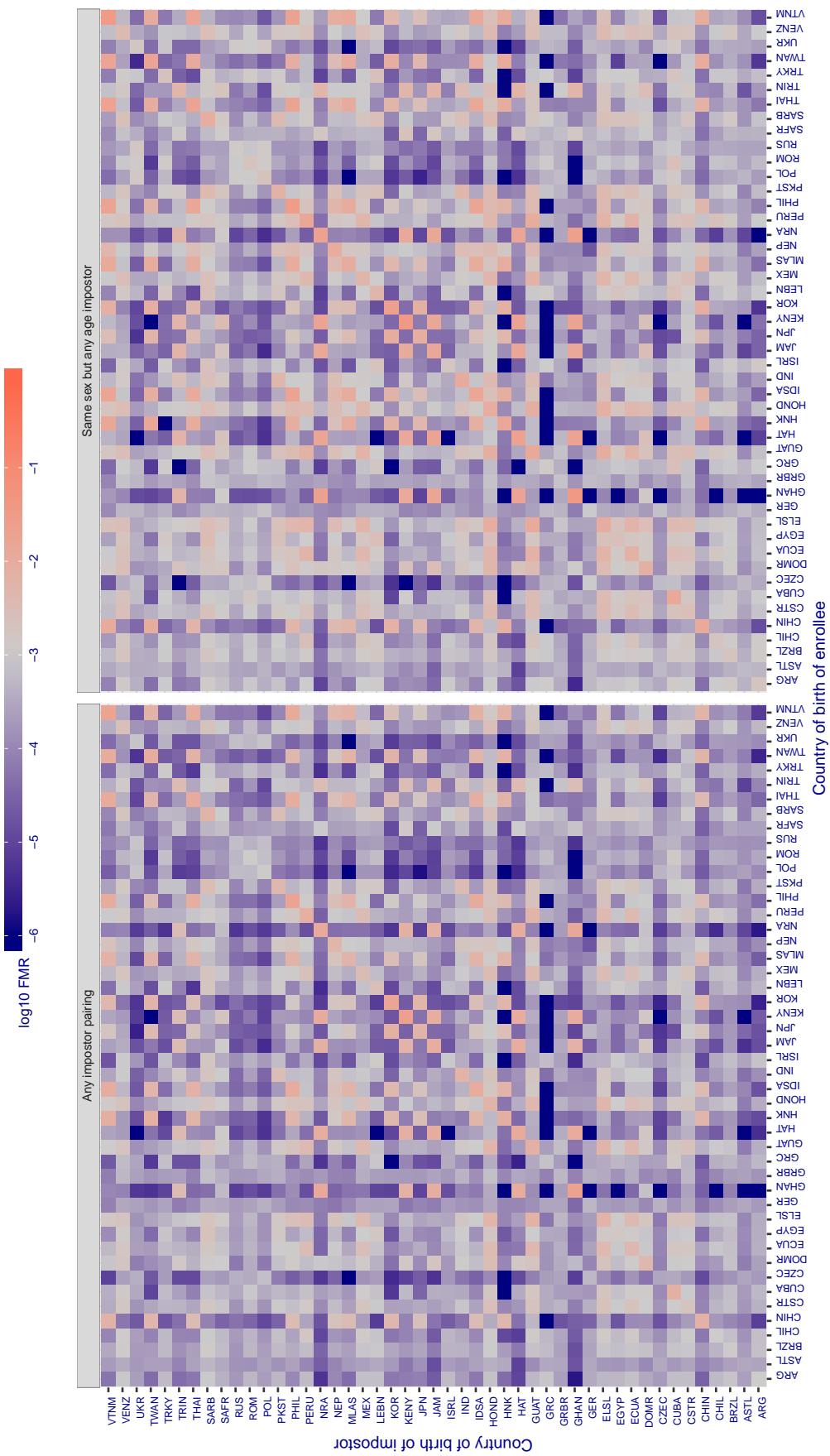
**Cross country FMR at threshold T = 1.431 for algorithm anyvision\_002, giving FMR(T) = 0.001 globally.**

Figure 218: For algorithm anyvision-002 operating on visa images, the heatmap shows false match rates observed over impostor comparisons of faces from different individuals who were born in the given country pair. False matches are counted against a recognition threshold fixed globally to give the target FMR in the plot title, computed over all on the order of  $10^{10}$  impostor comparisons. If text appears in each box it give the same quantity as that coded by the color. Grey indicates FMR is at the intended FMR target level. Light red colors present a security vulnerability to, for example, a passport gate. Each +1 increase in  $\log_{10} \text{FMR}$  corresponds to a factor of 10 increase in FMR. The matrix is not quite symmetric because images in the enrollment and verification sets are different.

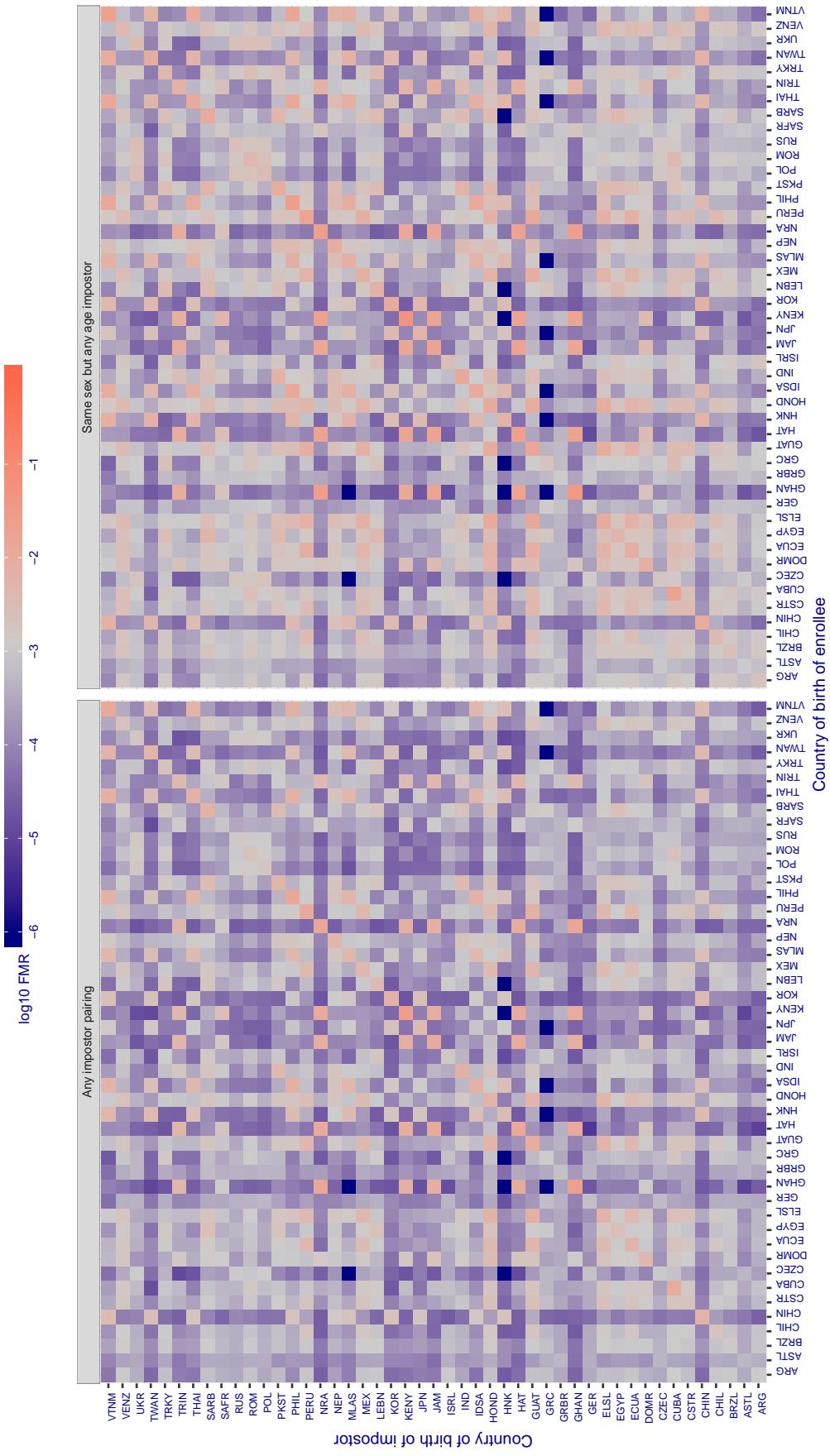
**Cross country FMR at threshold T = 1.297 for algorithm anyvision\_004, giving FMR(T) = 0.001 globally.**

Figure 219: For algorithm anyvision-004 operating on visa images, the heatmap shows false match rates observed over impostor comparisons of faces from different individuals who were born in the given country pair. False matches are counted against a recognition threshold fixed globally to give the target FMR in the plot title, computed over all on the order of  $10^{10}$  impostor comparisons. If text appears in each box it give the same quantity as that coded by the color. Grey indicates FMR is at the intended FMR target level. Light red colors present a security vulnerability to, for example, a passport gate. Each +1 increase in  $\log_{10} FMR$  corresponds to a factor of 10 increase in FMR. The matrix is not quite symmetric because images in the enrollment and verification sets are different.

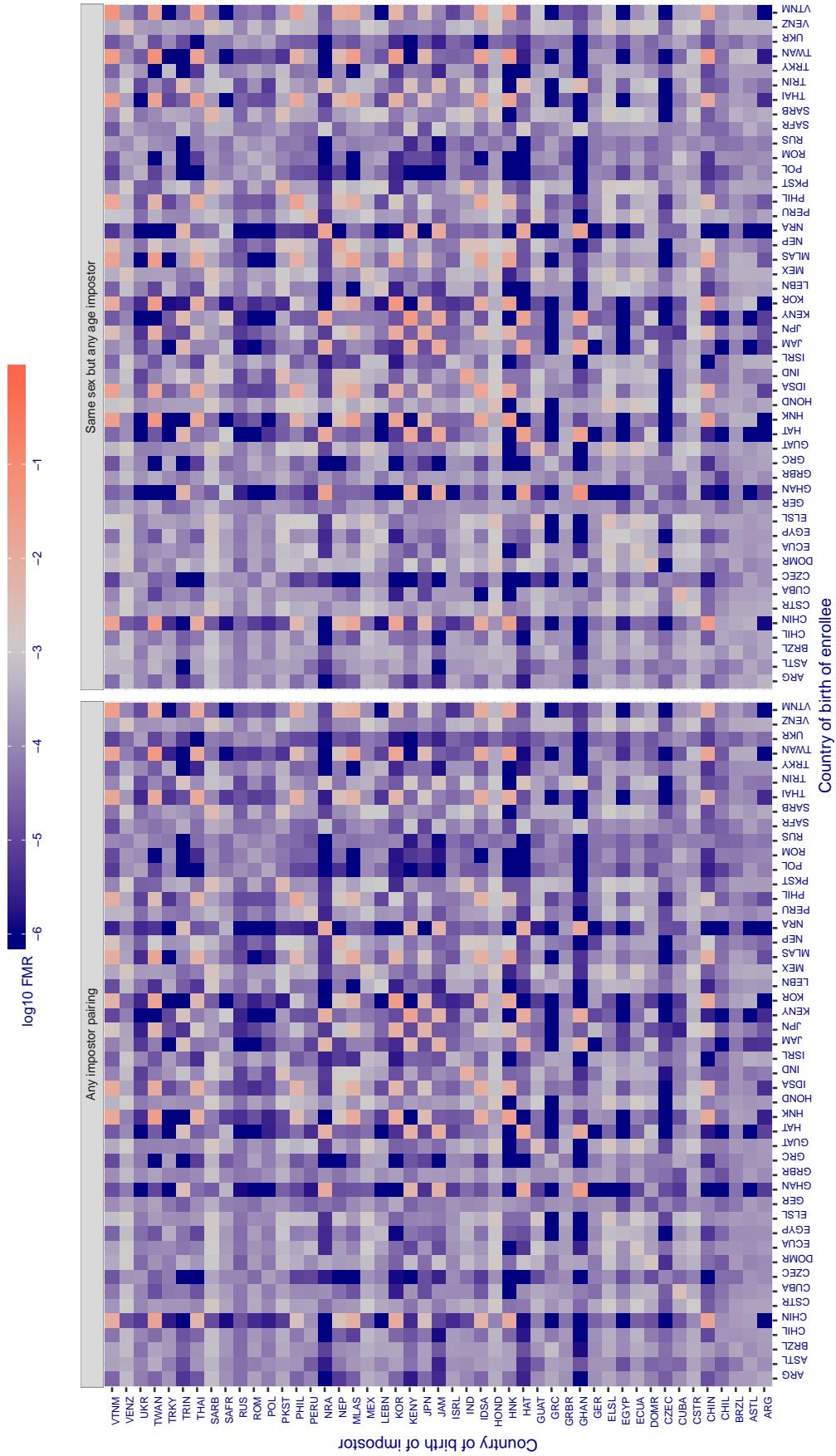
**Cross country FMR at threshold T = 2.758 for algorithm aware\_003, giving FMR(T) = 0.001 globally.**

Figure 220: For algorithm aware-003 operating on visa images, the heatmap shows false match rates observed over impostor comparisons of faces from different individuals who were born in the given country pair. False matches are counted against a recognition threshold fixed globally to give the target FMR in the plot title, computed over all on the order of  $10^{10}$  impostor comparisons. If text appears in each box it give the same quantity as that coded by the color. Grey indicates FMR is at the intended FMR target level. Light red colors present a security vulnerability to, for example, a passport gate. Each +1 increase in  $\log_{10} \text{FMR}$  corresponds to a factor of 10 increase in FMR. The matrix is not quite symmetric because images in the enrollment and verification sets are different.

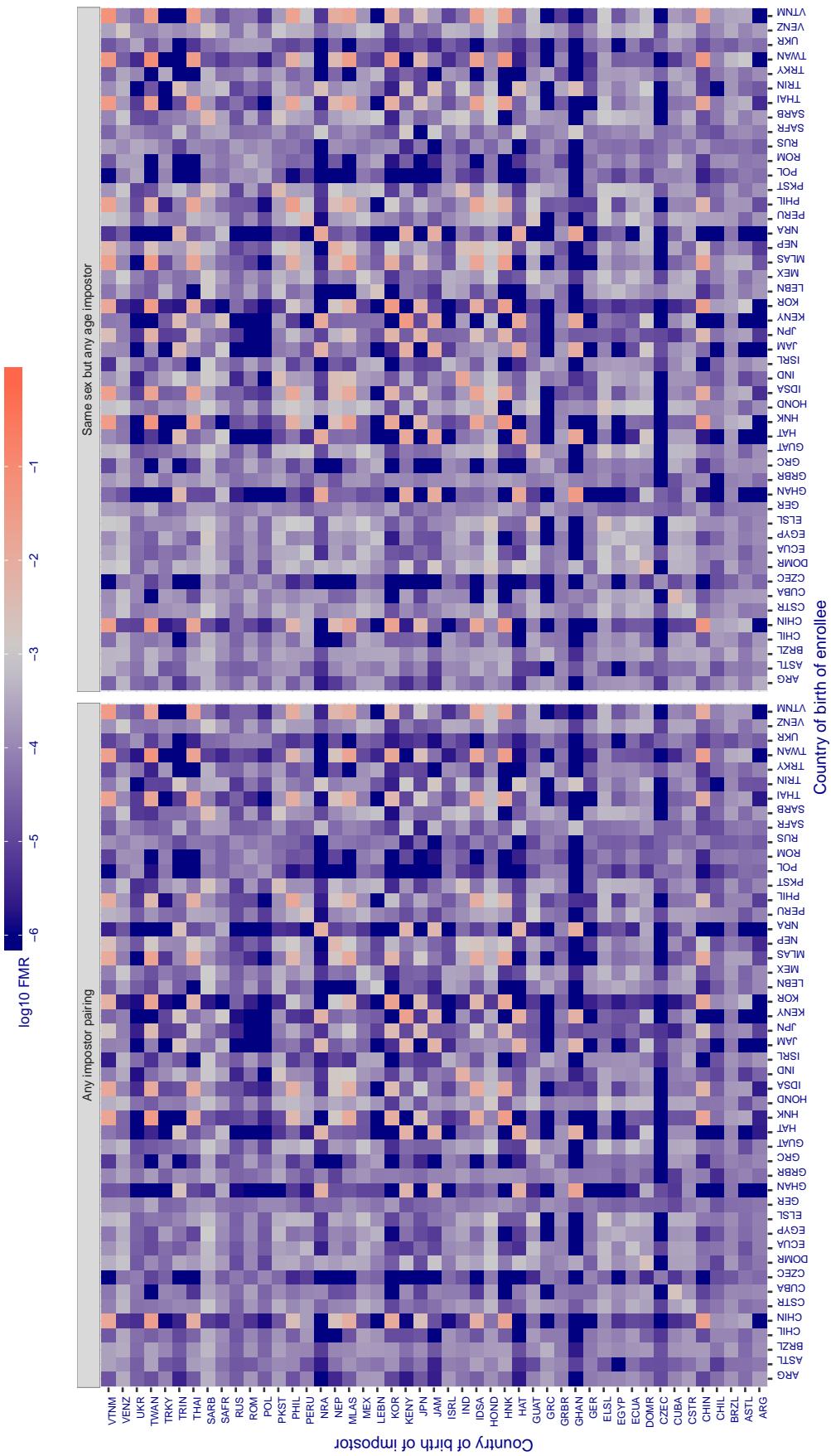
**Cross country FMR at threshold T = 3.681 for algorithm aware\_004, giving FMR(T) = 0.001 globally.**

Figure 221: For algorithm aware-004 operating on visa images, the heatmap shows false match rates observed over impostor comparisons of faces from different individuals who were born in the given country pair. False matches are counted against a recognition threshold fixed globally to give the target FMR in the plot title, computed over all on the order of  $10^{10}$  impostor comparisons. If text appears in each box it give the same quantity as that coded by the color. Grey indicates FMR is at the intended FMR target level. Light red colors present a security vulnerability to, for example, a passport gate. Each +1 increase in  $\log_{10} FMR$  corresponds to a factor of 10 increase in FMR. The matrix is not quite symmetric because images in the enrollment and verification sets are different.

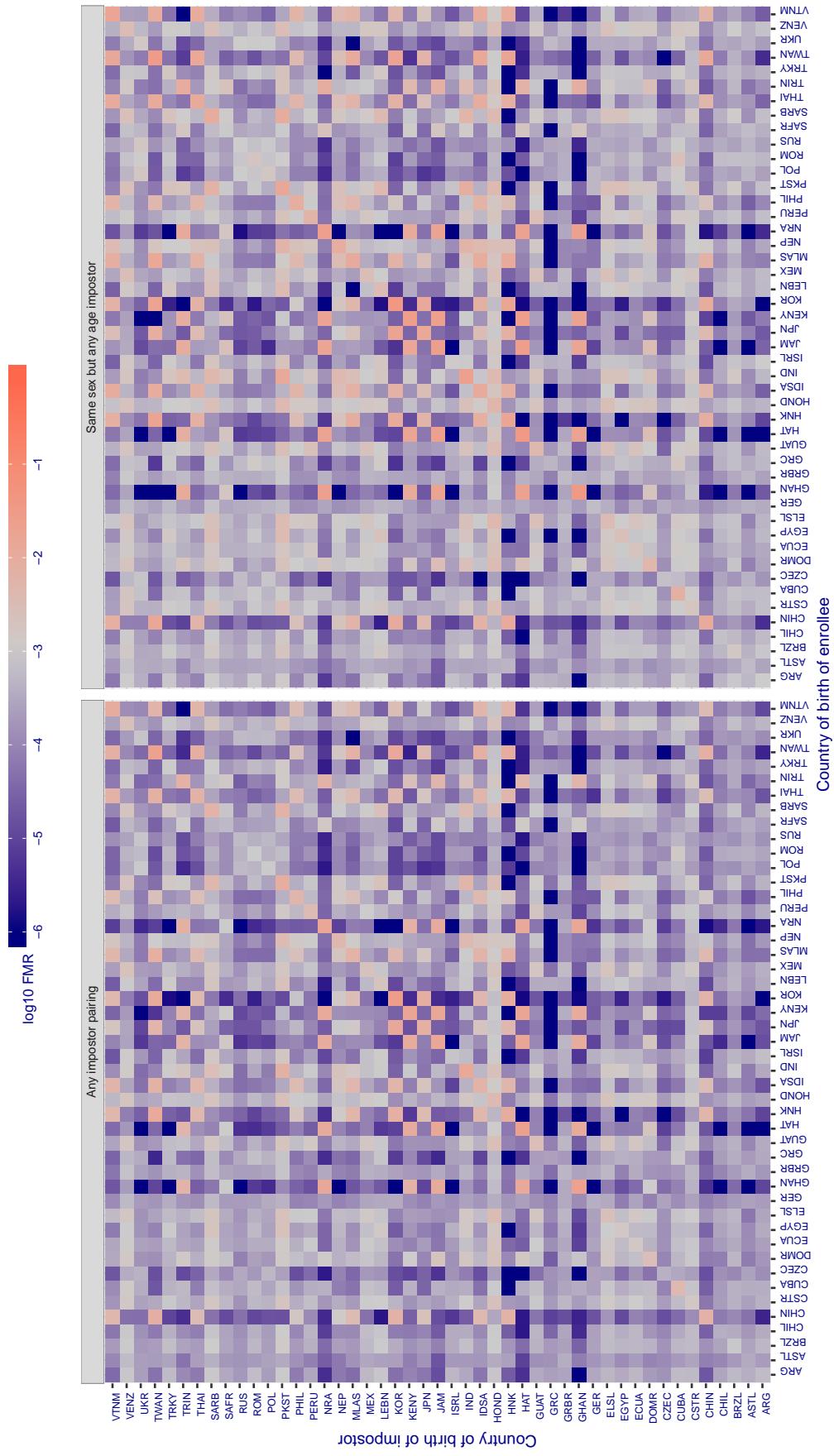
**Cross country FMR at threshold T = 0.800 for algorithm ayonix\_000, giving FMR(T) = 0.001 globally.**

Figure 222: For algorithm ayonix-000 operating on visa images, the heatmap shows false match rates observed over impostor comparisons of faces from different individuals who were born in the given country pair. False matches are counted against a recognition threshold fixed globally to give the target FMR in the plot title, computed over all on the order of  $10^{10}$  impostor comparisons. If text appears in each box it give the same quantity as that coded by the color. Grey indicates FMR is at the intended FMR target level. Light red colors present a security vulnerability to, for example, a passport gate. Each +1 increase in  $\log_{10} FMR$  corresponds to a factor of 10 increase in FMR. The matrix is not quite symmetric because images in the enrollment and verification sets are different.

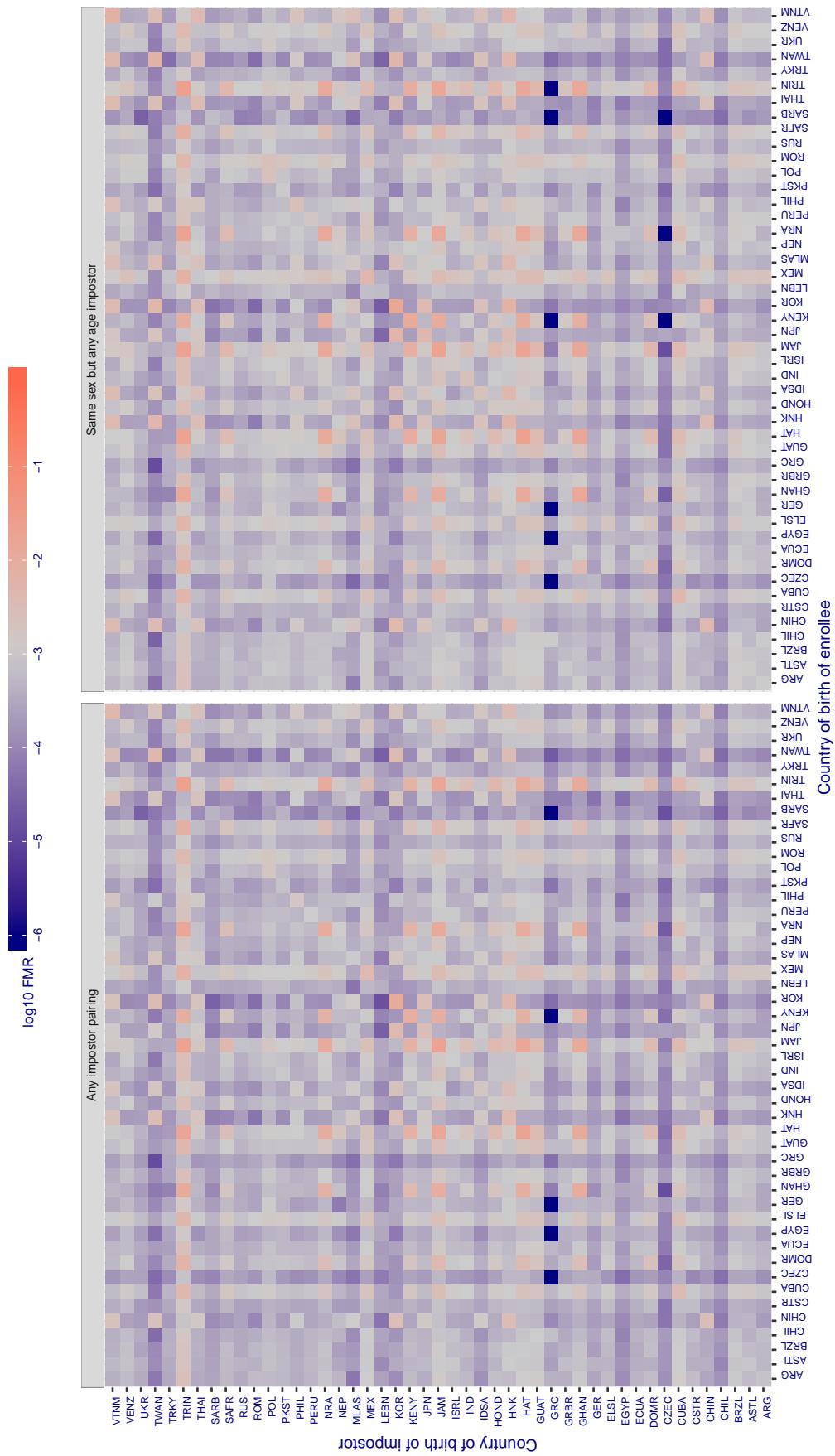
**Cross country FMR at threshold T = 0.649 for algorithm bm\_001, giving FMR(T) = 0.001 globally.**

Figure 223: For algorithm *bm-001* operating on visa images, the heatmap shows false match rates observed over impostor comparisons of faces from different individuals who were born in the given country pair. False matches are counted against a recognition threshold fixed globally to give the target FMR in the plot title, computed over all on the order of  $10^{10}$  impostor comparisons. If text appears in each box it give the same quantity as that coded by the color. Grey indicates FMR is at the intended FMR target level. Light red colors present a security vulnerability to, for example, a passport gate. Each +1 increase in  $\log_{10}$ FMR corresponds to a factor of 10 increase in FMR. The matrix is not quite symmetric because images in the enrollment and verification sets are different.

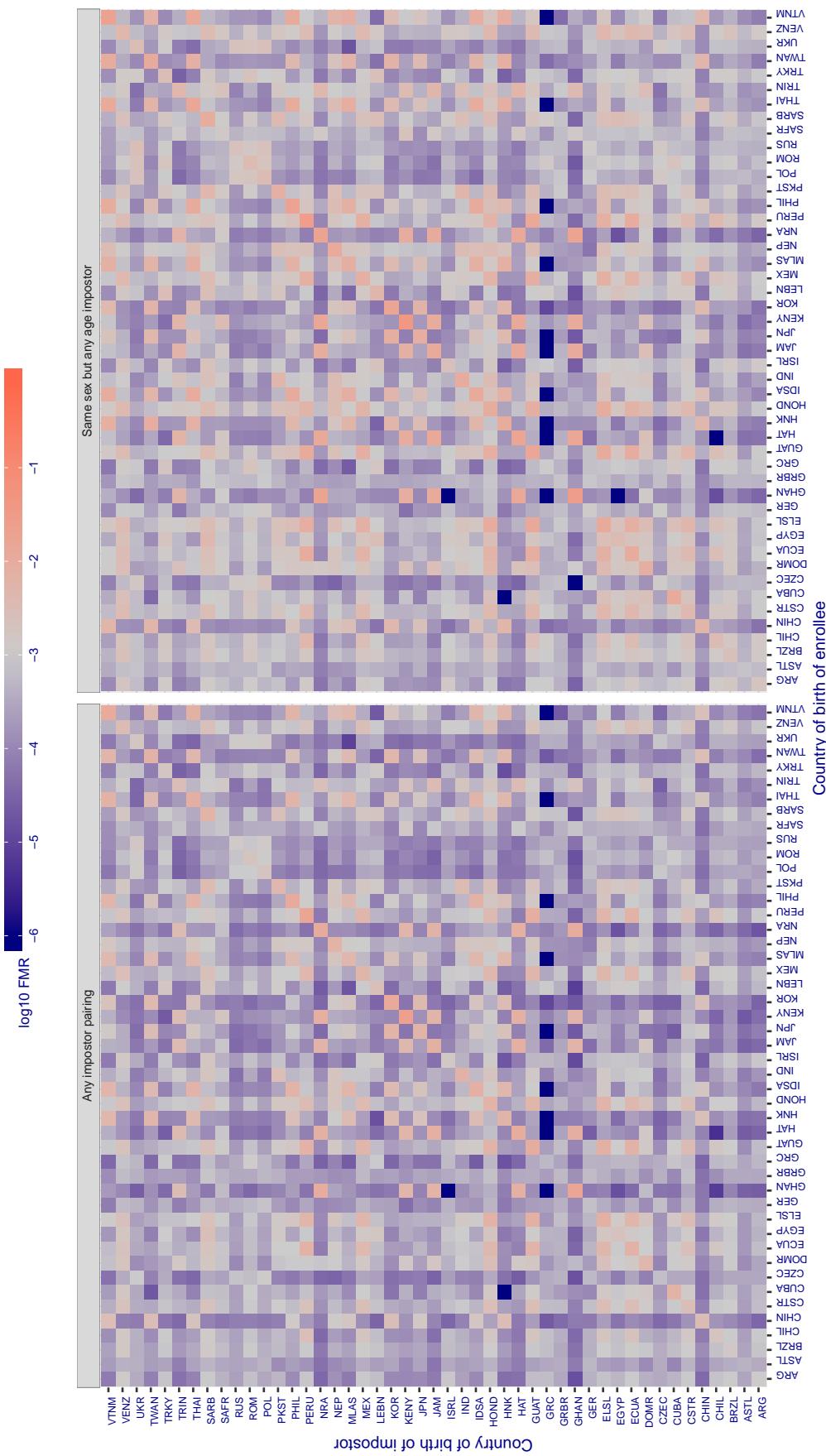
**Cross country FMR at threshold T = 0.306 for algorithm camvi\_002, giving  $\text{FMR}(T) = 0.001$  globally.**

Figure 224: For algorithm camvi-002 operating on visa images, the heatmap shows false match rates observed over impostor comparisons of faces from different individuals who were born in the given country pair. False matches are counted against a recognition threshold fixed globally to give the target FMR in the plot title, computed over all on the order of  $10^{10}$  impostor comparisons. If text appears in each box it give the same quantity as that coded by the color. Grey indicates FMR is at the intended FMR target level. Light red colors present a security vulnerability to, for example, a passport gate. Each +1 increase in  $\log_{10} \text{FMR}$  corresponds to a factor of 10 increase in FMR. The matrix is not quite symmetric because images in the enrollment and verification sets are different.

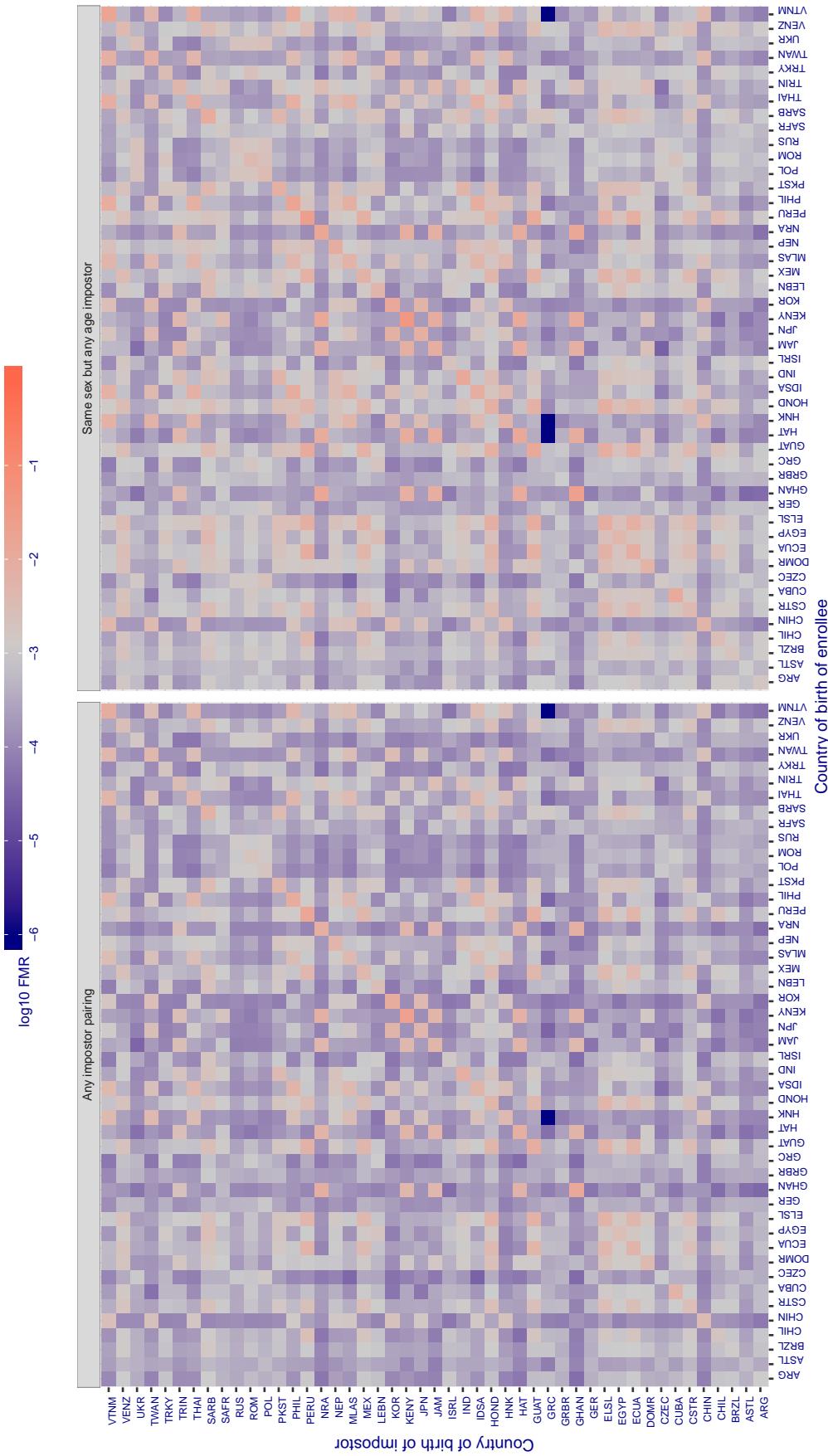
**Cross country FMR at threshold T = 0.301 for algorithm camvi\_003, giving  $\text{FMR}(T) = 0.001$  globally.**

Figure 225: For algorithm camvi-003 operating on visa images, the heatmap shows false match rates observed over impostor comparisons of faces from different individuals who were born in the given country pair. False matches are counted against a recognition threshold fixed globally to give the target  $\text{FMR}$  in the plot title, computed over all on the order of  $10^{10}$  impostor comparisons. If text appears in each box it give the same quantity as that coded by the color. Grey indicates  $\text{FMR}$  is at the intended  $\text{FMR}$  target level. Light red colors present a security vulnerability to, for example, a passport gate. Each +1 increase in  $\log_{10} \text{FMR}$  corresponds to a factor of 10 increase in  $\text{FMR}$ . The matrix is not quite symmetric because images in the enrollment and verification sets are different.

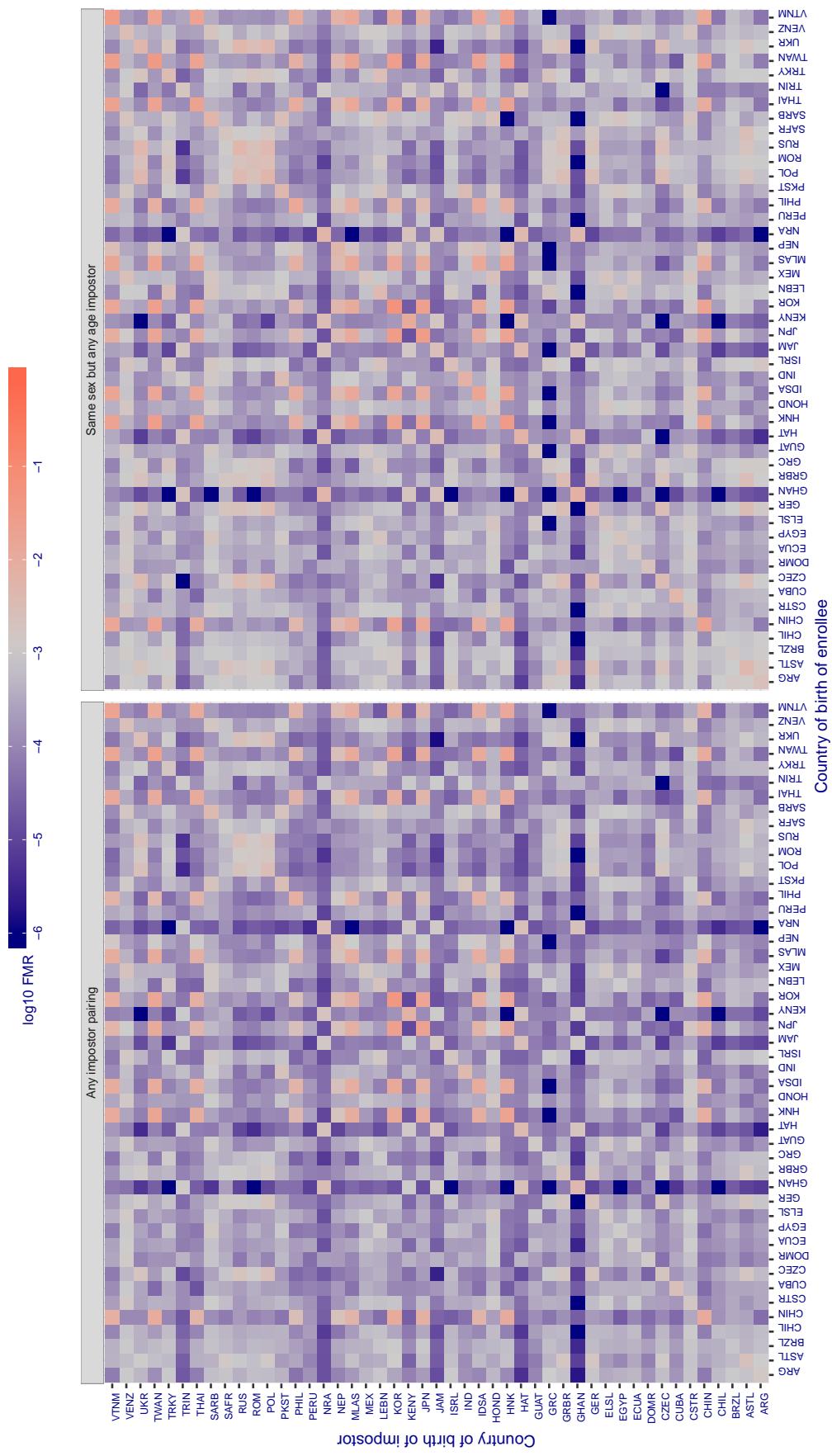
**Cross country FMR at threshold T = 0.346 for algorithm ceiec\_001, giving FMR(T) = 0.001 globally.**

Figure 226: For algorithm ceiec-001 operating on visa images, the heatmap shows false match rates observed over impostor comparisons of faces from different individuals who were born in the given country pair. False matches are counted against a recognition threshold fixed globally to give the target FMR in the plot title, computed over all on the order of  $10^{10}$  impostor comparisons. If text appears in each box it give the same quantity as that coded by the color. Grey indicates FMR is at the intended FMR target level. Light red colors present a security vulnerability to, for example, a passport gate. Each +1 increase in  $\log_{10}$  FMR corresponds to a factor of 10 increase in FMR. The matrix is not quite symmetric because images in the enrollment and verification sets are different.

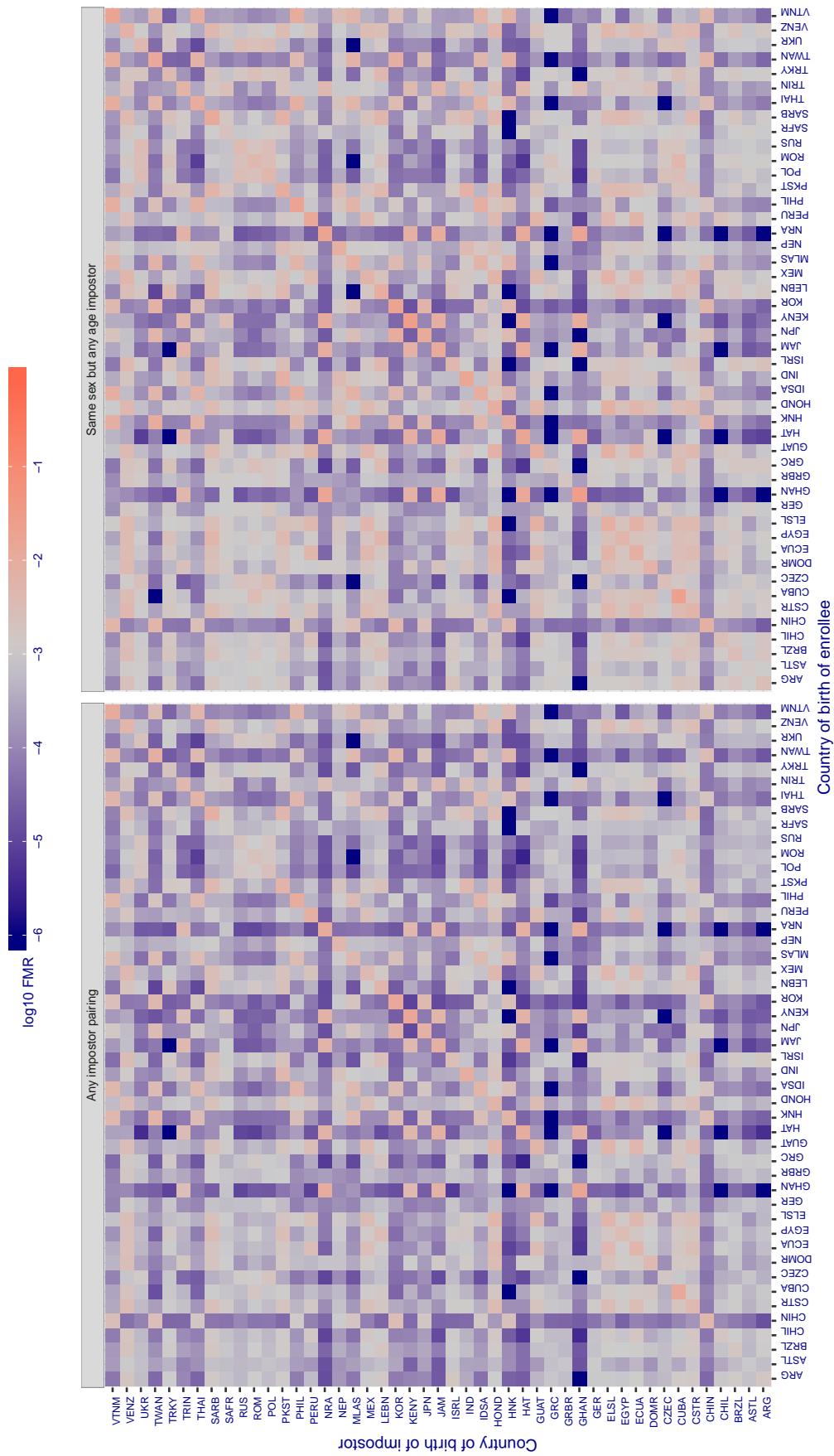
**Cross country FMR at threshold T = 3038.000 for algorithm cogent\_002, giving  $FMR(T) = 0.001$  globally.**

Figure 227: For algorithm cogent-002 operating on visa images, the heatmap shows false match rates observed over impostor comparisons of faces from different individuals who were born in the given country pair. False matches are counted against a recognition threshold fixed globally to give the target  $FMR$  in the plot title, computed over all on the order of  $10^{10}$  impostor comparisons. If text appears in each box it give the same quantity as that coded by the color. Grey indicates  $FMR$  is at the intended  $FMR$  target level. Light red colors present a security vulnerability to, for example, a passport gate. Each +1 increase in  $\log_{10} FMR$  corresponds to a factor of 10 increase in  $FMR$ . The matrix is not quite symmetric because images in the enrollment and verification sets are different.

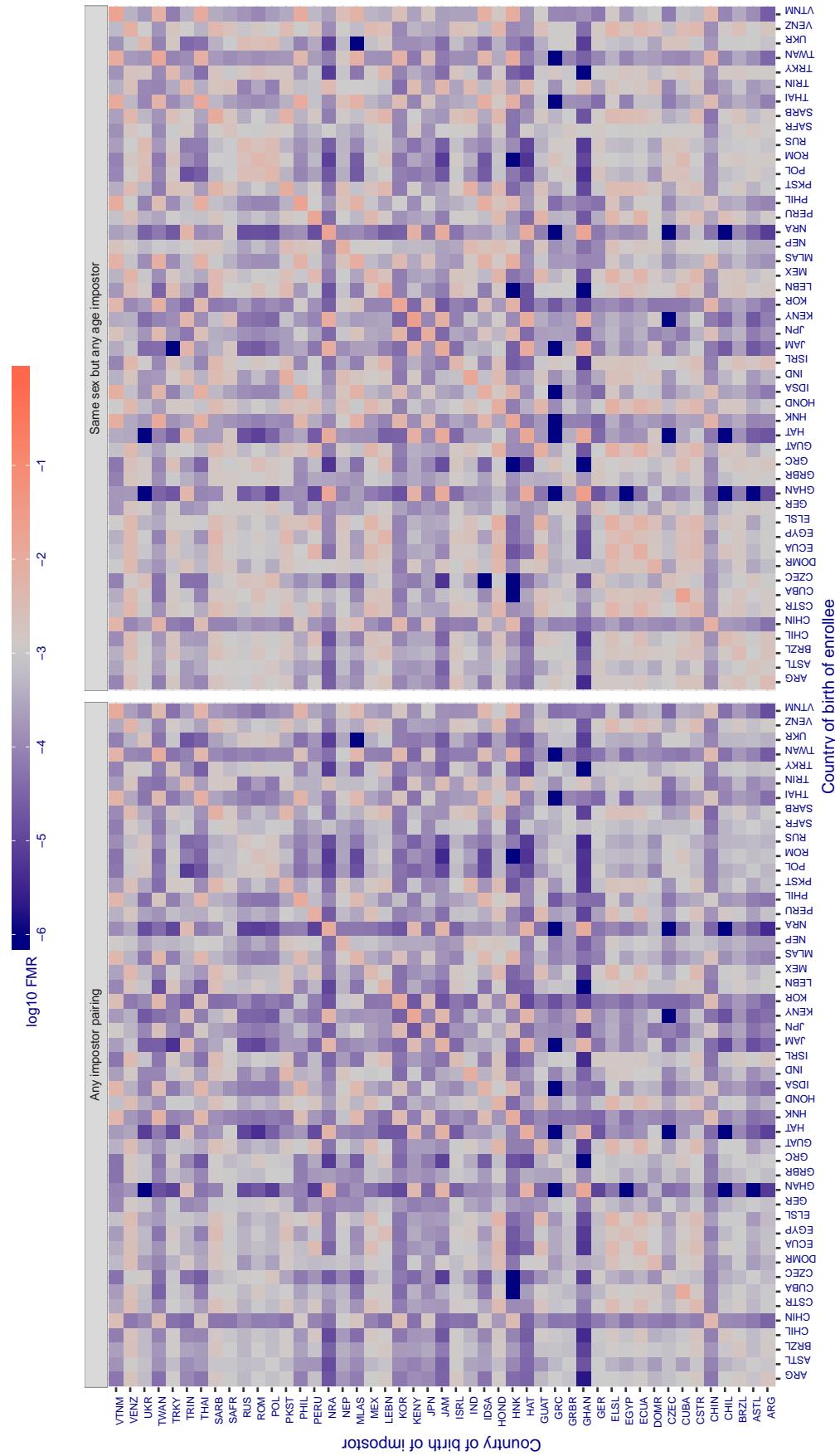
**Cross country FMR at threshold T = 2845.000 for algorithm cogent\_003, giving  $FMR(T) = 0.001$  globally.**

Figure 228: For algorithm cogent-003 operating on visa images, the heatmap shows false match rates observed over impostor comparisons of faces from different individuals who were born in the given country pair. False matches are counted against a recognition threshold fixed globally to give the target  $FMR$  in the plot title, computed over all on the order of  $10^{10}$  impostor comparisons. If text appears in each box it give the same quantity as that coded by the color. Grey indicates  $FMR$  is at the intended  $FMR$  target level. Light red colors present a security vulnerability to, for example, a passport gate. Each +1 increase in  $\log_{10} FMR$  corresponds to a factor of 10 increase in  $FMR$ . The matrix is not quite symmetric because images in the enrollment and verification sets are different.

**Cross country FMR at threshold  $T = 0.522$  for algorithm cognitec\_000, giving  $FMR(T) = 0.001$  globally.**

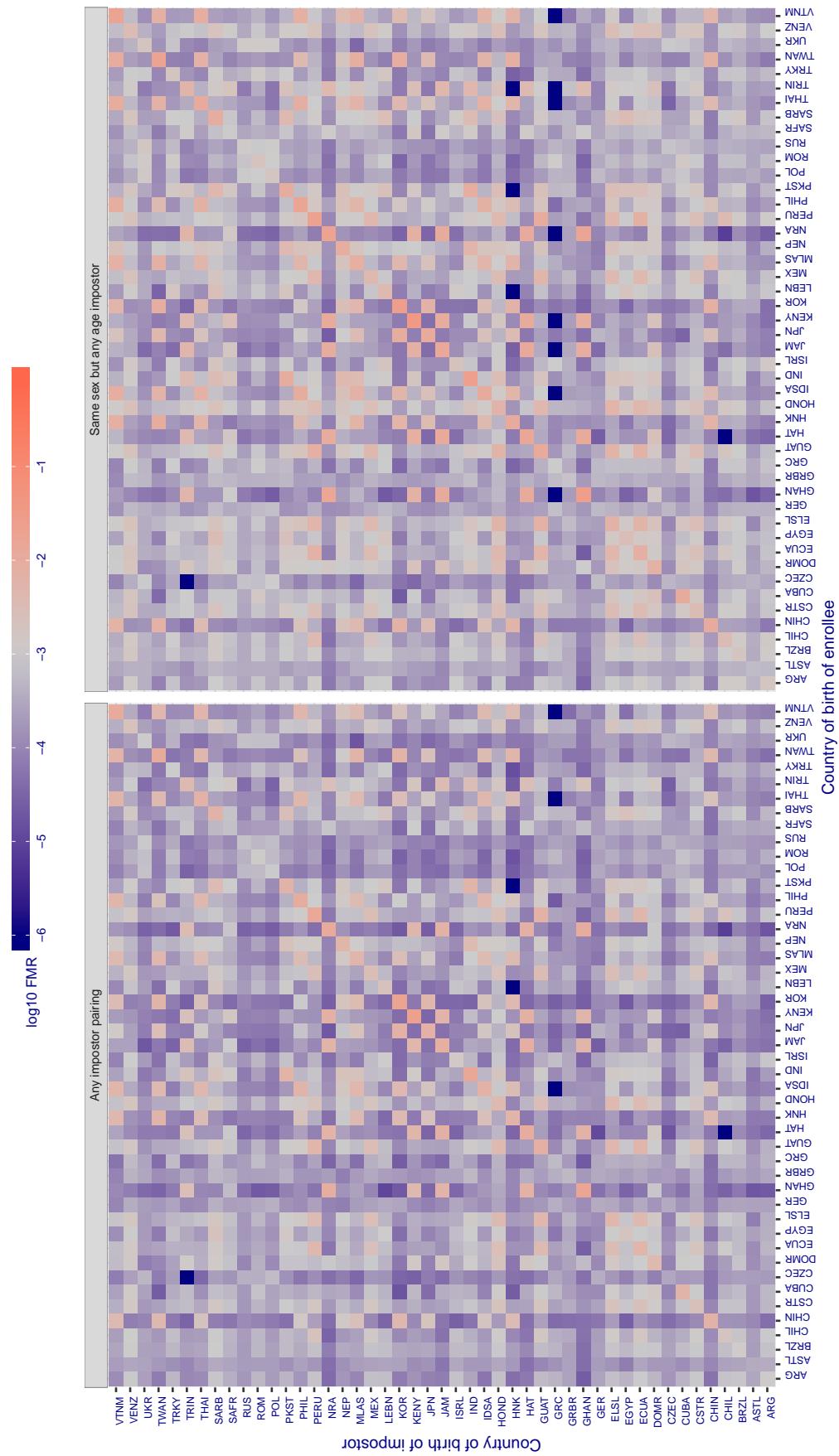


Figure 229: For algorithm cognitec-000 operating on visa images, the heatmap shows false match rates observed over impostor comparisons of faces from different individuals who were born in the given country pair. False matches are counted against a recognition threshold fixed globally to give the target FMR in the plot title, computed over all on the order of  $10^{10}$  impostor comparisons. If text appears in each box it give the same quantity as that coded by the color. Grey indicates FMR is at the intended FMR target level. Light red colors present a security vulnerability to, for example, a passport gate. Each +1 increase in  $\log_{10} FMR$  corresponds to a factor of 10 increase in FMR. The matrix is not quite symmetric because images in the enrollment and verification sets are different.

**Cross country FMR at threshold T = 0.522 for algorithm cognitec\_001, giving FMR(T) = 0.001 globally.**

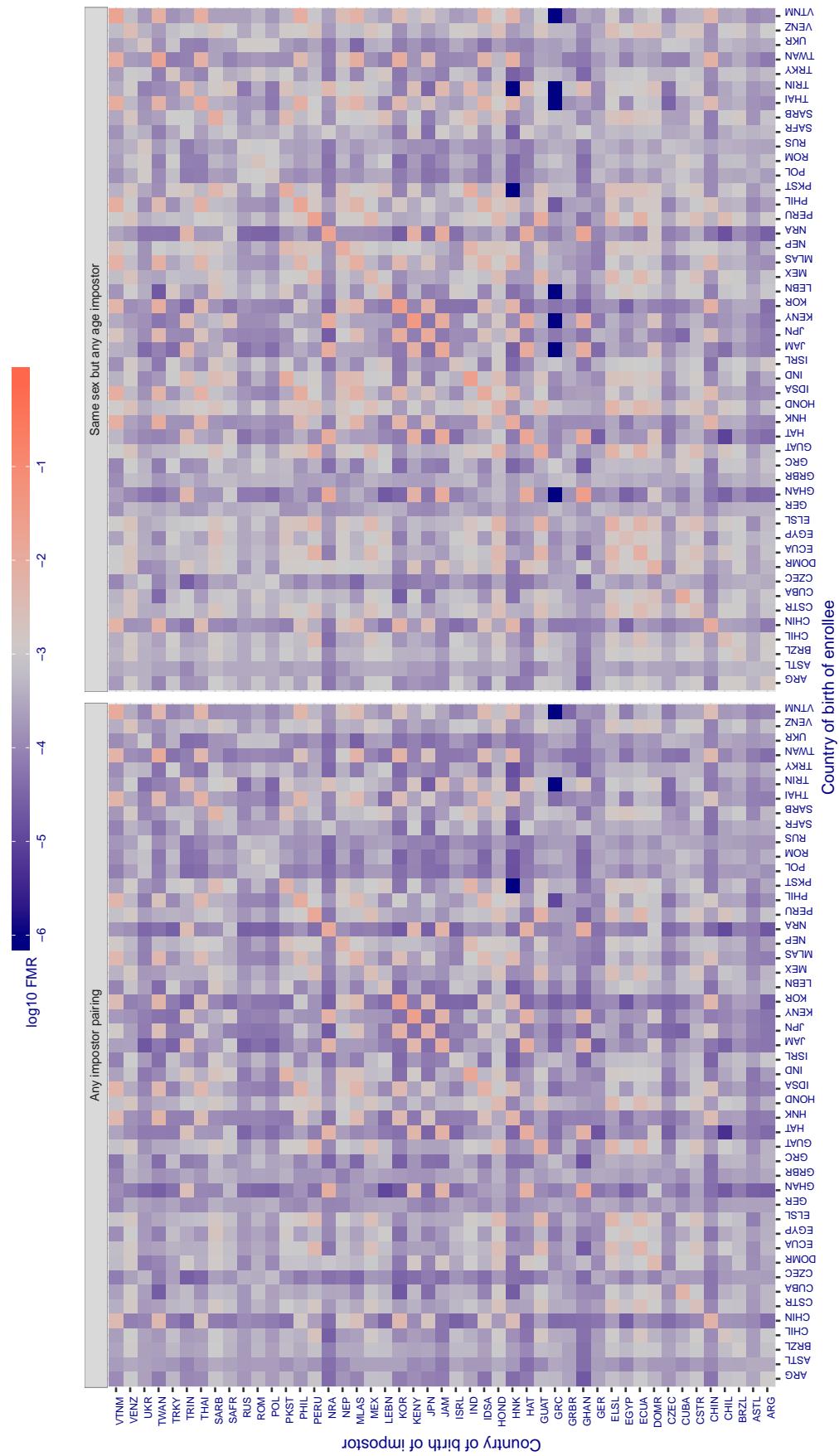


Figure 230: For algorithm cognitec-001 operating on visa images, the heatmap shows false match rates observed over impostor comparisons of faces from different individuals who were born in the given country pair. False matches are counted against a recognition threshold fixed globally to give the target FMR in the plot title, computed over all on the order of  $10^{10}$  impostor comparisons. If text appears in each box it give the same quantity as that coded by the color. Grey indicates FMR is at the intended FMR target level. Light red colors present a security vulnerability to, for example, a passport gate. Each +1 increase in  $\log_{10} FMR$  corresponds to a factor of 10 increase in FMR. The matrix is not quite symmetric because images in the enrollment and verification sets are different.

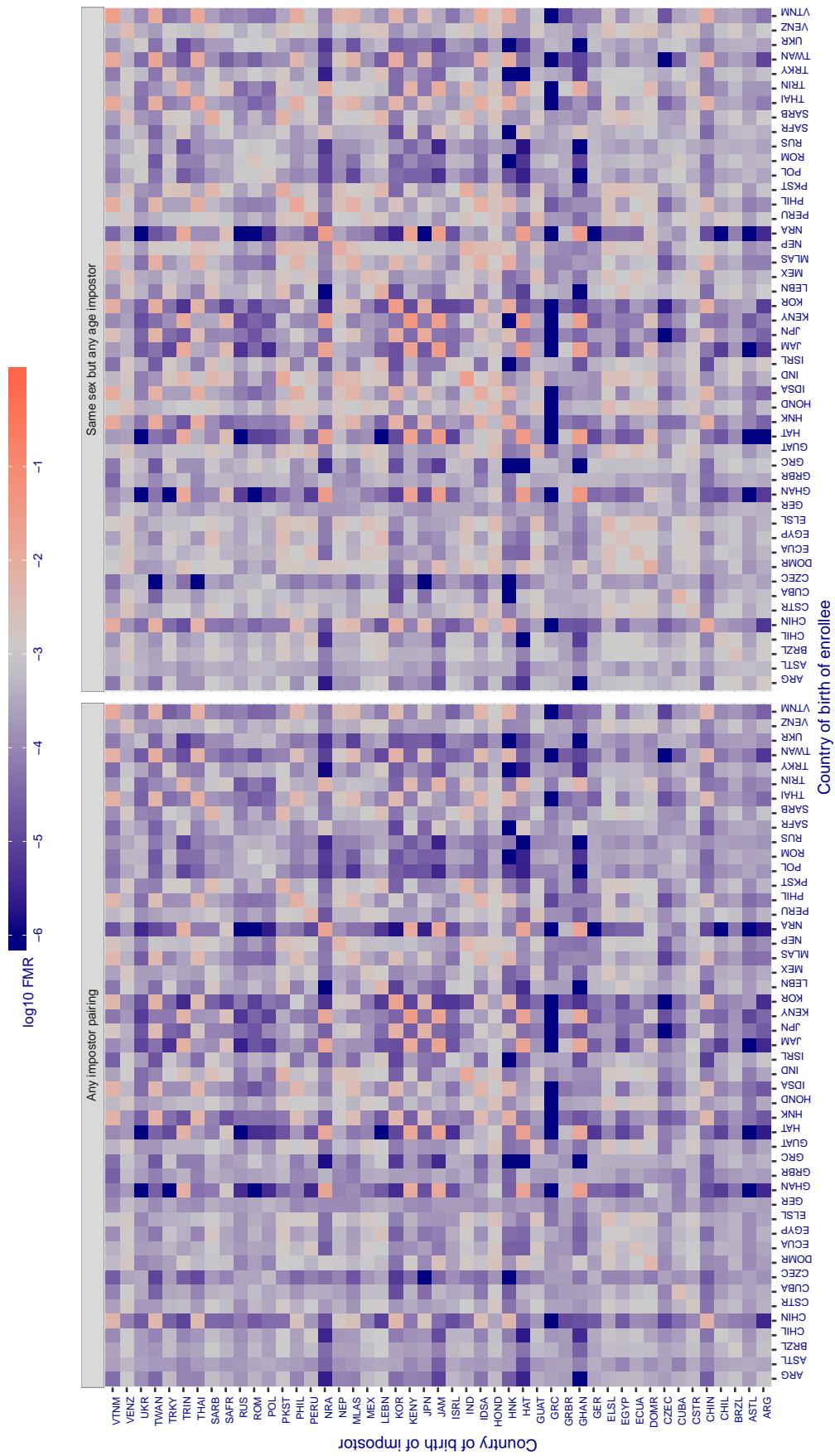
**Cross country FMR at threshold T = 0.702 for algorithm cyberextruder\_001, giving  $FMR(T) = 0.001$  globally.**

Figure 231: For algorithm cyberextruder-001 operating on visa images, the heatmap shows false match rates observed over impostor comparisons of faces from different individuals who were born in the given country pair. False matches are counted against a recognition threshold fixed globally to give the target FMR in the plot title, computed over all on the order of  $10^{10}$  impostor comparisons. If text appears in each box it give the same quantity as that coded by the color. Grey indicates FMR is at the intended FMR target level. Light red colors present a security vulnerability to, for example, a passport gate. Each +1 increase in  $\log_{10} FMR$  corresponds to a factor of 10 increase in FMR. The matrix is not quite symmetric because images in the enrollment and verification sets are different.

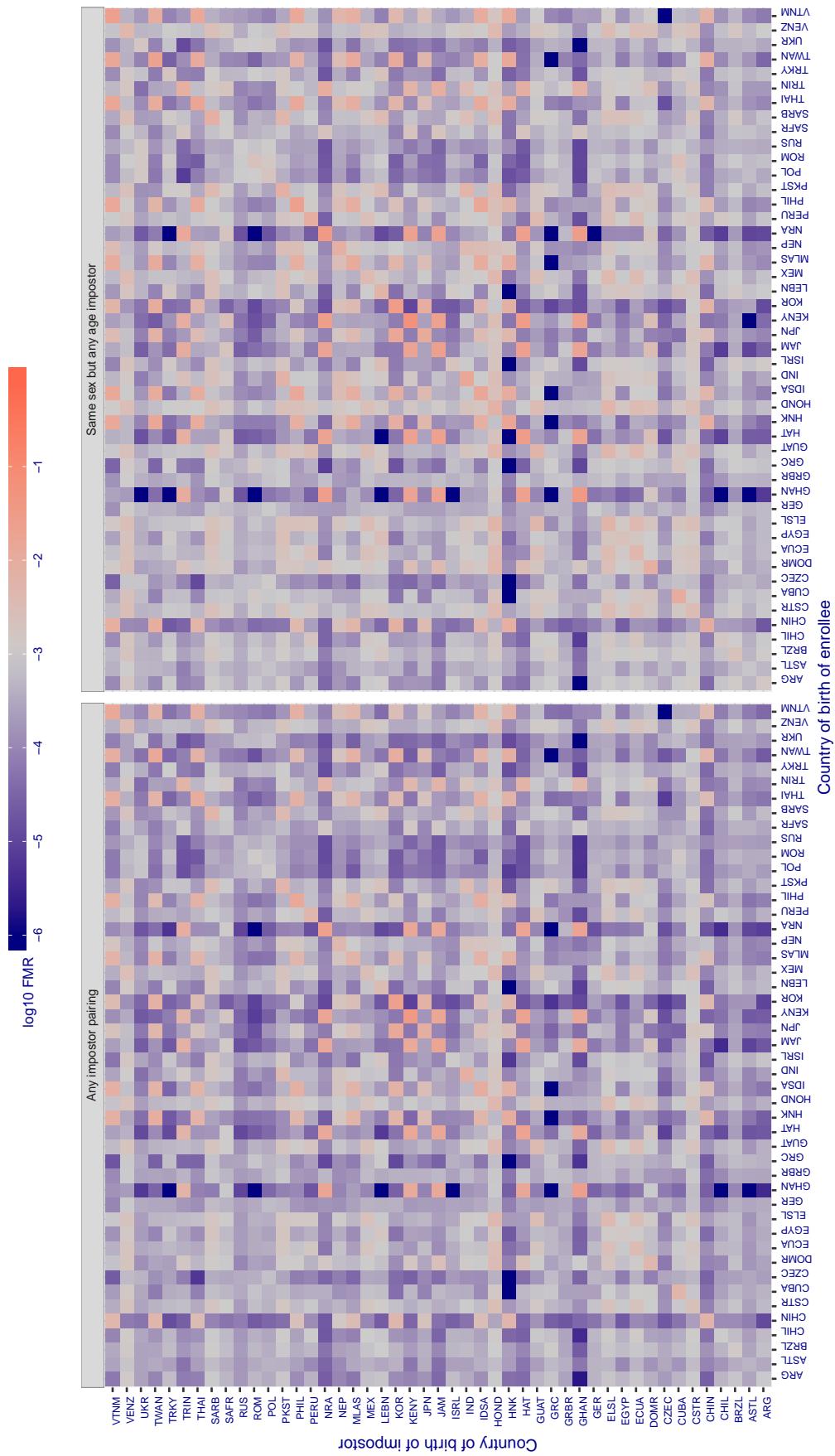
**Cross country FMR at threshold T = 0.408 for algorithm cyberextruder\_002, giving  $\text{FMR}(T) = 0.001$  globally.**

Figure 232: For algorithm cyberextruder-002 operating on visa images, the heatmap shows false match rates observed over impostor comparisons of faces from different individuals who were born in the given country pair. False matches are counted against a recognition threshold fixed globally to give the target  $\text{FMR}$  in the plot title, computed over all on the order of  $10^{10}$  impostor comparisons. If text appears in each box it give the same quantity as that coded by the color. Grey indicates  $\text{FMR}$  is at the intended  $\text{FMR}$  target level. Light red colors present a security vulnerability to, for example, a passport gate. Each +1 increase in  $\log_{10} \text{FMR}$  corresponds to a factor of 10 increase in  $\text{FMR}$ . The matrix is not quite symmetric because images in the enrollment and verification sets are different.

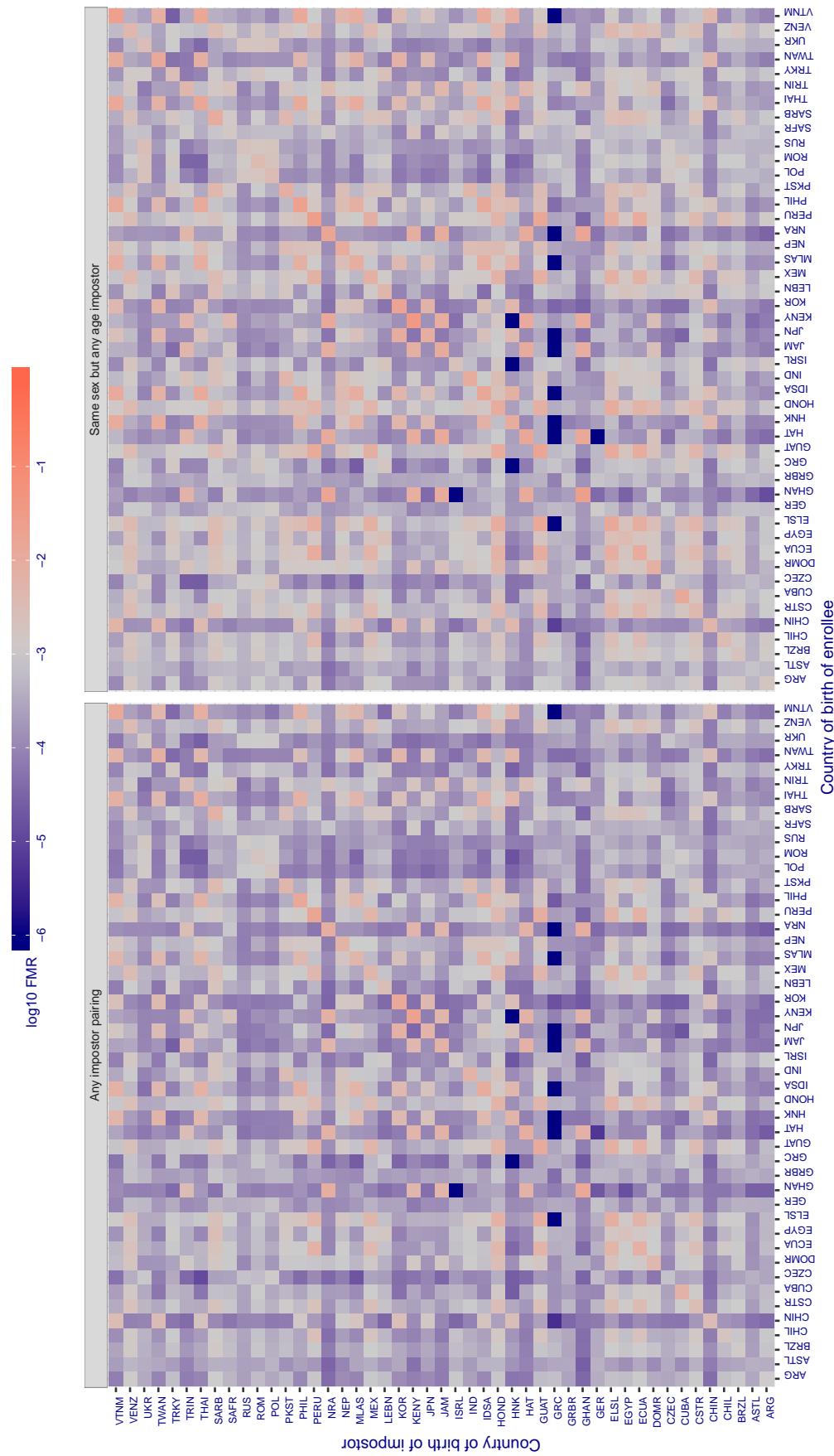
**Cross country FMR at threshold T = 1.322 for algorithm cyberlink\_000, giving  $\text{FMR}(T) = 0.001$  globally.**

Figure 233: For algorithm cyberlink-000 operating on visa images, the heatmap shows false match rates observed over impostor comparisons of faces from different individuals who were born in the given country pair. False matches are counted against a recognition threshold fixed globally to give the target FMR in the plot title, computed over all on the order of  $10^{10}$  impostor comparisons. If text appears in each box it give the same quantity as that coded by the color. Grey indicates FMR is at the intended FMR target level. Light red colors present a security vulnerability to, for example, a passport gate. Each +1 increase in  $\log_{10} \text{FMR}$  corresponds to a factor of 10 increase in FMR. The matrix is not quite symmetric because images in the enrollment and verification sets are different.

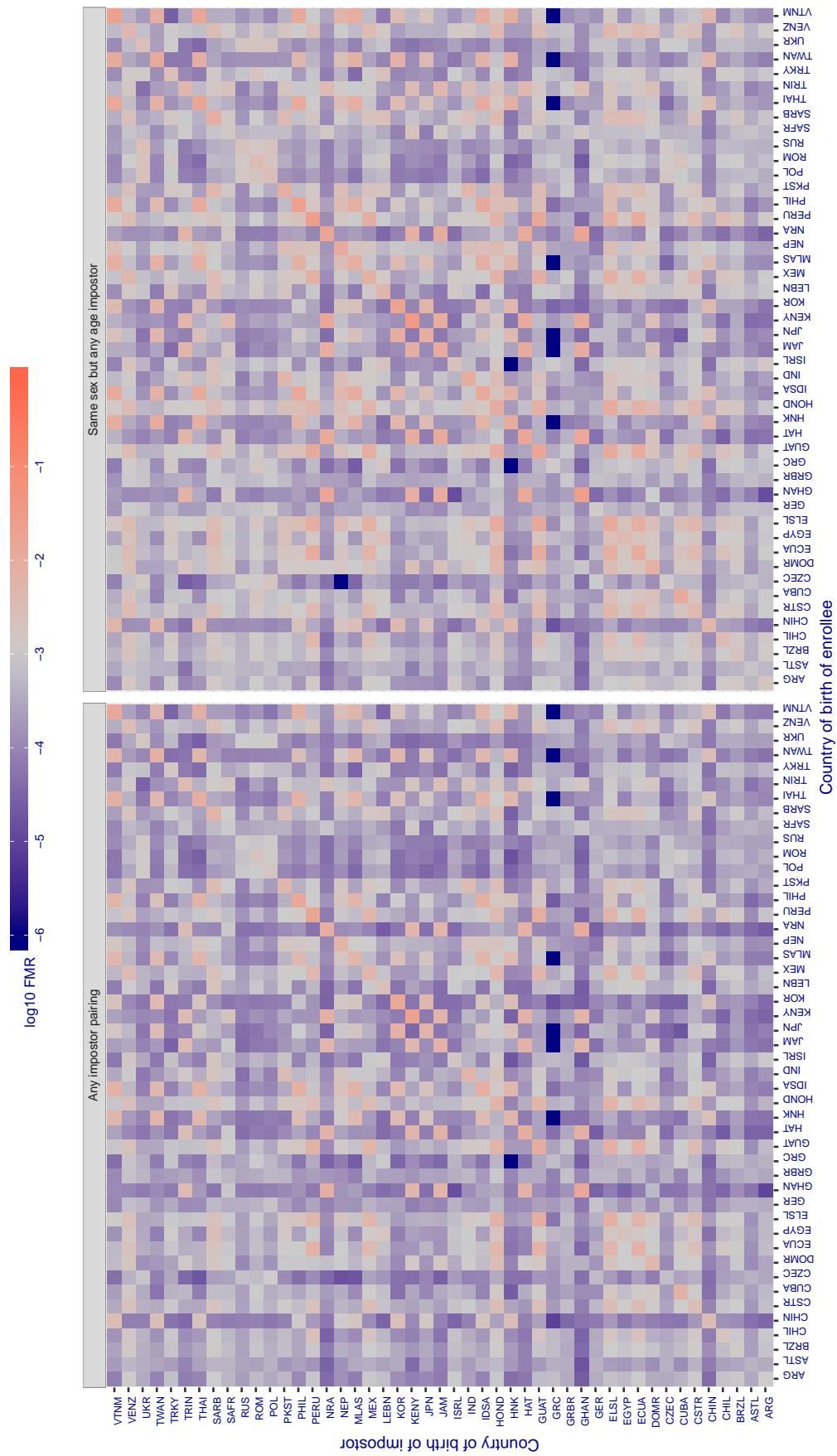
**Cross country FMR at threshold T = 1.322 for algorithm cyberlink\_001, giving  $\text{FMR}(T) = 0.001$  globally.**

Figure 234: For algorithm cyberlink-001 operating on visa images, the heatmap shows false match rates observed over impostor comparisons of faces from different individuals who were born in the given country pair. False matches are counted against a recognition threshold fixed globally to give the target  $\text{FMR}$  in the plot title, computed over all on the order of  $10^{10}$  impostor comparisons. If text appears in each box it give the same quantity as that coded by the color. Grey indicates  $\text{FMR}$  is at the intended  $\text{FMR}$  target level. Light red colors present a security vulnerability to, for example, a passport gate. Each +1 increase in  $\log_{10} \text{FMR}$  corresponds to a factor of 10 increase in  $\text{FMR}$ . The matrix is not quite symmetric because images in the enrollment and verification sets are different.

**Cross country FMR at threshold T = 6606.000 for algorithm dahua\_001, giving FMR(T) = 0.001 globally.**

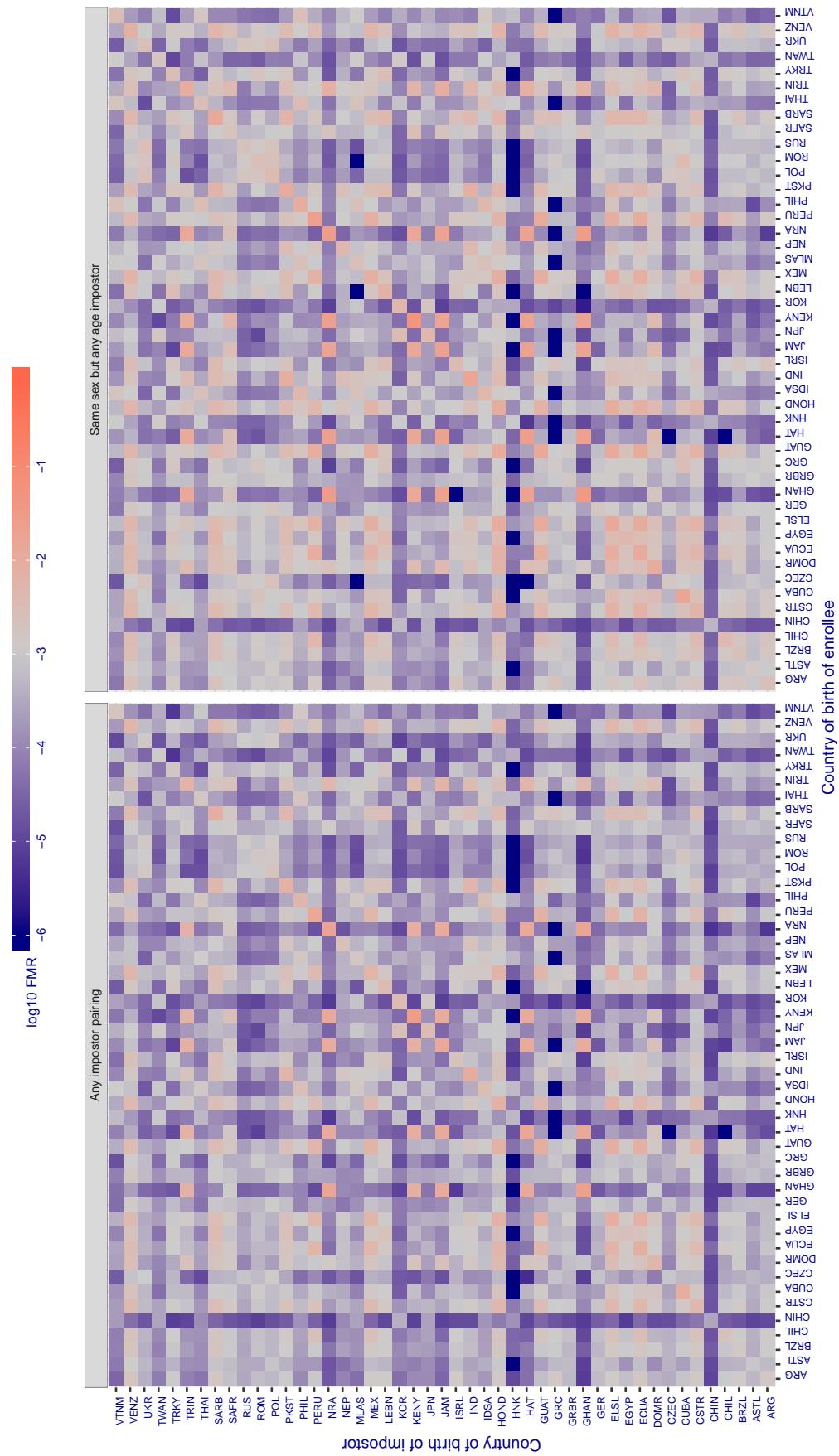


Figure 235: For algorithm dahua-001 operating on visa images, the heatmap shows false match rates observed over impostor comparisons of faces from different individuals who were born in the given country pair. False matches are counted against a recognition threshold fixed globally to give the target FMR in the plot title, computed over all on the order of  $10^{10}$  impostor comparisons. If text appears in each box it give the same quantity as that coded by the color. Grey indicates FMR is at the intended FMR target level. Light red colors present a security vulnerability to, for example, a passport gate. Each +1 increase in  $\log_{10} FMR$  corresponds to a factor of 10 increase in FMR. The matrix is not quite symmetric because images in the enrollment and verification sets are different.

**Cross country FMR at threshold T = 5958.000 for algorithm dahua\_002, giving FMR(T) = 0.001 globally.**

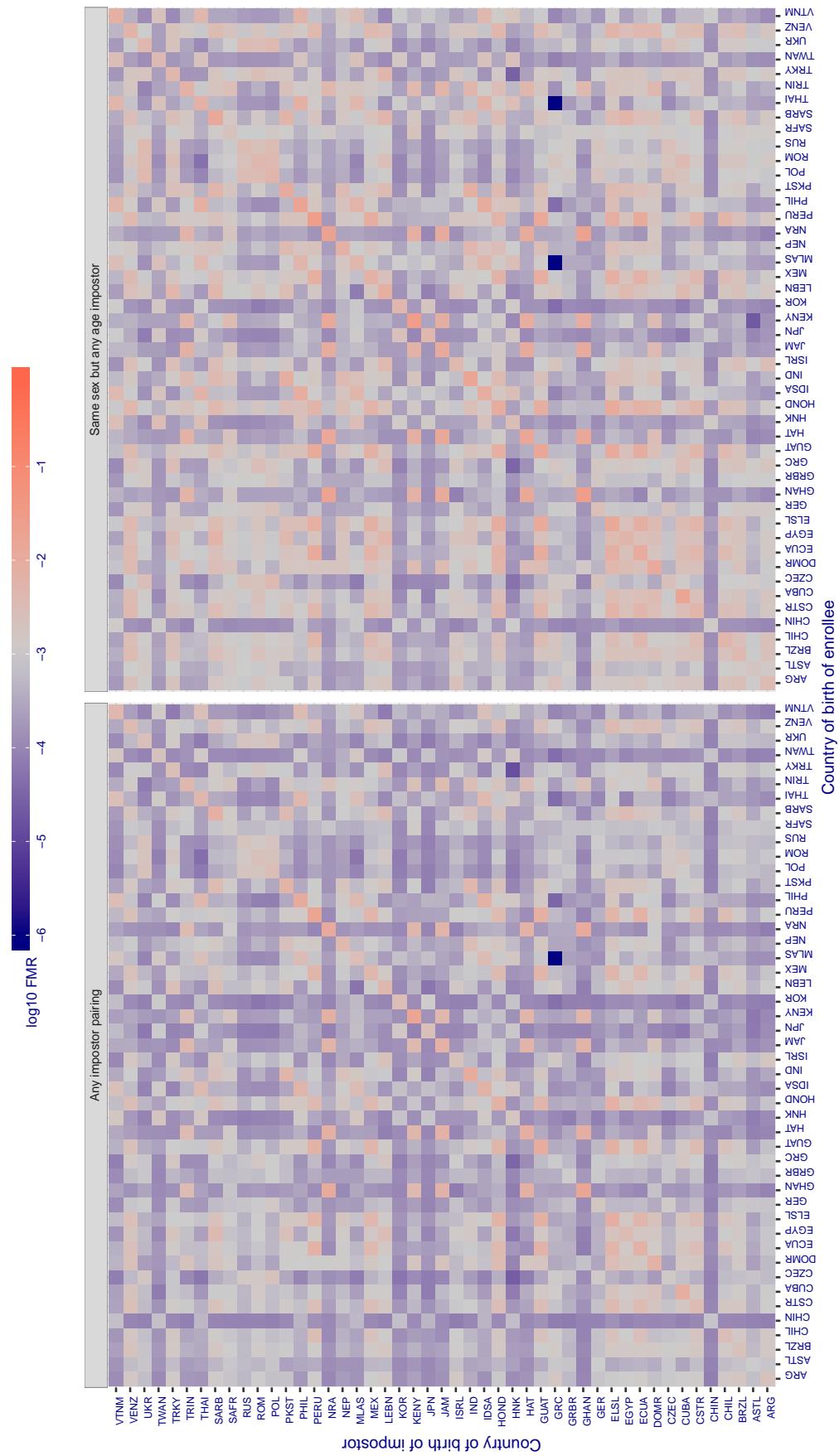


Figure 236: For algorithm dahua-002 operating on visa images, the heatmap shows false match rates observed over impostor comparisons of faces from different individuals who were born in the given country pair. False matches are counted against a recognition threshold fixed globally to give the target FMR in the plot title, computed over all on the order of  $10^{10}$  impostor comparisons. If text appears in each box it give the same quantity as that coded by the color. Grey indicates FMR is at the intended FMR target level. Light red colors present a security vulnerability to, for example, a passport gate. Each +1 increase in  $\log_{10} FMR$  corresponds to a factor of 10 increase in FMR. The matrix is not quite symmetric because images in the enrollment and verification sets are different.

**Cross country FMR at threshold T = 75.231 for algorithm dermalog\_005, giving  $\text{FMR}(T) = 0.001$  globally.**

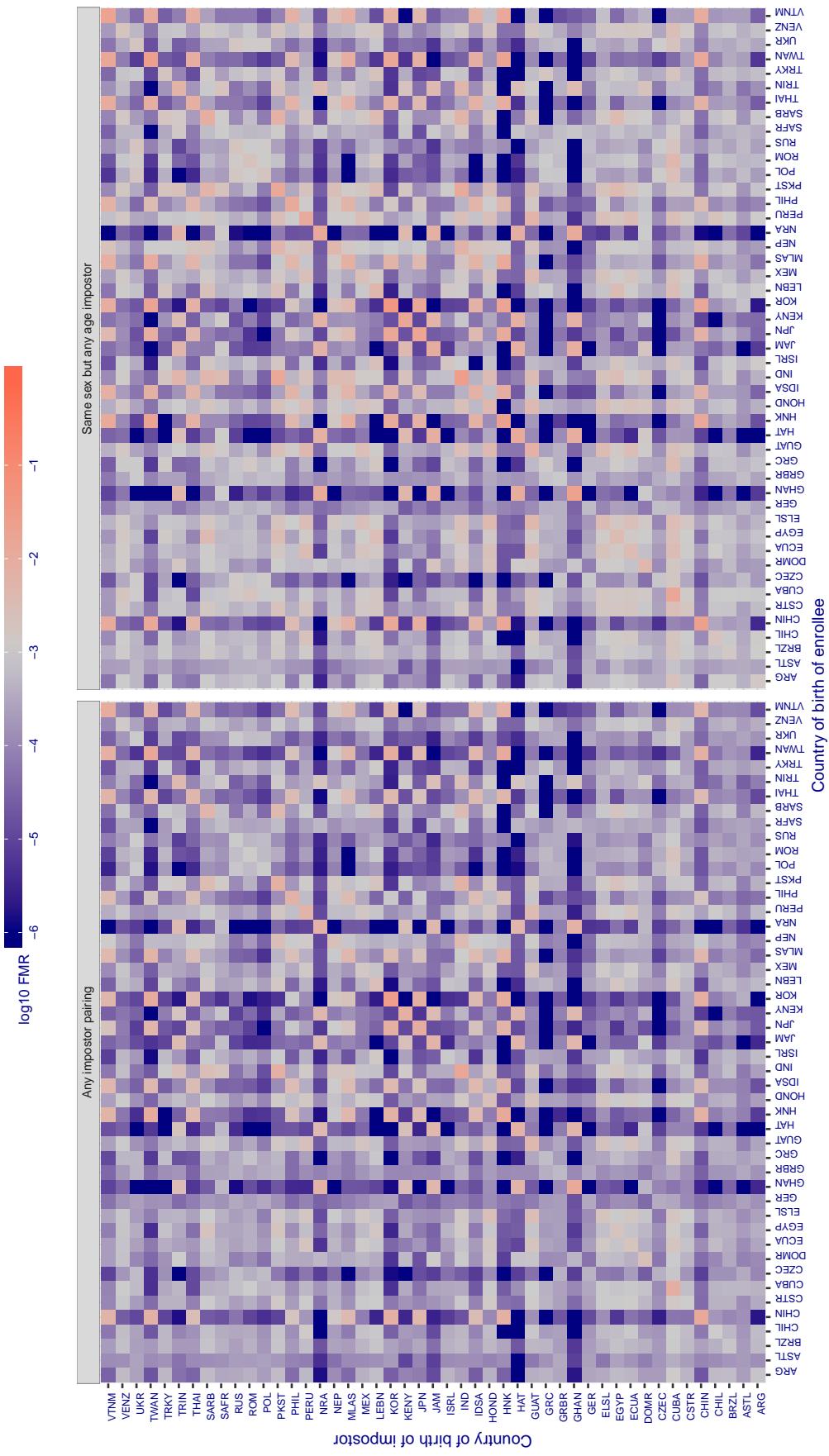


Figure 237: For algorithm dermalog-005 operating on visa images, the heatmap shows false match rates observed over impostor comparisons of faces from different individuals who were born in the given country pair. False matches are counted against a recognition threshold fixed globally to give the target  $\text{FMR}$  in the plot title, computed over all on the order of  $10^{10}$  impostor comparisons. If text appears in each box it give the same quantity as that coded by the color. Grey indicates  $\text{FMR}$  is at the intended  $\text{FMR}$  target level. Light red colors present a security vulnerability to, for example, a passport gate. Each +1 increase in  $\log_{10} \text{FMR}$  corresponds to a factor of 10 increase in  $\text{FMR}$ . The matrix is not quite symmetric because images in the enrollment and verification sets are different.

**Cross country FMR at threshold T = 76.496 for algorithm dermalog\_006, giving  $\text{FMR}(T) = 0.001$  globally.**

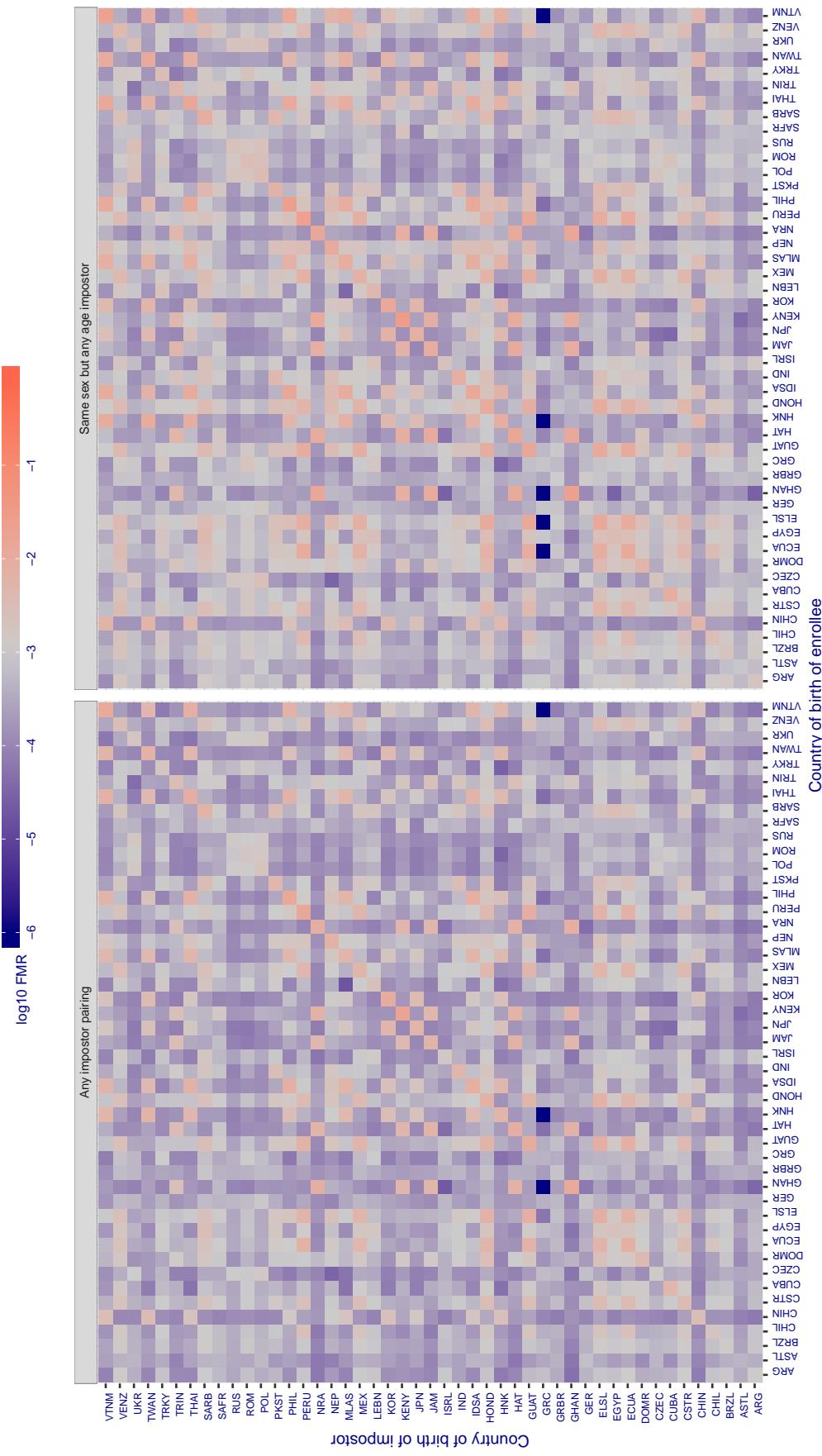


Figure 238: For algorithm dermalog-006 operating on visa images, the heatmap shows false match rates observed over impostor comparisons of faces from different individuals who were born in the given country pair. False matches are counted against a recognition threshold fixed globally to give the target  $\text{FMR}$  in the plot title, computed over all on the order of  $10^{10}$  impostor comparisons. If text appears in each box it give the same quantity as that coded by the color. Grey indicates  $\text{FMR}$  is at the intended  $\text{FMR}$  target level. Light red colors present a security vulnerability to, for example, a passport gate. Each +1 increase in  $\log_{10} \text{FMR}$  corresponds to a factor of 10 increase in  $\text{FMR}$ . The matrix is not quite symmetric because images in the enrollment and verification sets are different.

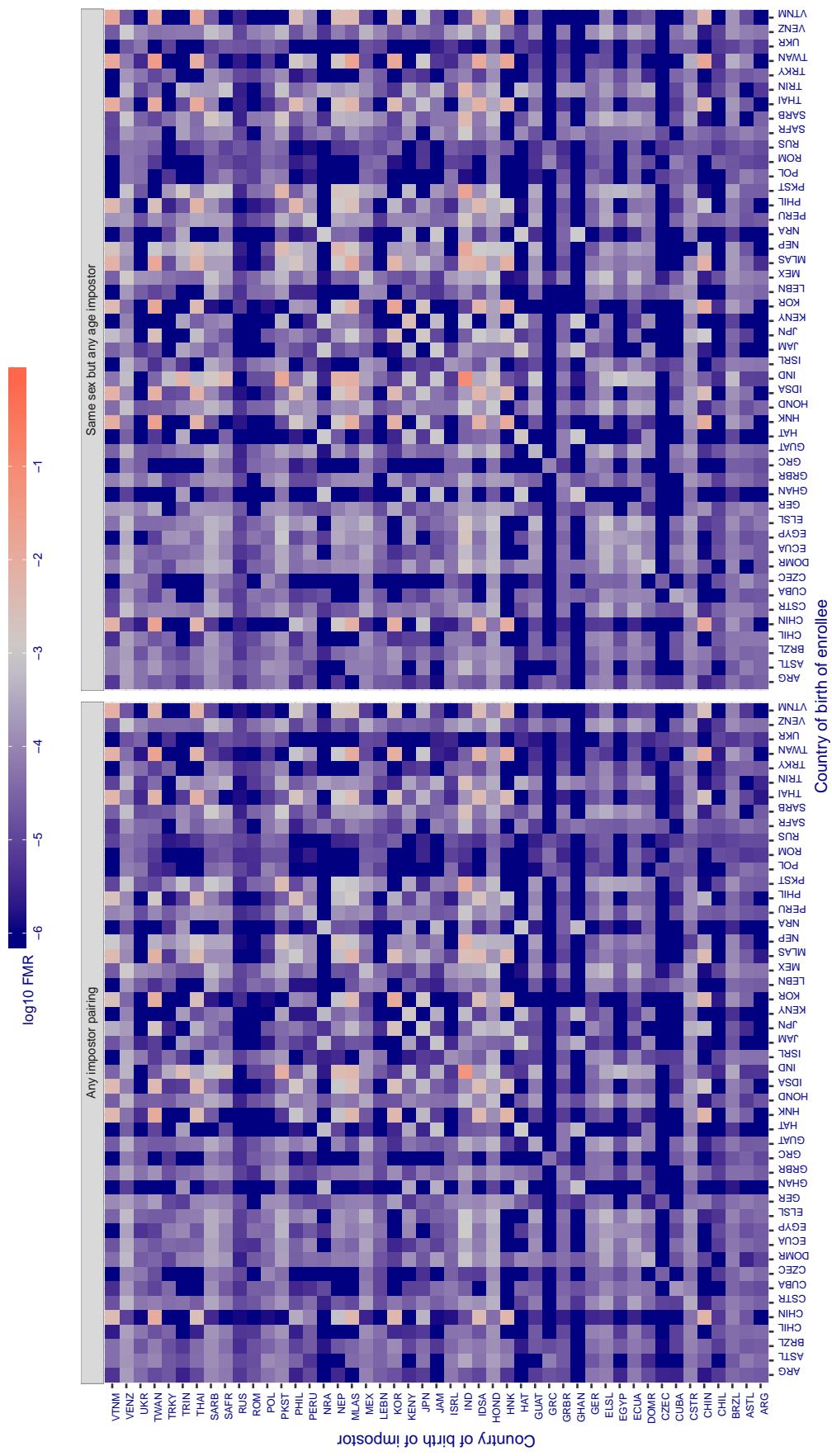
**Cross country FMR at threshold T = 0.547 for algorithm digitalbarriers\_002, giving  $FMR(T) = 0.001$  globally.**

Figure 239: For algorithm digitalbarriers-002 operating on visa images, the heatmap shows false match rates observed over impostor comparisons of faces from different individuals who were born in the given country pair. False matches are counted against a recognition threshold fixed globally to give the target  $FMR$  in the plot title, computed over all on the order of  $10^{10}$  impostor comparisons. If text appears in each box it give the same quantity as that coded by the color. Grey indicates  $FMR$  is at the intended  $FMR$  target level. Light red colors present a security vulnerability to, for example, a passport gate. Each +1 increase in  $\log_{10} FMR$  corresponds to a factor of 10 increase in  $FMR$ . The matrix is not quite symmetric because images in the enrollment and verification sets are different.

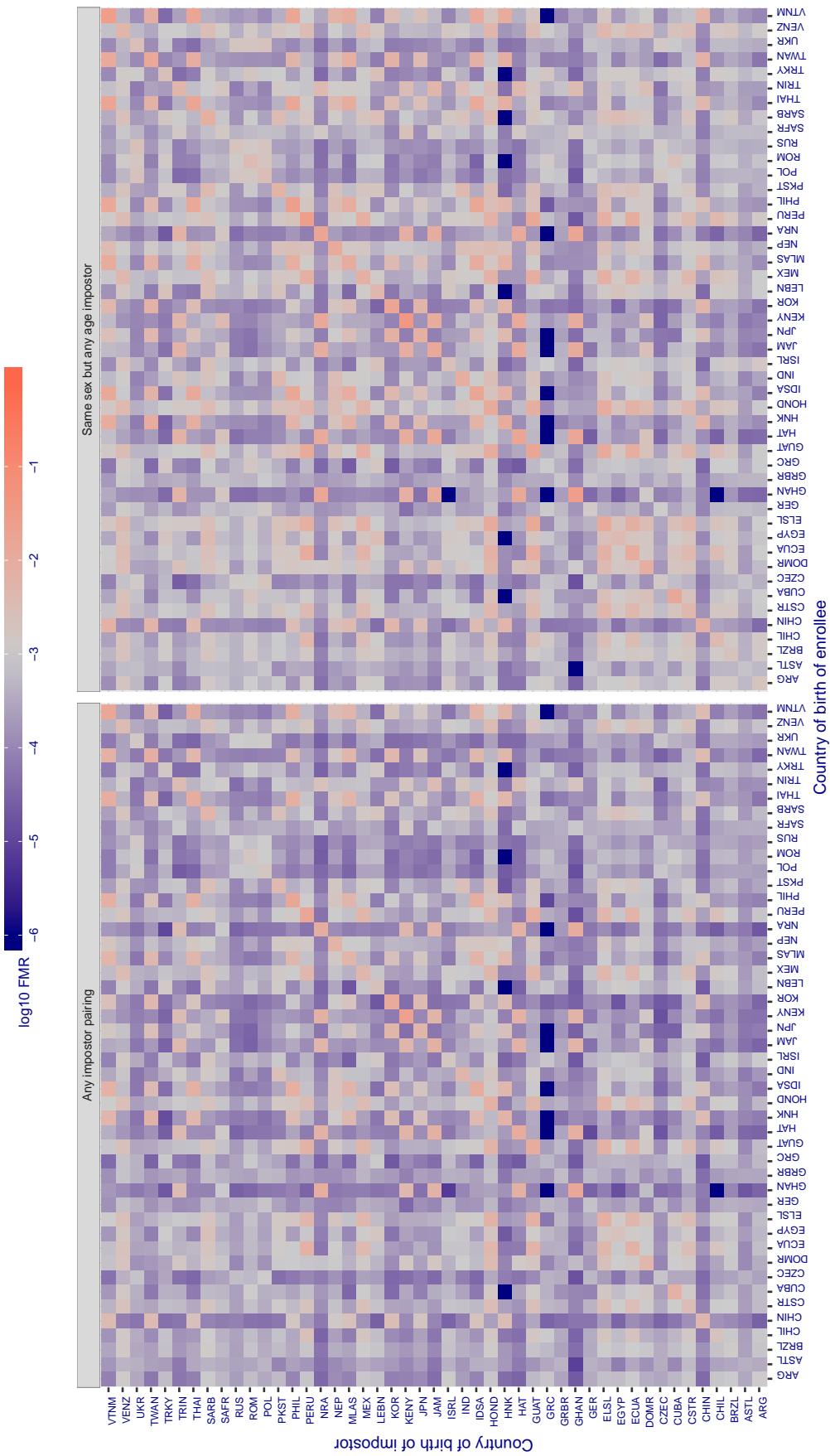
**Cross country FMR at threshold T = 2.510 for algorithm everai\_001, giving FMR(T) = 0.001 globally.**

Figure 240: For algorithm everai-001 operating on visa images, the heatmap shows false match rates observed over impostor comparisons of faces from different individuals who were born in the given country pair. False matches are counted against a recognition threshold fixed globally to give the target FMR in the plot title, computed over all on the order of  $10^{10}$  impostor comparisons. If text appears in each box it give the same quantity as that coded by the color. Grey indicates FMR is at the intended FMR target level. Light red colors present a security vulnerability to, for example, a passport gate. Each +1 increase in  $\log_{10} \text{FMR}$  corresponds to a factor of 10 increase in FMR. The matrix is not quite symmetric because images in the enrollment and verification sets are different.

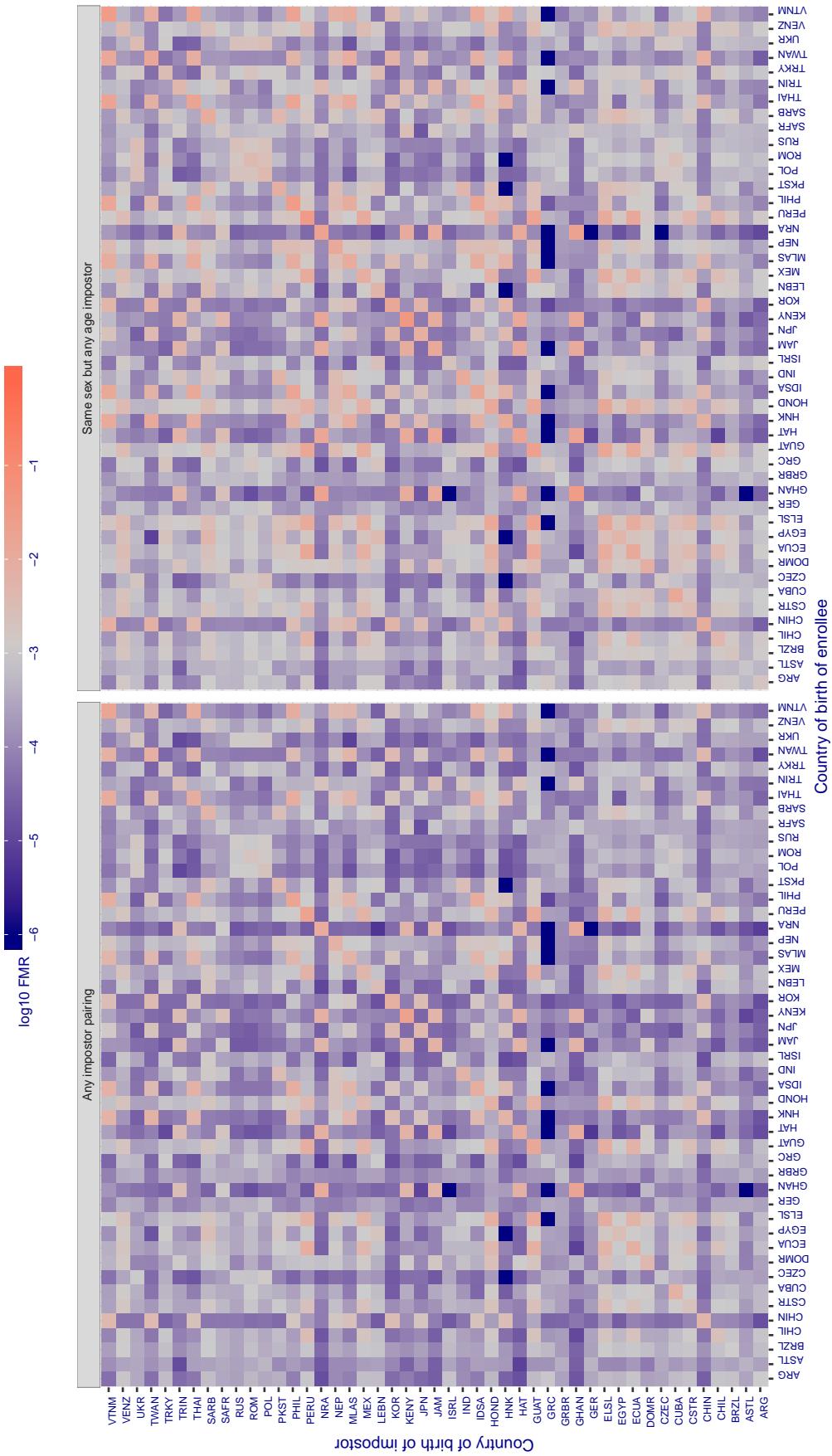
**Cross country FMR at threshold T = 2.426 for algorithm everai\_002, giving FMR(T) = 0.001 globally.**

Figure 241: For algorithm everai-002 operating on visa images, the heatmap shows false match rates observed over impostor comparisons of faces from different individuals who were born in the given country pair. False matches are counted against a recognition threshold fixed globally to give the target FMR in the plot title, computed over all on the order of  $10^{10}$  impostor comparisons. If text appears in each box it give the same quantity as that coded by the color. Grey indicates FMR is at the intended FMR target level. Light red colors present a security vulnerability to, for example, a passport gate. Each +1 increase in  $\log_{10} \text{FMR}$  corresponds to a factor of 10 increase in FMR. The matrix is not quite symmetric because images in the enrollment and verification sets are different.

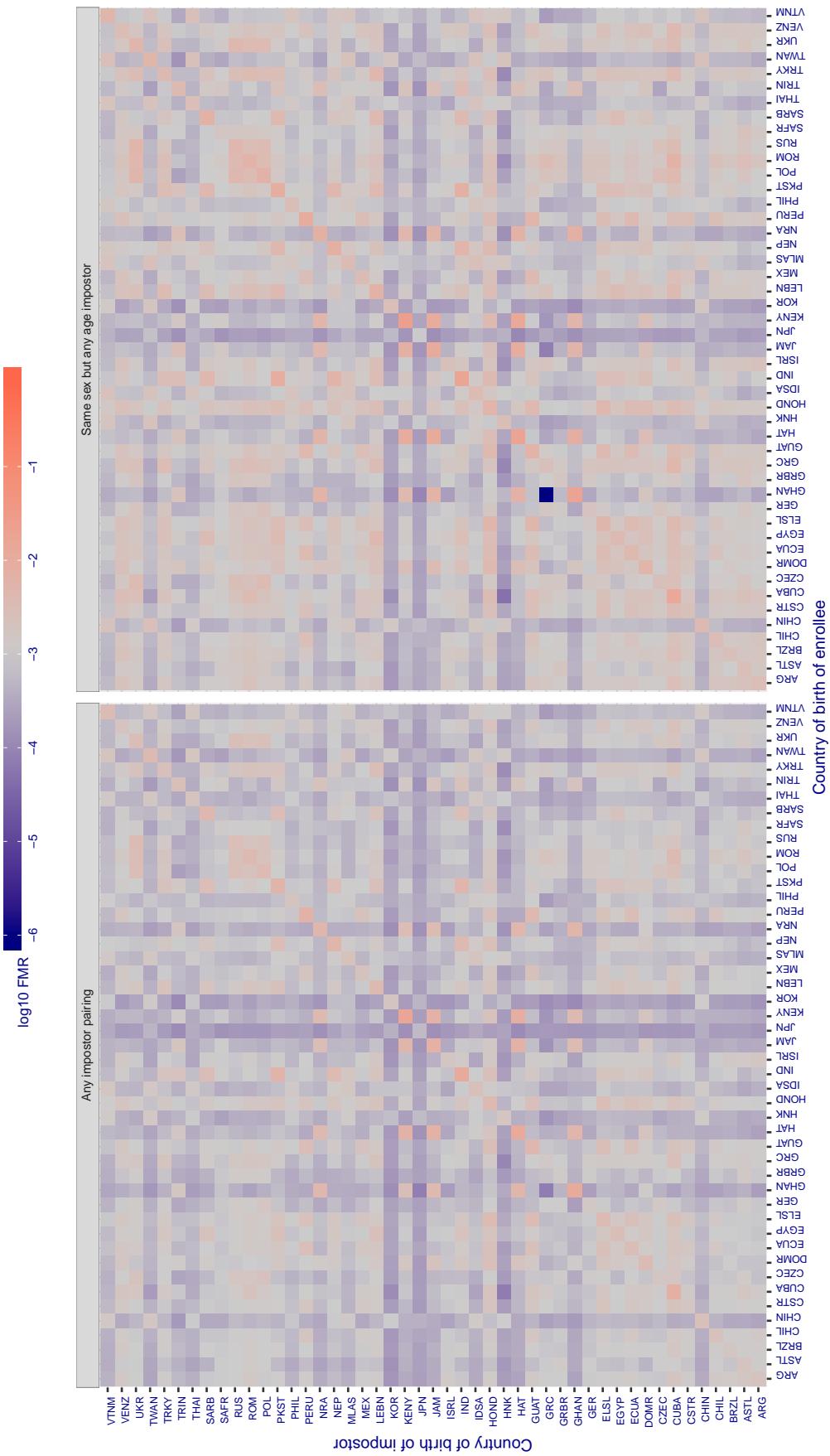
**Cross country FMR at threshold T = 0.591 for algorithm glory\_000, giving FMR(T) = 0.001 globally.**

Figure 242: For algorithm *glory-000* operating on visa images, the heatmap shows false match rates observed over impostor comparisons of faces from different individuals who were born in the given country pair. False matches are counted against a recognition threshold fixed globally to give the target FMR in the plot title, computed over all on the order of  $10^{10}$  impostor comparisons. If text appears in each box it give the same quantity as that coded by the color. Grey indicates FMR is at the intended FMR target level. Light red colors present a security vulnerability to, for example, a passport gate. Each +1 increase in  $\log_{10} FMR$  corresponds to a factor of 10 increase in FMR. The matrix is not quite symmetric because images in the enrollment and verification sets are different.

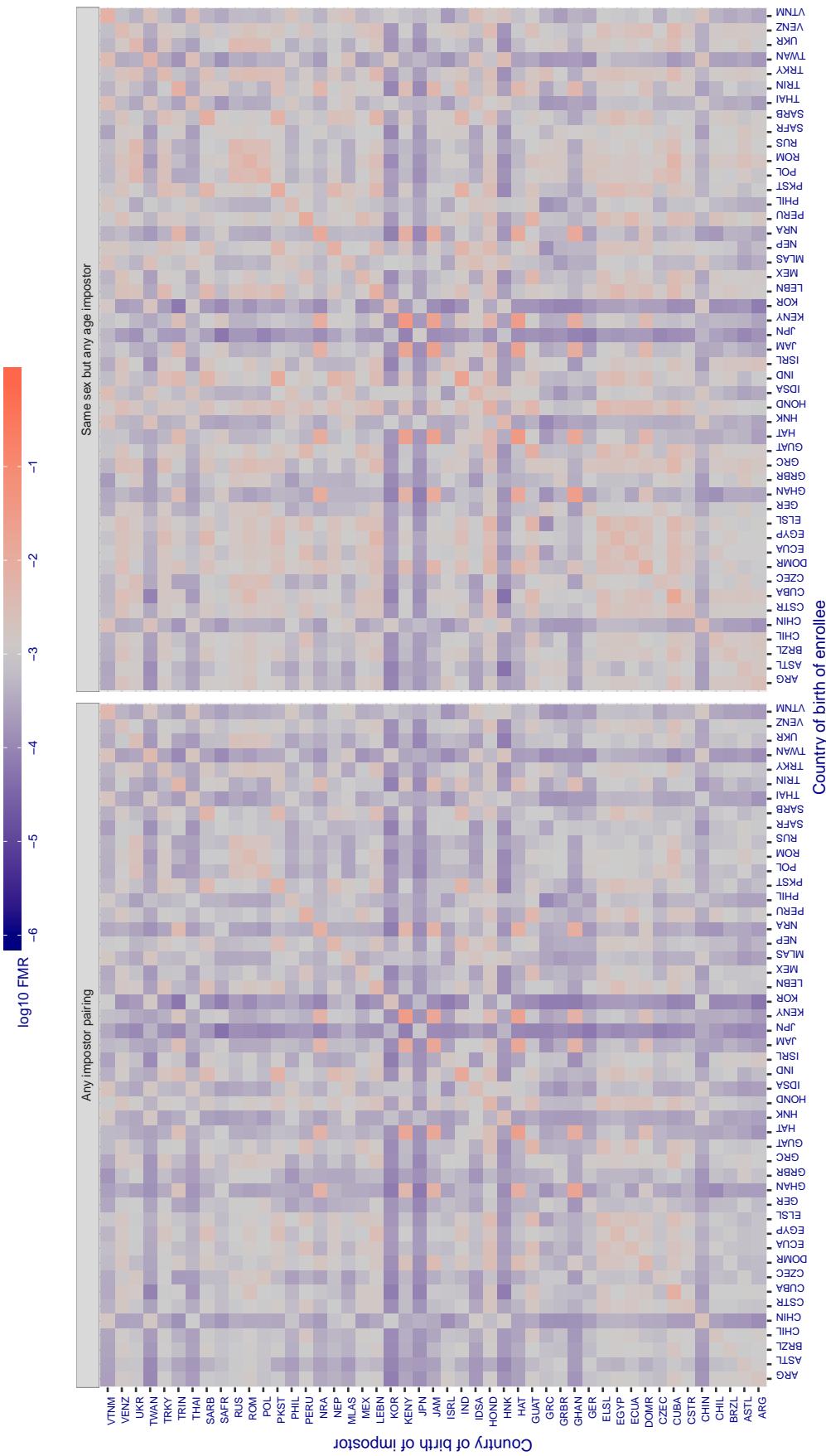
**Cross country FMR at threshold T = 0.596 for algorithm glory\_001, giving FMR(T) = 0.001 globally.**

Figure 243: For algorithm *glory-001* operating on visa images, the heatmap shows false match rates observed over impostor comparisons of faces from different individuals who were born in the given country pair. False matches are counted against a recognition threshold fixed globally to give the target FMR in the plot title, computed over all on the order of  $10^{10}$  impostor comparisons. If text appears in each box it give the same quantity as that coded by the color. Grey indicates FMR is at the intended FMR target level. Light red colors present a security vulnerability to, for example, a passport gate. Each +1 increase in  $\log_{10} FMR$  corresponds to a factor of 10 increase in FMR. The matrix is not quite symmetric because images in the enrollment and verification sets are different.

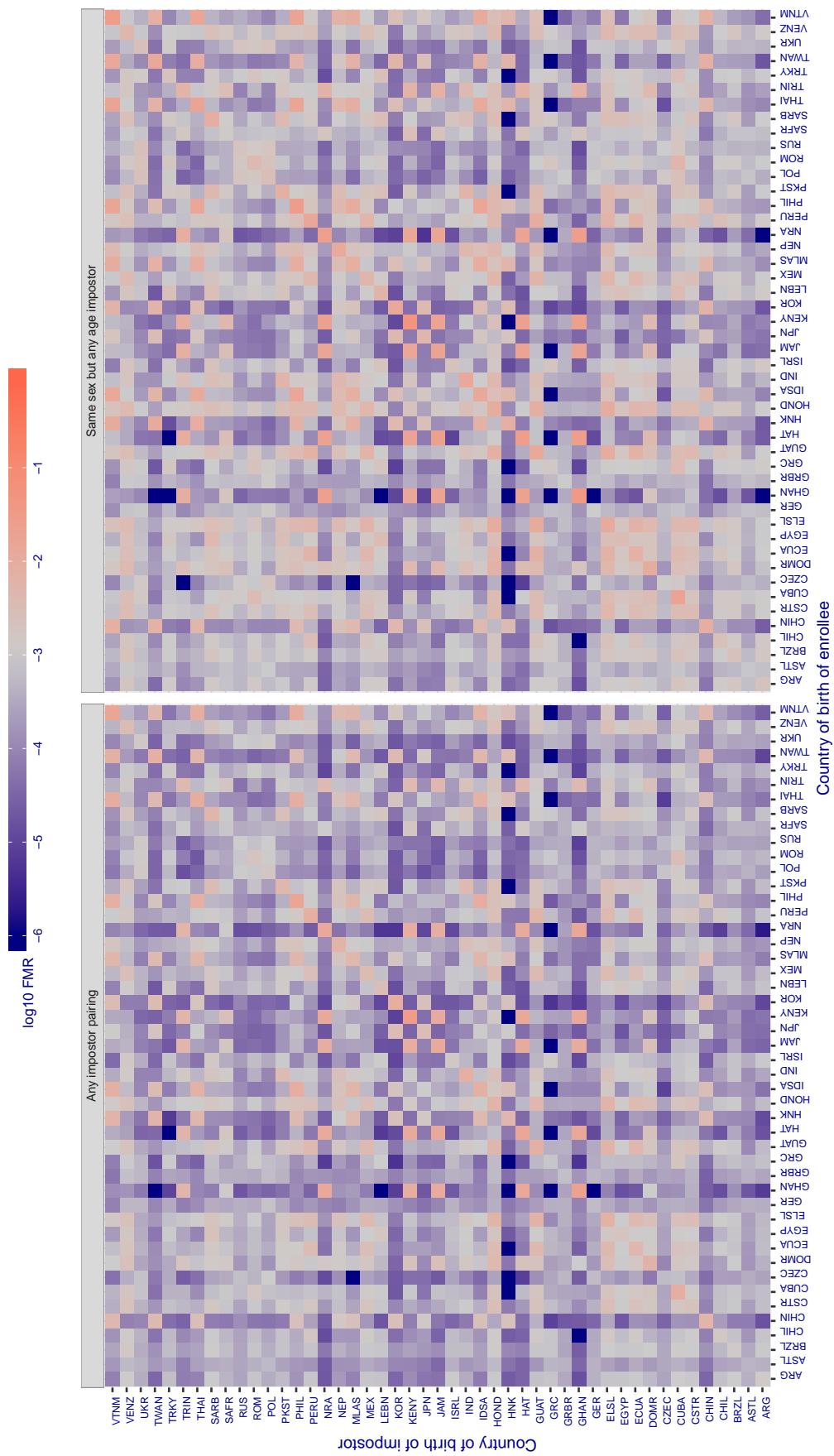
**Cross country FMR at threshold T = 0.474 for algorithm gorilla\_001, giving FMR(T) = 0.001 globally.**

Figure 244: For algorithm gorilla-001 operating on visa images, the heatmap shows false match rates observed over impostor comparisons of faces from different individuals who were born in the given country pair. False matches are counted against a recognition threshold fixed globally to give the target FMR in the plot title, computed over all on the order of  $10^{10}$  impostor comparisons. If text appears in each box it give the same quantity as that coded by the color. Grey indicates FMR is at the intended FMR target level. Light red colors present a security vulnerability to, for example, a passport gate. Each +1 increase in  $\log_{10}$  FMR corresponds to a factor of 10 increase in FMR. The matrix is not quite symmetric because images in the enrollment and verification sets are different.

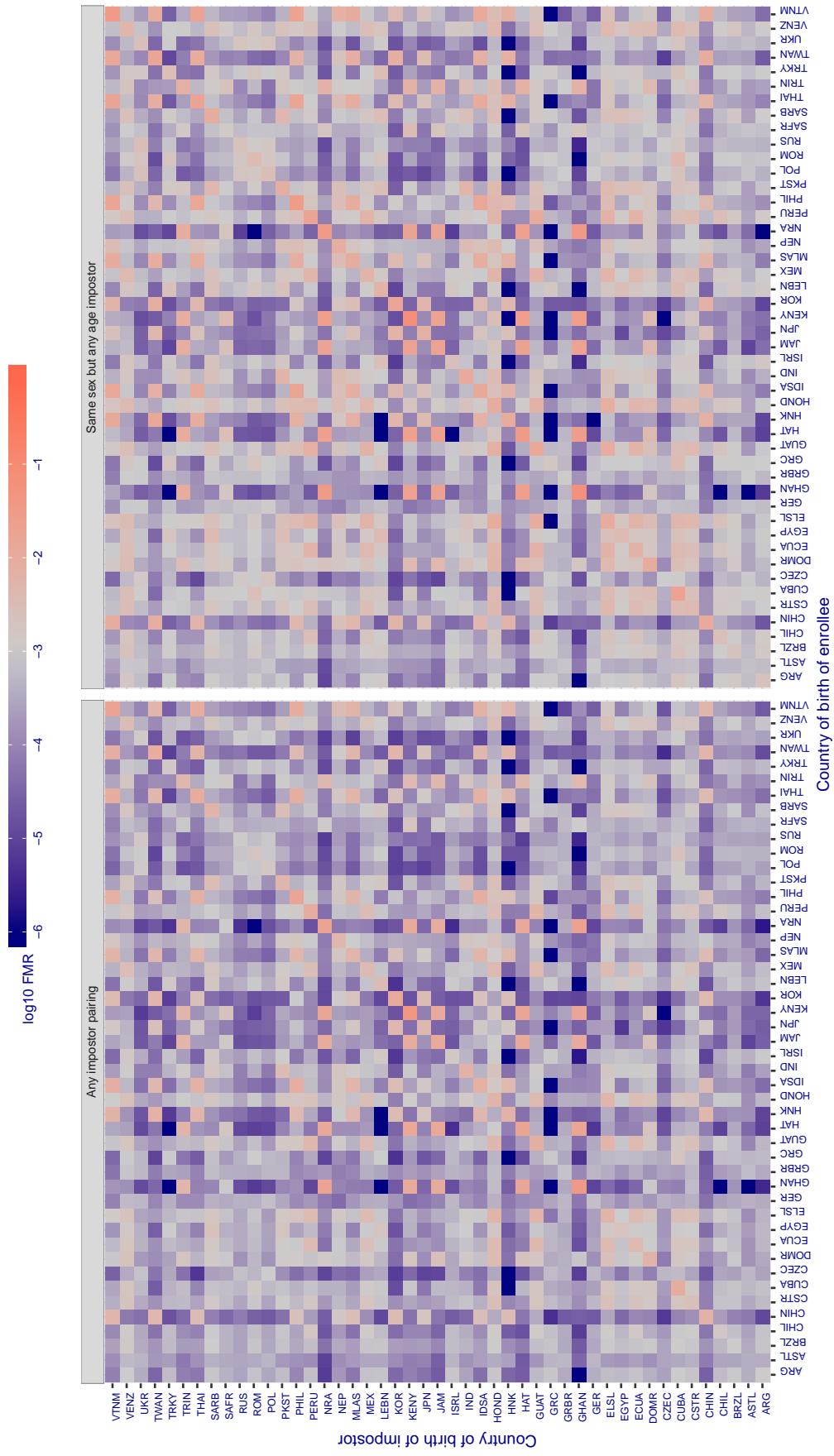
**Cross country FMR at threshold T = 0.402 for algorithm gorilla\_002, giving FMR(T) = 0.001 globally.**

Figure 245: For algorithm gorilla-002 operating on visa images, the heatmap shows false match rates observed over impostor comparisons of faces from different individuals who were born in the given country pair. False matches are counted against a recognition threshold fixed globally to give the target FMR in the plot title, computed over all on the order of  $10^{10}$  impostor comparisons. If text appears in each box it give the same quantity as that coded by the color. Grey indicates FMR is at the intended FMR target level. Light red colors present a security vulnerability to, for example, a passport gate. Each +1 increase in  $\log_{10} \text{FMR}$  corresponds to a factor of 10 increase in FMR. The matrix is not quite symmetric because images in the enrollment and verification sets are different.

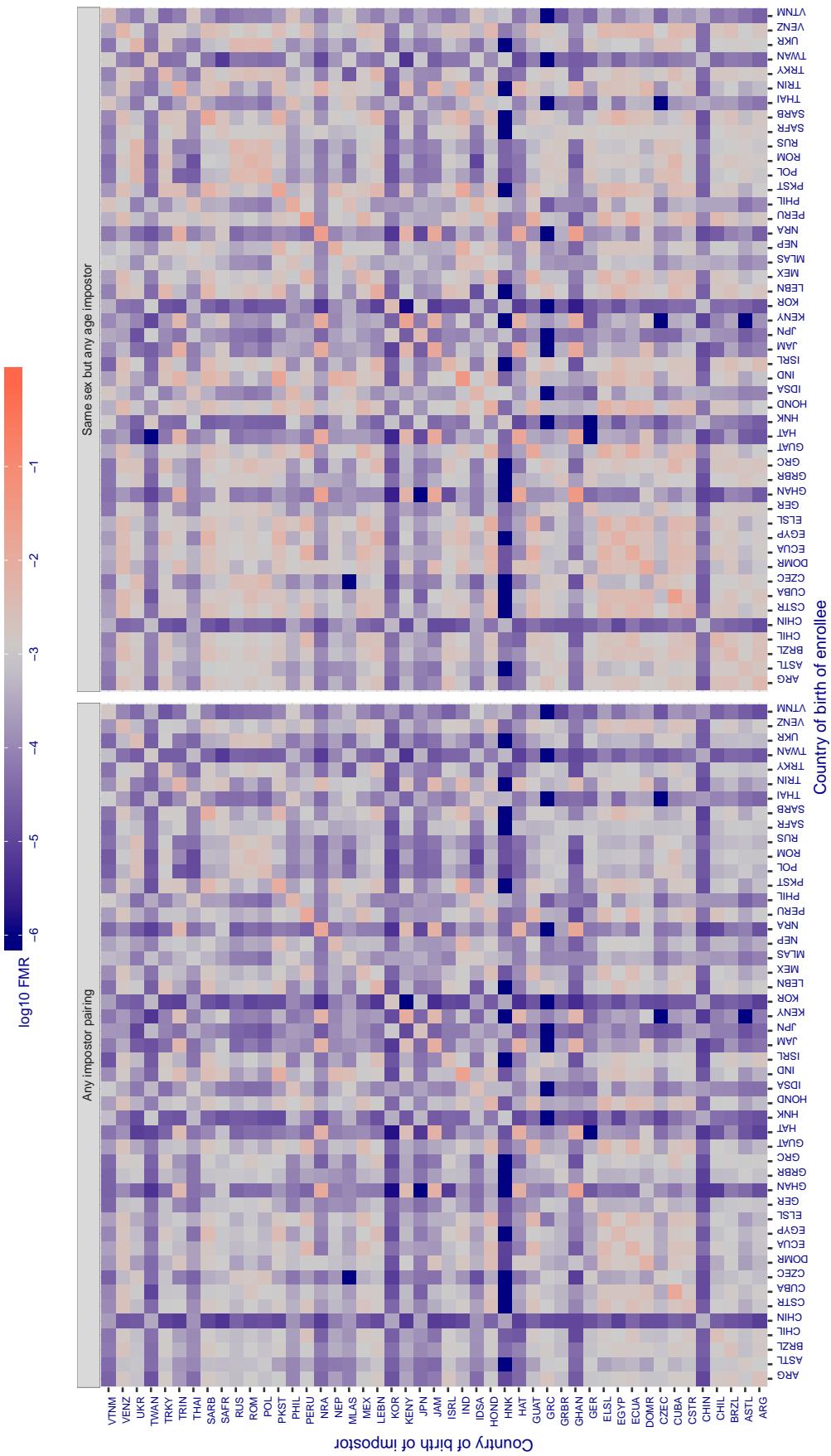
**Cross country FMR at threshold T = 63.025 for algorithm hik\_001, giving  $\text{FMR}(\text{T}) = 0.001$  globally.**

Figure 246: For algorithm hik-001 operating on visa images, the heatmap shows false match rates observed over impostor comparisons of faces from different individuals who were born in the given country pair. False matches are counted against a recognition threshold fixed globally to give the target FMR in the plot title, computed over all on the order of  $10^{10}$  impostor comparisons. If text appears in each box it give the same quantity as that coded by the color. Grey indicates  $\text{FMR}$  is at the intended  $\text{FMR}$  target level. Light red colors present a security vulnerability to, for example, a passport gate. Each +1 increase in  $\log_{10} \text{FMR}$  corresponds to a factor of 10 increase in  $\text{FMR}$ . The matrix is not quite symmetric because images in the enrollment and verification sets are different.

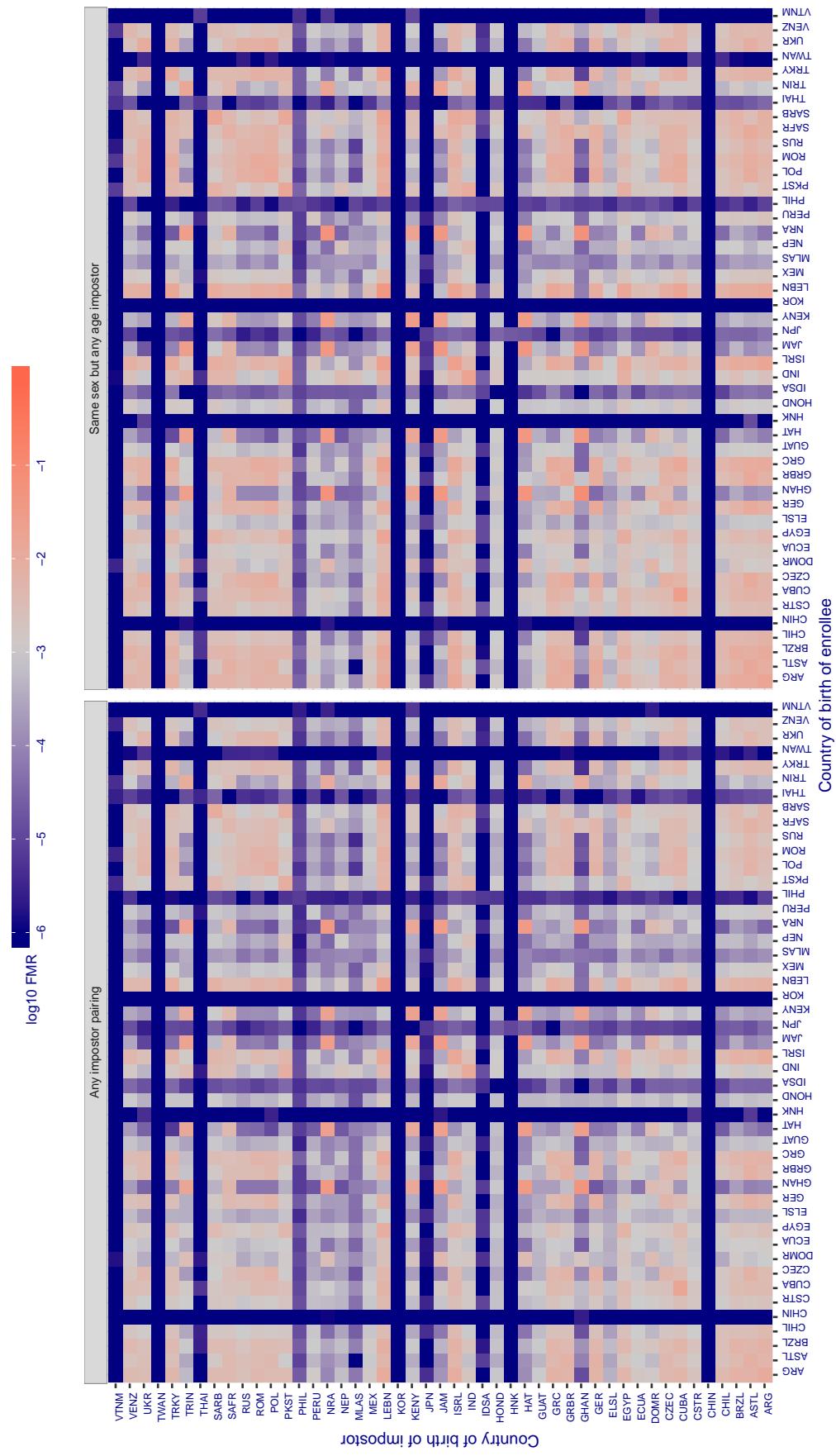
**Cross country FMR at threshold T = 0.949 for algorithm hr\_000, giving FMR(T) = 0.001 globally.**

Figure 247: For algorithm hr-000 operating on visa images, the heatmap shows false match rates observed over impostor comparisons of faces from different individuals who were born in the given country pair. False matches are counted against a recognition threshold fixed globally to give the target FMR in the plot title, computed over all on the order of  $10^{10}$  impostor comparisons. If text appears in each box it give the same quantity as that coded by the color. Grey indicates FMR is at the intended FMR target level. Light red colors present a security vulnerability to, for example, a passport gate. Each +1 increase in  $\log_{10}$  FMR corresponds to a factor of 10 increase in FMR. The matrix is not quite symmetric because images in the enrollment and verification sets are different.

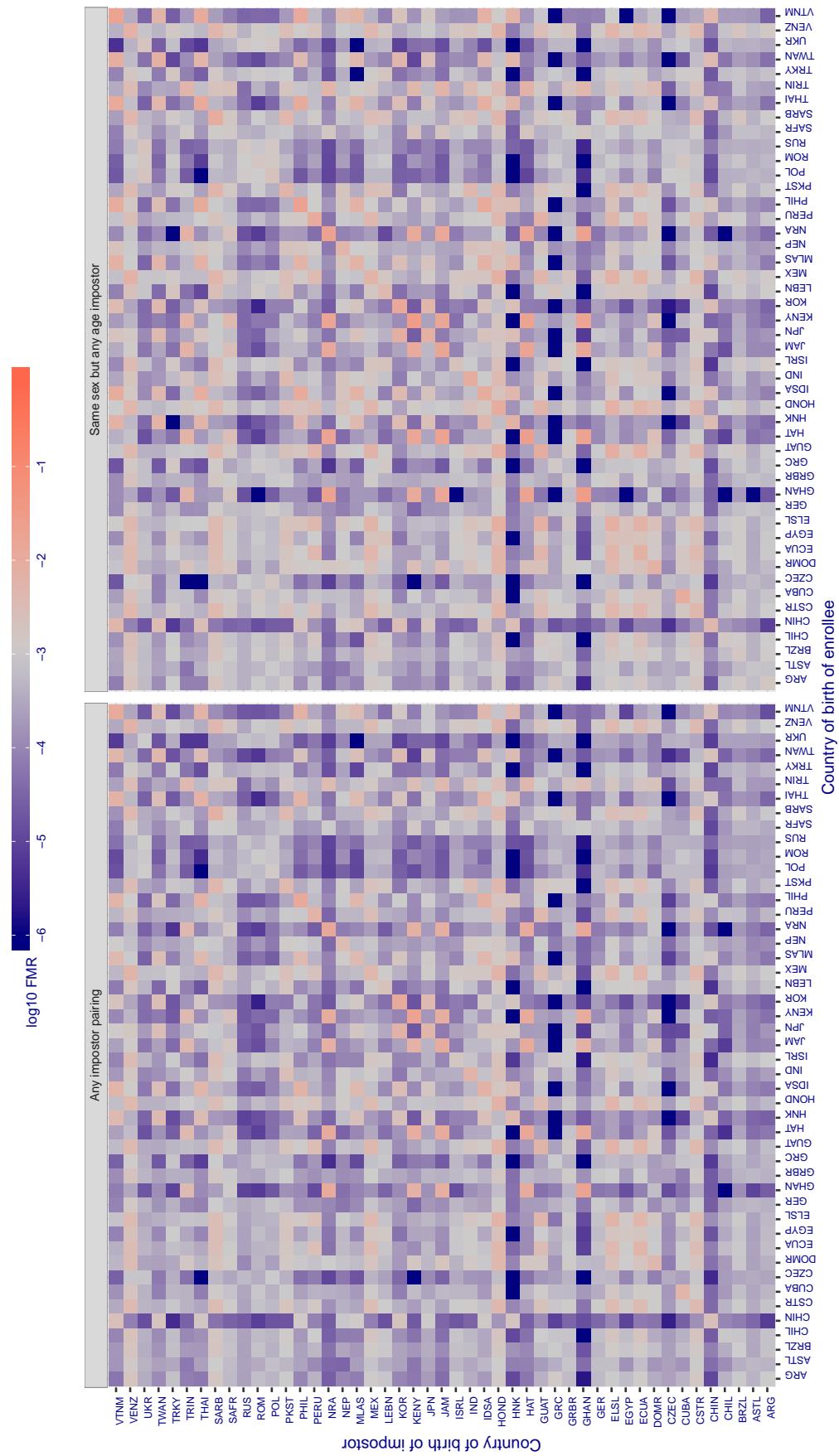
**Cross country FMR at threshold T = 36641.000 for algorithm id3\_003, giving FMR(T) = 0.001 globally.**

Figure 248: For algorithm id3\_003 operating on visa images, the heatmap shows false match rates observed over impostor comparisons of faces from different individuals who were born in the given country pair. False matches are counted against a recognition threshold fixed globally to give the target FMR in the plot title, computed over all on the order of  $10^{10}$  impostor comparisons. If text appears in each box it give the same quantity as that coded by the color. Grey indicates FMR is at the intended FMR target level. Light red colors present a security vulnerability to, for example, a passport gate. Each +1 increase in  $\log_{10} \text{FMR}$  corresponds to a factor of 10 increase in FMR. The matrix is not quite symmetric because images in the enrollment and verification sets are different.

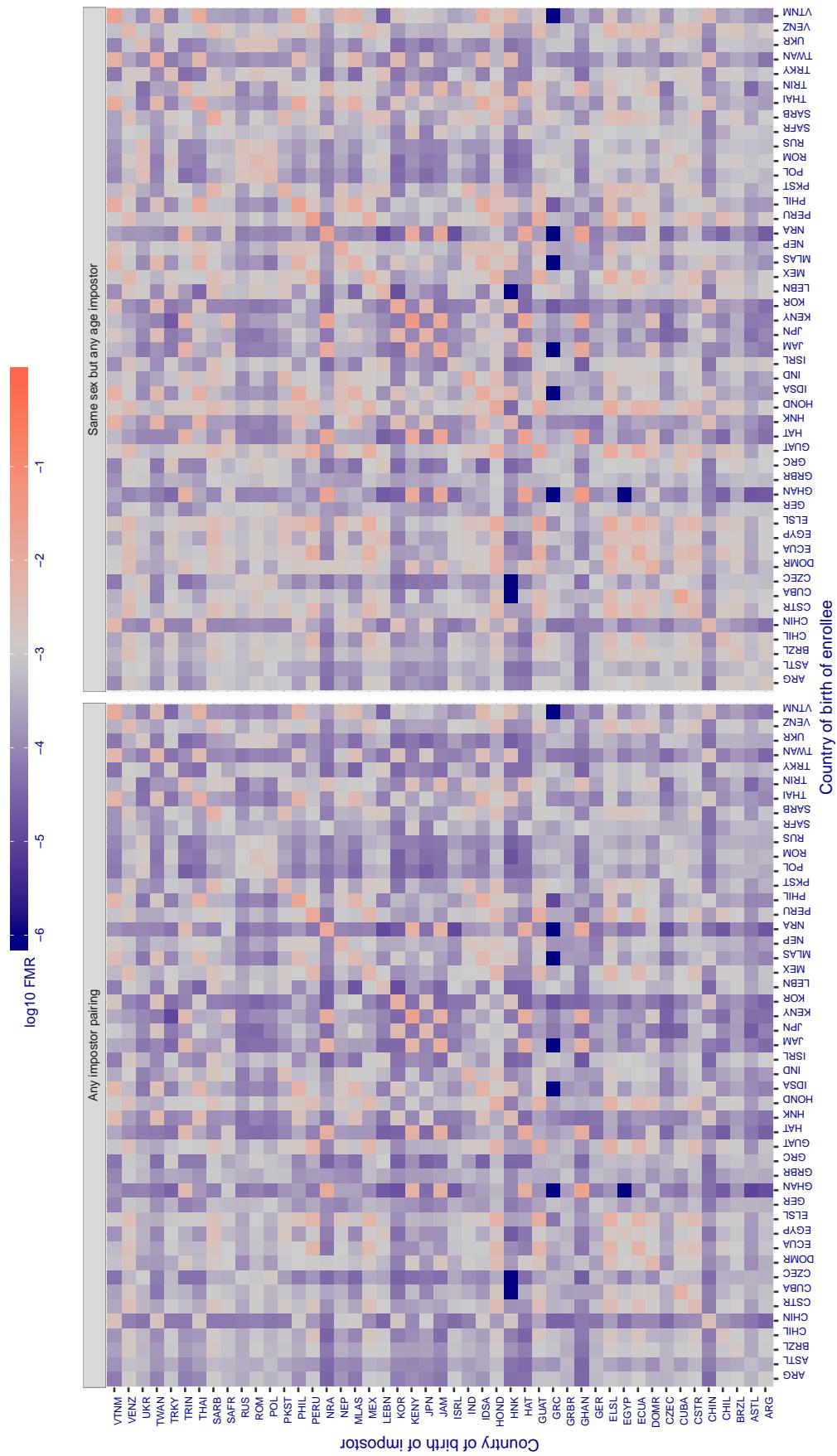
**Cross country FMR at threshold T = 36163.000 for algorithm id3\_004, giving FMR(T) = 0.001 globally.**

Figure 249: For algorithm id3\_004 operating on visa images, the heatmap shows false match rates observed over impostor comparisons of faces from different individuals who were born in the given country pair. False matches are counted against a recognition threshold fixed globally to give the target FMR in the plot title, computed over all on the order of  $10^{10}$  impostor comparisons. If text appears in each box it give the same quantity as that coded by the color. Grey indicates FMR is at the intended FMR target level. Light red colors present a security vulnerability to, for example, a passport gate. Each +1 increase in  $\log_{10}$  FMR corresponds to a factor of 10 increase in FMR. The matrix is not quite symmetric because images in the enrollment and verification sets are different.

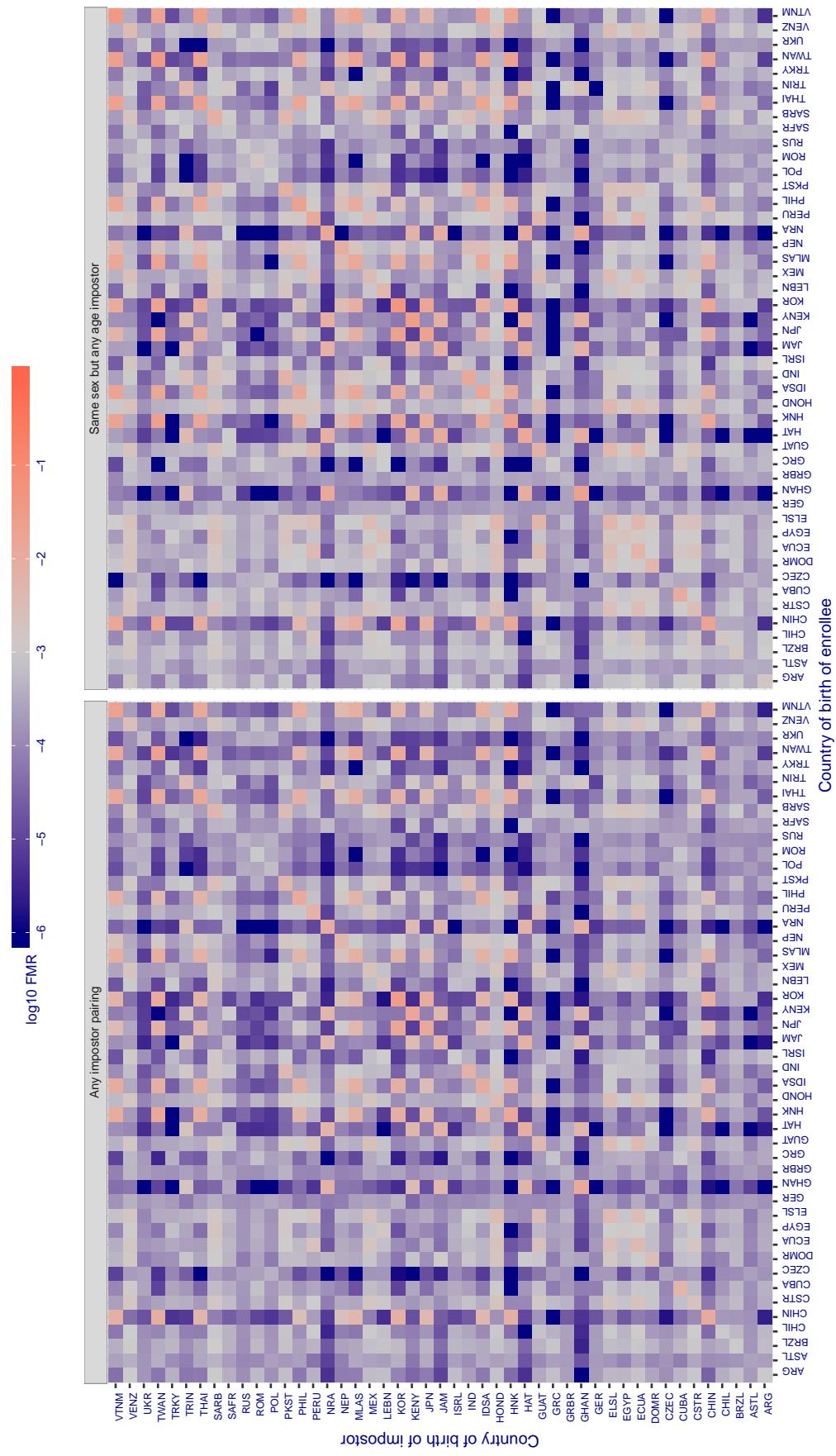
**Cross country FMR at threshold T = 3136.629 for algorithm idemia\_003, giving FMR(T) = 0.001 globally.**

Figure 250: For algorithm idemia-003 operating on visa images, the heatmap shows false match rates observed over impostor comparisons of faces from different individuals who were born in the given country pair. False matches are counted against a recognition threshold fixed globally to give the target FMR in the plot title, computed over all on the order of  $10^{10}$  impostor comparisons. If text appears in each box it give the same quantity as that coded by the color. Grey indicates FMR is at the intended FMR target level. Light red colors present a security vulnerability to, for example, a passport gate. Each +1 increase in  $\log_{10}$  FMR corresponds to a factor of 10 increase in FMR. The matrix is not quite symmetric because images in the enrollment and verification sets are different.

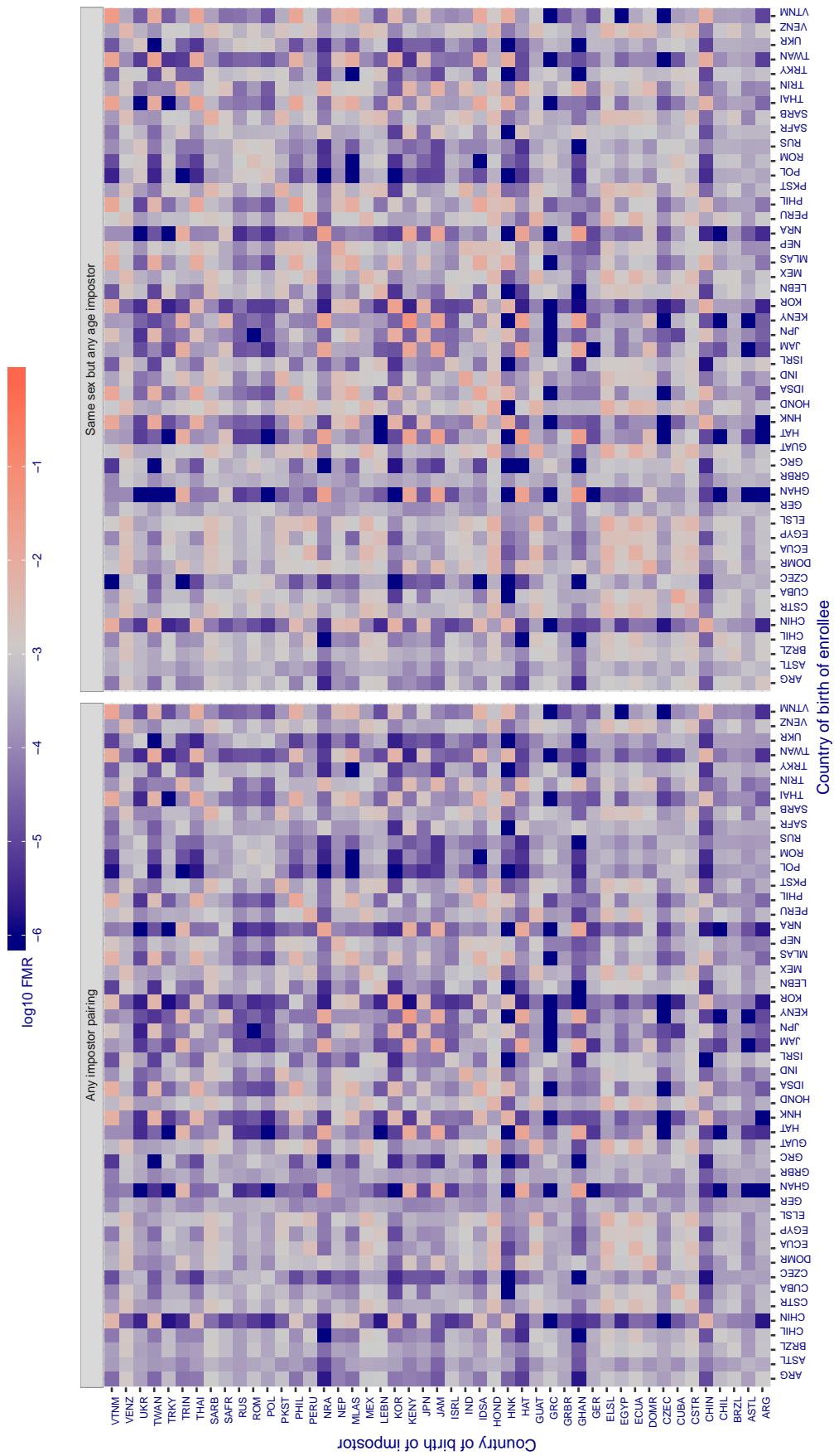
**Cross country FMR at threshold T = 3261.090 for algorithm idemia\_004, giving FMR(T) = 0.001 globally.**

Figure 251: For algorithm idemia-004 operating on visa images, the heatmap shows false match rates observed over impostor comparisons of faces from different individuals who were born in the given country pair. False matches are counted against a recognition threshold fixed globally to give the target FMR in the plot title, computed over all on the order of  $10^{10}$  impostor comparisons. If text appears in each box it give the same quantity as that coded by the color. Grey indicates FMR is at the intended FMR target level. Light red colors present a security vulnerability to, for example, a passport gate. Each +1 increase in  $\log_{10} FMR$  corresponds to a factor of 10 increase in FMR. The matrix is not quite symmetric because images in the enrollment and verification sets are different.

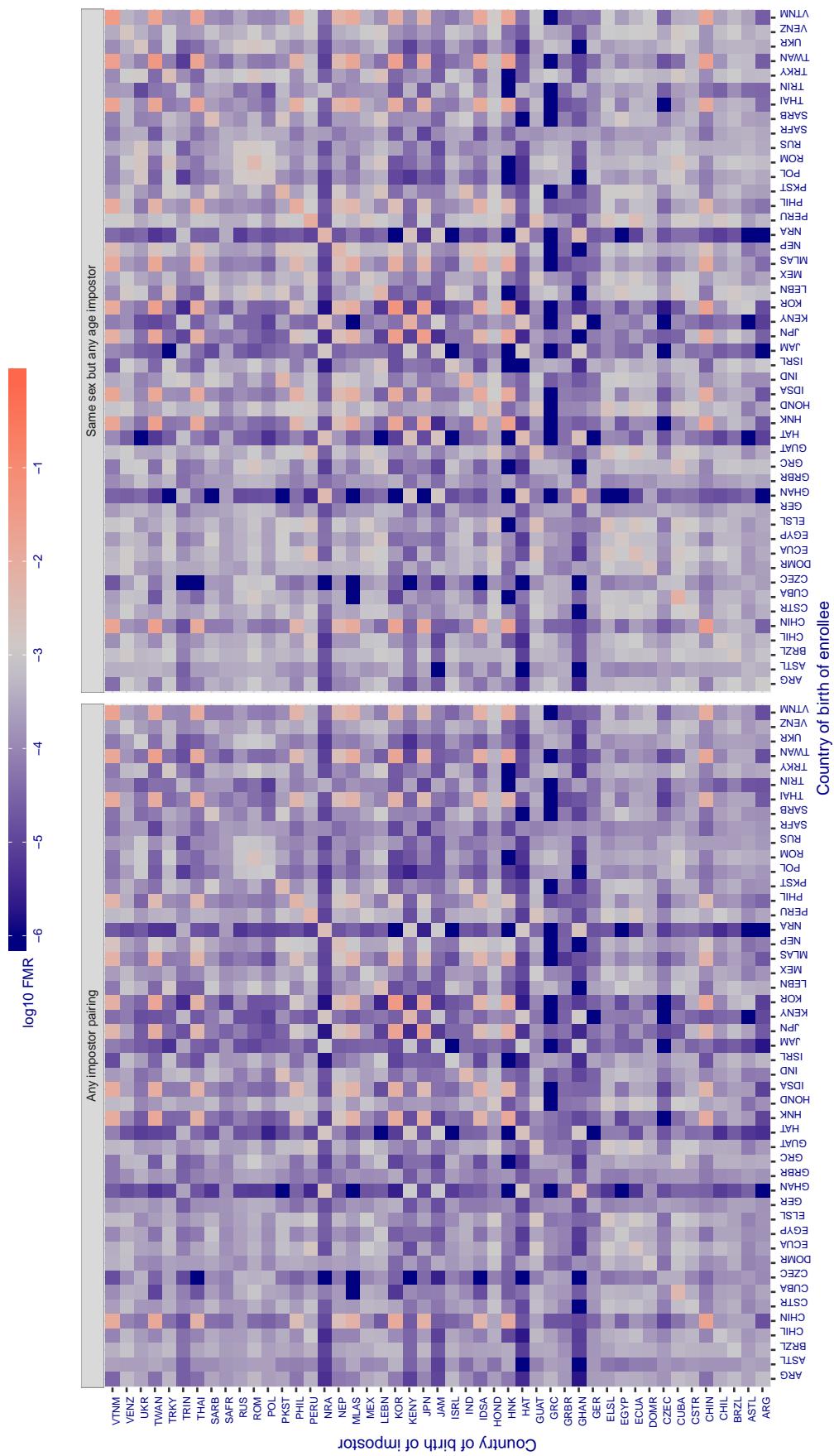
**Cross country FMR at threshold T = 0.721 for algorithm iit\_000, giving FMR(T) = 0.001 globally.**

Figure 252: For algorithm iit-000 operating on visa images, the heatmap shows false match rates observed over impostor comparisons of faces from different individuals who were born in the given country pair. False matches are counted against a recognition threshold fixed globally to give the target FMR in the plot title, computed over all on the order of  $10^{10}$  impostor comparisons. If text appears in each box it give the same quantity as that coded by the color. Grey indicates FMR is at the intended FMR target level. Light red colors present a security vulnerability to, for example, a passport gate. Each +1 increase in  $\log_{10} \text{FMR}$  corresponds to a factor of 10 increase in FMR. The matrix is not quite symmetric because images in the enrollment and verification sets are different.

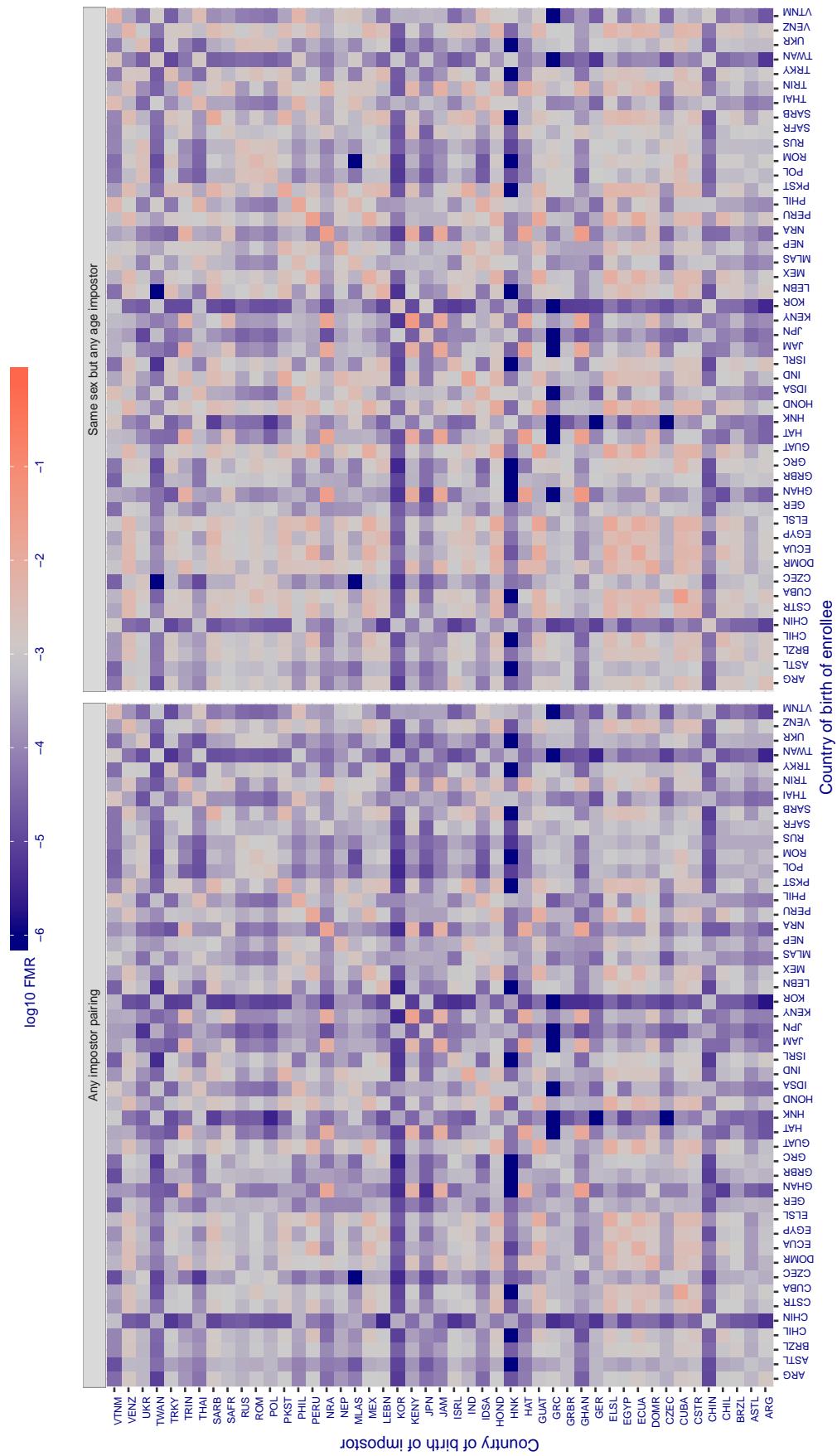
**Cross country FMR at threshold T = 1.302 for algorithm imperial\_000, giving FMR(T) = 0.001 globally.**

Figure 253: For algorithm imperial-000 operating on visa images, the heatmap shows false match rates observed over impostor comparisons of faces from different individuals who were born in the given country pair. False matches are counted against a recognition threshold fixed globally to give the target FMR in the plot title, computed over all on the order of  $10^{10}$  impostor comparisons. If text appears in each box it give the same quantity as that coded by the color. Grey indicates FMR is at the intended FMR target level. Light red colors present a security vulnerability to, for example, a passport gate. Each +1 increase in  $\log_{10} FMR$  corresponds to a factor of 10 increase in FMR. The matrix is not quite symmetric because images in the enrollment and verification sets are different.

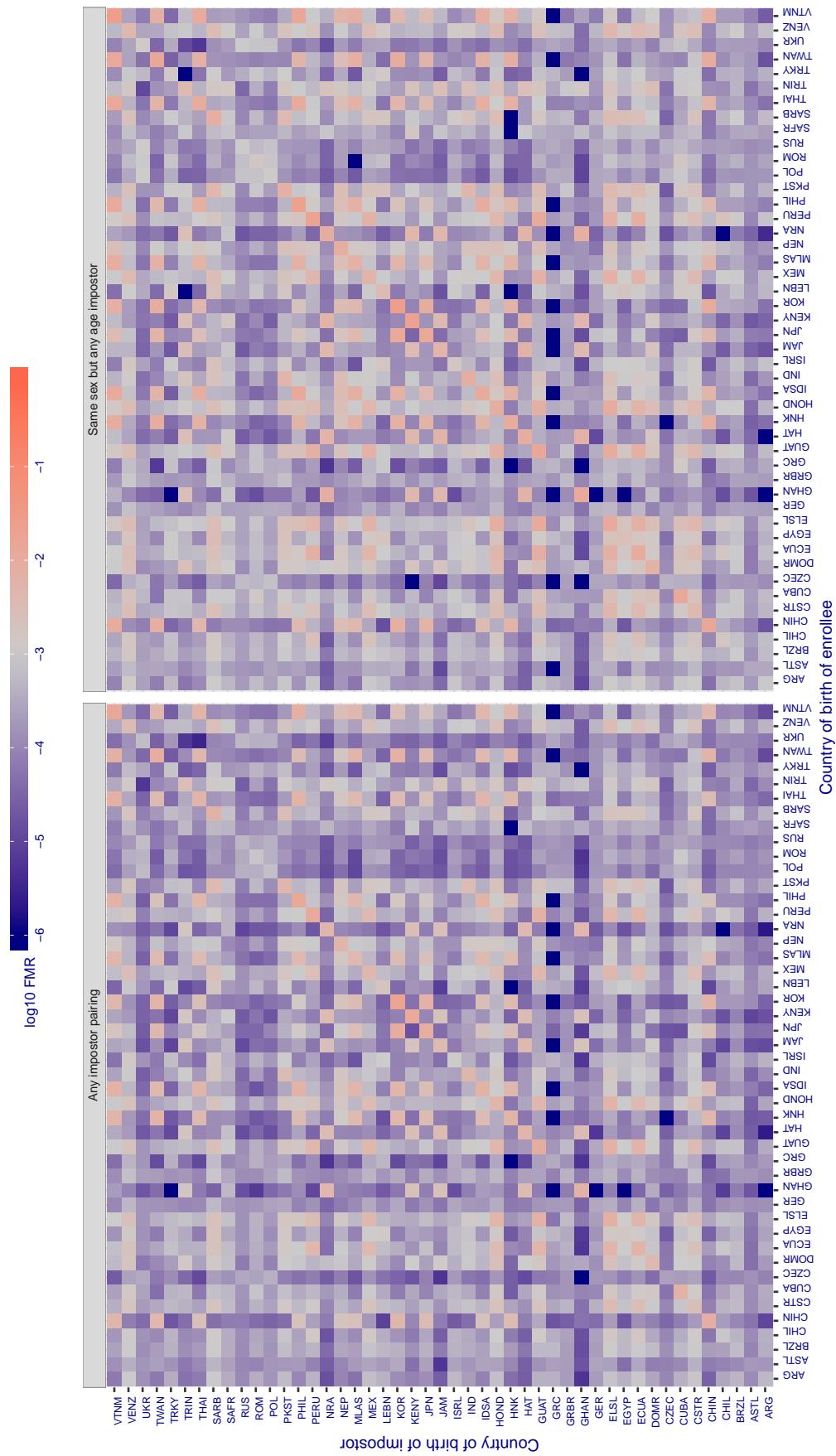
**Cross country FMR at threshold T = 1.320 for algorithm imperial\_001, giving FMR(T) = 0.001 globally.**

Figure 254: For algorithm imperial-001 operating on visa images, the heatmap shows false match rates observed over impostor comparisons of faces from different individuals who were born in the given country pair. False matches are counted against a recognition threshold fixed globally to give the target FMR in the plot title, computed over all on the order of  $10^{10}$  impostor comparisons. If text appears in each box it give the same quantity as that coded by the color. Grey indicates FMR is at the intended FMR target level. Light red colors present a security vulnerability to, for example, a passport gate. Each +1 increase in  $\log_{10} FMR$  corresponds to a factor of 10 increase in FMR. The matrix is not quite symmetric because images in the enrollment and verification sets are different.

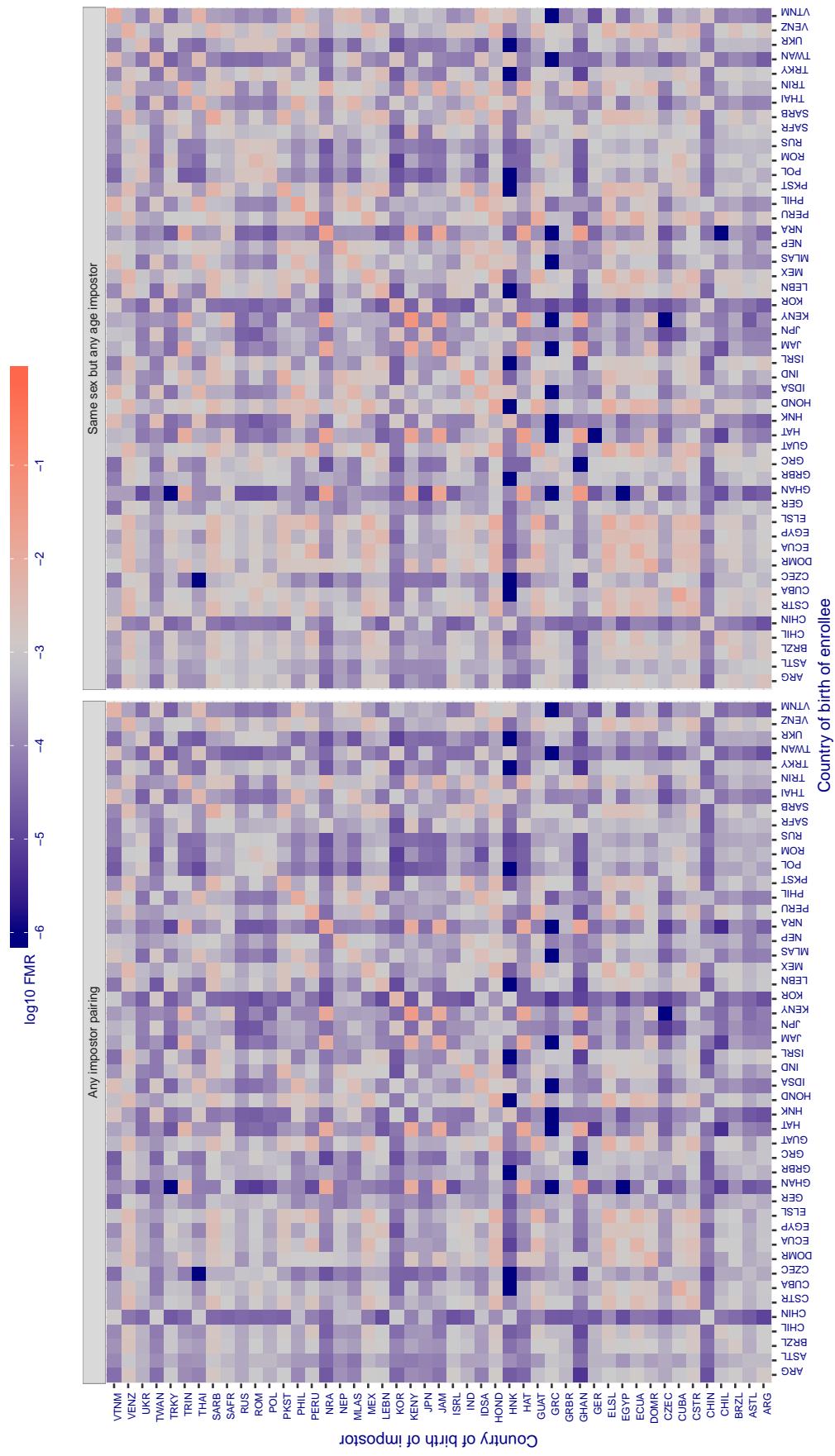
**Cross country FMR at threshold T = 1.288 for algorithm incode\_002, giving FMR(T) = 0.001 globally.**

Figure 255: For algorithm incode-002 operating on visa images, the heatmap shows false match rates observed over impostor comparisons of faces from different individuals who were born in the given country pair. False matches are counted against a recognition threshold fixed globally to give the target FMR in the plot title, computed over all on the order of  $10^{10}$  impostor comparisons. If text appears in each box it give the same quantity as that coded by the color. Grey indicates FMR is at the intended FMR target level. Light red colors present a security vulnerability to, for example, a passport gate. Each +1 increase in  $\log_{10} FMR$  corresponds to a factor of 10 increase in FMR. The matrix is not quite symmetric because images in the enrollment and verification sets are different.

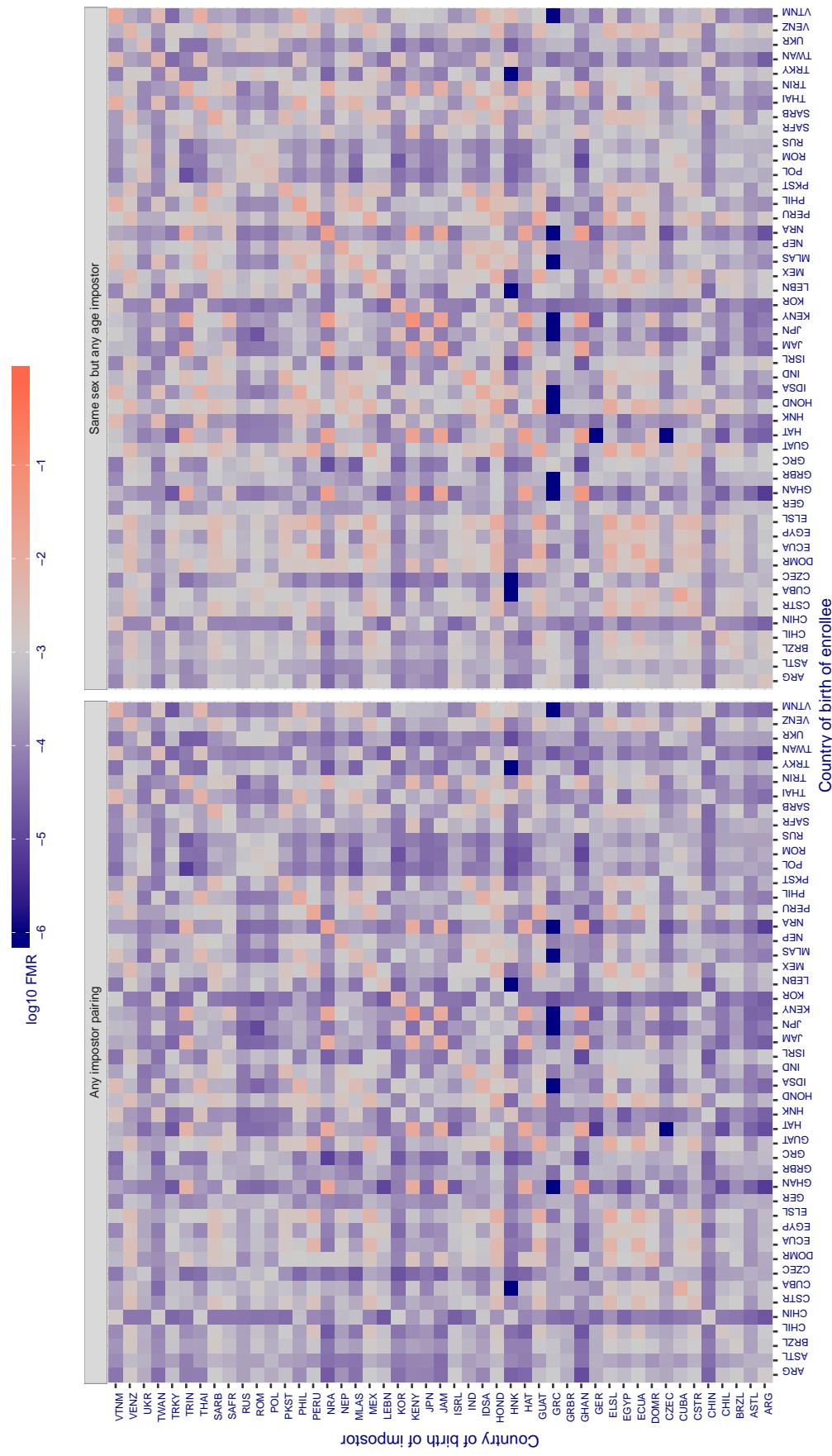
**Cross country FMR at threshold T = 1.340 for algorithm incode\_003, giving FMR(T) = 0.001 globally.**

Figure 256: For algorithm incode-003 operating on visa images, the heatmap shows false match rates observed over impostor comparisons of faces from different individuals who were born in the given country pair. False matches are counted against a recognition threshold fixed globally to give the target FMR in the plot title, computed over all on the order of  $10^{10}$  impostor comparisons. If text appears in each box it give the same quantity as that coded by the color. Grey indicates FMR is at the intended FMR target level. Light red colors present a security vulnerability to, for example, a passport gate. Each +1 increase in  $\log_{10} FMR$  corresponds to a factor of 10 increase in FMR. The matrix is not quite symmetric because images in the enrollment and verification sets are different.

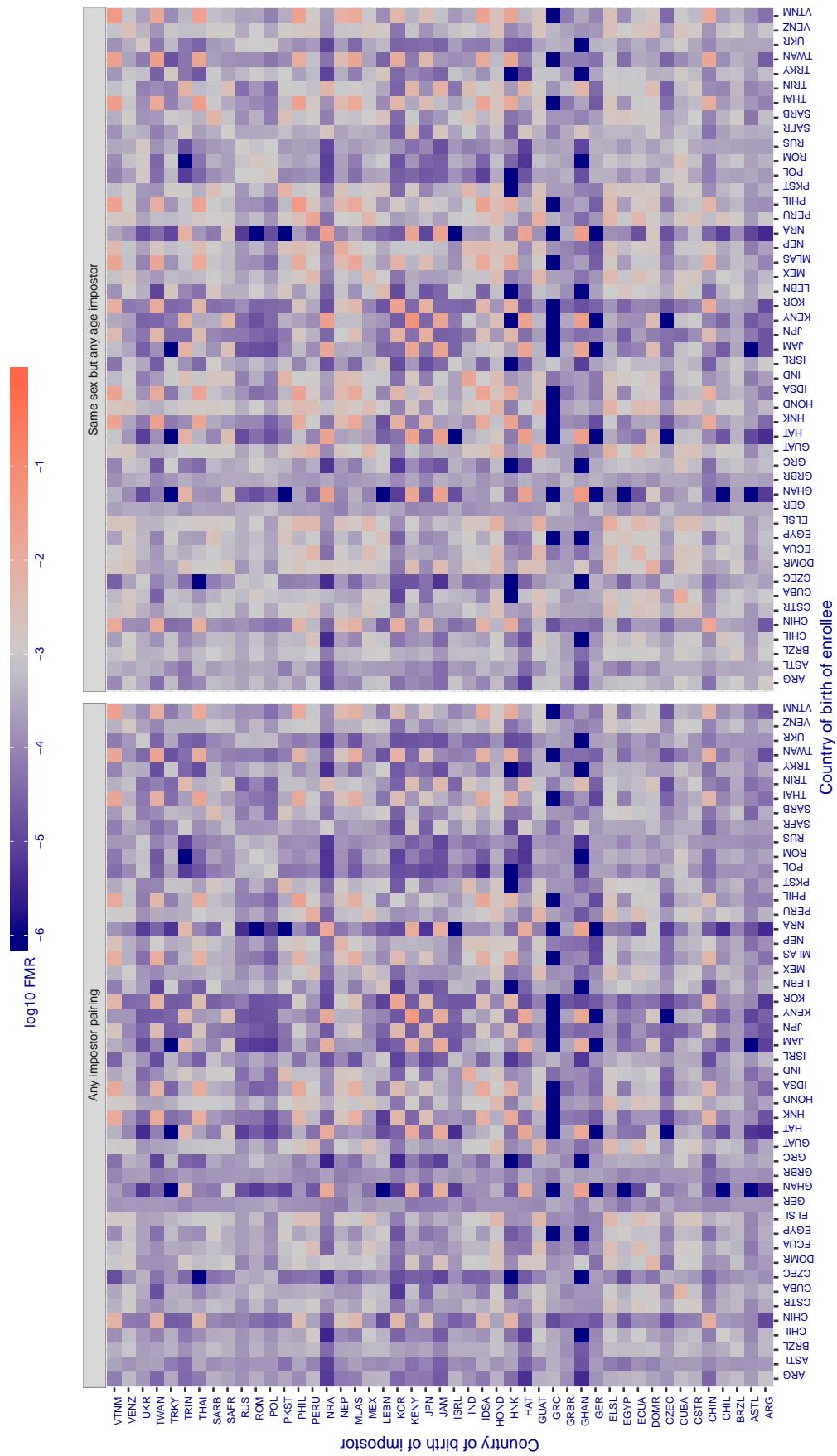
**Cross country FMR at threshold T = 21.422 for algorithm innovatrics\_004, giving FMR(T) = 0.001 globally.**

Figure 257: For algorithm innovatrics-004 operating on visa images, the heatmap shows false match rates observed over impostor comparisons of faces from different individuals who were born in the given country pair. False matches are counted against a recognition threshold fixed globally to give the target FMR in the plot title, computed over all on the order of  $10^{10}$  impostor comparisons. If text appears in each box it give the same quantity as that coded by the color. Grey indicates FMR is at the intended FMR target level. Light red colors present a security vulnerability to, for example, a passport gate. Each +1 increase in  $\log_{10} \text{FMR}$  corresponds to a factor of 10 increase in FMR. The matrix is not quite symmetric because images in the enrollment and verification sets are different.

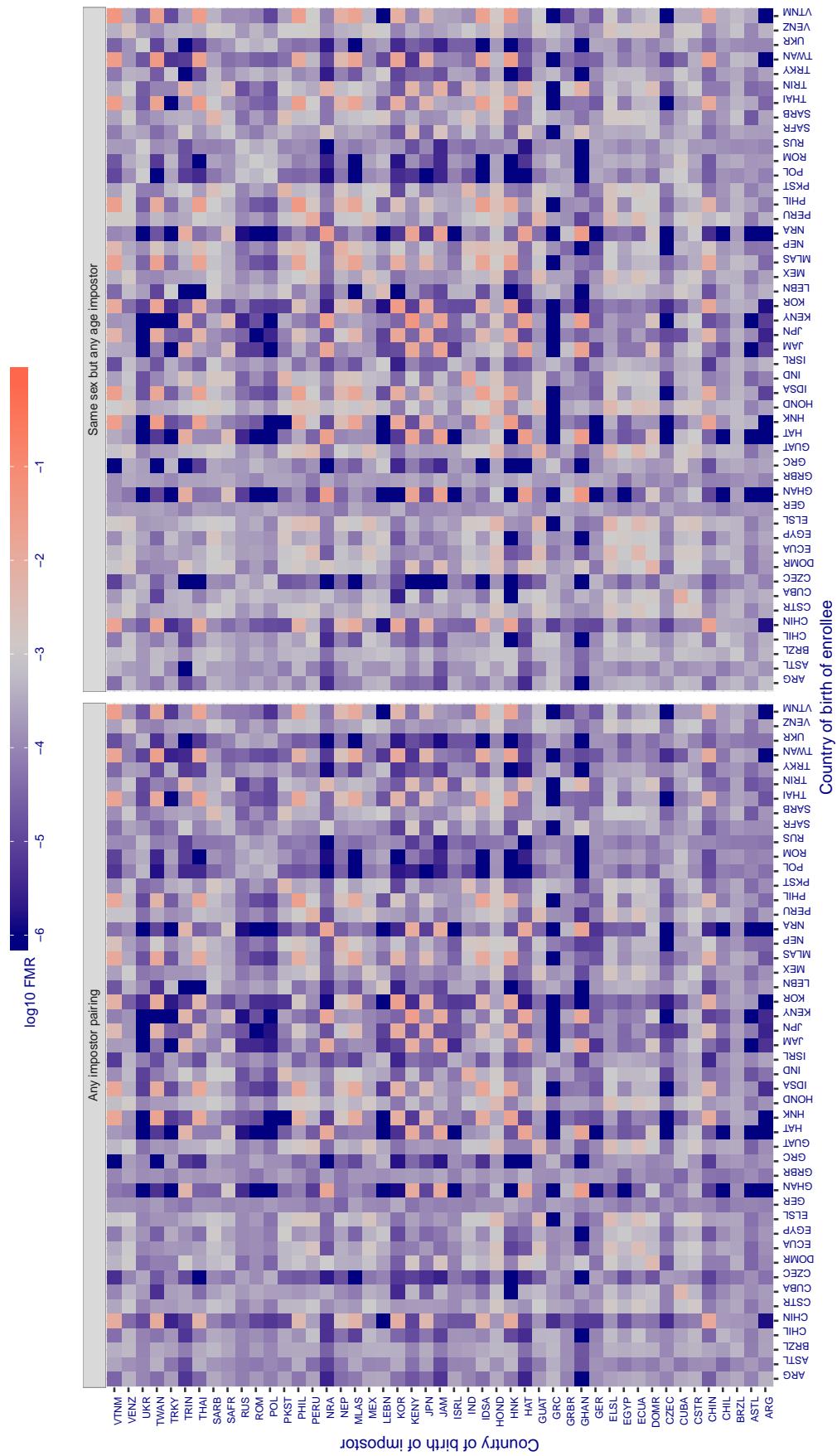
**Cross country FMR at threshold T = 28.706 for algorithm innovatrics\_005, giving FMR(T) = 0.001 globally.**

Figure 258: For algorithm innovatrics-005 operating on visa images, the heatmap shows false match rates observed over impostor comparisons of faces from different individuals who were born in the given country pair. False matches are counted against a recognition threshold fixed globally to give the target FMR in the plot title, computed over all on the order of  $10^{10}$  impostor comparisons. If text appears in each box it give the same quantity as that coded by the color. Grey indicates FMR is at the intended FMR target level. Light red colors present a security vulnerability to, for example, a passport gate. Each +1 increase in  $\log_{10} \text{FMR}$  corresponds to a factor of 10 increase in FMR. The matrix is not quite symmetric because images in the enrollment and verification sets are different.

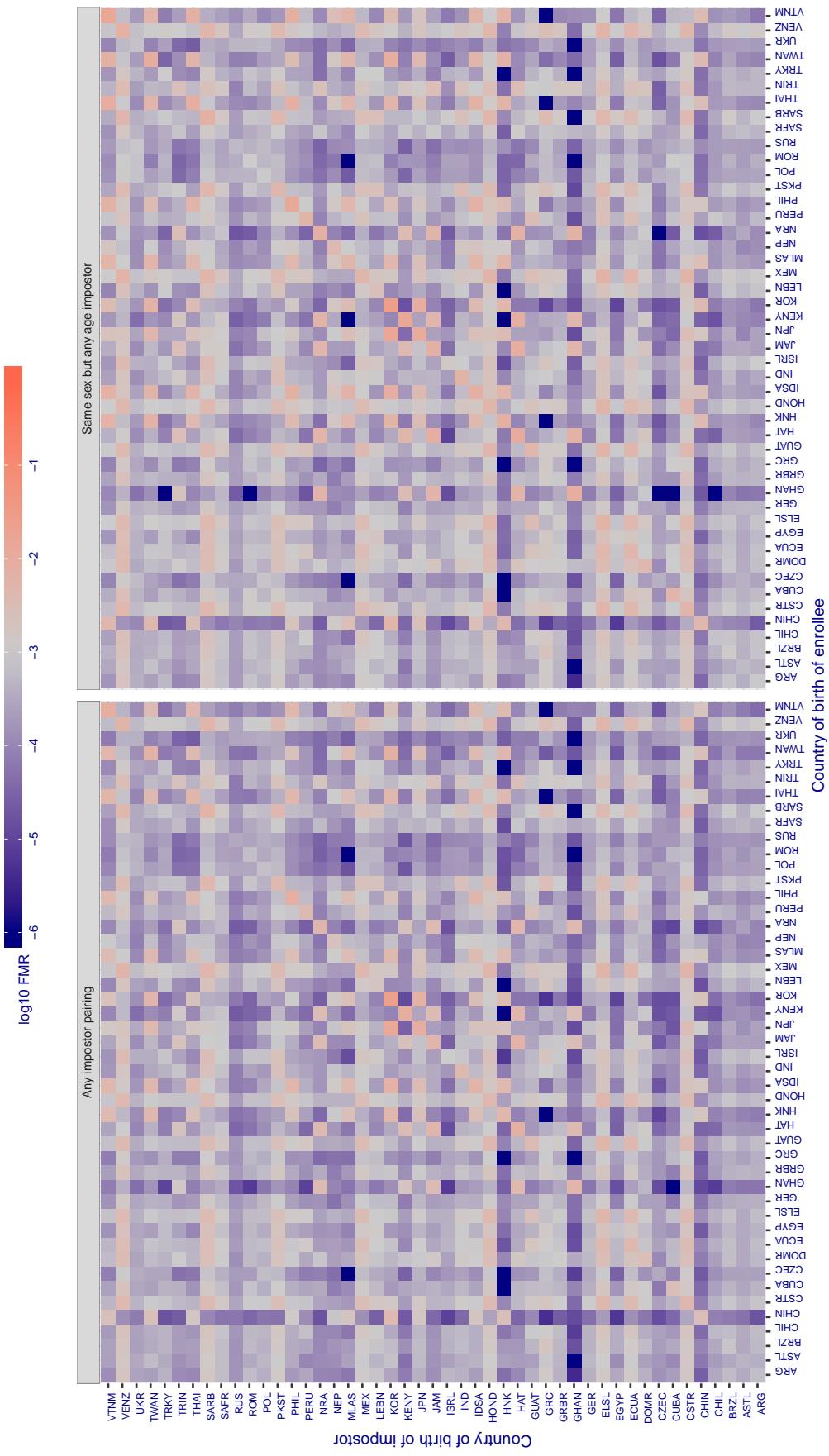
**Cross country FMR at threshold T = 37.554 for algorithm intellivision\_001, giving  $\text{FMR}(T) = 0.001$  globally.**

Figure 259: For algorithm intellivision-001 operating on visa images, the heatmap shows false match rates observed over impostor comparisons of faces from different individuals who were born in the given country pair. False matches are counted against a recognition threshold fixed globally to give the target  $\text{FMR}$  in the plot title, computed over all on the order of  $10^{10}$  impostor comparisons. If text appears in each box it give the same quantity as that coded by the color. Grey indicates  $\text{FMR}$  is at the intended  $\text{FMR}$  target level. Light red colors present a security vulnerability to, for example, a passport gate. Each +1 increase in  $\log_{10} \text{FMR}$  corresponds to a factor of 10 increase in  $\text{FMR}$ . The matrix is not quite symmetric because images in the enrollment and verification sets are different.

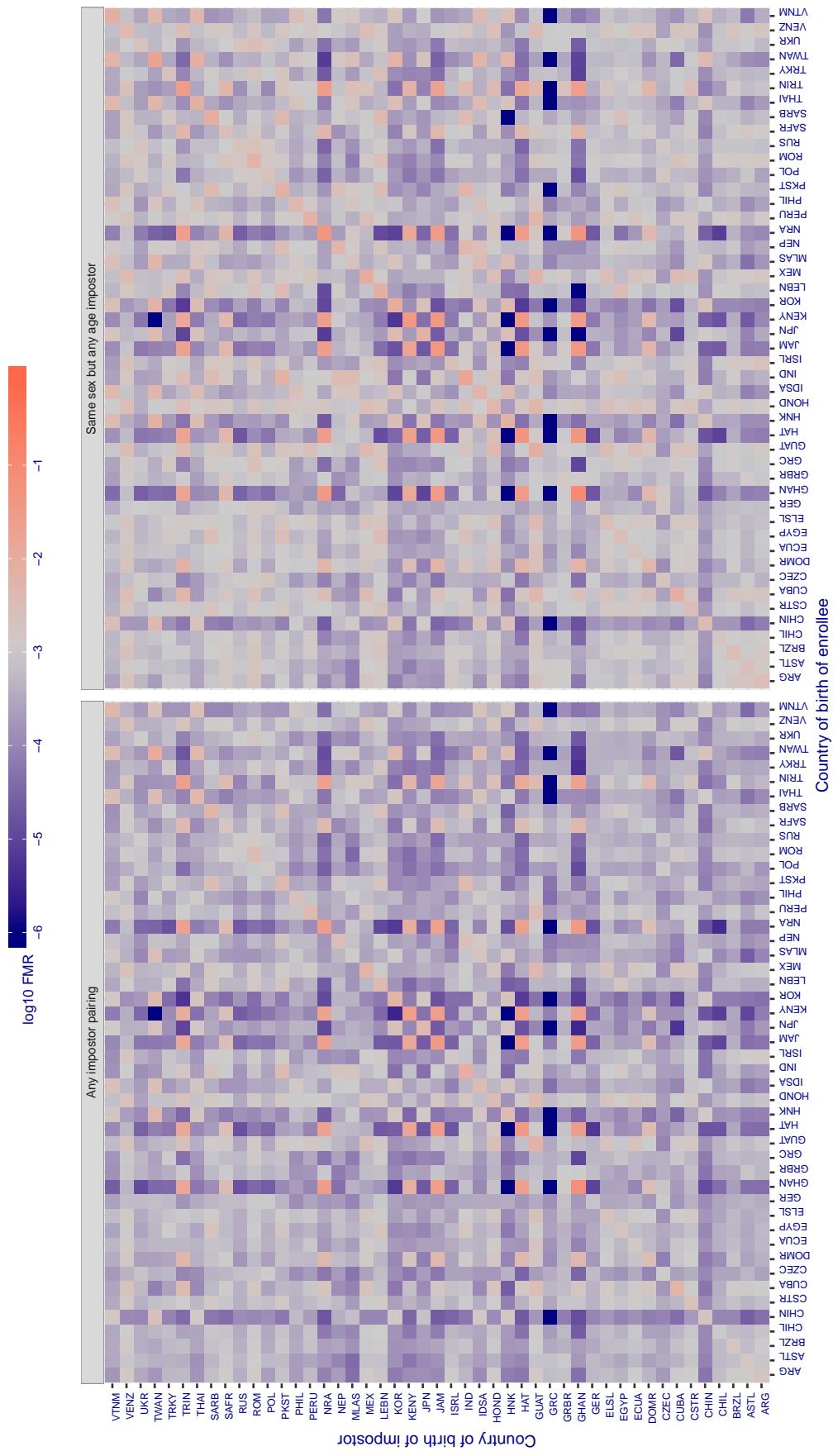
**Cross country FMR at threshold T = 20.648 for algorithm isityou\_000, giving FMR(T) = 0.001 globally.**

Figure 260: For algorithm isityou-000 operating on visa images, the heatmap shows false match rates observed over impostor comparisons of faces from different individuals who were born in the given country pair. False matches are counted against a recognition threshold fixed globally to give the target FMR in the plot title, computed over all on the order of  $10^{10}$  impostor comparisons. If text appears in each box it give the same quantity as that coded by the color. Grey indicates FMR is at the intended FMR target level. Light red colors present a security vulnerability to, for example, a passport gate. Each +1 increase in  $\log_{10}$  FMR corresponds to a factor of 10 increase in FMR. The matrix is not quite symmetric because images in the enrollment and verification sets are different.

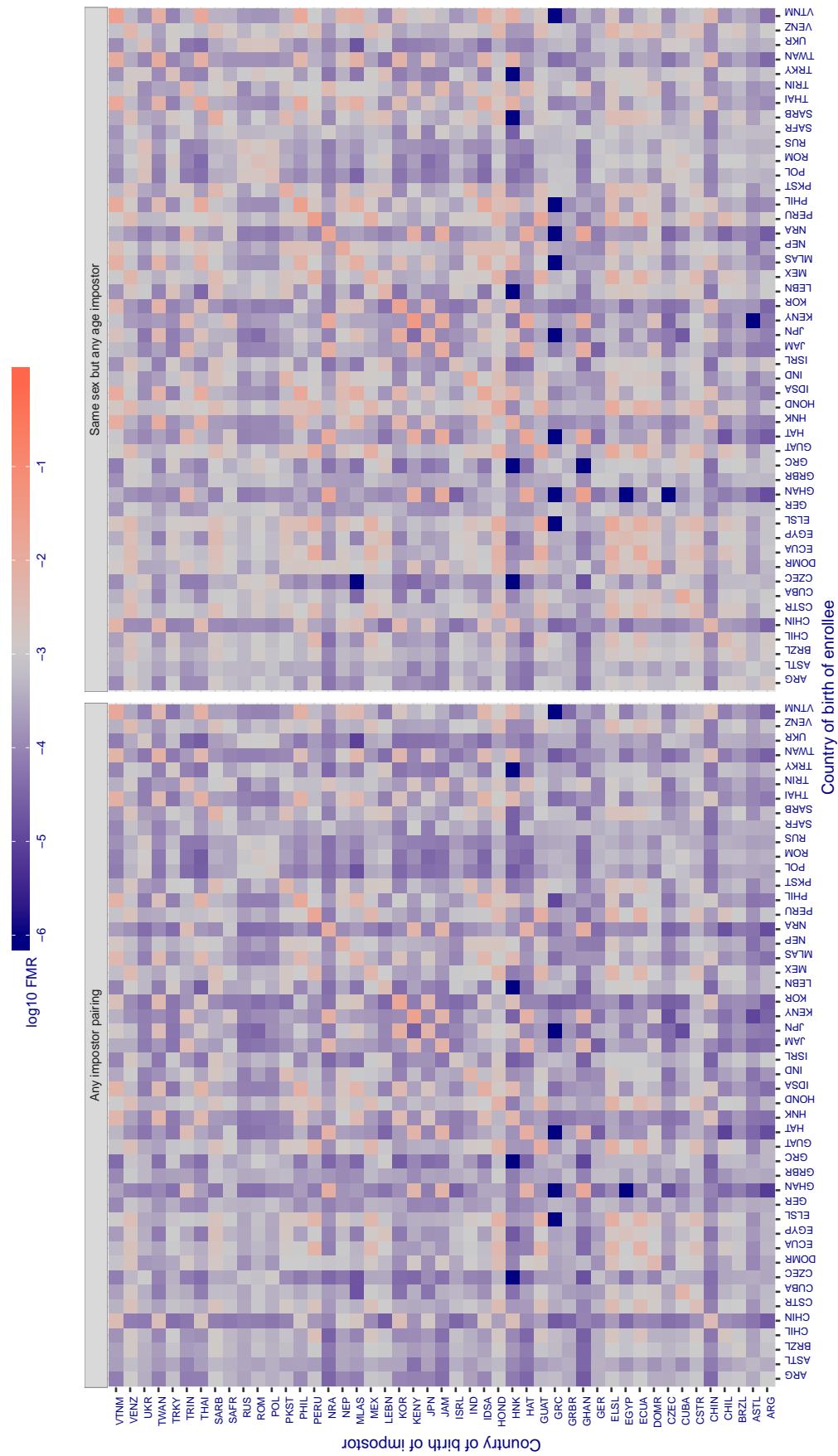
**Cross country FMR at threshold T = 0.649 for algorithm *systems\_001*, giving FMR(T) = 0.001 globally.**

Figure 261: For algorithm *systems-001* operating on visa images, the heatmap shows false match rates observed over impostor comparisons of faces from different individuals who were born in the given country pair. False matches are counted against a recognition threshold fixed globally to give the target FMR in the plot title, computed over all on the order of  $10^{10}$  impostor comparisons. If text appears in each box it give the same quantity as that coded by the color. Grey indicates FMR is at the intended FMR target level. Light red colors present a security vulnerability to, for example, a passport gate. Each +1 increase in  $\log_{10}$  FMR corresponds to a factor of 10 increase in FMR. The matrix is not quite symmetric because images in the enrollment and verification sets are different.

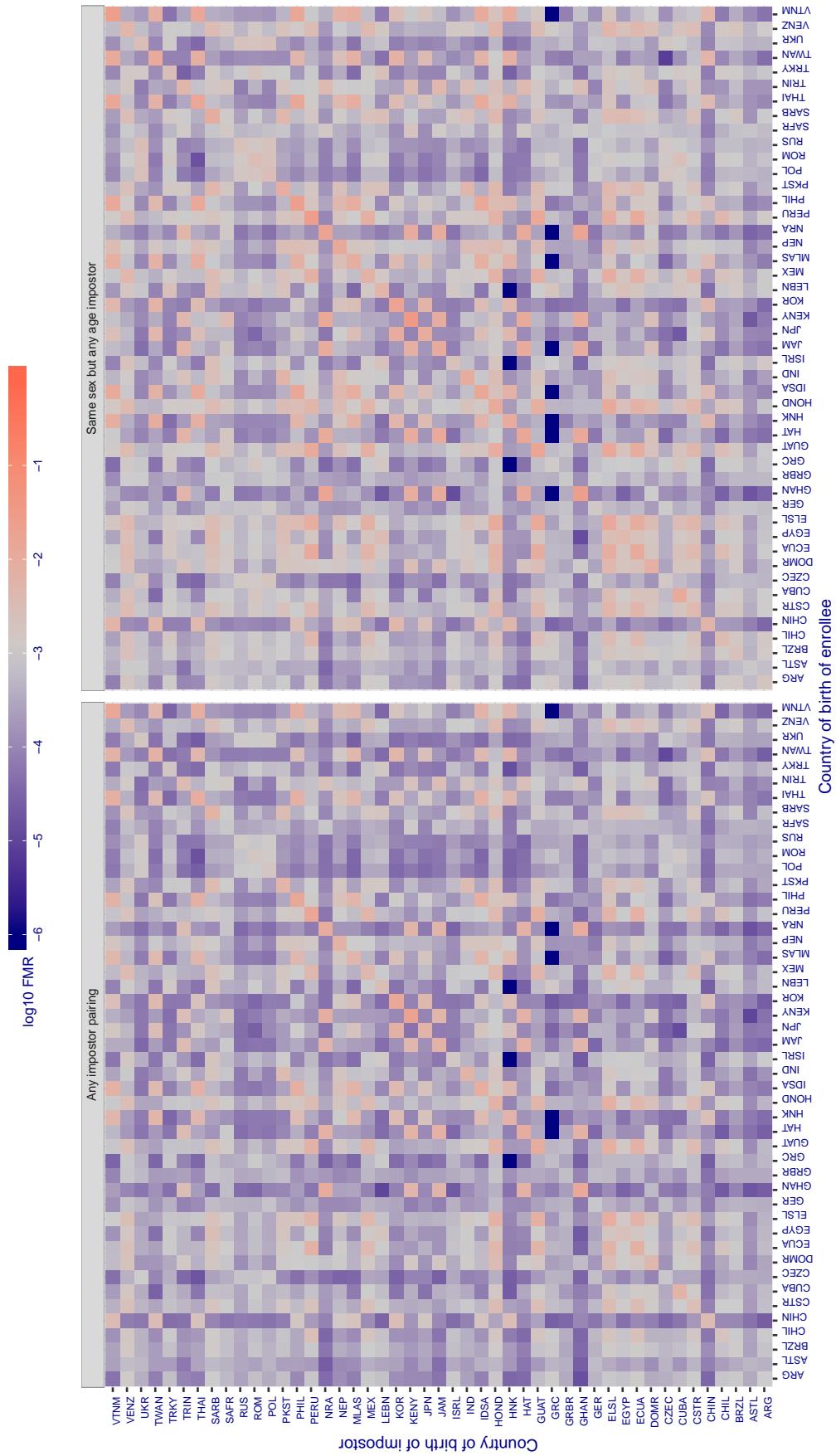
**Cross country FMR at threshold T = 0.647 for algorithm *systems\_002*, giving  $FMR(T) = 0.001$  globally.**

Figure 262: For algorithm *systems-002* operating on visa images, the heatmap shows false match rates observed over impostor comparisons of faces from different individuals who were born in the given country pair. False matches are counted against a recognition threshold fixed globally to give the target  $FMR$  in the plot title, computed over all on the order of  $10^{10}$  impostor comparisons. If text appears in each box it give the same quantity as that coded by the color. Grey indicates  $FMR$  is at the intended  $FMR$  target level. Light red colors present a security vulnerability to, for example, a passport gate. Each +1 increase in  $\log_{10} FMR$  corresponds to a factor of 10 increase in  $FMR$ . The matrix is not quite symmetric because images in the enrollment and verification sets are different.

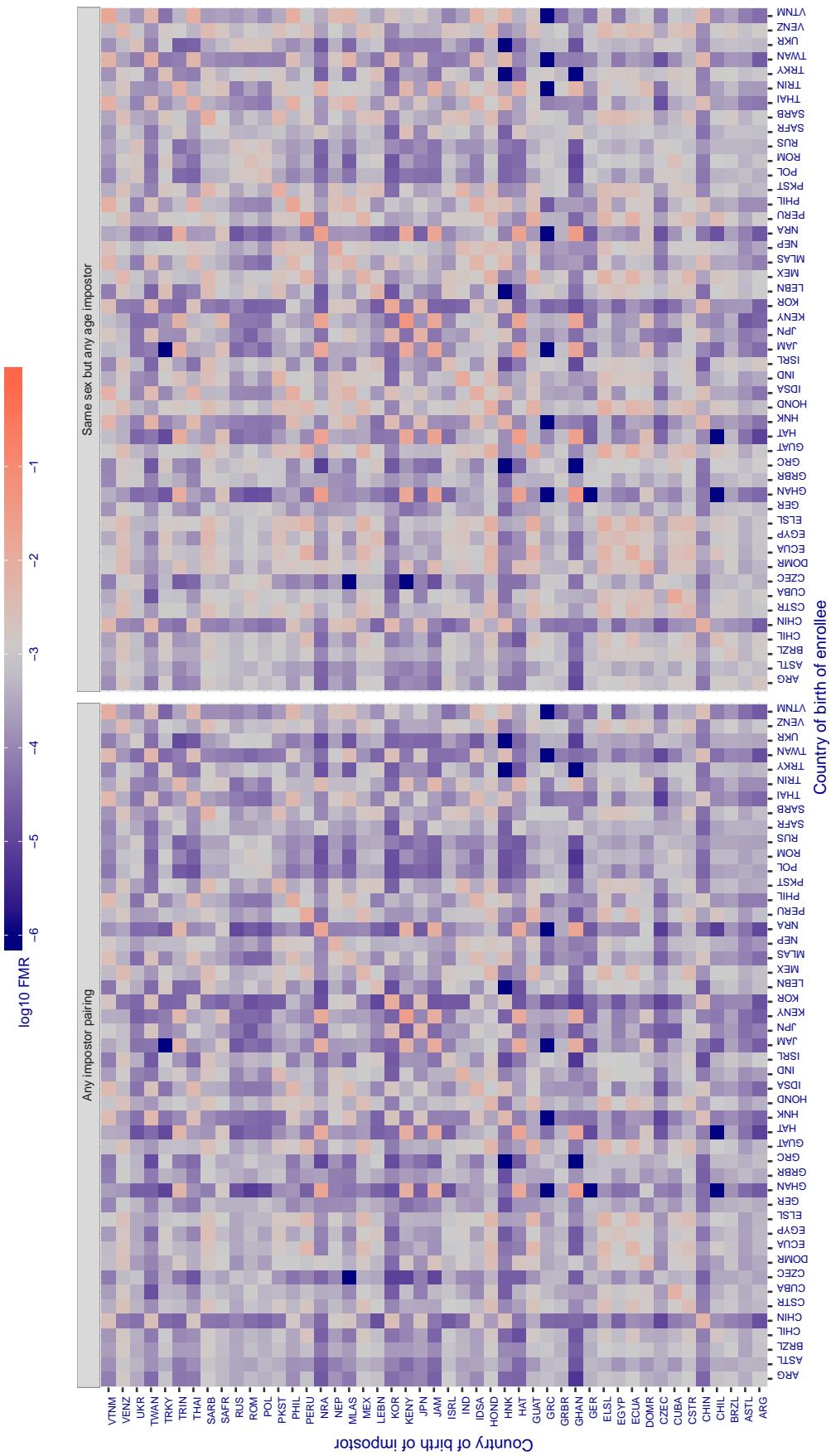
**Cross country FMR at threshold T = 10.316 for algorithm itmo\_005, giving FMR(T) = 0.001 globally.**

Figure 263: For algorithm itmo-005 operating on visa images, the heatmap shows false match rates observed over impostor comparisons of faces from different individuals who were born in the given country pair. False matches are counted against a recognition threshold fixed globally to give the target FMR in the plot title, computed over all on the order of  $10^{10}$  impostor comparisons. If text appears in each box it give the same quantity as that coded by the color. Grey indicates FMR is at the intended FMR target level. Light red colors present a security vulnerability to, for example, a passport gate. Each +1 increase in  $\log_{10}$  FMR corresponds to a factor of 10 increase in FMR. The matrix is not quite symmetric because images in the enrollment and verification sets are different.

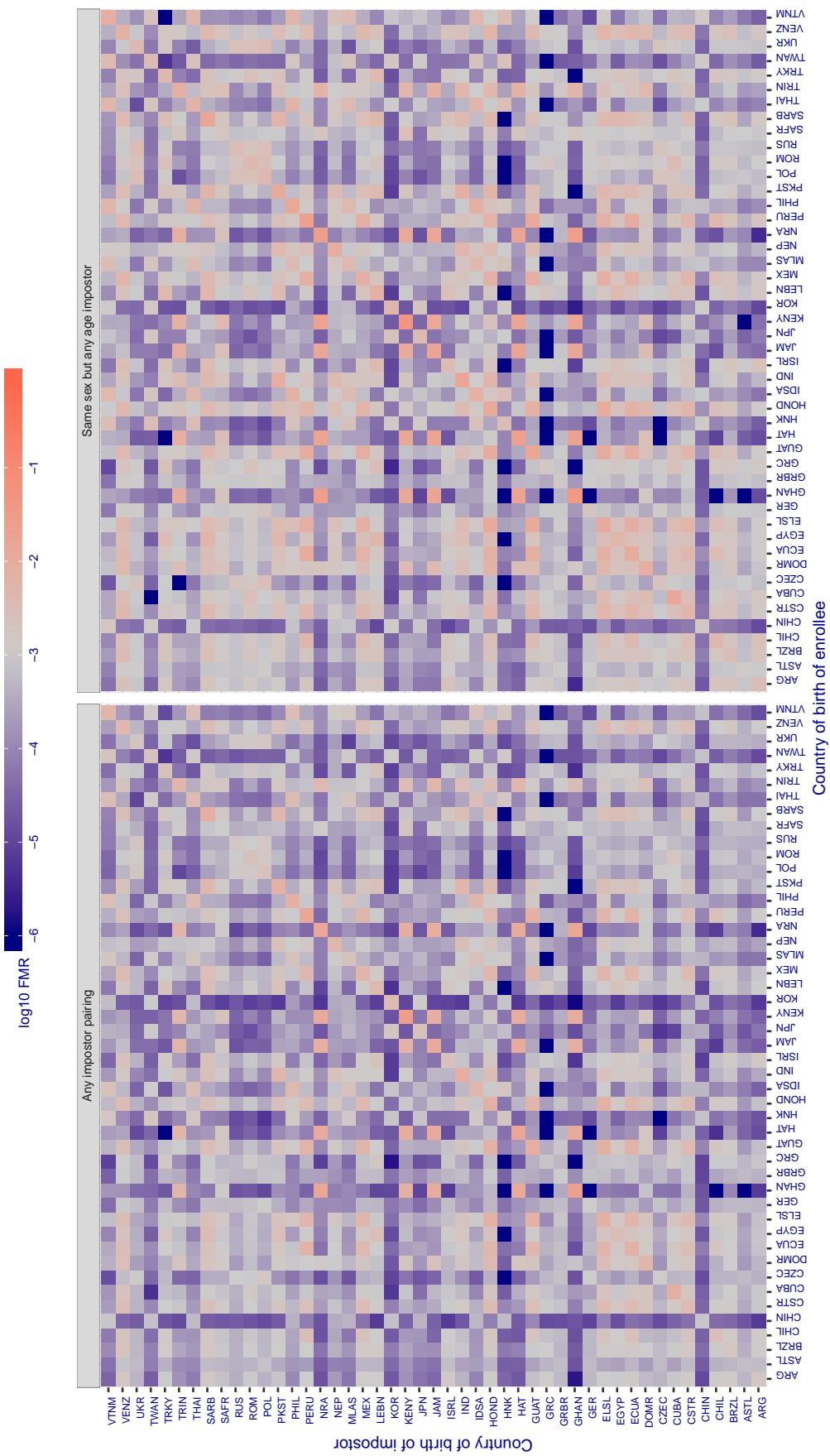
**Cross country FMR at threshold T = 12.030 for algorithm itmo\_006, giving FMR(T) = 0.001 globally.**

Figure 264: For algorithm itmo-006 operating on visa images, the heatmap shows false match rates observed over impostor comparisons of faces from different individuals who were born in the given country pair. False matches are counted against a recognition threshold fixed globally to give the target FMR in the plot title, computed over all on the order of  $10^{10}$  impostor comparisons. If text appears in each box it give the same quantity as that coded by the color. Grey indicates FMR is at the intended FMR target level. Light red colors present a security vulnerability to, for example, a passport gate. Each +1 increase in  $\log_{10} \text{FMR}$  corresponds to a factor of 10 increase in FMR. The matrix is not quite symmetric because images in the enrollment and verification sets are different.

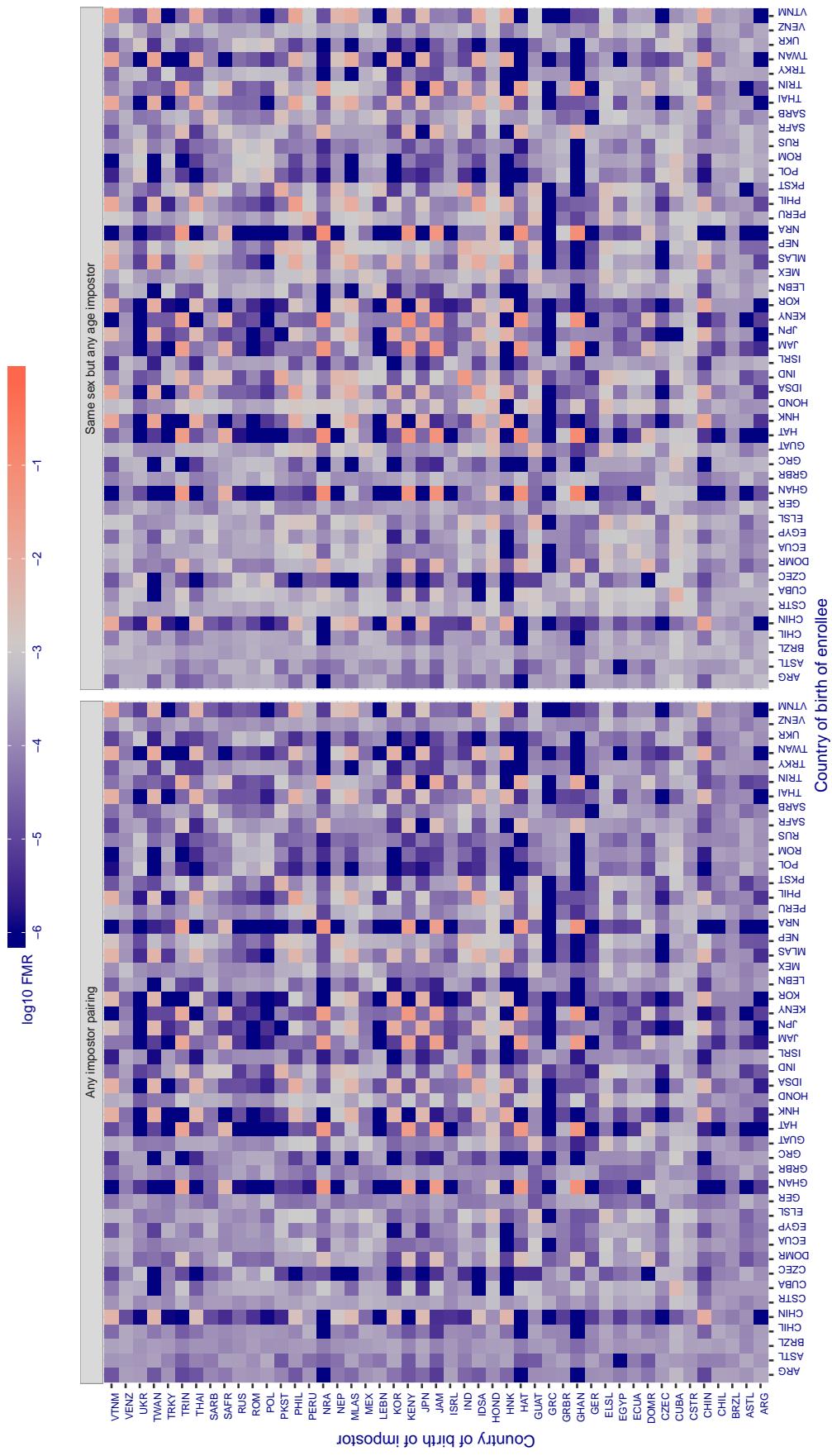
**Cross country FMR at threshold T = 1.192 for algorithm kakao\_001, giving  $FMR(T) = 0.001$  globally.**

Figure 265: For algorithm kakao-001 operating on visa images, the heatmap shows false match rates observed over impostor comparisons of faces from different individuals who were born in the given country pair. False matches are counted against a recognition threshold fixed globally to give the target FMR in the plot title, computed over all on the order of  $10^{10}$  impostor comparisons. If text appears in each box it give the same quantity as that coded by the color. Grey indicates FMR is at the intended FMR target level. Light red colors present a security vulnerability to, for example, a passport gate. Each +1 increase in  $\log_{10} FMR$  corresponds to a factor of 10 increase in FMR. The matrix is not quite symmetric because images in the enrollment and verification sets are different.

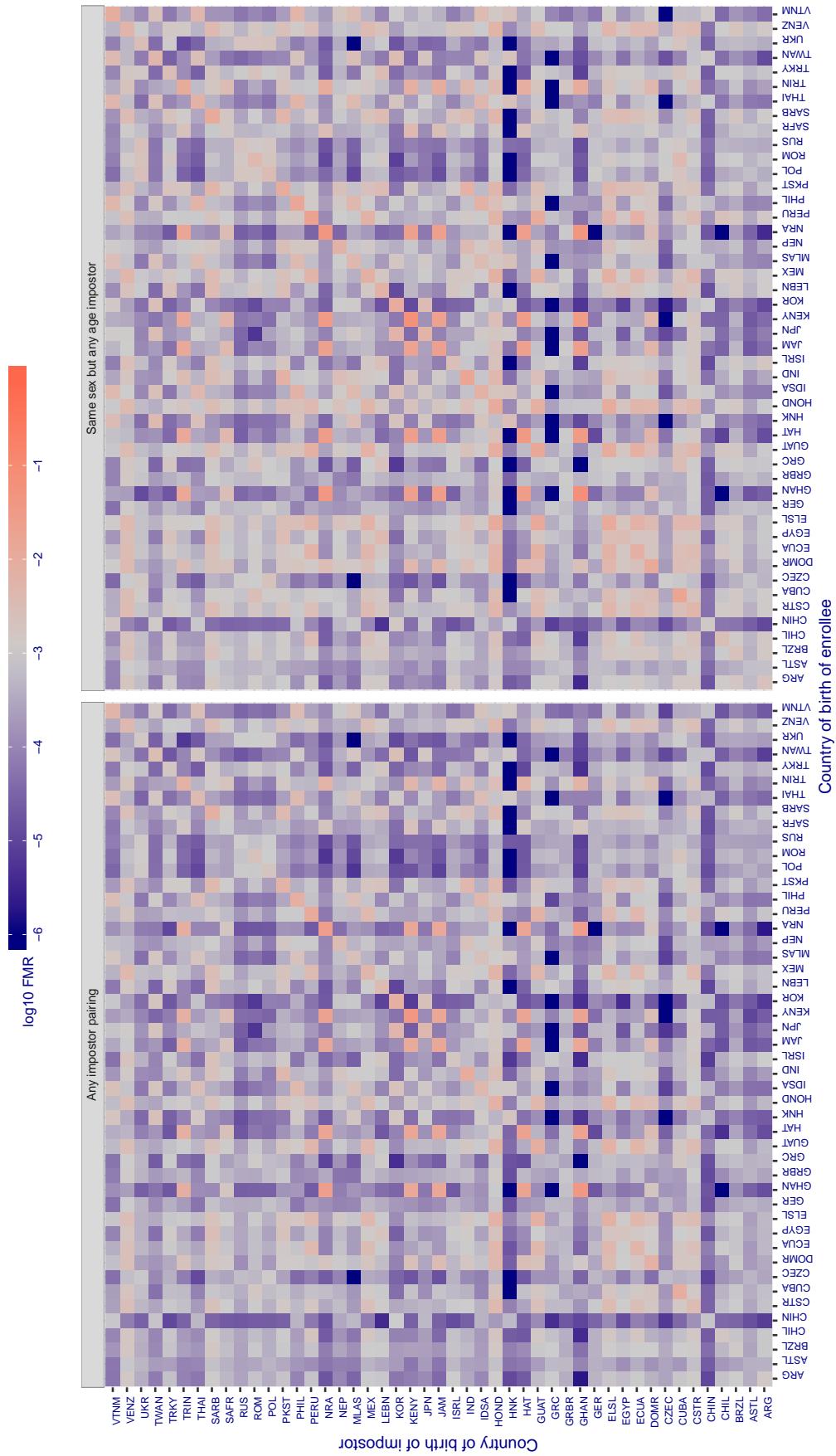
**Cross country FMR at threshold T = 0.656 for algorithm lookman\_002, giving  $FMR(T) = 0.001$  globally.**

Figure 266: For algorithm lookman-002 operating on visa images, the heatmap shows false match rates observed over impostor comparisons of faces from different individuals who were born in the given country pair. False matches are counted against a recognition threshold fixed globally to give the target  $FMR$  in the plot title, computed over all on the order of  $10^{10}$  impostor comparisons. If text appears in each box it give the same quantity as that coded by the color. Grey indicates  $FMR$  is at the intended  $FMR$  target level. Light red colors present a security vulnerability to, for example, a passport gate. Each +1 increase in  $\log_{10} FMR$  corresponds to a factor of 10 increase in  $FMR$ . The matrix is not quite symmetric because images in the enrollment and verification sets are different.

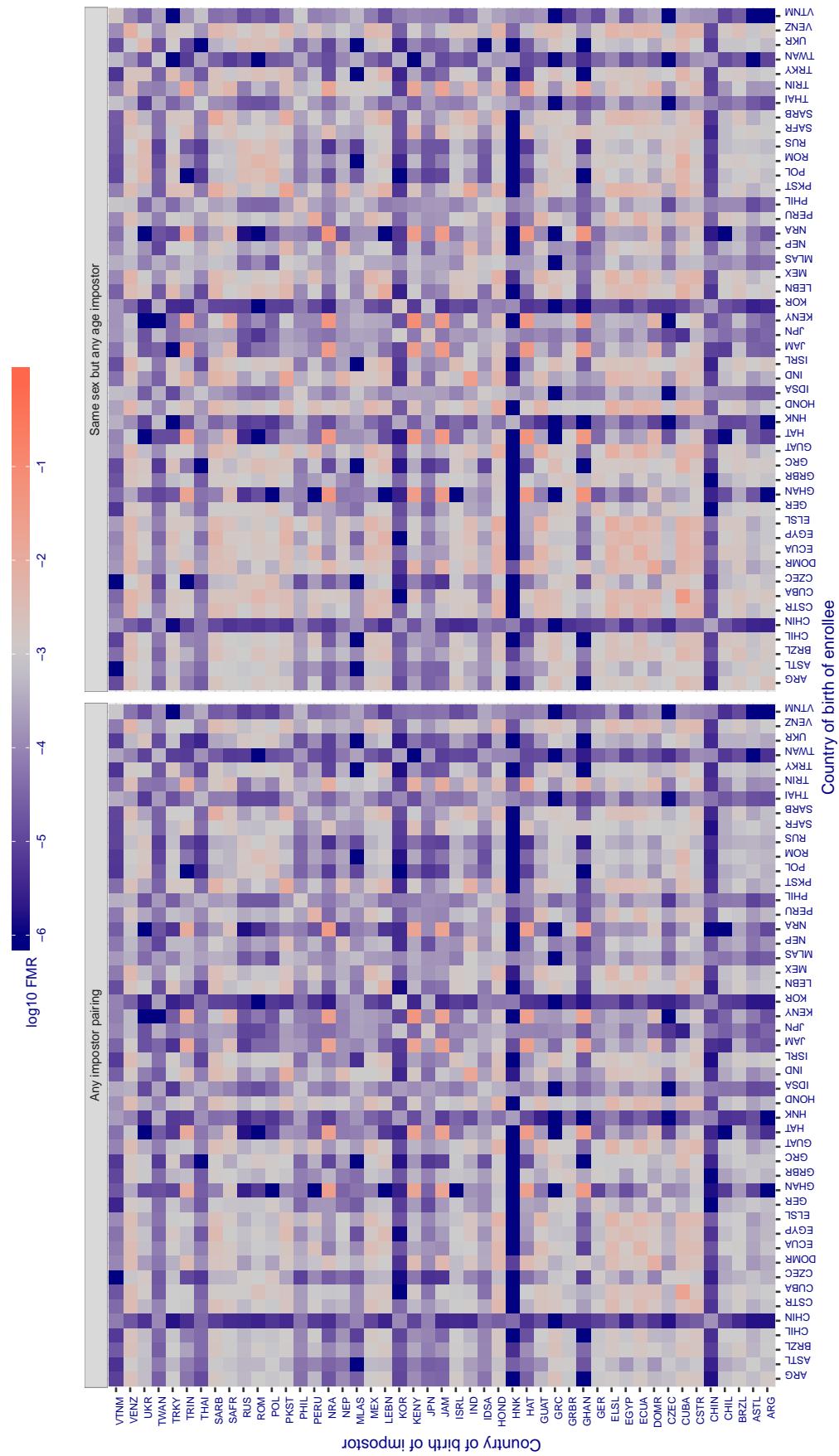
**Cross country FMR at threshold T = 66.706 for algorithm megvii\_001, giving FMR(T) = 0.001 globally.**

Figure 267: For algorithm megvii-001 operating on visa images, the heatmap shows false match rates observed over impostor comparisons of faces from different individuals who were born in the given country pair. False matches are counted against a recognition threshold fixed globally to give the target FMR in the plot title, computed over all on the order of  $10^{10}$  impostor comparisons. If text appears in each box it give the same quantity as that coded by the color. Grey indicates FMR is at the intended FMR target level. Light red colors present a security vulnerability to, for example, a passport gate. Each +1 increase in  $\log_{10} \text{FMR}$  corresponds to a factor of 10 increase in FMR. The matrix is not quite symmetric because images in the enrollment and verification sets are different.

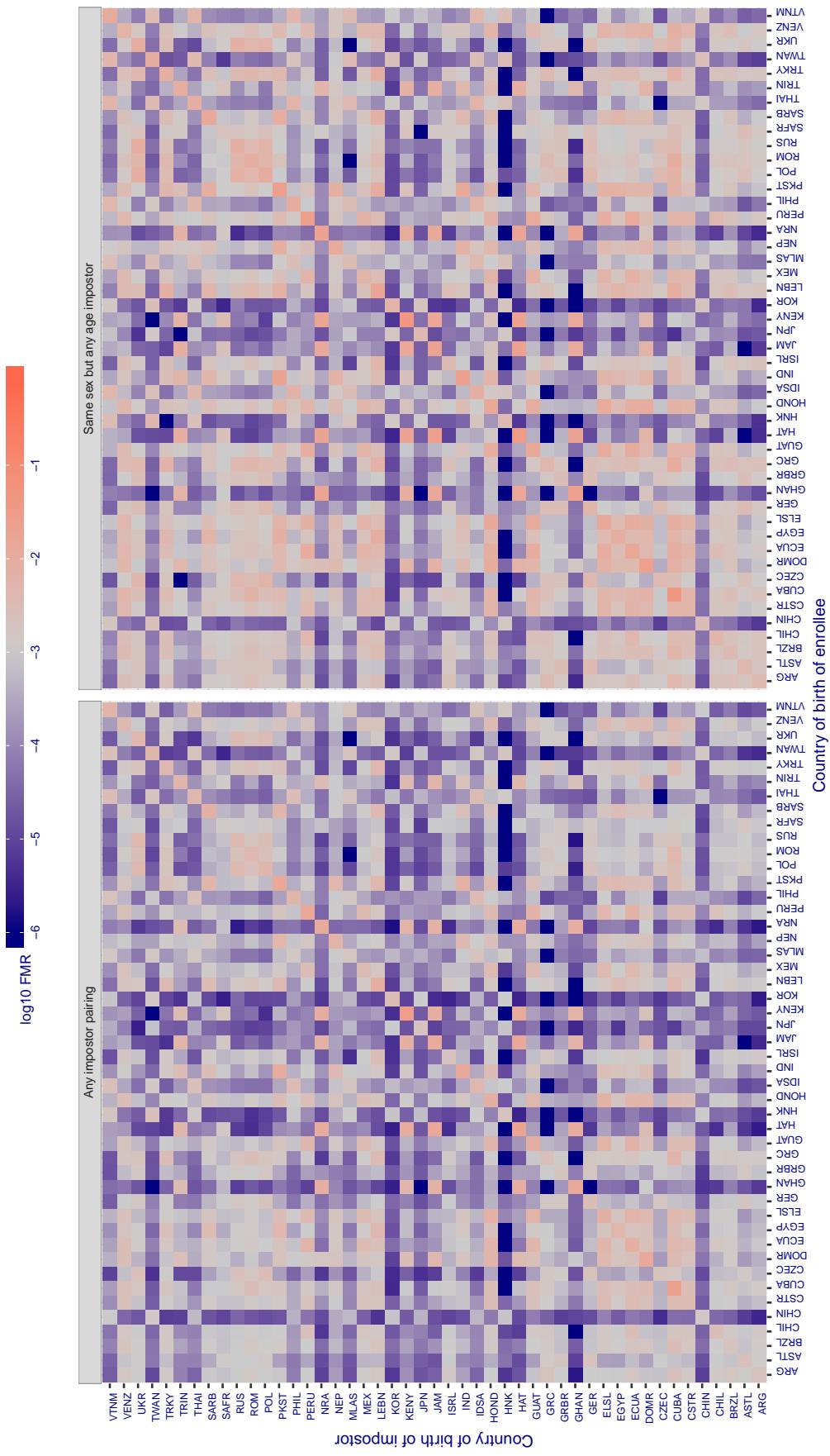
**Cross country FMR at threshold T = 58.026 for algorithm megvii\_002, giving FMR(T) = 0.001 globally.**

Figure 268: For algorithm megvii-002 operating on visa images, the heatmap shows false match rates observed over impostor comparisons of faces from different individuals who were born in the given country pair. False matches are counted against a recognition threshold fixed globally to give the target FMR in the plot title, computed over all on the order of  $10^{10}$  impostor comparisons. If text appears in each box it give the same quantity as that coded by the color. Grey indicates FMR is at the intended FMR target level. Light red colors present a security vulnerability to, for example, a passport gate. Each +1 increase in  $\log_{10}$  FMR corresponds to a factor of 10 increase in FMR. The matrix is not quite symmetric because images in the enrollment and verification sets are different.

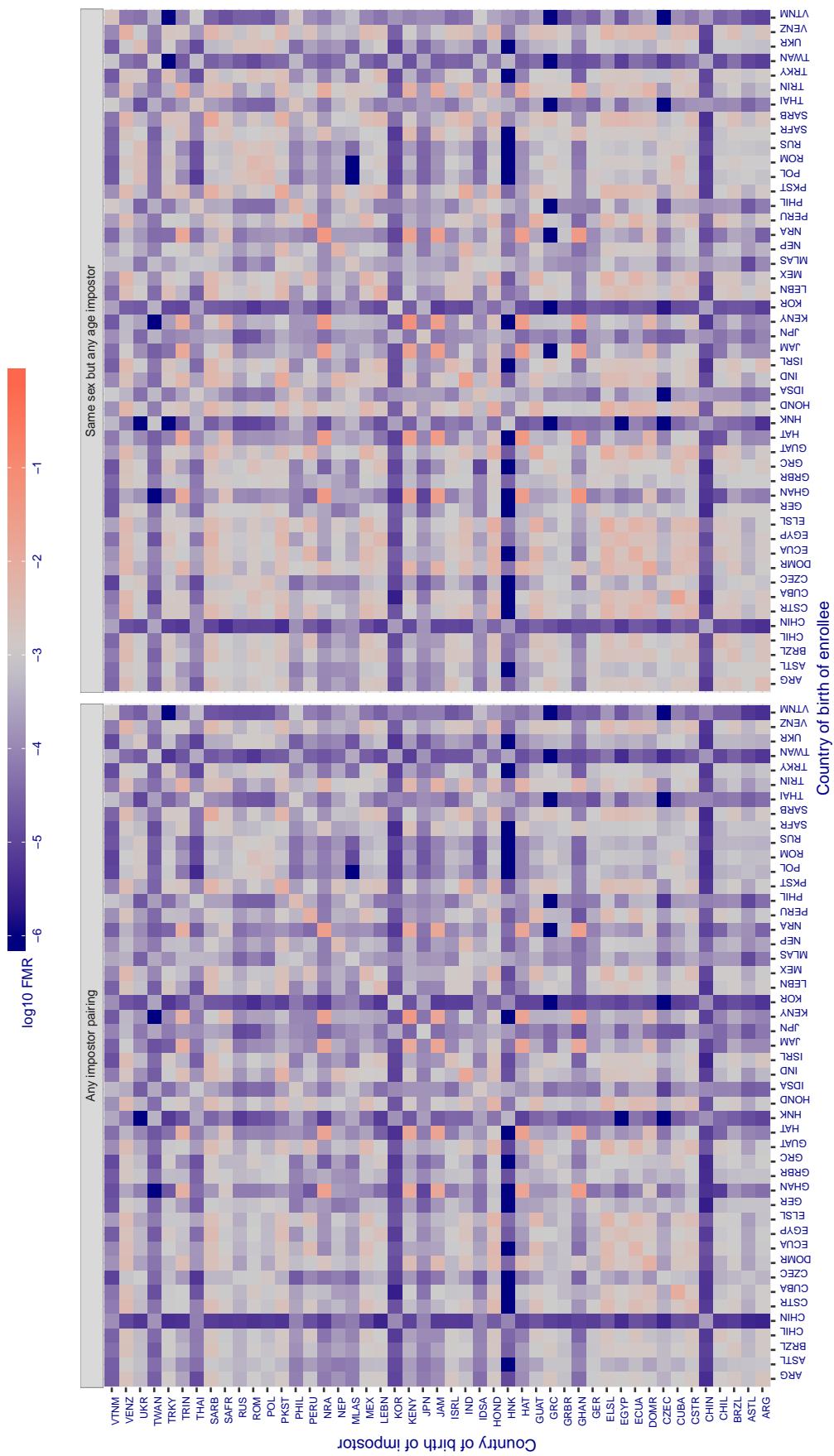
**Cross country FMR at threshold T = 0.345 for algorithm meiya\_001, giving FMR(T) = 0.001 globally.**

Figure 269: For algorithm meiya-001 operating on visa images, the heatmap shows false match rates observed over impostor comparisons of faces from different individuals who were born in the given country pair. False matches are counted against a recognition threshold fixed globally to give the target FMR in the plot title, computed over all on the order of  $10^{10}$  impostor comparisons. If text appears in each box it give the same quantity as that coded by the color. Grey indicates FMR is at the intended FMR target level. Light red colors present a security vulnerability to, for example, a passport gate. Each +1 increase in  $\log_{10} \text{FMR}$  corresponds to a factor of 10 increase in FMR. The matrix is not quite symmetric because images in the enrollment and verification sets are different.

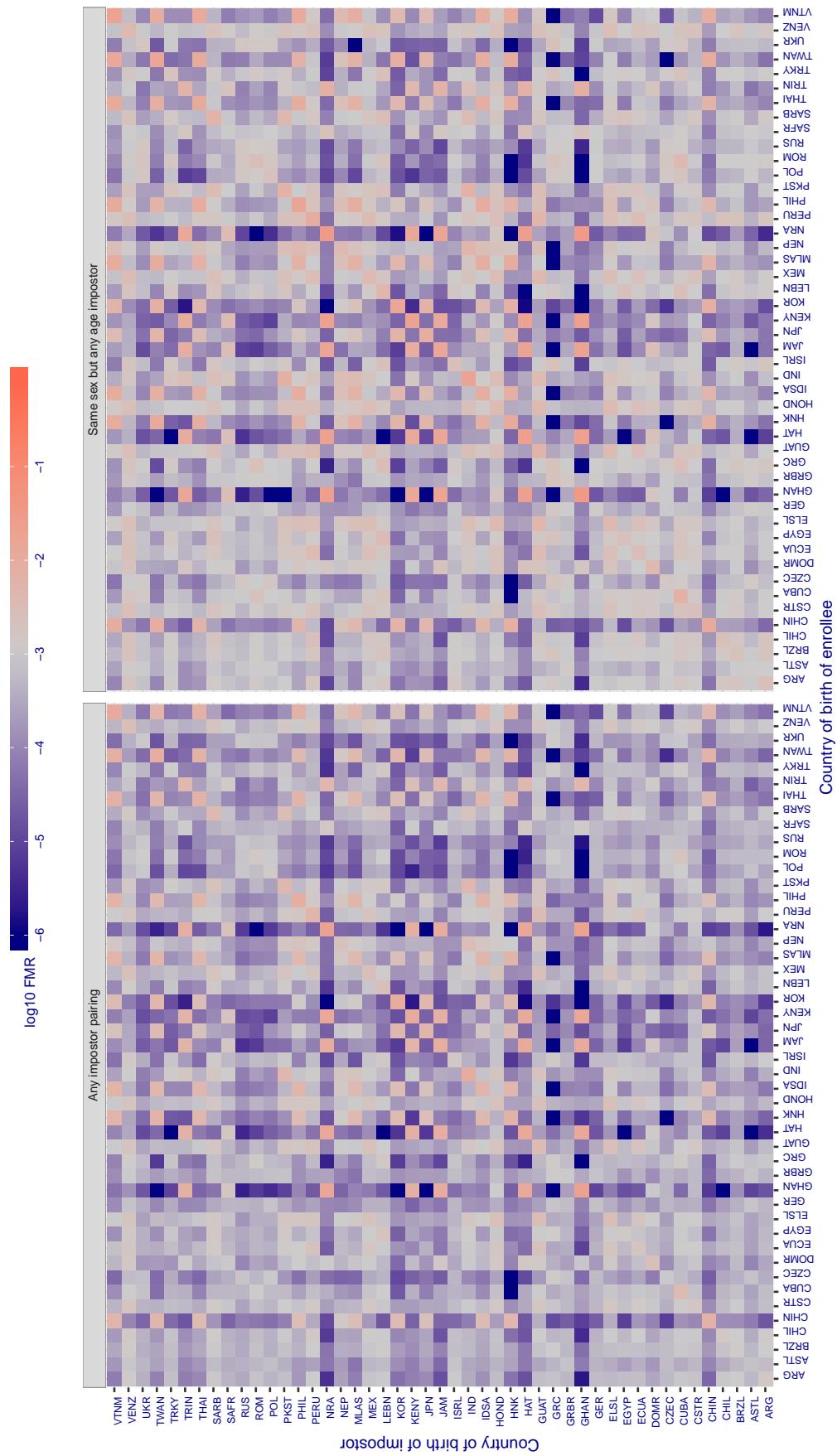
**Cross country FMR at threshold T = 0.624 for algorithm microfocus\_001, giving FMR(T) = 0.001 globally.**

Figure 270: For algorithm microfocus-001 operating on visa images, the heatmap shows false match rates observed over impostor comparisons of faces from different individuals who were born in the given country pair. False matches are counted against a recognition threshold fixed globally to give the target FMR in the plot title, computed over all on the order of  $10^{10}$  impostor comparisons. If text appears in each box it give the same quantity as that coded by the color. Grey indicates FMR is at the intended FMR target level. Light red colors present a security vulnerability to, for example, a passport gate. Each +1 increase in  $\log_{10} FMR$  corresponds to a factor of 10 increase in FMR. The matrix is not quite symmetric because images in the enrollment and verification sets are different.

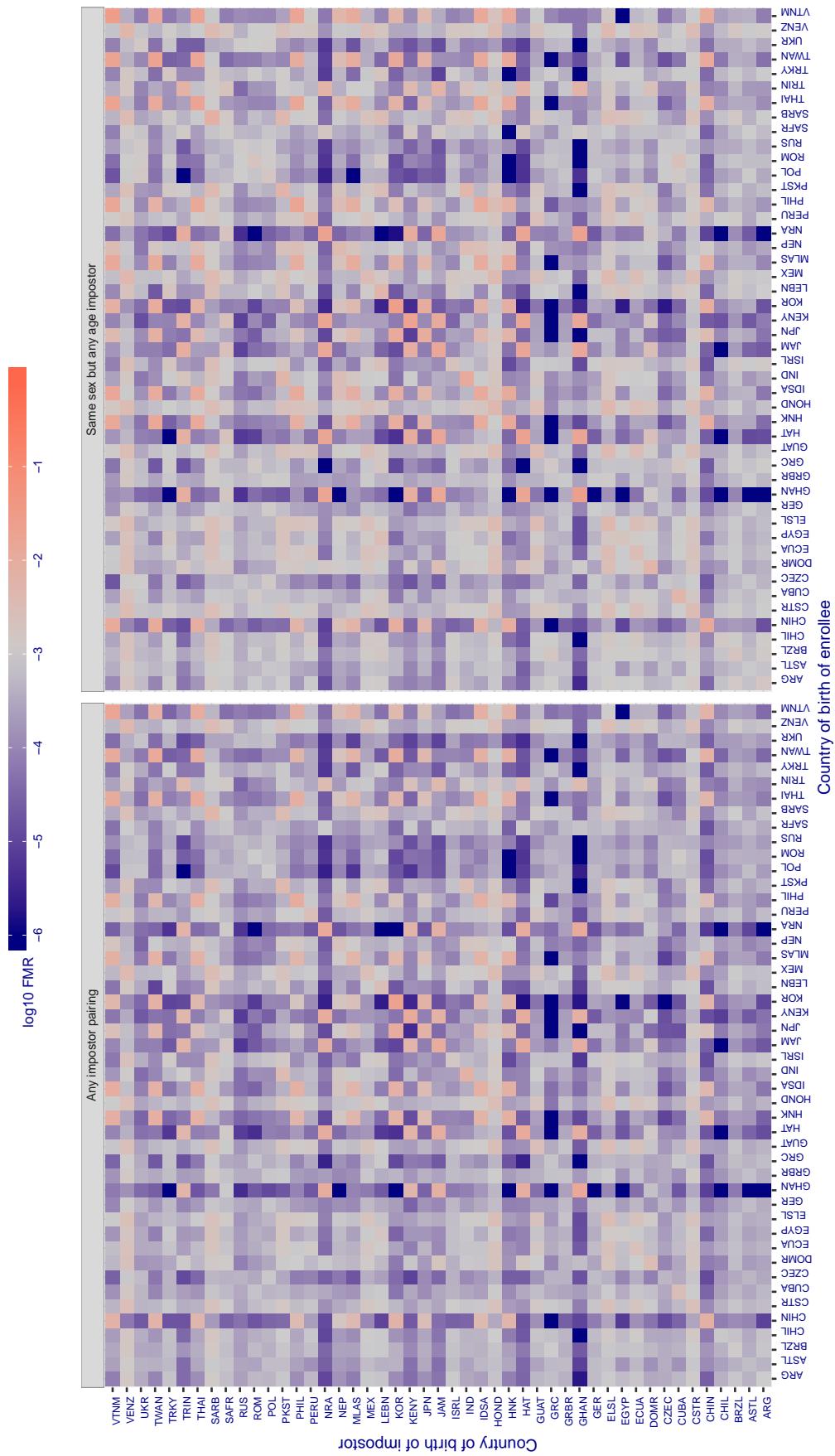
**Cross country FMR at threshold T = 0.542 for algorithm microfocus\_002, giving FMR(T) = 0.001 globally.**

Figure 271: For algorithm microfocus-002 operating on visa images, the heatmap shows false match rates observed over impostor comparisons of faces from different individuals who were born in the given country pair. False matches are counted against a recognition threshold fixed globally to give the target FMR in the plot title, computed over all on the order of  $10^{10}$  impostor comparisons. If text appears in each box it give the same quantity as that coded by the color. Grey indicates FMR is at the intended FMR target level. Light red colors present a security vulnerability to, for example, a passport gate. Each +1 increase in  $\log_{10} \text{FMR}$  corresponds to a factor of 10 increase in FMR. The matrix is not quite symmetric because images in the enrollment and verification sets are different.

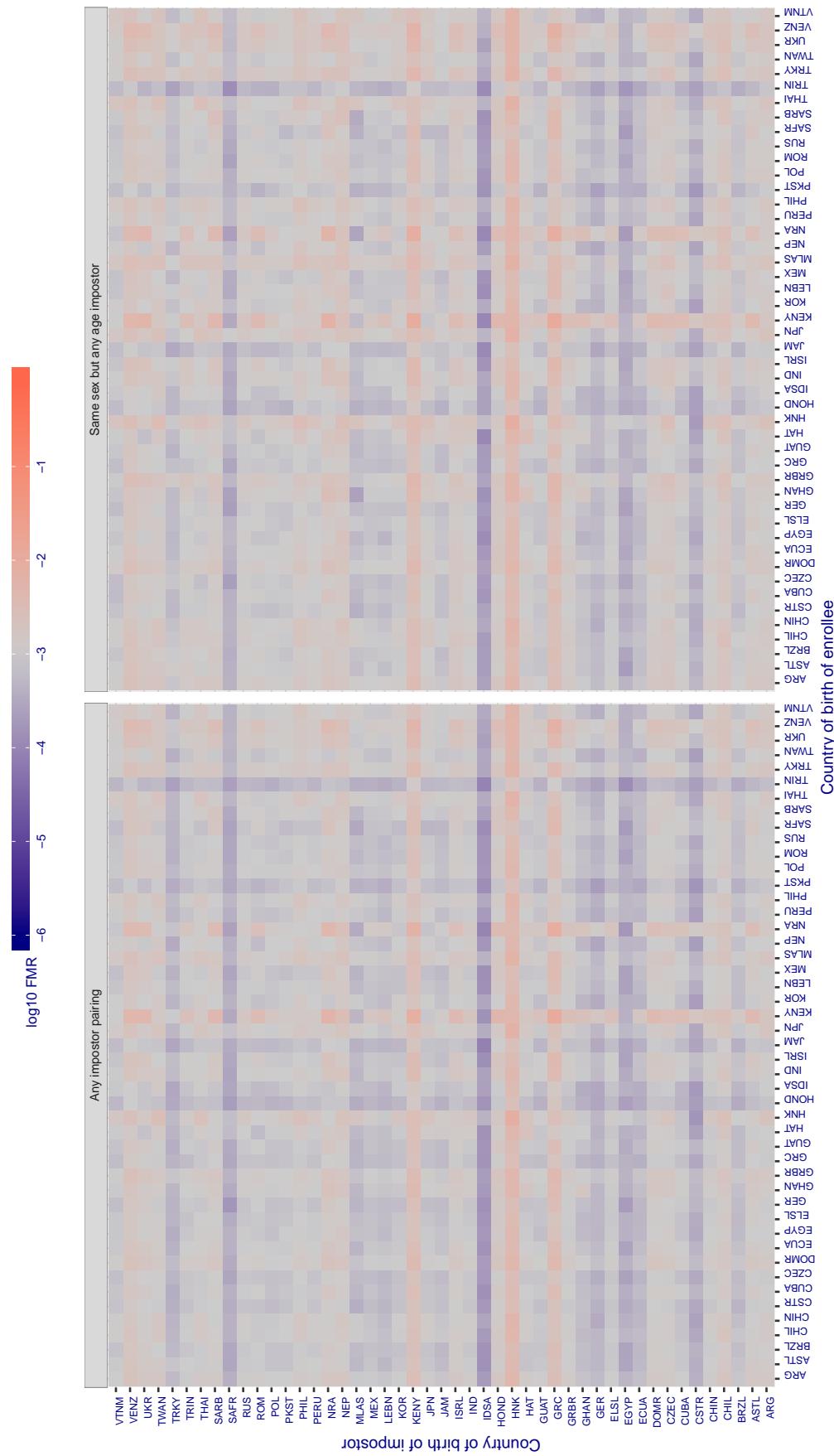
**Cross country FMR at threshold T = 0.693 for algorithm nodeflux\_001, giving FMR(T) = 0.001 globally.**

Figure 272: For algorithm nodeflux-001 operating on visa images, the heatmap shows false match rates observed over impostor comparisons of faces from different individuals who were born in the given country pair. False matches are counted against a recognition threshold fixed globally to give the target FMR in the plot title, computed over all on the order of  $10^{10}$  impostor comparisons. If text appears in each box it give the same quantity as that coded by the color. Grey indicates FMR is at the intended FMR target level. Light red colors present a security vulnerability to, for example, a passport gate. Each +1 increase in  $\log_{10} FMR$  corresponds to a factor of 10 increase in FMR. The matrix is not quite symmetric because images in the enrollment and verification sets are different.

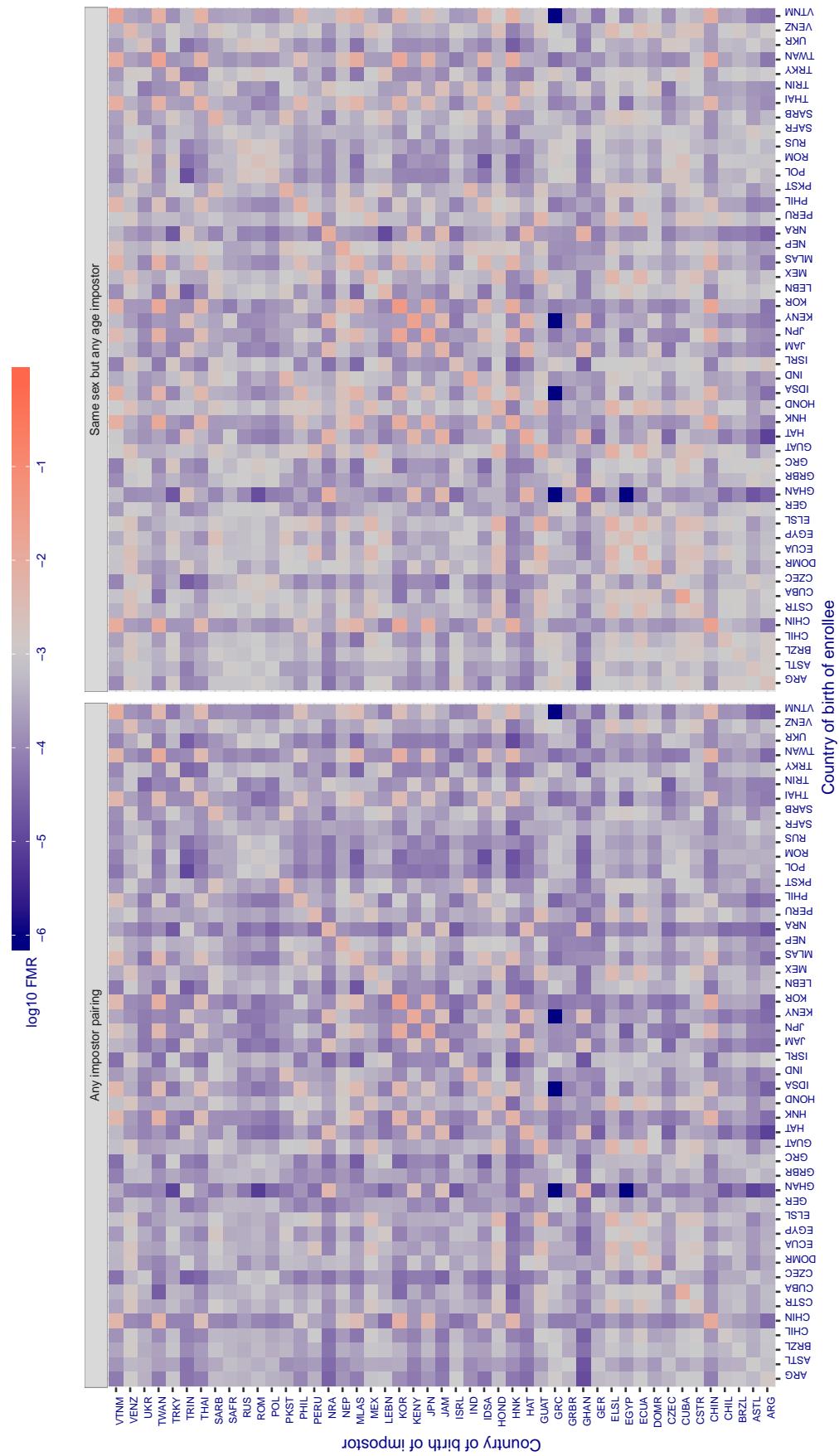
**Cross country FMR at threshold T = 1.369 for algorithm ntchlab\_005, giving FMR(T) = 0.001 globally.**

Figure 273: For algorithm ntchlab-005 operating on visa images, the heatmap shows false match rates observed over impostor comparisons of faces from different individuals who were born in the given country pair. False matches are counted against a recognition threshold fixed globally to give the target FMR in the plot title, computed over all on the order of  $10^{10}$  impostor comparisons. If text appears in each box it give the same quantity as that coded by the color. Grey indicates FMR is at the intended FMR target level. Light red colors present a security vulnerability to, for example, a passport gate. Each +1 increase in  $\log_{10} \text{FMR}$  corresponds to a factor of 10 increase in FMR. The matrix is not quite symmetric because images in the enrollment and verification sets are different.

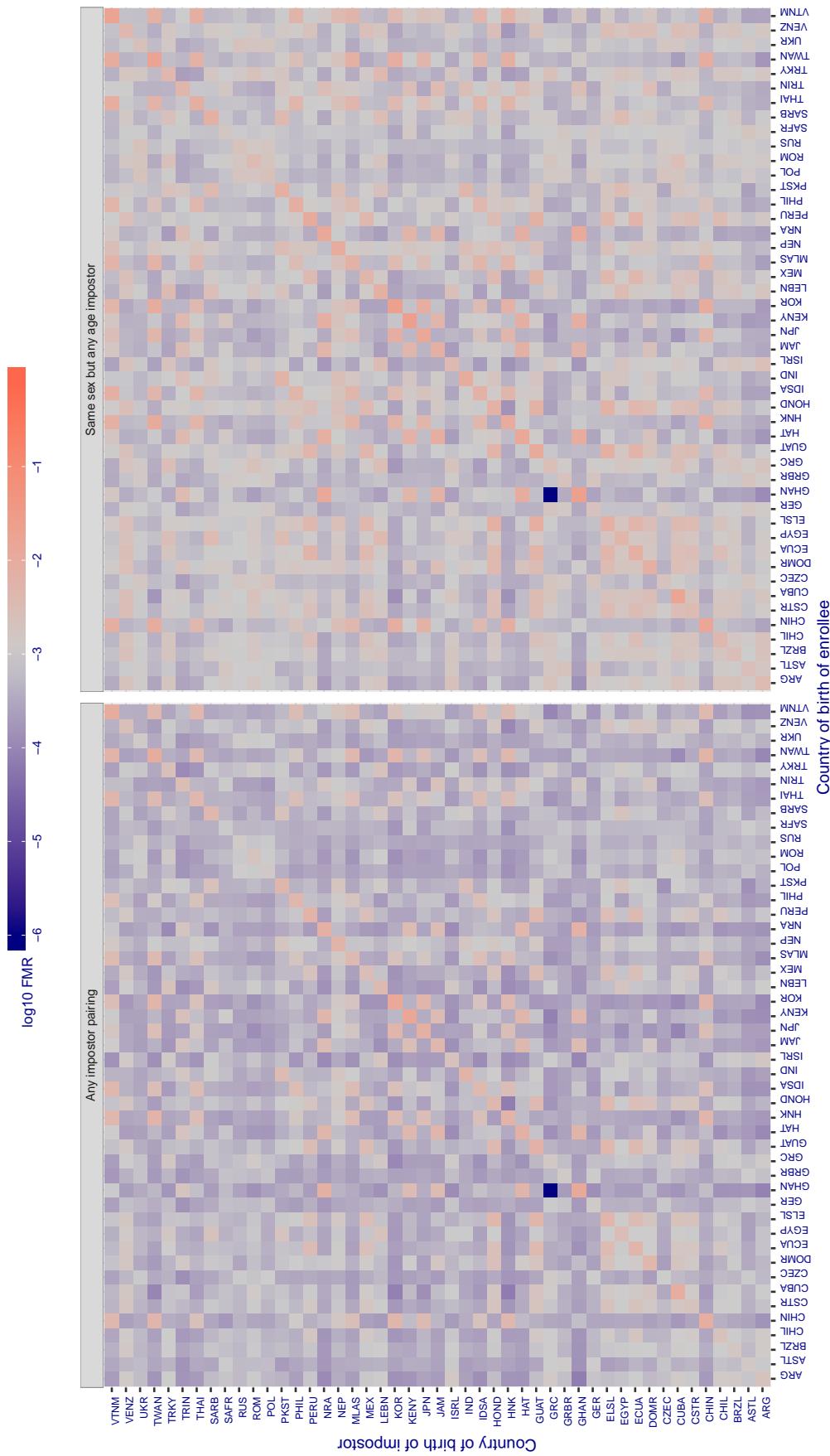
**Cross country FMR at threshold T = 1.929 for algorithm ntchlab\_006, giving FMR(T) = 0.001 globally.**

Figure 274: For algorithm ntchlab-006 operating on visa images, the heatmap shows false match rates observed over impostor comparisons of faces from different individuals who were born in the given country pair. False matches are counted against a recognition threshold fixed globally to give the target FMR in the plot title, computed over all on the order of  $10^{10}$  impostor comparisons. If text appears in each box it give the same quantity as that coded by the color. Grey indicates FMR is at the intended FMR target level. Light red colors present a security vulnerability to, for example, a passport gate. Each +1 increase in  $\log_{10} FMR$  corresponds to a factor of 10 increase in FMR. The matrix is not quite symmetric because images in the enrollment and verification sets are different.

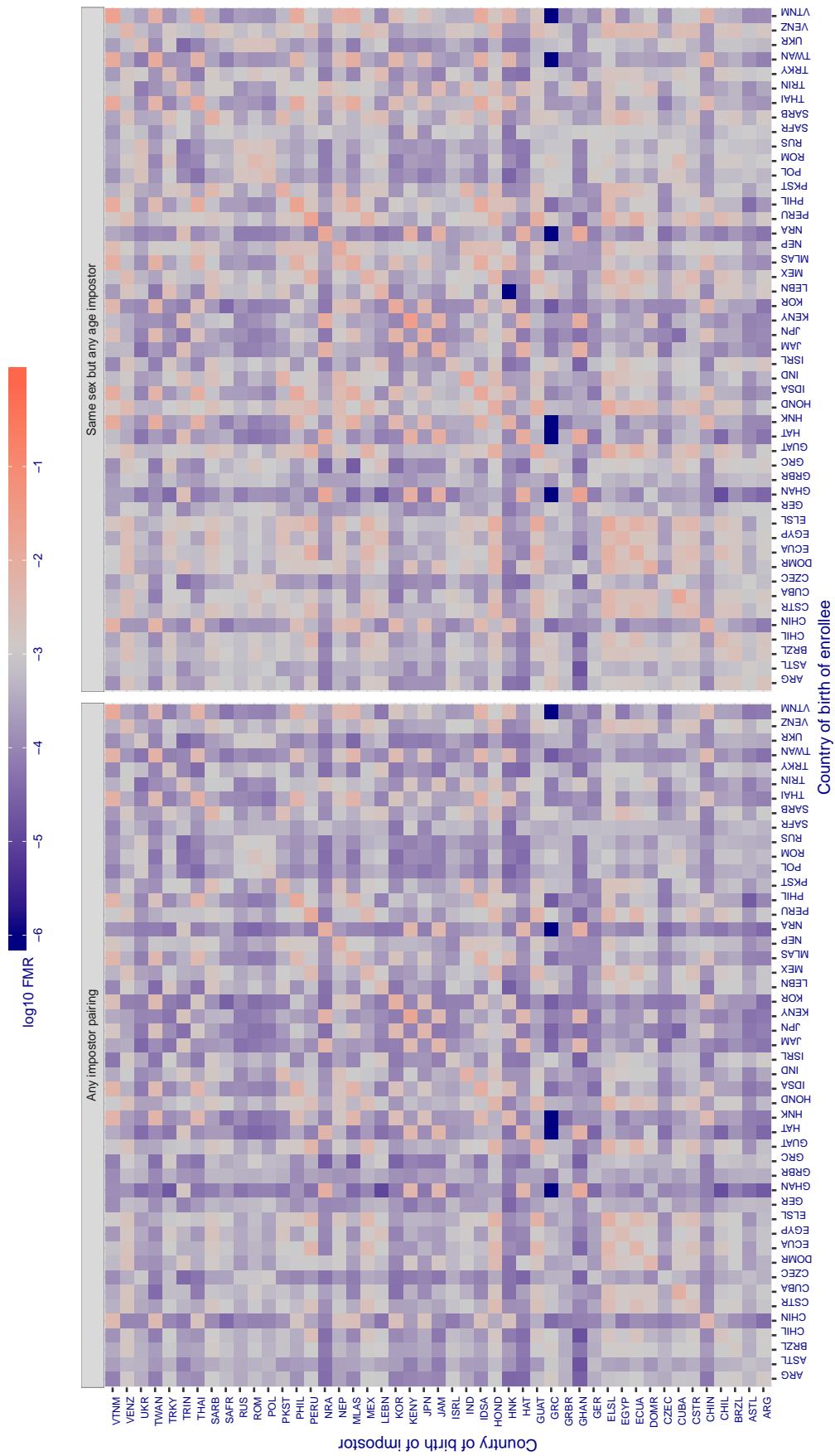
**Cross country FMR at threshold T = 0.253 for algorithm psl\_001, giving FMR(T) = 0.001 globally.**

Figure 275: For algorithm psl-001 operating on visa images, the heatmap shows false match rates observed over impostor comparisons of faces from different individuals who were born in the given country pair. False matches are counted against a recognition threshold fixed globally to give the target FMR in the plot title, computed over all on the order of  $10^{10}$  impostor comparisons. If text appears in each box it give the same quantity as that coded by the color. Grey indicates FMR is at the intended FMR target level. Light red colors present a security vulnerability to, for example, a passport gate. Each +1 increase in  $\log_{10} \text{FMR}$  corresponds to a factor of 10 increase in FMR. The matrix is not quite symmetric because images in the enrollment and verification sets are different.

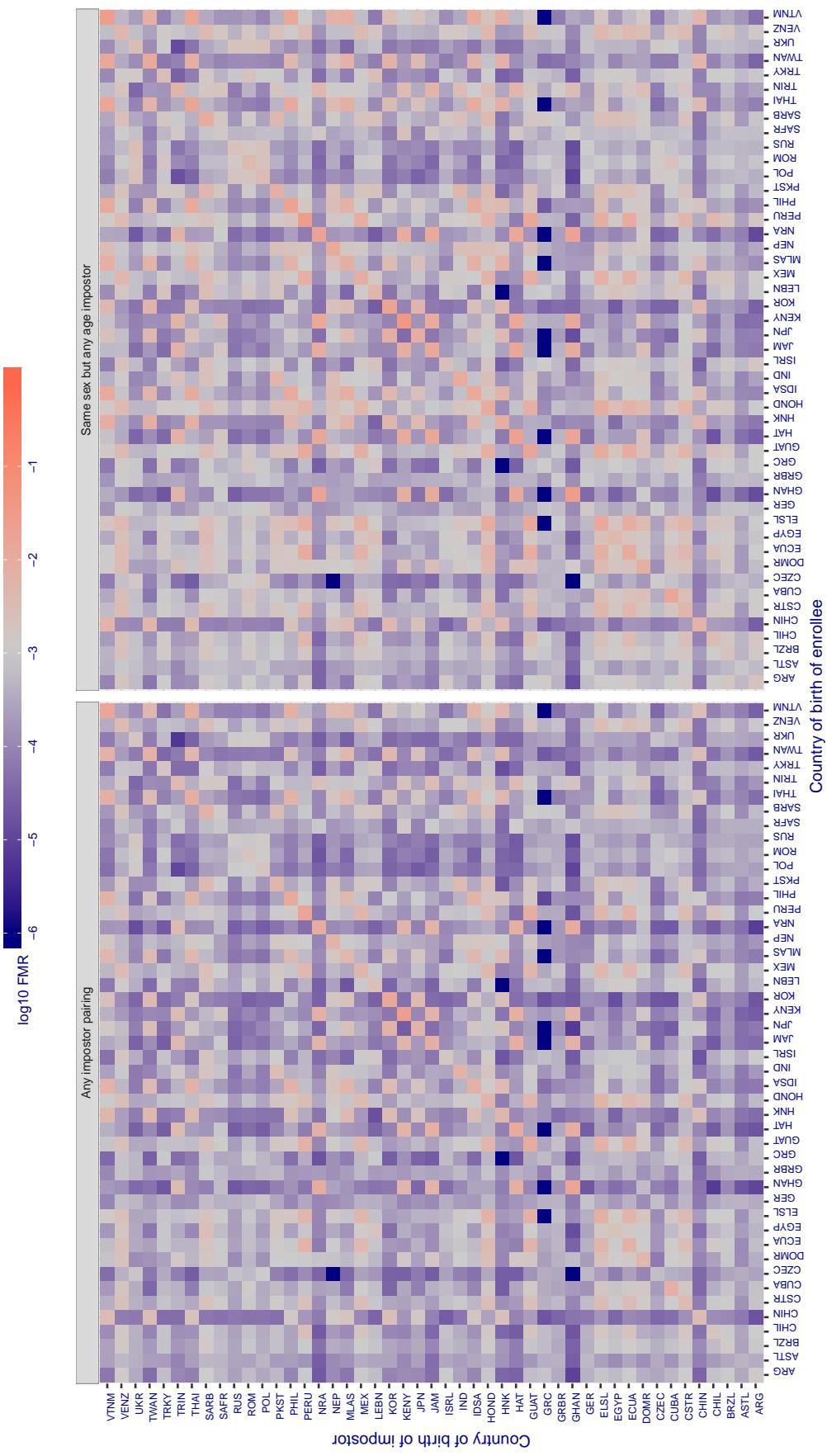
**Cross country FMR at threshold T = 0.272 for algorithm psl\_002, giving  $FMR(T) = 0.001$  globally.**

Figure 276: For algorithm psl\_002 operating on visa images, the heatmap shows false match rates observed over impostor comparisons of faces from different individuals who were born in the given country pair. False matches are counted against a recognition threshold fixed globally to give the target FMR in the plot title, computed over all on the order of  $10^{10}$  impostor comparisons. If text appears in each box it give the same quantity as that coded by the color. Grey indicates  $FMR$  is at the intended  $FMR$  target level. Light red colors present a security vulnerability to, for example, a passport gate. Each +1 increase in  $\log_{10} FMR$  corresponds to a factor of 10 increase in  $FMR$ . The matrix is not quite symmetric because images in the enrollment and verification sets are different.

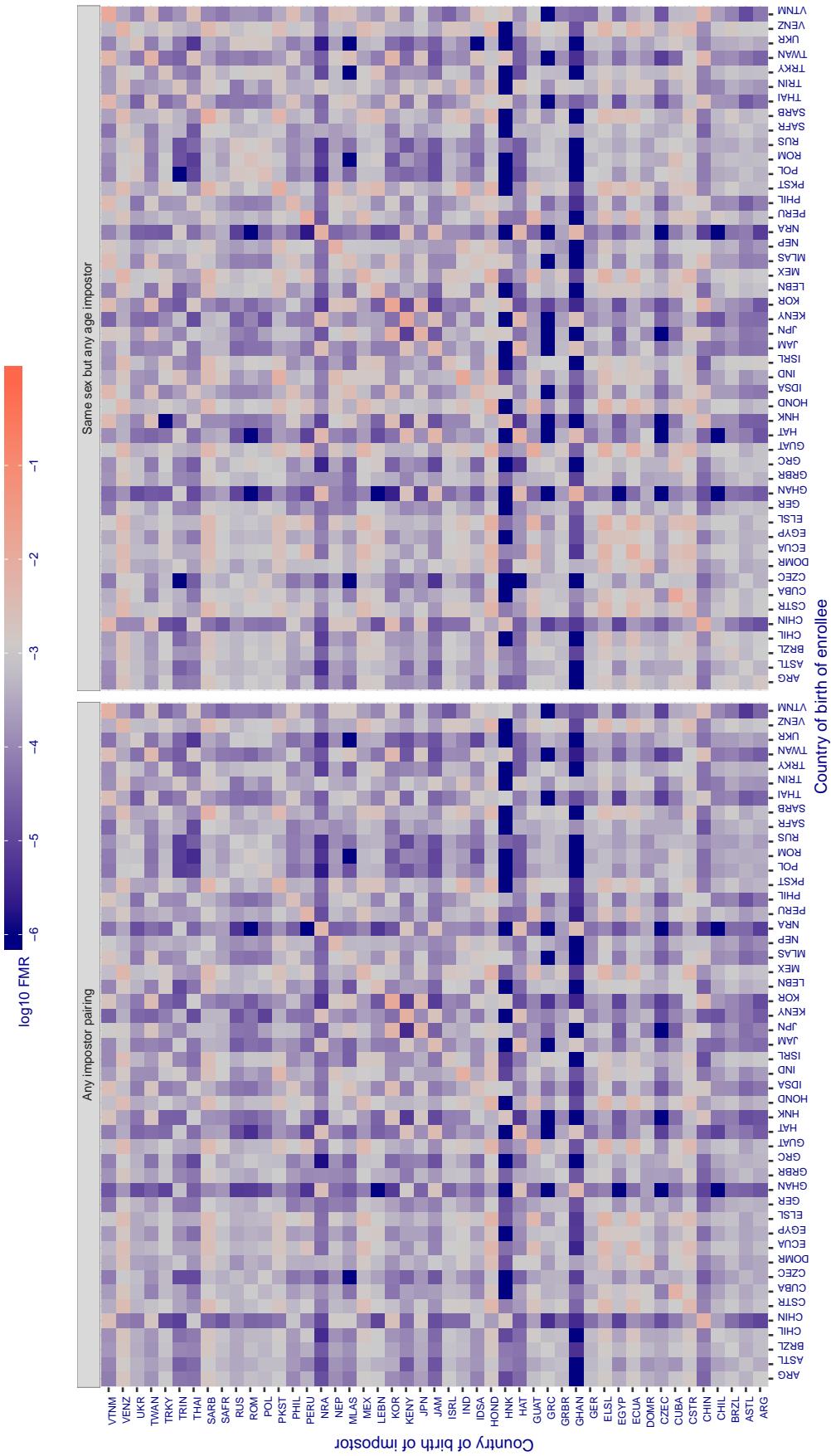
**Cross country FMR at threshold T = 0.613 for algorithm rankone\_006, giving FMR(T) = 0.001 globally.**

Figure 277: For algorithm rankone-006 operating on visa images, the heatmap shows false match rates observed over impostor comparisons of faces from different individuals who were born in the given country pair. False matches are counted against a recognition threshold fixed globally to give the target FMR in the plot title, computed over all on the order of  $10^{10}$  impostor comparisons. If text appears in each box it give the same quantity as that coded by the color. Grey indicates FMR is at the intended FMR target level. Light red colors present a security vulnerability to, for example, a passport gate. Each +1 increase in  $\log_{10} FMR$  corresponds to a factor of 10 increase in FMR. The matrix is not quite symmetric because images in the enrollment and verification sets are different.

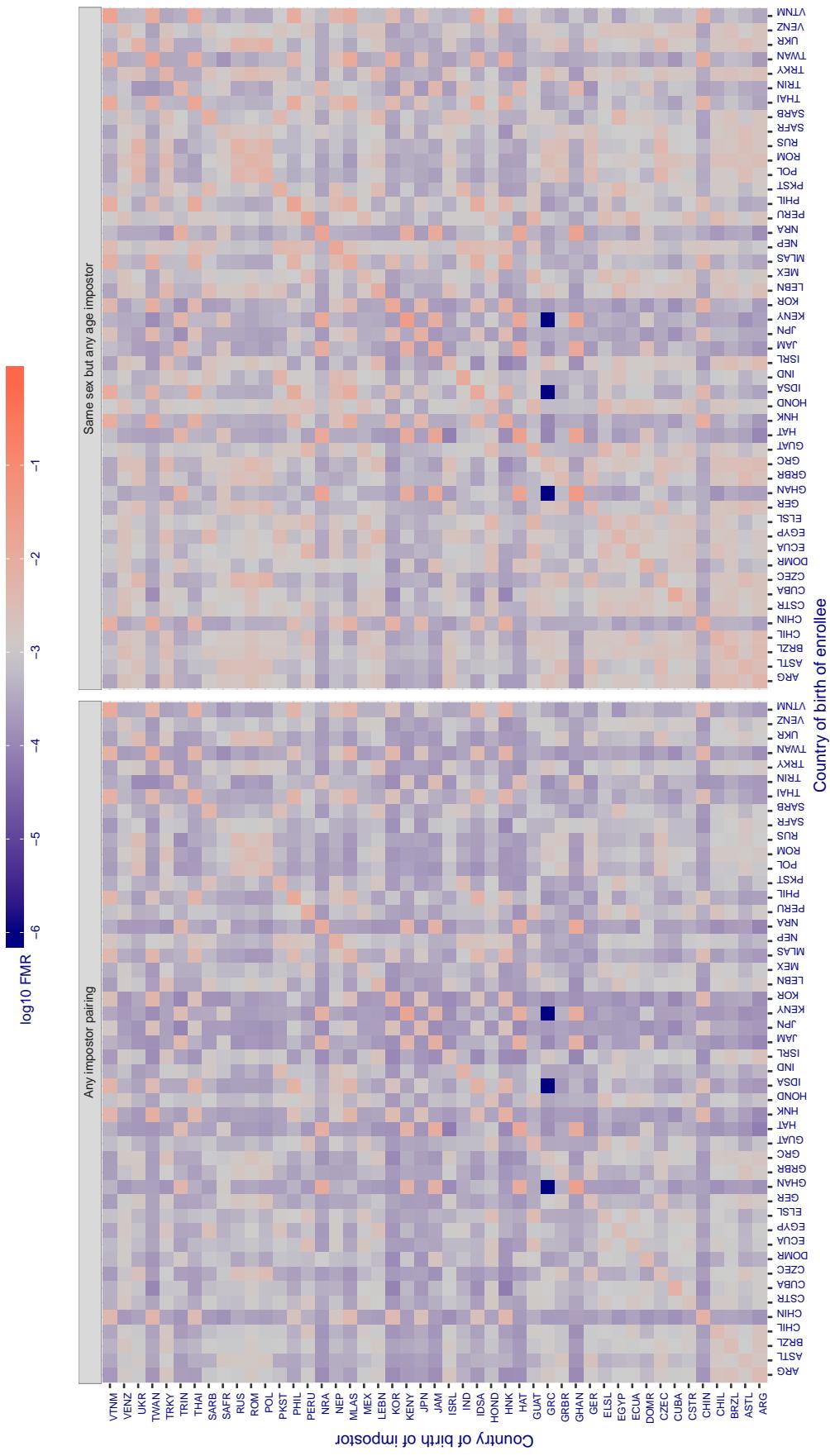
**Cross country FMR at threshold T = 0.814 for algorithm realnetworks\_001, giving FMR(T) = 0.001 globally.**

Figure 278: For algorithm realnetworks-001 operating on visa images, the heatmap shows false match rates observed over impostor comparisons of faces from different individuals who were born in the given country pair. False matches are counted against a recognition threshold fixed globally to give the target FMR in the plot title, computed over all on the order of  $10^{10}$  impostor comparisons. If text appears in each box it give the same quantity as that coded by the color. Grey indicates FMR is at the intended FMR target level. Light red colors present a security vulnerability to, for example, a passport gate. Each +1 increase in  $\log_{10} FMR$  corresponds to a factor of 10 increase in FMR. The matrix is not quite symmetric because images in the enrollment and verification sets are different.

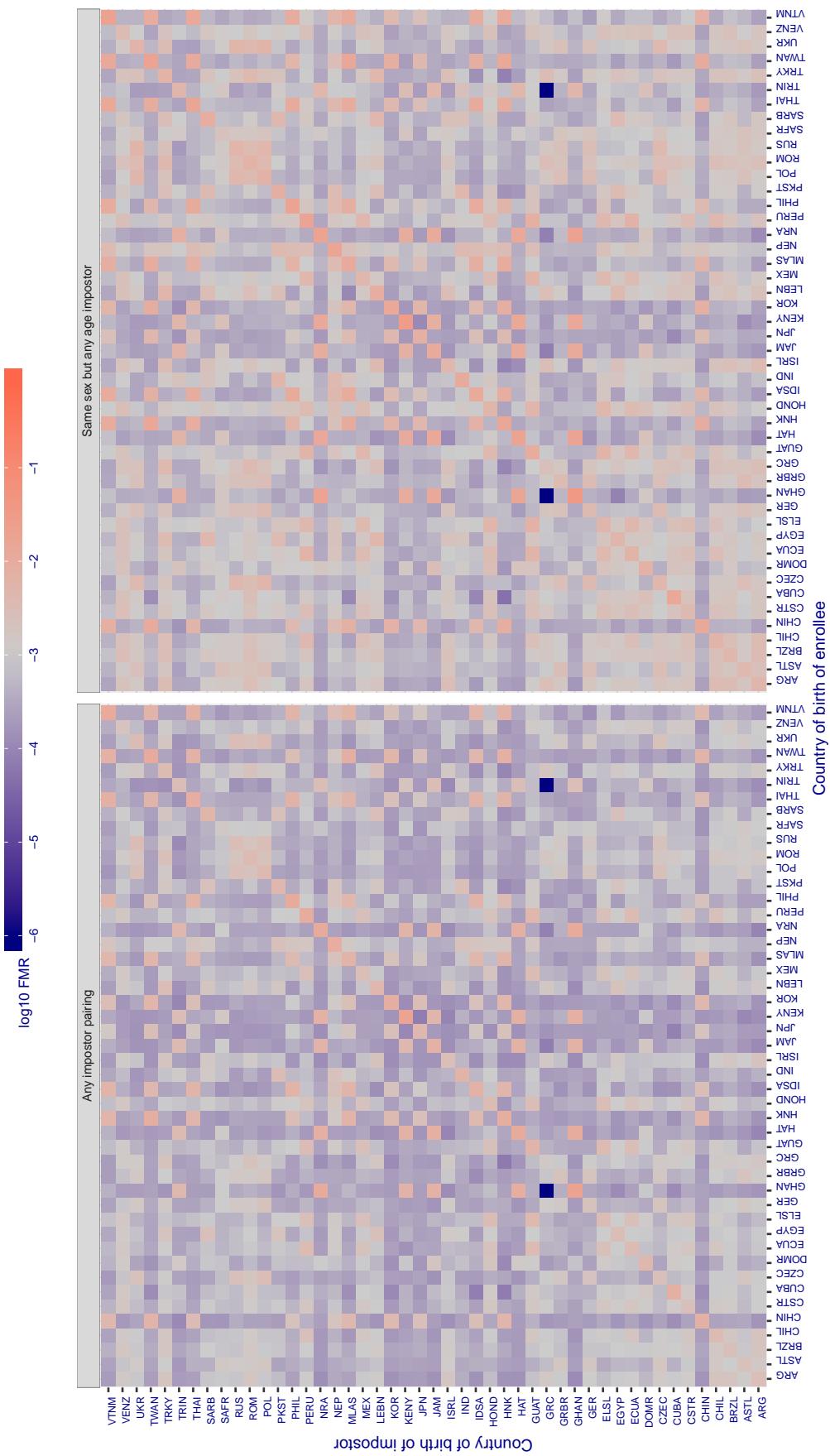
**Cross country FMR at threshold T = 0.814 for algorithm realnetworks\_002, giving FMR(T) = 0.001 globally.**

Figure 279: For algorithm realnetworks-002 operating on visa images, the heatmap shows false match rates observed over impostor comparisons of faces from different individuals who were born in the given country pair. False matches are counted against a recognition threshold fixed globally to give the target FMR in the plot title, computed over all on the order of  $10^{10}$  impostor comparisons. If text appears in each box it give the same quantity as that coded by the color. Grey indicates FMR is at the intended FMR target level. Light red colors present a security vulnerability to, for example, a passport gate. Each +1 increase in  $\log_{10} FMR$  corresponds to a factor of 10 increase in FMR. The matrix is not quite symmetric because images in the enrollment and verification sets are different.

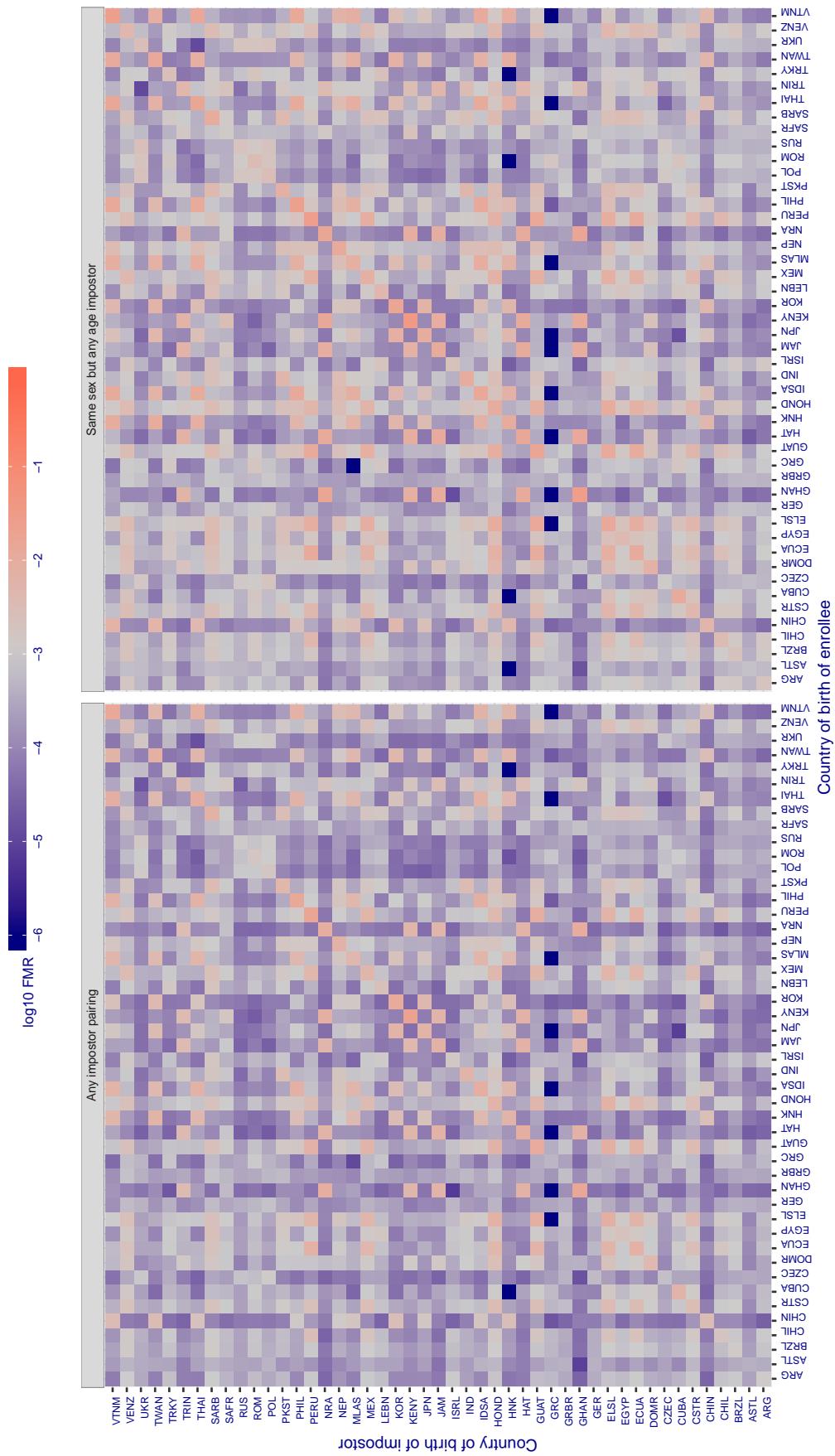
**Cross country FMR at threshold T = 65.920 for algorithm remarkai\_000, giving FMR(T) = 0.001 globally.**

Figure 280: For algorithm remarkai-000 operating on visa images, the heatmap shows false match rates observed over impostor comparisons of faces from different individuals who were born in the given country pair. False matches are counted against a recognition threshold fixed globally to give the target FMR in the plot title, computed over all on the order of  $10^{10}$  impostor comparisons. If text appears in each box it give the same quantity as that coded by the color. Grey indicates FMR is at the intended FMR target level. Light red colors present a security vulnerability to, for example, a passport gate. Each +1 increase in  $\log_{10} \text{FMR}$  corresponds to a factor of 10 increase in FMR. The matrix is not quite symmetric because images in the enrollment and verification sets are different.

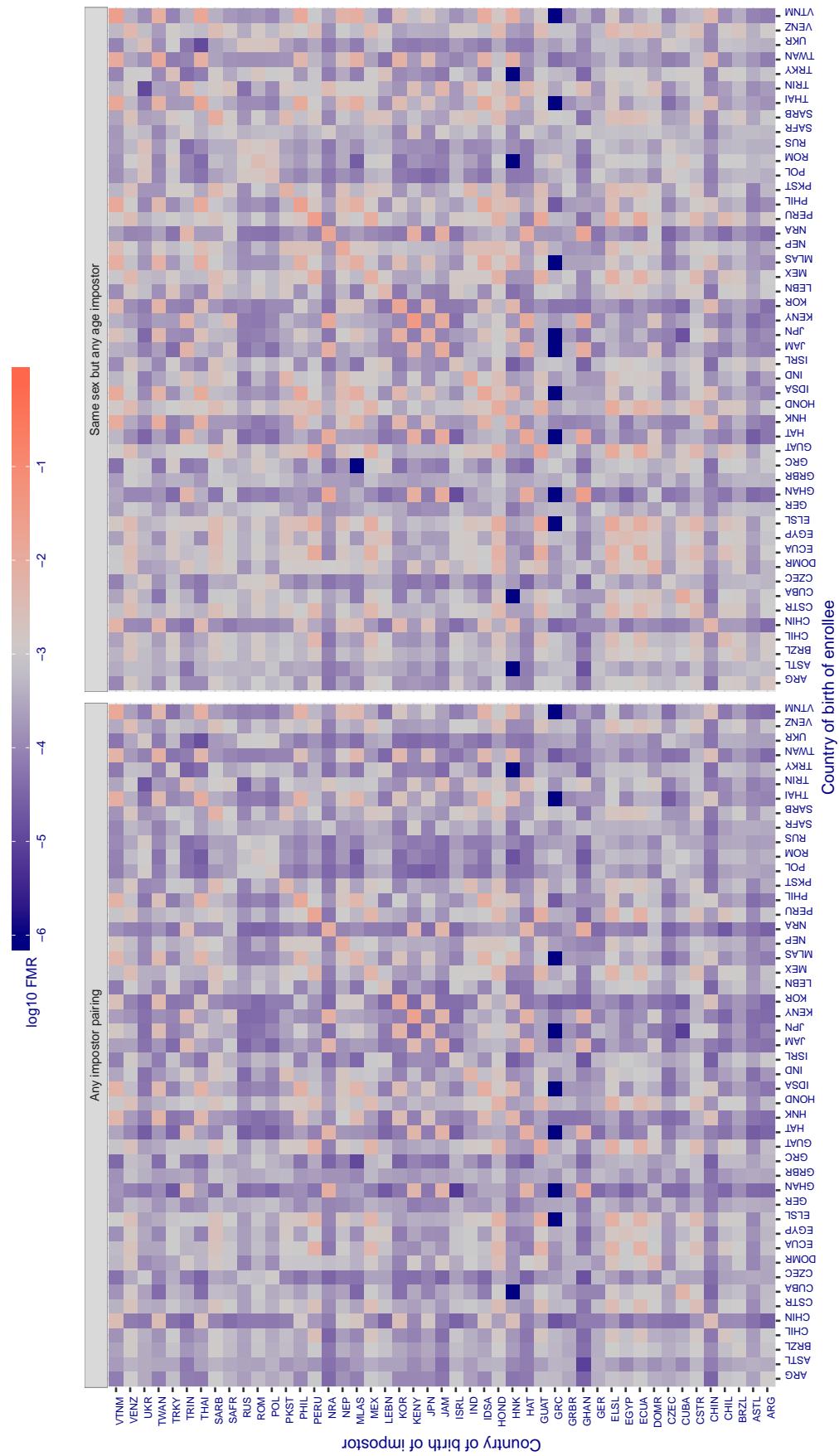
**Cross country FMR at threshold T = 65.928 for algorithm remarkai\_001, giving FMR(T) = 0.001 globally.**

Figure 281: For algorithm remarkai-001 operating on visa images, the heatmap shows false match rates observed over impostor comparisons of faces from different individuals who were born in the given country pair. False matches are counted against a recognition threshold fixed globally to give the target FMR in the plot title, computed over all on the order of  $10^{10}$  impostor comparisons. If text appears in each box it give the same quantity as that coded by the color. Grey indicates FMR is at the intended FMR target level. Light red colors present a security vulnerability to, for example, a passport gate. Each +1 increase in  $\log_{10} \text{FMR}$  corresponds to a factor of 10 increase in FMR. The matrix is not quite symmetric because images in the enrollment and verification sets are different.

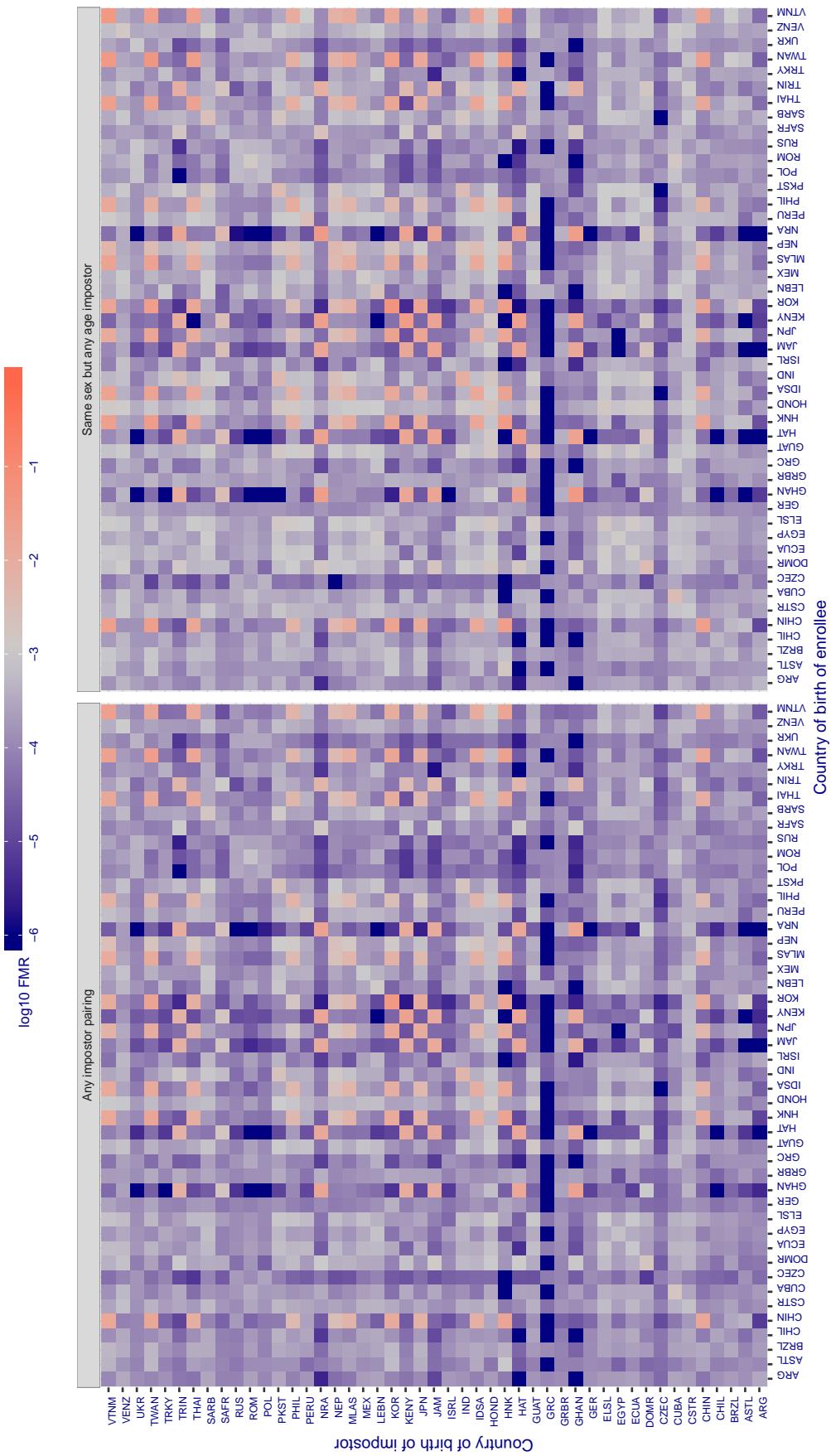
**Cross country FMR at threshold T = 0.609 for algorithm safe\_001, giving FMR(T) = 0.001 globally.**

Figure 282: For algorithm safe-001 operating on visa images, the heatmap shows false match rates observed over impostor comparisons of faces from different individuals who were born in the given country pair. False matches are counted against a recognition threshold fixed globally to give the target FMR in the plot title, computed over all on the order of  $10^{10}$  impostor comparisons. If text appears in each box it give the same quantity as that coded by the color. Grey indicates FMR is at the intended FMR target level. Light red colors present a security vulnerability to, for example, a passport gate. Each +1 increase in  $\log_{10} \text{FMR}$  corresponds to a factor of 10 increase in FMR. The matrix is not quite symmetric because images in the enrollment and verification sets are different.

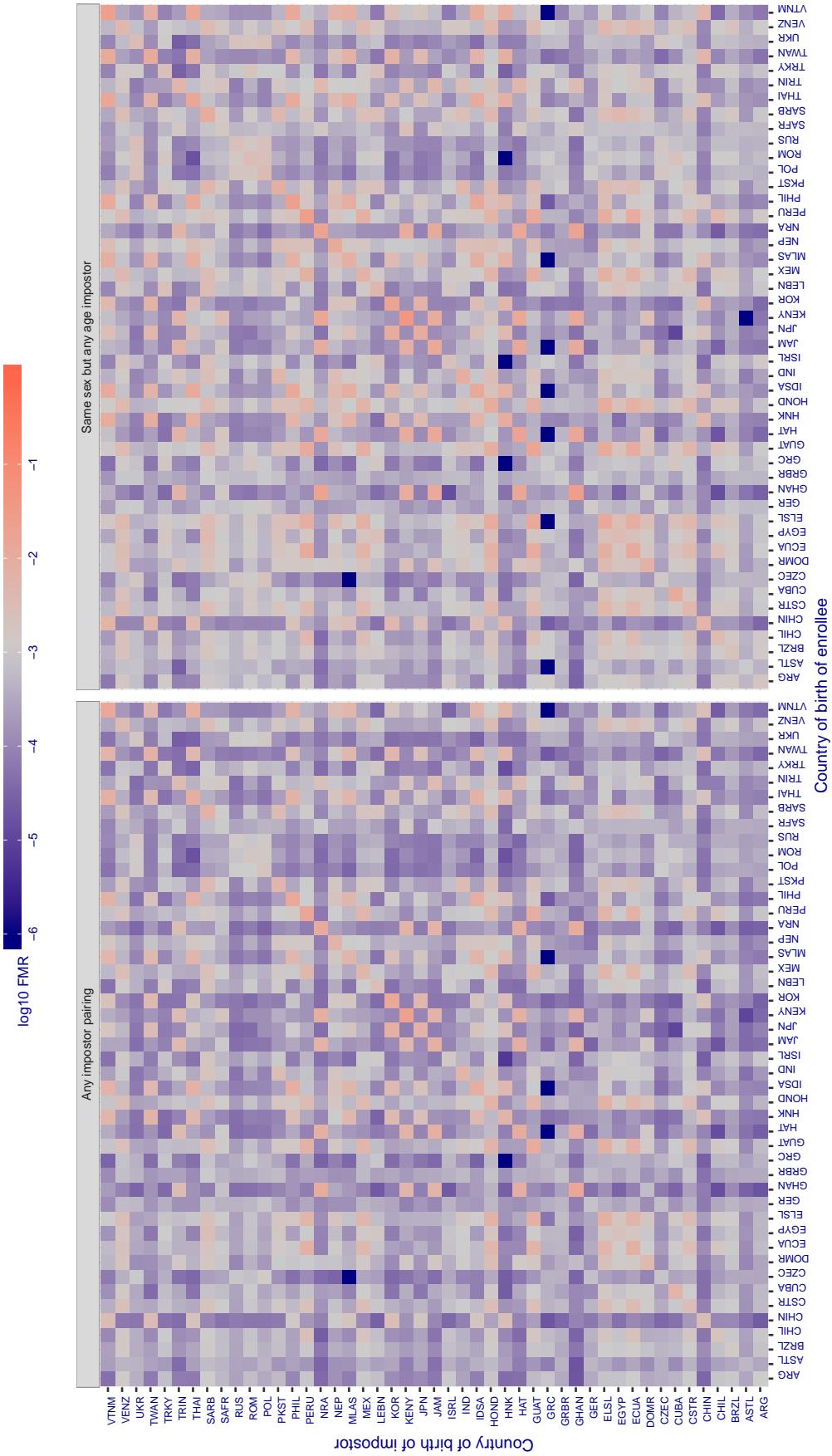
**Cross country FMR at threshold T = 0.295 for algorithm safe\_002, giving FMR(T) = 0.001 globally.**

Figure 283: For algorithm safe-002 operating on visa images, the heatmap shows false match rates observed over impostor comparisons of faces from different individuals who were born in the given country pair. False matches are counted against a recognition threshold fixed globally to give the target FMR in the plot title, computed over all on the order of  $10^{10}$  impostor comparisons. If text appears in each box it give the same quantity as that coded by the color. Grey indicates FMR is at the intended FMR target level. Light red colors present a security vulnerability to, for example, a passport gate. Each +1 increase in  $\log_{10} \text{FMR}$  corresponds to a factor of 10 increase in FMR. The matrix is not quite symmetric because images in the enrollment and verification sets are different.

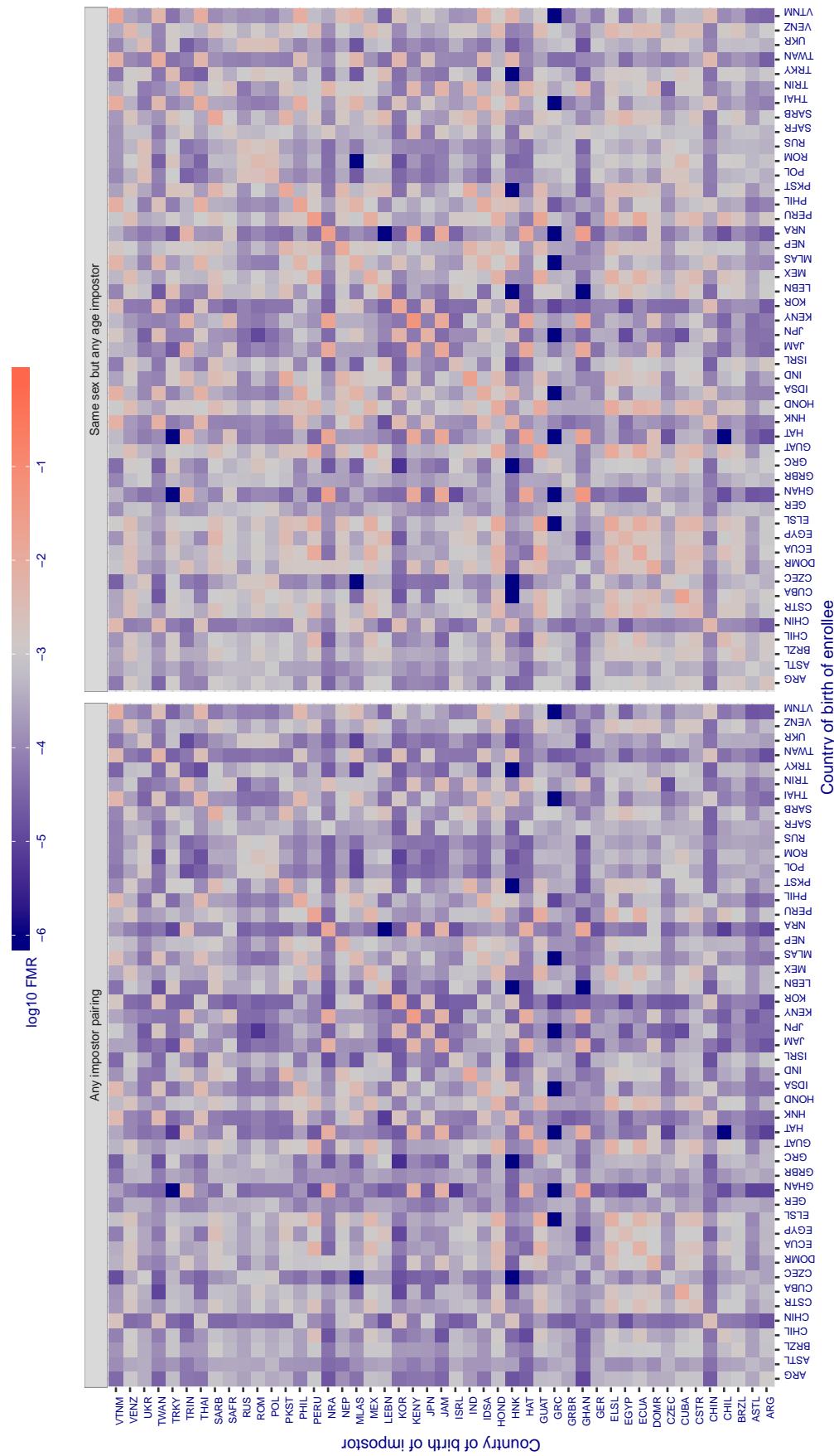
**Cross country FMR at threshold T = 0.368 for algorithm sensetime\_001, giving FMR(T) = 0.001 globally.**

Figure 284: For algorithm sensetime-001 operating on visa images, the heatmap shows false match rates observed over impostor comparisons of faces from different individuals who were born in the given country pair. False matches are counted against a recognition threshold fixed globally to give the target FMR in the plot title, computed over all on the order of  $10^{10}$  impostor comparisons. If text appears in each box it give the same quantity as that coded by the color. Grey indicates FMR is at the intended FMR target level. Light red colors present a security vulnerability to, for example, a passport gate. Each +1 increase in  $\log_{10} \text{FMR}$  corresponds to a factor of 10 increase in FMR. The matrix is not quite symmetric because images in the enrollment and verification sets are different.

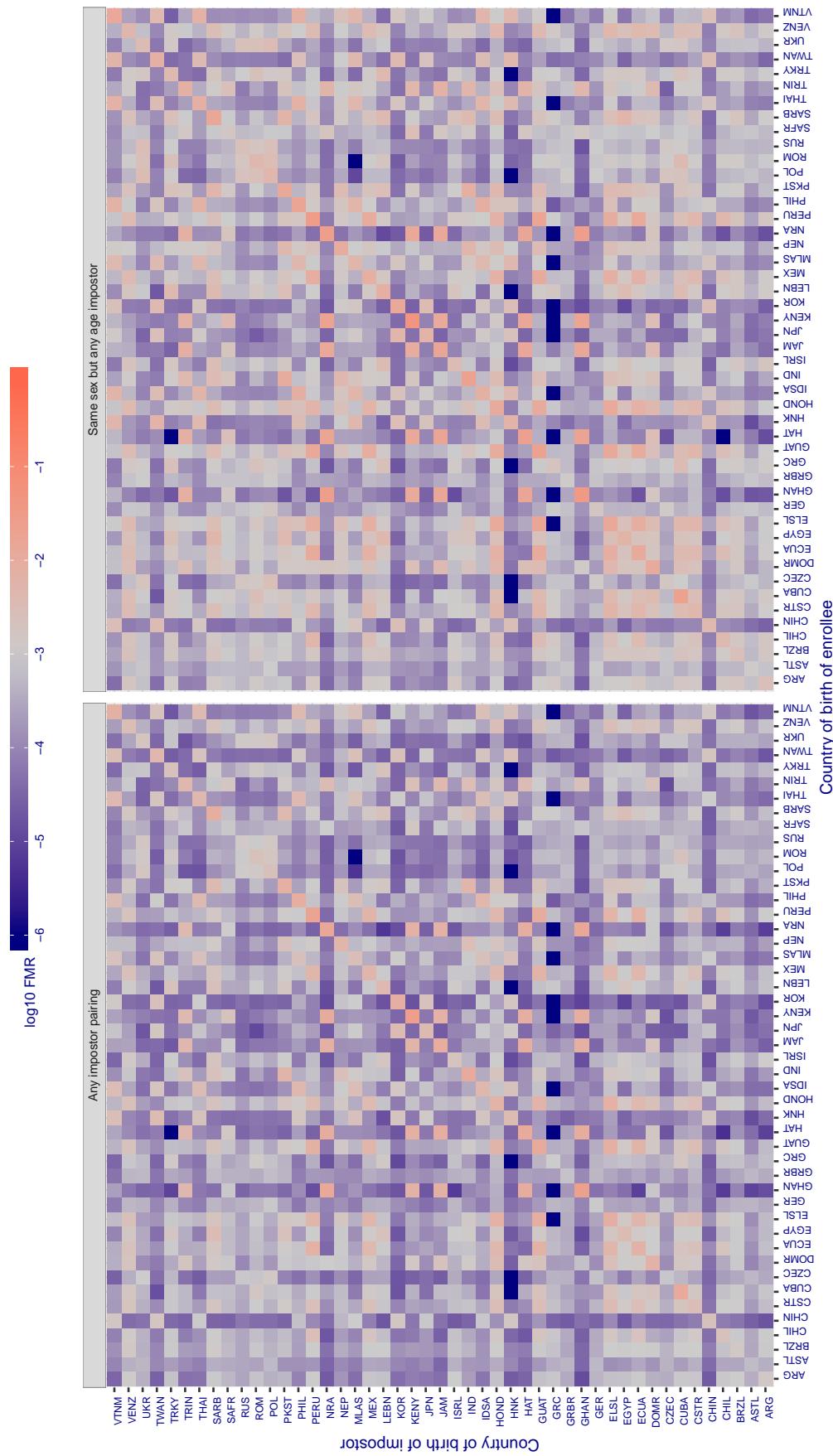
**Cross country FMR at threshold T = 0.369 for algorithm sensetime\_002, giving FMR(T) = 0.001 globally.**

Figure 285: For algorithm sensetime-002 operating on visa images, the heatmap shows false match rates observed over impostor comparisons of faces from different individuals who were born in the given country pair. False matches are counted against a recognition threshold fixed globally to give the target FMR in the plot title, computed over all on the order of  $10^{10}$  impostor comparisons. If text appears in each box it give the same quantity as that coded by the color. Grey indicates FMR is at the intended FMR target level. Light red colors present a security vulnerability to, for example, a passport gate. Each +1 increase in  $\log_{10} FMR$  corresponds to a factor of 10 increase in FMR. The matrix is not quite symmetric because images in the enrollment and verification sets are different.

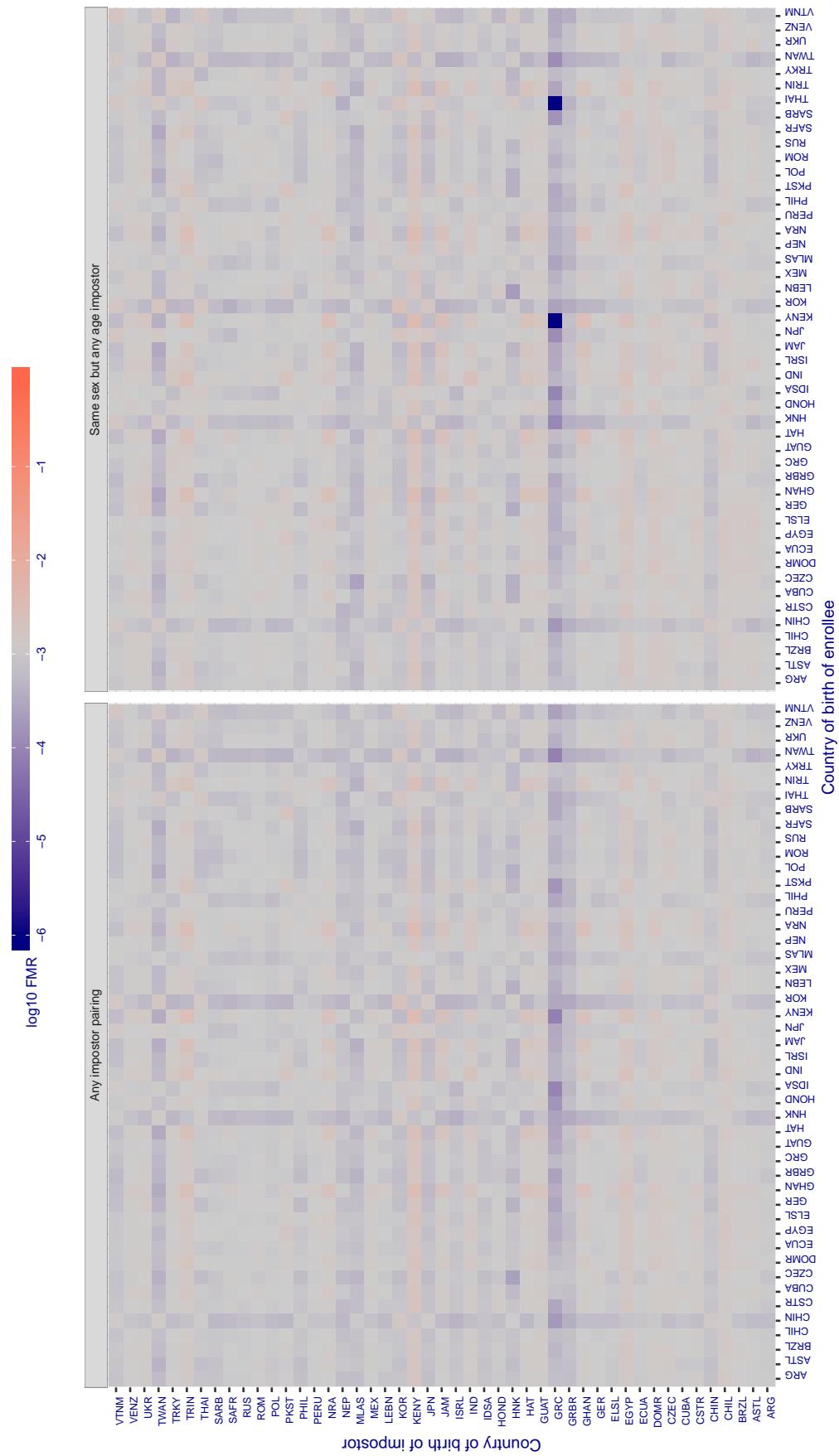
**Cross country FMR at threshold T = 0.939 for algorithm shaman\_000, giving FMR(T) = 0.001 globally.**

Figure 286: For algorithm shaman-000 operating on visa images, the heatmap shows false match rates observed over impostor comparisons of faces from different individuals who were born in the given country pair. False matches are counted against a recognition threshold fixed globally to give the target FMR in the plot title, computed over all on the order of  $10^{10}$  impostor comparisons. If text appears in each box it give the same quantity as that coded by the color. Grey indicates FMR is at the intended FMR target level. Light red colors present a security vulnerability to, for example, a passport gate. Each +1 increase in  $\log_{10} FMR$  corresponds to a factor of 10 increase in FMR. The matrix is not quite symmetric because images in the enrollment and verification sets are different.

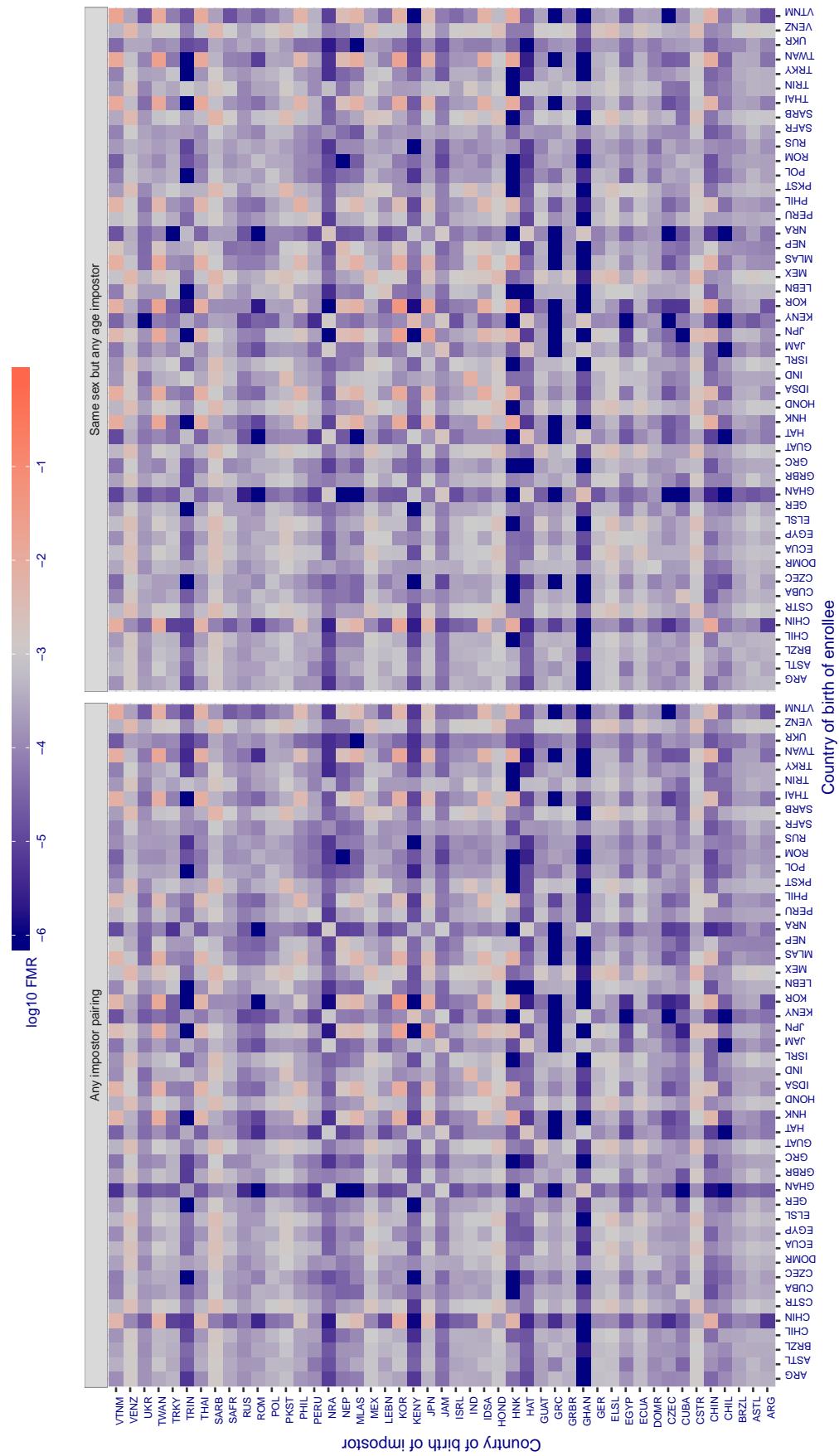
**Cross country FMR at threshold T = 0.599 for algorithm shaman\_001, giving  $FMR(T) = 0.001$  globally.**

Figure 287: For algorithm shaman-001 operating on visa images, the heatmap shows false match rates observed over impostor comparisons of faces from different individuals who were born in the given country pair. False matches are counted against a recognition threshold fixed globally to give the target  $FMR$  in the plot title, computed over all on the order of  $10^{10}$  impostor comparisons. If text appears in each box it give the same quantity as that coded by the color. Grey indicates  $FMR$  is at the intended  $FMR$  target level. Light red colors present a security vulnerability to, for example, a passport gate. Each +1 increase in  $\log_{10} FMR$  corresponds to a factor of 10 increase in  $FMR$ . The matrix is not quite symmetric because images in the enrollment and verification sets are different.

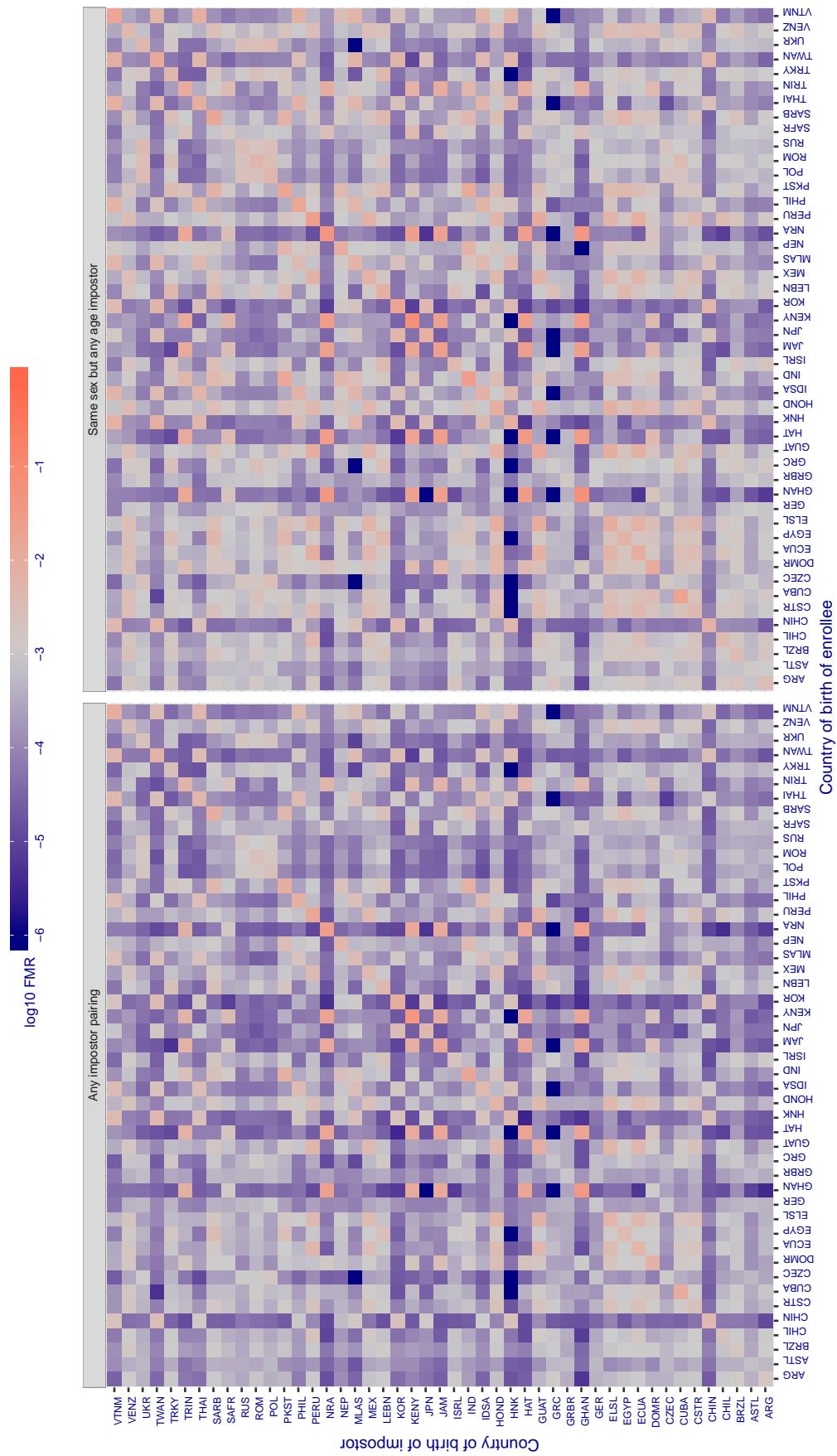
**Cross country FMR at threshold T = 0.370 for algorithm siat\_002, giving  $\text{FMR}(T) = 0.001$  globally.**

Figure 288: For algorithm siat-002 operating on visa images, the heatmap shows false match rates observed over impostor comparisons of faces from different individuals who were born in the given country pair. False matches are counted against a recognition threshold fixed globally to give the target FMR in the plot title, computed over all on the order of  $10^{10}$  impostor comparisons. If text appears in each box it give the same quantity as that coded by the color. Grey indicates FMR is at the intended FMR target level. Light red colors present a security vulnerability to, for example, a passport gate. Each +1 increase in  $\log_{10} \text{FMR}$  corresponds to a factor of 10 increase in FMR. The matrix is not quite symmetric because images in the enrollment and verification sets are different.

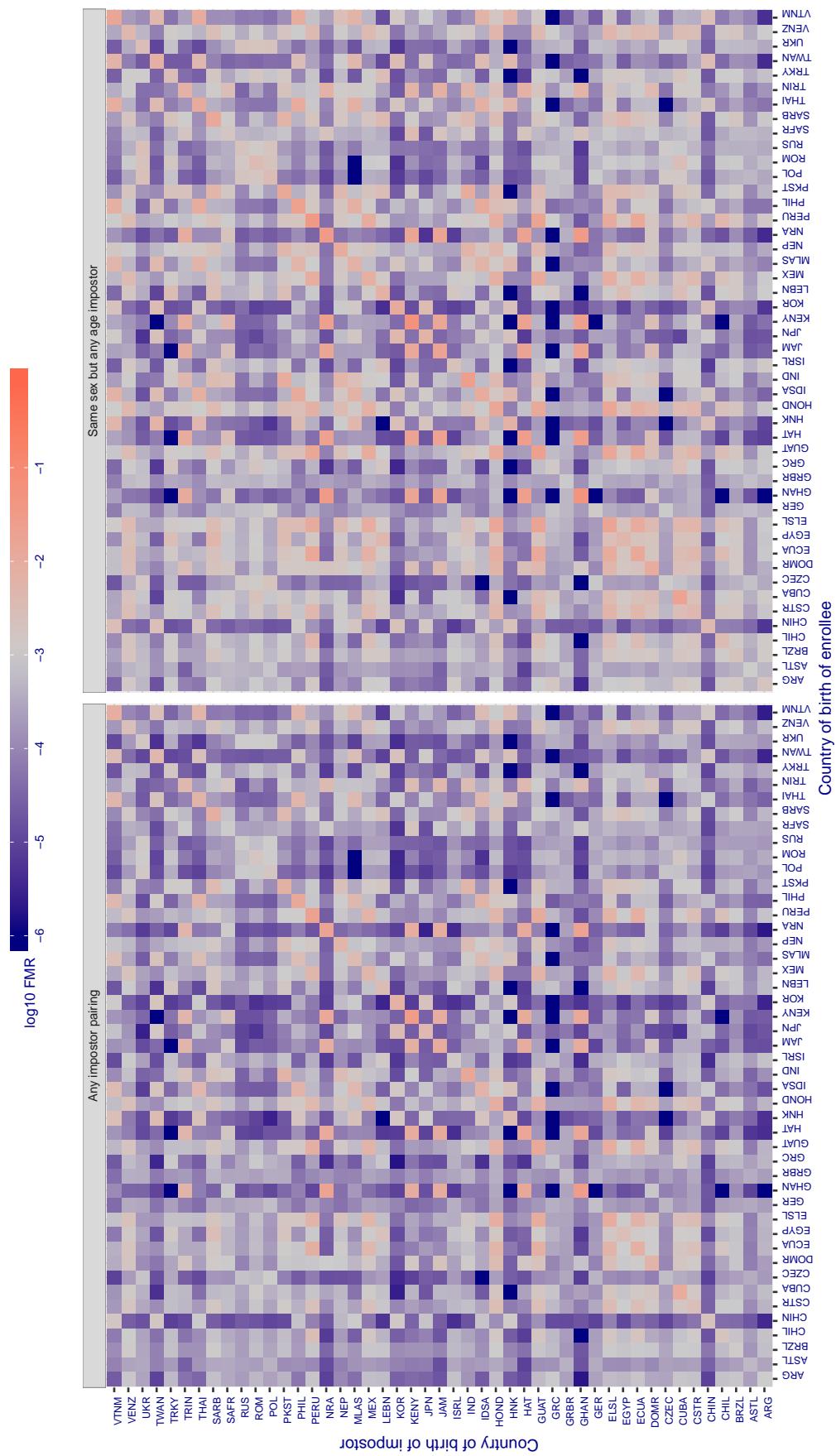
**Cross country FMR at threshold T = 0.371 for algorithm siat\_004, giving  $\text{FMR}(T) = 0.001$  globally.**

Figure 289: For algorithm siat-004 operating on visa images, the heatmap shows false match rates observed over impostor comparisons of faces from different individuals who were born in the given country pair. False matches are counted against a recognition threshold fixed globally to give the target FMR in the plot title, computed over all on the order of  $10^{10}$  impostor comparisons. If text appears in each box it give the same quantity as that coded by the color. Grey indicates  $\text{FMR}$  is at the intended  $\text{FMR}$  target level. Light red colors present a security vulnerability to, for example, a passport gate. Each +1 increase in  $\log_{10} \text{FMR}$  corresponds to a factor of 10 increase in  $\text{FMR}$ . The matrix is not quite symmetric because images in the enrollment and verification sets are different.

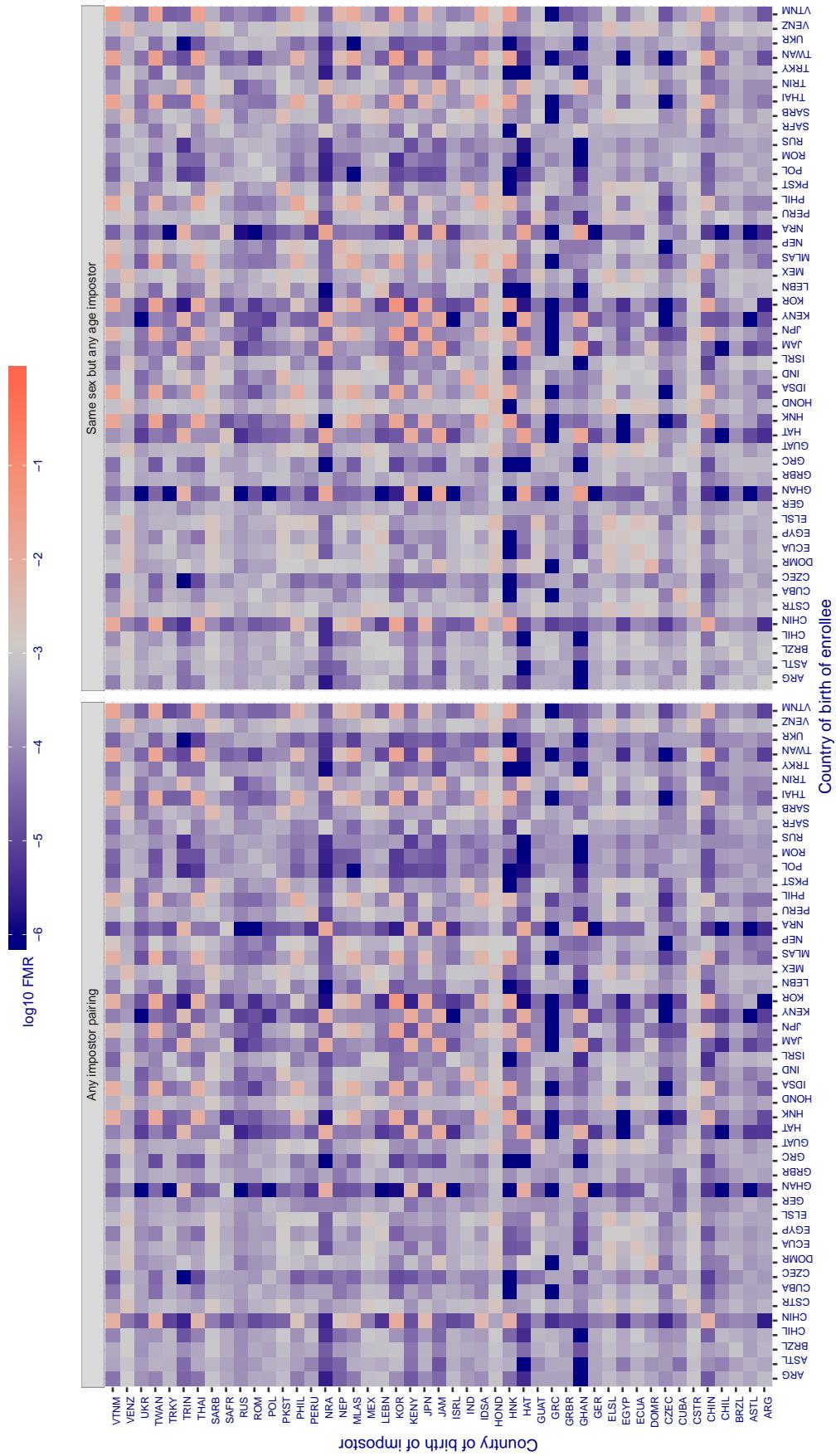
**Cross country FMR at threshold T = 0.488 for algorithm similart\_002, giving FMR(T) = 0.001 globally.**

Figure 290: For algorithm similart-002 operating on visa images, the heatmap shows false match rates observed over impostor comparisons of faces from different individuals who were born in the given country pair. False matches are counted against a recognition threshold fixed globally to give the target FMR in the plot title, computed over all on the order of  $10^{10}$  impostor comparisons. If text appears in each box it give the same quantity as that coded by the color. Grey indicates FMR is at the intended FMR target level. Light red colors present a security vulnerability to, for example, a passport gate. Each +1 increase in  $\log_{10} \text{FMR}$  corresponds to a factor of 10 increase in FMR. The matrix is not quite symmetric because images in the enrollment and verification sets are different.

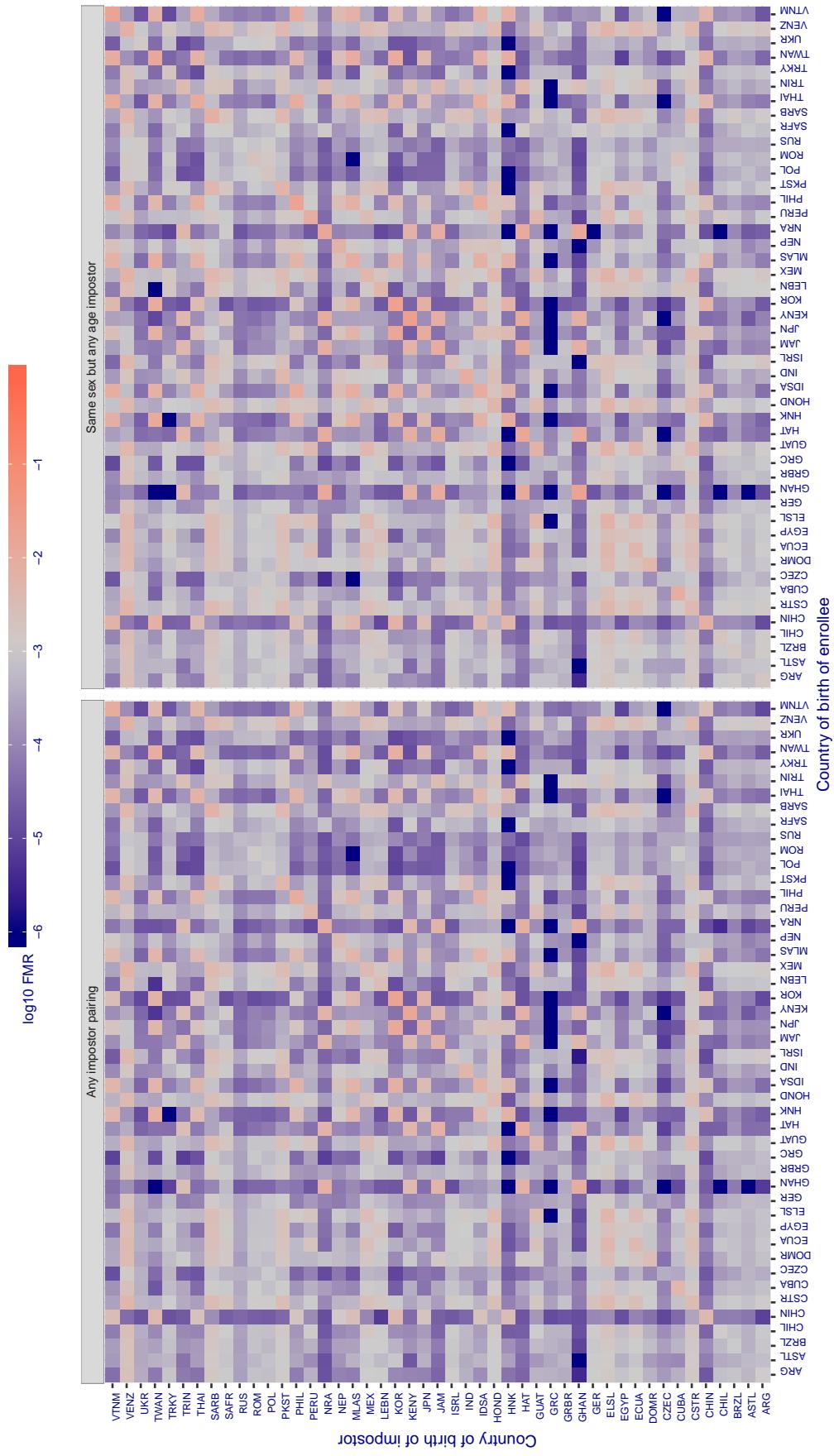
**Cross country FMR at threshold T = 0.388 for algorithm similart\_003, giving FMR(T) = 0.001 globally.**

Figure 291: For algorithm similart-003 operating on visa images, the heatmap shows false match rates observed over impostor comparisons of faces from different individuals who were born in the given country pair. False matches are counted against a recognition threshold fixed globally to give the target FMR in the plot title, computed over all on the order of  $10^{10}$  impostor comparisons. If text appears in each box it give the same quantity as that coded by the color. Grey indicates FMR is at the intended FMR target level. Light red colors present a security vulnerability to, for example, a passport gate. Each +1 increase in  $\log_{10} FMR$  corresponds to a factor of 10 increase in FMR. The matrix is not quite symmetric because images in the enrollment and verification sets are different.

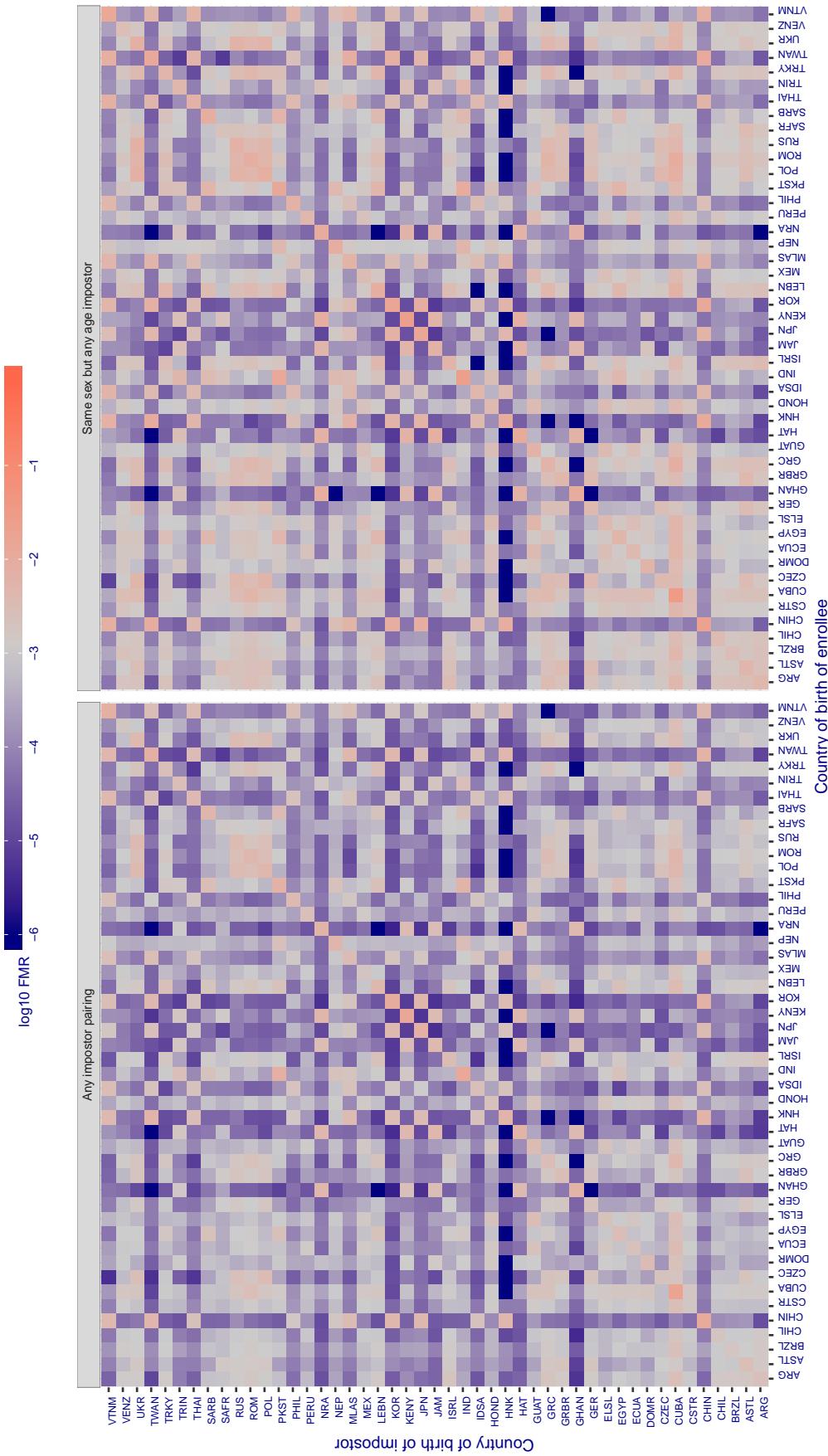
**Cross country FMR at threshold T = 148.095 for algorithm tech5\_001, giving FMR(T) = 0.001 globally.**

Figure 292: For algorithm tech5-001 operating on visa images, the heatmap shows false match rates observed over impostor comparisons of faces from different individuals who were born in the given country pair. False matches are counted against a recognition threshold fixed globally to give the target FMR in the plot title, computed over all on the order of  $10^{10}$  impostor comparisons. If text appears in each box it give the same quantity as that coded by the color. Grey indicates FMR is at the intended FMR target level. Light red colors present a security vulnerability to, for example, a passport gate. Each +1 increase in  $\log_{10} FMR$  corresponds to a factor of 10 increase in FMR. The matrix is not quite symmetric because images in the enrollment and verification sets are different.

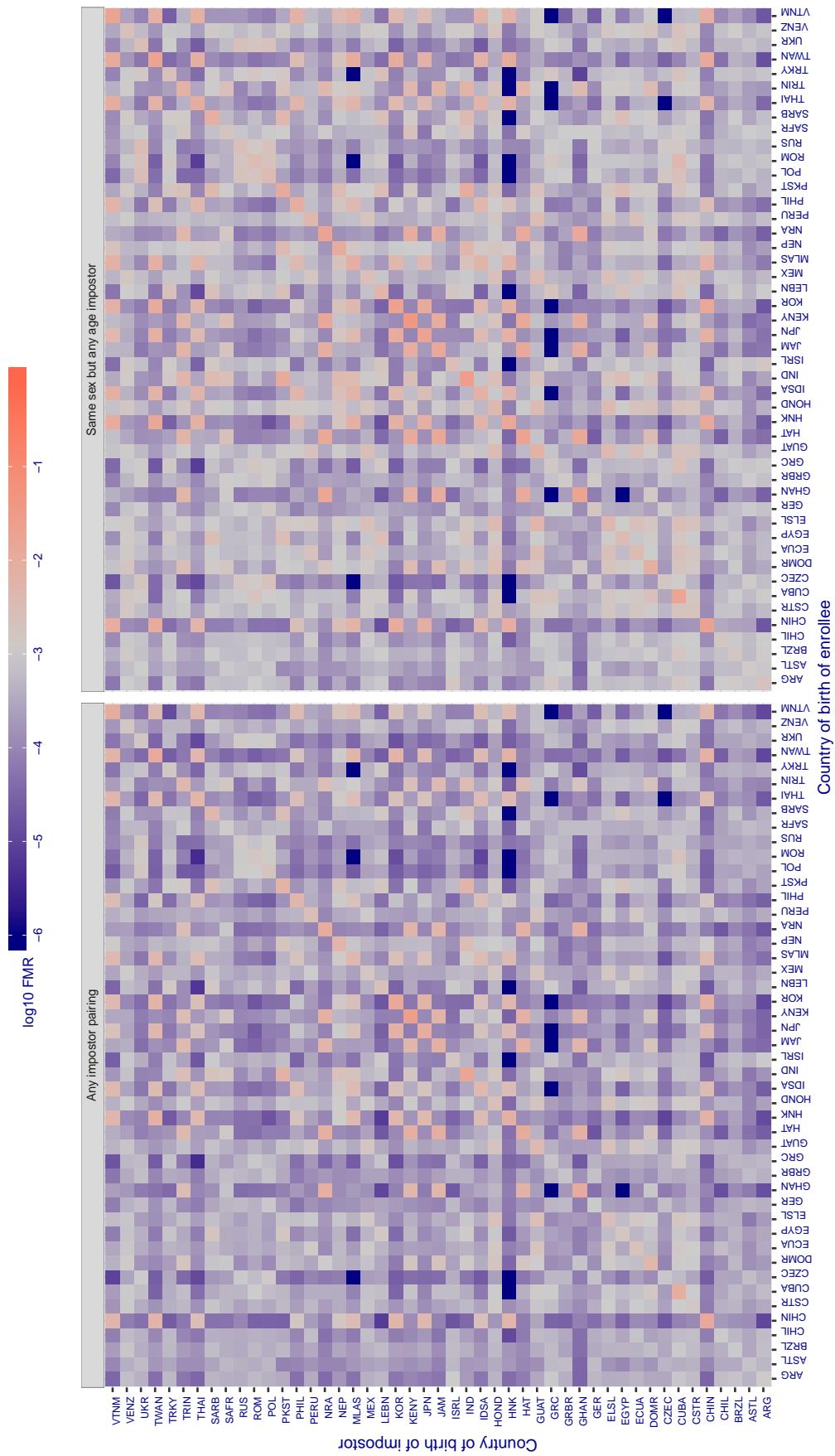
**Cross country FMR at threshold T = 147.234 for algorithm tech5\_002, giving FMR(T) = 0.001 globally.**

Figure 293: For algorithm tech5-002 operating on visa images, the heatmap shows false match rates observed over impostor comparisons of faces from different individuals who were born in the given country pair. False matches are counted against a recognition threshold fixed globally to give the target FMR in the plot title, computed over all on the order of  $10^{10}$  impostor comparisons. If text appears in each box it give the same quantity as that coded by the color. Grey indicates FMR is at the intended FMR target level. Light red colors present a security vulnerability to, for example, a passport gate. Each +1 increase in  $\log_{10}$  FMR corresponds to a factor of 10 increase in FMR. The matrix is not quite symmetric because images in the enrollment and verification sets are different.

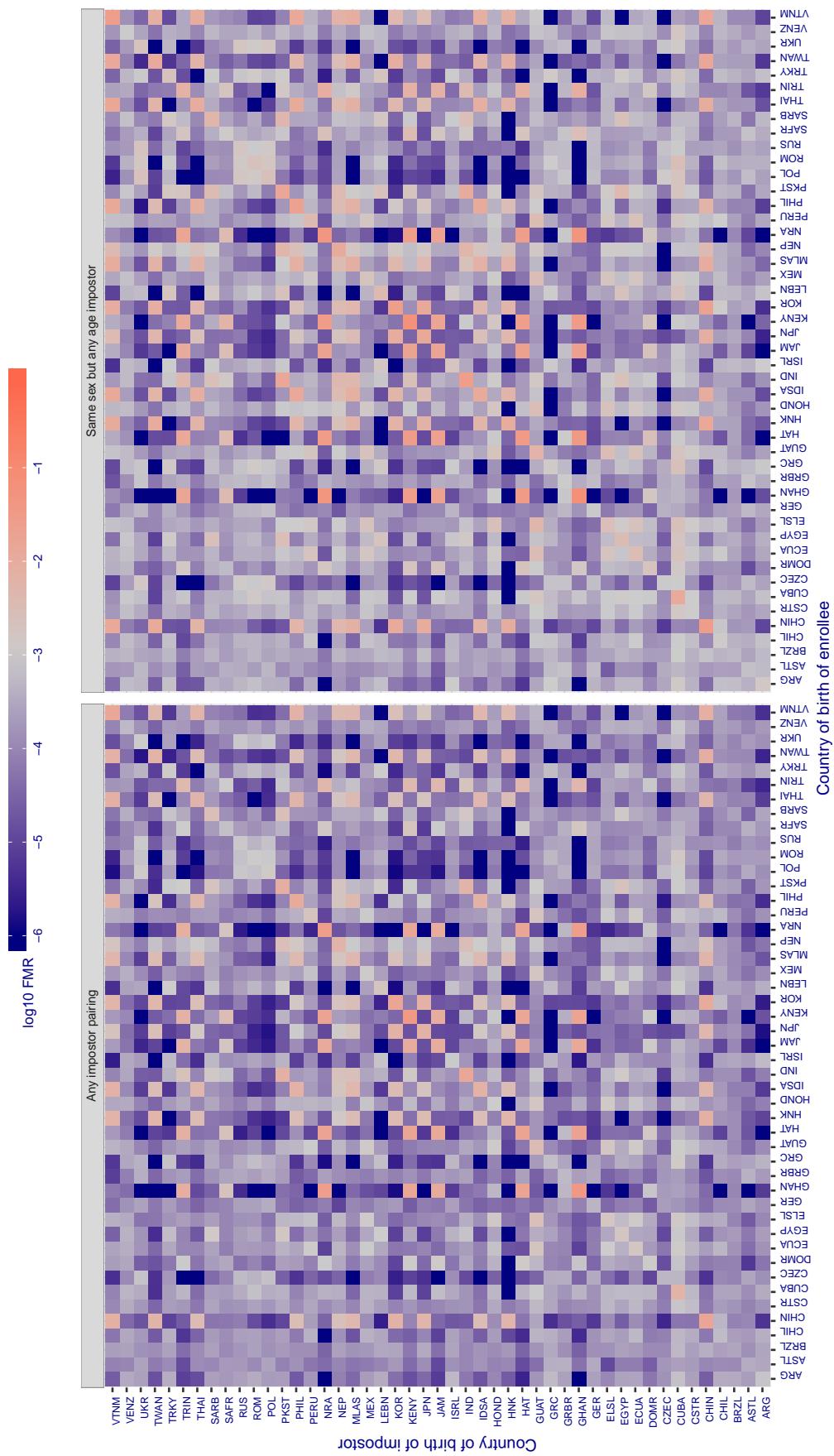
**Cross country FMR at threshold T = 0.769 for algorithm tevian\_003, giving  $FMR(T) = 0.001$  globally.**

Figure 294: For algorithm tevian-003 operating on visa images, the heatmap shows false match rates observed over impostor comparisons of faces from different individuals who were born in the given country pair. False matches are counted against a recognition threshold fixed globally to give the target  $FMR$  in the plot title, computed over all on the order of  $10^{10}$  impostor comparisons. If text appears in each box it give the same quantity as that coded by the color. Grey indicates  $FMR$  is at the intended  $FMR$  target level. Light red colors present a security vulnerability to, for example, a passport gate. Each +1 increase in  $\log_{10} FMR$  corresponds to a factor of 10 increase in  $FMR$ . The matrix is not quite symmetric because images in the enrollment and verification sets are different.

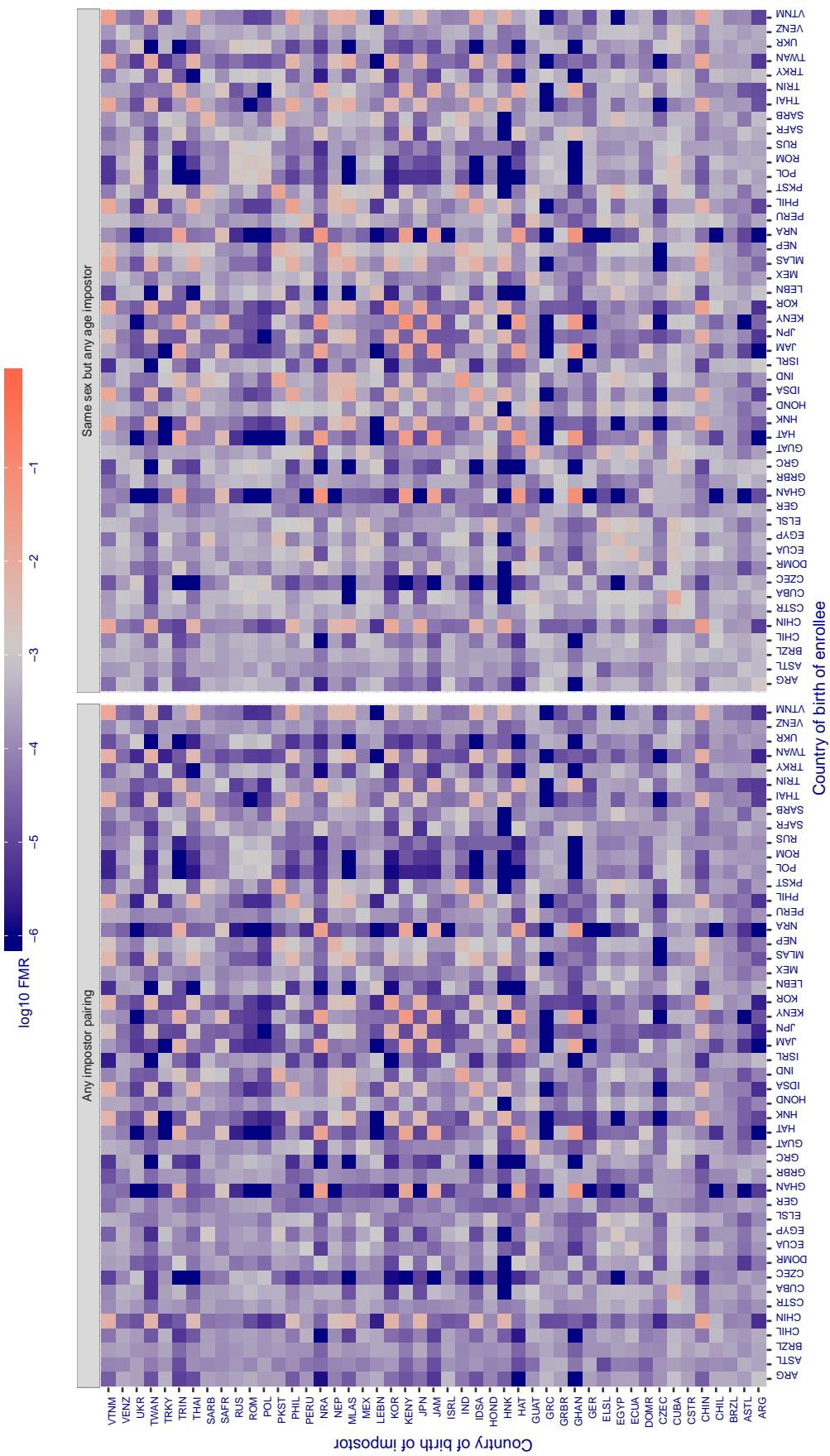
**Cross country FMR at threshold T = 0.769 for algorithm tevian\_004, giving FMR(T) = 0.001 globally.**

Figure 295: For algorithm tevian-004 operating on visa images, the heatmap shows false match rates observed over impostor comparisons of faces from different individuals who were born in the given country pair. False matches are counted against a recognition threshold fixed globally to give the target FMR in the plot title, computed over all on the order of  $10^{10}$  impostor comparisons. If text appears in each box it give the same quantity as that coded by the color. Grey indicates FMR is at the intended FMR target level. Light red colors present a security vulnerability to, for example, a passport gate. Each +1 increase in  $\log_{10} \text{FMR}$  corresponds to a factor of 10 increase in FMR. The matrix is not quite symmetric because images in the enrollment and verification sets are different.

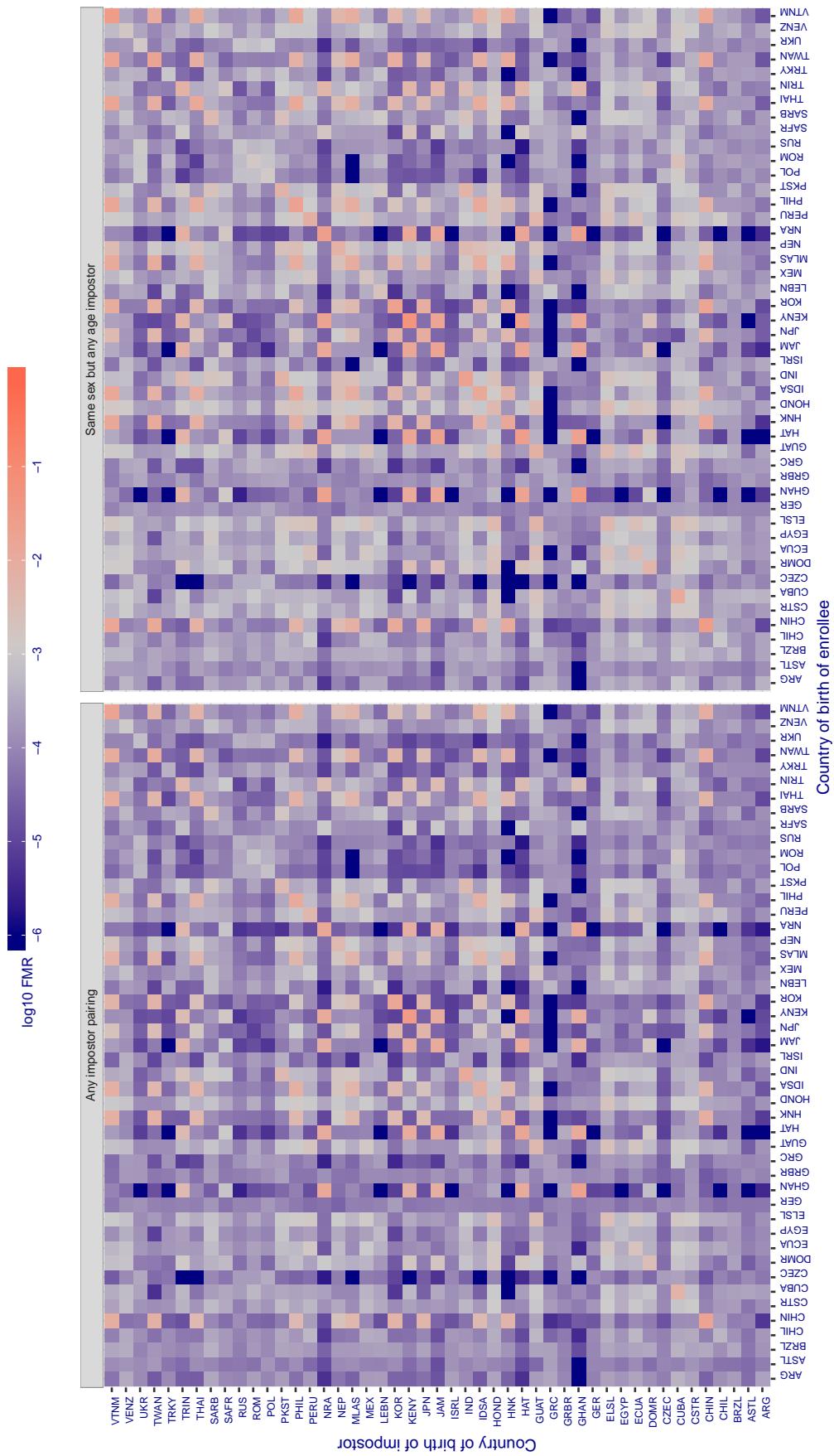
**Cross country FMR at threshold T = 143.194 for algorithm tiger\_002, giving FMR(T) = 0.001 globally.**

Figure 296: For algorithm tiger-002 operating on visa images, the heatmap shows false match rates observed over impostor comparisons of faces from different individuals who were born in the given country pair. False matches are counted against a recognition threshold fixed globally to give the target FMR in the plot title, computed over all on the order of  $10^{10}$  impostor comparisons. If text appears in each box it give the same quantity as that coded by the color. Grey indicates FMR is at the intended FMR target level. Light red colors present a security vulnerability to, for example, a passport gate. Each +1 increase in  $\log_{10} \text{FMR}$  corresponds to a factor of 10 increase in FMR. The matrix is not quite symmetric because images in the enrollment and verification sets are different.

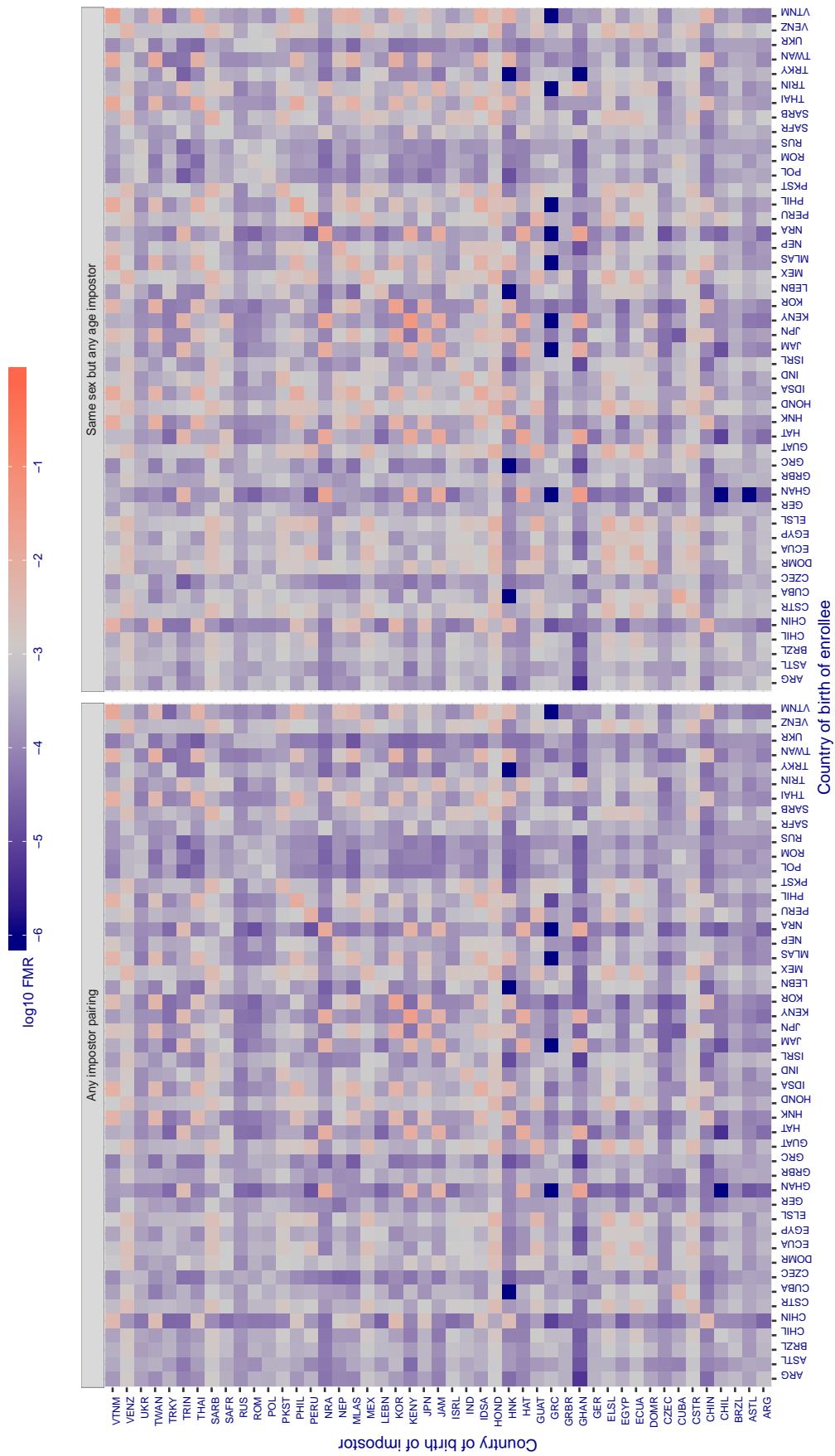
**Cross country FMR at threshold T = 139.101 for algorithm tiger\_003, giving FMR(T) = 0.001 globally.**

Figure 297: For algorithm tiger-003 operating on visa images, the heatmap shows false match rates observed over impostor comparisons of faces from different individuals who were born in the given country pair. False matches are counted against a recognition threshold fixed globally to give the target FMR in the plot title, computed over all on the order of  $10^{10}$  impostor comparisons. If text appears in each box it give the same quantity as that coded by the color. Grey indicates FMR is at the intended FMR target level. Light red colors present a security vulnerability to, for example, a passport gate. Each +1 increase in  $\log_{10} \text{FMR}$  corresponds to a factor of 10 increase in FMR. The matrix is not quite symmetric because images in the enrollment and verification sets are different.

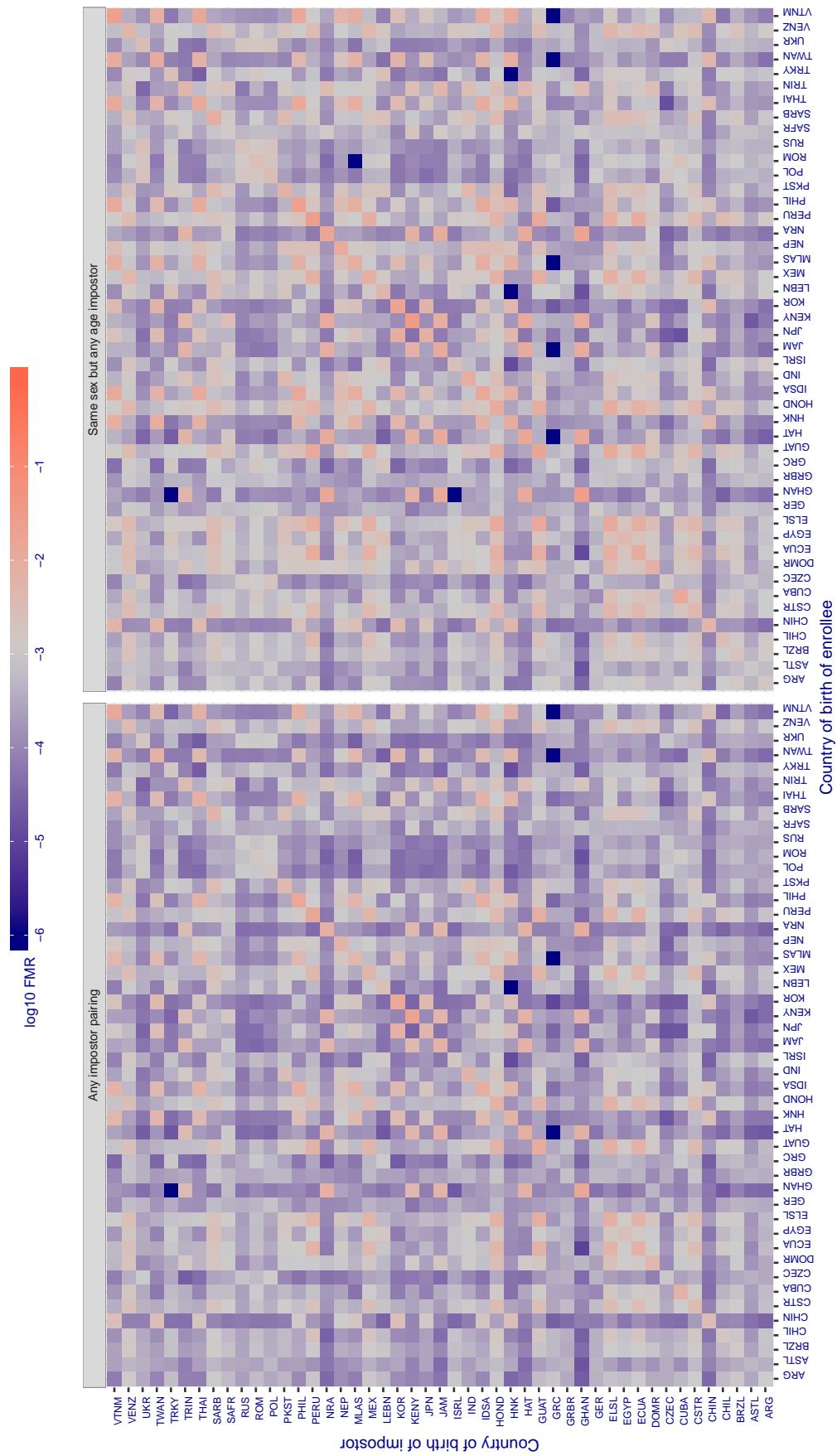
**Cross country FMR at threshold T = 0.599 for algorithm toshiba\_002, giving FMR(T) = 0.001 globally.**

Figure 298: For algorithm toshiba-002 operating on visa images, the heatmap shows false match rates observed over impostor comparisons of faces from different individuals who were born in the given country pair. False matches are counted against a recognition threshold fixed globally to give the target FMR in the plot title, computed over all on the order of  $10^{10}$  impostor comparisons. If text appears in each box it give the same quantity as that coded by the color. Grey indicates FMR is at the intended FMR target level. Light red colors present a security vulnerability to, for example, a passport gate. Each +1 increase in  $\log_{10}$  FMR corresponds to a factor of 10 increase in FMR. The matrix is not quite symmetric because images in the enrollment and verification sets are different.

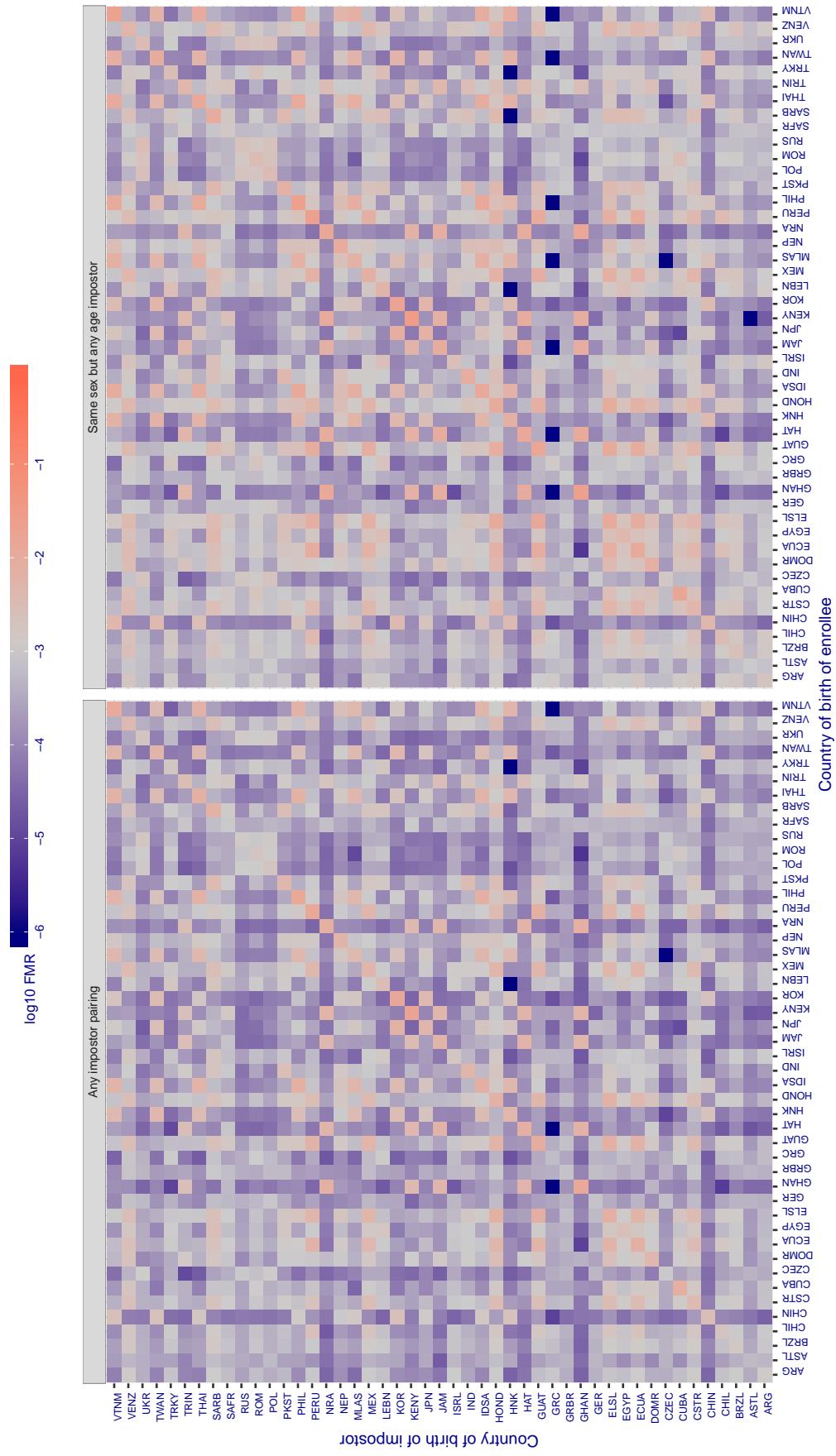
**Cross country FMR at threshold T = 0.596 for algorithm toshiba\_003, giving FMR(T) = 0.001 globally.**

Figure 299: For algorithm toshiba-003 operating on visa images, the heatmap shows false match rates observed over impostor comparisons of faces from different individuals who were born in the given country pair. False matches are counted against a recognition threshold fixed globally to give the target FMR in the plot title, computed over all on the order of  $10^{10}$  impostor comparisons. If text appears in each box it give the same quantity as that coded by the color. Grey indicates FMR is at the intended FMR target level. Light red colors present a security vulnerability to, for example, a passport gate. Each +1 increase in  $\log_{10} FMR$  corresponds to a factor of 10 increase in FMR. The matrix is not quite symmetric because images in the enrollment and verification sets are different.

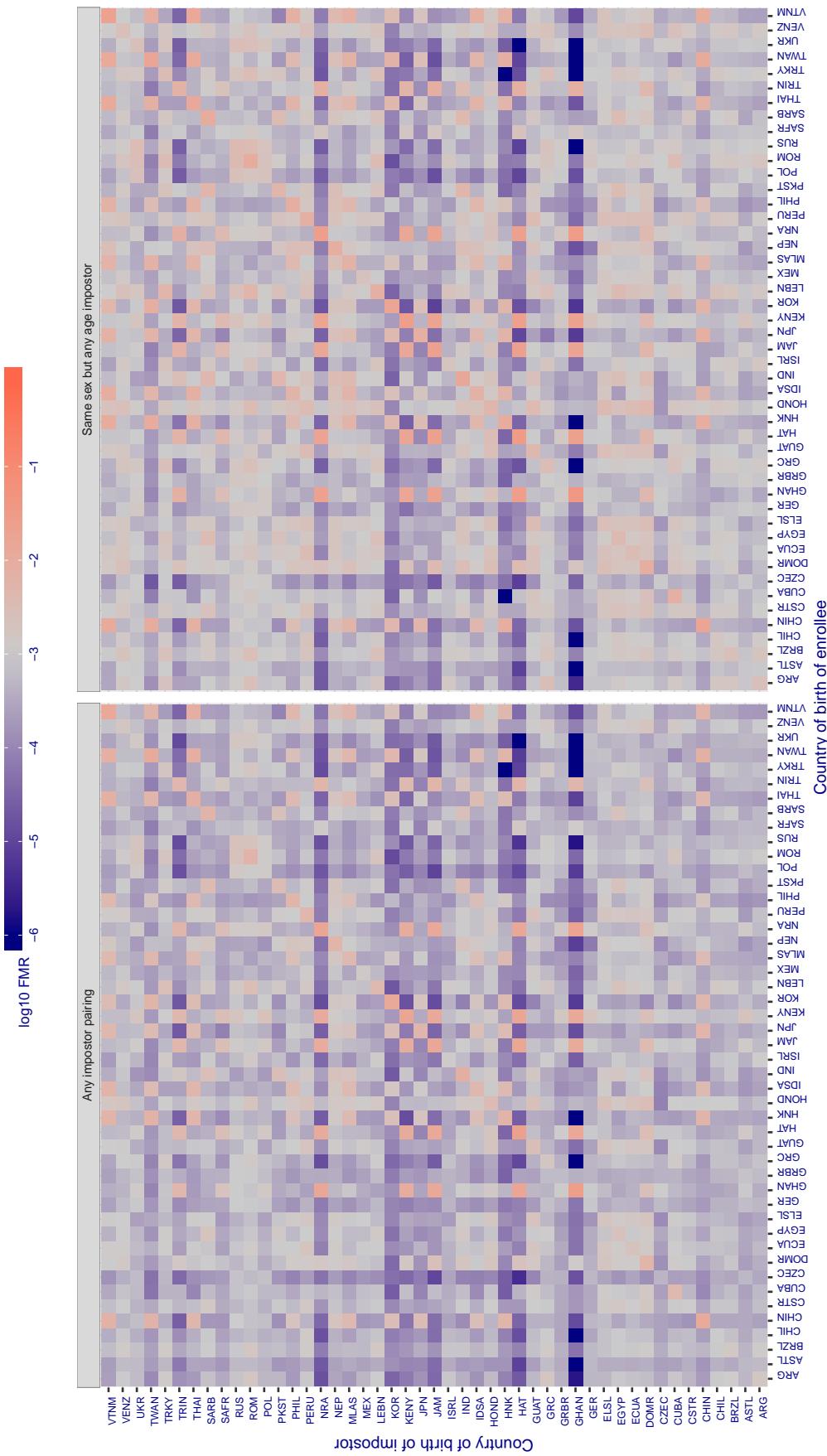
**Cross country FMR at threshold T = 0.310 for algorithm vcog\_002, giving FMR(T) = 0.001 globally.**

Figure 30: For algorithm vcog-002 operating on visa images, the heatmap shows false match rates observed over impostor comparisons of faces from different individuals who were born in the given country pair. False matches are counted against a recognition threshold fixed globally to give the target FMR in the plot title, computed over all on the order of  $10^{10}$  impostor comparisons. If text appears in each box it give the same quantity as that coded by the color. Grey indicates FMR is at the intended FMR target level. Light red colors present a security vulnerability to, for example, a passport gate. Each +1 increase in  $\log_{10}$  FMR corresponds to a factor of 10 increase in FMR. The matrix is not quite symmetric because images in the enrollment and verification sets are different.

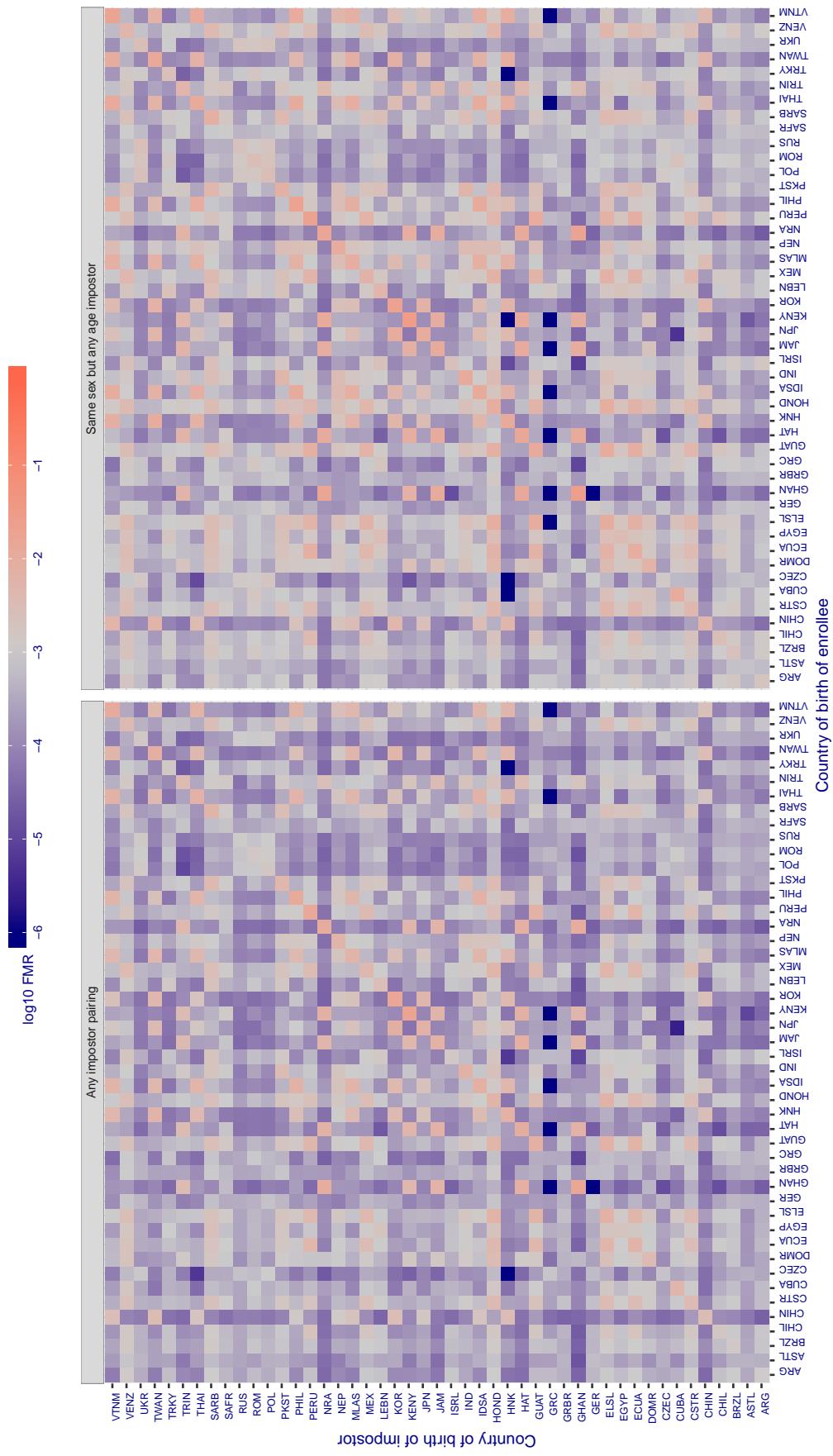
**Cross country FMR at threshold T = 66.962 for algorithm vd\_001, giving FMR(T) = 0.001 globally.**

Figure 301: For algorithm vd-001 operating on visa images, the heatmap shows false match rates observed over impostor comparisons of faces from different individuals who were born in the given country pair. False matches are counted against a recognition threshold fixed globally to give the target FMR in the plot title, computed over all on the order of  $10^{10}$  impostor comparisons. If text appears in each box it give the same quantity as that coded by the color. Grey indicates FMR is at the intended FMR target level. Light red colors present a security vulnerability to, for example, a passport gate. Each +1 increase in  $\log_{10} \text{FMR}$  corresponds to a factor of 10 increase in FMR. The matrix is not quite symmetric because images in the enrollment and verification sets are different.

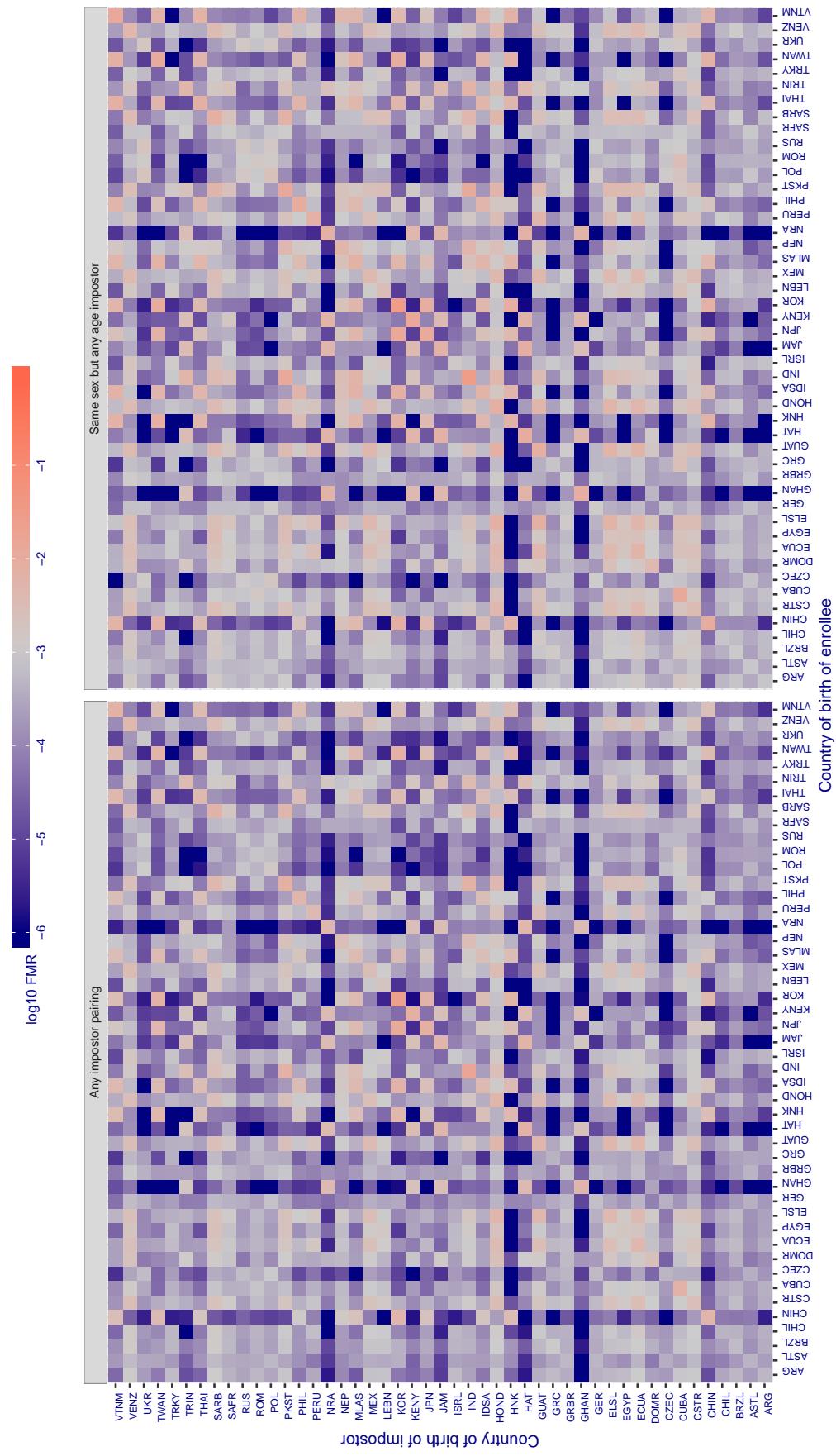
**Cross country FMR at threshold T = 2.897 for algorithm veridas\_001, giving FMR(T) = 0.001 globally.**

Figure 302: For algorithm veridas-001 operating on visa images, the heatmap shows false match rates observed over impostor comparisons of faces from different individuals who were born in the given country pair. False matches are counted against a recognition threshold fixed globally to give the target FMR in the plot title, computed over all on the order of  $10^{10}$  impostor comparisons. If text appears in each box it give the same quantity as that coded by the color. Grey indicates FMR is at the intended FMR target level. Light red colors present a security vulnerability to, for example, a passport gate. Each +1 increase in  $\log_{10} FMR$  corresponds to a factor of 10 increase in FMR. The matrix is not quite symmetric because images in the enrollment and verification sets are different.

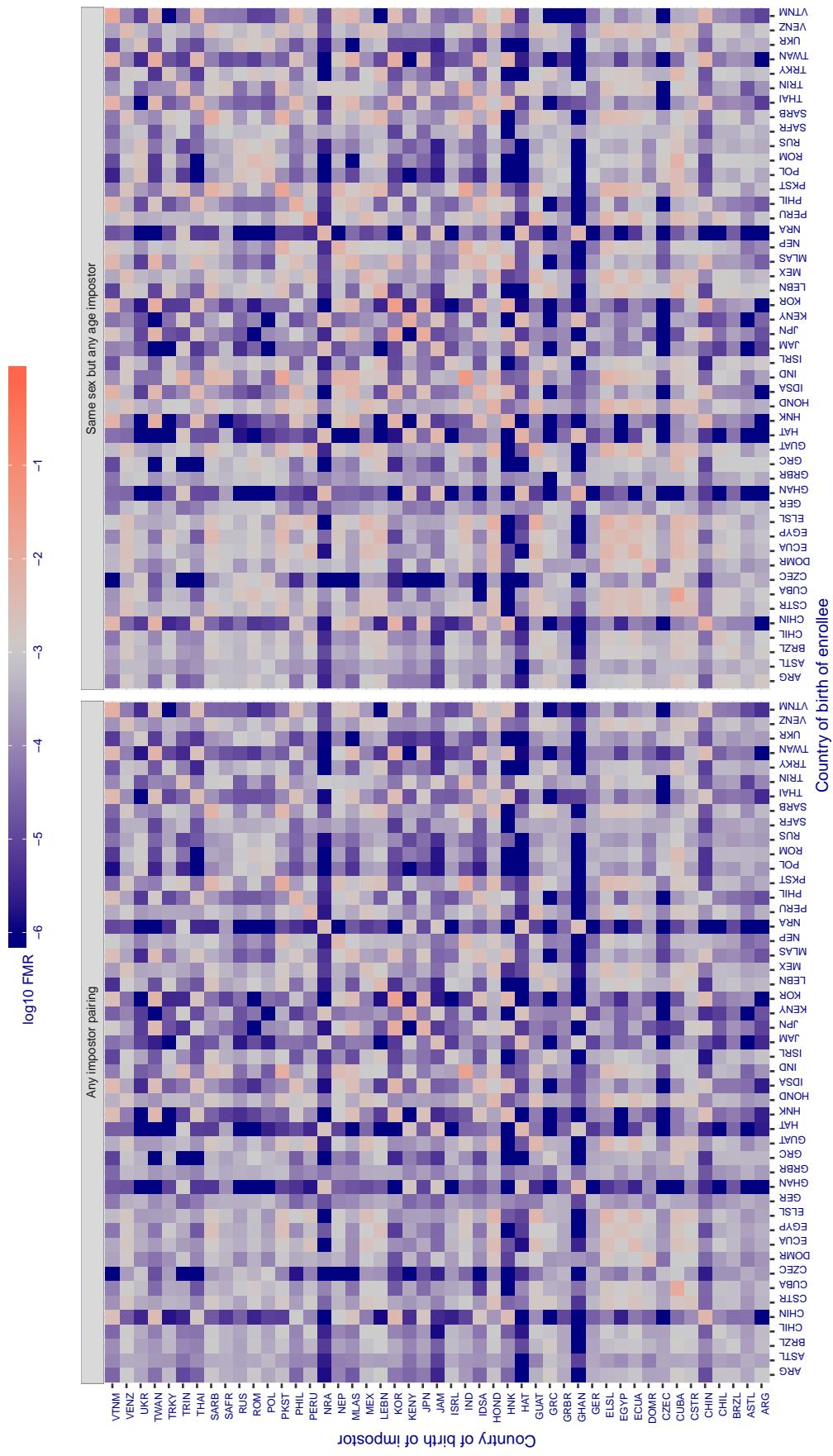
**Cross country FMR at threshold T = 3.010 for algorithm veridas\_002, giving FMR(T) = 0.001 globally.**

Figure 303: For algorithm veridas-002 operating on visa images, the heatmap shows false match rates observed over impostor comparisons of faces from different individuals who were born in the given country pair. False matches are counted against a recognition threshold fixed globally to give the target FMR in the plot title, computed over all on the order of  $10^{10}$  impostor comparisons. If text appears in each box it give the same quantity as that coded by the color. Grey indicates FMR is at the intended FMR target level. Light red colors present a security vulnerability to, for example, a passport gate. Each +1 increase in  $\log_{10}$  FMR corresponds to a factor of 10 increase in FMR. The matrix is not quite symmetric because images in the enrollment and verification sets are different.

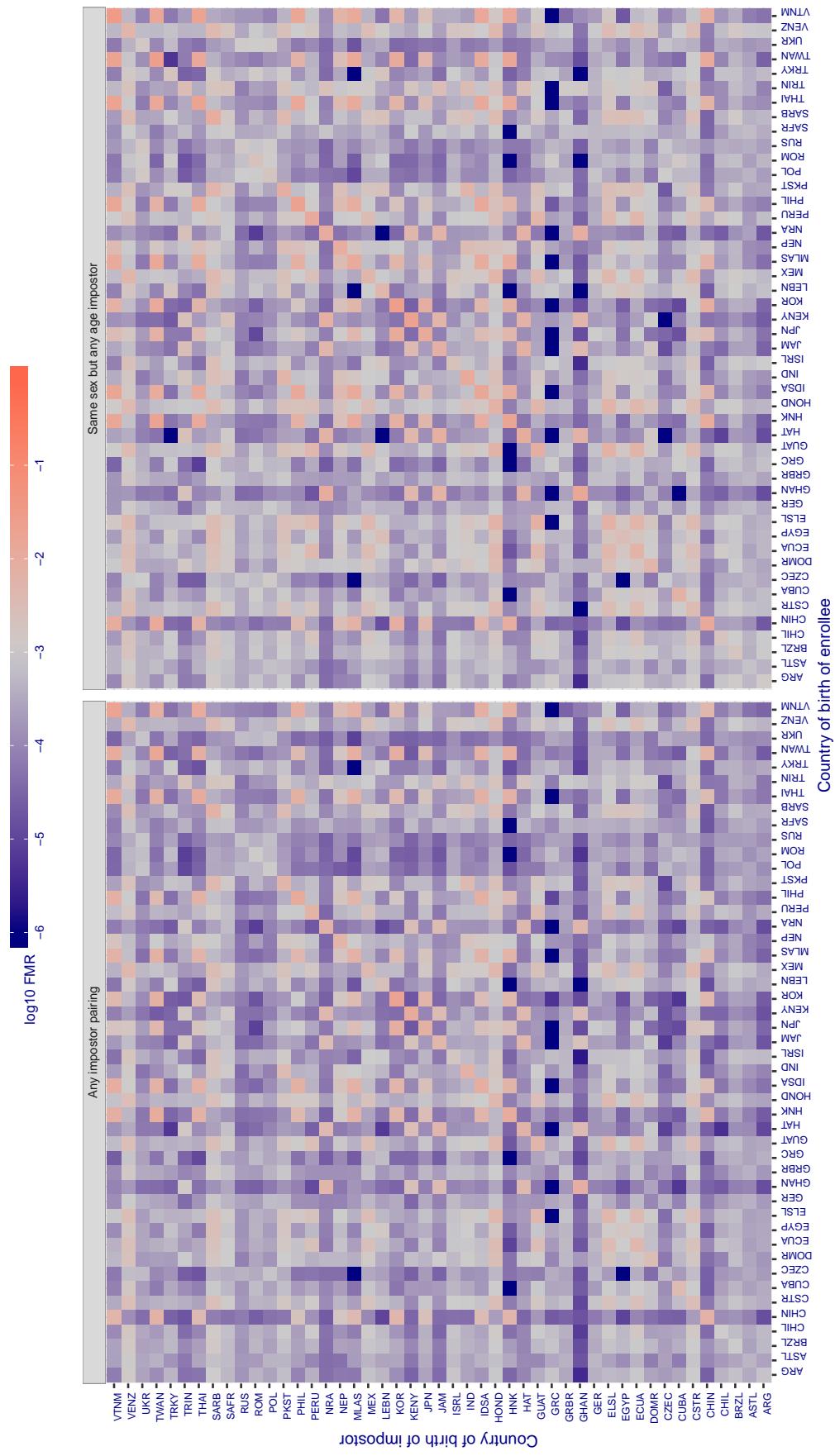
**Cross country FMR at threshold T = 2.800 for algorithm vigilantsolutions\_005, giving FMR(T) = 0.001 globally.**

Figure 304: For algorithm vigilantsolutions-005 operating on visa images, the heatmap shows false match rates observed over impostor comparisons of faces from different individuals who were born in the given country pair. False matches are counted against a recognition threshold fixed globally to give the target FMR in the plot title, computed over all on the order of  $10^{10}$  impostor comparisons. If text appears in each box it give the same quantity as that coded by the color. Grey indicates FMR is at the intended FMR target level. Light red colors present a security vulnerability to, for example, a passport gate. Each +1 increase in  $\log_{10}$  FMR corresponds to a factor of 10 increase in FMR. The matrix is not quite symmetric because images in the enrollment and verification sets are different.

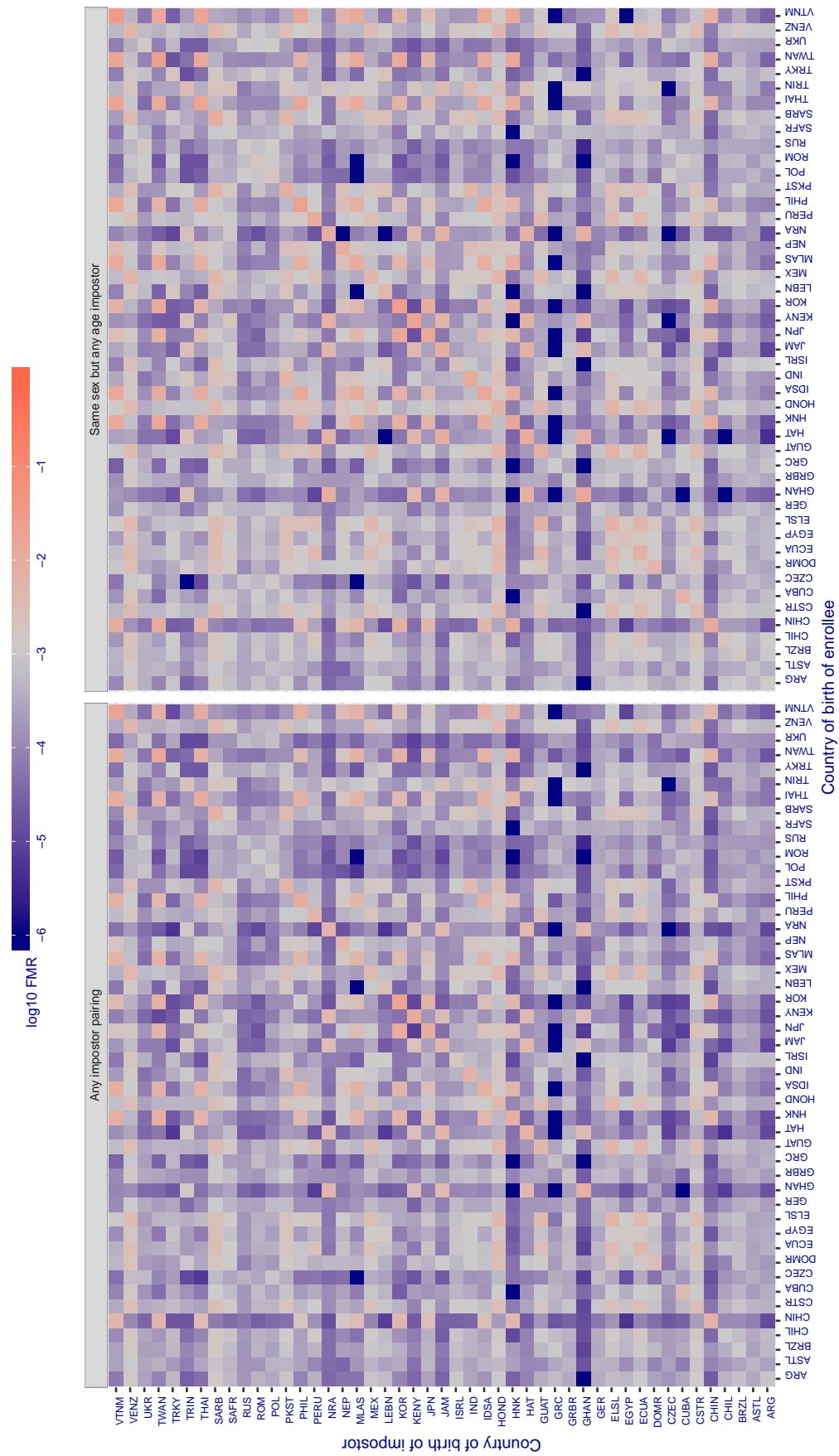
**Cross country FMR at threshold T = 2.809 for algorithm vigilantsolutions\_006, giving FMR(T) = 0.001 globally.**

Figure 305: For algorithm vigilantsolutions-006 operating on visa images, the heatmap shows false match rates observed over impostor comparisons of faces from different individuals who were born in the given country pair. False matches are counted against a recognition threshold fixed globally to give the target FMR in the plot title, computed over all on the order of  $10^{10}$  impostor comparisons. If text appears in each box it give the same quantity as that coded by the color. Grey indicates FMR is at the intended FMR target level. Light red colors present a security vulnerability to, for example, a passport gate. Each +1 increase in  $\log_{10} \text{FMR}$  corresponds to a factor of 10 increase in FMR. The matrix is not quite symmetric because images in the enrollment and verification sets are different.

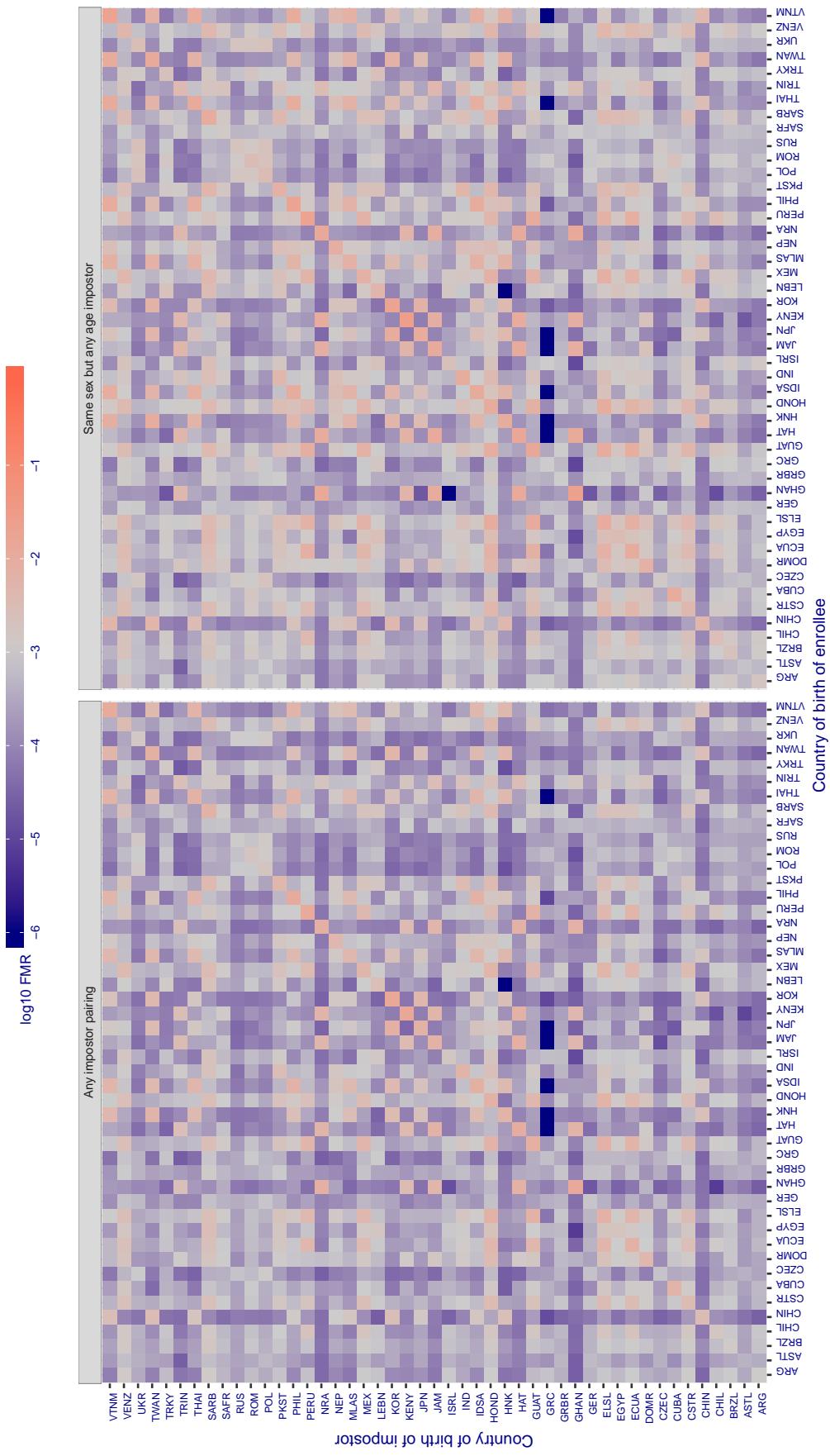
**Cross country FMR at threshold T = 0.336 for algorithm vion\_000, giving FMR(T) = 0.001 globally.**

Figure 306: For algorithm vion-000 operating on visa images, the heatmap shows false match rates observed over impostor comparisons of faces from different individuals who were born in the given country pair. False matches are counted against a recognition threshold fixed globally to give the target FMR in the plot title, computed over all on the order of  $10^{10}$  impostor comparisons. If text appears in each box it give the same quantity as that coded by the color. Grey indicates FMR is at the intended FMR target level. Light red colors present a security vulnerability to, for example, a passport gate. Each +1 increase in  $\log_{10} \text{FMR}$  corresponds to a factor of 10 increase in FMR. The matrix is not quite symmetric because images in the enrollment and verification sets are different.

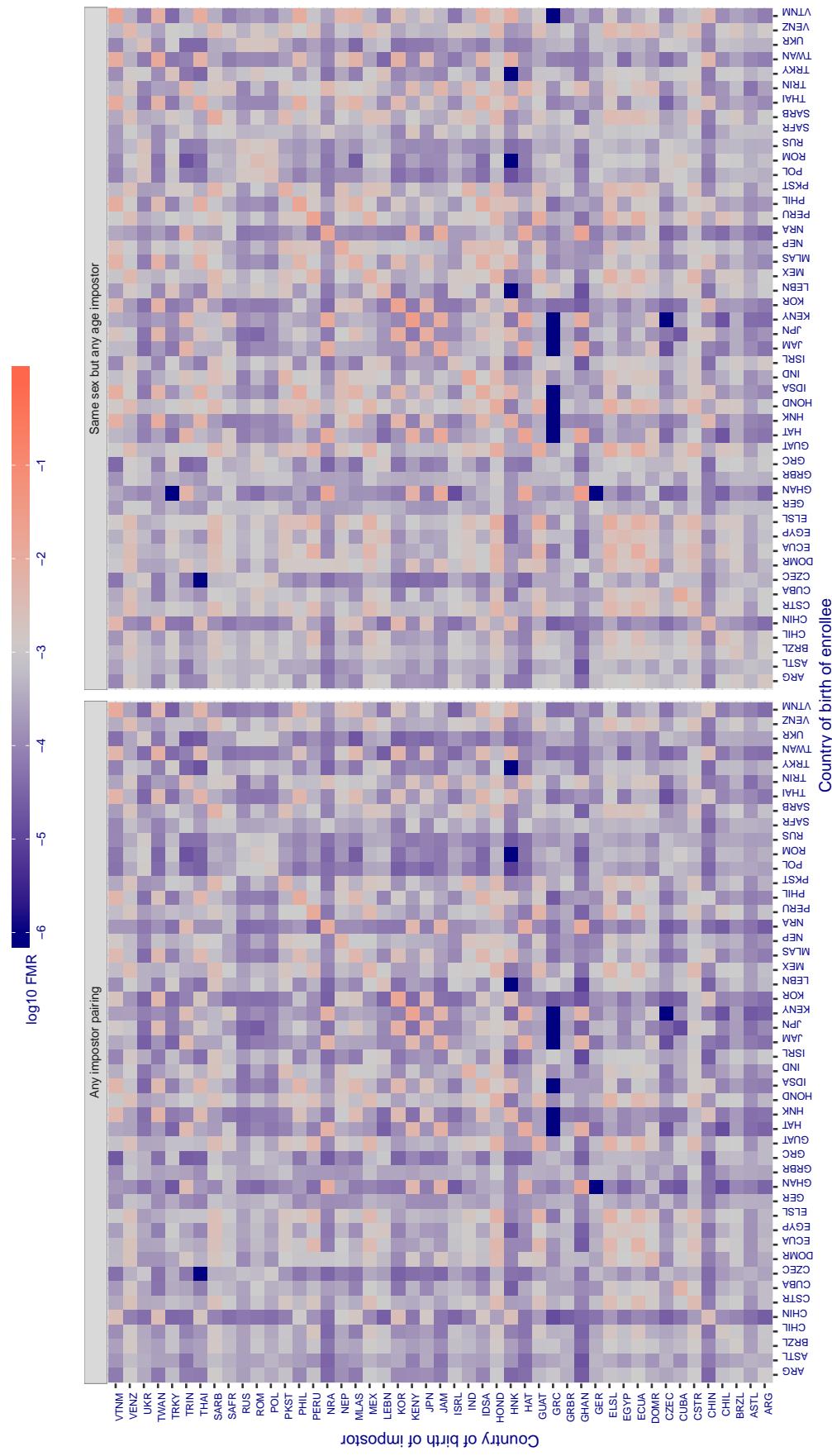
**Cross country FMR at threshold T = 0.340 for algorithm visionbox\_000, giving FMR(T) = 0.001 globally.**

Figure 307: For algorithm visionbox-000 operating on visa images, the heatmap shows false match rates observed over impostor comparisons of faces from different individuals who were born in the given country pair. False matches are counted against a recognition threshold fixed globally to give the target FMR in the plot title, computed over all on the order of  $10^{10}$  impostor comparisons. If text appears in each box it give the same quantity as that coded by the color. Grey indicates FMR is at the intended FMR target level. Light red colors present a security vulnerability to, for example, a passport gate. Each +1 increase in  $\log_{10} FMR$  corresponds to a factor of 10 increase in FMR. The matrix is not quite symmetric because images in the enrollment and verification sets are different.

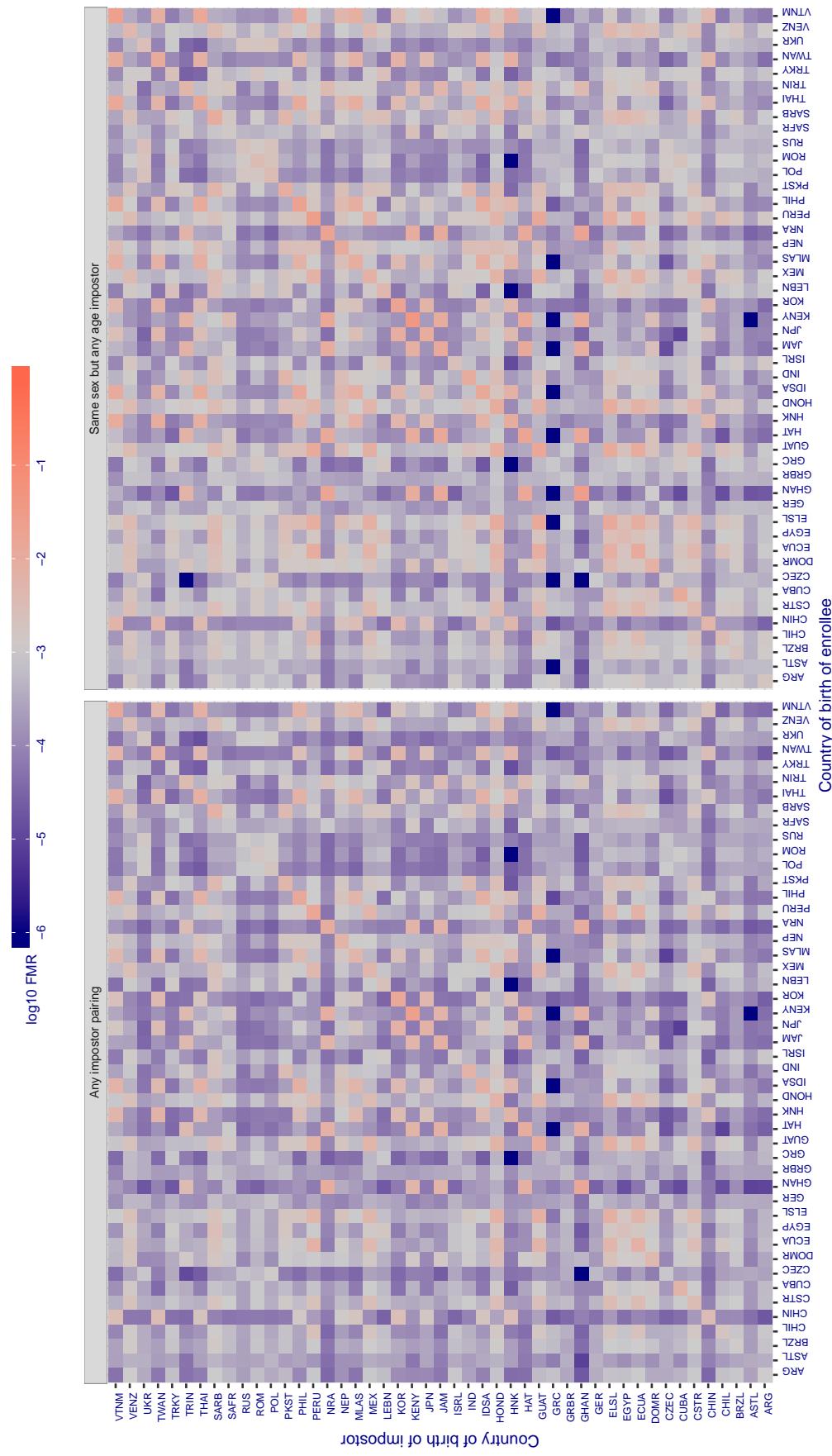
**Cross country FMR at threshold T = 0.296 for algorithm visionbox\_001, giving FMR(T) = 0.001 globally.**

Figure 308: For algorithm visionbox-001 operating on visa images, the heatmap shows false match rates observed over impostor comparisons of faces from different individuals who were born in the given country pair. False matches are counted against a recognition threshold fixed globally to give the target FMR in the plot title, computed over all on the order of  $10^{10}$  impostor comparisons. If text appears in each box it give the same quantity as that coded by the color. Grey indicates FMR is at the intended FMR target level. Light red colors present a security vulnerability to, for example, a passport gate. Each +1 increase in  $\log_{10} \text{FMR}$  corresponds to a factor of 10 increase in FMR. The matrix is not quite symmetric because images in the enrollment and verification sets are different.

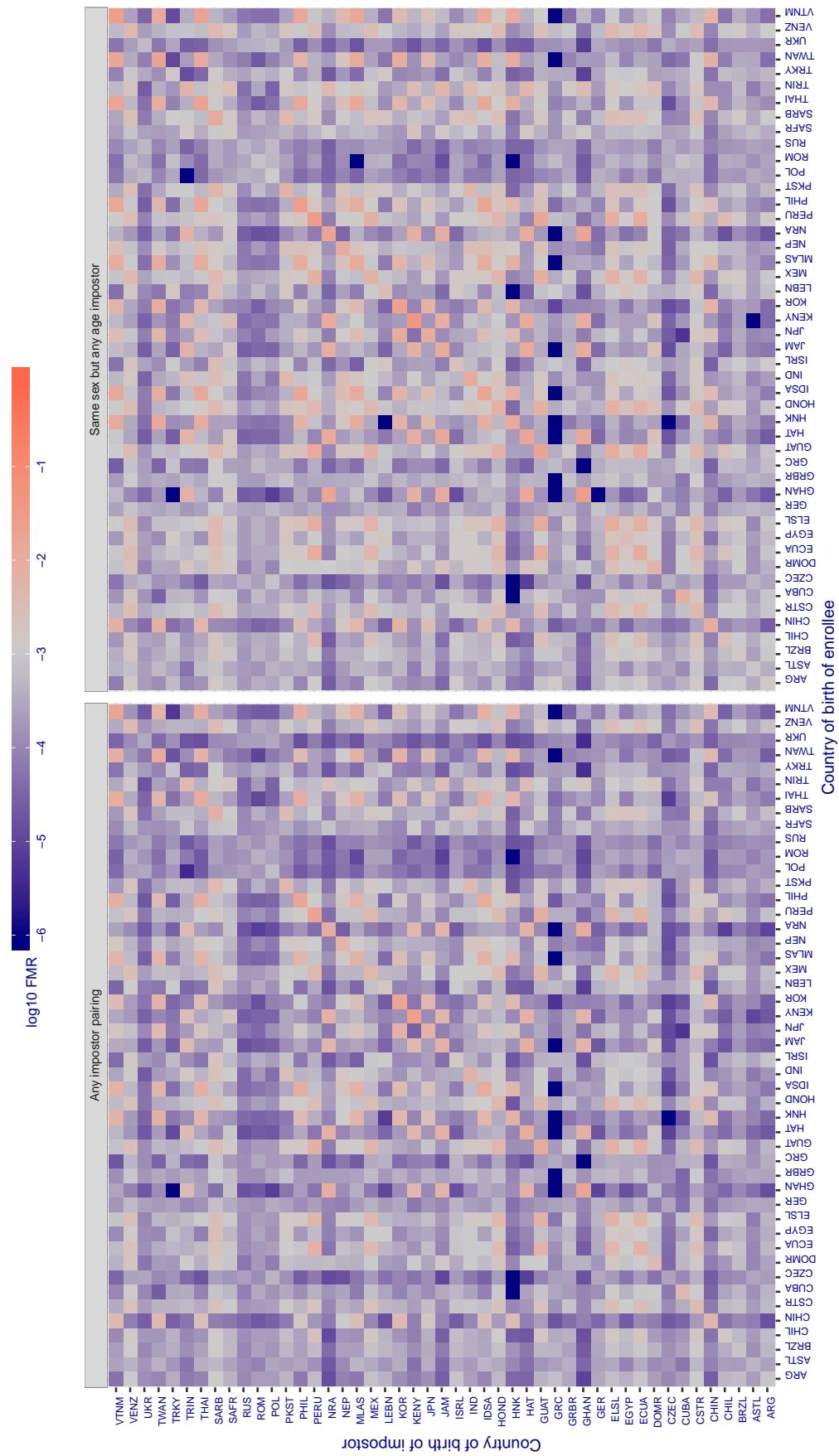
**Cross country FMR at threshold T = 0.000 for algorithm visionlabs\_005, giving FMR(T) = 0.001 globally.**

Figure 309: For algorithm visionlabs-005 operating on visa images, the heatmap shows false match rates observed over impostor comparisons of faces from different individuals who were born in the given country pair. False matches are counted against a recognition threshold fixed globally to give the target FMR in the plot title, computed over all on the order of  $10^{10}$  impostor comparisons. If text appears in each box it give the same quantity as that coded by the color. Grey indicates FMR is at the intended FMR target level. Light red colors present a security vulnerability to, for example, a passport gate. Each +1 increase in  $\log_{10} FMR$  corresponds to a factor of 10 increase in FMR. The matrix is not quite symmetric because images in the enrollment and verification sets are different.

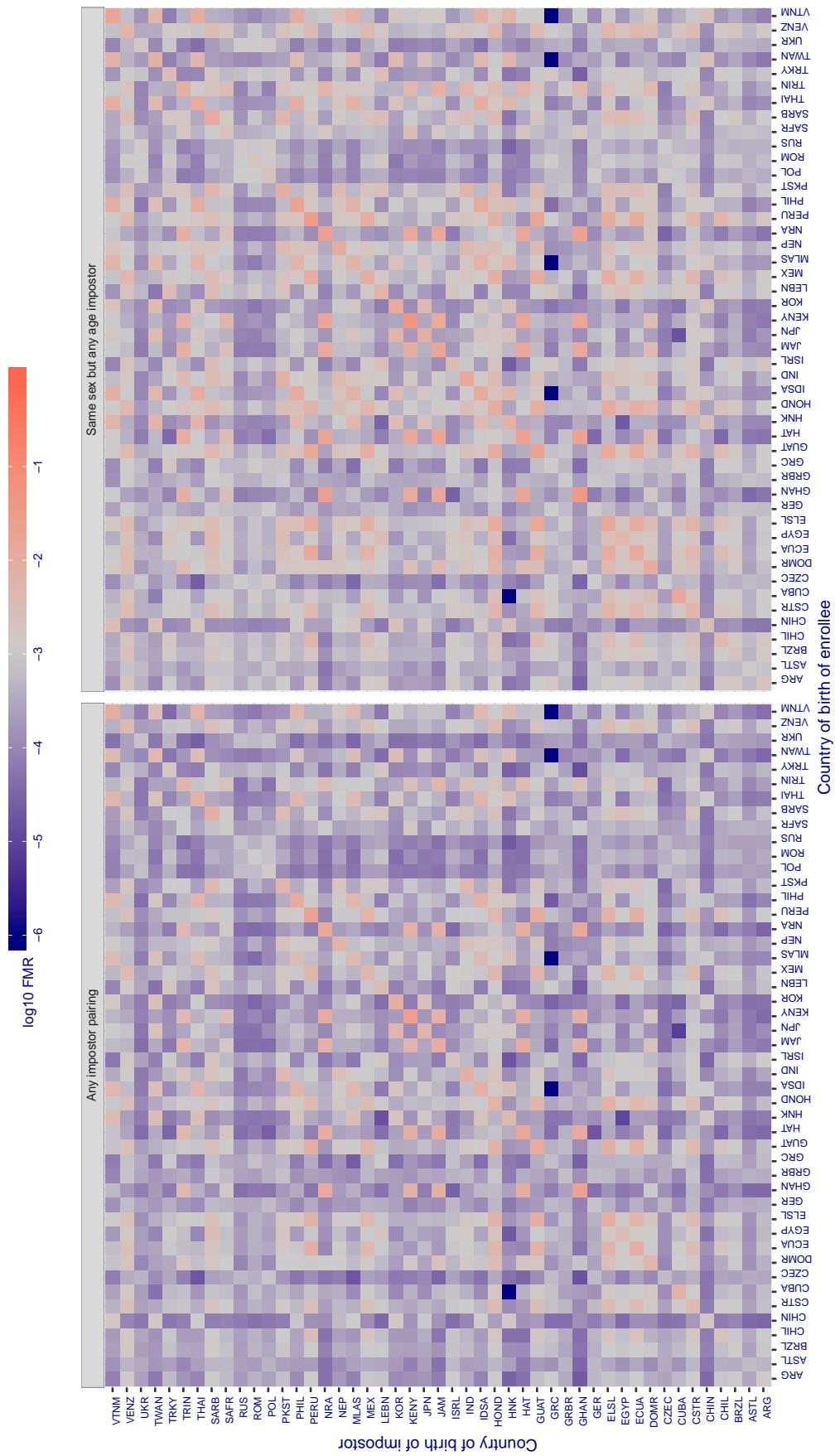
**Cross country FMR at threshold T = 0.444 for algorithm visionlabs\_006, giving  $\text{FMR}(T) = 0.001$  globally.**

Figure 310: For algorithm visionlabs-006 operating on visa images, the heatmap shows false match rates observed over impostor comparisons of faces from different individuals who were born in the given country pair. False matches are counted against a recognition threshold fixed globally to give the target  $\text{FMR}$  in the plot title, computed over all on the order of  $10^{10}$  impostor comparisons. If text appears in each box it give the same quantity as that coded by the color. Grey indicates  $\text{FMR}$  is at the intended  $\text{FMR}$  target level. Light red colors present a security vulnerability to, for example, a passport gate. Each +1 increase in  $\log_{10} \text{FMR}$  corresponds to a factor of 10 increase in  $\text{FMR}$ . The matrix is not quite symmetric because images in the enrollment and verification sets are different.

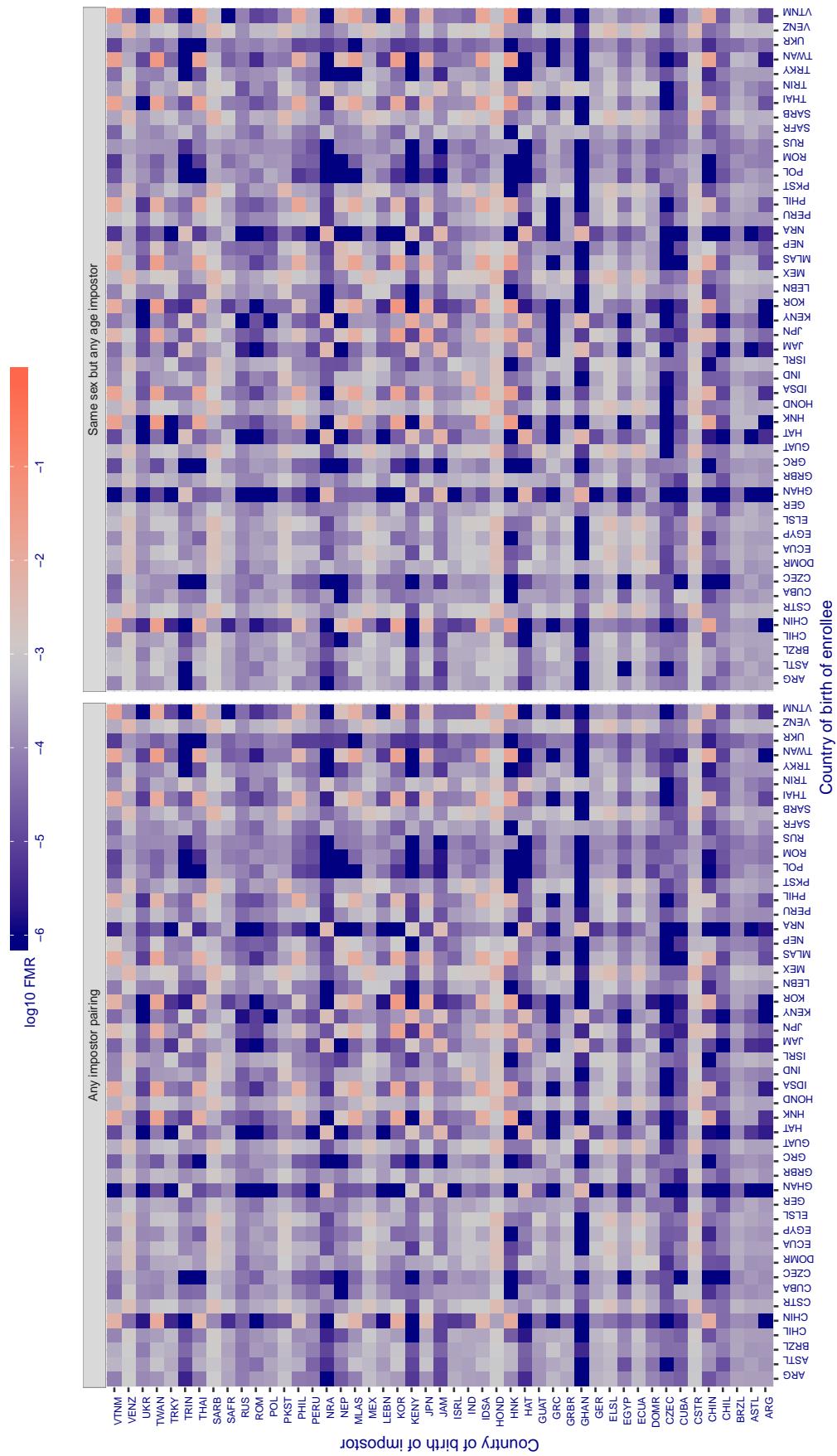
**Cross country FMR at threshold T = 5.333 for algorithm yisheng\_004, giving FMR(T) = 0.001 globally.**

Figure 311: For algorithm yisheng-004 operating on visa images, the heatmap shows false match rates observed over impostor comparisons of faces from different individuals who were born in the given country pair. False matches are counted against a recognition threshold fixed globally to give the target FMR in the plot title, computed over all on the order of  $10^{10}$  impostor comparisons. If text appears in each box it give the same quantity as that coded by the color. Grey indicates FMR is at the intended FMR target level. Light red colors present a security vulnerability to, for example, a passport gate. Each +1 increase in  $\log_{10} FMR$  corresponds to a factor of 10 increase in FMR. The matrix is not quite symmetric because images in the enrollment and verification sets are different.

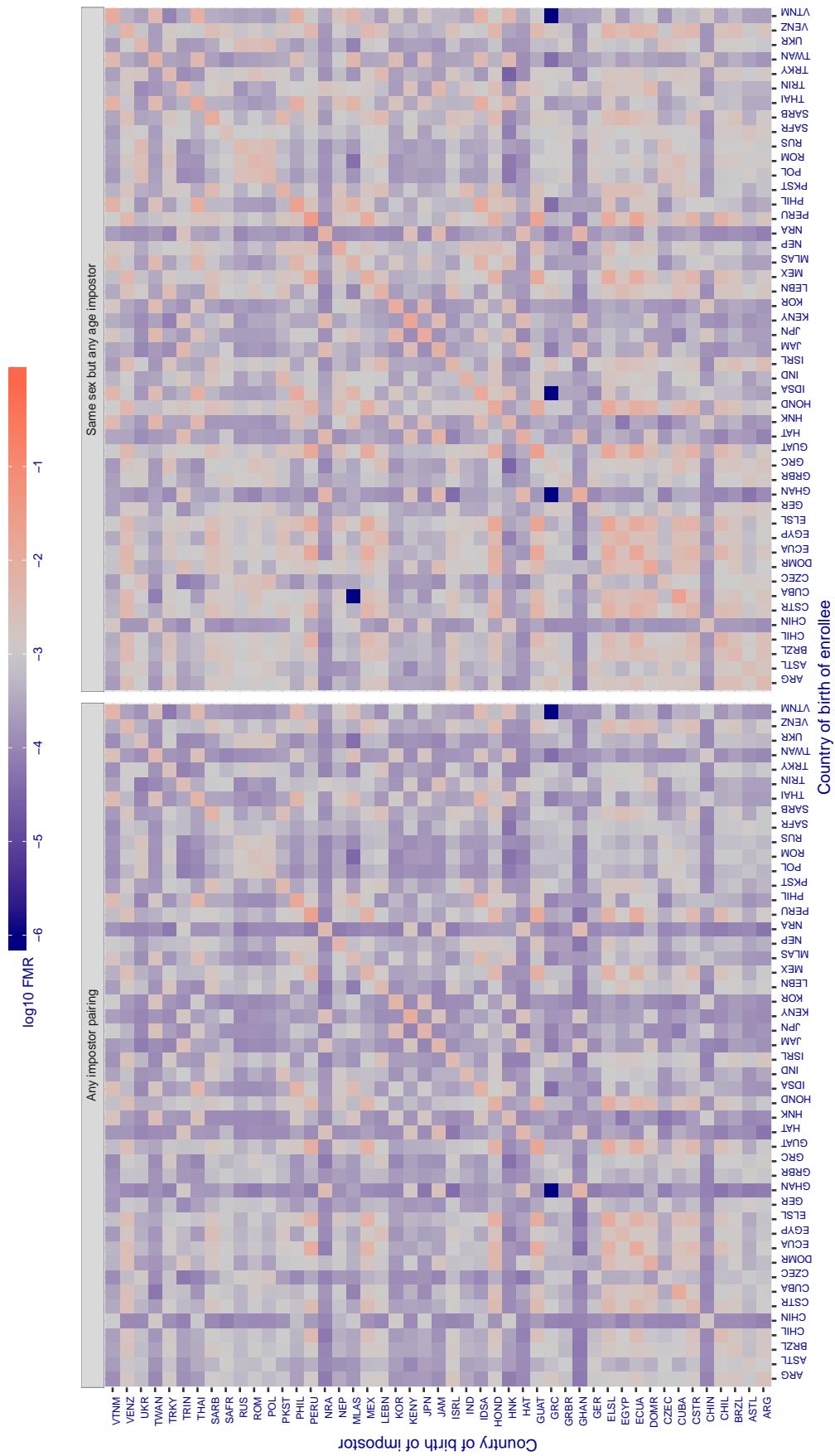
**Cross country FMR at threshold T = 37.550 for algorithm yitu\_003, giving FMR(T) = 0.001 globally.**

Figure 312: For algorithm yitu-003 operating on visa images, the heatmap shows false match rates observed over impostor comparisons of faces from different individuals who were born in the given country pair. False matches are counted against a recognition threshold fixed globally to give the target FMR in the plot title, computed over all on the order of  $10^{10}$  impostor comparisons. If text appears in each box it give the same quantity as that coded by the color. Grey indicates FMR is at the intended FMR target level. Light red colors present a security vulnerability to, for example, a passport gate. Each +1 increase in  $\log_{10} \text{FMR}$  corresponds to a factor of 10 increase in FMR. The matrix is not quite symmetric because images in the enrollment and verification sets are different.

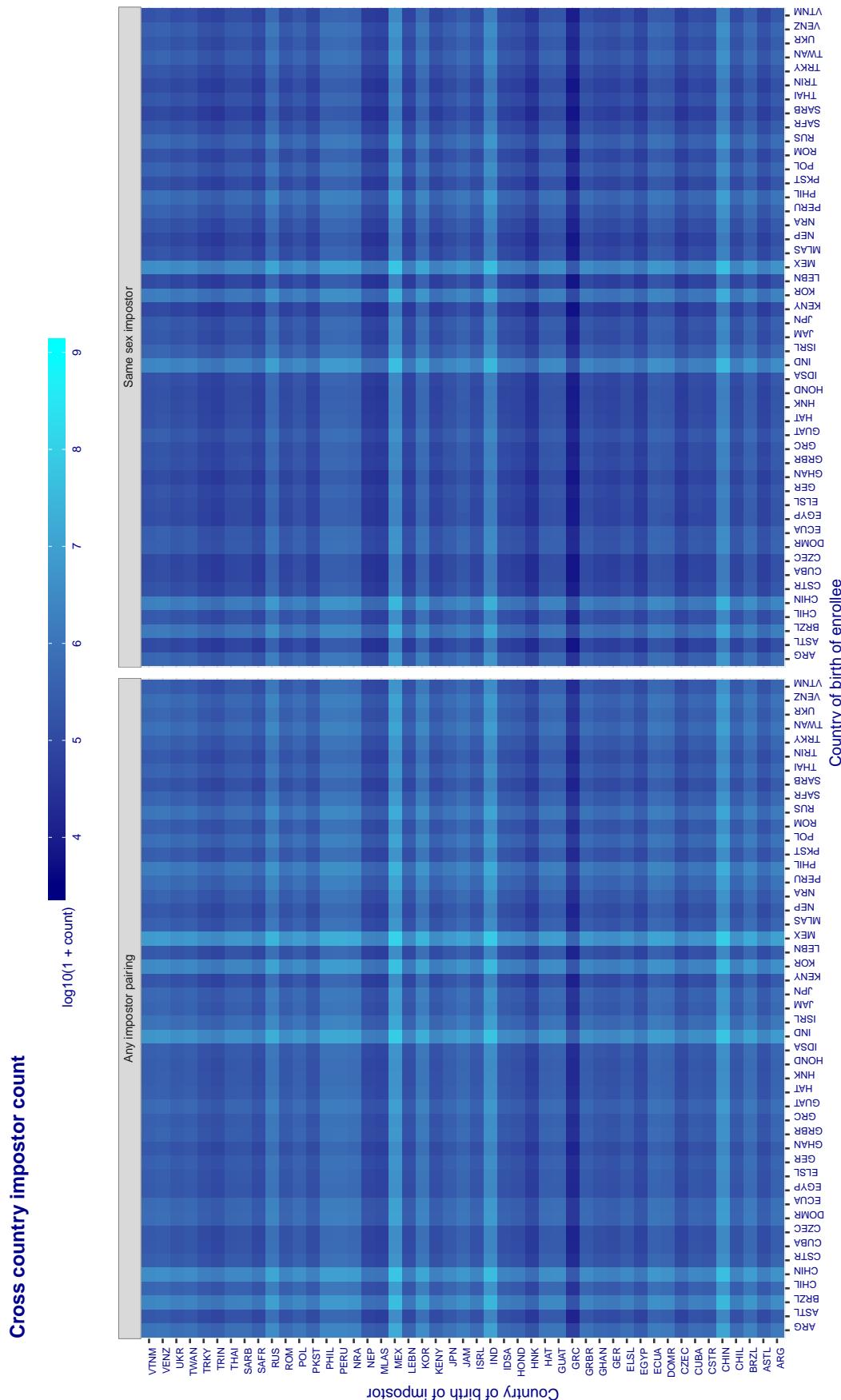


Figure 313: For visa images, the heatmap shows the count of impostor comparisons of faces from different individuals who were born in the given country pair.

### 3.6.2 Effect of age on impostors

**Background:** This section shows the effect of age on the impostor distribution. The ideal behaviour is that the age of the enrollee and the impostor would not affect impostor scores. This would support FMR stability over sub-populations.

**Goals:**

- ▷ To show the effect of relative ages of the impostor and enrollee on false match rates.
- ▷ To determine whether some algorithms have better impostor distribution stability.

**Methods:**

- ▷ Define 14 age group bins, spanning 0 to over 100 years old.
- ▷ Compute FMR over all impostor comparisons for which the subjects in the enrollee and impostor images have ages in two bins.
- ▷ Compute FMR over all impostor comparisons for which the subjects are additionally of the same sex, and born in the same geographic region.

**Results:**

The notable aspects are:

- ▷ Diagonal dominance: Impostors are more likely to be matched against their same age group.
- ▷ Same sex and same region impostors are more successful. On the diagonal, an impostor is more likely to succeed by posing as someone of the same sex. If  $\Delta \log_{10} \text{FMR} = 0.2$ , then same-sex same-region FMR exceeds the all-pairs FMR by factor of  $10^{0.2} = 1.6$ .
- ▷ Young children impostors give elevated FMR against young children. Older adult impostor give elevated FMR against older adults. These effects are quite large, for example if  $\Delta \log_{10} \text{FMR} = 1.0$  larger than a 32 year old, then these groups have higher FMR by a factor of  $10^1 = 10$ . This would imply an FMR above 0.01 for a nominal (global) FMR = 0.001.
- ▷ Algorithms vary.
- ▷ We computed the same quantities for a global FMR = 0.0001. The effects are similar.

Note the calculations in this section include impostors paired across all countries of birth.

Cross age FMR at threshold T = 2.740 for algorithm 3divi\_003, giving FMR(T) = 0.0001 globally.

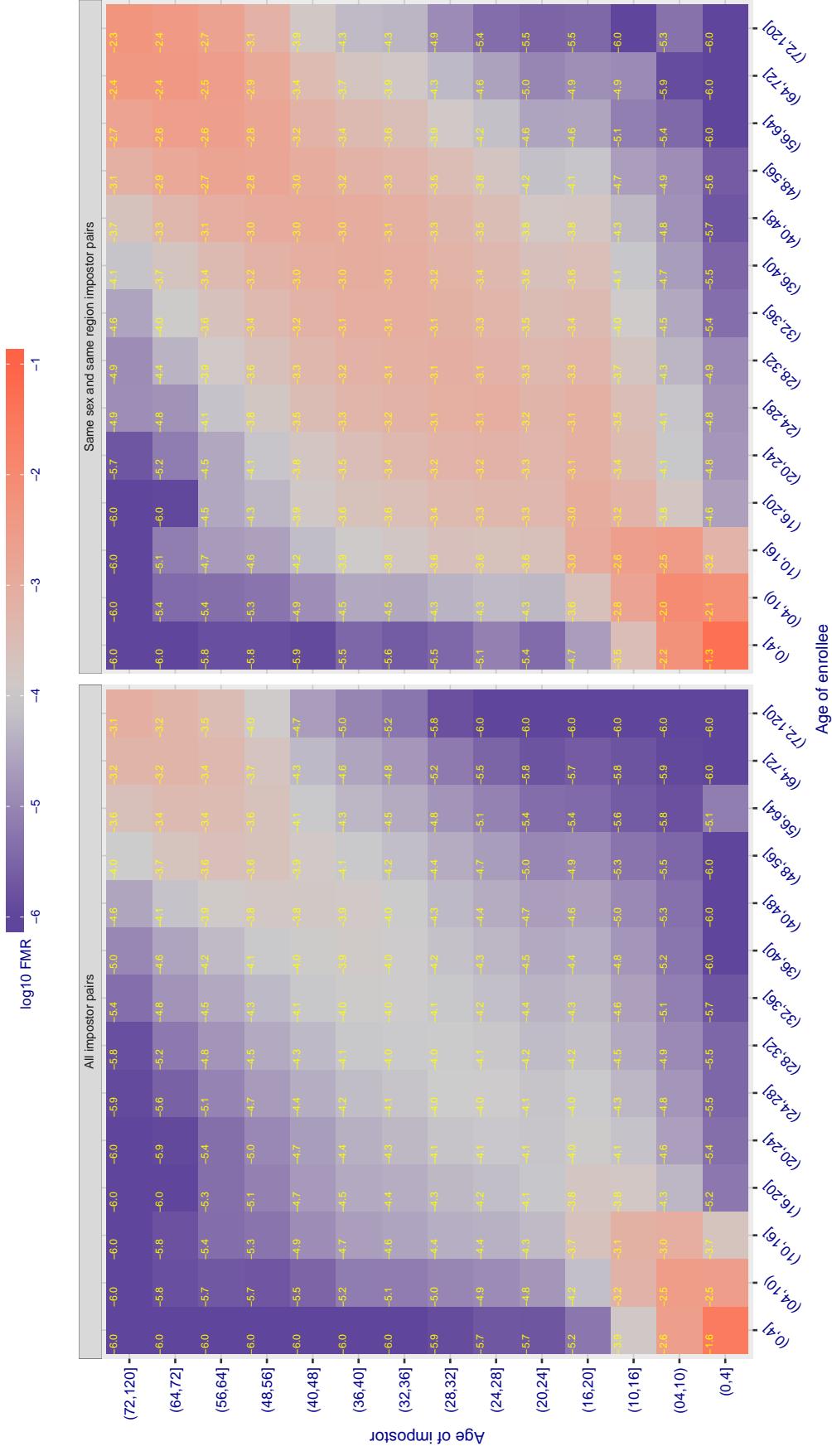


Figure 314: For algorithm 3divi-003 operating on visa images, the heatmap shows false match observed over impostor comparisons of faces from different individuals who have the given age pair. False matches are counted against a recognition threshold fixed globally to give  $FMR = 0.001$  over all on the order of  $10^{10}$  impostor comparisons. The text in each box gives the same quantity as that coded by the color. Light colors present a security vulnerability to, for example, a passport gate.

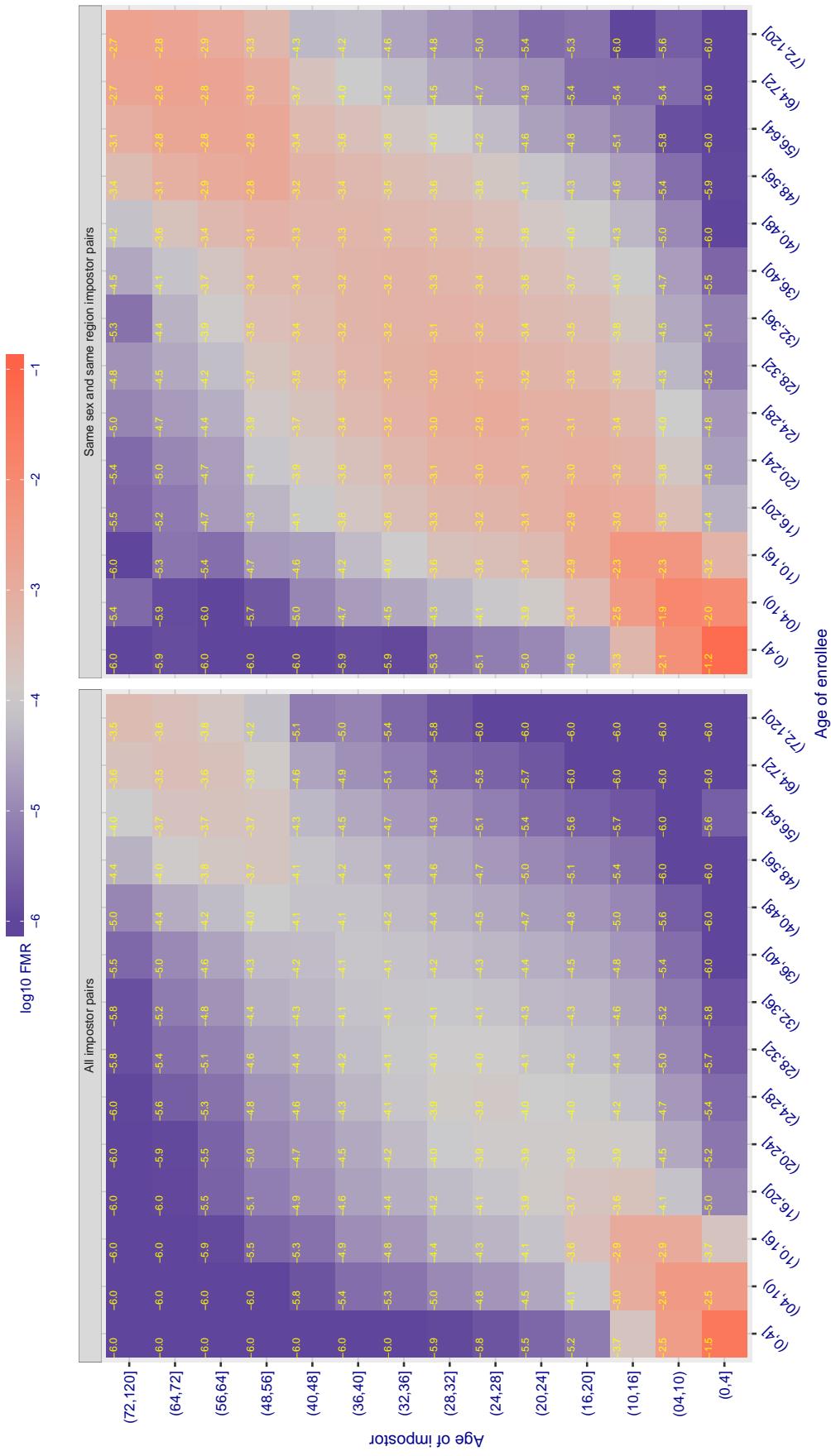
Cross age FMR at threshold T = 0.702 for algorithm alchera\_000, giving  $FMR(T) = 0.0001$  globally.

Figure 315: For algorithm alchera-000 operating on visa images, the heatmap shows false match observed over impostor comparisons of faces from different individuals who have the given age pair. False matches are counted against a recognition threshold fixed globally to give  $FMR = 0.001$  over all on the order of  $10^{10}$  impostor comparisons. The text in each box gives the same quantity as that coded by the color. Light colors present a security vulnerability to, for example, a passport gate.

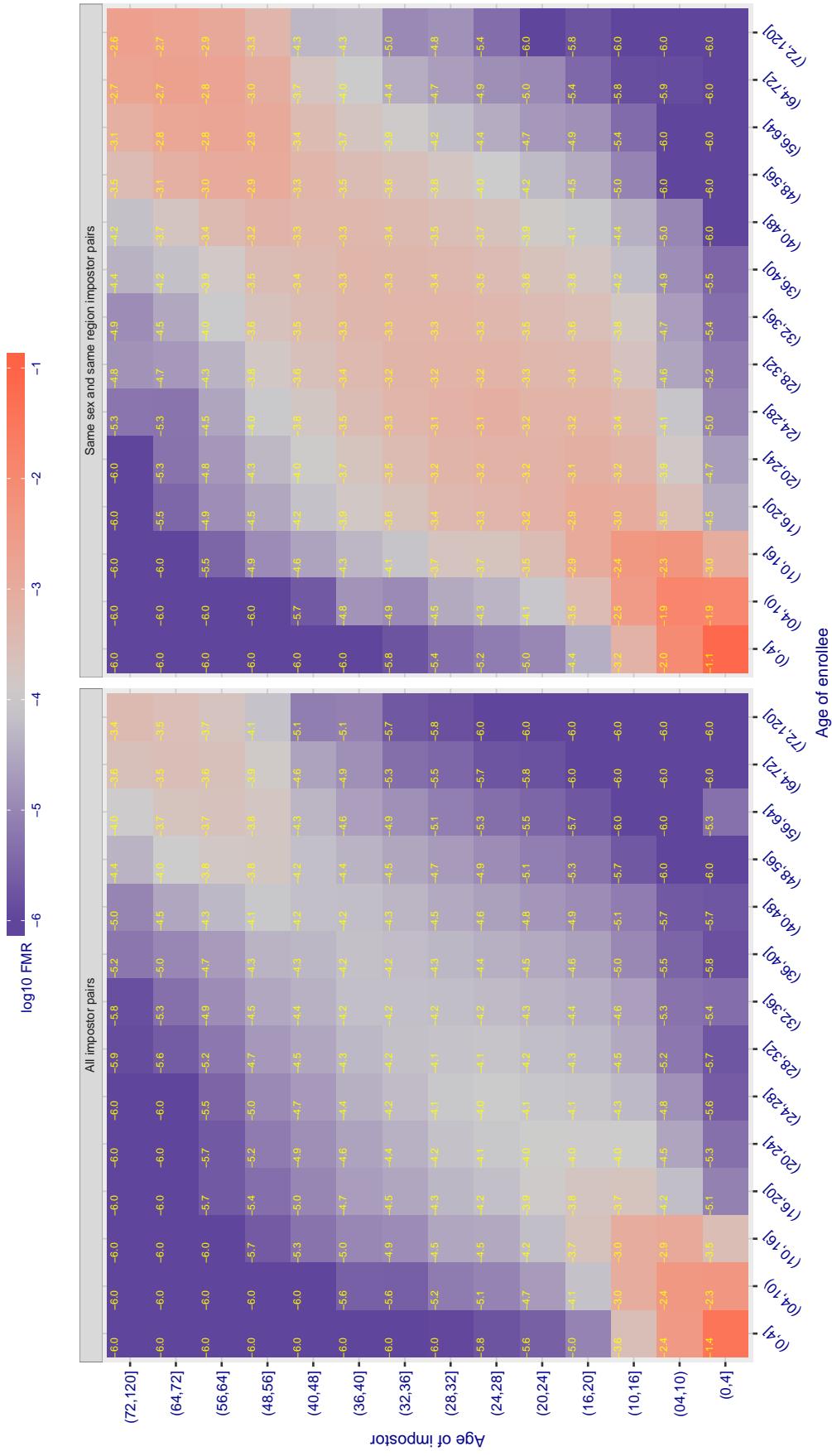
Cross age FMR at threshold T = 0.713 for algorithm alchera\_001, giving  $FMR(T) = 0.0001$  globally.

Figure 316: For algorithm alchera-001 operating on visa images, the heatmap shows false match observed over impostor comparisons of faces from different individuals who have the given age pair. False matches are counted against a recognition threshold fixed globally to give  $FMR = 0.001$  over all on the order of  $10^{10}$  impostor comparisons. The text in each box gives the same quantity as that coded by the color. Light colors present a security vulnerability to, for example, a passport gate.

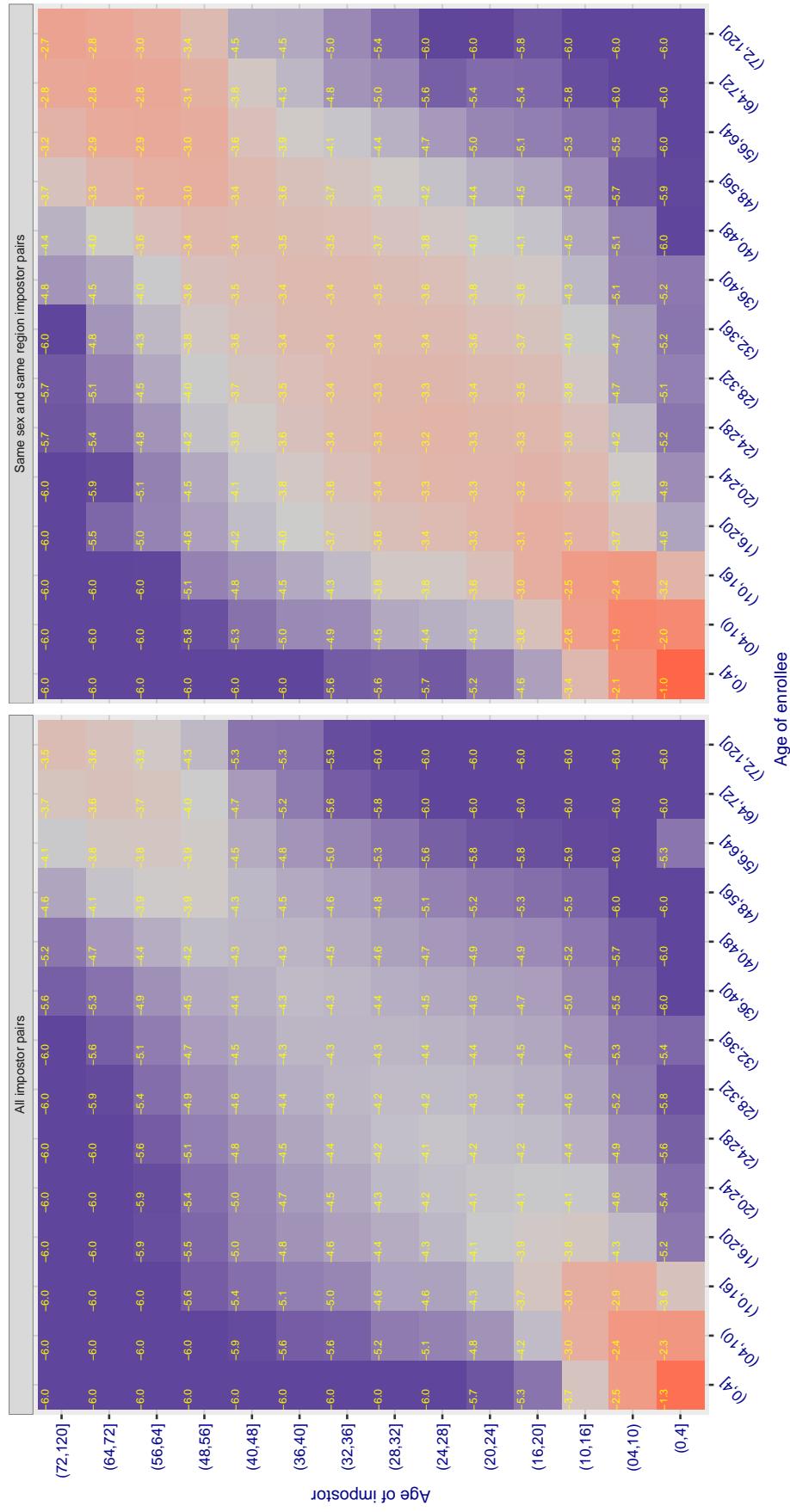
**Cross age FMR at threshold  $T = 0.433$  for algorithm allgovision\_000, giving  $FMR(T) = 0.0001$  globally.**

Figure 317: For algorithm allgovision-000 operating on visa images, the heatmap shows false match observed over imposter comparisons of faces from different individuals who have the given age pair. False matches are counted against a recognition threshold fixed globally to give  $FMR = 0.001$  over all on the order of  $10^{10}$  imposter comparisons. The text in each box gives the same quantity as that coded by the color. Light colors present a security vulnerability to, for example, a passport gate.

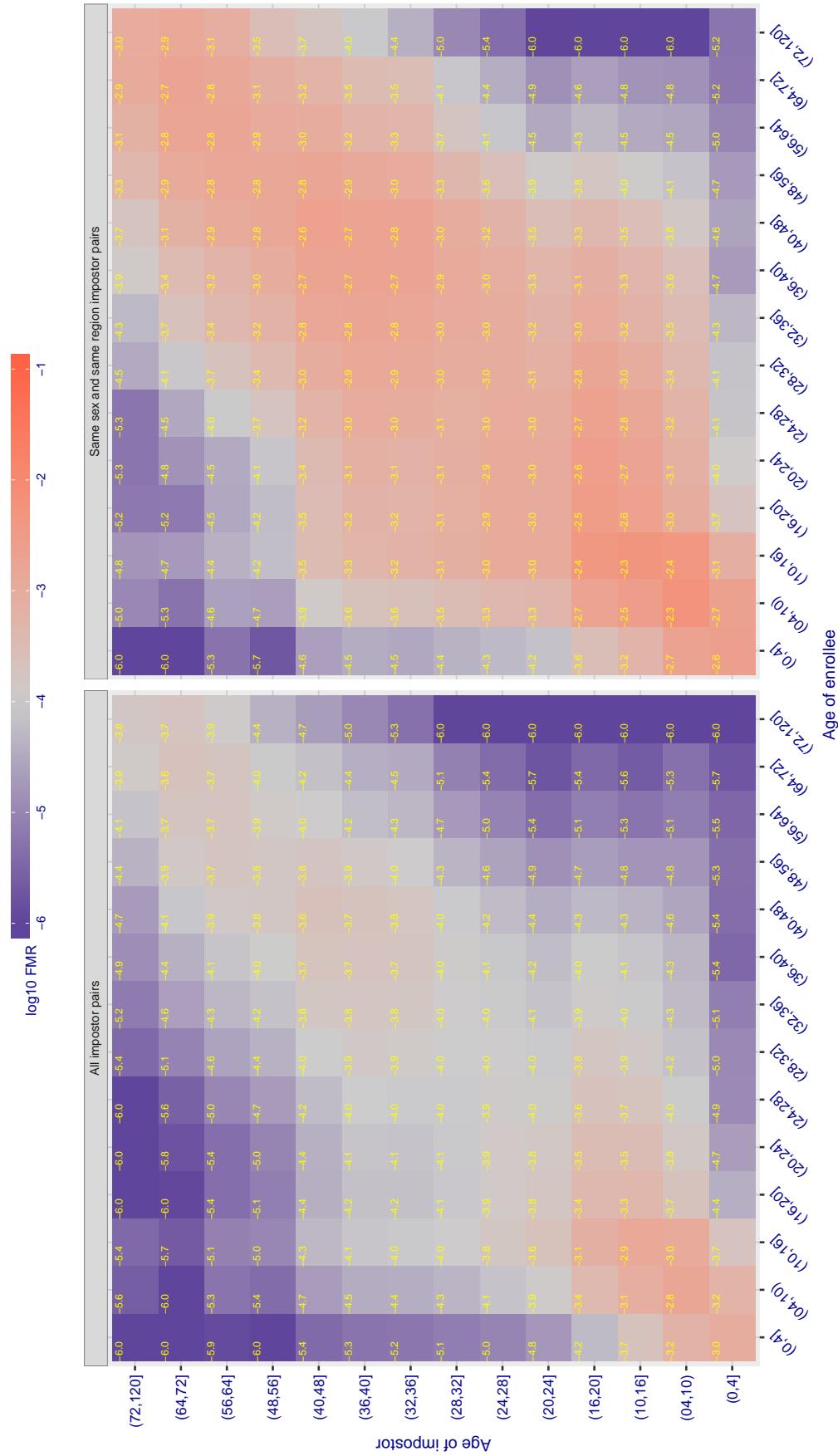
**Cross age FMR at threshold  $T = 3.640$  for algorithm amplifiedgroup\_001, giving  $FMR(T) = 0.0001$  globally.**

Figure 318: For algorithm amplifiedgroup-001 operating on visa images, the heatmap shows false match observed over impostor comparisons of faces from different individuals who have the given age pair. False matches are counted against a recognition threshold fixed globally to give  $FMR = 0.001$  over all on the order of  $10^{10}$  impostor comparisons. The text in each box gives the same quantity as that coded by the color. Light colors present a security vulnerability to, for example, a passport gate.

Cross age FMR at threshold T = 0.404 for algorithm anke\_002, giving FMR(T) = 0.0001 globally.

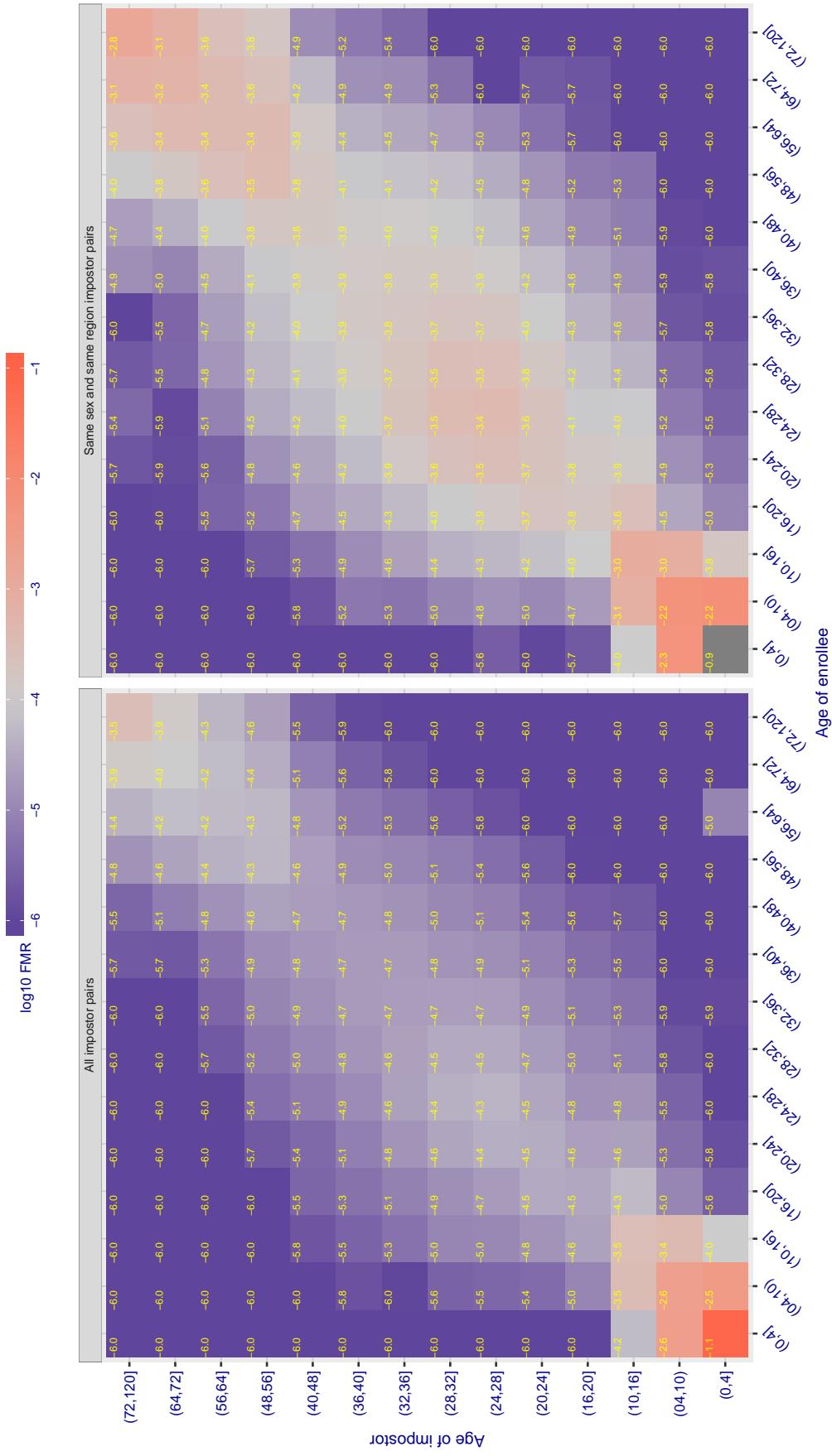


Figure 319: For algorithm anke-002 operating on visa images, the heatmap shows false match observed over impostor comparisons of faces from different individuals who have the given age pair. False matches are counted against a recognition threshold fixed globally to give  $FMR = 0.001$  over all on the order of  $10^{10}$  impostor comparisons. The text in each box gives the same quantity as that coded by the color. Light colors present a security vulnerability to, for example, a passport gate.

Cross age FMR at threshold T = 0.397 for algorithm anke\_003, giving FMR(T) = 0.0001 globally.

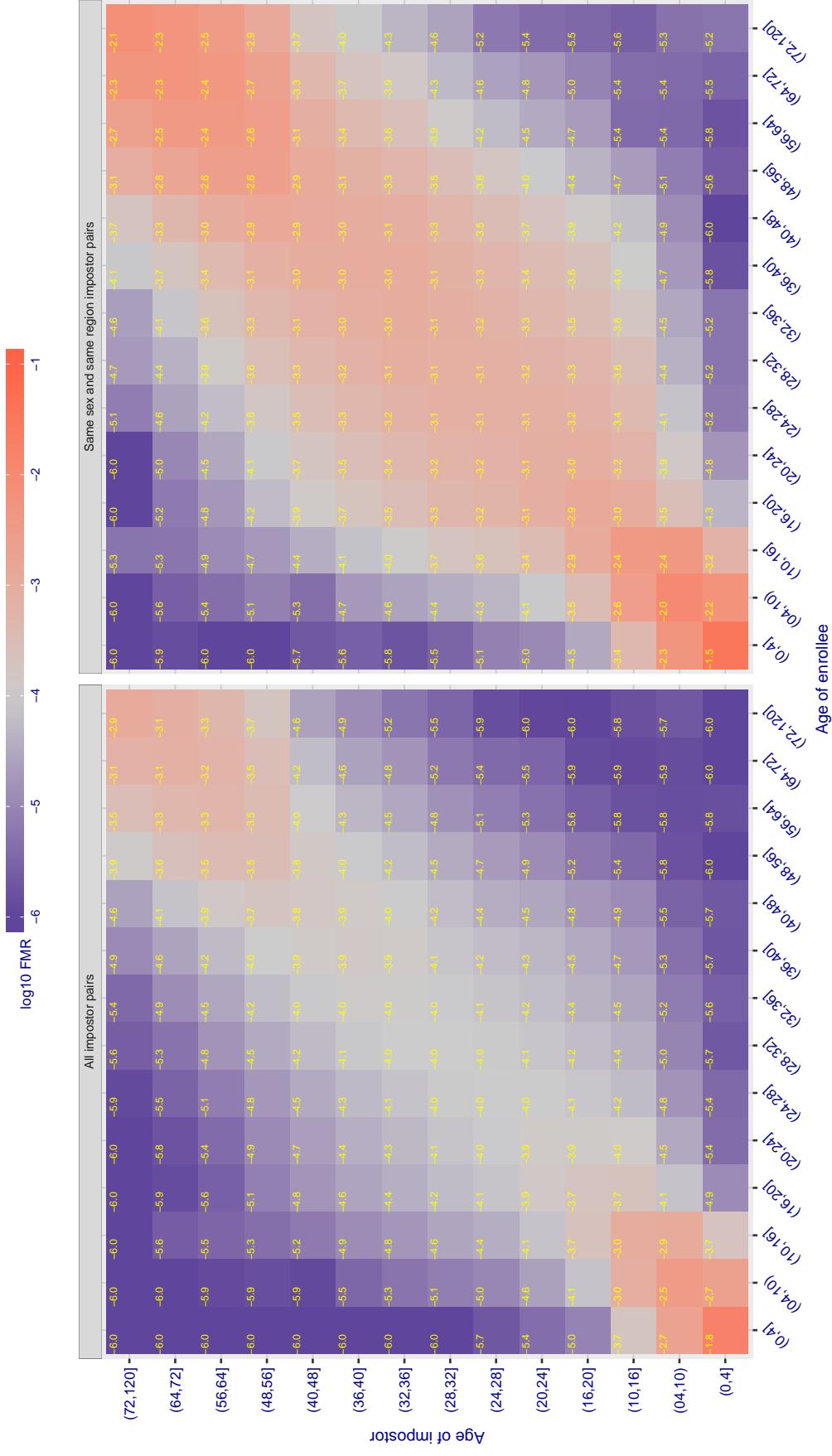


Figure 320: For algorithm anke\_003 operating on visa images, the heatmap shows false match observed over impostor comparisons of faces from different individuals who have the given age pair. False matches are counted against a recognition threshold fixed globally to give  $FMR = 0.001$  over all on the order of  $10^{10}$  impostor comparisons. The text in each box gives the same quantity as that coded by the color. Light colors present a security vulnerability to, for example, a passport gate.

Cross age FMR at threshold T = 1.526 for algorithm anyvision\_002, giving FMR(T) = 0.0001 globally.

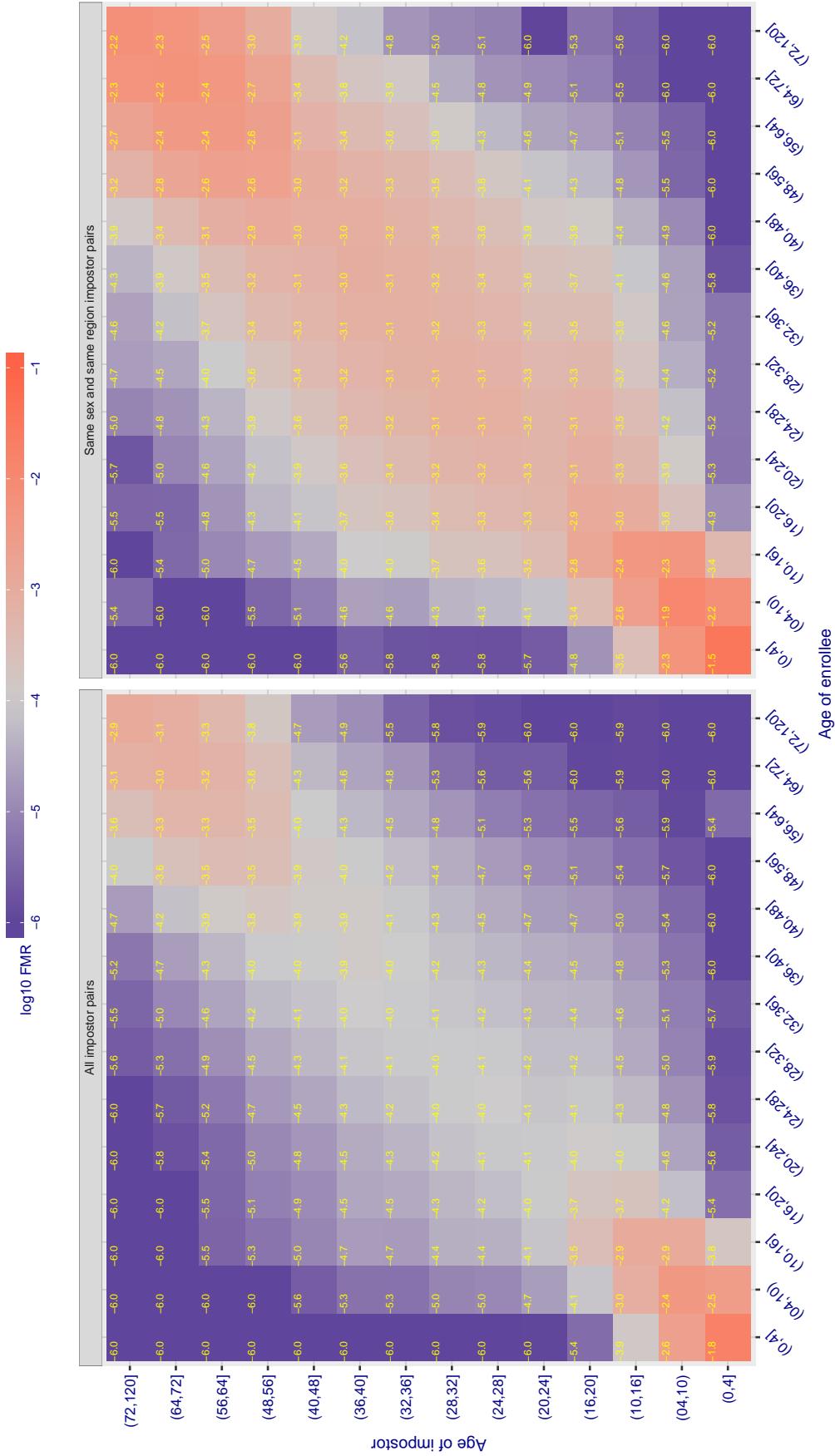
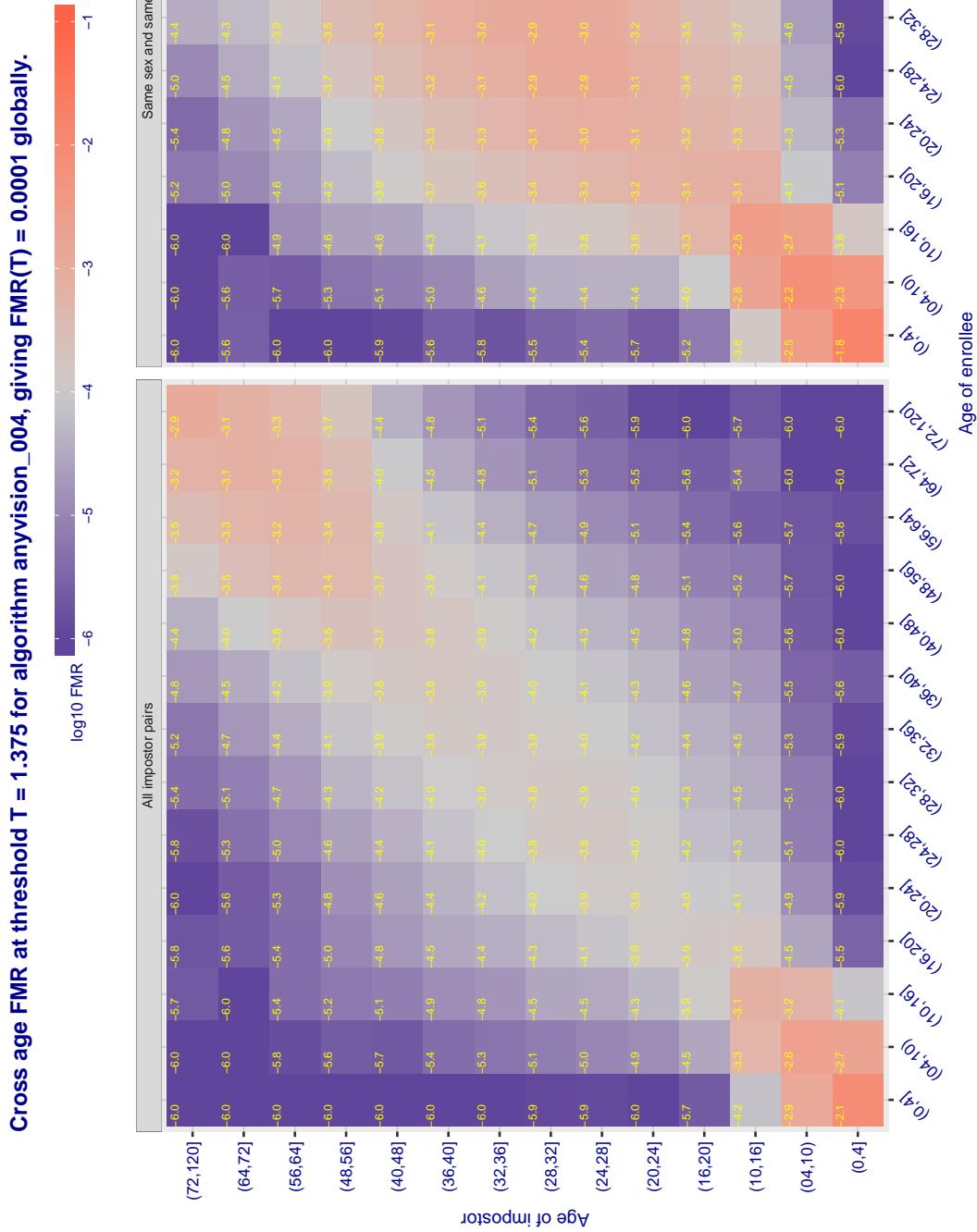
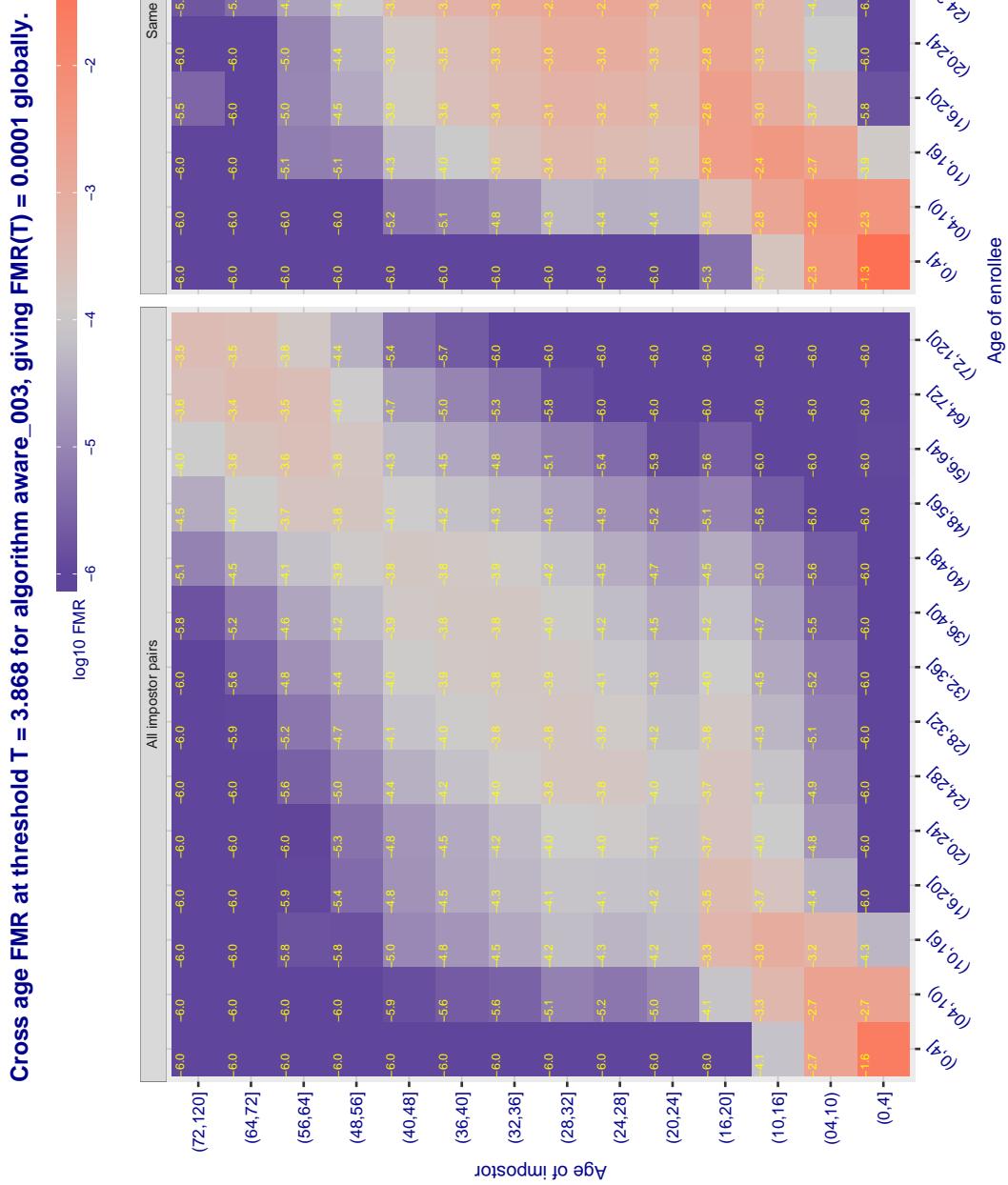


Figure 321: For algorithm anyvision-002 operating on visa images, the heatmap shows false match observed over impostor comparisons of faces from different individuals who have the given age pair. False matches are counted against a recognition threshold fixed globally to give  $FMR = 0.001$  over all on the order of  $10^{10}$  impostor comparisons. The text in each box gives the same quantity as that coded by the color. Light colors present a security vulnerability to, for example, a passport gate.



**Figure 322:** For algorithm anyvision-004 operating on visa images, the heatmap shows false match observed over impostor comparisons of faces from different individuals who have the given age pair. False matches are counted against a recognition threshold fixed globally to give  $FMR = 0.001$  over all on the order of  $10^{10}$  impostor comparisons. The text in each box gives the same quantity as that coded by the color. Light colors present a security vulnerability to, for example, a passport gate.



**Figure 323:** For algorithm aware-003 operating on visa images, the heatmap shows false match observed over impostor comparisons of faces from different individuals who have the given age pair. False matches are counted against a recognition threshold fixed globally to give  $FMR = 0.001$  over all on the order of  $10^{10}$  impostor comparisons. The text in each box gives the same quantity as that coded by the color. Light colors present a security vulnerability to, for example, a passport gate.

Cross age FMR at threshold T = 5.084 for algorithm aware\_004, giving FMR(T) = 0.0001 globally.

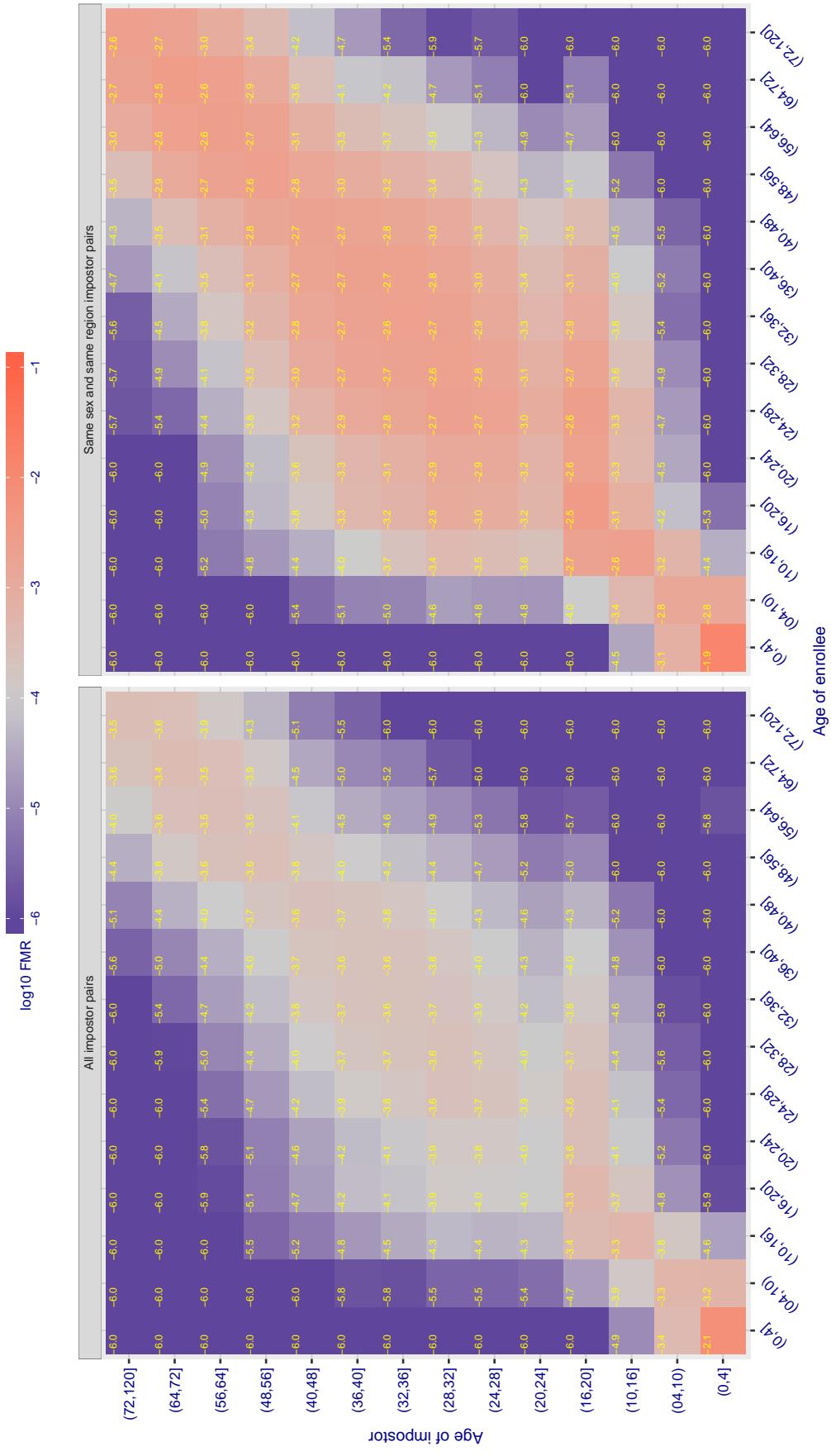
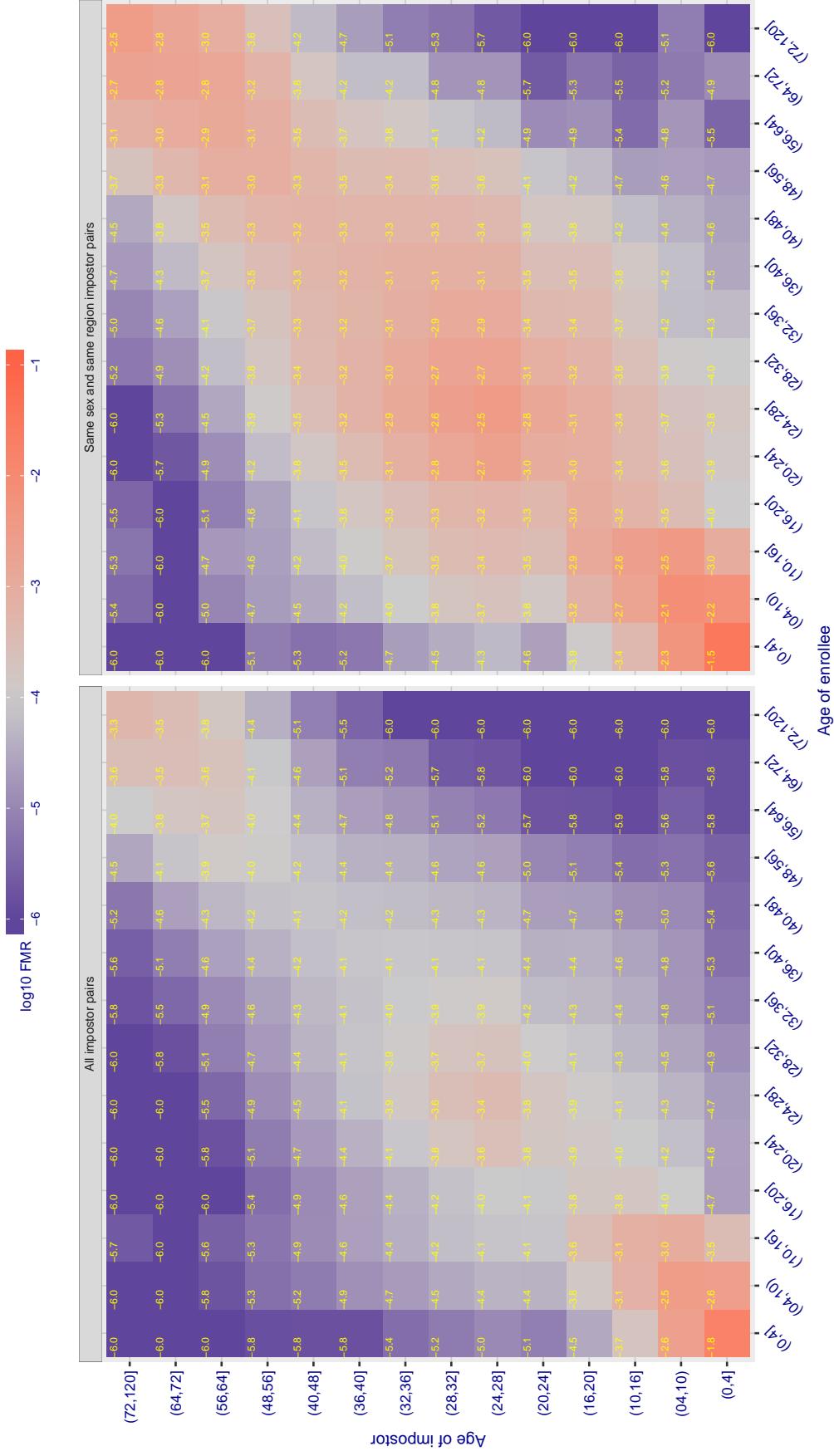


Figure 324: For algorithm aware-004 operating on visa images, the heatmap shows false match observed over impostor comparisons of faces from different individuals who have the given age pair. False matches are counted against a recognition threshold fixed globally to give  $\text{FMR} = 0.001$  over all on the order of  $10^{10}$  impostor comparisons. The text in each box gives the same quantity as that coded by the color. Light colors present a security vulnerability to, for example, a passport gate.

Cross age FMR at threshold T = 0.919 for algorithm ayonix\_000, giving  $\text{FMR}(\text{T}) = 0.0001$  globally.Figure 325: For algorithm ayonix-000 operating on visa images, the heatmap shows false match observed over impostor comparisons of faces from different individuals who have the given age pair. False matches are counted against a recognition threshold fixed globally to give  $\text{FMR} = 0.00$  over all on the order of  $10^{10}$  impostor comparisons. The text in each box gives the same quantity as that coded by the color. Light colors present a security vulnerability to, for example, a passport gate.

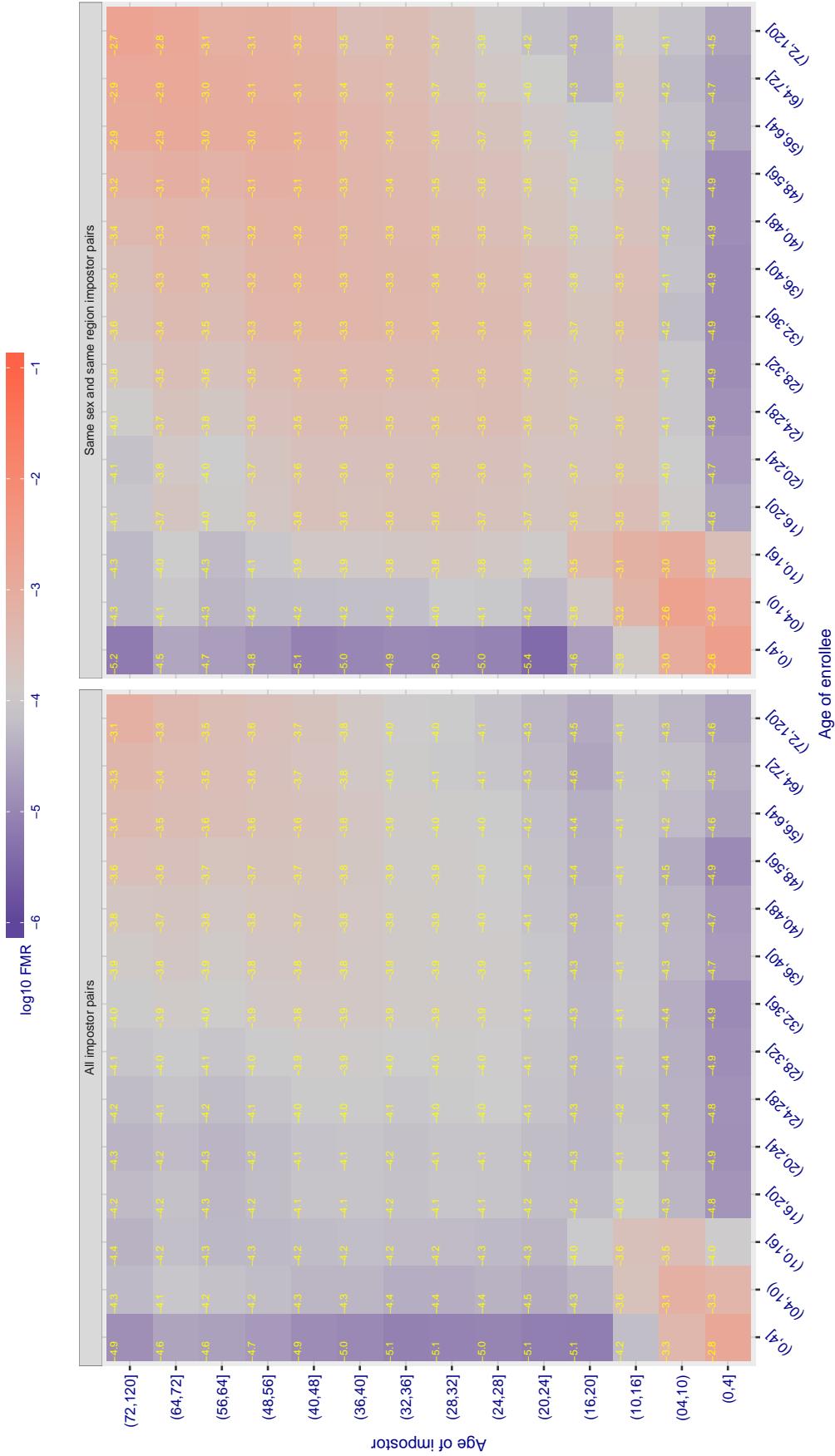
Cross age FMR at threshold T = 0.731 for algorithm bm\_001, giving  $\text{FMR}(T) = 0.00001$  globally.

Figure 326: For algorithm bm\_001 operating on visa images, the heatmap shows false match observed over impostor comparisons of faces from different individuals who have the given age pair. False matches are counted against a recognition threshold fixed globally to give  $\text{FMR} = 0.001$  over all on the order of  $10^{10}$  impostor comparisons. The text in each box gives the same quantity as that coded by the color. Light colors present a security vulnerability to, for example, a passport gate.

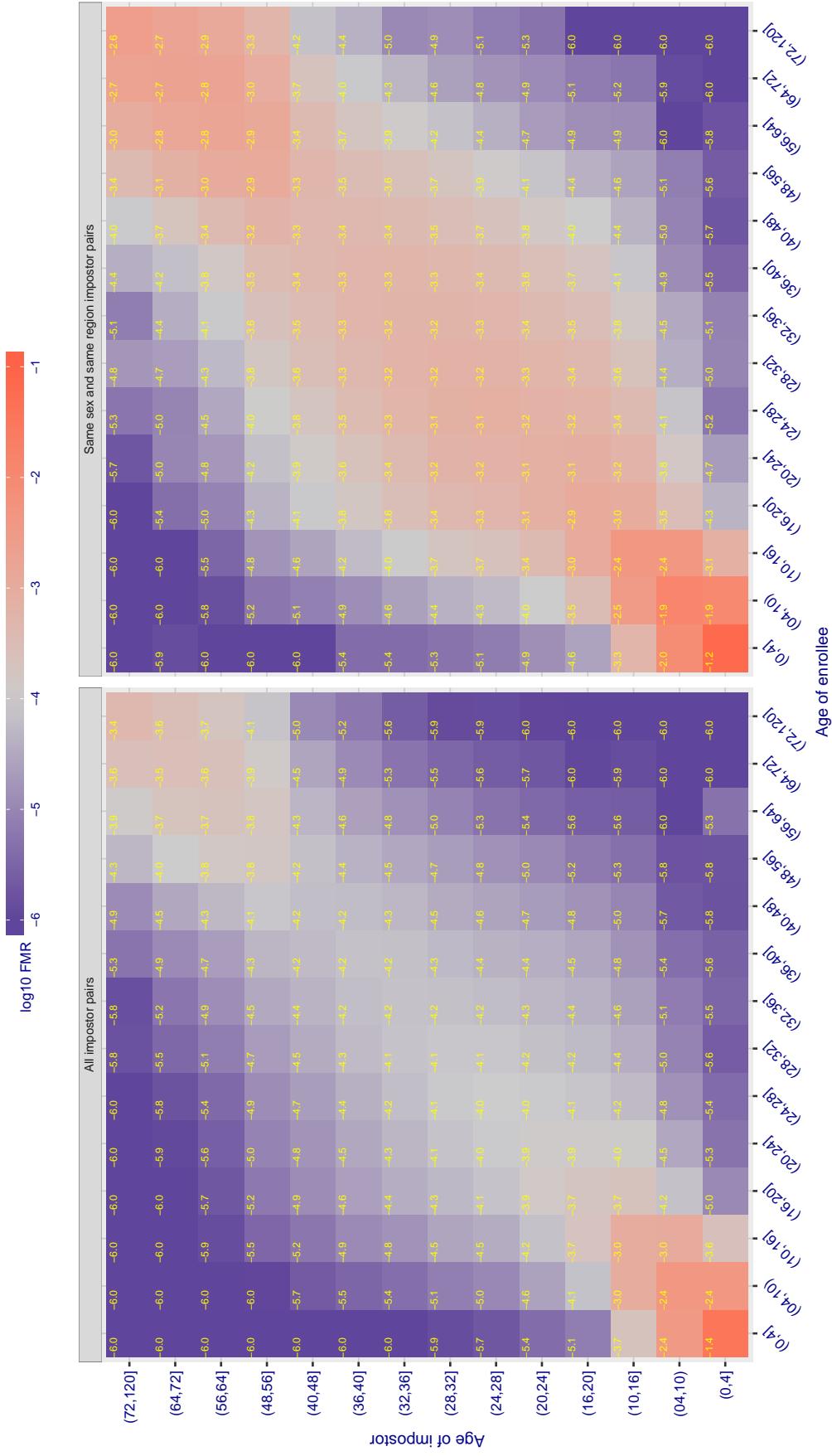
Cross age FMR at threshold T = 0.388 for algorithm camvi\_002, giving  $FMR(T) = 0.0001$  globally.

Figure 327: For algorithm camvi-002 operating on visa images, the heatmap shows false match observed over impostor comparisons of faces from different individuals who have the given age pair. False matches are counted against a recognition threshold fixed globally to give  $FMR = 0.001$  over all on the order of  $10^{10}$  impostor comparisons. The text in each box gives the same quantity as that coded by the color. Light colors present a security vulnerability to, for example, a passport gate.

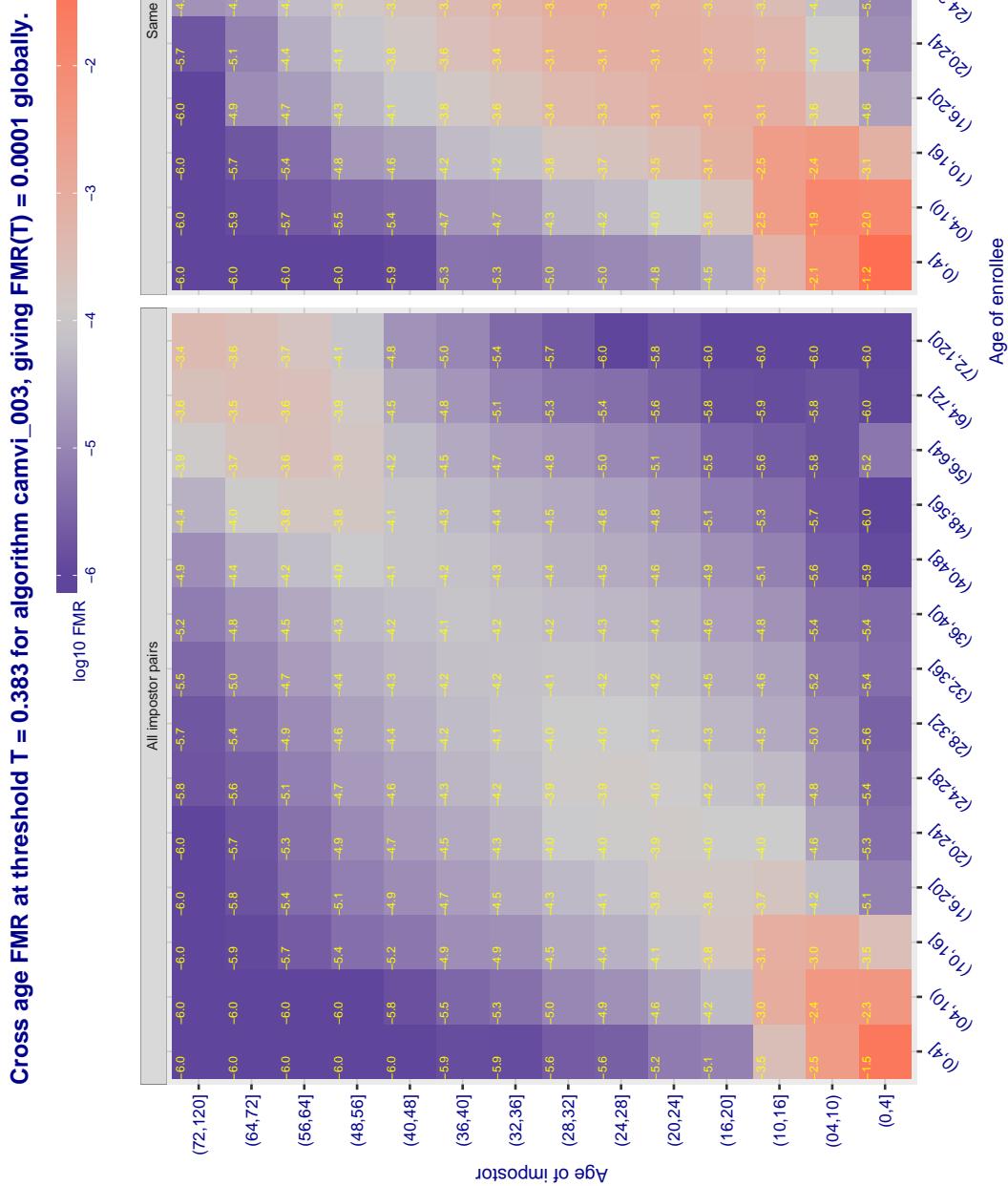


Figure 328: For algorithm camvi-003 operating on visa images, the heatmap shows false match observed over impostor comparisons of faces from different individuals who have the given age pair. False matches are counted against a recognition threshold fixed globally to give  $FMR = 0.001$  over all on the order of  $10^{10}$  impostor comparisons. The text in each box gives the same quantity as that coded by the color. Light colors present a security vulnerability to, for example, a passport gate.

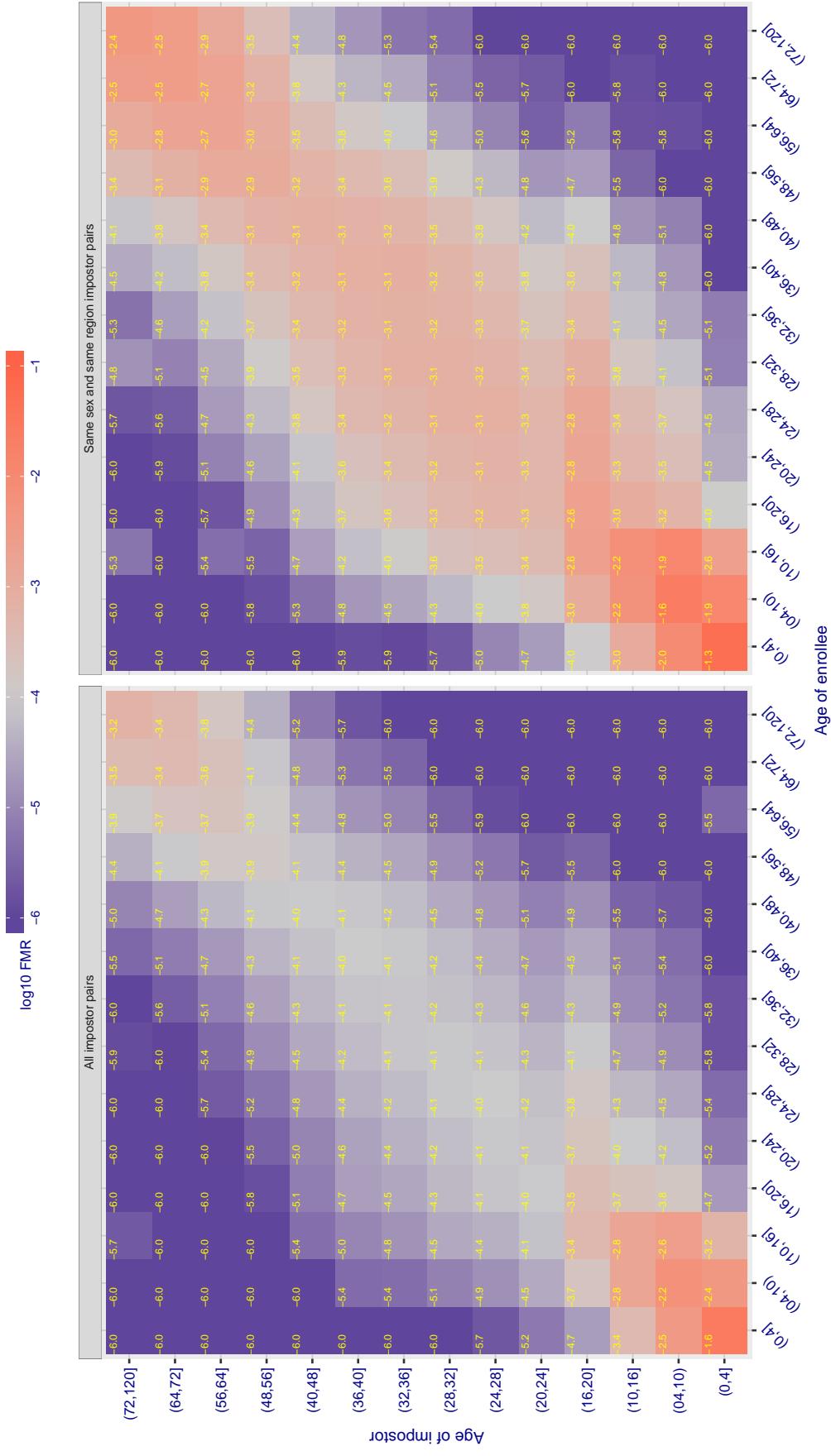
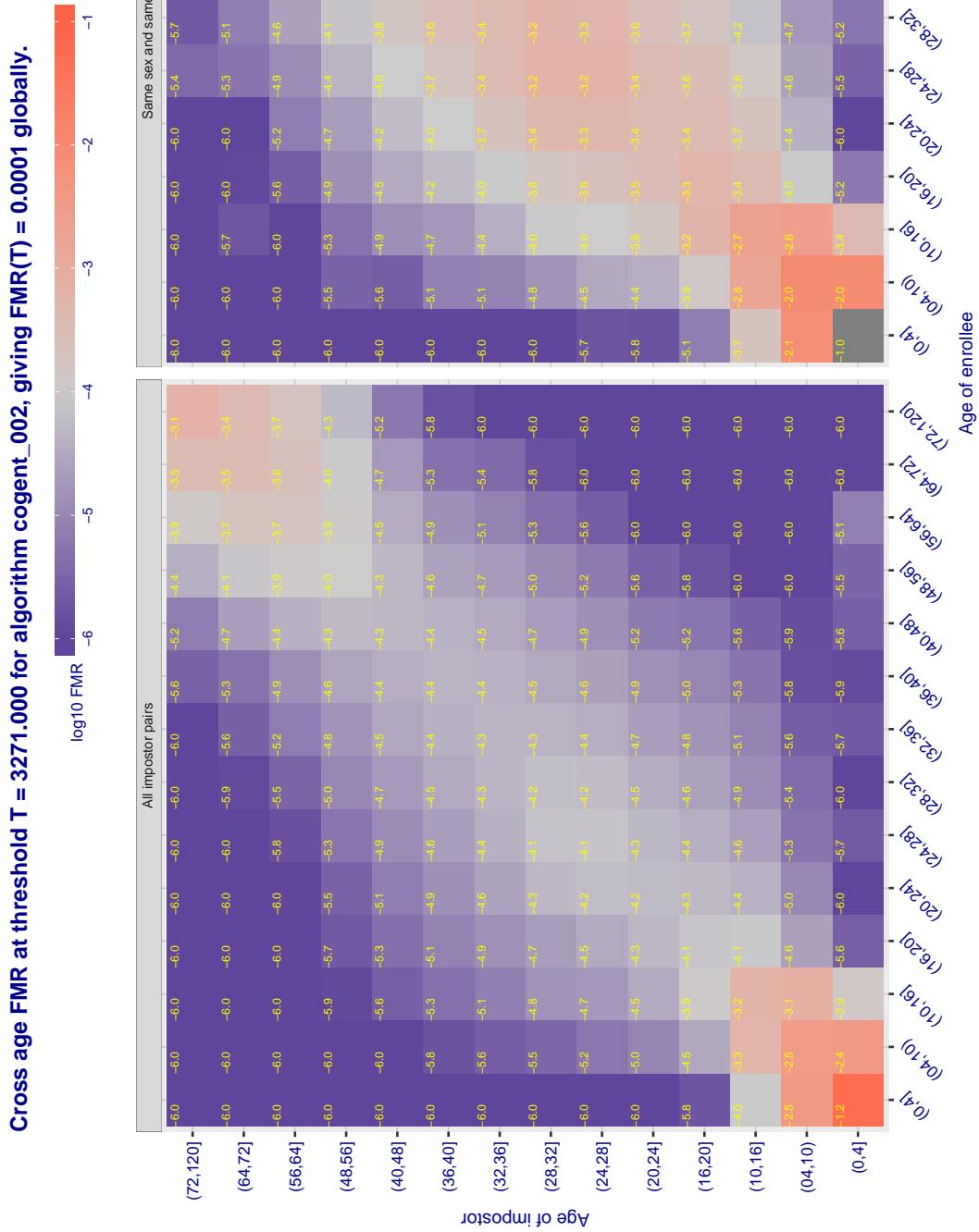
Cross age FMR at threshold T = 0.436 for algorithm ceiec\_001, giving  $\text{FMR}(\text{T}) = 0.0001$  globally.

Figure 329: For algorithm ceiec\_001 operating on visa images, the heatmap shows false match observed over impostor comparisons of faces from different individuals who have the given age pair. False matches are counted against a recognition threshold fixed globally to give  $\text{FMR} = 0.001$  over all on the order of  $10^{10}$  impostor comparisons. The text in each box gives the same quantity as that coded by the color. Light colors present a security vulnerability to, for example, a passport gate.



**Figure 330:** For algorithm cogent-002 operating on visa images, the heatmap shows false match observed over impostor comparisons of faces from different individuals who have the given age pair. False matches are counted against a recognition threshold fixed globally to give  $FMR = 0.001$  over all on the order of  $10^{10}$  impostor comparisons. The text in each box gives the same quantity as that coded by the color. Light colors present a security vulnerability to, for example, a passport gate.

Cross age FMR at threshold T = 2972.000 for algorithm cogent\_003, giving FMR(T) = 0.00001 globally.

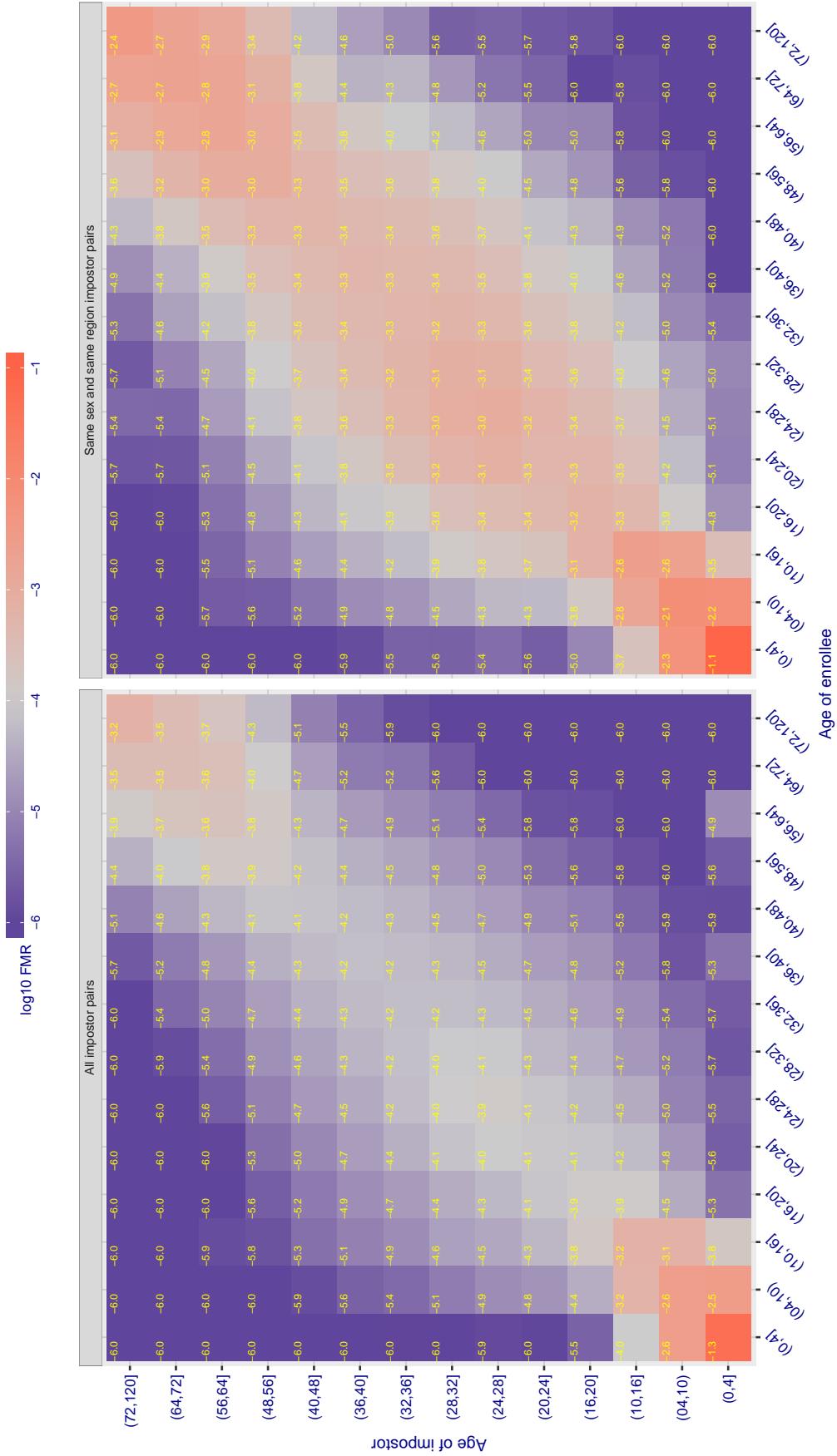


Figure 331: For algorithm cogent-003 operating on visa images, the heatmap shows false match observed over impostor comparisons of faces from different individuals who have the given age pair. False matches are counted against a recognition threshold fixed globally to give  $FMR = 0.001$  over all on the order of  $10^{10}$  impostor comparisons. The text in each box gives the same quantity as that coded by the color. Light colors present a security vulnerability to, for example, a passport gate.

Cross age FMR at threshold T = 0.565 for algorithm cognitec\_000, giving FMR(T) = 0.0001 globally.

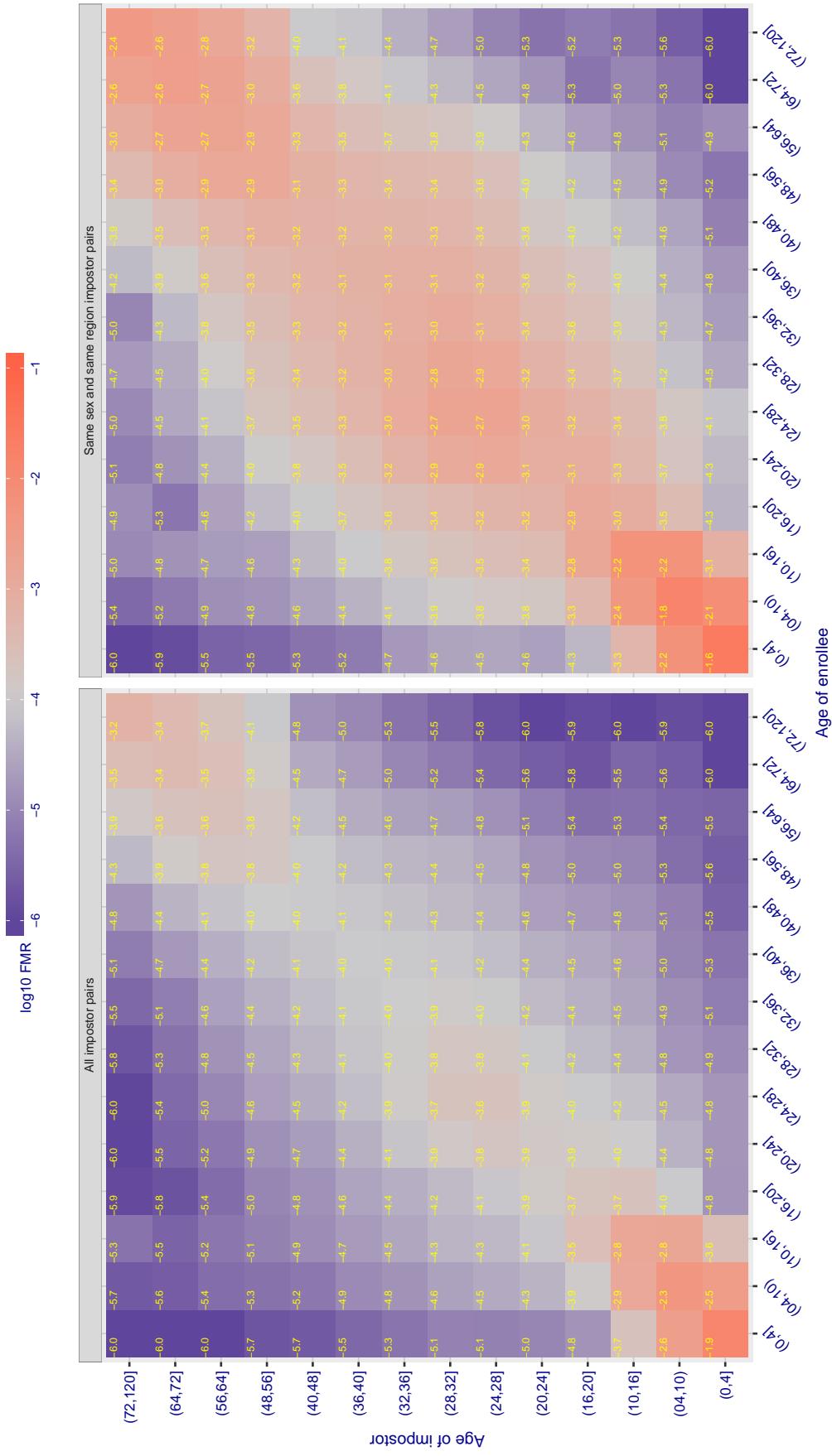


Figure 332: For algorithm cognitec-000 operating on visa images, the heatmap shows false match observed over impostor comparisons of faces from different individuals who have the given age pair. False matches are counted against a recognition threshold fixed globally to give FMR = 0.001 over all on the order of  $10^{10}$  impostor comparisons. The text in each box gives the same quantity as that coded by the color. Light colors present a security vulnerability to, for example, a passport gate.

Cross age FMR at threshold T = 0.565 for algorithm cognitec\_001, giving FMR(T) = 0.0001 globally.

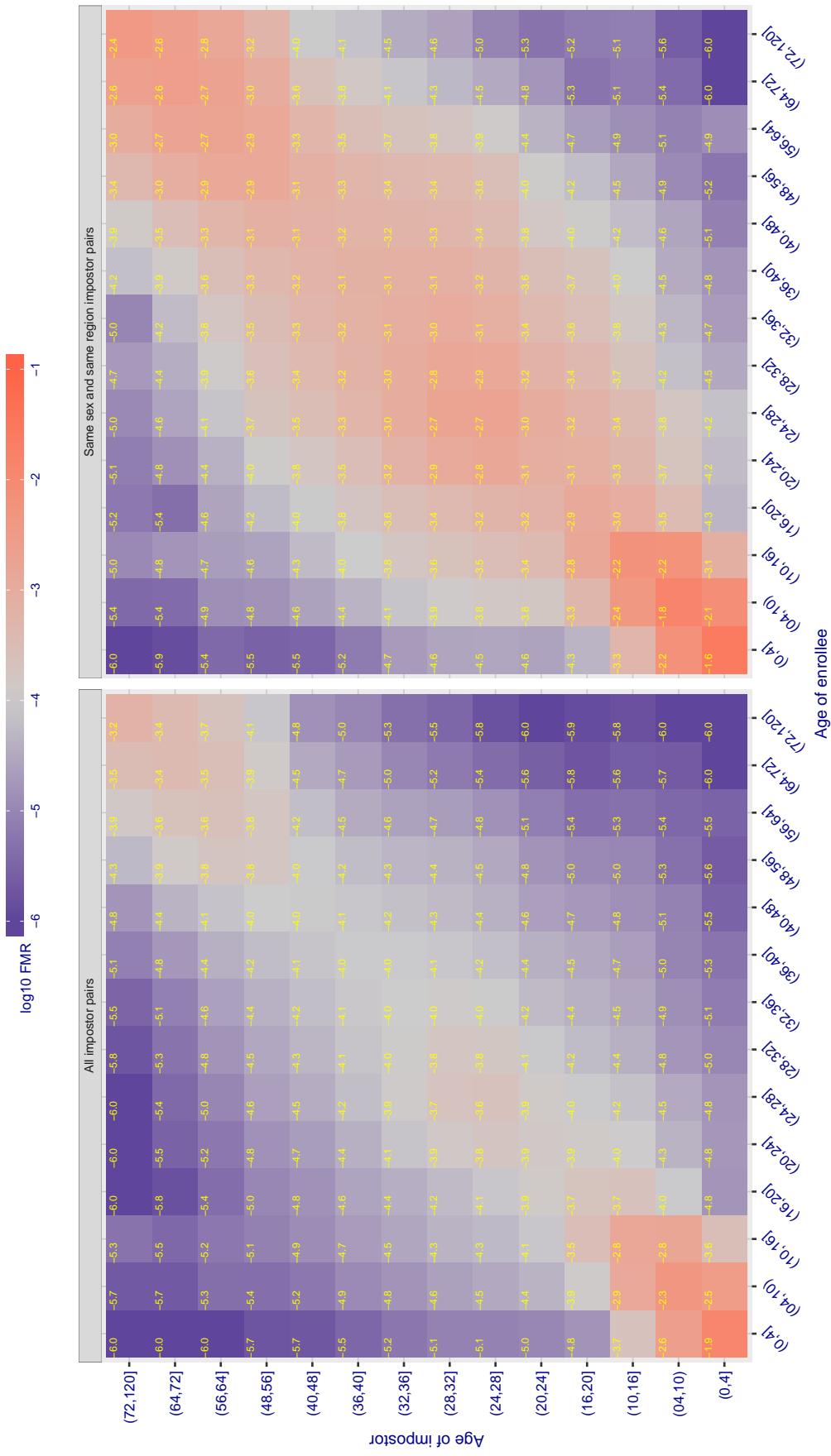


Figure 333: For algorithm cognitec-001 operating on visa images, the heatmap shows false match observed over impostor comparisons of faces from different individuals who have the given age pair. False matches are counted against a recognition threshold fixed globally to give FMR = 0.001 over all on the order of  $10^{10}$  impostor comparisons. The text in each box gives the same quantity as that coded by the color. Light colors present a security vulnerability to, for example, a passport gate.

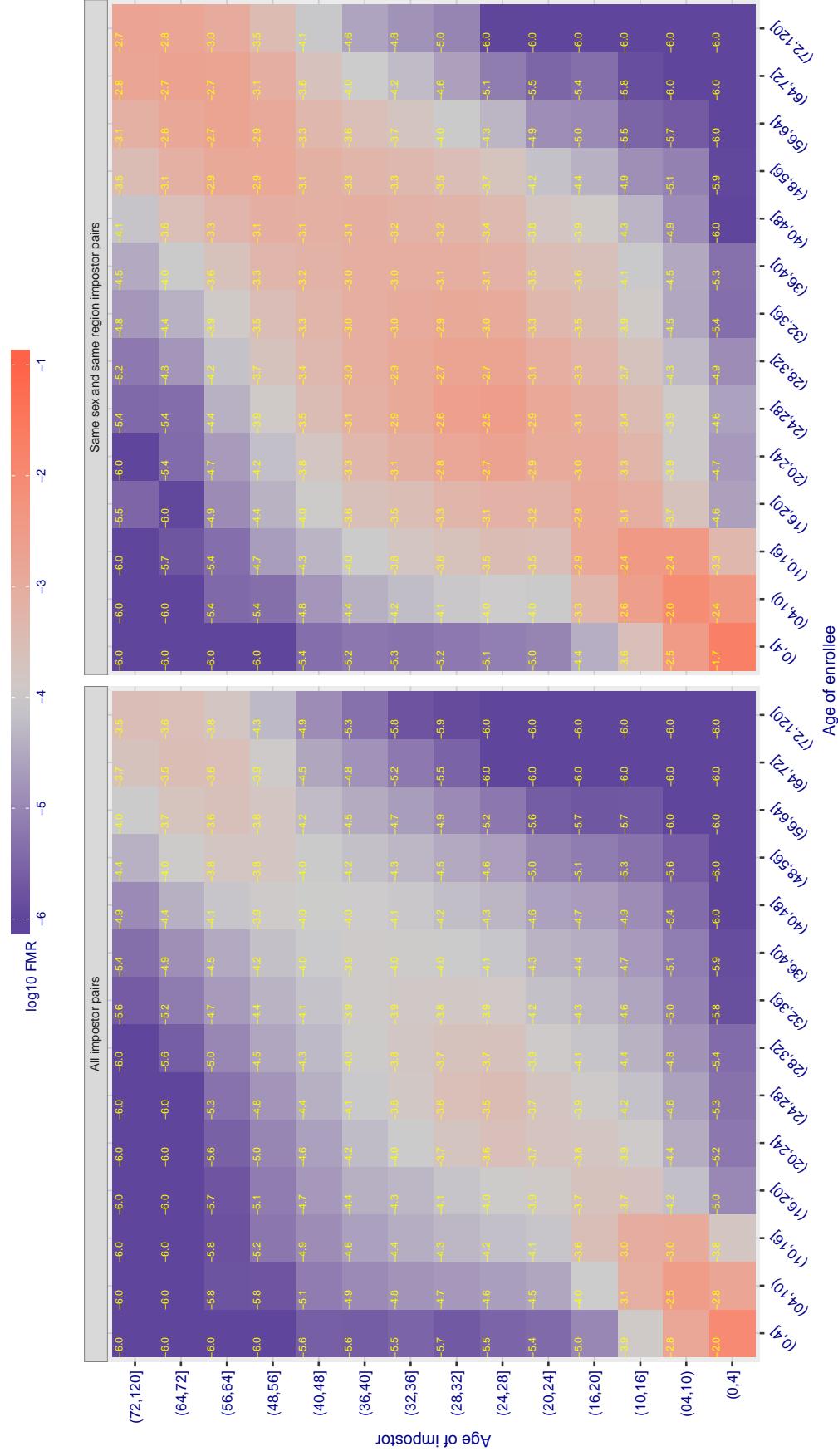
**Cross age FMR at threshold  $T = 0.762$  for algorithm cyberextruder\_001, giving  $FMR(T) = 0.0001$  globally.**

Figure 334: For algorithm cyberextruder-001 operating on visa images, the heatmap shows false match observed over impostor comparisons of faces from different individuals who have the given age pair. False matches are counted against a recognition threshold fixed globally to give  $FMR = 0.001$  over all on the order of  $10^{10}$  impostor comparisons. The text in each box gives the same quantity as that coded by the color. Light colors present a security vulnerability to, for example, a passport gate.

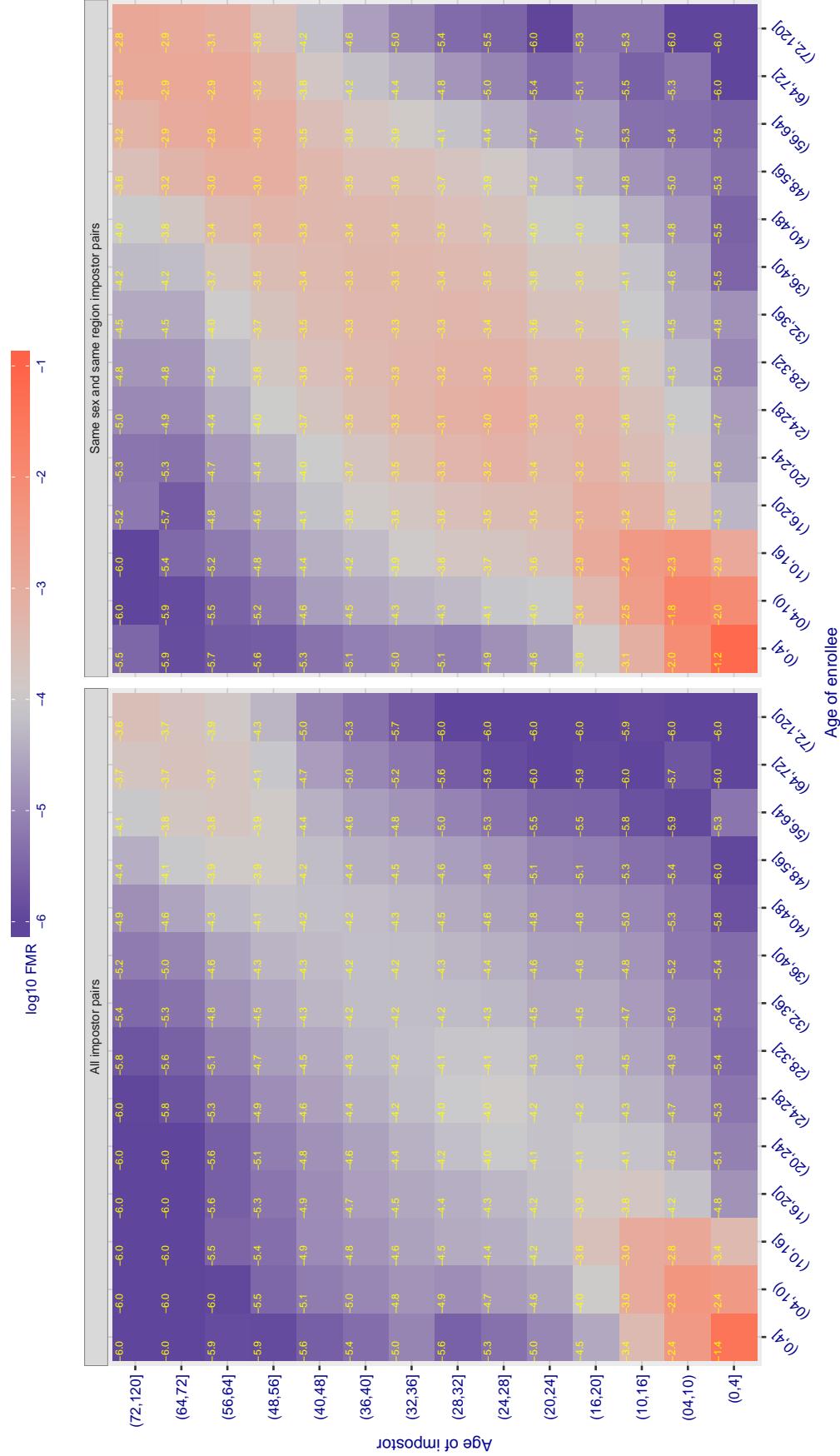
**Cross age FMR at threshold  $T = 0.500$  for algorithm cyberextruder\_002, giving  $FMR(T) = 0.0001$  globally.**

Figure 335: For algorithm cyberextruder-002 operating on visa images, the heatmap shows false match observed over impostor comparisons of faces from different individuals who have the given age pair. False matches are counted against a recognition threshold fixed globally to give  $FMR = 0.001$  over all on the order of  $10^{10}$  impostor comparisons. The text in each box gives the same quantity as that coded by the color. Light colors present a security vulnerability to, for example, a passport gate.

Cross age FMR at threshold T = 1.409 for algorithm cyberlink\_000, giving FMR(T) = 0.0001 globally.

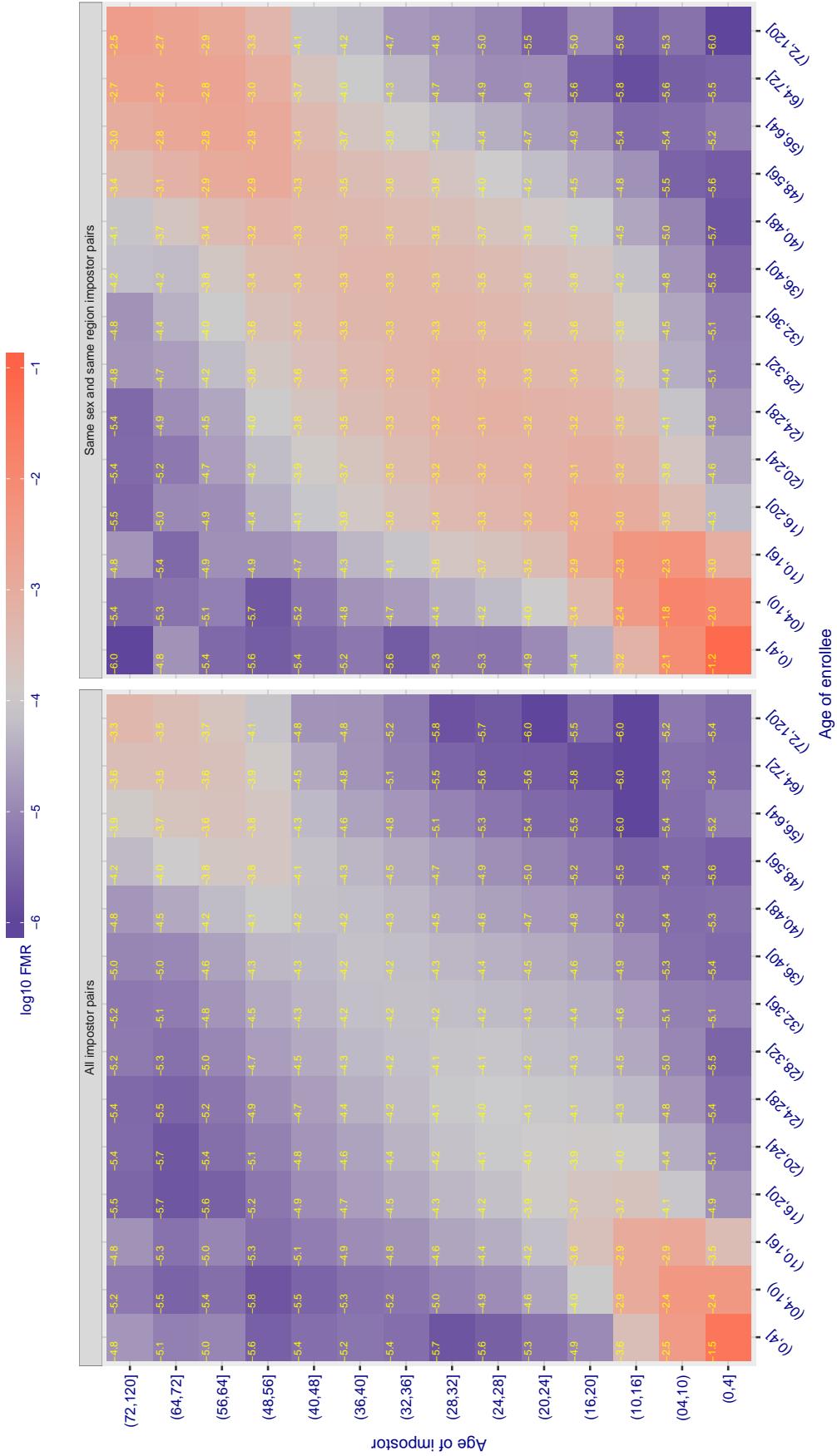


Figure 336: For algorithm cyberlink-000 operating on visa images, the heatmap shows false match observed over impostor comparisons of faces from different individuals who have the given age pair. False matches are counted against a recognition threshold fixed globally to give  $FMR = 0.001$  over all on the order of  $10^{10}$  impostor comparisons. The text in each box gives the same quantity as that coded by the color. Light colors present a security vulnerability to, for example, a passport gate.

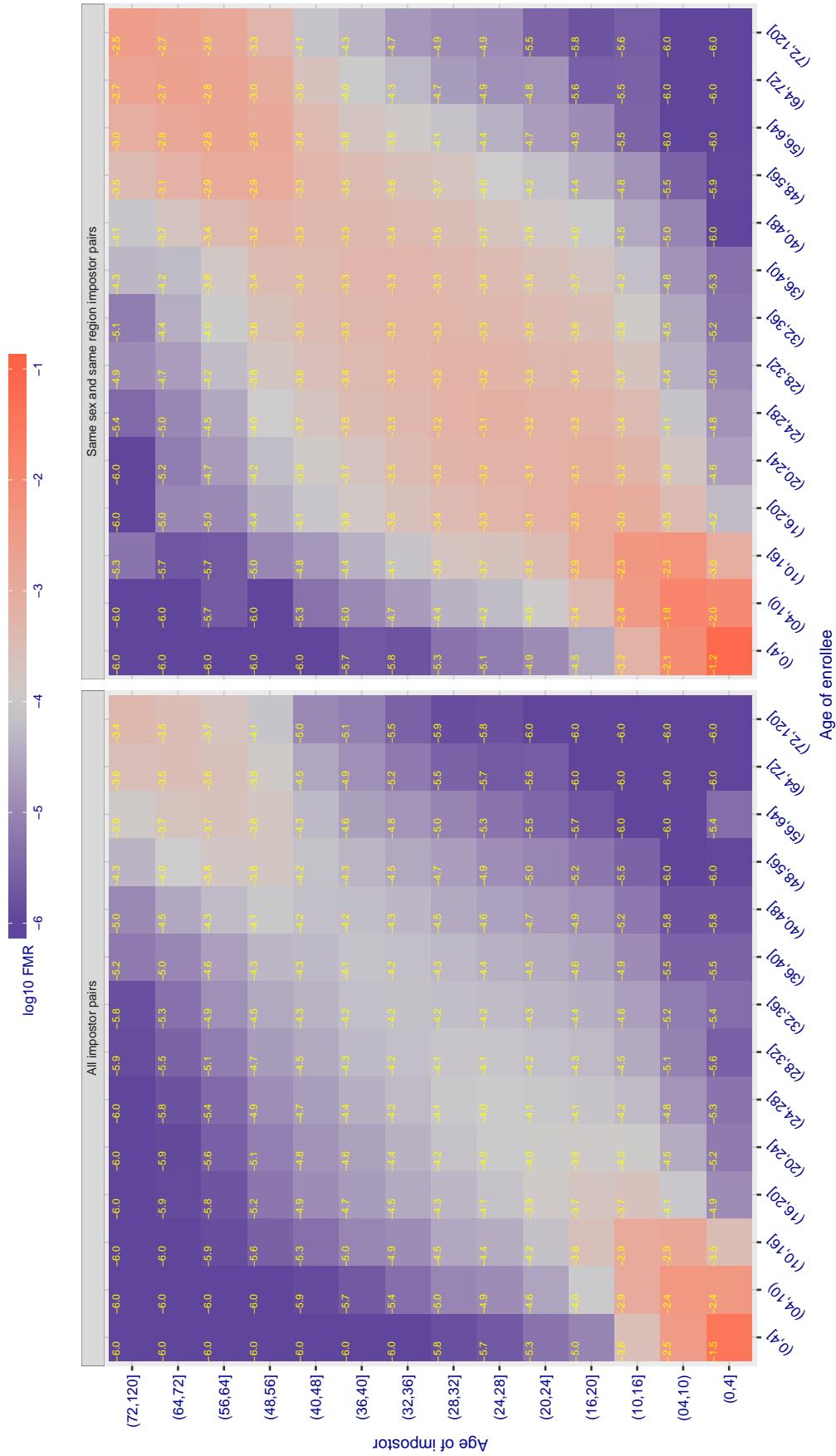
Cross age FMR at threshold T = 1.408 for algorithm cyberlink\_001, giving  $\text{FMR}(\text{T}) = 0.0001$  globally.

Figure 337: For algorithm cyberlink-001 operating on visa images, the heatmap shows false match observed over impostor comparisons of faces from different individuals who have the given age pair. False matches are counted against a recognition threshold fixed globally to give  $\text{FMR} = 0.001$  over all on the order of  $10^{10}$  impostor comparisons. The text in each box gives the same quantity as that coded by the color. Light colors present a security vulnerability to, for example, a passport gate.

Cross age FMR at threshold T = 7630.000 for algorithm dahua\_001, giving FMR(T) = 0.0001 globally.

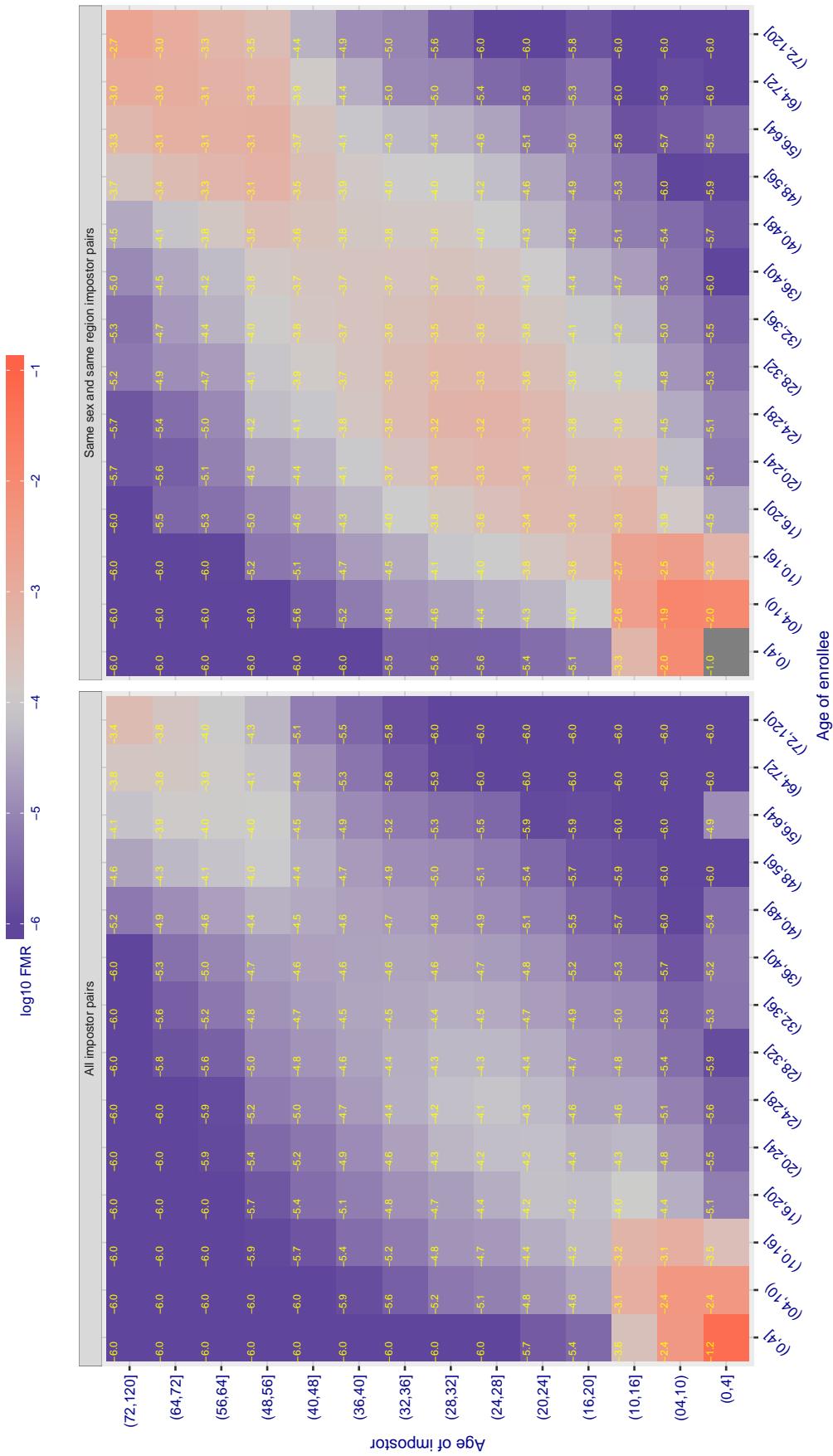
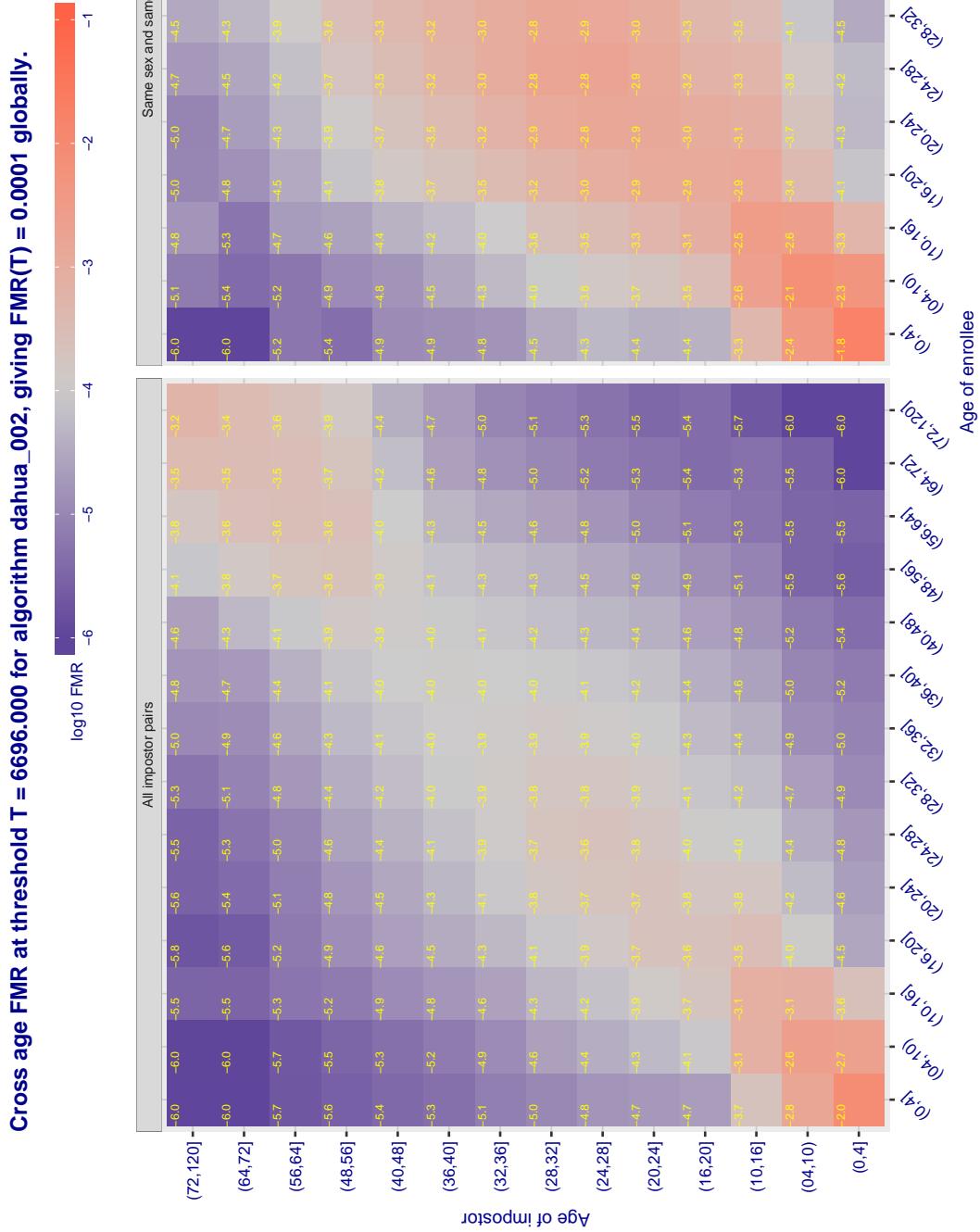


Figure 338: For algorithm dahua-001 operating on visa images, the heatmap shows false match observed over impostor comparisons of faces from different individuals who have the given age pair. False matches are counted against a recognition threshold fixed globally to give  $FMR = 0.001$  over all on the order of  $10^{10}$  impostor comparisons. The text in each box gives the same quantity as that coded by the color. Light colors present a security vulnerability to, for example, a passport gate.



**Figure 339:** For algorithm dahua-002 operating on visa images, the heatmap shows false match observed over impostor comparisons of faces from different individuals who have the given age pair. False matches are counted against a recognition threshold fixed globally to give  $FMR = 0.001$  over all on the order of  $10^{10}$  impostor comparisons. The text in each box gives the same quantity as that coded by the color. Light colors present a security vulnerability to, for example, a passport gate.

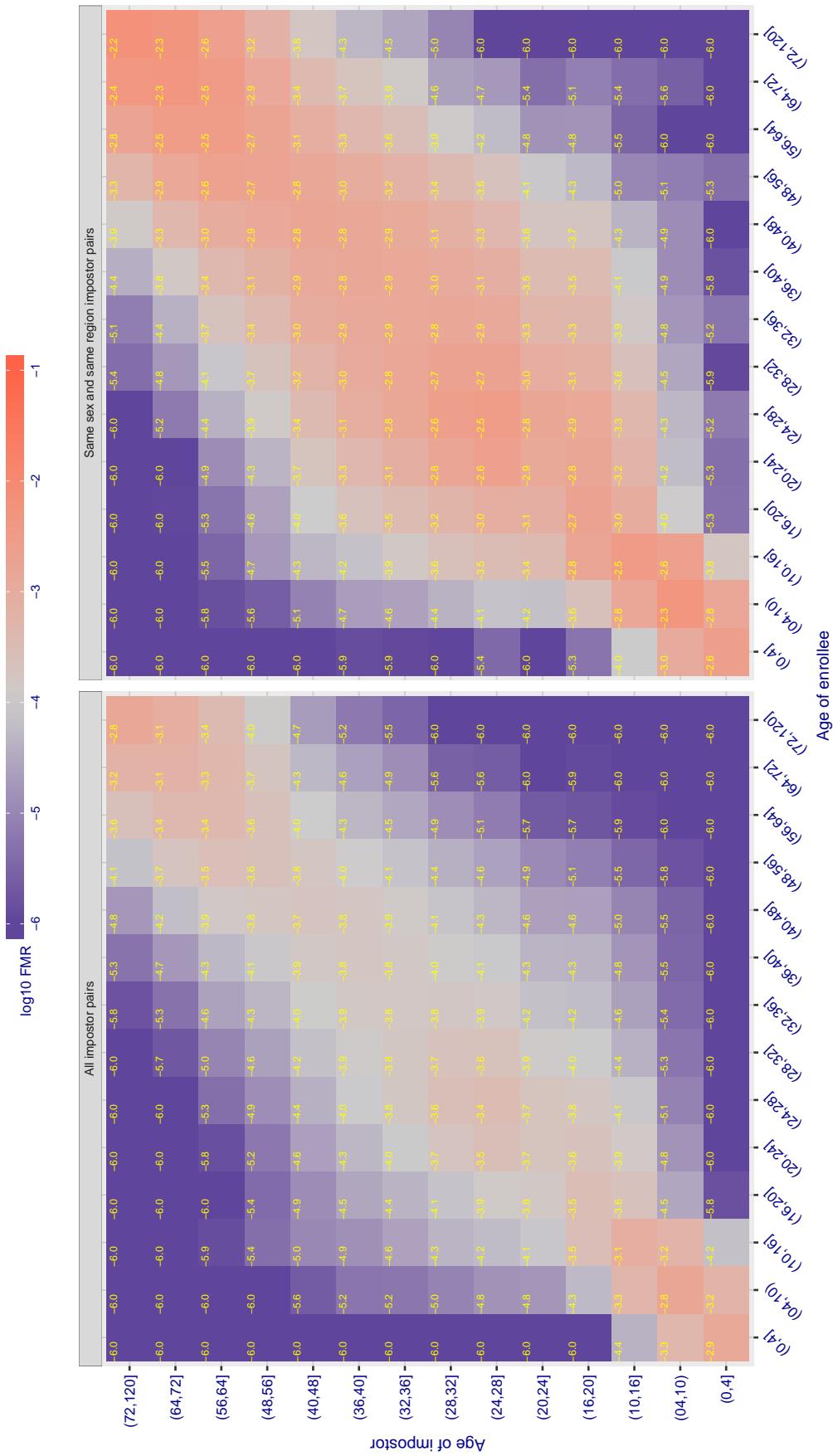
Cross age FMR at threshold T = 79.344 for algorithm dermalog\_005, giving  $FMR(T) = 0.0001$  globally.

Figure 340: For algorithm dermalog-005 operating on visa images, the heatmap shows false match observed over impostor comparisons of faces from different individuals who have the given age pair. False matches are counted against a recognition threshold fixed globally to give  $FMR = 0.001$  over all on the order of  $10^{10}$  impostor comparisons. The text in each box gives the same quantity as that coded by the color. Light colors present a security vulnerability to, for example, a passport gate.

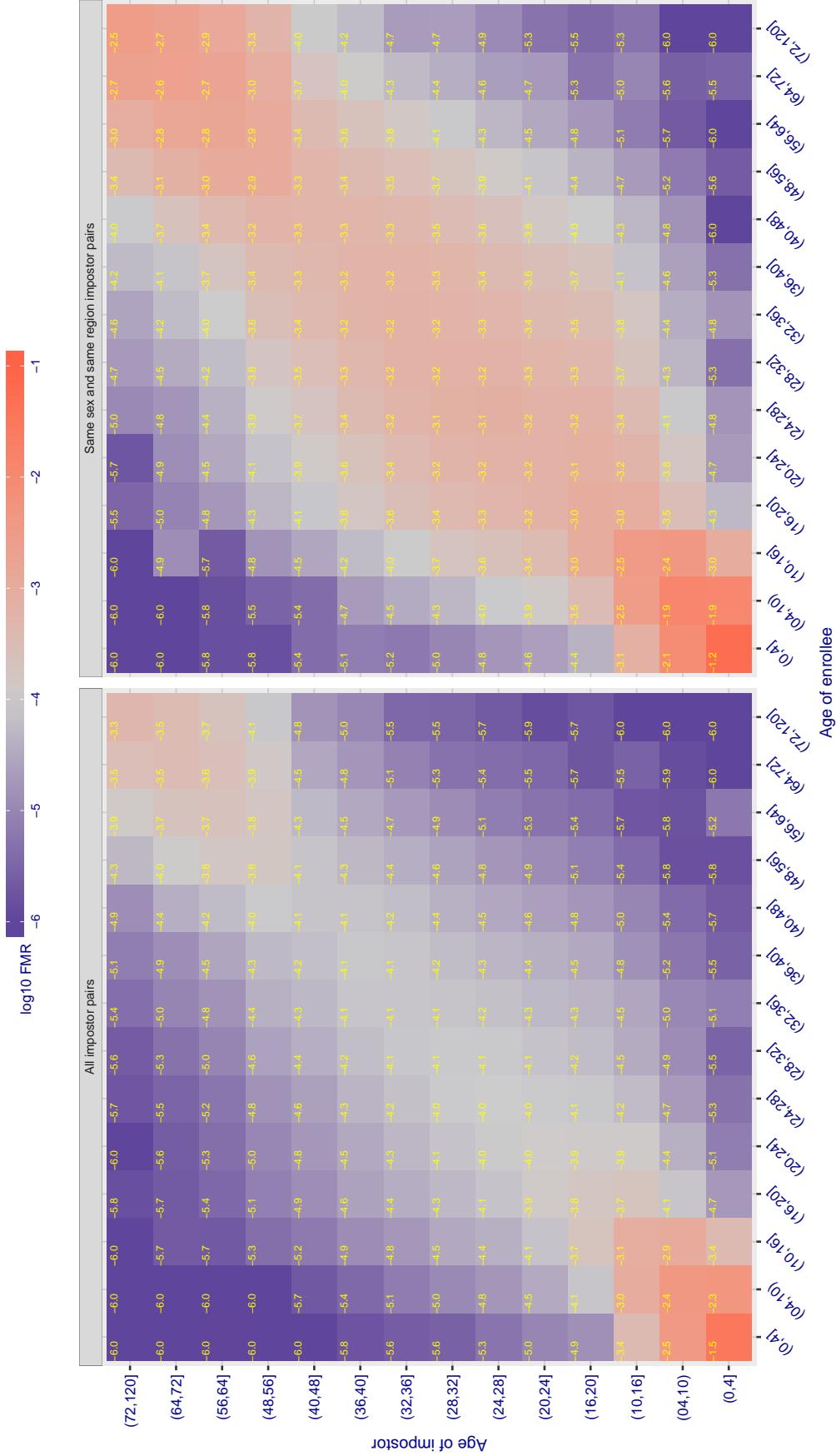
Cross age FMR at threshold T = 79.670 for algorithm dermalog\_006, giving  $FMR(T) = 0.0001$  globally.

Figure 341: For algorithm dermalog-006 operating on visa images, the heatmap shows false match observed over impostor comparisons of faces from different individuals who have the given age pair. False matches are counted against a recognition threshold fixed globally to give  $FMR = 0.001$  over all on the order of  $10^{10}$  impostor comparisons. The text in each box gives the same quantity as that coded by the color. Light colors present a security vulnerability to, for example, a passport gate.

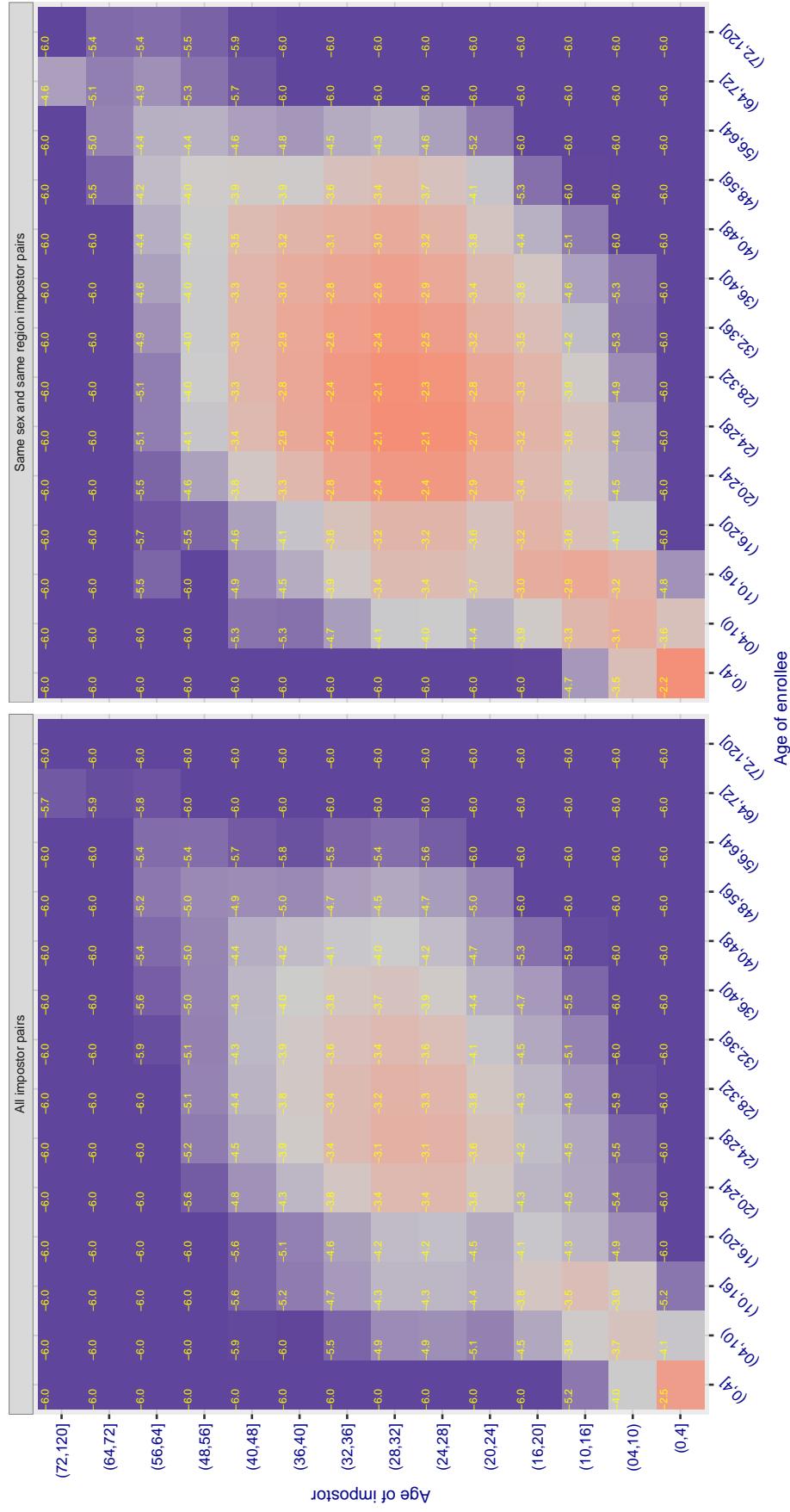
**Cross age FMR at threshold  $T = 0.675$  for algorithm digitalbarriers\_002, giving  $FMR(T) = 0.0001$  globally.**

Figure 342: For algorithm digitalBarriers-002 operating on visa images, the heatmap shows false match observed over impostor comparisons of faces from different individuals who have the given age pair. False matches are counted against a recognition threshold fixed globally to give  $FMR = 0.001$  over all on the order of  $10^{10}$  impostor comparisons. The text in each box gives the same quantity as that coded by the color. Light colors present a security vulnerability to, for example, a passport gate.

Cross age FMR at threshold T = 2.672 for algorithm everai\_001, giving FMR(T) = 0.0001 globally.

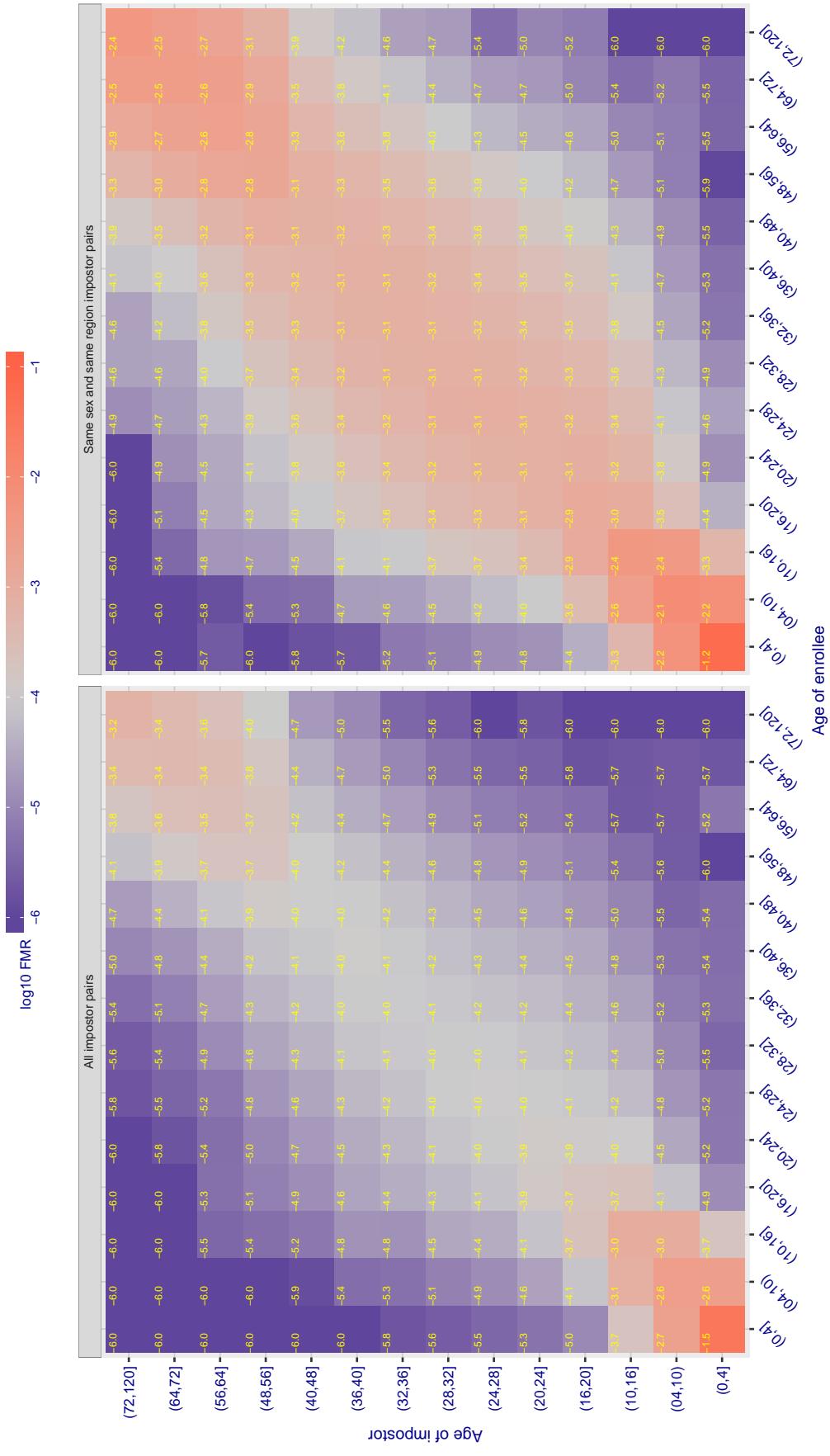


Figure 343: For algorithm everai-001 operating on visa images, the heatmap shows false match observed over impostor comparisons of faces from different individuals who have the given age pair. False matches are counted against a recognition threshold fixed globally to give  $FMR = 0.001$  over all on the order of  $10^{10}$  impostor comparisons. The text in each box gives the same quantity as that coded by the color. Light colors present a security vulnerability to, for example, a passport gate.

Cross age FMR at threshold T = 2.589 for algorithm everai\_002, giving FMR(T) = 0.0001 globally.

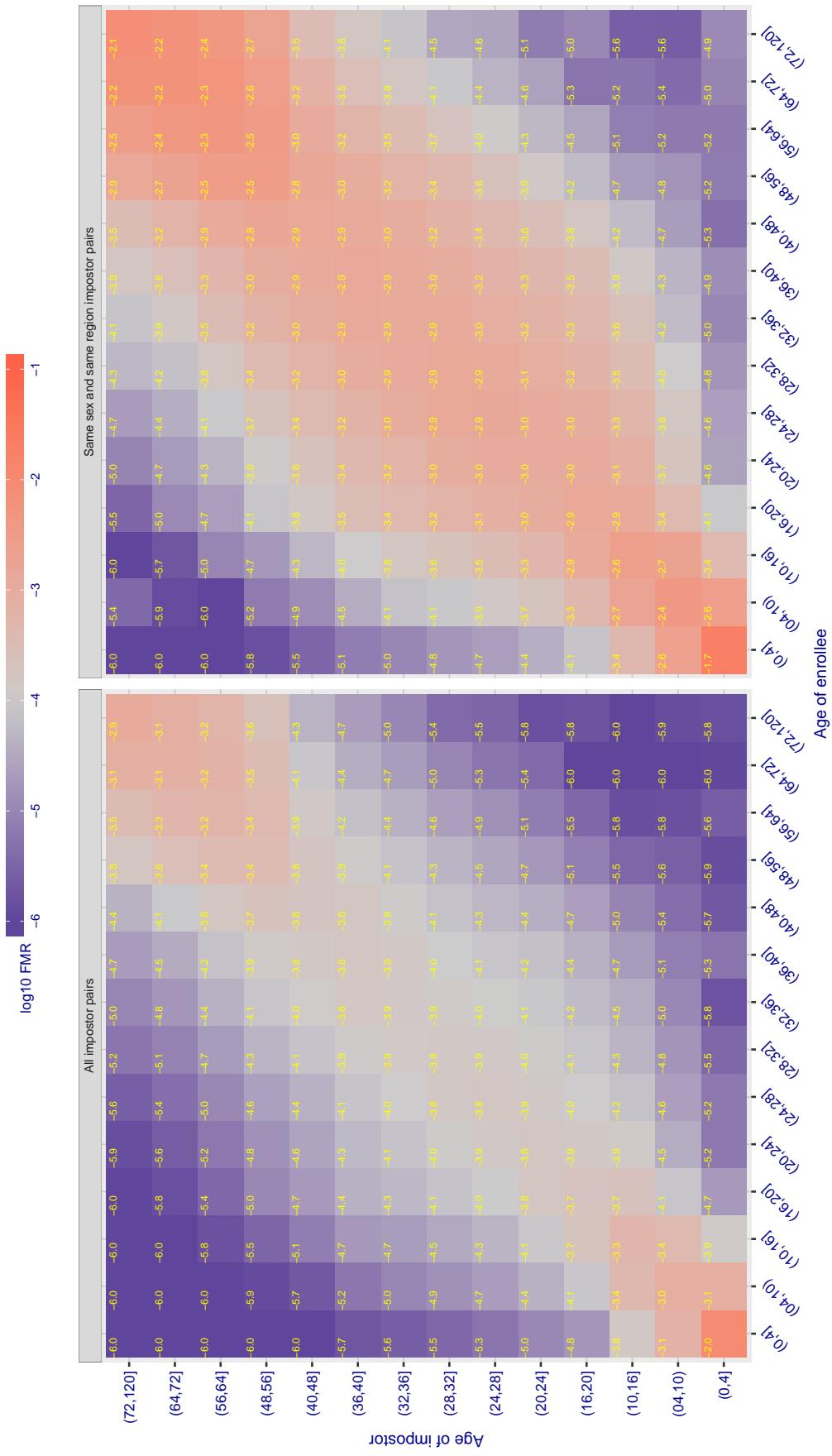


Figure 344: For algorithm everai-002 operating on visa images, the heatmap shows false match observed over impostor comparisons of faces from different individuals who have the given age pair. False matches are counted against a recognition threshold fixed globally to give  $FMR = 0.001$  over all on the order of  $10^{10}$  impostor comparisons. The text in each box gives the same quantity as that coded by the color. Light colors present a security vulnerability to, for example, a passport gate.

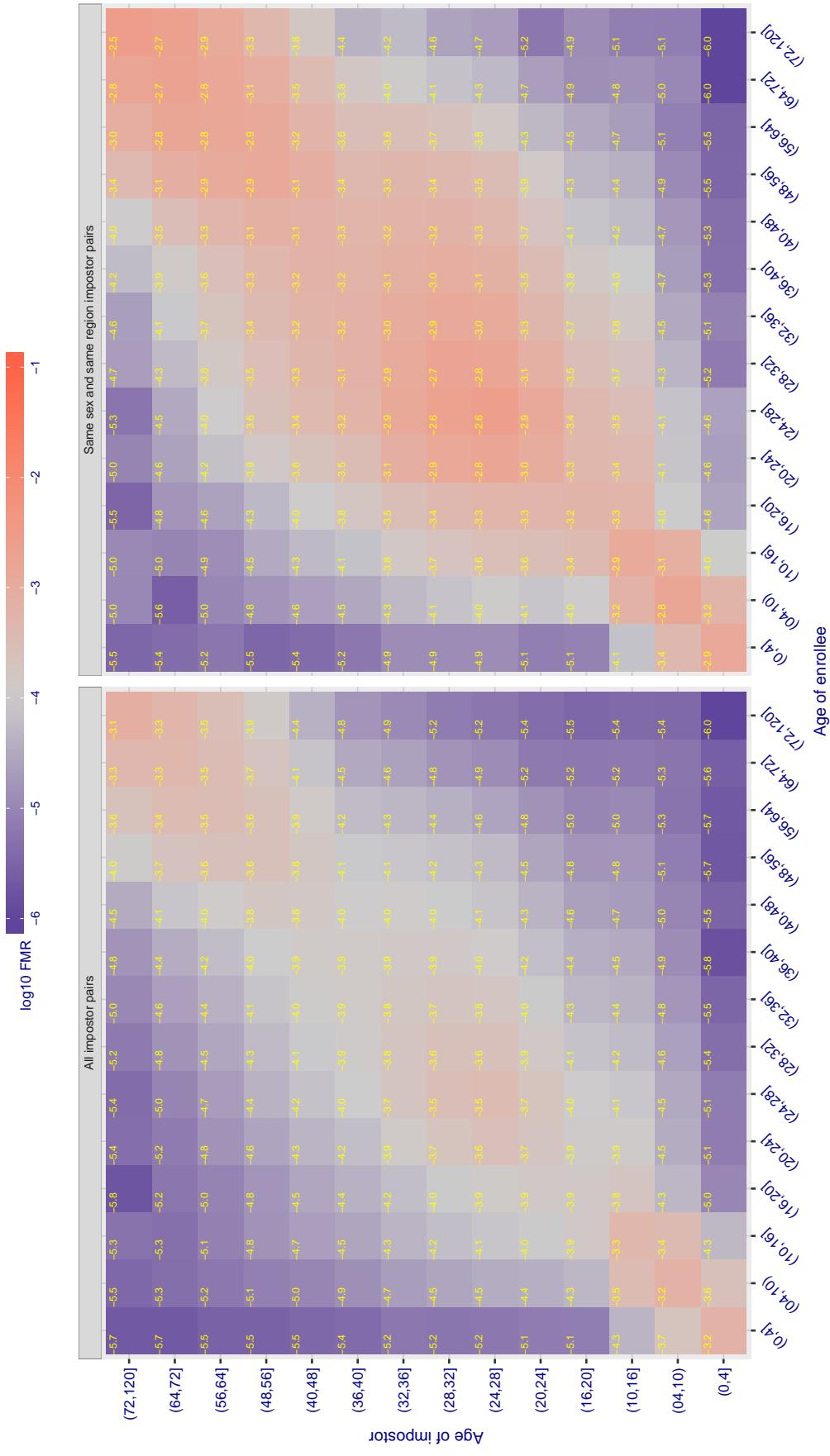
Cross age FMR at threshold T = 0.618 for algorithm glory\_001, giving  $FMR(T) = 0.0001$  globally.

Figure 345: For algorithm glory-001 operating on visa images, the heatmap shows false match observed over impostor comparisons of faces from different individuals who have the given age pair. False matches are counted against a recognition threshold fixed globally to give  $FMR = 0.001$  over all on the order of  $10^{10}$  impostor comparisons. The text in each box gives the same quantity as that coded by the color. Light colors present a security vulnerability to, for example, a passport gate.

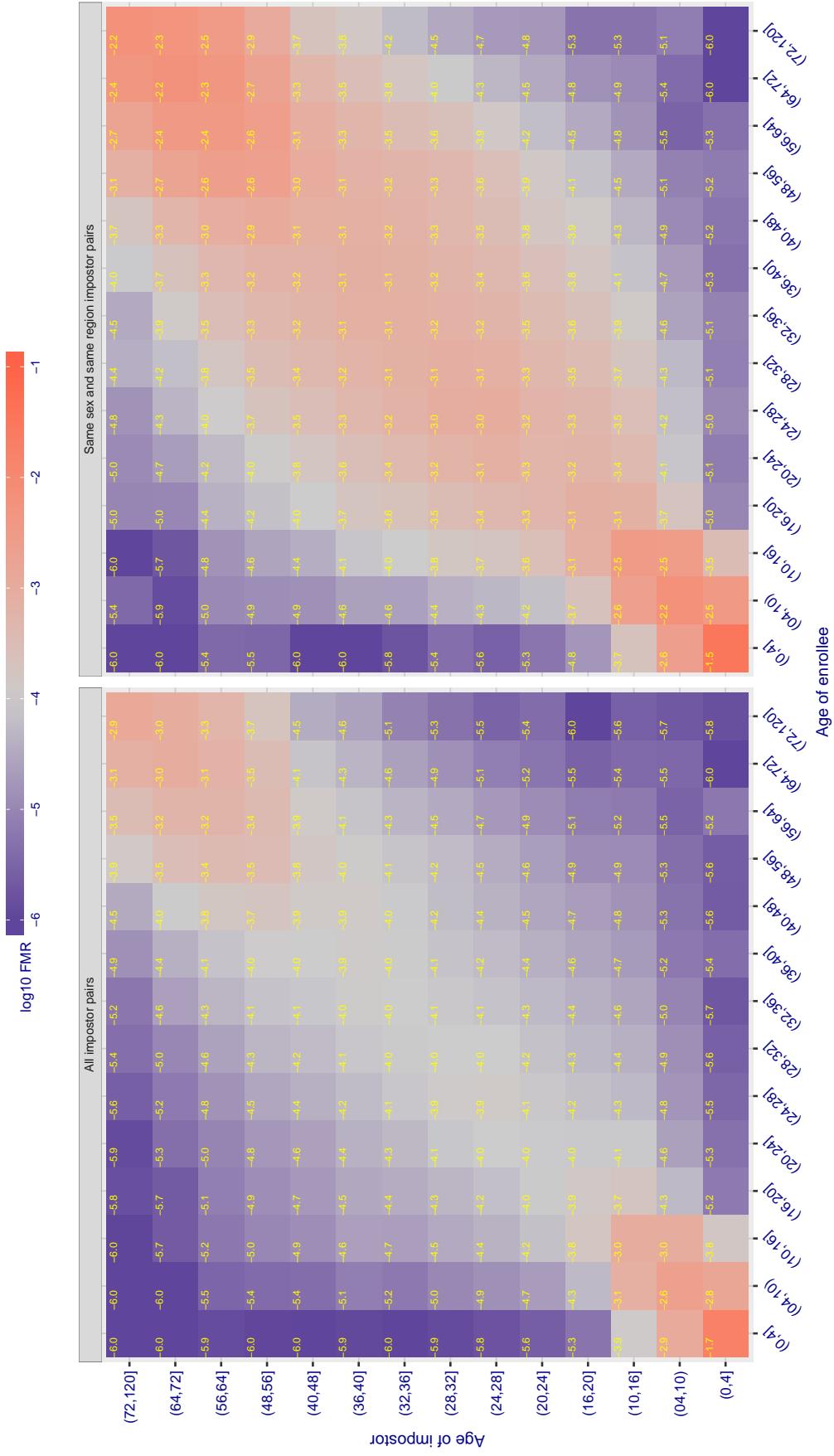
Cross age FMR at threshold T = 0.559 for algorithm gorilla\_001, giving  $FMR(T) = 0.0001$  globally.

Figure 346: For algorithm gorilla\_001 operating on visa images, the heatmap shows false match observed over impostor comparisons of faces from different individuals who have the given age pair. False matches are counted against a recognition threshold fixed globally to give  $FMR = 0.00$  over all on the order of  $10^{10}$  impostor comparisons. The text in each box gives the same quantity as that coded by the color. Light colors present a security vulnerability to, for example, a passport gate.

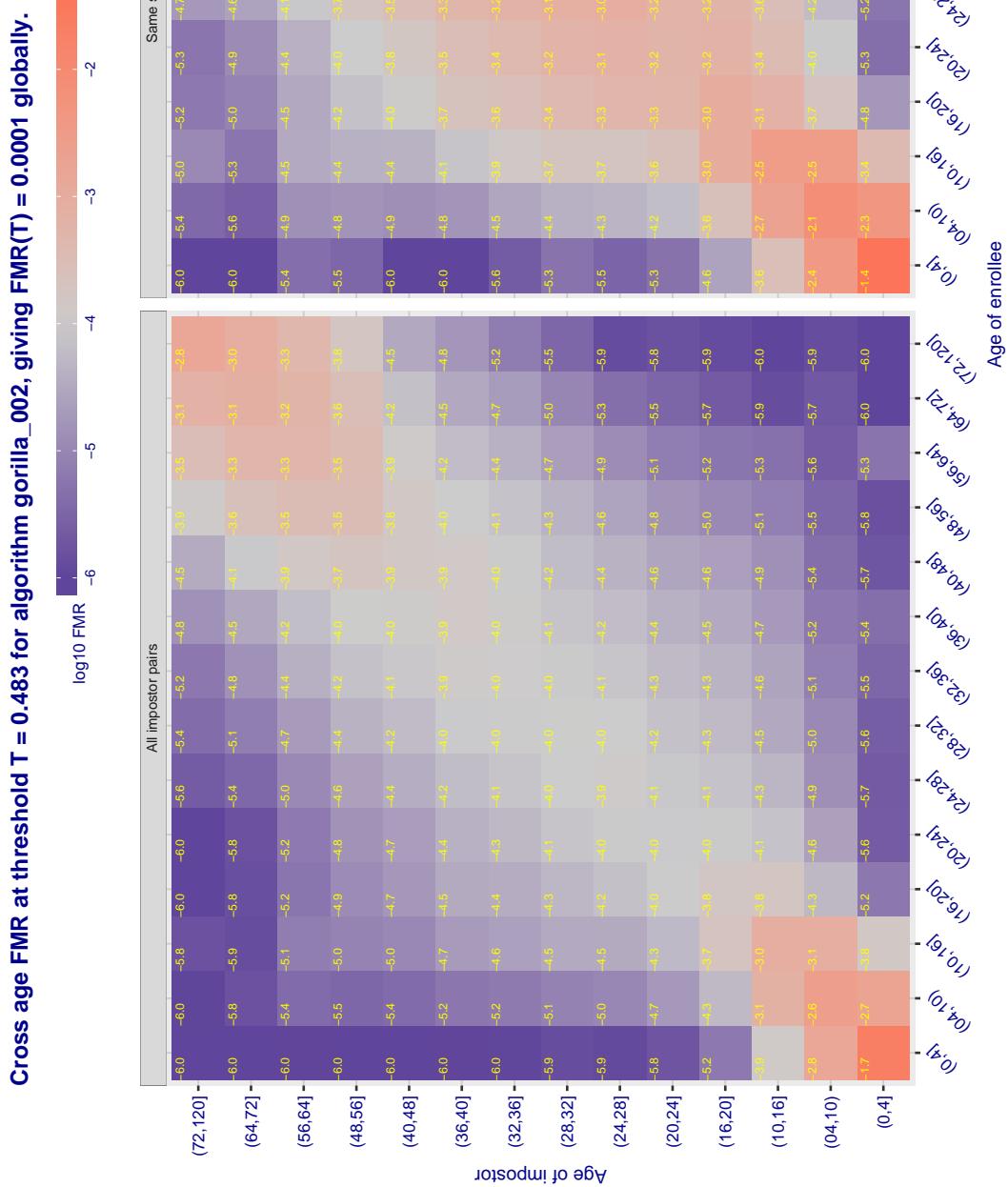


Figure 347: For algorithm gorilla-002 operating on visa images, the heatmap shows false match observed over impostor comparisons of faces from different individuals who have the given age pair. False matches are counted against a recognition threshold fixed globally to give  $FMR = 0.001$  over all on the order of  $10^{10}$  impostor comparisons. The text in each box gives the same quantity as that coded by the color. Light colors present a security vulnerability to, for example, a passport gate.

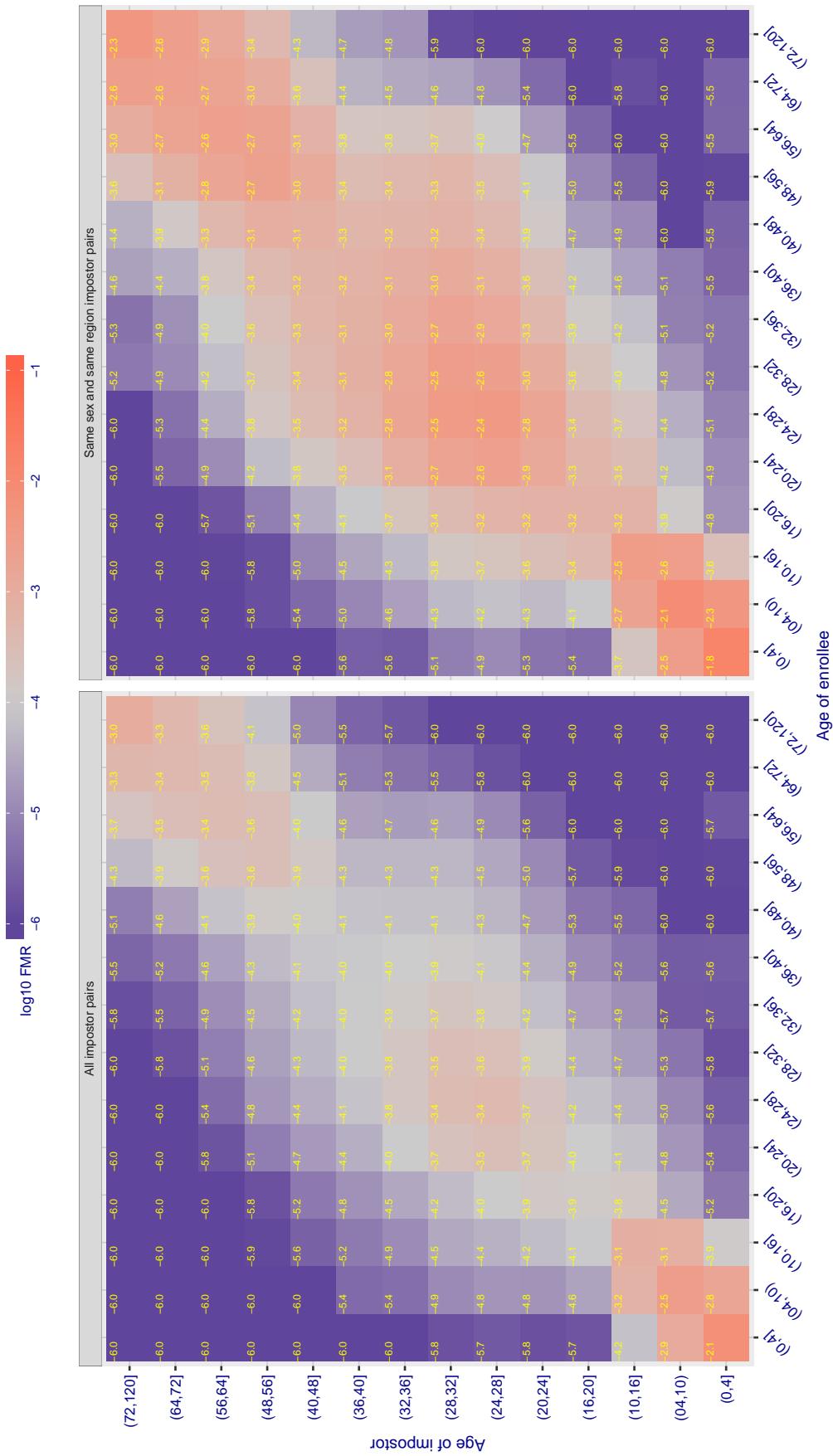
Cross age FMR at threshold T = 66.565 for algorithm hik\_001, giving  $\text{FMR}(T) = 0.0001$  globally.

Figure 348: For algorithm hik-001 operating on visa images, the heatmap shows false match observed over impostor comparisons of faces from different individuals who have the given age pair. False matches are counted against a recognition threshold fixed globally to give  $\text{FMR} = 0.001$  over all on the order of  $10^{10}$  impostor comparisons. The text in each box gives the same quantity as that coded by the color. Light colors represent a security vulnerability to, for example, a passport gate.

Cross age FMR at threshold T = 0.971 for algorithm hr\_000, giving FMR(T) = 0.0001 globally.

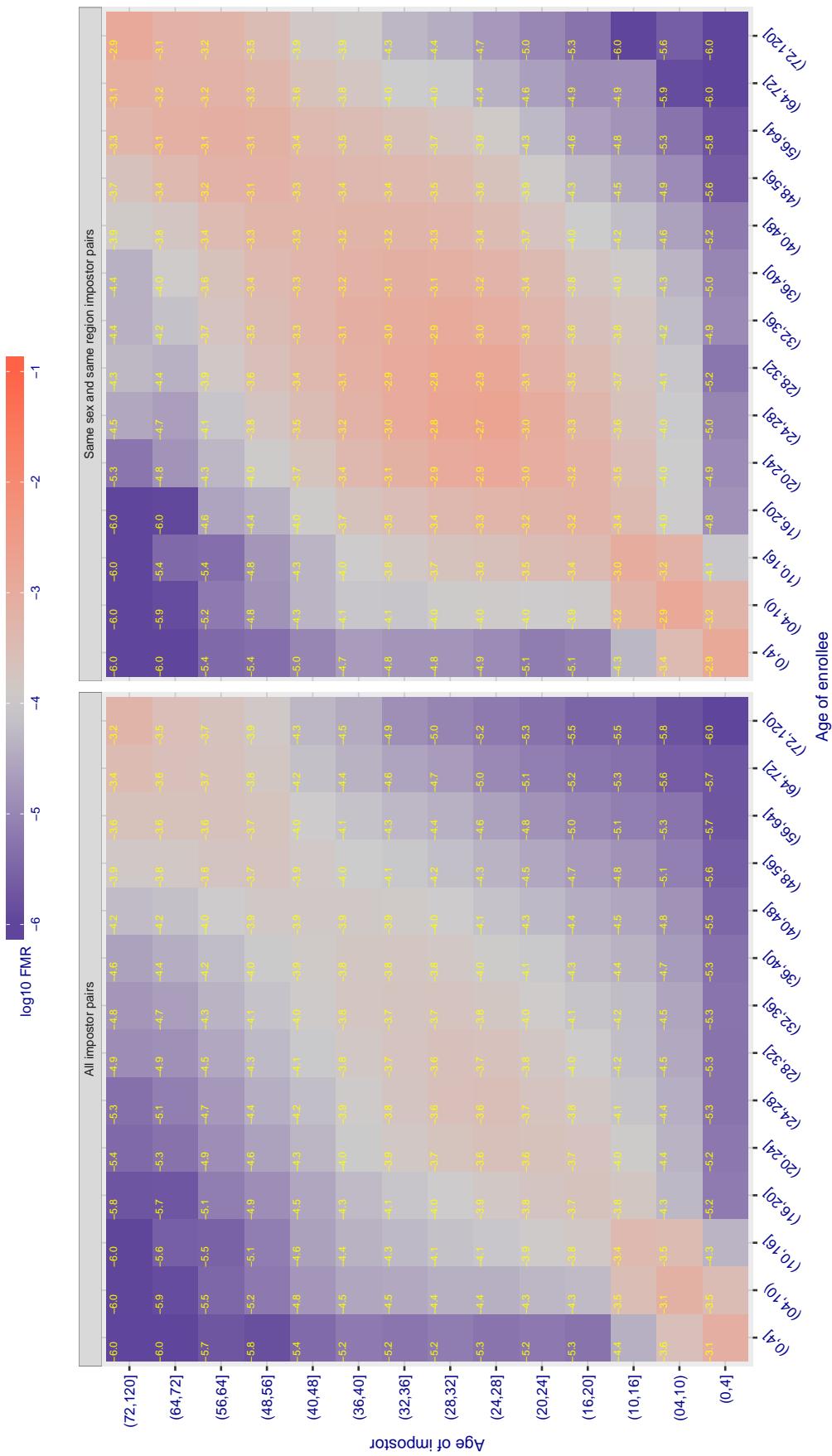
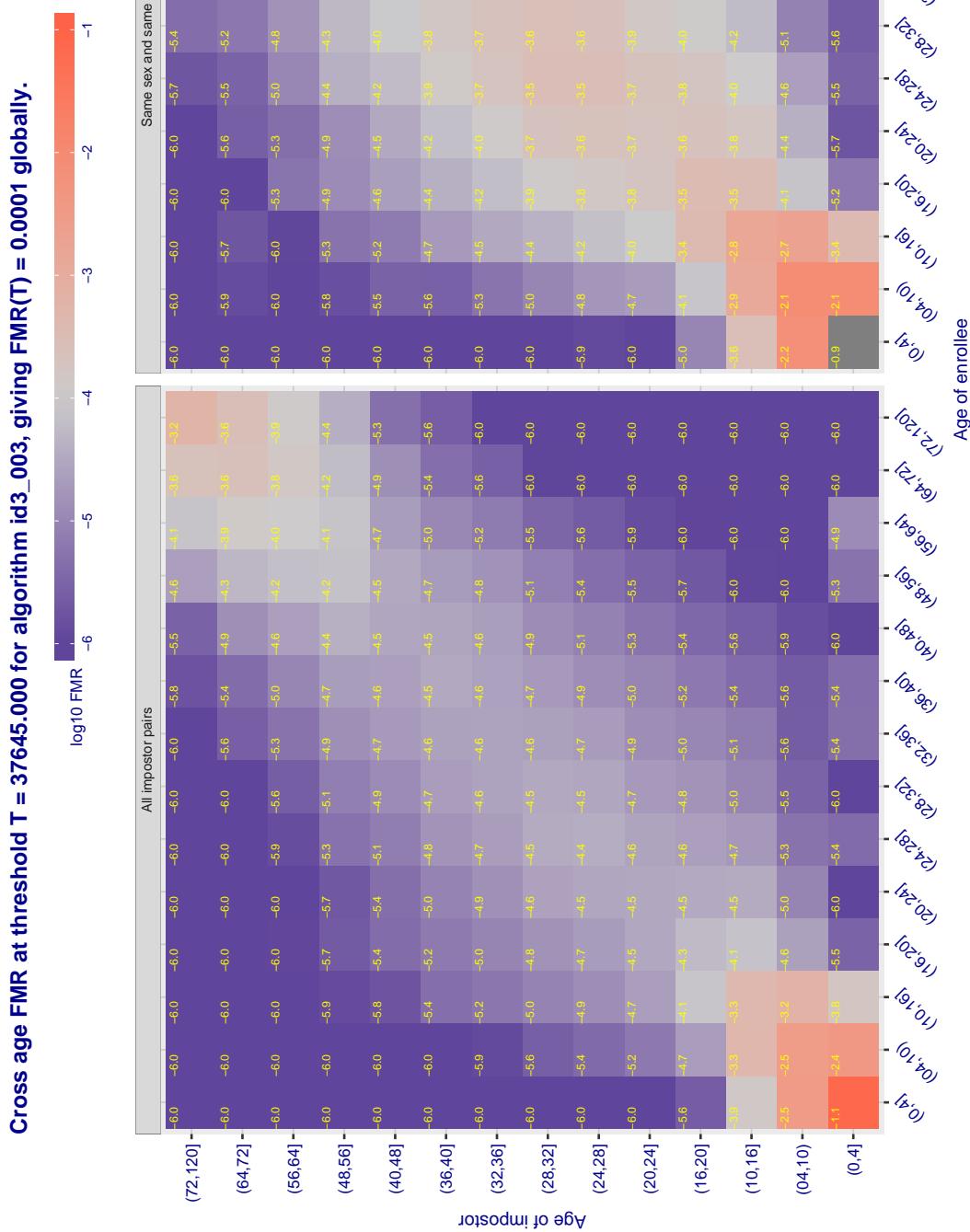
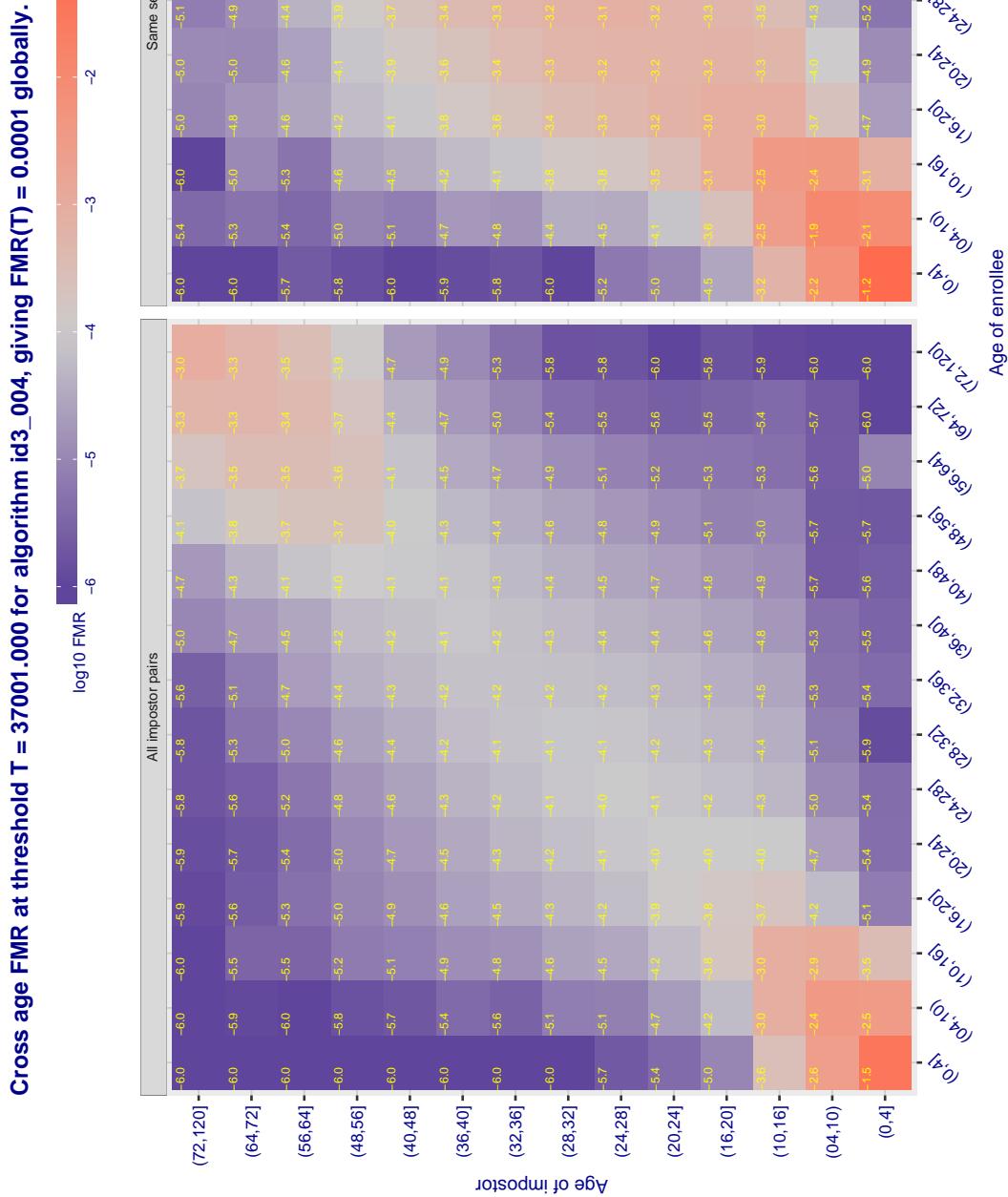


Figure 349: For algorithm hr-000 operating on visa images, the heatmap shows false match observed over impostor comparisons of faces from different individuals who have the given age pair. False matches are counted against a recognition threshold fixed globally to give FMR = 0.001 over all on the order of  $10^{10}$  impostor comparisons. The text in each box gives the same quantity as that coded by the color. Light colors present a security vulnerability to, for example, a passport gate.



**Figure 350:** For algorithm id3-003 operating on visa images, the heatmap shows false match observed over impostor comparisons of faces from different individuals who have the given age pair. False matches are counted against a recognition threshold fixed globally to give  $FMR = 0.001$  over all on the order of  $10^{10}$  impostor comparisons. The text in each box gives the same quantity as that coded by the color. Light colors present a security vulnerability to, for example, a passport gate.



**Figure 351:** For algorithm id3-004 operating on visa images, the heatmap shows false match observed over impostor comparisons of faces from different individuals who have the given age pair. False matches are counted against a recognition threshold fixed globally to give  $FMR = 0.001$  over all on the order of  $10^{10}$  impostor comparisons. The text in each box gives the same quantity as that coded by the color. Light colors present a security vulnerability to, for example, a passport gate.

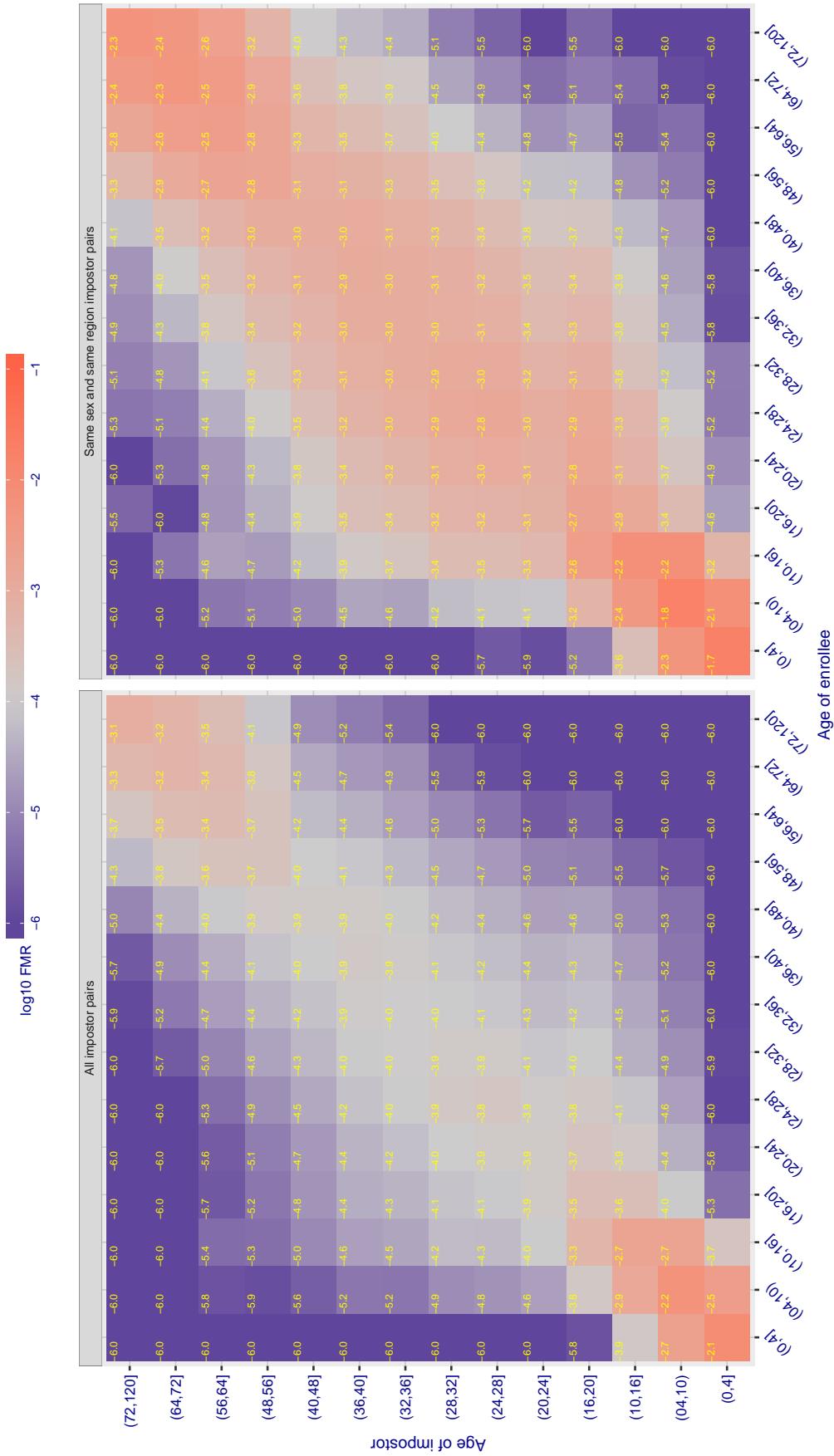
Cross age FMR at threshold T = 3664.380 for algorithm idemia\_003, giving  $\text{FMR}(\text{T}) = 0.00001$  globally.

Figure 352: For algorithm idemia-003 operating on visa images, the heatmap shows false match observed over impostor comparisons of faces from different individuals who have the given age pair. False matches are counted against a recognition threshold fixed globally to give  $\text{FMR} = 0.00$  over all on the order of  $10^{10}$  impostor comparisons. The text in each box gives the same quantity as that coded by the color. Light colors present a security vulnerability to, for example, a passport gate.

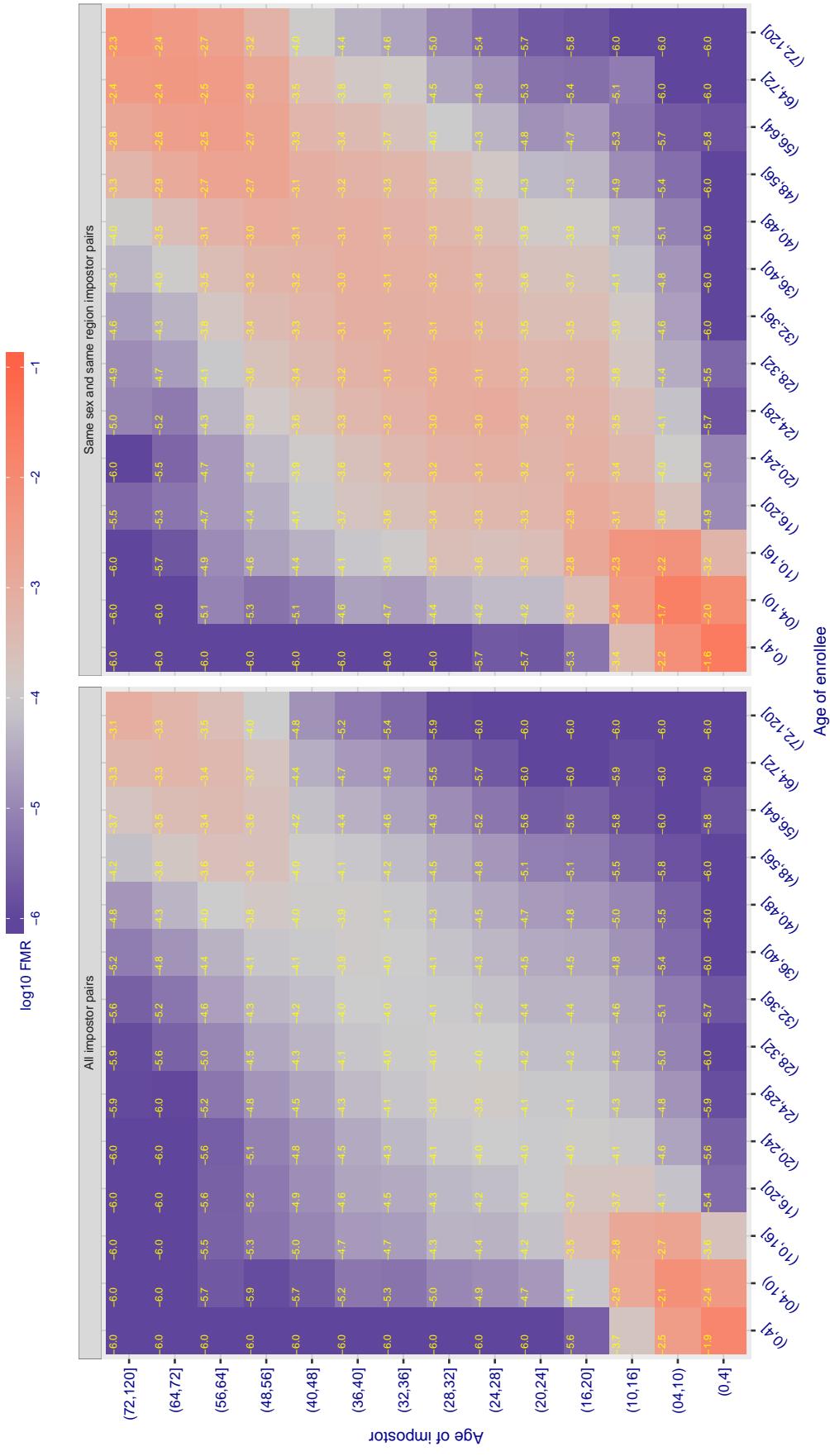
Cross age FMR at threshold T = 3925.463 for algorithm idemia\_004, giving  $\text{FMR}(\text{T}) = 0.00001$  globally.

Figure 353: For algorithm idemia-004 operating on visa images, the heatmap shows false match observed over impostor comparisons of faces from different individuals who have the given age pair. False matches are counted against a recognition threshold fixed globally to give  $\text{FMR} = 0.001$  over all on the order of  $10^{10}$  impostor comparisons. The text in each box gives the same quantity as that coded by the color. Light colors present a security vulnerability to, for example, a passport gate.

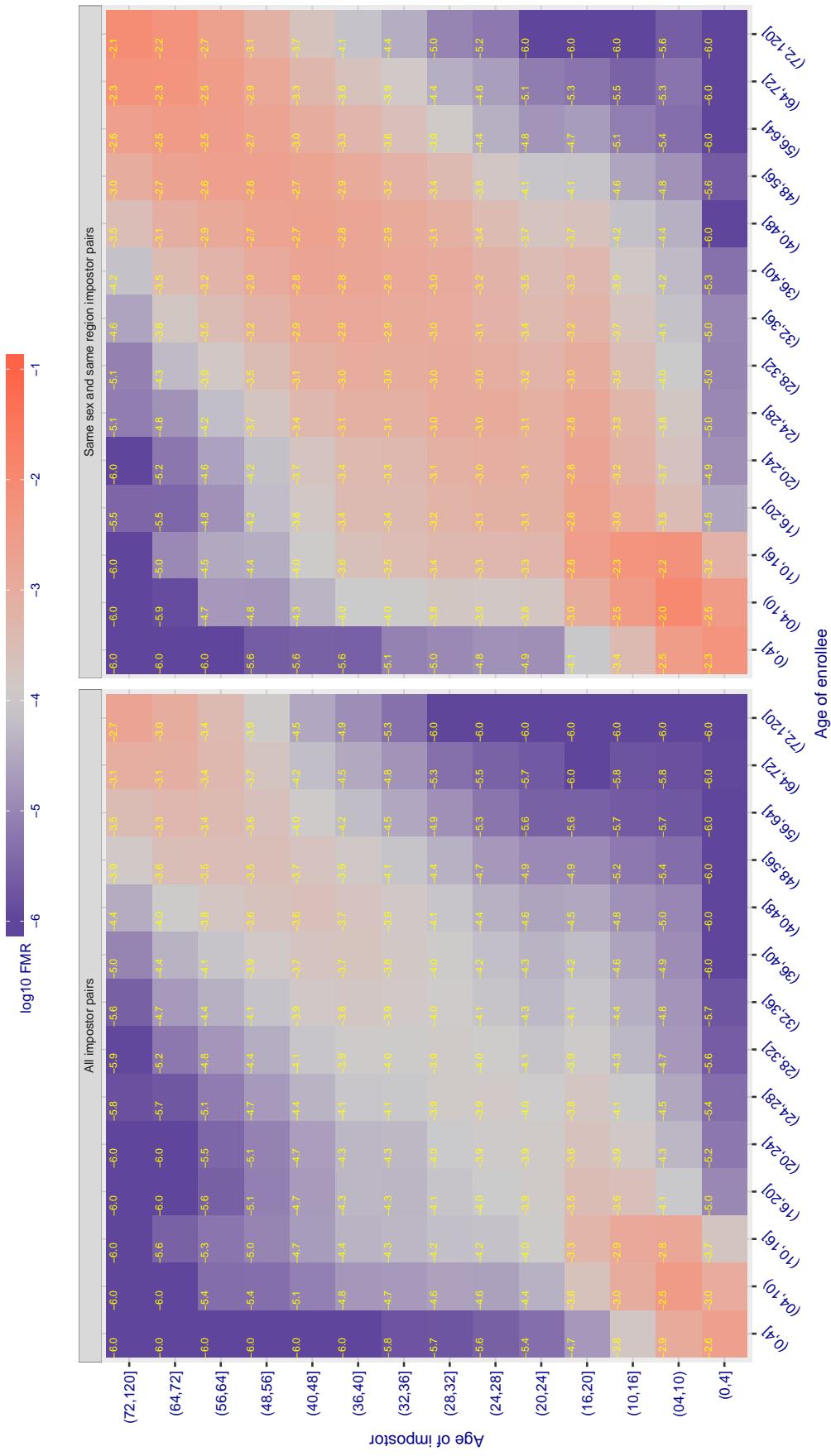
Cross age FMR at threshold T = 0.760 for algorithm iit\_000, giving  $\text{FMR}(T) = 0.0001$  globally.

Figure 354: For algorithm iit-000 operating on visa images, the heatmap shows false match observed over impostor comparisons of faces from different individuals who have the given age pair. False matches are counted against a recognition threshold fixed globally to give  $\text{FMR} = 0.001$  over all on the order of  $10^{10}$  impostor comparisons. The text in each box gives the same quantity as that coded by the color. Light colors present a security vulnerability to, for example, a passport gate.

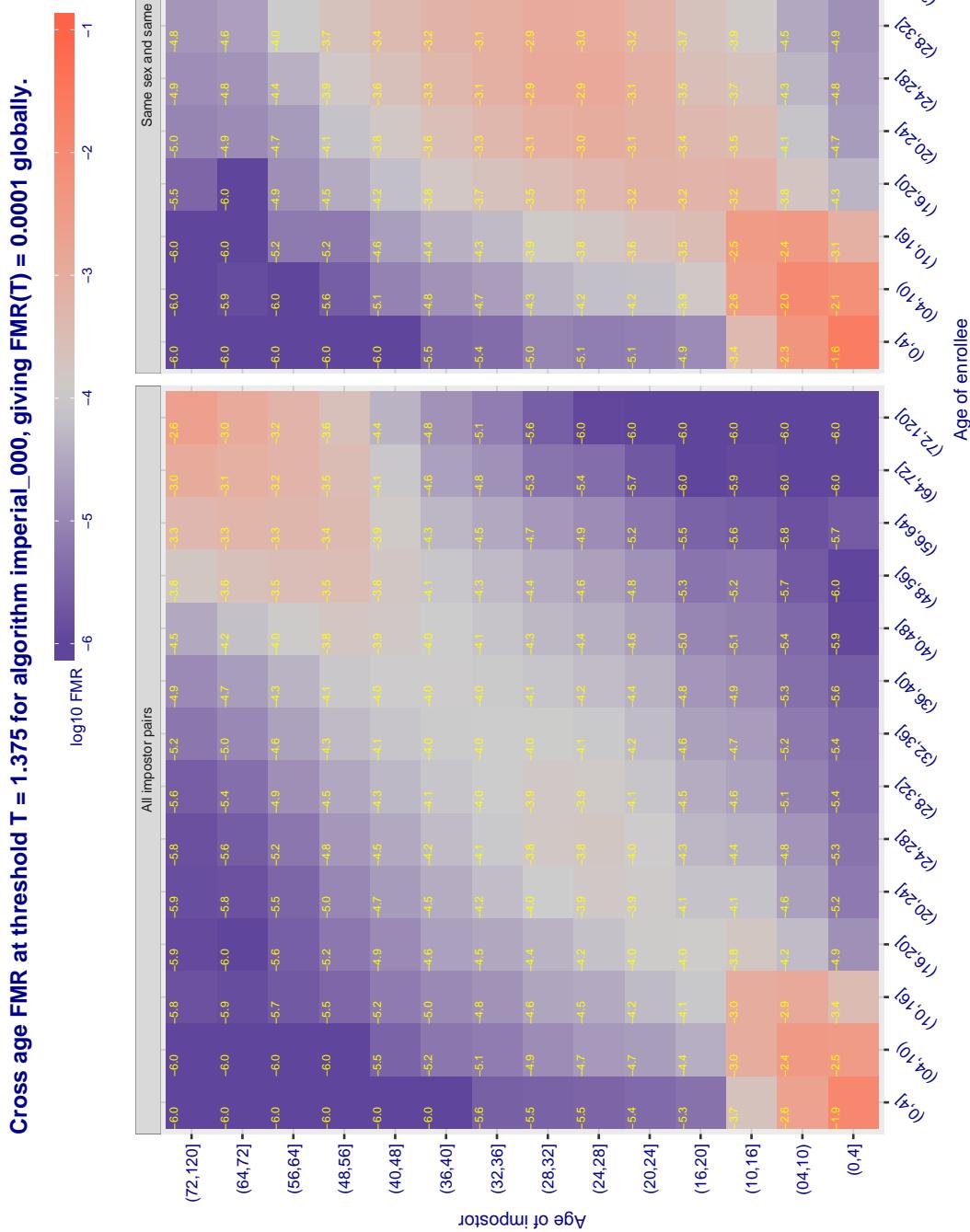


Figure 355: For algorithm imperial-000 operating on visa images, the heatmap shows false match observed over impostor comparisons of faces from different individuals who have the given age pair. False matches are counted against a recognition threshold fixed globally to give  $FMR = 0.001$  over all on the order of  $10^{10}$  impostor comparisons. The text in each box gives the same quantity as that coded by the color. Light colors present a security vulnerability to, for example, a passport gate.

Cross age FMR at threshold T = 1.402 for algorithm imperial\_001, giving FMR(T) = 0.0001 globally.

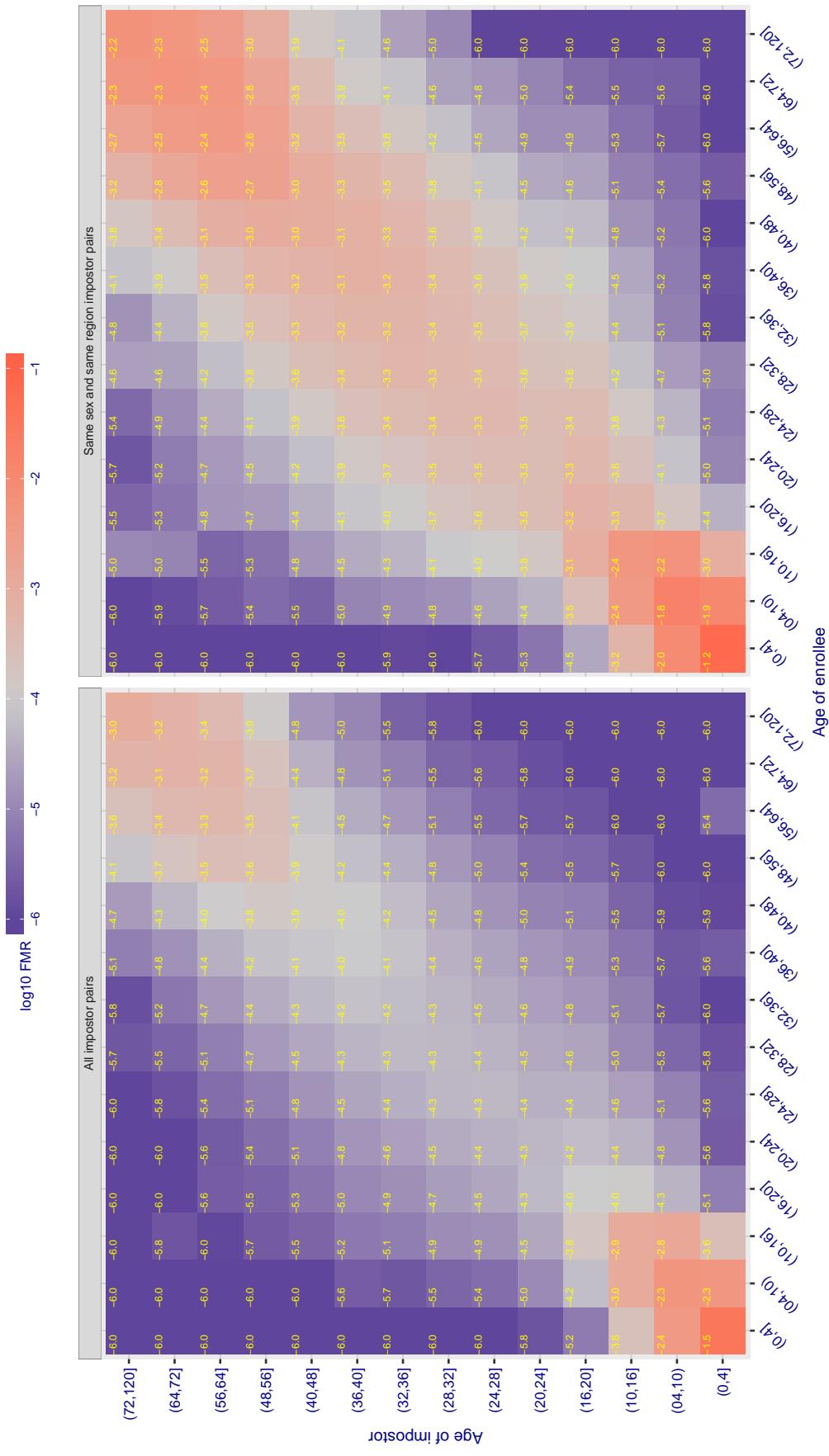


Figure 356: For algorithm imperial\_001 operating on visa images, the heatmap shows false match observed over impostor comparisons of faces from different individuals who have the given age pair. False matches are counted against a recognition threshold fixed globally to give FMR = 0.001 over all on the order of  $10^{10}$  impostor comparisons. The text in each box gives the same quantity as that coded by the color. Light colors present a security vulnerability to, for example, a passport gate.

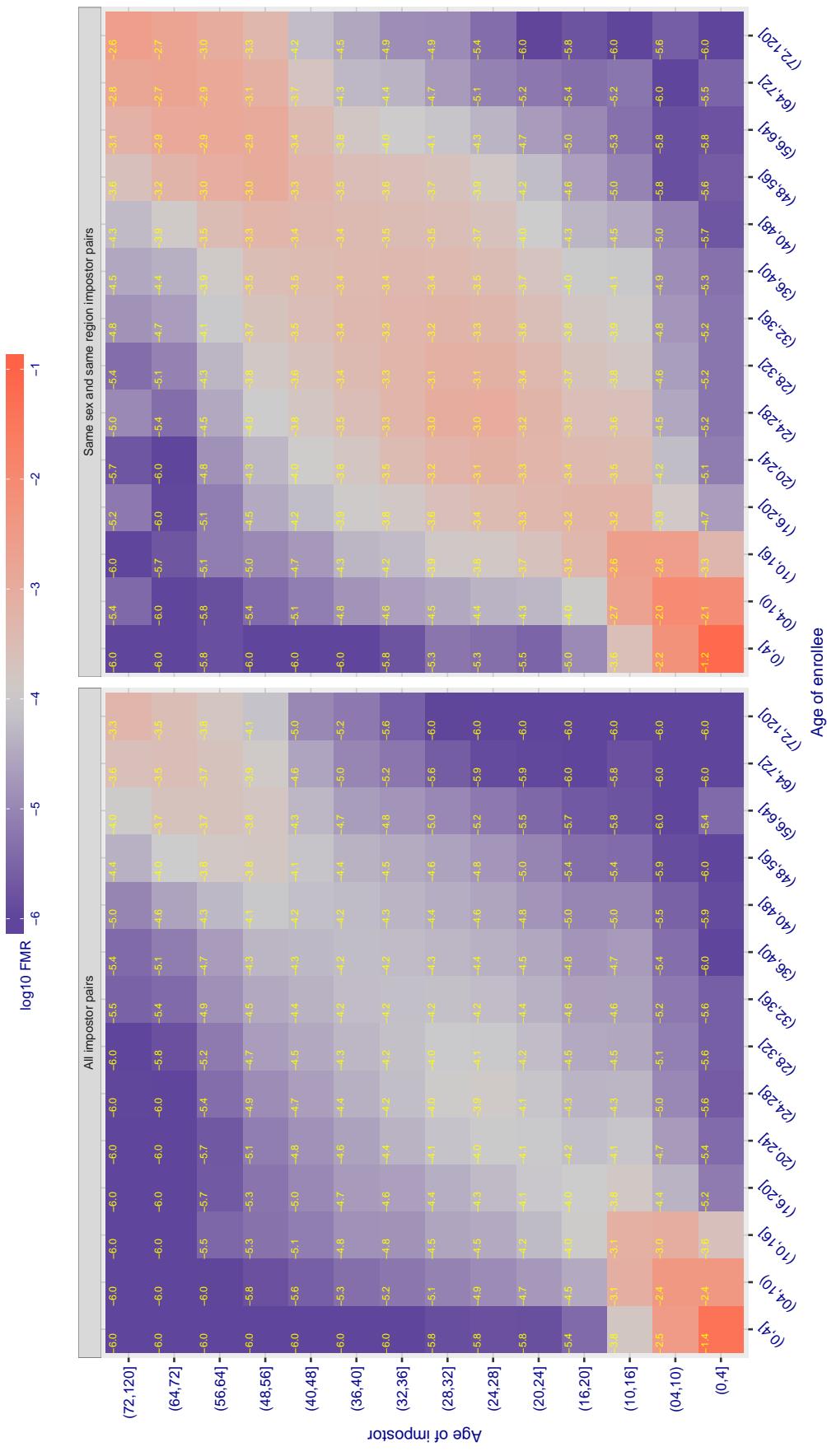
Cross age FMR at threshold T = 1.382 for algorithm incode\_002, giving  $FMR(T) = 0.0001$  globally.

Figure 357: For algorithm incode-002 operating on visa images, the heatmap shows false match observed over impostor comparisons of faces from different individuals who have the given age pair. False matches are counted against a recognition threshold fixed globally to give  $FMR = 0.00$  over all on the order of  $10^{10}$  impostor comparisons. The text in each box gives the same quantity as that coded by the color. Light colors present a security vulnerability to, for example, a passport gate.

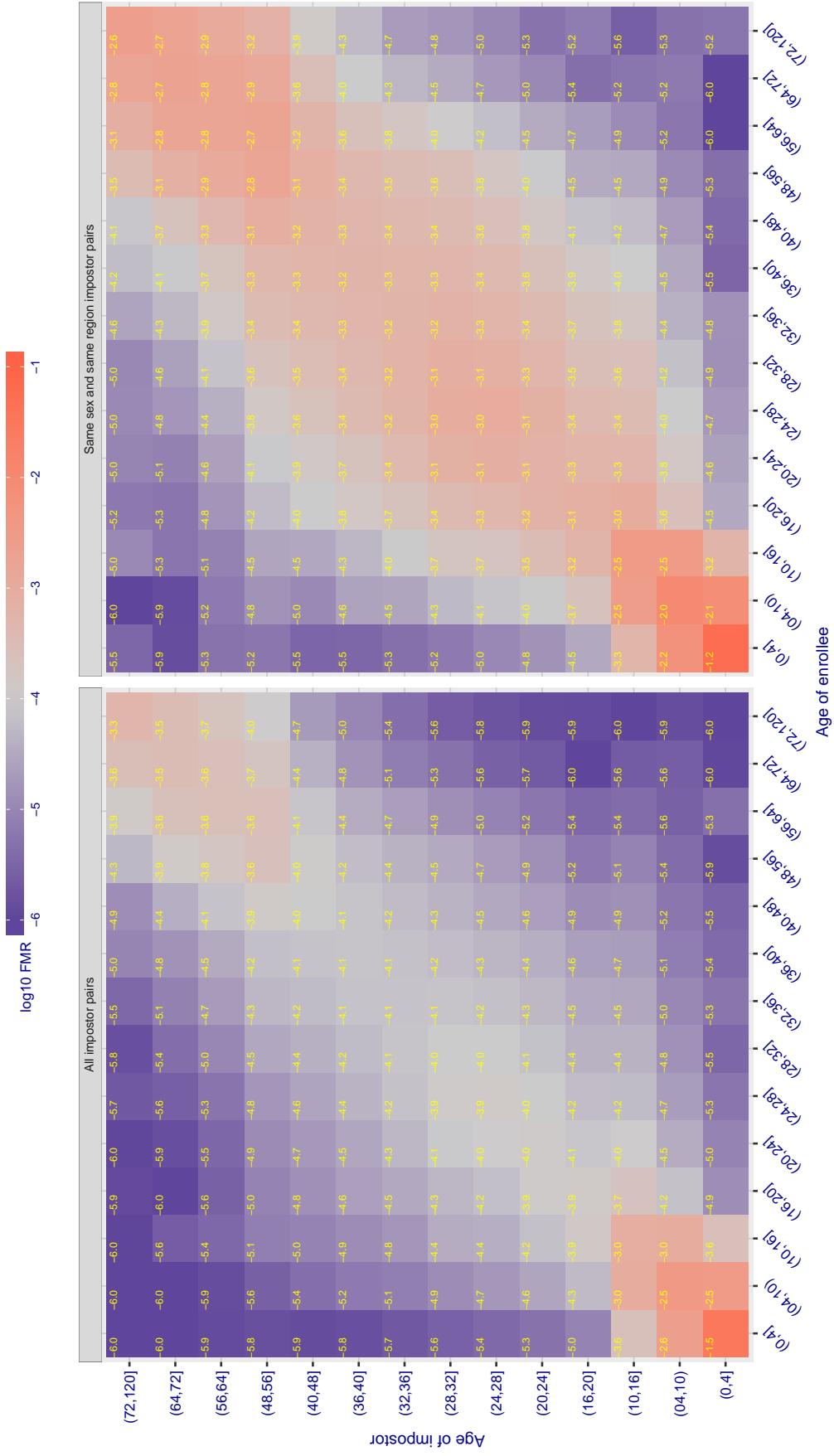
Cross age FMR at threshold T = 1.427 for algorithm incode\_003, giving  $FMR(T) = 0.0001$  globally.

Figure 358: For algorithm incode-003 operating on visa images, the heatmap shows false match observed over impostor comparisons of faces from different individuals who have the given age pair. False matches are counted against a recognition threshold fixed globally to give  $FMR = 0.001$  over all on the order of  $10^{10}$  impostor comparisons. The text in each box gives the same quantity as that coded by the color. Light colors present a security vulnerability to, for example, a passport gate.

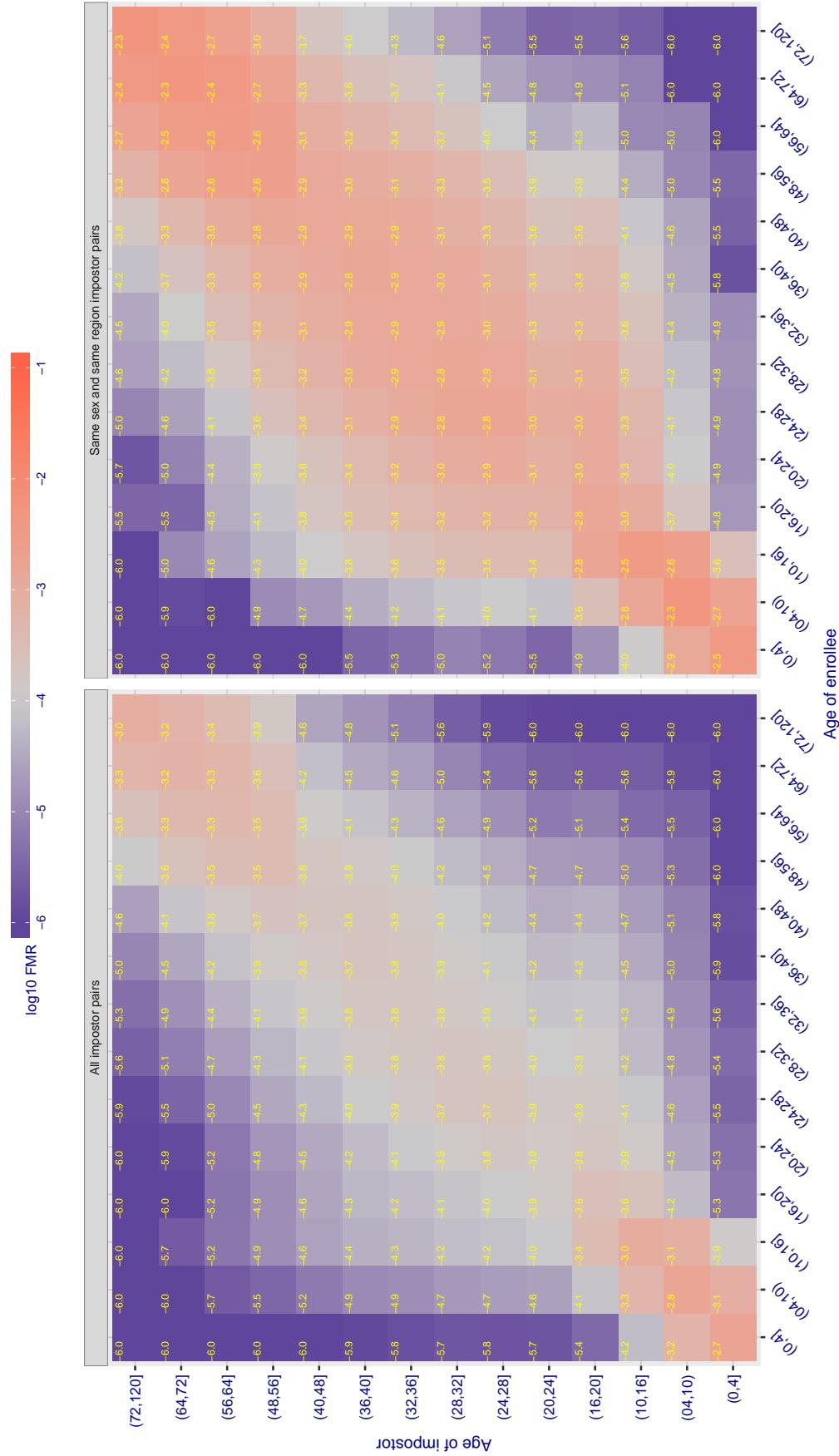
**Cross age FMR at threshold  $T = 29.232$  for algorithm innovatrics\_004, giving  $FMR(T) = 0.0001$  globally.**

Figure 359: For algorithm innovatrics-004 operating on visa images, the heatmap shows false match observed over imposter comparisons of faces from different individuals who have the given age pair. False matches are counted against a recognition threshold fixed globally to give  $FMR = 0.001$  over all on the order of  $10^{10}$  imposter comparisons. The text in each box gives the same quantity as that coded by the color. Light colors present a security vulnerability to, for example, a passport gate.

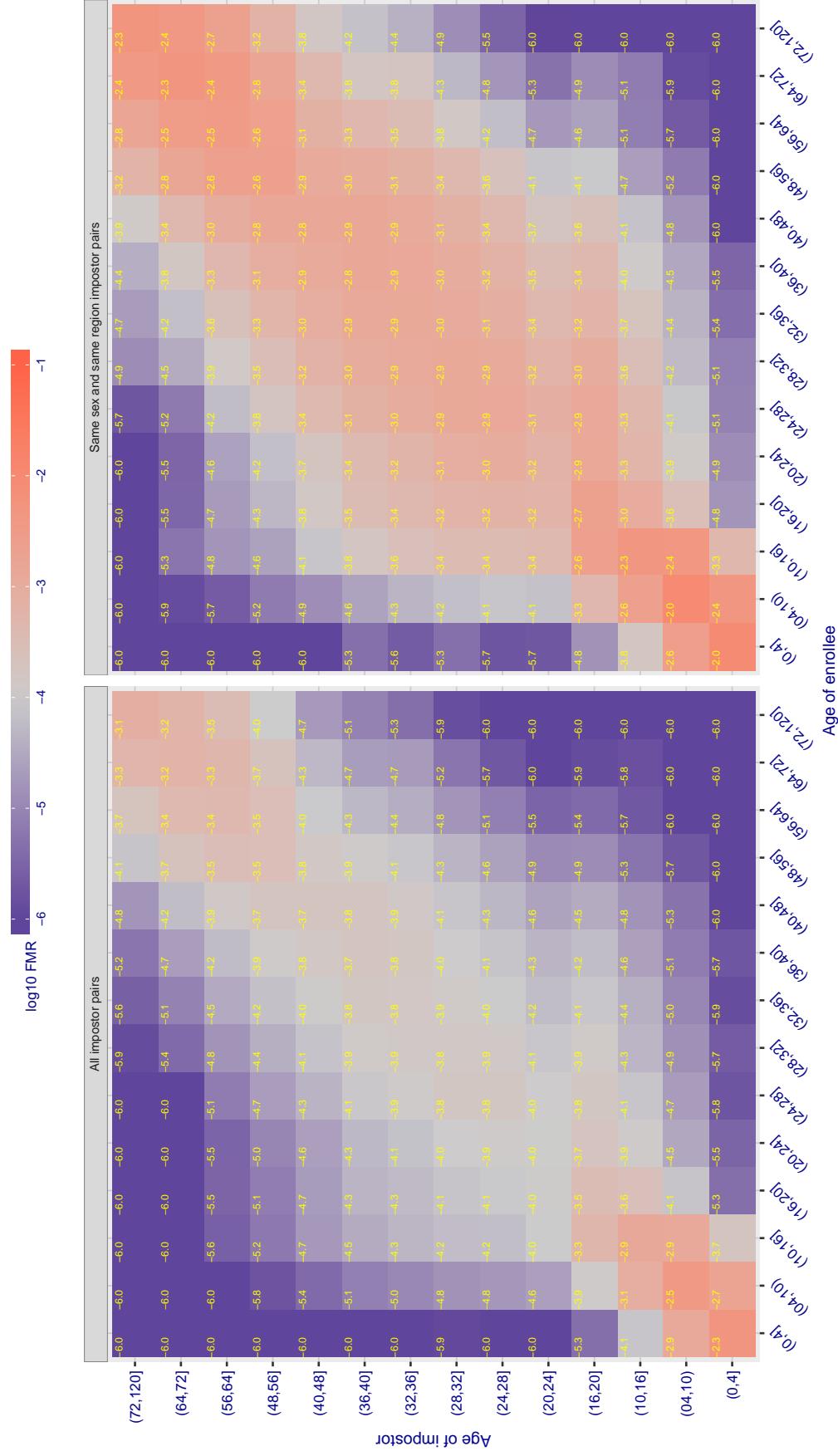
**Cross age FMR at threshold  $T = 40.157$  for algorithm innovatrics\_005, giving  $FMR(T) = 0.0001$  globally.**

Figure 360: For algorithm innovatrics-005 operating on visa images, the heatmap shows false match observed over imposter comparisons of faces from different individuals who have the given age pair. False matches are counted against a recognition threshold fixed globally to give  $FMR = 0.001$  over all on the order of  $10^{10}$  imposter comparisons. The text in each box gives the same quantity as that coded by the color. Light colors present a security vulnerability to, for example, a passport gate.

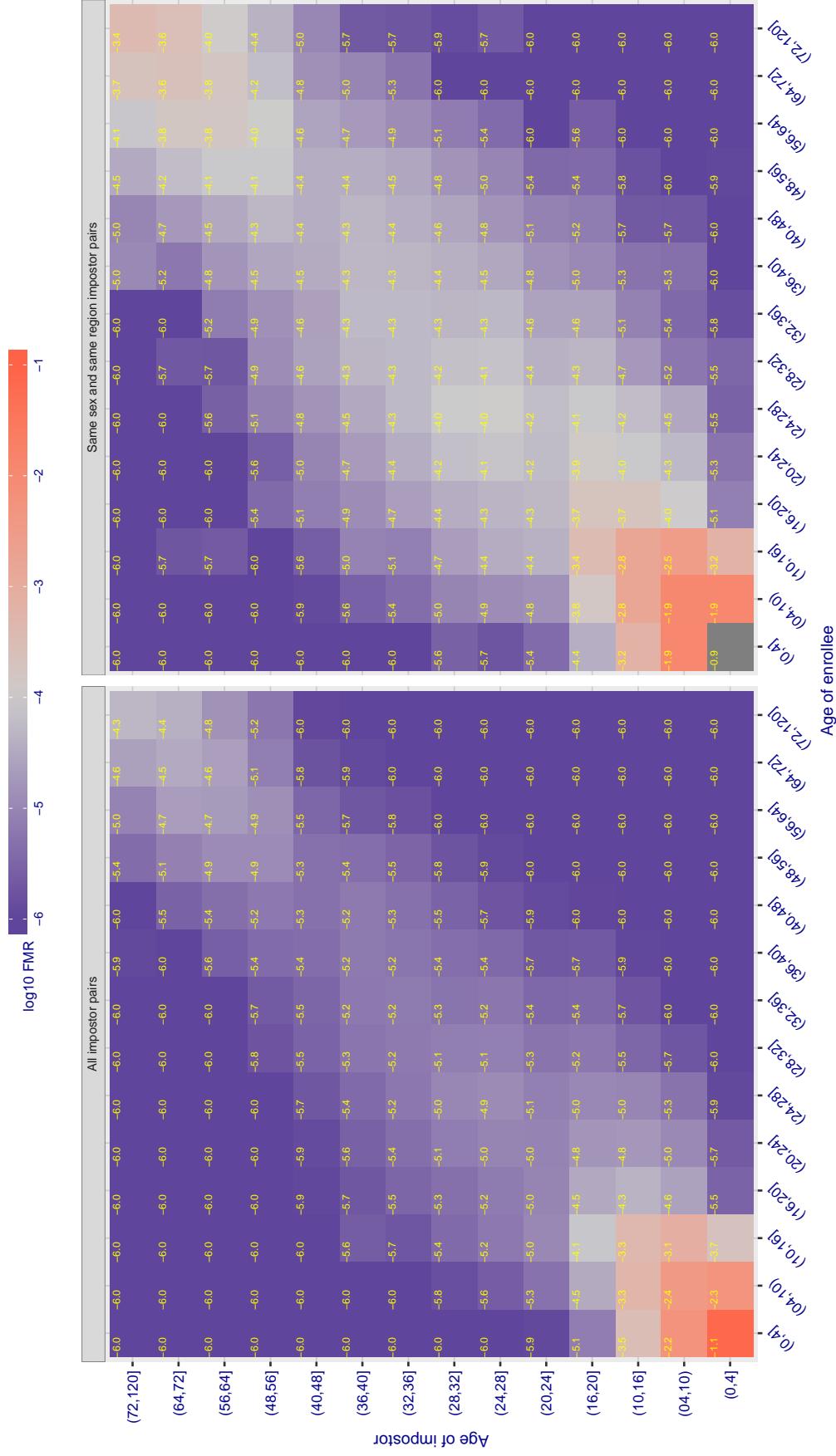
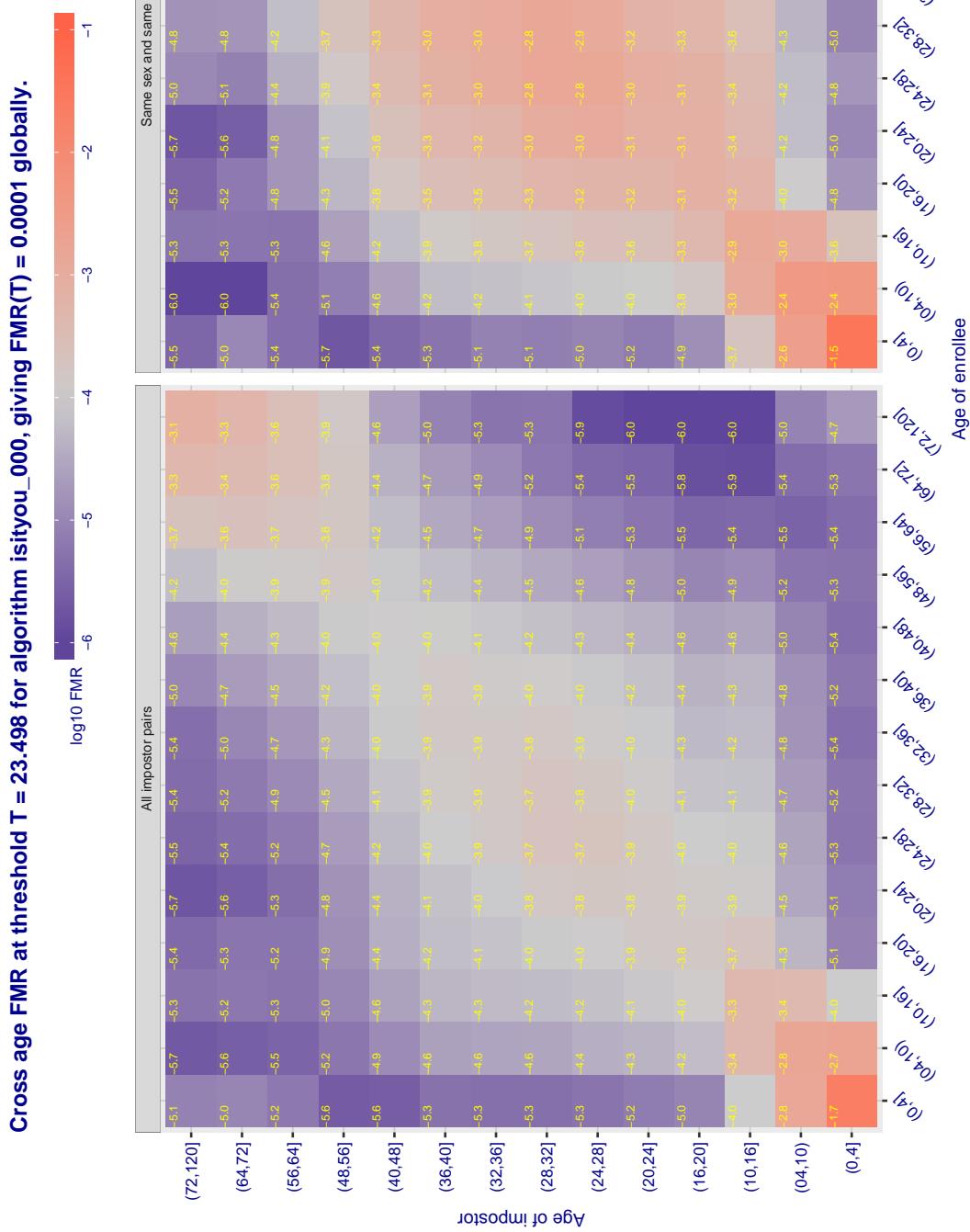
**Cross age FMR at threshold  $T = 49.664$  for algorithm intellivision\_001, giving  $\text{FMR}(T) = 0.00001$  globally.**

Figure 361: For algorithm intellivision\_001 operating on visa images, the heatmap shows false match observed over impostor comparisons of faces from different individuals who have the given age pair. False matches are counted against a recognition threshold fixed globally to give  $\text{FMR} = 0.001$  over all on the order of  $10^{10}$  impostor comparisons. The text in each box gives the same quantity as that coded by the color. Light colors present a security vulnerability to, for example, a passport gate.



**Figure 362:** For algorithm isityou-000 operating on visa images, the heatmap shows false match observed over impostor comparisons of faces from different individuals who have the given age pair. False matches are counted against a recognition threshold fixed globally to give  $FMR = 0.001$  over all on the order of  $10^{10}$  impostor comparisons. The text in each box gives the same quantity as that coded by the color. Light colors present a security vulnerability to, for example, a passport gate.

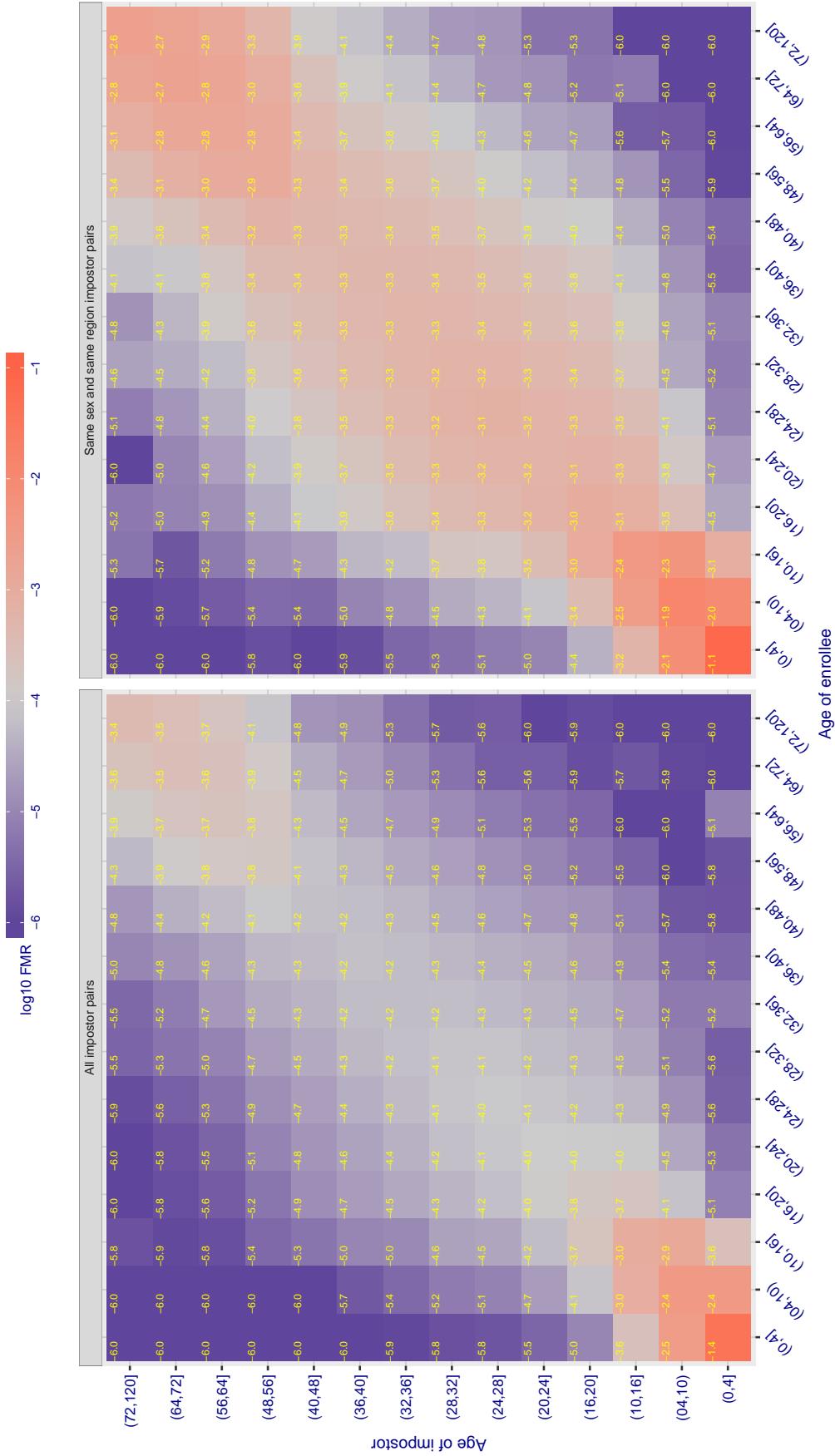
Cross age FMR at threshold T = 0.693 for algorithm systems\_001, giving  $FMR(T) = 0.0001$  globally.

Figure 363: For algorithm systems-001 operating on visa images, the heatmap shows false match observed over impostor comparisons of faces from different individuals who have the given age pair. False matches are counted against a recognition threshold fixed globally to give  $FMR = 0.001$  over all on the order of  $10^{10}$  impostor comparisons. The text in each box gives the same quantity as that coded by the color. Light colors present a security vulnerability to, for example, a passport gate.

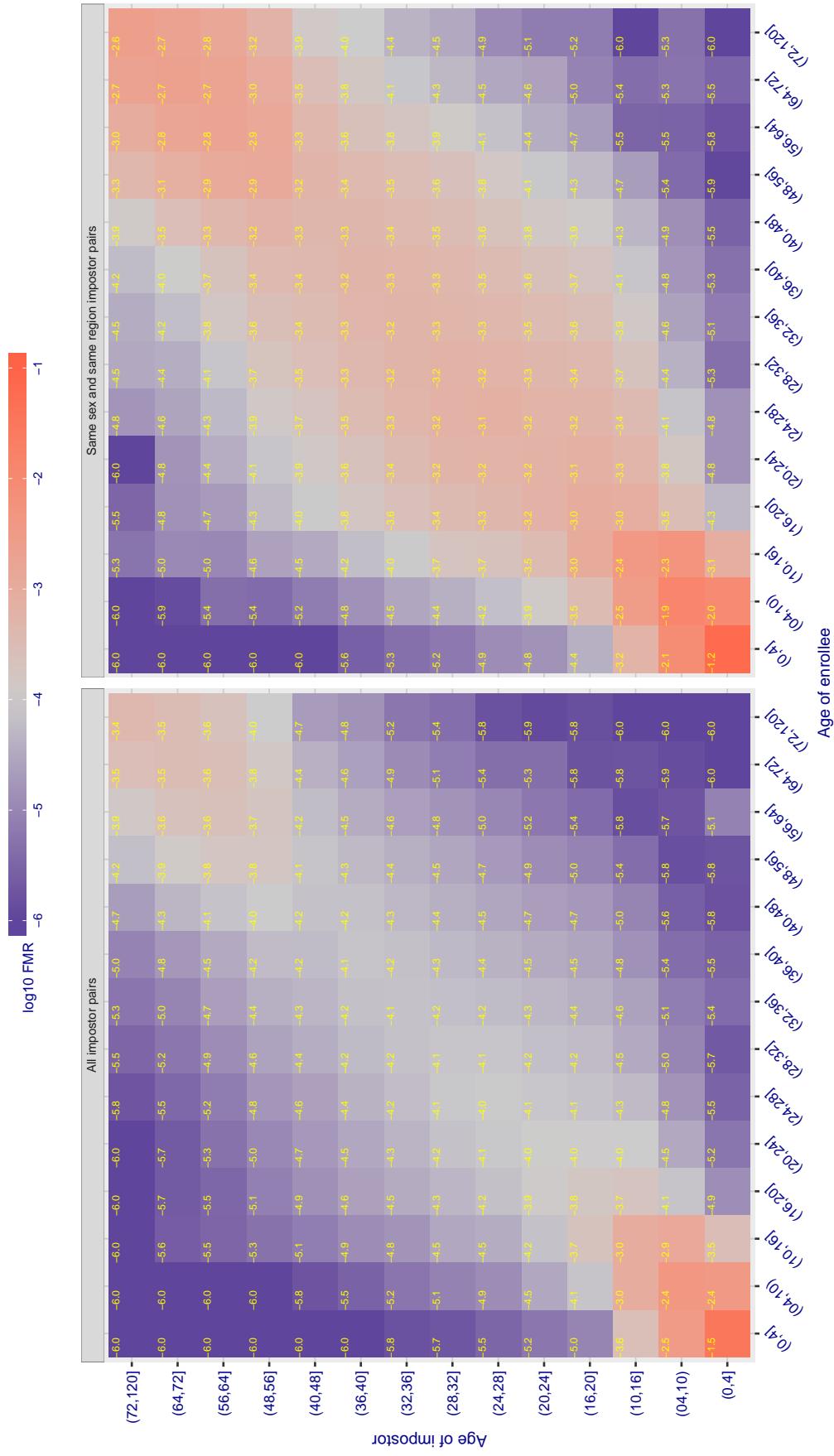
Cross age FMR at threshold T = 0.690 for algorithm systems\_002, giving  $FMR(T) = 0.0001$  globally.

Figure 364: For algorithm systems-002 operating on visa images, the heatmap shows false match observed over impostor comparisons of faces from different individuals who have the given age pair. False matches are counted against a recognition threshold fixed globally to give  $FMR = 0.001$  over all on the order of  $10^{10}$  impostor comparisons. The text in each box gives the same quantity as that coded by the color. Light colors present a security vulnerability to, for example, a passport gate.

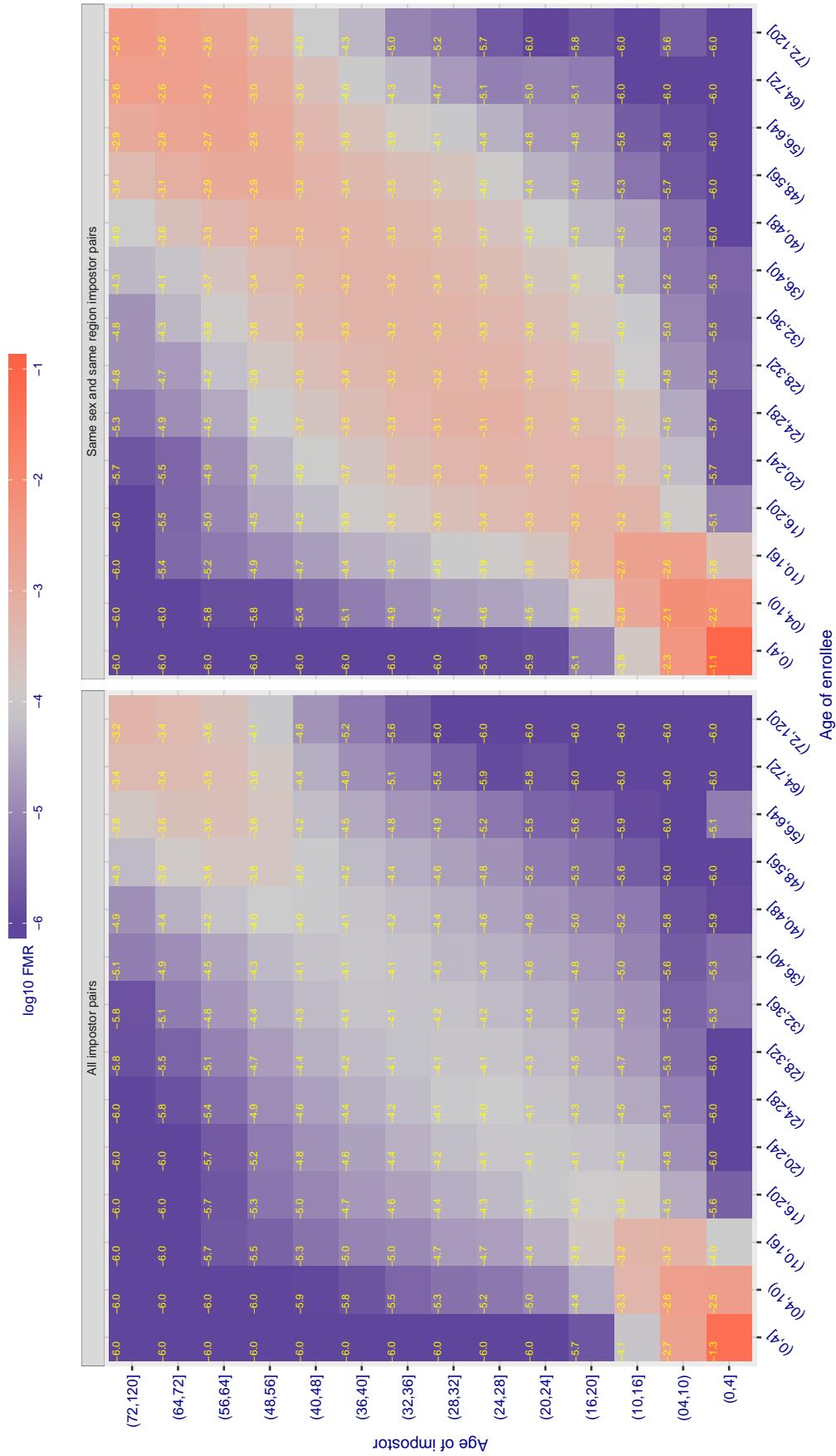
Cross age FMR at threshold T = 49.879 for algorithm itmo\_005, giving  $FMR(T) = 0.00001$  globally.

Figure 365: For algorithm itmo\_005 operating on visa images, the heatmap shows false match observed over impostor comparisons of faces from different individuals who have the given age pair. False matches are counted against a recognition threshold fixed globally to give  $FMR = 0.001$  over all on the order of  $10^{10}$  impostor comparisons. The text in each box gives the same quantity as that coded by the color. Light colors present a security vulnerability to, for example, a passport gate.

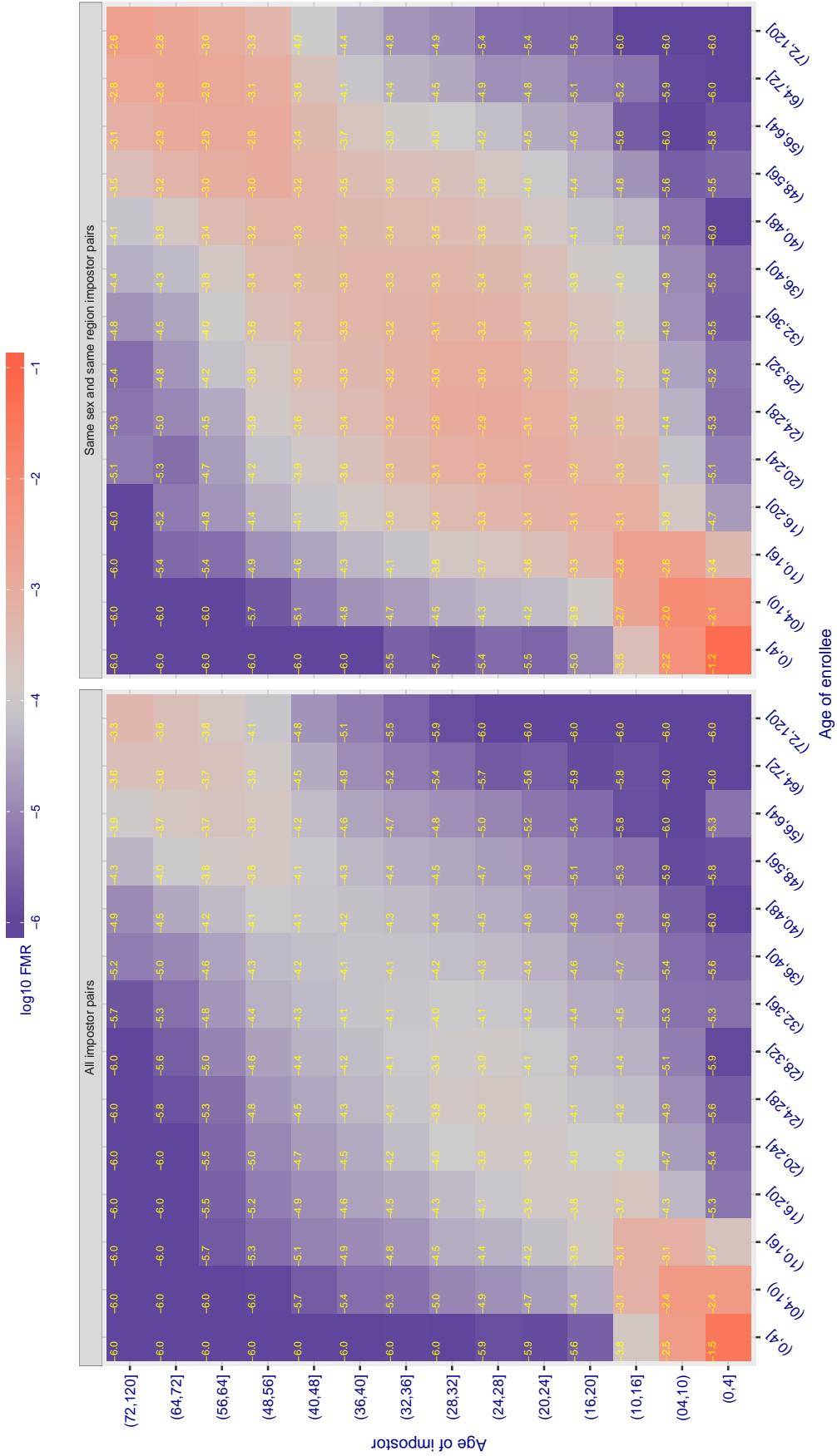
Cross age FMR at threshold T = 49.789 for algorithm itmo\_006, giving  $FMR(T) = 0.0001$  globally.

Figure 366: For algorithm itmo-006 operating on visa images, the heatmap shows false match observed over impostor comparisons of faces from different individuals who have the given age pair. False matches are counted against a recognition threshold fixed globally to give  $FMR = 0.001$  over all on the order of  $10^{10}$  impostor comparisons. The text in each box gives the same quantity as that coded by the color. Light colors present a security vulnerability to, for example, a passport gate.

Cross age FMR at threshold T = 1.301 for algorithm kakao\_001, giving FMR(T) = 0.0001 globally.

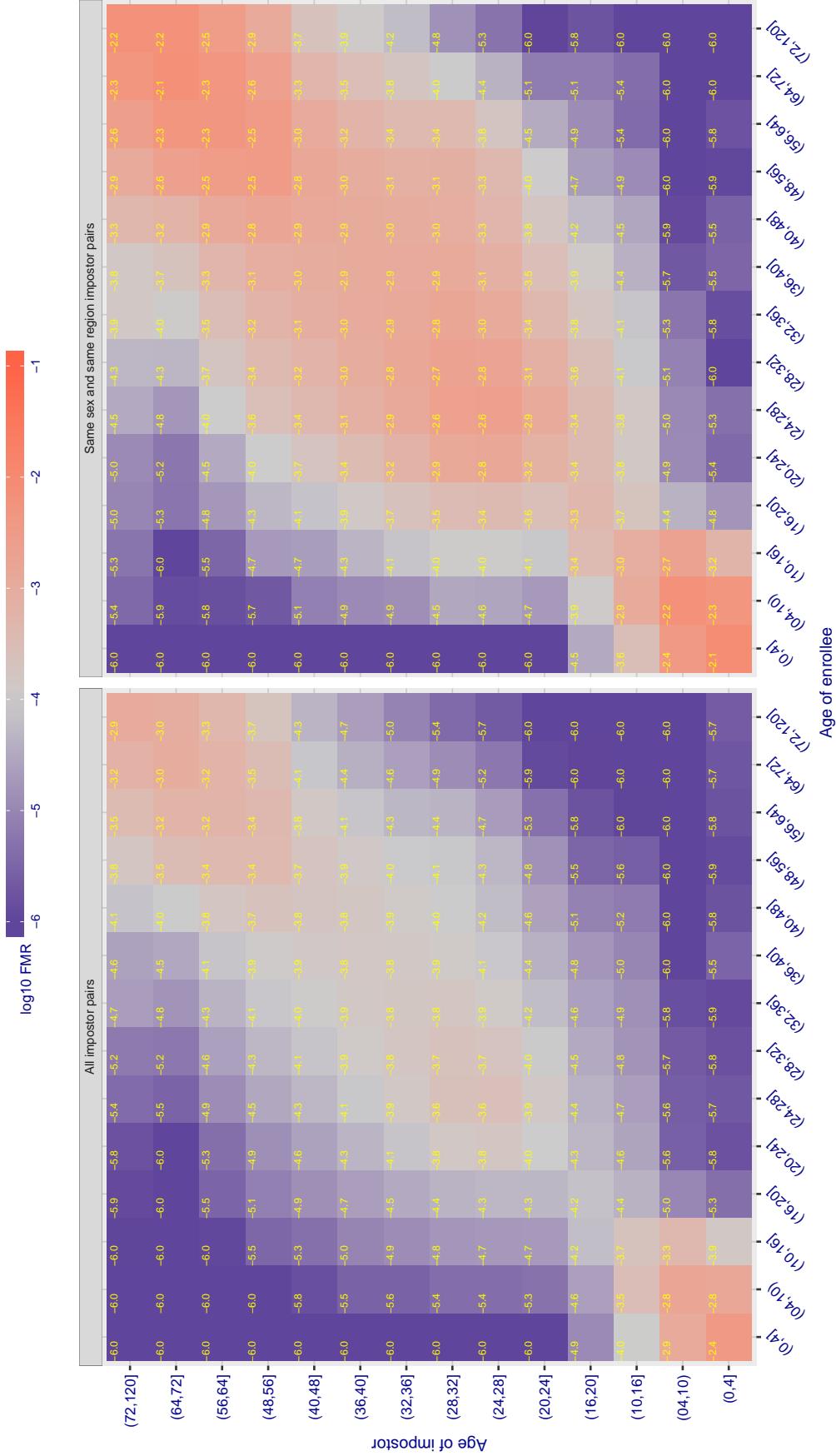


Figure 367: For algorithm kakao-001 operating on visa images, the heatmap shows false match observed over impostor comparisons of faces from different individuals who have the given age pair. False matches are counted against a recognition threshold fixed globally to give  $FMR = 0.001$  over all on the order of  $10^{10}$  impostor comparisons. The text in each box gives the same quantity as that coded by the color. Light colors present a security vulnerability to, for example, a passport gate.

Cross age FMR at threshold T = 0.701 for algorithm lookman\_002, giving FMR(T) = 0.0001 globally.

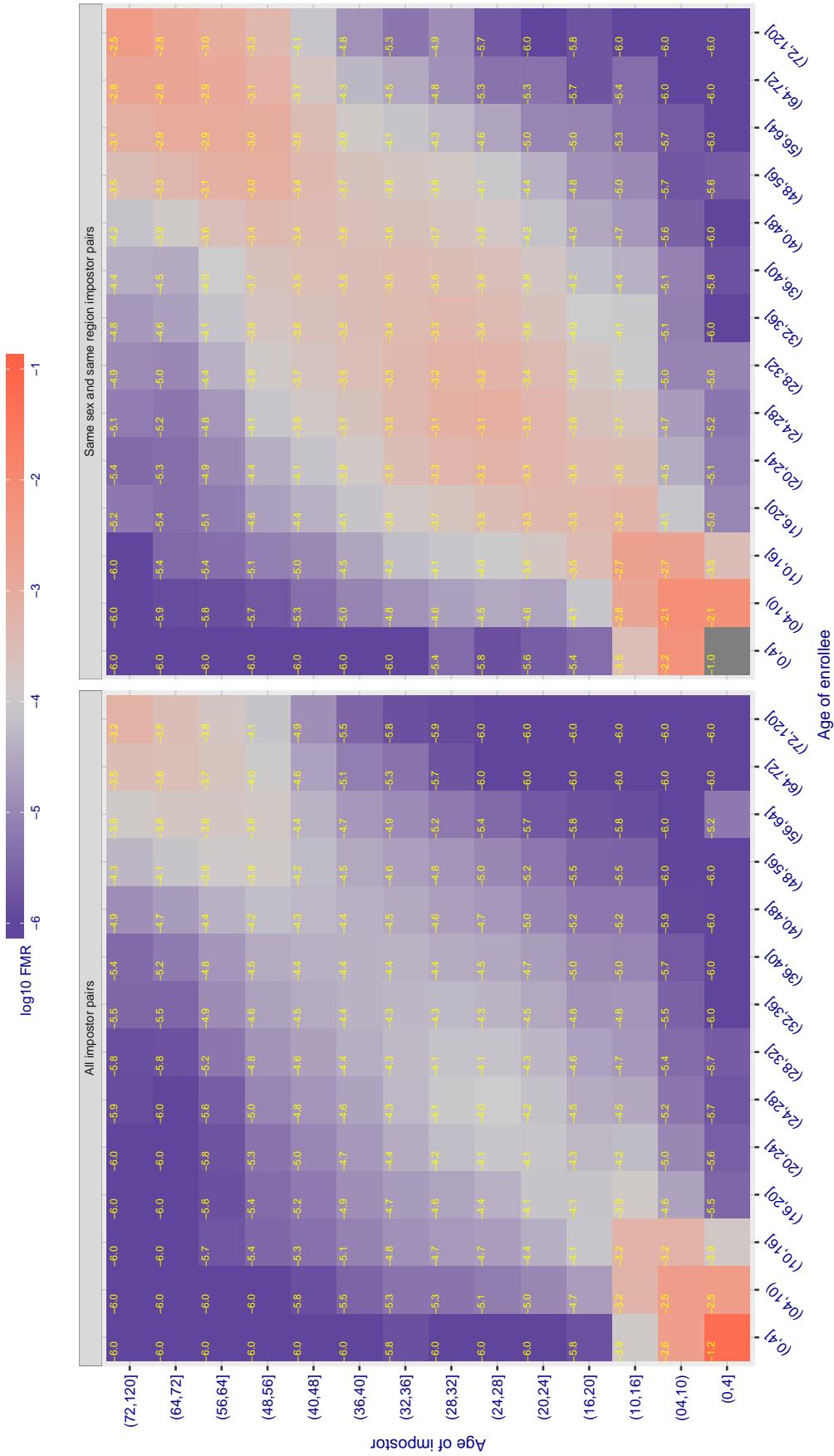


Figure 368: For algorithm lookman-002 operating on visa images, the heatmap shows false match observed over impostor comparisons of faces from different individuals who have the given age pair. False matches are counted against a recognition threshold fixed globally to give  $FMR = 0.001$  over all on the order of  $10^{10}$  impostor comparisons. The text in each box gives the same quantity as that coded by the color. Light colors present a security vulnerability to, for example, a passport gate.

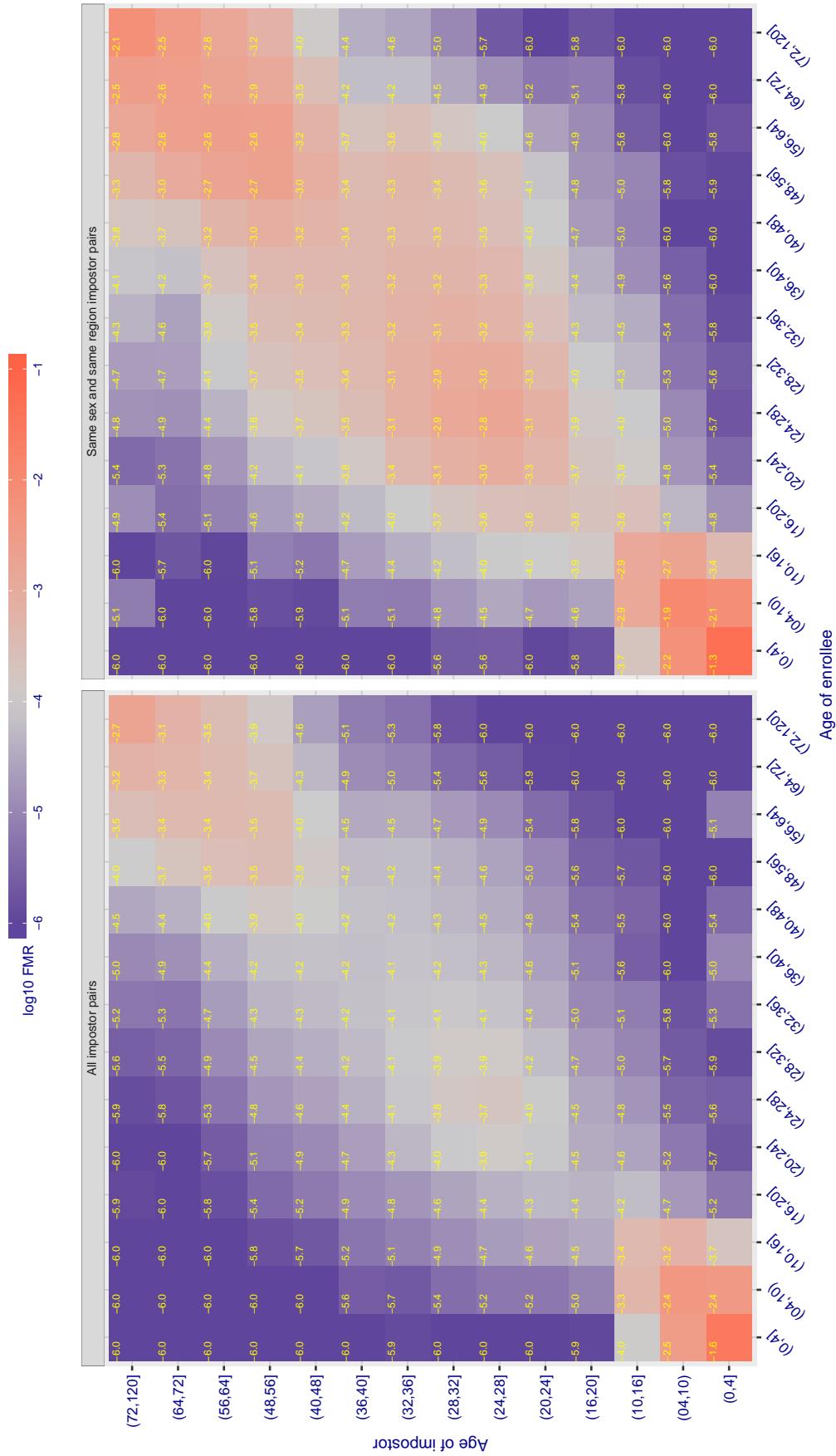
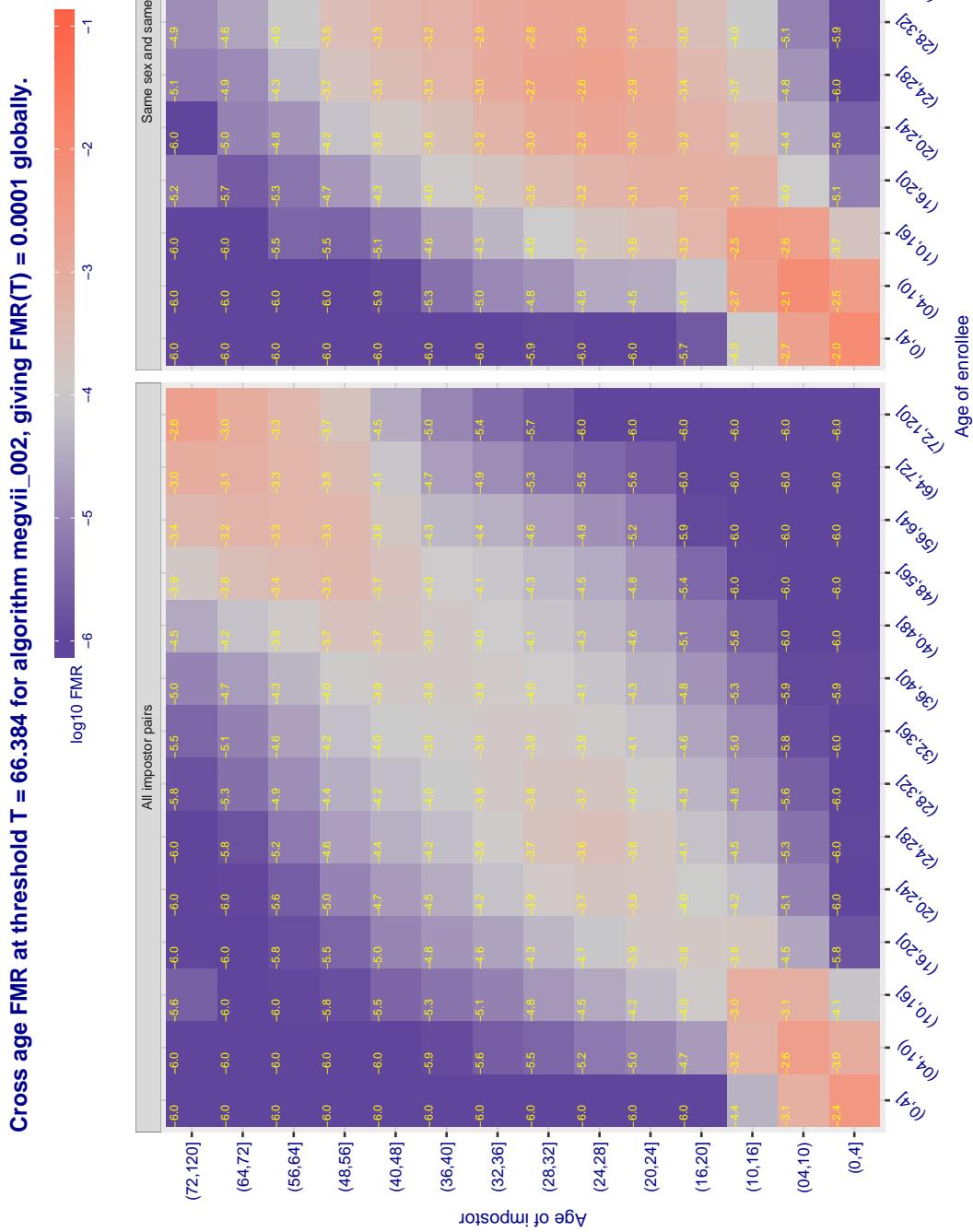
Cross age FMR at threshold T = 74.511 for algorithm megvii\_001, giving  $\text{FMR}(\text{T}) = 0.0001$  globally.

Figure 369: For algorithm megvii\_001 operating on visa images, the heatmap shows false match observed over impostor comparisons of faces from different individuals who have the given age pair. False matches are counted against a recognition threshold fixed globally to give  $\text{FMR} = 0.001$  over all on the order of  $10^{10}$  impostor comparisons. The text in each box gives the same quantity as that coded by the color. Light colors present a security vulnerability to, for example, a passport gate.



**Figure 370:** For algorithm megvii-002 operating on visa images, the heatmap shows false match observed over impostor comparisons of faces from different individuals who have the given age pair. False matches are counted against a recognition threshold fixed globally to give  $FMR = 0.001$  over all on the order of  $10^{10}$  impostor comparisons. The text in each box gives the same quantity as that coded by the color. Light colors present a security vulnerability to, for example, a passport gate.

Cross age FMR at threshold T = 0.425 for algorithm meiya\_001, giving FMR(T) = 0.0001 globally.

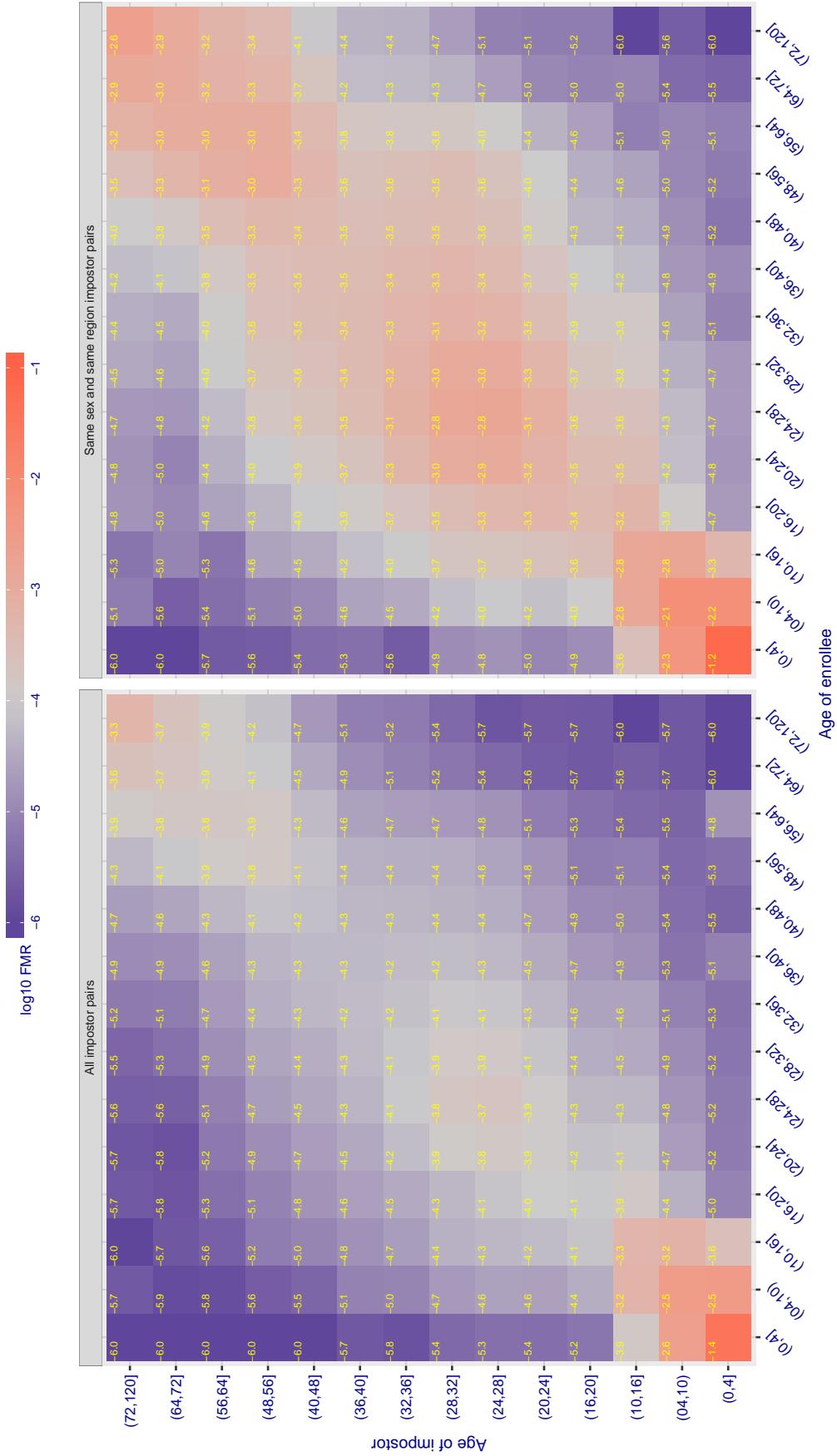


Figure 371: For algorithm meiya-001 operating on visa images, the heatmap shows false match observed over impostor comparisons of faces from different individuals who have the given age pair. False matches are counted against a recognition threshold fixed globally to give  $FMR = 0.001$  over all on the order of  $10^{10}$  impostor comparisons. The text in each box gives the same quantity as that coded by the color. Light colors present a security vulnerability to, for example, a passport gate.

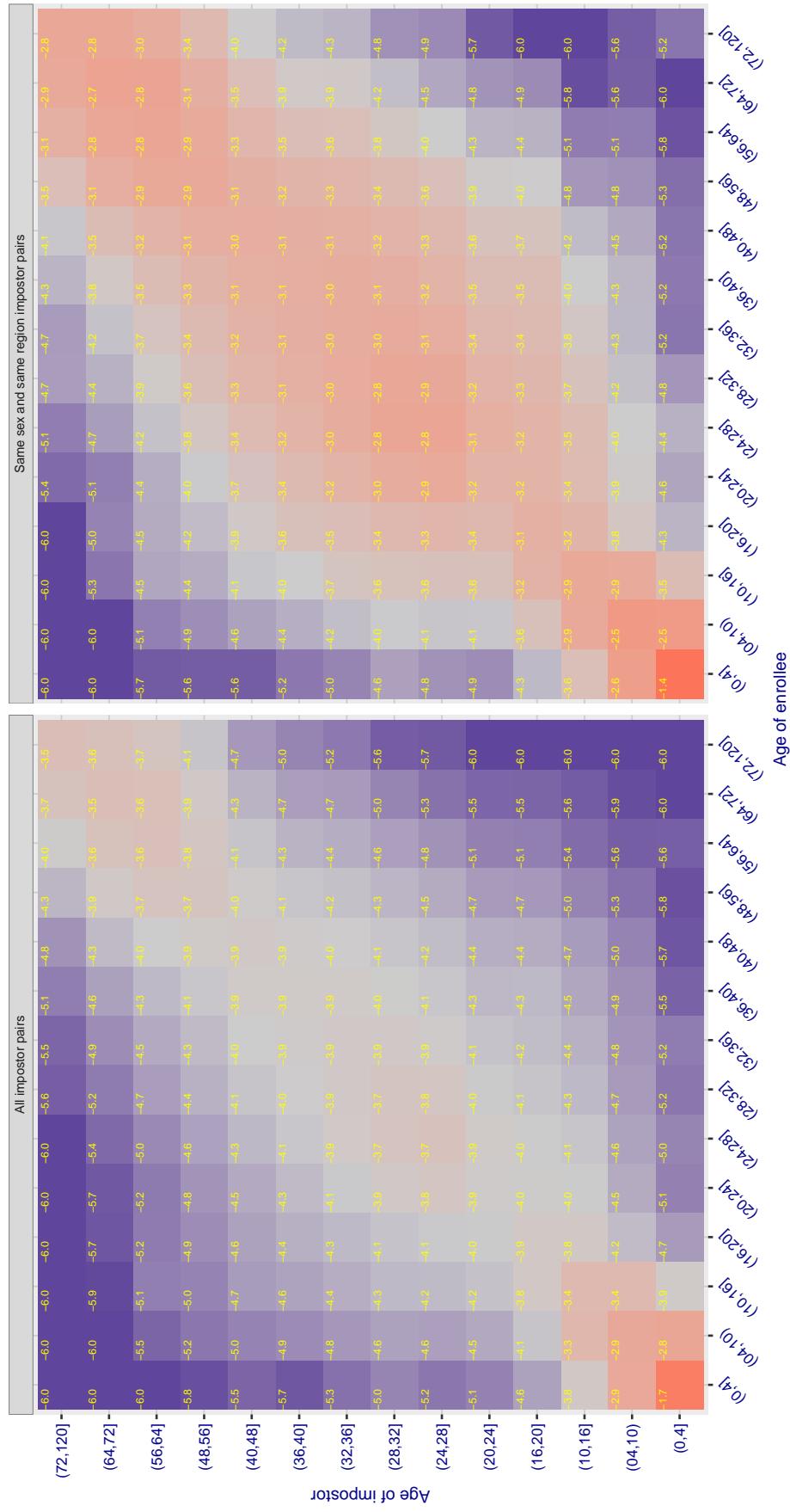
**Cross age FMR at threshold  $T = 0.668$  for algorithm microfocus\_001, giving  $\text{FMR}(T) = 0.0001$  globally.**

Figure 372: For algorithm microfocus-001 operating on visa images, the heatmap shows false match observed over imposter comparisons of faces from different individuals who have the given age pair. False matches are counted against a recognition threshold fixed globally to give  $\text{FMR} = 0.001$  over all on the order of  $10^{10}$  imposter comparisons. The text in each box gives the same quantity as that coded by the color. Light colors present a security vulnerability to, for example, a passport gate.

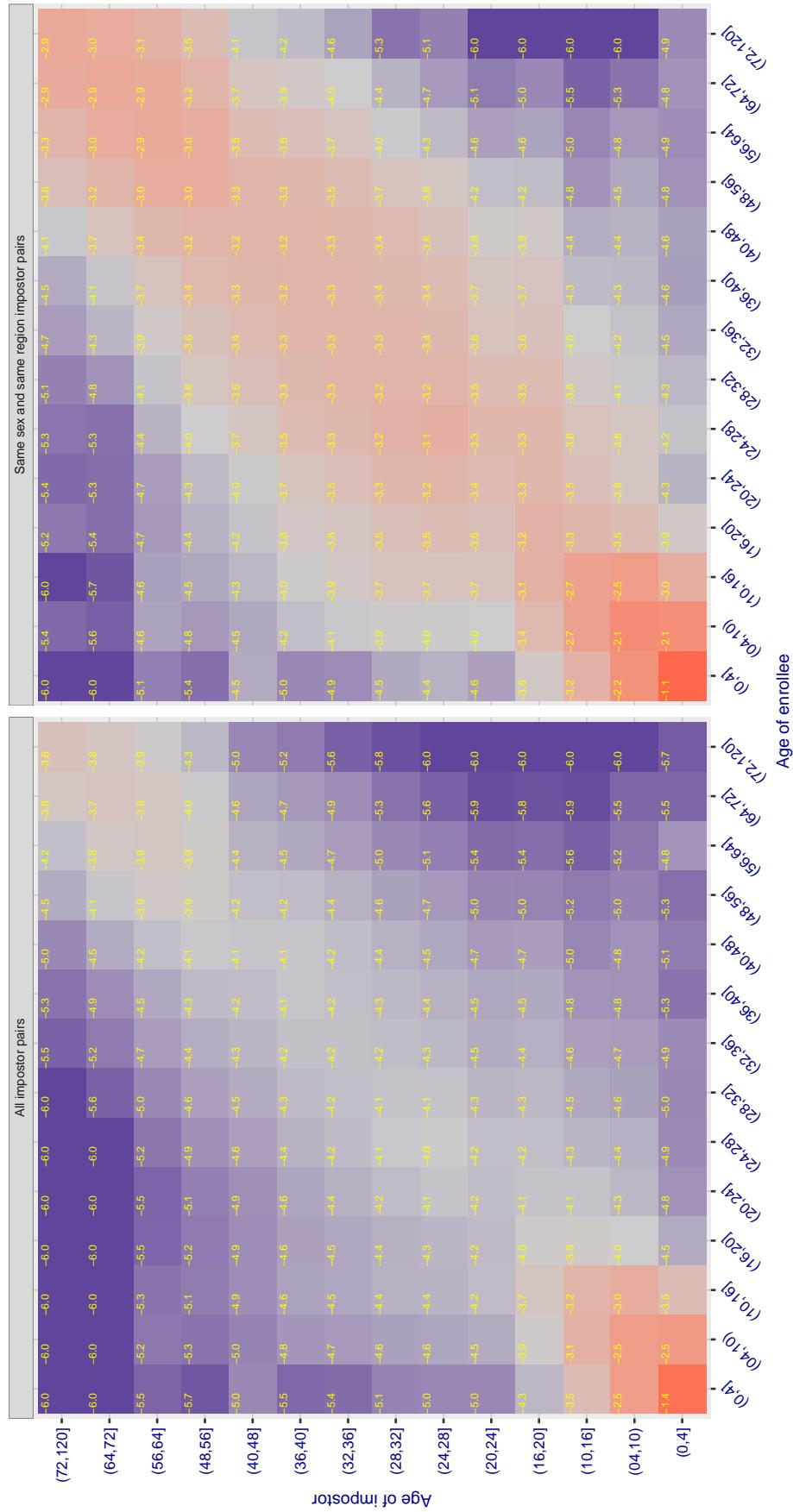
**Cross age FMR at threshold  $\tau = 0.602$  for algorithm microfocus\_002, giving  $FMR(T) = 0.0001$  globally.**

Figure 373: For algorithm microfocus-002 operating on visa images, the heatmap shows false match observed over imposter comparisons of faces from different individuals who have the given age pair. False matches are counted against a recognition threshold fixed globally to give  $FMR = 0.001$  over all on the order of  $10^{10}$  imposter comparisons. The text in each box gives the same quantity as that coded by the color. Light colors present a security vulnerability to, for example, a passport gate.

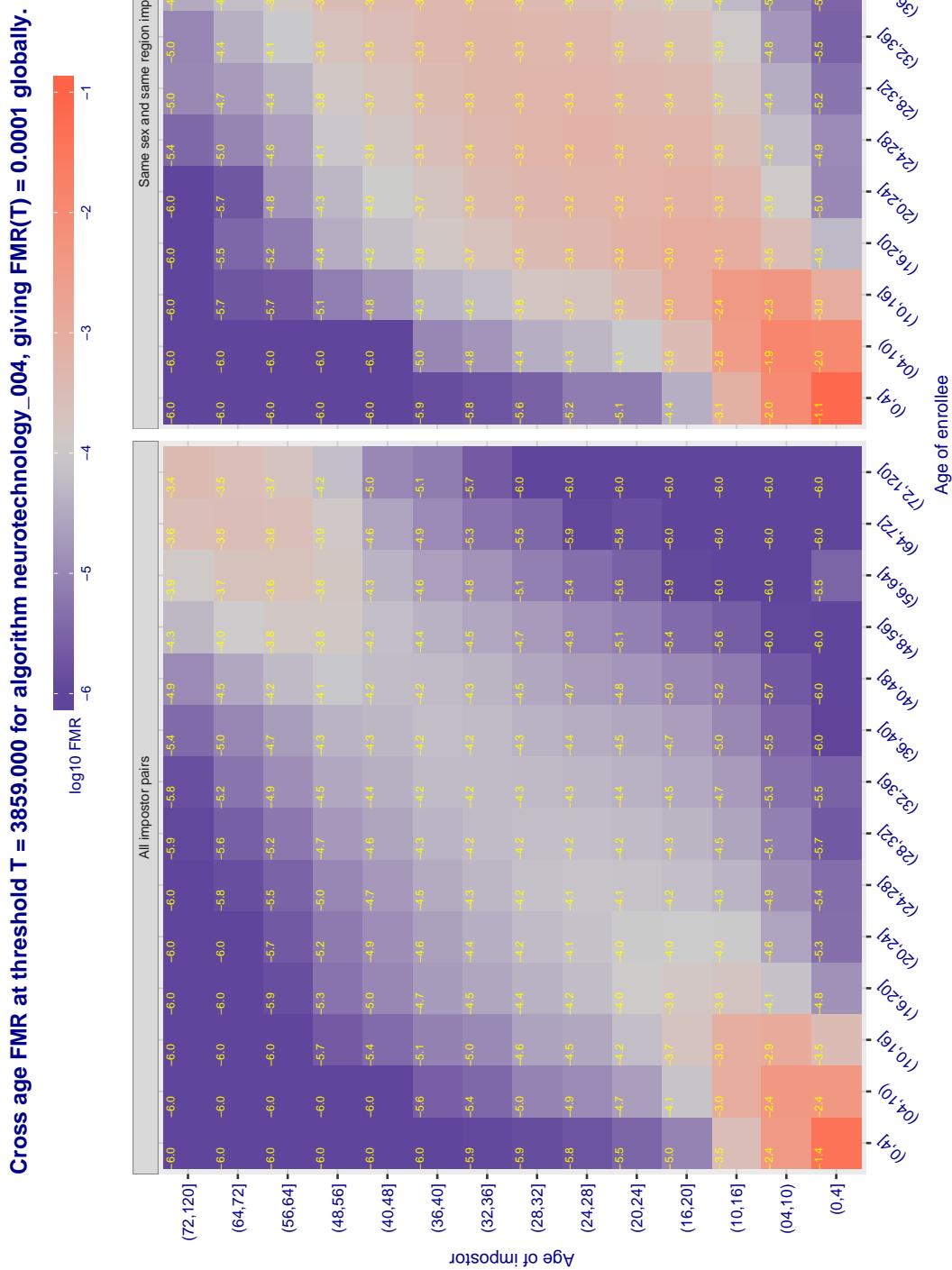


Figure 374: For algorithm neurotechnology-004 operating on visa images, the heatmap shows false match observed over impostor comparisons of faces from different individuals who have the given age pair. False matches are counted against a recognition threshold fixed globally to give  $FMR = 0.001$  over all on the order of  $10^{10}$  impostor comparisons. The text in each box gives the same quantity as that coded by the color. Light colors present a security vulnerability to, for example, a passport gate.

Cross age FMR at threshold T = 1.000 for algorithm nodeflux\_001, giving FMR(T) = 0.0001 globally.

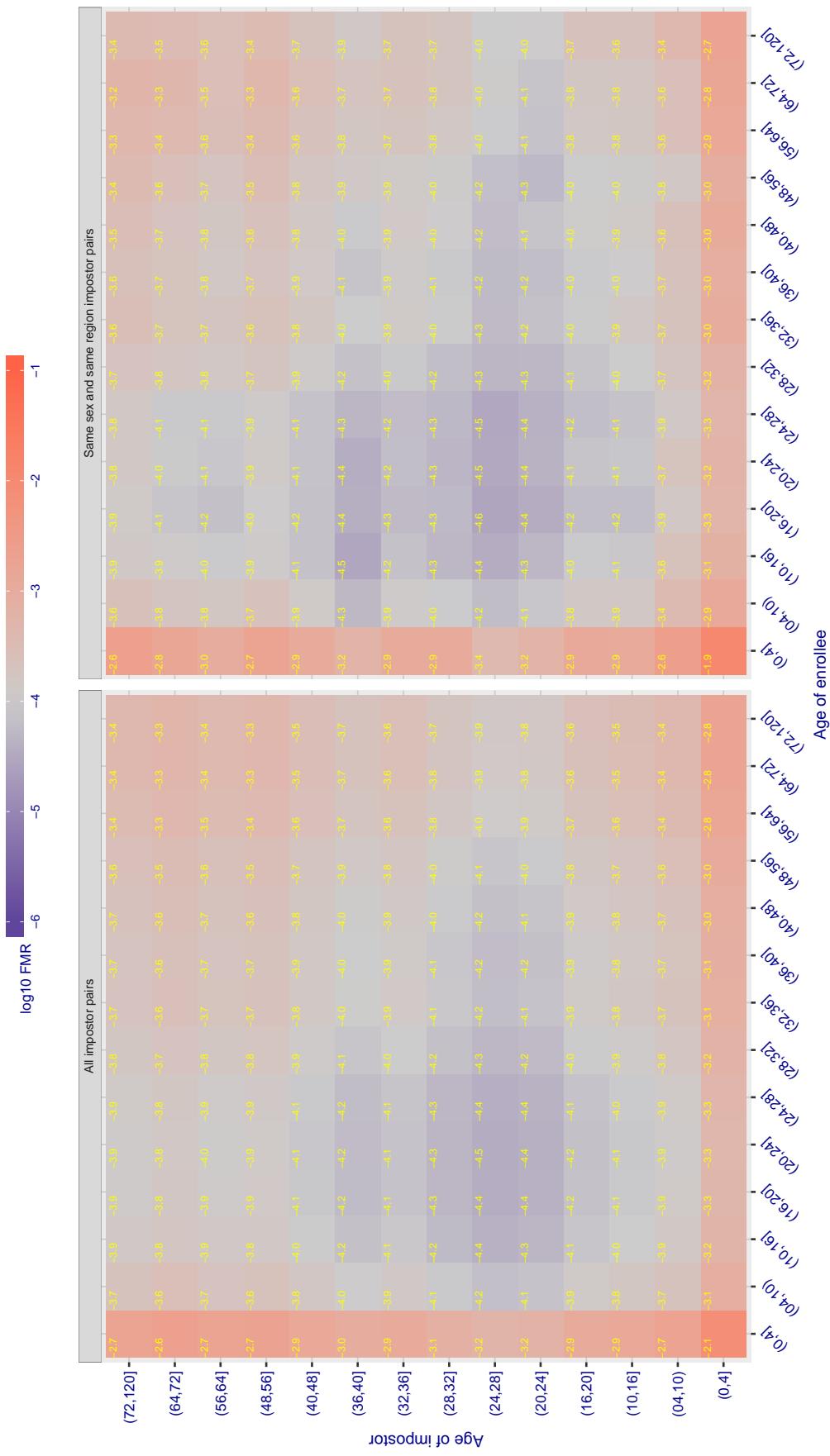


Figure 375: For algorithm nodeflux-001 operating on visa images, the heatmap shows false match observed over impostor comparisons of faces from different individuals who have the given age pair. False matches are counted against a recognition threshold fixed globally to give  $FMR = 0.001$  over all on the order of  $10^{10}$  impostor comparisons. The text in each box gives the same quantity as that coded by the color. Light colors present a security vulnerability to, for example, a passport gate.

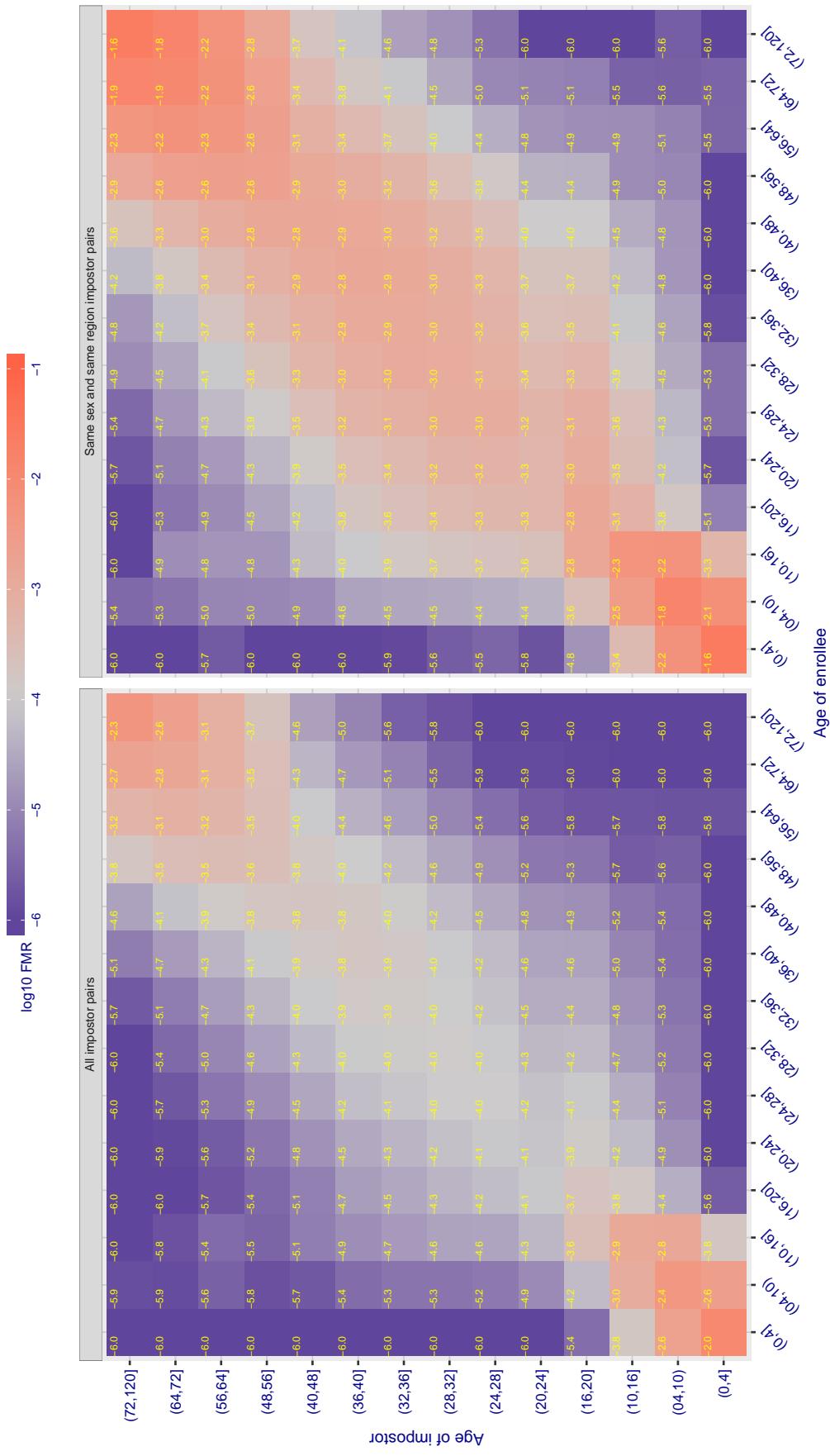
Cross age FMR at threshold T = 1.487 for algorithm ntechlab\_005, giving  $FMR(T) = 0.0001$  globally.

Figure 376: For algorithm ntechlab-005 operating on visa images, the heatmap shows false match observed over impostor comparisons of faces from different individuals who have the given age pair. False matches are counted against a recognition threshold fixed globally to give  $FMR = 0.001$  over all on the order of  $10^{10}$  impostor comparisons. The text in each box gives the same quantity as that coded by the color. Light colors present a security vulnerability to, for example, a passport gate.

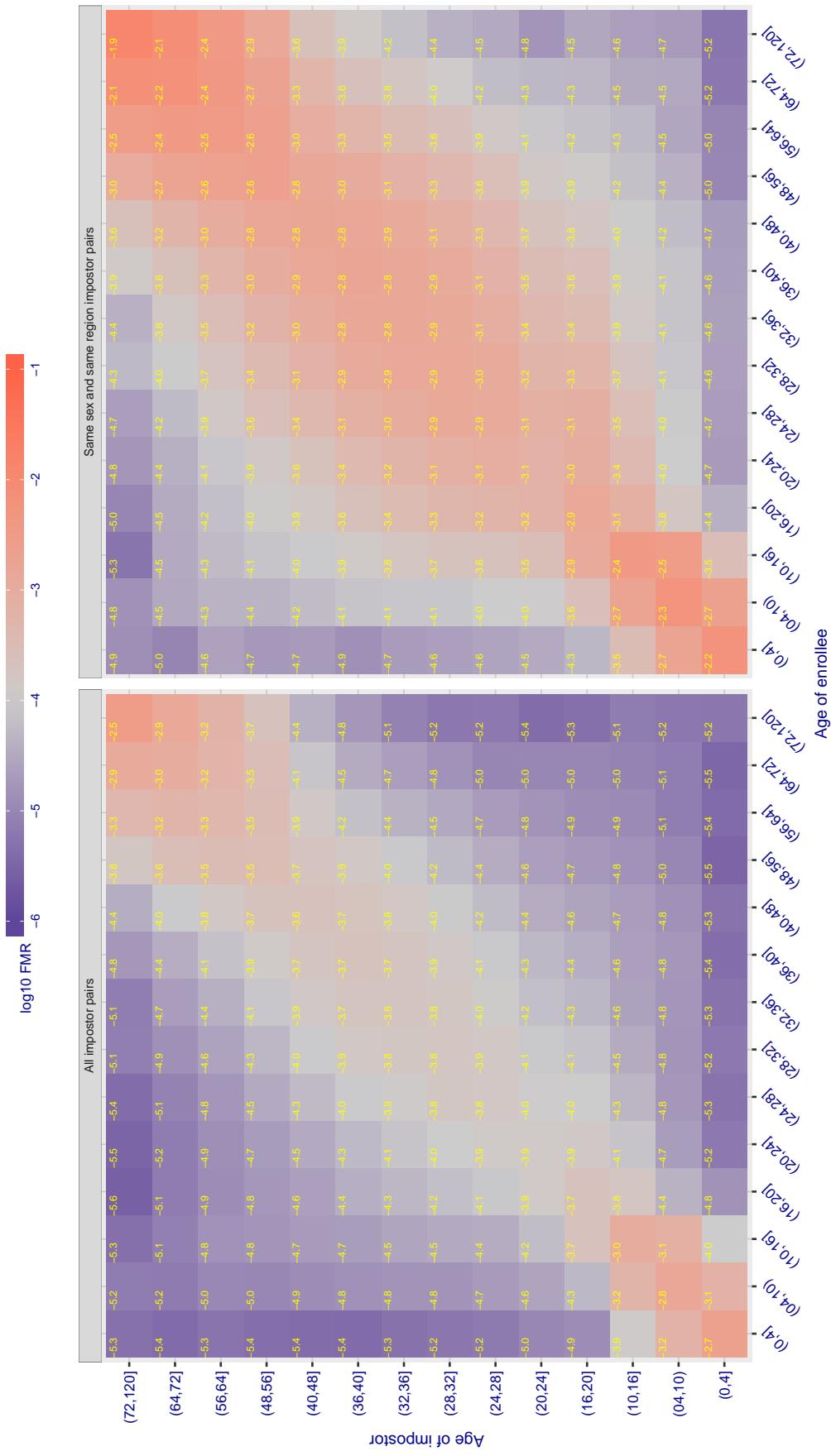
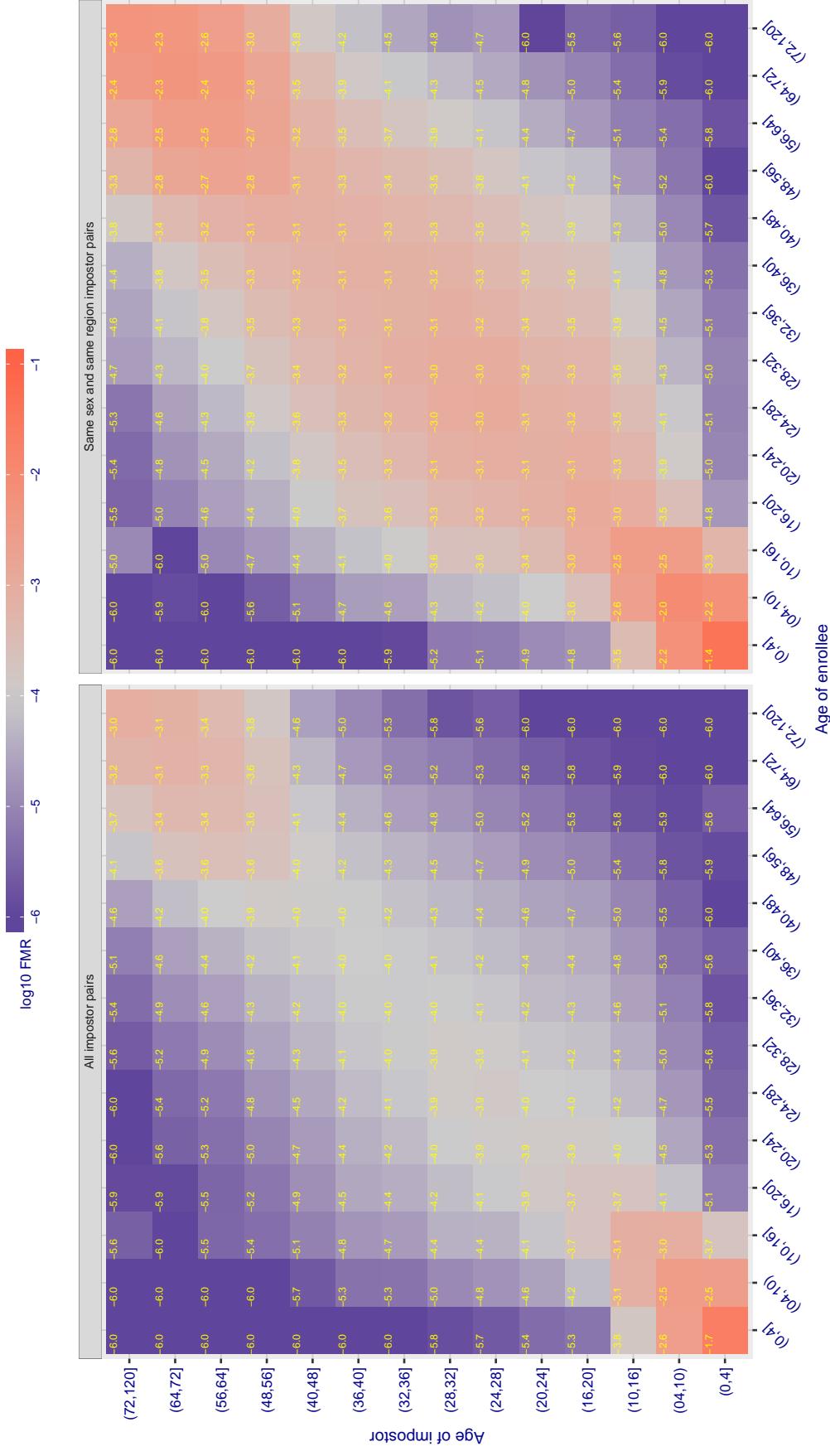
Cross age FMR at threshold T = 1.997 for algorithm ntechlab\_006, giving  $FMR(T) = 0.0001$  globally.

Figure 377: For algorithm ntechlab-006 operating on visa images, the heatmap shows false match observed over impostor comparisons of faces from different individuals who have the given age pair. False matches are counted against a recognition threshold fixed globally to give  $FMR = 0.001$  over all on the order of  $10^{10}$  impostor comparisons. The text in each box gives the same quantity as that coded by the color. Light colors present a security vulnerability to, for example, a passport gate.



**Figure 378:** For algorithm *psi-001* operating on visa images, the heatmap shows false match observed over impostor comparisons of faces from different individuals who have the given age pair. False matches are counted against a recognition threshold fixed globally to give  $FMR = 0.001$  over all on the order of  $10^{10}$  impostor comparisons. The text in each box gives the same quantity as that coded by the color. Light colors present a security vulnerability to, for example, a passport gate.

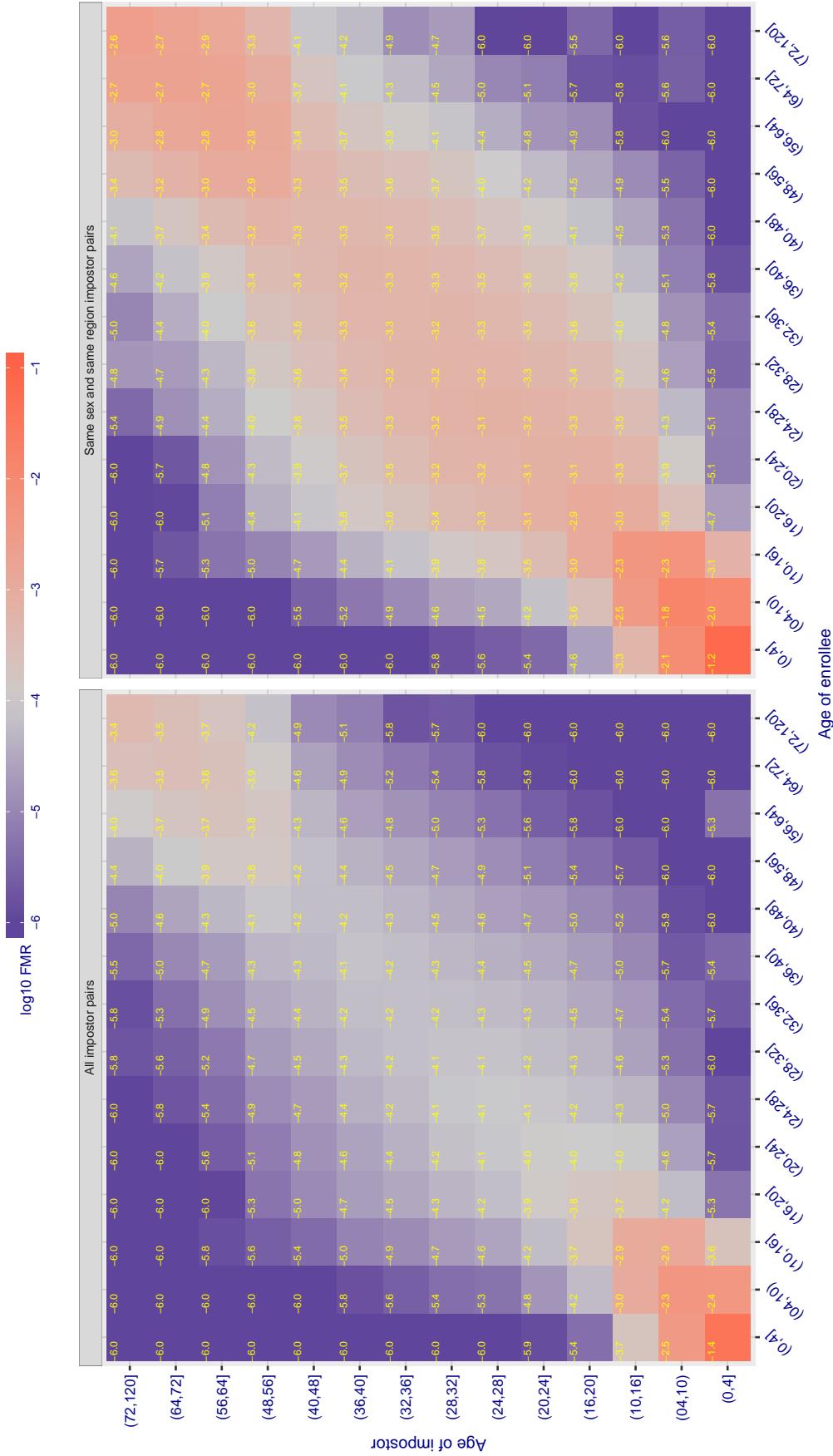
Cross age FMR at threshold T = 0.353 for algorithm psl\_002, giving  $\text{FMR}(\text{T}) = 0.00001$  globally.

Figure 379: For algorithm psl\_002 operating on visa images, the heatmap shows false match observed over impostor comparisons of faces from different individuals who have the given age pair. False matches are counted against a recognition threshold fixed globally to give  $\text{FMR} = 0.001$  over all on the order of  $10^{10}$  impostor comparisons. The text in each box gives the same quantity as that coded by the color. Light colors present a security vulnerability to, for example, a passport gate.

Cross age FMR at threshold T = 0.779 for algorithm rankone\_006, giving FMR(T) = 0.0001 globally.

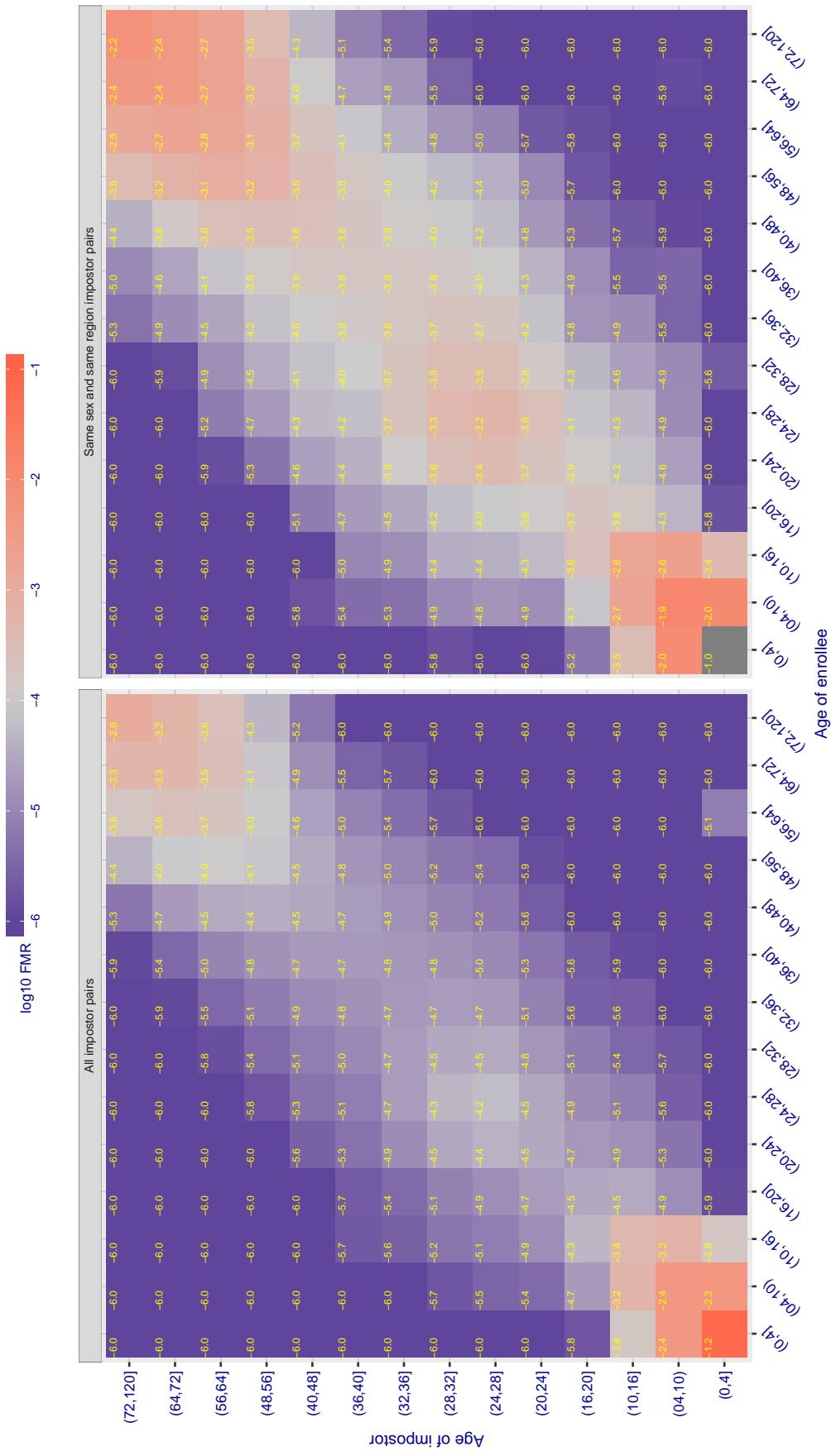


Figure 380: For algorithm rankone-006 operating on visa images, the heatmap shows false match observed over impostor comparisons of faces from different individuals who have the given age pair. False matches are counted against a recognition threshold fixed globally to give FMR = 0.001 over all on the order of  $10^{10}$  impostor comparisons. The text in each box gives the same quantity as that coded by the color. Light colors present a security vulnerability to, for example, a passport gate.

**Cross age FMR at threshold  $T = 0.885$  for algorithm `realmnetworks_001`, giving  $FMR(T) = 0.00001$  globally.**

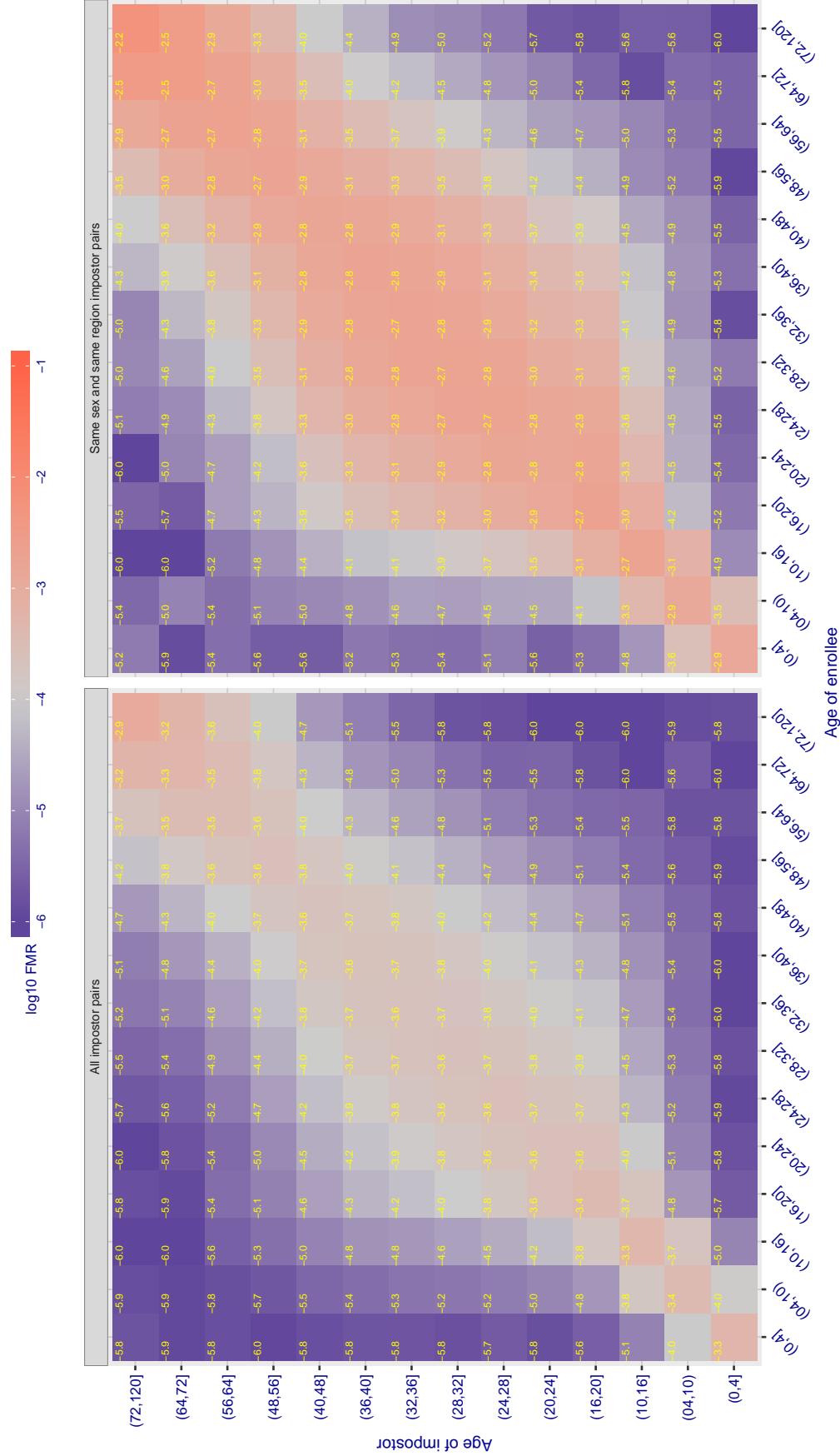


Figure 381: For algorithm `realmnetworks-001` operating on visa images, the heatmap shows false match observed over impostor comparisons of faces from different individuals who have the given age pair. False matches are counted against a recognition threshold fixed globally to give  $FMR = 0.001$  over all on the order of  $10^{10}$  impostor comparisons. The text in each box gives the same quantity as that coded by the color. Light colors present a security vulnerability to, for example, a passport gate.

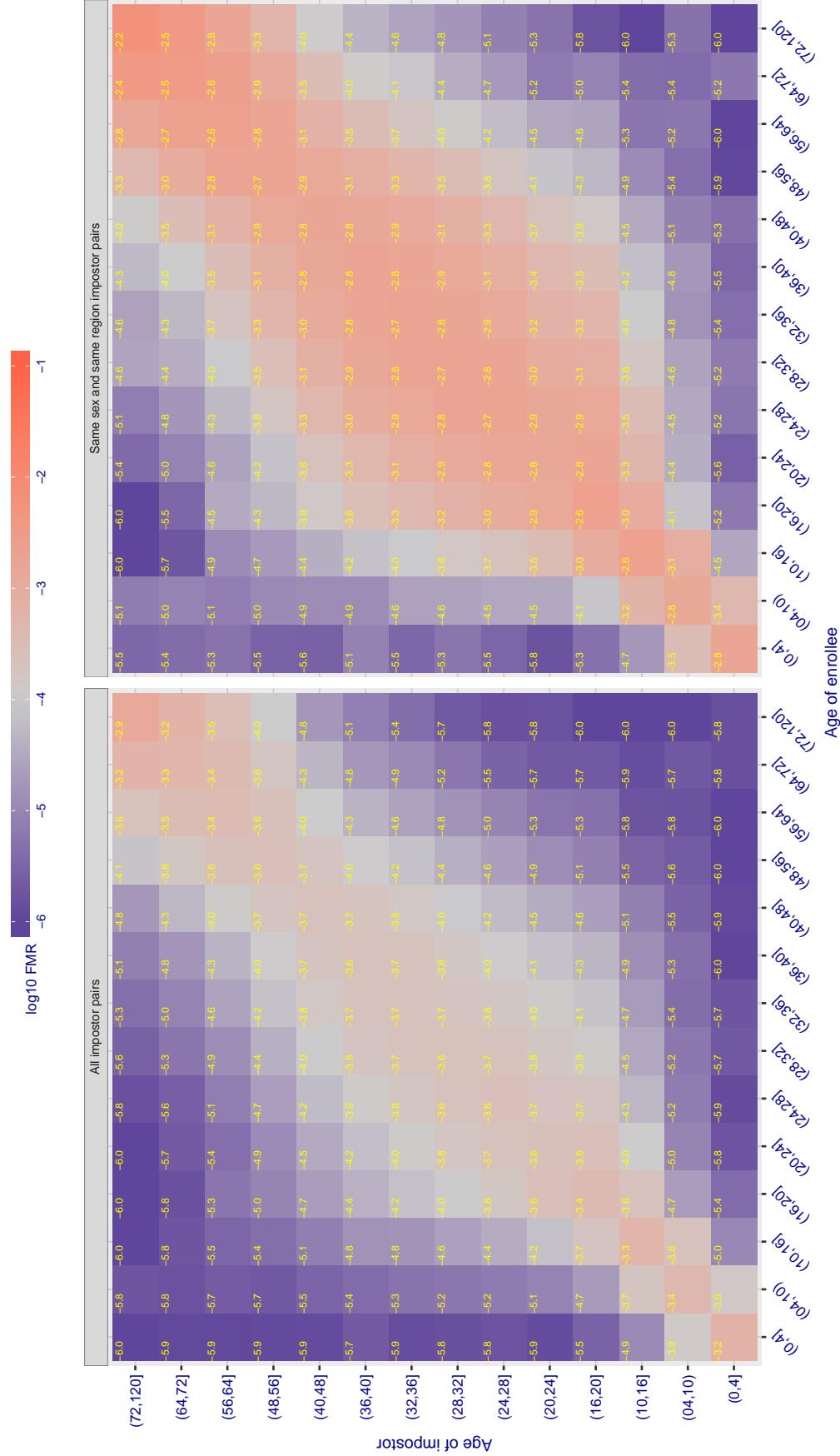
**Cross age FMR at threshold  $T = 0.883$  for algorithm reanetworks\_002, giving  $FMR(T) = 0.0001$  globally.**

Figure 382: For algorithm reanetworks-002 operating on visa images, the heatmap shows false match observed over impostor comparisons of faces from different individuals who have the given age pair. False matches are counted against a recognition threshold fixed globally to give  $FMR = 0.001$  over all on the order of  $10^{10}$  impostor comparisons. The text in each box gives the same quantity as that coded by the color. Light colors present a security vulnerability to, for example, a passport gate.

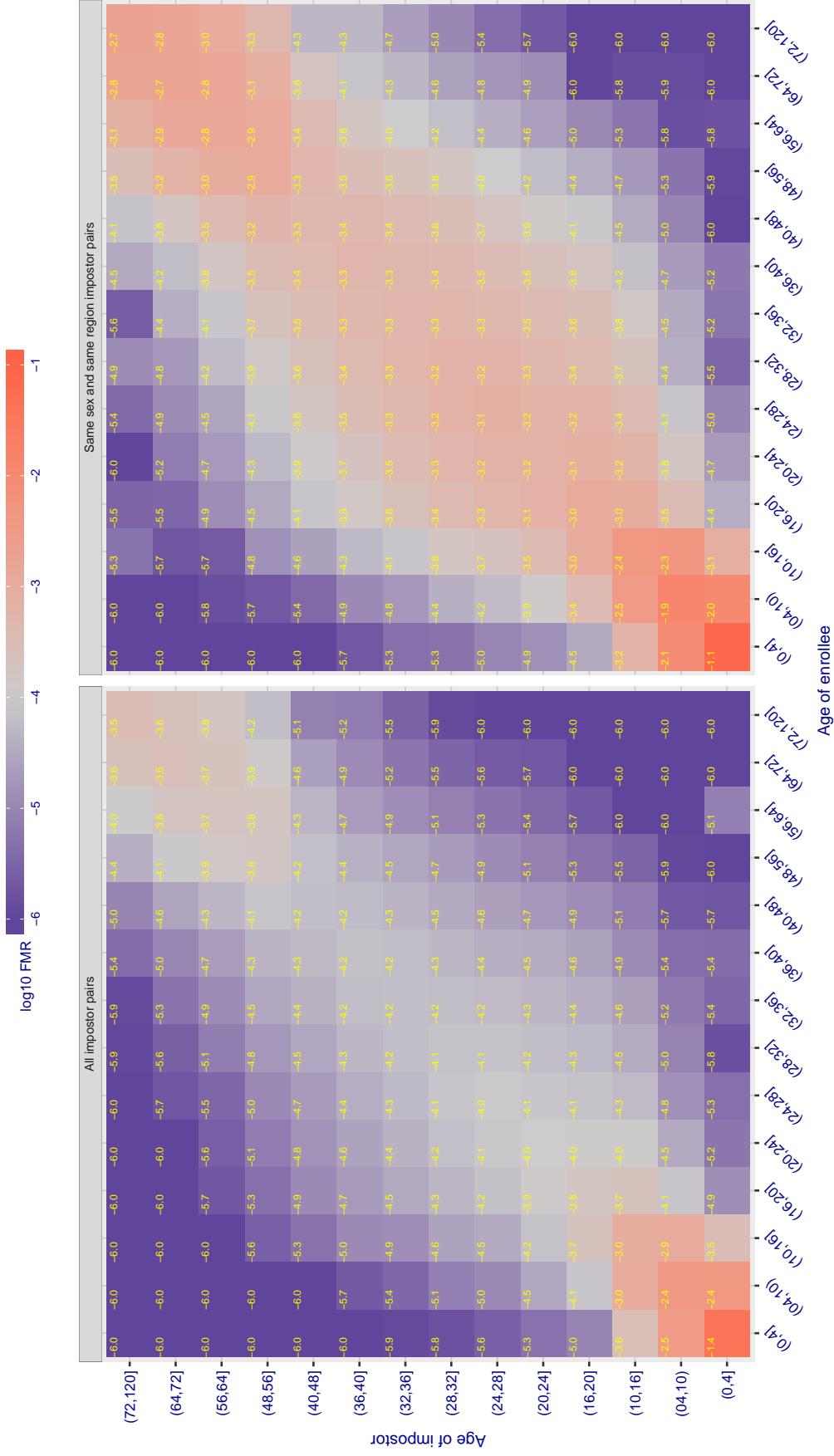
Cross age FMR at threshold T = 70.373 for algorithm remarkai\_000, giving  $\text{FMR}(T) = 0.0001$  globally.

Figure 383: For algorithm remarkai-000 operating on visa images, the heatmap shows false match observed over impostor comparisons of faces from different individuals who have the given age pair. False matches are counted against a recognition threshold fixed globally to give  $\text{FMR} = 0.001$  over all on the order of  $10^{10}$  impostor comparisons. The text in each box gives the same quantity as that coded by the color. Light colors present a security vulnerability to, for example, a passport gate.

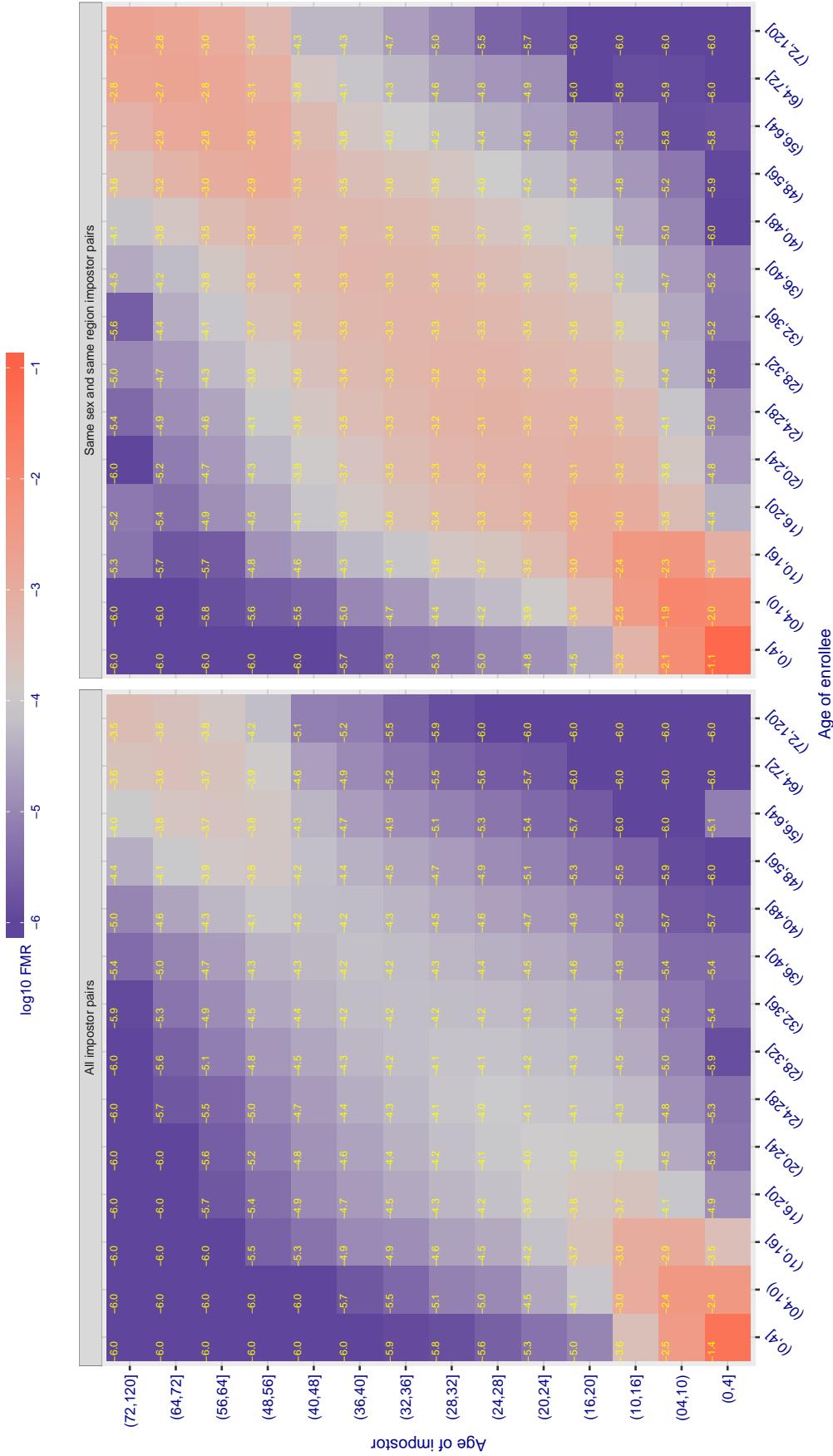
Cross age FMR at threshold T = 70.384 for algorithm remarkai\_001, giving  $\text{FMR}(T) = 0.0001$  globally.

Figure 384: For algorithm remarkai-001 operating on visa images, the heatmap shows false match observed over impostor comparisons of faces from different individuals who have the given age pair. False matches are counted against a recognition threshold fixed globally to give  $\text{FMR} = 0.001$  over all on the order of  $10^{10}$  impostor comparisons. The text in each box gives the same quantity as that coded by the color. Light colors present a security vulnerability to, for example, a passport gate.

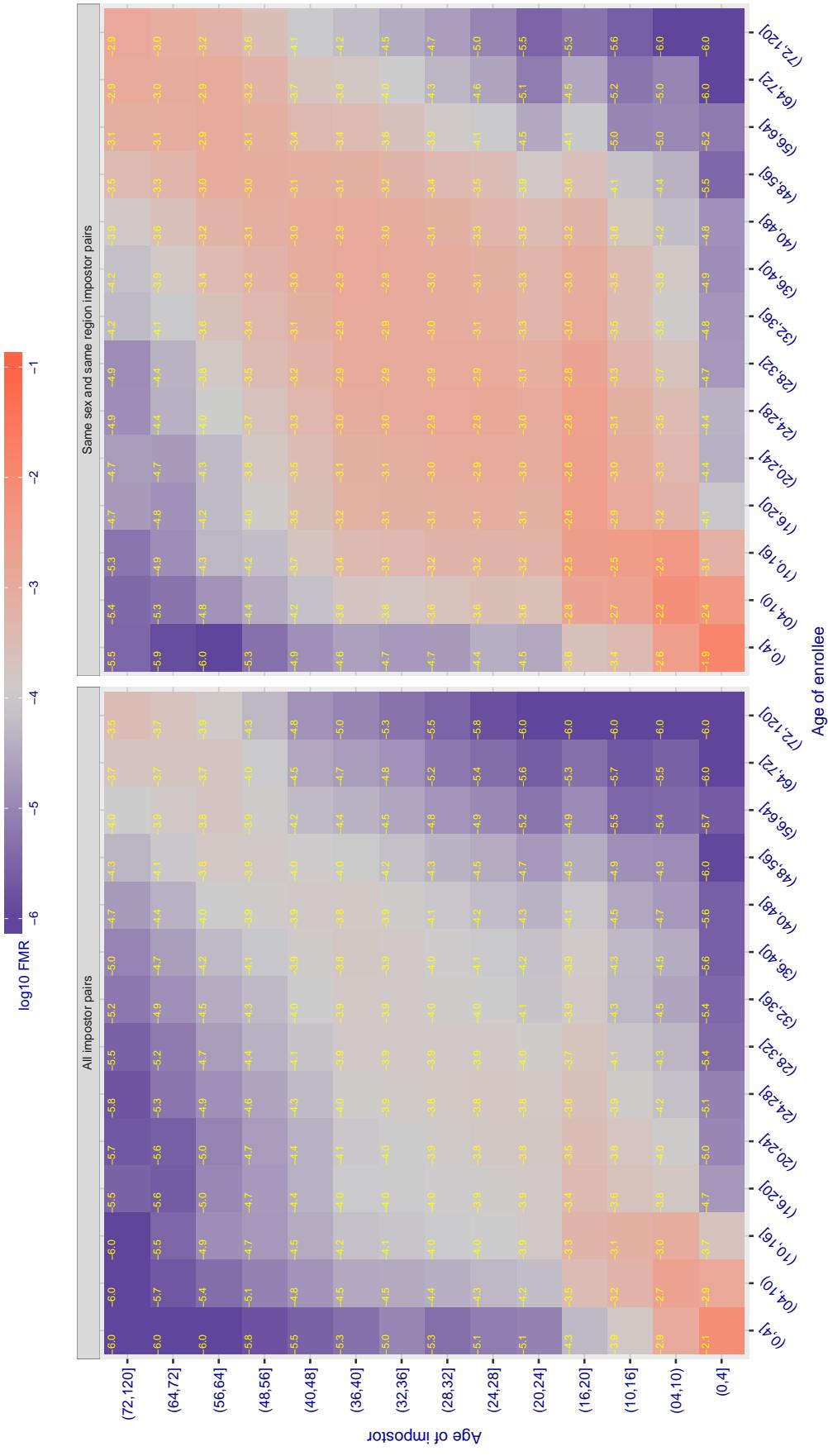


Figure 385: For algorithm safe-001 operating on visa images, the heatmap shows false match observed over impostor comparisons of faces from different individuals who have the given age pair. False matches are counted against a recognition threshold fixed globally to give  $FMR = 0.001$  over all on the order of  $10^{10}$  impostor comparisons. The text in each box gives the same quantity as that coded by the color. Light colors present a security vulnerability to, for example, a passport gate.

Cross age FMR at threshold T = 0.383 for algorithm saffe\_002, giving FMR(T) = 0.0001 globally.

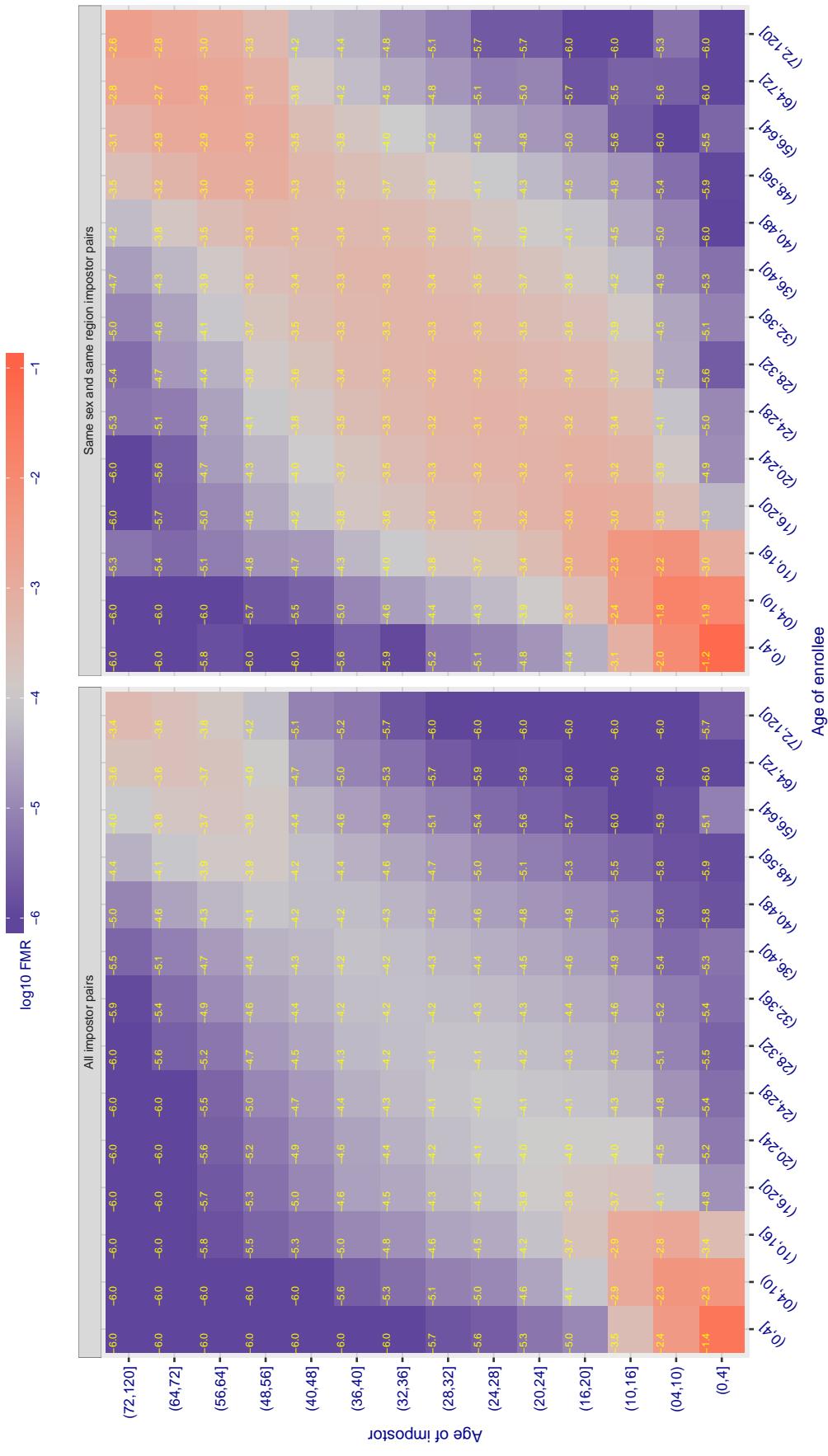


Figure 386: For algorithm saffe-002 operating on visa images, the heatmap shows false match observed over impostor comparisons of faces from different individuals who have the given age pair. False matches are counted against a recognition threshold fixed globally to give FMR = 0.001 over all on the order of  $10^{10}$  impostor comparisons. The text in each box gives the same quantity as that coded by the color. Light colors present a security vulnerability to, for example, a passport gate.

Cross age FMR at threshold T = 0.390 for algorithm sensetime\_001, giving  $\text{FMR}(T) = 0.00001$  globally.

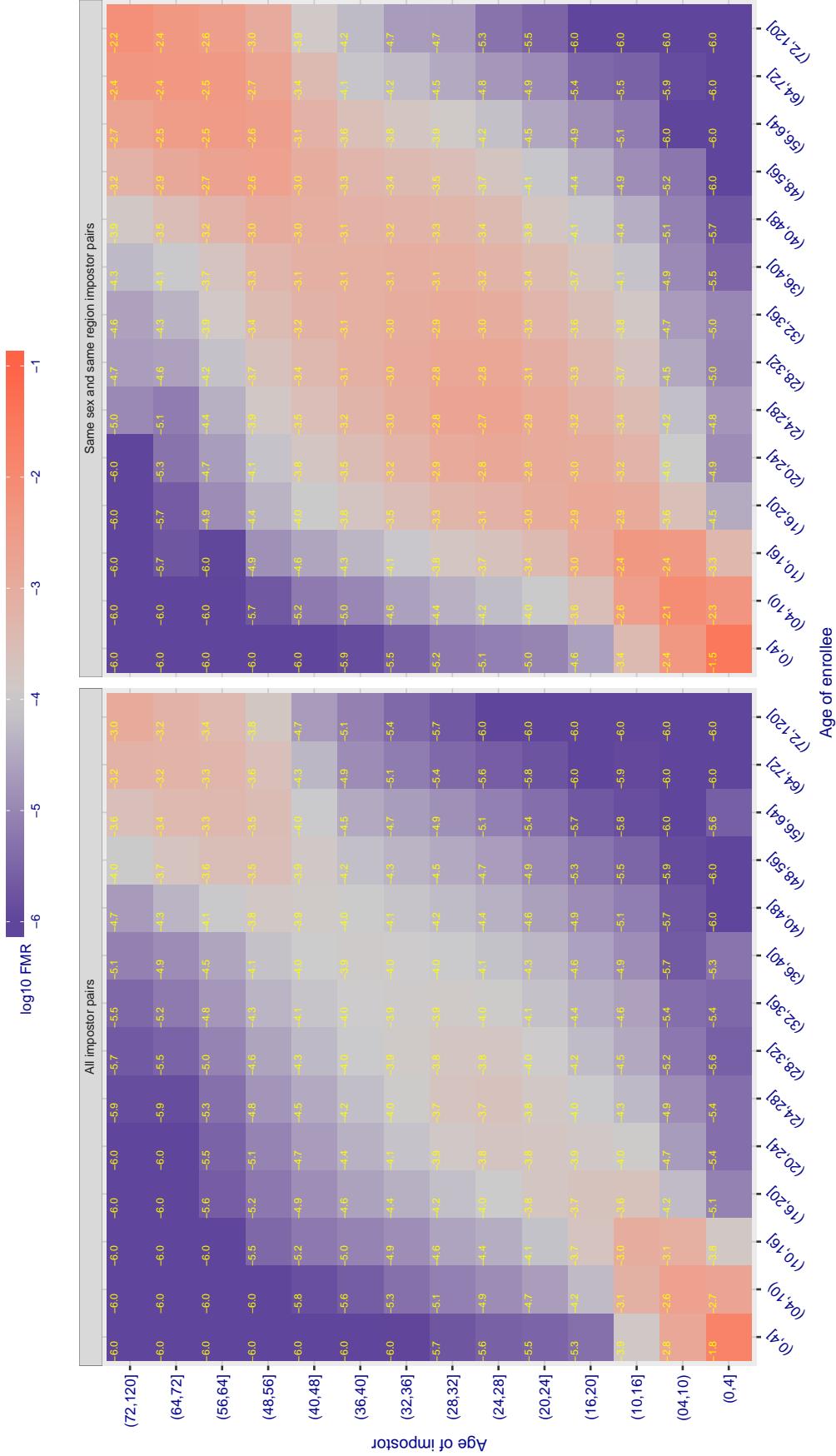


Figure 387: For algorithm sensetime-001 operating on visa images, the heatmap shows false match observed over impostor comparisons of faces from different individuals who have the given age pair. False matches are counted against a recognition threshold fixed globally to give  $\text{FMR} = 0.001$  over all on the order of  $10^{10}$  impostor comparisons. The text in each box gives the same quantity as that coded by the color. Light colors present a security vulnerability to, for example, a passport gate.

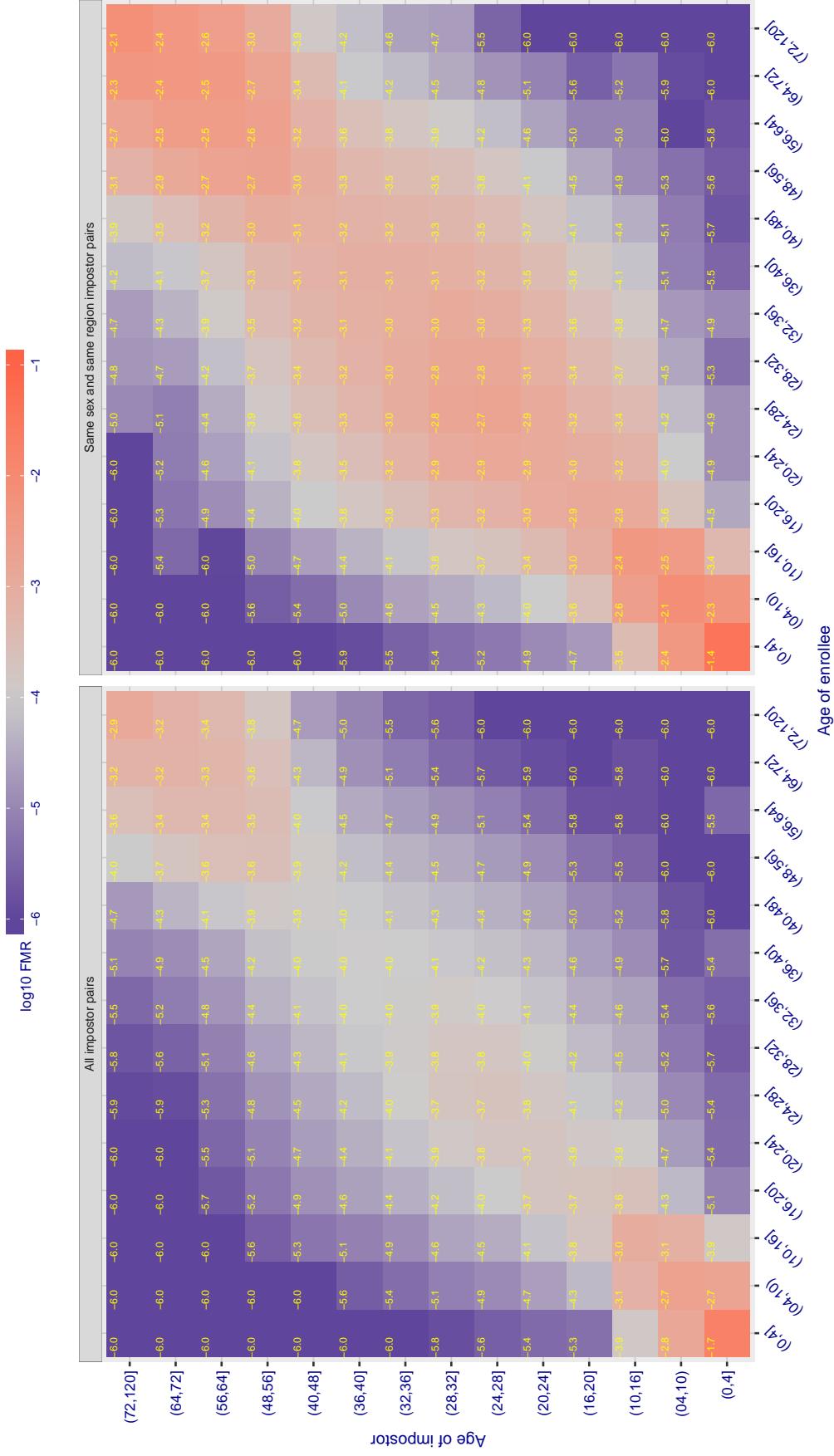
Cross age FMR at threshold T = 0.390 for algorithm sensetime\_002, giving  $FMR(T) = 0.00001$  globally.

Figure 388: For algorithm sensetime-002 operating on visa images, the heatmap shows false match observed over impostor comparisons of faces from different individuals who have the given age pair. False matches are counted against a recognition threshold fixed globally to give  $FMR = 0.001$  over all on the order of  $10^{10}$  impostor comparisons. The text in each box gives the same quantity as that coded by the color. Light colors present a security vulnerability to, for example, a passport gate.

Cross age FMR at threshold T = 0.970 for algorithm shaman\_000, giving FMR(T) = 0.0001 globally.

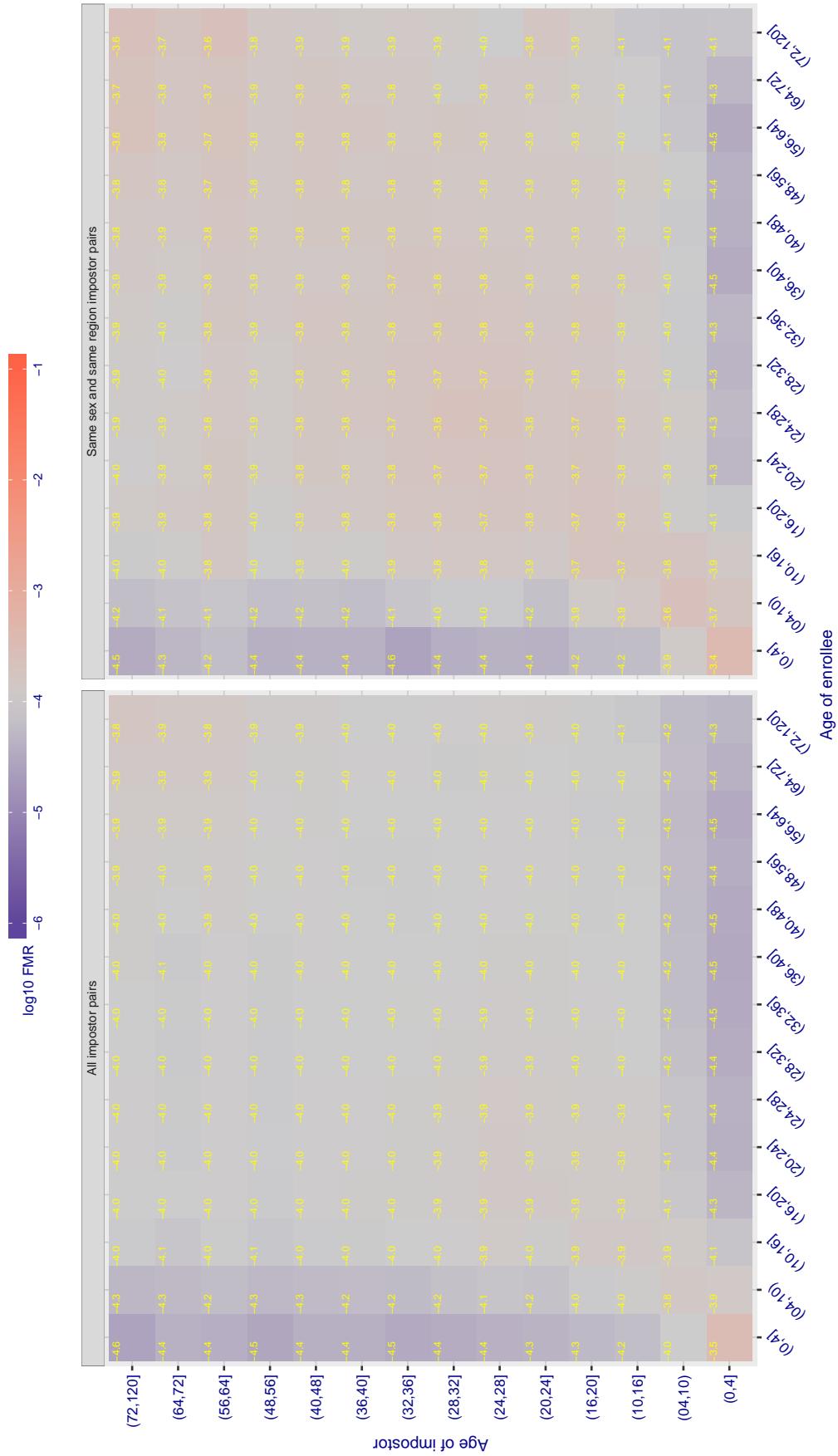


Figure 389: For algorithm shaman-000 operating on visa images, the heatmap shows false match observed over impostor comparisons of faces from different individuals who have the given age pair. False matches are counted against a recognition threshold fixed globally to give FMR = 0.001 over all on the order of  $10^{10}$  impostor comparisons. The text in each box gives the same quantity as that coded by the color. Light colors present a security vulnerability to, for example, a passport gate.

Cross age FMR at threshold T = 0.725 for algorithm shaman\_001, giving FMR(T) = 0.0001 globally.

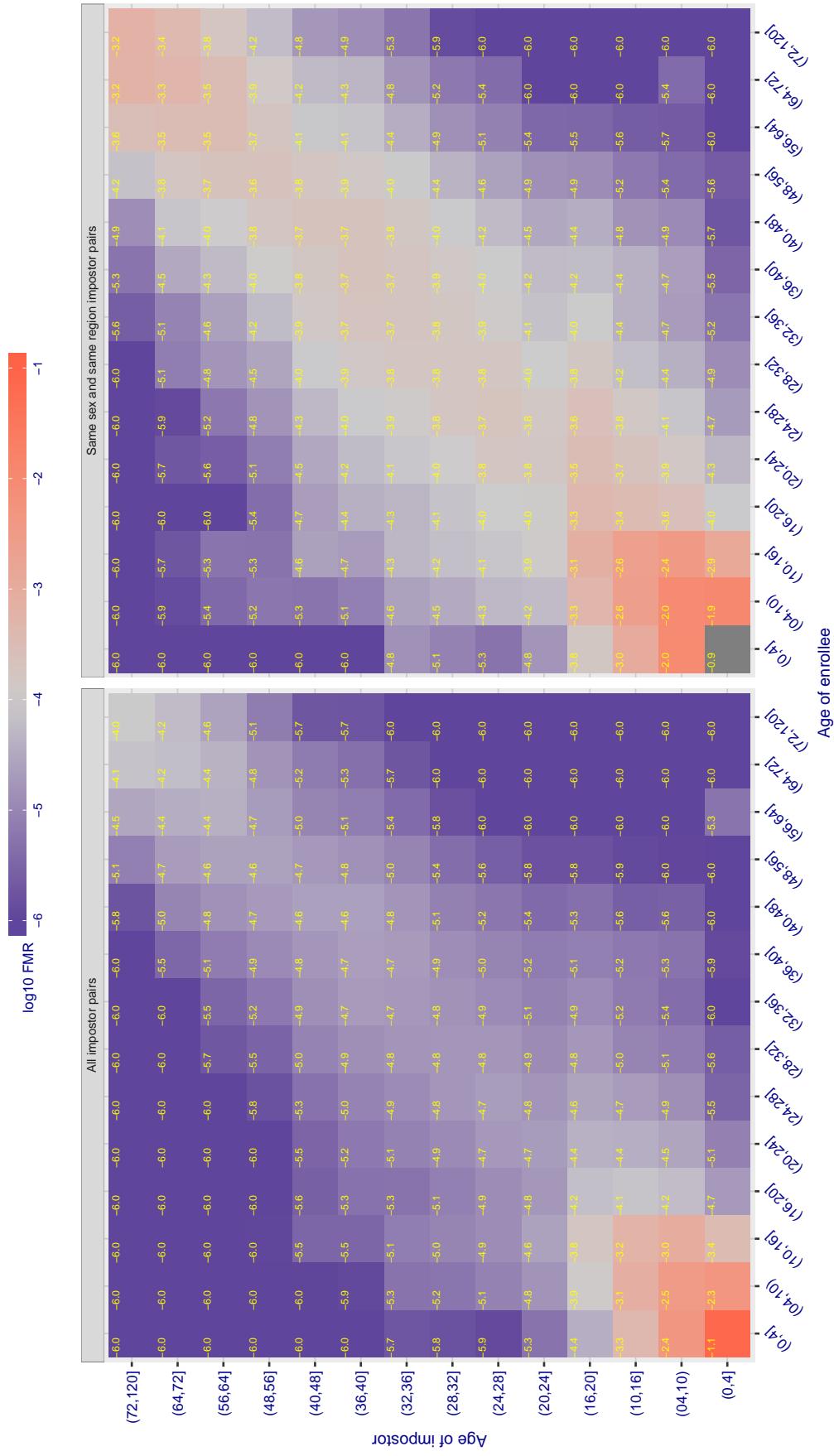


Figure 390: For algorithm shaman-001 operating on visa images, the heatmap shows false match observed over impostor comparisons of faces from different individuals who have the given age pair. False matches are counted against a recognition threshold fixed globally to give FMR = 0.001 over all on the order of  $10^{10}$  impostor comparisons. The text in each box gives the same quantity as that coded by the color. Light colors present a security vulnerability to, for example, a passport gate.

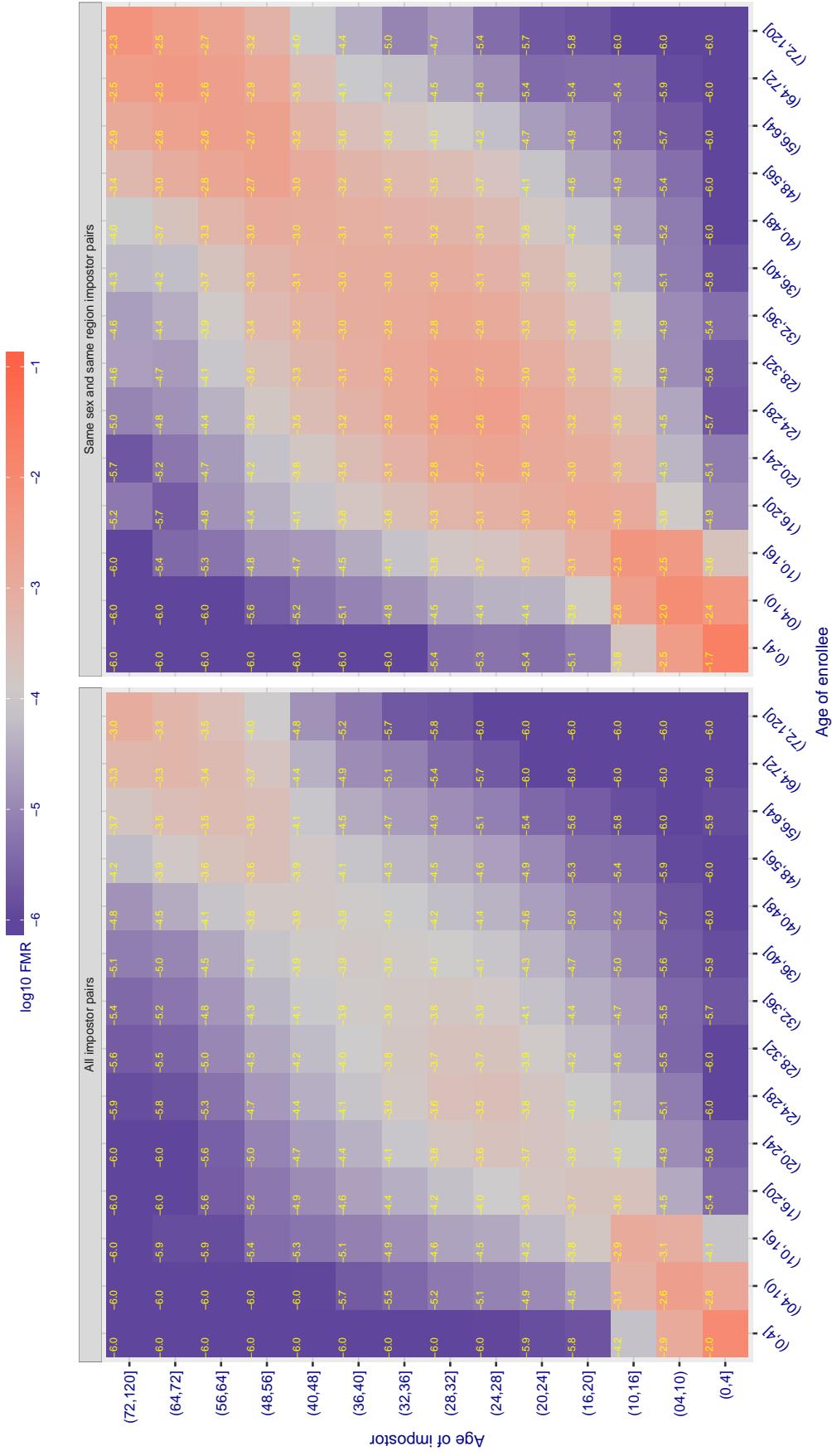
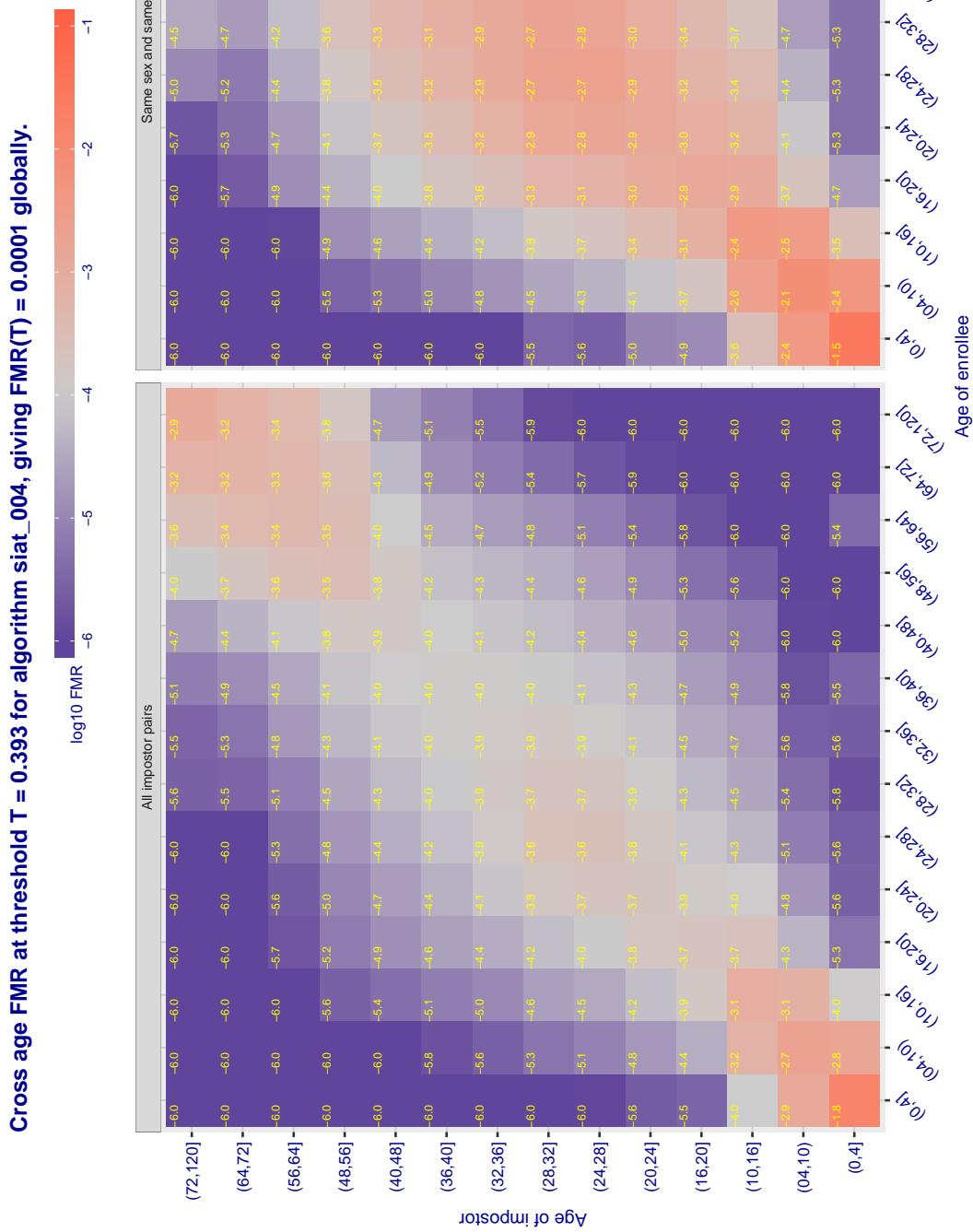
Cross age FMR at threshold T = 0.390 for algorithm siat\_002, giving  $FMR(T) = 0.0001$  globally.

Figure 391: For algorithm siat-002 operating on visa images, the heatmap shows false match observed over impostor comparisons of faces from different individuals who have the given age pair. False matches are counted against a recognition threshold fixed globally to give  $FMR = 0.001$  over all on the order of  $10^{10}$  impostor comparisons. The text in each box gives the same quantity as that coded by the color. Light colors present a security vulnerability to, for example, a passport gate.



**Figure 392:** For algorithm siat-004 operating on visa images, the heatmap shows false match observed over impostor comparisons of faces from different individuals who have the given age pair. False matches are counted against a recognition threshold fixed globally to give FMR = 0.001 over all on the order of  $10^{10}$  impostor comparisons. The text in each box gives the same quantity as that coded by the color. Light colors present a security vulnerability to, for example, a passport gate.

Cross age FMR at threshold T = 0.598 for algorithm smilart\_002, giving FMR(T) = 0.0001 globally.

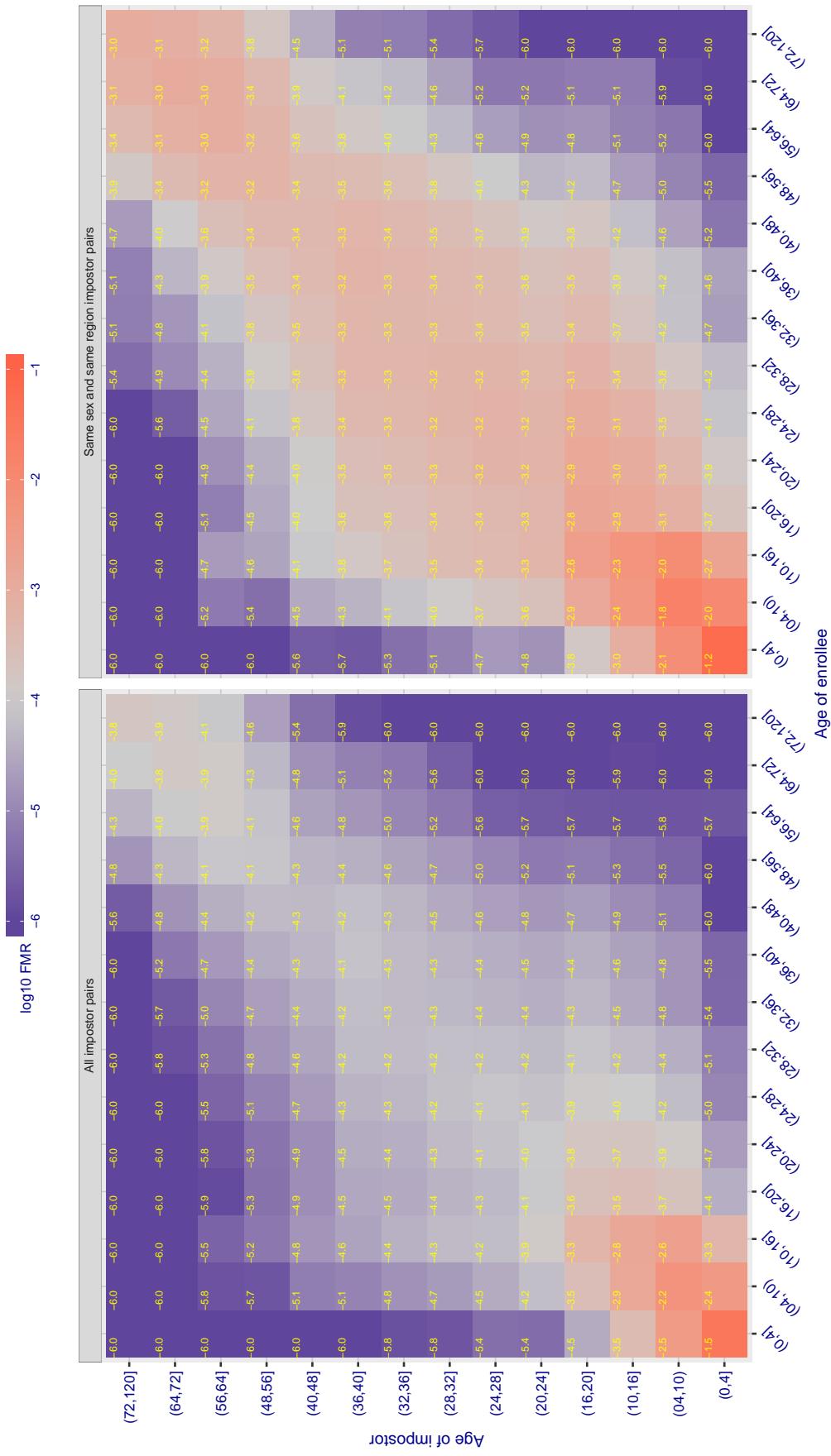
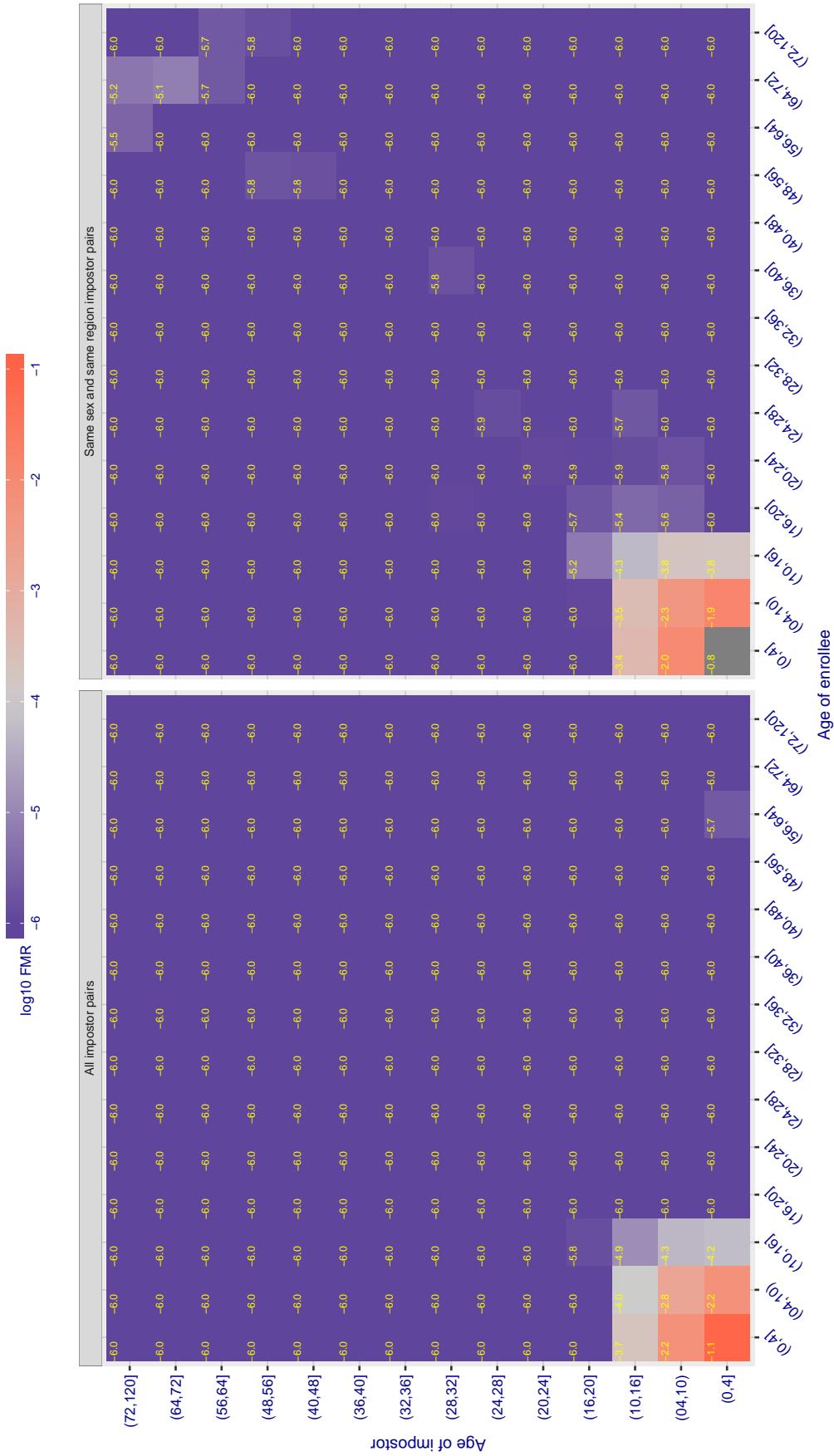


Figure 393: For algorithm smilart-002 operating on visa images, the heatmap shows false match observed over impostor comparisons of faces from different individuals who have the given age pair. False matches are counted against a recognition threshold fixed globally to give  $FMR = 0.001$  over all on the order of  $10^{10}$  impostor comparisons. The text in each box gives the same quantity as that coded by the color. Light colors present a security vulnerability to, for example, a passport gate.

Cross age FMR at threshold T = 0.654 for algorithm smilart\_003, giving  $FMR(T) = 0.0001$  globally.

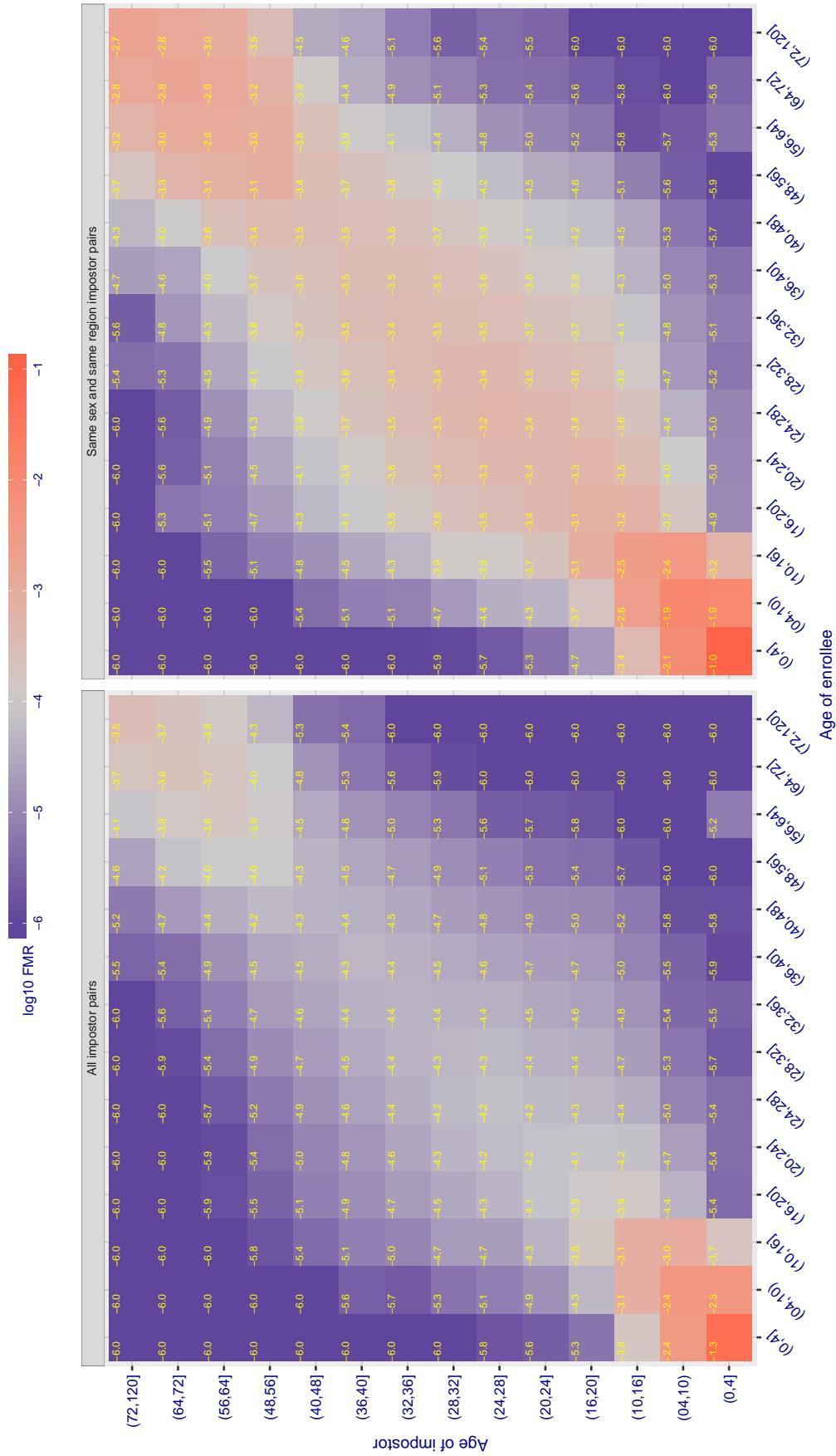
Cross age FMR at threshold T = 0.221 for algorithm synthesis\_004, giving  $FMR(T) = 0.0001$  globally.

Figure 395: For algorithm synthesis-004 operating on visa images, the heatmap shows false match observed over impostor comparisons of faces from different individuals who have the given age pair. False matches are counted against a recognition threshold fixed globally to give  $FMR = 0.001$  over all on the order of  $10^{10}$  impostor comparisons. The text in each box gives the same quantity as that coded by the color. Light colors present a security vulnerability to, for example, a passport gate.

Cross age FMR at threshold T = 148.416 for algorithm tech5\_001, giving  $FMR(T) = 0.00001$  globally.

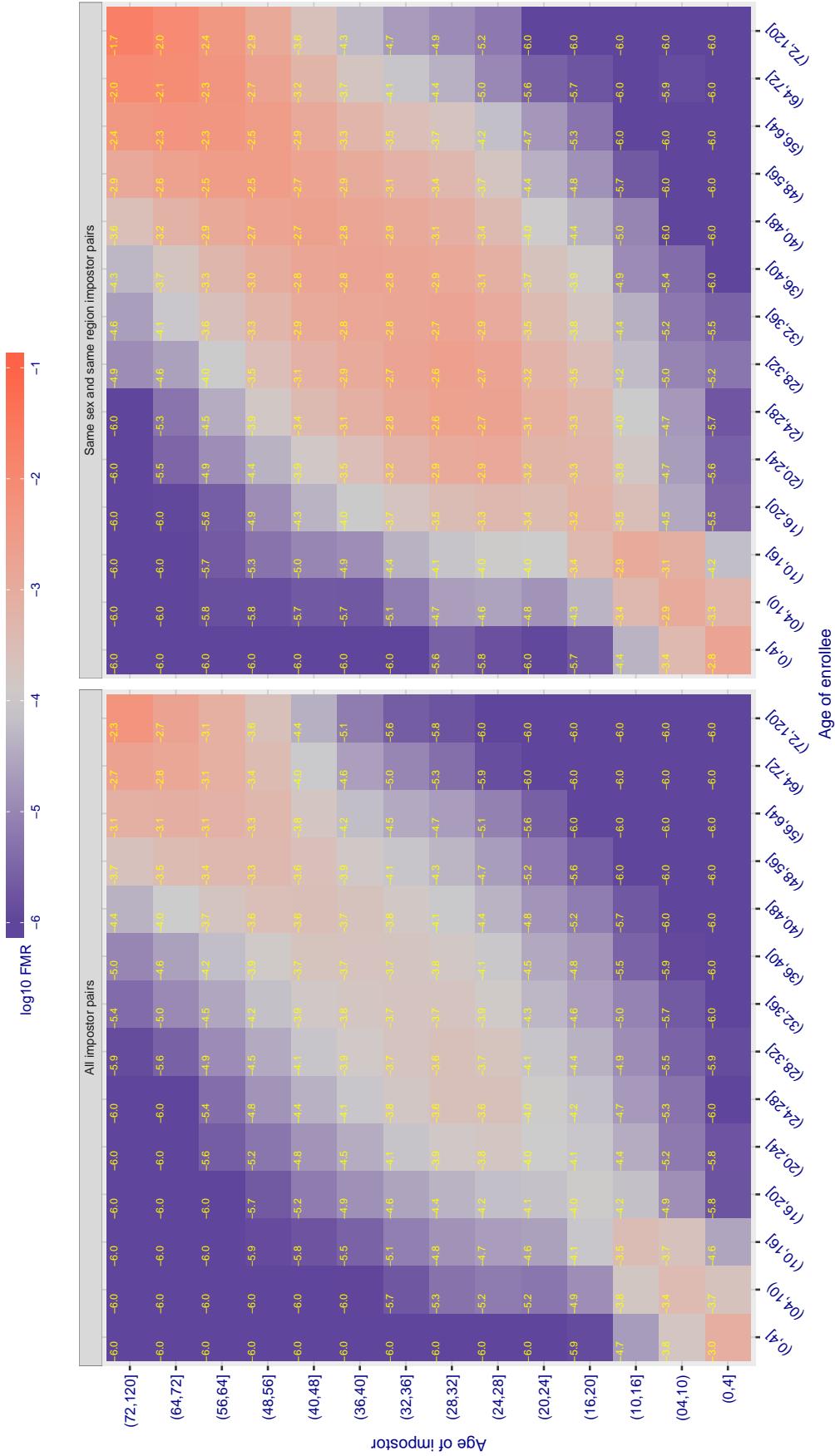


Figure 396: For algorithm tech5\_001 operating on visa images, the heatmap shows false match observed over impostor comparisons of faces from different individuals who have the given age pair. False matches are counted against a recognition threshold fixed globally to give  $FMR = 0.001$  over all on the order of  $10^{10}$  impostor comparisons. The text in each box gives the same quantity as that coded by the color. Light colors present a security vulnerability to, for example, a passport gate.

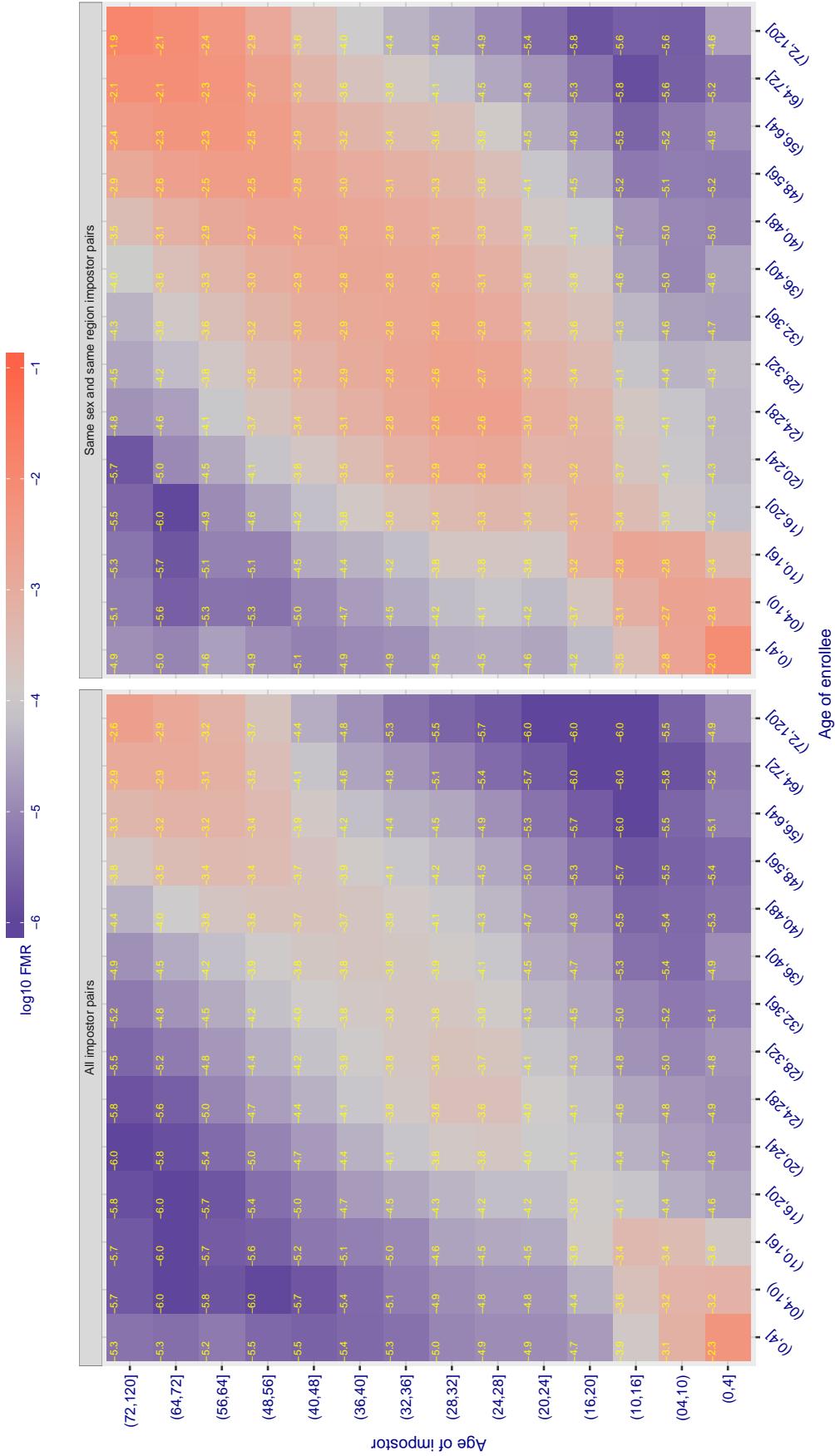
Cross age FMR at threshold T = 147.661 for algorithm tech5\_002, giving  $\text{FMR}(\text{T}) = 0.00001$  globally.

Figure 397: For algorithm tech5-002 operating on visa images, the heatmap shows false match observed over impostor comparisons of faces from different individuals who have the given age pair. False matches are counted against a recognition threshold fixed globally to give  $\text{FMR} = 0.001$  over all on the order of  $10^{10}$  impostor comparisons. The text in each box gives the same quantity as that coded by the color. Light colors present a security vulnerability to, for example, a passport gate.

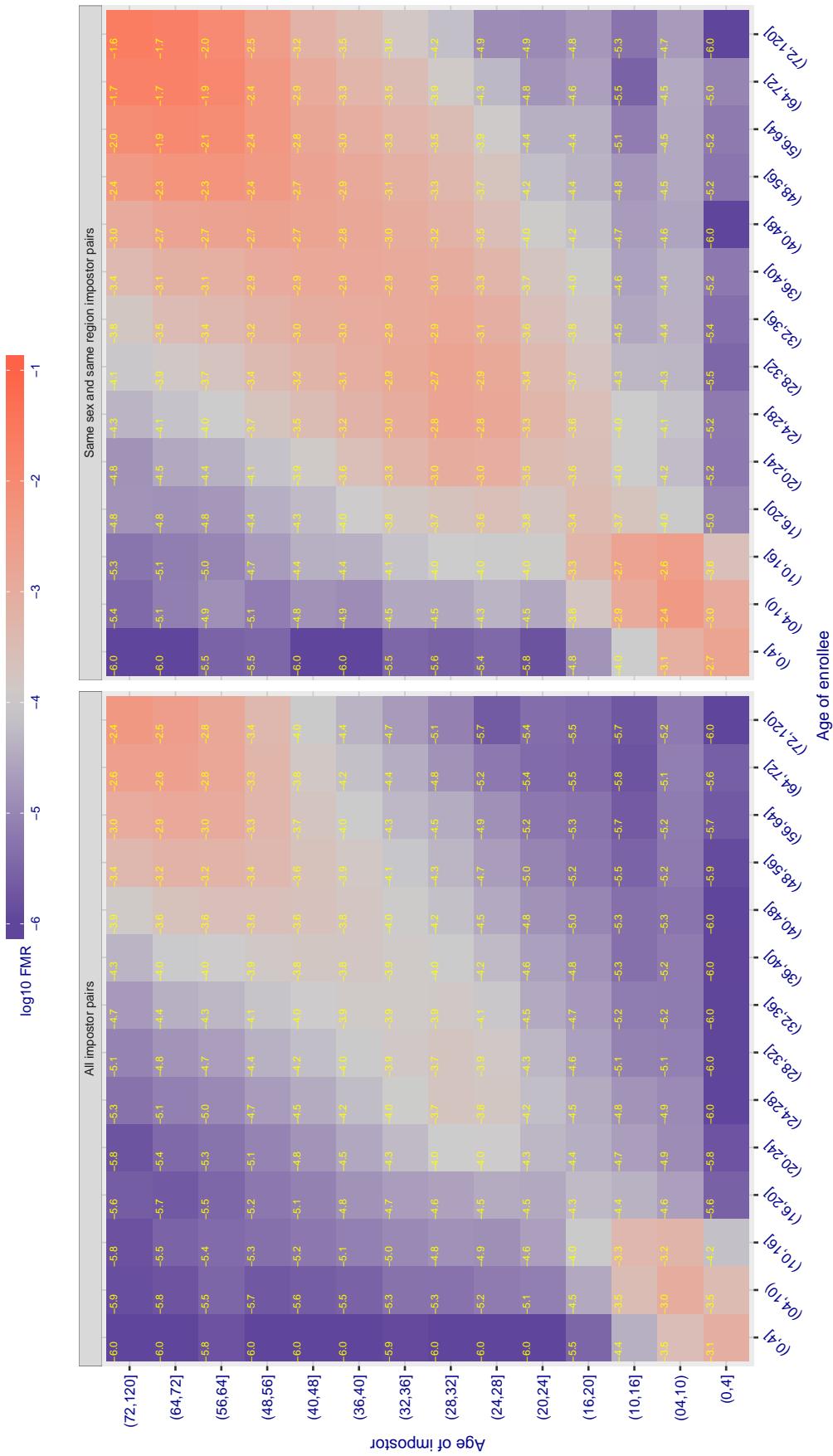
Cross age FMR at threshold T = 0.896 for algorithm tevian\_003, giving  $FMR(T) = 0.0001$  globally.

Figure 398: For algorithm tevian-003 operating on visa images, the heatmap shows false match observed over impostor comparisons of faces from different individuals who have the given age pair. False matches are counted against a recognition threshold fixed globally to give  $FMR = 0.001$  over all on the order of  $10^{10}$  impostor comparisons. The text in each box gives the same quantity as that coded by the color. Light colors represent a security vulnerability to, for example, a passport gate.

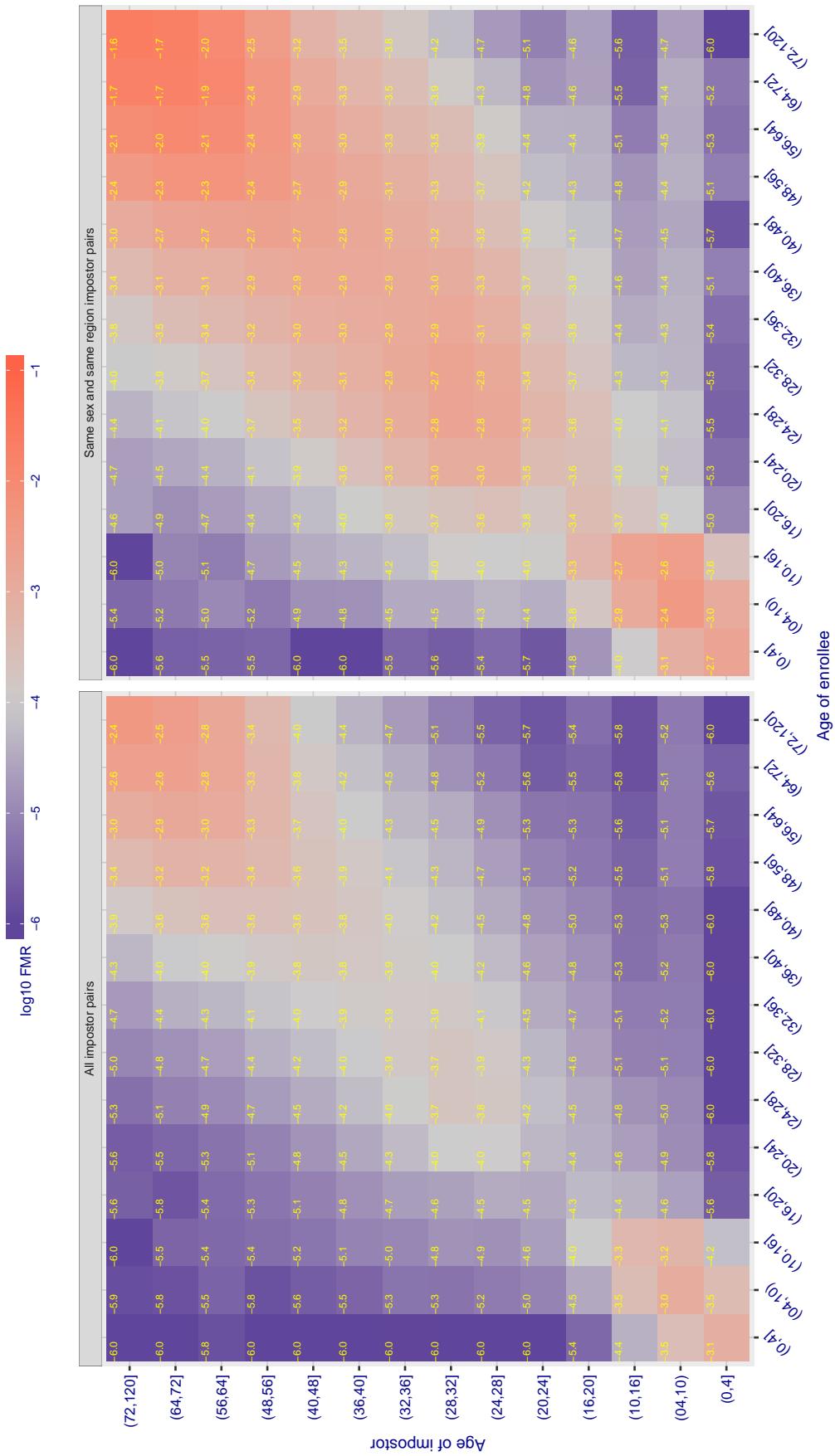
Cross age FMR at threshold T = 0.896 for algorithm tevian\_004, giving  $FMR(T) = 0.0001$  globally.

Figure 399: For algorithm tevian-004 operating on visa images, the heatmap shows false match observed over impostor comparisons of faces from different individuals who have the given age pair. False matches are counted against a recognition threshold fixed globally to give  $FMR = 0.001$  over all on the order of  $10^{10}$  impostor comparisons. The text in each box gives the same quantity as that coded by the color. Light colors present a security vulnerability to, for example, a passport gate.

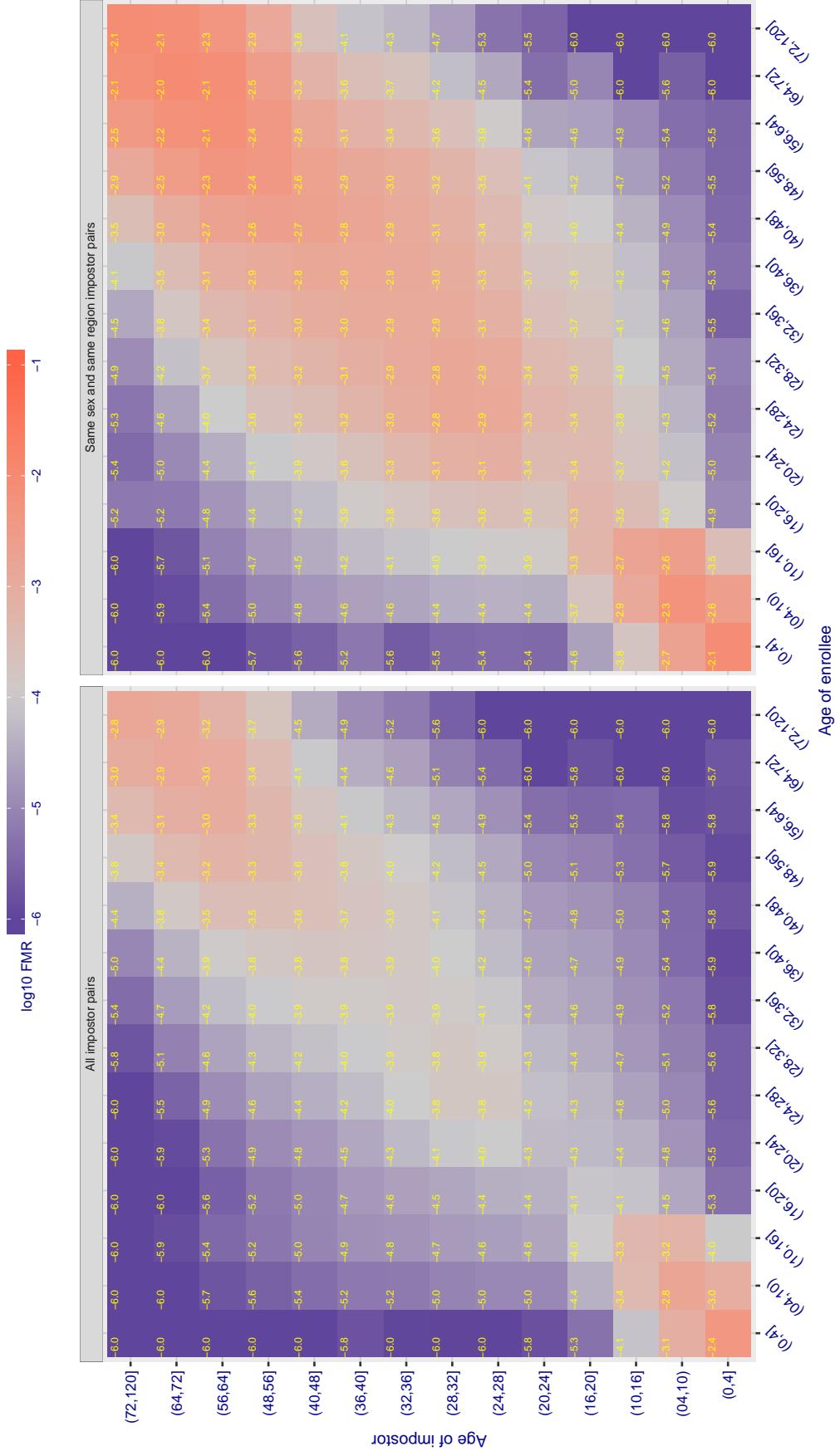
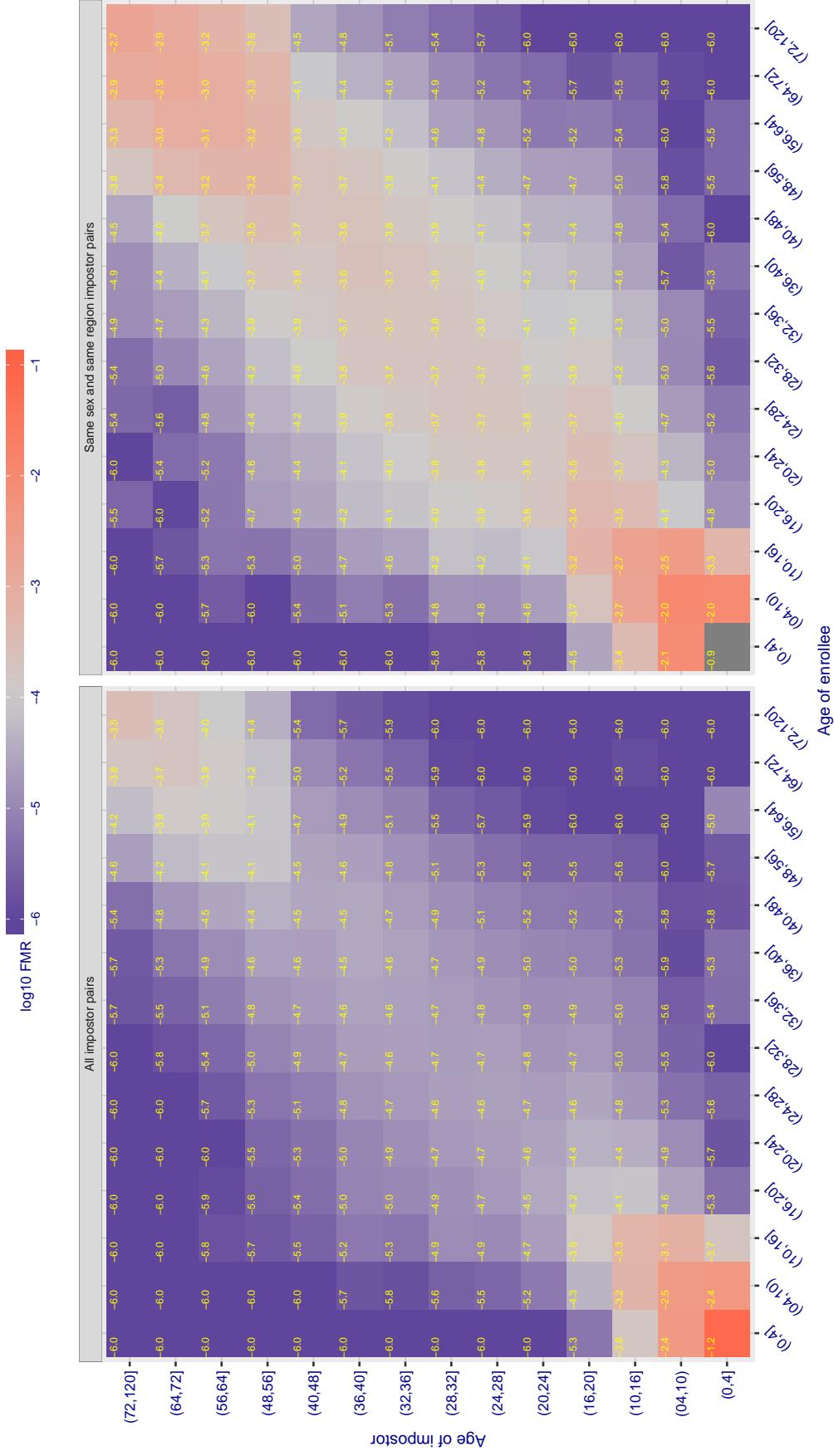
Cross age FMR at threshold T = 151.011 for algorithm tiger\_002, giving  $FMR(T) = 0.0001$  globally.

Figure 400: For algorithm tiger-002 operating on visa images, the heatmap shows false match observed over impostor comparisons of faces from different individuals who have the given age pair. False matches are counted against a recognition threshold fixed globally to give  $FMR = 0.001$  over all on the order of  $10^{10}$  impostor comparisons. The text in each box gives the same quantity as that coded by the color. Light colors present a security vulnerability to, for example, a passport gate.

Cross age FMR at threshold T = 149.313 for algorithm tiger\_003, giving  $FMR(T) = 0.0001$  globally.



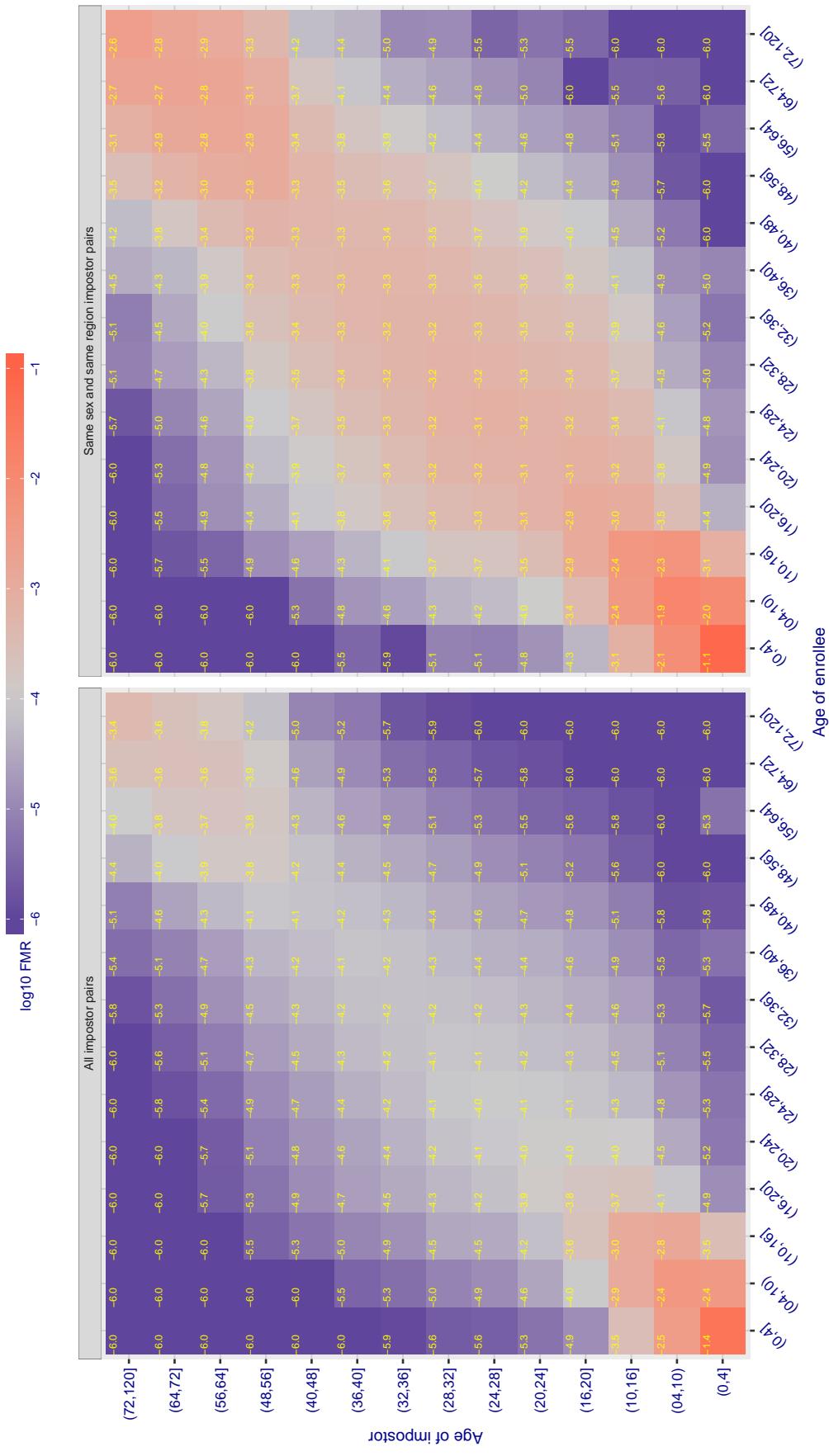
Cross age FMR at threshold T = 0.628 for algorithm toshiba\_002, giving  $FMR(T) = 0.0001$  globally.

Figure 402: For algorithm toshiba-002 operating on visa images, the heatmap shows false match observed over impostor comparisons of faces from different individuals who have the given age pair. False matches are counted against a recognition threshold fixed globally to give  $FMR = 0.001$  over all on the order of  $10^{10}$  impostor comparisons. The text in each box gives the same quantity as that coded by the color. Light colors present a security vulnerability to, for example, a passport gate.

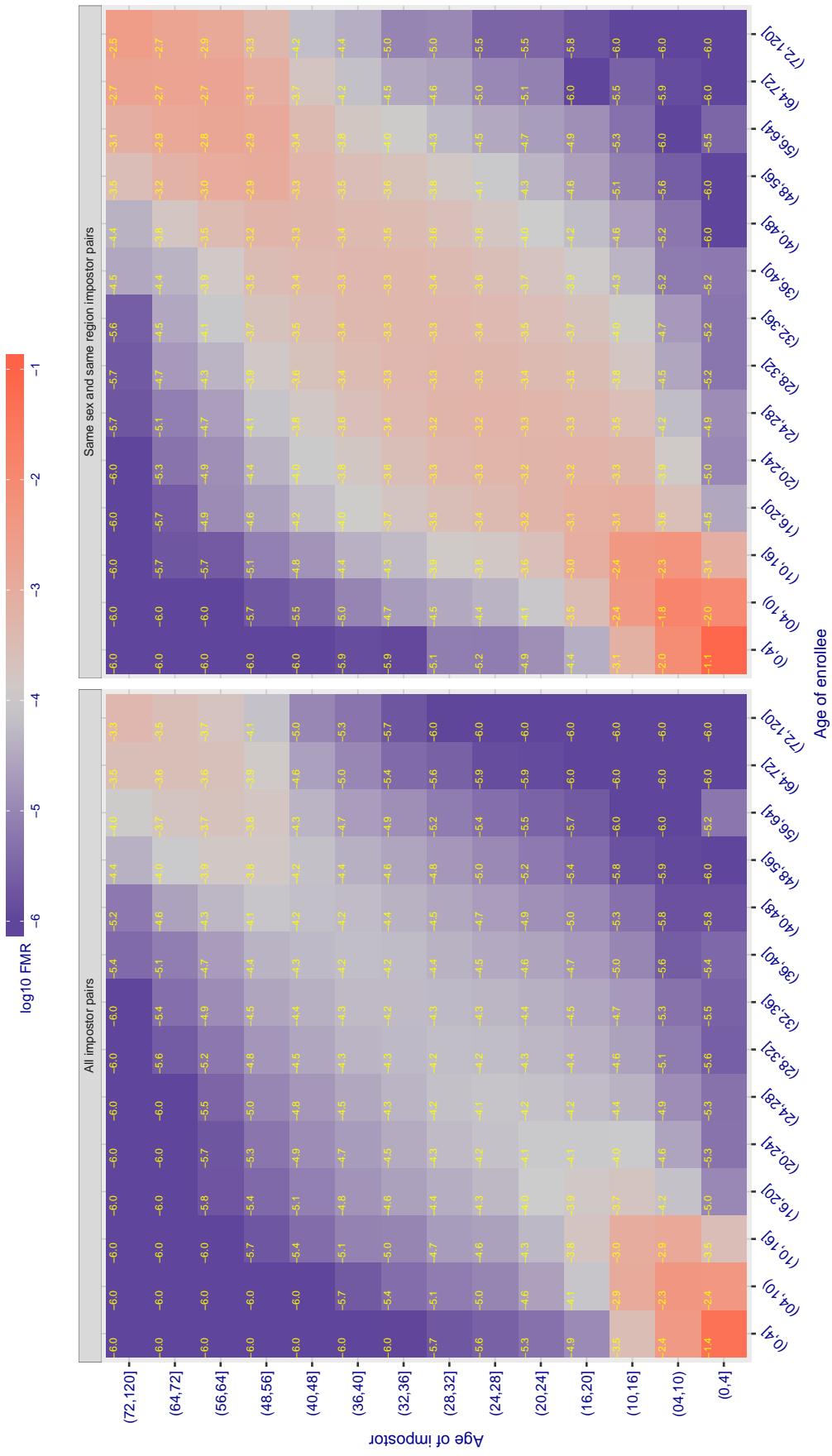
Cross age FMR at threshold T = 0.626 for algorithm toshiba\_003, giving  $FMR(T) = 0.0001$  globally.

Figure 403: For algorithm toshiba-003 operating on visa images, the heatmap shows false match observed over impostor comparisons of faces from different individuals who have the given age pair. False matches are counted against a recognition threshold fixed globally to give  $FMR = 0.00$  over all on the order of  $10^{10}$  impostor comparisons. The text in each box gives the same quantity as that coded by the color. Light colors present a security vulnerability to, for example, a passport gate.

Cross age FMR at threshold T = 0.428 for algorithm vcog\_002, giving FMR(T) = 0.0001 globally.

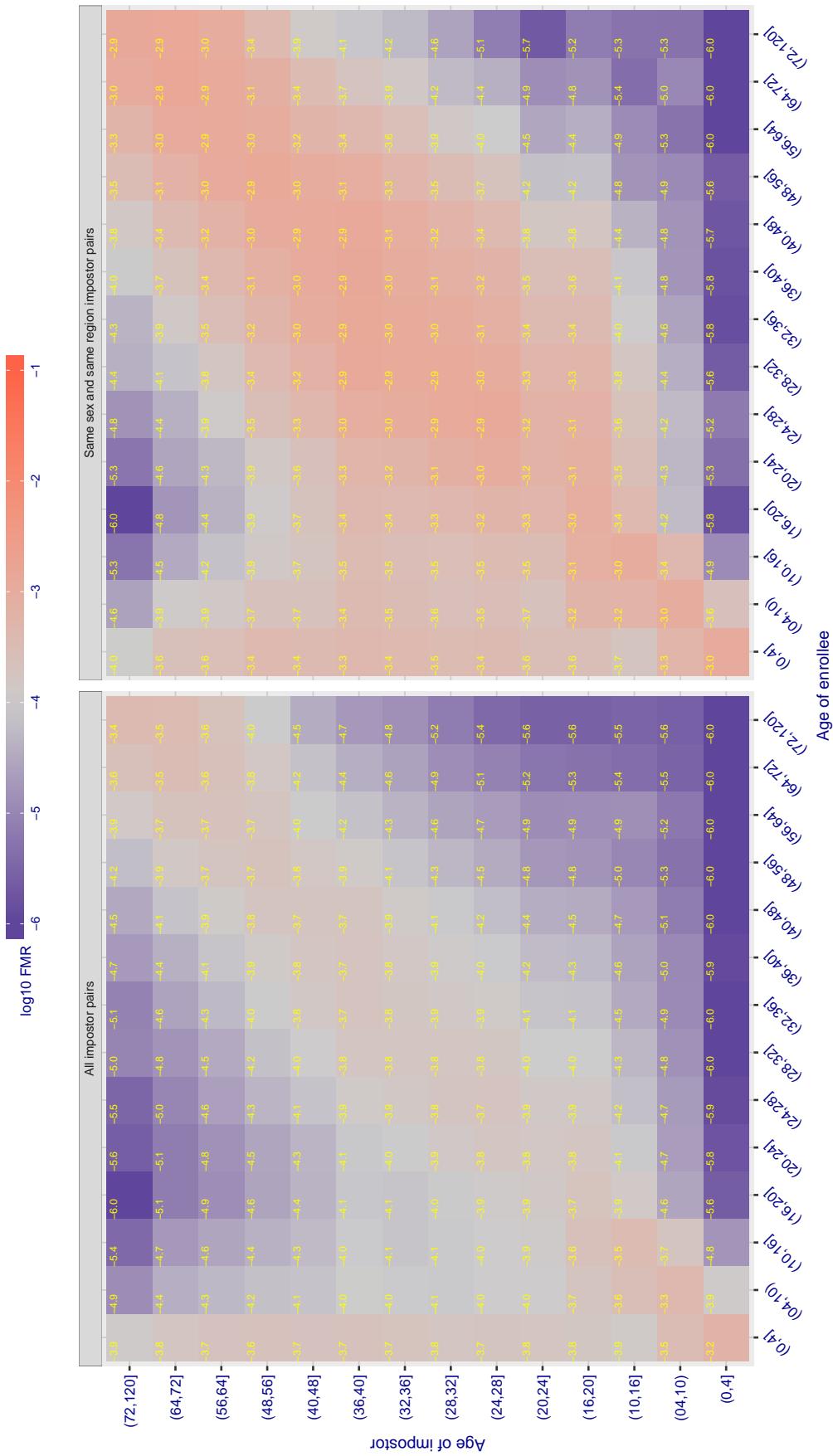


Figure 404: For algorithm vcog\_002 operating on visa images, the heatmap shows false match observed over impostor comparisons of faces from different individuals who have the given age pair. False matches are counted against a recognition threshold fixed globally to give FMR = 0.001 over all on the order of  $10^{10}$  impostor comparisons. The text in each box gives the same quantity as that coded by the color. Light colors present a security vulnerability to, for example, a passport gate.

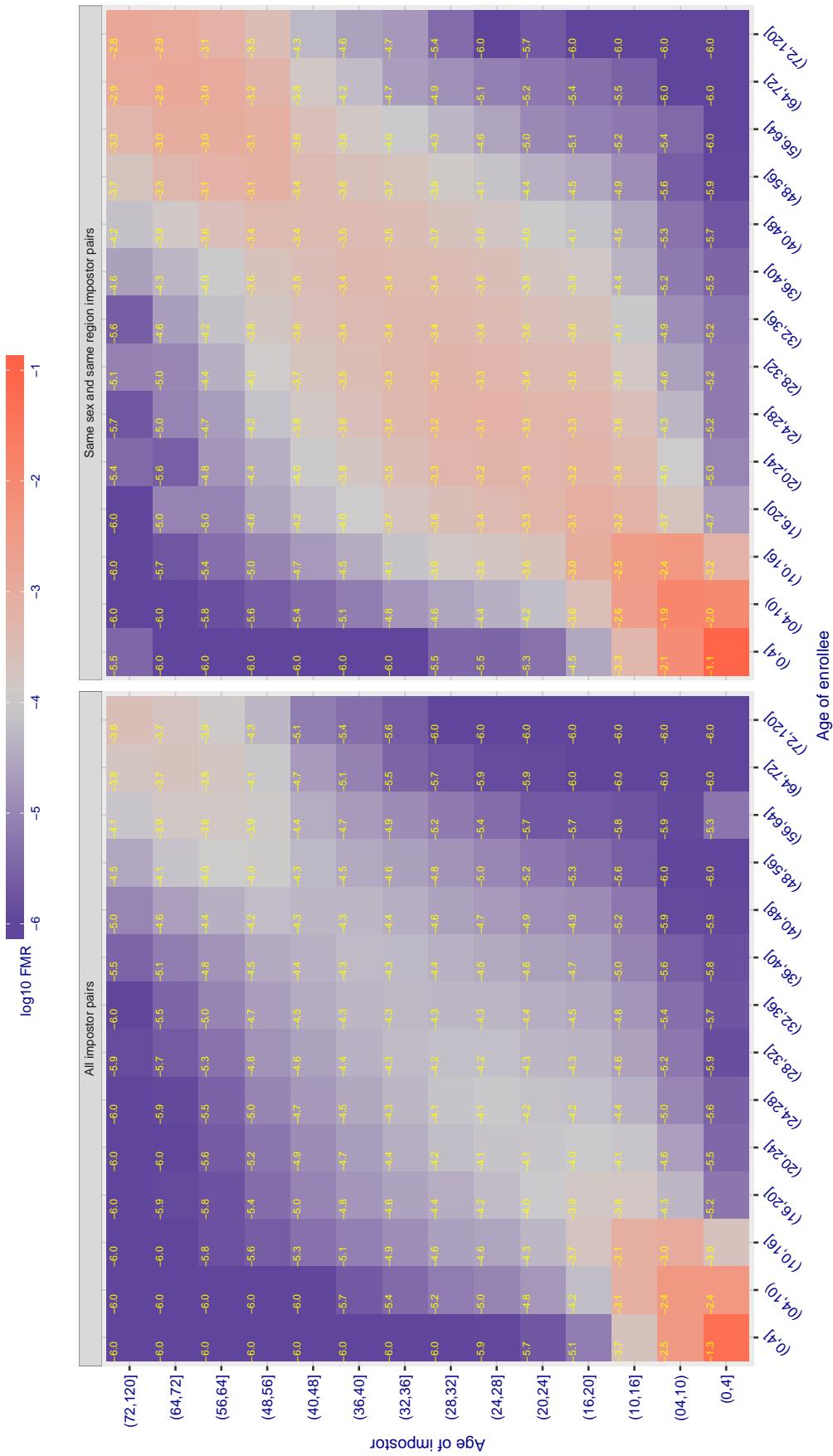
Cross age FMR at threshold T = 71.529 for algorithm vd\_001, giving  $FMR(T) = 0.0001$  globally.

Figure 405: For algorithm vd\_001 operating on visa images, the heatmap shows false match observed over impostor comparisons of faces from different individuals who have the given age pair. False matches are counted against a recognition threshold fixed globally to give  $FMR = 0.001$  over all on the order of  $10^{10}$  impostor comparisons. The text in each box gives the same quantity as that coded by the color. Light colors present a security vulnerability to, for example, a passport gate.

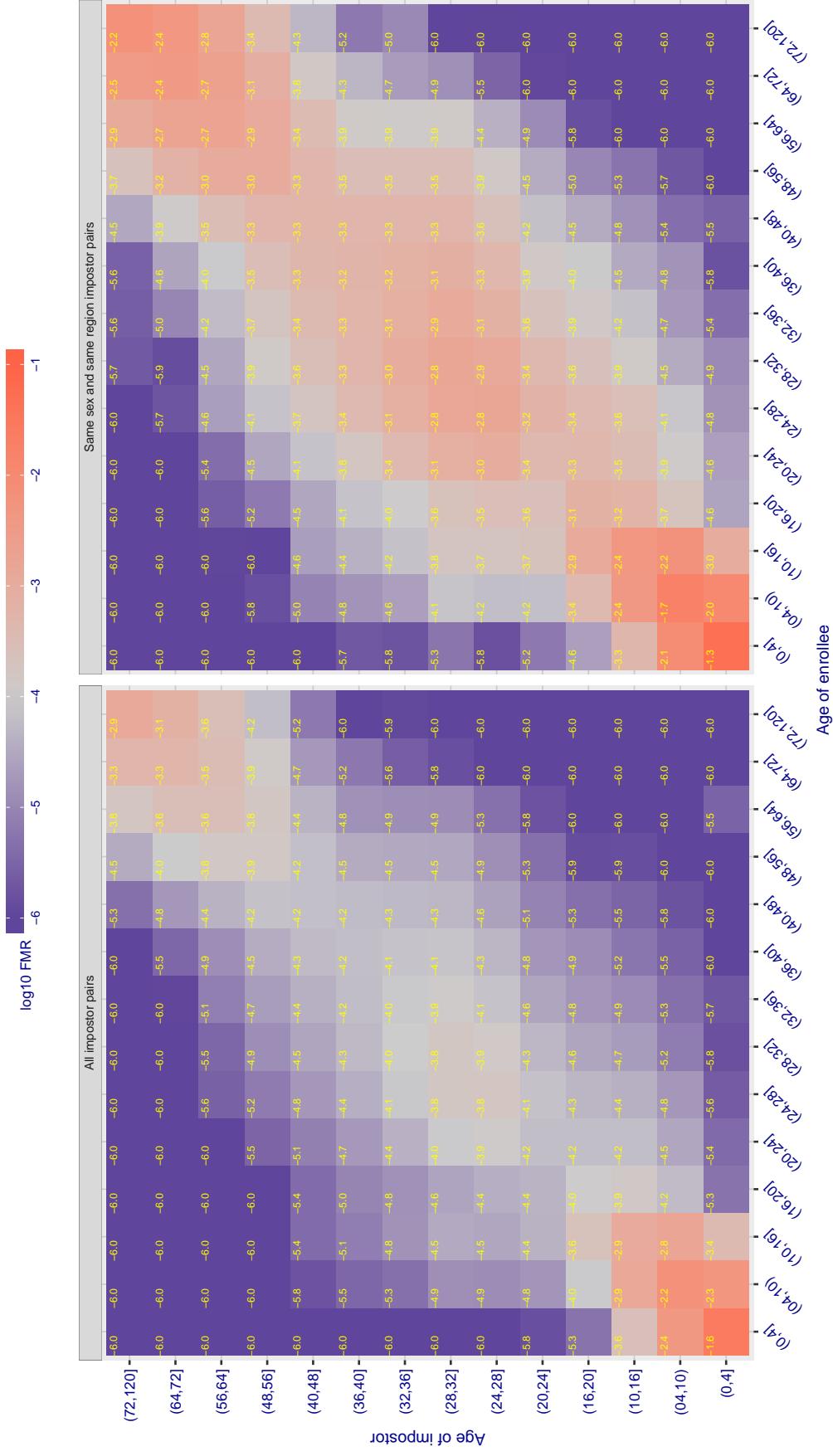
Cross age FMR at threshold T = 3.325 for algorithm veridas\_001, giving  $FMR(T) = 0.0001$  globally.

Figure 406: For algorithm veridas-001 operating on visa images, the heatmap shows false match observed over impostor comparisons of faces from different individuals who have the given age pair. False matches are counted against a recognition threshold fixed globally to give  $FMR = 0.001$  over all on the order of  $10^{10}$  impostor comparisons. The text in each box gives the same quantity as that coded by the color. Light colors present a security vulnerability to, for example, a passport gate.

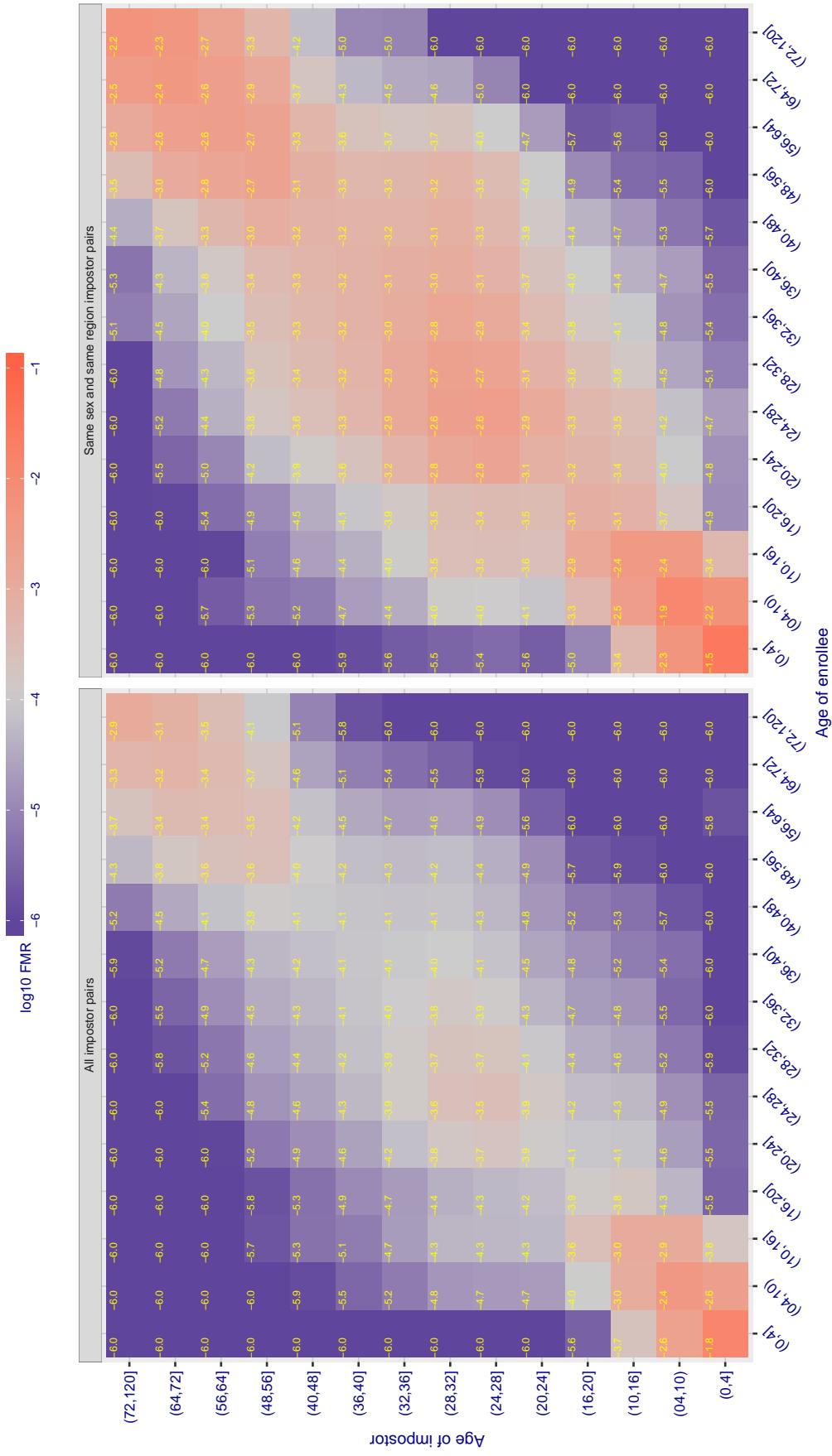
Cross age FMR at threshold T = 3.389 for algorithm veridas\_002, giving  $FMR(T) = 0.0001$  globally.

Figure 407: For algorithm veridas\_002 operating on visa images, the heatmap shows false match observed over impostor comparisons of faces from different individuals who have the given age pair. False matches are counted against a recognition threshold fixed globally to give  $FMR = 0.001$  over all on the order of  $10^{10}$  impostor comparisons. The text in each box gives the same quantity as that coded by the color. Light colors present a security vulnerability to, for example, a passport gate.

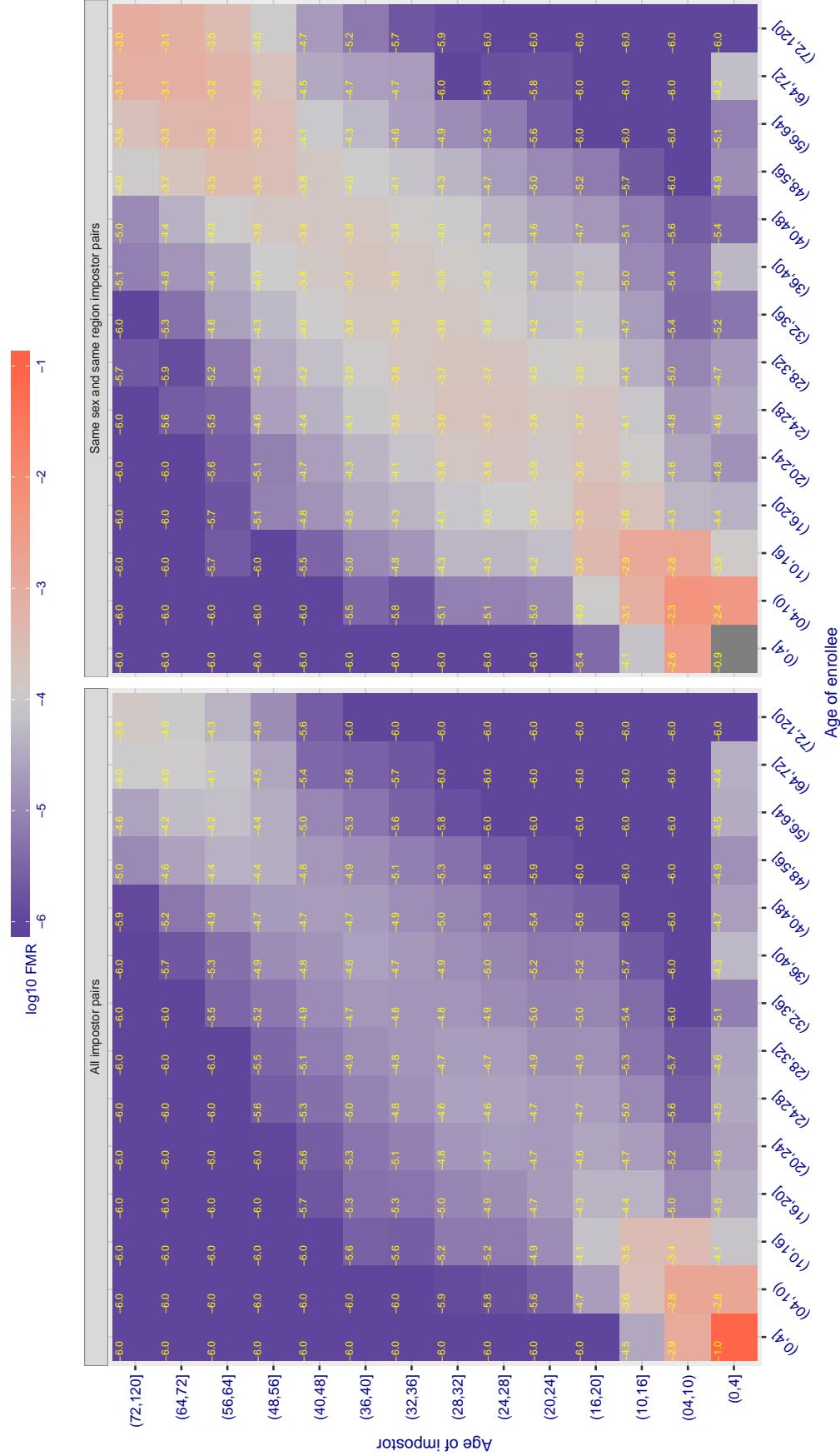
**Cross age FMR at threshold  $T = 3.051$  for algorithm vigilantsolutions\_005, giving  $FMR(T) = 0.0001$  globally.**

Figure 408: For algorithm vigilantsolutions-005 operating on visa images, the heatmap shows false match observed over impostor comparisons of faces from different individuals who have the given age pair. False matches are counted against a recognition threshold fixed globally to give  $FMR = 0.001$  over all on the order of  $10^{10}$  impostor comparisons. The text in each box gives the same quantity as that coded by the color. Light colors present a security vulnerability to, for example, a passport gate.

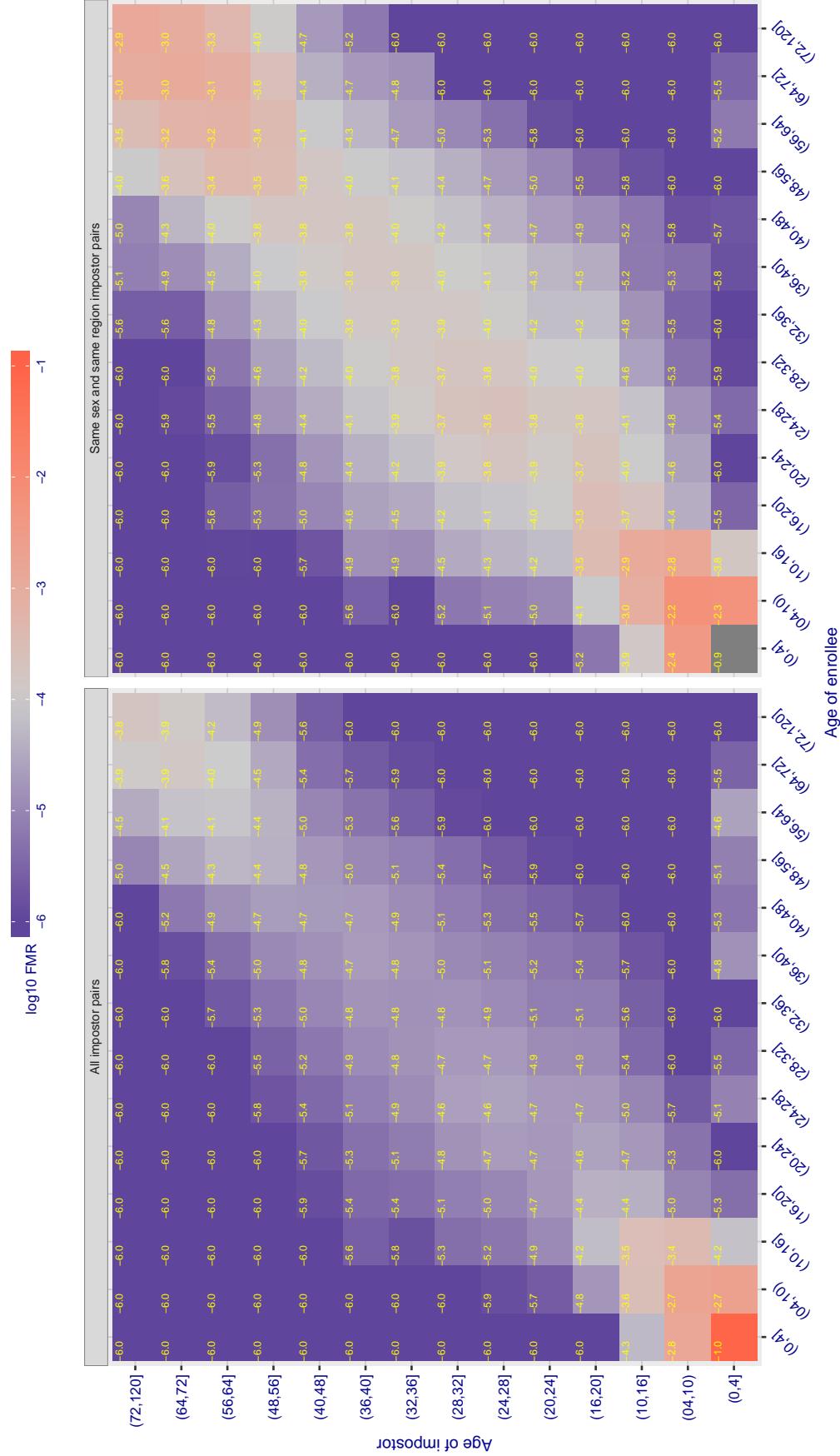
**Cross age FMR at threshold  $T = 3.057$  for algorithm vigilantsolutions\_006, giving  $FMR(T) = 0.0001$  globally.**

Figure 409: For algorithm vigilantsolutions-006 operating on visa images, the heatmap shows false match observed over impostor comparisons of faces from different individuals who have the given age pair. False matches are counted against a recognition threshold fixed globally to give  $FMR = 0.001$  over all on the order of  $10^{10}$  impostor comparisons. The text in each box gives the same quantity as that coded by the color. Light colors present a security vulnerability to, for example, a passport gate.

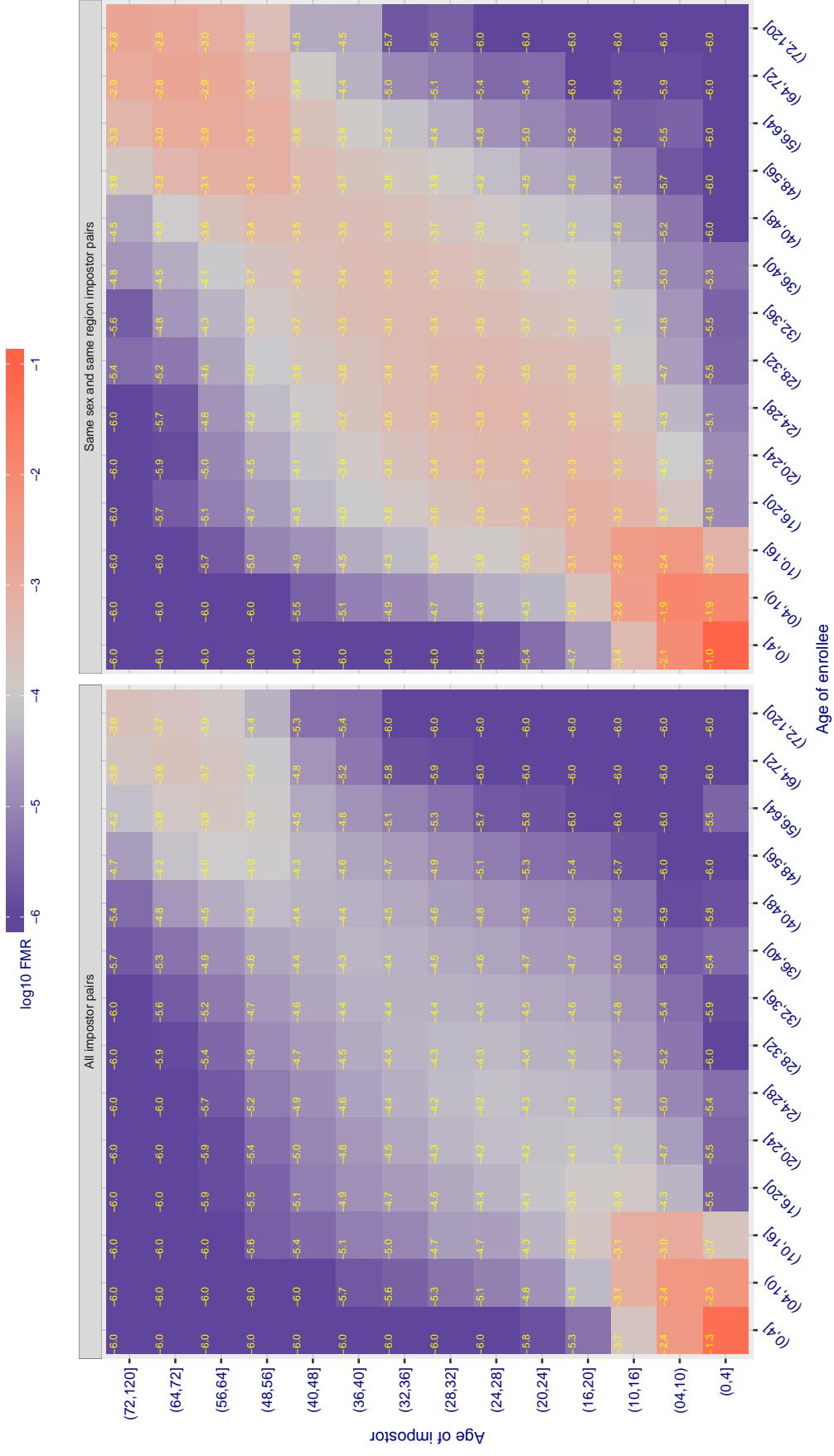
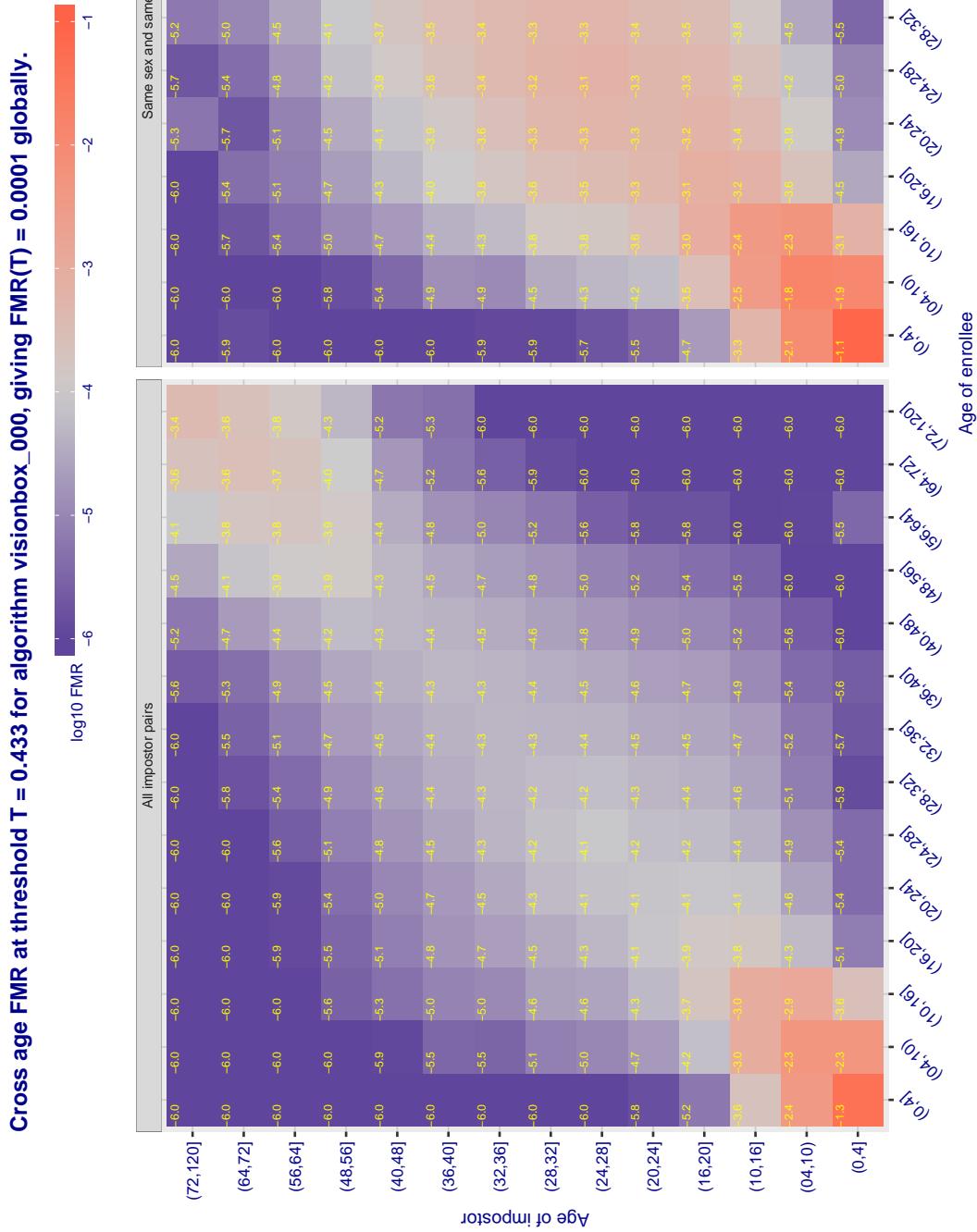
Cross age FMR at threshold T = 0.432 for algorithm vion\_000, giving  $FMR(T) = 0.0001$  globally.

Figure 410: For algorithm vion-000 operating on visa images, the heatmap shows false match observed over impostor comparisons of faces from different individuals who have the given age pair. False matches are counted against a recognition threshold fixed globally to give  $FMR = 0.001$  over all on the order of  $10^{10}$  impostor comparisons. The text in each box gives the same quantity as that coded by the color. Light colors present a security vulnerability to, for example, a passport gate.



**Figure 41:** For algorithm visionbox-000 operating on visa images, the heatmap shows false match observed over impostor comparisons of faces from different individuals who have the given age pair. False matches are counted against a recognition threshold fixed globally to give  $FMR = 0.001$  over all on the order of  $10^{10}$  impostor comparisons. The text in each box gives the same quantity as that coded by the color. Light colors present a security vulnerability to, for example, a passport gate.

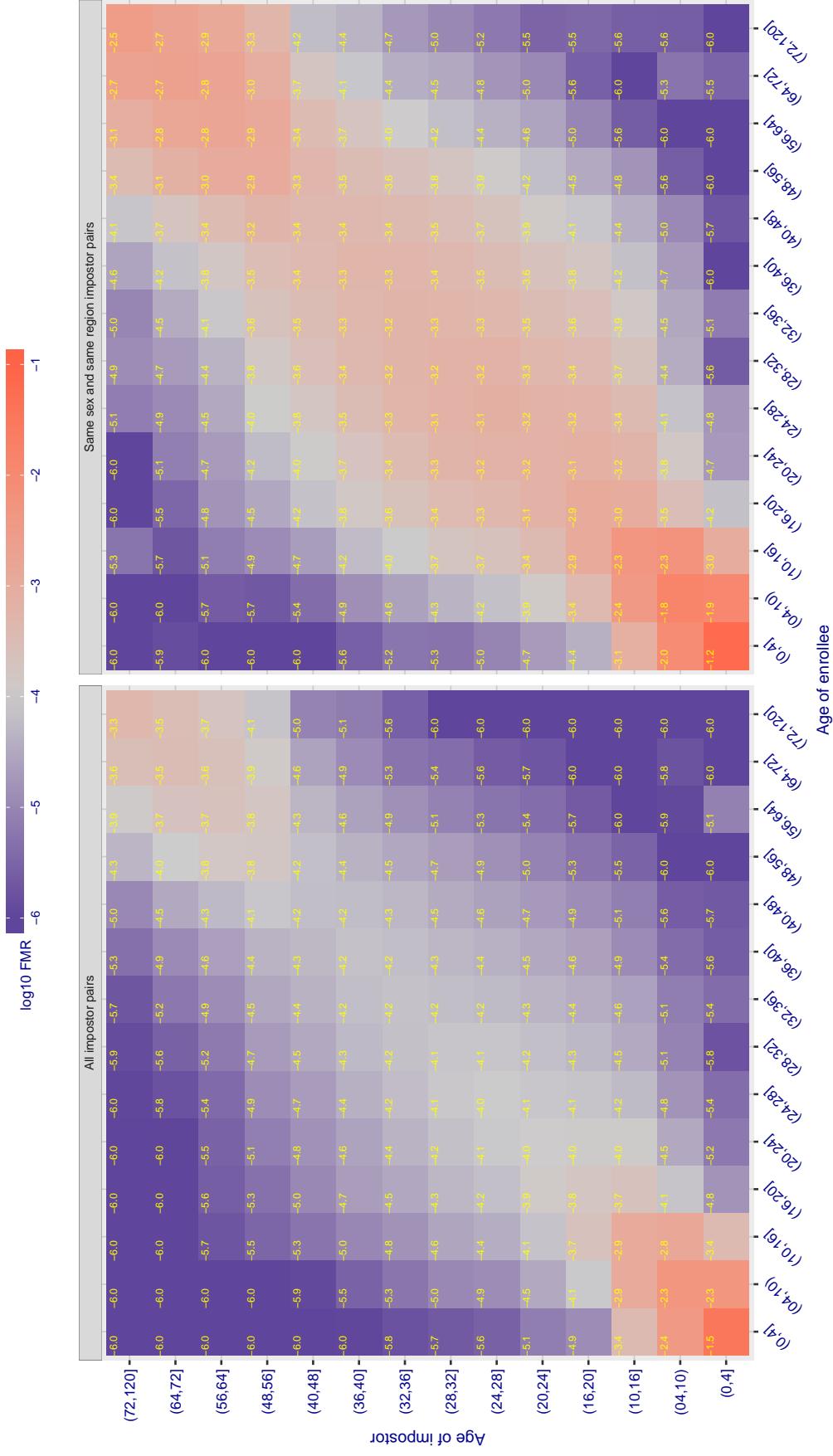
Cross age FMR at threshold T = 0.382 for algorithm visionbox\_001, giving  $\text{FMR}(\text{T}) = 0.0001$  globally.

Figure 412: For algorithm visionbox-001 operating on visa images, the heatmap shows false match observed over impostor comparisons of faces from different individuals who have the given age pair. False matches are counted against a recognition threshold fixed globally to give  $\text{FMR} = 0.001$  over all on the order of  $10^{10}$  impostor comparisons. The text in each box gives the same quantity as that coded by the color. Light colors present a security vulnerability to, for example, a passport gate.

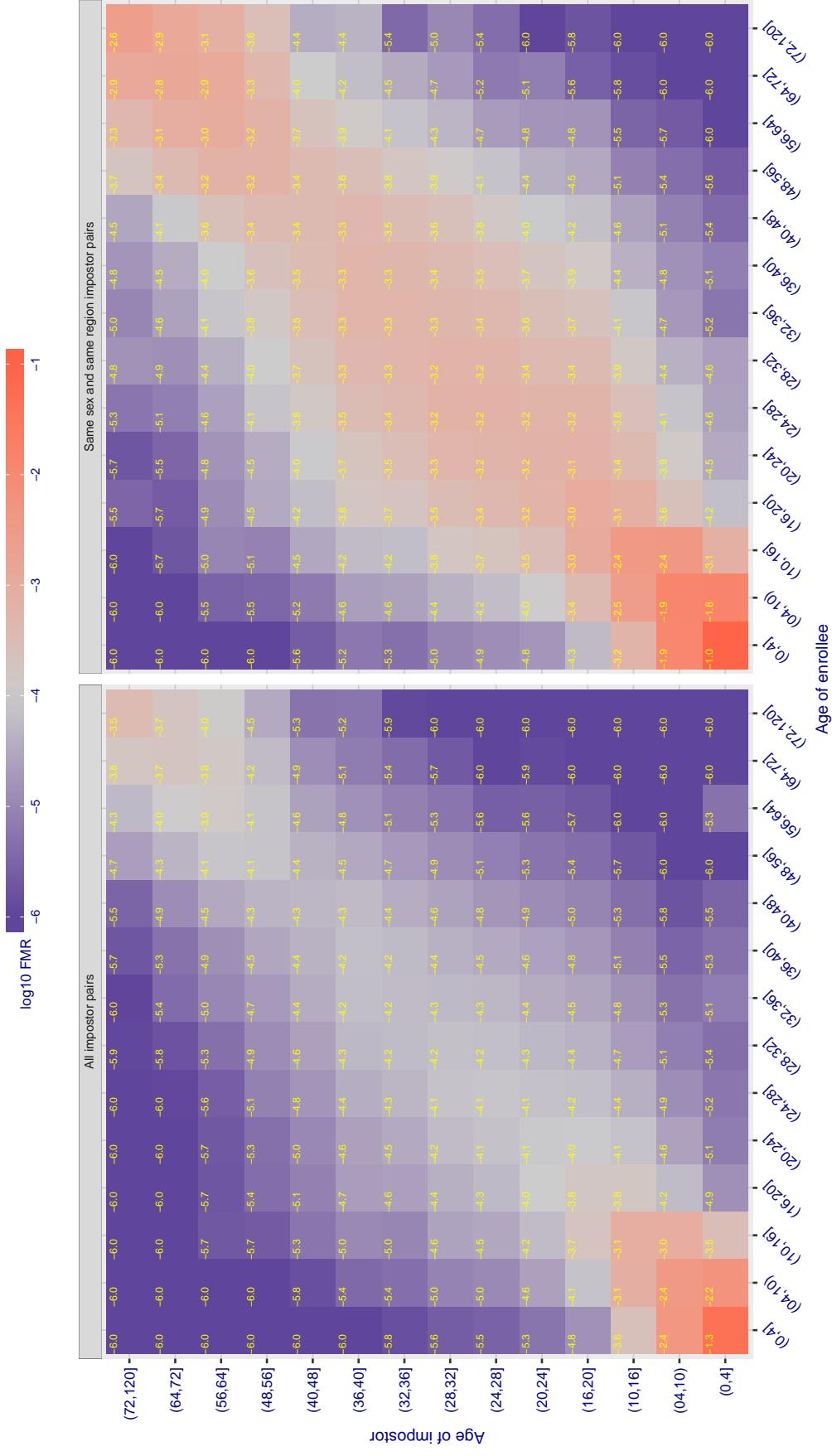
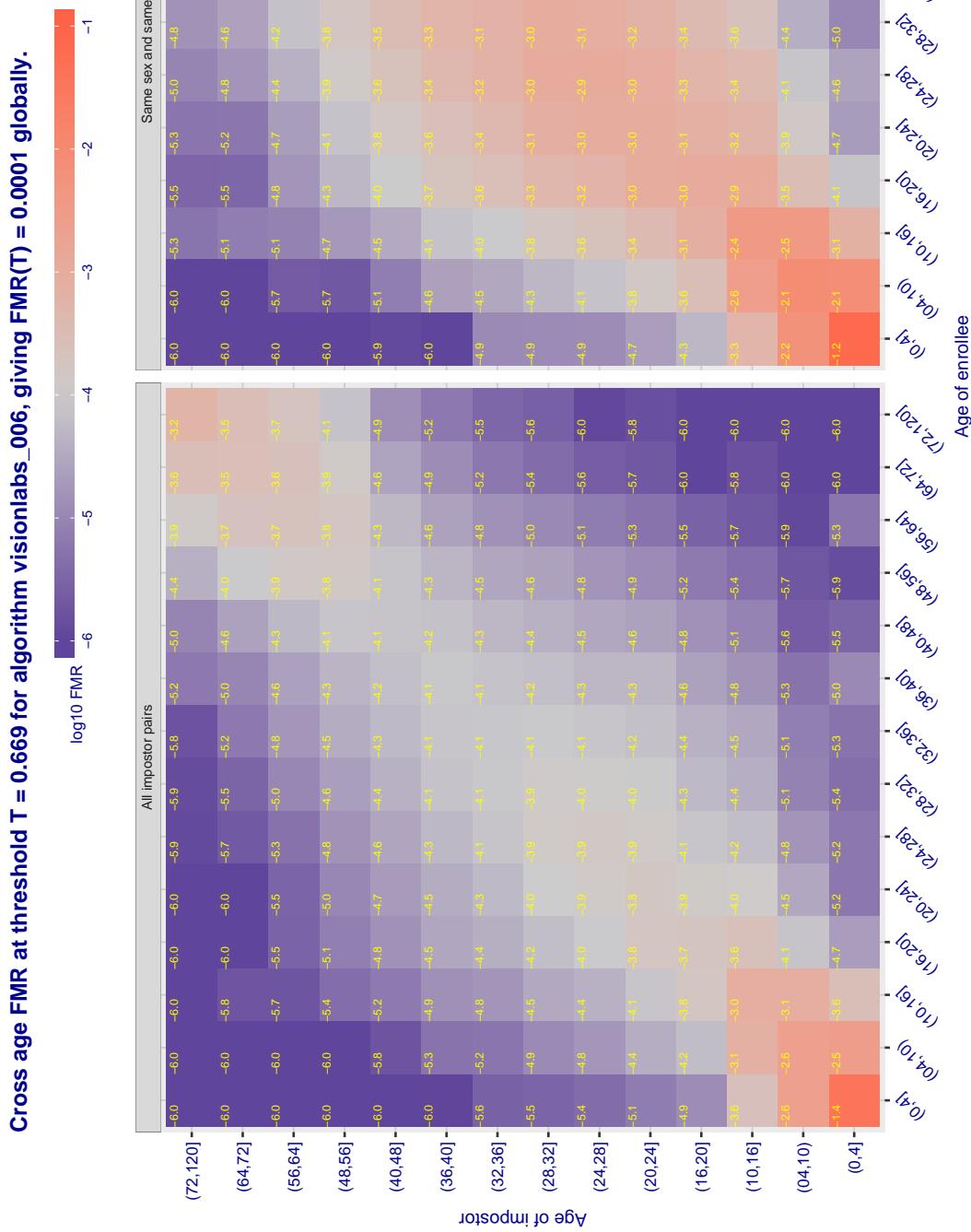
Cross age FMR at threshold T = 0.000 for algorithm visionlabs\_005, giving  $FMR(T) = 0.00001$  globally.

Figure 413: For algorithm visionlabs-005 operating on visa images, the heatmap shows false match observed over impostor comparisons of faces from different individuals who have the given age pair. False matches are counted against a recognition threshold fixed globally to give  $FMR = 0.001$  over all on the order of  $10^{10}$  impostor comparisons. The text in each box gives the same quantity as that coded by the color. Light colors present a security vulnerability to, for example, a passport gate.



**Figure 4-14:** For algorithm visionlabs-006 operating on visa images, the heatmap shows false match observed over impostor comparisons of faces from different individuals who have the given age pair. False matches are counted against a recognition threshold fixed globally to give  $FMR = 0.001$  over all on the order of  $10^{10}$  impostor comparisons. The text in each box gives the same quantity as that coded by the color. Light colors present a security vulnerability to, for example, a passport gate.

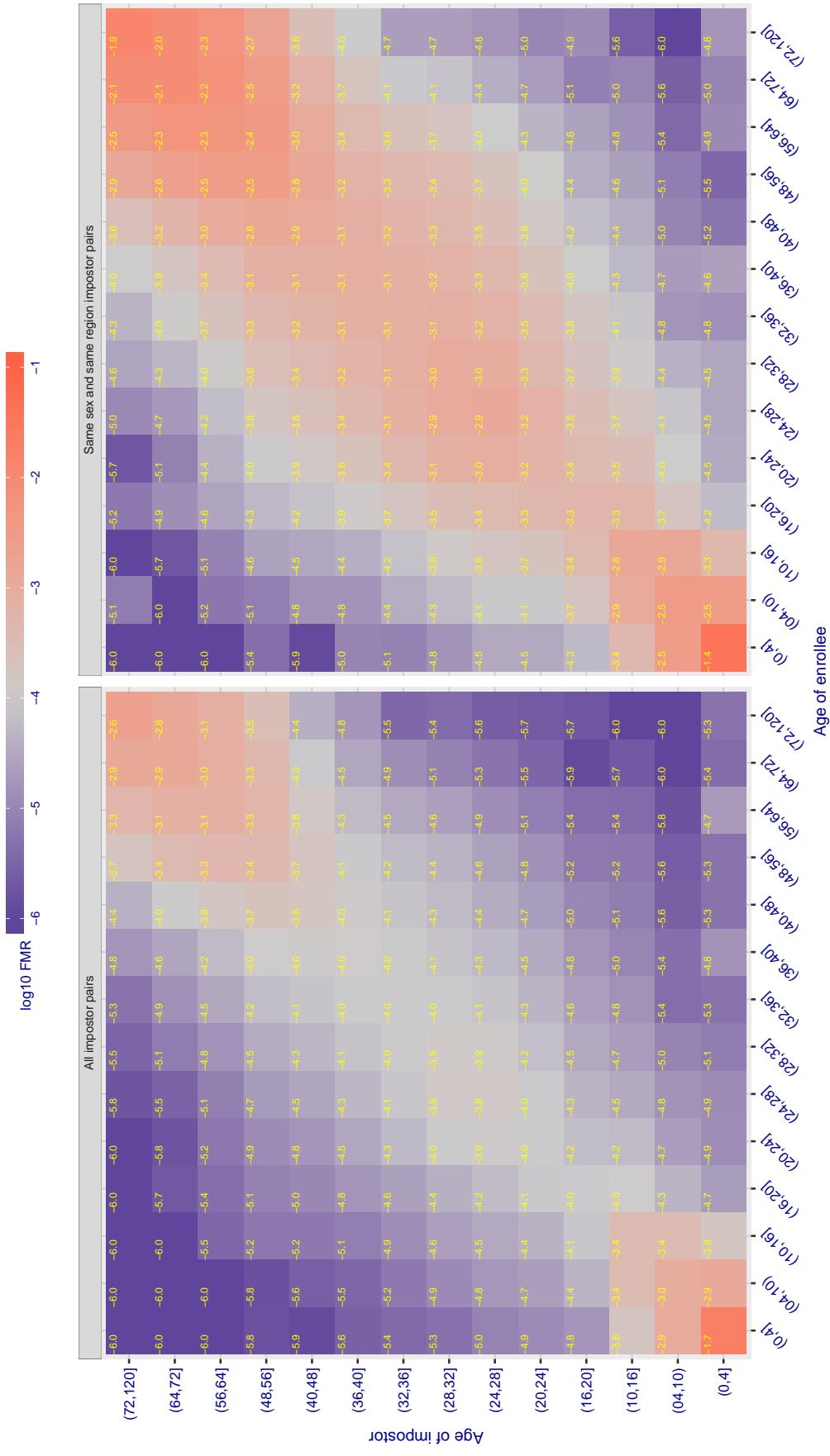
Cross age FMR at threshold T = 995.898 for algorithm vocord\_006, giving  $\text{FMR}(\text{T}) = 0.0001$  globally.

Figure 415: For algorithm vocord-006 operating on visa images, the heatmap shows false match observed over impostor comparisons of faces from different individuals who have the given age pair. False matches are counted against a recognition threshold fixed globally to give  $\text{FMR} = 0.00$  over all on the order of  $10^{10}$  impostor comparisons. The text in each box gives the same quantity as that coded by the color. Light colors present a security vulnerability to, for example, a passport gate.

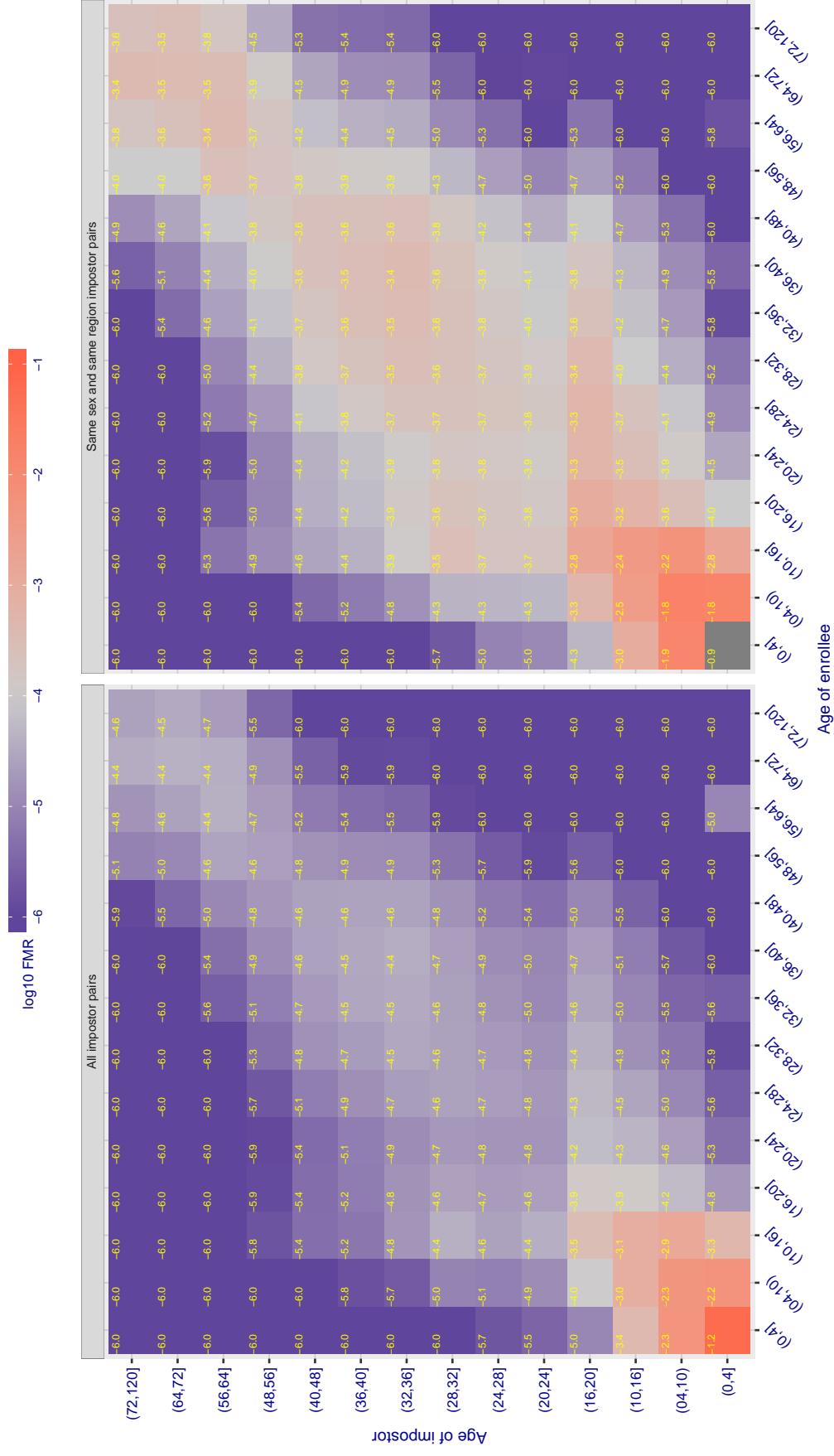
Cross age FMR at threshold T = 5.544 for algorithm *yisheng\_004*, giving  $FMR(T) = 0.0001$  globally.

Figure 416: For algorithm *yisheng-004* operating on visa images, the heatmap shows false match observed over impostor comparisons of faces from different individuals who have the given age pair. False matches are counted against a recognition threshold fixed globally to give  $FMR = 0.001$  over all on the order of  $10^{10}$  impostor comparisons. The text in each box gives the same quantity as that coded by the color. Light colors present a security vulnerability to, for example, a passport gate.

Cross age FMR at threshold T = 37.698 for algorithm yitu\_003, giving FMR(T) = 0.0001 globally.

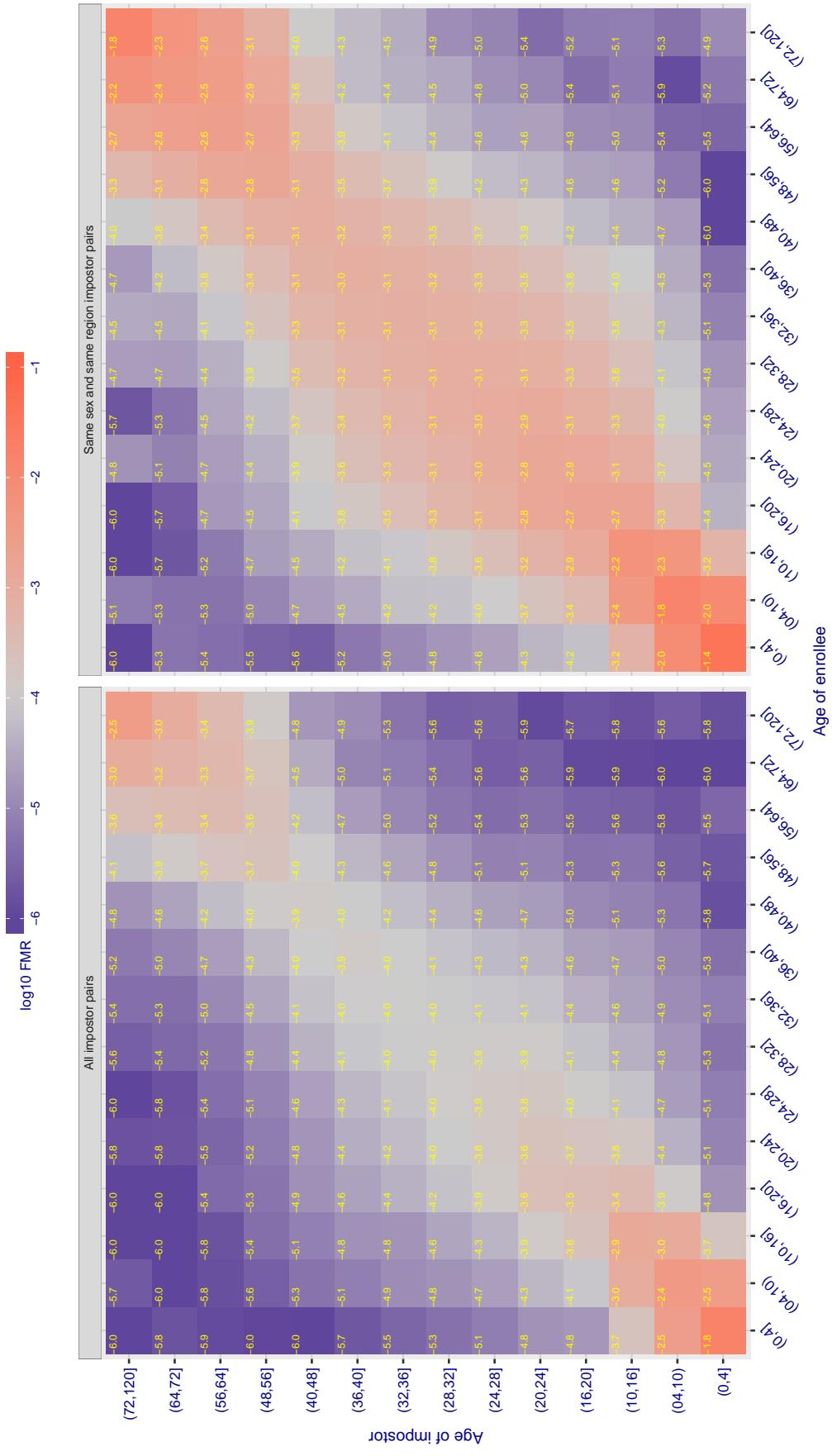


Figure 417: For algorithm yitu\_003 operating on visa images, the heatmap shows false match observed over impostor comparisons of faces from different individuals who have the given age pair. False matches are counted against a recognition threshold fixed globally to give FMR = 0.001 over all on the order of  $10^{10}$  impostor comparisons. The text in each box gives the same quantity as that coded by the color. Light colors present a security vulnerability to, for example, a passport gate.

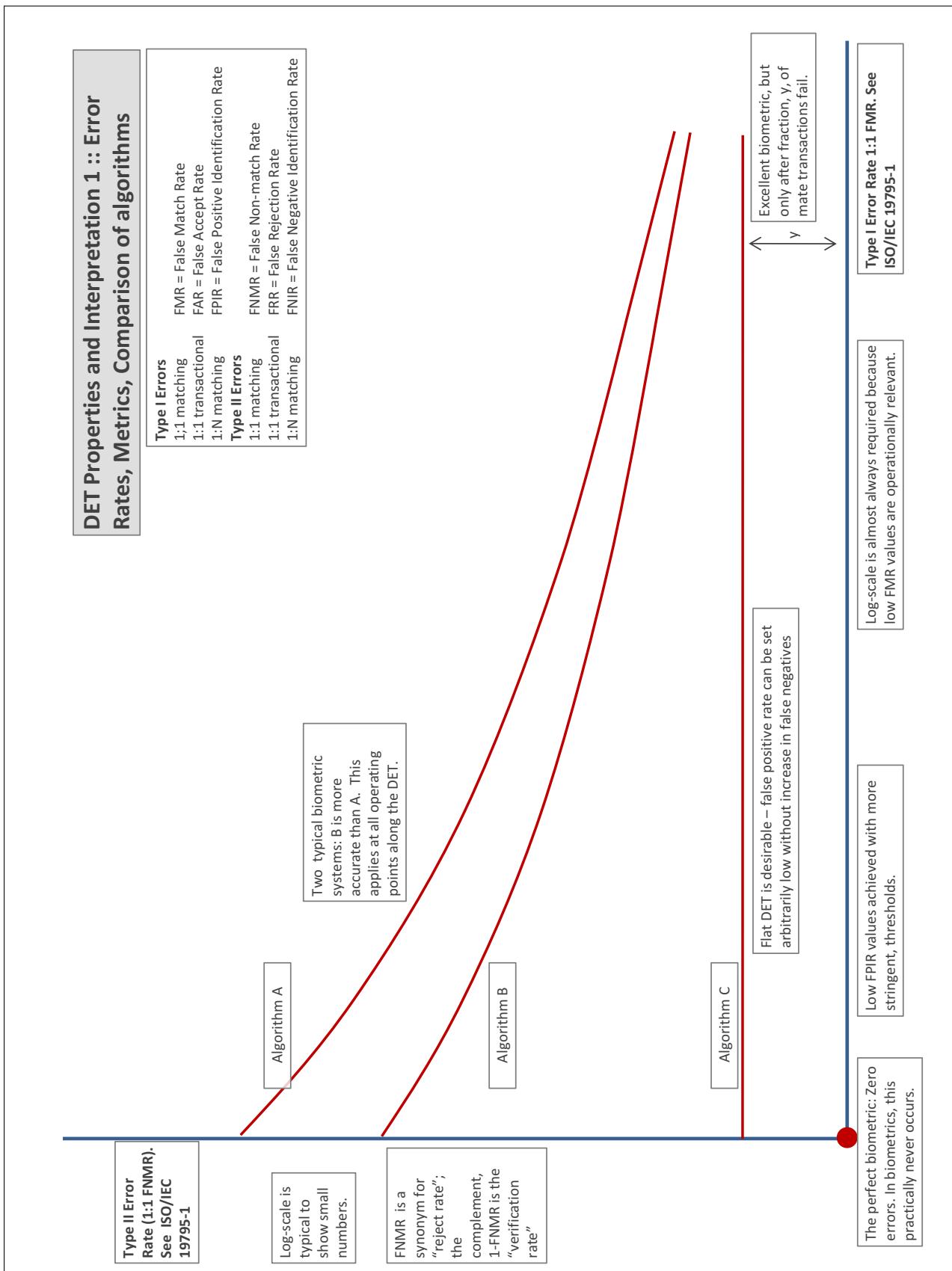
# Accuracy Terms + Definitions

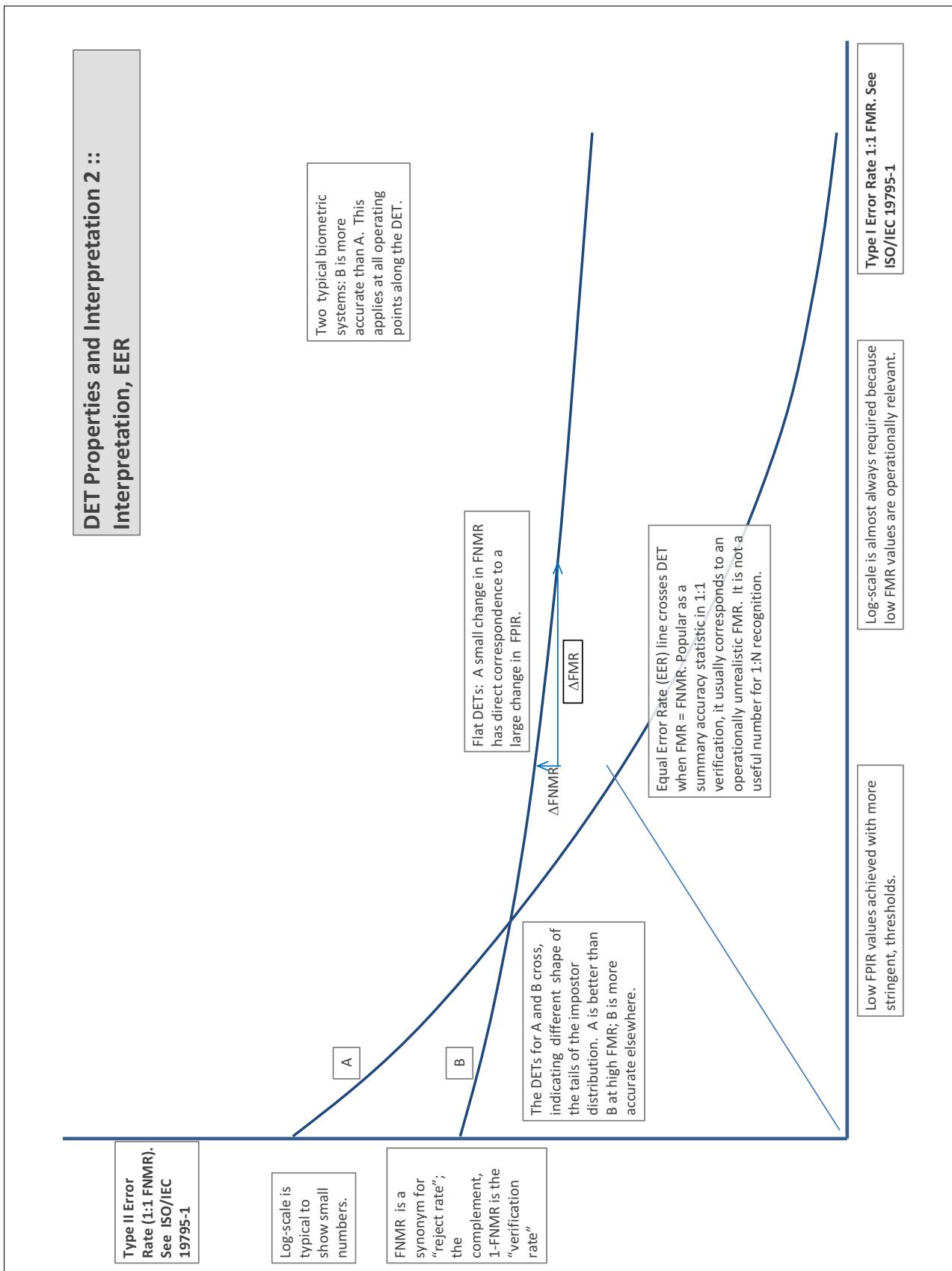
In biometrics, Type II errors occur when two samples of one person do not match – this is called a **false negative**. Correspondingly, Type I errors occur when samples from two persons do match – this is called a **false positive**. Matches are declared by a biometric system when the native comparison score from the recognition algorithm meets some **threshold**. Comparison scores can be either **similarity scores**, in which case higher values indicate that the samples are more likely to come from the same person, or **dissimilarity scores**, in which case higher values indicate different people. Similarity scores are traditionally computed by **fingerprint** and **face** recognition algorithms, while dissimilarities are used in **iris recognition**. In some cases, the dissimilarity score is a distance; this applies only when **metric** properties are obeyed. In any case, scores can be either **mate** scores, coming from a comparison of one person's samples, or **nonmate** scores, coming from comparison of different persons' samples. The words **genuine** or **authentic** are synonyms for mate, and the word **impostor** is used as a synonym for nonmatch. The words mate and nonmatch are traditionally used in identification applications (such as law enforcement search, or background checks) while genuine and impostor are used in verification applications (such as access control).

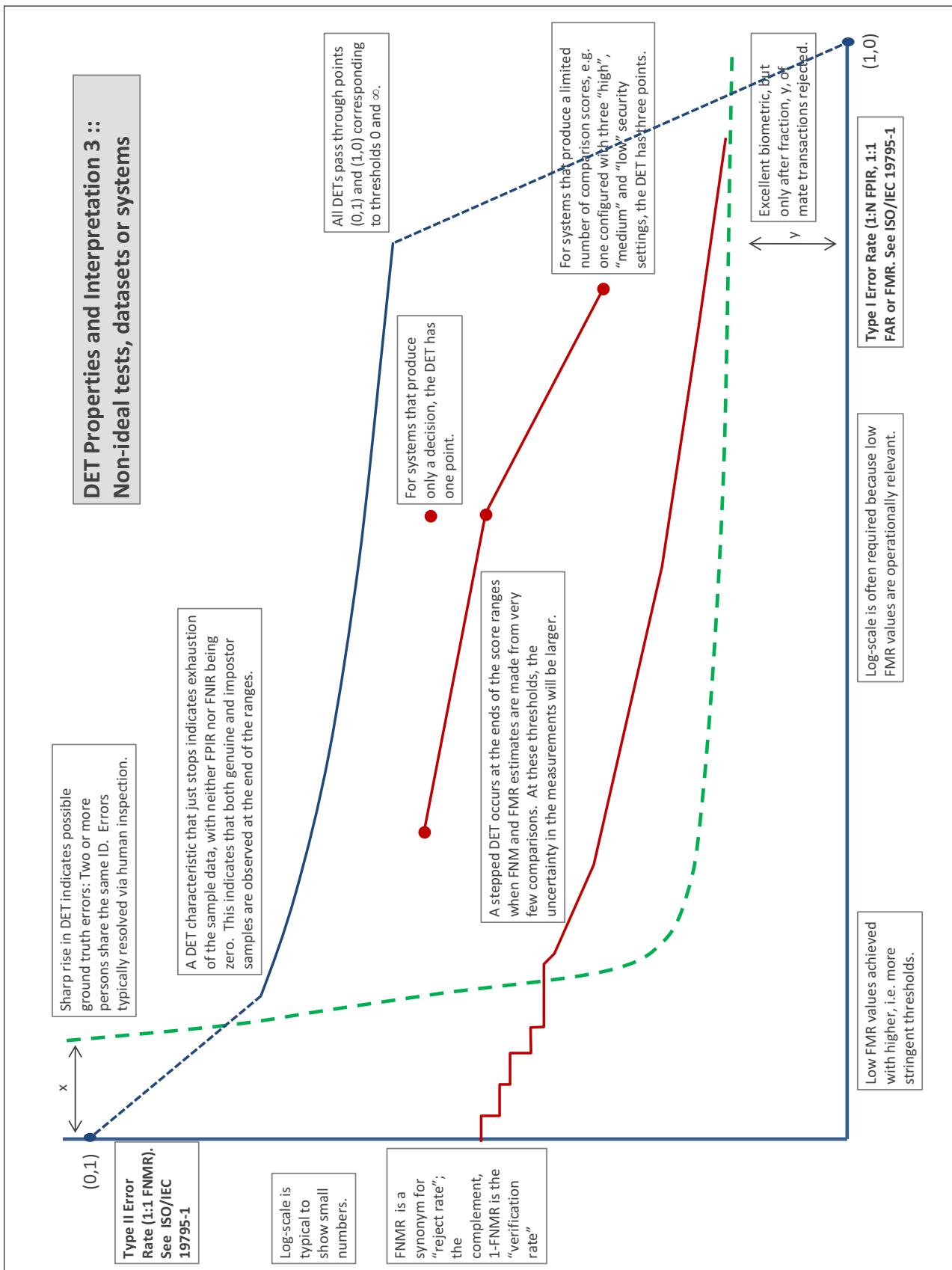
A **error tradeoff** characteristic represents the tradeoff between Type II and Type I classification errors. For verification this plots false non-match rate (FNMR) vs. false match rate (FMR) parametrically with T.

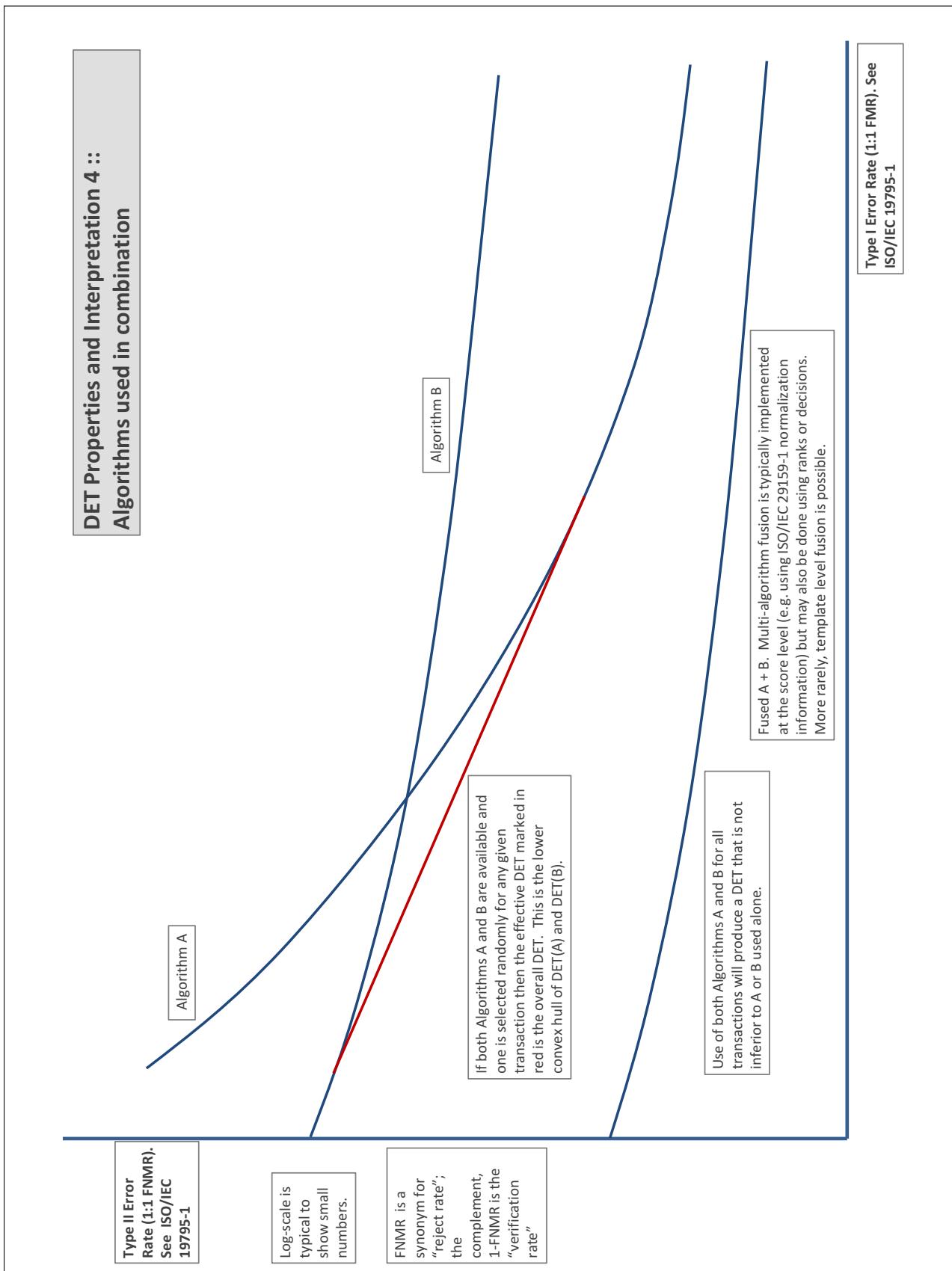
The error tradeoff plots are often called **detection error tradeoff (DET)** characteristics or **receiver operating characteristic (ROC)**. These serve the same function but differ, for example, in plotting the complement of an error rate (e.g.,  $TMR = 1 - FNMR$ ) and in transforming the axes most commonly using logarithms, to show multiple decades of FMR. More rarely, the function might be the inverse Gaussian function.

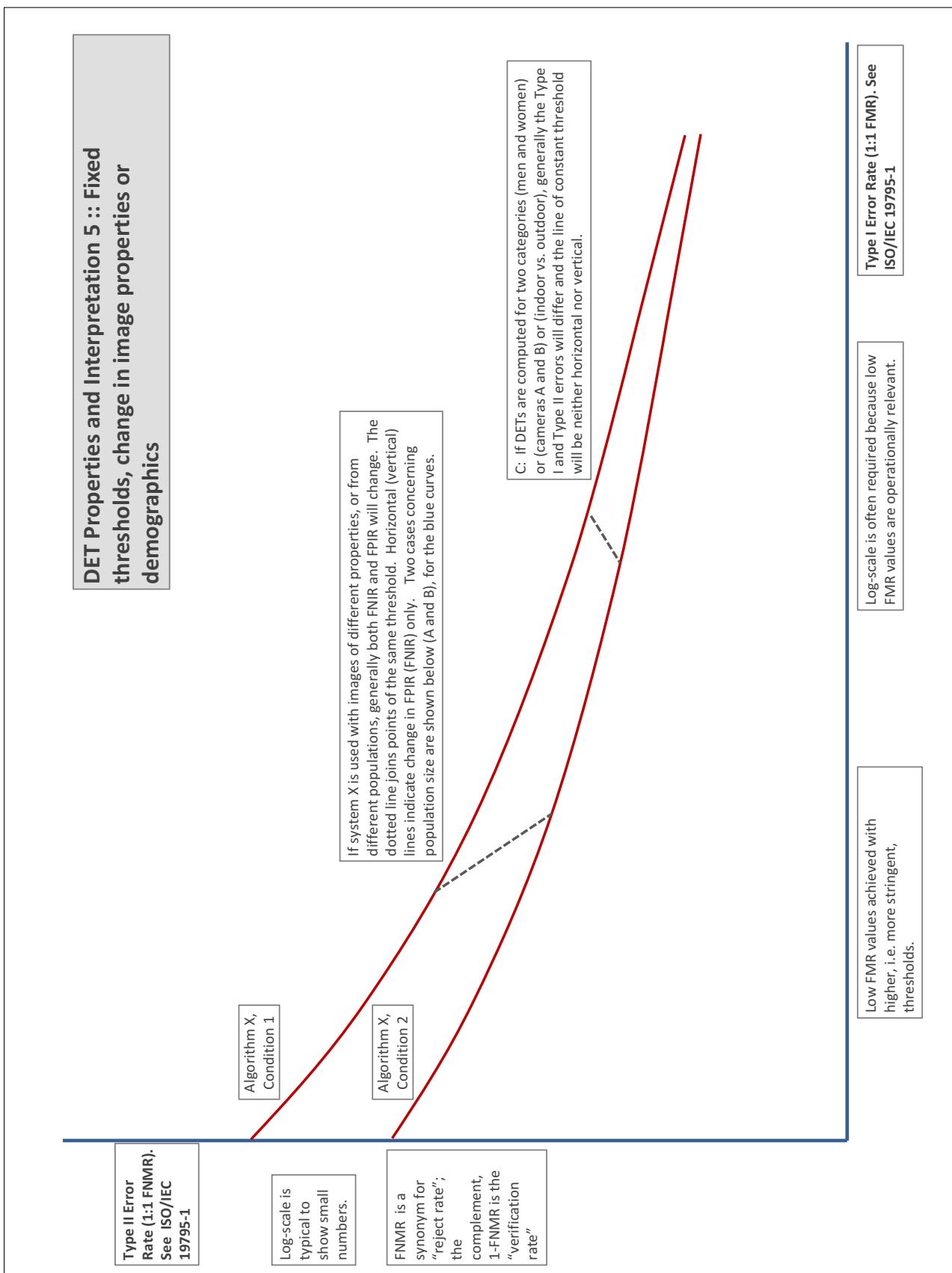
More detail and generality is provided in formal biometrics testing standards, see the various parts of [ISO/IEC 19795 Biometrics Testing and Reporting](#). More terms, including and beyond those to do with accuracy, see [ISO/IEC 2382-37 Information technology -- Vocabulary -- Part 37: Harmonized biometric vocabulary](#)











## References

- [1] P. Jonathon Phillips, Amy N. Yates, Ying Hu, Carina A. Hahn, Eilidh Noyes, Kelsey Jackson, Jacqueline G. Cavazos, Géraldine Jeckeln, Rajeev Ranjan, Swami Sankaranarayanan, Jun-Cheng Chen, Carlos D. Castillo, Rama Chellappa, David White, and Alice J. O'Toole. Face recognition accuracy of forensic examiners, superrecognizers, and face recognition algorithms. *Proceedings of the National Academy of Sciences*, 115(24):6171–6176, 2018.